IMMUNOBIOLOGY OF LEISHMANIASIS

EDITED BY: Herbert Leonel de Matos Guedes, Elvira Saraiva, Alexandre Barbosa Reis, Claudia Ida Brodskyn, Alda Maria Da-Cruz, Prof Sarman Singh and Anabela Cordeiro-da-Silva

PUBLISHED IN: Frontiers in Cellular and Infection Microbiology

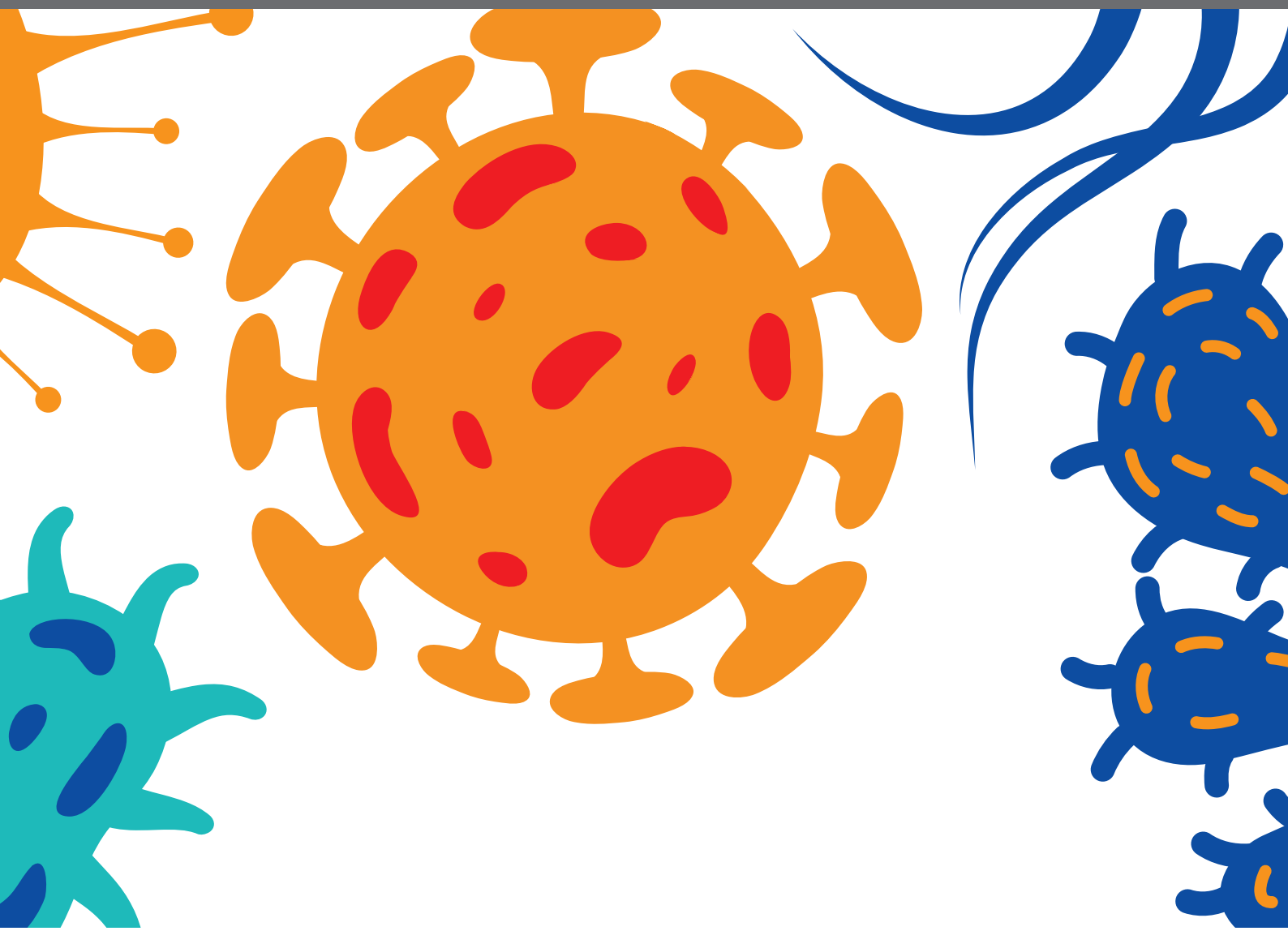

frontiers Research Topics

frontiers

ISSN 1664-8714
ISBN 978-2-88966-029-2
DOI 10.3389/978-2-88966-029-2

About Frontiers

Frontiers is more than just an open-access publisher of scholarly articles: it is a pioneering approach to the world of academia, radically improving the way scholarly research is managed. The grand vision of Frontiers is a world where all people have an equal opportunity to seek, share and generate knowledge. Frontiers provides immediate and permanent online open access to all its publications, but this alone is not enough to realize our grand goals.

Frontiers Journal Series

The Frontiers Journal Series is a multi-tier and interdisciplinary set of open-access, online journals, promising a paradigm shift from the current review, selection and dissemination processes in academic publishing. All Frontiers journals are driven by researchers for researchers; therefore, they constitute a service to the scholarly community. At the same time, the Frontiers Journal Series operates on a revolutionary invention, the tiered publishing system, initially addressing specific communities of scholars, and gradually climbing up to broader public understanding, thus serving the interests of the lay society, too.

Dedication to Quality

Each Frontiers article is a landmark of the highest quality, thanks to genuinely collaborative interactions between authors and review editors, who include some of the world's best academicians. Research must be certified by peers before entering a stream of knowledge that may eventually reach the public - and shape society; therefore, Frontiers only applies the most rigorous and unbiased reviews.
Frontiers revolutionizes research publishing by freely delivering the most outstanding research, evaluated with no bias from both the academic and social point of view. By applying the most advanced information technologies, Frontiers is catapulting scholarly publishing into a new generation.

What are Frontiers Research Topics?

Frontiers Research Topics are very popular trademarks of the Frontiers Journals Series: they are collections of at least ten articles, all centered on a particular subject. With their unique mix of varied contributions from Original Research to Review Articles, Frontiers Research Topics unify the most influential researchers, the latest key findings and historical advances in a hot research area! Find out more on how to host your own Frontiers Research Topic or contribute to one as an author by contacting the Frontiers Editorial Office: researchtopics@frontiersin.org

IMMUNOBIOLOGY OF LEISHMANIASIS

Topic Editors:
Herbert Leonel de Matos Guedes, Federal University of Rio de Janeiro, Brazil
Elvira Saraiva, Federal University of Rio de Janeiro, Brazil
Alexandre Barbosa Reis, Universidade Federal de Ouro Preto, Brazil
Claudia Ida Brodskyn, Gonçalo Moniz Institute (IGM), Brazil
Alda Maria Da-Cruz, Oswaldo Cruz Foundation (Fiocruz), Brazil
Prof Sarman Singh, All India Institute of Medical Sciences, India
Anabela Cordeiro-da-Silva, University of Porto, Portugal

Citation: de Matos Guedes, H. L., Saraiva, E., Reis, A. B., Brodskyn, C. I., Da-Cruz, A. M., Singh, P. S., Cordeiro-da-Silva, A., eds. (2018). Immunobiology of Leishmaniasis. Lausanne: Frontiers Media SA. doi: 10.3389/978-2-88966-029-2

Table of Contents

frontiers in Cellular and Infection Microbiology

ORIGINAL RESEARCH
published: 01 March 2019
doi: 10.3389/fcimb.2019.00030

Understanding Resistance vs. Susceptibility in Visceral Leishmaniasis Using Mouse Models of *Leishmania infantum* Infection

Begoña Pérez-Cabezas[1,2], *Pedro Cecílio*[1,2,3], *Tiago Bordeira Gaspar*[1,4,5,6], *Fátima Gärtner*[1,7,8], *Rita Vasconcellos*[9] *and Anabela Cordeiro-da-Silva*[1,2,3]*

[1] *Instituto de Investigação e Inovação em Saúde, Universidade do Porto, Porto, Portugal,* [2] *Parasite Disease Group, Instituto de Biologia Molecular e Celular, Universidade do Porto, Porto, Portugal,* [3] *Departamento de Ciências Biológicas, Faculdade de Farmácia, Universidade do Porto, Porto, Portugal,* [4] *Cancer Signalling and Metabolism Group, Institute of Molecular Pathology and Immunology of University of Porto, Porto, Portugal,* [5] *Faculdade de Medicina, Universidade do Porto, Porto, Portugal,* [6] *Instituto de Ciências Biomédicas Abel Salazar, Universidade do Porto, Porto, Portugal,* [7] *Department of Molecular Pathology and Immunology, Instituto de Ciências Biomédicas Abel Salazar, Universidade do Porto, Porto, Portugal,* [8] *Glycobiology in Cancer Group, Institute of Molecular Pathology and Immunology of University of Porto, Universidade do Porto, Porto, Portugal,* [9] *Immunobiology Department, Biology Institute, Universidade Federal Fluminense, Rio de Janeiro, Brazil*

OPEN ACCESS

Edited by:
Martin Craig Taylor, London School of Hygiene and Tropical Medicine, United Kingdom

Reviewed by:
Camila I. De Oliveira, Fundação Oswaldo Cruz, Brazil
Travis Bourret, Creighton University, United States

***Correspondence:**
Anabela Cordeiro-da-Silva
cordeiro@ibmc.up.pt

Specialty section:
This article was submitted to Parasite and Host, a section of the journal Frontiers in Cellular and Infection Microbiology

Received: *07 November 2018*
Accepted: *31 January 2019*
Published: *01 March 2019*

Citation:
Pérez-Cabezas B, Cecílio P, Gaspar TB, Gärtner F, Vasconcellos R and Cordeiro-da-Silva A (2019) Understanding Resistance vs. Susceptibility in Visceral Leishmaniasis Using Mouse Models of Leishmania infantum Infection. Front. Cell. Infect. Microbiol. 9:30. doi: 10.3389/fcimb.2019.00030

Every year, up to 90,000 new cases of Visceral Leishmaniasis and 30,000 resultant deaths are estimated to occur worldwide. Such numbers give relevance to the continuous study of this complex form of the disease: a zoonosis and an anthroponosis; two known etiological agents (*Leishmania infantum* and *L. donovani*, respectively); with an estimated average ratio of 1 symptomatic per 10 asymptomatic individuals; and sometimes associated with atypical clinical presentations. This complexity, which results from a long co-evolutionary process involving vector-host, host-pathogen, and pathogen-vector interactions, is still not completely understood. The determinants of visceralization are not fully defined and the dichotomy resistance vs. susceptibility remains unsolved, translating into obstacles that delay the progress of global disease control. Inbred mouse models, with different susceptibility patterns to *Leishmania* infection, have been very useful in exploring this dichotomy. BALB/c and C57BL/6 mice were described as susceptible strains to *L. donovani* visceral infection, while SV/129 was considered resistant. Here, we used these three mouse models, but in the context of *L. infantum* infection, the other *Leishmania* species that cause visceral disease in humans, and dynamically compared their local and systemic infection-induced immune responses in order to establish a parallel and to ultimately better understand susceptibility vs. resistance in visceral leishmaniasis. Overall, our results suggest that C57BL/6 mice develop an intermediate "infection-phenotype" in comparison to BALB/c and SV/129 mouse strains, considering both the splenic parasite burden and the determined target organs weights. However, the immune mechanisms associated with the control of infection seem to be different in each mouse strain. We observed that both BALB/c and SV/129, but not C57BL/6 mice, show an infection-induced increase of splenic T follicular helper cells. On the other hand, differences detected in terms of CD21 expression by B

cells early after infection, together with the quantified anti-*Leishmania* specific antibodies, suggest that SV/129 are faster than BALB/c and C57BL/6 mice in the assembly of an efficient B-cell response. Additionally, we observed an infection-induced increase in polyfunctional CD4+ T cells in the resistant SV/129 model, opposing an infection-induced increase in CD4+IL-10+ cells in susceptible BALB/c mice. Our data aligns with the observations reported for *L. donovani* infection and suggest that not only a single mechanism, but an interaction of several could be necessary for the control of this parasitic disease.

Keywords: *Leishmania*, visceral leishmaniasis, mouse models, susceptibility vs. resistance, immune regulation

INTRODUCTION

More than a century after the discovery of leishmaniasis and its vector-borne causative agent, *Leishmania* spp., a lot of ground remains to be covered. The number of species described associated with human disease has been increasing [around 20 species with clinical relevance (Akhoundi et al., 2016)] and, with them, the complexity of the host-parasite interactions equation. It is well-accepted that the infection outcome depends on a number of factors including the infecting parasite species, and the "equilibrium" between the host immune response and the parasite immune-evasion strategies (Cecílio et al., 2014). These aspects justify the different known leishmaniasis clinical manifestations (that vary from a localized cutaneous ulcer to skin and mucosa metastatic lesions, or to the colonization of internal organs such as the spleen, liver, and bone marrow), consequently associated with different pathological mechanisms (Bates, 2007; Hartley et al., 2014). Every year up to one million new cases and 30,000 deaths are associated with this spectrum of diseases (World Health Organization, 2017).

The quest for the missing vaccine and for better therapeutic options for human leishmaniasis requires the understanding of the infectious process (from the transmission of *Leishmania* parasites by their phlebotomine vector) which is still not completely understood. The determinants of metastization (diffuse cutaneous leishmaniasis; mucocutaneous leishmaniasis; PKDL) and visceralization (visceral leishmaniasis) are still ambiguous, while the susceptibility vs. resistance dichotomy remains unestablished for some disease forms (McCall et al., 2013; Hartley et al., 2014). The use of murine inbred animal models was indispensable for the establishment of the Th1/Th2 paradigm which explains resistance vs. susceptibility (respectively) to cutaneous disease (Sacks and Noben-Trauth, 2002), and for the disclosure of genetic resistance determinants in visceral disease, such as the expression of Nramp1 antiporter, that when functional, prevents parasite replication in the phagolysosome, by limiting their access to essential divalent cations (Lipoldova and Demant, 2006; Kumar and Nylén, 2012). Still, in visceral disease, the immunological aspects that condition parasite persistence and their connection with host genetic factors needs to be further explored, in a way to definitively understand resistance vs. susceptibility.

Here, taking advantage of three inbred mouse strains, with known different susceptibility patterns to infection by the viscerotropic *L. donovani* species (Lipoldova and Demant, 2006), we compared the development of experimental *L. infantum* infection, the main causative agent of visceral leishmaniasis in South America and the Mediterranean Basin (Ready, 2014). For this, at two different time-points, we quantified the parasite burdens in the main target organs; evaluated the liver's granulomatous responses; studied the splenic immune cell compartment composition and their infection-induced modifications, particularly emphasizing T and B lymphocyte's phenotypes; and assessed the development of specific humoral responses against the parasite, as a way to explore the above-mentioned dichotomy. The data obtained complement findings recently reported for *L. donovani* infection (Bodhale et al., 2018), important for the establishment of a parallel between the viscerotropic *Leishmania* strains in the context of *in vivo* infections.

MATERIALS AND METHODS

L. infantum Culture

A cloned line of virulent *Leishmania infantum* (MHOM/MA/67/ITMAP-263) freshly recovered from BALB/c mice was used for a total of 10 passages. Promastigotes were routinely maintained at 26°C in standard RPMI 1640 medium supplemented with 10% heat-inactivated Fetal Calf Serum (FCS; Biowest, Nuaillé, France), 2 mM L-glutamine, 100 U/ml penicillin, 100 μg/ml streptomycin and 20 mM HEPES buffer, all products from Lonza (Basel, Switzerland). All maintenance cultures were grown with a starting inoculum of 10^6 parasites/ml. Parasites for *in vivo* infections were always collected after 5 days of culture.

Mouse Strains, Infections, and Euthanasia

Six- to eight-week-old sex-matched BALB/c, C57BL/6 and SV/129 mice (Charles River Laboratories, France) were maintained under specific pathogen-free conditions at the i3S facilities, in sterile IVC cabinets, with food and water available *ad libitum*. The three mouse strains were always infected in parallel with the same parasite's preparation. Each animal was infected intraperitoneally with 1×10^8 stationary promastigotes, prepared as reported elsewhere (Faria et al., 2016). Two or eight weeks after infection, mice were anesthetized with isoflurane (Piramal healthcare, Northumberland, UK) and further manipulated only after the total loss of pedal reflex (firm

toe pinch). Euthanasia was performed by cervical dislocation (under volatile anesthesia). All the controls (non-infected) used in the experiments were strain-, age-, and sex-matched.

Blood and Organ Collection and Manipulation

Blood from mice was collected through intracardiac puncture under isoflurane anesthesia. Serum was collected and stored at −80°C for posterior analysis. Spleens and livers were aseptically collected from euthanized animals, weighed, and either homogenized using Falcon® 100 μm Cell Strainers (Corning Life Sciences, Tewksbury, MA, USA) and manual Potter-Elvehjem tissue homogenizers, respectively, or preserved in formalin for posterior histological evaluation.

Determination of Parasite Burdens

Splenic and hepatic parasite burdens were assessed using the limit dilution method, starting from 1 and 5 mg of organ, respectively. The "parasite titer" was considered the last dilution with >1 motile parasite. The number of parasites per gram of organ was calculated as previously described (Silvestre et al., 2007).

Histopathology

Livers were fixed in 10% formaldehyde (pH 7.4) for 48 h, followed by dehydration in ethanol and clarification in xylene (all from Sigma-Aldrich, MO, USA). Tissues were embedded in paraffin and cut to a thickness of 4 μm. All sections were stained with Hematoxylin and Eosin (H&E) for histopathological analysis. Slides were observed in an Axioskop 2 Zeiss microscope (Carl Zeiss, Jena, Germany) and photographs (100 and 400X magnifications) were acquired using a Nikon DS-L1 camera (Nikon, Tokyo, Japan). Two distinct observers blindly evaluated the preparations. The total number of granulomas was determined for each animal by accounting 20 microscopic fields (100x magnification). In cases with a very poor granulomatous response, the total number of granulomas *per* slide was accounted for.

Flow Cytometry

The anti-mouse monoclonal antibodies used to perform this study were all purchased from BioLegend (CA, USA) except if otherwise stated: FITC labeled anti-IgM (R6-60.2, BD Biosciences, NJ, USA), anti-CD8 (53-6.7), and anti-IFN-γ (XMG1.2); PE labeled anti-CD8 (53-6.7, BD), anti-CD44 (IM7), anti-CD19 (6D5) and anti-CXCR5 (L138D7); PerCP labeled anti-TNFα (MP6-XT22), anti-CD3 (17A2) and anti-CD4 (RM4-5); PE-Cy7 labeled anti-CD3 (HA2), anti-GL7 (GL7) and anti-PD1 (RMP1-30); APC labeled anti-CD19 (6D5), anti-CD23 (B3B4) and anti-IL-10 (JES5-16E3); BV510 labeled anti-CD4 (RM4-5), PB labeled anti-CD21 (7E9) and anti-IL-2 (JES6-5H4); and BV421 labeled anti-CD62L (MEL-14).

To analyze lymphoid cell populations, different antibody panels were designed. The general lymphoid panel was composed of anti-CD8, -CD3, -CD4, and -CD19. The T cell memory phenotype panel was composed of anti-CD8, -CD3, -CD4, -CD44, and -CD62L. The "T follicular" panel was composed of anti-CD3, -CD4 –PD1, and –CXCR5. The "B cell phenotype" panel was composed of anti-CD19, -IgM, -CD21, -CD23 and -GL7. Surface staining of splenic cells was performed in PBS + 0.5% BSA (20 min, 4°C) followed by 15 min fixation using 1% PFA. For intracellular staining, splenocytes were cultured for 4 h with PMA/Ionomycin (50/500 ng/ml) and Brefeldin A (10 μg/mL). Cells were surface-stained and then intracellularly after fixation and permeabilization with 1% saponin (all from Sigma-Aldrich, MO, USA). Isotype controls were always used for this study. Samples were acquired in a FACSCanto (BD, Franklin Lakes, NJ, USA) and analyzed with FlowJo software v10 (TreeStar, OR, USA).

Supplementary Figure 1 illustrates the gating strategies used in this work. Briefly, an initial gate plotting FSC-A vs. SSC-A was performed to exclude cell debris. Afterward, singlets were selected by plotting FSC-A vs. FSC-H and the remaining cell populations were resolved. T lymphoid cell populations were defined as CD3+/CD4+ and CD3+/CD8+ while B cells were defined as CD19+. Memory populations were defined as Naïve (CD62L+CD44-), T Effector Memory (TEM – CD62L-CD44+), and T Central Memory (TCM – CD62L+CD44+). Expression of CD21, CD23, and GL7 was evaluated within B cells. Cytokine production by T cells was assessed within CD3+/CD4+ and CD3+/CD8+ cells. Co-expression of PD1 and CXCR5 was evaluated within CD3+/CD4+ T cells.

Immunoglobulin Determination

Antigen-specific immunoglobulins were quantified by sandwich ELISA. Briefly, high protein binding 96-well plates (Greiner Bio-One, Kremsmünster, Austria) were coated overnight at 4°C with Soluble Total *Leishmania infantum* Antigens (Silvestre et al., 2008) prepared in NaHCO3 0.1 M to a final concentration of 40 μg/ml. Plates were then washed with PBS Tween 0.1%, blocked with 1% gelatin from porcine skin (Sigma-Aldrich, MO, USA) in PBS (blocking buffer) for 1 h at 37°C and re-washed. Each serum was then diluted 1:100 in blocking buffer and added to the plates in duplicate. Wells filled with just blocking buffer were used as blanks. Plates were incubated for 2 h at 37°C and re-washed. Afterward, IgG and IgG1 were detected using horseradish peroxidase (HRP) coupled α-mouse antibodies [diluted 1:5,000 (IgG1; Southern Biotech, AL, USA) or 1:8,000 (IgG; Southern Biotech, AL, USA) in blocking buffer; incubated for 1 h, at 37°C]. Plates were washed for the last time, and the substrate (ortho phenyl diamine (OPD) in citrate buffer) was added for 10 min, time after which the reaction was stopped with HCl 3 N. Absorbance values were determined at 492 nm in a Synergy™ 2 Multi-Mode Reader (BioTek instruments, VT, USA).

Statistical Analysis

Results are expressed per individual animals/samples and/or normalized in relation to the average values of the respective control groups, with a representation of the group mean-value ± standard deviation. Statistical differences were analyzed using GraphPad Prism v6.01 (CA, USA). One Way ANOVA (with Tukey's *post-hoc* analysis) was used for comparisons between the different murine strains (infected or non-infected), as well as for the comparison of normalized values; *t*-test

was used for comparison between infected animals and the respective controls.

RESULTS

Dynamics of *L. infantum* Infection in the Different Mouse Strains: Looking at the Main Target Organs

To study the determinants of visceral leishmaniasis resistance vs. susceptibility, we compared the evolution of experimental *L. infantum* infection in three inbred mouse strains. SV/129 is the strain described as resistant while C57BL/6 and BALB/c are defined as susceptible models in the context of *L. donovani* infection (Lipoldova and Demant, 2006). Two weeks after an intraperitoneal challenge with 1×10^8 *L. infantum* promastigotes, BALB/c mice showed significantly higher splenic parasite burdens in comparison with their SV/129 counterparts (**Figure 1A**, $p \leq 0.05$). This was accompanied by infection-induced increased hepatic and splenic weights in BALB/c, in a higher magnitude than the one observed for both C57BL/6 and SV/129 (**Figure 1B**, $p \leq 0.05$). Eight weeks post-infection, BALB/c mice still presented the highest splenic parasite counts, followed by C57BL/6 and last by SV/129 **Figure 1A**, $p \leq 0.05$), although at this time-point relative spleen weights were comparable among all the mouse strains (**Figure 1B**). Interestingly, at this later time point, relative liver weights were significantly different comparing the mouse strains (at least $p \leq 0.05$): BALB/c relative liver weight was the highest, while SV/129 was the lowest (**Figure 1B**) with a liver weight below the determined weight for control animals (**Supplementary Figure 2A**). However, such differences were not translated into different absolute hepatic parasite burdens, determined comparable among groups at both 2- and 8-weeks post-infection. Curiously, liver granulomatous response to *L. infantum* infection was consistently different between the mouse strains (**Figures 1C,D**, **Supplementary Figure 2B**). While BALB/c mice liver-sections contained on average 10 granulomas/field at both 2- and 8-weeks post-infection, in C57BL/6 we observed on average five hepatic granulomas/field (2- and 8 -weeks post-infection) and in SV/129 always less than five granulomas/field (**Figure 1D**). Additionally, we observed that SV/129 had rather less structured cell infiltrates when compared to the more susceptible mouse strains (**Figure 1C**).

Basal Differences in the Murine Strains Splenic Cell Compartments and Their Modification 2 Weeks Post-infection

It is known that the splenic cell compartments of different murine strains are not similar (Forni, 1988). To understand if such differences would influence the early response to *L. infantum* infection, we resolved by flow cytometry the splenic cell compartments of the three murine strains studied, comparing animals infected for 2 weeks with their non-infected counterparts. While regarding the lymphoid splenic cell populations, we observed differences comparing BALB/c, C57BL/6, and SV/129 both before and 2 weeks after infection (**Figures 2A,B**), this was not true for myeloid cell populations for which no major differences were observed (data not shown).

T lymphocytes (CD3+) represented more than 35% of spleen cells in BALB/c and SV/129 control mice, while in C57BL/6 this population accounted in average for 25% of this organ basal cell content (**Figure 2A**). Furthermore, within splenic T lymphocytes the basal levels of CD4+ cells were higher in BALB/c (50%) than in SV/129 (40%) and C57BL/6 (30%), while the basal levels of CD8+ were higher in C57BL/6 (55%) compared to both BALB/c and SV/129 mice (around 40%) (**Figure 2A**). Two weeks post-infection, these general tendencies were overall maintained, although an infection-induced effect was observed for BALB/c mice: CD3+ T cells decreased with infection (statistically different normalized numbers compared with SV/129, $p \leq 0.05$), as well as CD4+ T cells ($p \leq 0.05$ compared with non-infected values). We also resolved the T cell memory pool, and although we observed some differences comparing the strains, no major infection-induced effect was observed for CD4+ T cells, while for CD8+ T cells an infection-induced decrease in naïve and an increase in TEM and TCM populations was observed, particularly comparing C57BL/6 with BALB/c animals (**Supplementary Figure 3**). Additionally, we analyzed a subset of CD4+ T lymphocytes expressing CXCR5 and PD1, known as follicular helper T cells (Tfh), important for germinal center reaction related to T-B cell cognate interaction, since they may play an important role in the anti-*Leishmania* immune response (Rodrigues et al., 2014). Although the basal levels of this population were higher in C57BL/6 animals, 2 weeks post-infection this CD4 subset significantly increased in BALB/c and SV/129 mice, while it did not change in C57BL/6 mice (**Figure 1A**, $p \leq 0.05$ or $p \leq 0.01$, compared with BALB/c or SV/129, respectively).

Concerning total splenic B cells (CD19+) we observed that their basal levels in BALB/c mice were lower in comparison with C57BL/6 animals (**Figure 2B**). Furthermore, no major changes were observed in the frequencies of splenic B cells 2 weeks after infection (**Figure 2B**). Although most of these B cells expressed CD23 [important down-regulator of BCR signaling (Liu et al., 2016)], SV129 displayed a relatively larger population of CD19+CD23lo/- cells than BALB/c or C57BL/6. However, once again no significant changes in the frequency of CD19+CD23+ cells were observed as a consequence of *L. infantum* infection. CD21 is an important co-receptor molecule in BCR cognate stimulation (Roozendaal and Carroll, 2007). Although no significant differences were detected in terms of basal expression, comparing the three murine strains, a downregulation of this receptor 2 weeks after infection was detected for both BALB/c and C57BL/6 (**Figure 2B**), but not for SV129. Last but not least, we also observed a significant increase in the expression of the activation marker GL7 only in BALB/c mice 2 weeks after infection (**Figure 2B**; $p \leq 0.05$).

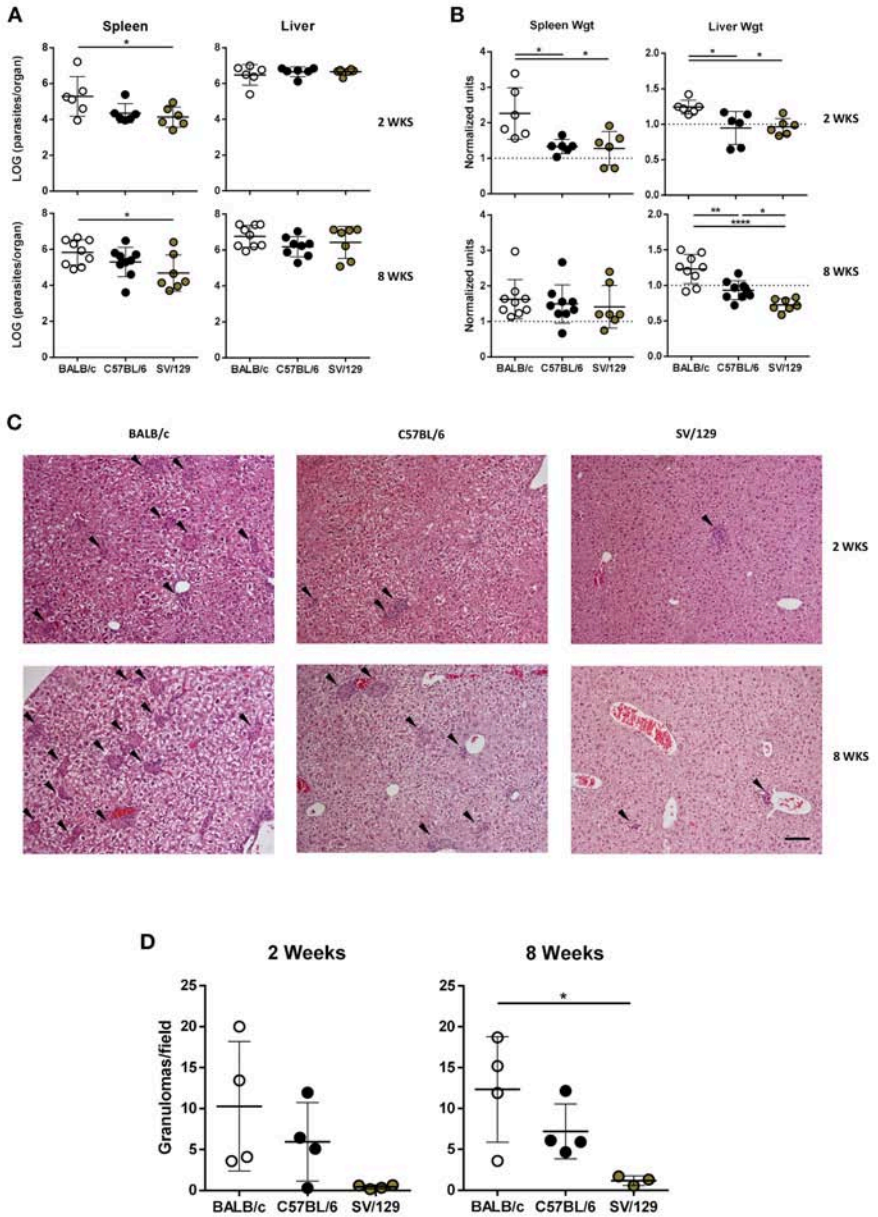

FIGURE 1 | Parasite burdens, organ weights, and hepatic granulomas quantification in the three murine strains 2 and 8 weeks after infection with *L. infantum*. BALB/c (white circles), C57BL/6 (black circles) and SV/129 (brown circles) mice were infected intraperitoneally with 1×10^8 *L. infantum* promastigotes and euthanized 2 or 8 weeks after. Aged matched non-infected controls were euthanized at the same time-points. **(A)** Hepatic and splenic total parasite burdens (determined by limiting dilution). **(B)** Relative splenic and hepatic weight alterations with infection (normalized by the controls average organ weights). **(C)** Hepatic granuloma morphology (representative images of H&E stained liver slides; 100X magnification; arrowheads point to granulomas; scale bar corresponds to 100 μm) and **(D)** quantification. Each dot represents an animal; average and SD of the values within each group are shown **(A,B,D)**. Results are representative of at least two independent experiments. Statistical differences are properly identified (One-Way ANOVA (with Tukey's *post-hoc* analysis): $^*p \leq 0.05$, $^{**}p \leq 0.01$, and $^{****}p \leq 0.0001$).

Murine Strains Splenic Cell Compartment Composition 8 Weeks Post-infection

To figure out if the murine strain's splenic cell compartments would differentially change with the course of *L. infantum* infection, we performed flow cytometry analysis in the spleens from age-matched BALB/c, C57BL/6 and SV/129 mice, at 8 weeks post-infection, always in comparison with the respective non-infected and age-matched controls. Once again, in the myeloid cell compartment no major infection-induced differences were seen at this later time-point (data not shown) while in the lymphoid cell compartment some alterations with the course of infection were observed (**Figure 3**). The CD3+

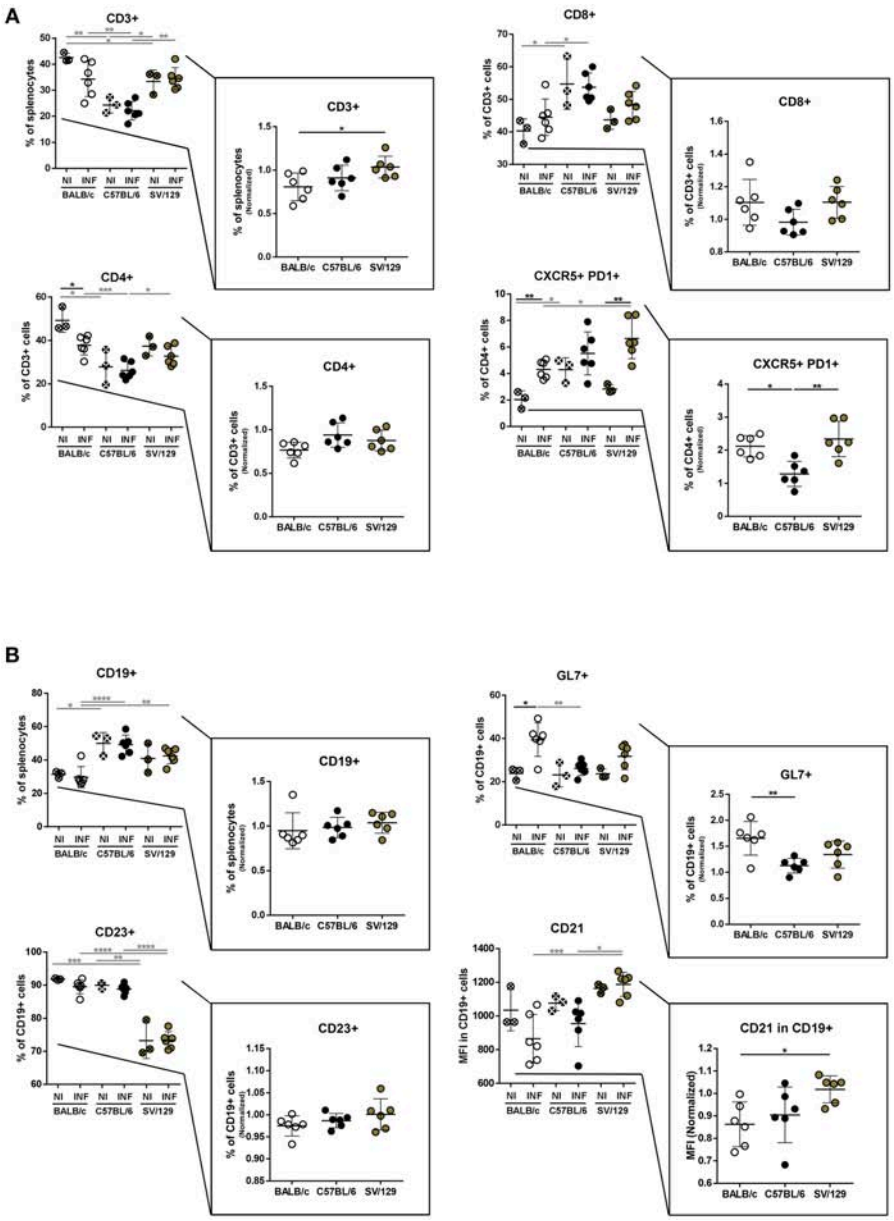

FIGURE 2 | Splenic lymphoid compartment of the different mouse strains and it's alteration 2 weeks post *L. infantum* infection. BALB/c (white circles), C57BL/6 (black circles), and SV/129 (brown circles) mice were infected intraperitoneally with 1×10^8 *L. infantum* promastigotes and euthanized 2 weeks after. Splenic lymphoid populations were resolved by flow cytometry: T cell **(A)** and B cell **(B)** compartments. Results, obtained in at least two independent experiments, are represented both in total percentages (infected and control animals) and normalized (infected in relation to control group average values) as a way to highlight the infection-induced alterations. Each dot represents an animal. Average and SD of the values within each group are shown. Statistical differences are properly identified. One Way ANOVA (with Tukey's *post-hoc* analysis) was used for comparisons between the different murine strains (infected or non-infected; gray lines), as well as for comparison of normalized values (black lines); *t*-tests (black lines) were performed for comparison between infected animals and controls from the same strain: $^*p \leq 0.05$, $^{**}p \leq 0.01$, $^{***}p \leq 0.001$, and $^{****}p \leq 0.0001$).

cells normalized levels at this time point were comparable among the groups, while the CD4+ and CD8+ normalized values were significantly different in C57BL/6 mice compared to both BALB/c and SV/129 strains: the infection induced an increase of CD4+ and a decrease of CD8+ T cells (**Figure 3A**). Furthermore, with respect to the T cell memory pool, apart from the previously observed strain-specific differences in basal levels, no major infection-induced alterations were observed (**Supplementary Figure 4**). Additionally, and as observed 2 weeks after infection, differences in CD4+CXCR5+PD1+ T cells were detected, comparing the different mouse strains, regarding both basal levels and the ones determined in 8-week-infected

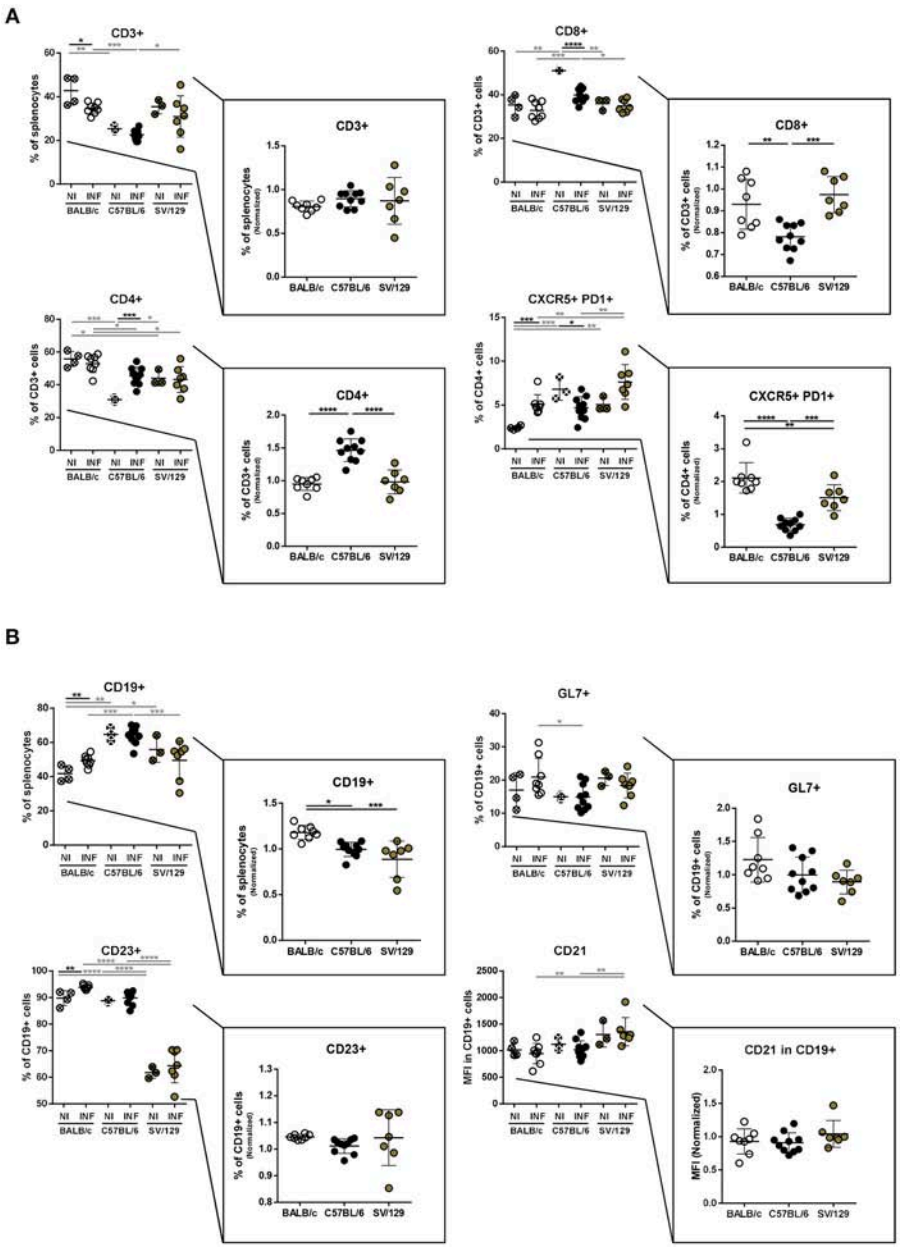

FIGURE 3 | Splenic lymphoid compartment of the different mouse strains and it's alteration 8 weeks post *L. infantum* infection. BALB/c (white circles), C57BL/6 (black circles), and SV/129 (brown circles) mice were infected intraperitoneally with 1×10^8 *L. infantum* promastigotes and euthanized 8 weeks after. Splenic lymphoid populations were resolved by flow cytometry: T cell **(A)** and B cell **(B)** compartments. Results, obtained in at least two independent experiments, are represented both in total percentages (infected and control animals) and normalized (infected in relation to control group average values) as a way to highlight the infection-induced alterations. Each dot represents an animal. Average and SD of the values within each group are shown. Statistical differences are properly identified. One Way ANOVA (with Tukey's *post-hoc* analysis) was used for comparisons between the different murine strains (infected or non-infected; gray lines), as well as for comparison of normalized values (black lines); *t*-tests (black lines) were performed for comparison between infected animals and controls from the same strain: $^*p \leq 0.05$, $^{**}p \leq 0.01$, $^{***}p \leq 0.001$, and $^{****}p \leq 0.0001$).

animals. While C57BL/6 mice showed a decrease of splenic Tfh cells ($p \leq 0.05$; compared with control counterparts), SV/129, and BALB/c mice showed an increase in this splenic T cell subset, more pronounced for the latest (**Figure 3A**; $p \leq 0.001$, compared with control counterparts). Finally, at this later time-point, an infection-induced increase in the splenic B cells was observed in BALB/c mice ($p \leq 0.01$) but not in C57BL/6 nor SV/129 animals, although phenotypically no alterations

were observed with infection comparing the different mouse strains (**Figure 3B**).

Dynamics of Splenic T Cell's Cytokine Response With the Course of Infection in the Different Mouse Strains

It is well-known that the inflammatory environment of target organs conditions parasite persistence or elimination (Rodrigues et al., 2016). These responses are particularly relevant in the spleen, organ used many times to distinguish between susceptible and resistant animal models, related to observations of infection progression or parasite elimination, respectively (Stanley and Engwerda, 2007). To extrapolate the infection-induced environment in the spleen of the different animal models used in this study, and to disclose potential differences between them, we evaluated by flow cytometry the cytokine production potential of splenic T cells at 2- and 8-weeks post-infection, always compared to non-infected matched controls.

Overall, no major differences were observed in the basal cytokine production by CD4+ T cells. Additionally, early after infection, all murine strains showed a similar capacity to produce IFN-γ. On the other hand, CD4+ T cells from infected BALB/c mice responded by producing significantly more IL-2 and IL-10 compared to both non-infected counterparts and infected C57BL/6 and SV/129 mice (**Figure 4A**; at least $p \leq 0.05$). No significant differences with respect to TNF-α producing CD4+ T cells were observed at this time-point, when comparing the different mouse strains, and consequently, no significant differences were observed when we looked at the frequencies of splenic polyfunctional CD4+ T cells (with the potential to produce simultaneously IFN-γ, IL-2, and TNF-α) (**Figure 4A**). However, 8 weeks after infection, SV/129 mice displayed a significant increase in the percentage of splenic CD4+ T cells with the capacity to secrete IFN-γ or TNF-α (**Figure 4B**; at least $p \leq 0.05$). This translated into a significant increase in the levels of splenic polyfunctional CD4+ T cells, comparing SV/129 animals with both BALB/c and C57BL/6 mice (**Figure 4B**; $p \leq 0.05$ and $p \leq 0.01$, respectively). Furthermore, at 8 weeks post-infection, the percentage of splenic CD4+ T cells showing the potential to secrete IL-10 was significantly and tendentiously increased in BALB/c and SV129 mice, respectively. Curiously, at this later time-point, the only infection-induced phenotype observed for C57BL/6 animals was the significant increase in the IL-2 production by splenic CD4+ T cells (**Figure 4B**).

Regarding the basal splenic CD8+ T cell cytokine-secreting potential, some differences were observed, particularly comparing SV/129 with the other models that show a higher response (**Figure 5A**). However, when we evaluated infection-induced effects 2 weeks post-challenge, splenic CD8+ T cells from C57BL/6 and SV/129 mice showed a greater potential of TNF-α secretion, when compared to BALB/c animals (**Figure 5A**; at least $p \leq 0.05$ comparing normalized values). Once again at this early time-point after infection, no major differences were observed in terms of infection-induced IFN-γ secretion (now by CD8+ T cells), while a significant increase in the splenic CD8+ T cells with the ability to produce either IL-10 or IL-2 was observed comparing BALB/c mice with both C57BL/6 and SV/129 animals (**Figure 5A**; at least $p \leq 0.05$ comparing normalized values). At 8 weeks post-infection we once again detected some differences in CD8+ T cell's cytokine-secretion potential when we compared the three mouse strains. While the infection-induced increase of CD8+ T cells producing IFN-γ was not strain related, TNF-α splenic CD8+ T cell secretion potential of SV/129 mice was significantly higher than the one of CD8+ T cells from both BALB/c and C57BL/6 animals (**Figure 5B**; $p \leq 0.0001$). Furthermore, as for CD4+ T cells at this time-point, splenic CD8+ T cells from C57BL/6 mice showed a significantly higher capacity of producing IL-2 than both CD8+ T cells from BALB/c and SV/129 (**Figure 5B**; at least $p \leq 0.001$). Finally, at this later time-point post-infection, CD8+ T cells from infected BALB/c mice maintained their capacity to secrete IL-10 (**Figure 5B**).

Anti-*Leishmania* Specific Immunoglobulin Response to Infection in the Three Murine Strains

The role of antibodies in leishmaniasis susceptibility vs. resistance is still not clear (Rodrigues et al., 2016). However, antibody responses, particularly having in consideration IgG isotypes, as the switch for IgG1 isotype is dependent on IL-4 and can be a marker of a Th2 response, may help us to better understand the immune response being mounted against *Leishmania* parasites (Tripathi et al., 2007). Because of this, we evaluated, using ELISA, the specific antibody responses generated upon *Leishmania* infection in the three mouse strains, at 2- and 8-weeks post-infection. Specific IgG response could be detected 2 weeks after *L. infantum* infection in mice from the three strains (**Figure 6A**). Curiously, SV/129 mice presented significantly higher levels of serum IgG that binds to *L. infantum* antigens, in comparison with both BALB/c and C57BL/6 strains (**Figure 6A**; $p \leq 0.001$). Importantly, this difference was not mediated by a significant increase of anti-*Leihmania* specific IgG1 antibodies (**Figure 6A**). Later, 8 weeks after infection, we did not observe any further difference in the levels of serum *L. infantum* specific IgG antibodies, comparing all mouse strains. However, at this later time-point, BALB/c mice presented significantly higher levels of serum *L. infantum* specific IgG1 antibodies, when compared to both C57BL/6 and SV129 infected mice (**Figure 6A**; at least $p \leq 0.05$). These results were evidenced by the calculation of specific immunoglobulin dynamics: BALB/c mice presented on average 5-fold more anti-*Leihmania* specific IgG1 antibodies at 8 vs. 2 weeks post-infection, while C57BL/6 and SV129 mice presented no more than a 2-fold increase.

DISCUSSION

One of the layers of complexity associated with leishmaniasis relates to the distinct known disease manifestations, a consequence of heterogeneous pathogen-host interactions that will condition the infectious process outcome (Loeuillet et al., 2016; Cecilio et al., 2018). While for some disease

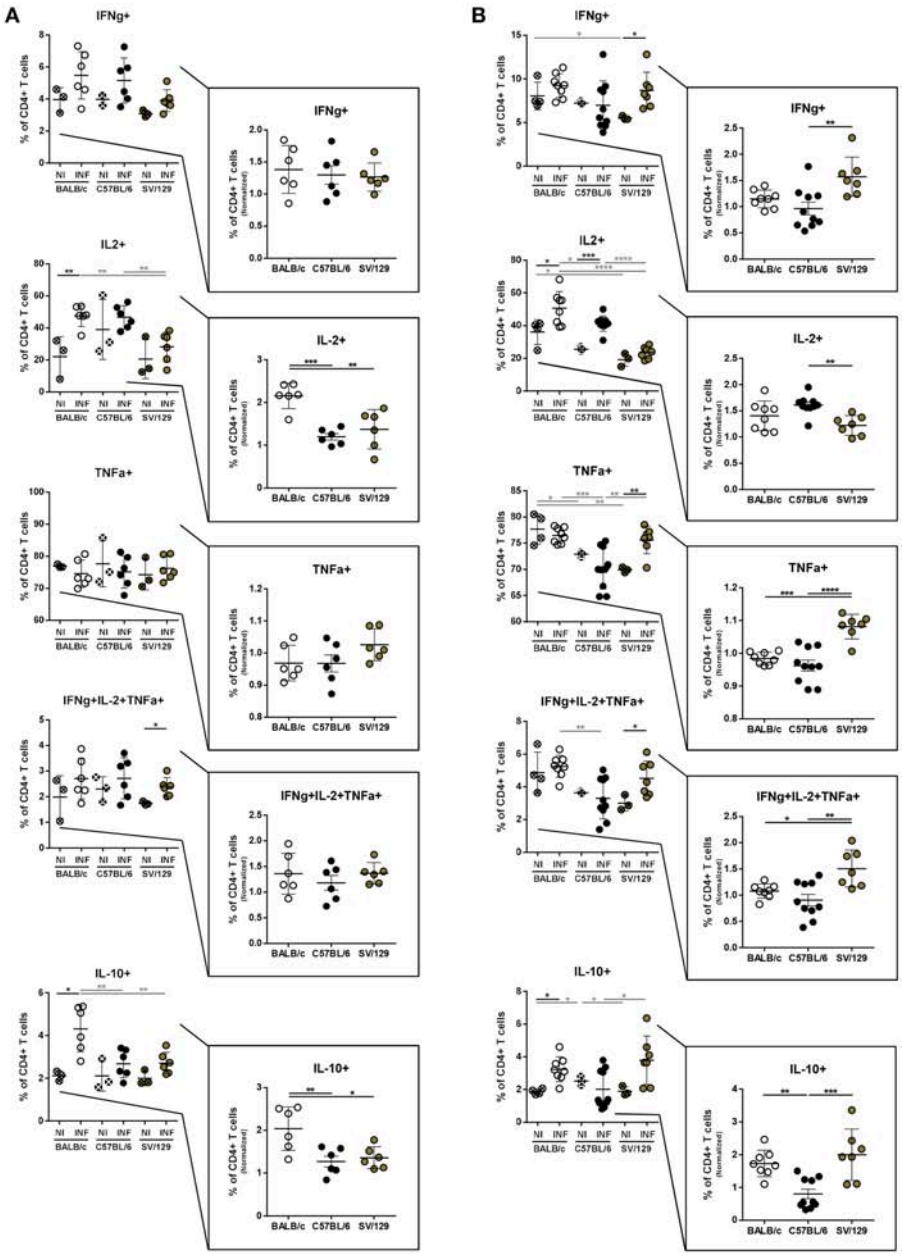

FIGURE 4 | Basal intracellular cytokine production by CD4+ T cells of the different mouse strains and it's alteration 2- and 8-weeks post *L. infantum* infection. BALB/c (white circles), C57BL/6 (black circles), and SV/129 (brown circles) mice were infected intraperitoneally with 1×10^8 *L. infantum* promastigotes and euthanized 2 or 8 weeks after. Splenocytes were cultured with PMA + Ionomycin + Brefeldin A for 4 h. CD4+ T cell frequencies producing IFN-γ, IL-2, TNF-α, and IL-10 were resolved by flow cytometry and are denoted for 2 **(A)** and 8 **(B)** weeks-infected animals and their respective controls. Results, obtained in at least two independent experiments, are represented both in total percentages (infected and control animals) and normalized (infected in relation to control group average values) as a way to highlight the infection-induced alterations. Each dot represents an animal. Average and SD of the values within each group are shown. Statistical differences are properly identified. One Way ANOVA (with Tukey's *post-hoc* analysis) was used for comparisons between the different murine strains (infected or non-infected; gray lines), as well as for comparison of normalized values (black lines); *t*-tests (black lines) were performed for comparison between infected animals and controls from the same strain: $^*p \leq 0.05$, $^{**}p \leq 0.01$, $^{***}p \leq 0.001$, and $^{****}p \leq 0.0001$).

forms, such as cutaneous leishmaniasis, we are close to understanding the determinants of resistance vs. susceptibility, for visceral leishmaniasis we are still unable to clearly establish this dichotomy. Here, trying to address this issue, we took advantage of different inbred mouse models, with known different susceptibility patterns to *Leishmania* spp. infection, and dynamically explored their splenic cell compartment's composition, in health, and after infection with

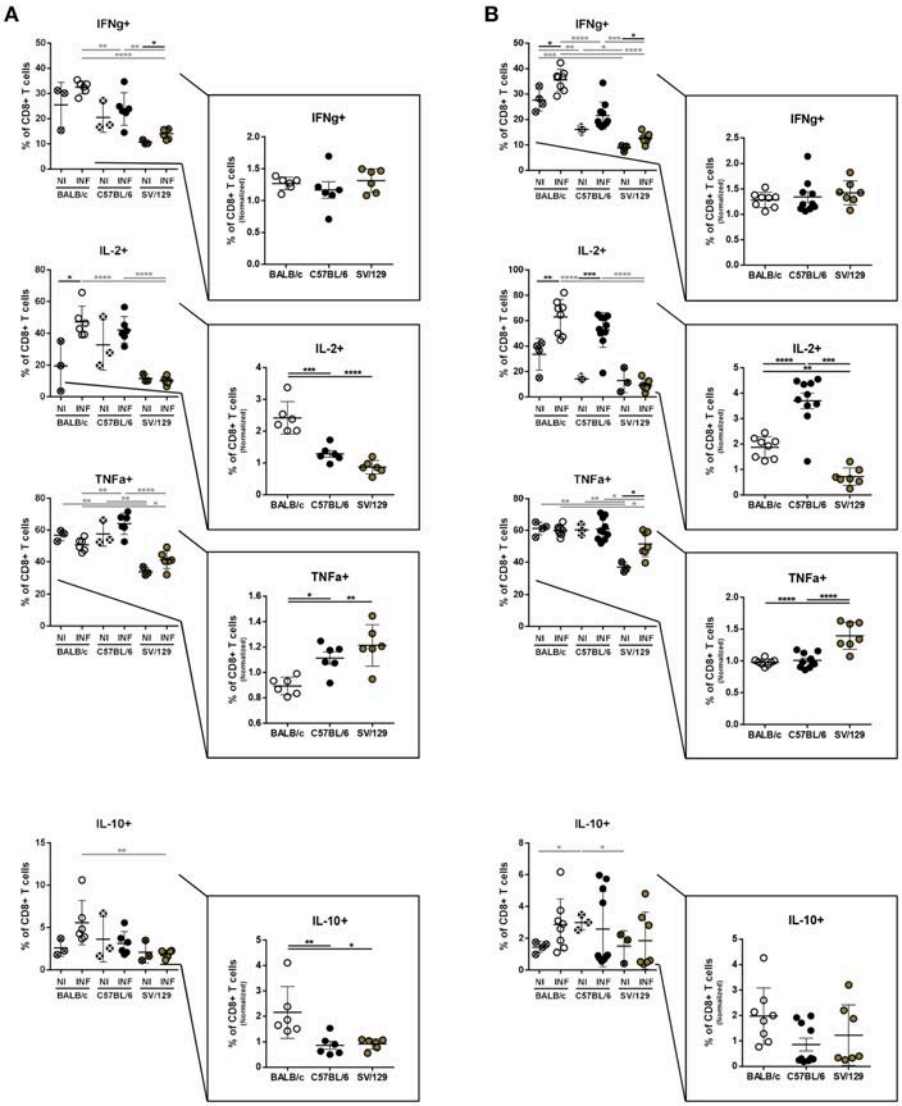

FIGURE 5 | Basal intracellular cytokine production by CD8+ T cells of the different mouse strains and it's alteration 2- and 8-weeks post *L. infantum* infection. BALB/c (white circles), C57BL/6 (black circles) and SV/129 (brown circles) mice were infected intraperitoneally with 1×10^8 *L. infantum* promastigotes and euthanized 2 or 8 weeks after. Splenocytes were cultured with PMA + Ionomycin + Brefeldin A for 4 h. CD8+ T cell frequencies producing IFN-γ, IL-2, TNF-α, and IL-10 were resolved by flow cytometry and are denoted for two **(A)** and 8 **(B)** weeks-infected animals and their respective controls. Results, obtained in at least two independent experiments, are represented both in total percentages (infected and control animals) and normalized (infected in relation to control group average values) as a way to highlight the infection-induced alterations. Each dot represents an animal. Average and SD of the values within each group are shown. Statistical differences are properly identified. One Way ANOVA (with Tukey's *post-hoc* analysis) was used for comparisons between the different murine strains (infected or non-infected; gray lines), as well as for comparison of normalized values (black lines); *t*-tests (black lines) were performed for comparison between infected animals and controls from the same strain: $^*p \leq 0.05$, $^{**}p \leq 0.01$, $^{***}p \leq 0.001$, and $^{****}p \leq 0.0001$).

L. infantum. Furthermore, we also looked at local and systemic infection-induced immune responses, comparing the different murine strains.

As expected, pathological differences were observed when we compared the different infected mouse strains. Two weeks post-infection BALB/c mice demonstrated hepatosplenomegaly, while both C57BL/6 and SV/129 mice kept their splenic and hepatic weights comparable to the respective controls (**Figure 1B**). Eight weeks post-infection, BALB/c mice continued to be the only model demonstrating hepatomegaly, while all of the strains showed similar signs of splenomegaly (**Figure 1B**). Interestingly, determined hepatic weights were in accordance with the granulomatous response quantified (**Figures 1C,D**), which may indicate a correlation between cell infiltrates and hepatic weight.

The above-mentioned results partially translated to the determined parasite burdens, particularly considering the splenic ones. As early as 2 weeks post-infection, we detected a significant difference when comparing the susceptible BALB/c model with

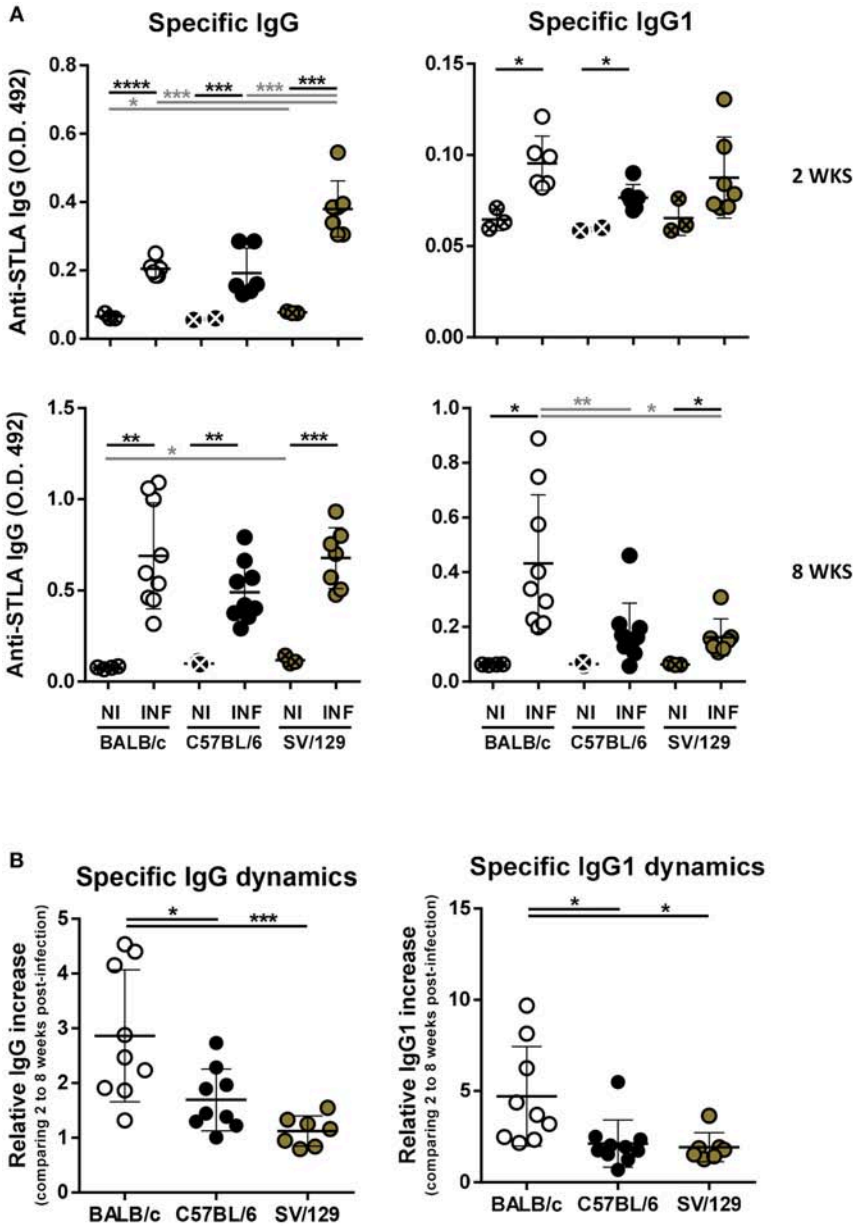

FIGURE 6 | Specific humoral response dynamics in the different *L. infantum* infection murine models. BALB/c (white circles), C57BL/6 (black circles), and SV/129 (brown circles) mice were infected intraperitoneally with 1×10^8 *L. infantum* promastigotes and euthanized 2 or 8 weeks after. **(A)** Specific seric IgG and IgG1 levels against parasite's soluble extract were determined by ELISA for the different infection models and the respective controls in the two time-points evaluated. **(B)** Specific immunoglobulin dynamics was calculated dividing the values obtained for 8 weeks-infected animals (normalized against the respective controls) by the average of the same values obtained for 2 weeks-infected animals. Results are representative of at least two independent experiments. Each dot represents an animal. Average and SD of the values within each group are shown. Statistical differences are properly identified. One Way ANOVA (with Tukey's *post-hoc* analysis) was used for comparisons between the different murine strains (infected or non-infected; gray lines), as well as for comparison of normalized values (black lines); *t*-tests (black lines) were performed for comparison between infected animals and controls from the same strain: $^*p \leq 0.05$, $^{**}p \leq 0.01$, $^{***}p \leq 0.001$, and $^{****}p \leq 0.0001$).

the resistant SV/129 (**Figure 1A**). These results are in line with the ones reported for the other viscerotropic *Leishmania* species, *L. donovani* (Bodhale et al., 2018). Interestingly, similar to what (Bodhale et al., 2018) reported, we also observed an increase of splenic parasite burdens with time in BALB/c and C57BL/6 mice, while for SV/129 mice we observed a plateau. Additionally, also similar with *L. donovani* infection, the splenic parasite burdens of C57BL/6 animals were always intermediate, compared with the other two animal models (Bodhale et al., 2018). Overall this may suggest that the pathogenic process of these two different parasite strains is similar, as will probably be the determinants of susceptibility vs. resistance. This gives relevance

to the convergent study of the two viscerotropic *Leishmania* spp. *in vivo*, as a way to tackle the many questions that still remain unanswered, that go beyond the dichotomy susceptibility vs. resistance (e.g., determinants of visceralization).

Regarding liver parasite burdens, no significant differences were detected among the mouse strains at both 2- and 8-weeks post-infection (**Figure 1A**). Most certainly, at a later time point post-infection, we would observe a reduction in hepatic parasite burdens, considering the organ-specific immunity associated with murine *Leishmania* infection models (Stanley and Engwerda, 2007), together with a milder granulomatous response. Although such a hepatic resolution of infection is observable at early time-points in other studies, we have to keep in mind that *Leishmania* spp. *in vivo* infection outcomes depend on a number of factors, including the parasite strain, the parasite dose, and the route of challenge (Loeuillet et al., 2016).

To understand if the infectious process differentially influences the immune response of different hosts and to try to infer how the host responds to the parasite, we resolved the splenic cell compartments of the three murine strains at two time-points after infection, always comparing with their basal (non-infected) statuses. And more than to identify the main cell types analyzed in host-*Leishmania* interaction studies, we looked at some functional markers of T and B cells. Interestingly, both BALB/c and SV/129 showed higher levels of infection-induced splenic Tfh cells than C57BL/6 mice (**Figures 2A**, **3A**). One possible explanation for such differences may be related to the generation, or absence thereof, of an environment favorable for Tfh differentiation, dependent, among other factors on cytokine secretion (Ma et al., 2012). Curiously, upon *Leishmania infantum* infection, BALB/c but not C57BL/6 mice, showed increased levels of IL-27 (Perez-Cabezas et al., 2016), one of the cytokines associated with Tfh differentiation (Ma et al., 2012). We may only speculate that the infection-induced expansion of the SV/129 Tfh cell compartment may be due to the same infection-induced IL-27 secretion observed in BALB/c mice. Regarding B cell functional markers, the infection-induced differences observed 2 weeks post-infection (comparing the different mouse strains) were absent at the 8 weeks post-infection time-point (**Figures 2B**, **3B**). Relevantly, 2 weeks post-infection, while splenic B cells from SV/129 mice retained the basal levels of CD21 expression, the ones from both BALB/c and C57BL/6 mice showed a downregulation of this surface marker, which may indicate a "more immature" B cell compartment (Thorarinsdottir et al., 2015). Such results are fittingly in line with the specific antibody titers determined against total parasite extract (**Figure 6A**), significantly higher in SV/129 mice early after infection, in comparison with the other two murine strains. This relation between CD21 expression levels and specific antibody titers is well-characterized in other infection models (Haas et al., 2002; Schauer et al., 2003). These results suggest that SV/129 are faster than BALB/c and C57BL/6 mice in the assembly of an efficient B-cell response that cannot be separated from a competent T-cell response (Crotty, 2015).

To disclose if possible, strain-related characteristics of the infection-induced splenic environment might justify the resistant vs. susceptible phenotypes, we further explored the dynamics of splenic T cell's cytokine response with the course of infection in the different mouse strains. It is well-known that IL-10 regulates the kinetics of visceral *Leishmania* infection (Nylén and Sacks, 2007). Relevantly, here we show that only CD4+ and CD8+ cells from BALB/c mice showed an infection-induced increase capacity of secreting IL-10, which is retained at 8 weeks post-infection (**Figures 4**, **5**). This is probably the main indirect justification of the differences in splenic parasite burdens determined, comparing BALB/c and SV/129 animals. On the other hand, and although also considered a susceptible model of VL, C57BL/6 mice never showed this IL-10 upregulation, while the resistant SV/129 mice showed an infection-induced IL-10 upregulation (in CD4+ T cells only) 8 weeks post-infection. Interestingly, when we looked at polyfunctional CD4+ T cells (Seder et al., 2008) we observed a significant increase in their frequency at 8 weeks post-infection in SV/129 mice compared to the susceptible murine models (**Figures 4**, **5**). Looking at the bigger picture, we may speculate that the control of infection observed in SV/129 mice is associated with this probable increase of T cell polyfunctionality, which is not well-explored in visceral leishmaniasis [only in a few vaccine studies, e.g., (Coler et al., 2015)], but is well-understood in other infectious diseases, such as the one caused by HIV-2 (Duvall et al., 2008). The infection-induced increased potential of IL-10 secretion detected for CD4+ T cells of SV/129 mice may also be an indirect indication of an effective anti-parasitic response, bearing in mind that accompanied with inflammation, regulatory mechanisms are expected to occur in order to limit tissue damage, and ultimately restore homeostasis (Iyer and Cheng, 2012).

Finally, we explored the specific anti-*Leishmania* humoral responses, also dynamically. Curiously, in BALB/c we observed a prevalent IgG1 response that increased with the course of infection (**Figure 6B**). It is certain that the Th1/Th2 paradigm explains resistance vs. susceptibility in cutaneous disease, but is not that straightforward in the visceral form of leishmaniasis (Wilson et al., 2005; Tripathi et al., 2007). This said, our results support the development of a prevalent Th2-like response in BALB/c mice, but not in C57BL/6 [as expected (Watanabe et al., 2004)] or SV/129 mice, a potential justification of the results observed regarding splenic parasite burdens.

Overall, our results suggest that C57BL/6 mice demonstrates an intermediate "infection-phenotype" compared to the susceptible and resistant BALB/c and SV/129 mouse strains respectively, in the context of *L. infantum* infection. It is difficult to draw a parallel between visceral leishmaniasis mouse models and human disease since the clinicopathological features of the last, are not recapitulated by the first (Loría-Cervera and Andrade-Narváez, 2014). Still, it is proposed by some authors that murine models of visceral disease may be translated to sub-clinical infection (Loría-Cervera and Andrade-Narváez, 2014) hypothesis, which is hard to confirm since most human individuals studied are either active patients or treated individuals. Allowing ourselves some speculation in convergence with this hypothesis,

these distinct mouse models may be representative of the spectrum of asymptomatic individuals: those with a higher probability to develop disease (BALB/c), those that remain asymptomatic (C57BL/6) and those that are able to resolve the infection (SV/129).

The genetic determinants of susceptibility vs. resistance in mouse models of visceral leishmaniasis, such as NRAMP functionality are well-known (Lipoldova and Demant, 2006; Loeuillet et al., 2016). However, we believe that regardless of the genetic background [which will obviously condition susceptibility/resistance to disease in humans (Blackwell, 1996), although not entirely], we need to understand the anti-parasitic immune response mounted by susceptible and resistant models of infection, which may or may not be influenced by the identified genetic susceptibility/resistance determinants, since infection establishment depends on a(n) (in)balance of parasite multiplication and elimination.

DATA AVAILABILITY

All relevant data are within the paper and its supplementary materials.

ETHICS STATEMENT

This study was carried out in accordance with the principles of the Basel Declaration and recommendations of the i3S Animal Ethics Committee and the Portuguese National Authorities for Animal Health guidelines, according to FELASA and AAALAC guidelines, and European legislation (63/2010). The protocol was approved by the i3S Animal Ethics Committee. BP-C and AC have accreditation for animal research given by the Portuguese Veterinary Direction (Ministerial Directive 1005/92).

AUTHOR CONTRIBUTIONS

BP-C, RV, and AC conceived and designed the experiments. BP-C, TG, and RV performed the experiments. BP-C, PC, TG, FG, RV, and AC analyzed the data. FG and AC contributed with the reagents, materials, and analysis tools. BP-C, PC, RV, and AC wrote the paper. BP-C, PC, TG, FG, RV, and AC critically revised and approved the paper.

FUNDING

The research leading to these results has received funding from the project NORTE-01-0145-FEDER-000012, supported by Norte Portugal Regional Operational Programme (NORTE 2020), under the PORTUGAL 2020 Partnership Agreement, through the European Regional Development Fund (ERDF). PC was supported by Foundation for Science and Technology (FCT), Portugal, through the individual grant SFRH/BD/121252/2016.

ACKNOWLEDGMENTS

We thank Dr. Catarina Leitão (Flow Cytometry Unit, i3S), Dr. Sofia Lamas (Animal Facility, i3S), and Rossana Correia (Histology service—HEMS, i3S) for all the technical assistance provided. We also acknowledge Kevin Muñoz for proofreading this manuscript.

SUPPLEMENTARY MATERIAL

The Supplementary Material for this article can be found online at: https://www.frontiersin.org/articles/10.3389/fcimb.2019.00030/full#supplementary-material

REFERENCES

Akhoundi, M., Kuhls, K., Cannet, A., Votypka, J., Marty, P., Delaunay, P., et al. (2016). A historical overview of the classification, evolution, and dispersion of leishmania parasites and sandflies. *PLoS. Negl. Trop. Dis.* 10:e0004349. doi: 10.1371/journal.pntd.0004349

Bates, P. A. (2007). Transmission of Leishmania metacyclic promastigotes by phlebotomine sand flies. *Int. J. Parasitol.* 37, 1097–1106. doi: 10.1016/j.ijpara.2007.04.003

Blackwell, J. M. (1996). Genetic susceptibility to leishmanial infections: studies in mice and man. *Parasitology* 112 (Suppl.), S67–74.

Bodhale, N. P., Pal, S., Kumar, S., Chattopadhyay, D., Saha, B., Chattopadhyay, N., et al. (2018). Inbred mouse strains differentially susceptible to *Leishmania donovani* infection differ in their immune cell metabolism. *Cytokine* 112, 12–15. doi: 10.1016/j.cyto.2018.06.003

Cecilio, P., Oliveira, F., and Cordeiro-da-Silva, A. (2018). "Vaccines for human leishmaniasis: where do we stand and what is still missing?" in *Leishmaniases as Re-emerging Diseases.* ed. F. Afrin (Rijeka: IntechOpen). doi: 10.5772/intechopen.75000

Cecílio, P., Pérez-Cabezas, B., Santarém N., Maciel, J., Rodrigues, V., and Cordeiro da Silva, A. (2014). Deception and manipulation: the arms of leishmania, a successful parasite. *Front. Immunol.* 5:480. doi: 10.3389/fimmu.2014.00480

Coler, R. N., Duthie, M. S., Hofmeyer, K. A., Guderian, J., Jayashankar, L., Vergara, J., et al. (2015). From mouse to man: safety, immunogenicity and efficacy of a candidate leishmaniasis vaccine LEISH-F3+GLA-SE. *Clin. Transl. Immunol.* 4:e35. doi: 10.1038/cti.2015.6

Crotty, S. (2015). A brief history of T cell help to B cells. *Nat. Rev. Immunol.* 15, 185–189. doi: 10.1038/nri3803

Duvall, M. G., Precopio, M. L., Ambrozak, D. A., Jaye, A., McMichael, A. J., Whittle, H. C., et al. (2008). Polyfunctional T cell responses are a hallmark of HIV-2 infection. *Eur. J. Immunol.* 38:350–363. doi: 10.1002/eji.200737768

Faria, J., Loureiro, I., Santarém N., Cecílio P., Macedo-Ribeiro, S., Tavares, J., et al. (2016). Disclosing the essentiality of ribose-5-phosphate isomerase B in Trypanosomatids. *Sci. Rep.* 6:26937. doi: 10.1038/srep26937

Forni, L. (1988). Strain differences in the postnatal development of the mouse splenic lymphoid system. *Ann. Inst. Pasteur Immunol.* 139, 257–266. doi: 10.1016/0769-2625(88)90139-0

Haas, K. M., Hasegawa, M., Steeber, D. A., Poe, J. C., Zabel, M. D., Bock, C. B., et al. (2002). Complement receptors CD21/35 link innate and protective immunity during *Streptococcus pneumoniae* infection by regulating IgG3 antibody responses. *Immunity* 17, 713–723. doi: 10.1016/S1074-7613(02)00483-1

Hartley, M. A., Drexler, S., Ronet, C., Beverley, S. M., and Fasel, N. (2014). The immunological, environmental, and phylogenetic perpetrators of metastatic leishmaniasis. *Trends Parasitol.* 30, 412–422. doi: 10.1016/j.pt.2014.05.006

Iyer, S. S., and Cheng, G. (2012). Role of interleukin 10 transcriptional regulation in inflammation and autoimmune disease. *Crit. Rev. Immunol.* 32, 23–63. doi: 10.1615/CritRevImmunol.v32.i1.30

Kumar, R., and Nylén, S. (2012). Immunobiology of visceral leishmaniasis. *Front. Immunol.* 3:251. doi: 10.3389/fimmu.2012.00251

Lipoldova, M., and Demant, P. (2006). Genetic susceptibility to infectious disease: lessons from mouse models of leishmaniasis. *Nat. Rev. Genet.* 7, 294–305. doi: 10.1038/nrg1832

Liu, C., Richard, K., Wiggins, M., Zhu, X., Conrad, D. H., and Song, W. (2016). CD23 can negatively regulate B-cell receptor signaling. *Sci. Rep.* 6:25629. doi: 10.1038/srep25629

Loeuillet, C., Bañuls, A. L., and Hide, M. (2016). Study of Leishmania pathogenesis in mice: experimental considerations. *Parasit. Vectors* 9:144. doi: 10.1186/s13071-016-1413-9

Loría-Cervera, E. N., and Andrade-Narváez, F. J. (2014). Animal models for the study of leishmaniasis immunology. *Rev. Inst. Med. Trop. Sao Paulo* 56, 1–11. doi: 10.1590/S0036-46652014000100001

Ma, C. S., Deenick, E. K., Batten, M., and Tangye, S. G. (2012). The origins, function, and regulation of T follicular helper cells. *J. Exp. Med.* 209, 1241–1253. doi: 10.1084/jem.20120994

McCall, L. I., Zhang, W. W., and Matlashewski, G. (2013). Determinants for the development of visceral leishmaniasis disease. *PLoS Pathog.* 9:e1003053. doi: 10.1371/journal.ppat.1003053

Nylén, S., and Sacks, D. (2007). Interleukin-10 and the pathogenesis of human visceral leishmaniasis. *Trends Immunol.* 28, 378–384. doi: 10.1016/j.it.2007.07.004

Perez-Cabezas, B., Cecilio, P., Robalo, A. L., Silvestre, R., Carrillo, E., Moreno, J., et al. (2016). Interleukin-27 early impacts leishmania infantum infection in mice and correlates with active visceral disease in humans. *Front. Immunol.* 7:478. doi: 10.3389/fimmu.2016.00478

Ready, P. D. (2014). Epidemiology of visceral leishmaniasis. *Clin. Epidemiol.* 6, 147–154. doi: 10.2147/CLEP.S44267

Rodrigues, V., Cordeiro-da-Silva, A., Laforge, M., Silvestre, R., and Estaquier, J. (2016). Regulation of immunity during visceral Leishmania infection. *Parasit. Vectors* 9:118. doi: 10.1186/s13071-016-1412-x

Rodrigues, V., Laforge, M., Campillo-Gimenez, L., Soundaramourty, C., Correia-de-Oliveira, A., Dinis-Oliveira, R. J., et al. (2014). Abortive T follicular helper development is associated with a defective humoral response in *Leishmania infantum*-infected macaques. *PLoS Pathog.* 10:e1004096. doi: 10.1371/journal.ppat.1004096

Roozendaal, R., and Carroll, M. C. (2007). Complement receptors CD21 and CD35 in humoral immunity. *Immunol. Rev.* 219, 157–166. doi: 10.1111/j.1600-065X.2007.00556.x

Sacks, D., and Noben-Trauth, N. (2002). The immunology of susceptibility and resistance to Leishmania major in mice. *Nat. Rev. Immunol.* 2, 845–858. doi: 10.1038/nri933

Schauer, U., Stemberg, F., Rieger, C. H., Büttner, W., Borte, M., Schubert, S., et al. (2003). Levels of antibodies specific to tetanus toxoid, Haemophilus influenzae type b, and pneumococcal capsular polysaccharide in healthy children and adults. *Clin. Diagn. Lab. Immunol.* 10, 202–207. doi: 10.1128/CDLI.10.2.202-207.2003

Seder, R. A., Darrah, P. A., and Roederer, M. (2008). T-cell quality in memory and protection: implications for vaccine design. *Nat. Rev. Immunol.* 8, 247–258. doi: 10.1038/nri2274

Silvestre, R., Cordeiro-Da-Silva, A.,Santarém, N., Vergnes, B., Sereno, D., and Ouaissi, A. (2007). SIR2-deficient *Leishmania infantum* induces a defined IFN-gamma/IL-10 pattern that correlates with protection. *J. Immunol.* 179, 3161–3170. doi: 10.4049/jimmunol.179.5.3161

Silvestre, R., Santarém, N., Cunha, J., Cardoso, L., Nieto, J., Carrillo, E., et al. (2008). Serological evaluation of experimentally infected dogs by LicTXNPx-ELISA and amastigote-flow cytometry. *Vet. Parasitol.* 158, 23–30. doi: 10.1016/j.vetpar.2008.09.001

Stanley, A. C., and Engwerda, C. R. (2007). Balancing immunity and pathology in visceral leishmaniasis. *Immunol. Cell Biol.* 85, 138–147. doi: 10.1038/sj.icb7100011

Thorarinsdottir, K., Camponeschi, A., Gjertsson, I., and Martensson, I. L. (2015). CD21 -/low B cells: a snapshot of a unique B cell subset in health and disease. *Scand. J. Immunol.* 82, 254–261. doi: 10.1111/sji.12339

Tripathi, P., Singh, V., and Naik, S. (2007). Immune response to leishmania: paradox rather than paradigm. *FEMS Immunol. Med. Microbiol.* 51, 229–242. doi: 10.1111/j.1574-695X.2007.00311.x

Watanabe, H., Numata, K., Ito, T., Takagi, K., and Matsukawa, A. (2004). Innate immune response in Th1- and Th2-dominant mouse strains. *Shock* 22, 460–466. doi: 10.1097/01.shk.0000142249.08135.e9

Wilson, M. E., Jeronimo, S. M., and Pearson, R. D. (2005). Immunopathogenesis of infection with the visceralizing Leishmania species. *Microb. Pathog.* 38, 147–160. doi: 10.1016/j.micpath.2004.11.002

World Health Organization (2017). *Leishmaniasis*. Fact sheet No 375 Available online at: http://www.who.int/mediacentre/factsheets/fs375/en/ (accessed January 10, 2018).

Conflict of Interest Statement: The authors declare that the research was conducted in the absence of any commercial or financial relationships that could be construed as a potential conflict of interest.

frontiers in Cellular and Infection Microbiology

ORIGINAL RESEARCH
published: 20 March 2019
doi: 10.3389/fcimb.2019.00060

Melatonin and *Leishmania amazonensis* Infection Altered miR-294, miR-30e, and miR-302d Impacting on *Tnf*, *Mcp-1,* and *Nos2* Expression

Juliane Cristina Ribeiro Fernandes[1,2†], *Juliana Ide Aoki*[1†], *Stephanie Maia Acuña*[1], *Ricardo Andrade Zampieri*[1], *Regina P. Markus*[1], *Lucile Maria Floeter-Winter*[1] *and Sandra Marcia Muxel*[1*]

[1] *Departamento de Fisiologia, Instituto de Biociências, Universidade de São Paulo, São Paulo, Brazil,* [2] *Instituto de Medicina Tropical, Universidade de São Paulo, São Paulo, Brazil*

OPEN ACCESS

Edited by:
Claudia Ida Brodskyn, Gonçalo Moniz Institute (IGM), Brazil

Reviewed by:
Renato Augusto DaMatta, Universidade Estadual do Norte Fluminense Darcy Ribeiro, Brazil
Elisa Azuara-Liceaga, Universidad Autónoma de la Ciudad de México, Mexico

***Correspondence:**
Sandra Marcia Muxel
sandrammuxel@usp.br

[†] *These authors have contributed equally to this work*

Specialty section:
This article was submitted to Parasite and Host, a section of the journal Frontiers in Cellular and Infection Microbiology

Received: *22 November 2018*
Accepted: *27 February 2019*
Published: *20 March 2019*

Citation:
Fernandes JCR, Aoki JI, Maia Acuña S, Zampieri RA, Markus RP, Floeter-Winter LM and Muxel SM (2019) Melatonin and Leishmania amazonensis Infection Altered miR-294, miR-30e, and miR-302d Impacting on Tnf, Mcp-1, and Nos2 Expression. Front. Cell. Infect. Microbiol. 9:60. doi: 10.3389/fcimb.2019.00060

Leishmaniases are neglected diseases that cause a large spectrum of clinical manifestations, from cutaneous to visceral lesions. The initial steps of the inflammatory response involve the phagocytosis of *Leishmania* and the parasite replication inside the macrophage phagolysosome. Melatonin, the darkness-signaling hormone, is involved in modulation of macrophage activation during infectious diseases, controlling the inflammatory response against parasites. In this work, we showed that exogenous melatonin treatment of BALB/c macrophages reduced *Leishmania amazonensis* infection and modulated host microRNA (miRNA) expression profile, as well as cytokine production such as IL-6, MCP-1/CCL2, and, RANTES/CCL9. The role of one of the regulated miRNA (miR-294-3p) in *L. amazonensis* BALB/c infection was confirmed with miRNA inhibition assays, which led to increased expression levels of *Tnf* and *Mcp*-1/*Ccl2* and diminished infectivity. Additionally, melatonin treatment or miR-30e-5p and miR-302d-3p inhibition increased nitric oxide synthase 2 (*Nos2*) mRNA expression levels and nitric oxide (NO) production, altering the macrophage activation state and reducing infection. Altogether, these data demonstrated the impact of melatonin treatment on the miRNA profile of BALB/c macrophage infected with *L. amazonensis* defining the infection outcome.

Keywords: polyamine pathway, nitric oxide synthase, arginase 1, interleukin, mRNA-miRNA interaction, melatonin and *Leishmania*

INTRODUCTION

Leishmaniases are neglected tropical diseases characterized by cutaneous, mucocutaneous, or visceral lesions (Alvar et al., 2012; Scott and Novais, 2016). The diseases are endemic in 98 countries worldwide (Alvar et al., 2012). According to the World Health Organization (WHO), approximately 12 million people are currently infected, and ∼20,000–30,000 deaths occur annually (Alvar et al., 2012; WHO, 2017). The etiological agents of leishmaniases are the protozoan parasites of *Leishmania* genus (Marsden, 1986; Ashford, 2000).

Leishmania amastigotes are obligatory intracellular parasites, which survive and replicate inside macrophage phagolysosomes, being able to modulate the host immune response by the reduction of inflammation and the development of an adaptive immune response (Nathan and Shiloh, 2000; Gregory and Olivier, 2005; Mosser and Edwards, 2008; Scott and Novais, 2016). Modulation of type 1 (Th1) or type 2 (Th2) polarization of T $CD4^+$ lymphocytes is essential to define the fate of infection, inducing death or proliferation of *Leishmania* amastigotes in the macrophages (Corraliza et al., 1995; Munder et al., 1998; Wanasen and Soong, 2008). Some enzymes, such as nitric oxide synthase 2 (NOS2) and arginase 1 (ARG1), are competitively regulated by Th1 or Th2 cytokines, and both enzymes use L-arginine as substrate. Stimulation with Th1-associated cytokines and chemokines, such as interferon gamma (IFN-γ), tumor necrosis factor (TNF) and granulocyte macrophage colony-stimulating factor (GM-CSF), polarize macrophages to the M1 phenotype by increasing NOS2 and decreasing ARG1 levels, leading to parasite control (Hrabak et al., 1996; Boucher et al., 1999; Mantovani et al., 2004; Wang et al., 2014). Conversely, Th2-associated cytokines and chemokines, such as interleukin 4 (IL-4), IL-13, tumor growth factor beta (TGF-β), IL-10 and macrophage colony-stimulating factor (M-CSF) (Verreck et al., 2004), induce M2 polarization by decreasing NOS2 and increasing ARG1 levels (Martinez et al., 2009), leading to parasite replication and survival (Hrabak et al., 1996; Boucher et al., 1999; Mantovani et al., 2004; Wang et al., 2014).

Melatonin, the darkness hormone, is synthesized during the night by the pineal gland under the control of the central clock, the suprachiasmatic nuclei of the hypothalamus. Melatonin is also synthesized by immune-competent cells and plays a role in surveillance against infection and in the recovery phase of acute defense responses (Markus et al., 2007, 2017; Carrillo-Vico et al., 2013). The interplay between timing and defense is a fine-tuned regulated process that involves melatonin-mediated restriction of leukocyte migration from the circulation to the tissues under normal conditions (Lotufo et al., 2001; Ren et al., 2015). However, suppression of pineal melatonin synthesis can occur in response to pathogen (bacteria and fungi)- and danger-associated molecular patterns (Da Silveira Cruz-Machado et al., 2010; Carvalho-Sousa et al., 2011) to allow migration of leukocytes to the lesion site at night as well as during the day. In addition, melatonin can be synthesized "on demand" by macrophages (Pontes et al., 2006; Muxel et al., 2012), dendritic cells (Pires-Lapa et al., 2018) and lymphocytes (Carrillo-Vico et al., 2004) during the recovery phase or under low-grade and chronic inflammatory conditions (Markus et al., 2017). This fine-tuned regulation of melatonin synthesis reduces susceptibility to bacterial infection (Rojas et al., 2002), lethal endotoxemia (Maestroni, 1996; Prendergast et al., 2003) and several parasite infections such as *Schistosoma mansoni* (El-Sokkary et al., 2002), *Plasmodium falciparum,* and *Plasmodium chabaudi* (Hotta et al., 2000), *Trypanosoma cruzi* (Santello et al., 2007), *Leishmania infantum* (Elmahallawy et al., 2014), and *Leishmania amazonensis* (Laranjeira-Silva et al., 2015). Melatonin promotes the expression of the immunoregulatory phenotype in immune-competent cells (Rojas et al., 2002; Kinsey et al., 2003), acting as a cytoprotector (Luchetti et al., 2010), an antioxidant (Reiter et al., 2013; Zhang and Zhang, 2014) and an immunomodulator (Reiter et al., 2000; Carrillo-Vico et al., 2005, 2013). Unlike bacteria and fungi, *L. amazonensis* did not suppress the nocturnal melatonin surge (Laranjeira-Silva et al., 2015), resulting in lower infectivity in the dark environment than in the day.

The immune response can also be modulated by microRNAs (miRNAs) participation (Baltimore et al., 2008; O'neill et al., 2011; Muxel et al., 2017b, 2018b). miRNAs are small non-coding RNAs that act as posttranscriptional regulators by targeting messenger RNAs (mRNAs) via 3′ untranslated region (UTR) sequence complementarity, leading to translational repression or mRNA degradation, among other mechanisms (Bagga et al., 2005; Lim et al., 2005). miRNAs are involved in macrophage activation and polarization (Baltimore et al., 2008; Graff et al., 2012; Banerjee et al., 2013; Wang et al., 2014). In recent years, some studies have been describing macrophage miRNA modulation during *Leishmania* infections (Ghosh et al., 2013; Lemaire et al., 2013; Frank et al., 2015; Geraci et al., 2015; Mukherjee et al., 2015; Muxel et al., 2017b). In this study, we demonstrated that the miRNA profile of *Leishmania*-infected macrophages was modified after melatonin treatment. Also, melatonin reduced the levels of cytokines and chemokines such as IL-6, MCP-1, MIP-2/CXCL2, and RANTES/CCL5. In contrast, melatonin increased *Nos2* mRNA expression and NO production during infection. Melatonin treatment, as well as functional inhibition of miRNAs in macrophages, impaired the infectivity of *L. amazonensis*.

MATERIALS AND METHODS

Parasite Culture

Leishmania amazonensis (MHOM/BR/1973/M2269) promastigotes were maintained in culture at 25°C in M199 medium (Invitrogen, Grand Island, NY, USA), supplemented with 10% heat-inactivated fetal bovine serum (FBS, Invitrogen), 5 ppm hemine, 100 μM adenine, 10 U/mL penicillin (Invitrogen), 10 μg/mL streptomycin (Life Technologies, Carlsbad, CA, USA), 40 mM HEPES-NaOH and 12 mM $NaHCO_3$ buffer (pH 6.85). The cultures were maintained for 7 days until the new subcultures and only in early passages (P1–P5) for infection assays.

In vitro Macrophage Infection

All experiments were performed with 6–8 weeks-old female BALB/c mice obtained from the Animal Center of the Institute of Bioscience of the University of São Paulo. Bone marrow-derived macrophages (BMDMs) were obtained from femurs and tibias by flushing with 2 mL of PBS. Then, the collected cells were centrifuged at 500 × g for 10 min at 4°C and resuspended in RPMI 1640 medium (LGC Biotecnologia, São Paulo, Brazil) supplemented with penicillin (100 U/ml) (Invitrogen, São Paulo, Brazil), streptomycin (100 μg/ml) (Life Technologies, Carlsbad, CA, USA), 10% heat-inactivated FBS (Invitrogen) and 20% of L929 cell supernatant. The cells were submitted to differentiation for 7–8 days at 34°C in an atmosphere of 5% CO_2. BMDMs

were used after phenotypic analysis by flow cytometry showing at least 95% F4/80- and CD11b-positive cells. Fluorescence detection was performed using an Amnis FlowSight (Merck-Millipore, Darmstadt, Germany) and analyzed using Ideas® Software (Amnis Corporation, Seattle, WA, USA).

For melatonin treatment assays, 2×10^5 cells were plated into 8-wells glass chamber slides (Lab-Teck Chamber Slide; Nunc, Naperville, IL, USA) and incubated at 34°C in an atmosphere of 5% CO_2. After, macrophages were treated with 3 or 30 nM melatonin (Tocris, Bristol, United Kingdom), vehicle (0.0005% ethanol in medium, Sigma-Aldrich, St. Louis, MO, USA) or medium only (untreated control) for 1, 2, or 4 h. Then, the macrophages were infected with promastigotes in the stationary growth phase (MOI 5:1), as previously described (Laranjeira-Silva et al., 2015). After 4 h of infection, the cells were washed to remove nonphagocytosed promastigotes, and then incubated with fresh RPMI medium supplemented as previously described, or removed for cell-fixation process. The infectivity was microscopically analyzed after 4 and 24 h of infection, cell-fixation was performed with acetone/methanol (1:1, v:v, Merck, Darmstadt, Germany) for 20 min at −20°C, followed by PBS washing and Panoptic-staining (Laborclin, Parana, Brazil). Infectivity was analyzed in phase-contrast microscopy (Nikon Eclipse E200, NJ, USA) counting the number of infected macrophages and amastigotes per macrophage in at least 1,000 macrophages/treatment in three independent experiments. The infection index was calculated by multiplying the mean number of amastigotes per macrophage by the rate of macrophage infection. The values were normalized based on the average values for the untreated infected macrophages.

For mRNA and miRNA expression analysis, 5×10^6 cells/well were plated into 6-well plates (SPL Life Sciences, Pocheon, Korea) and for cytokines quantification in supernatant, 1×10^6 cells/well were plated into 24-well plates (SPL Life Sciences), then the melatonin treatment (30 nM for 4 h before infection) and infection were performed as described above.

RNA Extraction, Reverse Transcription, and RT-qPCR for miRNA

Total RNA was extracted using a miRNeasy Mini Kit (Qiagen, Hilden, Germany) following the manufacturer's instructions. cDNA was synthesized from mature miRNA templates using a miScript II RT Kit (Qiagen), according the manufacturer's instructions. Briefly, 250 ng of total RNA was added to 2 μL of 5X miScript HiSpec Buffer, 1 μL of 10X Nucleics Mix and 1 μL of miScript Reverse Transcriptase Mix. RNase-free water was added to a final volume of 10 μL. The RNA was incubated for 60 min at 37°C to insert poly-A tail downstream of the miRNA sequence and to anneal a T-tail tag for the elongation of the cDNA. The enzyme was inactivated at 95°C for 5 min. The reaction was performed in Mastercycler Gradient thermocycler (Eppendorf, Hamburg, Germany), and the product was stored at −20°C until use.

An array of 84 miRNAs was measured using a Mouse Inflammatory Response and Autoimmunity miRNA PCR Array kit (MIMM-105Z, Qiagen) and miScript SYBR PCR Kit (Qiagen). The reaction was performed with 2X QuantiTect SYBR Green PCR Master Mix, 10X miScript Universal Primer and 105 μL of cDNA (triplicate samples of the 10-fold diluted cDNA). RNase-free water was added to a final volume of 2,625 μL (25 μL/well).

For specific amplification of miR-181c, miR-294-3p, miR-30e, miR-302d, and SNORD95A (used as a normalizer), reactions were prepared with 2X QuantiTect SYBR Green PCR Master Mix, 10X miScript Universal Primer, 10X specific primer, 5 μL of cDNA (3–4 samples 10-fold diluted) and RNase-free water to a final volume of 25 μL/well. qPCR started with activation of the HotStart DNA Polymerase for 15 s at 95°C and 40 cycles of 15 s at 94°C for denaturation, 30 s at 55°C for primer annealing and 30 s at 70°C for elongation. The reaction was performed in Thermocycler ABI Prism 7300 (Applied Biosystems, Carlsbad, CA, USA), and the relative Ct was analyzed using online tools provided with the kit (miScript miRNA PCR Array Data Analysis software). The geometric average Ct of the miRNAs was normalized based on the SNORD95A values, and then the fold changes were calculated to compare untreated, vehicle-treated or melatonin-treated and infected macrophages in relation to untreated and uninfected macrophages at the same time of culture. The RT-qPCR efficiencies were determined and a negative control reaction without reverse transcriptase enzyme was included to verify the absence of any DNA contamination in the RNA samples. The fold regulation (FR) was considered to be the negative inverse of the fold change [function = −1*(1/fold change value)]. FR ≥ 1.5 were considered to indicate upregulation, and levels ≤−1.5 were considered to indicate downregulation, as previously described (Muxel et al., 2017a).

Reverse Transcription and RT-qPCR for mRNA

Reverse transcription was performed using 2 μg of RNA and 20 nmol of random primer (Applied Biosystems) to a final volume of 13 μL. The mixture was incubated at 70°C for 5 min and then at 15°C for addition of the mix including 4 μL of 5X buffer, 2 μL of 10 mM dNTPs and 1 μL (2U) of RevertAid™ Reverse Transcriptase (Fermentas Life Sciences, Burlington, Ontario, Canada). The reaction was incubated at 37°C for 5 min and at 42°C for 60 min. The enzyme activity was blocked by heat inactivation at 75°C for 15 min, and the cDNA was stored at −20°C until use. A negative control reaction without reverse transcriptase enzyme was included to verify the presence of some DNA contamination in the RNA samples. Reactions were performed with 2X SYBR Green PCR Master Mix (Applied Biosystems), 200 nM of each primer pair, 5 μL of cDNA (100-fold diluted) and RNase-free water to a final volume of 25 μL. The reactions were performed in an Exicycler™ 96 Real-Time Quantitative Thermal Block (Bioneer, Daejeon, Korea). The mixture was incubated at 94°C for 5 min followed by 40 cycles of 94°C for 30 s and 60°C for 30 s. Quantification of target gene expression was performed based on a standard curve prepared from a 10-fold serial dilution of a quantified and linearized plasmid containing the target DNA. The following primer pairs were used for mouse mRNA analysis: *Nos2*:

5′-agagccacagtcctctttgc-3′ and 5′-gctcctcttccaaggtgctt-3′; *Arg1:* 5-agcactgaggaaagctggtc-3′ and 5′-cagaccgtgggttcttcaca-3′; *Cat-2b:* 5′-tatgttgtctcggcaggctc-3′ and 5′-gaaaagcaacccatcctccg-3′; *Cat1:* 5′-cgtaatcgccactgtgacct-3′ and 5′-ggctggtaccgtaagaccaa-3′; *Mcp-1/Ccl2:* 5′-tgatcccaatgagtaggctgg-3′ and 5′-gcacagacctctctcttgagc-3′, *Rantes/Ccl5:* 5′- ggagtatttctacaccagcagca-3′ and 5′-cccacttcttctctgggttgg-3′, *Tnf:* 5′- ccaccacgctcttctgtcta−3′ and 5′-agggtctgggccatagaact−3′ and *Gapdh*: 5′-ggcaaattcaacggcacagt-3′ and 5′-ccttttggctccacccttca-3′.

Transfection of miRNA Inhibitors

For miRNA expression analysis, 5×10^5 cells/well were plated into 24-well plates (SPL Life Sciences, Pocheon, Korea) and incubated at 34°C in an atmosphere of 5% CO_2. For infectivity analysis, 2×10^5 cells/well were plated into 8-well glass Lab-Teck chamber slides (Thermo Scientific, NY, USA) and incubated at 34°C in an atmosphere of 5% CO_2 for 18 h. Then, the cells were incubated with 30 or 100 nM of the inhibitors miR-181c-5p, miR-294-3p, miR-30e-5p, miR-302d-3p, the negative control (Ambion, Carlsbad, CA, USA) or only medium (untreated), which were previously incubated for 20 min at room temperature with 3 μL of the FuGENE HD transfection reagent (Roche, Madison, WI, USA) in 250 μL of 10% FBS RPMI 1640 medium (LGC Biotecnologia, São Paulo, Brazil). After 36 h of transfection, the cells were infected, as previously described.

Cytokine Quantification

The cytokines IL-1α, IL-1β, IL-4, IL-6, TNF-α, IL-13, IL-10, and IL-12; and the chemokines RANTES/CCL5, KC/CXCL1, MIP-2/CXCL2 and MCP-1/CCL2 were quantified using 25 μL of the supernatant of 1×10^6 cells of uninfected or infected macrophages that were untreated, vehicle-treated or melatonin-treated using a MILLIPLEX MAP Mouse Cytokine/Chemokine Panel I kit (Merck Millipore, MA, USA), according to the manufacturer's instructions.

NO Quantification

NO quantification was performed with DAF-FM (4-amino-5-methylamino-2′,7′-difluorofluorescein diacetate; Life Technologies, Eugene, OR, USA) labeling and analyzed by flow cytometry (FlowSight, Merck Millipore, Germany), as previously described (Muxel et al., 2017a,b).

In silico Analysis

To analyze miRNA-mRNA interactions, we used the miRecords platform (http://c1.accurascience.com/miRecords/), which provides information of predicted mRNA targets by integrating data from various tools: DIANA-microT, MicroInspector, miRanda, MirTarget2, miTarget, NBmiRTar, PicTar, PITA, RNA22, RNAhybrid, and TargetScan/TargetScanS.

Statistical Analysis

Statistical analyses were performed using GraphPad Prism Software (GraphPad Software Inc, La Jolla, CA, USA). Significance was determined based on Student's *t*-test and $p < 0.05$ was considered significant.

RESULTS

Melatonin Reduces macrophage-*Leishmania amazonensis* Infectivity in a Dose- and time-Dependent Manner

Melatonin treatment (3 or 30 nM) for 1 and 2 h did not modify the macrophage infection rate (as showed in the normalized data in **Figures 1A,B** and original data in **Supplementary Figure 1**), mean number of amastigotes per infected macrophage (3–5 amastigotes. **Figures 1D,E**) or infection index (**Figures 1G,H**) after 4 and 24 h of infection, compared to vehicle treatment.

Otherwise, melatonin (30 nM) treatment for 4 h showed reduction of 30% in the number of infected macrophages, while treatment with 3 nM of melatonin had no effect (**Figure 1C**; **Supplementary Figure 1**). The number of amastigotes per infected cell was reduced by the same percentage (20–25%) with 3 or 30 nM (**Figure 1F**), and the infection index was reduced at both concentrations (20–30% 3 nM, 60% 30 nM; **Figure 1I**). Subsequent analyses were performed based on treatment with 30 nM melatonin for 4 h.

Melatonin Modulates the Expression of Genes Related to L-arginine Transport and Metabolism in *Leishmania amazonensis*-Infected Macrophages

Considering that parasite survival in macrophages is affected by deviation of L-arginine metabolism to the production of polyamines (Muxel et al., 2018a), we evaluated the gene expression of melatonin-treated macrophages in comparison with vehicle-treated macrophages, by quantification of mRNA expression levels of *Cat2B* and *Cat1* (both involved in the macrophage L-arginine uptake), and of *Arg1* and *Nos2* (involved in the polyamine production and NO production, respectively) (**Figure 2**).

Based on these mRNA expression levels, we observed that at both times of infection, early (4 h) and established (24 h), *L. amazonensis* induced sustained expression of *Cat2B* and *Cat1* mRNA (**Figures 2A,B**). *Arg1* and *Nos*2 were transiently expressed in early (4 h) infected macrophages compared to uninfected macrophages. Exposure to vehicle and melatonin modulated mRNA levels in uninfected macrophages, increasing the basal levels of *Cat2B* and *Arg1* (**Figures 2A–C**). However, in infected macrophages, melatonin treatment did not alter the *Cat2B*, *Cat1,* or *Arg*1 mRNA levels (**Figures 2A–C**) compared to vehicle treatment. Still, melatonin sustained the levels of *Nos2* mRNA (**Figure 2D**) and increased the frequency of NO-producing cells (**Figure 2E**) and the amount of NO per cell (**Figure 2F**) at 24 h of infection. Our data revealed that melatonin treatment of macrophages promoted modulation of the expression of mRNA involved in L-arginine metabolism during infection, inducing *Nos2* to the detriment of *Arg1* and thus altering infectivity.

Melatonin Modifies Cytokine and Chemokine Production in *Leishmania amazonensis*-Infected Macrophages

Furthermore, we analyzed cytokine and chemokine production in response to melatonin treatment and *L. amazonensis* infection.

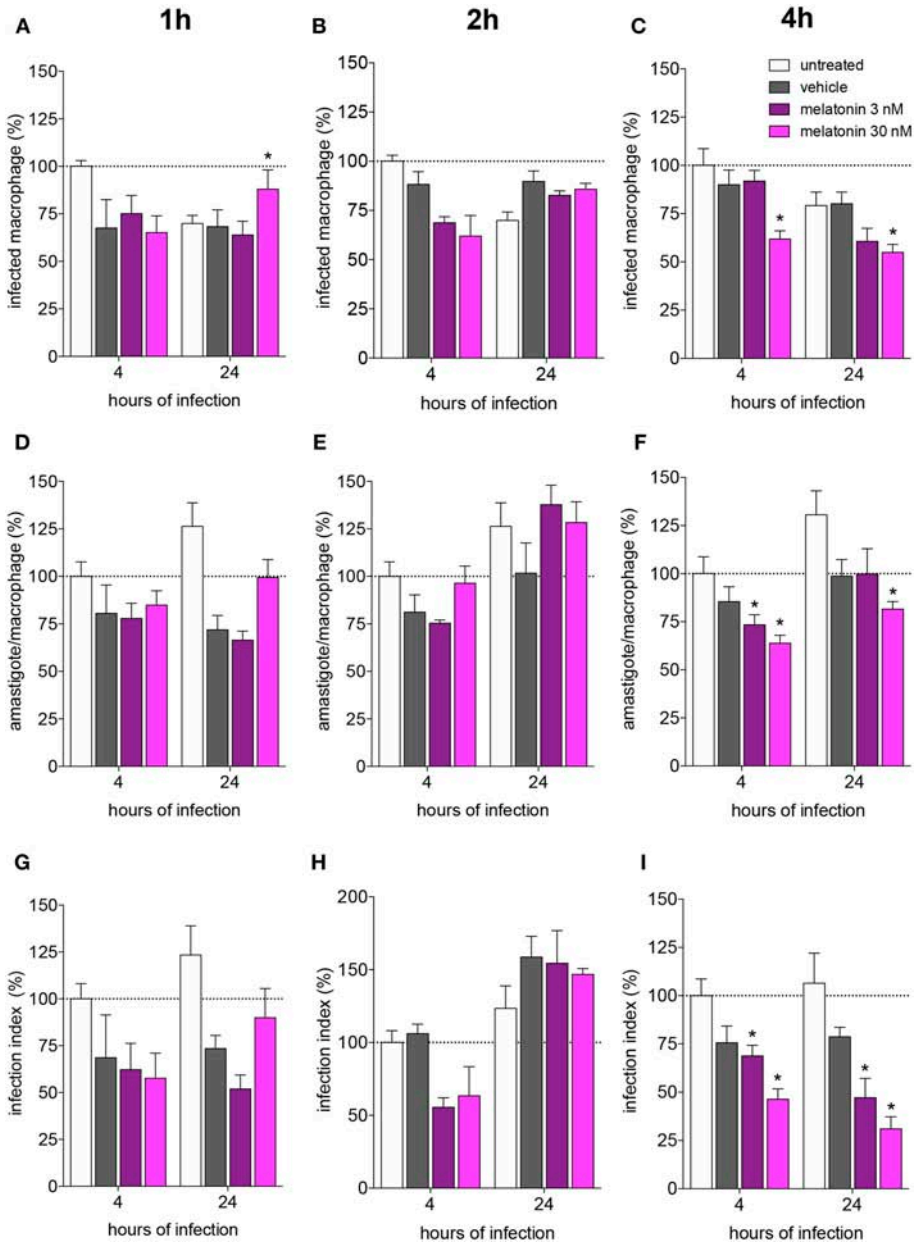

FIGURE 1 | Melatonin inhibition of *L. amazonensis* infectivity in a dose dependent manner. BALB/c macrophages (2×10^5 cells) were pre-incubated for 1, 2, or 4 h with medium (untreated, white bar), vehicle (ethanol 0.0005%, gray bar), or 3 (purple bar) or 30 (magenta bar) nM of melatonin. After, macrophages were infected with *L. amazonensis* (MOI 5:1) and analyzed after 4 and 24 h. **(A–C)**—Percentage of infected macrophages; **(D–F)**—number of amastigotes per infected macrophage; **(G–I)**—Infection index (rate of infected macrophages multiplied by the number of amastigotes per infected macrophage). Each bar represents the mean ± SEM of values normalized by untreated macrophages at 4 h of infection. The data were representative of three independent experiments ($n = 5$–8). *$p < 0.05$, comparing the melatonin treatment with the vehicle-treated macrophage at the same concentration and time.

The levels of the cytokines IL-4, IL-1β, IL-13, IL-6, TNF-α, and IL-12 and the chemokine RANTES/CCL5 did not changed after 4 and 24 h of infection, whereas IL-1α (2-fold), IL-10 (5-fold), MIP-2/CXCL2 (8-fold), and KC/CXCL1 (4-fold) showed decreased levels after 24 h of infection compared to those in uninfected macrophages (**Figure 3**). In contrast, MCP-1/CCL2 (2-fold) showed increased levels in infected macrophages (24 h of infection) compared to uninfected macrophages (**Figure 3**).

Melatonin treatment (30 nM) reduced the levels of IL-6 (2-fold), MCP-1/CCL2 (5-fold), and RANTES/CCL5 (6-fold) compared to vehicle treatment after both 4 and 24 h of infection, while both vehicle and melatonin treatment reduced the levels of IL-10, MIP-2/CXCL2, and KC/CXCL1 (**Figure 3**). Our data

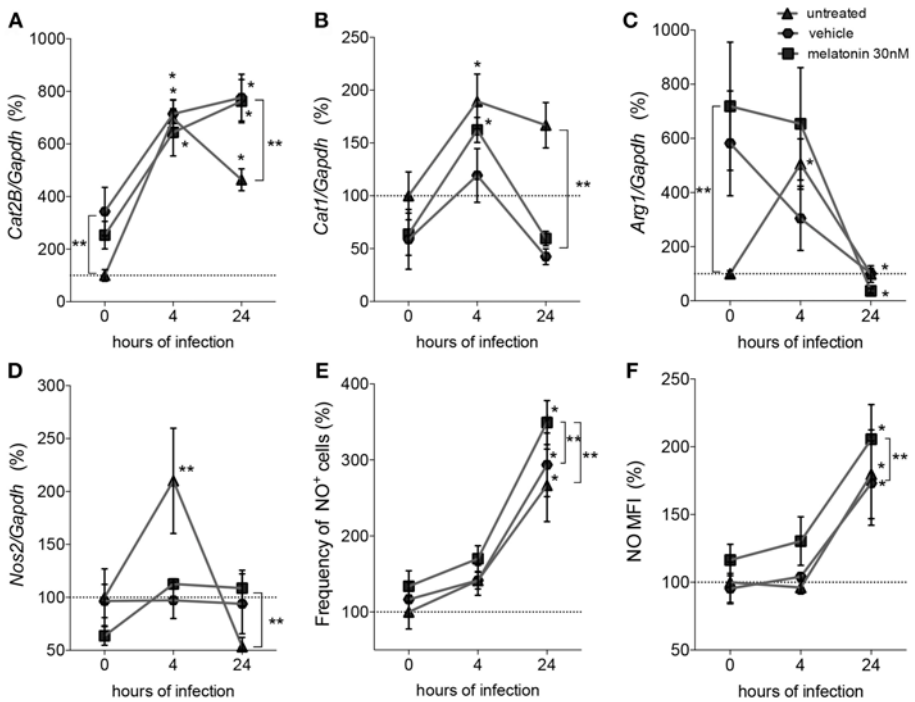

FIGURE 2 | Quantification of mRNA involved in L-arginine transport and metabolism and NO production. Macrophages (5×10^6) were treated with 30 nM of melatonin (squared dots), vehicle (5×10^{-6}% ethanol, hexagonal dots) or untreated (triangular dots) for 4 h, infected with *L. amazonensis* (MOI 5:1) and collected after 4 and 24 h of infection. RT-qPCR of *Cat2B* **(A)**, *Cat1* **(B)**, *Arg1* **(C)**, and *Nos2* **(D)** were normalized by *Gapdh* quantification and the values were normalized by untreated-uninfected condition (0 h); **(E)** Frequency of NO producing cells and **(F)** mean of fluorescence intensity (MFI) of NO were quantified by DAF-FM label using flow cytometry. Each bar represents the average ± SEM of the values obtained in three independent experiments ($n = 6$–8). Statistical significance was determined based on two-tailed Student's *t*-test. *$p < 0.05$, infected macrophages (4 h or 24 h) compared to non-infected (0 h) **$p < 0.05$, melatonin-treated compared to untreated or vehicle.

demonstrated that *L. amazonensis*-infection and melatonin could regulate the synthesis of these cytokines and chemokines.

Melatonin Antagonizes Changes in the miRNA Profile in *Leishmania amazonensis*-Infected Macrophages

The effect of melatonin on the miRNA expression profile was also evaluated after 4 and 24 h of infection. In untreated and 24 h-infected macrophages, only miR-294-3p, miR-410-3p, and miR-495-3p appeared upregulated. In vehicle-treated macrophages at 4 h of infection, miR-294-3p, miR-410-3p, miR-669h-3p, and miR-721 appeared upregulated, while miR-26a-5p, miR-130b-3p, and miR-181c-5p appeared downregulated (**Figure 4**, **Supplementary Table 1**). In addition, at 24 h of infection, the expression of miR-302d-3p, miR-30e-5p, and miR-669h-3p appeared upregulated, while miR-181c-5p and miR-26a-5p appeared downregulated.

Melatonin treatment and 4 h of *L. amazonensis* infection induced the expression of miR-294-3p, miR-410-3p, miR-694, and miR-669h-3p, while miR-26a-5p expression appeared reduced (**Figure 4**). Additionally, melatonin treatment at both 4 and 24 h of *L. amazonensis* infection reduced the expression of miR-26a-5p (**Figure 4**). However, only miR-694 was exclusively affected by melatonin treatment since it did not appear in vehicle treatment at early infection (**Figure 4**). These data indicated that melatonin blocked the upregulation of miR-721 and the downregulation of miR-130b-3p and miR-181c-5p after vehicle treatment at 4 h of infection, as well as the upregulation of miR-30e-5p, miR-302d-3p, and miR-669h-3p at 24 h of infection (**Figure 4**).

Our data demonstrated that melatonin treatment could modulate the miRNA profile of *L. amazonensis*-infected macrophages.

Inhibition of miR-181c-5p, miR-294-3p, miR-30e-5p, and miR-302d-3p Reduces the Infectivity of *Leishmania amazonensis* by Modulation of *Nos2*, *Tnf*, *Mcp-1*/*Ccl2,* and *Rantes*/*Ccl5* mRNA Expression

Since miR-181c-5p, miR-294-3p, miR-30e-5p, and miR-302d-3p appeared modulated in both vehicle and melatonin treatment, we performed validation assays to determine the impact of those miRNAs modulation on mRNA expression during infection.

Firstly, we performed *in silico* analysis, and based on a miRecord search, we identified miR-181c-5p, miR-294-3p, miR-30e-5p, and miR-302d-3p targeting thousands of mRNAs (**Supplementary Tables 2**–**5**). Among these interactions and

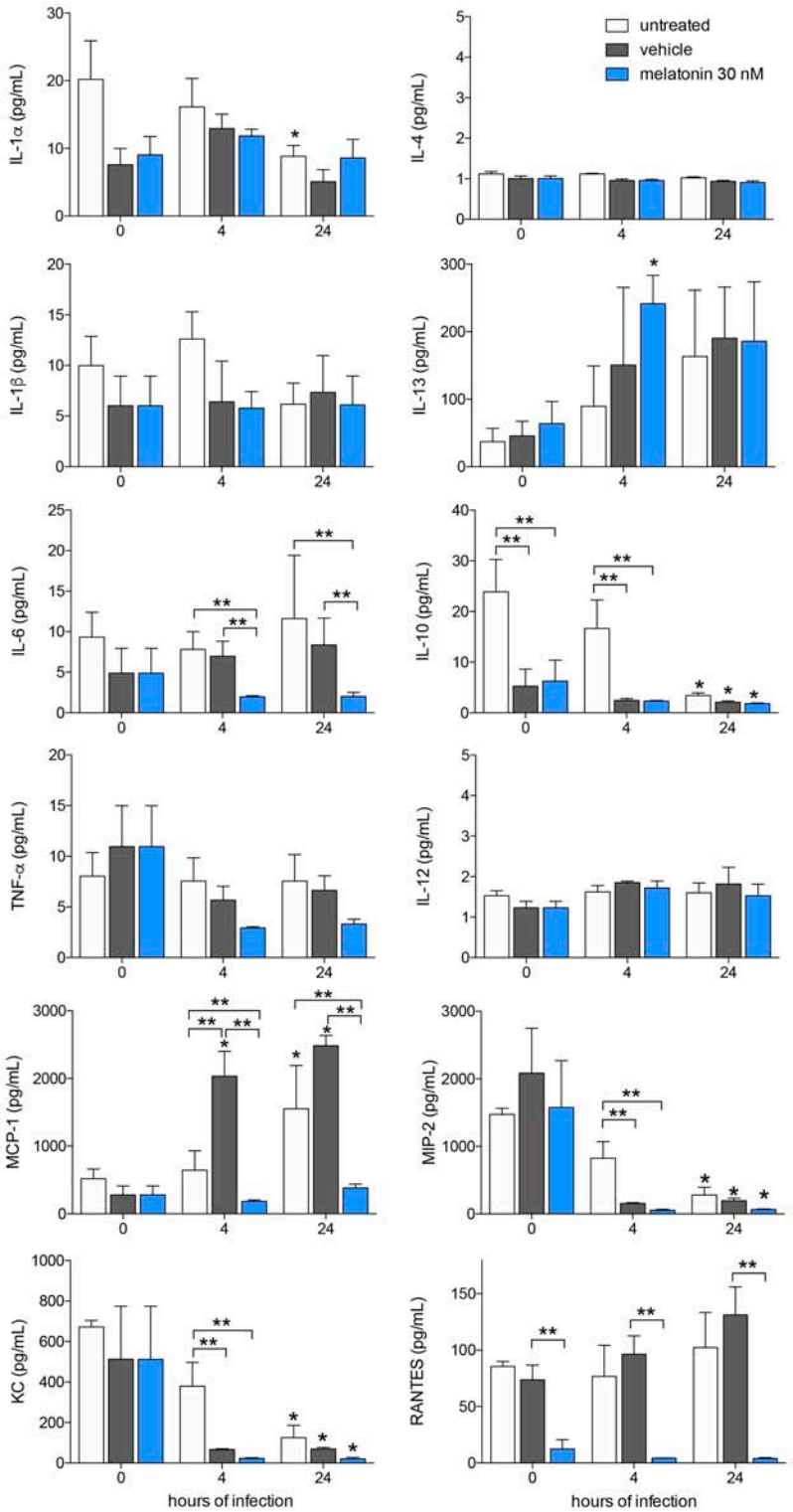

FIGURE 3 | Cytokine and chemokines production after melatonin treatment and *L. amazonensis* infection. Cytokine and chemokine quantifications were performed with macrophage supernatants (1×10^6/500 μL) treated with melatonin (30 nM, blue bar), vehicle (5×10^{-6}% ethanol, gray bar) or untreated (white bar) for 4 h, infected with *L. amazonensis* (MOI 5:1) and collected after 4 and 24 h of infection. The time 0 corresponds to non-infected macrophages. Each bar represents medium ± SEM of values obtained in three independent experiments ($n = 4$–5). *$p < 0.05$, infected compared to uninfected macrophages (0 h) **$p < 0.05$, melatonin-treated compared to untreated or vehicle.

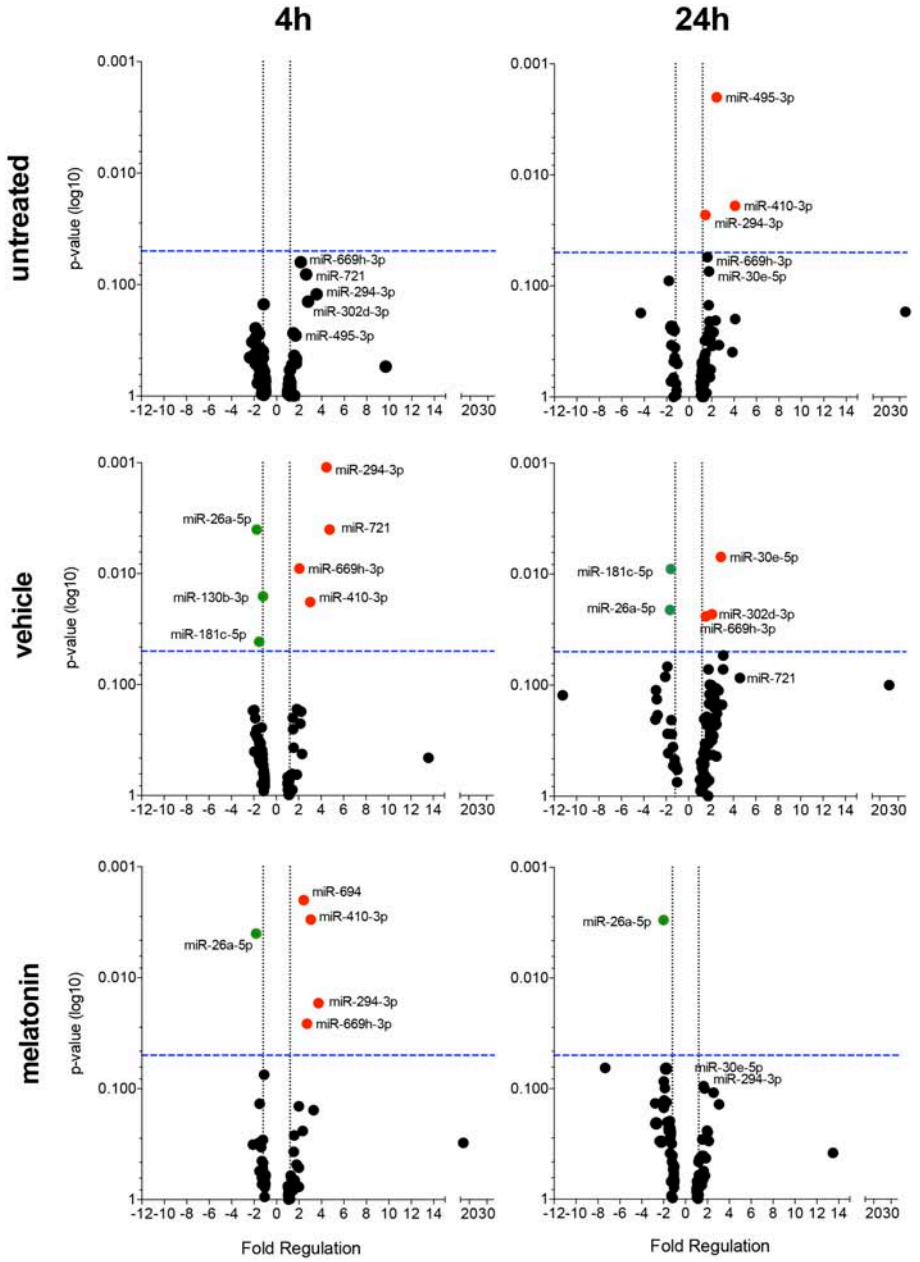

FIGURE 4 | Volcano plot showing melatonin modulation of miRNA profile in macrophages infected with *L. amazonensis* in a time dependent manner. Each dot represents one miRNA in untreated, vehicle or melatonin (30 nM) treated in macrophages infected for 4 or 24 h with *L. amazonensis*. The red dots indicate up-regulated miRNA and green dots indicate down-regulated miRNAs. Blue dotted line corresponds to $p = 0.05$, log 10. The relative up- and down-regulation of miRNAs, expressed as boundaries of 1.5 or −1.5 of Fold Regulation, respectively. *p*-value was determined based on unpaired two-tailed Student's *t*-test. The data are representative of three independent experiments ($n = 3$–4).

trial to focus on L-arginine metabolism and NO, cytokine and chemokine production, we identified that these miRNAs could target the following mRNAs: *Nos*2, *Tnf*, *Mcp*-1/*Ccl2,* and *Rantes/Ccl5*. Then, we performed *in vitro* validation through miRNA inhibition of infection-induced expression at 4 and 24 h. The miR-495-3p, miR-694, and miR-721 did not present *in silico* prediction on these mRNA, with exception of miR-721/*Nos*2 validated target (Muxel et al., 2017b), then we did not perform the validation assay (**Supplementary Tables 6–8**).

According to miRNA inhibition assays, we observed reduced levels of these miRNAs at 4 h, but not at 24 h of infection compared to untreated or negative control - transfected macrophages, indicating the efficiency of miRNA inhibition (**Figure 5A**).

Further, we evaluated the miRNA inhibitions and *Nos*2 mRNA expression levels, and we observed increased levels after inhibition of miR-30e-5p and miR-302d-3p compared to the negative control group (**Figure 5B**), indicating the interaction

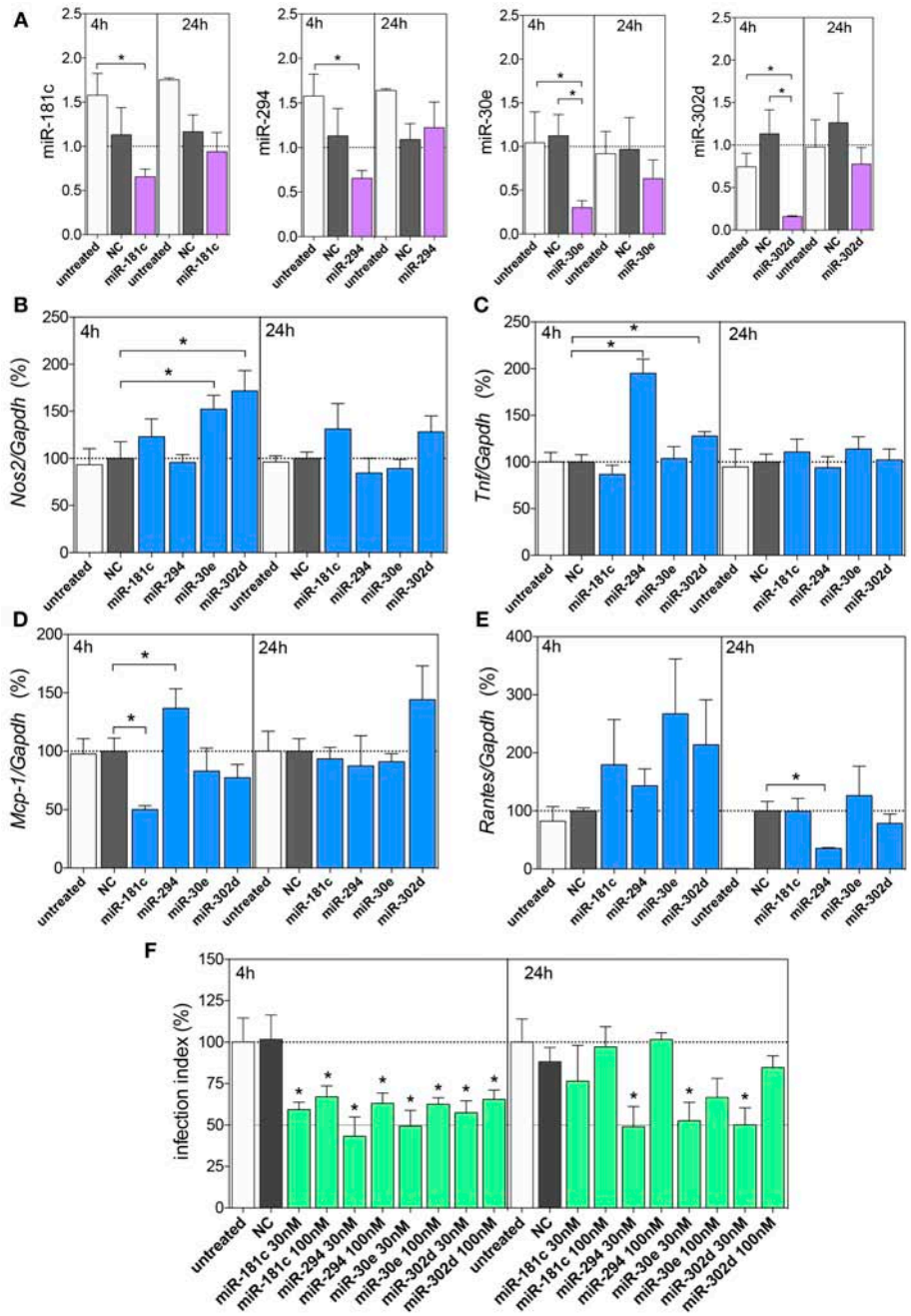

FIGURE 5 | Functional analysis of miR-181c, miR-294-5p, miR-30e, and miR302d inhibition. Macrophages (5×10^5) were transiently transfected with the negative control (NC, gray bars), 30 or 100 nM of miR-181c-5p, miR-294-3p, miR-30e-5p, or miR-302d-3p inhibitors (purple bars), or left non-transfected (untreated, white bars). After 36 h of incubation, the cells were infected with *L. amazonensis* (MOI 5:1) for 4 and 24 h. The inhibition with 100 nM of NC or miRNAs were performed to evaluated miR-181c-5p, miR-294-3p, miR-30e-5p, or miR-302d-3p expression **(A)** and for *Nos2* **(B)**, *Tnf*, **(C)** *Mcp-1* **(D),** and *Rantes* **(E)** mRNA expression, by qPCR; the inhibition with 30 or 100 nM of NC or miRNAs were also performed for infectivity evaluation **(F)** by microscopy analysis, counting the numbers of infected macrophages and amastigotes per macrophage ($n = 1{,}000$ macrophages/treatment). The values of miRNAs were represented by Fold change using SNORD95, as a normalizing endogenous control. The values of mRNAs were normalized (100%) based on the average values of the negative control (NC) at 4 h of infection. Each bar represents the average ± SEM of the values obtained in three independent experiments ($n = 4$–6). Statistical significance was determined based on unpaired two-tailed Student's *t*-test. In infectivity analysis **(F)**, $^*p < 0.05$, compared to negative control (NC) infected macrophages.

of these miRNAs with *Nos2*. The *Tnf* mRNA expression showed increased levels after inhibition of miR-294-3p and miR-302d-3p compared to those in the negative control group (**Figures 5C,D**), indicating the interaction of these miRNAs with *Tnf*. The *Mcp-1* mRNA expression showed increased levels after inhibition of miR-294-3p (**Figure 5D**), indicating

the interaction of this miRNA with *Mcp-1*. Interestingly, *Mcp-1* mRNA expression showed decreased levels after inhibition of miR-181c-5p (**Figure 5D**).

Since we observed no statistically significance in miRNA inhibitions at 24 h of infection, we did not infer a role for an interaction between miR-294-3p and *Rantes/Ccl5* mRNA targeting (**Figure 5E**).

The impact of miRNA inhibition assays were also evaluated in infection index and according to the **Figure 5F**, we observed that the inhibition of miR-181c-5p, miR-294-3p, miR-30e-5p, and miR-302d-3p at 30 or 100 nM inhibitors reduced the infection index at 4 h of infection, but only 30 nM of miR-294-3p, miR-30e-5p, and miR-302d-3p inhibitors presented reduction in the infection index at 24 h of infection (**Figure 5F**).

Altogether, the present data indicated that modulation of macrophage infection by melatonin is dependent of these miRNA expressions and therefore on changes in the cell defense program, rather than on only isolated effects at one enzyme or receptor.

DISCUSSION

Macrophages are essential components of innate immunity and are capable of differentiating into cells with a wide range of functions. These cells are able to respond to different stimuli, such as microbial molecules, damaged cell components, co-stimulatory molecules, cytokines, and chemokines by changing their phenotypes (Mosser and Edwards, 2008; Zhang and Mosser, 2008). In addition, melatonin can act as a pro- or anti-inflammatory agent depending on cell activation state and/or cell type. Melatonin also primes macrophages to a phenotype that reduces *L. amazonensis* infectivity (Laranjeira-Silva et al., 2015).

Melatonin can also act in the modulation of gene expression through transcriptional and posttranscriptional mechanisms, and these intricate regulatory mechanisms interfere with melatonin production. Several studies have shown the role of melatonin in inhibiting arginine uptake via CAT2B (Laranjeira-Silva et al., 2015), CAT1 (Gilad et al., 1998; Deng et al., 2006; Nair et al., 2011), and NOS2 activity (Xia et al., 2012). In contrast, our work showed that melatonin treatment of BALB/c BMDMs increased *Nos2* mRNA expression and NO production during infection, leading to a decreased infection index. Moreover, *Nos2* expression and NO production kill parasites and result in resistance to infection (Ghalib et al., 1995; Wei et al., 1995; Vieira et al., 1996; Wilhelm et al., 2001; Yang et al., 2007; Ben-Othman et al., 2009; Srivastava et al., 2012; Muxel et al., 2017b, 2018a,b).

In this work, we showed that melatonin treatment reduced IL-6, RANTES, MCP-1 and MIP-2 protein levels in infected macrophages, which could correlate with macrophage activation and cell recruitment to the inflammation site. In contrast, melatonin reduced IL-10 levels, which could correlate with immune response modulation induced by infection and pathogenesis. The melatonin treatment was previous described in the μM-mM range concentrations inhibiting IL-1β, TNF-α, IL-6, IL-8, IL-13, and IL-10 and attenuating NOS2 activation induced by LPS (Zhou et al., 2010; Xia et al., 2012). Additionally, melatonin treatment increased TNF-α, IFN-γ, and IL-12 production but reduced NO levels during *Trypanosoma cruzi* infection (Santello et al., 2008a,b). A recent study demonstrated that melatonin also inhibits the production of proinflammatory cytokines, such as TNF-α, IL-6, and IL-12, by TLR-9-stimulated peritoneal macrophages through ERK1/2 and AKT pathways (Xu et al., 2018). However, melatonin in the pM-nM range promotes increased phagocytosis of fungus-derived particles (zymosan) by macrophages (Muxel et al., 2012) and can also reduces the entrance and replication of *L. amazonensis* in peritoneal macrophages (Laranjeira-Silva et al., 2015).

Here, we show that *L. amazonensis* infection of BALB/c untreated-macrophages promoted a reduction in IL-1α production and did not alter IL-1β, IL-6, TNF-α, or IL-12 protein levels. However, in C57BL/6-macrophages, the levels of *Il1b*, *Tnf*, *Il10,* and *Il6* receptor transcripts increase during infection (Muxel et al., 2018b). IL-1β plays a role in macrophage activation, increasing NO production and leading to host resistance to *Leishmania* infection (Lima-Junior et al., 2013). Also, IL-1 receptor signaling induces NF-kB activation (Ikeda and Dikic, 2008; David et al., 2010; Roh et al., 2014; Fletcher et al., 2015), suggesting a negative regulation of inflammatory cytokine production in infected macrophages. This is in contrast to the upregulation of proinflammatory cytokine gene expression in human macrophages after infection with *L. amazonensis* and *L. major*, such as that of *Il-1b*, *Tnf,* and *Il-6* (Fernandes et al., 2016), and in murine macrophages after *L. major* infection, in which *Tnf*, *Il-1,* and *Il-6* are upregulated (Dillon et al., 2015). However, melatonin treatment reduced IL-6 levels in infected macrophages compared to untreated infected macrophages. Indeed, melatonin inhibits IL-1β, IL-6, and TNF production mediated via LPS-TLR4 signaling (Xia et al., 2012).

In this work, we showed that another effect of melatonin is related to modulation of miRNA profile imposed by *L. amazonensis* infection. Both miR-294-3p and miR-721 appeared upregulated in vehicle-treated macrophages after 4 h of infection, whereas miR-721 was downregulated in melatonin-treated infected macrophages. Our previous studies showed that these miRNAs reduce *Nos2* expression and NO production, enabling the establishment of infection (Muxel et al., 2017b). Additionally, melatonin blocked the downregulation of miR-130b-3p and miR-181c-5p compared to vehicle. Functional inhibition of miR-181c-5p, miR-30e-5p, and miR-302d-3p increased *Nos2* mRNA expression, impairing infectiveness.

Based on *in silico* analysis of miRNA-mRNA interactions, we performed functional validation through miRNA inhibition. In this way, the inhibition miR-30e-5p and miR-302d-3p increased the levels of *Nos*2 and also the inhibition of miR-294-3p and miR-302d-3p increased *Tnf* levels, which reduced infectivity. Indeed, miR-294 belongs to the miR-291/294 family and controls the cell cycle during embryogenesis (Houbaviy et al., 2003; Wang et al., 2008; Zheng et al., 2011). Previous functional validation of miR-294-3p in *L. amazonensis* infection of BALB/c-macrophages demonstrated that this miRNA targets *Nos*2 mRNA reducing NOS2 expression and NO production impacting in infectivity (Muxel et al., 2017b). Also, miR-294 shares the same putative binding site of miR-302d in *Nos*2 3′UTR, suggesting the competition to interact in the *Nos*2 3′UTR. The signaling via

TLR4 by LPS injection on mice downregulates miR-294 levels in blood and lung samples (Fernandes et al., 2016), whereas the miR-294-3p is overexpressed in C57BL/6-macrophages infected with *L. amazonensis* independently of TLR2, TLR4, and MyD88 (Muxel et al., 2018b), suggesting an alternative induction of this miRNA.

The miR-302d encompasses the miR-302/367 cluster that is highly conserved in vertebrates and plays a role in cell proliferation and differentiation (Xia et al., 2012). miR-302d is expressed at the early time and downregulated in late time of exudate during acute inflammation in murine peritonitis induced via TLR2/zymosan stimuli (Recchiuti et al., 2011). In contrast, miR-302d appears at lower levels in plasma of experimental autoimmune encephalomyelitis mouse model and systemic lupus erythematosus and regulates IFN type I gene expression targeting interferon regulator factor-9 (IRF-9) in murine model (Smith et al., 2017). Interestingly, the IRF9, STAT1, STA3, and NF-κB can bind to promoter region of *Nos*2 gene and induce its transcription during *Listeria monocytogenes* infection (Farlik et al., 2010), suggesting both direct and indirect routes for miR-302d regulation of *Nos*2 expression.

Moreover, miR-30e alters cell proliferation, colony formation and invasiveness in cancer cells, interfering with NF-κB/IκBα negative feedback and apoptosis (Jiang et al., 2012; Hershkovitz-Rokah et al., 2015; Zhuang et al., 2017), suggesting a putative role of NF-κB activation during miR-30e-5p inhibition and increased levels of *Nos*2. miR-30e leads to hyperactivation of NF-κB by targeting IκBα 3′UTR, which induces IFN-β and suppresses dengue virus replication (Zhu et al., 2014). miR-30e is overexpressed in *Mycobacterium tuberculosis*-infected THP-1-macrophages (Wu et al., 2017), and in neutrophils of traumatic injured patients correlating to systemic inflammation (Yang et al., 2013).

Additionally, infection and melatonin treatment reduced the levels of KC/CXCL1 and MIP-2/CXCL2 produced by macrophages. These chemokines recruit neutrophils to sites of *Leishmania* infection (Muller et al., 2001). RANTES/CCL5 levels produced by *L. amazonensis*-infected and non-infected macrophages were reduced in melatonin-treated macrophages compared with untreated macrophages. *Rantes/Ccl5* mRNA levels tended to increase after functional inhibition of miR-30e and miR-302d. The cytokines KC/CXCL1, MIP-2/CXCL2, and RANTES/CCL5 are associated with neutrophil, monocyte and lymphocyte recruitment to the inflammatory focus (Schall et al., 1993; Ohmori and Hamilton, 1994; Hornung et al., 1997, 2001; Lebovic et al., 2001), and nocturnal levels of melatonin reduce neutrophil and monocyte migration to inflammatory sites *in vivo* (Lotufo et al., 2001, 2006; Tamura et al., 2010; Marçola et al., 2013).

Interestingly, MCP-1/CCL2 levels were enhanced after infection with *L. amazonensis,* but melatonin treatment reduced this chemokine production in infected macrophages. Melatonin (pretreatment with 100 μM for 4 h) also reduces MCP-1/CCL2 levels and the levels of RANTES/CCL5 produced by PBMCs stimulated with LPS (Park et al., 2007). Corroborating the role of melatonin in miRNA modulation in infected macrophages, inhibition of miR-294-3p increased *Mcp-1* mRNA levels, impacting *Leishmania* infectivity. The validation of interactions of these miRNAs/mRNAs can be explored in the future.

Our data confirmed the previous idea that *Leishmania* infection may regulate cytokine, chemokine and NO production to prevent or delay macrophage activation, allowing parasite entrance and replication. These data reinforced the importance of studying miRNA expression in *L. amazonensis* infection and its role in macrophage activation. Additionally, we demonstrate that melatonin treatment can modulate the miRNA profile and consequently alter the activation phenotype of infected macrophages.

DATA AVAILABILITY

All datasets generated for this study are included in the manuscript and/or the supplementary files.

ETHICS STATEMENT

Experimental protocols using animals were approved by the Animal Care and Use Committee of the Institute of Bioscience of the University of São Paulo (CEUA 169/2012 and 233/2014). This study was carried out in strict accordance with the recommendations in the guide and policies for the care and use of laboratory animals of the state of São Paulo (Lei Estadual 11.977 de 25/08/2005) and the Brazilian government (Lei Federal 11.794 de 08/10/2008).

AUTHOR CONTRIBUTIONS

JF, JA, StM, RZ, and SaM performed experiments. JF, JA, StM, RZ, RM, LF-W, and SaM analyzed data and statistics. SaM and JF prepared the figures. JA, JF, LF-W, and SaM wrote the manuscript. All authors reviewed the manuscript.

FUNDING

This work was supported by grants from the Conselho Nacional de Desenvolvimento Científico e Tecnológico (CNPq. www.cnpq.br: 479399/2012-3, 307587/2014-2 and 406351/2018-0.) and Fundação de Amparo à Pesquisa do Estado de São Paulo (FAPESP. www.fapesp.br: 2012/15263-4, 2014/50717-1, 2016/19815-2, 2016/03273-6, 2017/201906-9, and 2017/23519-2).

SUPPLEMENTARY MATERIAL

The Supplementary Material for this article can be found online at: https://www.frontiersin.org/articles/10.3389/fcimb.2019.00060/full#supplementary-material

Supplementary Figure 1 | *Leishmania* infectivity in melatonin-treated macrophages**.** BALB/c macrophages (2×10^5 cells) were pre-incubated for 1, 2, or 4 h with medium (untreated, white bar), vehicle (ethanol 0.0005%, gray bar), or 3 (blue bar) or 30 (light blue bar) nM of melatonin. After, macrophages were infected with *L. amazonensis* (MOI 5:1) and analyzed after 4 and 24 h. **(A–C)**—percentage of infected macrophages; **(D–F)**—number of amastigotes per infected macrophage; **(G–I)**—infection index (rate of infected macrophages

multiplied by the number of amastigotes per infected macrophage). Each bar represents the mean ± SEM of three independent experiments ($n = 5$–8). $^*p < 0.05$, comparing the melatonin treatment with the vehicle-treated macrophage at the same concentration and time.

Supplementary Table 1 | miRNAs Up-Down Regulation in melatonin and infected *L. amazonensis* infected macrophages compared to uninfected. The relative up- and down-regulation of miRNAs, expressed as boundaries of 1.5 and −1.5 of Fold Regulation, respectively. $p < 0.05$ was considered statistically significant. *p*-value was determined based on two-tailed Student's *t*-test. The data are representative of three independent experiments. Untreated: only 10% FBS RMPI 1640 medium; Vehicle: ethanol 0.0005% in 10% FBS RMPI 1640 medium; Melatonin 30 nM diluted 10% FBS RMPI 1640 medium.

Supplementary Table 2 | Predicted mRNA-targets for miR-30e. The miRNA-mRNA interaction was predicted using miRecord tools (http://c1.accurascience.com/miRecords/) based in the integration of various prediction tools: DIANA-microT, MicroInspector, miRanda, MirTarget2, miTarget, NBmiRTar, PicTar, PITA, RNA22, RNAhybrid, and TargetScan/TargertScanS.

Supplementary Table 3 | Predicted mRNA-targets for miR-181c. The miRNA-mRNA interaction was predicted using miRecord tools (http://c1.accurascience.com/miRecords/) based in the integration of various prediction tools: DIANA-microT, MicroInspector, miRanda, MirTarget2, miTarget, NBmiRTar, PicTar, PITA, RNA22, RNAhybrid, and TargetScan/TargertScanS.

Supplementary Table 4 | Predicted mRNA-targets for miR-294. The miRNA-mRNA interaction was predicted using miRecord tools (http://c1.accurascience.com/miRecords/) based in the integration of various prediction tools: DIANA-microT, MicroInspector, miRanda, MirTarget2, miTarget, NBmiRTar, PicTar, PITA, RNA22, RNAhybrid, and TargetScan/TargertScanS.

Supplementary Table 5 | Predicted mRNA-targets for miR-302d. The miRNA-mRNA interaction was predicted using miRecord tools (http://c1.accurascience.com/miRecords/) based in the integration of various prediction tools: DIANA-microT, MicroInspector, miRanda, MirTarget2, miTarget, NBmiRTar, PicTar, PITA, RNA22, RNAhybrid, and TargetScan/TargertScanS.

Supplementary Table 6 | Predicted mRNA-targets for miR-495. The miRNA-mRNA interaction was predicted using miRecord tools (http://c1.accurascience.com/miRecords/) based in the integration of various prediction tools: DIANA-microT, MicroInspector, miRanda, MirTarget2, miTarget, NBmiRTar, PicTar, PITA, RNA22, RNAhybrid, and TargetScan/TargertScanS.

Supplementary Table 7 | Predicted mRNA-targets for miR-694. The miRNA-mRNA interaction was predicted using miRecord tools (http://c1.accurascience.com/miRecords/) based in the integration of various prediction tools: DIANA-microT, MicroInspector, miRanda, MirTarget2, miTarget, NBmiRTar, PicTar, PITA, RNA22, RNAhybrid, and TargetScan/TargertScanS.

Supplementary Table 8 | Predicted mRNA-targets for miR-721. The miRNA-mRNA interaction was predicted using miRecord tools (http://c1.accurascience.com/miRecords/) based in the integration of various prediction tools: DIANA-microT, MicroInspector, miRanda, MirTarget2, miTarget, NBmiRTar, PicTar, PITA, RNA22, RNAhybrid, and TargetScan/TargertScanS.

REFERENCES

Alvar, J., Velez, I. D., Bern, C., Herrero, M., Desjeux, P., Cano, J., et al. (2012). Leishmaniasis worldwide and global estimates of its incidence. *PLoS ONE* 7:e35671. doi: 10.1371/journal.pone.0035671

Ashford, R.W. (2000). The leishmaniases as emerging and reemerging zoonoses. *Int. J. Parasitol.* 30, 1269–1281. doi: 10.1016/S0020-7519(00)00136-3

Bagga, S., Bracht, J., Hunter, S., Massirer, K., Holtz, J., Eachus, R., et al. (2005). Regulation by let-7 and lin-4 miRNAs results in target mRNA degradation. *Cell* 122, 553–563. doi: 10.1016/j.cell.2005.07.031

Baltimore, D., Boldin, M. P., O'connell, R. M., Rao, D. S., and Taganov, K. D. (2008). MicroRNAs: new regulators of immune cell development and function. *Nat. Immunol.* 9, 839–845. doi: 10.1038/ni.f.209

Banerjee, S., Xie, N., Cui, H., Tan, Z., Yang, S., Icyuz, M., et al. (2013). MicroRNA let-7c regulates macrophage polarization. *J. Immunol.* 190, 6542–6549. doi: 10.4049/jimmunol.1202496

Ben-Othman, R., Dellagi, K., and Guizani-Tabbane, L. (2009). Leishmania major parasites induced macrophage tolerance: implication of MAPK and NF-kappaB pathways. *Mol. Immunol.* 46, 3438–3444. doi: 10.1016/j.molimm.2009.05.337

Boucher, J. L., Moali, C., and Tenu, J. P. (1999). Nitric oxide biosynthesis, nitric oxide synthase inhibitors and arginase competition for L-arginine utilization. *Cell. Mol. Life Sci.* 55, 1015–1028. doi: 10.1007/s000180050352

Carrillo-Vico, A., Calvo, J. R., Abreu, P., Lardone, P. J., Garcia-Maurino, S., Reiter, R. J., et al. (2004). Evidence of melatonin synthesis by human lymphocytes and its physiological significance: possible role as intracrine, autocrine, and/or paracrine substance. *FASEB J.* 18, 537–539. doi: 10.1096/fj.03-0694fje

Carrillo-Vico, A., Guerrero, J. M., Lardone, P. J., and Reiter, R. J. (2005). A review of the multiple actions of melatonin on the immune system. *Endocrine* 27, 189–200. doi: 10.1385/ENDO:27:2:189

Carrillo-Vico, A., Lardone, P. J., Alvarez-Sanchez, N., Rodriguez-Rodriguez, A., and Guerrero, J. M. (2013). Melatonin: buffering the immune system. *Int. J. Mol. Sci.* 14, 8638–8683. doi: 10.3390/ijms14048638

Carvalho-Sousa, C. E., Da Silveira Cruz-Machado, S., Tamura, E. K., Fernandes, P. A., Pinato, L., Muxel, S. M., et al. (2011). Molecular basis for defining the pineal gland and pinealocytes as targets for tumor necrosis factor. *Front. Endocrinol.* 2:10. doi: 10.3389/fendo.2011.00010

Corraliza, I. M., Soler, G., Eichmann, K., and Modolell, M. (1995). Arginase induction by suppressors of nitric oxide synthesis (IL-4, IL-10 and PGE2) in murine bone-marrow-derived macrophages. *Biochem. Biophys. Res. Commun.* 206, 667–673. doi: 10.1006/bbrc.1995.1094

Da Silveira Cruz-Machado, S., Carvalho-Sousa, C. E., Tamura, E. K., Pinato, L., Cecon, E., Fernandes, P. A., et al. (2010). TLR4 and CD14 receptors expressed in rat pineal gland trigger NFKB pathway. *J. Pineal Res.* 49, 183–192. doi: 10.1111/j.1600-079X.2010.00785.x

David, Y., Ziv, T., Admon, A., and Navon, A. (2010). The E2 ubiquitin-conjugating enzymes direct polyubiquitination to preferred lysines. *J. Biol. Chem.* 285, 8595–8604. doi: 10.1074/jbc.M109.089003

Deng, W. G., Tang, S. T., Tseng, H. P., and Wu, K. K. (2006). Melatonin suppresses macrophage cyclooxygenase-2 and inducible nitric oxide synthase expression by inhibiting p52 acetylation and binding. *Blood* 108, 518–524. doi: 10.1182/blood-2005-09-3691

Dillon, L. A., Suresh, R., Okrah, K., Corrada Bravo, H., Mosser, D. M., and El-Sayed, N. M. (2015). Simultaneous transcriptional profiling of Leishmania major and its murine macrophage host cell reveals insights into host-pathogen interactions. *BMC Genomics* 16:1108. doi: 10.1186/s12864-015-2237-2

Elmahallawy, E. K., Jimenez-Aranda, A., Martinez, A. S., Rodriguez-Granger, J., Navarro-Alarcon, M., Gutierrez-Fernandez, J., et al. (2014). Activity of melatonin against *Leishmania infantum* promastigotes by mitochondrial dependent pathway. *Chem. Biol. Interact.* 220, 84–93. doi: 10.1016/j.cbi.2014.06.016

El-Sokkary, G. H., Omar, H. M., Hassanein, A. F., Cuzzocrea, S., and Reiter, R. J. (2002). Melatonin reduces oxidative damage and increases survival of mice infected with Schistosoma mansoni. *Free Radic. Biol. Med.* 32, 319–332. doi: 10.1016/S0891-5849(01)00753-5

Farlik, M., Reutterer, B., Schindler, C., Greten, F., Vogl, C., Muller, M., et al. (2010). Nonconventional initiation complex assembly by STAT and NF-kappaB transcription factors regulates nitric oxide synthase expression. *Immunity* 33, 25–34. doi: 10.1016/j.immuni.2010.07.001

Fernandes, M. C., Dillon, L. A., Belew, A. T., Bravo, H. C., Mosser, D. M., and El-Sayed, N. M. (2016). Dual transcriptome profiling of leishmania-infected human macrophages reveals distinct reprogramming signatures. *MBio* 7:e00027-16. doi: 10.1128/mBio.00027-16

Fletcher, A. J., Mallery, D. L., Watkinson, R. E., Dickson, C. F., and James, L. C. (2015). Sequential ubiquitination and deubiquitination enzymes synchronize the dual sensor and effector functions of TRIM21. *Proc. Natl. Acad. Sci. U S A.* 112, 10014–10019. doi: 10.1073/pnas.1507534112

Frank, B., Marcu, A., De Oliveira Almeida Petersen, A. L., Weber, H., Stigloher, C., Mottram, J. C., et al. (2015). Autophagic digestion of Leishmania major by host macrophages is associated with differential expression of BNIP3, CTSE, and the miRNAs miR-101c, miR-129, and miR-210. *Parasit. Vectors* 8:404. doi: 10.1186/s13071-015-0974-3

Geraci, N. S., Tan, J. C., and Mcdowell, M. A. (2015). Characterization of microRNA expression profiles in Leishmania-infected human phagocytes. *Parasite Immunol.* 37, 43–51. doi: 10.1111/pim.12156

Ghalib, H. W., Whittle, J. A., Kubin, M., Hashim, F. A., El-Hassan, A. M., Grabstein, K. H., et al. (1995). IL-12 enhances Th1-type responses in human *Leishmania donovani* infections. *J. Immunol.* 154, 4623–4629.

Ghosh, J., Bose, M., Roy, S., and Bhattacharyya, S. N. (2013). *Leishmania donovani* targets Dicer1 to downregulate miR-122, lower serum cholesterol, and facilitate murine liver infection. *Cell Host Microbe* 13, 277–288. doi: 10.1016/j.chom.2013.02.005

Gilad, E., Wong, H. R., Zingarelli, B., Virag, L., O'connor, M., Salzman, A. L., et al. (1998). Melatonin inhibits expression of the inducible isoform of nitric oxide synthase in murine macrophages: role of inhibition of NFkappaB activation. *FASEB J.* 12, 685–693. doi: 10.1096/fasebj.12.9.685

Graff, J. W., Dickson, A. M., Clay, G., Mccaffrey, A. P., and Wilson, M. E. (2012). Identifying functional microRNAs in macrophages with polarized phenotypes. *J. Biol. Chem.* 287, 21816–21825. doi: 10.1074/jbc.M111.327031

Gregory, D. J., and Olivier, M. (2005). Subversion of host cell signalling by the protozoan parasite *Leishmania*. *Parasitology* 130, S27–S35. doi: 10.1017/S0031182005008139

Hershkovitz-Rokah, O., Modai, S., Pasmanik-Chor, M., Toren, A., Shomron, N., Raanani, P., et al. (2015). MiR-30e induces apoptosis and sensitizes K562 cells to imatinib treatment via regulation of the BCR-ABL protein. *Cancer Lett.* 356, 597–605. doi: 10.1016/j.canlet.2014.10.006

Hornung, D., Bentzien, F., Wallwiener, D., Kiesel, L., and Taylor, R. N. (2001). Chemokine bioactivity of RANTES in endometriotic and normal endometrial stromal cells and peritoneal fluid. *Mol. Hum. Reprod.* 7, 163–168. doi: 10.1093/molehr/7.2.163

Hornung, D., Ryan, I. P., Chao, V. A., Vigne, J. L., Schriock, E. D., and Taylor, R. N. (1997). Immunolocalization and regulation of the chemokine RANTES in human endometrial and endometriosis tissues and cells. *J. Clin. Endocrinol. Metab.* 82, 1621–1628. doi: 10.1210/jc.82.5.1621

Hotta, C. T., Gazarini, M. L., Beraldo, F. H., Varotti, F. P., Lopes, C., Markus, R. P., et al. (2000). Calcium-dependent modulation by melatonin of the circadian rhythm in malarial parasites. *Nat. Cell Biol.* 2, 466–468. doi: 10.1038/35017112

Houbaviy, H. B., Murray, M. F., and Sharp, P. A. (2003). Embryonic stem cell-specific MicroRNAs. *Dev. Cell* 5, 351–358. doi: 10.1016/S1534-5807(03)00227-2

Hrabak, A., Bajor, T., Temesi, A., and Meszaros, G. (1996). The inhibitory effect of nitrite, a stable product of nitric oxide (NO) formation, on arginase. *FEBS Lett.* 390, 203–206. doi: 10.1016/0014-5793(96)00659-X

Ikeda, F., and Dikic, I. (2008). Atypical ubiquitin chains: new molecular signals. 'Protein modifications: beyond the usual suspects' review series. *EMBO Rep.* 9, 536–542. doi: 10.1038/embor.2008.93

Jiang, L., Lin, C., Song, L., Wu, J., Chen, B., Ying, Z., et al. (2012). MicroRNA-30e* promotes human glioma cell invasiveness in an orthotopic xenotransplantation model by disrupting the NF-kappaB/IkappaBalpha negative feedback loop. *J. Clin. Invest.* 122, 33–47. doi: 10.1172/JCI58849

Kinsey, S. G., Prendergast, B. J., and Nelson, R. J. (2003). Photoperiod and stress affect wound healing in Siberian hamsters. *Physiol. Behav.* 78, 205–211. doi: 10.1016/S0031-9384(02)00967-8

Laranjeira-Silva, M. F., Zampieri, R. A., Muxel, S. M., Floeter-Winter, L. M., and Markus, R. P. (2015). Melatonin attenuates *Leishmania* (L.) amazonensis infection by modulating arginine metabolism. *J. Pineal Res.* 59, 478–487. doi: 10.1111/jpi.12279

Lebovic, D. I., Chao, V. A., Martini, J. F., and Taylor, R. N. (2001). IL-1beta induction of RANTES (regulated upon activation, normal T cell expressed and secreted) chemokine gene expression in endometriotic stromal cells depends on a nuclear factor-kappaB site in the proximal promoter. *J. Clin. Endocrinol. Metab.* 86, 4759–4764. doi: 10.1210/jcem.86.10.7890

Lemaire, J., Mkannez, G., Guerfali, F. Z., Gustin, C., Attia, H., Sghaier, R. M., et al. (2013). MicroRNA expression profile in human macrophages in response to *Leishmania* major infection. *PLoS Negl. Trop. Dis.* 7:e2478. doi: 10.1371/journal.pntd.0002478

Lim, L. P., Lau, N. C., Garrett-Engele, P., Grimson, A., Schelter, J. M., Castle, J., et al. (2005). Microarray analysis shows that some microRNAs downregulate large numbers of target mRNAs. *Nature* 433, 769–773. doi: 10.1038/nature03315

Lima-Junior, D. S., Costa, D. L., Carregaro, V., Cunha, L. D., Silva, A. L., Mineo, T. W., et al. (2013). Inflammasome-derived IL-1beta production induces nitric oxide-mediated resistance to Leishmania. *Nat. Med.* 19, 909–915. doi: 10.1038/nm.3221

Lotufo, C. M., Lopes, C., Dubocovich, M. L., Farsky, S. H., and Markus, R. P. (2001). Melatonin and N-acetylserotonin inhibit leukocyte rolling and adhesion to rat microcirculation. *Eur. J. Pharmacol.* 430, 351–357. doi: 10.1016/S0014-2999(01)01369-3

Lotufo, C. M., Yamashita, C. E., Farsky, S. H., and Markus, R. P. (2006). Melatonin effect on endothelial cells reduces vascular permeability increase induced by leukotriene B4. *Eur. J. Pharmacol.* 534, 258–263. doi: 10.1016/j.ejphar.2006.01.050

Luchetti, F., Canonico, B., Betti, M., Arcangeletti, M., Pilolli, F., Piroddi, M., et al. (2010). Melatonin signaling and cell protection function. *FASEB J.* 24, 3603–3624. doi: 10.1096/fj.10-154450

Maestroni, G. J. (1996). Melatonin as a therapeutic agent in experimental endotoxic shock. *J. Pineal Res.* 20, 84–89. doi: 10.1111/j.1600-079X.1996.tb00244.x

Mantovani, A., Sica, A., Sozzani, S., Allavena, P., Vecchi, A., and Locati, M. (2004). The chemokine system in diverse forms of macrophage activation and polarization. *Trends Immunol.* 25, 677–686. doi: 10.1016/j.it.2004.09.015

Marçola, M., Da Silveira Cruz-Machado, S., Fernandes, P. A., Monteiro, A. W., Markus, R. P., and Tamura, E. K. (2013). Endothelial cell adhesiveness is a function of environmental lighting and melatonin level. *J. Pineal Res.* 54, 162–169. doi: 10.1111/j.1600-079X.2012.01025.x

Markus, R. P., Fernandes, P. A., Kinker, G. S., Da Silveira Cruz-Machado, S., and Marcola, M. (2017). Immune-Pineal Axis - Acute inflammatory responses coordinate melatonin synthesis by pinealocytes and phagocytes. *Br. J. Pharmacol.* 175, 3239–3250. doi: 10.1111/bph.14083

Markus, R. P., Ferreira, Z. S., Fernandes, P. A., and Cecon, E. (2007). The immune-pineal axis: a shuttle between endocrine and paracrine melatonin sources. *Neuroimmunomodulation* 14, 126–133. doi: 10.1159/000110635

Marsden, P. D. (1986). Mucosal leishmaniasis ("espundia" Escomel, 1911). *Trans. R. Soc. Trop. Med. Hyg.* 80, 859–876. doi: 10.1016/0035-9203(86)90243-9

Martinez, F. O., Helming, L., and Gordon, S. (2009). Alternative activation of macrophages: an immunologic functional perspective. *Annu. Rev. Immunol.* 27, 451–483. doi: 10.1146/annurev.immunol.021908.132532

Mosser, D. M., and Edwards, J. P. (2008). Exploring the full spectrum of macrophage activation. *Nat. Rev. Immunol.* 8, 958–969. doi: 10.1038/nri2448

Mukherjee, B., Paul, J., Mukherjee, S., Mukhopadhyay, R., Das, S., Naskar, K., et al. (2015). Antimony-resistant *Leishmania donovani* exploits miR-466i to deactivate host MyD88 for regulating IL-10/IL-12 levels during early hours of infection. *J. Immunol.* 195, 2731–2742. doi: 10.4049/jimmunol.1402585

Muller, K., Van Zandbergen, G., Hansen, B., Laufs, H., Jahnke, N., Solbach, W., et al. (2001). Chemokines, natural killer cells and granulocytes in the early course of *Leishmania* major infection in mice. *Med. Microbiol. Immunol.* 190, 73–76. doi: 10.1007/s004300100084

Munder, M., Eichmann, K., and Modolell, M. (1998). Alternative metabolic states in murine macrophages reflected by the nitric oxide synthase/arginase balance: competitive regulation by CD4+ T cells correlates with Th1/Th2 phenotype. *J. Immunol.* 160, 5347–5354.

Muxel, S. M., Acuna, S. M., Aoki, J. I., Zampieri, R. A., and Floeter-Winter, L. M. (2018b). Toll-like receptor and miRNA-let-7e expression alter the inflammatory response in *Leishmania amazonensis*-infected macrophages. *Front. Immunol.* 9:2792. doi: 10.3389/fimmu.2018.02792

Muxel, S. M., Aoki, J. I., Fernandes, J. C. R., Laranjeira-Silva, M. F., Zampieri, R. A., Acuna, S. M., et al. (2018a). Arginine and polyamines fate in *Leishmania* infection. *Front. Microbiol.* 8:2682. doi: 10.3389/fmicb.2017.02682

Muxel, S. M., Laranjeira-Silva, M. F., Zampieri, R. A., Aoki, J. I., Acuña, S. M., and Floeter-Winter, L. M. (2017a). Functional validation of miRNA-mRNA interactions in macrophages by inhibition/competition assays based in transient transfection. *Protoc. Exchange*. 1–14. doi: 10.1038/protex.2017.034

Muxel, S. M., Laranjeira-Silva, M. F., Zampieri, R. A., and Floeter-Winter, L. M. (2017b). *Leishmania* (Leishmania) *amazonensis* induces macrophage miR-294 and miR-721 expression and modulates infection by targeting NOS2 and L-arginine metabolism. *Sci. Rep.* 7:44141. doi: 10.1038/srep44141

Muxel, S. M., Pires-Lapa, M. A., Monteiro, A. W., Cecon, E., Tamura, E. K., Floeter-Winter, L. M., et al. (2012). NF-kappaB drives the synthesis of melatonin in RAW 264.7 macrophages by inducing the transcription of the arylalkylamine-N-acetyltransferase (AA-NAT) gene. *PLoS ONE* 7:e52010. doi: 10.1371/journal.pone.0052010

Nair, S. M., Rahman, R. M., Clarkson, A. N., Sutherland, B. A., Taurin, S., Sammut, I. A., et al. (2011). Melatonin treatment following stroke induction modulates L-arginine metabolism. *J. Pineal Res.* 51, 313–323. doi: 10.1111/j.1600-079X.2011.00891.x

Nathan, C., and Shiloh, M. U. (2000). Reactive oxygen and nitrogen intermediates in the relationship between mammalian hosts and microbial pathogens. *Proc. Natl. Acad. Sci. U S A.* 97, 8841–8848. doi: 10.1073/pnas.97.16.8841

Ohmori, Y., and Hamilton, T. A. (1994). IFN-gamma selectively inhibits lipopolysaccharide-inducible JE/monocyte chemoattractant protein-1 and KC/GRO/melanoma growth-stimulating activity gene expression in mouse peritoneal macrophages. *J. Immunol.* 153, 2204–2212.

O'neill, L. A., Sheedy, F. J., and Mccoy, C. E. (2011). MicroRNAs: the fine-tuners of Toll-like receptor signalling. *Nat. Rev. Immunol.* 11, 163–175. doi: 10.1038/nri2957

Park, H. J., Kim, H. J., Ra, J., Hong, S. J., Baik, H. H., Park, H. K., et al. (2007). Melatonin inhibits lipopolysaccharide-induced CC chemokine subfamily gene expression in human peripheral blood mononuclear cells in a microarray analysis. *J. Pineal Res.* 43, 121–129. doi: 10.1111/j.1600-079X.2007.00452.x

Pires-Lapa, M. A., Carvalho-Sousa, C. E., Cecon, E., Fernandes, P. A., and Markus, R. P. (2018). β-adrenoceptors trigger melatonin synthesis in phagocytes. *Int. J. Mol. Sci.* 19:E2182. doi: 10.3390/ijms19082182

Pontes, G. N., Cardoso, E. C., Carneiro-Sampaio, M. M., and Markus, R. P. (2006). Injury switches melatonin production source from endocrine (pineal) to paracrine (phagocytes) - melatonin in human colostrum and colostrum phagocytes. *J. Pineal Res.* 41, 136–141. doi: 10.1111/j.1600-079X.2006.00345.x

Prendergast, B. J., Hotchkiss, A. K., Bilbo, S. D., Kinsey, S. G., and Nelson, R. J. (2003). Photoperiodic adjustments in immune function protect Siberian hamsters from lethal endotoxemia. *J. Biol. Rhythms* 18, 51–62. doi: 10.1177/0748730402239676

Recchiuti, A., Krishnamoorthy, S., Fredman, G., Chiang, N., and Serhan, C.N. (2011). MicroRNAs in resolution of acute inflammation: identification of novel resolvin D1-miRNA circuits. *FASEB J.* 25, 544–560. doi: 10.1096/fj.10-169599

Reiter, R. J., Calvo, J. R., Karbownik, M., Qi, W., and Tan, D. X. (2000). Melatonin and its relation to the immune system and inflammation. *Ann. N. Y. Acad. Sci.* 917, 376–386. doi: 10.1111/j.1749-6632.2000.tb05402.x

Reiter, R. J., Tan, D. X., Rosales-Corral, S., and Manchester, L. C. (2013). The universal nature, unequal distribution and antioxidant functions of melatonin and its derivatives. *Mini Rev. Med. Chem.* 13, 373–384. doi: 10.2174/1389557511313030006

Ren, D. L., Li, Y. J., Hu, B. B., Wang, H., and Hu, B. (2015). Melatonin regulates the rhythmic migration of neutrophils in live zebrafish. *J. Pineal Res.* 58, 452–460. doi: 10.1111/jpi.12230

Roh, Y. S., Song, J., and Seki, E. (2014). TAK1 regulates hepatic cell survival and carcinogenesis. *J. Gastroenterol.* 49, 185–194. doi: 10.1007/s00535-013-0931-x

Rojas, I. G., Padgett, D. A., Sheridan, J. F., and Marucha, P. T. (2002). Stress-induced susceptibility to bacterial infection during cutaneous wound healing. *Brain Behav. Immun.* 16, 74–84. doi: 10.1006/brbi.2000.0619

Santello, F. H., Frare, E. O., Caetano, L. C., Alonsotoldo, M. P., and Do Prado, J. C. Jr. (2008a). Melatonin enhances pro-inflammatory cytokine levels and protects against Chagas disease. *J. Pineal Res.* 45, 79–85. doi: 10.1111/j.1600-079X.2008.00558.x

Santello, F. H., Frare, E. O., Dos Santos, C. D., Caetano, L. C., Alonso Toldo, M. P., and Do Prado, J. C. Jr. (2008b). Suppressive action of melatonin on the TH-2 immune response in rats infected with Trypanosoma cruzi. *J. Pineal Res.* 45, 291–296. doi: 10.1111/j.1600-079X.2008.00589.x

Santello, F. H., Frare, E. O., Dos Santos, C. D., Toldo, M. P., Kawasse, L. M., Zucoloto, S., et al. (2007). Melatonin treatment reduces the severity of experimental Trypanosoma cruzi infection. *J. Pineal Res.* 42, 359–363. doi: 10.1111/j.1600-079X.2007.00427.x

Schall, T. J., Bacon, K., Camp, R. D., Kaspari, J. W., and Goeddel, D. V. (1993). Human macrophage inflammatory protein alpha (MIP-1 alpha) and MIP-1 beta chemokines attract distinct populations of lymphocytes. *J. Exp. Med.* 177, 1821–1826. doi: 10.1084/jem.177.6.1821

Scott, P., and Novais, F. O. (2016). Cutaneous leishmaniasis: immune responses in protection and pathogenesis. *Nat. Rev. Immunol.* 16, 581–592. doi: 10.1038/nri.2016.72

Smith, S., Fernando, T., Wu, P. W., Seo, J., Ni Gabhann, J., Piskareva, O., et al. (2017). MicroRNA-302d targets IRF9 to regulate the IFN-induced gene expression in SLE. *J. Autoimmun.* 79, 105–111. doi: 10.1016/j.jaut.2017.03.003

Srivastava, A., Singh, N., Mishra, M., Kumar, V., Gour, J. K., Bajpai, S., et al. (2012). Identification of TLR inducing Th1-responsive *Leishmania donovani* amastigote-specific antigens. *Mol. Cell. Biochem.* 359, 359–368. doi: 10.1007/s11010-011-1029-5

Tamura, E. K., Fernandes, P. A., Marçola, M., Da Silveira Cruz-Machado, S., and Markus, R. P. (2010). Long-lasting priming of endothelial cells by plasma melatonin levels. *PLoS ONE* 5:e13958. doi: 10.1371/journal.pone.0013958

Verreck, F. A., De Boer, T., Langenberg, D. M., Hoeve, M. A., Kramer, M., Vaisberg, E., et al. (2004). Human IL-23-producing type 1 macrophages promote but IL-10-producing type 2 macrophages subvert immunity to (myco)bacteria. *Proc. Natl. Acad. Sci. U S A.* 101, 4560–4565. doi: 10.1073/pnas.0400983101

Vieira, L. Q., Goldschmidt, M., Nashleanas, M., Pfeffer, K., Mak, T., and Scott, P. (1996). Mice lacking the TNF receptor p55 fail to resolve lesions caused by infection with *Leishmania* major, but control parasite replication. *J. Immunol.* 157, 827–835.

Wanasen, N., and Soong, L. (2008). L-arginine metabolism and its impact on host immunity against Leishmania infection. *Immunol. Res.* 41, 15–25. doi: 10.1007/s12026-007-8012-y

Wang, N., Liang, H., and Zen, K. (2014). Molecular mechanisms that influence the macrophage m1-m2 polarization balance. *Front. Immunol.* 5:614. doi: 10.3389/fimmu.2014.00614

Wang, Y., Liang, Y., and Lu, Q. (2008). MicroRNA epigenetic alterations: predicting biomarkers and therapeutic targets in human diseases. *Clin. Genet.* 74, 307–315. doi: 10.1111/j.1399-0004.2008.01075.x

Wei, X. Q., Charles, I. G., Smith, A., Ure, J., Feng, G. J., Huang, F. P., et al. (1995). Altered immune responses in mice lacking inducible nitric oxide synthase. *Nature* 375, 408–411. doi: 10.1038/375408a0

WHO (2017). *Leishmaniasis*.

Wilhelm, P., Ritter, U., Labbow, S., Donhauser, N., Rollinghoff, M., Bogdan, C., et al. (2001). Rapidly fatal leishmaniasis in resistant C57BL/6 mice lacking TNF. *J. Immunol.* 166, 4012–4019. doi: 10.4049/jimmunol.166.6.4012

Wu, Y., Sun, Q., and Dai, L. (2017). Immune regulation of miR-30 on the Mycobacterium tuberculosis-induced TLR/MyD88 signaling pathway in THP-1 cells. *Exp. Ther. Med.* 14, 3299–3303. doi: 10.3892/etm.2017.4872

Xia, M. Z., Liang, Y. L., Wang, H., Chen, X., Huang, Y. Y., Zhang, Z. H., et al. (2012). Melatonin modulates TLR4-mediated inflammatory genes through MyD88- and TRIF-dependent signaling pathways in lipopolysaccharide-stimulated RAW264.7 cells. *J. Pineal Res.* 53, 325–334. doi: 10.1111/j.1600-079X.2012.01002.x

Xu, X., Wang, G., Ai, L., Shi, J., Zhang, J., and Chen, Y. X. (2018). Melatonin suppresses TLR9-triggered proinflammatory cytokine production in macrophages by inhibiting ERK1/2 and AKT activation. *Sci. Rep.* 8:15579. doi: 10.1038/s41598-018-34011-8

Yang, J., Liang, Y., Han, H., and Qin, H. (2013). Identification of a miRNA signature in neutrophils after traumatic injury. *Acta Biochim. Biophys. Sin.* 45, 938–945. doi: 10.1093/abbs/gmt100

Yang, Z., Mosser, D. M., and Zhang, X. (2007). Activation of the MAPK, ERK, following *Leishmania amazonensis* infection of macrophages. *J. Immunol.* 178, 1077–1085. doi: 10.4049/jimmunol.178.2.1077

Zhang, H. M., and Zhang, Y. (2014). Melatonin: a well-documented antioxidant with conditional pro-oxidant actions. *J. Pineal Res.* 57, 131–146. doi: 10.1111/jpi.12162

Zhang, X., and Mosser, D.M. (2008). Macrophage activation by endogenous danger signals. *J. Pathol.* 214, 161–178. doi: 10.1002/path.2284

Zheng, G. X., Ravi, A., Calabrese, J. M., Medeiros, L. A., Kirak, O., Dennis, L. M., et al. (2011). A latent pro-survival function for the mir-290-295 cluster in mouse embryonic stem cells. *PLoS Genet.* 7:e1002054. doi: 10.1371/journal.pgen.1002054

Zhou, L. L., Wei, W., Si, J. F., and Yuan, D. P. (2010). Regulatory effect of melatonin on cytokine disturbances in the pristane-induced lupus mice. *Mediat. Inflamm.* 2010:951210. doi: 10.1155/2010/951210

Zhu, X., He, Z., Hu, Y., Wen, W., Lin, C., Yu, J., et al. (2014). MicroRNA-30e* suppresses dengue virus replication by promoting NF-kappaB-dependent IFN production. *PLoS Negl. Trop. Dis.* 8:e3088. doi: 10.1371/journal.pntd.0003088

Zhuang, L., Shou, T., Li, K., Gao, C. L., Duan, L. C., Fang, L. Z., et al. (2017). MicroRNA-30e-5p promotes cell growth by targeting PTPN13 and indicates poor survival and recurrence in lung adenocarcinoma. *J. Cell. Mol. Med.* 21, 2852–2862. doi: 10.1111/jcmm.13198

Conflict of Interest Statement: The authors declare that the research was conducted in the absence of any commercial or financial relationships that could be construed as a potential conflict of interest.

frontiers in Cellular and Infection Microbiology

ORIGINAL RESEARCH
published: 27 March 2019
doi: 10.3389/fcimb.2019.00071

Lutzomyia longipalpis TGF-β Has a Role in *Leishmania infantum chagasi* Survival in the Vector

*Tatiana Di-Blasi[1], Erich Loza Telleria[1,2], Christiane Marques[1], Rodrigo de Macedo Couto[1], Monique da Silva-Neves[1], Magdalena Jancarova[2], Petr Volf[2], Antonio Jorge Tempone[1] and Yara Maria Traub-Csekö[1]**

[1] Laboratório de Biologia Molecular de Parasitas e Vetores, Instituto Oswaldo Cruz, Rio de Janeiro, Brazil, [2] Parasitology Department, Faculty of Science, Charles University, Prague, Czechia

Despite the increasing number of studies concerning insect immunity, *Lutzomyia longipalpis* immune responses in the presence of *Leishmania infantum chagasi* infection has not been widely investigated. The few available studies analyzed the role of the Toll and IMD pathways involved in response against *Leishmania* and microbial infections. Nevertheless, effector molecules responsible for controlling sand fly infections have not been identified. In the present study we investigated the role a signal transduction pathway, the Transforming Growth Factor-beta (TGF-β) pathway, on the interrelation between *L. longipalpis* and *L. i. chagasi*. We identified an *L. longipalpis* homolog belonging to the multifunctional cytokine TGF-β gene family (*LITGF-β*), which is closely related to the activin/inhibin subfamily and potentially involved in responses to infections. We investigated this gene expression through the insect development and in adult flies infected with *L. i. chagasi*. Our results showed that *LITGF-β* was expressed in all *L. longipalpis* developmental stages and was upregulated at the third day post *L. i. chagasi* infection, when protein levels were also higher as compared to uninfected insects. At this point blood digestion is finished and parasites are in close contact with the insect gut. In addition, we investigated the role of LITGF-β on *L. longipalpis* infection by *L. i. chagasi* using either gene silencing by RNAi or pathway inactivation by addition of the TGF-β receptor inhibitor SB431542. The blockage of the LITGF-β pathway increased significantly antimicrobial peptides expression and nitric oxide levels in the insect gut, as expected. Both methods led to a decreased *L. i. chagasi* infection. Our results show that inactivation of the *L. longipalpis* TGF-β signal transduction pathway reduce *L. i. chagasi* survival, therefore suggesting that under natural conditions the parasite benefits from the insect LITGF-β pathway, as already seen in *Plamodium* infection of mosquitoes.

Keywords: ***Lutzomyia longipalpis*, *Leishmania*, vector-parasite interaction, innate immunity, TGF-β, activin**

OPEN ACCESS

Edited by:
Claudia Ida Brodskyn, Gonçalo Moniz Institute (IGM), Brazil

Reviewed by:
Diego Luis Costa, National Institute of Allergy and Infectious Diseases (NIAID), United States
Isabel Mauricio, Instituto de Higiene e Medicina Tropical, Universidade NOVA de Lisboa, Portugal

***Correspondence:**
Yara Maria Traub-Csekö
ytraub@ioc.fiocruz.br

Specialty section:
This article was submitted to Parasite and Host, a section of the journal Frontiers in Cellular and Infection Microbiology

Received: *12 December 2018*
Accepted: *04 March 2019*
Published: *27 March 2019*

Citation:
Di-Blasi T, Telleria EL, Marques C, Couto RM, Silva-Neves M, Jancarova M, Volf P, Tempone AJ and Traub-Csekö YM (2019) Lutzomyia longipalpis TGF-β Has a Role in Leishmania infantum chagasi Survival in the Vector. Front. Cell. Infect. Microbiol. 9:71. doi: 10.3389/fcimb.2019.00071

INTRODUCTION

Leishmaniasis is a serious public health concern, affecting millions of people every year. Leishmaniasis is caused by parasites from the genus *Leishmania*. These parasites are transmitted in the New and Old World by phlebotomine sand flies belonging to the *Lutzomyia* and *Phlebotomus* genera, respectively. When a female sand fly feeds on an infected vertebrate host,

macrophages containing amastigote parasites are ingested. Inside the insect gut, the aflagellated immotile rounded parasites transform into flagellated motile promastigotes that multiply and then migrate to the anterior midgut (Lainson and Rangel, 2005). To prevent being eliminated these parasites must resist the blood digestion process (Pruzinova et al., 2018) and adhere to the midgut epithelium prior to insect defecation (Wilson et al., 2010). The presence of *Leishmania* parasites in the insect gut is not harmless to the vector. For instance, parasites secrete a chitinolytic enzyme that attack and damage the sand fly stomodeal valve, leading to the regurgitation of the gut content at the bite site (Rogers et al., 2008). The intricate interactions among *Leishmania* parasites, gut microbioma and the insect immunity are complex, and evolved to avoid the harmful consequences of an eventual uncontrolled microbial or leishmanial growth inside the insect gut (Sant'Anna et al., 2014; Kelly et al., 2017; Telleria et al., 2018).

Most of the knowledge on insect immune responses was acquired from *Drosophila* studies. Pathogens in the insect midgut elicit immune responses that have evolved to eliminate or control infections. These immune responses initiate when the insect innate immune system recognizes the invader. This recognition occurs when pathogen-associated molecular patterns (PAMPs) binds to host-derived pattern recognition receptors (PPRs), leading to the activation of signal transduction pathways. These pathways intensify the immune responses, induce the synthesis of antimicrobial molecules and potentiate effector mechanisms. Among these widely conserved receptor-mediated immune mechanisms, Toll, IMD, and Jak-Stat pathways are the most studied in insects. They are regulators and mediators of insect humoral and cellular immune responses, with intracellular negative regulators that keep these pathways under control (reviewed in Lemaitre and Hoffmann, 2007; Kleino and Silverman, 2014; Lindsay and Wasserman, 2014; Myllymäki and Rämet M, 2014). To date few studies have addressed *L. longipalpis* immunity. The Toll and IMD pathways can be activated in *L. longipalpis* LL5 embryonic cells in response to microbial and *L. i. chagasi* infections (Tinoco-Nunes et al., 2016). Bacterial challenges in *L. longipalpis* larvae leads to a positive modulation of Pirk gene, a suppressor of the IMD pathway at the signal transduction level (Heerman et al., 2015). In adult *L. longipalpis* the RNAi-mediated gene silencing of the IMD pathway repressor Caspar decreased *Leishmania* survival (Telleria et al., 2012). Furthermore the expression of a sand fly defensin was upregulated after artificial infection with different bacteria (Boulanger et al., 2004; Telleria et al., 2013). In insects another important strategy for infection control is the gut environment oxidative stress modulation. The oxidative stress is a consequence of aerobic processes that lead to the production of reactive oxygen species (ROS) such as superoxide, hydrogen peroxide, and nitric oxide (NO), among others (reviewed in Murphy et al., 2011, Kodrik et al., 2015). While aerobic processes occur autonomously in many organisms, some stimuli during development and pathogen challenges can induce ROS production as a result of growth factor receptors and activation of cytokines such as mitogen, integrin and wingless (reviewed in Covarrubias et al., 2008).

The Transforming Growth Factor-beta (TGF-β) pathway, a highly conserved signal transduction pathway in animals, has received very little attention in insects. This cytokine superfamily comprises more than 40 members, grouped into subfamilies according to structure or function: TGF-β *stritu sensu*, bone morphogenic protein (BMP), decapentaplegic (Dpp), Mullerian inhibiting substance, and activin/inhibin (Massague, 1990). These cytokines are involved in several aspects of animal biology including embryonic development, organogenesis, stress responses, and immune modulation (Huminiecki et al., 2009; Massague, 2012; Chen and Ten Dijke, 2016; Morikawa et al., 2016; Mullen and Wrana, 2017). Activins and BMPs are key regulators of immune response having pro- and anti-inflammatory roles (reviewed in Jones et al., 2004; Aleman-Muench and Soldevila, 2012; Lee et al., 2012; Spottiswoode et al., 2017). Activins are secreted in stimulated immune cells and they can act as immune response activator or repressor depending on the which cell type is stimulated (Ogawa and Funaba, 2011).

Although we have some information regarding immunity effectors in sand flies, there is little information on the cytokine-like molecules possibly involved in their regulation. In the present work, we characterized a *L. longipalpis TGF-β* gene (*LlTGF-β*). We also investigated the involvement of *LlTGF-β* in *L. i. chagasi* infection. The blockage of this signal transduction pathway revealed an effect on insect immune related molecules and NO production with consequences to *L. i chagasi* infection.

MATERIALS AND METHODS

Insects

Sand flies were obtained from a laboratory colony of *L. longipalpis* established from sand flies caught in Jacobina (Bahia, Brazil). Insects were fed on 50–70 % sucrose *ad libitum* and females were blood fed on anesthetized hamsters or mice once a week. Females 2–3 day old were used on experimental procedures. All procedures involving animals were performed in accordance with the Brazilian Ethics Committee for Animal Use at FIOCRUZ (CEUA L-016/2018).

Artificial Infection With *Leishmania*

L. i. chagasi (MHOM/BR/1974/PP75) were cultured in M199 medium, pH 7.4, supplemented with 10% fetal bovine serum and collected at exponential growth phase, washed with PBS, and resuspended in inactivated rabbit blood at 10^7 parasites/mL. Sand flies were infected with promastigotes for practical reasons, since there is evidence that infections initiated with *Leishmania* promastigotes, axenic amastigotes or macrophage-derived amastigotes yield to equally successful infections of sand flies (Freitas et al., 2012; Sadlova et al., 2017). Insects were fed on infective blood through chick skin using a Hemotek artificial feeder. As control group, insects were fed on blood.

For the LlTGF-β receptor inhibition assays, the flies were fed with blood containing *L. i. chagasi* and 10 μM of the TGF-β receptor inhibitor SB431542 (TOCRYS Biosciences). As control the flies were fed with the same volume of the vehicle dimethyl sulfoxide (DMSO) added to the infective blood meal. For these

experiments, pools of 10 fully engorged females were collected at 24, 72, and 144 h post infection.

LITGF-β Gene Identification

Partial *L. longipalpis TGF-β* gene (*LlTGF-β*) sequence was identified through the screening of a *L. longipalpis* EST library. Sequence identity was determined by similarity using the blastx search tool (Altschul et al., 1990) against the NCBI GenBank. Full cDNA sequence was obtained by PCR using an existing cDNA library (Ramalho-Ortigao et al., 2001) with a *LlTGF-β* internal primers (LlTGFblibrary1-R or LlTGFblibrary2-R) and cDNA library plasmid primer (T3) (**Table 1**). Phylogeny analysis of *LlTGF-β* was performed utilizing Mega 6.06 software, using Maximum Likelihood statistical method with bootstrap method with 500 replicates as phylogeny test. The mutation model used was Jones-Taylor-Thornton with Gamma distribution with invariant sites, and 5 rate categories was chosen according to MEGA 6.06 best mutation model analysis.

LITGF-β Double Stranded RNA Synthesis

LlTGF-β cDNA template was amplified by PCR using primers containing the T7 promoter at the 5' end (dsTGFb-F and dsTGFb-R—**Table 1**). The control dsRNA cDNA template was obtained from β-galactosidase gene amplified from plasmid pGEM T-easy vector (PROMEGA) (Tinoco-Nunes et al., 2016). The PCR products were used as templates for transcription reactions with the Megascript RNAi Kit (Ambion) according to the manufacturer's instructions and subsequently concentrated to 40 μg/μL using a vacuum microcentrifuge concentrator.

TABLE 1 | Primers.

Primer name	Sequence
LlTGFblibrary1-R	GCAGTTGATGTTCCGC
LlTGFblibrary2-R	CTGCGTAATCTTCCCGTAGT
T3	AATTAACCCTCACTAAAGGG
LlTGFb-F	CTCTTCTACTTGGACAGCAA
LlTGFb-R	CATACAGCCGCATCCTTC
LlRP49-F	GACCGATATGCCAAGCTAAAGCA
LlRP49-R	GGGGAGCATGTGGCGTGTCTT
LlHistone-F	GAAAAGCAGGCAAACACTCC
LlHistone-R	GAAGGATGGGTGGAAAGAAG
LlCecropin-F	TGGCAGTCCTGACCACTGGA
LlCecropin-R	CTTCTCCACTGAACGGTGAACG
LlDefensin2-F	ATCCATCCTTTATGCAACCG
LlDefensin2-R	GCCTTTGAGTCGCAGTATCC
LliNOS-F	TGGCTGTCGCAATTTGTGTG
LliNOS-R	CCGCAATGTTCACCTCAACC
dsTGFb-F	TAATACGACTCACTATAGGGGGCTATCATGCCTACTTC
dsTGFb-R	TAATACGACTCACTATAGGGGGCAAAACTTTCTGTGTG
dsBgal-F	TGGCGCCCCTAGATGTGATGGCACCCTGATTGA
dsBgal-R	TGGCGCCCCTAGATGTCATTGCCCAGAGACCAGA
T7-adaptor	CCGTAATACGACTCACTATAGGGTGGCGCCCCTAGATG
Leish-Actin-F	GTCGTCGATAAAGCCGAAGGTGGTT
Leish-Actin-R	TTGGGCCAGACTCGTCGTACTCGCT

Sandfly Microinjections

L. longipalpis female dsRNA microinjection procedure was adapted from Sant'Anna et al. (2008). Shortly, 3 day old sandflies were microinjected with 32 nL of 4 μg/μL ds-LlTGF-β or control dsRNA solution using micro-capillary glass needle coupled to a Nanoject II microinjector (Drummond). Injected flies were artificially blood fed or infected with *Leishmania* as previously described and pools of 5 females were collected at the time-points of 24, 48, and 72 h after feeding.

RNA Extraction and cDNA Synthesis

Total RNA was extracted with TRIzol reagent (Invitrogen-Life Technologies) according to the manufacturer's protocol, from groups of 5 to 10 fully engorged females collected at 24, 48, 72, and 144 h after blood feeding, after artificial *L. i. chagasi* infection, or after dsRNA microinjection. Total RNA was also extracted from pools of unfed females (0 h), males, eggs, and larvae (L1, L2, L3, and L4 instars). RNA was treated with RQ1 RNase-Free DNase (Promega). First strand cDNA was synthetized with SuperScript III First-Strand Synthesis System for RT-PCR (Invitrogen), oligo dT(16) primer, and up to 1 μg of total RNA.

Semi-Quantitative PCR of Larvae and Blood Fed or Infected Sand Flies cDNA

Semi-quantitative PCR was carried out using cDNA samples under the following cycling conditions: 96°C/3 min, followed by 25 cycles at 96°C for 45 s, 60°C for 45 s and 72°C for 45 s, and a final extension of 72°C for 5 min. Primers for *LlTGF-β* and constitutive expression controls, histone (Telleria et al., 2007) and RP49 (Tinoco-Nunes et al., 2016), are listed in **Table 1**. PCR products were separated in 2.0% ethidium bromide-stained agarose gel. The intensity of amplified products was determined by densitometry using the ImageJ software 1.48 software (Schneider et al., 2012). *LlTGF-β* transcription was normalized to histone or RP49 amplification, plotted on GraphPad Prism software (version 6.05—GraphPad Software, Inc). RT-PCR procedures were performed at least 3 times with consistent results. Significance was evaluated by *t*-test and Mann-Whitney post-test, with $p < 0.05$.

Quantitative PCR Using cDNA From *L. longipalpis* Silenced for *LlTGF-β* or Fed With TGF-β Receptor Inhibitor SB431542

Quantitative PCR was performed using the kit iQTM SYBR Green Supermix (Applied Biosystems) under the following cycling conditions: 96°C/3 min, followed by 42 cycles at 96°C for 30 s, 60°C for 20 s. All experiments were performed using three biological cDNA replicates. The primers used are listed on **Table 1**. Expression was normalized using the *L. longipalpis* reference gene RP49, relative levels of RNA expressed were calculated using the ΔΔCT method (Schefe et al., 2006) and plotted on GraphPad Prism software. Q-PCR procedures were performed with 3 replicates with consistent results. Significant differences were evaluated by *t*-test and Mann-Whitney post-test, with $p < 0.05$.

LITGF-β Recombinant Protein (LITGF-β*rec*)

A 3′-end fragment (359 bp) of the *LlTGF-β* gene was amplified by PCR using specific primers (TGF-beta-His-F and TGF-beta-His-R), the PCR product was cloned in pGEM-T easy plasmid (Promega), excised with BamH-I and Hind-III restriction enzymes and then subcloned in pET28a expression plasmid. Protein expression was carried out in *E. coli* (BL21 DE3 strain) system by IPTG induction followed by purification with Ni^{2+}-NTA Agarose His-tagged protein purification system (QIAGEN). The expressed recombinant protein (∼15 kDa) was sequenced for identity confirmation by mass spectrometry at the protein sequencing platform at FIOCRUZ.

LITGF-β Anti-serum Production

LlTGF-β*rec* (1 mg) was inoculated into 45 days old New Zealand male rabbit with Freund's complete adjuvant, with two subsequent boosts using incomplete Freund's adjuvant. Animal use was approved by the Instituto Oswaldo Cruz Ethical Commitee on Animal Use (CEUA/IOC-010/2018). Serum titration was carried out by immuno-dot blot (not shown), using the corresponding antigen, and revealed with horseradish peroxydase (HRP)-labeled goat anti-rabbit IgG as the secondary antibody. Western blot assays were also carried to verify LlTGF-β anti-serum specificity in sand fly dissected gut samples (**Figure S2**).

ELISA

ELISA high binding microplates (NOH® ELISA Plate—LBEP196) were coated overnight in a moist chamber with the protein extract of 12 midguts from *L. longipalpis* 72 h after feeding on blood or blood containing *L. i. chagasi*. 5 μg of LlTGF-β*rec* was also used as a positive control. Wells were blocked overnight at 4°C with 1% BSA in PBS. On the following day, wells were incubated overnight at 4°C with anti-LlTGF-β serum 1:100 diluted in 1% BSA in PBS. Wells were washed three times with PBS and incubated overnight at 4°C with 1:40.000 dilution of goat anti-rabbit IgG peroxidase-conjugated antibody. After washing, plates were revealed by adding to each well 50 μl of 3,3′,5,5′-Tetramethylbenzidine (TMP) substrate solution followed by a 15 min incubation at room temperature. Following this step, 50 μl of stop solution (0.2 M H_2SO_4) was added to each well and incubated for 30 min. The endpoint absorbance was measured at 450 nm.

Nitrite Detection in Sand Fly Guts

Detection of Nitrite-derived NO was performed with pools of 10 midguts (with Malpighian tubules removed) dissected from *LlTGF-β* or β-gal (control group) dsRNA injected flies artificially fed on defibrinated rabbit blood, or non-injected insects fed on blood containing 10 μM of the TGF-β receptor inhibitor SB431542 or DMSO (control group). Samples were collected at 24, 48, and 72 h after feeding, homogenized in 0.9% NaCl solution, and centrifuged. The supernatant was split in 2 replicates of 50 μL, loaded in a clear polystyrene medium-binding flat bottom 96-well plate (Corning, SIGMA) for Griess Reagent nitrite detection in 150 μL final volume assay following standard procedures. Nitrite levels were measured under 550 nm wave-length in an Infinite M2000 plate reader (TECAN, Switzerland).

RESULTS

LITGF-β Sequence and Phylogenetic Tree

The full *LlTGF-β* sequence (GenBank: MF074142) contains 1,158 nucleotides that encode a 386 amino acid sequence (**Figure S1**). The amino acid sequence contains eight conserved cysteine residues involved in disulfide bonds and a RXXR motif that is a putative catalytic domain. The TGF-β superfamily domain was identified from amino acids 280 to 385.

TGF-β family aminoacid sequences available on NCBI data base were aligned in order to create a TGF-β family tree and assess subgroup similarities. Sequences obtained from organisms of different taxa but belonging to the same TGF-β subfamily were grouped such as activin/inhibin, TGF-β *sensu stricto*, and glass bottom boat (GBB) member of the BMP subfamily (**Figure 1**). *LlTGF-β* grouped with *G. morsitans* and *P. papatasi* activin/inhibin sequences with high bootstrap support.

LITGF-β Gene Expression in Immature and Adult Insects, and in Infected Females

Due to the activin/inhibin subfamily association to growth and development regulation we investigated its expression in sand fly larval and adult stages. The *LlTGF-β* gene was ubiquitously expressed in all *L. longipalpis* developmental stages (**Figure 2A**), with a slight non-significant increase in adult male and female insects. Comparison among sugar fed, blood fed and *Leishmania* infected sand flies females revealed that blood ingestion induced *LlTGF-β* expression when compared to sugar fed females (**Figure 2B**). Additionally, *LlTGF-β* gene was significantly upregulated in *Leishmania* infected females when compared to blood fed insects at 72 h post feeding (**Figure 2B**). This increased *LlTGF-β* transcription occurred in both carcass and dissected gut (**Figure 2C**). Our attempts to use Western blot to verify the presence of LlTGF-β in *L. longipalpis* guts were hindered by the recognition of mammal TGF-β in blood fed insects (**Figure S2**). Nevertheless, these bands disappeared rapidly and were totally absent at 24, 48, and 72 h post-blood-feeding. Using the more sensitive ELISA detection we also observed an increased production of LlTGF-β at the protein level in *Leishmania* infected compared to blood fed females at 72 h after feeding (**Figure 2D**).

Leishmania Infection of Sandflies Silenced for LITGF-β or Fed With TGF-β Receptor Inhibitor SB431542

To investigate the involvement of the TGF-β signal transduction pathway on the evolution of *Leishmania* infection in *L. longipalpis* this pathway was abrogated using RNAi to silence *LlTGF-β* (**Figure S3A**) or employing a TGF-β receptor inhibitor. After each treatment *L. longipalpis* were infected with *L. i. chagasi*. Both approaches had as consequence a significant decrease in *Leishmania* infection at 72 and 144 h post infection (**Figures 3A,B**).

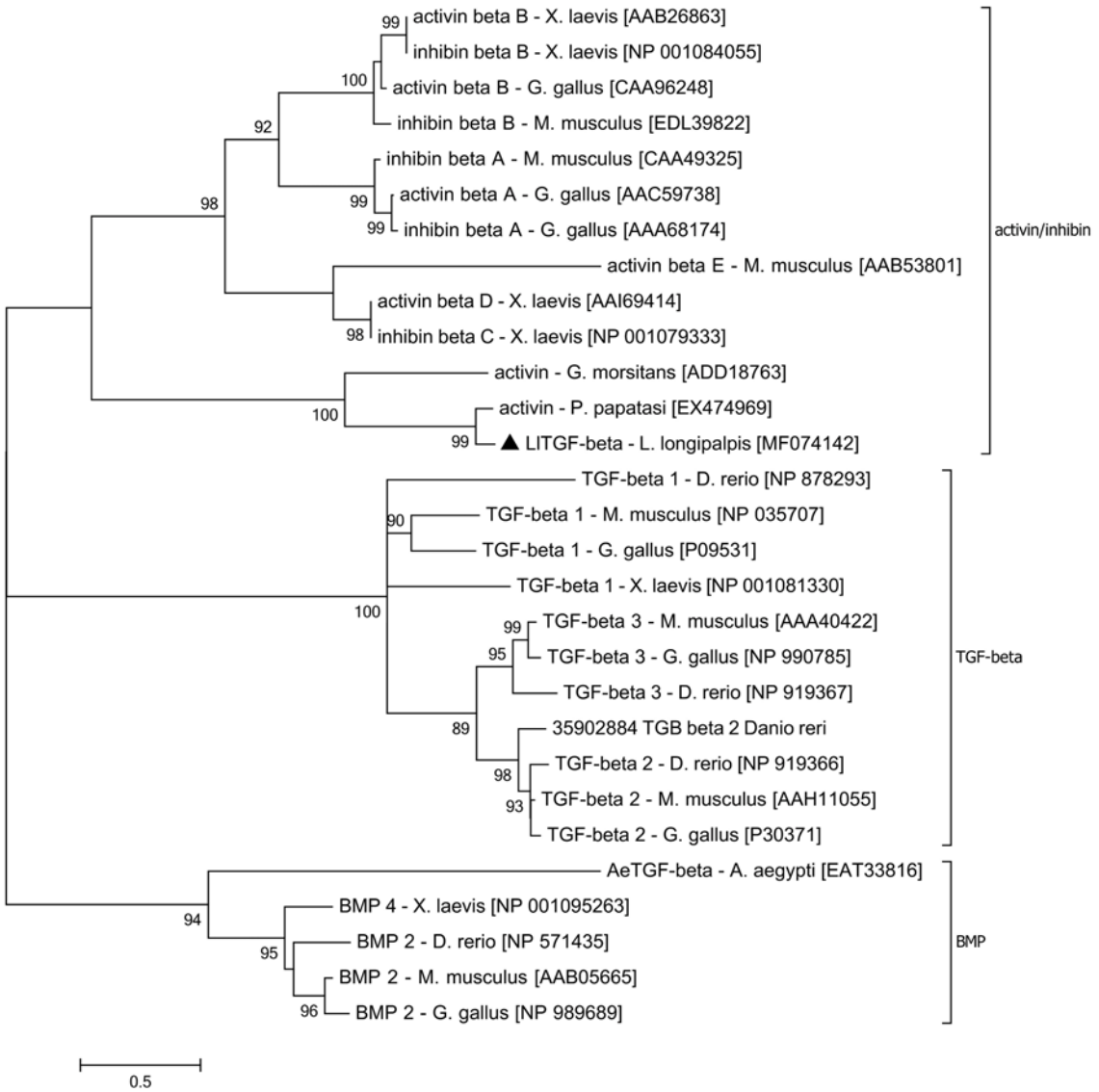

FIGURE 1 | LITGF-β phylogenetic tree. The LITGF-β deduced amino acid sequence was aligned with other TGF-β sequences from the insect vectors *Aedes aegypti*, *Glossina morsitans*, *Phlebotomus papatasi*, and the vertebrates *Danio rerio*, *Gallus gallus*, *Mus musculus*, *Xenopus laevis*. The evolutionary history was inferred using MEGA 6.06 software with Maximum Likelihood method based on the JTT matrix-based model. Evolutionary rate differences among sites [5 categories (+G, parameter = 3.2942)] were modeled by discrete Gamma distribution. The rate variation model allowed for some sites to be evolutionarily invariable ([+I], 2.1884% sites). Positions with gaps and missing data were eliminated. The TGF-β subfamily groups are indicated on the right side of the phylogram. Each sequence is labeled with species name followed by GenBank accession number. Branch length represents numbers of substitutions per site. Numbers on the tree nodes indicate bootstrap values higher than 85% (500 replicates).

Gene Expression of Immune Effectors After LITGF-β Knock-Down or Feeding With TGF-β Receptor Inhibitor SB431542 Followed by *Leishmania* Infection

The decreased *L. longipalpis* infection by *Leishmania* upon the TGF-β signaling pathway inhibition led us to investigate the expression of some effector molecules. We assessed the effect of *LlTGF-β* silencing or TGF-β receptor inhibitor treatment on Toll regulated AMPs, such as defensin 2 and cecropin. In sand flies with TGF-beta silenced and infected with *L. i. chagasi* a statistically significant increase of both cecropin (**Figure 3C**) and defensin 2 (**Figures 3E,F**) expression was observed only at 24 h post infection, with a significant decrease at 72 and 144, respectively. In sand flies fed with the TGF-β receptor inhibitor and infected with *Leishmania*, cecropin expression levels increased at 24 h, although not significantly (**Figure 3D**).

Regulation of NO Production by LITGF-β

To test the possible role of LlTGF-β transduction signaling pathway on NO production, we assessed iNOS expression by

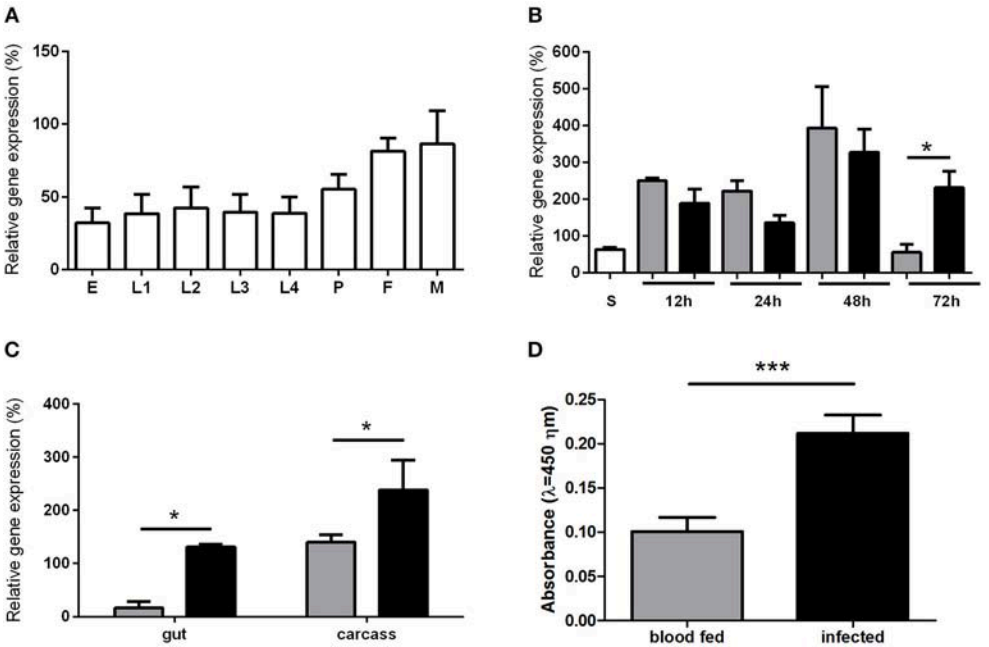

FIGURE 2 | *LlTGF-β* gene expression in sand flies. **(A)** *L. longipalpis* development stages: egg (E), larval stages (L1, L2, L3, L4), pupae (P), adult female (F), and male (M). **(B)** *L. longipalpis* fed on sucrose (S) are represented by white bar. Flies collected at 12, 24, 48, and 72 h post blood meal are represented by gray bars or after feeding on infective blood represented by black bars. **(C)** *LlTGF-β* expression in gut and carcass 72 h after ingestion of blood without (gray bars) or with (black bars) *Leishmania*. Gene expression by semi-quantitative PCR was calculated relative to histone or RP49 *L. longipalpis* reference genes. **(D)** ELISA for detection of LlTGF-β protein 72 h after blood or infective meal. Bars represent mean with standard error of 3 replicates. Significant differences were evaluated by *t*-test and Mann-Whitney post-test (*$p < 0.05$; ***$p < 0.001$).

qPCR. iNOS levels were increased in LlTGF-β silenced insects at 24 h post infection (**Figure 4A**) and presented a slight but not significant increase on TGF-β receptor inhibitor SB431542 fed insects at 24 h post infection (**Figure 4B**). We tested the nitrite production levels in LlTGF-β silenced insects. In non-fed silenced insects nitrite levels were very low and no detectable modulation occurred (**Figure S3B**). Since the insect acquire *Leishmania* parasites through blood feeding we also measured the nitrite levels after LlTGF-β gene silencing or TGF-β receptor inhibitor treatements on blood fed *L. longipalpis*. LlTGF-β gene silencing was followed by an increase of nitrite levels in sand fly guts at 48 h post blood feeding when compared to control groups (**Figure 4C**). A similar result was obtained in TGF-β receptor inhibitor treated females, with an increase of nitrite at 48 h post blood feeding (**Figure 4D**).

DISCUSSION

TGF-β belongs to a family of multifunctional cytokines found in organisms that go from arthropods to mammals (Massague, 1990). TGF-β molecules belonging to different subfamilies has been identified in many insect species including *Bombyx mori* (Hu et al., 2016), *Drosophila* (reviewed in Hinck et al., 2016), and the mosquitoes *Culex pipiens* (Hickner et al., 2015) and *Anopheles stephensi* (Crampton and Luckhart, 2001). In the malaria vector *A. stephensi*, a TGF-β homolog named As60A was implicated in the insect immune response to *Plasmodium* (Crampton and Luckhart, 2001). It was also determined that the mammalian TGF-β 1 present in the ingested blood regulates NO production, modulating the *A. stephensi* immune response against the parasite (Luckhart et al., 2003).

In sand flies, this is the first report on the characterization of a TGF-β family gene. The identified *LlTGF-β* sequence contains the catalytic and conserved signature domains of the TGF-β superfamily. Phylogenetic analysis showed LlTGF-β to be highly similar to the activin/inhibin subfamily.

In insects, as much as in other organisms, TGF-β family molecules are involved in ontogeny (O'Connor et al., 2006). The expression profile of the *L. longipalpis* TGF-β gene shows that it is expressed in all developmental stages and may thus be involved in sand fly ontogeny as well. Additionaly, members of the TGF-β family have a role in nutrient detection and therefore may regulate nutrient acquisition (Chng et al., 2014). In the case of *L. longipalpis LlTGF-β* expression in blood fed females was increased after blood intake, indicating that the presence of nutrients stimulates activin production. Regarding the effect of *L. longipalpis* infection with *Leishmania*, LlTGF-β expression was increased at 3 days post infection, when parasites are in close contact with the insect midgut epithelium, shown both by RT-PCR as well as by ELISA. This is in line with the fact that the activin/inhibin subfamily may be involved in immune response.

TGF-β is considered an anti-inflammatory and immunosuppressive cytokine in mammals. When mice chronically infected with *L. major* were treated with an antibody

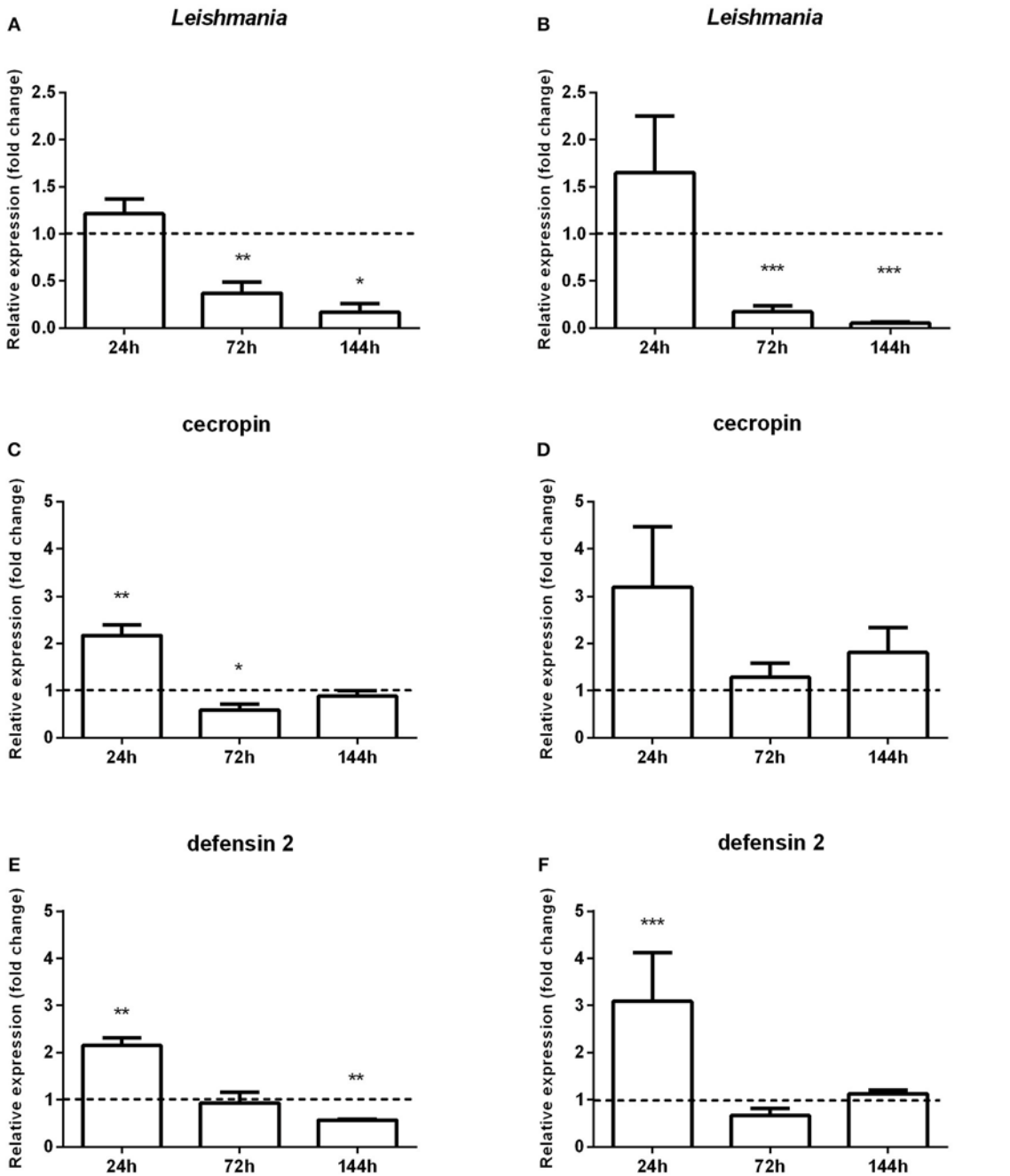

FIGURE 3 | Gene expression in sand flies infected by *L. i. chagasi* after abrogation of the LITGF-β signaling pathway. **(A,C,E)** Gene expression of LITGF-β silenced insects. **(B,D,F)** Gene expression of insects fed with TGF-β receptor inhibitor. **(A,B)** Quantification of *L. i. chagasi* in sand flies. **(C,D)** Relative expression of cecropin. **(E,F)** Relative expression of defensin 2. Samples were collected at 24, 72, and 144 h post infection. Dotted lines indicate gene expression of β-galactosidase dsRNA injected **(A,C,E)** or DMSO fed flies **(B,D,F)** control groups, or. Both test and control groups were infected by *L. i. chagasi*. Comparisons were done between silenced vs. non-silenced, or inhibitor treated vs. non-treated sand fly groups. Bars represent mean with standard error of fold change in gene expression relative to control groups of 3 independent experiments. Significant differences were evaluated by *t*-test and Mann–Whitney post-test (*$p < 0.05$; **$p < 0.01$; ***$p < 0.001$).

anti-TGF-β a pro-inflammatory environment was created with consequent decrease of parasite numbers at the lesion site (Li et al., 2018). In addition, *in vitro* assays showed that the incubation of recombinant TGF-β with *L. braziliensis* infected macrophages increased parasite loads (Barral et al., 1995). In an inflammatory situation, Toll-like receptors (TLRs) mediate the

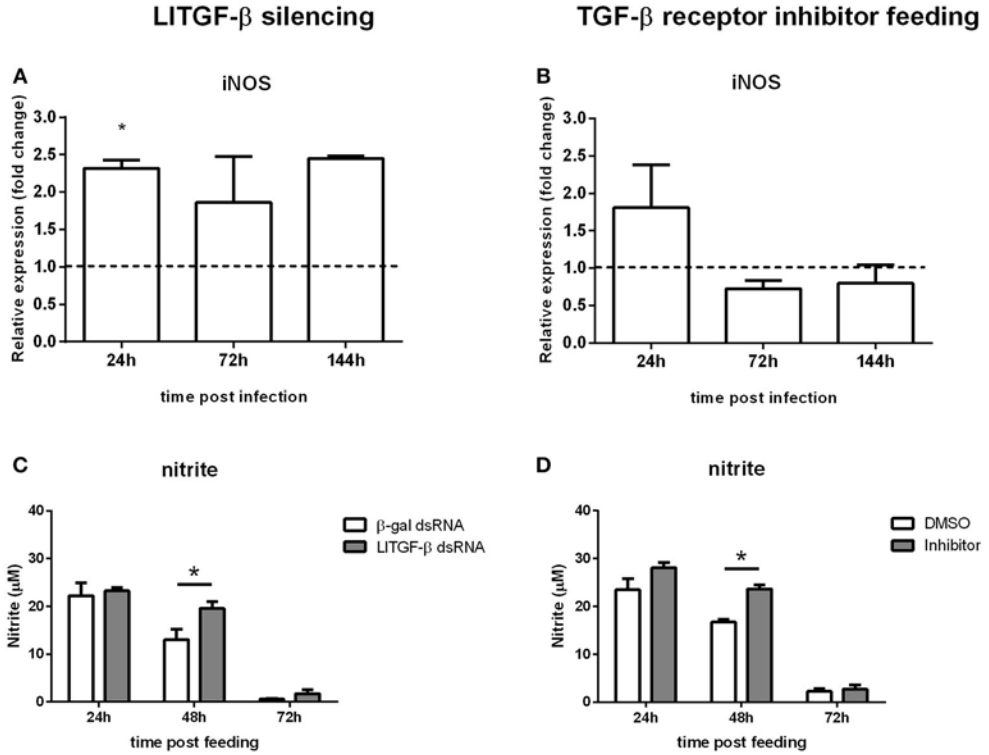

FIGURE 4 | Nitric oxide production in sand flies abrogated for the LITGF-β signaling pathway. **(A)** iNOS gene expression of LITGF-β silenced insects, **(B)** fed with blood containing TGF-β receptor inhibitor, both **(A,B)** infected by *L. i. chagasi*. Samples were collected at 24, 72, and 144 h post infection. Dotted line indicates gene expression of control group, β-gal dsRNA injected or blood containing DMSO fed flies. Bars represent mean with standard error of fold change in gene expression relative to control groups of three independent experiments. Significant differences were evaluated by *t*-test and Mann-Whitney post-test. **(C)** NO measurement in LITGF-β silenced sand flies fed on blood. **(D)** Nitrite measurement in flies fed on blood containing TGF-β receptor inhibitor. Bars represent mean with standard error of nitrite measurements in test and control groups of 3 independent experiments. Significant differences were evaluated by *t*-test and Mann-Whitney post-test (*$p <$ 0.05).

activation of activins that consequently suppresses the immune response (negative feedback; Sideras et al., 2013).

To investigate the putative participation of the insect LlTGF-β signaling pathway in response to parasitic infection, we blocked this signaling pathway. Both blocking gene translation or protein interaction with a receptor generated a strong decrease on parasite numbers in late time points, revealing that the suppression of this cytokine-like has a deleterious effect on the parasite. This indicates that this molecule most probably has an anti-inflammatory role in *L. longipalpis*, as already seen in mammals.

We assessed the effects of suppressing the TGF-β signaling on sand fly immune effector molecules. The silencing of *LlTGF-β* or inhibition of a TGF-β receptor resulted in an early increased expression of the AMPs cecropin and defensin suggesting that the *L. longipalpis* activin-like molecule can have a suppressing effect over AMPs expression. AMPs production is one of the main responses against infection in insects and is regulated mainly by the Toll and IMD pathways (Leulier et al., 2003; Kaneko et al., 2004). In *Drosophila*, AMPs are crucial for the maintenance of gut homeostasis, especially in what concerns microbiota regulation (Bosco-Drayon et al., 2012), and the *dpp* and *dawdle*, members of the TGF-β family, have a suppressing effect on AMPs expression (Coggins et al., 2012).

Besides the repressor effect on the insect immunity, activins were previously shown to be involved in immune response regulation throught other pathways. Studies with parasitic infections in vertebrates showed that TGF-β family members are responsible not only for regulating initial pro-inflammatory and late anti-inflammatory responses (Vodovotz et al., 2004), but are also involved in repressing inducible nitric oxide synthase (iNOS) expression, stability and activity in different cell types through mechanisms that were not fully understood (Berg et al., 2007; Aleman-Muench and Soldevila, 2012).

In *A. stephensi*, the TGF-β gene As60A expression was induced by infection with *Plasmodium berghei* (Crampton and Luckhart, 2001). Interestingly, human blood derived TGF-β was able to activate the mosquito TGF-β pathway leading to the activation of the MAPK/ERK cascade and downregulation of NO production (Surachetpong et al., 2009). Both *A. stephensi* and *Drosophila* are able to modulate ROS

levels to combat pathogen infections (Luckhart et al., 1998; Ha et al., 2005; Shrinet et al., 2014). On the other hand, NO mediated an early *Drosophila* innate immune responses through diptericin and drosomycin expression (Foley and O'Farrell, 2003) indicating that it is an important signaling molecule.

ROS production in *L. longipalpis* immune response against two different pathogens, *Leishmania mexicana* and *Serratia marcescens*, elicited different immune responses. *S. marcescens* infection increased ROS levels in the insect gut whereas *L. mexicana* did not (Diaz-Albiter et al., 2012). The RNAi gene silencing of *L. longipalpis* catalase, a ROS-detoxifying gene, led to decreased *L. mexicana* infection. These results suggest that ROS are harmful to *Leishmania* and *S. marcescens* but *Leishmania* is able to modulate the *L. longipalpis* oxidative stress response while *S. marcescens* is not (Diaz-Albiter et al., 2012).

Our results showed that blocking the TGF-β pathway increased iNOS expression in early times post *Leishmania* infection. In the following days infection levels were reduced indicating that, in the absence of an intact TGF-β pathway, increased iNOS levels can be deleterious to *Leishmania*. We would expect that under normal LlTGF-β conditions it would control iNOS expression and consequently nitrite levels. To test this hypothesis we measured nitrite levels in blood fed flies under the effect of both TGF-β pathway blockage methods. We observed that there was a significant increase of nitrite levels 2 days post blood feeding. In hematophagous insects blood digestion requires an efficient control of oxidative stress (Souza et al., 1997) and in *L. longipalpis* the nitrite levels in blood fed gut reached nearly 100 times higher than sugar fed insects. In order to control the harmful effects of these free radicals insects have a plethora of mechanisms to keep the ROS balance in the gut. In *L. longipalpis* the TGF-β blockade significantly hindered the nitrite balance in the gut on the second day of blood feeding, time when the subproducts of blood digestion are released in high levels (Graça-Souza et al., 2006). High doses of NO are implicated in parasite killing, but in the case of *Leishmania* infection the parasites proliferate in the insect gut apparently benefitting from LlTGF-β controlling NO levels.

Our results show the conservation of the TGF-β-mediated signaling in the presence of *Leishmania* infection in vector and vertebrate hosts, and a role for this citokine-like molecule in the regulation of AMPs expression and nitrite levels.

DATA AVAILABILITY

The datasets generated for this study can be found in GenBank, MF074142.

AUTHOR CONTRIBUTIONS

TD-B, ET, AT, YT-C contributed conception and design of the study; TD-B, ET, CM, RMC, MS-N, MJ performed experiments; TD-B, ET, AT, YT-C participated in manuscript writing; PV contributed with reagents. All authors contributed to manuscript revision, read and approved the submitted version.

FUNDING

This work was supported by Instituto Oswaldo Cruz-Fiocruz, PAPES VI Fiocruz, and CNPq. This study was financed in part by the Coordenação de Aperfeiçoamento de Pessoal de Nível Superior—Brasil (CAPES)—Finance Code 001. ET was also supported by the International Mobility of Researchers at Charles University number CZ.02.2.69/0.0/0.0/16_027/0008495.

ACKNOWLEDGMENTS

We thank Adriana Oliveira de Araujo, Daiana Zucoloto, and Rute Maria Julio for rearing insects and Nikola Polanska for technical support on nitrite detection assays. We are also grateful to the Genomic Platform—DNA Sequencing—RPT01A, and Mass Spectometry—RPT02A (Rede de Plataformas Tecnológicas FIOCRUZ) and Dr. Mariana Waghabi, IOC-Fiocruz, for the generous gift of the TGF-β receptor inhibitor.

SUPPLEMENTARY MATERIAL

The Supplementary Material for this article can be found online at: https://www.frontiersin.org/articles/10.3389/fcimb.2019.00071/full#supplementary-material

Figure S1 | *LITGF-β* cDNA and deduced amino acid sequences. Numbers on the left side indicate nucleotides. Numbers on right indicate amino acid residues. Cleavage signal peptide site is indicated by a black triangle (between residues 24 and 25). Conserved cysteine residues are shown in bold characters (residues 282, 283, 311, 315, 350, 351, 383, and 385). Putative catalytic domain motif is indicted by a rectangle (residues 268 to 271). The TGF-β superfamily domain is indicated by underlined characters (residues 280 to 385).

Figure S2 | LITGF-β antiserum assay detecting a single polypeptide from *L. longipalpis* gut samples. Samples corresponding to 2 guts dissected at 0 (non-fed), 2, 6, 12, 24, 48, and 72 h after blood feeding, and recombinant LITGF-β as positive control (750 ng) were separated by 12% SDS-PAGE under constant 100 V, and transferred to nitrocellulose membrane during 1 h at 4°C. Membranes were blocked with 5% low-fat dried milk in Tris buffered saline (TBS) supplemented with 0.05% Tween-20. Membranes were washed three times with TBS and incubated for 1 h with anti-LITGF-β serum at 1:500 dilution. HRP-conjugated goat anti-rabbit IgG at a 1:40,000 dilution was used as secondary antibody. The relative molecular mass of the reactive polypeptides was calculated by comparison with the mobility of molecular mass standards, using ImageJ 1.42q software (NIH, USA).

Figure S3 | LITGF-β silencing: Non-blood fed flies were injected with LITGF-β dsRNA or β-gal dsRNA (control group) and kept with sugar meal *ad libitum*. **(A)** LITGF-β gene expression in non-blood fed females after LITGF-β dsRNA microinjection is expressed relative to control group indicated by dotted line as described previously in manuscript qPCR methods; **(B)** Guts were dissected at 24, 48, and 72 h pos dsRNA injection for nitrite detection assays. Gray bars represent nitrite levels in LITGF-β dsRNA injected insects. White bars represent nitrite levels in β-gal dsRNA injected insects. Graphics represent mean with standard error of 3 independent experiments. Significant differences were evaluated by *t*-test and Mann-Whitney post-test (*$p < 0.05$; **$p < 0.01$).

REFERENCES

Aleman-Muench, G. R., and Soldevila, G. (2012). When versatility matters: activins/inhibins as key regulators of immunity. *Immunol. Cell. Biol.* 90, 137–148. doi: 10.1038/icb.2011.32

Altschul, S. F., Gish, W., Miller, W., Myers, E. W., and Lipman, D. J. (1990). Basic local alignment search tool. *J. Mol. Biol.* 215, 403–410. doi: 10.1016/S0022-2836(05)80360-2

Barral, A., Teixeira, M., Reis, P., Vinhas, V., Costa, J., Lessa, H., et al. (1995). Transforming growth factor-beta in human cutaneous leishmaniasis. *Am. J. Pathol.* 147, 947–954.

Berg, D. T., Gupta, A., Richardson, M. A., O'Brien, L. A., Calnek, D., and Grinnell, B. W. (2007). Negative regulation of inducible nitric-oxide synthase expression mediated through transforming growth factor-beta-dependent modulation of transcription factor TCF11. *J. Biol. Chem.* 282, 36837–36844. doi: 10.1074/jbc.M706909200

Bosco-Drayon, V., Poidevin, M., Boneca, I. G., Narbonne-Reveau, K., Royet, J., and Charroux, B. (2012). Peptidoglycan sensing by the receptor PGRP-LE in the Drosophila gut induces immune responses to infectious bacteria and tolerance to microbiota. *Cell Host Microbe* 12, 153–165. doi: 10.1016/j.chom.2012.06.002

Boulanger, N., Lowenberger, C., Volf, P., Ursic, R., Sigutova, L., Sabatier, L., et al. (2004). Characterization of a defensin from the sand fly Phlebotomus duboscqi induced by challenge with bacteria or the protozoan parasite Leishmania major. *Infect. Immun.* 72, 7140–7146. doi: 10.1128/IAI.72.12.7140-7146.2004

Chen, W., and Ten Dijke, P. (2016). Immunoregulation by members of the TGFbeta superfamily. *Nat. Rev. Immunol.* 16, 723–740. doi: 10.1038/nri.2016.112

Chng, W. A., Sleiman, M. S. B., Schüpfer, F., and Lemaitre, B. (2014). Transforming growth factor beta/activin signaling functions as a sugar-sensing feedback loop to regulate digestive enzyme expression. *Cell Rep.* 9, 336–348. doi: 10.1016/j.celrep.2014.08.064

Coggins, S. A., Estévez-Lao, T. Y., and Hillyer, J. F. (2012). Increased survivorship following bacterial infection by the mosquito *Aedes aegypti* as compared to *Anopheles gambiae* correlates with increased transcriptional induction of antimicrobial peptides. *Dev. Comp. Immunol.* 37, 390–401. doi: 10.1016/j.dci.2012.01.005

Covarrubias, L., Hernandez-Garcia, D., Schnabel, D., Salas-Vidal, E., and Castro-Obregon, S. (2008). Function of reactive oxygen species during animal development: passive or active? *Dev. Biol.* 320, 1–11. doi: 10.1016/j.ydbio.2008.04.041

Crampton, A., and Luckhart, S. (2001). The role of As60A, a TGF-beta homolog, in Anopheles stephensi innate immunity and defense against Plasmodium infection. *Infect. Genet. Evol.* 1, 131–141. doi: 10.1016/S1567-1348(01)00017-X

Diaz-Albiter, H., Sant' Anna, M. R., Genta, F. A., and Dillon, R. J. (2012). Reactive oxygen species-mediated immunity against Leishmania mexicana and Serratia marcescens in the phlebotomine sand fly Lutzomyia longipalpis. *J. Biol. Chem.* 287, 23995–24003. doi: 10.1074/jbc.M112.376095

Foley, E., and O'Farrell, P. H. (2003). Nitric oxide contributes to induction of innate immune responses to gram-negative bacteria in Drosophila. *Genes Dev.* 17, 115–125. doi: 10.1101/gad.1018503

Freitas, V. C., Parreiras, K. P., Duarte, A. P., Secundino, N. F., and Pimenta, P. F. (2012). Development of Leishmania (Leishmania) infantum chagasi in its natural sandfly vector Lutzomyia longipalpis. *Am. J. Trop. Med. Hyg.* 86, 606–612. doi: 10.4269/ajtmh.2012.11-0386

Graça-Souza, A. V., Maya-Monteiro, C., Paiva-Silva, G. O., Braz, G. R., Paes, M. C., Sorgine, M. H., et al. (2006). Adaptations against heme toxicity in blood-feeding arthropods. *Insect Biochem. Mol. Biol.* 36, 322–335. doi: 10.1016/j.ibmb.2006.01.009

Ha, E. M., Oh, C. T., Ryu, J. H., Bae, Y. S., Kang, S. W., Jang, I. H., et al. (2005). An antioxidant system required for host protection against gut infection in Drosophila. *Dev. Cell.* 8, 125–132. doi: 10.1016/j.devcel.2004.11.007

Heerman, M., Weng, J. L., Hurwitz, I., Durvasula, R., and Ramalho-Ortigao, M. (2015). Bacterial infection and immune responses in lutzomyia longipalpis sand fly larvae midgut. *PLoS Negl. Trop. Dis.* 9:e0003923. doi: 10.1371/journal.pntd.0003923

Hickner, P. V., Mori, A., Zeng, E., Tan, J. C., and Severson, D. W. (2015). Whole transcriptome responses among females of the filariasis and arbovirus vector mosquito Culex pipiens implicate TGF-beta signaling and chromatin modification as key drivers of diapause induction. *Funct. Integr. Genomics* 15, 439–447. doi: 10.1007/s10142-015-0432-5

Hinck, A. P., Mueller, T. D., and Springer, T. A. (2016). Structural biology and evolution of the TGF-beta family. *Cold Spring Harb Perspect. Biol.* 8:12. doi: 10.1101/cshperspect.a022103

Hu, X., Jiang, Y., Gong, Y., Zhu, M., Zhu, L., Chen, F., et al. (2016). Important roles played by TGF-beta member of Bmdpp and Bmdaw in BmNPV infection. *Mol. Immunol.* 73, 122–129. doi: 10.1016/j.molimm.2016.04.004

Huminiecki, L., Goldovsky, L., Freilich, S., Moustakas, A., Ouzounis, C., Heldin, C., et al. (2009). Emergence, development and diversification of the TGF-beta signalling pathway within the animal kingdom. *BMC Evol. Biol.* 9:28. doi: 10.1186/1471-2148-9-28

Jones, K. L., de Kretser, D. M., Patella, S., and Phillips, D. J. (2004). Activin A and follistatin in systemic inflammation. *Mol. Cell. Endocrinol.* 225, 119–125. doi: 10.1016/j.mce.2004.07.010

Kaneko, T., Goldman, W. E., Mellroth, P., Steiner, H., Fukase, K., Kusumoto, S., et al. (2004). Monomeric and polymeric gram-negative peptidoglycan but not purified LPS stimulate the Drosophila IMD pathway. *Immunity* 20, 637–649. doi: 10.1016/S1074-7613(04)00104-9

Kelly, P. H., Bahr, S. M., Serafim, T. D., Ajami, N. J., Petrosino, J. F., Meneses, C., et al. (2017). The gut microbiome of the vector lutzomyia longipalpis is essential for survival of leishmania infantum. *MBio* 8:1. doi: 10.1128/mBio.01121-16

Kleino, A., and Silverman, N. (2014). The Drosophila IMD pathway in the activation of the humoral immune response. *Dev. Comp. Immunol.* 42, 25–35. doi: 10.1016/j.dci.2013.05.014

Kodrík, D., Bednárová, A., Zemanová, M., and Krishnan, N. (2015). Hormonal regulation of response to oxidative stress in insects-an update. *Int. J. Mol. Sci.* 16, 25788–25816. doi: 10.3390/ijms161025788

Lainson, R., and Rangel, E. F. (2005). Lutzomyia longipalpis and the eco-epidemiology of American visceral leishmaniasis, with particular reference to Brazil: a review. *Mem. Inst. Oswaldo Cruz* 100, 811–827. doi: 10.1590/S0074-02762005000800001

Lee, K. B., Taghavi, C. E., Murray, S. S., Song, K. J., Keorochana, G., and Wang, J. C. (2012). BMP induced inflammation: a comparison of rhBMP-7 and rhBMP-2. *J. Orthop. Res.* 30, 1985–1994. doi: 10.1002/jor.22160

Lemaitre, B., and Hoffmann, J. (2007). The host defense of Drosophila melanogaster. *Annu. Rev. Immunol.* 25, 697–743. doi: 10.1146/annurev.immunol.25.022106.141615

Leulier, F., Parquet, C., Pili-Floury, S., Ryu, J. H., Caroff, M., Lee, W. J., et al. (2003). The Drosophila immune system detects bacteria through specific peptidoglycan recognition. *Nat. Immunol.* 4, 478–484. doi: 10.1038/ni922

Li, H. Y., Lin, X. W., Geng, S. L., and Xu, W. H. (2018). TGF-beta and BMP signals regulate insect diapause through Smad1-POU-TFAM pathway. *Biochim. Biophys. Acta Mol. Cell. Res.* 1865, 1239–1249. doi: 10.1016/j.bbamcr.2018.06.002

Lindsay, S. A., and Wasserman, S. A. (2014). Conventional and non-conventional Drosophila Toll signaling. *Dev. Comp. Immunol.* 42, 16–24. doi: 10.1016/j.dci.2013.04.011

Luckhart, S., Crampton, A. L., Zamora, R., Lieber, M. J., Dos Santos, P. C., Peterson, T. M., et al. (2003). Mammalian transforming growth factor beta1 activated after ingestion by Anopheles stephensi modulates mosquito immunity. *Infect. Immun.* 71, 3000–3009. doi: 10.1128/IAI.71.6.3000-3009.2003

Luckhart, S., Vodovotz, Y., Cui, L., and Rosenberg, R. (1998). The mosquito Anopheles stephensi limits malaria parasite development with inducible synthesis of nitric oxide. *Proc. Natl. Acad. Sci. U.S.A.* 95, 5700–5705. doi: 10.1073/pnas.95.10.5700

Massague, J. (1990). The transforming growth factor-beta family. *Annu. Rev. Cell. Biol.* 6, 597–641. doi: 10.1146/annurev.cb.06.110190.003121

Massague, J. (2012). TGFbeta signalling in context. *Nat. Rev. Mol. Cell. Biol.* 13, 616–630. doi: 10.1038/nrm3434

Morikawa, M., Derynck, R., and Miyazono, K. (2016). TGF-beta and the TGF-beta family: context-dependent roles in cell and tissue physiology. *Cold Spring Harb. Perspect. Biol.* 8:5. doi: 10.1101/cshperspect.a021873

Mullen, A. C., and Wrana, J. L. (2017). TGF-beta family signaling in embryonic and somatic stem-cell renewal and differentiation. *Cold Spring Harb. Perspect. Biol.* 9:7. doi: 10.1101/cshperspect.a022186

Murphy, M. P., Holmgren, A., Larsson, N. G., Halliwell, B., Chang, C. J., Kalyanaraman, B., et al. (2011). Unraveling the biological roles of reactive oxygen species. *Cell. Metab.* 13, 361–366. doi: 10.1016/j.cmet.2011.03.010

Myllymäki, H., and Rämet M, M. (2014). JAK/STAT pathway in Drosophila immunity. *Scand. J. Immunol.* 79, 377–385. doi: 10.1111/sji.12170

O'Connor, M. B., Umulis, D., Othmer, H. G., and Blair, S. S. (2006). Shaping BMP morphogen gradients in the Drosophila embryo and pupal wing. *Development* 133, 183–193. doi: 10.1242/dev.02214

Ogawa, K., and Funaba, M. (2011). Activin in humoral immune responses. *Vitam. Horm.* 85, 235–253. doi: 10.1016/B978-0-12-385961-7.00012-3

Pruzinova, K., Sadlova, J., Myskova, J., Lestinova, T., Janda, J., and Volf, P. (2018). Leishmania mortality in sand fly blood meal is not species-specific and does not result from direct effect of proteinases. *Parasit. Vectors* 11:37. doi: 10.1186/s13071-018-2613-2

Ramalho-Ortigao, J. M., Temporal, P., de Oliveira, S. M. P., Barbosa, A. F., Vilela, M. L., Rangel, E., et al. (2001). Characterization of constitutive and putative differentially expressed mRNAs by means of expressed sequence tags, differential display reverse transcriptase-PCR and randomly amplified polymorphic DNA-PCR from the sand fly vector Lutzomyia longipalpis. *Mem. Inst. Oswaldo Cruz.* 96, 105–111. doi: 10.1590/S0074-02762001000100012

Rogers, M. E., Hajmová, M., Joshi, M. B., Sadlova, J., Dwyer, D. M., Volf, P., et al. (2008). Leishmania chitinase facilitates colonization of sand fly vectors and enhances transmission to mice. *Cell Microbiol.* 10, 1363–1372. doi: 10.1111/j.1462-5822.2008.01132.x

Sadlova, J., Myskova, J., Lestinova, T., Votypka, J., Yeo, M., and Volf, P. (2017). Leishmania donovani development in Phlebotomus argentipes: comparison of promastigote- and amastigote-initiated infections. *Parasitology* 144, 403–410. doi: 10.1017/S0031182016002067

Sant'Anna, M. R., Alexander, B., Bates, P. A., and Dillon, R. J. (2008). Gene silencing in phlebotomine sand flies: xanthine dehydrogenase knock down by dsRNA microinjections. *Insect Biochem. Mol. Biol.* 38, 652–660. doi: 10.1016/j.ibmb.2008.03.012

Sant'Anna, M. R., Diaz-Albiter, H., Aguiar-Martins, K., Al Salem, W. S., Cavalcante, R. R., Dillon, V., et al. (2014). Colonisation resistance in the sand fly gut: *Leishmania* protects *Lutzomyia longipalpis* from bacterial infection. *Parasit. Vectors* 7:329. doi: 10.1186/1756-3305-7-329

Schefe, J. H., Lehmann, K. E., Buschmann, I. R., Unger, T., and Funke-Kaiser, H. (2006). Quantitative real-time RT-PCR data analysis: current concepts and the novel gene expression's CT difference formula. *J. Mol. Med.* 84, 901–910. doi: 10.1007/s00109-006-0097-6

Schneider, C. A., Rasband, W. S., and Eliceiri, K. W. (2012). NIH Image to ImageJ: 25 years of image analysis. *Nat. Methods* 9, 671–675.

Shrinet, J., Nandal, U. K., Adak, T., Bhatnagar, R. K., and Sunil, S. (2014). Inference of the oxidative stress network in Anopheles stephensi upon Plasmodium infection. *PLoS ONE* 9:e114461. doi: 10.1371/journal.pone.0114461

Sideras, P., Apostolou, E., Stavropoulos, A., Sountoulidis, A., Gavriil, A., Apostolidou, A., et al. (2013). Activin, neutrophils, and inflammation: just coincidence? *Semin. Immunopathol.* 35, 481–499. doi: 10.1007/s00281-013-0365-9

Souza, A. V., Petretski, J. H., Demasi, M., Bechara, E. J., and Oliveira, P. L. (1997). Urate protects a blood-sucking insect against hemin-induced oxidative stress. *Free Radic. Biol. Med.* 22, 209–214. doi: 10.1016/S0891-5849(96)00293-6

Spottiswoode, N., Armitage, A. E., Williams, A. R., Fyfe, A. J., Biswas, S., Hodgson, S. H., et al. (2017). Role of activins in hepcidin regulation during malaria. *Infect. Immun.* 85:12. doi: 10.1128/IAI.00191-17

Surachetpong, W., Singh, N., Cheung, K. W., and Luckhart, S. (2009). MAPK ERK signaling regulates the TGF-beta1-dependent mosquito response to *Plasmodium falciparum*. *PLoS Pathog.* 5:e1000366. doi: 10.1371/journal.ppat.1000366

Telleria, E. L., Martins-da-Silva, A., Tempone, A. J., and Traub-Cseko, Y. M. (2018). Leishmania, microbiota and sand fly immunity. *Parasitology* 2018, 1–18. doi: 10.1017/S0031182018001014

Telleria, E. L., Pitaluga, A., O Ortigão-Farias, N. J., de Araújo, R. A. P., Ramalho-Ortigão, J. M., and Traub-Cseko, Y. M. (2007). Constitutive and blood meal-induced trypsin genes in Lutzomyia longipalpis. *Arch. Insect. Biochem. Physiol.* 66, 53–63. doi: 10.1002/arch.20198

Telleria, E. L., Sant'Anna, M. R., Alkurbi, M. O., Pitaluga, A. N., Dillon, R. J., and Traub-Cseko, Y. M. (2013). Bacterial feeding, Leishmania infection and distinct infection routes induce differential defensin expression in Lutzomyia longipalpis. *Parasit. Vectors* 6:12. doi: 10.1186/1756-3305-6-12

Telleria, E. L., Sant'Anna, M. R. V., Ortigao-Farias, J. R., Pitaluga, A. N., Dillon, V. M., Bates, P. A., et al. (2012). Caspar-like gene depletion reduces leishmania infection in sand fly host lutzomyia longipalpis. *J. Biol. Chem.* 287, 12985–12993. doi: 10.1074/jbc.M111.331561

Tinoco-Nunes, B., Telleria, E. L., Silva-Neves, M., Marques, C., Azevedo-Brito, D. A., Pitaluga, A. N. (2016). The sandfly *Lutzomyia longipalpis* LL5 embryonic cell line has active Toll and Imd pathways and shows immune responses to bacteria, yeast and *Leishmania*. *Parasit Vectors* 9:4. doi: 10.1186/s13071-016-1507-4

Vodovotz, Y., Zamora, R., Lieber, M. J., and Luckhart, S. (2004). Cross-talk between nitric oxide and transforming growth factor-beta1 in malaria. *Curr. Mol. Med.* 4, 787–797. doi: 10.2174/1566524043359999

Wilson, R., Bates, M. D., Dostalova, A., Jecna, L., Dillon, R. J., Volf, P., et al. (2010). Stage-specific adhesion of Leishmania promastigotes to sand fly midguts assessed using an improved comparative binding assay. *PLoS Negl. Trop. Dis.* 4:9. doi: 10.1371/journal.pntd.0000816

Conflict of Interest Statement: The authors declare that the research was conducted in the absence of any commercial or financial relationships that could be construed as a potential conflict of interest.

frontiers in Cellular and Infection Microbiology

ORIGINAL RESEARCH
published: 09 April 2019
doi: 10.3389/fcimb.2019.00088

Dietary Vitamin D3 Deficiency Increases Resistance to *Leishmania (Leishmania) amazonensis* Infection in Mice

Izabella Pereira da Silva Bezerra[1†], *Gabriel Oliveira-Silva*[1†], *Danielle Sophia Ferreira Santos Braga*[1], *Mirian França de Mello*[1], *Juliana Elena Silveira Pratti*[1], *Joyce Carvalho Pereira*[1], *Alessandra Marcia da Fonseca-Martins*[1], *Luan Firmino-Cruz*[1], *Diogo Maciel-Oliveira*[1], *Tadeu Diniz Ramos*[1], *André Macedo Vale*[1], *Daniel Claudio Oliveira Gomes*[2], *Bartira Rossi-Bergmann*[1] *and Herbert Leonel de Matos Guedes*[1,3*]

[1] *Instituto de Biofísica Carlos Chagas Filho, Universidade Federal do Rio de Janeiro, Rio de Janeiro, Brazil,* [2] *Núcleo de Doenças Infecciosas/Núcleo de Biotecnologia, Universidade Federal do Espírito Santo, Vitória, Brazil,* [3] *Núcleo Multidisciplinar de Pesquisa UFRJ – Xerém em Biologia, UFRJ Campus Duque de Caxias Professor Geraldo Cidade – Universidade Federal do Rio de Janeiro, Duque de Caxias, Brazil*

The leishmaniases are a group of diseases caused by *Leishmania* parasites, which have different clinical manifestations. *Leishmania (Leishmania) amazonensis* is endemic in South America and causes cutaneous leishmaniasis (CL), which can evolve into a diffuse form, characterized by an anergic immune response. Since the leishmaniases mainly affect poor populations, it is important to understand the involvement of immunonutrition, how the immune system is modulated by dietary nutrients and the effect this has on *Leishmania* infection. Vitamin D3 (VitD) is an immunonutrient obtained from diet or endogenously synthesized, which suppresses Th1 and Th17 responses by favoring T helper (Th) 2 and regulatory T cell (Treg) generation. Based on these findings, this study aims to evaluate dietary VitD influence on *L. (L.) amazonensis* experimental infection in C57BL/6 and BALB/c mice. Thus, C57BL/6 and BALB/c VitD deficient (VDD) mice were generated through dietary VitD restriction 45 days prior to infection. Both strains of VDD mice showed a more controlled lesion development compared to mice on a regular diet (Ctrl). There were no differences in serum levels of anti-*Leishmania* IgG1 and IgG2a, but there was a decrease in IgE levels in BALB/c VDD mice. Although $CD4^+$ T cell number was not changed, the $CD4^+$ IFN-γ^+ T cell population was increased in both absolute number and percentage in C57BL/6 and BALB/c VDD mice compared to Ctrl mice. There was also no difference in IL-4 and IL-17 production, however, there was reduction of IL-10 production in VDD mice. Together, our data indicate that VitD contributes to murine cutaneous leishmaniasis susceptibility and that the Th1 cell population may be related to the resistance of VDD mice to *L. (L.) amazonensis* infection.

Keywords: leishmaniasis, *Leishmania amazonensis*, vitamin D, Th1, immunonutrition, IL-10

OPEN ACCESS

Edited by:
Justin Boddey, Walter and Eliza Hall Institute of Medical Research, Australia

Reviewed by:
Manuel Soto, Autonomous University of Madrid, Spain
Clara Lúcia Barbiéri, Federal University of São Paulo, Brazil

***Correspondence:**
Herbert Leonel de Matos Guedes
herbert@biof.ufrj.br;
herbert@xerem.ufrj.br;
hlmguedes@gmail.com

[†]*These authors have contributed equally to this work*

Specialty section:
This article was submitted to Parasite and Host, a section of the journal Frontiers in Cellular and Infection Microbiology

Received: *15 January 2019*
Accepted: *12 March 2019*
Published: *09 April 2019*

Citation:
Bezerra IPS, Oliveira-Silva G, Braga DSFS, de Mello MF, Pratti JES, Pereira JC, da Fonseca-Martins AM, Firmino-Cruz L, Maciel-Oliveira D, Ramos TD, Vale AM, Gomes DCO, Rossi-Bergmann B and de Matos Guedes HL (2019) Dietary Vitamin D3 Deficiency Increases Resistance to Leishmania (Leishmania) amazonensis Infection in Mice. Front. Cell. Infect. Microbiol. 9:88. doi: 10.3389/fcimb.2019.00088

INTRODUCTION

The leishmaniases are a group of diseases caused by protozoans of the *Leishmania* genus, which are transmitted to mammalian hosts by female sandflies of the Phlebotominae family. Each year, 0.7 to 1 million new cases occur worldwide and clinical manifestations are divided into cutaneous and the lethal visceral leishmaniasis (VL) (Burza et al., 2018). Cutaneous leishmaniasis (CL) is generally characterized by a single self-healing ulcer. However, depending on the parasite species involved in infection and on the host immune status, it can evolve into a more severe manifestation (Scott and Novais, 2016). *Leishmania* (*Leishmania*) *amazonensis*, a species of the *L.* (*L.*) *mexicana* complex, is endemic in many South American countries and can cause diffuse CL, characterized by an anergic immune response and excess of parasites in multiple lesions. Moreover, cases of VL caused by *L. (L.) amazonensis* have been reported previously (Silveira et al., 2004).

Since *Leishmania* spp. amastigote forms are intracellular and mainly infect macrophages, the development of a T helper (Th) 1 immune response is desirable for disease control. Although BALB/c mice are susceptible and C57BL/6 mice are resistant to *L. (L.) major* infection, developing a Th2, and a Th1 immune response, respectively (Heinzel et al., 1989; Launois et al., 1997; Scott and Novais, 2016), this dichotomy is not observed in *L. (L.) amazonensis* infection. Most mice strains are susceptible and develop a mixed Th1/Th2 immune response with low cellular activation, as is observed in humans (Ji et al., 2002; Silveira et al., 2009; Velasquez et al., 2016).

Available treatments against leishmaniases are based on drug repositioning and have many problems such as high toxicity, high cost and development of resistant parasite strains. In addition, there is still no human vaccine approved (Rossi and Fasel, 2018). Thus, understanding disease immunobiology is necessary for the development of strategies that promote infection control.

In this context, immunonutrition is a key factor to be considered to better understand the immune system modulation by dietary nutrients, particularly in diseases that affect poor populations (McCarthy and Martindale, 2018), such as the leishmaniases.

Vitamin D3 (VitD) is an important immunonutrient that can be obtained from the diet or can be endogenously synthesized from a cholesterol precursor (7-dehydrocholesterol) through incidence of sun-UVB rays on the skin. This vitamin and its metabolites are essential for calcium homeostasis and also affect cell growth, differentiation, and function in many tissues, including the immune system (Baeke et al., 2010; Bikle, 2011).

VitD binds to the nuclear VitD receptor (VDR), which forms a complex with retinoic acid X receptor (RXR) and promotes transcription of several genes through VitD response elements (VDREs) (Pike and Meyer, 2012). VitD also induces non-genomics effects related to cell maturation, including growth factor and cytokine modulation through cytosolic pathways (Hii and Ferrante, 2016). Immune cells express VDR and they are capable of metabolizing circulating VitD to the active form 1,25-dihydroxycholecalciferol [$1,25(OH)_2D_3$], which suppresses the immune response by blocking dendritic cell (DC) differentiation and maturation, inducing a stable tolerogenic phenotype (Piemonti et al., 2000; Penna et al., 2005; Széles et al., 2009; Ferreira et al., 2012). Moreover, DCs treated with $1,25(OH)_2D_3$ stimulate regulatory T cell (Treg) generation and impair autoreactive T cell activation (van Halteren et al., 2004; Penna et al., 2005; Unger et al., 2009). Active $1,25(OH)_2D_3$ also induces CCR10 expression and skin-homing through the CCL27 chemokine, imprinting T cell epidermotropism (Sigmundsdottir et al., 2007). These are fundamental functions in the context of autoimmune diseases, allergies, and immunopathologies, such as leishmaniases.

A previous study demonstrated that VitD treatment has a beneficial effect on *L. (L.) mexicana* infection, controlling lesion development in BALB/c mice (Ramos-Martínez et al., 2013). In addition, VitD also plays a favorable role in canine infection by *L. (L.) infantum*, since disease progression is strongly associated with VitD deficiency in dogs (Rodriguez-Cortes et al., 2017). On the other hand, BALB/c VDR knockout mice have increased resistance to *L. (L.) major* infection (Whitcomb et al., 2012), suggesting a negative role for VitD. Overall, the role of VitD in *Leishmania* infection seems to depend on the parasite species involved. Thus, this study aims to evaluate the effect that dietary VitD has on experimental infection with *L. (L.) amazonensis* in both C57BL/6 and BALB/c mice, including its role in the development of an immune response to the parasite.

MATERIALS AND METHODS

Mice

Female C57BL/6 and BALB/c mice of 6–8 weeks old from Instituto de Biofísica Carlos Chagas Filho, Universidade Federal do Rio de Janeiro (Brazil) were maintained in sterilized cages and received filtered water and regular pelleted food (AIN-93M, Pragsoluções, Brazil). Dietary VitD deficient (VDD) mice were subjected to a commercial diet without VitD (AIN-93M, Pragsoluções, Brazil) for 45 days before infection. The diet was maintained throughout the experiment. All procedures performed are in accordance with the "Basic Principles for Research Involving Animal Use," approved and registered by the Ethics Committee on Animal Use in Research (CEUA/UFRJ number 157).

Parasites

Leishmania (L.) amazonensis promastigotes (MHOM/BR/75) were maintained at 26°C in Minimum Essential Medium 199 (MEM 199, Cultilab, Brazil) supplemented with 10% heat inactivated fetal bovine serum (HIFBS, Cultilab, Brazil), penicillin and streptomycin (100 U/mL and 100 µg/mL, respectively, Stemcell Technologies, USA) and hemin (5 µg/mL, Sigma-Aldrich, USA). To ensure infectivity, parasites were used at most until the fourth culture passage, after which, parasites were reisolated from pre-infected BALB/c mice.

Infection

Culture promastigotes in the stationary growth phase were used for infection. Parasites were washed with PBS by centrifugation at 1500 g. Mice were subcutaneously injected into the hind footpad

with 2×10^5 *L. (L.) amazonensis* promastigotes in a volume of 20 μL. Lesion development was monitored by measurement with a caliper (No. 7301, Mitutoyo, Japan) once every 7 days for 92 (C57BL/6 mice) or 99 (BALB/c mice) days.

Parasite Load

Parasite loads were evaluated by limiting dilution assay as previously described (Torres-Santos et al., 1999). Briefly, on day 92 (C57BL/6 mice) or 99 (BALB/c mice) post-infection, footpads were individually homogenized (2 mL/footpad), and diluted 1:100 (only BALB/c mice samples) in MEM 199. Homogenates were serially diluted 1:4 in microplates for 16 dilutions (final volume of 200 μL/well), performed in triplicate for each sample, and incubated at 26°C for 14 days. The original number of amastigotes per footpad was calculated taking as reference the last dilution in which promastigotes were observed under optical microscope, theoretically equivalent to a single amastigote.

Cytokines

IL-4, IL-17, and IL-10 were measured in supernatants of lesion homogenates by Enzyme-Linked Immunosorbent Assay (ELISA). Cytokine concentrations were determined from standard curves using recombinant cytokines and murine antibodies, according to manufacturer's instructions (BD Systems, USA).

Antibodies

On day 92 (C57BL/6 mice) or 99 (BALB/c mice) post-infection, blood samples were collected, and after standing at room temperature for 2 h, then centrifuged at 2000 g to obtain serum. Seric IgG1, IgG2a, IgA, and IgE antibodies specific for *L. (L.) amazonensis* promastigote antigens (LaAg) were quantified by ELISA. LaAg was prepared as described before (Pratti et al., 2016). Briefly, plates were pretreated with LaAg (1 μg/well) and incubated overnight at 4°C. Samples were diluted 250x for evaluation and biotinylated antibodies were used for detection (Goat Anti-Mouse IgG1-UNLB: Cat. No. 1071-01, Goat Anti-Mouse IgG2a-UNLB: Cat. No. 1101-01, Goat Anti-Mouse IgE-UNLB: Cat. No. 1110-05, Goat Anti-Mouse IgA-UNLB: Cat. No. 1040-05, SouthernBiotec) according to the manufacturer's recommendations.

Flow Cytometry

On day 92 (C57BL/6 mice) or 99 (BALB/c mice) post-infection, popliteal lesion-draining lymph nodes homogenates were prepared, cellularity was performed by manual counting on a Neubauer chamber and single cell suspensions were incubated with anti-CD3 (Peridinin Chlorophyll Protein Complex; Percp-conjugated), anti-CD4 [R-phycoerythrin PE and the cyanine dye Cy7 combined; PE-Cy7-conjugated], and anti-IFN-γ (Allophycocyanin; APC-conjugated) monoclonal antibodies according to manufacturer's instructions from eBioscience. The analyzes were performed in the software Summit. Gate strategy is demonstrated in **Supplementary Figure 5**.

Statistical Analysis

Results were analyzed using GraphPad PRISM® version 6.0 software. Student *t*-test was used. For lesion development kinetics a Two-way ANOVA with Bonferroni post-test was used. Results are expressed as mean ± standard deviation (SD) and the differences between means with $P < 0.05$ are considered significant. All data are representative of three independent experiments.

RESULTS

VDD Mice Are More Resistant to *L. (L.) amazonensis* Infection

The development of *L. (L.) amazonensis* infection was evaluated in partially susceptible C57BL/6 and susceptible BALB/c mice submitted to dietary VitD restriction (VDD) or fed a regular diet (Ctrl). Both C57BL/6 and BALB/c VDD mice showed a more controlled lesion development compared to those on the regular diet (**Figures 1A,B**) when mice were infected with 2×10^5 promastigotes. In C57BL/6 VDD the lesions began to resolve by day 60, whereas in the Ctrl mice this did not occur until day 75. In BALB/c mice, the lesions continued to develop until the endpoint of the experiment, with BALB/c VDD mice showing a significantly smaller lesion over this time. There was no significant difference in the parasite loads at the infection site of the C57BL/6 VDD compared to C57BL/6 ctrl (day 92) or BALB/c VDD compared to BALB/c ctrl (day 99) (**Figures 1C,D**). We also evaluated parasite load in lymph nodes, and no difference was observed between the infected Ctrl and VDD mice for either C57BL/6 and BALB/c mice (**Supplementary Figure 1**). It is important to note that dietary VitD restriction did not interfere in the appearance or body weight of the mice (**Supplementary Figure 2**). Moreover, when a high challenge model of infection with 2×10^6 promastigotes was used, no difference was observed in lesion size between the Ctrl and VDD mice for each mouse strain (**Supplementary Figure 3**). Based on that, subsequent experiments were performed using an infection dose of 2×10^5 parasites. However, as we had already observed that the lesion resolution was more accelerated in the C57BL/6 VDD mice (**Figure 1**), we further evaluated the infection profile of these mice for 149 days to assess whether there was complete resolution of the lesion. In the beginning of chronic phase there was no difference between the VDD and Ctrl mice, however, later in the chronic phase, VDD mice presented significantly smaller lesions in comparison to the Ctrl mice (**Supplementary Figure 4**) indicating a reduction of lesion size at both the peak of infection and in late chronic phase. However, again, there was no significant difference in the parasite loads at this late chronic phase time-points.

Increase in $CD4^+$ IFN-γ^+ T Cell Population in the Lesion-Draining Lymph Nodes of VDD Mice

To better understand the role of VitD in the immune response to infection, cell phenotype in lesion-draining popliteal lymph nodes was evaluated at the endpoint of infection, day 92 for C57BL/6, and day 99 for BALB/c. There was no difference in the total number of lymph node cells between VDD and Ctrl mice, in both mouse strains, C57BL/6 (**Figure 2A**) and BALB/c

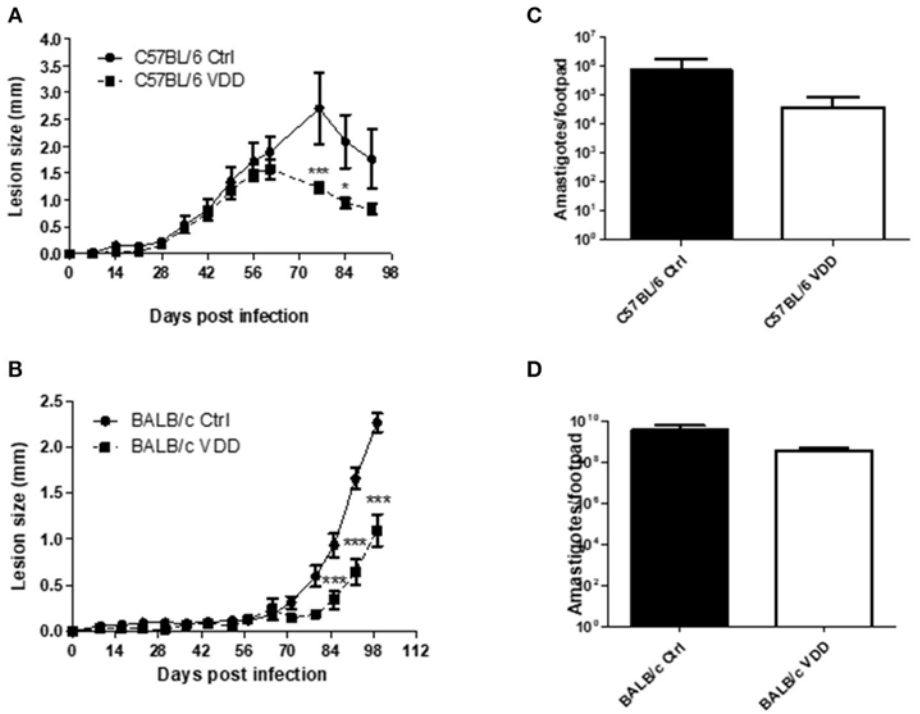

FIGURE 1 | VDD mice are more resistant to *L. (L.) amazonensis* infection. C57BL/6 and BALB/c mice normally fed (Ctrl) or on a Vitamin D-deficient diet (VDD) were subcutaneously infected in the footpad with 2×10^5 *L. (L.) amazonensis* promastigotes and lesion development was followed weekly **(A,B)**. On day 92 (C57BL/6) or 99 (BALB/c) post-infection, parasite loads in the infection site were evaluated by limiting dilution assay **(C,D)**. The data (means ± SD; $n = 5$ $^{***}P < 0.0001$; $^{*}P < 0.05$) are representative of three independent experiments producing the same result profile.

(**Figure 2B**). There was also no difference in the number of $CD4^+$ cells between VDD and Ctrl mice (**Figures 2C,D**), but in terms of the percentage of $CD4^+$ cells in the total cell population, there was a reduction in C57BL/6 VDD (**Figure 2E**) and an increase in BALB/c VDD (**Figure 2F**) compared to their respective controls. Since *Leishmania* spp. are intracellular parasites and induction of Th1 response is generally associated with disease control, the number and percentage of the $CD4^+$ cell population producing IFN-γ was further evaluated. The $CD4^+$ IFN-γ^+ cell population was increased in both absolute number (**Figures 2G,H**) and the percentage within the $CD4^+$ population (**Figures 2I,J**) in C57BL/6 VDD and BALB/c VDD mice compared to respective controls. This cell population may be associated with resistance of mice to *L. (L.) amazonensis* infection.

BALB/c VDD Exhibit a Reduction in IL-10 and IgE Levels, Without Affecting IgG1 and IL-4 Production

Cytokine and antibody production at the endpoint of infection, day 92 for C57BL/6 and day 99 for BALB/c, were also evaluated. Both C57BL/6 VDD and BALB/c VDD mice showed no difference in IL-4 and IL-17 production compared to respective controls (**Figures 3A–D**), however, a decrease of IL-10 was observed in VDD mice in comparison with Ctrl mice (**Figures 3E,F**). Moreover, both C57BL6 VDD and BALB/c VDD mice had no difference in the production of IgG1, IgG2a, and IgA antibodies specific for *L. (L.) amazonensis* antigens compared to respective controls (**Figures 4A–F**). However, BALB/c VDD mice showed reduced levels of IgE compared to the control mice on the regular diet (**Figure 4H**).

DISCUSSION

Since the leishmaniases are neglected diseases that mainly affect poor populations, dietary factors could likely influence the development of infection. The hypothesis of a possible VitD involvement in the regulation of immune processes was due to the presence of an abundance of VDR receptors in different cell types of the immune system, such as $CD4^+$ and $CD8^+$ T lymphocytes, neutrophils, dendritic cells, and macrophages (Baeke et al., 2010). In addition, VitD plays a role in the development of Th2 and Treg immune responses, and in the induction of lymphocyte expression of molecules that target homing of cells to the skin (Sassi et al., 2018).

VDD mice exhibited a smaller lesion progression profile, although they did not present a significant reduction in the parasite load, compared to control mice fed on a regular diet (**Figure 1**). This profile was observed in both partially susceptible C57BL/6 and susceptible BALB/c mice. A previous study described that C57BL/6 VitD-receptor knockout (VDRKO) mice are also more resistant to *L. (L.) major* infection compared to wild-type (WT) mice (Ehrchen et al., 2007; Whitcomb et al.,

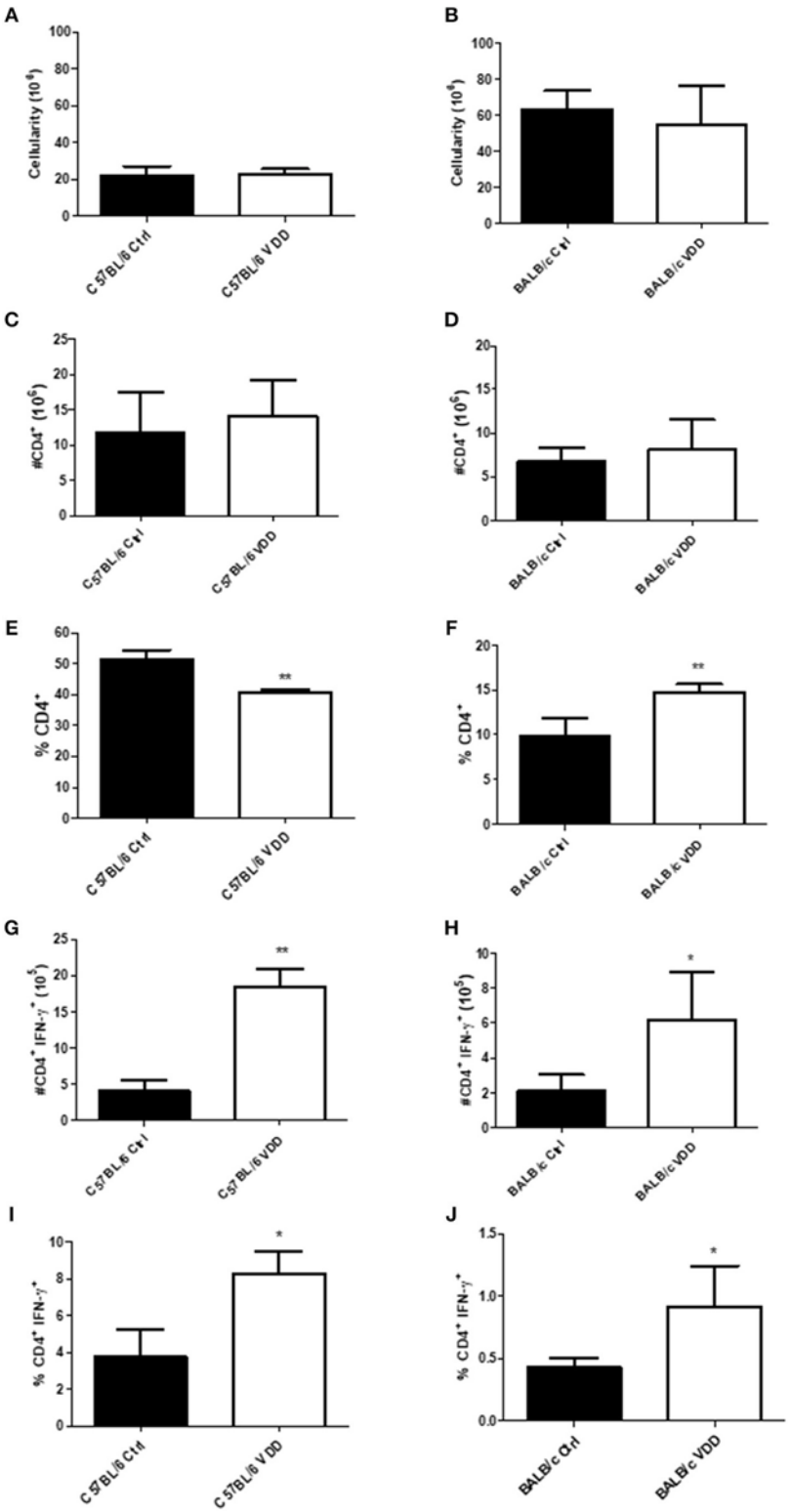

FIGURE 2 | Increase in the T CD4$^+$ IFN-γ^+ cell population in lesion-draining lymph nodes of *L. (L.) amazonensis*-infected VDD mice. C57BL/6 and BALB/c mice normally fed (Ctrl) or on a Vitamin D-deficient diet (VDD) were subcutaneously infected in the footpad with 2×10^5 *L. (L.) amazonensis* promastigotes. On day 92 (C57BL/6) or 99 (BALB/c) post-infection, lesion-draining lymph node cellularity **(A,B)**, number of T CD4$^+$ lymphocytes **(C,D)**, percentage of T CD4$^+$ lymphocytes **(E,F)**, number of IFN-γ producing T CD4$^+$ lymphocytes **(G,H)** and percentage of IFN-γ producing T CD4$^+$ lymphocytes **(I,J)** were assessed by flow cytometry. The data (means ± SD; $n = 5$ $^{**}P < 0.0001$) are representative of two independent experiments producing the same result profile.

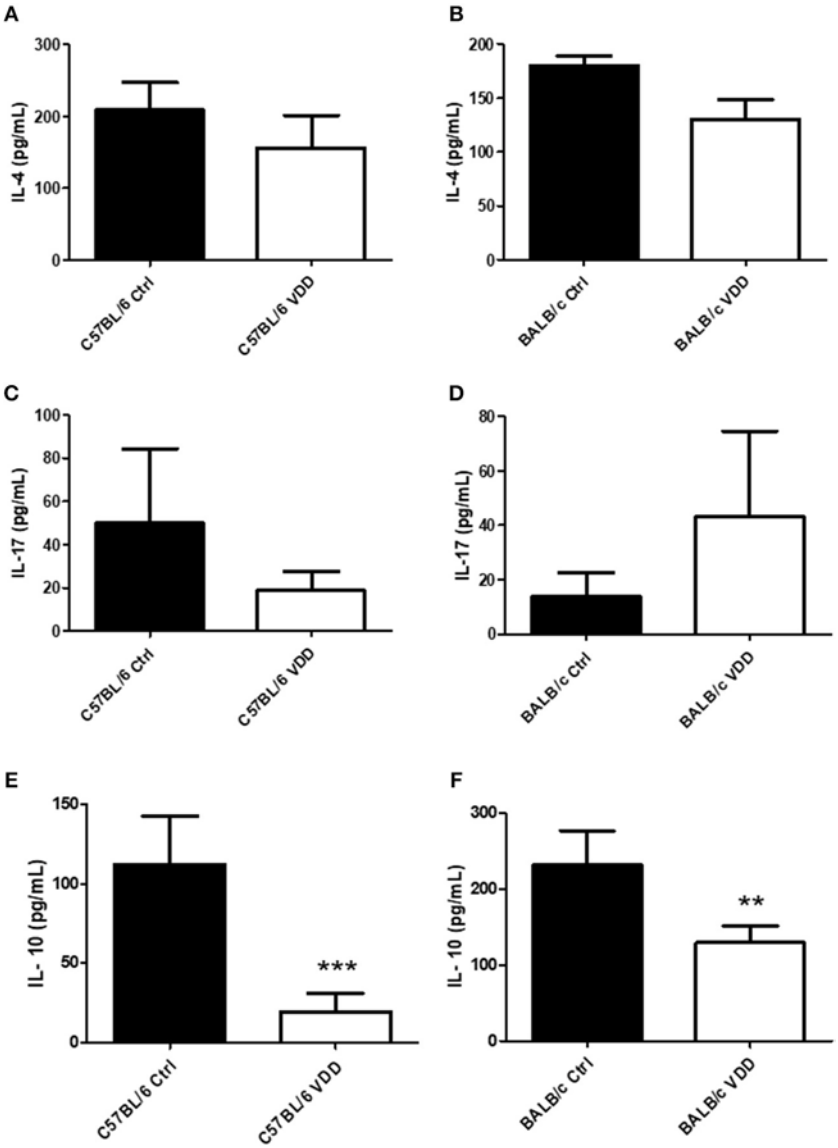

FIGURE 3 | Cytokine profile in the lesions of *L. (L.) amazonensis*-infected VDD mice. C57BL/6 and BALB/c mice normally fed (Ctrl) or on a Vitamin D-deficient diet (VDD) were subcutaneously infected in the footpad with 2×10^5 *L. (L.) amazonensis* promastigotes. On day 92 (C57BL/6) or 99 (BALB/c) post-infection, the cytokine profile in the lesions was evaluated by ELISA. IL-4 **(A,B)**, IL-17 **(C,D),** and IL-10 **(E,F)** levels in tissue homogenates were quantified. The data (means ± SD; $n = 5$; $^{***}P < 0.001$, $^{**}P < 0.01$) are representative of two independent experiments producing the same result profile.

2012). However, BALB/c VDRKO mice present no difference in lesion development during *L. (L.) major* infection compared WT mice (Whitcomb et al., 2012). Together, these data indicate that VDD, either through dietary VitD depletion or the ablation of VitD-signaling, leads to an increased resistance to *Leishmania* infection. It is important to note that experimental models lacking VDR expression are quite different from the dietary VitD deprivation model used in this study. VDRKO animals have an absence of a systemic response to VitD, affecting cell differentiation and impacting on the innate and adaptive immune system. On the other hand, the use of a deficient diet does not impair the endogenous synthesis of VitD or its signaling pathway, being the best model to study the nutritional impact. Our data show that using VDD mice, either in a C57BL/6 or BALB/c background, a similar resistance to *L. (L.) amazonensis* infection was observed, indicating a strong phenotype using the VitD deficient diet.

Contrary to what was observed in CL, VitD deficiency is related to the progression of VL in dogs (Rodriguez-Cortes et al., 2017), suggesting clear differences in the involvement of macrophages from skin and the visceral organs, such as spleen, liver, and bone marrow. Clinical studies in humans should be performed to better comprehend the impact of VitD deficiency in CL and VL.

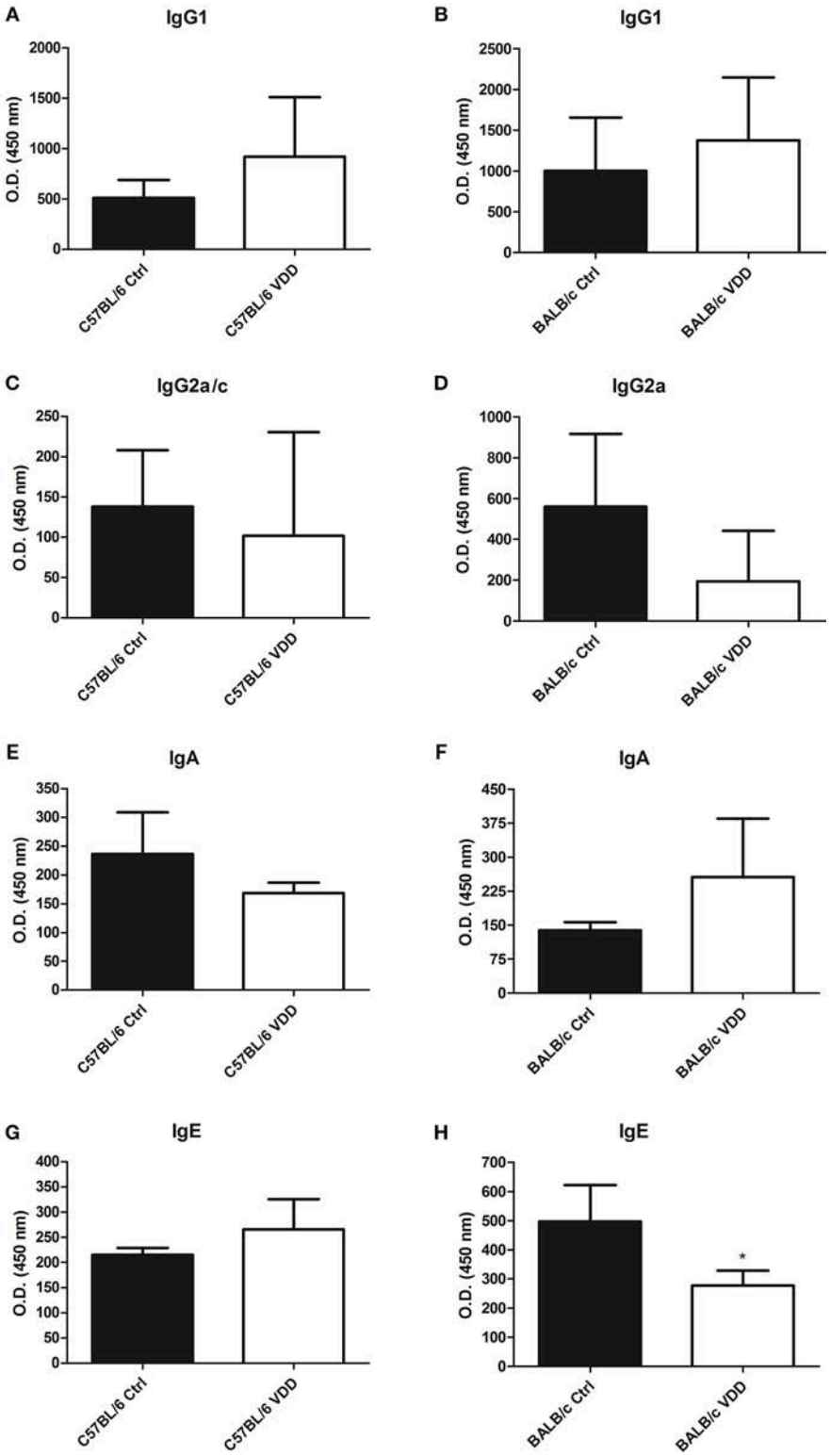

FIGURE 4 | *L. (L.) amazonensis*-specific antibody production in VDD mice. C57BL/6 and BALB/c mice normally fed (Ctrl) or on a Vitamin D-deficient diet (VDD) were subcutaneously infected in the footpad with 2×10^5 *L. (L.) amazonensis* promastigotes. On day 92 (C57BL/6) or 99 (BALB/c) post-infection, *L. (L.) amazonensis*-specific antibody production in the serum was evaluated by ELISA. IgG1 **(A,B)**, IgG2a **(C,D)**, IgA **(E,F)**, and IgE **(G,H)** levels were quantified. Mean ± SD; $n = 5$. The data (means ± SD; $n = 5$; $^*P < 0.05$) are representative of two independent experiments producing the same result profile.

A different approach showed that intraperitoneal treatment with the active form of VitD, 1,25-dihydroxycholecalciferol [$1,25(OH)_2D_3$] significantly reduces lesion size in BALB/c mice infected with *L. (L.) mexicana*, but without reducing the parasite load. Treatment with $1,25(OH)_2D_3$ is associated with a healing profile, increasing eosinophils and fibroblasts in the lesions, enhancing collagen production, and decreasing pro-inflammatory cytokines levels compared to untreated control mice, without affecting parasite elimination (Ramos-Martínez et al., 2013). However, this model uses the active form of VitD after infection, while the VitD deficient diet affects immunity in the mice prior to infection. Thus, it is not adequate to compare results between these different approaches, and dietary VitD deficiency is the most appropriate model to evaluate the impact of nutrition on immunity against leishmaniasis.

Comparing C57BL/6 ctrl mice (partially resistant) to BALB/c ctrl mice (susceptible), C57BL/6 mice exhibited higher numbers of IFN-γ-producing $CD4^+$ cells, which are related to leishmaniasis control (**Figure 2**). It has been demonstrated that VitD suppresses the Th1 response (Cantorna et al., 2015). Corroborating this data, our results show that both C57BL/6 and BALB/c VDD have an increased frequency and number of IFN-γ-producing $CD4^+$ cells (**Figure 2**). This increased Th1 response is probably related to the more controlled lesion development in infected VDD mice. However, the increase of IFN-γ-producing cells was not enough to control the parasite load, so perhaps other mechanisms are necessary, such as reactive oxygen species production by macrophages. Whereas, VDRKO mice also exhibit an increase in IFN-γ production by $CD4^+$ and $CD8^+$ T cells during *L. (L.) major* infection, this controls both lesion development and parasite load (Ehrchen et al., 2007). In our experiments, no difference in $CD8^+$ T cells was observed (data not shown), which may be associated to the failure to control parasite load.

Evaluation of cytokine production at the site of infection in the chronic phase showed that VDD mice, both C57BL/6, and BALB/c, have no difference in IL-4 (**Figure 3**), which has also been observed in *L. (L.) major* infection of C57BL/6 VDRKO mice (Whitcomb et al., 2012). *In vitro* studies indicate that VitD upregulates the activity of Th2 cells (Boonstra et al., 2001; Staeva-Vieira and Freedman, 2002). IL-4 is a cytokine associated with susceptibility to *L. (L.) amazonensis* infection and IL-4-deficient BALB/c mice are more resistant to infection, depending on the initial parasite inoculum, developing smaller lesions and a higher Th1 response, with higher IFN-γ, and IgG2a production than WT mice (Guimarães et al., 2006). In addition, leishmaniasis pathogenesis is associated with the blockage of a Th1 response development, leading to a greater number of IL-4 and IL-10-producing cells in the lesions (Carvalho et al., 2016). Studies with C57BL/6 mice show that only 30% of IL-4-receptor-deficient animals develop a lesion after inoculation of *L. (L.) amazonensis* and they have higher IFN-γ production compared to WT mice (Felizardo et al., 2012). Despite the fact that VitD is related to a Th2 immune response development, dietary VitD deficiency did not impact IL-4 production during *L. (L.) amazonensis* infection. It has also been demonstrated that VitD suppresses Th17 cell differentiation (Korf et al., 2012; Fawaz et al., 2016), a cytokine related to pathogenesis of *L. (L.) mexicana* infection (Pedraza-Zamora et al., 2017). However, no difference in the level of IL-17 was observed between VDD and Ctrl mice.

We demonstrated that VDD mice presented a reduction of IL-10 in comparison to Ctrl mice (**Figures 3E,F**). A similar phenotype was observed in C57BL6 VDRKO mice, with a decrease of IL-10 by Real Time PCR in comparison to WT mice (Whitcomb et al., 2012). IL-10 production has been associated to susceptibility to *L. (L) amazonensis* infection (Padigel et al., 2003) and reduction of IL-10 is related to a decrease of lesion size (Padigel et al., 2003; Firmino-Cruz et al., 2018). In addition, the production of IFN-γ inhibits the production of IL-10 by macrophages (Herrero et al., 2003). Therefore, we suggest VitD deficiency promotes the increase of IFN-γ that inhibits the production of IL-10, which is associated with reduction of lesion size.

Antibody production has been associated to pathogenesis in *L. (L.) amazonensis* infection (Firmino-Cruz et al., 2018). Our results show that VDD mice had no difference in antigen specific-IgG1 and IgG2a production compared to Ctrl mice (**Figure 4**). However, it has been shown that C57BL/6 VDRKO mice infected with *L. (L.) major* produce more IgG2a in comparison to WT mice (Whitcomb et al., 2012). With regards to BALB/c VDD mice, there was a higher serum level of IgE compared to Ctrl mice, which is related to a Th2 immune response. In humans, VitD deficiency is related to increased IgE with direct effect on B cells during allergy (James et al., 2016; Guo et al., 2018).

Studies using experimental models have demonstrated that lack of VitD also interferes with the immune response to other pathogens. VDD mice have increased susceptibility to lung infection by *Aspergillus fumigatus*, developing an excessive inflammatory response (Li et al., 2014). VitD also plays a key role in the immunity against *Mycobacterium tuberculosis* in mice. Following BCG stimulation, IFN-γ levels significantly increased and IL-10 levels significantly decreased in the VDD mice compared to control mice (Yang et al., 2013). On the other hand, $1,25(OH)_2D_3$ treatment inhibited the inflammatory infiltrates and expression of IL-2, IFN-γ and TNF-β in the spleen of VDD mice following vaccination with BCG (Zhang et al., 2018). These findings corroborate that Th1 cells are strongly activated under VDD conditions.

CONCLUSION

Altogether, our results indicate that dietary VitD deficiency is able to decrease lesion growth and provide an increase in Th1 response in C57BL/6 and BALB/c mice upon *L. (L.) amazonensis* infection, although it does not decrease parasite burden in either of the murine models used. Thus, VitD may contribute to host susceptibility to murine tegumentary leishmaniasis. Further studies on the influence of immunonutrition in the leishmaniases are needed to better understand the immunobiology of these diseases.

AUTHOR CONTRIBUTIONS

HdMG conceived and designed the experiments. GO-S, DB, MM, JEP, JCP, TR, AdF-M, and LF-C performed the experiments. GO-S, MM, LF-C, TR, and AdF-M analyzed data. IB, GO-S, DG, BR-B, and HdMG scientific discussion. HdMG, BR-B, and AV contributed reagents, materials and analysis tools. IB and HdMG wrote the paper.

FUNDING

We received financial support from Programa Jovem Cientista do Nosso Estado (Faperj – E-26/203.215/2015); Productivity Fellowships from Conselho Nacional de Desenvolvimento Científico e Tecnológico (304712/2016-7) and Agency for Support and Evaluation of Graduate Education (CAPES) Finance code 001.

SUPPLEMENTARY MATERIAL

The Supplementary Material for this article can be found online at: https://www.frontiersin.org/articles/10.3389/fcimb.2019.00088/full#supplementary-material

Supplementary Figure 1 | Parasite loads in draining lymph nodes. C57BL/6 and BALB/c mice normally fed (Ctrl) or on a Vitamin D-deficient diet (VDD) were subcutaneously infected in the footpad with 2×10^5 *L. (L.) amazonensis* promastigotes and lesion development was followed weekly as in **Figure 1**. On day 92 (C57BL/6) or 99 (BALB/c) post-infection, parasite loads in the draining lymph nodes were evaluated by limiting dilution assay **(A,B)**. The data are representative of three independent experiments producing the same result profile.

Supplementary Figure 2 | Body weight variation upon *L. (L.) amazonensis* infection. C57BL/6 **(A)** and BALB/c **(B)** mice fed normally (Ctrl) or on a Vitamin D-deficient diet (VDD) were subcutaneously infected in the footpad with 2×10^5 *L. (L.) amazonensis* promastigotes 45 days after starting the diet. Body weight was evaluated weekly throughout the experiment. The data (means ± SD; $n = 5$) are representative of three independent experiments producing the same result profile.

Supplementary Figure 3 | Evaluation of VDD mice on high challenge model of infection. C57BL/6 and BALB/c mice normally fed (Ctrl) or on a Vitamin D-deficient diet (VDD) were subcutaneously infected in the footpad with 2×10^6 *L. (L.) amazonensis* promastigotes and lesion development was followed weekly **(A,B)**. The data (means ± SD; $n = 5$) are representative of two independent experiments producing the same result profile.

Supplementary Figure 4 | C57BL/6 VDD mice are more resistant to *L. (L.) amazonensis* infection in late chronic phase. C57BL/6 normally fed (Ctrl) or on a Vitamin D-deficient diet (VDD) were subcutaneously infected in the footpad with 2×10^5 *L. (L.) amazonensis* promastigotes and lesion development was followed weekly **(A)**. On day 149 post-infection, parasite loads in the infection site were evaluated by limiting dilution assay **(B)**. The data (means ± SD; $n = 5$ $^{**}P < 0.001$; $^{*}P < 0.05$) are representative of two independent experiments producing the same result profile.

Supplementary Figure 5 | Gate strategy used for lymph node $CD4^+$ cells. Lymph node cells from infected Ctrl and VDD mice were plated at 5×10^5 per well and stained for flow cytometry to determine the percentage of $CD4^+$ and $CD4^+$ IFN-γ^+ cells.

REFERENCES

Baeke, F., Takiishi, T., Korf, H., Gysemans, C., and Mathieu, C. (2010). Vitamin D: modulator of the immune system. *Curr. Opin. Pharmacol.* 10, 482–496. doi: 10.1016/j.coph.2010.04.001

Bikle, D. D. (2011). Vitamin D regulation of immune function. *Vitam. Horm.* 86, 1–21. doi: 10.1016/B978-0-12-386960-9.00001-0

Boonstra, A., Barrat, F. J., Crain, C., Heath, V. L., Savelkoul, H. F., and O'Garra, A. (2001). 1alpha,25-Dihydroxyvitamin d3 has a direct effect on naive CD4(+) T cells to enhance the development of Th2 cells. *J. Immunol.* 167, 4974–80. doi: 10.4049/jimmunol.167.9.4974

Burza, S., Croft, S. L., and Boelaert, M. (2018). Leishmaniasis. *Lancet* 392, 951–970. doi: 10.1016/S0140-6736(18)31204-2

Cantorna, M. T., Snyder, L., Lin, Y. D., and Yang, L. (2015). Vitamin D and 1,25(OH)2D regulation of T cells. *Nutrients* 7, 3011–3021. doi: 10.3390/nu7043011

Carvalho, A. K., Carvalho, K., Passero, L. F. D., Sousa, M. G. T., da Matta, V. L. R., Gomes, C. M. C., et al. (2016). Differential recruitment of dendritic cells subsets to lymph nodes correlates with a protective or permissive T-cell response during *Leishmania* (*Viannia*) *Braziliensis* or *Leishmania* (*Leishmania*) *Amazonensis* infection. *Mediat. Inflamm.* 2016, 1–12. doi: 10.1155/2016/7068287

Ehrchen, J., Helming, L., Varga, G., Pasche, B., Loser, K., Gunzer, M., et al. (2007). Vitamin D receptor signaling contributes to susceptibility to infection with *Leishmania* major. *FASEB J.* 21, 3208–3218. doi: 10.1096/fj.06-7261com

Fawaz, L., Mrad, M. F., Kazan, J. M., Sayegh, S., Akika, R., and Khoury, S. J. (2016). Comparative effect of 25(OH)D3 and 1,25(OH)2D3 on Th17 cell differentiation. *Clin. Immunol.* 166–167, 59–71. doi: 10.1016/j.clim.2016.02.011

Felizardo, T. C., Gaspar-Elsas, M. I., Lima, G. M., and Abrahamsohn, I. A. (2012). Lack of signaling by IL-4 or by IL-4/IL-13 has more attenuating effects on *Leishmania* amazonensis dorsal skin – than on footpad-infected mice. *Exp. Parasitol.* 130, 48–57. doi: 10.1016/j.exppara.2011.09.015

Ferreira, G. B., Kleijwegt, F. S., Waelkens, E., Lage, K., Nikolic, T., Hansen, D. A., et al. (2012). Differential protein pathways in 1,25-dihydroxyvitamin d(3) and dexamethasone modulated tolerogenic human dendritic cells. *J. Proteome Res.* 11, 941–71. doi: 10.1021/pr200724e

Firmino-Cruz, L., Ramos, T. D., da Fonseca-Martins, A. M., Maciel-Oliveira, D., Oliveira-Silva, G., Pratti, J. E. S., et al. (2018). Immunomodulating role of IL-10-producing B cells in *Leishmania amazonensis* infection. *Cell. Immunol.* 334, 20–30. doi: 10.1016/j.cellimm.2018.08.014

Guimarães, E. T., Santos, L. A., Ribeiro dos Santos, R., Teixeira, M. M., dos Santos, W. L., and Soares, M. B. (2006). Role of interleukin-4 and prostaglandin E2 in *Leishmania amazonensis* infection of BALB/c mice. *Microb. Infect.* 8, 1219–1226. doi: 10.1016/j.micinf.2005.11.011

Guo, H., Zheng, Y., Cai, X., Yang, H., Zhang, Y., Hao, L., et al. (2018). Correlation between serum vitamin D status and immunological changes in children affected by gastrointestinal food allergy. *Allergol. Immunopathol.* 46, 39–44. doi: 10.1016/j.aller.2017.03.005

Heinzel, F. P., Sadick, M. D., Holaday, B. J., Coffman, R. L., and Locksley, R. M. (1989). Reciprocal expression of interferon gamma or interleukin 4 during the resolution or progression of murine leishmaniasis. Evidence for expansion of distinct helper T cell subsets. *J. Exp. Med.* 169, 59–72. doi: 10.1084/jem.169.1.59

Herrero, C., Hu, X., Li, W. P., Samuels, S., Sharif, M. N., Kotenko, S., et al. (2003). Reprogramming of IL-10 activity and signaling by IFN-gamma. *J Immunol.* 171, 5034–41.doi: 10.4049/jimmunol.171.10.5034

Hii, C., and Ferrante, A. (2016). The Non-Genomic Actions of Vitamin D. *Nutrients* 8:135. doi: 10.3390/nu8030135

James, J., Weaver, V., and Cantorna, M. T. (2016). Control of circulating IgE by the vitamin D receptor in vivo involves B cell intrinsic and extrinsic mechanisms. *J. Immunol.* 198, 1164–1171. doi: 10.4049/jimmunol.1601213

Ji, J., Sun, J., Qi, H., and Soong, L. (2002). Analysis of T helper cell responses during infection with *Leishmania amazonensis*. *Am. J. Trop. Med. Hyg.* 66, 338–45. doi: 10.4269/ajtmh.2002.66.338

Korf, H., Wenes, M., Stijlemans, B., Takiishi, T., Robert, S., Miani, M., et al. (2012). 1,25-Dihydroxyvitamin D3 curtails the inflammatory and T cell stimulatory capacity of macrophages through an IL-10-dependent mechanism. *Immunobiology* 217, 1292–1300. doi: 10.1016/j.imbio.2012.07.018

Launois, P., Maillard, I., Pingel, S., Swihart, K. G., Xénarios, I., Acha-Orbea, H., et al. (1997). IL-4 rapidly produced by V beta 4 V alpha 8 CD4+ T cells instructs Th2 development and susceptibility to *Leishmania* major in BALB/c mice. *Immunity* 6, 541–9. doi: 10.1016/S1074-7613(00)80342-8

Li, P., Xu, X., Cao, E., Yu, B., Li, W., Fan, M., et al. (2014). Vitamin D deficiency causes defective resistance to *Aspergillus fumigatus* in mice via aggravated and sustained inflammation. *PLoS ONE* 9:e99805. doi: 10.1371/journal.pone.0099805

McCarthy, M. S., and Martindale, R. G. (2018). Immunonutrition in critical illness: what is the role? *Nutri. Clin. Pract.* 33, 348–358. doi: 10.1002/ncp.10102

Padigel, U. M., Alexander, J., and Farrell, J. P. (2003). The role of interleukin-10 in susceptibility of BALB/c mice to infection with *Leishmania* mexicana and *Leishmania amazonensis*. *J Immunol.* 171:3705–10. doi: 10.4049/jimmunol.171.7.3705

Pedraza-Zamora, C. P., Delgado-Domínguez, J., Zamora-Chimal, J., and Becker, I. (2017). Th17 cells and neutrophils: close collaborators in chronic *Leishmania mexicana* infections leading to disease severity. *Parasite Immunol.* 39:e12420. doi: 10.1111/pim.12420

Penna, G., Roncari, A., Amuchastegui, S., Daniel, K. C., Berti, E., Colonna, M., et al. (2005). Expression of the inhibitory receptor ILT3 on dendritic cells is dispensable for induction of CD4+Foxp3+ regulatory T cells by 1,25-dihydroxyvitamin D3. *Blood* 106, 3490–3497. doi: 10.1182/blood-2005-05-2044

Piemonti, L., Monti, P., Sironi, M., Fraticelli, P., Leone, B. E., Dal Cin, E., et al. (2000). Vitamin D3 affects differentiation, maturation, and function of human monocyte-derived dendritic cells. *J. Immunol.* 164, 4443–51. doi: 10.4049/jimmunol.164.9.4443

Pike, J. W., and Meyer, M. B. (2012). The vitamin D receptor: new paradigms for the regulation of gene expression by 1,25-dihydroxyvitamin D3. *Rheum Dis Clin North Am.* 38, 13–27. doi: 10.1016/j.rdc.2012.03.004

Pratti, J. E., Ramos, T. D., Pereira, J. C., da Fonseca-Martins, A. M., Maciel-Oliveira, D., Oliveira-Silva, G., et al. (2016). Efficacy of intranasal LaAg vaccine against *Leishmania* amazonensis infection in partially resistant C57Bl/6 mice. *Parasit Vectors*. 9:534. doi: 10.1186/s13071-016-1822-9

Ramos-Martínez, E., Villaseñor-Cardoso, M. I., López-Vancell, M. R., García-Vázquez, F. J., Pérez-Torres, A., Salaiza-Suazo, N., et al. (2013). Effect of 1,25(OH)2D3 on BALB/c mice infected with *Leishmania mexicana*. *Exp. Parasitol.* 134, 413–421. doi: 10.1016/j.exppara.2013.05.009

Rodriguez-Cortes, A., Martori, C., Martinez-Florez, A., Clop, A., Amills, M., Kubejko, J., et al. (2017). Canine Leishmaniasis progression is associated with vitamin D deficiency. *Sci. Rep.* 7:3346. doi: 10.1038/s41598-017-03662-4

Rossi, M., and Fasel, N. (2018). How to master the host immune system? *Leishmania* parasites have the solutions! *Int. Immunol.* 30, 103–111. doi: 10.1093/intimm/dxx075

Sassi, F., Tamone, C., and D'Amelio, P. (2018). Vitamin D: nutrient, hormone, and immunomodulator. *Nutrients* 10:1656. doi: 10.3390/nu10111656

Scott, P., and Novais, F. O. (2016). Cutaneous leishmaniasis: immune responses in protection and pathogenesis. *Nat. Rev. Immunol.* 16, 581–592. doi: 10.1038/nri.2016.72

Sigmundsdottir, H., Pan, J., Debes, G. F., Alt, C., Habtezion, A., Soler, D., et al. (2007). DCs metabolize sunlight-induced vitamin D3 to "program" T cell attraction to the epidermal chemokine CCL27. *Nat. Immunol.* 8, 285–293. doi: 10.1038/ni1433

Silveira, F. T., Lainson, R., and Corbett, C. E. (2004). Clinical and immunopathological spectrum of American cutaneous leishmaniasis with special reference to the disease in Amazonian Brazil: a review. *Memorias Do Instituto Oswaldo Cruz* 99, 239–251. doi: 10.1590/S0074-02762004000300001

Silveira, F. T., Lainson, R., De Castro Gomes, C. M., Laurenti, M. D., and Corbett, C. E. (2009). Immunopathogenic competences of *Leishmania* (V.) braziliensis and L. *(L.) amazonensis* in American cutaneous leishmaniasis. *Parasite Immunol.* 31, 423–431. doi: 10.1111/j.1365-3024.2009.01116.x

Staeva-Vieira, T. P., and Freedman, L. P. (2002). 1,25-dihydroxyvitamin D3 inhibits IFN-gamma and IL-4 levels during *in vitro* polarization of primary murine CD4+ T cells. *J. Immunol.* 168, 1181–9. doi: 10.4049/jimmunol.168.3.1181

Széles, L., Keresztes, G., Töröcsik, D., Balajthy, Z., Krenács, L., Póliska, S., et al. (2009). 1,25-dihydroxyvitamin D3 is an autonomous regulator of the transcriptional changes leading to a tolerogenic dendritic cell phenotype. *J. Immunol.* 182, 2074–83. doi: 10.4049/jimmunol.0803345

Torres-Santos, E. C., Rodrigues, J. M., Moreira, D. L., Kaplan, M. A., and Rossi-Bergmann, B. (1999). Improvement of *in vitro* and *in vivo* antileishmanial activities of 2', 6'-dihydroxy-4'-methoxychalcone by entrapment in poly(D,L-lactide) nanoparticles. *Antimicrob. Agents Chemother.* 43, 1776–8.

Unger, W. W., Laban, S., Kleijwegt, F. S., van der Slik, A. R., and Roep, B. O. (2009). Induction of Treg by monocyte-derived DC modulated by vitamin D3 or dexamethasone: differential role for PD-L1. *Eur. J. Immunol.* 39, 3147–3159. doi: 10.1002/eji.200839103

van Halteren, A. G. S., Tysma, O. M., van Etten, E., Mathieu, C., and Roep, B. O. (2004). 1α,25-Dihydroxyvitamin D3 or analogue treated dendritic cells modulate human autoreactive T cells via the selective induction of apoptosis. *J. Autoimmun.* 23, 233–239. doi: 10.1016/j.jaut.2004.06.004

Velasquez, L. G., Galuppo, M. K., De Rezende, E., Brandão, W. N., Peron, J. P., Uliana, S. R., et al. (2016). Distinct courses of infection with *Leishmania* (L.) *amazonensis* are observed in BALB/c, BALB/c nude and C57BL/6 mice. *Parasitology* 143, 692–703. doi: 10.1017/S003118201600024X

Whitcomb, J. P., Deagostino, M., Ballentine, M., Fu, J., Tenniswood, M., Welsh, J., et al. (2012). The role of vitamin D., and vitamin D receptor in immunity to *Leishmania* major infection. *J. Parasitol. Res.* 2012:134645. doi: 10.1155/2012/134645

Yang, H. F., Zhang, Z. H., Chang, Z. Q., Tang, K. L., Lin, D. Z., and Xu, J. Z. (2013). Vitamin D deficiency affects the immunity against *Mycobacterium tuberculosis* infection in mice. *Clin. Exp. Med.* 13, 265–270. doi: 10.1007/s10238-012-0204-7

Zhang, Z., Chen, F., Li, J., Luo, F., Hou, T., and Xu, J. (2018). 1,25(OH)2D3 suppresses proinflammatory responses by inhibiting Th1 cell differentiation and cytokine production through the JAK/STAT pathway. *Am. J. Transl. Res.* 10, 2737–2746.

Conflict of Interest Statement: The authors declare that the research was conducted in the absence of any commercial or financial relationships that could be construed as a potential conflict of interest.

frontiers in Cellular and Infection Microbiology

REVIEW
published: 11 April 2019
doi: 10.3389/fcimb.2019.00100

Modulation of Host-Pathogen Communication by Extracellular Vesicles (EVs) of the Protozoan Parasite *Leishmania*

George Dong†*, Alonso Lira Filho*† *and Martin Olivier**

Infectious Diseases and Immunity in Global Heath Program, The Research Institute of the McGill University Health Centre, Montreal, QC, Canada

Leishmania genus protozoan parasites have developed various strategies to overcome host cell protective mechanisms favoring their survival and propagation. Recent findings in the field propose a new player in this infectious strategy, the *Leishmania* exosomes. Exosomes are eukaryotic extracellular vesicles essential to cell communication in various biological contexts. In fact, there have been an increasing number of reports over the last 10 years regarding the role of protozoan parasite exosomes, *Leishmania* exosomes included, in their capacity to favor infection and propagation within their hosts. In this review, we will discuss the latest findings regarding *Leishmania* exosome function during infectious conditions with a strong focus on *Leishmania*-host interaction from a mammalian perspective. We also compare the immunomodulatory properties of *Leishmania* exosomes to other parasite exosomes, demonstrating the conserved, important role that exosomes play during parasite infection.

Keywords: ***Leishmania*, macrophage, exosome, host-pathogen interaction, immunomodulation**

OPEN ACCESS

Edited by:
Claudia Ida Brodskyn, Gonçalo Moniz Institute (IGM), Brazil

Reviewed by:
Xing-Quan Zhu, Lanzhou Veterinary Research Institute (CAAS), China
Maria Fernanda Laranjeira-Silva, University of São Paulo, Brazil

****Correspondence:***
Martin Olivier
martin.olivier@mcgill.ca

†*These authors share equal co-authorship*

Specialty section:
This article was submitted to Parasite and Host, a section of the journal Frontiers in Cellular and Infection Microbiology

Received: *18 December 2018*
Accepted: *25 March 2019*
Published: *11 April 2019*

Citation:
Dong G, Filho AL and Olivier M (2019) Modulation of Host-Pathogen Communication by Extracellular Vesicles (EVs) of the Protozoan Parasite Leishmania. Front. Cell. Infect. Microbiol. 9:100. doi: 10.3389/fcimb.2019.00100

INTRODUCTION

Leishmaniasis is a complex pattern of diseases caused by sand fly-transmitted *Leishmania sp*. With more than 300 million people living in *Leishmani*a-endemic areas (Alvar et al., 2012), there are over 2 million new cases of leishmaniasis every year resulting in 30 000 deaths each year (WHO, 2015). In mammals, *Leishmania* parasites establish a persistent infection by inducing macrophage dysfunction through direct manipulation of macrophage signaling. We have deciphered the mechanisms whereby *Leishmania* exploits macrophage signaling pathways to block microbicidal functions and innate inflammatory responses during infection (Olivier et al., 2005; Isnard et al., 2012). Our lab has previously demonstrated how *Leishmania* major surface protease GP63 manipulates macrophage responses to promote infection through direct activation of protein tyrosine phosphatases (Gomez et al., 2009), thus negatively downregulating JAK and MAP kinase pathways and cleaving key signaling molecules such as the transcription factors AP-1 and NF-κB (Abu-Dayyeh et al., 2008; Contreras et al., 2010; Shio et al., 2015).

Additional investigation from our lab has demonstrated how *Leishmania* parasites, like the majority of eukaryotic cells and other protozoan parasites, release extracellular vesicles (EVs) that play a key role in macrophage modulation. These cellular entities are a vehicle for biologically active macromolecules, such as proteins and nucleic acids, which, once delivered, act on the physiology and function of host cells. Generally grouped according to various criteria including

size, density, and location within cells, these vesicles originate from the cell membrane. They have been termed microparticles, microvesicles, or even ectosomes. On the other hand, exosomes are produced inside and released by multivesicular bodies (MVB) when the latter merge with the plasma membrane (Tkach and Thery, 2016). In scientific literature, the term "exosome" is generally used in reference to a group of mixed EVs regardless of their intracellular provenance. Advanced scientific techniques should soon be capable of distinguishing the many types of EVs (Thery et al., 2009; Raposo and Stoorvogel, 2013; Tkach and Thery, 2016). Recently, the universality of exosomes and their numerous possible applications in medicine (diagnostics or treatment) have garnered them special consideration.

40–120 nm in size, ultracentrifugation (at 100,000 g or greater) is necessary to the sedimentation of exosomes (Johnstone et al., 1987). Linear sucrose gradients can be used for additional purification given their specific density in the medium (1.13–1.19 g/ml) (Raposo et al., 1996). Exosomes occur when the endosomal membrane invaginates into MVBs. Melding of the latter with the plasma membrane (PM) leads to exosome secretion (Thery et al., 2002). This novel EV biogenesis pathway was first noted in transferrin secretion by reticulocytes (Harding et al., 1983; Pan et al., 1985). This distinguished exosomes from other EVs that were thought to simply bud from the PM. The mechanism of protein sorting into these vesicles is remarkably organized as well as contingent on the type and biological status of the original cell (Thery et al., 2002). That said, given their frequent enrichment within exosomes, select proteins are thought to be necessary to exosome generation in MVBs. This suggests some conservation in terms of the sorting and biogenesis pathway (Baietti et al., 2012).

Exosomes originating from distinct cell varieties consist of different endosome-associated proteins. Rab GTPases are one example, or proteins included in MVB synthesis (Alix, Tsg101) (Thery et al., 2009; Taylor and Gercel-Taylor, 2011; Raposo and Stoorvogel, 2013). Additionally, within exosomes there are numerous categories of proteins that are constantly present: heat shock proteins (HSP60, HSP70, HSP90), proteins with adhesion activity (tetraspanins CD81, CD63, CD37), annexins (I, II, V, VI), cytoskeletal proteins (actin, tubulin), metabolic enzymes, and proteins with translational (Elongation Factors 1, 2) or signaling activity (Schorey and Bhatnagar, 2008; Simpson et al., 2008; Thery et al., 2009; Silverman et al., 2010a; Hassani et al., 2011; Taylor and Gercel-Taylor, 2011; Yang and Robbins, 2011; Raposo and Stoorvogel, 2013; Atayde et al., 2015). Exosomes also contain mRNAs and microRNAs (miRNA) that can be transmitted to cells of interest in a functional state (Valadi et al., 2007; Zomer et al., 2010).

THE CRITICAL ROLE OF EXOSOMES IN CELL-CELL COMMUNICATION

Exosomes play a role in numerous biological processes, both pathophysiological and physiological. They have been identified in many types of biological material including saliva, urine, plasma, breast milk, and amniotic fluid (Admyre et al., 2007; Keller et al., 2007, 2011; Looze et al., 2009; Moon et al., 2011). Currently, uses for exosomes in the treatment of cancer and infectious diseases are being extensively studied, as well as their possible function in regenerative therapy, targeted therapy, and more (Lener et al., 2015). With the popularity of exosome research, the International Society for Extracellular Vesicles (ISEV) has implemented a gold standard for the isolation and analysis of extracellular vesicles, exosomes included. For instance, this includes the use of nanovesicle tracking assay (NTA) for the determination of population homogeneity, use of transmission electron microscopy (TEM) for morphological observation, use of linear sucrose gradients to assess their density, as well as the use of mass spectrometry, western blotting, and high throughput sequencing to precisely analyze their protein and RNA contents (Lötvall et al., 2014). Classification of *Leishmania* exosomes requires such analyses.

The enrichment of certain molecules in exosomes, including tetraspanins and integrins (involved in adhesion and cell communication), suggests that the cooperation between said proteins and their counterparts found on the plasma membrane of the target cell facilitates exosome delivery. Moreover, various stimuli can induce changes in tetraspanin composition that impacts the selection of targets by exosomes (Rana and Zoller, 2011; Andreu and Yanez-Mo, 2014). Exosomes merge with the plasma membrane of the target cell for direct cargo transfer (Silverman et al., 2010a) or undergo endocytosis or phagocytosis (Feng et al., 2010; Bastos-Amador et al., 2012). Additionally, certain exosomes can deliver their information through simple attachment to target cells (fusion, endocytosis, or phagocytosis are unnecessary); specifically exosomes expressing MHC II in their interaction with T-cells (Yang and Robbins, 2011). That said, demonstration of the majority of the aforementioned methods of interaction came from experiments performed *in vitro*; as such, the mechanisms taking place *in vivo* are still in question.

SECRETION OF EXOSOMES CONTAINING *Leishmania* PROTEINS

As with higher eukaryotes, the parasite *Leishmania* and members of the trypanosomatids use the ER/Golgi-mediated secretion system (McConville et al., 2002; Corrales et al., 2010), polarizing parasite proteins toward the parasites' flagellar pocket (Field et al., 2007) Several *Leishmania* virulence factors, including the metalloprotease GP63 and other immunomodulatory proteins, use this pathway to exit the host cell (Yao et al., 2003; Joshi et al., 2005). For example, the cysteine proteases of *L. mexicana* are sorted to lysosomes and then released via the flagellar pocket upon their passage into the Golgi apparatus (Brooks et al., 2000).

One of the first pieces of evidence for the use of non-conventional secretory mechanisms in trypanosomatids was revealed while studying their hydrophilic acylated surface proteins (HSAPs). HSAPB is a surface protein found in many *Leishmania,* possessing the unique characteristic of lacking a signal peptide, a transmembrane domain, and a GPI-anchor site. Denny et al. revealed a sequence of amino acids in the protein's N-terminal region that seems to act as a signal peptide, allowing

HSAPB distribution to the plasma membrane. To support this, they transferred a fluorescent GFP protein to the parasite surface by simply adding this sequence of amino acids. Interestingly, HSAPB transfection of mammalian cells also brought about its cell surface translocation, establishing that similar protein trafficking can occur in higher eukaryotes (Denny et al., 2000).

Included among non-conventional mechanisms of protein secretion is the exosomal pathway, since the majority of exosome proteins do not bear a predicted signal peptide (Thery et al., 2009; Hassani et al., 2011; Atayde et al., 2015). Importantly, this pathway is not rare and found to be a cardinal mechanism utilized by a great number of eukaryotic organisms, including protozoan parasites such as *Leishmania*.

The accurate analysis of the complex proteins of exosomes is now possible by advanced mass spectrometry. This further applies to the identification of a myriad of proteins belonging to the secretomes of various cell types (Skalnikova et al., 2011), microscopic unicellular (Silverman et al., 2008; Cuervo et al., 2009; Atyame Nten et al., 2010; Geiger et al., 2010) and multicellular organisms (Moreno et al., 2011), and various tissues (Pardo et al., 2012). Information stemming from these analyses is of paramount importance for our understanding of the mechanisms of secretion and responses of cells to diverse stimuli. Notably, different laboratories have reported that, similar to higher eukaryotes, the majority of *Leishmania* species studied to date also have a low percentage of exosomal proteins that bear a signal peptide (Thery et al., 2009; Hassani et al., 2011; Atayde et al., 2015). This suggests that a great majority of proteins belonging to the secretome of various organisms are non-conventionally secreted (Silverman et al., 2008; Cuervo et al., 2009; Atyame Nten et al., 2010; Geiger et al., 2010).

Vesicle release, common to organisms including prokaryotes, protozoans, fungi, archaea, and higher eukaryotes, has been proposed as universal (Deatherage and Cookson, 2012). Exosomes are special in that they are derived from the endocytic pathway, rather than from direct budding from the plasma membrane like other EVs (Tkach and Thery, 2016). In mammalian cells, the most important pathway requires the action of endosomal sorting complexes necessary for transport (ESCRT) proteins. These ESCRT proteins were first discovered in yeast by selecting for mutant yeasts deficient in vacuole biogenesis and sorting, resulting in the discovery of vacuolar sorting proteins (VPS) (Banta et al., 1988). There are 4 ESCRT complexes, ESCRT 0-III, and they are responsible for the formation of MVBs, as well as the sequestration of ubiquitinated proteins into the intraluminal vesicles (ILVs) (Raposo and Stoorvogel, 2013).

Interestingly, this ESCRT machinery seems common to eukaryotes, including trypanosomatids (Leung et al., 2008). In trypanosomatids, the exact processes responsible for secretion of exosomes are still unclear, but they appear comparable biochemically to those of mammalian exosomes in terms of density and morphology (Silverman et al., 2008, 2010a; Trocoli Torrecilhas et al., 2009). Furthermore, TEM analyses offer convincing arguments for the direct, *in vivo* secretion of exosomes by *Leishmania* through MVBs (Atayde et al., 2015), while Rab GTPases, Alix, and ESCRT orthologs were found through proteomic analyses of *Leishmania* exosomes/exoproteome (Silverman et al., 2008, 2010a; Corrales et al., 2010; Deatherage and Cookson, 2012; Atayde et al., 2015); this suggests a pathway analogous to that of the mammalian ESCRT-dependent pathway previously reported. Although ESCRT-independent exosome biogenesis pathways have been described in mammalian cells and other parasites, this area has yet to be explored in depth in *Leishmania* (Theos et al., 2006; Trajkovic et al., 2008). For example, sphingomyelinase and tetraspanin CD63 have been identified in *Fasciola hepatica*, the common liver fluke, which represent an alternative pathway for cargo sorting and invagination of the endosome for MVB formation (Cwiklinski et al., 2015). The mechanisms for exosome secretion itself remain unclear, though soluble NSF-attachment protein receptor (SNARE) complexes and the RAB family of small GTPases have been suggested to be involved in mammalian cells (Thery et al., 2009; Raposo and Stoorvogel, 2013).

Leishmania EXOSOMES: ITS IMPACT ON CUTANEOUS LEISHMANIASIS PROGRESSION

In the last 10 years, several groups reported that various *Leishmania* species secrete exosomes in culture and in the midgut of its sand fly vector. These vesicles are actively manipulating host signaling and immune cell functions, as per the enrichment by *Leishmania* exosomes of virulence factors such as GP63 (Silverman et al., 2010a,b; Hassani et al., 2014; Atayde et al., 2015). Experiments performed on macrophages *in vitro* and with mice *in vivo* brought clear evidences that enrichment of *Leishmania* virulence factors by exosomes is of cardinal importance for the infectious process and the development of pathologies related to leishmaniasis.

Our interest, in regards to the study of *Leishmania* exosomes, was initially triggered by the observation of intra-macrophage vesicles clustering around the *Leishmania* surface protease GP63, leading us to hypothesis that *Leishmania* parasite can form and release extracellular vesicles, including exosomes (Gomez et al., 2009; Gomez and Olivier, 2010). Initial evidence for *Leishmania* exosome secretion was obtained through the study of *L. mexicana* exoproteome (Hassani et al., 2011), but Silverman et al. were the first to report *bona fide* secretion of *Leishmania* exosomes (Silverman et al., 2010a). However, in our study, we found that temperature shift (TS) mimicking the conditions for inoculation of *Leishmania* into its host was sufficient to cause a rapid and important augmentation in protein release from the *Leishmania* parasite in culture alongside a clear increase of exosome-like vesicles being released from the parasites' surface (see **Figure 1**). Additionally, the majority of *Leishmania* exosomal proteins were found to be secreted non-conventionally, as per their proteomic analysis (Hassani et al., 2011). We further showed that *L. mexicana* exosomes released upon TS possessed a similar capacity to inhibit several macrophage microbicidal functions as the parasite *per se*, relying on the induction of PTP activity concurring to the alteration of key host cell signaling pathways.

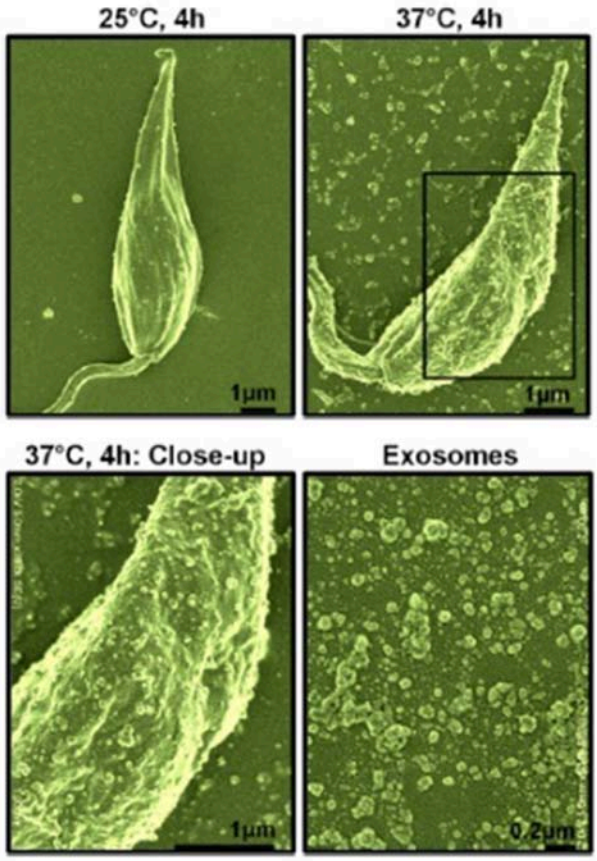

FIGURE 1 | Scanning electron microscopy of *L. mexicana* parasites before and after temperature shift. Top left, Parasites at 25◦C for 4 h; Top right, Parasites at 37◦C for 4 h; Bottom left, Close-up of parasite surface at 37◦C; Bottom right, purified exosomes. Exosomes were of 40–100 nm in size as per electron microscopy observation [from Hassani et al. (2011)].

Thereafter, the role of exosome-enriched *Leishmania* GP63 and its impact on immune cell functions was explored. Using a *L. major* gp63$^{-/-}$ (KO), it was found that the immunomodulatory capacities of leishmanial exosomes deficient in the metalloprotease GP63 were strikingly abrogated in comparison to *L. major* wild type (WT). This strongly supports the cardinal role of exosome-enriched *Leishmania* virulence factors in the infectious process. Using qRT-PCR analysis, this was further confirmed by the divergent capacity of WT and KO exosomes to induce macrophage gene expression, such as cytokines and chemokines. Of utmost interest is how the proteomic analysis of WT and KO exosomes revealed such drastic modification of their protein contents, suggesting that GP63 in *Leishmania* participates in the regulation of exosomal protein sorting (Hassani et al., 2014).

Studies performed in Reiner's lab further established the impact of *Leishmania* exosomes on host immune responses (Silverman et al., 2010a,b). For instance, they observed that exosomes from *Leishmania donovani* can modify the secretion of IL-10 and TNF-α by human monocytes subjected to IFN-γ stimulation. Furthermore, they found that mice treated with *L. donovani* exosomes will have an augmented production of CD4^{+} T-cells producing IL-10 and IL-4 once challenged with infectious *Leishmania*, which could explain in part the exacerbated skin inflammation they observed (Silverman et al., 2010b). Findings stemming from these studies suggested that *Leishmania* exosomes are mainly favoring an immunosuppressive status permitting the parasite to better propagate within its infected host. More recently, a study by Lambertz et al. reported enrichment of small RNAs originating from non-coding RNAs in various *Leishmania* species' exosomes. Unfortunately, the role for this cargo has not been investigated in depth, therefore its potential impact in the infectious process remains uncertain (Lambertz et al., 2015).

RELEASE OF *Leishmania* EXOSOMES WITHIN SAND FLY MIDGUTS

For many years, a great number of investigations dealing with extracellular vesicles were done with vesicles obtained from diverse biological fluids and supernatants from cells cultured *in vitro*. Until recently, the observation of exosome biogenesis and their exit from the cell in an *in vivo* context has proved to be an incredible challenge. After years of effort, we have been able to report a seminal finding demonstrating that *Leishmania* exosomes were produced and released in the sandfly vector midgut and are egested during blood meals together with *Leishmania* parasites (see **Figure 2**). This co-inoculation was found to significantly augment skin lesion due to the synthesis of key pro-inflammatory cytokines, such as IL-17a (Atayde et al., 2015). Of utmost importance, this work represents the first demonstration that GP63-enriched *Leishmania* exosomes are critical vector-inoculated virulence factors and solidly places these *Leishmania* vesicles as important infectious agents necessary for proper progression of the *Leishmania* life cycle.

Contrasting with the work of Silverman et al. using *L. major* exosomes (Silverman et al., 2010b), we found the induction of IL-17a to be increased relative to IL-4 (Atayde et al., 2015). This can be in part due to the fact that instead of vaccinating mice with exosomes, we directly co-injected exosomes and parasites together, therefore better mimicking what is happening in natural conditions. IL-17a is known to be a hallmark of neutrophil recruitment during the development of *Leishmania*-induced human and murine lesions (Lopez Kostka et al., 2009; Boaventura et al., 2010). Previous findings from our laboratory are in accordance with the fact that *Leishmania* exosome inoculation trigger neutrophil recruitment at the site of injection (Deatherage and Cookson, 2012).

Leishmania RNA VIRUS 1 ENHANCES MUCOCUTANEOUS LEISHMANIASIS USING EXOSOMES

Leishmania, being eukaryotic organisms themselves, are a host to infectious agents as well, including viruses like *Leishmania* RNA Virus 1 (LRV1) (Guilbride et al., 1992). The significance

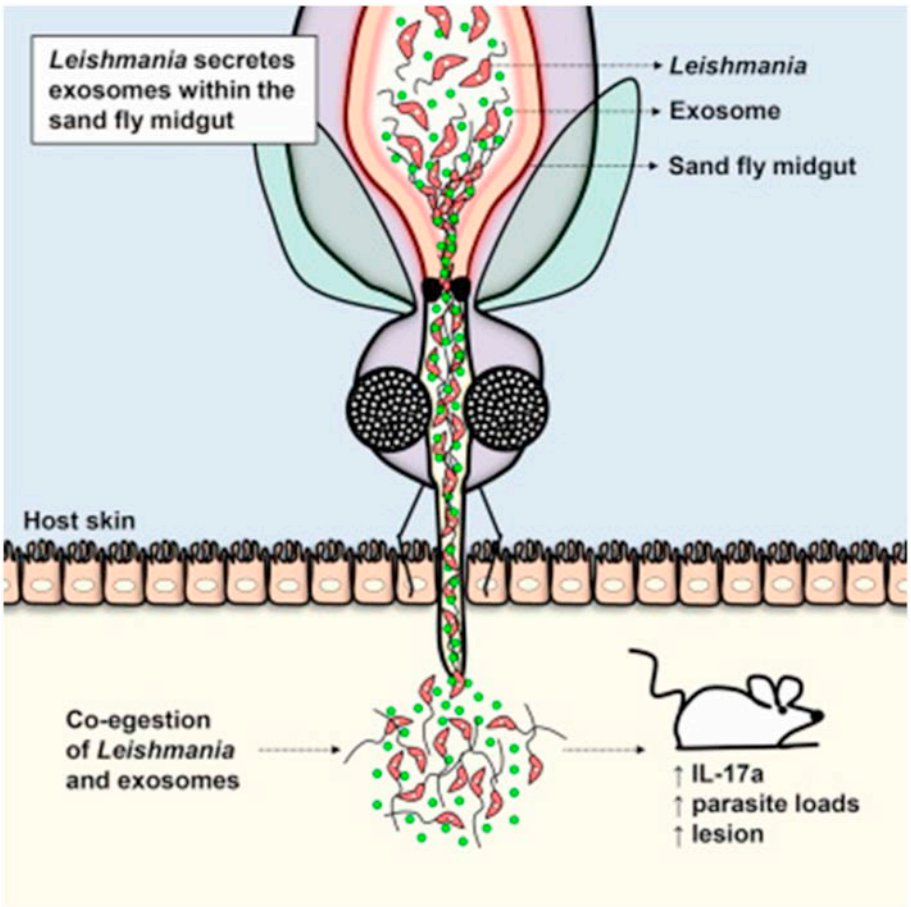

FIGURE 2 | Cartoon depicting the release of *Leishmania* exosomes within the sand fly midguts and their egestion during the insect blood meal. Their co-inoculation seems to favor skin hyperinflammation and increase in parasitic load [from Atayde et al. (2015)].

of this was revealed when Ives et al. reported that LRV1 modulates mucocutaneous leishmaniasis when investigating *L. guyanensis*, a member of the *L. Viannia* subgenus and a common cause of mucocutaneous leishmaniasis (Ives et al., 2011). They identified two groups of *L. guyanensis* clones, metastatic (LgM^+) and non-metastatic (LgM^-), based on their ability to cause secondary lesion formation in hamsters. When investigating the role of macrophage Toll-like receptors (TLR), they found that metastasis caused by LgM^+ was dependent on TLR3 and enhanced by TLR7. This was particularly interesting since TLR3 and TLR7 recognize double stranded and single stranded RNA, respectively (Doyle and O'Neill, 2006), implicating a viral infection taking place in the LgM^+ infected macrophages. Ives et al. were able to quantify LRV1 infection of *L. guyanensis* by RT-qPCR, and showed that LgM^+ had higher viral load compared to LgM^-. They further demonstrated that $TLR3^{-/-}$ and $TLR7^{-/-}$ mice did not display enhanced inflammation or pathology when infected with LgM^+ compared to LgM^- and $LgLRV^-$.

Building upon this discovery, our group recently demonstrated that *Leishmania* exosomes play an important role in the LRV1 life cycle by protecting the whole LRV1 virion from a potential dangerous external environment (e.g., from the action of RNAses) (Atayde et al., 2019). Another defense mechanism that this exosomal coating confers to the virus is the ability to disguise LRV1 since these *Leishmania* exosomes are naturally integrated into the naive recipient parasites, leading to an increase of in infectivity. In this way, *Leishmania* exosomes act both as a protecting and facilitating viral carrier. Exosomes bear a striking resemblance to viral particles on many levels, including their structure and physical properties. This similarity is a possible reason why exosomes are exploited by HIV to facilitate their distribution (Teow et al., 2016). In fact, a variety of viruses, including HCV, HAV, HSV, and EBV, have all had exosome release in the course of infection linked to their pathological processes (Meckes and Raab-Traub, 2011; Alenquer and Amorim, 2015). However, this is the first time exosomes have been shown to carry the whole virion. We could also conclude that the newly LRV1-infected parasites generated a more aggressive form of leishmaniasis in a mice infection model, demonstrating how this exosomal coating process used by LRV1 is also important in the context of the mammalian host; it can be

said that *Leishmania* and LRV1 have a mutualistic relationship facilitated by exosomes.

PARASITE-DERIVED EXOSOMES/EVS

The prospective uses of exosomes and various pathogen-secreted vesicles as immunomodulators are countless; they are being further explored for their potential in treatments or vaccine development. Combined with cutting-edge genomics techniques like CRISPR, a better understanding of pathogen-derived EVs may allow the engineering of exosomes and other EVs that stimulate and promote an immune response and host protection in the hopes of combatting infectious diseases.

Exosomes have been shown to possess both immune-stimulatory and -inhibitory effects in eukaryote pathogens. For example, Oliveira et al. recently demonstrated that *Cryptococcus neoformans* produces exosome-like vesicles that lead to the release of TNF, IL-10, and NO through stimulation of macrophages. Macrophage priming with the aforementioned vesicles facilitates the killing of fungi (Oliveira et al., 2010). In contrast, extracellular vesicles originating from *T. cruzi* and administered to mice led to a worsened infection; lower iNOS and higher IL-4 and IL-10 levels were observed, as well as greater localization of parasites to the viscera and heart (Trocoli Torrecilhas et al., 2009).

In addition, another parasite of the genus *Trypanosoma*, *T. brucei,* has been reported to use extracellular vesicles in their pathogenesis. In the study performed by Szempruch et al., bloodstream parasites could be observed producing extracellular vesicles enriched in flagellar proteins and virulence factors including serum resistance-associated protein (SRA), a well-defined protein of this group (Trocoli Torrecilhas et al., 2009). More interestingly, when stimulating non-human infectious trypanosomes with these vesicles, SRA was transferred to these parasites, giving them the ability to evade the innate immune response. Finally, these extracellular vesicles were able to fuse with erythrocytes and make them express Variant Surface Glycoprotein (VSG), leading to a rapid clearance of these cells by the immune system and resulting in anemia in two distinct mouse strains. In a more recent study by another group, these vesicles were also found to affect the social motility of parasites; they drove parasites away, repelling them from overstressed or compromised cells, thus providing a novel function for these vesicles in the parasite life cycle (Eliaz et al., 2017).

In a similar fashion, *Trichomonas vaginalis* exosomes were found to be produced and released with similar biophysical properties to mammalian vesicles, sharing many proteins found in the mammalian exosome proteome (e.g., tetraspanins, Alix, and Rabs) (Twu et al., 2013). In addition to their ability to fuse and deliver proteins to vaginal epithelial cells, exosomes from strains of very adherent parasites improved the adherence of strains of less adherent parasites. Furthermore, the extracted exosomes led to production of IL-6 in stimulated epithelial cells while down-regulating IL-8 yield. This potential immune modulation was further studied by Olmos-Ortiz et al. (2017), who showed *T. vaginalis* exosomes not only increased IL-6 production but highly increased IL-10 production in macrophages. The possible anti-inflammatory role of *T. vaginalis* exosomes was tested in a murine *in-vivo* model, which showed that pre-treatment with these vesicles lead to a diminished inflammatory response after *T. vaginalis* infection, favoring the persistence and viability of the parasite.

IMPACT OF IMMUNE CELL EXOSOMES AND CONTROL OVER INFECTIOUS AGENTS

The function of host exosomes during infection by related parasites has also been explored during this time period. While most in-depth studies were related to cancer, reports of exosomes playing unique, crucial roles during host viral, bacterial, or protozoan infection are accumulating.

Schorey lab reported that exosomes containing glycopeptidolipids derived from *Mycobacterium* can be released from macrophages infected by various species of the bacteria, and contain numerous *Mycobacterium*-derived proteins (Bhatnagar and Schorey, 2007; Giri et al., 2010). Particularly, it was demonstrated that said exosomes can lead to protection against infection by *M. tuberculosis* in mice through production of iNOS and TNF-α by naive macrophages; a pro-inflammatory response (Bhatnagar and Schorey, 2007; Cheng and Schorey, 2013). Further testing by said group explored infection of macrophages with *Mycobacterium* ssp., *Salmonella typhimurium*, and *Toxoplasma gondii* (protozoan parasite) and demonstrated that the produced exosomes also prompted MyD88- and TLR-dependent production of TNF-α by naive macrophages (Bhatnagar et al., 2007). Interestingly, exosomes from dendritic cells infected with *T. gondii* used to vaccinate mouse fetuses were reported to offer protection against congenital infection (Beauvillain et al., 2009).

Infection of reticulocytes by *Plasmodium yoelii* and immunization with the released exosomes was investigated by Martin-Jaular et al. Said exosomes had previously been shown to incorporate the parasites' proteins, and authors noted impressive protection of immunized mice when later challenged with infection by *P. yoelii* (Martin-Jaular et al., 2011). Research from 2013 demonstrated how *P. falciparum*-infected erythrocytes are capable of using released exosomes to communicate with certain parasites among a population, evidence suggesting that exosomes may be crucial to the transfer of *P. falciparum* to its insect vector (Regev-Rudzki et al., 2011). Likewise, a newer investigation performed by the aforementioned researchers showed that these vesicles contain small RNA and genomic DNA of the parasite and can reach human monocytes, which will lead to a STING-dependent DNA sensing, possibly acting as an immune decoy, favoring parasite survival (Sisquella et al., 2017).

In this same time period, we studied the outcome of infection by *Leishmania* on release of exosomes by macrophages (Hassani and Olivier, 2013). Exosome production by macrophages (untreated, LPS-stimulated, and *L. mexicana*-infected) was compared using proteomic analyses. We noted that stimulation by LPS and infection by *Leishmania* lead to both similar

and dissimilar variations in protein function group sorting (particularly plasma membrane-associated proteins) into exosomes; additionally, signaling molecules (including MAPK) were differentially induced in naive macrophages by said exosomes. This work demonstrated that, within exosomes liberated by infected macrophages, *Leishmania* GP63 was the sole enriched *Leishmania* protein (Hassani and Olivier, 2013).

Importantly, from the perspective of all the work performed up to now, it is clear that *Leishmania* exosomes are pro-active components of this parasitic infection, both *in vitro* and *in vivo*, mainly influencing the early innate immune response during *Leishmania* infection to favor the parasite's survival, allowing it to fully establish itself within the mammalian host. Although it has been suggested that non-vesicular components display immunomodulatory potential (Perez-Cabezas et al., 2019), offering the counterpoint that EVs are not the sole effector of immunomodulation, the vast majority of findings stemming from these various studies fully establish *Leishmania* exosomes as cardinal virulence factors.

In conclusion, we hope that this review brings about a new and more in-depth understanding of the part that *Leishmania* exosomes and various infectious agents play in the context of host-parasite interactions, with a particular focus on the establishment of infection. Future research in this field of investigations is critical for the development of new vaccine and diagnostic tools.

AUTHOR CONTRIBUTIONS

The first draft was done by MO. AF and GD added new information.

FUNDING

Research in MO laboratory is supported by the Canadian Institute of Health Research (grant number: PJT-159765) and the Natural Sciences and Engineering Research Council (grant number: RGPIN-2018-03849) of Canada. AF is recipient of a studentship from Science without Border (Brazil). GD is recipient of a studentship from the experimental medicine program of McGill University.

REFERENCES

Abu-Dayyeh, I., Shio, M. T., Sato, S., Akira, S., Cousineau, B., and Olivier, M. (2008). *Leishmania*-induced IRAK-1 inactivation is mediated by SHP-1 interacting with an evolutionarily conserved KTIM motif. *PLoS Negl. Trop. Dis.* 2:e305. doi: 10.1371/journal.pntd.0000305

Admyre, C., Johansson, S. M., Qazi, K. R., Filen, J. J., Lahesmaa, R., Norman, M., et al. (2007). Exosomes with immune modulatory features are present in human breast milk. *J. Immunol.* 179, 1969–1978. doi: 10.4049/jimmunol.179.3.1969

Alenquer, M., and Amorim, M. J. (2015). Exosome biogenesis, regulation, and function in viral infection. *Viruses* 7, 5066–5083. doi: 10.3390/v7092862

Alvar, J., Velez, I. D., Bern, C., Herrero, M., Desjeux, P., Cano, J., et al. (2012). Leishmaniasis worldwide and global estimates of its incidence. *PLoS ONE* 7:e35671. doi: 10.1371/journal.pone.0035671

Andreu, Z., and Yanez-Mo, M. (2014). Tetraspanins in extracellular vesicle formation and function. *Front. Immunol.* 5:442. doi: 10.3389/fimmu.2014.00442

Atayde, V. D., Aslan, H., Townsend, S., Hassani, K., Kamhawi, S., and Olivier, M. (2015). Exosome secretion by the parasitic protozoan *Leishmania* within the sand fly midgut. *Cell Rep.* 13, 957–967. doi: 10.1016/j.celrep.2015.09.058

Atayde, V. D., da Silva Lira Filho, A., Chaparro, V., Zimmermann, A., Martel, C., Jaramillo, M., et al. (2019). Exploitation of the *Leishmania* exosomal pathway by *Leishmania* RNA virus 1. *Nat. Microbiol.* 4, 714–723. doi: 10.1038/s41564-018-0352-y

Atyame Nten, C. M., Sommerer, N., Rofidal, V., Hirtz, C., Rossignol, M., Cuny, G., et al. (2010). Excreted/secreted proteins from trypanosome procyclic strains. *J. Biomed. Biotechnol.* 2010:212817. doi: 10.1155/2010/212817

Baietti, M. F., Zhang, Z., Mortier, E., Melchior, A., Degeest, G., Geeraerts, A., et al. (2012). Syndecan-syntenin-ALIX regulates the biogenesis of exosomes. *Nat. Cell. Biol.* 14, 677–685. doi: 10.1038/ncb2502

Banta, L. M., Robinson, J. S., Klionsky, D. J., and Emr, S. D. (1988). Organelle assembly in yeast: characterization of yeast mutants defective in vacuolar biogenesis and protein sorting. *J. Cell Biol.* 107:1369.

Bastos-Amador, P., Perez-Cabezas, B., Izquierdo-Useros, N., Puertas, M. C., Martinez-Picado, J., Pujol-Borrell, R., et al. (2012). Capture of cell-derived microvesicles (exosomes and apoptotic bodies) by human plasmacytoid dendritic cells. *J. Leukoc. Biol.* 91, 751–758. doi: 10.1189/jlb.0111054

Beauvillain, C., Juste, M. O., Dion, S., Pierre, J., and Dimier-Poisson, I. (2009). Exosomes are an effective vaccine against congenital toxoplasmosis in mice. *Vaccine* 27, 1750–1757. doi: 10.1016/j.vaccine.2009.01.022

Bhatnagar, S., and Schorey, J. S. (2007). Exosomes released from infected macrophages contain Mycobacterium avium glycopeptidolipids and are proinflammatory. *J. Biol. Chem.* 282, 25779–25789. doi: 10.1074/jbc.M702277200

Bhatnagar, S., Shinagawa, K., Castellino, F. J., and Schorey, J. S. (2007). Exosomes released from macrophages infected with intracellular pathogens stimulate a proinflammatory response *in vitro* and *in vivo*. *Blood* 110, 3234–3244. doi: 10.1182/blood-2007-03-079152

Boaventura, V. S., Santos, C. S., Cardoso, C. R., de Andrade, J., Dos Santos, W. L., Clarencio, J., et al. (2010). Human mucosal leishmaniasis: neutrophils infiltrate areas of tissue damage that express high levels of Th17-related cytokines. *Eur. J. Immunol.* 40, 2830–2836. doi: 10.1002/eji.200940115

Brooks, D. R., Tetley, L., Coombs, G. H., and Mottram, J. C. (2000). Processing and trafficking of cysteine proteases in *Leishmania mexicana*. *J. Cell. Sci.* 113 (Pt 22), 4035–4041.

Cheng, Y., and Schorey, J. S. (2013). Exosomes carrying mycobacterial antigens can protect mice against *Mycobacterium tuberculosis* infection. *Eur. J. Immunol.* 43, 3279–3290. doi: 10.1002/eji.201343727

Contreras, I., Gomez, M. A., Nguyen, O., Shio, M. T., McMaster, R. W., and Olivier, M. (2010). *Leishmania*-induced inactivation of the macrophage transcription factor AP-1 is mediated by the parasite metalloprotease GP63. *PLoS Pathog.* 6:e1001148. doi: 10.1371/journal.ppat.1001148

Corrales, R. M., Sereno, D., and Mathieu-Daude, F. (2010). Deciphering the *Leishmania* exoproteome: what we know and what we can learn. *FEMS Immunol. Med. Microbiol.* 58, 27–38. doi: 10.1111/j.1574-695X.2009.00608.x

Cuervo, P., De Jesus, J. B., Saboia-Vahia, L., Mendonca-Lima, L., Domont, G. B., and Cupolillo, E. (2009). Proteomic characterization of the released/secreted proteins of *Leishmania* (Viannia) braziliensis promastigotes. *J. Proteomics* 73, 79–92. doi: 10.1016/j.jprot.2009.08.006

Cwiklinski, K., de la Torre-Escudero, E., Trelis, M., Bernal, D., Dufresne, P. J., Brennan, G. P., et al. (2015). The extracellular vesicles of the helminth pathogen, *Fasciola hepatica*: biogenesis pathways and cargo molecules involved in parasite pathogenesis. *Mol. Cell. Proteomics* 14, 3258–3273. doi: 10.1074/mcp.M115.053934

Deatherage, B. L., and Cookson, B. T. (2012). Membrane vesicle release in Bacteria, Eukaryotes and Archaea: a conserved yet underappreciated aspect of microbial life. *Infect. Immun.* 80, 1948–1957. doi: 10.1128/IAI.06014-11

Denny, P. W., Gokool, S., Russell, D. G., Field, M. C., and Smith, D. F. (2000). Acylation-dependent protein export in *Leishmania*. *J. Biol. Chem.* 275, 11017–11025. doi: 10.1074/jbc.275.15.11017

Doyle, S. L., and O'Neill, L. A. (2006). Toll-like receptors: from the discovery of NFkappaB to new insights into transcriptional regulations in innate immunity. *Biochem. Pharmacol.* 72, 1102–1113. doi: 10.1016/j.bcp.2006.07.010

Eliaz, D., Kannan, S., Shaked, H., Arvatz, G., Tkacz, I. D., Binder, L., et al. (2017). Exosome secretion affects social motility in *Trypanosoma brucei*. *PLoS Pathog.* 13:e1006245. doi: 10.1371/journal.ppat.1006245

Feng, D., Zhao, W. L., Ye, Y. Y., Bai, X. C., Liu, R. Q., Chang, L. F., et al. (2010). Cellular internalization of exosomes occurs through phagocytosis. *Traffic* 11, 675–687. doi: 10.1111/j.1600-0854.2010.01041.x

Field, M. C., Natesan, S. K., Gabernet-Castello, C., and Koumandou, V. L. (2007). Intracellular trafficking in the trypanosomatids. *Traffic* 8, 629–639. doi: 10.1111/j.1600-0854.2007.00558.x

Geiger, A., Hirtz, C., Becue, T., Bellard, E., Centeno, D., Gargani, D., et al. (2010). Exocytosis and protein secretion in Trypanosoma. *BMC Microbiol.* 10:20. doi: 10.1186/1471-2180-10-20

Giri, P. K., Kruh, N. A., Dobos, K. M., and Schorey, J. S. (2010). Proteomic analysis identifies highly antigenic proteins in exosomes from *M. tuberculosis*-infected and culture filtrate protein-treated macrophages. *Proteomics* 10, 3190–3202. doi: 10.1002/pmic.200900840

Gomez, M. A., Contreras, I., Halle, M., Tremblay, M. L., McMaster, R. W., and Olivier, M. (2009). *Leishmania* GP63 alters host signaling through cleavage-activated protein tyrosine phosphatases. *Sci. Signal.* 2:ra58. doi: 10.1126/scisignal.2000213

Gomez, M. A., and Olivier, M. (2010). Proteases and phosphatases during *Leishmania*-macrophage interaction: paving the road for pathogenesis. *Virulence* 1, 314–318. doi: 10.4161/viru.1.4.12194

Guilbride, L., Myler, P. J., and Stuart, K. (1992). Distribution and sequence divergence of LRV1 viruses among different *Leishmania* species. *Mol. Biochem. Parasitol.* 54, 101–104. doi: 10.1016/0166-6851(92)90099-6

Harding, C., Heuser, J., and Stahl, P. (1983). Receptor-mediated endocytosis of transferrin and recycling of the transferrin receptor in rat reticulocytes. *J. Cell. Biol.* 97, 329–339. doi: 10.1083/jcb.97.2.329

Hassani, K., Antoniak, E., Jardim, A., and Olivier, M. (2011). Temperature-induced protein secretion by *Leishmania mexicana* modulates macrophage signalling and function. *PLoS ONE* 6:e18724. doi: 10.1371/journal.pone.0018724

Hassani, K., and Olivier, M. (2013). Immunomodulatory impact of *Leishmania*-induced macrophage exosomes: a comparative proteomic and functional analysis. *PLoS Neglect. Trop. Dis.* 7:e2185. doi: 10.1371/journal.pntd.0002185

Hassani, K., Shio, M. T., Martel, C., Faubert, D., and Olivier, M. (2014). Absence of metalloprotease GP63 alters the protein content of *Leishmania* exosomes. *PLoS ONE* 9:e95007. doi: 10.1371/journal.pone.0095007

Isnard, A., Shio, M. T., and Olivier, M. (2012). Impact of *Leishmania* metalloprotease GP63 on macrophage signaling. *Front. Cell. Infect. Microbiol.* 2:72. doi: 10.3389/fcimb.2012.00072

Ives, A., Ronet, C., Prevel, F., Ruzzante, G., Fuertes-Marraco, S., Schutz, F., et al. (2011). *Leishmania* RNA virus controls the severity of mucocutaneous leishmaniasis. *Science* 331, 775–778. doi: 10.1126/science.1199326

Johnstone, R. M., Adam, M., Hammond, J. R., Orr, L., and Turbide, C. (1987). Vesicle formation during reticulocyte maturation. Association of plasma membrane activities with released vesicles (exosomes). *J. Biol. Chem.* 262, 9412–9420.

Joshi, M. B., Rogers, M. E., Shakarian, A. M., Yamage, M., Al-Harthi, S. A., Bates, P. A., et al. (2005). Molecular characterization, expression, and *in vivo* analysis of LmexCht1: the chitinase of the human pathogen, *Leishmania mexicana*. *J. Biol. Chem.* 280, 3847–3861. doi: 10.1074/jbc.M412299200

Keller, S., Ridinger, J., Rupp, A. K., Janssen, J. W., and Altevogt, P. (2011). Body fluid derived exosomes as a novel template for clinical diagnostics. *J. Transl. Med.* 9:86. doi: 10.1186/1479-5876-9-86

Keller, S., Rupp, C., Stoeck, A., Runz, S., Fogel, M., Lugert, S., et al. (2007). CD24 is a marker of exosomes secreted into urine and amniotic fluid. *Kidney Int.* 72, 1095–1102. doi: 10.1038/sj.ki.5002486

Lambertz, U., Oviedo Ovando, M. E., Vasconcelos, E. J., Unrau, P. J., Myler, P. J., and Reiner, N. E. (2015). Small RNAs derived from tRNAs and rRNAs are highly enriched in exosomes from both old and new world *Leishmania* providing evidence for conserved exosomal RNA Packaging. *BMC Genomics* 16:151. doi: 10.1186/s12864-015-1260-7

Lener, T., Gimona, M., Aigner, L., Borger, V., Buzas, E., Camussi, G., et al. (2015). Applying extracellular vesicles based therapeutics in clinical trials—an ISEV position paper. *J. Extracellular Vesicles* 4:30087. doi: 10.3402/jev.v4.30087

Leung, K. F., Dacks, J. B., and Field, M. C. (2008). Evolution of the multivesicular body ESCRT machinery; retention across the eukaryotic lineage. *Traffic* 9, 1698–1716. doi: 10.1111/j.1600-0854.2008.00797.x

Looze, C., Yui, D., Leung, L., Ingham, M., Kaler, M., Yao, X., et al. (2009). Proteomic profiling of human plasma exosomes identifies PPARgamma as an exosome-associated protein. *Biochem. Biophys. Res. Commun.* 378, 433–438. doi: 10.1016/j.bbrc.2008.11.050

Lopez Kostka, S., Dinges, S., Griewank, K., Iwakura, Y., Udey, M. C., and von Stebut, E. (2009). IL-17 promotes progression of cutaneous leishmaniasis in susceptible mice. *J. Immunol.* 182, 3039–3046. doi: 10.4049/jimmunol.0713598

Lötvall, J., Hill, A. F., Hochberg, F., Buzás, E. I., Di Vizio, D., Gardiner, C., et al. (2014). Minimal experimental requirements for definition of extracellular vesicles and their functions: a position statement from the International Society for Extracellular Vesicles. *J. Extracellular Vesicles* 3:26913. doi: 10.3402/jev.v3.26913

Martin-Jaular, L., Nakayasu, E. S., Ferrer, M., Almeida, I. C., and Del Portillo, H. A. (2011). Exosomes from *Plasmodium yoelii*-infected reticulocytes protect mice from lethal infections. *PLoS ONE* 6:e26588. doi: 10.1371/journal.pone.0026588

McConville, M. J., Mullin, K. A., Ilgoutz, S. C., and Teasdale, R. D. (2002). Secretory pathway of trypanosomatid parasites. *Microbiol. Mol. Biol. Rev.* 66, 122–154. doi: 10.1128/MMBR.66.1.122-154.2002

Meckes, D. G. Jr., and Raab-Traub, N. (2011). Microvesicles and viral infection. *J. Virol.* 85, 12844–12854. doi: 10.1128/JVI.05853-11

Moon, P. G., You, S., Lee, J. E., Hwang, D., and Baek, M. C. (2011). Urinary exosomes and proteomics. *Mass Spectrometry Rev.* 30, 1185–1202. doi: 10.1002/mas.20319

Moreno, Y., Gros, P. P., Tam, M., Segura, M., Valanparambil, R., Geary, T. G., et al. (2011). Proteomic analysis of excretory-secretory products of *Heligmosomoides polygyrus* assessed with next-generation sequencing transcriptomic information. *PLoS Negl. Trop. Dis.* 5:e1370. doi: 10.1371/journal.pntd.0001370

Oliveira, D. L., Freire-de-Lima, C. G., Nosanchuk, J. D., Casadevall, A., Rodrigues, M. L., and Nimrichter, L. (2010). Extracellular vesicles from *Cryptococcus neoformans* modulate macrophage functions. *Infect. Immun.* 78, 1601–1609. doi: 10.1128/IAI.01171-09

Olivier, M., Gregory, D. J., and Forget, G. (2005). Subversion mechanisms by which *Leishmania* parasites can escape the host immune response: a signaling point of view. *Clin. Microbiol. Rev.* 18, 293–305. doi: 10.1128/CMR.18.2.293-305.2005

Olmos-Ortiz, L. M., Barajas-Mendiola, M. A., Barrios-Rodiles, M., Castellano, L. E., Arias-Negrete, S., Avila, E. E., et al. (2017). Trichomonas vaginalis exosome-like vesicles modify the cytokine profile and reduce inflammation in parasite-infected mice. *Parasite Immunol.* 39:12426. doi: 10.1111/pim.12426

Pan, B. T., Teng, K., Wu, C., Adam, M., and Johnstone, R. M. (1985). Electron microscopic evidence for externalization of the transferrin receptor in vesicular form in sheep reticulocytes. *J. Cell. Biol.* 101, 942–948. doi: 10.1083/jcb.101.3.942

Pardo, M., Roca-Rivada, A., Seoane, L. M., and Casanueva, F. F. (2012). Obesidomics: contribution of adipose tissue secretome analysis to obesity research. *Endocrine* 41, 374–383. doi: 10.1007/s12020-012-9617-z

Perez-Cabezas, B., Santarem, N., Cecilio, P., Silva, C., Silvestre, R., Catita, J. A. M., et al. (2019). More than just exosomes: distinct *Leishmania infantum* extracellular products potentiate the establishment of infection. *J. Extracell Vesicles* 8:1541708. doi: 10.1080/20013078.2018.1541708

Rana, S., and Zoller, M. (2011). Exosome target cell selection and the importance of exosomal tetraspanins: a hypothesis. *Biochem. Soc. Trans.* 39, 559–562. doi: 10.1042/BST0390559

Raposo, G., Nijman, H. W., Stoorvogel, W., Liejendekker, R., Harding, C. V., Melief, C. J., et al. (1996). B lymphocytes secrete antigen-presenting vesicles. *J. Exp. Med.* 183:1161.

Raposo, G., and Stoorvogel, W. (2013). Extracellular vesicles: exosomes, microvesicles, and friends. *J. Cell. Biol.* 200, 373–383. doi: 10.1083/jcb.201211138

Regev-Rudzki, N., Wilson, D. W., Carvalho, T. G., Sisquella, X., Coleman, B. M., Rug, M., et al. (2011). Cell-cell communication between malaria-infected red blood cells via exosome-like vesicles. *Cell* 153, 1120–1133. doi: 10.1016/j.cell.2013.04.029

Schorey, J. S., and Bhatnagar, S. (2008). Exosome function: from tumor immunology to pathogen biology. *Traffic* 9, 871–881. doi: 10.1111/j.1600-0854.2008.00734.x

Shio, M. T., Christian, J. G., Jung, J. Y., Chang, K. P., and Olivier, M. (2015). PKC/ROS-mediated NLRP3 inflammasome activation is attenuated by *Leishmania* zinc-metalloprotease during infection. *PLoS Negl. Trop. Dis.* 9:e0003868. doi: 10.1371/journal.pntd.0003868

Silverman, J. M., Chan, S. K., Robinson, D. P., Dwyer, D. M., Nandan, D., Foster, L. J., et al. (2008). Proteomic analysis of the secretome of *Leishmania donovani*. *Genome Biol.* 9:R35. doi: 10.1186/gb-2008-9-2-r35

Silverman, J. M., Clos, J., de'Oliveira, C. C., Shirvani, O., Fang, Y., Wang, C., et al. (2010a). An exosome-based secretion pathway is responsible for protein export from *Leishmania* and communication with macrophages. *J. Cell. Sci.* 123, 842–852. doi: 10.1242/jcs.056465

Silverman, J. M., Clos, J., Horakova, E., Wang, A. Y., Wiesgigl, M., Kelly, I., et al. (2010b). *Leishmania* exosomes modulate innate and adaptive immune responses through effects on monocytes and dendritic cells. *J. Immunol.* 185, 5011–5022. doi: 10.4049/jimmunol.1000541

Simpson, R. J., Jensen, S. S., and Lim, J. W. (2008). Proteomic profiling of exosomes: current perspectives. *Proteomics* 8, 4083–4099. doi: 10.1002/pmic.200800109

Sisquella, X., Ofir-Birin, Y., Pimentel, M. A., Cheng, L., Abou Karam, P., Sampaio, N. G., et al. (2017). Malaria parasite DNA-harbouring vesicles activate cytosolic immune sensors. *Nat. Commun.* 8:1985. doi: 10.1038/s41467-017-02083-1

Skalnikova, H., Motlik, J., Gadher, S. J., and Kovarova, H. (2011). Mapping of the secretome of primary isolates of mammalian cells, stem cells and derived cell lines. *Proteomics* 11, 691–708. doi: 10.1002/pmic.201000402

Taylor, D. D., and Gercel-Taylor, C. (2011). Exosomes/microvesicles: mediators of cancer-associated immunosuppressive microenvironments. *Semin. Immunopathol.* 33, 441–454. doi: 10.1007/s00281-010-0234-8

Teow, S. Y., Nordin, A. C., Ali, S. A., and Khoo, A. S. (2016). Exosomes in human immunodeficiency virus type I pathogenesis: threat or opportunity? *Adv. Virol.* 2016:9852494. doi: 10.1155/2016/9852494

Theos, A. C., Truschel, S. T., Tenza, D., Hurbain, I., Harper, D. C., Berson, J. F., et al. (2006). A lumenal domain-dependent pathway for sorting to intralumenal vesicles of multivesicular endosomes involved in organelle morphogenesis. *Dev. Cell.* 10, 343–354. doi: 10.1016/j.devcel.2006.01.012

Thery, C., Ostrowski, M., and Segura, E. (2009). Membrane vesicles as conveyors of immune responses. *Nat. Rev.* 9, 581–593. doi: 10.1038/nri2567

Thery, C., Zitvogel, L., and Amigorena, S. (2002). Exosomes: composition, biogenesis and function. *Nat. Rev. Immunol.* 2, 569–579. doi: 10.1038/nri855

Tkach, M., and Thery, C. (2016). Communication by extracellular vesicles: where we are and where we need to go. *Cell* 164, 1226–1232. doi: 10.1016/j.cell.2016.01.043

Trajkovic, K., Hsu, C., Chiantia, S., Rajendran, L., Wenzel, D., Wieland, F., et al. (2008). Ceramide triggers budding of exosome vesicles into multivesicular endosomes. *Science* 319:1244. doi: 10.1126/science.1153124

Trocoli Torrecilhas, A. C., Tonelli, R. R., Pavanelli, W. R., da Silva, J. S., Schumacher, R. I., de Souza, W., et al. (2009). *Trypanosoma cruzi*: parasite shed vesicles increase heart parasitism and generate an intense inflammatory response. *Microbes Infect.* 11, 29–39. doi: 10.1016/j.micinf.2008.10.003

Twu, O., de Miguel, N., Lustig, G., Stevens, G. C., Vashisht, A. A., Wohlschlegel, J. A., et al. (2013). *Trichomonas vaginalis* exosomes deliver cargo to host cells and mediate host:parasite interactions. *PLoS Pathogens* 9:e1003482. doi: 10.1371/journal.ppat.1003482

Valadi, H., Ekstrom, K., Bossios, A., Sjostrand, M., Lee, J. J., and Lotvall, J. O. (2007). Exosome-mediated transfer of mRNAs and microRNAs is a novel mechanism of genetic exchange between cells. *Nat. Cell. Biol.* 9, 654–659. doi: 10.1038/ncb1596

WHO (2015). *Leishmaniasis Fact Sheet No. 375*. Geneva: World Health Organization.

Yang, C., and Robbins, P. D. (2011). The roles of tumor-derived exosomes in cancer pathogenesis. *Clin. Dev. Immunol.* 2011:842849. doi: 10.1155/2011/842849

Yao, C., Donelson, J. E., and Wilson, M. E. (2003). The major surface protease (MSP or GP63) of *Leishmania* sp. Biosynthesis, regulation of expression, and function. *Mol. Biochem. Parasitol.* 132, 1–16. https://doi.org/10.1016/S0166-6851(03)00211-1

Zomer, A., Vendrig, T., Hopmans, E. S., van Eijndhoven, M., Middeldorp, J. M., and Pegtel, D. M. (2010). Exosomes: fit to deliver small RNA. *Commun. Integr. Biol.* 3, 447–450. doi: 10.4161/cib.3.5.12339

Conflict of Interest Statement: The authors declare that the research was conducted in the absence of any commercial or financial relationships that could be construed as a potential conflict of interest.

frontiers in Cellular and Infection Microbiology

ORIGINAL RESEARCH
published: 12 April 2019
doi: 10.3389/fcimb.2019.00105

CD4$^+$ T Cell-Dependent Macrophage Activation Modulates Sustained PS Exposure on Intracellular Amastigotes of *Leishmania amazonensis*

Joao Luiz Mendes Wanderley[1], Poliana Deolindo[2], Eric Carlsen[3], Arieli Bernardo Portugal[1], Renato Augusto DaMatta[4], Marcello Andre Barcinski[5†] and Lynn Soong[6*†]*

[1] Laboratório de Imunoparasitologia, Unidade de Pesquisa Integrada em Produtos Bioativos e Biociências, Universidade Federal do Rio de Janeiro, Macaé, Brazil, [2] Laboratório de Biologia Molecular de Parasitas e Vetores, Fundação Oswaldo Cruz, Rio de Janeiro, Brazil, [3] Department of Pathology, University of Pittsburgh Medical Center, Pittsburgh, PA, United States, [4] Laboratório de Biologia Celular e Tecidual, Universidade Estadual do Norte Fluminense, Campos dos Goytacazes, Brazil, [5] Instituto de Biofísica Carlos Chagas Filho, Universidade Federal do Rio de Janeiro, Rio de Janeiro, Brazil, [6] Department of Microbiology and Immunology, Center for Tropical Diseases, Institute for Human Infections and Immunity, University of Texas Medical Branch, Galveston, TX, United States

Leishmania amazonensis amastigotes can make use of surface-exposed phosphatidylserine (PS) molecules to promote infection and non-classical activation of macrophages (MΦ), leading to uncontrolled intracellular proliferation of the parasites. This mechanism was quoted as apoptotic mimicry. Moreover, the amount of PS molecules exposed on the surface of amastigotes correlates with the susceptibility of the host. In this study, we tested whether host cellular responses influence PS expression on intracellular amastigotes. We found that the level of PS exposure on intracellular amastigotes was modulated by CD4$^+$ T cell and MΦ activation status *in vitro* and *in vivo*. *L. amazonensis* infection generated a Th1/Th2-mixed cytokine profile, providing the optimal MΦ stimulation that favored PS exposure on intracellular amastigotes. Maintenance of PS exposed on the parasite was dependent on low, but sustained, levels of nitric oxide and polyamine production. Amastigotes obtained from lymphopenic nude mice did not expose PS on their surface, and adoptive transfer of CD4$^+$ T cells reversed this phenotype. In addition, histopathological analysis of mice treated with anti-PS antibodies showed increased inflammation and similarities to nude mouse lesions. Collectively, our data confirm the role of pathogenic CD4$^+$ T cells for disease progression and point to PS as a critical parasite strategy to subvert host immune responses.

Keywords: phosphatidylserine, amastigote, T cell, parasitophorous vacuole, macrophage, immune evasion

OPEN ACCESS

Edited by:
Claudia Ida Brodskyn, Gonçalo Moniz Institute (IGM), Brazil

Reviewed by:
Veronica Jimenez, California State University, Fullerton, United States
Fabiano Oliveira, National Institute of Allergy and Infectious Diseases (NIAID), United States

****Correspondence:***
Joao Luiz Mendes Wanderley
lmwjoao@macae.ufrj.br
Lynn Soong
lysoong@utmb.edu

† These authors have contributed equally to this work

Specialty section:
This article was submitted to Parasite and Host, a section of the journal Frontiers in Cellular and Infection Microbiology

Received: *16 December 2018*
Accepted: *26 March 2019*
Published: *12 April 2019*

Citation:
Wanderley JLM, Deolindo P, Carlsen E, Portugal AB, DaMatta RA, Barcinski MA and Soong L (2019) CD4$^+$ T Cell-Dependent Macrophage Activation Modulates Sustained PS Exposure on Intracellular Amastigotes of Leishmania amazonensis. Front. Cell. Infect. Microbiol. 9:105. doi: 10.3389/fcimb.2019.00105

INTRODUCTION

Leishmania amazonensis (*L. amazonensis*) is the causative agent of cutaneous Leishmaniasis in South America. This species is associated with most cases of diffuse/disseminated cutaneous Leishmaniasis (DCL), a very severe clinical manifestation (Leon et al., 1990). Experimentally, most inbred mouse strains develop progressive cutaneous lesions, although the disease severity varies among mice of different genetic backgrounds (Terabe et al., 2004). Both DCL patients and experimentally infected mice show deficient cellular immune responses to the pathogen, as judged by delayed-type hypersensitivity (DTH) responses or cytokine/chemokine profiles (Ji et al., 2003; Silveira et al., 2005). In fact, when compared to the classical *L. major* infection models, *L. amazonensis*-infected mice failed to elicit a polarized Th response because activated $CD4^+$ T cells produced a mix of Th1/Th2/Th17 and modulatory cytokines (Ji et al., 2003; Ramer et al., 2006; Vargas-Inchaustegui et al., 2009). This phenotype is consistent with the poor activation presented by infected dendritic cells, which is not sufficient to turn these cells into efficient, functional antigen-presenting cells (Xin et al., 2008; Wanderley et al., 2013). Consequently, macrophages (MΦs), the preferential host cells for parasite growth, are not efficiently activated and not capable of controlling the infection. Competent MΦ activation is necessary for disease control, since those cells are the main effector cells for parasite killing, usually dependent on the expression of nitric oxide synthase (iNOS) (Xie et al., 1993) or the production of reactive oxygen species (Carneiro et al., 2018). On the other hand, alternative or non-classical MΦ activation leads to an increased activation of arginase I, an enzyme responsible for the first step of polyamine synthesis, which is mandatory for parasite growth (Franca-Costa et al., 2015) and restrains NO production by competing for the same substrate, L-arginine (Wanasen and Soong, 2008). Those intracellular pathways control the fate of the intracellular parasite.

Apoptotic cells are known to display several distinctive molecular patterns, which are recognized by phagocytic cells for efficient internalization (Poon et al., 2014). In addition, phagocytes stimulated by apoptotic cell recognition are prompted to produce modulatory cytokines such as TGF-β and IL-10 (Fadok et al., 1998). Phosphatidylserine (PS) is a structural phospholipid that is actively maintained in the cytoplasmic leaflet of the plasma membrane but is translocated to the surface at the early stages of apoptotic death (Fadok et al., 1992). Recognition of PS exposed at the surface of apoptotic cells is sufficient to induce apoptotic cell clearance and non-classical activation of phagocytic cells (Hoffmann et al., 2001). We had previously shown that the amastigote forms of *L. amazonensis*, when purified from mice lesions, exposed PS at their surface without additional signs of apoptotic death. Since PS-exposing amastigotes are fully viable and highly competent in infecting and maintaining a productive disease in mice, we termed this phenotype apoptotic mimicry (de Freitas Balanco et al., 2001). As in the case of apoptotic cell/phagocyte interactions, the host cell is induced to produce immunosuppressive cytokines, which, in turn, signal for MΦ non-classical activation and consequent parasite growth (de Freitas Balanco et al., 2001; Wanderley et al., 2006). PS exposure on *L. amazonensis* amastigotes correlates with the severity of the disease, since amastigotes purified from BALB/c mice, which are highly susceptible to the infection, exhibit a higher density of PS moieties than do those from parasites purified from semi-resistant C57BL/6 mice (Wanderley et al., 2006). In addition, *in vivo* treatment of infected mice with anti-PS monoclonal antibodies delays disease progression and up-regulates the efficiency of dendritic cells to present antigen and activate parasite-specific T cells (Wanderley et al., 2013). PS exposure on pathogens operates in several different models of infection, such as those using *Trypanosoma cruzi* (Damatta et al., 2007), *Toxoplasma gondii* (Seabra et al., 2004), enveloped and non-enveloped viruses in which they confirm PS as a strategy to silently invade host cells (Seabra et al., 2004; Damatta et al., 2007; Mercer and Helenius, 2008; Feng et al., 2013). Additionally, by inducing transient PS exposure on the surface of host cells, viral infections can spread signals derived from PS recognition, such as TGF-β and IL-10 production by neighbor phagocytes, to avoid full activation of the immune system (Soares et al., 2008).

In this study, we tested whether PS exposure is an adaptive response of *L. amazonensis* amastigotes to the hostile environment of the parasitophorous vacuole generated by MΦ immune activation. We observed that intracellular amastigotes infecting activated MΦs are able to increase PS exposure. This is dependent on iNOS and arginase I concomitant expression. We confirmed our findings by demonstrating that PS exposure on amastigotes purified from lesions of T cell-deficient nude mice was nearly absent, but the adoptive transfer of primed $CD4^+$ T cells recovered this phenotype. We also demonstrated that lesions of anti-PS antibody-treated infected mice were similar to lesions of immunodeficient mice. Our data lead us to conclude that PS exposed by intracellular amastigotes of *L. amazonensis* is a phenotype acquired as a response to host immune activation, and thus an important adaptive strategy employed by those intracellular parasites.

MATERIALS AND METHODS

Mice and Parasites

Female nude BALB/c mice (C.Cg/AnNTac-*Foxn1*^{nu} NE9), C57BL/6 mice deficient in iNOS (C57BL/6NTac-Nos2^{tm}1N12), and their corresponding wide-type (WT) controls were purchased from Taconic Farms (Germantown, NY) or Harlan Sprague Dawley (Indianapolis, IN), respectively. All mice were maintained under specific pathogen-free conditions and used at 6–8 weeks of age, according to the protocols approved by the Animal Care and Use Committee of the University of Texas Medical Branch (#9803016A). Promastigotes of *L. amazonensis* (LV78) were cultured at 23°C in Schneider's *Drosophila* medium (Invitrogen, Carlsbad, CA), pH 7.0, supplemented with 20% FBS (Sigma, St. Louis, MO) and 50 μg/ml of gentamicin. Axenic amastigotes of *L. amazonensis* (LV78) were cultured at 33°C in complete Grace's insect cell culture medium (Invitrogen), pH 5.0, supplemented with 20% FBS. Parasite infectivity was maintained by *in vivo* passages in BALB/c mice, and cultures of <6 passages were used for infection.

Reagents

Otherwise stated, all recombinant cytokines were purchased from Peprotech (Rocky Hill, NJ, USA). Superoxide scavenger MnTBAP (Mn^3 tetrakis (4-benzoic acid) porphyrin chloride) was purchased from Enzo Life Sciences (Farmingdale, NY, USA), iNOS inhibitor L-NIL- [L-N^6-(1iminoethyl) lysine], and (ODC) decarboxylase inhibitor DFMO (DL-α-Difluoromethylornithine, Hydrochloride) were purchased from Calbiochem (Darmstadt, Germany).

Amastigote Purification

Infected tissues or infected MΦs were finely minced and homogenized with a tissue grinder (Thomas Scientific, NJ). The cell suspension was centrifuged at 50 g for 10 min at 4°C. The supernatant was carefully collected, and further centrifuged and washed for 3 more times at 1,450 g for 17 min at 4°C. After 2 h incubation under rotation at 34°C to liberate endocytic membranes (Saraiva et al., 1983), amastigotes were further centrifuged and incubated for 16 h at 34°C to complete release of endocytic membranes and to test for bacterial contamination. After this time, they were centrifuged and washed 3 times before use. Prior to amastigote purification from *in vitro* infected cells, MΦs were thoroughly washed with HBSS.

Generation of Bone Marrow-Derived Macrophages (BMMΦs)

BMMΦs were generated from mice by cultivating fresh bone marrow cells in complete IMDM (Invitrogen) containing 10% FBS, supplemented with 20 ng/ml of recombinant M-CSF (eBioscience, San Diego, CA). To generate BMMΦs, we replaced the medium at 5–6 days of culture and harvested adhered cells after 10–12 days. To recover adhered MΦs, we washed the petri dishes twice with warm PBS (Invitrogen) and incubated the cells with 5 ml of cell dissociation solution (CellGro, Manassas, VA) for 20 min at room temperature. We detached the cells by pipetting up and down and washed the cell pellet twice with complete medium prior to use.

Flow Cytometry

Parasites were quantified and 10^6 amastigotes were washed and suspended in annexin V binding buffer, which contains 10 mM HEPES, 150 mM NaCl, and 2.5 mM $CaCl_2$, at pH 7.2. Cells were incubated at room temperature for 15 min with annexin V-FITC (Molecular Probes, Eugene, OR) at the concentration indicated by the manufacturer and diluted in the binding buffer. All incubation procedures were performed on ice. At the time of acquisition, 0.4 μg/ml of propidium iodide (PI, Sigma) was added to the control and Annexin V-FITC-labeled samples to determine parasite viability. Data were collected in a BD FACSCalibur® (20,000 gated events per sample) and analyzed by Cellquest Pro® (BD Biosciences, San Jose, CA) and FlowJo software (TreeStar, Ashland, OR).

Generation of Supernatant (SN) From Stimulated Lymph Node Cells

Mice were infected in the footpad with 2×10^6 promastigote forms of *L. amazonensis*. After 5–7 weeks of infection, popliteal lymph nodes (LNs) were harvested, and a single-cell suspension was obtained. Total LN cells from infected or naïve mice were plated in U-bottomed, 96-well plates, 4×10^5 cells per well, in the presence of 40 μg/ml of soluble *Leishmania*l antigens (SLA). After 4 days of culture, supernatants from stimulated LN cells from naïve mice or infected mice were pooled, filtered, and stored in aliquots at −70°C. To generate SLA, promastigote forms were submitted to 5 cycles of freeze-and-thaw and centrifugation to dispose of insoluble materials.

Adoptive Cell Transfer

BALB/c WT or nude mice were infected in the footpad with $1–2 \times 10^6$ promastigote forms of *L. amazonensis*. After 6–8 weeks of infection, popliteal LNs from WT mice were harvested and a single-cell suspension was obtained. $CD4^+$ or $CD8^+$ T cells were purified by selected cell isolation kits (Miltenyi Biotech, Alburn, CA), following the manufacturer's instructions. Infected BALB/c nude mice were i.v. injected with $1–3 \times 10^6$ purified $CD4^+$ or $CD8^+$ T cells. At 2–3 weeks post-transfer, mice were euthanized to obtain popliteal LNs and lesion-derived amastigotes to evaluate T cell activation and PS exposure on amastigotes, respectively.

Macrophage Infection

Thioglycolate-elicited peritoneal MΦs or BMMΦs were placed on 24-well plates and allowed to attach overnight. Cells were incubated with axenic amastigotes or promastigotes in a 3:1 ratio. After 4 h at 33°C, free parasites were removed by washing and, if necessary, cells were activated and/or treated with SNs, cytokines or drugs. Cultures proceeded for an additional 24-h period. In some cases, MΦs were attached on 13-mm^2 glass coverslips (Fisher Scientific, Pittsburgh, PA) and, after infection and activation/treatment, were stained with Giemsa (Sigma) to evaluate host cell morphology and infection efficiency.

Polymerase Chain Reaction (PCR)

Total RNA was extracted from 1×10^6 MΦs 24 h post-infection and/or activation by using the RNeasy system (QIAGEN, Valencia, CA). Immediately cDNA was generated by using up to 5 μg of total RNA and the Superscript III Synthesis System (Invitrogen) and following the manufacturer's instructions. Amplifications of specific cDNAs were performed by using the GoTaq® Green Master Mix system (Promega, San Luis Obispo, CA). Briefly, Arginase I cDNA was subsequently amplified by use of the following cDNA primers: sense, 5′-AGACATCGTGTACATTG-3′ and antisense, 5′-GAGTTCCGAAGCAAGCCAAG-3′. Amplification occurred over 30 cycles, with the first cycle for primary denaturing at 95°C for 2 min; the next 28 cycles each comprising three steps for denaturing (94°C, 35 s), primer annealing (59°C for 45 s) and primer extension (72°C, 45 s); and a final cycle of denaturing (95°C, 30 s), annealing (69°C, 30 s), and extension (72°C, 5 min). To amplify inducible nitric oxide synthase (iNOS) and β-actin cDNA, we used the following cDNA primers: iNOS sense, 5′-GTTTCTGGCAGCAGCGGCTC-3′; antisense, 5′-GCTCCTCGCTCAAGTTCAGC-3′. β-actin sense, 5′-CGTGGGCCGCCCTAGGCACCAGGG-3′; antisense,

5′-GGGAGGAAGAGGATGCCGCAGTGG-3′. Amplification occurred over 36 cycles, by using the following approaches:the first cycle for primary denaturing at 95°C for 2 min; 34 cycles each comprising three steps for denaturing (95°C, 30 s), annealing (69°C, 30 s), extension (72°C, 20 s); and a final cycle of denaturing (95°C, 30 s), annealing (69°C, 30 s), and extension (72°C, 5 min). All reactions were performed by using a GeneAmp PCR System 2700 (Applied Biosystems, Foster City, CA), and the PCR products were separated by electrophoresis on 1.2% agarose gels. Real-time RT-PCR assays were performed with TaqMan Universal PCR Master Mix (Applied Biosystems, Foster City, CA, USA), using the following primer-probe sets purchased from Applied Biosystems: *inos* (Mm00440502_m1), *arginase I* (Mm00475988_m1), and *β-actin* endogenous control. The reactions were performed using Bio-Rad CFX96 Real-Time PCR detection system. Data were normalized to the expression of *β-actin*.

Cytokine Production

Cytokine production was measured in the supernatant of LN cell or MΦ cultures by using the Bio-Plex Pro-Mouse Cytokine 23-plex Assay from Bio-Rad (Hercules, CA) and following the manufacturer's instructions. Total and biologically reactive TGF-β_1 were measured by using the ELISA Ready-SET-Go system (eBioscience), and data for biological reactive TGF-β_1 are presented, The level of nitric oxide was measured by using a Griess assay (Caymann Chemical, Ann Arbor, MI).

Parasite Quantification by Real-Time PCR

Parasite loads were quantified by measuring the gene of *L. amazonensis* cysteine proteinase isoform 1 (*Llacys1*), which is a single-copy gene per haploid genome and expressed in both developmental stages (Lasakosvitsch et al., 2003). Infected MΦs were collected for DNA extraction with a DNeasy kit (Qiagen, Valencia, CA). DNA (10 ng) was used for parasite detection by the UTMB Real-time PCR Core Facility (all reagents were purchased from Applied Biosystems, Foster City, CA). Each sample was run in duplicate and normalized by the amount of total DNA extracted. The number of parasites per sample was calculated based on a standard curve, as described in our previous studies (Xin et al., 2010).

Histopathological Analysis

Mice were infected i.d. in the right ear with 10^6 promastigotes. After 2 weeks of infection and every 3 days thereafter they were given i.p. injections of 100 μg of PGN635, a second-generation fully humanized anti-PS monoclonal antibody (Zhou et al., 2014). Other groups of mice received PBS or the isotype control C44 antibody that binds to colchicine (Edmond Rouan et al., 1989). Mice were treated for 6 weeks and the infected ears were collected, fixed in 4% paraformaldehyde, dehydrated, embedded in paraffin, and mounted slides were stained with hematoxylin and eosin.

Parasitophorous Vacuole Morphometric Evaluation

The sizes parasitophorous vacuoles from lesions of mice treated with anti-PS, isotype antibodies or PBS were observed under an Axioplan (Zeiss) microscopy and images were captured using a MRc5 AxioCam digital camera and processed with the software ImageJ version 1.47t (Wayne Rasband–NIH). Values are shown as the area in μm^2 for at least 200 PVs in each tested sample.

Western Blot

BMMΦs (1×10^6) were infected with axenic amastigotes at a 3:1 parasite-to-cell ratio. At 24 h post-infection and/or indicated treatments, cells were harvested, washed, and suspended in 10 μl of PBS and 10 μl of 2X lysis buffer (2% Triton X-100, 100 mM Tris-Cl, 600 mM NaCl, 10 mM EDTA, 2 mM PMSF, 250 mM sucrose) that contained an inhibitor cocktail (Roche, Indianapolis, IN). Protein concentrations were determined by using the BCA protein assay kit (Pierce Biotechnology). Equal amounts of proteins were loaded onto 10% SDS-polyacrylamide gels, and then transferred to polyvinylidene difluoride membranes (BioRad Laboratories, Hercules, CA). Rabbit anti-mouse iNOS and arginase I antibodies were purchased from Santa Cruz Biotechnology (Santa Cruz, CA). Mouse anti-actin mAb (Sigma) was obtained from Dr. Jiaren Sun (Department of Microbiology and Immunology, UTMB, TX). Membranes were incubated with primary Abs (diluted 1:200 in TBS buffer containing 5% non-fat milk and 0.05% Tween-20) at 4°C overnight, washed, and incubated with an HRP-conjugated secondary Ab (1:2000) for 1 h. Blots were developed with the enzyme chemiluminescence kit ECL (Amersham Biosciences, Piscataway, NJ).

Statistical Analysis

One- or two-way ANOVA was used for multiple group comparisons (GraphPad Software v5.0, San Diego, CA). Statistically significant values are referred to as follows: *, $p < 0.05$; **, $p < 0.01$; ***, $p < 0.001$.

RESULTS

Increase of PS Exposure on Intracellular Amastigotes Depends on Macrophage Interactions With Lymph Node Cells

We previously showed that lesion-derived amastigotes purified from BALB/c mice expose higher amounts of PS than do those parasites derived from C57BL/6 mice (Wanderley et al., 2006), a finding that may indicate that the host can modulate this phenotype of the parasite. To evaluate the role of host macrophages (MΦs) in modulating PS exposure on the parasite, we obtained thioglycollate-elicited peritoneal MΦs from BALB/c and C57BL/6 mice, infected them either with promastigotes or lesion-derived amastigotes and collected intracellular amastigotes every 24 h to evaluate PS exposure by flow cytometry. We found no major differences between parasites derived from BALB/c vs. C57BL/6 MΦs (**Figure 1A**), regardless of the form of parasite used for infection or the time

post-infection. Consequently, we suspected that the interaction between MΦs and other types of immune cells was responsible for the differential levels of PS on lesion-derived parasites *in vivo*. To investigate this possibility, we obtained lymph node (LN) cells from infected BALB/c mice and incubated them with peritoneal MΦs infected with lesion-derived amastigotes. These interactions stimulated an about 30% higher PS exposure on intracellular amastigotes compared to that in parasites obtained from isolated MΦs, in a dose-dependent manner (**Figure 1B**).

To determine whether cytokine production by LN cells was a requirement to induce PS exposure on intracellular parasites, we generated supernatants from LN cells obtained from naïve (nSN) or infected (iSN) mice and stimulated with SLA for 4 days. We treated MΦs infected with axenic amastigotes with different concentrations of those supernatants (SNs) and evaluate PS exposure on intracellular amastigotes 24 h post-infection and stimulation. As shown in **Figure 1C**, axenic amastigotes exposed very low amounts of PS, which represented a technical advantage for minimizing background levels of PS exposure and indicated that parasite-host interactions should be necessary to stimulate PS exposure on amastigotes. Indeed, intracellular amastigotes from unstimulated MΦs ("no SN") increased PS on their surface, 24 h post-infection. In addition, treatment of infected MΦs with iSNs induced PS exposure on intracellular amastigotes. This effect was dependent on the activation of those LN cells, since iSN was significantly more efficient than nSN and a clear positive correlation with the concentration of SN was observed: 10% of iSN added to the culture induced a 50% increase, while 25% of iSN induced about a 70% increase in PS exposure on intracellular amastigotes (**Figure 1C**).

As expected, the cytokine profile of those SNs corroborated the previous data regarding T cell activation during *L. amazonensis* infection in the mice (Ji et al., 2003). Moderate amounts of Th1, Th2, and modulatory cytokines such as IL-4, IL-13, IFNγ, IL-1β, TGF-β_1, and IL-10 (**Figure 1D**), were present, especially in the SN generated from re-stimulated, *in vivo*-primed cells (iSN), which indicates that this response is antigen-specific. One of the hallmarks of the apoptotic mimicry, described to operate during amastigote infection, is the fact that amastigotes exposing PS are perfectly viable and infective and do not display any other sign of apoptotic death (de Freitas Balanco et al., 2001; Wanderley et al., 2006). To evaluate whether MΦ activation leads to PS exposure on intracellular amastigotes due to apoptotic mimicry, we measured parasite loads on infected MΦs at 24 and 72 h post-infection. As shown in **Figure 2A**, MΦ activation with SNs derived from stimulated LN cells from either infected or naïve mice promoted parasite proliferation 72 h post-infection, as opposed to LPS and IFNγ activation. In addition, the morphological characteristics of *L. amazonensis* infection are maintained, and include, for example, enlarged parasitophorous vacuoles with parasites attached to the vacuole internal membrane (**Figure 2B**). Our data suggest that MΦ activation through interactions with primed LN cells and their soluble products modulate active PS exposure by intracellular amastigotes in an apoptotic mimicry fashion.

Balanced Expression of iNOS and Arginase I Controls cytokine-Dependent PS Exposure on Amastigotes and Parasite Survival

It is known that the survival of *Leishmania* parasites inside macrophages (MΦs) is mostly mediated by the balance between iNOS and arginase I activation. These are induced enzymes and therefore their activity is directly related to their cellular expression. Arginase I is the first enzyme in the polyamine synthesis pathway, while iNOS is the enzyme responsible for all steps of NO synthesis. Those intracellular signaling pathways compete with each other, since they depend on the same substrate. In addition, some molecules, produced as secondary metabolites, act as cross-inhibitors (Wanasen and Soong, 2008). Interactions between infected MΦs and other immune cells determine which pathway is activated, since inflammatory cytokines stimulate iNOS expression and decrease mRNA levels of arginase I and vice-versa (Corraliza et al., 1995; Modolell et al., 1995). Since MΦ activation seems to be important for the cytokine-dependent PS exposure by intracellular parasites, we aimed to understand the role of those pathways in this mechanism. We observed that SN from re-stimulated, *in vivo*-primed LN cells induced the expression of both arginase I and iNOS at the mRNA and protein levels (**Figures 3A,B** and **Figure S1**). The expression of both enzymes was the highest when 25% of iSN was used to stimulate infected MΦs, the same concentration that induced an optimal increase of PS exposure on intracellular amastigotes. However, iSN stimulation was weak, when compared to that in the positive controls for arginase I and iNOS expression, TGFβ_1+IL-4 or IFNγ+TNFα, respectively (**Figures 3A,B**). The expression of both enzymes by activated MΦs correlates with the profile of cytokines present on those SNs, since they are constituted by a mix of Th1/Th2/modulatory cytokines (**Figure 1D**).

To understand the contribution of both pathways individually, we activated infected MΦs in the presence of L-NIL, a relatively selective inhibitor of iNOS, or, as a control, we used MnTBAP, a superoxide scavenger molecule. L-NIL has IC_{50} values of 0.4–3.3 μM for iNOS as opposed to 8–38 and 17–92 μM for eNOS and nNOS, respectively (Moore et al., 1994; Stenger et al., 1995). At 24 h of infection, we evaluated PS exposure on purified intracellular amastigotes. The iNOS inhibitor abrogated the cytokine-dependent induction of PS exposure, while scavenging superoxide molecules had no effect (**Figure 4A**). Treatment with both inhibitors brought the levels of PS exposure on amastigotes to the same levels of L-NIL alone, indicating that there was no synergistic effect between NO and superoxide to induce PS exposure on the parasite (**Figure 4A**). To further demonstrate the role of iNOS expression by MΦs in the induction of PS exposure on amastigotes, we generated BMMΦs from wild-type (WT) and $iNOS^{-/-}$ C57BL/6 mice, infected them, and purified intracellular amastigotes from activated MΦs to evaluate PS exposure on the parasite. C57BL/6-derived MΦs were more sensitive to activation, since 25% of nSN was able to induce the same levels of PS on the parasite when compared with iSN (**Figure 4B**). Activation

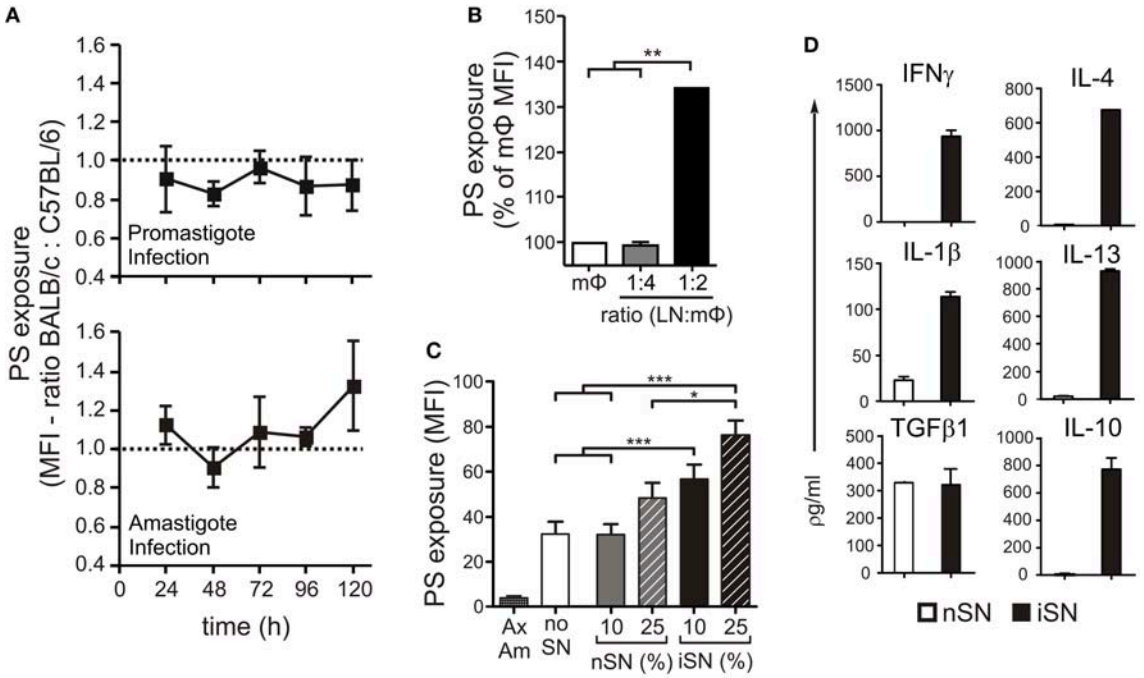

FIGURE 1 | PS exposure on the surface of intracellular amastigotes is induced through MΦ activation by lymph node cells. **(A)** BALB/c- or C57BL/6-derived peritoneal MΦs were infected with stationary-phase promastigotes (upper panel) or amastigotes (lower panel). Every 24 h post-infection, intracellular parasites were purified, and PS exposure was analyzed by flow cytometry. Results are shown as the ratio between the MFIs of annexin V staining of amastigotes derived from BALB/c and C57BL/6 MΦs. BALB/c-derived BMMΦs were infected with amastigotes in the absence or presence of **(B)** LN cells from infected BALB/c mice (at indicated LN cell-to-MΦ ratios), or **(C)** supernatants of *in vitro*-stimulated LN cells from naïve BALB/c mice (nSN) or infected mice (iSN). After 24 h of treatment, amastigotes were purified for PS exposure analysis by flow cytometry. Results are pooled from 3 to 5 independent experiments. **(D)** Cytokine levels in supernatants of *in vitro*-stimulated LN cells from naïve BALB/c mice (nSN) or infected mice (iSN) were measured by bioplex assays. Graph represents data from 3 independent batches of SNs, produced from LNs of 2 mice per batch. $^{*}p < 0.05$, $^{**}p < 0.01$, $^{***}p < 0.001$.

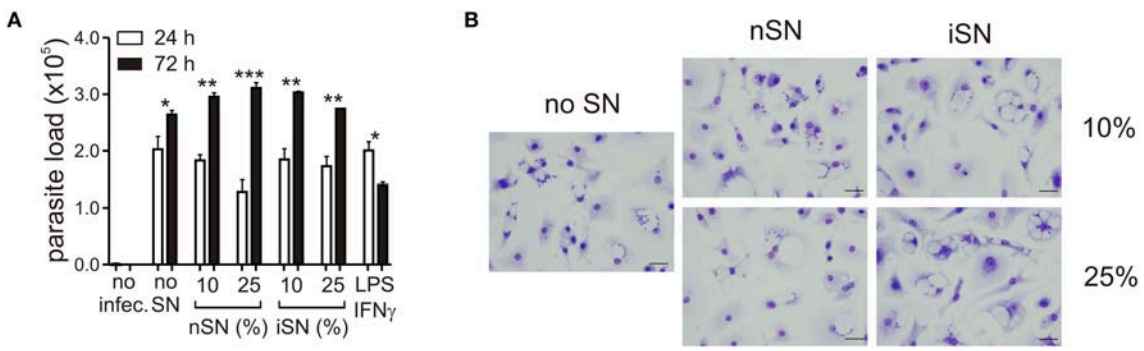

FIGURE 2 | PS exposure on intracellular amastigotes, induced by MΦ stimulation is not due to apoptotic death. **(A)** Parasite loads in infected BALB/c-derived BMMΦs activated with different concentrations of nSN and iSN were measured by real-time PCR. Asterisks indicate comparison between black and white bars. LPS (100 ng/ml) plus IFN-γ (100 ng/ml) was used as positive control. $^{*}p < 0.05$, $^{**}p < 0.01$, $^{***}p < 0.001$. All comparisons were made among the same samples at 24 and 72 h post infection. **(B)** Photomicrography of infected BMMΦs activated with different concentrations of nSN and iSN. Bars indicate 10 μm. Graph represents data from 5 independent experiments.

of infected iNOS$^{-/-}$ MΦs did not increase PS exposure on amastigotes regardless of the source or the concentration of SN (**Figure 4B**). Similar to what happened in BALB/c-derived MΦs, the differences observed on amastigotes purified from WT or iNOS$^{-/-}$ C57BL/6 MΦs were not related to the death of the amastigotes, since parasite loads 72 h post-infection were not altered among the different SN treatments (**Figure 4C**). Despite the increased iNOS expression, MΦ activation with 10 or 25% of iSN or nSN did not induce detectable amounts of NO, evaluated by Griess reaction (**Figure 4D**). To test whether polyamines

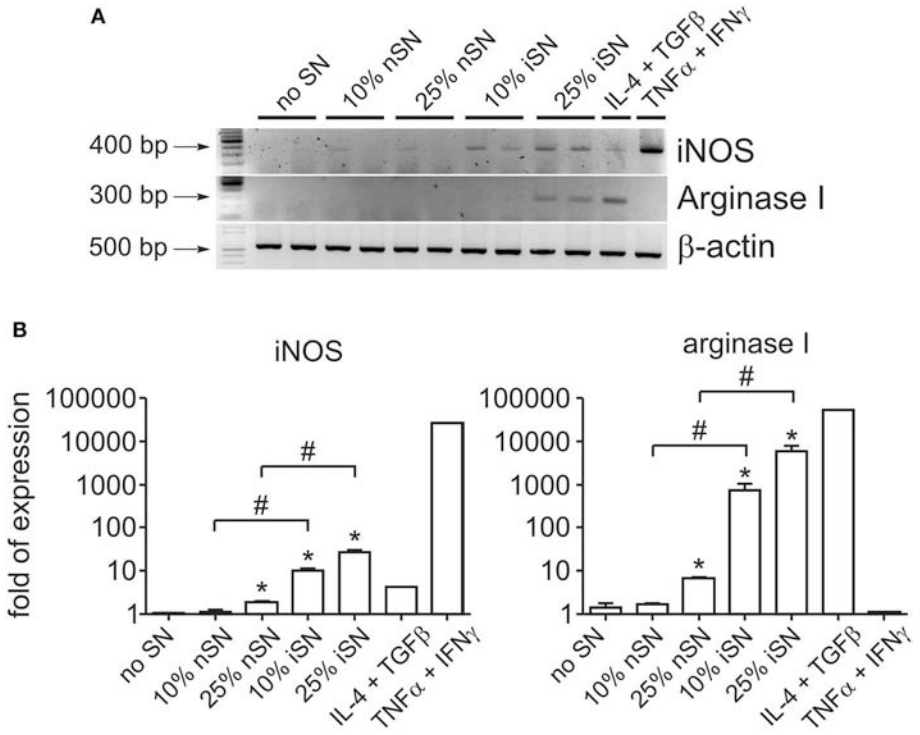

FIGURE 3 | Macrophage stimulation leads to concomitant expression of iNOS and arginase I. **(A)** RT-PCR and **(B)** real-time RT-PCR analyses of iNOS and Arginase I expression by BALB/c-derived BMMΦs at 24 h post-infection and activation with SNs from SLA-stimulated, naïve LN cells (nSN) or re-stimulated, *in vivo*-primed LN cells (iSN). **(A)** Representative photographs of 2–3 experiments. TGF-β (10 ng/ml) plus IL-4 (1 ng/ml) stimulation was used as a positive control for arginase expression and IFN-γ (100 ng/ml) plus TNF-α (10 ng/ml) stimulation for iNOS expression. $^{*}p < 0.05$ (compared with medium controls), $^{\#}p < 0.05$ (between the groups).

play a role in the induction of PS exposure on amastigotes, we purified amastigotes from infected- and activated-MΦs treated with different concentrations of difluoromethylornithine (DFMO), an specific and irreversible inhibitor of ornithine decarboxylase, the enzyme responsible for metabolizing L-arginine-derived ornithine into the polyamine putrescine (Canellakis et al., 1979). Independent on the concentration of DFMO used, this drug had no effect on the PS exposure on the amastigotes (**Figure 4E**). However, when we quantified parasite loads on infected-MΦs activated with 25% of iSN, we observed that DFMO treatment was detrimental for the proliferation of intracellular parasites at 72 h post-infection (**Figure 4F**). This finding may indicate that polyamine synthesis is a requirement for parasite proliferation and maintenance in these conditions, as described in other models (Majumder and Kierszenbaum, 1993; Vannier-Santos et al., 2008). Nevertheless, our data imply that PS exposure on intracellular amastigotes is modulated by cytokine-mediated, iNOS-dependent MΦ activation, rather than by arginase I expression. Arginase I, however, is necessary for parasite proliferation and survival in activated MΦs.

CD4^{+} T Cells Are Required for PS Exposure on Intracellular Amastigotes *in vivo*

To further understand the role of different cellular populations present in the lymph nodes (LNs) for the modulation of PS exposure on intracellular amastigotes, we infected WT or nude BALB/c mice in the footpad and purified lesion-derived amastigotes to evaluate PS exposure on a weekly basis. Confirming previous data from the literature, we observed a delay in the development of lesions in immunodeficient mice, which, eventually, reached the same size of lesions from WT mice (Soong et al., 1997; **Figure 5A**). PS exposure on lesion-derived amastigotes purified from WT mice was 2- to 6-times higher than on parasites obtained from nude mice, depending on the time post infection (**Figure 5B**), confirming previous results (Franca-Costa et al., 2012). Since CD4^{+} T cells are the major regulators of host immune response to *Leishmania* infection, we hypothesized that the modulation of PS exposure on intracellular parasites observed by incubating infected MΦs with LN cells or culture SNs was due to CD4^{+} T cell-dependent MΦ activation. To test this hypothesis, we purified CD4^{+} T cells from draining LNs of infected WT mice and adoptively transferred these cells to infected nude mice. After 2–3 weeks post-transfer, we purified lesion-derived amastigotes to evaluate PS exposure. The adoptive transfer of CD4^{+} T cells increased PS exposure on the amastigotes by 2- or 3-fold, whereas transfer of CD8^{+} T cells, used as a control, did not alter the parasite phenotype (**Figures 5C,D**).

In addition to the decreased PS exposure on amastigotes derived from nude mice (Franca-Costa et al., 2012; **Figure 5B**), histopathological analysis of BALB/c nude mice lesions showed a marked decrease in the size of the parasitophorous vacuoles of

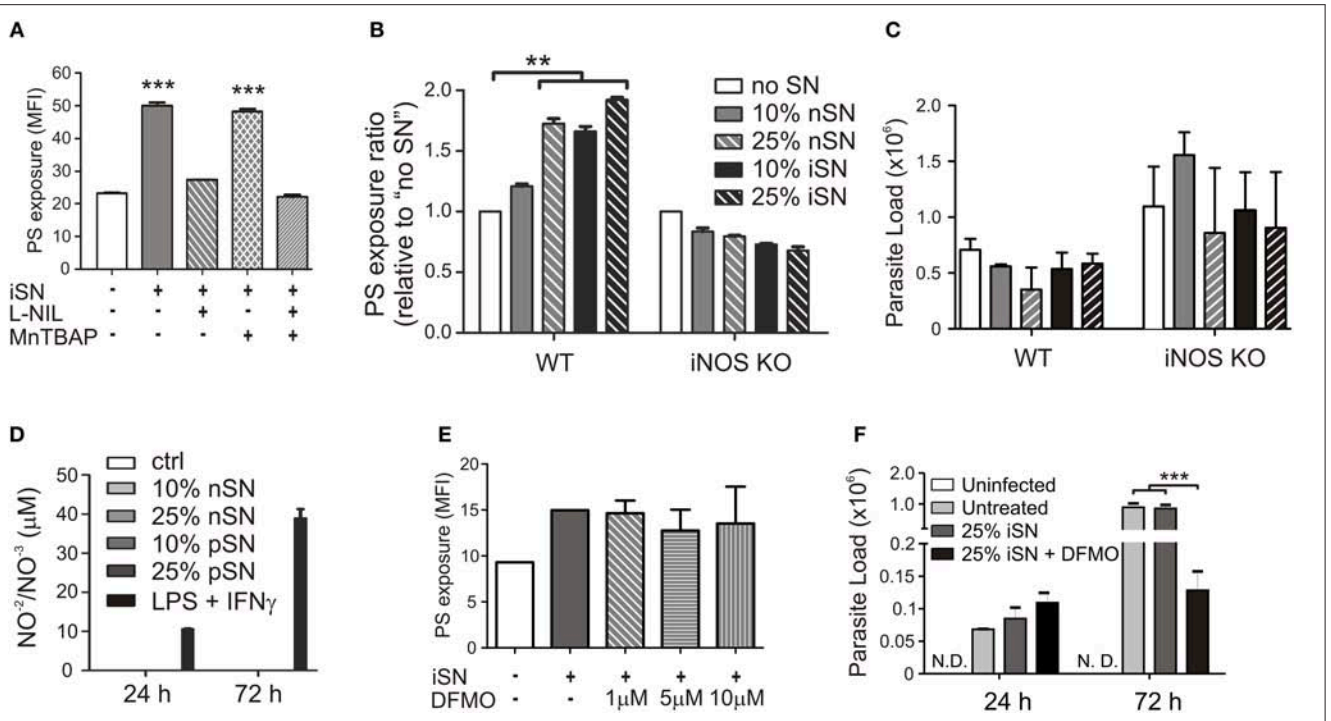

FIGURE 4 | Cytokine-induced PS exposure on amastigotes depends on iNOS function. Infected BALB/c-derived BMMΦs were activated with SNs from re-stimulated, *in vivo*-primed LN cells (iSN) in the presence of **(A)** 50 μg/ml of L-NIL (a selective inhibitor of iNOS), 200 μM of MnTBAP (a superoxide scavenger molecule), or **(E)** different concentrations of DFMO (a selective ODC inhibitor). After 24 h of infection, amastigotes were purified for PS exposure analysis by flow cytometry. **(B)** BMMΦs were obtained from WT or iNOS KO mice, infected and activated with different concentrations of iSN and nSNs. After 24 h of infection, amastigotes were purified for PS exposure analysis by flow cytometry. Parasite loads in infected BMMΦs **(F)** treated with 10 μM of DFMO or **(C)** obtained from iNOS KO mice and activated with iSN were measured by real-time PCR. **(D)** NO production by BMMΦs stimulated with different concentrations of iSN, nSNs or LPS+IFN-γ (100 ng/ml for both), measured by Griess reaction. **(A)** Asterisks indicate comparison with untreated MΦs. Graphs represent data from 3 to 5 pooled experiments. $^{**}p < 0.01$, $^{***}p < 0.001$.

infected MΦs (Franca-Costa et al., 2012). This is also observed in lesions from MHC class $II^{-/-}$ mice (Soong et al., 1997). We observed that infected mice treated intraperitoneally with anti-PS mAb displayed decreased parasitophorous vacuole size (**Figures 6D–F**) when compared to untreated mice (**Figures 6A–C**). The difference in the vacuole size was not observed in infected mice treated with isotype control antibodies (**Figure 6G** and **Supplementary Table 1**). Our data demonstrate that PS exposure on intracellular amastigotes is a response of the parasite when it senses MΦ activation through primed $CD4^+$ T cells.

DISCUSSION

L. amazonensis, particularly its amastigotes, can infect host cells without triggering overt cellular activation. Actually, those parasites are able to down-modulate signaling pathways involved in dendritic cell activation, suppress cytokine production and expression of MHC class II molecules and, therefore, to inhibit antigen presentation (Prina et al., 2004; Xin et al., 2008). In addition, the inhibitory effects of *L. amazonensis* amastigotes on macrophages (MΦs) are also well known, including sequestration and degradation of MHC class II molecules, inhibition of endosomal proteases and blocking of NO production (Prina et al., 1990, 1993; Antoine et al., 1999). Consequently, *L. amazonensis* infection models are typically characterized by presenting a weak and non-polarized T cell response that is not sufficient to induce proper MΦ activation and control of parasite loads (Soong et al., 1997; Ji et al., 2002, 2003).

Our group has previously shown that the ability of amastigotes of *L. amazonensis* to silently infect host cells is mainly due to the exposure of PS molecules at their surface in a mechanism referred to as apoptotic mimicry (de Freitas Balanco et al., 2001; Wanderley et al., 2006). The recognition of this molecule and opsonizing ligands such as antibodies and complement factors mediate amastigote uptake by MΦs. In addition PS is highly effective in triggering anti-inflammatory cytokine production by MΦs, creating a permissive environment for parasite intracellular proliferation (de Freitas Balanco et al., 2001; Wanderley et al., 2006; Birge et al., 2016). Interestingly, PS exposure on amastigotes is correlated with disease severity, since amastigotes derived from BALB/c mice, which develop a more severe disease when exposed to higher amounts of PS than do those obtained from moderately susceptible C57BL/6 mice (Wanderley et al., 2006). In the context of parasite/host interactions, there are several reports showing a similar effect in the opposite direction: infection modulating host cell functions such as apoptosis, and expression of molecules involved with microbicidal effects or immune functions (Osorio y Fortea et al., 2007; Soong, 2008; Lecoeur et al., 2010; Muxel et al., 2017b).

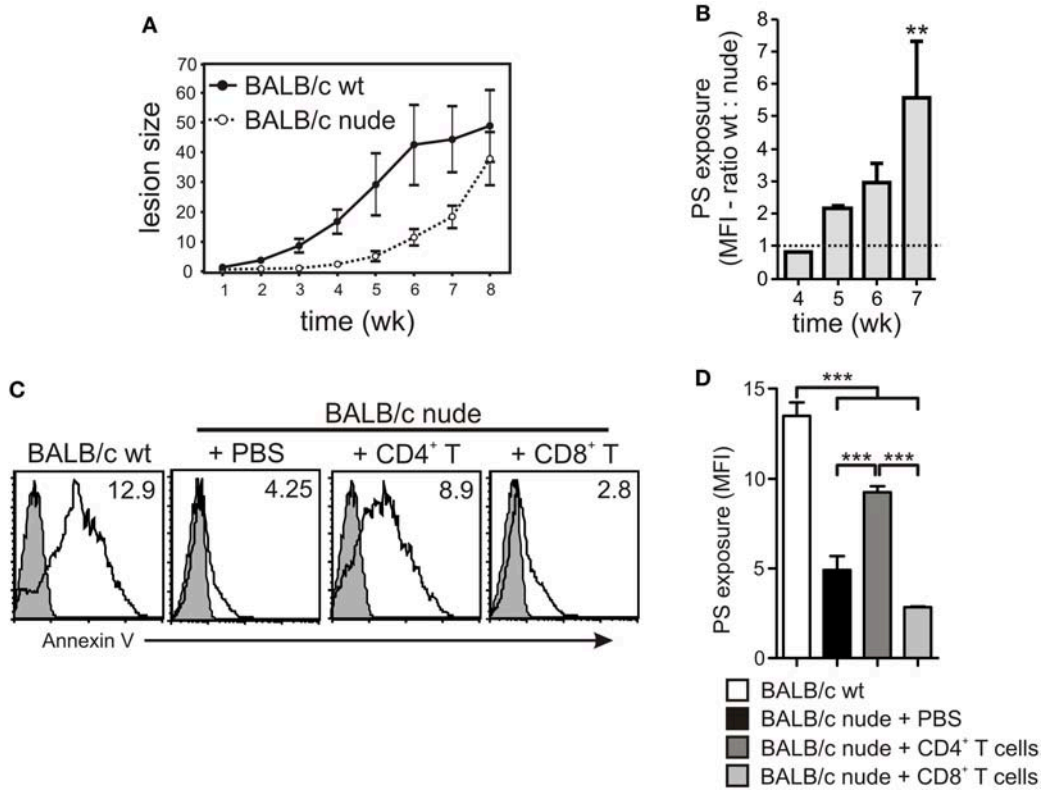

FIGURE 5 | PS exposure on intracellular amastigotes is dependent on the presence of $CD4^+$ T cells *in vivo*. **(A)** WT or nude BALB/c mice were infected with 2×10^6 stationary-phase promastigotes on the hind footpad. Lesion sizes were measured weekly by using a Vernon caliper. **(B)** PS exposure on lesion-derived amastigotes was assessed by flow cytometry. Results are shown as the ratio between the MFIs of annexin V staining of amastigotes derived from WT vs. nude mice. **(C,D)** After 7–8 weeks of infection, 4×10^6 $CD4^+$ or $CD8^+$ T cells, purified from draining LNs of infected WT BALB/c mice, were adoptively transferred to infected nude mice. At 2–3 weeks post-transfer, lesion-derived amastigotes were purified for PS exposure analysis by flow cytometry. **(C)** The shaded histograms represent amastigotes stained with annexin V in the absence of $CaCl_2$. $^{**}p < 0.01$, $^{***}p < 0.001$. **(B,D)** Graphs represent data from 2 to 3 pooled experiments.

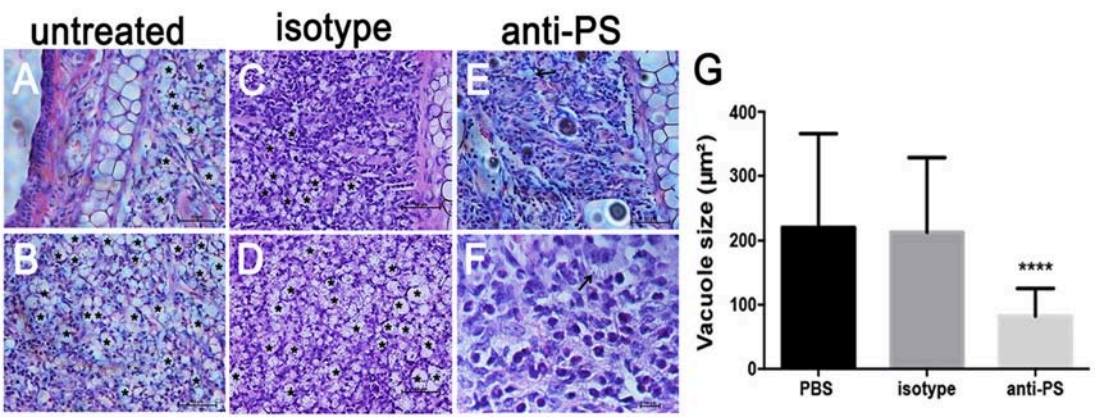

FIGURE 6 | Histopathological analysis of mice lesions treated with anti-PS blocking monoclonal antibodies. **(A–F)** Mice were infected in the ear dermis with 10^6 stationary-phase promastigotes. After 2 weeks of infection and every 3 days thereafter, mice were given i.p. injections of 100 µg of anti-PS or isotype control antibody. After 6 weeks of treatment the lesions were processed for histopathological analysis. **(A–D)** Asterisks in the images indicate large vacuoles containing amastigotes, **(E,F)** arrows indicate vacuoles containing parasites in anti PS treated infected mice. **(G)** Quantification of parasitophorous vacuole size from 2 independent experiments. $^{****}p < 0.0001$ compared to isotype and PBS treated mice.

However, the presence of this phenotype suggests that, in the case of BALB/c mice infection, the host is able to modulate parasite virulence by inducing or selecting amastigotes with an increased capacity to expose PS. Definitely, this modulation depends on host cell types and activation status, since the internalization of axenically-cultured amastigotes by MΦs induces a basal level of PS exposure on these parasites, which is absent *in vitro*. However, MΦs with different genetic backgrounds are not able, by themselves, to differentially modulate PS exposure by the intracellular parasites. Differential modulation only occurs in the presence of lymph node (LN) cells or soluble molecules produced by antigen-stimulated LN cells.

PS recognition is clearly related to the internalization of amastigotes by MΦs (de Freitas Balanco et al., 2001; Wanderley et al., 2006) and to the modulation of dendritic cells and MΦ responses by both promastigotes and amastigotes (Wanderley et al., 2006, 2009, 2013; Franca-Costa et al., 2012). These events are dependent on PS recognition by surface receptors expressed by MΦs and other phagocytic cells. However, our results indicate that PS exposure on intracellular amastigotes is a counteraction of MΦ activation, suggesting that the parasite is able to modulate the host cells from within the parasitophorous vacuole. Therefore it should be determined whether there are endosomal PS receptors expressed by the MΦ, especially those ones involved in the regulation of host cell inflammatory activation such as TAM receptors (Axl, Tyro3, and Mer; Rothlin et al., 2007). Since signal transduction can be mediated by endosomal receptors it is likely to assume that PS receptors either coopted from the plasma membrane during parasite uptake or specifically trafficked to the parasitophorous vacuole.

It is known that the T cells response elicited by *L. amazonensis* infection is not sufficient to induce parasite killing, which was confirmed by our results. Cytokines produced by both *in vivo* primed (iSNs) or naïve LN cells (nSNs) stimulated with SLA were able to induce increased PS exposure, although this effect is prominent when *in vivo* primed cells were used, due to higher cytokine concentrations. In addition to this effect, we are demonstrating that MΦ stimulation with soluble factors produced by LN cells stimulated with *L. amazonensis* antigens generates a unique condition that triggers PS exposure on intracellular amastigotes, thereby increasing parasite virulence (Wanderley et al., 2006). We tried to activate infected MΦs with different combinations of cytokines, such as IFN-γ and TNF-α, in an attempt to create the exact conditions that drive PS exposure on the intracellular parasites. Although some induction of PS exposure was observed, it did not reach the same efficiency when compared to iSN (data not shown). We understand that PS exposure depends on a very unique combination of time-dependent and concentration-dependent cytokines, which favor parasite survival over parasite killing, but maintain stress-signals sufficient to induce PS exposure. This issue could be addressed by using SNs from LN cells from other infected mice strains, such as C57BL/6 or C3H.He mice (de Oliveira Cardoso et al., 2010). There are several reports demonstrating that $CD4^+$ T cells are pathogenic for *L. amazonensis* infection; however, the mechanisms underlying this effect are not fully understood. It is well known that C57BL/6 mice deficient in the CIITA, MHC class II, and RAG2 genes or nude C57BL/6 mice exhibit a delay in lesion development and smaller parasite loads in infected tissues, indicating that $CD4^+$ T cells play a role in lesion pathology and disease progression (Soong et al., 1997). However, those mice are persistently infected, developing lesions at later time points. The administration of competent $CD4^+CD25^+$ regulatory T cells is capable of transiently inhibiting those pathogenic effector cells, ameliorating the disease (Ji et al., 2005). Actually, amastigotes derived from BALB/c nude mice expose low amounts of PS, when compared to those in parasites obtained from their WT counterparts (Franca-Costa et al., 2012). The adoptive transfer of $CD4^+$ T cells to infected nude mice stimulated PS exposure on lesion-derived amastigotes. These data reinforce the assertion that pathogenic $CD4^+$ T cells affect *Leishmania* infection and suggest that these cells are necessary to generate amastigotes with high amounts of PS at their surface that, therefore, are highly capable of re-infecting new host cells, modulating MΦ functions and avoiding immune surveillance.

The outcome of *Leishmania* infection is determined by the efficiency of MΦ activation and by the enzyme metabolizing the aminoacid L-arginine. Classical MΦ activation through inflammatory cytokines leads to iNOS expression, NO production and parasite killing, whereas regulatory or anti-inflammatory cytokines lead to non-classical MΦ activation, arginase I expression, polyamine production and parasite survival and growth (Wanasen and Soong, 2008; Acuna et al., 2017; Muxel et al., 2017a). Both pathways use L-arginine as a primary substrate. Infected MΦs stimulated with supernatants from re-stimulated LN cells led to the simultaneous expression of iNOS and arginase I. This activation provides the necessary stimuli to increase PS exposure on intracellular amastigotes without interfering with the parasites' viability and proliferative capacity. The presence of very low concentrations of NO as a result of iNOS activation was sensed by intracellular amastigotes, triggering PS exposure, while arginase I expression and possible polyamine synthesis were necessary for maintenance of parasite viability and persistence in the host. NO is known to induce apoptosis in intracellular amastigotes (Murray and Nathan, 1999). However, it is possible that the low levels of NO produced, undetected by the Griess reaction, are sufficient to trigger PS exposure that does not lead to cell death due to the simultaneous presence of polyamines derived from arginase I/ODC activity. The latter can act as a protective factor, through DNA stabilization, protecting cells from DNA degradation or inducing autophagic processes, as shown in other models (Rowlatt and Smith, 1981; Ha et al., 1998; Madeo et al., 2010). However, our data do not exclude a possible participation polyamines derived from the parasite, since treatment with DFMO could block ODC expressed by the parasite. We are currently determining the optimal concentration of different NO-donor molecules, to induce PS exposure on axenic amastigotes. This information is necessary to study both the ability of NO to induce this phenotype and to better understand the role of polyamines for parasite survival. This mechanism configures a positive feedback cycle that is beneficial for the parasite. The poor activation of specific $CD4^+$ T cell responses generates stimulatory conditions that induce non-classical MΦ

activation, leading to concomitant and low expression of both iNOS and arginase I. Non-classical MΦ activation in turn, stimulates increased and sustained PS exposure on intracellular amastigotes, generating parasites more competent to infect new host cells and spread the anti-inflammatory signals derived from PS recognition. This mechanism seems to operate in BALB/c mice. The differential activation of $CD4^+$ T cells in other mouse strains, such as C57BL/6, can explain the variations on PS exposure described in lesion-derived parasites from different mouse strains (Wanderley et al., 2006), and need to be further investigated. In addition, it is important to determine the impact of PS-dependent infection in human infections. Previous work showed that there is a positive correlation between PS exposure on parasites isolated from patients and the development of diffuse cutaneous Leishmaniasis (DCL). This correlation is also observed when comparing the level of PS on the surface of the isolated parasites and the number of lesions in the patient and the duration of the disease (Franca-Costa et al., 2012). DCL patients are characterized by low inflammatory and T cell response that leads to uncontrolled parasite dissemination and lesion development (Barroso et al., 2018). It is possible to suppose that in DCL patients, there is a unique combination of cytokines that induce augmented PS exposure on the parasite therefore leading to more severe disease.

One of the hallmarks of *L. amazonensis* infection is the peculiar parasitophorous vacuoles formed in infected MΦs. These vacuoles are large organelles shared by several parasites that continuously undergo fusion with lysosomes, exosomes and endosomes (Veras et al., 1996; Real et al., 2008). This feature is important for amastigotes to uptake nutrients (Borges et al., 1998), to dilute microbicidal molecules (Sacks and Sher, 2002; Wilson et al., 2008) and to evade the immune response (Antoine et al., 1999). Interestingly, different authors showed that enlarged vacuoles are less present in immunodeficient mice (Soong et al., 1997; Franca-Costa et al., 2012), suggesting that vacuole enlargement is also a counteractive response from amastigotes against a stressful environment. We observed that mice treated with anti-PS antibodies showed a marked and significant decrease in vacuole size when compared to untreated or isotype-treated mice. Surely, the antibodies are binding to released amastigotes since they do not have access to the parasitophorous vacuole. PS blockade could lead to a deviation in the endocytic pathway of parasite internalization since PS-dependent amastigote internalization occurs by macropinocytosis (Wanderley et al., 2006), which is characterized by the formation of enlarged endosomes (Basagiannis et al., 2016). The effect of anti-PS blocking antibodies on vacuole size provides a further explanation for the decreased parasite load of mice treated with anti-PS blocking antibodies (Wanderley et al., 2013). These results suggest that MΦ activation by T lymphocytes stimulate PS exposure and the consequences of this exposure are the alternative activation of MΦs, increase amastigote infectivity and enlargement of the parasitophorous vacuoles. The direct mechanism that link PS exposure and vacuole enlargement warrant further investigation.

In summary, this work describes that cytokine-dependent interactions between $CD4^+$ T cells and infected MΦs are sensed by intracellular parasites, which counteract by exposing PS. Exposed PS, in turn, down-regulates the MΦ microbicidal capacity (Wanderley et al., 2006, 2013). Such cross-talk is obtained by a fine-tuned balance between iNOS activation, sufficient for stress-induced PS exposure, and arginase I activation, required for maintaining parasite survival and proliferation. We provide evidence that the increased PS exposure observed on amastigotes *in vitro* or from mouse lesions is due to MΦ stimulation by cytokines produced by $CD4^+$ T cells. Therefore, the cellular immune response against the parasite can be exploited by the pathogen, generating amastigotes that are more competent to disseminate the disease and to escape from the host's immune system (Wanderley et al., 2006). In addition, we have provided further explanation for the pathogenic role of $CD4^+$ T cells during *L. amazonensis* infection.

ETHICS STATEMENT

This study was carried out in accordance with the recommendations of University of Texas Medical Branch Animal Care and Use Committee. The protocol was approved by the University of Texas Medical Branch Animal Care and Use Committee under the number #9803016A.

AUTHOR CONTRIBUTIONS

JW and PD performed *in vitro* infections, cell cultures, and *in vivo* adoptive transfer experiments. EC performed qPCR and western blot analysis of iNOS and arginase I expression. AP performed the anti-PS *in vivo* treatment and histopathological analysis. JW, RD, MB, and LS designed experiments, wrote the manuscript, and made helpful critiques.

FUNDING

This study was supported by NIH grant AI043003 to LS, NIH training grant T32AI007526 to EDC, a Brazilian National Research Council Scholarship (CNPq) to JW, a scholarship to AP (Coordenação de Aperfeiçoamento de Pessoal de Nível Superior—Brasil (CAPES)—Finance Code 001, a MCT/CNPq grant 471144/2008 and a CNPq senior investigator grant to MB.

ACKNOWLEDGMENTS

We thank Dr. Lijun Xin and Dr. Yingwei Wang for technical assistance and helpful discussion, Eulógio Carlos Queiroz de Carvalho for assistance with histopathology sample processing, and Peregrine Pharmaceuticals for kindly donate anti-PS antibodies.

SUPPLEMENTARY MATERIAL

The Supplementary Material for this article can be found online at: https://www.frontiersin.org/articles/10.3389/fcimb.2019.00105/full#supplementary-material

REFERENCES

Acuna, S. M., Aoki, J. I., Laranjeira-Silva, M. F., Zampieri, R. A., Fernandes, J. C. R., Muxel, S. M., et al. (2017). Arginase expression modulates nitric oxide production in *Leishmania (Leishmania) amazonensis*. *PLoS ONE* 12:e0187186. doi: 10.1371/journal.pone.0187186

Antoine, J. C., Lang, T., Prina, E., Courret, N., and Hellio, R. (1999). H-2M molecules, like MHC class II molecules, are targeted to parasitophorous vacuoles of *Leishmania*-infected macrophages and internalized by amastigotes of *L. amazonensis* and *L. mexicana*. *J. Cell. Sci.* 112(Pt 15), 2559–2570.

Barroso, D. H., Falcao, S. A. C., da Motta, J. O. C., Sevilha Dos Santos, L., Takano, G. H. S., Gomes, C. M., et al. (2018). PD-L1 may mediate T-cell exhaustion in a case of early diffuse leishmaniasis caused by *Leishmania (L.) amazonensis*. *Front. Immunol.* 9:1021. doi: 10.3389/fimmu.2018.01021

Basagiannis, D., Zografou, S., Murphy, C., Fotsis, T., Morbidelli, L., Ziche, M., et al. (2016). VEGF induces signalling and angiogenesis by directing VEGFR2 internalisation through macropinocytosis. *J. Cell. Sci.* 129, 4091–4104. doi: 10.1242/jcs.188219

Birge, R. B., Boeltz, S., Kumar, S., Carlson, J., Wanderley, J., Calianese, D., et al. (2016). Phosphatidylserine is a global immunosuppressive signal in efferocytosis, infectious disease, and cancer. *Cell. Death Differ.* 23, 962–978. doi: 10.1038/cdd.2016.11

Borges, V. M., Vannier-Santos, M. A., and de Souza, W. (1998). Subverted transferrin trafficking in *Leishmania*-infected macrophages. *Parasitol. Res.* 84, 811–822. doi: 10.1007/s004360050493

Canellakis, E. S., Viceps-Madore, D., Kyriakidis, D. A., and Heller, J. S. (1979). The regulation and function of ornithine decarboxylase and of the polyamines. *Curr. Top. Cell. Regul.* 15, 155–202. doi: 10.1016/B978-0-12-152815-7.50009-0

Carneiro, M. B. H., Roma, E. H., Ranson, A. J., Doria, N. A., Debrabant, A., Sacks, D. L., et al. (2018). NOX2-derived reactive oxygen species control inflammation during *Leishmania amazonensis* infection by mediating infection-induced neutrophil apoptosis. *J. Immunol.* 200, 196–208. doi: 10.4049/jimmunol.1700899

Corraliza, I. M., Soler, G., Eichmann, K., and Modolell, M. (1995). Arginase induction by suppressors of nitric oxide synthesis (IL-4, IL-10 and PGE2) in murine bone-marrow-derived macrophages. *Biochem. Biophys. Res. Commun.* 206, 667–673. doi: 10.1006/bbrc.1995.1094

Damatta, R. A., Seabra, S. H., Deolindo, P., Arnholdt, A. C., Manhaes, L., Goldenberg, S., et al. (2007). *Trypanosoma cruzi* exposes phosphatidylserine as an evasion mechanism. *FEMS Microbiol. Lett.* 266, 29–33. doi: 10.1111/j.1574-6968.2006.00495.x

de Freitas Balanco, J. M., Moreira, M. E., Bonomo, A., Bozza, P. T., Amarante-Mendes, G., Pirmez, C., et al. (2001). Apoptotic mimicry by an obligate intracellular parasite downregulates macrophage microbicidal activity. *Curr. Biol.* 11, 1870–1873. doi: 10.1016/S0960-9822(01)00563-2

de Oliveira Cardoso, F., de Souza Cda, S., Mendes, V. G., Abreu-Silva, A. L., Goncalves da Costa, S. C., and Calabrese, K. S. (2010). Immunopathological studies of *Leishmania amazonensis* infection in resistant and in susceptible mice. *J. Infect. Dis.* 201, 1933–1940. doi: 10.1086/652870

Edmond Rouan, S. K., Otterness, I. G., Cunningham, A. C., and Rhodes, C. T. (1989). Specific, high affinity colchicine binding monoclonal antibodies: development and characterization of the antibodies. *Hybridoma* 8, 435–448. doi: 10.1089/hyb.1989.8.435

Fadok, V. A., Bratton, D. L., Konowal, A., Freed, P. W., Westcott, J. Y., and Henson, P. M. (1998). Macrophages that have ingested apoptotic cells *in vitro* inhibit proinflammatory cytokine production through autocrine/paracrine mechanisms involving TGF-beta, PGE2, and PAF. *J. Clin. Invest.* 101, 890–898. doi: 10.1172/JCI1112

Fadok, V. A., Voelker, D. R., Campbell, P. A., Cohen, J. J., Bratton, D. L., and Henson, P. M. (1992). Exposure of phosphatidylserine on the surface of apoptotic lymphocytes triggers specific recognition and removal by macrophages. *J. Immunol.* 148, 2207–2216.

Feng, Z., Hensley, L., McKnight, K. L., Hu, F., Madden, V., Ping, L., et al. (2013). A pathogenic picornavirus acquires an envelope by hijacking cellular membranes. *Nature* 496, 367–371. doi: 10.1038/nature12029

Franca-Costa, J., Van Weyenbergh, J., Boaventura, V. S., Luz, N. F., Malta-Santos, H., Oliveira, M. C., et al. (2015). Arginase I, polyamine, and prostaglandin E2 pathways suppress the inflammatory response and contribute to diffuse cutaneous Leishmaniasis. *J. Infect. Dis.* 211, 426–435. doi: 10.1093/infdis/jiu455

Franca-Costa, J., Wanderley, J. L., Deolindo, P., Zarattini, J. B., Costa, J., Soong, L., et al. (2012). Exposure of phosphatidylserine on *Leishmania amazonensis* isolates is associated with diffuse cutaneous Leishmaniasis and parasite infectivity. *PLoS ONE* 7:e36595. doi: 10.1371/journal.pone.0036595

Ha, H. C., Yager, J. D., Woster, P. A., and Casero, R. A. Jr. (1998). Structural specificity of polyamines and polyamine analogues in the protection of DNA from strand breaks induced by reactive oxygen species. *Biochem. Biophys. Res. Commun.* 244, 298–303. doi: 10.1006/bbrc.1998.8258

Hoffmann, P. R., deCathelineau, A. M., Ogden, C. A., Leverrier, Y., Bratton, D. L., Daleke, D. L., et al. (2001). Phosphatidylserine (PS) induces PS receptor-mediated macropinocytosis and promotes clearance of apoptotic cells. *J. Cell. Biol.* 155, 649–659. doi: 10.1083/jcb.200108080

Ji, J., Masterson, J., Sun, J., and Soong, L. (2005). CD4+CD25+ regulatory T cells restrain pathogenic responses during *Leishmania amazonensis* infection. *J. Immunol.* 174, 7147–7153. doi: 10.4049/jimmunol.174.11.7147

Ji, J., Sun, J., Qi, H., and Soong, L. (2002). Analysis of T helper cell responses during infection with *Leishmania amazonensis*. *Am. J. Trop. Med. Hyg.* 66, 338–345. doi: 10.4269/ajtmh.2002.66.338

Ji, J., Sun, J., and Soong, L. (2003). Impaired expression of inflammatory cytokines and chemokines at early stages of infection with *Leishmania amazonensis*. *Infect. Immun.* 71, 4278–4288. doi: 10.1128/IAI.71.8.4278-4288.2003

Lasakosvitsch, F., Gentil, L. G., dos Santos, M. R., da Silveira, J. F., and Barbieri, C. L. (2003). Cloning and characterisation of a cysteine proteinase gene expressed in amastigotes of *Leishmania* (*L.*) *amazonensis*. *Int. J. Parasitol.* 33, 445–454. doi: 10.1016/S0020-7519(03)00010-9

Lecoeur, H., de La Llave, E., Osorio, Y. F. J., Goyard, S., Kiefer-Biasizzo, H., Balazuc, A. M., et al. (2010). Sorting of *Leishmania*-bearing dendritic cells reveals subtle parasite-induced modulation of host-cell gene expression. *Microbes Infect.* 12, 46–54. doi: 10.1016/j.micinf.2009.09.014

Leon, L. L., Machado, G. M., Paes, L. E., and Grimaldi Junior, G. (1990). Antigenic differences of *Leishmania amazonensis* isolates causing diffuse cutaneous Leishmaniasis. *Trans. R. Soc. Trop. Med. Hyg.* 84, 678–680. doi: 10.1016/0035-9203(90)90144-4

Madeo, F., Tavernarakis, N., and Kroemer, G. (2010). Can autophagy promote longevity? *Nat. Cell. Biol.* 12, 842–846. doi: 10.1038/ncb0910-842

Majumder, S., and Kierszenbaum, F. (1993). Inhibition of host cell invasion and intracellular replication of *Trypanosoma cruzi* by N,N'-bis(benzyl)-substituted polyamine analogs. *Antimicrob. Agents Chemother.* 37, 2235–2238. doi: 10.1128/AAC.37.10.2235

Mercer, J., and Helenius, A. (2008). Vaccinia virus uses macropinocytosis and apoptotic mimicry to enter host cells. *Science* 320, 531–535. doi: 10.1126/science.1155164

Modolell, M., Corraliza, I. M., Link, F., Soler, G., and Eichmann, K. (1995). Reciprocal regulation of the nitric oxide synthase/arginase balance in mouse bone marrow-derived macrophages by TH1 and TH2 cytokines. *Eur. J. Immunol.* 25, 1101–1104. doi: 10.1002/eji.1830250436

Moore, W. M., Webber, R. K., Jerome, G. M., Tjoeng, F. S., Misko, T. P., and Currie, M. G. (1994). L-N6-(1-iminoethyl)lysine: a selective inhibitor of inducible nitric oxide synthase. *J. Med. Chem.* 37, 3886–3888. doi: 10.1021/jm00049a007

Murray, H. W., and Nathan, C. F. (1999). Macrophage microbicidal mechanisms in vivo: reactive nitrogen versus oxygen intermediates in the killing of intracellular visceral *Leishmania donovani*. *J. Exp. Med.* 189, 741–746. doi: 10.1084/jem.189.4.741

Muxel, S. M., Aoki, J. I., Fernandes, J. C. R., Laranjeira-Silva, M. F., Zampieri, R. A., Acuna, S. M., et al. (2017a). Arginine and Polyamines Fate in *Leishmania* Infection. *Front. Microbiol.* 8:2682. doi: 10.3389/fmicb.2017.02682

Muxel, S. M., Laranjeira-Silva, M. F., Zampieri, R. A., and Floeter-Winter, L. M. (2017b). *Leishmania* (*Leishmania*) *amazonensis* induces macrophage miR-294 and miR-721 expression and modulates infection by targeting NOS2 and L-arginine metabolism. *Sci. Rep.* 7:44141. doi: 10.1038/srep44141

Osorio y Fortea, J., Prina, E., de La Llave, E., Lecoeur, H., Lang, T., and Milon, G. (2007). Unveiling pathways used by *Leishmania amazonensis* amastigotes to subvert macrophage function. *Immunol. Rev.* 219, 66–74. doi: 10.1111/j.1600-065X.2007.00559.x

Poon, I. K., Lucas, C. D., Rossi, A. G., and Ravichandran, K. S. (2014). Apoptotic cell clearance: basic biology and therapeutic potential. *Nat. Rev. Immunol.* 14, 166–180. doi: 10.1038/nri3607

Prina, E., Abdi, S. Z., Lebastard, M., Perret, E., Winter, N., and Antoine, J. C. (2004). Dendritic cells as host cells for the promastigote and amastigote stages of *Leishmania amazonensis*: the role of opsonins in parasite uptake and dendritic cell maturation. *J. Cell. Sci.* 117(Pt 2), 315–325. doi: 10.1242/jcs.00860

Prina, E., Antoine, J. C., Wiederanders, B., and Kirschke, H. (1990). Localization and activity of various lysosomal proteases in *Leishmania amazonensis*-infected macrophages. *Infect. Immun.* 58, 1730–1737.

Prina, E., Jouanne, C., de Souza Lao, S., Szabo, A., Guillet, J. G., and Antoine, J. C. (1993). Antigen presentation capacity of murine macrophages infected with *Leishmania amazonensis* amastigotes. *J. Immunol.* 151, 2050–2061.

Ramer, A. E., Vanloubbeeck, Y. F., and Jones, D. E. (2006). Antigen-responsive CD4+ T cells from C3H mice chronically infected with *Leishmania amazonensis* are impaired in the transition to an effector phenotype. *Infect. Immun.* 74, 1547–1554. doi: 10.1128/IAI.74.3.1547-1554.2006

Real, F., Pouchelet, M., and Rabinovitch, M. (2008). *Leishmania* (*L.*) *amazonensis*: fusion between parasitophorous vacuoles in infected bone-marrow derived mouse macrophages. *Exp. Parasitol.* 119, 15–23. doi: 10.1016/j.exppara.2007.12.013

Rothlin, C. V., Ghosh, S., Zuniga, E. I., Oldstone, M. B., and Lemke, G. (2007). TAM receptors are pleiotropic inhibitors of the innate immune response. *Cell* 131, 1124–1136. doi: 10.1016/j.cell.2007.10.034

Rowlatt, C., and Smith, G. J. (1981). Ultrastructural studies on chromatin digestion by micrococcal nuclease in the presence of polyamines. *J. Cell. Sci.* 48, 171–179.

Sacks, D., and Sher, A. (2002). Evasion of innate immunity by parasitic protozoa. *Nat. Immunol.* 3, 1041–1047. doi: 10.1038/ni1102-1041

Saraiva, E. M., Pimenta, P. F., Pereira, M. E., and de Souza, W. (1983). Isolation and purification of amastigotes of *Leishmania mexicana amazonensis* by a gradient of Metrizamide. *J. Parasitol.* 69, 627–629. doi: 10.2307/3281388

Seabra, S. H., de Souza, W., and Damatta, R. A. (2004). *Toxoplasma gondii* exposes phosphatidylserine inducing a TGF-beta1 autocrine effect orchestrating macrophage evasion. *Biochem. Biophys. Res. Commun.* 324, 744–752. doi: 10.1016/j.bbrc.2004.09.114

Silveira, F. T., Lainson, R., and Corbett, C. E. (2005). Further observations on clinical, histopathological, and immunological features of borderline disseminated cutaneous Leishmaniasis caused by *Leishmania* (*Leishmania*) *amazonensis*. *Mem. Inst. Oswaldo Cruz.* 100, 525–534. doi: 10.1590/S0074-02762005000500013

Soares, M. M., King, S. W., and Thorpe, P. E. (2008). Targeting inside-out phosphatidylserine as a therapeutic strategy for viral diseases. *Nat. Med.* 14, 1357–1362. doi: 10.1038/nm.1885

Soong, L. (2008). Modulation of dendritic cell function by *Leishmania* parasites. *J. Immunol.* 180, 4355–4360. doi: 10.4049/jimmunol.180.7.4355

Soong, L., Chang, C. H., Sun, J., Longley, B. J. Jr., Ruddle, N. H., Flavell, R. A., et al. (1997). Role of CD4+ T cells in pathogenesis associated with *Leishmania amazonensis* infection. *J. Immunol.* 158, 5374–5383.

Stenger, S., Thuring, H., Rollinghoff, M., Manning, P., and Bogdan, C. (1995). L-N6-(1-iminoethyl)-lysine potently inhibits inducible nitric oxide synthase and is superior to NG-monomethyl-arginine *in vitro* and *in vivo*. *Eur. J. Pharmacol.* 294, 703–712. doi: 10.1016/0014-2999(95)00618-4

Terabe, M., Wakana, S., Katakura, K., Onodera, T., Matsumoto, Y., and Ito, M. (2004). Influence of H2 complex and non-H2 genes on progression of cutaneous lesions in mice infected with *Leishmania amazonensis*. *Parasitol. Int.* 53, 217–221. doi: 10.1016/j.parint.2003.12.002

Vannier-Santos, M. A., Menezes, D., Oliveira, M. F., and de Mello, F. G. (2008). The putrescine analogue 1,4-diamino-2-butanone affects polyamine synthesis, transport, ultrastructure and intracellular survival in *Leishmania amazonensis*. *Microbiology* 154(Pt 10), 3104–3111. doi: 10.1099/mic.0.2007/013896-0

Vargas-Inchaustegui, D. A., Tai, W., Xin, L., Hogg, A. E., Corry, D. B., and Soong, L. (2009). Distinct roles for MyD88 and Toll-like receptor 2 during *Leishmania braziliensis* infection in mice. *Infect. Immun.* 77, 2948–2956. doi: 10.1128/IAI.00154-09

Veras, P. S., Topilko, A., Gouhier, N., Moreau, M. F., Rabinovitch, M., and Pouchelet, M. (1996). Fusion of *Leishmania amazonensis* parasitophorous vacuoles with phagosomes containing zymosan particles: cinemicrographic and ultrastructural observations. *Braz. J. Med. Biol. Res.* 29, 1009–1018.

Wanasen, N., and Soong, L. (2008). L-arginine metabolism and its impact on host immunity against *Leishmania* infection. *Immunol. Res.* 41, 15–25. doi: 10.1007/s12026-007-8012-y

Wanderley, J. L., Moreira, M. E., Benjamin, A., Bonomo, A. C., and Barcinski, M. A. (2006). Mimicry of apoptotic cells by exposing phosphatidylserine participates in the establishment of amastigotes of *Leishmania* (*L*) *amazonensis* in mammalian hosts. *J. Immunol.* 176, 1834–1839. doi: 10.4049/jimmunol.176.3.1834

Wanderley, J. L., Pinto da Silva, L. H., Deolindo, P., Soong, L., Borges, V. M., Prates, D. B., et al. (2009). Cooperation between apoptotic and viable metacyclics enhances the pathogenesis of Leishmaniasis. *PLoS ONE* 4:e5733. doi: 10.1371/journal.pone.0005733

Wanderley, J. L. M., Thorpe, P. E., Barcinski, M. A., and Soong, L. (2013). Phosphatidylserine exposure on the surface of *Leishmania amazonensis* amastigotes modulates *in vivo* infection and dendritic cell function. *Parasite Immunol.* 35, 109–119. doi: 10.1111/pim.12019

Wilson, J., Huynh, C., Kennedy, K. A., Ward, D. M., Kaplan, J., Aderem, A., et al. (2008). Control of parasitophorous vacuole expansion by LYST/Beige restricts the intracellular growth of *Leishmania amazonensis*. *PLoS Pathog.* 4:e1000179. doi: 10.1371/journal.ppat.1000179

Xie, Q. W., Whisnant, R., and Nathan, C. (1993). Promoter of the mouse gene encoding calcium-independent nitric oxide synthase confers inducibility by interferon gamma and bacterial lipopolysaccharide. *J. Exp. Med.* 177, 1779–1784. doi: 10.1084/jem.177.6.1779

Xin, L., Li, K., and Soong, L. (2008). Down-regulation of dendritic cell signaling pathways by *Leishmania amazonensis* amastigotes. *Mol. Immunol.* 45, 3371–3382. doi: 10.1016/j.molimm.2008.04.018

Xin, L., Vargas-Inchaustegui, D. A., Raimer, S. S., Kelly, B. C., Hu, J., Zhu, L., et al. (2010). Type I IFN receptor regulates neutrophil functions and innate immunity to *Leishmania* parasites. *J. Immunol.* 184, 7047–7056. doi: 10.4049/jimmunol.0903273

Zhou, H., Stafford, J. H., Hallac, R. R., Zhang, L., Huang, G., Mason, R. P., et al. (2014). Phosphatidylserine-targeted molecular imaging of tumor vasculature by magnetic resonance imaging. *J. Biomed. Nanotechnol.* 10, 846–855. doi: 10.1166/jbn.2014.1851

Conflict of Interest Statement: The authors declare that the research was conducted in the absence of any commercial or financial relationships that could be construed as a potential conflict of interest.

frontiers in Cellular and Infection Microbiology

ORIGINAL RESEARCH
published: 02 May 2019
doi: 10.3389/fcimb.2019.00120

Leishmania braziliensis Infection Enhances Toll-Like Receptors 2 and 4 Expression and Triggers TNF-α and IL-10 Production in Human Cutaneous Leishmaniasis

Ludmila P. Polari[1], *Pedro Paulo Carneiro*[1,2], *Michael Macedo*[1], *Paulo R. L. Machado*[1,2], *Phillip Scott*[3], *Edgar M. Carvalho*[2,4] *and Olivia Bacellar*[1,2]*

[1] Serviço de Imunologia, Complexo Hospitalar Universitário Prof. Edgard Santos, Universidade Federal da Bahia, Salvador, Brazil, [2] Instituto Nacional de Ciência e Tecnologia de Doenças Tropicais - INCT-DT (CNPq/MCT), Salvador, Brazil, [3] Department of Pathobiology, School of Veterinary Medicine, University of Pennsylvania, Philadelphia, PA, United States, [4] Instituto Pesquisa Gonçalo Moniz – Fiocruz-Bahia, Salvador, Brazil

OPEN ACCESS

Edited by:
Anabela Cordeiro-da-Silva, Universidade do Porto, Portugal

Reviewed by:
Fátima Ribeiro-Dias, Universidade Federal de Goiás, Brazil
Julio Scharfstein, Federal University of Rio de Janeiro, Brazil

***Correspondence:**
Olivia Bacellar
olivinhaufba@gmail.com

Specialty section:
This article was submitted to Parasite and Host, a section of the journal Frontiers in Cellular and Infection Microbiology

Received: 31 October 2018
Accepted: 04 April 2019
Published: 02 May 2019

Citation:
Polari LP, Carneiro PP, Macedo M, Machado PRL, Scott P, Carvalho EM and Bacellar O (2019) Leishmania braziliensis Infection Enhances Toll-Like Receptors 2 and 4 Expression and Triggers TNF-α and IL-10 Production in Human Cutaneous Leishmaniasis. Front. Cell. Infect. Microbiol. 9:120. doi: 10.3389/fcimb.2019.00120

Cutaneous leishmaniasis (CL) caused by infection with *Leishmania braziliensis* is characterized by an exaggerated inflammatory response that controls the parasite burden, but also contributes to pathology. While myeloid cells are required to eliminate the parasite, recent studies indicate that they may also participate in the inflammatory response driving disease progression. The innate immune response to leishmania is driven in part by the Toll-like receptors (TLRs) TLR2, TLR4, and TLR9. In this study, we used flow cytometric analysis to compare TLR2 and TLR4 expression in monocyte subsets (classical, intermediate, and non-classical) from CL patients and healthy subjects (HS). We also determined if there was an association of either the pro-inflammatory cytokine TNF or the anti-inflammatory cytokine IL-10 with TLR2 or TLR4 expression levels after *L. braziliensis* infection. *In vitro* infection with *L. braziliensis* caused CL monocytes to up-regulate TLR2 and TLR4 expression. We also found that intermediate monocytes expressed the highest levels of TLR2 and TLR4 and that infected monocytes produced more TNF and IL-10 than uninfected monocytes. Finally, while classical and intermediate monocytes were mainly responsible for TNF production, classical monocytes were the main source of IL-10. Collectively, our studies revealed that up-regulated TLR2/4 expression and TNF production by intermediate/inflammatory subsets of monocytes from patients correlates with detrimental outcome of cutaneous leishmaniasis.

Keywords: human cutaneous leishmaniasis, *Leishmania braziliensis*, toll like receptor 2, toll like receptor 4, inflammation, monocytes subsets

INTRODUCTION

The protozoan parasite leishmania is the causal agent of tegumentary and visceral leishmaniasis. Cutaneous leishmaniasis (CL), characterized by a well-delimited ulcer, is the most common form of American Tegumentary Leishmaniasis, and *Leishmania braziliensis* is the most important species associated with CL in the New World (Alvar et al., 2012). The immune response to *L. braziliensis* is characterized by a strong Th1 response with high production of IFN-γ, TNF and other pro-inflammatory cytokines (Bacellar et al., 2002; Gomes-Silva et al., 2007; Faria et al., 2012; Gonzalez-Lombana et al., 2013). This defense mechanism is important to control parasite growth and dissemination, but the exaggerated inflammation, mainly due the reduced ability of IL-10 to appropriately down regulate the immune response to leishmania antigens (Bacellar et al., 2002; Gonzalez-Lombana et al., 2013; Oliveira et al., 2014), contributes to the pathology of CL (Antonelli et al., 2005; Santos Cda et al., 2013; Cardoso et al., 2015; Novais et al., 2017).

Myeloid cells, including monocytes, dendritic cells, and macrophages, act as the principal host cells for *Leishmania*. Myeloid cells play a central role in the development of the immune response against these parasites via antigen presentation as well as the secretion of cytokines, chemokines, and microbicidal products. Early interactions between leishmania and macrophages can determine the outcome of the infection (Bosque et al., 2000). In *L. braziliensis* infection we have shown that macrophages from CL patients produce high amounts of TNF, CXCL9, CXCL10, and CCL3 after leishmania infection but their ability to kill the parasite is impaired (Giudice et al., 2012; Muniz et al., 2016).

Monocytes are macrophage precursors. Based on the expression of CD14 and the high affinity Fc receptor for IgG (CD16), monocytes are differentiated into three subsets: classical monocytes($CD14^{high}CD16^{-}$), intermediate or inflammatory monocytes ($CD14^{high}CD16^{+}$), and non-classical monocytes, also known as patrolling monocytes ($CD14^{low}CD16^{++}$)(Ziegler-Heitbrock et al., 2010). Intermediate monocytes are increased in CL and are the major source of TNF, a cytokine involved in the pathology of CL (Soares et al., 2006; Passos et al., 2015). These data point to the participation of myeloid-lineage cells, in addition to T cells, in the pathology of CL.

The Toll-like receptors (TLR) are a well-characterized class of pattern recognition receptors (PRRs) and the TLR signaling pathway is one the first defense mechanisms against *Leishmania* (Medzhitov and Janeway, 2000; Tuon et al., 2008). TLRs bind to myeloid differentiation factor 88 (MyD88), resulting in downstream activation of NF-κB and the subsequent transcription of inflammatory mediators such as TNF, IL-6, and IL-1 (Medzhitov and Janeway, 2000). Macrophages recognize *Leishmania* mainly through TLR2, TLR4, and TLR9 (Becker et al., 2003; de Veer et al., 2003; Kropf et al., 2004a,b; Faria et al., 2005; Flandin et al., 2006; Viana et al., 2017).

Most of the studies about TLRs in leishmaniasis are in experimental models with different species of the parasite. For instance, C57Bl/6 MyD88-null mice are more susceptible to infection with *L. major* than wild type animals (de Veer et al., 2003) while C57BL/6J $TLR2^{-/-}$ mice infected with *L. braziliensis* are more resistant to infection than C57BL/6J wild type mice (Vargas-Inchaustegui et al., 2009). Also, in C57BL/6 $TLR2^{-/-}$ mice infected with *Leishmania amazonensis*, the parasite burden is reduced when compared with C57BL/ 6 wild type mice which were more susceptible to the infection (Guerra et al., 2010). Studies performed in BALB/c mice infected with *Leishmania donovani* showed an increase in TLR2 and TLR4 mRNA, which was correlated with parasite load (Cezário et al., 2011). In contrast, TLR4-deficient mice are unable to control *L. major* infection and develop lesions that are more severe as compared to wild type animals (Kropf et al., 2004b). Additionally, in BALB/c mice infected with *Leishmania pifanoi,* the TNF production in the infected TLR4 $^{-/-}$ bone marrow-derived macrophages was significantly lower and *in vivo* the number of parasites in footpad lesions was higher than their wild type counterpart (Whitaker et al., 2008). In CL patients, the exposure to soluble *Leishmania* antigen (SLA) enhances TLR9 expression on monocytes [30]. Moreover, the frequency of $TLR9^{+}$ monocytes is correlated with greater lesion size (Vieira et al., 2013). However, in the lesion site, TLR9 was associated with granuloma formation (Tuon et al., 2010). These studies show that depending on the mice strain and the leishmania species, TLR expression may have either a protective or a deleterious effect on leishmania infection.

We have previously shown that *ex vivo* expression of TLR2 and TLR4 is higher on monocytes from CL patients as compared to monocytes from healthy subjects (HS) (Carneiro et al., 2016). In the present study, we investigate the expression of TLR2 and TLR4 on *L. braziliensis* infected monocyte subsets from CL patients and assess if TLR expression in monocyte subsets is associated with the production of TNF and IL-10. Our results reveal that infection with *L. braziliensis* increases the expression of TLR2 and TLR4 on inflammatory monocyte subsets and this increase is accomplished mainly by TNF production. These findings suggest that TLR expression contributes to an enhancement in the inflammatory response and pathology in the *L. braziliensis* infection.

MATERIALS AND METHODS

Patients

A total of 30 patients with CL were included in this study. These patients sought medical attention from the Health Post of Corte de Pedra, municipality of Tancredo Neves, Bahia, Brazil, a known area of *L. braziliensis* transmission. Patients were diagnosed with CL if they presented with a clinical picture characteristic of the disease in conjunction with one of the following positive test results: parasite isolation in culture, parasite identification in histopathologic analysis, or the presence of parasite DNA by polymerase chain reaction (PCR) (Weirather et al., 2011). The CL group was composed of 25 males and 5 females. The median of age was 31 ranging between 18 and 54 years of age. A control group was formed by 20 healthy subjects (HS) living in an urban area of no exposure to leishmania, with 5 males and 15 females. The median of age was 31, ranging between 23 and 45 years.

All the experiments were performed prior to therapy. All patients were treated with i.v. meglumine antimoniate (Sanofi-Aventis, Paris, France) in a dose of 20 mg/kg body weight daily for 20 days.

Ethics Statement

This study was carried out in accordance with the recommendations of Institutional Review Board of the Federal University of Bahia, Brazil, with written informed consent from all subjects. All subjects gave written informed consent in accordance with the Declaration of Helsinki. The protocol was approved by the Institutional Review Board of the Federal University of Bahia, Brazil (approval number 693.111).

Human Blood Samples and Preparation of Peripheral Blood Cells

Peripheral blood mononuclear cells (PBMC) were separated from heparinized venous blood by Ficoll-Hypaque gradient centrifugation. Cells were then washed in saline and resuspended in RPMI 1640 (supplemented with 5% of fetal calf serum, 100 U penicillin/mL, 100 ug streptomycin/ mL) (GIBCO BRL., Grand Island, NY, USA).

Parasites

An isolate of leishmania obtained from a skin lesion of a CL patient from Corte de Pedra (MHOM/BR/LTCP11245) was characterized as *L. brazilensis* using PCR and multicolus enzyme electrophoresis (Cupolillo et al., 1994). Parasites were initially grown in biphasic medium (NNN). After isolation, the parasite was cryopreserved in liquid nitrogen. The parasites selected for this study had not been previously passaged in liquid culture medium. After selection, the parasites were expanded in complete Schneider's medium (Aldrch Sigma, St. Louis, MO) supplemented with 10% fetal bovine serum (FBS) (Gilco BRL) and 2% sterile urine. For *in vitro* infection of PBMC, the promastigotes in the stationary growth phase were stained with 5 mM Carboxyfluorescein succinimidyl ester (CFSE) to identify cells infected by *L. braziliensis* (Chang et al., 2007). All the reagents and Schneider medium are endotoxin free as determined by Endotoxin Testing (LAL) (BioReliance, SIGMA-ALDRICH).

Infection of Monocytes With *L. braziliensis*

PBMC (1×10^6 cells / tube) of CL patients and healthy subjects were infected with *L. braziliensis* labeled with CFSE (as described above) at a ratio of 5:1 parasites per cell and incubated for 1 h at 37°C in a 5% CO_2 atmosphere. After this period, extracellular parasites were washed with 0.9% saline containing 10% FBS. The cells were placed in complete RPMI 1640 medium and incubated at 37°C in an atmosphere of 5% CO_2 for 4 h and 24 h. The infection was assessed by CFSE fluorescence (FITC) by flow cytometry.

Expression of CD14, CD16, TLR4, and TLR2 in Monocytes From Peripheral Blood by Flow Cytometry

CL patient and healthy subject peripheral blood monocyte expression of CD14, CD16, TLR2, and TLR4 was analyzed *in vitro* after 4 h incubation with CFSE-labeled *L. braziliensis* or stimulation with one of the following reagents: lipopolysaccharide (LPS) (100 ng/ml) or synthetic TLR2 ligands tripalmitoyl-S- glycerol-Cys-(Lys)4 (Pam3Cys) (100 ng/ml). The analysis was performed by flow cytometry. The following antibodies were used: anti-CD14 conjugated with PerCP-Cy5.5 (clone 61D3) and anti-CD16 conjugated to APC (clone CB16) (eBioscience, San Diego, CA, USA); anti-TLR2 conjugated to PE (clone TL2.1) and anti-TLR4 PE-conjugated (clone HTA125) (IMGENEX, San Diego, CA, USA). Analysis of TLR2 and TLR4 expression was undertaken in separate tubes. After staining, cells were washed and resuspended in 4% paraformaldehyde solution. We acquired at least 200,000 events on the flow cytometry BD FACS CANTOII. Data analysis was performed using FlowJo software (Free Star Inc.).

Analysis of the Expression of TNF and IL-10 in Monocytes by Flow Cytometry

PBMCs were either infected with parasites of *L braziliensis* or left uninfected. Infected and uninfected PBMCs were then incubated separately for 8 h and 24 h at 37°C, 5% CO_2. Cells were then stained with anti-CD14 monoclonal antibodies (PerCP Cy-5.5), anti-CD16 (APC), anti-TLR2 (PE) and anti-TLR4 (PE) for 15 min 4°C in the dark (BD-Bioscience). The cells were washed with PBS (1,500 rpm, 5 min, 4°C), fixed with 4% paraformaldehyde, and permeabilized with Perm Wash solution for 15 min at 4°C in the dark (BD-Bioscience). Intracellular staining was performed with anti-TNF and anti-IL-10 (FITC) antibodies for 30 min. After this period, the cells were washed and suspended in 400 µl PBS for flow cytometry analysis on BD FACS CANTOII. A total of 200,000 events were acquired. Data analysis was performed using FlowJo program (Free Star Inc.).

Statistical Analysis

Data analyses were performed using GraphPad Prism 5.0 (GraphPad Software, Inc., San Diego, CA, USA). The comparison between groups was performed using the non-parametric Mann-Whitney U test. Analysis of variance (Kruskal-Wallis) was calculated to assess the differences between three or more groups, with Dunn's post-test. Analysis of variance (ANOVA) with Bonferroni post-test's was performed when the data presented normal Gaussian distribution. An error below 5% ($p < 0.05\%$) was used for statistical significance.

RESULTS

Ex vivo Expression of TLR2 and TLR4 on Different Monocytes Subsets

We had shown that e*x vivo* expression of TLR2 and TLR4 on monocytes from CL patients was higher than on monocytes from HS (Carneiro et al., 2016). Monocytes are a heterogeneous population of cells and there are three monocytes subsets based on the expression of CD14 and CD16. The expression and CD14 CD16 was not modified after infection with *L.braziliensis* (data not shown) but it known that the frequency of intermediate (inflammatory) monocytes is higher in CL patients than in HS (Soares et al., 2006; Passos et al., 2015). In the present study, to determine if the expression of TLRs differs among

monocyte subsets, we analyzed the *ex vivo* expression of TLR2 and TLR4 on classical, intermediate, and non-classical monocytes (**Figure 1**). In CL patients, TLR2 expression, represented by the mean fluorescence intensity (MFI), was more intense in classical and intermediate monocytes than in non-classical monocytes, although only the latter achieved statistical significance, $p < 0.001$ (**Figure 1B**). The MFI for TLR4 (**Figure 1C**) in CL patients was similar in classical and intermediate monocytes and both subpopulations expressed more TLR4 than non-classical monocytes ($p < 0.01$). In HS, the MFI for TLR2 and TLR4 was higher in classical and intermediate monocytes than in non-classical monocytes (**Figures 1B,C**). In HS group, the expression of these receptors in all monocytes subsets was lower than in CL monocytes ($p < 0.01$ and $p < 0.001$). A comparative analysis of the MFI for TLR2 and TLR4 in CL patients vs. HS in intermediate monocytes showed that cells from CL patients expressed more TLR2 and TLR4 than cells from the HS group ($p < 0.001$).

Infection With *L. braziliensis* Increase TLR2 and TLR4 Expression on Monocytes From CL Patients

To assess if the infection with *L. braziliensis* modifies either TLR2 or TLR4 expression in CL monocytes, the expression of these receptors was evaluated on *L. braziliensis*-infected monocytes. First, the infection rate on monocytes from CL and HS was compared. The frequency of *L. braziliensis*-infected monocytes was similar in CL cells and in HS cells, 55and 62%, respectively, $p > 0.05$ (**Figure 2A**). Also, we found that classical and intermediate monocytes were more infected than non-classical monocytes and there was no difference in CL and HS (**Figure 2B**)

Next, the expression of these receptors was evaluated on non-infected cells and *L. braziliensis*-infected cells from CL patients. The median MFI of TLR2 and TLR4 on infected monocytes was significantly higher ($p < 0.001$) than that observed in uninfected monocytes (**Figures 3A,B**). We also evaluated the expression of TLR2 and TLR4 on monocytes from HS after infection with *L.braziliensis*. The infection with *L.braziliensis* increased the expression of TLR2 and TLR4 on monocytes from HS. However, the expression of TLR2 and TLR4 was lower than that observed in CL patients, 25 (22-29); (Whitaker et al., 2008; Guerra et al., 2010; Cezário et al., 2011) vs. 70 (27–150, < 0.05) and 43 (24–56) vs. 54 (25–72, p <0.05), respectively. There was no difference in the expression of these receptors between the different periods of infection in both groups, CL and HS (**Supplementary Figure 1**).

TLR2 and TLR4 Expression on Different Monocytes Subsets After Infection With *L. braziliensis*

Because the *ex vivo* expression of these receptors was higher on inflammatory monocytes from CL patients, further experiments evaluating the expression of TLR2 and TLR4 on monocyte subsets after infection with *L. braziliensis* were performed.

The intensity of expression of TLR2 and TLR4 on different monocyte subsets from CL patients and HS after infection with *L. braziliensis* is shown in **Figure 4**.

In fact, the infection with *L. braziliensis* increased the expression of TLR2 and TLR4 on intermediate monocytes. Again, in CL patients, TLR2 expression was more intense in classical and intermediate monocytes than in non-classical monocytes (**Figure 4B**), Also, the expression of TLR4 was higher on intermediate monocytes than in classical and non-classical monocytes. However, the expression of TLR2 and TLR4 on *L. braziliensis* infected intermediate monocytes from CL patients was higher than that observed on monocyte subsets from HS individuals (**Figures 4A,B**). In uninfected monocytes the expression of these receptors was lower than in infected cells in both groups. Additionally, we evaluate the expression of TLR2 and TLR4 after 24 h of infection and the expression of these receptors was similar to that obtained after 4 h of infection. The expression of these receptors was also higher in intermediate monocytes (**Supplementary Figure 2**).

So far, these results indicate that in human CL, in addition to TLR2 and TLR4 are preferentially expressed in intermediate monocytes, the infection with *L. braziliensis* increases the expression of these receptors on this monocyte subset. Thus, increased expression of TLR2 and TLR4 in the CL patient's intermediate monocytes may result in an enhancement of the inflammatory response.

Evaluation of the Intracellular Expression of TNF and IL-10 in Monocytes From CL Patients Expressing TLR2 and TLR4 After Infection With *L. braziliensis*

TLRs initiate innate immune responses in a variety of ways, leading to the production of inflammatory cytokines, such as TNF, by dendritic cells, macrophages, and monocytes (Kuniyoshi et al., 2014). IL-10 is the most important regulatory cytokine in leishmaniasis (Carvalho et al., 1994b; Bomfim et al., 1996; Bacellar et al., 2002). The high levels of TNF and the decreased ability of IL-10 to down regulate cytokine production leads to an exacerbation of the inflammatory reaction and development of cutaneous and mucosal leishmaniasis following infection with *L. braziliensis* (Da-Cruz et al., 1996; Bacellar et al., 2002; Antonelli et al., 2005). Thus, we asked if the increased expression of TLR2 and TLR4 on infected-monocytes was associated with an increase in production of TNF and IL-10 by these cells. While the frequency of infected monocytes co-expressing TLR2 and TNF was 44% (19–74%) and TLR4 and TNF was 61% (39–75%), in non-infected monocytes co-expression of these receptors and TNF was 7% (3–75%) and 7% (4–33%), respectively (**Figure 5A**). Similar data was observed regarding IL-10. The frequency of cells expressing IL-10 in TLR2 $^{(+)}$ and TLR4 $^{(+)}$ infected monocytes was higher than that observed in non-infected monocytes expressing these receptors (**Figure 5B**). These data reveal that expression of TLR2 and TLR4 up regulate TNF and IL-10 expression in infected monocytes from CL patients.

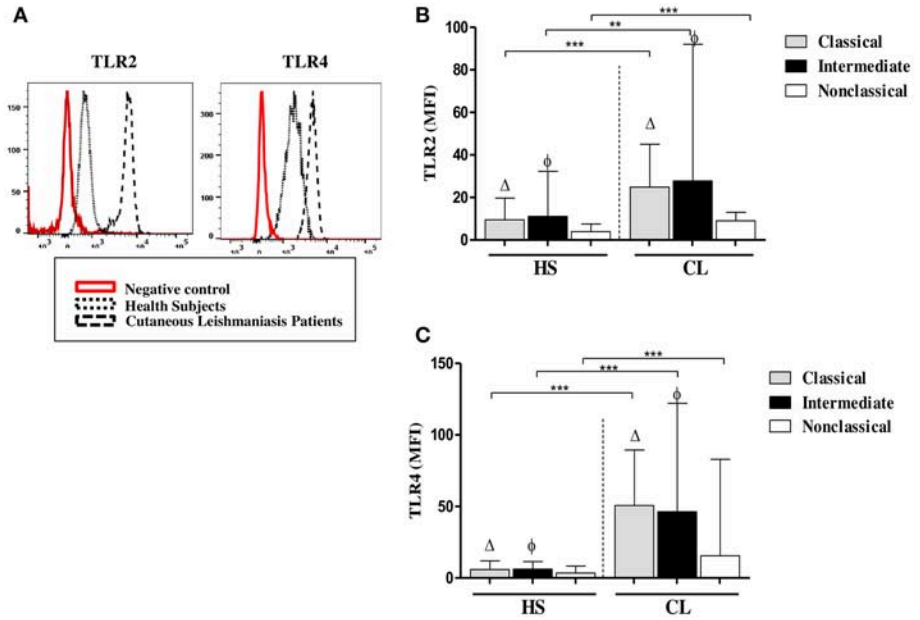

FIGURE 1 | Classical ($CD14^{high}CD16^{-}$) and intermediate monocytes ($CD14^{high}CD16^{+}$) express more TLR2 and TLR4 than non-classical ($CD14^{low}CD16^{+}$) monocytes. **(A)** Representative strategy analysis for the TLR2 and TLR4 expression. **(B)** *Ex vivo* expression of TLR2 on monocytes subsets from CL patients and HS group ($n = 10$). **(C)** *Ex vivo* expression of TLR4 in monocytes subsets from CL patients and HS group ($n = 10$). Data are represented by the median of the mean intensity of fluorescence (MIF).Mann-Whitney and Kruskal-Wallis with Dunn's post-test was used for statistical analyses. (Δ) classical vs. non-classical monocytes, (φ) intermediate vs. non-classical monocytes, (**$P < 0.01$, ***$P < 0.001$).

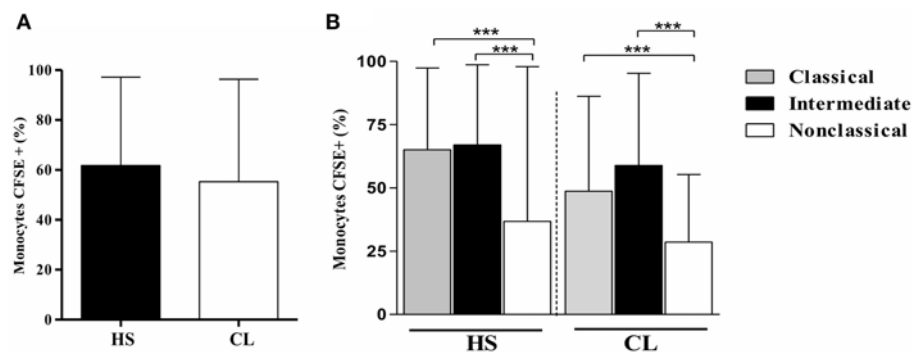

FIGURE 2 | The frequency of *L. braziliensis*-infected monocytes is similar in CL and HS cells. Classical and intermediate monocytes are more infected than non-classical monocytes in CL and HS groups. **(A)** Frequency of PBMC-derived monocytes ($CD14^{+}CD16^{+}$) from CL patients ($n = 8$) and HS ($n = 8$) infected with CFSE-labeled parasites after 4 h of culture. **(B)** Frequency of infected classical ($CD14^{high}CD16^{-}$), intermediate ($CD14^{high}CD16^{+}$), and non-classical monocytes ($CD14^{low}CD16^{+}$) from CL patients and HS after 4 h of culture. Data are represented by the median of the frequency of cells infected. Kruskal-Wallis with Dunn's post-test was used for statistical analyses (***$P < 0.001$).

TNF and IL-10 Are Expressing Mainly in TLR2 $^{(+)}$ and TLR4 $^{(+)}$ Infected Monocytes

Due to the observation that TNF and IL-10 expression was enhanced in TLR2 $^{(+)}$ and TLR4 $^{(+)}$ infected cells, we evaluated the expression of TNF and IL-10 in TLR $^{(+)}$ and in TLR $^{(-)}$ infected monocytes in order to investigate if these cytokines are preferentially expressed on TLR2 $^{(+)}$ and TLR4 $^{(+)}$ infected monocytes.

The frequency of cells expressing intracellular TNF was higher in TLR2 $^{(+)}$ and TLR4 $^{(+)}$ infected monocytes, 44%(19–74%) and 61%(39–75%), respectively, than TLR2 $^{(-)}$ and TLR4 $^{(-)}$ infected monocytes, 13%(7–28%) and 7%(3–17%), respectively (**Figure 6A**). Similarly, the frequency of cells expressing intracellular IL-10 was higher on TLR2 $^{(+)}$ and TLR4 $^{(+)}$ infected monocytes than on TLR2 $^{(-)}$ and TLR4 $^{(-)}$ infected monocytes (**Figure 6B**). In a small number of patients we also evaluate the expression of these cytokines

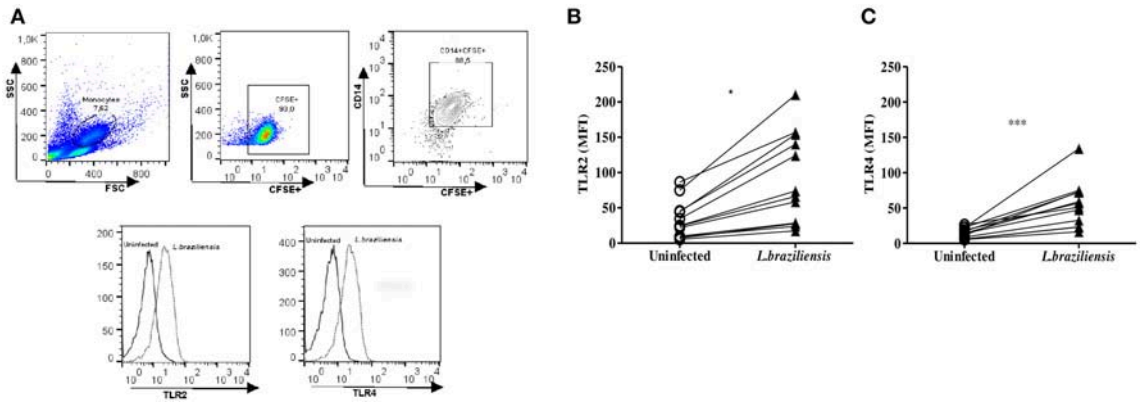

FIGURE 3 | *L. braziliensis* up regulate the expression of TLR2 and TLR4 on monocytes from CL patients**.** PBMC-derived monocytes from CL patients ($n = 08$) and HS ($n = 08$) were infected for 4 h with *L. braziliensis* (ratio 5:1) stained with CFSE. **(A)** Representative strategy analysis for the TLR2 and TLR4 expression after infection by *L. braziliensis* **(B)** TLR2 and **(C)** TLR4 expression in monocytes from CL after infection with *L. braziliensis*. Data are represented by the median of the mean intensity of fluorescence (MIF). Wilcoxon test were used for statistical analyses (*$P < 0.05$, ***$P < 0.01$).

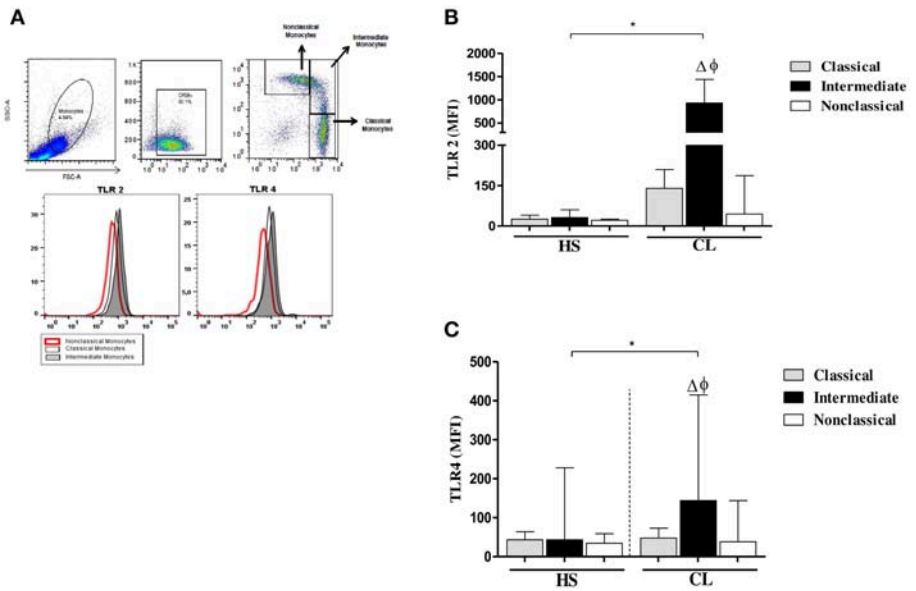

FIGURE 4 | TLR2 and TLR4 expression in monocytes subsets from CL patients after infection by *L. braziliensis***.** PBMC-derived monocytes from CL patients ($n = 08$) and HS ($n = 08$) were infected for 4 h with *L.braziliensis* (ratio 5:1) stained with CFSE for 4 h. **(A)** Representative strategy analysis for the selection of monocytes subsets and TLR2 and TLR4 expression. **(B)** TLR2 expression in classical ($CD14^{high}CD16^{-}$), intermediate ($CD14^{high}CD16^{+}$), and non-classical monocytes ($CD14^{low}CD16^{+}$) from CL patients and HS after infection by *L. braziliensis*.**(C)** TLR4 expression in monocytes subsets from CL patients and HS after infection by *L. braziliensis*. Data are represented by the median of the mean intensity of fluorescence (MIF). (Δ) Intermediate vs. classical monocytes, $P < 0.01$ (φ) Intermediate vs. non-classical monocytes, $P < 0.01$. Mann-Whitney and Kruskal-Wallis with Dunn's post-test was used for statistical test was used for statistical analyses (*$P < 0.05$).

after 24 h of infection and as expected there was a decrease in the intracellular expression of TNF and IL-10 as these cytokines are predominantly detected early after infection (**Supplementary Figure 3**).

Together, these data reinforce the idea that the up regulation of these receptors, after infection with leishmania, activates the monocytes to produce TNF and IL-10.

Intracellular Expression of TNF and IL-10 on Monocytes Subsets From CL Patients After Infection With *L. braziliensis*

The classical $CD14^{++}CD16^{-}$ monocytes specialize in phagocytosis, production of reactive oxygen species, and secretion of IL-10, CCL2, IL-6, and TNF in response to ligands for extracellular TLRs (such as the bacterial product LPS) (Saha and

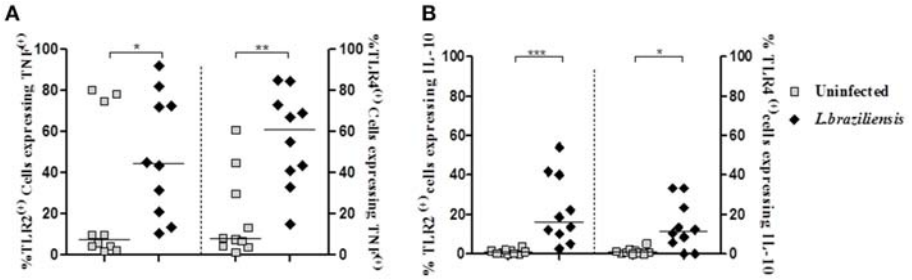

FIGURE 5 | Infection with *L. braziliensis* increases the frequency of TLR2 $^{(+)}$ and TLR4 $^{(+)}$ monocytes expressing TNF and IL-10**.** PBMC-derived monocytes from CL patients ($n = 9$) were infected with *L. braziliensis* (ratio 5:1) for 8 h. The data represent the frequency of TLR2 $^{(+)}$ and TLR4 $^{(+)}$ on monocytes (CD14+) from CL patients ($n = 9$) expressing TNF **(A)** and IL-10 **(B)**. The percentage of CD14+ cells expressing cytokines in non-infected and infected cells was determined by gating on the corresponding population. The results are expressed as median and Mann-Whitney test was used for statistical analyses (*$P < 0.05$, **$P < 0.01$, ***$P < 0.001$).

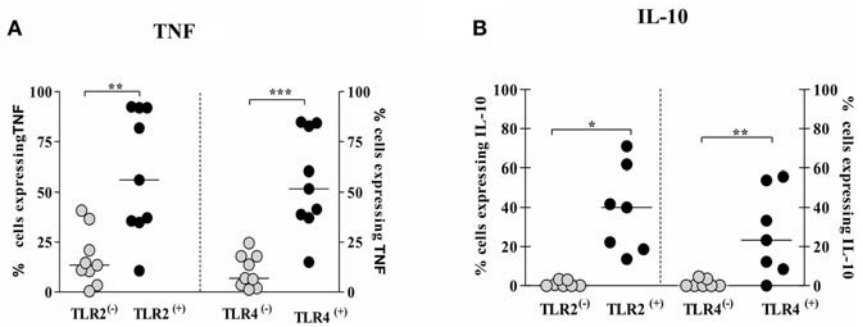

FIGURE 6 | Monocytes from CL patients expressing TLR2 and TLR4 produce more TNF and IL-10 after *L.braziliensis infection*. PBMC-derived monocytes from CL patients ($n = 9$) were infected with *L.braziliensis* (ratio 5:1) for 8 h. The data represent the frequency of cells expressing TNF **(A)** and IL-10 **(B)** on monocytes TLR$^{(+)}$ or TLR$^{(-)}$. The frequency of CD14+ cells expressing cytokines on cells TLR$^{(+)}$ or TLR$^{(-)}$ was determined by gating on the corresponding population. The results are expressed as median and Mann-Whitney test was used for statistical analyses (*$P < 0.05$, **$P < 0.01$, ***$P < 0.001$).

Geissmann, 2011; Wong et al., 2012). The intermediate subset displays the characteristics of activated cells. Such cells have elevated intracytoplasmic levels of pro-inflammatory cytokines such as TNF (Hristov and Weber, 2011; Wong et al., 2012).

Because we observed that intermediate monocytes express more TLR2 and TLR4 than classical and non-classical monocytes after infection with leishmania, we analyzed the frequency of cells expressing TNF and IL-10 on monocyte subsets expressing TLR2 and TLR4. **Figure 7** shows the percentage of cells within each monocyte subset that express these cytokines. There was no difference in TNF expression on monocyte subsets expressing TLR2 (**Figure 7A**). However, the percentage of TLR4 $^{(+)}$ classical and intermediate monocytes expressing TNF was higher than TLR4 $^{(+)}$ non-classical monocytes. Moreover, TLR2 $^{(+)}$ and TLR4 $^{(+)}$ classical monocytes were the main source of IL-10 (**Figure 7B**).

We recognized that experimental design adopted in this study may simulate the scenario of reinfection as the patients remained in the endemic area and could be continually exposure to sandflies bites. In such case, the *ex vivo* expression of TLR2 and TLR4 and cytokines spontaneously produced by the intermediate monocytes could also reflect stimulation of NLRP3 inflammasome by pro-inflammatory molecules derived from sandflies derived-microbiota (Dey et al., 2018).

DISCUSSION

The TLRs are a well-characterized class of pattern recognition receptors that are expressed on phagocytes and interact with PAMPs expressed on the surface of infectious agents (Ozinsky et al., 2000). TLR activation by parasite molecules trigger nuclear factor the nuclear localization of transcription factor NF-κB and mitogen activated protein kinase (MAPk) signaling pathways, to induce expression of pro-inflammatory cytokines genes that are essential for controlling parasite replication (Tuon et al., 2008). However, in several infectious diseases, such as tuberculosis, malaria, and toxoplasmosis, TLR2 and TLR4 have been considered important in the development of the inflammatory response and pathology (Mukherjee et al., 2016). We have previously described that *ex vivo* expression of TLR2 and TLR4 was higher on monocytes from CL patients than on HS cells (Carneiro et al., 2016). In this study we show that the expression of these receptors was higher on classical and intermediate monocytes from CL patients. The expression of TLR2 and TLR4

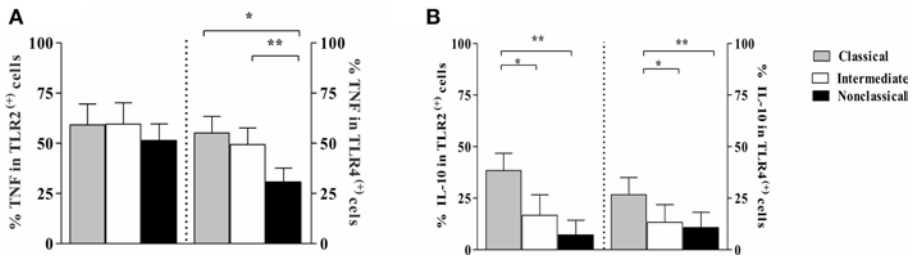

FIGURE 7 | Frequency of monocytes subsets from CL patients expressing TNF and IL-10 in cells TLR2 $^{(+)}$ and TLR4 $^{(+)}$ after *L. braziliensis infection*. PBMC-derived monocytes from CL patients ($n = 9$) were infected with *L. braziliensis* (ratio 5:1) and stained with CFSE for 8 h. The data represent the frequency of cells expressing TNF **(A)** and IL-10 **(B)** on classical ($CD14^{high}CD16^{-}$), intermediate ($CD14^{high}CD16^{+}$), and non-classical monocytes ($CD14^{low}CD16^{+}$) after infection with *L. braziliensis*. The percentage of monocytes expressing cytokines on cells TLR $^{(+)}$ was determined by gating on the corresponding population. The results are expressed as median. Kruskal-Wallis with Dunn's post-test were used for statistical analyses (*$P < 0.05$, **$P < 0.01$).

was higher on intermediate monocytes from CL patients than on cells from the HS group. We also demonstrate that following *in vitro* infection with *L. braziliensis*, TLR2 and TLR4 expression is up-regulated in cells from CL patient monocytes as compared to HS monocytes.

On cells from CL patients the expression of TLR2 and TLR4 was highest on classical and intermediate monocyte subsets. As the infection rate was similar between monocyte subsets from CL and HS (**Figure 2A**), the up regulation of these receptors on cells from CL after infection with *L. braziliensis* suggests that peripheral blood monocytes are already activated and the interaction with the parasite induces the increased expression of these receptors. Also, the increased expression of TLRs may be due to recognition of *Leishmania* lipophosphoglycans (LPGs) by the innate immune system (Tuon et al., 2008). *L. braziliensis* LPG is a strong agonist of TLR2, inducing TNF, IL-1β, and IL-6 production (Ibraim et al., 2013). Our results give support to the finding of increased expression of TLR2 and TLR4 in skin lesions from CL patients caused by *L.braziliensis* (Campos et al., 2018).

Previous studies have evaluated the importance of the TLR in mice infected with leishmania, but the functional role of TLRs in human leishmaniasis still needs to be elucidated. TLR signaling has been linked to pro-inflammatory responses (Medzhitov and Janeway, 2000). For instance, macrophages from $MyD88^{-/-}TRIF^{-/-}$ *L. panamensis* infected C57BL/6 mice, which are unable to activate TLR-dependent pathways, have a decreased ability to secrete TNF and an increased parasite burden early in the infection (Gallego et al., 2011). In contrast, in TLR2-deficient C57BL/6 mice infected with *L. amazonensis*, a decrease in parasitic load and in the recruitment of inflammatory cells at the infection site was observed in the early stages of infection, suggesting that absence of this receptor decreases inflammation and favors the control of parasitic burden (Guerra et al., 2010). The results found in the studies involving TLR4 are also controversial. TLR4-deficient C57BL/10ScN mice are more susceptible to *L. major* infection, presenting with more severe lesions and higher parasitic load than TLR4-competent mice, an observation that was associated with an increase in IL-10 synthesis and IL-4 receptor expression (Kropf et al., 2004a). However, macrophages from $TLR4^{-/-}$ C57BL/6 infected with *L. panamensis* are able to clear amastigotes (Gallego et al., 2011).

IFN-γ is the main cytokine that activates macrophages to kill parasites. However, clearance of the leishmania parasite is also mediated by TNF. Monocytes are the main source of TNF and the importance of this cytokine in the pathology of CL and ML caused by *L. braziliensis,* has been well documented (Lessa et al., 2001; Antonelli et al., 2005; Oliveira et al., 2014; Passos et al., 2015).

To further assess the potential roles of TLR signaling and cytokine production by distinct monocyte subsets in *L. braziliensis* infection, we evaluated their expression in CL monocytes before and after infection with *L. braziliensis.* First, we showed that after infection with *L. braziliensis* there is an increase in TNF expression and it occurs predominantly in TLR2 $^{(+)}$ and TLR4 $^{(+)}$ cells. Giving support to the role of TLR4 in cytokine secretion, Galdino et al. demonstrated that infection with *L. braziliensis* increases the production of TNF and IL-10 by human cells in a TLR4 dependent manner (Galdino et al., 2016). However, a small number of both TLR $^{(-)}$ and uninfected monocytes also expressed TNF. This observation is likely due to the ability of *L. braziliensis* infected cells to induce TNF production in uninfected bystander cells (Carvalho et al., 2008).

Previously, we have shown that while classical monocytes have the ability to kill leishmania, intermediate monocytes were the main source of TNF (Novais et al., 2014; Passos et al., 2015). Here we demonstrated the importance of TLR2 and TLR4 in cytokine secretion and that in addition to intermediate monocytes, classical monocytes expressing TLR4 also produce TNF. Moreover, while all monocyte subsets express TNF, classical and intermediate monocytes expressing TLR4 were the main source of this cytokine. We also show that TLR2 $^{(+)}$ and TLR4 $^{(+)}$ cells express TNF and IL-10. As more than 60% of TLR2 $^{(+)}$ or TLR4 $^{(+)}$ cells expressed TNF and a large percentage of TLR $^{(+)}$ monocytes also expressed IL-10, it is likely that some cells express both inflammatory and anti-inflammatory cytokines.

IL-10 is the major regulatory cytokine in human leishmaniasis (Carvalho et al., 1994a; Bacellar et al., 2002; Gautam et al., 2011). Although IL-10 is associated with parasite persistence and dissemination (Bomfim et al., 1996; Anderson et al.,

2008), it is also important for controlling the exaggerated inflammatory response associated with pathology observed in parasitic diseases such as malaria, Chagas disease, and leishmaniasis (Li et al., 2003; Costa et al., 2009, 2015; Gautam et al., 2011). Classical monocytes are the main source of IL-10 after stimulation with LPS (Wong et al., 2011). Therefore, the increased expression of IL-10 in classical monocytes may have two explanations. As classical monocytes are cells responsible for leishmania killing (Novais et al., 2013), the increase in IL-10 may be one way leishmania is able to escape host defense mechanisms. Alternatively, IL-10 production may represent an attempt of the classical monocytes to attenuate pathology mediated by the exaggerated pro-inflammatory response of the intermediate monocyte (Cyktor and Turner, 2011).

As the experiments in this study were performed with promastigotes in the stationary phase and it known that this population contain about 20% of the parasites that are not metacyclics promastigotes (Viana et al., 2017), there is a minor chance that the results obtained with such global parasite populations might be shaped by pro-inflammatory molecules produced by the stationary promastigotes, rather than from the 80% metacyclics parasites.

While TLRs participate in host defense mechanisms by promoting secretion of pro-inflammatory molecules and development of a Th1 type immune response, their role in the pathology of human CL has not been clearly documented. Comparing expression of TLR2 and TLR4 in macrophages from patients infected with *L. major*, Tolouei et al. showed that on macrophages from patients who had healing lesions with no history of treatment, TLR2 and TLR4 expression was higher than macrophages from CL patients with non-healing lesions and with an illness duration of more than 1 year (Tolouei et al., 2013). While this finding suggests that a decrease in TLR expression may impair the control of the infection, the patients evaluated in this study with no healing lesions had history of at least two full courses of treatment with Glucantime which could explain the decreased expression of these receptors on cells from these patients. Here, we showed the importance of TLR2 and TLR4 expression in the production of TNF, a cytokine associated with pathology in human CL caused by *L. braziliensis*.

We add to the body of knowledge about TLRs in *L. braziliensis* infection and about different monocyte subset functions. *L. braziliensis* infection enhanced TLR2 and TLR4 receptors as well as the frequency of classical and intermediate monocytes expressing these receptors. Moreover, while classical and intermediate monocytes expressing TLR2 and TLR4 are the main cells secreting TNF, the classical monocytes are the major cell source of IL-10. This study also has implications in immunotherapy for infectious diseases. As TLRs trigger inflammatory responses, agonists of TLRs have been used as adjuvants in vaccines against leishmania infection in experimental animals (Calvopina et al., 2006; Raman et al., 2010). However, our data show that *L. braziliensis* enhances TLR2 and TLR4 which leads to a pro-inflammatory environment that does not prevent the appearance of the disease. Thus, it is possible that over expression of TLRs may be more related to pathology than protection in human CL. As TLR antagonist molecules have been used in the treatment of inflammatory diseases (Gao et al., 2017), studies evaluating the role of TLR2 and TLR4 antagonists in the modulation of the inflammatory response in patients with CL should be performed.

ETHICS STATEMENT

This study was carried out in accordance with the recommendations of Institutional Review Board of the Federal University of Bahia, Brazil, with written informed consent from all subjects. All subjects gave written informed consent in accordance with the Declaration of Helsinki. The protocol was approved by the Institutional Review Board of the Federal University of Bahia, Brazil (approval number 693.111).

AUTHOR CONTRIBUTIONS

LP, PC, and OB participated equally in the study design and in the writing of the manuscript. LP and PC participated equally in all experiments. MM participated in the human macrophages infection and processing of samples on the flow cytometer. PM is a dermatologist and participated in the diagnostic of the patients in the endemic area and in the discussion of the results. EC and OB are the principal investigators of this work and followed the work from the beginning to the end and also participated in the writing of the manuscript. PS participated in the discussion of the results and in the writing of the manuscript.

FUNDING

This work was supported by the National Institute of Health (NIH) grant AI136032. The funders had no role in study design, data collection and analysis, decision to publish, or preparation of the manuscript.

ACKNOWLEDGMENTS

We deeply thank all personnel of the Jackson Costa Health Post in Corte de Pedra, Bahia, Brazil, for their careful help with patient management.

SUPPLEMENTARY MATERIAL

The Supplementary Material for this article can be found online at: https://www.frontiersin.org/articles/10.3389/fcimb.2019.00120/full#supplementary-material

REFERENCES

Alvar, J., Velez, I. D., Bern, C., Herrero, M., Desjeux, P., Cano, J., et al. (2012). Leishmaniasis worldwide and global estimates of its incidence. *PLoS ONE* 7:e35671. doi: 10.1371/journal.pone.0035671

Anderson, C. F., Lira, R., Kamhawi, S., Belkaid, Y., Wynn, T.A., and Sacks, D. (2008). IL-10 and TGF-β control the establishment of persistent and transmissible infections produced by *Leishmania tropica* in C57BL/6 mice. *J. Immunol.* 180, 4090–4097. doi: 10.4049/jimmunol.180.6.4090

Antonelli, L. R., Dutra, W. O., Almeida, R. P., Bacellar, O., Carvalho, E. M., and Gollob, K. J. (2005). Activated inflammatory T cells correlate with lesion size in human cutaneous leishmaniasis. *Immunol. Lett.* 101, 226–230. doi: 10.1016/j.imlet.2005.06.004

Bacellar, O., Lessa, H., Schriefer, A., Machado, P., Ribeiro de Jesus, A., Dutra, W. O., et al. (2002). Up-regulation of Th1-type responses in mucosal leishmaniasis patients. *Infect. Immun.* 70, 6734–6740. doi: 10.1128/IAI.70.12.6734-6740.2002

Becker, I., Salaiza, N., Aguirre, M., Delgado, J., Carrillo-Carrasco, N., Kobeh, L. G., et al. (2003). *Leishmania* lipophosphoglycan (LPG) activates NK cells through toll-like receptor-2. *Mol. Biochem. Parasitol.* 130, 65–74. doi: 10.1016/S0166-6851(03)00160-9

Bomfim, G., Nascimento, C., Costa, J., Carvalho, E. M., Barral-Netto, M., and Barral, A. (1996). Variation of cytokine patterns related to therapeutic response in diffuse cutaneous leishmaniasis. *Exp. Parasitol.* 84, 188–194. doi: 10.1006/expr.1996.0104

Bosque, F., Saravia, N. G., Valderrama, L., and Milon, G. (2000). Distinct innate and acquired immune responses to Leishmania in putative susceptible and resistant human populations endemically exposed to L. (Viannia) panamensis infection. *Scand. J. Immunol.* 51, 533–541.

Calvopina, M., Barroso, P. A., Marco, J. D., Korenaga, M., Cooper, P. J., Nonaka, S., et al. (2006). Efficacy of vaccination with a combination of Leishmania amastigote antigens and the lipid A-analogue ONO- for immunoprophylaxis and immunotherapy against Leishmania amazonensis infection in a murine model of New World cutaneous leishmaniasis. *Vaccine* 24, 5645–5652. doi: 10.1016/j.vaccine.2006.03.023

Campos, M. B., Lima, L., de Lima, A. C. S., Vasconcelos Dos Santos, T., Ramos, P. K. S., Gomes, C. M. C., et al. (2018). Toll-like receptors 2, 4, and 9 expressions over the entire clinical and immunopathological spectrum of American cutaneous leishmaniasis due to Leishmania(V.) braziliensis and Leishmania (L.) amazonensis. *PLoS ONE* 13:e0194383. doi: 10.1371/journal.pone.0194383

Cardoso, T. M., Machado, A., Costa, D. L., Carvalho, L. P., Queiroz, A., Machado, P., et al. (2015). Protective and pathological functions of $CD8^+$ T cells in Leishmania braziliensis infection. *Infect. Immun.* 83, 898–906. doi: 10.1128/IAI.02404-14

Carneiro, P. P., Conceicao, J., Macedo, M., Magalhaes, V., Carvalho, E. M., and Bacellar, O. (2016). The role of nitric oxide and reactive oxygen species in the killing of leishmania braziliensis by monocytes from patients with cutaneous leishmaniasis. *PLoS ONE* 11:e0148084. doi: 10.1371/journal.pone.0148084

Carvalho, E. M., Bacellar, O., Brownell, C., Regis, T., Coffman, R. L., and Reed, S. G. (1994a). Restoration of IFN-gamma production and lymphocyte proliferation in visceral leishmaniasis. *J. Immunol.* 152, 5949–5956.

Carvalho, E. M., Barral, A., Costa, J. M., Bittencourt, A., and Marsden, P. (1994b). Clinical and immunopathological aspects of disseminated cutaneous leishmaniasis. *Acta Trop.* 56, 315–325.

Carvalho, L. P., Pearce, E. J., and Scott, P. (2008). Functional dichotomy of dendritic cells following interaction with *Leishmania braziliensis*: infected cells produce high levels of TNF-α, whereas bystander dendritic cells are activated to promote T cell responses. *J. Immunol.* 181, 6473–6480. doi: 10.4049/jimmunol.181.9.6473

Cezário, G. A., de Oliveira, L. R., Peresi, E., Nicolete, V. C., Polettini, J., de Lima, C. R., et al. (2011). Analysis of the expression of toll-like receptors 2 and 4 and cytokine production during experimental *Leishmania chagasi* infection. *Mem. Inst. Oswaldo. Cruz.* 106, 573–583. doi: 10.1590/S0074-02762011000500010

Chang, H. K., Thalhofer, C., Duerkop, B. A., Mehling, J. S., Verma, S., Gollob, K. J., et al. (2007). Oxidant generation by single infected monocytes after short-term fluorescence labeling of a protozoan parasite. *Infect. Immun.* 75, 1017–1024. doi: 10.1128/IAI.00914-06

Costa, D. L., Cardoso, T. M., Queiroz, A., Milanezi, C. M., Bacellar, O., Carvalho, E. M., et al. (2015). Tr-1-like $CD4^+CD25^-CD127^{-/low}FOXP3^-$ cells are the main source of interleukin 10 in patients with cutaneous leishmaniasis due to Leishmania braziliensis. *J. Infect. Dis.* 211, 708–718. doi: 10.1093/infdis/jiu406

Costa, G.C., da Costa Rocha, M.O., Moreira, P.R., Menezes, C.A., Silva, M.R., Gollob, K.J., et al. (2009). Functional IL-10 gene polymorphism is associated with Chagas disease cardiomyopathy. *J. Infect. Dis.* 199, 451–454. doi: 10.1086/596061

Cupolillo, E., Grimaldi, G. Jr., and Momen, H. (1994). A general classification of New World Leishmania using numerical zymotaxonomy. *Am. J. Trop. Med. Hyg.* 50, 296–311.

Cyktor, J. C., and Turner, J. (2011). Interleukin-10 and immunity against prokaryotic and eukaryotic intracellular pathogens. *Infect. Immun.* 79, 2964–2973. doi: 10.1128/IAI.00047-11

Da-Cruz, A. M., de Oliveira, M. P., De Luca, P. M., Mendonca, S. C., and Coutinho, S. G. (1996). Tumor necrosis factor-alpha in human american tegumentary leishmaniasis. *Mem. Inst. Oswaldo Cruz.* 91, 225–229.

de Veer, M. J., Curtis, J. M., Baldwin, T. M., DiDonato, J. A., Sexton, A., McConville, M. J., et al. (2003). MyD88 is essential for clearance of Leishmania major: possible role for lipophosphoglycan and Toll-like receptor 2 signaling. *Eur. J. Immunol.* 33, 2822–2831. doi: 10.1002/eji.200324128

Dey, R., Joshi, AB., Oliveira, F., Pereira, L., Guimarães-Costa, AB., Serafim, TD., et al. (2018). Gut microbes egested during bites of infected sand flies augment severity of leishmaniasis via inflammasome-derived IL-1β. *Cell Host Microbe.* 23, 134–143.e6. doi: 10.1016/j.chom.2017.12.002.

Faria, D. R., Gollob, K. J., Barbosa, J. Jr., Schriefer, A., Machado, P. R., Lessa, H., et al. (2005). Decreased in situ expression of interleukin-10 receptor is correlated with the exacerbated inflammatory and cytotoxic responses observed in mucosal leishmaniasis. *Infect. Immun.* 73, 7853–7859. doi: 10.1128/IAI.73.12.7853-7859.2005

Faria, M. S., Reis, F. C., and Lima, A. P. (2012). Toll-like receptors in leishmania infections: guardians or promoters? *J. Parasitol. Res.* 12:930257. doi: 10.1155/2012/930257

Flandin, J. F., Chano, F., and Descoteaux, A. (2006). RNA interference reveals a role for TLR2 and TLR3 in the recognition of Leishmania donovani promastigotes by interferon-gamma-primed macrophages. *Eur. J. Immunol.* 36, 411–420. doi: 10.1002/eji.200535079

Galdino, H. Jr., Saar Gomes, R., Dos Santos, J. C., Pessoni, L. L., Maldaner, A. E., Marques, S. M., et al. (2016). Leishmania (Viannia) braziliensis amastigotes induces the expression of TNFalpha and IL-10 by human peripheral blood mononuclear cells in vitro in a TLR4-dependent manner. *Cytokine* 88, 184–192. doi: 10.1016/j.cyto.2016.09.009

Gallego, C., Golenbock, D., Gomez, M. A., and Saravia, N. G. (2011). Toll-like receptors participate in macrophage activation and intracellular control of Leishmania (Viannia) panamensis. *Infect. Immun.* 79, 2871–2879. doi: 10.1128/IAI.01388-10

Gao, W., Xiong, Y., Li, Q., and Yang, H. (2017). Inhibition of toll-like receptor signaling as a promising therapy for inflammatory diseases: a journey from molecular to nano therapeutics. *Front. Physiol.* 8, 508. doi: 10.3389/fphys.2017.00508

Gautam, S., Kumar, R., Maurya, R., Nylen, S., Ansari, N., Rai, M., et al. (2011). IL-10 neutralization promotes parasite clearance in splenic aspirate cells from patients with visceral leishmaniasis. *J. Infect. Dis.* 204, 1134–1137. doi: 10.1093/infdis/jir461

Giudice, A., Vendrame, C., Bezerra, C., Carvalho, L. P., Delavechia, T., Carvalho, E. M., et al. (2012). Macrophages participate in host protection and the disease pathology associated with *Leishmania braziliensis* infection. *BMC Infect. Dis.* 12, 75. doi: 10.1186/1471-2334-12-75

Gomes-Silva, A., de Cassia Bittar, R., Dos Santos Nogueira, R., Amato, V. S., da Silva Mattos, M., Oliveira-Neto, M. P., et al. (2007). Can interferon-gamma and interleukin-10 balance be associated with severity of human Leishmania (Viannia) braziliensis infection? *Clin. Exp. Immunol.* 149, 440–444. doi: 10.1111/j.1365-2249.2007.03436.x

Gonzalez-Lombana, C., Gimblet, C., Bacellar, O., Oliveira, W. W., Passos, S., Carvalho, L. P., et al. (2013). IL-17 mediates immunopathology in the absence of IL-10 following Leishmania major infection. *PLoS Pathog.* 9:e1003243. doi: 10.1371/journal.ppat.1003243

Guerra, C. S., Silva, R. M., Carvalho, L. O., Calabrese, K. S., Bozza, P. T., and Corte-Real, S. (2010). Histopathological analysis of initial cellular response in TLR-2 deficient mice experimentally infected by Leishmania (L.) amazonensis. *Int. J. Exp. Pathol.* 91, 451–459. doi: 10.1111/j.1365-2613.2010.00717.x

Hristov, M., and Weber, C. (2011). Differential role of monocyte subsets in atherosclerosis. *Thromb. Haemost.* 106, 757–762. doi: 10.1160/TH11-07-0500

Ibraim, I.C., de Assis, R.R., Pessoa, N.L., Campos, M.A., Melo, M. N., Turco, S. J., et al. (2013). Two biochemically distinct lipophosphoglycans from Leishmania braziliensis and Leishmania infantum trigger different innate immune responses in murine macrophages. *Parasit. Vectors* 6:54. doi: 10.1186/1756-3305-6-54

Kropf, P., Freudenberg, M. A., Modolell, M., Price, H. P., Herath, S., Antoniazi, S., et al. (2004a). Toll-like receptor 4 contributes to efficient control of infection with the protozoan parasite *Leishmania major*. *Infect. Immun.* 72, 1920–1928. doi: 10.1128/IAI.72.4.1920-1928.2004

Kropf, P., Freudenberg, N., Kalis, C., Modolell, M., Herath, S., Galanos, C., et al. (2004b). Infection of C57BL/10ScCr and C57BL/10ScNCr mice with Leishmania major reveals a role for Toll-like receptor 4 in the control of parasite replication. *J. Leukoc. Biol.* 76, 48–57. doi: 10.1189/jlb.1003484

Kuniyoshi, K., Takeuchi, O., Pandey, S., Satoh, T., Iwasaki, H., Akira, S., et al. (2014). Pivotal role of RNA-binding E3 ubiquitin ligase MEX3C in RIG-I-mediated antiviral innate immunity. *Proc. Natl. Acad. Sci. U.S.A.* 111, 5646–5651. doi: 10.1073/pnas.1401674111

Lessa, H. A., Machado, P., Lima, F., Cruz, A. A., Bacellar, O., Guerreiro, J., et al. (2001). Successful treatment of refractory mucosal leishmaniasis with pentoxifylline plus antimony. *Am. J. Trop. Med. Hyg.* 65, 87–89. doi: 10.4269/ajtmh.2001.65.87

Li, C., Sanni, L.A., Omer, F., Riley, E., and Langhorne, J. (2003). Pathology of *Plasmodium chabaudi chabaudi* infection and mortality in interleukin-10-deficient mice are ameliorated by anti-tumor necrosis factor alpha and exacerbated by anti-transforming growth factor beta antibodies. *Infect. Immun.* 71, 4850–4856. doi: 10.1128/IAI.71.9.4850-4856.2003

Medzhitov, R., and Janeway, C. Jr. (2000). The Toll receptor family and microbial recognition. *Trends Microbiol.* 8, 452–456. doi: 10.1016/S0966-842X(00)01845-X

Mukherjee, S., Karmakar, S., and Babu, S.P. (2016). TLR2 and TLR4 mediated host immune responses in major infectious diseases: a review. *Braz. J. Infect. Dis.* 20, 193–204. doi: 10.1016/j.bjid.2015.10.011

Muniz, A. C., Bacellar, O., Lago, E. L., Carvalho, A. M., Carneiro, P. P., Guimaraes, L. H., et al. (2016). Immunologic markers of protection in Leishmania (Viannia) braziliensis Infection: A 5-Year cohort study. *J. Infect. Dis.* 214, 570–576. doi: 10.1093/infdis/jiw196

Novais, F. O., Carvalho, A. M., Clark, M. L., Carvalho, L. P., Beiting, D. P., Brodsky, I. E., et al. (2017). CD8+ T cell cytotoxicity mediates pathology in the skin by inflammasome activation and IL-1beta production. *PLoS Pathog* 13:e1006196. doi: 10.1371/journal.ppat.1006196

Novais, F. O., Carvalho, L. P., Graff, J. W., Beiting, D. P., Ruthel, G., Roos, D. S., et al. (2013). Cytotoxic T cells mediate pathology and metastasis in cutaneous leishmaniasis. *PLoS Pathog* 9:e1003504. doi: 10.1371/journal.ppat.1003504

Novais, F. O., Nguyen, B. T., Beiting, D. P., Carvalho, L. P., Glennie, N. D., Passos, S., et al. (2014). Human classical monocytes control the intracellular stage of Leishmania braziliensis by reactive oxygen species. *J. Infect. Dis.* 209, 1288–1296. doi: 10.1093/infdis/jiu013

Oliveira, W. N., Ribeiro, L. E., Schrieffer, A., Machado, P., Carvalho, E. M., and Bacellar, O. (2014). The role of inflammatory and anti-inflammatory cytokines in the pathogenesis of human tegumentary leishmaniasis. *Cytokine* 66, 127–132. doi: 10.1016/j.cyto.2013.12.016

Ozinsky, A., Underhill, D. M., Fontenot, J. D., Hajjar, A. M., Smith, K. D., Wilson, C.B., et al. (2000). The repertoire for pattern recognition of pathogens by the innate immune system is defined by cooperation between toll-like receptors. *Proc. Natl. Acad. Sci. U.S.A.* 97, 13766–13771. doi: 10.1073/pnas.250476497

Passos, S., Carvalho, L. P., Costa, R. S., Campos, T. M., Novais, F. O., Magalhaes, A., et al. (2015). Intermediate monocytes contribute to pathologic immune response in Leishmania braziliensis infections. *J. Infect. Dis.* 211, 274–282. doi: 10.1093/infdis/jiu439

Raman, V. S., Bhatia, A., Picone, A., Whittle, J., Bailor, H. R., O'Donnell, J., et al. (2010). Applying TLR synergy in immunotherapy: implications in cutaneous leishmaniasis. *J. Immunol.* 185, 1701–1710. doi: 10.4049/jimmunol.1000238

Saha, P., and Geissmann, F. (2011). Toward a functional characterization of blood monocytes. *Immunol. Cell Biol.* 89, 2–4. doi: 10.1038/icb.2010.130

Santos Cda, S., Boaventura, V., Ribeiro Cardoso, C., Tavares, N., Lordelo, M. J., Noronha, A., et al. (2013). CD8(+) granzyme B(+)-mediated tissue injury vs. CD4(+)IFNgamma(+)-mediated parasite killing in human cutaneous leishmaniasis. *J. Invest. Dermatol.* 133, 1533–40. doi: 10.1038/jid.2013.4

Soares, N. M., Ferraz, T. P., Nascimento, E. G., Carvalho, E. M., and Pontes-de-Carvalho, L. (2006). The major circulating immunosuppressive activity in American visceral leishmaniasis patients is associated with a high-molecular weight fraction and is not mediated by IgG, IgG immune complexes or lipoproteins. *Microb. Pathog.* 40, 254–260. doi: 10.1016/j.micpath.2006.02.005

Tolouei, S., Hejazi, S. H., Ghaedi, K., Khamesipour, A., and Hasheminia, S. J. (2013). TLR2 and TLR4 in cutaneous leishmaniasis caused by Leishmania major. *Scand. J. Immunol.* 78, 478–484. doi: 10.1111/sji.12105

Tuon, F. F., Fernandes, E. R., Duarte, M. I., and Amato, V. S. (2010). The expression of TLR2, TLR4 and TLR9 in the epidermis of patients with cutaneous leishmaniasis. *J. Dermatol. Sci.* 59, 55–57. doi: 10.1016/j.jdermsci.2010.04.009

Tuon, F. F., Gomes-Silva, A., Da-Cruz, A. M., Duarte, M. I., Neto, V. A., and Amato, V. S. (2008). Local immunological factors associated with recurrence of mucosal leishmaniasis. (1016). *Clin. Immunol.* 128, 442–446. doi: 10./j.clim.2008.05.007

Vargas-Inchaustegui, D. A., Tai, W., Xin, L., Hogg, A. E., Corry, D. B., and Soong, L. (2009). Distinct roles for MyD88 and Toll-like receptor 2 during Leishmania braziliensis infection in mice. *Infect. Immun.* 77, 2948–2956. doi: 10.1128/IAI.00154-09

Viana, A. G., Magalhaes, L. M. D., Giunchetti, R. C., Dutra, W. O., and Gollob, K. J. (2017). Infection of human monocytes with leishmania infantum strains induces a downmodulated response when compared with infection with *Leishmania braziliensis*. *Front. Immunol.* 8:1896. doi: 10.3389/fimmu.2017.01896

Vieira, E. L., Keesen, T. S., Machado, P. R., Guimaraes, L. H., Carvalho, E. M., Dutra, W. O., et al. (2013). Immunoregulatory profile of monocytes from cutaneous leishmaniasis patients and association with lesion size. *Parasite Immunol.* 35, 65–72. doi: 10.1111/pim.12012

Weirather, J. L., Jeronimo, S. M., Gautam, S., Sundar, S., Kang, M., Kurtz, M. A., et al. (2011). Serial quantitative PCR assay for detection, species discrimination, and quantification of Leishmania spp. in human samples. *J. Clin. Microbiol.* 49, 3892–3904. doi: 10.1128/JCM.r00764-11

Whitaker, S. M., Colmenares, M., Pestana, K. G., and McMahon-Pratt, D. (2008). Leishmania pifanoi proteoglycolipid complex P8 induces macrophage cytokine production through Toll-like receptor 4. *Infect. Immun.* 76, 2149–2156. doi: 10.1128/IAI.01528-07

Wong, K. L., Tai, J. J., Wong, W. C., Han, H., Sem, X., Yeap, W. H., Kourilsky, P, and Wong, S. C. (2011). Gene expression profiling reveals the defining features of the classical,intermediate, and nonclassical human monocyte subsets. *Blood* 118:e16–31. doi: 10.1182/blood-2010-12-326355

Wong, K. L., Yeap, W. H., Tai, J. J., Ong, S. M., Dang, T. M., and Wong, S. C. (2012). The three human monocyte subsets: implications for health and disease. *Immunol Res.* 53:41–57. doi: 10.1007/s12026-012-8297-3

Ziegler-Heitbrock, L., Ancuta, P., Crowe, S., Dalod, M., Grau, V., Hart, D. N., et al. (2010). Nomenclature of monocytes and dendritic cells in blood. *Blood* 116, e74–80. doi: 10.1182/blood-2010-02-258558

Conflict of Interest Statement: The authors declare that the research was conducted in the absence of any commercial or financial relationships that could be construed as a potential conflict of interest.

frontiers in Cellular and Infection Microbiology

ORIGINAL RESEARCH
published: 03 May 2019
doi: 10.3389/fcimb.2019.00115

Immunomodulation From Moderate Exercise Promotes Control of Experimental Cutaneous Leishmaniasis

Rodrigo Terra[1†], Pedro J. F. Alves[1‡], Ana K. C. Lima[1], Shayane M. R. Gomes[1], Luciana S. Rodrigues[2], Verônica P. Salerno[3], Silvia A. G. Da-Silva[1] and Patricia M. L. Dutra[1]*

[1] Discipline of Parasitology, Department of Microbiology, Immunology and Parasitology, State University of Rio de Janeiro, Rio de Janeiro, Brazil, [2] Discipline of General Pathology, Department of Pathology and Laboratories, State University of Rio de Janeiro, Rio de Janeiro, Brazil, [3] Laboratory of Exercise Biochemistry and Molecular Motors, School of Physical Education and Sports, Universidade Federal do Rio de Janeiro, Rio de Janeiro, Brazil

OPEN ACCESS

Edited by:
Claudia Ida Brodskyn,
Gonçalo Moniz Institute (IGM), Brazil

Reviewed by:
Manuel Soto,
Autonomous University of Madrid, Spain
Bellisa Freitas Barbosa,
Federal University of Uberlandia, Brazil

***Correspondence:**
Patricia M. L. Dutra
pmldutra@gmail.com

[†]Programa de Pós-Graduação em Fisiopatologia Clínica e Experimental (FISCLINEX – UERJ)

[‡]Programa de Pós-Graduação em Ciências do Exercício e do Esporte (PPGCEE – UERJ)

Specialty section:
This article was submitted to Parasite and Host, a section of the journal Frontiers in Cellular and Infection Microbiology

Received: 17 December 2018
Accepted: 02 April 2019
Published: 03 May 2019

Citation:
Terra R, Alves PJF, Lima AKC, Gomes SMR, Rodrigues LS, Salerno VP, Da-Silva SAG and Dutra PML (2019) Immunomodulation From Moderate Exercise Promotes Control of Experimental Cutaneous Leishmaniasis. Front. Cell. Infect. Microbiol. 9:115. doi: 10.3389/fcimb.2019.00115

Physical exercise has been described as an important tool in the prevention and treatment of numerous diseases as it promotes a range of responses and adaptations in several biological systems, including the immune system. Studies on the effect of exercise on the immune system could play a critical role in improving public health. Current literature suggests that moderate intensity exercise can modulate the Th1/Th2 dichotomy directing the immune system to a Th1 cellular immune response, which favors the resolution of infections caused by intracellular microorganisms. Leishmaniasis is a group of diseases presenting a wide spectrum of clinical manifestations that range from self-limiting lesions to visceral injuries whose severity can lead to death. The etiological agents responsible for this group of diseases are protozoa of the genus Leishmania. Infections by the parasite *Leishmania major* in mice (Balb/c) provide a prototype model for the polarization of CD4+ T cell responses of both Th1 (resistance) or Th2 (susceptibility), which determines the progression of infections. The aim of this study was to evaluate the effect of exercise on the development of *L. major* experimental infections by scanning the pattern of immune response caused by exercise. Groups of Balb/c mice infected with *L. major* were divided into groups that preformed a physical exercise of swimming three times a week or were sedentary along with treatment or not with the reference drug, meglumine antimoniate. Animals in groups submitted to physical exercise did not appear to develop lesions and presented a significantly lower parasite load independent of drug treatment. They also showed a positive delayed hypersensitivity response to a specific *Leishmania* antigen compared to control animals. The IFN-γ/IL-4 and IFN-γ/IL10 ratios in trained animals were clearly tilted to a Th1 response in lymph node cells. These data suggest that moderate intensity exercise is able to modulate the Th1 response that provides a protective effect against the development of leishmanial lesions.

Keywords: exercise, leishmaniasis, immune response, Balb/c, control of infection

INTRODUCTION

Regular physical exercise promotes a series of responses and physiological adaptations that are dependent on different aspects of the activity such as volume and intensity (American College of Sports Medicine Position Stand American Heart Association, 1998, 2007; Walsh et al., 2011b). The metabolic changes from exercise have been associated to alterations in immune function (Pedersen and Hoffman-Goetz, 2000), which can directly influence the immune response of a host to an infectious agent (Lili and Cheng, 2007). Intense exercise favors the resolution of bacterial infections by promoting a predominance to a Th2 type response (Malm, 2004, reviewed by Terra et al., 2012). Prolonged and strenuous exercise decreases the expression of Toll-Like Receptors in macrophages and compromises the presentation of antigens to T lymphocytes, which diminishes the Th1 inflammatory response. This anti-inflammatory effect prevents tissue damage caused by inflammatory mediators and reduces the risk of chronic inflammatory diseases, but increases the susceptibility to infections by intracellular microorganisms (Gleeson, 2006). Moderate exercise, in contrast, induces the immune system to a predominately Th1 type response that favors the resolution of viral infections and control of infections caused by intracellular microorganisms (Gleeson, 2006, 2007), which can include the bacteria *Mycobacterium tuberculosis* and *Listeria monocytogenis* along with the protozoa *Toxoplasma gondii, Trypanosoma cruzi,* and *Leishmania* spp. (Bogdan, 2008).

Parasites from the *Leishmania* genus are the etiological agents responsible for leishmaniasis, a vector-borne group of diseases that are endemic in 102 countries and territories distributed throughout Europe, Africa, Asia, and the Americas (Alvar et al., 2012; World Health Organization, 2018). Approximately 350 million people are at risk of infection with an annual incidence of around 1.6 million and a prevalence of 12 million individuals (World Health Organization, 2018). Phlebotomine sandflies are the principle vector of transmission and the macrophages of an infected person are the main host cell (Lainson et al., 1997). Based on the clinical manifestations and the parasites species involved, leishmaniasis can be present three main forms: visceral (also known as kala-azar, the most serious form that can be lethal), cutaneous (the most common), and mucosal (Stark et al., 2006; Shah et al., 2010; Badirzadeh et al., 2013; McCall et al., 2013; Organização Pan Amaricana De Saúde and, 2018). Cutaneous leishmaniasis (CL) is caused by several species of dermotropic *Leishmania*, such as *L. tropica* and *L. major* in the Old World along with *L. braziliensis* and *L. amazonesis* in the New World (Carvalho et al., 2005; Samy et al., 2014; Kahime et al., 2016). Mucosal leishmaniasis, also known as or mucocutaneous, is most commonly observed with infections by species restricted to South America, principally from the sub-genius *Viannia*, such as *L. braziliensis* and *L. panamensis* (Miranda Lessa et al., 2007). Visceral leishmaniasis is caused by viscerotropic species as *L. donovani* (Old World) and *L. infantum* (New World) (Momen et al., 1993).

Control of all the clinical forms of leishmaniasis appears to depend on type 1 immune response. Interferon-gamma (IFN-γ) and tumor necrosis factor (TNF) -α and -β, from the Th1 profile, are known to be involved in the resistance and elimination of the parasites, while Th2 cytokines such as IL-4 and IL-10 are linked to susceptibility to infections by *Leishmania* (Von Stebut, 2007; de Assis Souza et al., 2013). However, an exacerbation of the Th1 type response (hyperergia) leads to increased tissue destruction as observed in mucocutaneous leishmaniasis (Martin and Leibovich, 2005; Mendes et al., 2013).

The mouse strain Balb/c provides a laboratory model for the study of *Leishmania* infections, because this strain toward a Th2 (susceptibility) response, which determines the progression of infections (Fritzche et al., 2010; Barthelmann et al., 2011). The aim of the current study was to evaluate the effect of moderate exercise on the development of *L. major* experimental infections in Balb/c. Mice were infected with *L. major* and divided into a number of cohorts to analyse the impact of a swimming exercise (three times a week for 12 weeks) in combination or not with treatment with the reference drug, meglumine antimoniate (Glucantime®). In addition, the pattern of immune response caused by exercise was measured. The data obtained demonstrate that moderate intensity exercise was able to modulate the Th1 response, suggesting a protective effect of exercise on the development of leishmanial lesions.

MATERIALS AND METHODS

Chemicals

Kits for measuring cytokines were purchased from R&D Systems (Minneapolis, MN, USA). Fetal calf serum (FCS) was purchased from Cultilab Co (Campinas, São Paulo, Brazil). DMEM culture medium, Schneider medium, bacterial lipopolysaccharide (LPS), concanavalin A (ConA), and all other chemicals used in this study were purchased from Sigma (St. Louis, MO, USA). The Glucantime® and the Ketamine were kindly provided by Oswaldo Cruz Institute and University Hospital Pedro Ernesto, respectively.

Animals

A total of 94 male BALB/c mice (*Mus musculus*) were included in this study. Animals were housed in mini-isolators at 22–24°C on shelves ventilated by an IVC filter system (Model Domi AL20 system; Alesco®) with a 12 h light/dark cycle. Food and water was provided *ad libitum*. Animals were sacrificed using ketamine hydrochloride (7.5 mg), 48 h after the last training session. Popliteal lymph nodes and paws were immediately isolated following the sacrifice. This study was approved by the Ethics Committee for Experimental Use and Animal Care at the Biology Institute Roberto Alcântara Gomes (Protocol number CEA/043/2009). Animals were divided into eight cohorts ($N = 8$). In the case of lactate and MDA (lipid peroxidation) dosages, the animals were divided into three cohorts ($N = 5$). After 12 weeks of infection, the mice were scarified using CO_2 chamber.

Microorganisms

Promastigotes of the LV39 strain of *Leishmania major* were grown as previously described (Terra et al., 2013). Briefly, parasites were cultured in Schneider's medium supplemented with 2 mM glutamine, 100 units/mL penicillin, 100 mg/mL

streptomycin and 20% fetal calf serum in a humidified incubator at 26°C. This strain was kindly provided by Dr. George dos Reis.

Infection Model

Mice were infected in the plantar cushion with 2×10^6 *L. major* promastigotes suspended in 20 μl of PBS. Lesion development was measured weekly using a caliper ruler (Mitutoyo, Brazil). The lesion size was calculated by the difference between the sizes of infected paw in relation to non-infected one.

Groups

C—Control, E—Exercised—animals trained for 12 weeks, I—Infected—animals infected with 2×10^6 *L. major* promastigotes, IE—Infected and exercised—infected animals trained for 12 weeks, from the first week of infection. IT—Infected with treatment—Animals infected and treated with therapeutic dose (8 mg) of Glucantime® after the onset of injury. ITE—Infected with treatment and exercised post-lesion—Animals infected, treated with therapeutic dose (8 mg) of Glucantime® and exercised after the onset of injury (from 6th week). IEP—Infected and exercised post-lesion—infected animals trained (for 6 weeks) after the onset of injury (from 6th week). EAPI -Trained during 6 weeks, infected and exercised—Animals trained for 6 weeks, infected and trained for 12 weeks.

Treatment Protocol

Animals were treated with a therapeutic dose (8 mg @ ∼500 mg/kg) of Glucantime® by an intraperitoneal application 5 times/week over a 12 week span. The treatment started after the onset of injury (6th week).

Exercise Protocol and Physical Tests

Animals were subjected to a previously described swimming exercise protocol for 30 min X 3 times per week for 6 or 12 weeks with some modifications (Terra et al., 2013). The training started 6 weeks before the infection (EAPI), 48 h after the infection (IE) or after 6 weeks from the infection (ITE and IEP). Animals were introduced into a tank (50 × 50 × 40 cm) with a water depth of 30 cm and a temperature of 32 ± 2°C that stimulated swimming, herein referred to as the study protocol. To meet the desired exercise intensity, weight was attached to their tails. The initial mass was 2% of the measured body mass (BM) of each individual animal. The load was increased to 4% BM in week 4 and 6% BM in week 6. Animal BM was measured weekly.

Animals in the exercise groups (E, IE, ITE, IEP, and EAPI) were submitted to multiple physical capacity tests starting on the initial week and repeated on the fourth, 8th and 12th weeks. The other groups (C, I and IT) were submitted to physical capacity tests just in starting on the initial week and repeated on the 12th week. The test consisted of a timed swimming session with a 2% BM load until the point of fatigue, which was defined as the moment when the animal remained submerged for 10 s without returning to the surface for breath. An intense exercise test was also applied prior to measure lactate and MDA levels that consisted of a swimming session until the exhaustion with the addition of weight equal to 6% BM.

Lactate

To verify that the study protocol reflected a protocol of moderate intensity, we measured the blood lactate in the animals after three different situations: rest, submitted to study protocol and submitted to a strenuous exercise protocol. The animals used in this evaluation ($N = 15$) did not participate of the experimental groups. Blood lactate levels were measured using a lactometer (Accusport®) from a whole blood sample (∼10 μl) collected from a small incision in the tail. Measurement were performed on three groups: sedentary, moderate exercise and intense exercise, at rest and, for the exercise groups, immediately after an exercise session (acutely, before beginning training).

Evaluation of Lipid Peroxidation Indices

The lipid peroxidation dosage (thiobarbituric acid reactive substances-TBARs) was performed as previously described (Keles et al., 2001). Three groups were used: rest, moderate exercise and intense exercise. The animals used in this dosage ($N = 15$) did not participate of the experimental groups. Immediately after the exercise session, animals were anesthetized with ketamine hydrochloride (7.5 mg) and blood was collected by a cardiac puncture into tubes with EDTA. The blood was centrifuged for 10 min at 1,000 g and the plasma was isolated to perform an assay for lipid peroxidation. The plasma (50 μL) was mixed with 200 μL of 10% TCA and 150 μL of potassium phosphate buffer (100 mM, pH 7.4) and incubated at room temperature for 10 min before centrifugation (2,000 × g for 15 min). The supernatant was collected and then, 500 μL thiobarbituric acid (0.67%) was added followed by an additional incubation at 95°C for 60 min. The samples were then cooled for 5 min and subjected to vortex. Finally, the absorbance was measured at 532 nm in a microplate reader, TP reader Thermo Plate. The MDA (malondialdehyde) concentrations were evaluated using a TMP (1,1,3,3-Tetramethoxypropane) standard curve.

Antigen Parasite Preparation

After obtaining sufficient numbers of parasites in the first culture pass (P1) at the beginning of the stationary phase (determined by a growth curve), they were centrifuged at 1,300 g for 10 min and washed twice with PBS to remove serum. The pellet was resuspended in DMEM medium and the parasite number adjusted to 2×10^8/mL. The promastigotes were submitted to three cycles of freezing-thawing in liquid nitrogen for complete lysis. The total antigen thus obtained was aliquoted and stored at −20°C until use. For the quantification of protein in the lysate, the Lowry method (Lowry et al., 1951) was used.

Delayed Type Hypersensitivity (DTH)

DTH was evaluated using total antigen of *L. major* (1 μg/μl). The antigen (20 μl) was inoculated into the plantar cushion of non-infected paw. The extent of swelling was measured using a caliper rule (Mitutoyo, Brazil) 48 h after inoculation. The DTH was expressed as the difference between the paw sizes before and after the antigen inoculation.

Lymph Node Cell Culture

The popliteal lymph nodes were harvested as previously described (Terra et al., 2013). Briefly, after the excision of the lymph nodes, a single cell suspension for each group was prepared by forcing tissue fragments through a stainless-steel mesh. The cell suspension (500 μL) was plated at 2 × 10^6 cells/mL in 24-well plates in the absence or presence of the parasite antigen (10 μg/mL) and incubated at 37°C in atmosphere of 5% CO_2 for 48 h. Supernatants were collected for cytokine measurements.

Infected Paws

After sacrifice, infected paws were collected and weighed. After removal of claws and skin, a single cell suspension for each group was prepared by forcing tissue fragments through a stainless-steel mesh into Schneider medium. The product of maceration was separated by centrifugation (1,300 × g for 20 min). From the supernatant, measurements for cytokines levels were made and the parasite load determined.

Measurement of Cytokine Production

The levels of the cytokines IFN-y, IL-4, IL-10, TNF, TGF-β, and IL-12 in the supernatants of cultured lymph node cells and isolated infected paws were measured by sandwich ELISA (R&D Systems, USA) utilizing a standard curve of recombinant murine cytokines and antibodies according to the manufacturer's instructions. Briefly, capture antibodies were plated into a 96-well ELISA plates and incubated at room temperature for 18 h (TNF-α = 0.8 μg/mL, other cytokines - 4 μg/mL), washed 3 times with PBS pH 7, 2, TWEEN 20 (0.05%) and blocked with PBS (pH 7.2) with 1% bovine serum albumin (BSA) for 1 h at room temperature. For TGF-β, the blocking solution also contained TWEEN 20 (5%) and sodium azide (0.05%) and that of IFN-γ, 0.05% sodium azide. After blocking, the plates were washed 3 times with wash buffer and the samples added (TGF-β dosing samples were previously activated by 1N HCl solution and neutralized by the addition of 1.2 N NaOH, 0.5 M HEPES). Then, the systems were incubated at room temperature for 2 h, washed three times with wash buffer and followed by the addition of biotinylated antibodies to cytokines TGF-β, TNF-α (200 ng/ml each), IL-10, IL-12p40 (400 ng/ml), IFN-γ (800 ng/ml), and IL-4 (600 ng/ml). Again, the samples were incubated for 2 h at room temperature and subsequently washed 3 times. The detection was achieved with Streptavidin HRP (conjugated to peroxidase and diluted 1:250). After washing, 0.1 M sodium citrate-acetate buffer, pH 4.0, containing 0.02% Tetramethylbenzidine (TMB), 0.02% hydrogen peroxide (H_2O_2) and 5% DMSO was added in the absence of light, for 20 min at room temperature. After this period, the reaction was stopped by adding 2N sulfuric acid (H_2SO_4) and read at 450 nm in a microplate reader, TP reader Thermo Plate.

Parasite Load

To obtain an estimative from number of live parasites, these were quantified as described before, with modifications (Kalama and Nanda, 2009). Briefly, to obtain the parasites, after the sacrifice of the animals, the infected paws were cut, weighed, had claws, and skin removed and were macerated in Schneider's medium (8 mL), with samples of the eight animals per group grouped as a pool. The resultant supernatant was used for parasites quantification. A volume of this supernatant was distributed into a 96-well plate through a serial dilution of 1:10 to 1:10,000 using Schneider medium supplemented with 100 units/mL of penicillin, 100 mg/mL of streptomycin and 20% fetal calf serum. Plates were cultured at 26°C until the presence of parasites was observed in group I (7th day). Then, the parasites were quantified in Neubauer Chamber, and the number of parasites obtained was divided by the total weight (gram) of infected paws tissue.

Statistical Analysis

Normality testing was performed for all samples. One-way ANOVA followed by the Tukey multiple comparisons test were used to analyze the statistical significance of cytokine concentrations from cultured lymph node cells and supernatant of infected paws. One-way ANOVA followed by the Dunnet test were used to analyze the statistical significance of DTH and parasite load. Differences were considered significant when $P < 0.05$.

RESULTS

Control of Exercise Intensity Through Physical Capacity Tests, Blood Lactate Concentration, and Lipid Peroxidation

Animal physical performance was evaluated by a maximum physical capacity test that was executed every 4 weeks to verify the adaptation of each animals to the swimming exercise. Exercise intensity was adjusted by an increase in the weight overload (% BM) or time of the exercise to maintain a moderate level of physical exertion. By the 8th week of exercise, the IEP, EAPI groups did not adapt satisfactorily to the increase of the overload to 6% of BM. The weight overload of 4% BM was maintained with an increase in time, since this was significantly different from the previous test for the same overload ($P < 0.05$). There was no significant difference in the maximum exercise time for the IE and E groups as a function of the overload increase over the weeks. However, the exercised groups showed an improvement in swimming capacity when compared to control groups (**Table 1**). All trained groups showed a significant increase in swimming time (>100%) during the physical fitness test. This data indicated that the exercise protocol used here, the study protocol, was able to produce positive training effects.

The blood lactate levels were measured under three different conditions to verify that the study protocol imposed an exercise of moderate intensity; (1) animals at rest, (2) animals immediately after being submitted to the study protocol, and (3) animals immediately after being submitted to a known strenuous exercise protocol. At rest, the blood lactate concentration was 1.78 mmol/L. Following the study protocol, the measured concentraton was 3.23 mmol/L and it was 5.63 mmol/L after

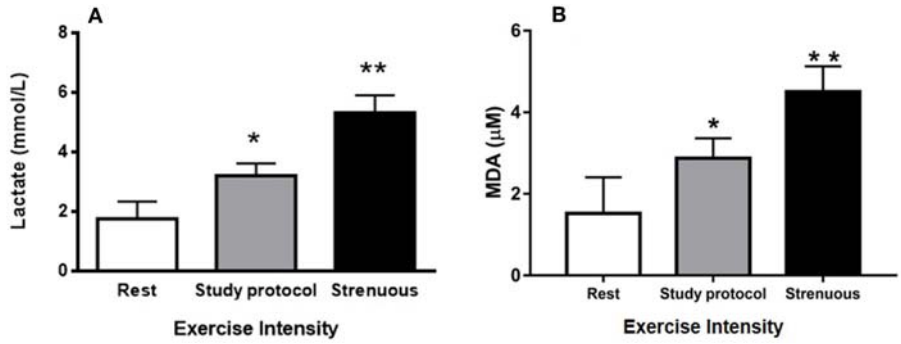

FIGURE 1 | Control of exercise intensity [blood lactate concentrations **(A)** and TBARs **(B)**]: **(A)** Blood lactate concentrations were measured at rest as well as after a session of study protocol and intense exercise. **(B)** MDA concentrations (lipid peroxidation) were measured at rest as well as after a session of study protocol and intense exercise. The animals used in these dosages, lactate ($n = 15$) and lipid peroxidation ($n = 15$), did not participate of the experimental groups. (*$P < 0.01$ compared to rest, **$P < 0.001$ compared to rest and study protocol). Values are expressed as mean and ± SD. Data were analyzed by one-way ANOVA followed by Tukey's multiple comparison test.

TABLE 1 | Maximal physical capacity of animal groups in a timed swim test at the start and end of the study.

Group	Swim time (min)		Differences (%)
	Initial week	Final week	
C	16.41 ± 4.45	22.02 ± 11.77	↑34
E	30.98 ± 11.31	62.29 ± 3.16*	↑101
I	41.82 ± 7.79	35.57 ± 9.07	↓15
IT	43.09 ± 5.80	40.00 ± 7.21	↓7
ITE	38.23 ± 6.95	69.73 ± 8.87*	↑82
IE	22.02 ± 11.78	59.37 ± 12.32*	↑170
IEP	23.28 ± 12.57	60.39 ± 11.77*	↑159
EAPI	40.23 ± 7.47	69.45 ± 6.29*	↑73

*$P < 0.05$. The animals were submitted to maximal physical capacity test in the starting and at the final of experiment. In the case of E, IE, ITE, IEP, and EAPI groups, the test also was applied every 4 weeks from the initial week. The time was measured in minutes. *$P < 0.05$. Arrows indicate increase or decrease in exercise time in relation to the first week.

a strenuous exercise (**Figure 1A**). These data suggest that the exercise protocol employed in this study was associated with moderate intensity, since the lactate level of animals submitted to strenuous exercise was significantly greater than level of the study protocol. In addition, there was a change of 88% in lipid peroxidation from the rest group (1.52 μM of MDA) to moderate exercised group (2.87 μM of MDA). However, the strenuous exercised mice (4.50 μM of MDA) presented an increase of 196% in lipid peroxidation when compared to rest group (**Figure 1B**). These data suggest the animals did not suffer much oxidative stress from our study protocol.

Effect of Exercise on Development of Murine Leishmaniasis

After 12 weeks of infection, it was observed that treatment with therapeutic dose of Glucantime® after the appearance of the lesion (IT) led to a regression in the lesion size consistent with inhibiting their progression (**Figure 2A**). This was considered our experimental control that represented current practice for clinical care. The development of lesion size due to infection in control animals (I) was significant only from the 6th week after injection of the inoculum of *L. major* ($P < 0.01$ compared to the first week of infection). Animals that performed exercise from the beginning of study period when the infection was introduce (IE) displayed a complete inhibition in the progression of the lesion (**Figure 2B**). Even when exercise was begun at 6 weeks post-infection, when a lesion had been visually established (IEP), a regression was observed in the lesions (**Figure 2B**). The animals in the ITE group, which were treated with Glucantime® and submitted to the training protocol after the onset of injury, showed the same pattern presented by the IT group (**Figure 2A**). Interestingly, the prophylaxis group that was subjected to 6 weeks of training before infection (EAPI) did not develop lesion (**Figure 2C**). These data suggest that exercise may modulate the immune response to leishmaniasis.

Intradermal Response to Total Leishmania Antigen

The DTH response was measured 48 h after an inoculum of *L. major* was injected into the uninfected paw (**Figure 3**). IE and IEP groups had significant differences compared to control infection (I) showing a positive DTH. The group treated with a therapeutic dose of Glucantime® showed no positive DTH as well as EAPI and ITE groups.

Parasite Load

We observed that the number of promastigotes grown from the parasites isolated in the infected control group (I) was, at least, 230 times higher than in the other groups, reaching this difference, at 7,000 times when compared with IE group (**Figure 4**).

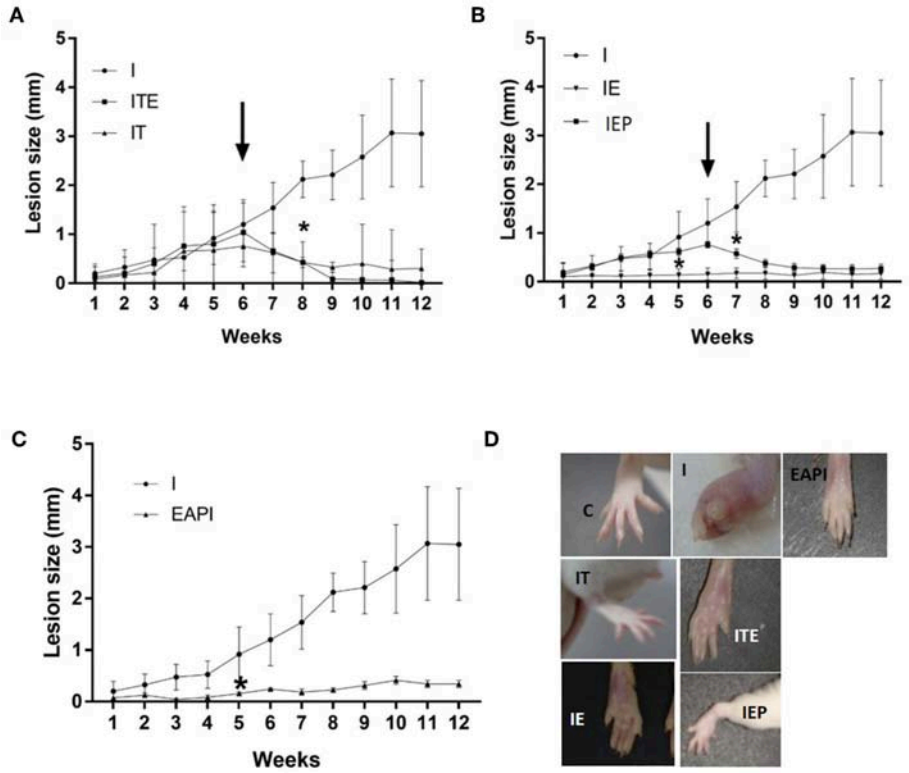

FIGURE 2 | Effect of exercise on the development of lesions on the paws of BALB/c mice that were infected with L. major (2 x 106 promastigotes): **(A–C)** The size of paws was measured weekly for 12 weeks with a pachymeter (Mitutoyo). Results are expressed as the difference between the contralateral paw and infected paw (mm). The arrow indicates the start of training and/or treatment. Values represent the average of two experiments with 8 animals per group in each experiment. **(D)** A representative image of the infected footpad from 1 animal of each different group at the end of the assay (13th week). Values were expressed as mean ± SD. I—Infected. IT—Animals infected and treated with therapeutic dose (8 mg) of Glucantime® after the onset of injury. ITE - Animals infected, trained and treated with therapeutic dose (8 mg) of Glucantime® after the onset of injury. IE—infected animals trained from the first week of infection. IEP—infected animals trained after the onset of injury (6th week). EAPI—Animals trained for 6 weeks, infected and trained for 12 weeks. * The week displaying significant difference ($P < 0.001$) from the control group (I).

Effect of Exercise on the Production of Cytokines by Infected Animals

Cytokine Production in Lymph Node Cells Draining the Lesion

The IL-4 cytokine was not detected in the C and IEP, with very similar concentrations in the other groups (**Figure 5A**). The IE, IT, and ITE groups had IL-4 production inhibited after stimulation with the parasite antigen (**Figure 5A**), where the other groups showed no significant difference from group I. The production of IL-10 was greatest in the infection control group (I), which was significantly stimulated by the parasite antigen (**Figure 5B**). Although this profile was also presented by groups E, IE, IT, and ITE, the increase promoted in I was significantly higher (**Figure 5B**). The production of TGF-β was very similar in all groups that were not stimulated, and was more pronounced in group I after stimulation with the parasite antigen (**Figure 5C**). The presence of IFN-γ was not detected in the supernatant of both cells, non-stimulated cells and stimulated by the *L. major* antigen in group C (**Figure 5D**). In groups E and IE, this cytokine was shown to be increased in comparison to its respective C and I controls in both, non-stimulated and stimulated cells (**Figure 5D**). The cytokine IL-12 was not detected in the both systems non-stimulated and stimulated from C group (**Figure 5E**). Again, in the E and IE groups, the cytokine in question was shown to be increased in relation to its respective C and I controls in the system stimulated by *L. major* antigen (**Figure 5E**). The Group I presented the highest TNF production in both systems, where the differences with the other groups, although statistically significant, were not very pronounced (**Figure 5F**). To compare the cytokines pattern production (Th1 and Th2), we calculated the ratio of IFN-γ/IL-4 and IFN-γ/IL-10. The groups IT, ITE and IE showed a higher ratio for IFN-γ/IL-4 (**Figure 5G**), while for IFN-γ/IL-10, the largest ratios were observed for the exercised mice (ITE, IE, and IEP) (**Figure 5H**).

Cytokine Production in Infected Paw Cells

The animals submitted to physical exercise presented an increase in the production of inflammatory cytokines IL-12, IFN-γ, and TNF, with an exception for IEP for IL-12 and TNF and ITE for IFN-γ (**Figures 6C–E**). Though group I presented a production

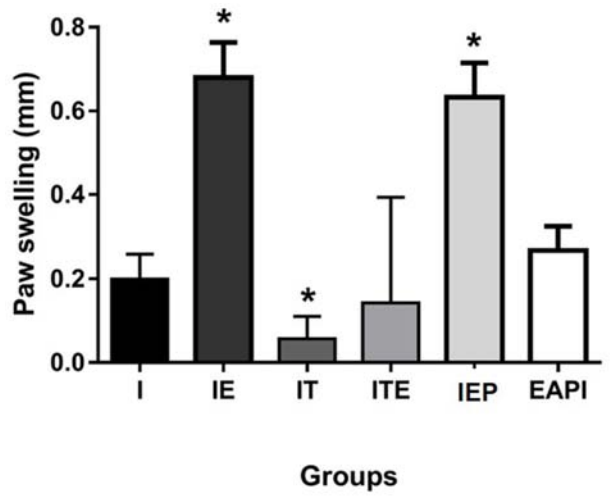

FIGURE 3 | Delayed type hypersensitivity (DTH) to total Leishmania major antigen in BALB / c mice trained and/or treated with Glucantime®. DTH was carried out in the 13th week, at the end of the experiment. The DTH was evaluated using 20 μg of total L. major antigen in 20 μL of saline inoculated into the contralateral non-infected paw. Results obtained after 48 h of antigen inoculum of L. major. Values are expressed as mean ± SD. Data were analyzed by one-way ANOVA followed by Tukey's multiple comparison test. *$P < 0.05$ compared to (I).

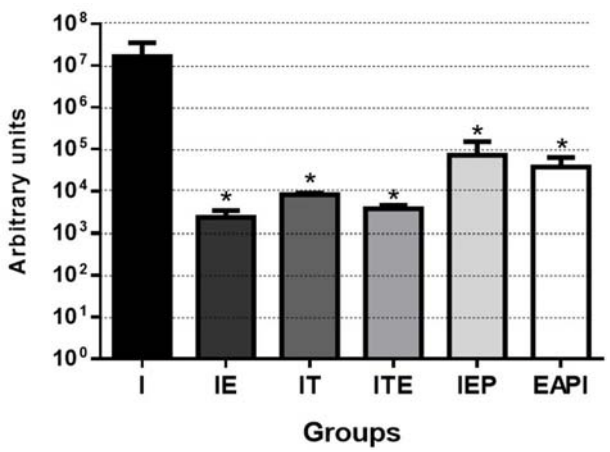

FIGURE 4 | Parasitic burden of infected mice. Parasites were isolated from the paws after 13 weeks of infection and quantified by serial dilution in Schneider's medium plus 20% FBS. After isolation, they were kept at 26°C until the presence of parasites was observed in group I (7th day). Then, the parasites were quantified in Neubauer Chamber, and the number of parasites obtained was divided by the total weight (gram) of infected paws tissue. Values are expressed as the mean of two experiments with the samples of eight animals per group grouped as a pool. The bars represent the standard error of the mean. I—Infected. IT—Animals infected and treated with a therapeutic dose (8 mg) of Glucantime®, after the onset of the lesion. ITE—Animals infected, trained and treated with therapeutic dose (8 mg) of Glucantime® after the onset of injury. IE—Animals infected and trained from the first week of infection. IEP—Animals infected and trained after the appearance of the lesion (6th week). EAPI—Animals trained for 6 weeks, infected and trained for another 12 weeks. *$P < 0.05$ with respect to I.

of inflammatory cytokines lower than the exercised groups, it cannot be said that this group presents an anti-inflammatory profile because the production of these cytokines in the paw of infected animals was higher in the groups submitted to the exercise. The EAPI group showed a more pro-inflammatory pattern, with the concentrations of the anti-inflammatory cytokines IL-4 (**Figure 6A**) and TGF-β (**Figure 6C**) lesser than I and the regulatory cytokine IL-10 (**Figure 6B**) higher than I.

DISCUSSION

The potential benefits promoted by physical exercise with regards to immune response appears to depend on the level of exertion experienced by the individual. In practice, the absence of training control can lead to overtraining such as in the case of strenuous training that may not promote the beneficials adaptations (Kellman, 2010; Walsh et al., 2011a). As a consequence, there is a possibility of an increase in viral infections or intracellular microorganisms, since high intensity exercises direct the immune system to a predominance of humoral response (Th2), which is not able to overcome these types of infection. In contrast, the practice of controlled exercise to provide a moderate physical intensity, results in a predominance of the cellular response pattern (Th1), controlling these kind of infections (Walsh et al., 2011b).

There are several parameters currently used to control exercise volume and intensity. The gold standard is represented by the maximum oxygen consumption (VO_2max). However, heart rate, subjective perception of effort, blood lactate concentration and specific physical capacity tests can also be employed (ACSM, 2011). Here, the blood lactate concentration in mice submitted to a session of exercise (moderate or strenuous) were evaluated to verify that the study protocol reflected a moderate exercise. In the post-exercise period of study protocol (3.23 mmol/L), the lactate level was characteristic of a moderate intensity exercise, since the concentration for a protocol of intense exercise until fatigue (5.63 mmol/L) was significantly larger (**Figure 1A**). Other protocols of moderate intensity presented lactate values very similar to those found in this work. Balb/c mice submitted to a moderately intensive run (25 m/min) presented a blood lactate concentration of 2.61 mmol/L, whereas at rest the value found was 1.81 mmol/L (Haramizu et al., 2009). This value is similar to the value measured in this work (1.78 mmol/L at rest). In addition, the mice submitted to a strenuous exercise presented a lipid peroxidation level that was 196% greater than the rest group, while the study protocol group increased 88% (**Figure 1B**). This is a further indication that the intensity of the protocol used was moderate, since the production of reactive oxygen species (ROS) by the muscle is directly proportional to the increase in exercise intensity (Bloomer and Fisher-Wellman, 2008). The levels of lipid peroxidation are increased after exhaustive aerobic exercise and resistance exercise (Alessio et al., 2000; Pinho et al., 2010).

Additional factors associated to increases in lipid peroxidation include the physical fitness level and the antioxidant capacity (Pinho et al., 2010). The training protocol implemented in this study included an adjustment to the overload weight applied

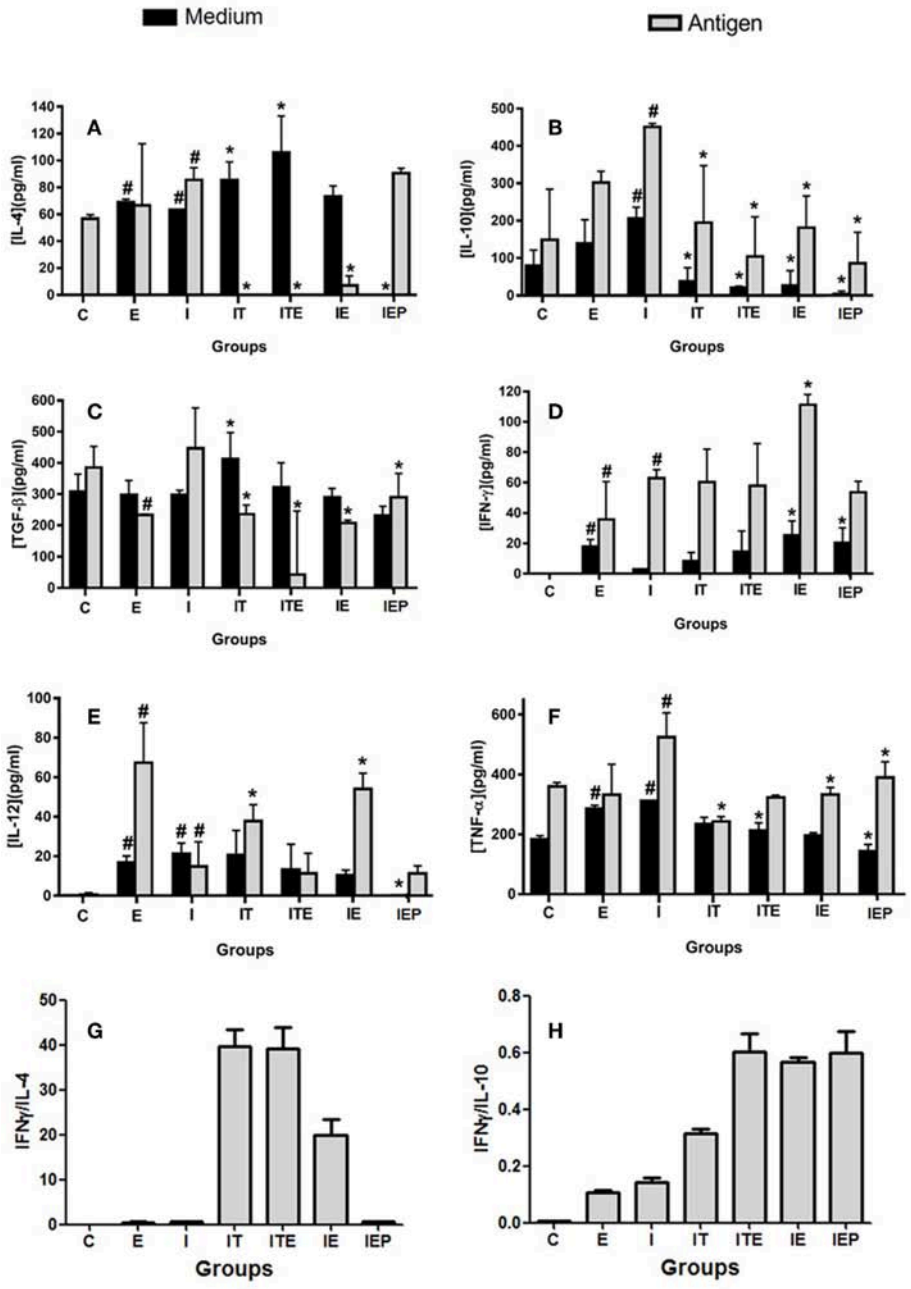

FIGURE 5 | Effect of physical exercise on cytokine production by lymph node cells of BALB/c mice. The concentration of cytokines was determined by ELISA according to Material and Methods. Values represent the mean of two experiments with samples of the eight animals per group grouped as a pool. **(A)** IL-4; **(B)** IL-10; **(C)** TGF-β; **(D)** IFN-γ; **(E)** IL-12; **(F)** TNF-α; **(G)** IFN-γ/IL-4 ratio; **(H)** IFN-γ/IL-10 ratio. The bars represent the standard error. C—Sedentary and uninfected. E—Trained not infected. I—Infected. IT—Animals infected and treated with a therapeutic dose (8 mg) of Glucantime®, after the onset of the lesion. ITE—Animals infected, trained and treated with therapeutic dose (8 mg) of Glucantime® after the onset of injury. IE—Animals infected and trained from the first week of infection. IEP—Animals infected and trained after the appearance of the lesion (6th week). #$P < 0.05$ in relation to C and in *$P < 0.05$ in relation to I.

to the animals during swimming every four weeks to maintain the desired intensity. This load adjustment is necessary for two reasons: (1) the timeframe of the experiments was during a growth phase of the animals when their weight increased and the extra loads are relative to body weight; and (2) the animals adapt to exercise through improved fitness. Thus, a greater stressor stimulus was required for homeostasis breakdown. These changes reflected an adaptation of the animals to the exercise, which was confirmed by the increased fitness level of the animals (**Table 1**). These adaptations are generally associated

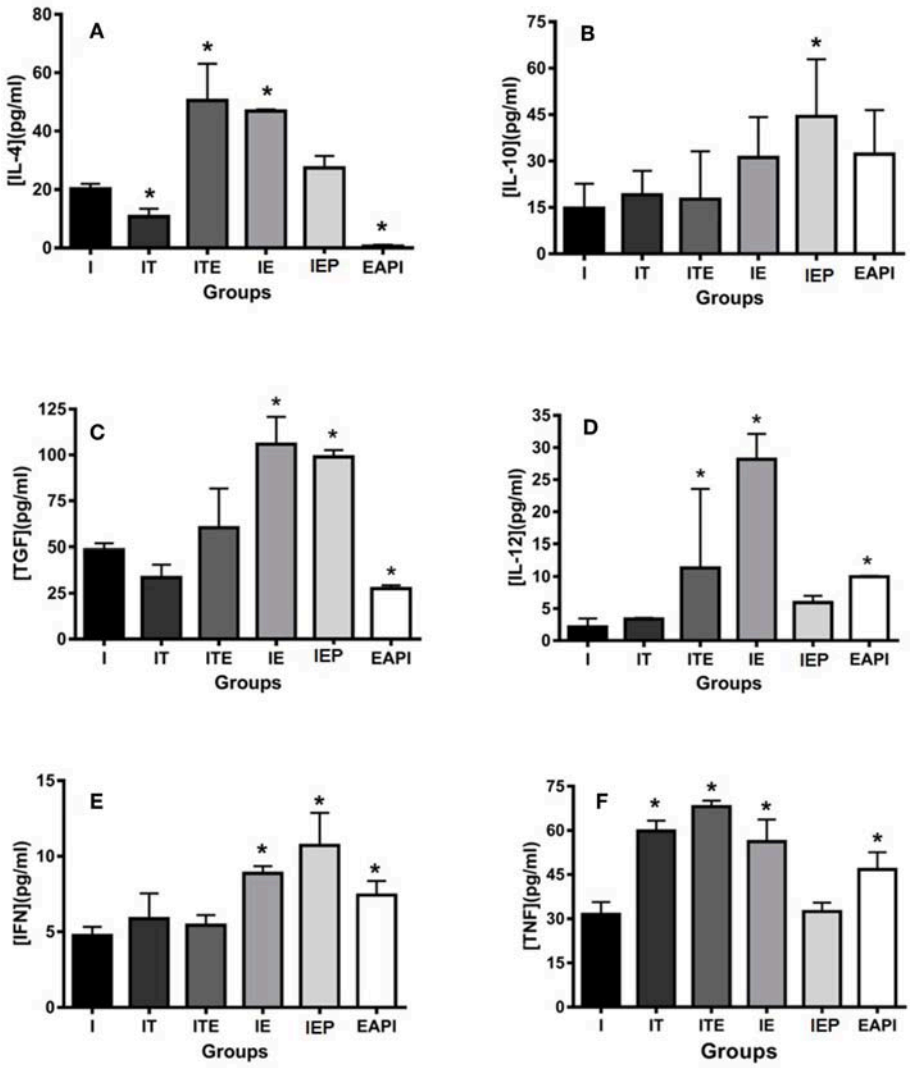

FIGURE 6 | Effect of physical exercise on cytokine production by cells in the paws of infected BALB/c mice. The cytokines IL-4 **(A)**, IL-10 **(B)**, TGF-β **(C)**, IL-12 **(D)**, IFN-γ **(E)** and TNF **(F)** were determined by ELISA (see Material and Methods). Values represent the mean of two experiments with samples of the eight animals per group grouped as a pool. The bars represent the standard error. C—Non-infected sedentary. E—Trained not infected. I—Infected. IT—Animals infected and treated with a therapeutic dose (8 mg) of Glucantime®, after the onset of the lesion. ITE—Animals infected, trained and treated with therapeutic dose (8 mg) of Glucantime® after the onset of injury. IE—Animals infected and trained from the first week of infection. IEP—Animals infected and trained after the appearance of the lesion (6 th week). EAPI—Animals trained for 6 weeks, infected and trained for another 12 weeks. *$P < 0.05$ with respect to I.

with increases in antioxidant capacity. Since the maintenance of the intensity and volume parameters of an exercise is essential to achieve the adaptations promoted by it (Walsh et al., 2011a) and the official positioning of the International Society for Exercise and Immunology (ISEI) establishes that a program of physical exercises of mild/moderate intensity improves immune function (Walsh et al., 2011b), the parameters of the swimming protocol executed by the trained animals provided a moderate exertion level that positively modified their immune response to an infection with *Leishmania*. This is consistent with multiple studies on exercise that show, when prescribed according to ACSM recommendations, reduces episodes of infection (Karper and Boschen, 1993; Nieman et al., 1993; Rowbottom and Green, 2000).

Our physical training protocol was able to not only able to avoid the development of lesions (EAPI and IE—**Figure 2**), it also appeared to reverse an established infection (IEP and ITE—**Figure 2**) along with a reduction in parasitic burden (**Figure 4**). Mice trained after a lesion was established displayed a disease progression that was similar to animals treated with Glucantime® over the same period. The delayed hypersensitivity response (DTH) in the trained Balb/c mice (IE and IEP) was significantly higher in relation to the infected group (I) (**Figure 3**). The positive DTH is indicative of a cellular immune

response (Th1), which appears generally to correlate with protection against parasites of the genus *Leishmania* (Naderer and Mcconville, 2008; Mougneau et al., 2011). Although the infection was also contained in the IT and ITE groups, the DTH appeared equal to or less than group I (**Figure 3**). The IT and ITE groups were treated with the reference drug Glucantime®, therefore the direct antiparasite effect of the drug induced control of infection. However, the literature is not clear on this issue and the mechanism of action of pentavalent antimonials has not yet been fully elucidated (Baiocco et al., 2009; Kaur and Rajput, 2014; Brazilian Ministry of Health, 2017). Likewise, the correlation between a therapeutic response and immunity is unclear (Conceição-Silva et al., 2018). Similar findings have been achieved in *L.major*-infected mice after immunization with lpg2- *L. major* (Uzonna et al., 2004) and Lmp27$^{-/-}$ mutant (Elikaee et al., 2018), where protection and DTH are not necessarily correlated.

The infected group (I) had a high prevalence of parasites in the infected paw how can be observed in the estimate of parasite load (**Figure 4**). Animals that underwent the moderate exercise protocol at the time of lesion appearance presented an estimate parasite load nearly 300-fold lower than that of infected animals (IEP and EAPI—**Figure 4**) or 4,000 fold lower in the case of ITE. Animals that began the exercises at the time of the infection, the difference was 7,000 fold (IE—**Figure 4**). The estimate parasite load appeared to be inversely proportional to DTH, except for the animals treated with the drug (IT—**Figures 3**, **4**). In a previous study on the development of leishmaniotic lesions caused by *L. major* (2×10^6 promastigotes) injections in susceptible Balb/c and resistant C57BL/6 mice (Barthelmann et al., 2011), the course of the lesion size, DTH and parasite in resistant animals presented positive DTH and low parasite load similar to that found in this study for susceptible mice submitted to exercise. These observations corroborate our hypothesis that moderate exercise can promote a protective and curative effect against *Leishmania*. Although we have not evaluated the parasitic load in the draining lymph nodes, it is known that even in cured animals the persistence of parasites in the draining lymph node occurs for long periods. The persistence of parasites seems to be important for the maintenance of the cellular immune response and generation of T cell memory (Mandell and Beverley, 2016; Conceição-Silva et al., 2018).

During a Th1 response, the increased production of IFN-γ stimulates the expression of the enzyme iNOS resulting in the production of nitric oxide (NO) by macrophages. The expression of this enzyme is induced by various stimuli, including IL-1, TNF, IFN-γ, and LPS (Stafford et al., 2002; Mansueto et al., 2007). The NO appears to be the main molecule involved in leishmanicidal mechanisms (Liew et al., 1990). In an anterior study from our group using the same exercise protocol, macrophages from 12 weeks trained Balb/c mice showed a significant increase in NO production after LPS stimulation (Terra et al., 2013). Here, mice infected and submitted to physical exercise (IE) had significantly higher concentrations of Th1 cytokines than the infected sedentary (I) in the isolated cells of the popliteal lymph node. This pattern was also observed for the uninfected animals submitted to exercise (E) when compared to the control system (C) (**Figure 5**). There was a significant decrease in IL-10 production by lymphocytes isolated from trained animals (**Figure 5B**), mainly in animals that were trained from the 6th week of infection (IEP).

Qualitatively, the production of these cytokines can be compared to the Th1/Th2 dichotomy models afforded by the resistant C57BL/6 mouse (Fritzche et al., 2010) and the susceptible Balb/c mouse (Barthelmann et al., 2011). In Balb/c mice, IL-10 is associated with the phenomena of susceptibility to infection by intracellular microorganisms, such as *Leishmania major* (Sacks and Noben-Trauth, 2002). The cytokine IL-10 was initially described as a Th2-type cytokine (Belkaid, 2007). Additional evidence has shown that its production is associated with regulatory T cell response (Treg) (Vignali et al., 2008). However, IL-10 production is not Th2 or Treg specific. It can also be expressed by other cells including Th1, Th17 subgroups, CD8$^+$ cells and B lymphocytes (Maloy and Maloy and Powrie, 2001; Roncarolo et al., 2006; O'Garra and Vieira, 2007; Trinchieri, 2007; Saraiva and O'Garra, 2010). Further, IL-10 can also be produced by cells participating in the innate immune response such as dendritic cells (DCs), macrophages, mast cells, NK cells, eosinophils and neutrophils (Saraiva and O'Garra, 2010). The decrease in IL-10 and TGF-β measured in the IEP group may play an important role in the resolution of the infection since the inflammatory cytokines IFN-γ and IL-12 were not modified in this group at the end of 12 weeks of infection in the systems stimulated by the parasitic antigen (popliteal lymph node) (**Figures 5D,E**). This was significantly different from that presented by the group that was trained from the first week of infection (IE), where the decrease in IL-10 and TGF-β (**Figures 5B,C**), production and the increase in IFN-γ and IL-12 production occurred concurrently (**Figures 5D,E**). It is possible that this difference may be due to the shorter training time to which this group (IEP) was submitted (6 weeks only). However, this hypothesis can be confirmed only if the IE cytokine training pattern is analyzed in the 6th week. Although TNF is an inflammatory cytokine (Mougneau et al., 2011), it has been decreased in the systems of mice submitted to exercise (IE and IEP) compared to infected animals (I) (**Figure 5F**). Our findings are in agreement with the literature where it has been widely argued that the practice of moderate-intensity physical exercise leads to a predominance of Th1 cytokines (Pedersen and Hoffman-Goetz, 2000; Walsh et al., 2011b).

Although the levels of IFN-γ detected of the trained (ITE, IEP)/treated (IT) groups were relatively similar to infected group (I), the levels of anti-inflammatory cytokines as IL-4, IL-10, and TGF-β were significantly lower. We hypothesize that in the absence of a strong IL-4 or IL-10 response, the low levels of IFN-γ produced may be sufficient for protection. When we performed the IFN-γ/IL-4 and IFN-γ/IL10 ratio, we observed a clear slope for the Th1 response (**Figures 5G,H**). These data are consistent with the cytokine patterns of the lymph node cells after 12 weeks training of Balb/c mice, when compared with sedentary group (Terra et al., 2013).

A similar scheme can be observed at the site of infection. When we analyzed the cytokine profile produced in the

infected paw (**Figure 6**), we observed that the response tended to be of a Th1 type where cytokines associated with this pattern (IL-12 and IFN-γ) are increased in the three of the four exercised groups studied including IEP. The local increase in this group could possibly contribute to the resolution of the infection. The presented EAPI cytokine profile at the site of infection seems characteristically to trend toward the Th1 pattern. The inflammatory cytokines IL-12 and IFN-γ, as well as TNF, were found to be increased (**Figures 6D–F**), whereas those associated with the Th2 pattern were significantly decreased (IL-4 and TGF-β) (**Figures 6A,C**) or without significant difference (IL-10) (**Figure 6B**). One possibility for this well-established pattern could be associated to training time, since this group began the practice of physical exercise at 6 weeks before the infection, and maintained their training throughout the course of the experiments. Data from the EAPI group suggest that regular physical exercise of moderate intensity can modulate the Th1 response and provide protection against *L. major* infection.

A regulatory response also appears to be present, especially in the IEP group, where IL-10 and TGF-β cytokines have been found to be increased (**Figures 6B,C**). The phenomena of resistance and susceptibility in all forms of leishmaniasis have been related to immune responses mediated by cells (Belosevic et al., 1989). Individuals with cutaneous leishmaniasis in the New World present a positive prognosis when their cellular immune response is balanced (Brazilian Ministry of Health, 2017). On the other hand, susceptibility is associated with an activation response of Th2-type lymphocytes (T helper 2), with production of interleukin 4 (Bogdan et al., 1996; Romagnani and Abbas, 1996; Lanouis et al., 2002; Mansueto et al., 2007). Diffuse cutaneous leishmaniasis and visceral leishmaniasis present non-protective Th2 responses (Romagnani and Abbas, 1996; Mansueto et al., 2007). However, an exacerbation of the Th1 type response (hypererygia) leads to increased tissue destruction where parasite antigen is present. This is characteristic of classical mucosal leishmaniasis, where IFN-γ and TNF levels are very high, associated with a relatively low production of IL-10. In addition, cells from individuals with this parasite have low ability to respond to cytokines inhibiting IFN-γ secretion (Brazilian Ministry of Health, 2017).

Overall, our data clearly shows a protective effect from moderate exercise on the development of experimental leishmaniasis. A potential mechanism for this protection is a modulation in the cytokine pattern during the immune response that was promoted by exercise. Further studies are needed to elucidate additional details in these complex, interconnected mechanisms.

ETHICS STATEMENT

This study was approved by the Ethics Committee for Experimental Use and Animal Care at the Biology Institute Roberto Alcântara Gomes (UERJ) (Protocol number CEUA/019/2015).

AUTHOR CONTRIBUTIONS

RT conducted experiments and contributed to the writing of the manuscript. PA, AL and SG, conducted the experiments. LR contributed to the execution and discussion of cytokine production analysis. VS conducted co-orientation and contributed to the writing of the manuscript. SD-S conducted experiments, co-orientation and contributed to the writing of the manuscript. PD conducted orientation, experimentation and contributed to the writing of the manuscript.

FUNDING

Edital FAPERJ N° 10/2014 - Support Program for the Study of Neglected and Reemerging Diseases - (E-26/010.002549/2014); Edital FAPERJ N° 08/2009 - Program Young Scientist of Our State- (E26/102.266/2009).

ACKNOWLEDGMENTS

We thank CAPES (Coordenação de Aperfeiçoamento de Pessoal de Nível Superior) and FAPERJ (Fundação Carlos Chagas Filho de Amparo à Pesquisa do Estado do Rio de Janeiro) for their support and scholarships granted.

REFERENCES

ACSM (2011). American College of Sports Medicine position stand. Quantity and quality of exercise for developing and maintaining cardiorespiratory, musculoskeletal, and neuromotor fitness in apparently healthy adults: guidance for prescribing exercise. *Med. Sci. Sports Exerc.* 43, 1334–1359. doi: 10.1249/MSS.0b013e318213fefb

Alessio, H. M., Hagerman, A. E., Fulkerson, B. K., Ambrose, J., Rice, R. E., and Wiley, R. L., (2000). Generation of reactive oxygen species after exhaustive aerobic and isometric exercise. *Med. Sci. Sports. Exerc.* 32, 1576-81. doi: 10.1097/00005768-200009000-00008

Alvar, J., Vélez, I. D., Bern, C., Herrero, M., Desjeux, P., Cano, J., et al. (2012). Leishmaniasis worldwide and global estimates of its incidence. *PLoS ONE*. 7:5. doi: 10.1371/journal.pone.0035671

American College of Sports Medicine Position Stand and American Heart Association, - ACSM/AHA (1998). Recommendations for cardiovascular screening, staffing, and emergency policies at health/fitness facilities. *Med. Sci. Sports. Exerc.* 30, 1009–1018.

American College of Sports Medicine Position Stand and American Heart Association, - ACSM/AHA (2007). Exercise and acute cardiovascular events: placing the risks into perspective. *Med. Sci. Sports Exerc.* 115, 2358–2368. doi: 10.1161/CIRCULATIONAHA.107.181485

Badirzadeh, A., Mohebali, M., Ghasemian, M., Amini, H., Zarei, Z., Akhoundi, B., et al. (2013). Cutaneous and post kala-azar dermal leishmaniasis caused by *Leishmania infantum* in endemic areas of visceral leishmaniasis, northwestern Iran 2002e2011: a case series. *Pathog. Glob. Health*. 107, 194–197. doi: 10.1179/2047773213Y.0000000097

Baiocco, P., Franceschini, S., Ilari, A., and Colotti, G. (2009). Trypanothione reductase from *Leishmania infantun*: cloning, expression, purification, crystallization and preliminary X-ray data analysis. *Protein Pept. Lett.* 16, 196–200. doi: 10.2174/092986609787316306

Barthelmann, J., Nietsch, J., Blessenohl, M., Laskay, T., van Zandbergen, G., Westermann, J., et al. (2011). The protective Th1 response in mice is induced in the T-cell zone only three weeks after infection with *Leishmania major* and not during early T-cell activation. *Med. Microbiol. Immunol.* 201, 25–35. doi: 10.1007/s00430-011-0201-6

Belkaid, Y. (2007). Regulatory T cells and infection: a dangerous necessity. *Nat. Rev. Immunol.* 7, 875–888. doi: 10.1038/nri2189

Belosevic, M., Finbloom, D. S., Van Der Meide, P. H., Slayter, M. V., and Nacy, C. A., (1989). Administration of monoclonal anti-IFN-gamma antibodies *in vivo* abrogates natural resistance of C3H/HeN mice to infection with Leishmania major. *J Immunol*. 143, 266–274.

Bloomer, R. J., and Fisher-Wellman, K. H. (2008). Blood oxidative stress biomarkers: influence of sex, exercise training status, and dietary intake. *Gend. Med*. 5, 218–228. doi: 10.1016/j.genm.2008.07.002

Bogdan, C. (2008). Mechanisms and consequences of persistence of intracellular pathogens: lesihmaniasis as an example. *Cell. Microbiol.* 10, 1221–1234. doi: 10.1111/j.1462-5822.2008.01146.x

Bogdan, C., Gessner, A., Solbach, W., and Rollinghoff, M. (1996). Invasion, control and persistence of *Leishmania* parasites. *Curr. Opin. Immun*. 8, 517–525. doi: 10.1016/S0952-7915(96)80040-9

Brazilian Ministry of Health, (2017). *Manual de Vigilância da Leishmaniose Tegumentar Americana. 2, 77-82*. Techinical note No: 233/2013 (Updated in 12/04/2015).

Carvalho, L. P., Passos, S., Dutra, W. O., Soto, M., Alonso, C., Gollob, K. J., et al. (2005). Effect of LACK and KMP11 on IFN-γ production by peripheral blood mononuclear cells from cutaneous and mucosal leishmaniasis patients. *Scand. J. Immunol*. 61, 337–342. doi: 10.1111/j.1365-3083.2005.01581.x

Conceição-Silva, F., Leite-Silva, J., and Morgado, F. N. (2018). The binomial parasite-host immunity in the healing process and in reactivation of human tegumentary leishmaniasis. *Front. Microbiol.* 9:1308. doi: 10.3389/fmicb.2018.01308

de Assis Souza, M., de Castro, M. C., de Oliveira, A. P., de Almeida, A. F., de Almeida, T. M., Reis, L. C., et al. (2013). Cytokines and NO in American tegumentary leishmaniasis patients: profiles in active disease, after therapy and in self-healed individuals. *Microb. Pathog.* 57, 27–32. doi: 10.1016/j.micpath.2013.02.004

Elikaee, S., Mohebali, M., Rezaei, S., Eslami, H., Khamesipour, A., Keshavarz, H., et al. (2018). Development of a new live attenuated Leishmania major p27 gene knockout: Safety and immunogenicity evaluation in BALB/c mice. *Cell. Immunol.* 332, 24–31. doi: 10.1016/j.cellimm.2018.07.002

Fritzche, C., Schleicher, U., and Bogdan, C. (2010). Endothelial nitric oxide synthase limits the inflammatory response in mouse cutaneous leishmaniasis. *Immunobiology* 215, 826–832. doi: 10.1016/j.imbio.2010.05.022

Gleeson, M. (2006). Immune system adaptation in elite athletes. *Curr. Opin. Clin. Nutr. Metab. Care*. 9, 659–665. doi: 10.1097/01.mco.0000247476.02650.18

Gleeson, M. (2007). Exercise and immune function. *J. Appl. Physiol*. 103, 693–699. doi: 10.1152/japplphysiol.00008.2007

Haramizu, S., Nagasawa, A., Ota, N., Hase, T., Tokimitsu, I., and Murase, T., (2009). Different contribution of muscle and liver lipid metabolism to endurance capacity and obesity susceptibility of mice. *J. Appl. Physiol*. 106, 871–879. doi: 10.1152/japplphysiol.90804.2008

Kahime, K., Boussaa, S., Laamrani-El Idrissi, A., Nhammi, H., and Boumezzough, A. (2016). Epidemiological study on acute cutaneous leishmaniasis in Morocco. *J. Acute Dis*. 5, 41–45. doi: 10.1016/j.joad.2015.08.004

Kalama, T., and Nanda, N. K. (2009). Protective response to leishmania major in BALB/c mice requires antigen processing in the absence of DM^1. *J. Immunol.* 182, 4882–4890. doi: 10.4049/jimmunol.0803956

Karper, W. B., and Boschen, M. B. (1993). Effects of exercise on acute respiratory tract infections and related symptoms. Moderate exercise may boast an elder's natural defenses against common illnesses. *Geriatr Nurs*. 14, 15–8. doi: 10.1016/S0197-4572(06)80071-6

Kaur, G., and Rajput, B. (2014). Comparative analysis of the omics technologies used to study antimonial, amphotericin B, and pentamidine resistance in leishmania. *J. Parasitol. Res.* 2014:726328. doi: 10.1155/2014/726328

Keles, M. S., Taysi, S., Sen, N., Aksoy, H., and Akcay, F. (2001). Effect of corticosteroid therapy on serum and CSF malondialdehyde and antioxidant proteins in multiple sclerosis. *Can. J. Neurol. Sci.* 28, 141–143. doi: 10.1017/S0317167100052823

Kellman, M. (2010). Preventing overtraining in athletes in high-intensity sports and stress/recovery monitoring. *Scand. J. Med. Sci. Sports*. 20, 95–102. doi: 10.1111/j.1600-0838.2010.01192.x

Lainson, R., Ward, R. D., and Shaw, J. J. (1997). Leishmania in phlebotomid sandflies: VI. Importance of hindgut development in distinguishing between parasites of the *Leishmaniamexicana* and L. braziliensis complexes. *Proc. R. Soc. Lond. Biol. Sci.* 199:309. doi: 10.1098/rspb.1977.0141

Lanouis, P., Gumy, A., Himmelrich, H., Locksley, R. M., Röcken, M., and Louis, J. A. (2002). Rapid IL-4 production by Leishmania homolog of mammalian RACK1-reactive CD4(+) T cells in resistant mice treated once with anti-IL-12 or -IFN-gamma antibodies at the onset of infection with *Leishmania* major instructs Th2 cell development, resulting in nonhealing lesions. *J. Immunol.* 168, 4628–4635. doi: 10.4049/jimmunol.168.9.4628

Liew, F. Y., Millott, S., Parkinson, C., Palmer, R. M., and Moncada, S. (1990). Macrophage killing of Leishmania parasite *in vivo* is mediated by nitric oxide from L-arginine. *J. Immunol.* 144, 4794–4797.

Lili, T., and Cheng, P. (2007). Alterations of immunoendocrine responses during the recovery period after acute prolonged cycling. *Eur. J. Appl. Physiol.* 101, 539–546. doi: 10.1007/s00421-007-0529-1

Lowry, O., Rosebrough, N. J., Farr, A. L., and Randall, R. J. (1951). Protein measurement with the Folin phenol reagent. *J. Biol. Chem.* 193, 265–275.

Malm, C. (2004). Exercise immunology: the current state of man and mouse. *Sports Med*. 34, 555–566. doi: 10.2165/00007256-200434090-00001

Maloy, K. J., and Powrie, F. (2001). Regulatory T cells in the control of immune pathology. *Nat. Immunol.* 2, 816–822. doi: 10.1038/ni0901-816

Mandell, M. A., and Beverley, S. M. (2016). Concomitant immunity induced by persistent Leishmania major does not preclude secondary re-infection: implications for genetic exchange, diversity and vaccination. *PLoS Negl. Trop. Dis*. 10:e0004811. doi: 10.1371/journal.pntd.0004811

Mansueto, P., Vitale, G., Di Lorenzo, G., Rini, G. B., Mansueto, S., and Cillari, E. (2007). Immunopathology of leishmaniasis: an update. *Int. J. Immun. Pharma*. 20, 435–445. doi: 10.1177/039463200702000302

Martin, P., and Leibovich, S. J. (2005). Inflammatory cells during wound repair: the good, the bad and the ugly. *Trend Cell Biol*. 15, 599– 607. doi: 10.1016/j.tcb.2005.09.002

McCall, L., Zhang, W., and Matlashewski, G. (2013). Determinants for the development of visceral leishmaniasis disease. *PLoS Pathog.* 9:1003053. doi: 10.1371/journal.ppat.1003053

Mendes, D. S., Dantas, M. L., Gomes, J. M., dos Santos, W. L., Silva, A. Q., Guimaraes, L. H., et al. (2013). Inflammation in disseminated lesions: an analysis of CD4+, CD20+, CD68+, CD31+ and vW+ cells in non-ulcerated lesions of disseminated leishmaniasis. *Memorias. Inst. Oswaldo. Cruz*. 108, 18–22. doi: 10.1016/j.cyto.2013.12.016

Miranda Lessa, M., Andrade Lessa, H., Castro, T. W. N., Oliveira, A., Scherifer, A., Machado, P., et al. (2007). Mucosal leishmaniasis: epidemiological and clinical aspects. *Braz. J. Otorhinolaryngol*. 73, 843–847. doi: 10.1016/S1808-8694(15)31181-2

Momen, H., Pacheco, R. S., Cupolillo, E., and Grimaldi Junior, G. (1993). Molecular evidence for the importation of World Leishmania into the Americas. *Biol. Res.* 26, 249–255.

Mougneau, E., Bihl, F., and Glaichenhaus, N. (2011). Cell biology and immunology of *Leishmania*. *Immunol. Rev.* 240, 286–296. doi: 10.1111/j.1600-065X.2010.00983.x

Naderer, T., and Mcconville, M. J. (2008). The *Leishmania*-macrophage interaction: a metabolic perspective. *Cell. Microbiol.* 10, 301–308. doi: 10.1111/j.1462-5822.2007.01096.x

Nieman, D. C., Henson, D. A., Gusewitch, G., Warren, B. J., Dotson, R. C., Butterworth, D. E., et al. (1993). Physical activity and immune function in elderly women. *Med. Sci. Sports. Exerc*. 25, 823–31. doi: 10.1249/00005768-199307000-00011

O'Garra, A., and Vieira, P. (2007). T(H)1 cells control themselves by producing interleukin-10. *Nat. Rev. Immunol.* 7, 425–428. doi: 10.1038/nri2097

Organização Pan Amaricana De Saúde and, Organização Mundial De Saúde. (2018). *Leishmanioses: Informe Epidemiológico das Américas*. 6. Available online at: http://iris.paho.org/xmlui/bitstream/handle/123456789/34857/LeishReport6_por.pdf?sequence=5&isAllowed=y

Pedersen, B. K., and Hoffman-Goetz, L. (2000). Exercise and the immune system: regulation, integration, and adaptation. *Physiol. Rev*. 80, 1055–1081. doi: 10.1152/physrev.2000.80.3.1055

Pinho, R. A., Silva, L. A., Pinho, C. A., Scheffer, D. L., Souza, C. T., Benetti, M., et al. (2010). Oxidative stress and inflammatory parameters after an Ironman race. *Clin. J. Sport Med*. 20, 306–311. doi: 10.1097/JSM.0b013e3181e413df

Romagnani, S., and Abbas, A. K. (1996). IV international conference on cytokines. ares-serono foundation (under the auspices of the European Cytokine Society). Florence, Italy. Report and abstracts. *Eur Cytokine Netw*. 7, 801–27.

Roncarolo, M. G., Gregori, S., Battaglia, M., Bacchetta, R., Fleischhauer, K., Levings, M. K., et al. (2006). Interleukin-10-secreting type 1 regulatory T cells in rodents and humans. *Immunol. Rev*. 212, 28-50. doi: 10.1111/j.0105-2896.2006.00420.x

Rowbottom, D. G., and Green, K. J. (2000). Acute exercise effects on the immune system. *Med. Sci. Sports. Exerc*. 32, 396–405. doi: 10.1097/00005768-200007001-00004

Sacks, D., and Noben-Trauth, N. (2002). The immunology of susceptibility and resistance to *Leishmania major* in mice. *Nat. Rev. Immunol*. 2, 845–858. doi: 10.1038/nri933

Samy, A. M., Doha, S., and Kenawy, M. A. (2014). Ecology of cutaneous leishmaniasis in Sinai: linking parasites, vectors and hosts. *Mem. Inst. Oswaldo Cruz*. 109, 299–306. doi: 10.1590/0074-0276130426

Saraiva, M., and O'Garra, A. (2010). The regulation of IL-10 production by immune cells. *Nat. Rev. Immunol*. 10, 170–181. doi: 10.1038/nri2711

Shah, S., Shah, A., Prajapati, S., and Bilimoria, F. (2010). Post-kala-azar dermal leishmaniasis in HIV-positive patients: a study of two cases. *Indian J. Sex. Transm. Dis AIDS*. 31, 42–44. doi: 10.4103/0253-7184.69001

Stafford, J. L., Neumann, N. F., and Belosevic, M. (2002). Macrophage-mediated innate host defense against protozoan parasites. *Crit. R. Microbiol*. 28, 187–248. doi: 10.1080/1040-840291046731

Stark, D., Pett, S., Marriott, D., and Harkness, J. (2006). Post-kala-azar dermal leishmaniasis due to leishmania infantum in a human immunodeficiency virus type 1- infected patient. *J. Clin. Microbiol*. 44, 1178–1180. doi: 10.1128/JCM.44.3.1178-1180.2006

Terra, R., Alves, P. J. F., Gonçalves da Silva, S. A., Salerno, V. P., and Dutra, P. M. L. (2013). Exercise improves the Th1 response by modulating cytokine and NO production in BALB/c Mice. *Sports Med*. 34, 661–666. doi: 10.1055/s-0032-1329992

Terra, R., Silva, S. A. G., da Pinto, V. S., and Dutra, P. M. L. (2012). Efeito do exercício no sistema imune: resposta, adaptação e sinalização celular. *Rev .Bras. Med. Esporte*. 18, 208–214. doi: 10.1590/S1517-869220120003 00015

Trinchieri, G. (2007). Interleukin-10 production by effector T cells: Th1 cells show self control. *J. Exp. Med.*. 204, 239–243. doi: 10.1084/jem.200 70104

Uzonna, J. E., Späth, G. F., Beverley, S. M., and Scott, P. (2004) Vaccination with phosphoglycan deficient *Leishmania major* protects highly susceptible mice from virulent challenge without inducing a strong Th1 response. *J. Immunol*. (2004) 172, 3793–3797. doi: 10.4049/jimmunol.172. 6.3793

Vignali, D. A., Collison, L. W., and Workman, C. J. (2008). How regulatory T cells work. *Nat. Rev. Immunol*. 8, 523–532. doi: 10.1038/nri2343

Von Stebut, E. (2007). Cutaneous *Leishmania* infection: progress in pathogenesis research and experimental therapy. *Exp Dermato*. 16, 349–346. doi: 10.1111/j.1600-0625.2007.00554.x

Walsh, N. P., Gleeson, M., Pyne, D. B., Nieman, D. C., Dhabhar, F. S., Shephard, R. J., et al. (2011b). Position statement part two: maintaining immune health. *Exerc. Immunol. Rev*. 17, 64-103.

Walsh, N. P., Gleeson, M., Shephard, R. J., Gleeson, M., Woods, J. A., Bishop, N. C., et al. (2011a). Position statement: part one: immune function and exercise. *Exerc. Immunol. Rev*. 17, 6-63.

World Health Organization (2018) Available online at: https://www.who.int/en/news-room/fact-sheets/detail/leishmaniasis; https://www.afro.who.int/health-topics/Leishmaniasis (accessed July, 11 2018).

Conflict of Interest Statement: The authors declare that the research was conducted in the absence of any commercial or financial relationships that could be construed as a potential conflict of interest.

frontiers in Cellular and Infection Microbiology

ORIGINAL RESEARCH
published: 10 May 2019
doi: 10.3389/fcimb.2019.00153

Infection of Human Neutrophils With *Leishmania infantum* or *Leishmania major* Strains Triggers Activation and Differential Cytokines Release

Rafeh Oualha[1,2], *Mourad Barhoumi*[1], *Soumaya Marzouki*[3], *Emna Harigua-Souiai*[1], *Melika Ben Ahmed*[3] *and Ikram Guizani*[1]*

[1] *Laboratory of Molecular Epidemiology and Experimental Pathology - LR16IPT04, Institut Pasteur de Tunis, Université de Tunis El Manar, Tunis, Tunisia,* [2] *Faculté des Sciences de Bizerte, Université de Carthage, Tunis, Tunisia,* [3] *Laboratory of Transmission, Control and Immunobiology of Infections - LR16IPT02, Institut Pasteur de Tunis, Université de Tunis El Manar, Tunis, Tunisia*

Leishmaniases are neglected diseases, caused by intracellular protozoan parasites of the *Leishmania* (*L.*) genus. Although the principal host cells of the parasites are macrophages, neutrophils are the first cells rapidly recruited to the site of parasites inoculation, where they play an important role in the early recognition and elimination of the parasites. The nature of early interactions between neutrophils and *Leishmania* could influence the outcome of infection. Herein we aimed to evaluate whether different *Leishmania* strains, responsible for distinct clinical manifestations, could influence *ex vivo* functional activity of neutrophils. Human polymorphonuclear leukocytes were isolated from 14 healthy volunteers and the *ex vivo* infection of these cells was done with two *L. infantum* and one *L. major* strains. Infection parameters were determined and neutrophils activation was assessed by oxidative burst, degranulation, DNA release and apoptosis; cytokine production was measured by a multiplex flow cytometry analysis. Intracellular amastigotes were rescued to determine *Leishmania* strains survival. The results showed that *L. infantum* and *L. major* promastigotes similarly infected the neutrophils. Oxidative burst, neutrophil elastase, myeloperoxidase activity and apoptosis were significantly increased in infected neutrophils but with no differences between strains. The *L. infantum*-infected neutrophils induced more DNA release than those infected by *L. major*. Furthermore, *Leishmania* strains induced high amounts of IL-8 and stimulated the production of IL-1β, TNF-α, and TGF-β by human neutrophils. We observed that only one strain promoted IL-6 release by these neutrophils. The production of TNF-α was also differently induced by the parasites strains. All these results demonstrate that *L. infantum* and *L. major* strains were able to induce globally a similar *ex vivo* activation and apoptosis of neutrophils; however, they differentially triggered cytokines release from these cells. In addition, rescue of intracellular parasites indicated different survival rates further emphasizing on the influence of parasite strains within a species on the fate of infection.

Keywords: *Leishmania* spp., neutrophils, oxidative burst, degranulation, DNA release, apoptosis, multiplex cytokine bead array, amastigote survival

OPEN ACCESS

Edited by:
Claudia Ida Brodskyn, Gonçalo Moniz Institute (IGM), Brazil

Reviewed by:
Fabienne Tacchini-Cottier, Université de Lausanne, Switzerland
Sima Rafati, Pasteur Institute of Iran (PII), Iran

***Correspondence:**
Ikram Guizani
ikram.guizani@pasteur.rns.tn

Specialty section:
This article was submitted to Parasite and Host, a section of the journal Frontiers in Cellular and Infection Microbiology

Received: *08 February 2019*
Accepted: *24 April 2019*
Published: *10 May 2019*

Citation:
Oualha R, Barhoumi M, Marzouki S, Harigua-Souiai E, Ben Ahmed M and Guizani I (2019) Infection of Human Neutrophils With Leishmania infantum or Leishmania major Strains Triggers Activation and Differential Cytokines Release. Front. Cell. Infect. Microbiol. 9:153. doi: 10.3389/fcimb.2019.00153

INTRODUCTION

Leishmaniases are a complex group of neglected diseases, caused by the intracellular protozoan parasites of the genus *Leishmania*. They are endemic in more than 98 countries and cause significant morbidity and mortality worldwide. They are characterized by a spectrum of clinical manifestations of the disease ranging from the self-healing skin lesions of cutaneous leishmaniasis (CL) to the visceral leishmaniasis (VL) that is fatal in the absence of treatment. The different clinical manifestations depend on the *Leishmania* parasite species and on the immune response of the host among other factors (Herwaldt, 1999; Guizani et al., 2011; Alvar et al., 2012). An estimated 700,000 to 1 million new cases and some 26,000 to 65,000 deaths occur annually (Who, 2019). In addition, the Global Burden of Disease 2017 study estimated the prevalence of leishmaniases to be 4.130 Million (95 % Uncertainty Interval 3.515–4.966) (Diseases, 2018). Maps presenting the global distribution of these diseases and their local risk factors were recently updated; based on such maps computer modeling predicted that 1.7 billion are living in areas at risk for leishmaniases (Pigott et al., 2014). In spite of sustained efforts, no effective human vaccine is yet available (Kumar and Engwerda, 2014; Didwania et al., 2017; Seyed et al., 2018). The mainstay therapy is based on the use of pentavalent antimonials, which present adverse effects and increasingly induce drug resistance (Hefnawy et al., 2017; Ghorbani and Farhoudi, 2018). Studies in animal models have shown that protection against the disease is associated with the production of IL-12 by innate cells, which induces the proliferation of CD4+ Th1 cells, which in turn produce IFN-γ to activate macrophages to kill the parasites (Sacks and Noben-Trauth, 2002; Kaye and Scott, 2011). Furthermore, it seems that early events that occur during the establishment of the infection in the skin are very important to the development of an effective immune response against *Leishmania* infection (Peters and Sacks, 2006). Infectious *Leishmania* promastigotes are inoculated to the mammalian host by sand fly bites, then these parasites transform into amastigotes inside parasitophorous vacuoles within a range of host cells: macrophages, dendritic cells and neutrophils as result of complex host/pathogen/ vector interactions (Rodríguez and Wilson, 2014; Martínez-López et al., 2018). Studies on animal models have shown that neutrophils are massively and rapidly recruited to the site of infection and are the first cells to encounter the parasites (Müller et al., 2001; Peters et al., 2008). Neutrophils constitute the first line of defense against these pathogens. They participate in their elimination by several mechanisms including the production of reactive oxygen species (ROS), the release of azurophilic granules that contain antimicrobial proteins such as Neutrophil Elastase (NE) and myeloperoxidase (MPO) (Segal, 2005; Nauseef, 2007). In addition, neutrophils can release extracellular traps (NETs) composed of histones, fibrous DNA and granule proteins (Brinkmann et al., 2004), which can trap extracellular pathogens and in some cases kill them (Kolaczkowska and Kubes, 2013; Bardoel et al., 2014). The role of neutrophils in host defense against leishmaniases has been well studied in animal models. Both protective and non-protective roles against *Leishmania* infection have been reported for these cells, which depend on *Leishmania* species and host immune responses (Peters and Sacks, 2009; Charmoy et al., 2010; Ribeiro-Gomes and Sacks, 2012; Carlsen et al., 2015b; Hurrell et al., 2016). Indeed, it was shown that at the time of *L. major* infection, depletion of neutrophils in susceptible BALB/c mice reduced the parasite load and induced resistance to *L. major* infection (Tacchini-Cottier et al., 2000). In contrast, at the same time, the depletion of neutrophils in resistant C57Bl/6 exacerbated parasite load and footpad lesion (Tacchini-Cottier et al., 2000; Ribeiro-Gomes et al., 2004; Chen et al., 2005). The use of neutropenic *Genista* mice that lack mature neutrophils has provided further information about the role of neutrophils in disease progression. Indeed, these mice were able to control parasite load and resolve their lesion after *L. mexicana* infection suggesting that neutrophils impaired the development of effective immune response against this species (Hurrell et al., 2015). The neutrophils can also influence the development of the immune response against *Leishmania* by secreting cytokines and chemokines. These cytokines can influence the subsequent T cell differentiation (Tacchini-Cottier et al., 2000). In addition, the chemokines can attract other innate immune cells to the site of infection where they interact with neutrophils, which can influence the early anti-*Leishmania* response (Ribeiro-Gomes and Sacks, 2012; Hurrell et al., 2016). *Ex vivo* studies have shown that the impact of neutrophils on parasite survival depends on the *Leishmania* species. Indeed, *L. major* can escape killing by neutrophils, which act as "Trojan horses" providing to the parasites a silent entry into macrophages (Van Zandbergen et al., 2004; Ritter et al., 2009). Furthermore, the NETs release induced *in vitro* can trap the parasites but could kill them or not (Guimarães-Costa et al., 2009; Gabriel et al., 2010). Thus, we believe that understanding the interaction between *Leishmania* species and neutrophils could help understanding the mechanisms controlling these parasites. In this context, as a first step we aimed to evaluate whether *Leishmania* strains that belong to *L. infantum* and *L. major* species, responsible for distinct clinical manifestations in the Old World, could influence *ex vivo* functional activity of human neutrophils. The interactions were addressed by the characterization of infection parameters (percentage of infection, index of infection), by measuring the oxidative burst, degranulation, neutrophils extracellular traps (NETs) release and apoptosis. The cytokine production was also measured by a multiplex flow cytometry analysis. Viability of intracellular parasites was also assessed by an MTT assay on rescued amastigotes.

MATERIALS AND METHODS

Ethical Statement

Blood sample collection was done from fourteen informed healthy volunteers that consented by writing to participate to the study. The Ethical committee of the Institut Pasteur de Tunis approved this study (2018/07/I/LR11IPT04).

Parasites

Three laboratory strains were used in this study: *Leishmania (L.) infantum* LV50 (MHOM/TN/94/LV50) was isolated

from a visceral leishmaniasis case, *L. infantum* Drep-14 (MHOM/TN/96/Drep-14) from the lesion of a sporadic cutaneous leishmaniasis patient (CL patient only), and *L. major* Empa-12 (MHOM/TN/2012/Empa-12) from a zoonotic cutaneous leishmaniasis case. Virulence of these parasites was maintained by regular passages through BALB/c mice. Mice were subcutaneously (s.c.) infected with 1×10^6 *L. major* (Empa-12) stationary phase promastigotes. While 1×10^7 *L. infantum* strains Drep-14 or LV50 stationary phase promastigotes were injected intravenously (i.v.) in the lateral tail vein of BALB/c mice. The *L. major* Empa-12 strain was isolated from the infected footpad lesion. While *L. infantum* LV50 and Drep-14 strains were isolated from the mouse inguinal lymph node. Samples taken from the lesion (in the case of *L. major*) or lymph nodes (in the case of *L. infantum*) were cultured at 22 °C in RPMI-1640/ Glutamax medium (Gibco BRL, Germany) containing penicillin (100 U/mL) and streptomycin (100 μg/mL) supplemented with 10 % heat-inactivated Fetal Bovine Serum (FBS) (Gibco BRL, Germany). Cultures were monitored every 3–4 days for the presence of flagellated promastigotes forms by microscope. The growing parasites were cryopreserved to constitute the stocks used in this study. The growth kinetics of each strain was established to determine the stationary growth phase. Promastigotes at this phase were used in the infection experiments.

Polymorphonuclear Neutrophil (PMN) Isolation and Purification

Neutrophils granulocytes from fourteen healthy volunteer donors were isolated based on density gradient centrifugation using Ficoll-Paque density gradients and dextran sedimentation as previously described (Kuhns et al., 2015). Briefly, with no delay between sampling and purification, platelet-rich plasma was removed from EDTA-anticoagulated (BD Vacutainer, BD Bioscience, UK) blood by centrifugation at 500 g for 10 min. The blood cells then were overlayed on Ficoll-Paque (GE Healthcare, Sweden) and the mononuclear cells were aspirated and eliminated after centrifugation at 500 g for 30 min at +4 °C. The red blood cells were separated from the neutrophils by sedimentation for 35 min at room temperature in 6 % dextran (Sigma, Denmark). The neutrophils rich supernatant was collected by centrifugation at 300 g at +4 °C. The remaining red blood cells were removed by a hypotonic lysis Buffer (Sigma, Denmark). Finally, the neutrophils were collected and washed two times with phosphate buffer saline (PBS) and centrifuged at 300 g for 5 min. The viability counts of the PMNs were systematically checked by trypan blue dye exclusion [0.4 % trypan blue solution (Sigma)]; viability was estimated as > 99 %. The purity of granulocytes was > 97 % as determined microscopically by morphological analysis after May-Grunwald-Giemsa staining with RAL 555 Kit (RAL DIAGNOSTICS, France). The **Supplementary Table 1** summarizes the contribution of the donors to the experiments.

Leishmania Infection of PMN

2×10^6 PMN were cultured in 24 wells plates for 18 h at 37 °C and 5 % CO_2 in RPMI-1640/ Glutamax medium containing penicillin (100 U/mL) and streptomycin (100 μg/mL) supplemented with 5 % FBS, in the presence or absence of stationary phase *Leishmania* promastigotes at a ratio of 10 parasites per 1 neutrophil (Multiplicity Of Infection (MOI) 10 or otherwise as indicated). After 18 h of incubation, the cultures were washed to remove extracellular parasites. Cells were then fixed and stained with RAL 555 kit (RAL DIAGNOSTICS, France) following the manufacturer's instructions. The numbers of infected cells and intracellular amastigotes within infected cells were quantified by counting at least 100 cells under optical microscopy. Infection index was calculated as: the percentage of infected cells x mean amastigotes number per cell.

Measurement of Oxidative Burst

Superoxide anion (O_2^-) production was measured using a colorimetric nitroblue tetrazolium (NBT) assay, in which the soluble yellow dye NBT is reduced by intracellular O_2^- generated upon activation of phagocytes forming insoluble blue black formazan crystals. The oxidative burst assay was performed as described previously (Marques et al., 2015). Briefly, the neutrophils and the infected neutrophils, or the positive control neutrophils that were stimulated with 100 nM Phorbol 12-Myristate 13-Acetate (PMA), were incubated in triplicate in 1 mL of RPMI-1640/ Glutamax medium containing penicillin (100 U/mL) and streptomycin (100 μg/mL) supplemented with 5 % FBS containing 0.2 % NBT (Sigma, China), at 37 °C and 5 % CO_2 for 18 h, or at different time points: 1, 2, 3, 4, 5, 6, and 18 h when we performed a kinetic analysis of O_2^- production. Following this incubation, the cells were washed with warm PBS and the NBT deposited inside the PMNs was solubilized with 10 % SDS and 0.1 N HCl. Absorbance of dissolved NBT solution was measured at 570 nm using a microplate reader (MULTISCAN GO, Thermo Scientific, Finland). Results are expressed as the mean values of O_2^- production from 14 donors ± standard deviation (SD).

Degranulation Assays

Myeloperoxidase (MPO) and elastase activity of neutrophils were measured spectrophotometrically in supernatants of PMN and PMN infected with *Leishmania* parasites during 18 h, by adding specific substrates. Neutrophils stimulated with 100 nM PMA were used as a positive control. When we did kinetics of enzymes release, we incubated the cells for 2, 4, 6, and 18 h. The activity of MPO was assessed in the supernatants as described previously (Kumar et al., 2002). Briefly, 100 μL of the substrate cocktail containing *o*-Dianisidine/H_2O_2 was added to 100 μL of culture supernatants. The mixture was kept at room temperature for 10 min and the absorbance of oxidized *o*-Dianisidine was measured at 450 nm. Elastase activity was quantified by addition of 100 μL of 1mM elastase substrate [N-methoxysuccinyl-Ala-Ala-Pro-Val p-nitroanilide (Sigma, USA)] to 100 μL of supernatants (Marques et al., 2015). After 3 h of incubation at 37 °C, absorbance of the cleaved p-nitroanilide was measured at 405 nm in a microplate reader (MULTISCAN GO, Thermo Scientific, Finland). Results are expressed as mean values of MPO and elastase production from 14 donors ± standard deviation (SD).

Quantification of DNA Released in the Culture Medium

Neutrophils were incubated with *Leishmania* promastigotes as described above or with 100 nM PMA as positive control, for 18 h. To quantify the release of DNA (hallmark of NET release) into the culture supernatant, *EcoR1* and *HindIII* (20 U/mL) restriction enzymes (GE Health care, Amersham, Greece) were added to the cultures as described (Guimarães-Costa et al., 2009) to digest any released DNA, and were incubated for additional 4 h at 37 °C. Then, the cells were centrifuged and DNA release was quantified in the culture supernatants, using the Qubit 1x double stranded HS Assay kit (Invitrogen, USA), by Qubit 4 Fluorometer following the manufacturer instructions. Results are expressed as mean values of NETs DNA release from seven donors ± standard deviation (SD). To visualize the DNA, we also did electrophoresis on 0.7 % agarose gels in presence of ethidium bromide (0.5 μg/mL) at 40 V/cm, and observation under UV light.

Measurement of Neutrophils Apoptosis

For the detection of apoptotic or necrotic cell death, the PE-Annexin V / 7-amino-actinomycin D (7-AAD) apoptosis detection kit (BD Biosciences, San Diego, CA) was used according to the manufacturer's protocol. Briefly neutrophils (1×10^6 cells/mL) were incubated in the presence or absence of promastigotes (MOI of 10). After 18 h of incubation, the extracellular parasites were removed as described above. Then, the PMNs were washed with cold PBS and stained with PE-Annexin V / PerCP-cy5.5-(7-AAD). After 15 min of incubation in the dark at room temperature, the cells were re-suspended in 1x binding Buffer and the samples were acquired by flow cytometry (FACS Canto II, BD Biosciences).

Cytometric Bead Array Assay (CBA)

Interleukin-8 (IL-8), interleukin-1β (IL-1β), interleukin-6 (IL-6), interleukin-10 (IL-10), tumor necrosis factor alpha (TNF-α), and interleukin-12p70 (IL-12p70) protein levels were detected and quantified in culture supernatants of neutrophils infected or not by *Leishmania* promastigotes after 18 h of incubation at 37 °C in the presence of 5 % CO_2, by multiplex flow cytometry using the BD Cytometric Bead Array (CBA): Human Inflammation Cytokines kit according to the instructions of the manufacturer (BD Biosciences, San Diego, CA). Briefly, 50 μL of mixed antibody conjugated capture beads were incubated with 50 μL supernatants or cytokine standard dilutions containing a mixture of each recombinant protein, and with 50 μL of phycoerythrin (PE)-conjugated detection antibodies. After 3 h of incubation, the mixture was washed, centrifuged and re-suspended in 300 μL of wash buffer. Finally, fluorescence signals of the beads were acquired by flow cytometry (FACS Canto II, BD Biosciences, San Diego, CA). Results were expressed as the cytokine concentration obtained for each of ten tested donors.

ELISA Quantification of TGF-β

Active form of transforming growth factor beta (TGF-β) levels were quantified, in culture supernatants of non-infected and infected cells collected after 18 h of incubation, by Enzyme-linked immunosorbent assay (ELISA) using Human TGF-β ELISA Sets (BD Biosciences, San Diego, CA) according to manufacturer's instructions. All supernatants were activated by acidification using 1 N HCl and incubated for 60 min at +4 °C. The activated samples were then neutralized with 1 N NaOH as recommended by manufacturer's instructions. The TGF-β concentrations in the supernatants were interpolated from a standard curve using known amounts of the recombinant cytokine. Results were expressed as the mean cytokine concentration of technical replicates, obtained for each of seven tested donors.

Statistical Assessment and Principal Component Analysis

Most graphs were prepared using GraphPad Prism version 7.0 (GraphPad Software). Data were shown as mean values ± standard deviation (SD). The non-parametric Mann–Whitney test was used to assess the differences between two groups. These differences were considered significant when the *p*-value was < 0.05. $^{*}p < 0.05$, $^{**}p < 0.01$, $^{***}p < 0.001$ on the figures indicate statistically significant differences at the indicated *p*-values.

Principal component analysis (PCA) was performed using R3.4 under the RStudio environment. Since PCA can only be performed on complete data, we considered through this analysis data collected from healthy donors, out of the fourteen, for which data was available for all the observations**.** Thus, data collected from ten donors about the infection parameters and the cytokine production under the non-infected (NI) and the infected conditions were formatted into a data frame. This led to 40 individuals (10 donors in 4 conditions) for which 11 variables were observed (infection index, percentage of infection, Oxidative burst, Elastase, MPO, IL-12p70, IL-8, IL-6, IL-10, IL1-β, and TNF-α). The observations "TGF-β" and "NETs" were discarded in the analysis as it only concerned seven donors and no missing data could be considered for PCA. An additional observation, called "species," was used as a supplementary qualitative variable to generate the groups of individuals according to the infection condition (NI, Drep-14, LV50, and Empa-12). The package *FactoMineR* was used for PCA calculation and the package *factoextra* was used to generate the corresponding figures.

Measure of Neutrophils Leishmanicidal Activity Against Intracellular *L. infantum* and *L. major*

To evaluate the impact of neutrophils activity on intracellular *Leishmania* survival, promastigotes of each strain were incubated with an excess of neutrophils at a ratio of 1 parasite per 10 neutrophils to allow efficient parasite internalization as described previously (Carlsen et al., 2015a). Briefly, 2×10^6 neutrophils isolated from three donors were infected with 0.2×10^6 promastigotes (MOI of 0.1) in technical replicates in 24 well-plates. After 18 h of infection, the cultures were washed to remove the extracellular parasites. Cells were then fixed and stained with RAL 555 kit, and the infected cells and the intracellular amastigotes per infected cells were quantified by counting at least 100 cells under optical microscope. The remaining cells were lysed by SDS (0.01 %), and the pellets were

washed with PBS and resuspended in 100 μL Schneider medium supplemented with 10 % FBS and cultured at 22 °C in 96 well-plates. Parasites viability was assessed right after the lysis of the cells and 24 h later, by a Methylthiazolyldiphenyl-tetrazolium bromide (MTT) assay as described previously (Harigua-Souiai et al., 2018). Briefly, 20 μL of MTT (5 mg/mL) were added to each well and incubated at 22 °C. After 4 h of incubation, the MTT is reduced to formazan crystals by the mitochondrial dehydrogenases of the live parasites, and 150 μL of DMSO was added to dissolve the formazan crystals. Absorbance was measured at 570 nm using a microplate reader (MULTISCAN GO, Thermo Scientific, Finland). A range of serial dilutions of counted promastigotes (1:2) were performed and submitted to MTT assays. The resulting linear equation was used to interpolate the number of parasites recovered from the infected PMNs, having an active metabolism and thus which are viable. Results are expressed as mean number of viable parasites ± standard deviation (SD).

RESULTS

Human Neutrophils Similarly Uptake *Leishmania* Promastigotes From Different Strains

To investigate the interaction between neutrophils and *Leishmania* promastigotes, 2×10^6 PMN were infected with stationary phase *Leishmania* promastigotes at various MOI (3, 5, 10, and 15) and incubation times (2, 4, 6, 18, and 24 h). The cultures were washed to discard un-internalized parasites. PMN were then fixed and stained with May Grunwald Giemsa and assessed for the percentage of infected cells and parasite burden. The optimum number of infected PMN and intracellular parasites were obtained with 10:1 ratio and after 18 h of incubation (**Supplementary Figure 1A**). Thus, the experimental conditions at MOI of 10 and 18 h of incubation were chosen for the rest of our study. Neutrophils isolated from 14 healthy donors were infected *ex vivo* with Drep-14, LV50 and Empa-12 strains and infection parameters were determined. Their comparison showed that the neutrophils were similarly infected (**Figure 1**), according to all parameters tested: the percentage of infection (**Figure 1A**), the infection index (**Figure 1B**) and the parasite load (**Figure 1C**). Intracellular parasites had an amastigote-like morphology and were therefore designated as amastigotes (**Supplementary Figure 1B**). The percentage of infected neutrophils was in average 56 % [50–68] with Drep-14, 64.2 % [55–72] with LV50, and 60 % [54–67] with Empa-12. The infection index was in average of 115 [88–177] with Drep-14, 146 [129–183] with LV50, and 127 [114–142] with Empa-12. The number of amastigotes within infected cell (**Figure 1C**) showed that of the infected cells nearly 66 % [63–69] carried only one to two parasites, while approximately 34 % [30–36] of them had multiple parasites (3 to 6 parasites). The mean amastigote number per cell was also similar for each strain, in the range of [2.05–2.27]. Therefore, the mean percentage of infected neutrophils and infection index were similar in neutrophils infected with each strain ($p > 0.05$). Taken together these results demonstrated that in these experimental conditions there were no differences in the ability of the three tested strains to infect human neutrophils.

Leishmania Promastigotes Upregulate Neutrophil Oxidative Burst

Reactive oxygen species (ROS) are a critical component of the microbicidal activity of neutrophils (Robinson, 2008; Winterbourn et al., 2016). We investigated the effects of infection with the different *Leishmania* strains on superoxide anion (O_2^-) generation in human neutrophils. We incubated infected and non-infected cells isolated from 14 healthy donors with NBT as described above. As shown in **Figure 2**, a significant increase in O_2^- production was observed following infection with the three *Leishmania* strains or exposure to PMA as compared with PMN alone, whereas no differences could be observed in superoxide anion production by neutrophils infected with the

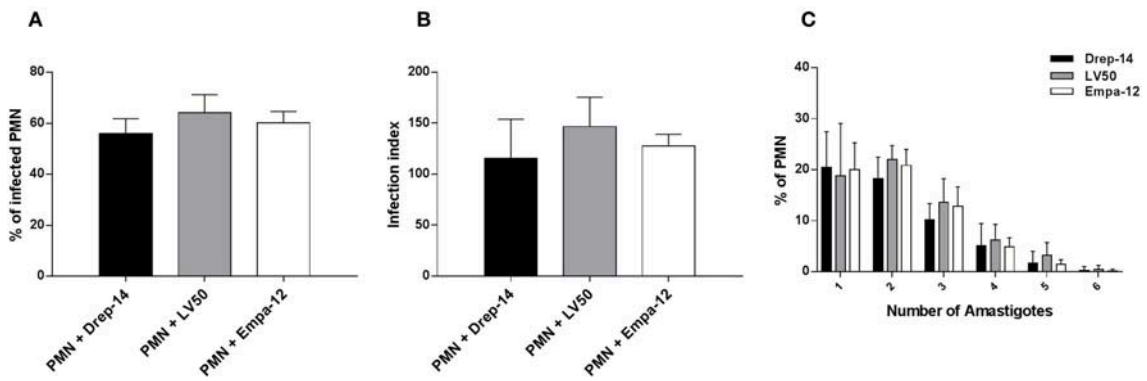

FIGURE 1 | *Leishmania* infection of PMNs. Human neutrophils were infected with *Leishmania* promastigotes (MOI of 10) for 18 h. Then, extracellular parasites were removed and the cells were fixed and stained with May-Grünwald Giemsa kit. **(A)** The percentage of infected PMN, **(B)** the infection index and **(C)** the percentage of cells carrying the designated number of amastigotes were quantified using optical microscopy, by counting at least 100 neutrophils. Data are shown as the mean values from fourteen donors ± standard deviation (SD). Statistical comparisons were performed using the non-parametric Mann-Whitney test.

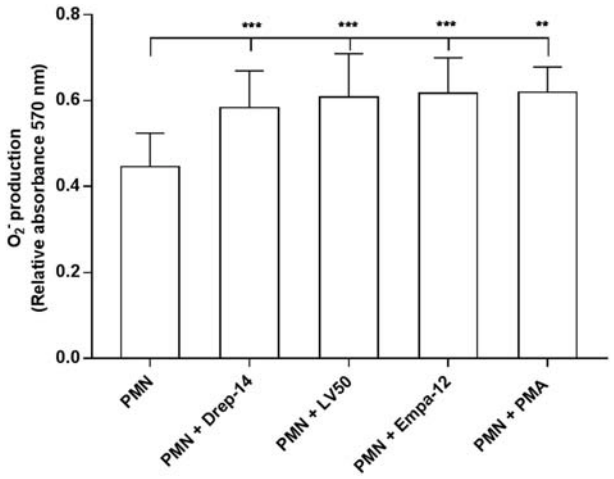

FIGURE 2 | Measures of oxidative burst in *Leishmania* infected neutrophils. PMNs, PMNs exposed to *Leishmania* promastigotes, and PMNs stimulated with 100 nM PMA were incubated in triplicate in 96 well-plates in 100 μL of RPMI-1640/ Glutamax medium plus penicillin (100 U/mL) and streptomycin (100 μg/mL) supplemented with 5 % FBS containing 0.2 % NBT solution to quantify intracellular O_2^- production. After 18 h of incubation at 37 °C, in presence of 5 % CO_2, blue formazan particles were generated after NBT reduction in activated neutrophils. Intracellular formazan deposits were then solubilized by adding 100 μL of 10 % SDS / 0.1 N HCl, and the absorbance of the solution was measured at 570 nm. Data are shown as the mean values of O_2^- production from fourteen donors ± SD. Mann-Whitney test was used to compare the absorbance of *Leishmania* infected PMNs to control PMN cultures, and of the infected PMNs in a pair-wise manner; $^{**}p < 0.01$ and $^{***}p < 0.001$ indicate statistically significant differences at the indicated *p*-values.

Drep-14, LV50 or Empa-12 strains ($p > 0.05$). These results suggested that the three *Leishmania* strains induced in the same manner O_2^- production from human neutrophils. To confirm that at 18 h after infection the O_2^- production did not reach a plateau, a kinetics of O_2^- production (1, 2, 3, 4, 5, 6, and 18 h) was performed for three of the 14 donors. As shown in the **Supplementary Figure 2**, the tested parasites were able to similarly induce significant O_2^- production at all times tested.

Leishmania Promastigotes Trigger Neutrophils Degranulation

Degranulation of vesicles into the phagolysosome or in the extracellular space is a key event for microbicidal activity. Contents release of neutrophil granules contributes to the elimination of pathogens (Kumar and Sharma, 2010). To evaluate degranulation, we examined the release of MPO and Neutrophil elastase, which are both azurophilic granule contents, by neutrophils isolated from the 14 healthy donors in the culture medium upon their infection by the different *Leishmania* strains. Enzymatic activities were measured spectrophotometrically in supernatants of non-infected and promastigote-infected PMN through addition of the appropriate substrates (**Figure 3**). The MPO (**Figure 3A**) and elastase activities (**Figure 3B**) were 2.4 and 2 fold higher, respectively, in the supernatants from *Leishmania*- infected neutrophils as compared to the non-infected neutrophils. We also found greater levels of MPO and elastase activity in supernatants from PMA stimulated cells in comparison to untreated neutrophils. Therefore, infection with each of the three strains triggered in the same manner the extracellular release of myeloperoxidase and elastase by human neutrophils. Furthermore, to assess the absence of significant differences in MPO and elastase production between strains within the first hours of infection, a kinetics of released MPO and elastase activities (2, 4, 6, and 18 h) was performed in case of three of the 14 donors. As shown in the **Supplementary Figure 3**, the three strains significantly, and similarly, increased MPO and elastase release at all-times tested. In conclusion, our data showed that all the tested strains induced in the same way the degranulation of human neutrophils.

Leishmania Promastigotes Induce DNA Release

NETs were described as a host defense mechanism of the innate immune response. NETs involve the release of DNA into the extracellular environment associated with nuclear and granular proteins (Brinkmann et al., 2004; Guimarães-Costa et al., 2009). To determine whether *Leishmania* strains trigger the extracellular release of DNA, neutrophils purified from seven healthy donors were infected or not with parasites for 18 h. Upon this time, extracellular DNA was digested with two restriction enzymes and the DNA released in the supernatants were quantified by fluorometry on a Qubit.

The results showed that all parasite strains significantly induced DNA (and thus likely NETs) release, in higher amounts than non-infected neutrophils and PMA-stimulated neutrophils ($p < 0.01$) (**Figure 4**). Moreover, the two *L. infantum* strains induced more DNA release from infected neutrophils than the *L. major* strain ($p < 0.05$). Furthermore, to prove the presence of DNA in the supernatants, we did electrophoresis on agarose gels. As shown on **Supplementary Figure 4**, the supernatants showed the presence of DNA smears ranging from high molecular weight DNA (> 10 Kb) to lower DNA sizes as observed in other studies (Sousa-Rocha et al., 2015; Stephan et al., 2016).

Leishmania Promastigotes Infection Increases Neutrophils Apoptosis Rates

Neutrophils have a very short life span and they rapidly die via apoptosis. Apoptotic cells express phosphatidylserine (PS), which could be detected by PE Annexin V. To evaluate the effect of *Leishmania* strains on neutrophils apoptosis, neutrophils purified from three healthy donors (among the 14 selected) were infected or not with parasites for 18 h. Then, cells were double stained with Annexin V and the vital dye (7-ADD) to differentiate between viable (PE-Annexin V^-/ 7-ADD^-), necrotic (PE-Annexin V^-/ 7-ADD^+), early apoptotic (PE-Annexin V^+/ 7-ADD^-) and late apoptotic and/or already dead PMN (PE-Annexin V^+/ 7-ADD^+). The results showed a significant increase in the percentage of apoptotic cells (PE-Annexin V^+) following exposure to *Leishmania* strains as compared to PMN alone (**Figure 5**). Neutrophils viability was significantly decreased in

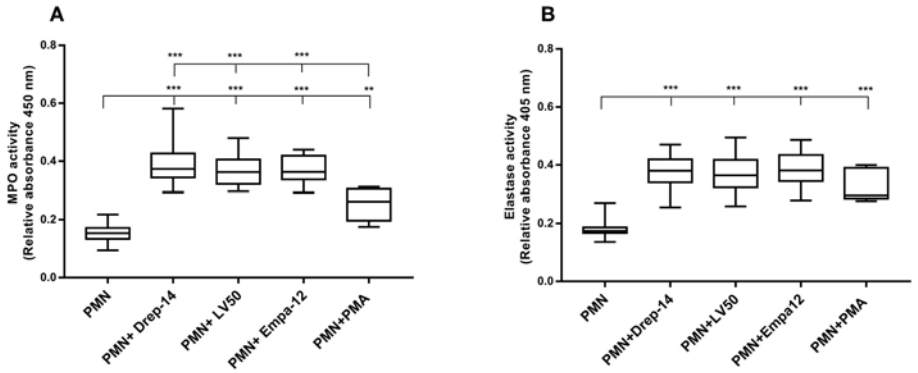

FIGURE 3 | *Leishmania* promastigotes stimulate the degranulation of human PMNs. PMN cultures were infected with stationary phase promastigotes of *Leishmania* strains or incubated with PMA (0 nM & 100 nM, as negative and positive control, respectively) for 18 h, at 37 °C in presence of 5 % CO_2. Then, supernatants were collected and tested for the presence of enzymes released in the culture medium. **(A)** The enzymatic activity of MPO was quantified by an enzyme-substrate reaction using *o*-Dianisidine and hydrogen peroxide. The absorbance of oxidized *o*-Dianisidine was measured at 450 nm after 10 min of substrate incubation at room temperature. **(B)** The enzymatic activity of neutrophil elastase was determined from the same culture supernatants using a specific synthetic peptide substrate of elastase that is cleaved to colorimetric p-nitroanilide (pNA). The release of pNA was measured at 405 nm after 3 h of incubation at 37 °C. Data are shown as the mean values from fourteen donors ± SD. Mann-Whitney test was used to compare the absorbance of (PMN) vs. each (PMN-*Leishmania* strain) or (PMN-PMA) supernatants, and of the infected PMNs in a pair-wise manner; $^{**}p < 0.01$ and $^{***}p < 0.001$ indicate statistically significant differences at the indicated *p*-values.

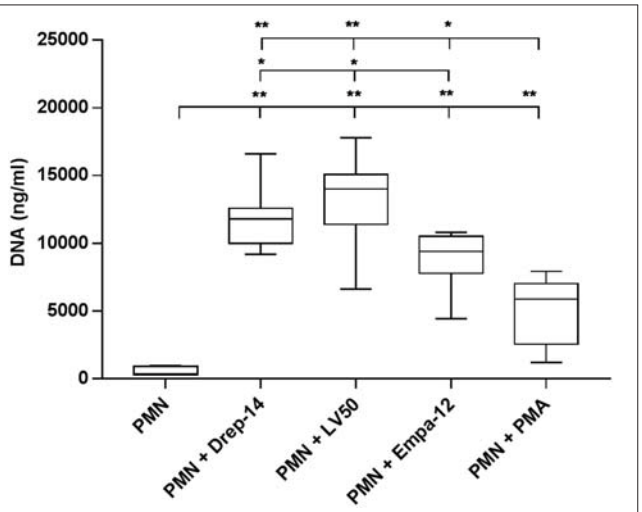

FIGURE 4 | *Leishmania* promastigotes induce DNA release. Neutrophils (2×10^5) were infected with *Leishmania* strains at a 10:1 ratio or with 100 nM PMA as a positive control (0 nM PMA was the negative control) for 18 h at 37 °C in presence of 5 % CO_2. Then, *EcoR1* and *HindIII* (20 U/mL) were added to the medium to digest the DNA trapped in the released NETs. After 4 h of incubation at 37 °C, the cells were centrifuged and released DNA was quantified in the culture supernatant by DNA quantification using a dsDNA High Sensibility Assay Kit on a Qubit. Data are shown as mean values from seven donors ± SD. Pair wise comparisons of PMN vs. each strain-infected PMNs or vs. PMN-PMA, and of infected PMNs between each other were performed using the Mann–Whitney test; $^{*}p < 0.05$ and $^{**}p < 0.01$ indicate statistically significant differences at the indicated *p*-values.

the presence of all tested *Leishmania* strains, whereas we detected low percentages of both necrotic and late apoptotic PMN that were not affected upon *Leishmania* infection (**Figure 5A**). No statistically significant differences could be observed in apoptosis of neutrophils infected with Drep-14, LV50, or Empa-12 strains (**Figure 5B**). In conclusion, our data showed that the three *L. infantum* and *L. major* strains tested in our study were able to similarly increase the apoptosis of the tested human neutrophils.

Leishmania Strains Differently Induce Cytokines Release From Neutrophils

As neutrophils are the first cells to arrive at the sites of infection, they may influence the development of the anti-*Leishmania* immune response by producing cytokines and chemokines, which in turn can influence the outcome of disease (Ribeiro-Gomes and Sacks, 2012; Hurrell et al., 2016). In order to evaluate the immune response triggered by the three *Leishmania* strains through the release of cytokines, neutrophils purified from ten healthy donors were incubated in the presence (MOI 10) or absence of each *Leishmania* strain. Supernatants were then collected 18 h after infection, and a cytokine multiplex analysis of culture supernatants was performed by flow cytometry (**Figure 6**). As shown in **Figure 6A**, infected neutrophils with each *Leishmania* strain produced approximately 150 fold higher IL-8 amounts than the non-infected neutrophils (**Figure 6A**). Additionally, IL-1β and (active form) TGF-β production by neutrophils were significantly induced by all strains (**Figures 6C,G**). Interestingly, we observed that only Drep-14 strain promoted IL-6 release (**Figure 6B**) by the neutrophils. The production of TNF-α was also significantly induced by all parasite strains (**Figure 6D**), whereas Drep-14 induced the highest TNF-α amounts as compared to LV50 and Empa-12. The IL-10 and IL-12p70 cytokines (**Figures 6E,F**) were neither produced in the supernatant of the non-infected nor of the infected neutrophils. All these results demonstrated that the three *Leishmania* strains have differently affected the pattern of cytokines production by the human neutrophils.

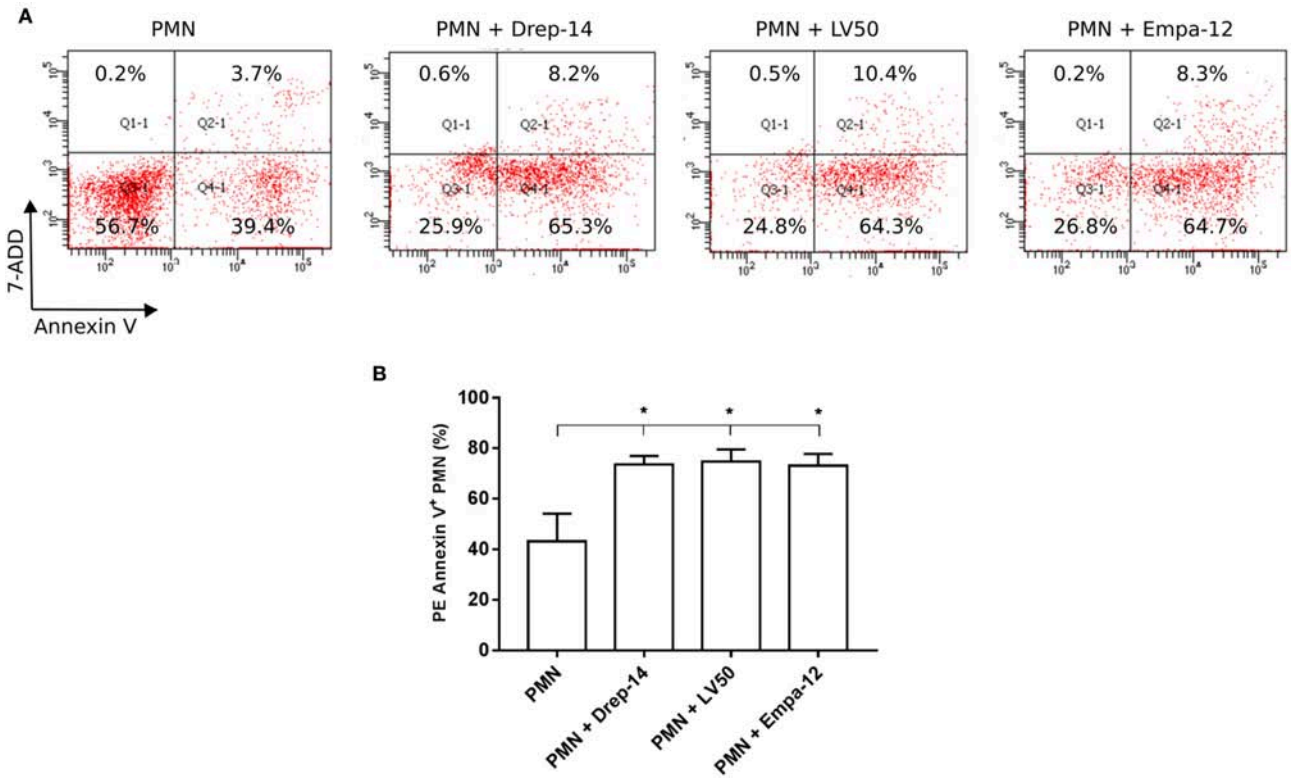

FIGURE 5 | Increased neutrophils apoptosis upon *Leishmania* promastigotes infection. Neutrophils isolated from three donors were infected or not with *Leishmania* parasites (MOI of 10). After 18 h of infection, the cells were labeled with PE Annexin V / 7-ADD and analyzed by FACS. **(A)** Representative dot plots of non-infected PMN and PMN infected with Drep-14 (PMN+Drep-14), with LV50 (PMN+LV50) or with Empa-12 (PMN+Empa-12) were labeled with Annexin V vs. 7-ADD. The plots illustrate the results obtained for one of three donors tested. **(B)** Percentage of PMN Annexin V^+ of non- infected and infected PMN of three donors. Data are shown as mean percentage of apoptotic PMN ± SD. Pair- wise comparisons of the non-infected PMN vs. each strain- infected PMN were performed using the Mann–Whitney test; $^*p < 0.05$ indicates statistically significant differences.

Principal Component Analysis Reveals Strain-Dependent Cytokine Production Profiles

In order to compare the effect of each donor immune response to the effect of the *Leishmania* strain on the cytokine production profiles by human neutrophils, we generated 3D histograms of the data (**Supplementary Figure 5**). The histograms suggested no donor-specific variability in cytokines production from one side and a possible strain-specific variability from the other. To statistically confirm such observations, we performed a principal component analysis (PCA) using data from ten individuals (donors) for which 11 observations could be collected under four conditions (non-infected (NI), infected with Drep-14, LV50, or Empa-12 strains). This analysis consisted in an orthogonal linear transformation of the data that led to its projection in a new coordinates system, composed of linearly uncorrelated variables called the principal components (PCs). The objective was to observe a maximum of variance of the data on the first PCs, and thus to be able to reduce the dimension of the data while observing the possible variations among the individuals. Herein, the PCA resulted in 69.6 % of the total variation on the first two principal components (PC1: 51 % and PC2: 18.6 %), which indicated reliability of the analysis. The projection of the individuals on the 2D plot composed by PC1 and PC2, presented a clear separation of the non-infected vs. *Leishmania*-infected individuals (**Figure 7A**). Observations on all individuals infected by each strain were presented in different colors. The centroids of each strain group and the geometry of the projections suggested that no significant difference could be observed between the LV50 and the Empa-12-infected individuals. Both groups were centered and mostly aggregated in the same plane quarter with a slight diffusion along PC2. Whereas, the Drep14-infected individuals presented a more diffuse geometry along PC1 and PC2, simultaneously. Noticeably, PC1 mostly segregated the non-infected vs. infected populations (**Figure 7B**) and PC2 distinguished the infection parameters (infection index, percentage of infection, oxidative burst, Elastase, and MPO) vs. the cytokines IL-6, IL-10, IL1-β, and TNF-α production. This suggested that all three strains induced the infection in an equivalent manner, whilst Drep-14 induced different cytokine production profiles as compared to LV50 and Empa-12. IL-8 production presented the least variation between the strains. IL-12p70 production appeared as non-correlated to the infection conditions. Thus, this statistical analysis of all

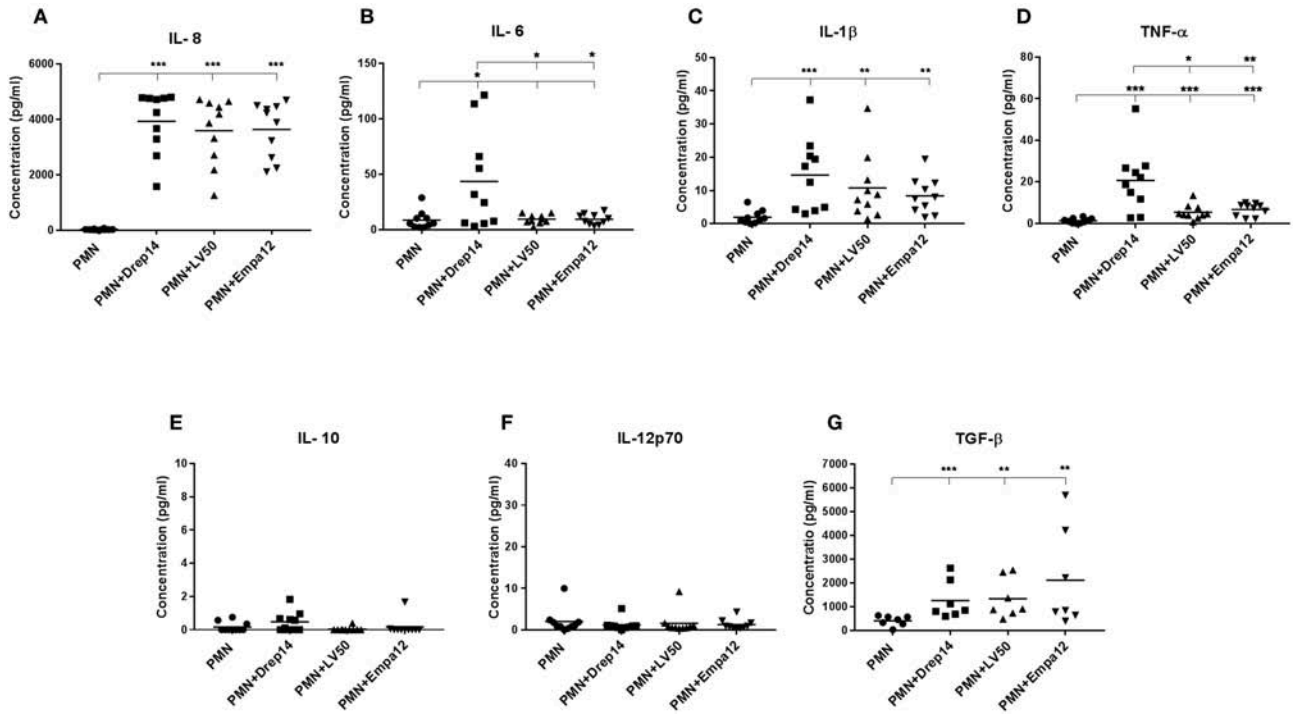

FIGURE 6 | Effect of *Leishmania* strains on cytokines production after *ex vivo* infection of human PMNs**.** Neutrophils were infected or not by *Leishmania* parasites (MOI of 10). Then, supernatants were collected after 18 h of incubation. The amounts of **(A)** IL-8, **(B)** IL-6, **(C)** IL-1β, **(D)** TNF-α, **(E)** IL-10, and **(F)** IL-12p70 protein were quantified from (50 μL) culture supernatants using the BD Cytometric Bead Array (CBA) Human Inflammation Cytokines kit. The amount of **(G)** TGF-β was quantified from the supernatants (100 μL) by Enzyme-linked immunosorbent assay (ELISA). Results were expressed as the cytokine concentration obtained from seven (TGF-β) or ten sampled donors. The horizontal bars indicate the median value of cytokine production. Statistical pair- wise comparisons of PMN vs. each strain-infected PMN, and of strain- infected PMNs were performed using the Mann–Whitney test; $^{*}p < 0.05$, $^{**}p < 0.01$, and $^{***}p < 0.001$ indicate statistically significant differences at the indicated *p*-values.

the results together reveals a strain (and species) dependent cytokine production.

Leishmania Strain Dependent Survival Within Infected Neutrophils

Our previous results indicated that the neutrophils differently responded to the strains tested. So we assessed whether the neutrophils differently impair intracellular parasite survival using a model of infection where most parasites would be internalized, thus leaving very few extracellular ones (Carlsen et al., 2015a). To this end, 2×10^6 neutrophils purified from three donors were infected with 0.2×10^6 parasites (MOI of 0.1) for 18 h and the number of internalized parasites was quantified using optical microscopy. The percentage of infected cells was similar for the 3 strains ≈8 % (**Figure 8A**). The number of intracellular parasites was estimated to be 0.18×10^6 for the strains Drep-14 and Empa-12, and 0.19×10^6 for LV50 (**Figure 8B**). These values are considered as equivalent. Thus, all strains had a similar infectivity index in average 28.5 [28–29]. Internalized parasites were then recovered from the infected PMN after cellular lysis, and their viability was assessed right after the lysis and after 24 h of incubation at 22 °C, using an MTT assay. The interpolated number of viable parasites was compared to the intracellular amastigotes counts by microscope and the percentage of viability was determined at the 2 time points (**Figure 8C**). Whereas, 87.8 and 82 % of LV50 parasites were viable at lysis and 24 h later, respectively, the estimates were significantly reduced in case of the other two strains, Drep-14 (43.6 % vs. 30.4 %) and Empa-12 (48.2 and 48.3 %). The difference in survival of the Drep-14 and EMPA-12 strains *vs.* LV50 was considered to be significant at the two time points tested.

Therefore, while all strains presented the same infectivity, the results clearly indicated that their intracellular survival was different. Noticeably, both dermotropic strains that belong to two different species: *L. infantum* and *L. major* showed poorer survival rates as compared to the viscerotropic LV50 strain (*L. infantum*).

In conclusion, our results suggest that intracellular leishmanicidal ability of the tested human neutrophils will depend on the *Leishmania* strains, even for the same species.

DISCUSSION

Our objectives were to assess effect of strains of the *L. infantum* and *L. major* species that cause different clinical manifestations (VL or CL) on *ex vivo* human neutrophils. To this end, we

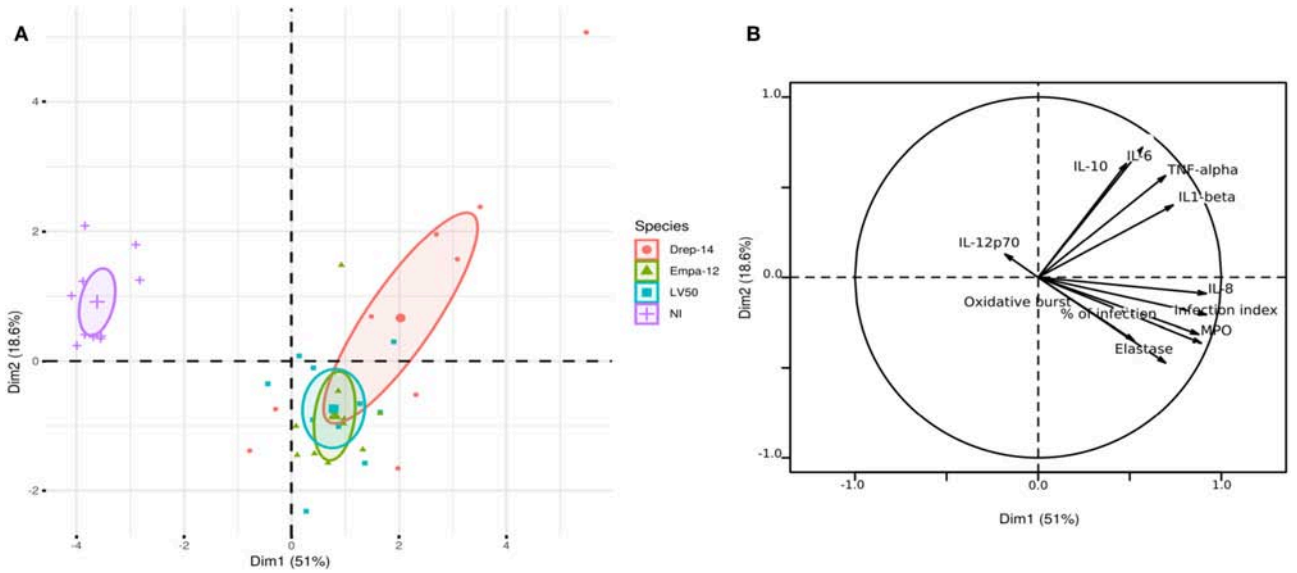

FIGURE 7 | Principal component analysis results. The PCA was performed using data from ten donors for eleven observations (infection index, percentage of infection, Oxidative burst, Elastase, MPO, IL-12p70, IL-8, IL-6, IL-10, IL1-β, and TNF-α) under four conditions (NI= Non-Infected, and three infected conditions with the Drep-14, LV50 or Empa-12 strains). **(A)** The individuals' map shows the distribution of the population projected on the 2D plane composed of the first two principal components PC1 and PC2 (Dim1 and Dim2, respectively). **(B)** The variable factors map shows the projection on the first two principal components (PC1 and PC2) of the different observations.

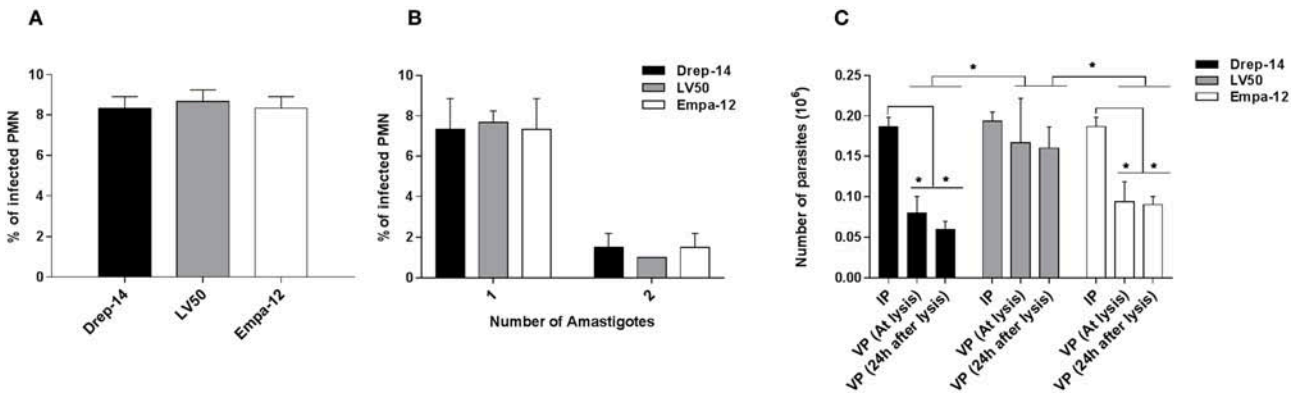

FIGURE 8 | Intracellular *Leishmania* survival in *ex vivo* infected neutrophils. Neutrophils isolated from three donors were infected or not by *Leishmania* parasites (MOI of 0.1) for 18 h. Then, the extracellular parasites were removed and cells were fixed and stained with May-Grünwald Giemsa kit to determine, under optical microscope, the percentage of infected PMN **(A)** and the percentage of cells carrying the designated number of amastigotes **(B)** by counting at least 100 neutrophils. The PMN cultures were lysed at 18 h, by 0.01 % SDS, washed with PBS and resuspended in 100 μL Schneider medium supplemented with 10 % FBS and cultured at 22 °C. **(C)** Parasites viability was assessed right after the lysis of the cells and 24 h later by an MTT assay. Data are shown as mean values of number ± SD. We performed the non-parametric Mann–Whitney test to compare infection parameters **(A,B)**, and in **(C)**: (i) for each strain, the number of Internalized Parasites (IP) within the infected cells vs. the number of Viable Parasites (VP) after lysis at each time point, and (ii) between strains, in a pair- wise manner, the number of surviving parasites at each time point; $^*p < 0.05$ indicates statistically significant differences.

have used neutrophils purified from healthy human donors and established conditions that allowed optimal infection of the cells by using stationary phase promastigotes. We reached 65 % infection upon 18 h incubation at an MOI 10. With a higher MOI we observed an extensive cell lysis and so we retained the MOI 10 condition. Previous studies provided evidence that either human or murine neutrophils internalize promastigotes of a range of *Leishmania* species including *L. major* (Laufs et al., 2002; Van Zandbergen et al., 2004; Peters et al., 2008; Mollinedo et al., 2010; Ricci-Azevedo et al., 2016; Ronet et al., 2018) and *L. infantum* (Rousseau et al., 2001; Thalhofer et al., 2011; Marques et al., 2015; Quintela-Carvalho et al., 2017; Sacramento et al., 2017; Valério-Bolas et al., 2019). Species of the *Viannia* subgenus internalized more parasites than those of the *Leishmania*

subgenus (*L. infantum*; *L. amazonensis*) (Valério-Bolas et al., 2019). Here we confirmed infection of human neutrophils by *in vitro* promastigote forms of strains of the *L. major* or *L. infantum* species. The intracellular parasites had an amastigote-like morphology and were therefore designated as amastigotes. This indicated that in our experiments the parasites underwent morphological transformation within the neutrophils. Previous studies also observed "amastigotes or amastigote- like forms" within promastigote- infected neutrophils as soon as after 3 h incubation (Marques et al., 2015; Quintela-Carvalho et al., 2017; Valério-Bolas et al., 2019). In addition, we did not observe any significant differences between the strains in the different infection parameters measured at two different MOIs (10 and 0.1). Interestingly, with the MOI 10 experiments, 34 % of the infected cells were found to contain 3 to 6 amastigotes. This may be correlated with the fact that more than 2 parasites were uptaken at this higher MOI. Amastigotes were also seen to replicate within neutrophils (Hurrell et al., 2017) but we cannot ascertain it was the case here.

Neutrophils, as key component of the innate immune system, play a pivotal role in first line defense against invading pathogens through phagocytosis, the release of granule contents (Segal, 2005; Nauseef, 2007) and the production of NETs (Brinkmann et al., 2004; Guimarães-Costa et al., 2009). Upon phagocytosis, neutrophils NADPH oxidase is activated and produces the superoxide anion (O_2^-) (Pham, 2006) leading to the production of antimicrobial molecules such as ROS, which contribute to the killing of intracellular parasites such as *L. donovani* and *L. major* (Pearson and Steigbigel, 1981; Laufs et al., 2002). Neutrophils from VL patients displayed impaired effector functions but they were able to phagocyte *L. donovani* similarly to neutrophils from healthy controls, which suggested a role in the survival and dissemination of *L. donovani* (Yizengaw et al., 2016). In contrast, other studies documented differences in the induction of oxidative burst response depending on *Leishmania* species. It was significantly higher in *L. braziliensis*-infected murine neutrophils than in those infected by *L. amazonensis* (Carlsen et al., 2015a). Herein, we report that the tested *L. infantum* and *L. major* strains similarly induced high oxidative burst in the infected human neutrophils at different time points.

Release of azurophilic granules that contain antimicrobial proteins such as NE and MPO, into the phagolysosome or the extracellular space of infected neutrophils, plays a crucial role in pathogens elimination (Segal, 2005; Nauseef, 2007). Degranulation was observed in human, murine and in canine neutrophils infected by different *Leishmania* species: *L. braziliensis* (Carlsen et al., 2015a; Falcão et al., 2015), *L. amazonensis* (Tavares et al., 2014; Carlsen et al., 2015a), *L. infantum* (Marques et al., 2015; Pereira et al., 2017). Here, we have observed that the tested *L. infantum* and *L. major* strains induced the neutrophils degranulation with similar NE and MPO production.

The release of NETs, also known as NETosis, in response to different *Leishmania* species has been described in human or murine neutrophils. These extracellular structures made of fiber-, web- and tube- like elements emitted by activated neutrophils are rich in histones (toxic proteins to pathogens), DNA, and granular and cytosolic proteins such as NE or MPO, and are able to entrap the parasites (Guimarães-Costa et al., 2009; Valério-Bolas et al., 2019). In case of *L. infantum*, it appeared that tube-like structures could allow coiling phagocytosis of promastigotes by murine neutrophils (Valério-Bolas et al., 2019), an unconventional phagocytosis mechanism also used by macrophages to internalize the parasites (Hsiao et al., 2011). *L. amazonensis* induced the formation of NETs by a mechanism involving surface lipophosphoglycan (LPG) and was killed by them (Guimarães-Costa et al., 2009). *L. donovani* and *L. infantum* were also shown to induce NETs release but they escaped NETs killing owing to their LPG (Gabriel et al., 2010) or their 3'-nucleotidase/nuclease activity (Guimarães-Costa et al., 2014), respectively. Furthermore, *L. mexicana* induced the formation of NETs but was also not killed by them through a not reported mechanism (Hurrell et al., 2015). We here report that the 3 *L. infantum* and *L. major* strains induced the release of DNA in the extracellular medium by human neutrophils, suggesting the presence of NETs. *L. infantum* released more DNA amounts than *L. major* suggesting that the intensity of this release may be species-specific. A difference between the DNA amounts released by the two *L. infantum* strains was also noticed although not considered significant. In line with this observation, it was recently shown that murine neutrophils exposed to *L. amazonensis* emitted fewer NETs than those exposed to *L. shawi* or *L. guyanensis* (Valério-Bolas et al., 2019). *L. infantum* also induced more NETs release than *L. major* in human neutrophils (Guimarães-Costa et al., 2009).

Different studies reported that *L. major*, *L. donovani* and *L. infantum* can delay human, murine or canine neutrophils apoptosis and prolong the cell's life span to ensure an intracellular environment favorable to parasites survival, and their silent entry in macrophages (Aga et al., 2002; Gueirard et al., 2008; Sarkar et al., 2013; Marques et al., 2015; Pereira et al., 2017). In contrast, *L. amazonensis* and *L. braziliensis* induced murine neutrophils apoptosis and accelerated their death (Carlsen et al., 2013; Falcão et al., 2015). In the present study the tested *L. infantum* and *L. major* strains increased apoptosis in the donors tested. This difference between our results and those reported in previous studies for these species could be due to the difference between strains, the genetic background of the donors and/or the experimental conditions (MOI, infection time, etc). Further studies are necessary to further investigate apoptosis induced by these species and cellular mechanisms involved in death. Notably *L. infantum* infected neutrophils were shown to undergo necroptosis in presence of specific caspase 8 inhibitor (and so when apoptosis was inhibited) (Barbosa et al., 2018).

In addition to the classical functions of phagocytosis and killing of invading pathogens, neutrophils can modulate the immune responses against *Leishmania* infection by secreting chemokines that attract macrophages and dendritic cells to the site of infection (Ribeiro-Gomes and Sacks, 2012; Hurrell et al., 2016), and also cytokines that influence T cells differentiation (Tacchini-Cottier et al., 2000). Indeed, the early wave of neutrophils in *L. major*-infected BALB/c was shown to express IL-4, and to induce the development of a Th2 response and the partial control of the disease (Tacchini-Cottier et al., 2000) or its

exacerbation (Chen et al., 2005). Furthermore, the interactions between neutrophils and macrophages or dendritic cells were shown to influence the outcome of *L. major* infection in animal models (Ribeiro-Gomes et al., 2004, 2012). To our knowledge, the present study is the first addressing the determination of cytokines produced by human neutrophils exposed to different *Leishmania* species using cytometry bead assays (CBA). The choice of this method rather than more classical ones: ELISA or real time PCR (RT-PCR), relied on the limited sample volume needed for the CBA assays, their high sensitivity, the time gain and the diminution of inter assay variations (Faresjö, 2014).

IL-8 enhances the early recruitment of neutrophils to the site of infection (Müller et al., 2001) and activates their functions, such as the phagocytosis (Scapini et al., 2000). IL-8 produced by neutrophils seems to have a limited role in human leishmaniasis as neutrophils from either asymptomatic or non-healing individuals produced high and similar levels of IL-8 after exposure to *L. major* (Safaiyan et al., 2011). Here, we report that human neutrophils exposed to *L. infantum* or *L. major* also produced high amount of IL-8 as in previously reported studies (Laufs et al., 2002; Van Zandbergen et al., 2002; Safaiyan et al., 2011; Keyhani et al., 2014).

TNF-α produced by neutrophils plays an important role for leucocytes migration and for DC and macrophages activation and differentiation (Nathan, 2006). Furthermore, it can induce the neutrophils degranulation at the site of infection, thus it influences the development of an efficient immune response against the parasite (Nathan, 2006). Our results showed that all *Leishmania* strains tested induced the production of TNF-α by the neutrophils of the healthy donors of this study as previously described in case of *L. major* exposed human neutrophils (Safaiyan et al., 2011), or *L. braziliensis*- exposed murine neutrophils (Falcão et al., 2015). Notably, TNF-α release was significantly higher from Drep-14- infected neutrophils than from LV50 and Empa-12- infected ones.

IL-12 and IL-10, which are important immune modulatory cytokines known to favor Th1 or Th2 type responses, respectively, were not induced by the strains tested as reported in previous studies using human and murine neutrophils (Van Zandbergen et al., 2006; Falcão et al., 2015). In contrast, neutrophils from *L. major* infected C57BL6 mice were able to induce the secretion of IL-12p70 and IL-10 (Charmoy et al., 2007). This discrepancy could be due to the host origin of the neutrophils. In line with this hypothesis, in the same study, *L. major*-infected BALB/c neutrophils were unable to induce the secretion of IL-12p70 and IL-10 (Charmoy et al., 2007).

The production of anti-inflammatory TGF-β was associated to the development of non-protective response against *L. major* infection (Van Zandbergen et al., 2006). Furthermore, it was shown that TGF-β favors the uptake of apoptotic cells by macrophages (Fadok et al., 1998). Our observation that human neutrophils produced high amounts of TGF-β after exposure to *L. infantum* or *L. major* strains is consistent with previous studies that highlighted the prominent role of neutrophils in the creation of a microenvironment favorable for parasite survival and the exacerbation of the disease (Safaiyan et al., 2011; Hurrell et al., 2015). In contrast to our results and other studies, Keyhani et al. reported that *L. major* failed to induce expression of TGF-β mRNA in human neutrophils (Keyhani et al., 2014). This discrepancy could be due to the methods used for quantification of cytokine expression: CBA in our study and RT-PCR in the mentioned one, and the other experimental conditions.

IL-1β is a pro-inflammatory cytokine that has a controversial role in murine leishmaniasis. IL-1β promotes the development of leishmaniasis in *L. major* infected susceptible BALB/c mice (Voronov et al., 2010). Furthermore, the inflammasome -derived IL-1β production was important to develop an efficient immune response against *L. braziliensis*, *L. amazonensis*, and *L. chagasi* infection (Lima-Junior et al., 2013) but it failed to induce resistance against the infection of the resistant C57BL/6 mice by *L. major* Seidman strain (*Lm*Sd) (Charmoy et al., 2016) or the hamster infection by *L. donovani* (Dey et al., 2018). Both studies highlighted the role of the early production of IL-1β in sustaining the recruitment of neutrophils and in inducing the exacerbation of the disease (Charmoy et al., 2016; Dey et al., 2018). Few studies assessed the production of IL-1β by human neutrophils. Our results showed that human neutrophils exposed to *L. infantum* or to *L. major* were able to produce IL-1β as previously described (Keyhani et al., 2014). Contrary to our results, it was also shown that *L. infantum* down regulates the expression of IL-1β in murine neutrophils (Marques et al., 2015). This discrepancy could be due to the strains, the host origin of the neutrophils, or the methods used for the detection of this cytokine: CBA detection of the protein vs. quantitative measure of the transcript, or to the time of detection: 18 h here and 3 h in the mentioned study.

IL-6 is a pleiotropic cytokine produced by many cells that is involved in B cell maturation, macrophages differentiation and promotion of Th2 differentiation (Kishimoto, 2005; Kopf et al., 2010). In addition, with TGF-β, IL-6 induces the differentiation of Th17 cells and inhibits regulatory T cells generation (Bettelli et al., 2006; Kimura and Kishimoto, 2010). IL-6 plays also a pivotal role in the regulation of neutrophils trafficking during inflammation, by regulating the production of chemokines and by inducing neutrophils apoptosis (Fielding et al., 2008). The role of IL-6 in leishmaniases has been assessed in animal models. It was shown that BALB.B mice that are deficient for IL-6 were still susceptible to *L. major* infection, and they were not able to resolve their infection (Titus et al., 2001). In contrast, IL-6 deficient C57BL/6 mice were able to control the infection by *L. major* as the wild type corresponding mice (Moskowitz et al., 1997). Furthermore, multiple studies have shown a correlation between the high level of some cytokines, including IL-6, and the severity of visceral leishmaniasis (Ansari et al., 2006; Van Den Bogaart et al., 2014; Dos Santos et al., 2016; Ramos et al., 2016) and cutaneous leishmaniasis (Latifynia et al., 2012; Espir et al., 2014). To our knowledge, this is the first study addressing the determination of IL-6 protein levels produced by human neutrophils after exposure to *Leishmania* species. Our results showed that only the Drep-14 strain induced the production of IL-6 by human neutrophils. Notably, this strain also induced higher levels of TNF-α and IL-1β than the other two strains, LV50 and Empa-12 while the levels were comparable in case of the 4 other cytokines measured.

Collectively, our results suggest that the response of human neutrophils *in vitro*, at least for the production of cytokines and DNA release, seem to depend on the *Leishmania* strains and species. Although, the three *Leishmania* strains used in the present study induced very high and comparable levels of TGF-β, there was a differential production of the other inflammatory cytokines: TNF-α, IL-1β, and IL-6 according to the strain and species. Importantly, the statistical analysis of our results consolidated the fact that the strain (within the same species) appeared as the main drive in influencing the donors' cell response to the infection. This is further corroborated by the measures of parasite survival. In our experiment, while all strains presented similar infection index, the number of viable parasites was significantly lower in case of the dermotropic strains Drep-14 and Empa-12 that belong to two different species, *L. infantum* and *L. major*. Whereas, in case of the viscerotropic *L. infantum* (LV50 strain) the number of rescued parasites was similar to the number of internalized ones. This indicates that different leishmanicidal mechanisms are may be triggered within the infected cells according to the parasite strains and species. Importantly, our results point that in the interaction of a *Leishmania* species with human blood neutrophils, the parasite strains may differently influence the fate of the infection. Taking account that only three laboratory strains of two species were used in the present study, it would be interesting to assess the effect of more strains and clinical isolates of these species on human neutrophils infection and activation. Interestingly, this would also open ways to study relationship between clinical origin or genetic background of the strains (/species) and the immune response induced.

In conclusion, the present study established an infection model of human neutrophils to evaluate *ex vivo* their responses to *L. infantum* or *L. major* strains infection. Our study clearly demonstrated that the strains were able to induce similar *ex vivo* activation and apoptosis of the tested human neutrophils. However, they differently triggered DNA and inflammatory cytokines release from the neutrophils suggesting that these responses are *Leishmania* species- and strain- specific notably in case of *L. infantum*. Intracellular survival of the parasites also depended on the strains and species. Further study on the mechanisms involved in the responses triggered by these strains needs to be developed. Likewise, the effect of these differentially activated neutrophils and different parasite survival on macrophage infection needs investigation.

ETHICS STATEMENT

This study was carried out in accordance with the recommendations of The Ethical committee of the Institut Pasteur de Tunis with written informed consent from all subjects. All subjects gave written informed consent in accordance with the Declaration of Helsinki. The protocol was approved by The Ethical committee of the Institut Pasteur de Tunis.

AUTHOR CONTRIBUTIONS

IG, MB, and RO conceived and designed the experiments. RO performed the experiments. RO and SM performed the ELISA experiment. RO and EH-S performed the statistical analysis. RO, MB, SM, and MBA performed the FACS experiments. RO, MB, EH-S, MBA, and IG analyzed the data. RO, EH-S, IG, and MB drafted the manuscript. All authors read, edited, and approved the final manuscript.

FUNDING

This work was supported by funds from the Ministry of Higher Education and Research (MERST) in Tunisia (LR16IPT04) and by a grant from the Agence Universitaire de la Francophonie in frame of the Thématiques intégrées en Santé Publique to IG. RO is a recipient of a PhD fellowship from the MERST. EH-S is supported by the USAID-NAS -PEER cycle 5 program (PEER 518).

ACKNOWLEDGMENTS

We thank Dr. Makram Essafi and Dr. Khadija Essafi-Benkhadir for helpful discussions, reagent sharing and advice.

SUPPLEMENTARY MATERIAL

The Supplementary Material for this article can be found online at: https://www.frontiersin.org/articles/10.3389/fcimb.2019.00153/full#supplementary-material

REFERENCES

Aga, E., Katschinski, D. M., Van Zandbergen, G., Laufs, H., Hansen, B., Müller, K., et al. (2002). Inhibition of the spontaneous apoptosis of neutrophil granulocytes by the intracellular parasite *Leishmania* major. *J. Immunol.* 169, 898–905. doi: 10.4049/jimmunol.169.2.898

Alvar, J., Vélez, I. D., Bern, C., Herrero, M., Desjeux, P., Cano, J., et al. (2012). Leishmaniasis worldwide and global estimates of its incidence. *PLoS ONE* 7:e35671. doi: 10.1371/journal.pone.0035671f

Ansari, N. A., Saluja, S., and Salotra, P. (2006). Elevated levels of interferon-gamma, interleukin-10, and interleukin-6 during active disease in Indian kala azar. *Clin. Immunol.* 119, 339–345. doi: 10.1016/j.clim.2006.01.017

Barbosa, L. A., Fiuza, P. P., Borges, L. J., Rolim, F. A., Andrade, M. B., Luz, N. F., et al. (2018). RIPK1-RIPK3-MLKL-Associated Necroptosis Drives *Leishmania* infantum Killing in Neutrophils. *Front. Immunol.* 9:1818. doi: 10.3389/fimmu.2018.01818

Bardoel, B. W., Kenny, E. F., Sollberger, G., and Zychlinsky, A. (2014). The balancing act of neutrophils. *Cell Host Microbe.* 15, 526–536. doi: 10.1016/j.chom.2014.04.011

Bettelli, E., Carrier, Y., Gao, W., Korn, T., Strom, T. B., Oukka, M., et al. (2006). Reciprocal developmental pathways for the generation of pathogenic effector TH17 and regulatory T cells. *Nature* 441, 235–238. doi: 10.1038/nature04753

Brinkmann, V., Reichard, U., Goosmann, C., Fauler, B., Uhlemann, Y., Weiss, D. S., et al. (2004). Neutrophil extracellular traps kill bacteria. *Science* 303, 1532–1535. doi: 10.1126/science.1092385

Carlsen, E. D., Hay, C., Henard, C. A., Popov, V., Garg, N. J., and Soong, L. (2013). *Leishmania* amazonensis amastigotes trigger neutrophil activation but resist neutrophil microbicidal mechanisms. *Infect. Immun*. 81, 3966–3974. doi: 10.1128/IAI.00770-13

Carlsen, E. D., Jie, Z., Liang, Y., Henard, C. A., Hay, C., Sun, J., et al. (2015a). Interactions between neutrophils and *Leishmania braziliensis* amastigotes facilitate cell activation and parasite clearance. *J. Innate. Immun*. 7, 354–363. doi: 10.1159/000373923

Carlsen, E. D., Liang, Y., Shelite, T. R., Walker, D. H., Melby, P. C., and Soong, L. (2015b). Permissive and protective roles for neutrophils in leishmaniasis. *Clin. Exp. Immunol*. 182, 109–118. doi: 10.1111/cei.12674

Charmoy, M., Auderset, F., Allenbach, C., and Tacchini-Cottier, F. (2010). The prominent role of neutrophils during the initial phase of infection by *Leishmania* parasites. *J. Biomed. Biotechnol*. 2010:719361. doi: 10.1155/2010/719361

Charmoy, M., Hurrell, B. P., Romano, A., Lee, S. H., Ribeiro-Gomes, F., Riteau, N., et al. (2016). The Nlrp3 inflammasome, IL-1beta, and neutrophil recruitment are required for susceptibility to a nonhealing strain of *Leishmania* major in C57BL/6 mice. *Eur. J. Immunol*. 46, 897–911. doi: 10.1002/eji.201546015

Charmoy, M., Megnekou, R., Allenbach, C., Zweifel, C., Perez, C., Monnat, K., et al. (2007). *Leishmania* major induces distinct neutrophil phenotypes in mice that are resistant or susceptible to infection. *J. Leukoc. Biol*. 82, 288–299. doi: 10.1189/jlb.0706440

Chen, L., Zhang, Z. H., Watanabe, T., Yamashita, T., Kobayakawa, T., Kaneko, A., et al. (2005). The involvement of neutrophils in the resistance to *Leishmania* major infection in susceptible but not in resistant mice. *Parasitol. Int*. 54, 109–118. doi: 10.1016/j.parint.2005.02.001

Dey, R., Joshi, A. B., Oliveira, F., Pereira, L., Guimarães-Costa, A. B., Serafim, T. D., et al. (2018). Gut microbes egested during bites of infected sand flies augment severity of leishmaniasis via inflammasome-derived IL-1beta. *Cell Host Microbe* 23:e136. doi: 10.1016/j.chom.2017.12.002

Didwania, N., Shadab, M., Sabur, A., and Ali, N. (2017). Alternative to chemotherapy-the unmet demand against leishmaniasis. *Front. Immunol*. 8:1779. doi: 10.3389/fimmu.2017.01779

Diseases (2018). Global, regional, and national incidence, prevalence, and years lived with disability for 354 diseases and injuries for 195 countries and territories, 1990-2017: a systematic analysis for the Global Burden of Disease Study 2017. *Lancet* 392**,** 1789–1858. doi: 10.1016/S0140-6736(18)32279-7

Dos Santos, P. L., De Oliveira, F. A., Santos, M. L., Cunha, L. C., Lino, M. T., De Oliveira, M. F., et al. (2016). The severity of visceral leishmaniasis correlates with elevated levels of serum IL-6, IL-27 and sCD14. *PLoS. Negl. Trop. Dis*. 10:e0004375. doi: 10.1371/journal.pntd.0004375

Espir, T. T., Figueira Lde, P., Naiff Mde, F., da Costa, A. G., Ramalho-Ortigão, M., Malheiro, A., et al. (2014). The role of inflammatory, anti-inflammatory, and regulatory cytokines in patients infected with cutaneous leishmaniasis in Amazonas State, Brazil. *J. Immunol. Res*. 2014:481750. doi: 10.1155/2014/481750

Fadok, V. A., Bratton, D. L., Konowal, A., Freed, P. W., Westcott, J. Y., and Henson, P. M. (1998). Macrophages that have ingested apoptotic cells *in vitro* inhibit proinflammatory cytokine production through autocrine/paracrine mechanisms involving TGF-beta, PGE2, and PAF. *J. Clin. Invest*. 101, 890–898. doi: 10.1172/JCI1112

Falcão, S. A., Weinkopff, T., Hurrell, B. P., Celes, F. S., Curvelo, R. P., Prates, D. B., et al. (2015). Exposure to *Leishmania braziliensis* triggers neutrophil activation and apoptosis. *PLoS. Negl. Trop. Dis*. 9:e0003601. doi: 10.1371/journal.pntd.0003601

Faresjö, M. (2014). A useful guide for analysis of immune markers by fluorochrome (Luminex) technique. *Methods Mol. Biol*. 1172, 87–96. doi: 10.1007/978-1-4939-0928-5_7

Fielding, C. A., Mcloughlin, R. M., Mcleod, L., Colmont, C. S., Najdovska, M., Grail, D., et al. (2008). IL-6 regulates neutrophil trafficking during acute inflammation via STAT3. *J. Immunol*. 181, 2189–2195. doi: 10.4049/jimmunol.181.3.2189

Gabriel, C., Mcmaster, W. R., Girard, D., and Descoteaux, A. (2010). *Leishmania donovani* promastigotes evade the antimicrobial activity of neutrophil extracellular traps. *J. Immunol*. 185, 4319–4327. doi: 10.4049/jimmunol.1000893

Ghorbani, M., and Farhoudi, R. (2018). Leishmaniasis in humans: drug or vaccine therapy? *Drug Des. Devel. Ther*. 12, 25–40. doi: 10.2147/DDDT.S146521

Gueirard, P., Laplante, A., Rondeau, C., Milon, G., and Desjardins, M. (2008). Trafficking of *Leishmania* donovani promastigotes in non-lytic compartments in neutrophils enables the subsequent transfer of parasites to macrophages. *Cell Microbiol*. 10, 100–111. doi: 10.1111/j.1462-5822.2007.01018.x

Guimarães-Costa, A. B., Desouza-Vieira, T. S., Paletta-Silva, R., Freitas-Mesquita, A. L., Meyer-Fernandes, J. R., and Saraiva, E. M. (2014). 3'-nucleotidase/nuclease activity allows *Leishmania* parasites to escape killing by neutrophil extracellular traps. *Infect. Immun*. 82, 1732–1740. doi: 10.1128/IAI.01232-13

Guimarães-Costa, A. B., Nascimento, M. T., Froment, G. S., Soares, R. P., Morgado, F. N., Conceição-Silva, F., et al. (2009). *Leishmania* amazonensis promastigotes induce and are killed by neutrophil extracellular traps. *Proc. Natl. Acad. Sci. U.S.A*. 106, 6748–6753. doi: 10.1073/pnas.09002 26106

Guizani, I., Mukhtar, M., Alvar, J., Ben Abderrazak, S., and Shaw, J. (2011). "Leishmaniases," in *Encyclopedia of Environmental Health,* ed J. O. Nriagu (Burlington: Elsevier), 435–480. doi: 10.1016/B978-0-444-52272-6.00524-9

Harigua-Souiai, E., Abdelkrim, Y. Z., Bassoumi-Jamoussi, I., Zakraoui, O., Bouvier, G., Essafi-Benkhadir, K., et al. (2018). Identification of novel leishmanicidal molecules by virtual and biochemical screenings targeting *Leishmania* eukaryotic translation initiation factor 4A. *PLoS. Negl. Trop. Dis*. 12 :e0006160. doi: 10.1371/journal.pntd.0006160

Hefnawy, A., Berg, M., Dujardin, J. C., and De Muylder, G. (2017). Exploiting knowledge on *Leishmania* drug resistance to support the quest for new drugs. *Trends Parasitol*. 33, 162–174. doi: 10.1016/j.pt.2016.11.003

Herwaldt, B. L. (1999). Leishmaniasis. *Lancet* 354, 1191–1199. doi: 10.1016/S0140-6736(98)10178-2

Hsiao, C. H., Ueno, N., Shao, J. Q., Schroeder, K. R., Moore, K. C., Donelson, J. E., et al. (2011). The effects of macrophage source on the mechanism of phagocytosis and intracellular survival of Leishmania. *Microbes Infect*. 13, 1033–1044. doi: 10.1016/j.micinf.2011.05.014

Hurrell, B. P., Beaumann, M., Heyde, S., Regli, I. B., Müller, A. J., and Tacchini-Cottier, F. (2017). Frontline Science: *Leishmania* mexicana amastigotes can replicate within neutrophils. *J. Leukoc. Biol*. 102, 1187–1198. doi: 10.1189/jlb.4HI0417-158R

Hurrell, B. P., Regli, I. B., and Tacchini-Cottier, F. (2016). Different *Leishmania* species drive distinct neutrophil functions. *Trends Parasitol*. 32, 392–401. doi: 10.1016/j.pt.2016.02.003

Hurrell, B. P., Schuster, S., Grün, E., Coutaz, M., Williams, R. A., Held, W., et al. and Tacchini-Cottier, F. (2015). Rapid Sequestration of *Leishmania mexicana* by neutrophils contributes to the development of chronic lesion. *PLoS Pathog*. 11:e1004929. doi: 10.1371/journal.ppat.1004929

Kaye, P., and Scott, P. (2011). Leishmaniasis: complexity at the host-pathogen interface. *Nat. Rev. Microbiol*. 9, 604–615. doi: 10.1038/nrmicro2608

Keyhani, A., Riazi-Rad, F., Pakzad, S. R., and Ajdary, S. (2014). Human polymorphonuclear leukocytes produce cytokines in response to *Leishmania* major promastigotes. *APMIS* 122, 891–897. doi: 10.1111/apm. 12252

Kimura, A., and Kishimoto, T. (2010). IL-6: regulator of Treg/Th17 balance. *Eur. J. Immunol*. 40, 1830–1835. doi: 10.1002/eji.201040391

Kishimoto, T. (2005). IL-6: from laboratory to bedside. *Clin. Rev. Allergy. Immunol*. 28, 177–186. doi: 10.1385/CRIAI:28:3:177

Kolaczkowska, E., and Kubes, P. (2013). Neutrophil recruitment and function in health and inflammation. *Nat. Rev. Immunol*. 13, 159–175. doi: 10.1038/nri3399

Kopf, M., Bachmann, M. F., and Marsland, B. J. (2010). Averting inflammation by targeting the cytokine environment. *Nat. Rev. Drug Discov*. 9, 703–718. doi: 10.1038/nrd2805

Kuhns, D. B., Long Priel, D. A., Chu, J., and Zarember, K. A. (2015). Isolation and functional analysis of human neutrophils. *Curr. Protoc. Immunol. 111*, 21–16. doi: 10.1002/0471142735.im0723s111

Kumar, P., Pai, K., Pandey, H. P., and Sundar, S. (2002). NADH-oxidase, NADPH-oxidase and myeloperoxidase activity of visceral leishmaniasis patients. *J. Med. Microbiol*. 51, 832–836. doi: 10.1099/0022-1317-51-10-832

Kumar, R., and Engwerda, C. (2014). Vaccines to prevent leishmaniasis. *Clin. Transl. Immunology*. 3:e13. doi: 10.1038/cti.2014.4

Kumar, V., and Sharma, A. (2010). Neutrophils: Cinderella of innate immune system. *Int. Immunopharmacol*. 10, 1325–1334. doi: 10.1016/j.intimp.2010.08.012

Latifynia, A., Khamesipour, A., Bokaie, S., and Khansari, N. (2012). Antioxidants and proinflamatory cytokines in the sera of patients with cutaneous leishmaniasis. *Iran J. Immunol*. 9, 208–214.

Laufs, H., Müller, K., Fleischer, J., Reiling, N., Jahnke, N., Jensenius, J. C., et al. (2002). Intracellular survival of *Leishmania* major in neutrophil granulocytes after uptake in the absence of heat-labile serum factors. *Infect. Immun*. 70, 826–835. doi: 10.1128/IAI.70.2.826-835.2002

Lima-Junior, D. S., Costa, D. L., Carregaro, V., Cunha, L. D., Silva, A. L., Mineo, T. W., et al. and Zamboni, D. S. (2013). Inflammasome-derived IL-1beta production induces nitric oxide-mediated resistance to *Leishmania*. *Nat. Med*. 19, 909–915. doi: 10.1038/nm.3221

Marques, C. S., Passero, L. F., Vale-Gato, I., Rodrigues, A., Rodrigues, O. R., Martins, C., et al. (2015). New insights into neutrophil and *Leishmania* infantum *in vitro* immune interactions. *Comp. Immunol. Microbiol. Infect. Dis*. 40, 19–29. doi: 10.1016/j.cimid.2015.03.003

Martínez-López, M., Soto, M., Iborra, S., and Sancho, D. (2018). *Leishmania* hijacks myeloid cells for immune escape. *Front. Microbiol*. 9:883. doi: 10.3389/fmicb.2018.00883

Mollinedo, F., Janssen, H., de La Iglesia-Vicente, J., Villa-Pulgarin, J. A., and Calafat, J. (2010). Selective fusion of azurophilic granules with *Leishmania*-containing phagosomes in human neutrophils. *J. Biol. Chem*. 285, 34528–34536. doi: 10.1074/jbc.M110.125302

Moskowitz, N. H., Brown, D. R., and Reiner, S. L. (1997). Efficient immunity against *Leishmania* major in the absence of interleukin-6. *Infect. Immun*. 65, 2448–2450.

Müller, K., Van Zandbergen, G., Hansen, B., Laufs, H., Jahnke, N., Solbach, W., et al. (2001). Chemokines, natural killer cells and granulocytes in the early course of *Leishmania* major infection in mice. *Med. Microbiol. Immunol*. 190, 73–76. doi: 10.1007/s004300100084

Nathan, C. (2006). Neutrophils and immunity: challenges and opportunities. *Nat. Rev. Immunol*. 6, 173–182. doi: 10.1038/nri1785

Nauseef, W. M. (2007). How human neutrophils kill and degrade microbes: an integrated view. *Immunol. Rev*. 219, 88–102. doi: 10.1111/j.1600-065X.2007.00550.x

Pearson, R. D., and Steigbigel, R. T. (1981). Phagocytosis and killing of the protozoan *Leishmania* donovani by human polymorphonuclear leukocytes. *J. Immunol*. 127, 1438–1443.

Pereira, M., Valério-Bolas, A., Santos-Mateus, D., Alexandre-Pires, G., Santos, M., Rodrigues, A., et al. (2017). Canine neutrophils activate effector mechanisms in response to *Leishmania* infantum. *Vet. Parasitol*. 248, 10–20. doi: 10.1016/j.vetpar.2017.10.008

Peters, N., and Sacks, D. (2006). Immune privilege in sites of chronic infection: *Leishmania* and regulatory T cells. *Immunol. Rev*. 213, 159–179. doi: 10.1111/j.1600-065X.2006.00432.x

Peters, N. C., Egen, J. G., Secundino, N., Debrabant, A., Kimblin, N., Kamhawi, S., et al. (2008). *In vivo* imaging reveals an essential role for neutrophils in leishmaniasis transmitted by sand flies. *Science* 321, 970–974. doi: 10.1126/science.1159194

Peters, N. C., and Sacks, D. L. (2009). The impact of vector-mediated neutrophil recruitment on cutaneous leishmaniasis. *Cell Microbiol*. 11, 1290–1296. doi: 10.1111/j.1462-5822.2009.01348.x

Pham, C. T. (2006). Neutrophil serine proteases: specific regulators of inflammation. *Nat. Rev. Immunol*. 6, 541–550. doi: 10.1038/nri1841

Pigott, D. M., Bhatt, S., Golding, N., Duda, K. A., Battle, K. E., Brady, O. J., et al. (2014). Global distribution maps of the leishmaniases. *Elife* 3:e02851. doi: 10.7554/eLife.02851

Quintela-Carvalho, G., Luz, N. F., Celes, F. S., Zanette, D. L., Andrade, D., Menezes, D., et al. (2017). Heme drives oxidative stress-associated cell death in human neutrophils infected with *Leishmania* infantum. *Front. Immunol*. 8:1620. doi: 10.3389/fimmu.2017.01620

Ramos, P. K., Carvalho, K. I., Rosa, D. S., Rodrigues, A. P., Lima, L. V., Campos, M. B., et al. (2016). Serum cytokine responses over the entire clinical-immunological spectrum of human *Leishmania* (L.) infantum chagasi Infection. *Biomed. Res. Int*. 2016:6937980. doi: 10.1155/2016/6937980

Ribeiro-Gomes, F. L., Otero, A. C., Gomes, N. A., Moniz-De-Souza, M. C., Cysne-Finkelstein, L., Arnholdt, A. C., et al. (2004). Macrophage interactions with neutrophils regulate *Leishmania* major infection. *J. Immunol*. 172, 4454–4462. doi: 10.4049/jimmunol.172.7.4454

Ribeiro-Gomes, F. L., Peters, N. C., Debrabant, A., and Sacks, D. L. (2012). Efficient capture of infected neutrophils by dendritic cells in the skin inhibits the early anti-*leishmania* response. *PLoS Pathog*. 8:e1002536. doi: 10.1371/journal.ppat.1002536

Ribeiro-Gomes, F. L., and Sacks, D. (2012). The influence of early neutrophil-*Leishmania* interactions on the host immune response to infection. *Front. Cell Infect. Microbiol*. 2:59. doi: 10.3389/fcimb.2012.00059

Ricci-Azevedo, R., Oliveira, A. F., Conrado, M. C., Carvalho, F. C., and Roque-Barreira, M. C. (2016). Neutrophils contribute to the protection conferred by ArtinM against intracellular pathogens: a study on *Leishmania* major. *PLoS. Negl. Trop. Dis*. 10:e0004609. doi: 10.1371/journal.pntd.0004609

Ritter, U., Frischknecht, F., and Van Zandbergen, G. (2009). Are neutrophils important host cells for *Leishmania* parasites? *Trends Parasitol*. 25, 505–510. doi: 10.1016/j.pt.2009.08.003

Robinson, J. M. (2008). Reactive oxygen species in phagocytic leukocytes. *Histochem. Cell Biol* . 130, 281–297. doi: 10.1007/s00418-008-0461-4

Rodríguez, N. E., and Wilson, M. E. (2014). Eosinophils and mast cells in leishmaniasis. *Immunol. Res*. 59, 129–141. doi: 10.1007/s12026-014-8536-x

Ronet, C., Passelli, K., Charmoy, M., Scarpellino, L., Myburgh, E., Hauyon La Torre, Y., et al. (2018). TLR2 signaling in skin nonhematopoietic cells induces early neutrophil recruitment in response to Leishmania major Infection. *J Invest Dermatol*. doi: 10.1016/j.jid.2018.12.012. [Epub ahead of print].

Rousseau, D., Demartino, S., Ferrua, B., Michiels, J. F., Anjuère, F., Fragaki, K., et al. (2001). *In vivo* involvement of polymorphonuclear neutrophils in *Leishmania* infantum infection. *BMC Microbiol*. 1:17. doi: 10.1186/1471-2180-1-17

Sacks, D., and Noben-Trauth, N. (2002). The immunology of susceptibility and resistance to Leishmania major in mice. *Nat. Rev. Immunol*. 2, 845–858. doi: 10.1038/nri933

Sacramento, L. A., Da Costa, J. L., De Lima, M. H., Sampaio, P. A., Almeida, R. P., Cunha, F. Q., et al. (2017). Toll-like receptor 2 is required for inflammatory process development during leishmania infantum infection. *Front. Microbiol*. 8:262. doi: 10.3389/fmicb.2017.00262

Safaiyan, S., Bolhassani, A., Nylen, S., Akuffo, H., and Rafati, S. (2011). Contribution of human neutrophils in the development of protective immune response during *in vitro Leishmania* major infection. *Parasite Immunol*. 33, 609–620. doi: 10.1111/j.1365-3024.2011.01321.x

Sarkar, A., Aga, E., Bussmeyer, U., Bhattacharyya, A., Möller, S., Hellberg, L., et al. and Laskay, T. (2013). Infection of neutrophil granulocytes with *Leishmania* major activates ERK 1/2 and modulates multiple apoptotic pathways to inhibit apoptosis. *Med. Microbiol. Immunol*. 202, 25–35. doi: 10.1007/s00430-012-0246-1

Scapini, P., Lapinet-Vera, J. A., Gasperini, S., Calzetti, F., Bazzoni, F., and Cassatella, M. A. (2000). The neutrophil as a cellular source of chemokines. *Immunol. Rev*. 177, 195–203. doi: 10.1034/j.1600-065X.2000.17706.x

Segal, A. W. (2005). How neutrophils kill microbes. *Annu. Rev. Immunol*. 23, 197–223. doi: 10.1146/annurev.immunol.23.021704.115653

Seyed, N., Peters, N. C., and Rafati, S. (2018). Translating observations from leishmanization into non-living vaccines: the potential of dendritic cell-based vaccination strategies against *Leishmania*. *Front. Immunol*. 9, 1227. doi: 10.3389/fimmu.2018.01227

Sousa-Rocha, D., Thomaz-Tobias, M., Diniz, L. F., Souza, P. S., Pinge-Filho, P., and Toledo, K. A. (2015). Trypanosoma cruzi and Its soluble antigens induce NET release by stimulating toll-like receptors. *PLoS ONE* 10:e0139569. doi: 10.1371/journal.pone.0139569

Stephan, A., Batinica, M., Steiger, J., Hartmann, P., Zaucke, F., Bloch, W., and Fabri, M. (2016). LL37:DNA complexes provide antimicrobial activity against intracellular bacteria in human macrophages. *Immunology* 148, 420–432. doi: 10.1111/imm.12620

Tacchini-Cottier, F., Zweifel, C., Belkaid, Y., Mukankundiye, C., Vasei, M., Launois, P., et al. (2000). An immunomodulatory function for neutrophils during the induction of a CD4+ Th2 response in BALB/c mice infected with *Leishmania* major. *J. Immunol*. 165, 2628–2636. doi: 10.4049/jimmunol.165.5.2628

Tavares, N. M., Araújo-Santos, T., Afonso, L., Nogueira, P. M., Lopes, U. G., Soares, R. P., et al. (2014). Understanding the mechanisms controlling *Leishmania* amazonensis infection *in vitro*: the role of LTB4 derived from human neutrophils. *J. Infect. Dis*. 210, 656–666. doi: 10.1093/infdis/jiu158

Thalhofer, C. J., Chen, Y., Sudan, B., Love-Homan, L., and Wilson, M. E. (2011). Leukocytes infiltrate the skin and draining lymph nodes in response to the protozoan *Leishmania* infantum chagasi. *Infect. Immun.* 79, 108–117. doi: 10.1128/IAI.00338-10

Titus, R. G., Dekrey, G. K., Morris, R. V., and Soares, M. B. (2001). Interleukin-6 deficiency influences cytokine expression in susceptible BALB mice infected with *Leishmania* major but does not alter the outcome of disease. *Infect. Immun.* 69, 5189–5192. doi: 10.1128/IAI.69.8.5189-5192.2001

Valério-Bolas, A., Pereira, M., Alexandre-Pires, G., Santos-Mateus, D., Rodrigues, A., Rafael-Fernandes, M., et al. (2019). Intracellular and extracellular effector activity of mouse neutrophils in response to cutaneous and visceral *Leishmania* parasites. *Cell. Immunol.* 335, 76–84. doi: 10.1016/j.cellimm.2018.11.003

Van Den Bogaart, E., Talha, A. B., Straetemans, M., Mens, P. F., Adams, E. R., Grobusch, M. P., et al. and Schallig, H. D. (2014). Cytokine profiles amongst Sudanese patients with visceral leishmaniasis and malaria co-infections. *BMC Immunol.* 15:16. doi: 10.1186/1471-2172-15-16

Van Zandbergen, G., Bollinger, A., Wenzel, A., Kamhawi, S., Voll, R., Klinger, M., et al. (2006). *Leishmania* disease development depends on the presence of apoptotic promastigotes in the virulent inoculum. *Proc. Natl. Acad. Sci. U.S.A.* 103, 13837–13842. doi: 10.1073/pnas.0600843103

Van Zandbergen, G., Hermann, N., Laufs, H., Solbach, W., and Laskay, T. (2002). *Leishmania* promastigotes release a granulocyte chemotactic factor and induce interleukin-8 release but inhibit gamma interferon-inducible protein 10 production by neutrophil granulocytes. *Infect. Immun.* 70, 4177–4184. doi: 10.1128/IAI.70.8.4177-4184.2002

Van Zandbergen, G., Klinger, M., Mueller, A., Dannenberg, S., Gebert, A., Solbach, W., and Laskay, T. (2004). Cutting edge: neutrophil granulocyte serves as a vector for *Leishmania* entry into macrophages. *J. Immunol.* 173, 6521–6525. doi: 10.4049/jimmunol.173.11.6521

Voronov, E., Dotan, S., Gayvoronsky, L., White, R. M., Cohen, I., Krelin, Y., et al. (2010). IL-1-induced inflammation promotes development of leishmaniasis in susceptible BALB/c mice. *Int. Immunol.* 22, 245–257. doi: 10.1093/intimm/dxq006

Who (2019). *World Health Organization/Leishmaniasis/Fact sheet/Detail. Available online at: https://www.who.int/en/news-room/fact-sheets/detail/leishmaniasis* (*accessed* March 27, 2019).

Winterbourn, C. C., Kettle, A. J., and Hampton, M. B. (2016). Reactive oxygen species and neutrophil function. *Annu. Rev. Biochem.* 85**,** 765–792. doi: 10.1146/annurev-biochem-060815-014442

Yizengaw, E., Getahun, M., Tajebe, F., Cruz Cervera, E., Adem, E., Mesfin, G., et al. and Kropf, P. (2016). Visceral leishmaniasis patients display altered composition and maturity of neutrophils as well as impaired neutrophil effector functions. *Front. Immunol.* 7:517. doi: 10.3389/fimmu.2016.00517

Conflict of Interest Statement: The authors declare that the research was conducted in the absence of any commercial or financial relationships that could be construed as a potential conflict of interest.

frontiers in Cellular and Infection Microbiology

BRIEF RESEARCH REPORT
published: 26 June 2019
doi: 10.3389/fcimb.2019.00237

The Paradoxical Leishmanicidal Effects of Superoxide Dismutase (SOD)-Mimetic Tempol in *Leishmania braziliensis* Infection *in vitro*

Laíse B. Oliveira[1], *Fabiana S. Celes*[1], *Claudia N. Paiva*[2] *and Camila I. de Oliveira*[1,3]*

[1] *Instituto Gonçalo Moniz-IGM/FIOCRUZ, Salvador, Brazil,* [2] *Instituto de Microbiologia, Universidade Federal do Rio de Janeiro, Rio de Janeiro, Brazil,* [3] *Instituto de Investigação em Imunologia, São Paulo, Brazil*

Leishmaniasis is an infectious disease caused by protozoans of the genus *Leishmania*. The macrophage is the resident cell in which the parasite replicates and it is important to identify new compounds that can aid in parasite elimination since the drugs used to treat leishmaniasis are toxic and present side effects. We have previously shown that treatment of *Leishmania braziliensis*-infected macrophages with DETC (Diethyldithiocarbamate) induces parasite killing, *in vivo*. Thus, the objective of this study was to further evaluate the effect of oxidants and antioxidants in *L. braziliensis*-infected macrophages, following treatment with either oxidizing Hydrogen Peroxide, Menadione, DETC, or antioxidant [NAC (N-Acetyl-Cyteine), Apocynin, and Tempol] compounds. We determined the percentage of infected macrophages and number of amastigotes. Promastigote survival was also evaluated. Both DETC (SOD-inhibitor) and Tempol (SOD-mimetic) decreased the percentage of infected cells and parasite load. Hydrogen peroxide did not interfere with parasite burden, while superoxide-generator Menadione had a reducing effect. On the other hand, NAC (GSH-replenisher) and Apocynin (NADPH-oxidase inhibitor) increased parasite burden. Tempol surfaces as an interesting candidate for the chemotherapy of CL with an IC_{50} of 0.66 ± 0.08 mM and selectivity index of 151. While it remains obscure how a SOD-mimetic may induce leishmanicidal effects, we suggest the possibility of developing Tempol-based topical applications for the treatment of cutaneous leishmaniasis caused by *L. braziliensis*.

Keywords: *L. braziliensis*, oxidants, anti-oxidants, leishmaniasis, chemotherapy

OPEN ACCESS

Edited by:
Alexandre Barbosa Reis, Universidade Federal de Ouro Preto, Brazil

Reviewed by:
Isabel Mauricio, New University of Lisbon, Portugal
Rodrigo Soares, Oswaldo Cruz Foundation (Fiocruz), Brazil

***Correspondence:**
Camila I. de Oliveira
camila@bahia.fiocruz.br

Specialty section:
This article was submitted to Parasite and Host, a section of the journal Frontiers in Cellular and Infection Microbiology

Received: *01 December 2018*
Accepted: *14 June 2019*
Published: *26 June 2019*

Citation:
Oliveira LB, Celes FS, Paiva CN and de Oliveira CI (2019) The Paradoxical Leishmanicidal Effects of Superoxide Dismutase (SOD)-Mimetic Tempol in Leishmania braziliensis Infection in vitro. Front. Cell. Infect. Microbiol. 9:237. doi: 10.3389/fcimb.2019.00237

INTRODUCTION

Leishmaniasis is zoonotic infection widely distributed from Asia to America which exhibits a high mortality rate. The clinical forms of leishmaniasis depend on the infecting organism and the general state of the host's immune response and are divided in visceral leishmaniasis (VL) and tegumentary leishmaniasis (TL). TL is characterized by cutaneous or mucosal lesions with low lethality, but with high morbidity. CL caused by *Leishmania braziliensis* is distinguished from other leishmaniasis by its chronicity, latency, and tendency to metastasize in the human host (Bittencourt et al., 2003). Brazil along with nine other countries account for 70–75% of the global CL incidence (Alvar et al., 2012). First choice drugs for leishmaniasis chemotherapy are pentavalent antimonials (Sb^V)

[Meglumine Antimoniate (Glucantime®) and Sodium Stibogluconate (Pentostam®) (Croft and Coombs, 2003)] which are significantly toxic and with reported drug resistance (Llanos-Cuentas et al., 2008). Amphotericin B (Annaloro et al., 2009) and Miltefosine (Machado et al., 2010) are also limited with regards to toxicity, cost, and/or time of treatment, reinforcing the need for new chemotherapeutic alternatives.

Leishmania promastigotes infect both resident macrophages and monocytes recruited to the infection site. Macrophages are the main host cell, where the parasite differentiates into replicating amastigotes. Upon macrophage activation by IFN-γ, NADPH oxidase generates $O_2^{-\bullet}$ through the transfer of electrons from NADPH, coupling them to O_2. In a phagosome where leishmania parasites reside, $O_2^{-\bullet}$ may either undergo SOD degradation to form H_2O_2 or be used to generate other ROS, depending on expressed enzymes/cofactors availability and the imbalance between oxidants and antioxidants results in oxidative damage (Sies, 1993). ROS inhibits the growth of *L. braziliensis* amastigotes and contribute to parasite killing (Novais et al., 2014), while NO production alone does not suffice to control infection (Carneiro et al., 2016).

As an evasion strategy, *Leishmania* induces IFN-β production by infected macrophages, which on its turn induces the expression of the enzyme superoxide dismutase (SOD1). The enzyme SOD1 has an antioxidant function: it converts $O_2^{-\bullet}$ into molecular oxygen (O_2) and hydrogen peroxide (H_2O_2), the latter degraded by catalase. Survival of *L. amazonensis* and *L. braziliensis* in the host depends on this process (Khouri et al., 2009).

The SOD1-inhibitor diethyldithiocarbamate (DETC) kills intracellular parasites *in vitro* and *in vivo* in a murine model of cutaneous leishmaniasis (Khouri et al., 2010). We have previously shown that DETC can be used as a topical treatment in the cutaneous lesions caused by *L. braziliensis* (Celes et al., 2016), suggesting that manipulation of the redox status during *in vitro* infection with *L. braziliensis* can contribute to the identification of novel therapeutic alternatives. To this purpose, we incubated promastigotes and infected macrophages with Glutahtione replenisher N-acetyl-cysteine (NAC) (Aldini et al., 2018), SOD-mimetic Tempol (Wilcox, 2010) and $O_2^{-\bullet}$-generator menadione (Hassan, 2013). Much to our surprise, we observed that Tempol, a SOD-mimetic, was as effective as DETC (SOD-inhibitor) and menadione (superoxide generator via redox cycling (Criddle et al., 2006) with regards to its ability to reduce macrophage infection by *L. braziliensis*, suggesting novel yet unexplained effects of antioxidants over *Leishmania* infection.

MATERIALS AND METHODS

Ethics Statements

Female BALB/c mice, 6–8 weeks of age, were obtained from IGM/FIOCRUZ animal facility where they were maintained under pathogen-free conditions. All animal work was conducted according to the Guidelines for Animal Experimentation of the Colégio Brasileiro de Experimentação Animal and of the Conselho Nacional de Controle de Experimentação Animal. The local Ethics Committee on Animal Care and Utilization (CEUA) approved all procedures involving animals (CEUA L001/12 IGM/FIOCRUZ).

Parasites

Leishmania braziliensis (MHOM /BR/00/BA788/GFP) were grown in Schneider Insect medium (ThermoFisher Scientific) supplemented with 100 U/mL penicillin, 100 mg/mL streptomycin and 10% inactivated FBS (ThermoFisher Scientific) at 26°C until the stationary phase.

Infection of Bone Marrow-Derived Macrophages (BMDM) With *L. braziliensis* and Treatment With Oxidants and Anti-oxidants

Bone marrow derived macrophages were obtained as described (Weischenfeldt and Porse, 2008) and were resuspended in DMEM medium (ThermoFisher Scientific) supplemented with 100 U/ml penicillin, 100 ug/ml streptomycin, and 10% inactivated FBS (ThermoFisher Scientific) and seeded at density of 3×10^5 cells per well in 24-well tissue plates. Monolayers received 3×10^6 *L. braziliensis* promastigotes and were incubated at 35 °C in supplemented DMEM medium for 24 h. Infected macrophages were washed to remove non-internalized parasites. Cultures were treated with Diethyldithiocarbamate (DETC) (1 or 2 mM) (Khouri et al., 2010; Celes et al., 2016), Hydrogen Peroxide (100 or 150 μM), N-acetyl cysteine (NAC) (1, 5, or 10 mM), Apocynin (APO) (20 mM) (Paiva et al., 2012), Tempol (4-Hydroxy-TEMPO) (0.5, 1, or 5 mM) (Hahn et al., 1997; Shilo and Tirosh, 2003; Kim et al., 2017) and Menadione (1, 10, or 20 μM) (Mittra et al., 2013), all from SIGMA. Compounds were diluted in DMSO (vehicle). Amphotericin B (0.25 μg/mL, Invitrogen) was used as positive control. After 48 h, cells were extensively washed, fixed, and stained with hematoxylin and eosin (Fischer et al., 2008). The number of infected cells and intracellular amastigotes were counted by optical microscopy in 200 macrophages. Cultures (control and infected macrophages) were performed in quintuplicate. Alternatively, the rate of infection was evaluated by flow cytometry. Briefly, cells were fixed in PBS with 2% paraformaldehyde for 10 min, and kept at 4°C in the dark until acquisition. Data were acquired in a Fortessa flow cytometer (BD Biosciences, USA), for analysis by using FlowJo software (Tree Star, Version 10.2).

Treatment of *L. braziliensis* Promastigotes With Tempol, DETC, and Menadione

Stationary-phase promastigotes (3×10^5) were cultured in supplemented Schneider in the presence of Tempol (1, 3, or 5 mM), DETC (0.1, 0.5, or 1 mM) and Menadione (2, 5, 10, or 20 μM), all from SIGMA. Promastigotes were cultured in 96-well plates for up to 3 days and the number of viable promastigotes was determined daily using hemocytometer. All assays were performed in quadruplicate and Schneider's medium alone or medium containing vehicle alone were used as a negative control. The half-maximal

cytotoxic concentration (CC_{50}) and half maximal effective concentration (EC_{50}) values of Tempol were determined by a non-linear regression of the concentration-responses curves using GraphPad Software. The selectivity index (SI) was calculated as a ratio between CC_{50}/EC_{50} obtained with murine macrophages and intracellular *L. braziliensis* amastigotes, respectively.

Statistical Analysis

For non-parametric data, analyzes were performed using the Kruskal-Wallis test, followed by the Dunn's multiple comparisons test, for comparisons between three or more groups. For all the analyzes the confidence interval of 95% was established, being the values considered statistically significant when $p<0.05$. Three biological replicates were performed for each experiment. All analyzes were done using GraphPad Prism Software version 5.0. Flow cytometric analyzes were performed using FlowJo software version 10.

RESULTS AND DISCUSSION

Herein, we tested a number of compounds for their ability to modulate the oxidative stress in macrophages infected with *L. braziliensis*. We hypothesized that compounds able to increase ROS induce parasite elimination, building on previous studies showing that such effect can be applied to the development of topical formulations for the treatment of cutaneous leishmaniasis (Celes et al., 2016).

BMDM were infected with *L. braziliensis* and treated with DETC. DETC significantly reduced the percentage of infected cells (**Figure 1A**) and the number of intracellular parasites (**Figure 1B**). DETC (2 mM) showed a leishmanicidal effect similar to that of Amphotericin B, used to treat human leishmaniasis and employed here as a positive control, corroborating our previous findings that the elevation of $O_2^{-\bullet}$ levels by DETC-mediated inhibition of SOD1 induces *L. braziliensis* killing (Khouri et al., 2010; Celes et al., 2016). H_2O_2 significantly reduced the number of infected cells nor the number of amastigotes (**Figures 1C,D**, respectively), indicating that the ROS responsible for parasite killing induced by DETC is $O_2^{-\bullet}$ itself or another species which uses $O_2^{-\bullet}$ as a substrate. These results are in accordance with the killing of *L. braziliensis* amastigotes by EGCG (Inacio et al., 2014), shown to induce the production of superoxide anions, hydrogen peroxide, and other reactive oxygen species (ROS) (Suh et al., 2010), an effect inhibited by catalase-PEG. *L. donovani* was reported to evade oxidative conditions by removing H_2O_2 and allowing parasite survival (Channon and Blackwell, 1985). More recently, resistance of *L. donovani*-infected macrophages to H_2O_{2-} mediated apoptosis was shown to be due to upregulation of thioredoxin and SOCS (Srivastav et al., 2014).

Tempol is an antioxidant able to promote $O_2^{-\bullet}$ metabolism at rates similar to SOD and able to permeate membranes freely (Batinic-Haberle et al., 2010). It acts as an $O_2^{-\bullet}$ scavenger that crosses cell membranes and therefore can be used to scavenge $O_2^{-\bullet}$ in living phagocyte (Gariboldi et al., 1998). We thus expected that Tempol, as an antioxidant molecule, would also favor infection by *L. braziliensis*. Strinkingly, exposure to Tempol significantly reduced the percentage of infected cells (**Figure 1E**) and the number of amastigotes (**Figure 1F**), controlling *L. braziliensis* infection, as seen with DETC. Moreover, the combination DETC+Tempol also reduced the percentage of infected cells (**Supplemental Figure 1**), as seen individually with DETC (**Figure 1**). Tempol mimics superoxide dismutase activity thus generating hydrogen peroxide and water, destabilizing the oxidation. We can speculate that the presence of Tempol increased H_2O_2 levels, interfering with parasite viability. In this case, the concentrations of H_2O_2 reached inside the phagosome would need to be significantly higher than those obtained herein following macrophage incubation with 50 μM H_2O_2 (**Figures 1C,D**). Alternatively, Tempol may have off-target leishmanicidal effects superimposed to its anti-oxidant effects. Treatment with Menadione also significantly decreased the percentage of *L. braziliensis*-infected cells (**Figure 1G**) and the number of intracellular parasites (**Figure 1H**). We can speculate that, as seen with DETC (Celes et al., 2016), the presence of Menadione may have elevated superoxide levels, leading to parasite elimination.

In *L. infantum*-infected BMDM macrophages, addition of Tempol during phagocytosis increases intracellular infection (Gantt et al., 2001). In *L. amazonensis*-infected mice, SOD-mimetic Tempol exacerbated lesion development and increased parasite load after oral administration. This was associated with reduction of nitric oxide and sequestration of oxidizing molecules (Linares et al., 2008). Differences in the pathogenesis of CL caused by *L. amazonensis* and *L. braziliensis* have been reported regarding the role of neutrophils, for example (Novais et al., 2009; Roma et al., 2016; Carneiro et al., 2018). Therefore, we can speculate that the microbicidal effect of Tempol observed herein, *in vitro*, recapitulate such differences and thus warrant further *in vivo* experiments, especially given Tempol's ability to modulate H_2O_2 levels.

We also verified the leishmanicidal effect of oxidants on *L. braziliensis* promastigotes: DETC significantly reduced *L. braziliensis* proliferation at all DETC concentrations tested (**Supplemental Figure 2A**). As seen with amastigotes (**Figures 1E,F**), SOD-mimetic Tempol also inhibited the proliferation of *L. braziliensis* promastigotes (**Supplemental Figure 2B**), similarly to SOD-inhibitor DETC, although we did not observe clear-cut dose-dependent effects. Menadione induced promastigote killing (**Supplemental Figure 2C**). Lastly, a combination of Tempol+DETC strongly reduced parasite survival as seen with combinations of Menadione + Tempol and Menadione + DETC combinations (**Supplemental Figure 2D**).

In parallel to the oxidants, we examined the effect of antioxidants: N-Acetyl-Cysteine (NAC) is a synthetic precursor of intracellular cysteine and glutathione, and its anti-ROS activity results from its ability to directly remove free radicals

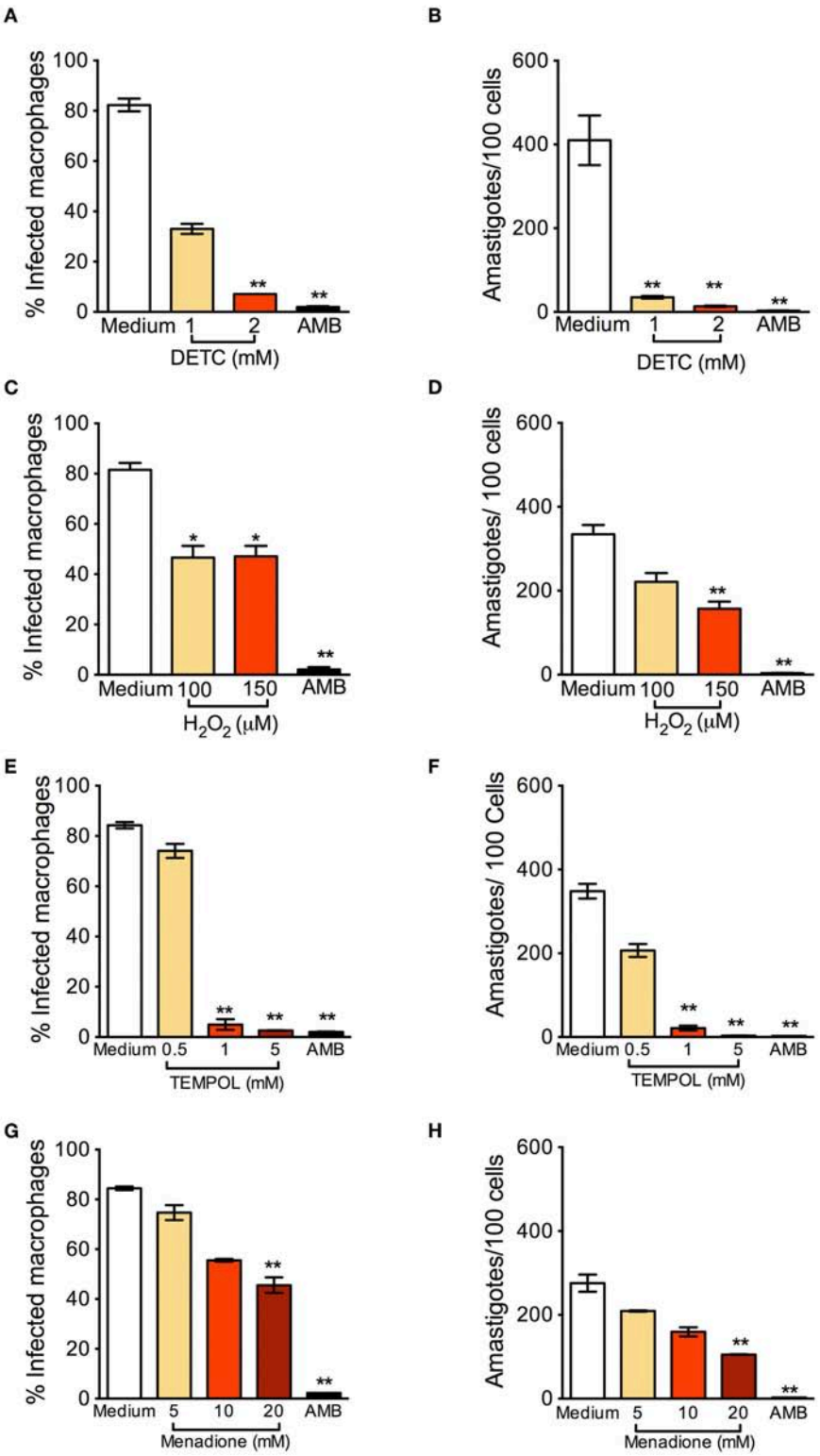

FIGURE 1 | Oxidants reduce *Leishmania braziliensis* infection *in vitro*. Macrophages were infected with *L. braziliensis* for 24 h, and then exposed to different concentrations of DETC **(A,B)**, H_2O_2 **(C,D)** for 24 h, Tempol **(E,F)**, and Menadione **(G,H)** for 24 h. Cells were stained with H&E and assessed for the percentage of infection **(A,C,E,F)** and the number of amastigotes per 100 macrophages **(B,D,G,H)** by optical microscopy. Infected macrophages treated with Amphotericin B (AMB) were used as positive controls. Data are shown as mean ± SEM. $^{*}p < 0.05$; $^{**}p < 0.01$, $^{***}p < 0.001$, all comparisons were against negative control (medium).

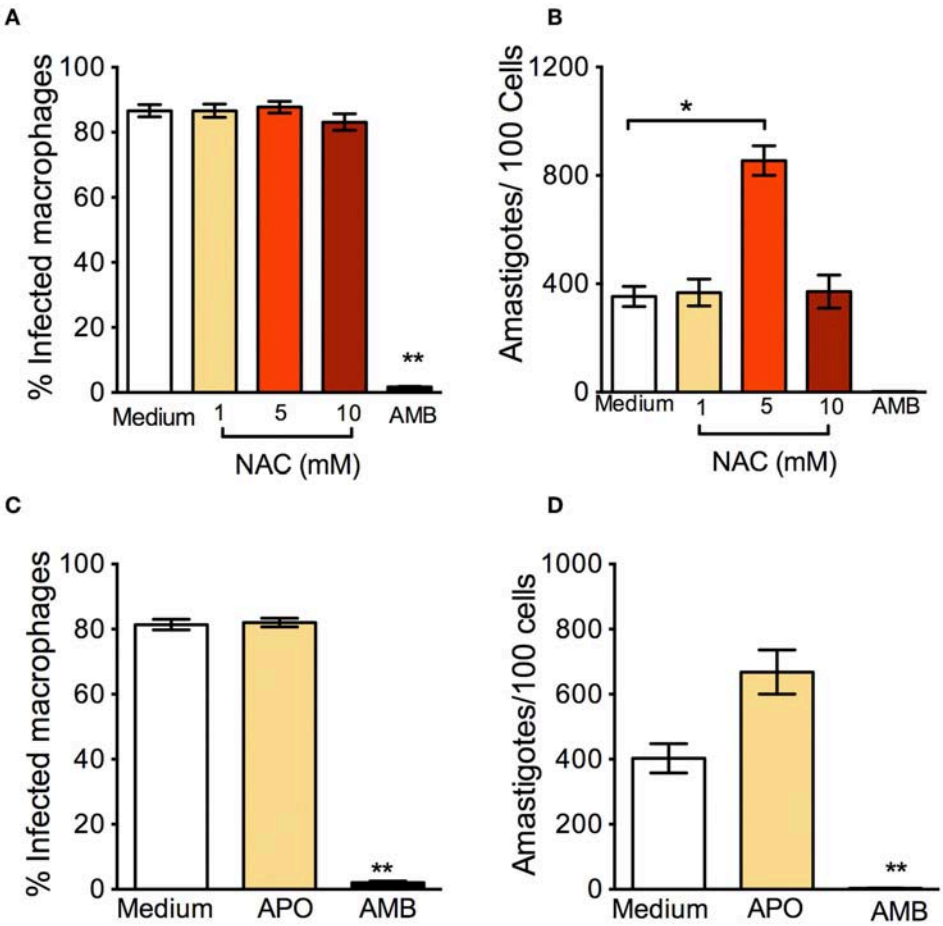

FIGURE 2 | Anti-oxidants enhance *in vitro* infection with *L. braziliensis*. Macrophages were infected with *L. braziliensis* for 24 h, and then exposed to different concentrations of NAC **(A,B)** and Apocycin **(C,D)** for 48 h. Cells were stained with H&E and assessed for **(A,C)** the percentage of infected macrophages and **(B,D)** the number of amastigotes per 100 macrophages by optical microscopy. Infected macrophages treated with Amphotericin B (AMB) were used as positive controls. Data are shown as mean ± SEM. $^{*}p < 0.05$, $^{**}p < 0.01$, all comparisons were against negative control (medium).

through the redox potential of thiols and indirectly by increasing levels of glutathione in cells (Sun, 2010). *L. braziliensis*-infected macrophages treated with NAC had a significantly higher percentage of infection (**Figure 2A**) and a significantly increased parasite load (**Figure 2B**). Similar results were reported in human monocytes infected with *L. braziliensis* and incubated with NAC (Novais et al., 2014). We believe that these effects are due to the neutralization of ROS, since NAC restores glutathione (GSH) and NAC may protect *L. braziliensis* from oxidative stress just as it does with human red blood cells (Grinberg et al., 2005). Alike NAC, exposure of *L. braziliensis*-infected macrophages to APO did not change the percentage of infected cells (**Figure 2C**), but induced an increase in the number of amastigotes in cells, indicating that the source of ROS in infected macrophages is indeed NADPH-oxidase respiratory burst (**Figure 2D**).

Although news studies are needed to understand the mechanisms by which Tempol acts to eliminate *L. braziliensis*, we believe Tempol is an interesting candidate for the chemotherapy of CL. Of note in BMDM, the IC_{50} of Tempol was determined at 0.66 mM ± 0.08 mM, the CC_{50} was calculated as >100 mM and the selectivity index was established at 151. Tempol presents low toxicity and has successfully completed phase I clinical trials to be used topically against tissue damage (Metz et al., 2004). Given that treatment options for CL are currently limited and that the number of refractory cases has increased, Tempol surfaces as a viable alternative for further investigation.

ETHICS STATEMENT

All animal work was conducted according to the Guidelines for Animal Experimentation of the Colégio Brasileiro de Experimentação Animal and of the Conselho Nacional de Controle de Experimentação Animal. The local Ethics Committee on Animal Care and Utilization (CEUA) approved all procedures involving animals (CEUA L001/12 IGM/FIOCRUZ).

AUTHOR CONTRIBUTIONS

LO and FC performed experiments. LO, CP, and CO drafted the manuscript. CP contributed reagents.

FUNDING

LO was the recipient of a CNPq fellowship (Iniciação Científica). FC was financed by the Coordenação de Aperfeiçoamento de pessoal de Nível Superior—Brasil (CAPES)—Finance Code 001. CO is a senior investigator from CNPq. This work was funded in part by Instituto Gonçalo Moniz (IGM)-Fiocruz.

ACKNOWLEDGMENTS

We thank the flow cytometery core.

SUPPLEMENTARY MATERIAL

The Supplementary Material for this article can be found online at: https://www.frontiersin.org/articles/10.3389/fcimb.2019.00237/full#supplementary-material

REFERENCES

Aldini, G., Altomare, A., Baron, G., Vistoli, G., Carini, M., Borsani, L., et al. (2018). N-Acetylcysteine as an antioxidant and disulphide breaking agent: the reasons why. *Free Radic. Res.* 52, 751–762. doi: 10.1080/10715762.2018.1468564

Alvar, J., Velez, I. D., Bern, C., Herrero, M., Desjeux, P., Cano, J., et al. (2012). Leishmaniasis worldwide and global estimates of its incidence. *PLoS ONE* 7:e35671. doi: 10.1371/journal.pone.0035671

Annaloro, C., Olivares, C., Usardi, P., Onida, F., Della Volpe, A., Tagliaferri, E., et al. (2009). Retrospective evaluation of amphotericin B deoxycholate toxicity in a single centre series of haematopoietic stem cell transplantation recipients. *J. Antimicrob. Chemother.* 63, 625–626. doi: 10.1093/jac/dkn549

Batinic-Haberle, I., Reboucas, J. S., and Spasojevic, I. (2010). Superoxide dismutase mimics: chemistry, pharmacology, and therapeutic potential. *Antioxid. Redox. Signal.* 13, 877–918. doi: 10.1089/ars.2009.2876

Bittencourt, A., Silva, N., Straatmann, A., Nunes, V. L., Follador, I., and Badaro, R. (2003). Post-kala-azar dermal leishmaniasis associated with AIDS. *Braz. J. Infect. Dis.* 7, 229–233. doi: 10.1590/S1413-86702003000300009

Carneiro, M. B. H., Roma, E. H., Ranson, A. J., Doria, N. A., Debrabant, A., Sacks, D. L., et al. (2018). NOX2-derived reactive oxygen species control inflammation during *Leishmania amazonensis* infection by mediating infection-induced neutrophil apoptosis. *J. Immunol.* 200, 196–208. doi: 10.4049/jimmunol.1700899

Carneiro, P. P., Conceicao, J., Macedo, M., Magalhaes, V., Carvalho, E. M., and Bacellar, O. (2016). The role of nitric oxide and reactive oxygen species in the killing of *Leishmania braziliensis* by monocytes from patients with cutaneous leishmaniasis. *PLoS ONE* 11:e0148084. doi: 10.1371/journal.pone.0148084

Celes, F. S., Trovatti, E., Khouri, R., Van Weyenbergh, J., Ribeiro, S. J., Borges, V. M., et al. (2016). DETC-based bacterial cellulose bio-curatives for topical treatment of cutaneous leishmaniasis. *Sci. Rep.* 6:38330. doi: 10.1038/srep38330

Channon, J. Y., and Blackwell, J. M. (1985). A study of the sensitivity of Leishmania donovani promastigotes and amastigotes to hydrogen peroxide. II. Possible mechanisms involved in protective H2O2 scavenging. *Parasitology* 91 (Pt 2), 207–217. doi: 10.1017/S0031182000057310

Criddle, D. N., Gillies, S., Baumgartner-Wilson, H. K., Jaffar, M., Chinje, E. C., Passmore, S., et al. (2006). Menadione-induced reactive oxygen species generation via redox cycling promotes apoptosis of murine pancreatic acinar cells. *J. Biol. Chem.* 281, 40485–40492. doi: 10.1074/jbc.M607704200

Croft, S. L., and Coombs, G. H. (2003). Leishmaniasis–current chemotherapy and recent advances in the search for novel drugs. *Trends Parasitol.* 19, 502–508. doi: 10.1016/j.pt.2003.09.008

Fischer, A. H., Jacobson, K. A., Rose, J., and Zeller, R. (2008). Hematoxylin and eosin staining of tissue and cell sections. *CSH Protoc.* 2008:pdb prot4986. doi: 10.1101/pdb.prot4986

Gantt, K. R., Goldman, T. L., Mccormick, M. L., Miller, M. A., Jeronimo, S. M., Nascimento, E. T., et al. (2001). Oxidative responses of human and murine macrophages during phagocytosis of *Leishmania chagasi*. *J. Immunol.* 167, 893–901. doi: 10.4049/jimmunol.167.2.893

Gariboldi, M. B., Lucchi, S., Caserini, C., Supino, R., Oliva, C., and Monti, E. (1998). Antiproliferative effect of the piperidine nitroxide TEMPOL on neoplastic and nonneoplastic mammalian cell lines. *Free Radic. Biol. Med.* 24, 913–923. doi: 10.1016/S0891-5849(97)00372-9

Grinberg, L., Fibach, E., Amer, J., and Atlas, D. (2005). N-acetylcysteine amide, a novel cell-permeating thiol, restores cellular glutathione and protects human red blood cells from oxidative stress. *Free Radic. Biol. Med.* 38, 136–145. doi: 10.1016/j.freeradbiomed.2004.09.025

Hahn, S. M., Mitchell, J. B., and Shacter, E. (1997). Tempol inhibits neutrophil and hydrogen peroxide-mediated DNA damage. *Free Radic. Biol. Med.* 23, 879–884. doi: 10.1016/S0891-5849(97)00079-8

Hassan, G. S. (2013). Menadione. *Profiles Drug. Subst. Excip. Relat. Methodol.* 38, 227–313. doi: 10.1016/B978-0-12-407691-4.00006-X

Inacio, J. D., Gervazoni, L., Canto-Cavalheiro, M. M., and Almeida-Amaral, E. E. (2014). The effect of (-)-epigallocatechin 3-O–gallate *in vitro* and *in vivo* in *Leishmania braziliensis*: involvement of reactive oxygen species as a mechanism of action. *PLoS Negl. Trop Dis.* 8:e3093. doi: 10.1371/journal.pntd.0003093

Khouri, R., Bafica, A., Silva Mda, P., Noronha, A., Kolb, J. P., Wietzerbin, J., et al. (2009). IFN-beta impairs superoxide-dependent parasite killing in human macrophages: evidence for a deleterious role of SOD1 in cutaneous leishmaniasis. *J. Immunol.* 182, 2525–2531. doi: 10.4049/jimmunol.0802860

Khouri, R., Novais, F., Santana, G., De Oliveira, C. I., Vannier Dos Santos, M. A., Barral, A., et al. (2010). DETC induces Leishmania parasite killing in human *in vitro* and murine *in vivo* models: a promising therapeutic alternative in Leishmaniasis. *PLoS ONE* 5:e14394. doi: 10.1371/journal.pone.0014394

Kim, J. Y., Choi, G. E., Yoo, H. J., and Kim, H. S. (2017). Interferon potentiates toll-like receptor-induced prostaglandin D2 production through positive feedback regulation between signal transducer and activators of transcription 1 and reactive oxygen species. *Front. Immunol.* 8:1720. doi: 10.3389/fimmu.2017.01720

Linares, E., Giorgio, S., and Augusto, O. (2008). Inhibition of *in vivo* leishmanicidal mechanisms by tempol: nitric oxide down-regulation and oxidant scavenging. *Free Radic. Biol. Med.* 44, 1668–1676. doi: 10.1016/j.freeradbiomed.2008.01.027

Llanos-Cuentas, A., Tulliano, G., Araujo-Castillo, R., Miranda-Verastegui, C., Santamaria-Castrellon, G., Ramirez, L., et al. (2008). Clinical and parasite species risk factors for pentavalent antimonial treatment failure in cutaneous leishmaniasis in Peru. *Clin. Infect. Dis.* 46, 223–231. doi: 10.1086/524042

Machado, P. R., Ampuero, J., Guimaraes, L. H., Villasboas, L., Rocha, A. T., Schriefer, A., et al. (2010). Miltefosine in the treatment of cutaneous leishmaniasis caused by *Leishmania braziliensis* in Brazil: a randomized and controlled trial. *PLoS Negl. Trop. Dis.* 4:e912. doi: 10.1371/journal.pntd.0000912

Metz, J. M., Smith, D., Mick, R., Lustig, R., Mitchell, J., Cherakuri, M., et al. (2004). A phase I study of topical Tempol for the prevention of alopecia induced by whole brain radiotherapy. *Clin. Cancer Res.* 10, 6411–6417. doi: 10.1158/1078-0432.CCR-04-0658

Mittra, B., Cortez, M., Haydock, A., Ramasamy, G., Myler, P. J., and Andrews, N. W. (2013). Iron uptake controls the generation of Leishmania infective forms through regulation of ROS levels. *J. Exp. Med.* 210, 401–416. doi: 10.1084/jem.20121368

Novais, F. O., Nguyen, B. T., Beiting, D. P., Carvalho, L. P., Glennie, N. D., Passos, S., et al. (2014). Human classical monocytes control the intracellular

stage of *Leishmania braziliensis* by reactive oxygen species. *J. Infect. Dis.* 209, 1288–1296. doi: 10.1093/infdis/jiu013

Novais, F. O., Santiago, R. C., Bafica, A., Khouri, R., Afonso, L., Borges, V. M., et al. (2009). Neutrophils and macrophages cooperate in host resistance against *Leishmania braziliensis* infection. *J. Immunol.* 183, 8088–8098. doi: 10.4049/jimmunol.0803720

Paiva, C. N., Feijo, D. F., Dutra, F. F., Carneiro, V. C., Freitas, G. B., Alves, L. S., et al. (2012). Oxidative stress fuels *Trypanosoma cruzi* infection in mice. *J. Clin. Invest.* 122, 2531–2542. doi: 10.1172/JCI58525

Roma, E. H., Macedo, J. P., Goes, G. R., Goncalves, J. L., Castro, W., Cisalpino, D., et al. (2016). Impact of reactive oxygen species (ROS) on the control of parasite loads and inflammation in Leishmania amazonensis infection. *Parasit. Vectors* 9:193. doi: 10.1186/s13071-016-1472-y

Shilo, S., and Tirosh, O. (2003). Selenite activates caspase-independent necrotic cell death in Jurkat T cells and J774.2 macrophages by affecting mitochondrial oxidant generation. *Antioxid. Redox Signal* 5, 273–279. doi: 10.1089/152308603322110850

Sies, H. (1993). Strategies of antioxidant defense. *Eur. J. Biochem.* 215, 213–219. doi: 10.1111/j.1432-1033.1993.tb18025.x

Srivastav, S., Basu Ball, W., Gupta, P., Giri, J., Ukil, A., and Das, P. K. (2014). *Leishmania donovani* prevents oxidative burst-mediated apoptosis of host macrophages through selective induction of suppressors of cytokine signaling (SOCS) proteins. *J. Biol. Chem.* 289, 1092–1105. doi: 10.1074/jbc.M113.496323

Suh, K. S., Chon, S., Oh, S., Kim, S. W., Kim, J. W., Kim, Y. S., et al. (2010). Prooxidative effects of green tea polyphenol (-)-epigallocatechin-3-gallate on the HIT-T15 pancreatic beta cell line. *Cell Biol. Toxicol.* 26, 189–199. doi: 10.1007/s10565-009-9137-7

Sun, S. Y. (2010). N-acetylcysteine, reactive oxygen species and beyond. *Cancer Biol. Ther.* 9, 109–110. doi: 10.4161/cbt.9.2.10583

Weischenfeldt, J., and Porse, B. (2008). Bone Marrow-Derived Macrophages (BMM): isolation and applications. *Cold Spring Harbor. Protocols* 2008:pdb.prot5080-pdb.prot5080. doi: 10.1101/pdb.prot5080

Wilcox, C. S. (2010). Effects of tempol and redox-cycling nitroxides in models of oxidative stress. *Pharmacol. Ther.* 126, 119–145. doi: 10.1016/j.pharmthera.2010.01.003

Conflict of Interest Statement: The authors declare that the research was conducted in the absence of any commercial or financial relationships that could be construed as a potential conflict of interest.

frontiers in Cellular and Infection Microbiology

ORIGINAL RESEARCH
published: 28 June 2019
doi: 10.3389/fcimb.2019.00229

Miltefosine-Lopinavir Combination Therapy Against *Leishmania infantum* Infection: *In vitro* and *in vivo* Approaches

Karina M. Rebello[1], *Valter V. Andrade-Neto*[2], *Claudia Regina B. Gomes*[3], *Marcos Vinícius N. de Souza*[3], *Marta H. Branquinha*[4], *André L. S. Santos*[4], *Eduardo Caio Torres-Santos*[2‡] *and Claudia M. d'Avila-Levy*[1*†‡]

[1] *Laboratório de Estudos Integrados em Protozoologia, Instituto Oswaldo Cruz, Fundação Oswaldo Cruz (FIOCRUZ), Rio de Janeiro, Brazil,* [2] *Laboratório de Bioquímica de Tripanosomatídeos, Instituto Oswaldo Cruz, FIOCRUZ, Rio de Janeiro, Brazil,* [3] *Laboratório de Síntese de Substâncias no Combate a Doenças Tropicais, Farmanguinhos, FIOCRUZ, Rio de Janeiro, Brazil,* [4] *Laboratório de Estudos Avançados de Microrganismos Emergentes e Resistentes, Instituto de Microbiologia Paulo de Góes, UFRJ, Rio de Janeiro, Brazil*

Concurrently, leishmaniasis and AIDS are global public health issues and the overlap between these diseases adds additional treats to the management of co-infected patients. Lopinavir (LPV) has a well characterized anti-HIV and leishmanicidal action, and to analyze its combined action with miltefosine (MFS) could help to envisage strategies to the management of co-infected patients. Here, we evaluate the interaction between LPV and MFS against *Leishmania infantum* infection by *in vitro* and *in vivo* approaches. The effect of the compounds alone or in association was assessed for 72 h in mouse peritoneal macrophages infected with *L. infantum* by the determination of the IC_{50}s and FICIs. Subsequently, mice were orally treated twice daily during 5 days with the compounds alone or in association and evaluated after 30 days. The *in vitro* assays revealed an IC_{50} of 0.24 μM and 9.89 μM of MFS and LPV, respectively, and an additive effect of the compounds (FICI 1.28). The *in vivo* assays revealed that LPV alone reduced the parasite load in the spleen and liver by 52 and 40%, respectively. The combined treatment of infected BALB/c mice revealed that the compounds alone required at least two times higher doses than when administered in association to virtually eliminate the parasite. Mice plasma biochemical parameters assessed revealed that the combined therapy did not present any relevant hepatotoxicity. In conclusion, the association of MFS with LPV allowed a reduction in each compound concentration to achieve the same outcome in the treatment of visceral leishmaniasis. Although a pronounced synergistic effect was not evidenced, it does not discard that such combination could be useful in humans co-infected with HIV and *Leishmania* parasites.

Keywords: chemotherapy, co-infection, HIV, HIV-PI, leishmaniasis, treatment

OPEN ACCESS

Edited by:
Herbert Leonel de Matos Guedes, Federal University of Rio de Janeiro, Brazil

Reviewed by:
Peter Epeh Kima, University of Florida, United States
Manuel Soto, Autonomous University of Madrid, Spain

***Correspondence:**
Claudia M. d'Avila-Levy
davila.levy@ioc.fiocruz.br

†Present Address:
Claudia M. d'Avila-Levy, de Duve Institute, Université Catholique de Louvain, Brussels, Belgium

‡*These authors share senior authorship*

Specialty section:
This article was submitted to Parasite and Host, a section of the journal Frontiers in Cellular and Infection Microbiology

Received: *15 April 2019*
Accepted: *11 June 2019*
Published: *28 June 2019*

Citation:
Rebello KM, Andrade-Neto VV, Gomes CRB, de Souza MVN, Branquinha MH, Santos ALS, Torres-Santos EC and d'Avila-Levy CM (2019) Miltefosine-Lopinavir Combination Therapy Against Leishmania infantum Infection: In vitro and in vivo Approaches. Front. Cell. Infect. Microbiol. 9:229. doi: 10.3389/fcimb.2019.00229

INTRODUCTION

Visceral leishmaniasis (VL), also known as kala-azar, is a vector-borne disseminated protozoan infection caused by species of the *Leishmania donovani* complex (Lukes et al., 2007; Burza et al., 2018). It is a an important but neglected tropical disease that occurs worldwide (Ready, 2014). In 2015, more than 90% of VL occurred in only seven countries: Brazil, Ethiopia, India, Kenya, Somalia, South Sudan, and Sudan (Burza et al., 2018). Notwithstanding, VL remains prevalent in more than 60 countries worldwide (Burza et al., 2018).

VL is an opportunist disease in human immunodeficiency virus (HIV) infected patients and this co-infection is one of the major challenges for VL control (Alvar et al., 2008). The re-emergence of VL in Europe in the 1990's was caused by immigration and HIV infection worsened the scenario (Agostoni et al., 1998). Since then, co-infection cases have been reported in 35 countries worldwide (Lindoso et al., 2016), being more prevalent in the East Africa region, especially Ethiopia (Van Griensven et al., 2014b; Yimer et al., 2014), in Brazil (Nascimento et al., 2011; Lima et al., 2018), and in India (Burza et al., 2014; Singh, 2014). VL promotes an increase in viral load and accelerates the clinical progression of acquired immunodeficiency syndrome (AIDS), thereby reducing the life quality and expectancy of these patients. On the other hand, HIV co-infection significantly increases the risk of progression to VL disease in asymptomatic or subclinical individuals (Alvar et al., 2008; Ezra et al., 2010; Adriaensen et al., 2017). Indeed, it has been shown that the immunological status of HIV patients is favorable for the multiplication of *Leishmania* parasites (Adriaensen et al., 2017). Thus, both pathogens exert synergistic detrimental effect on the immune response of co-infected patients (Ezra et al., 2010).

Despite VL/HIV co-infection representing a significant public health burden, the current therapies are inefficient, and an effective treatment is remaining a challenge (Ritmeijer et al., 2011; Sinha et al., 2011; Van Griensven et al., 2014a). VL/HIV co-infection cases have higher rates of treatment failure, greater susceptibility to drug toxicity and higher lethality and relapse than in VL infected patients without HIV infection (Monge-Maillo et al., 2014; Van Griensven, 2014; Van Griensven et al., 2014c). The advent of the highly active antiretroviral therapy (HAART) improved the life quality, increased the life expectancy of HIV patients, as well as promoted a substantial reduction on the incidence of opportunistic infections (Crabtree-Ramírez et al., 2016; Lindoso et al., 2016). Particularly, HIV-aspartyl peptidase inhibitors (HIV-PIs) have been described as a powerful *in vitro* antiproliferative agents against several opportunistic pathogens (Pozio and Morales, 2005; Trudel et al., 2008; Santos et al., 2009; Santos, 2010; Lindoso et al., 2016). Previous data from our research group demonstrated that nelfinavir is an effective antileishmanial agent against promastigotes of several *Leishmania* species (Santos et al., 2013), as well as that lopinavir (LPV) affects *Leishmania*-macrophage interaction (Santos et al., 2009).

The combination therapy may be an interesting strategy to deal with the co-infection. Previous studies have shown that drug association can be very effective, reducing side effects, decreasing the induction of resistance, and allowing the prescription of lower doses to achieve the same outcome (Perron et al., 2012; Stone et al., 2014; Trinconi et al., 2014; Sun et al., 2016). Driven by the necessity of finding alternative therapeutic strategies for VL/HIV co-infection, we evaluated the combination treatment with LPV, an HIV-PI, and miltefosine (MFS) in *L. infantum* infection. Our results suggest that LPV- MFS combination therapy can be effective in the treatment of VL/HIV co-infected patients and provides data that can help to guide a possible therapeutic strategy in VL/HIV co-infection.

MATERIALS AND METHODS

Drugs and Chemicals

LPV was synthesized in the Laboratory of Chemical Synthesis, Farmanguinhos, FIOCRUZ. MFS, heat inactivated fetal bovine serum (FBS), RPMI-1640 medium, streptomycin, penicillin, hemin, D-biotin, adenine, folic acid, AlamarBlue®, and dimethylsulfoxide (DMSO) were purchased from Sigma Aldrich Chemical (St. Louis, MO, USA). Drugs were prepared in DMSO, aliquoted, and kept at −20°C until use. All other reagents were analytical grade or superior.

Parasites

Leishmania infantum (strain MHOM/MA/67/ITMAP-263) was cultivated at 26°C in RPMI medium supplemented with 10% FBS, streptomycin (100 μg/mL), penicillin (100 U/mL), hemin (5 mg/mL), D-biotin (0.2 mg/mL), adenine (4 mg/mL), and folic acid (0.5 mg/mL).

Experimental Animals and Ethics Statement

BALB/c mice (female, 6–8 weeks old) were obtained from the Institute of Science and Technology in Biomodels (ICTB-FIOCRUZ). Mice were housed five per cage and maintained in standard environmental conditions (12:12 h light:dark cycle at 22 ± 2°C) with access to food and water *ad libitum*.

Cytotoxicity Assay

The AlamarBlue® assay was used to determine the cytotoxicity of LPV and MFS in uninfected mouse macrophages. Resident peritoneal macrophages from BALB/c mice were seeded at 1×10^6 cells/mL in 200 μL supplemented RPMI into 96 well-plates at 37°C in 5% CO_2 for 4 h for adherence. Then, the plates were gently washed two times with PBS (phosphate buffered saline, 150 mM NaCl, 20 mM phosphate buffer, pH 7.2) to remove non-adherent cells, and treated with 2-fold serial dilutions of LPV and MFS concentration ranging from 400 to 3.125 μM and 40 to 0.3125 μM, respectively. After 72 h, AlamarBlue® was added to the macrophage cultures to a final concentration of 10% v/v, and the plates were then incubated at 37°C for additional 4 h. The absorbance was measured at excitation/emission of 560/590 nm (Kulshrestha et al., 2013; Cunha-Júnior et al., 2017). The results were expressed as the percentage of viable cells compared to the control cells treated with the highest DMSO dose used to dissolve the compounds.

Evaluation of *in vitro* Antileishmanial Activity

Resident peritoneal macrophages from BALB/c mice were resuspended in supplemented RPMI medium. 8×10^5 cells/well were plated in eight chamber Lab-Tek chambers (Nunc, Roskilde, Denmark). *L. infantum* promastigotes collected at the stationary phase were washed three times in PBS (3,000 × g for 10 min) and added to adherent cells at a parasite/macrophage ratio of 5:1 and incubated for 4 h at 37°C in 5% CO_2. Next, free promastigotes were removed by washing with RPMI medium and the macrophages were incubated with LPV alone or in combination with MFS at 37°C for 72 h. The solutions were prepared in proportions of 5:0, 4:1, 3:2, 2:3, 1:4, and 0:5 of LPV and MFS drugs, respectively, which were serially diluted (base 2) six times. The initial drug concentrations were 25 and 2 μM of LPV and MFS, respectively. LPV initial concentration was the highest non cytotoxic to macrophages, while for MFS, we chose the most potent (non-cytotoxic) concentration that did not completely eliminate parasites from macrophages in the single compound assays. Three independent experiments, in triplicate, were performed for each drug combination and susceptibility assay.

Finally, the slides were fixed, stained with Panoptic and the amastigotes were counted using light microscopy. The infection rate was calculated using the formula: (% of infected macrophages × average number of amastigotes per macrophage). Control experiments were performed with infected macrophages incubated with DMSO at the highest dose used to dissolve the compounds. The 50% inhibitory concentration (IC_{50}), i.e., the minimum drug concentration that caused a 50% reduction in infection rate in comparison with that in control infection without the compound, was obtained by non-linear regression using GraphPad Prism software. Each point was tested in duplicate with three biological replicates.

Fractional Inhibitory Concentration Determination and Isobologram Construction

The four fractional inhibitory concentration indexes (FICIs) of LPV, derived from association curves, were calculated using the following equation: concentration of LPV in each association curve (4:1, 3:2, 2:3, 1:4) able to inhibit 50% of the parasite growth/IC_{50} of LPV alone. The same formula was applied to MFS. The sum FICIs (ΣFICIs) were calculated as FICI of LPV plus FICI of MFS and the arithmetic mean of the FICIs obtained was compared to the reference values and reported as synergism (FICI≤ 0.5), antagonism (FICI ≥ 4.0) and additive effect of the compounds (0.5 < FICI < 4.0) (Odds, 2003). The interaction between drugs was expressed graphically as an isobologram.

Mice Infection and Treatment

BALB/c mice were infected intraperitoneally with 1.0×10^8 stationary-phase *L. infantum* promastigotes. After 7 days, animals were treated by oral gavage twice daily for 5 days with a 12 h interval between doses following the dosages described below (Katsuno et al., 2015; Cunha-Júnior et al., 2017). Thirty days post infection, the animals were euthanized, and the spleen and liver were aseptically removed, weighed, and homogenized in supplemented RPMI medium. The parasite load was estimated by limiting dilution assay (LDA) (Buffet et al., 1995). Plasma biochemical parameters investigated were aspartate aminotransferase (AST) and alanine aminotransferase (ALT), creatinine (CREA), urea, total bilirubin and cholesterol, which were measured by the Program of Technological Development in Tools for Heath PDTIS-Fiocruz.

Therapeutic Scheme

The animals were treated with either MFS, LPV or the combination of both drugs by the oral route twice daily (at 12 h intervals) for 5 days (Katsuno et al., 2015) at day seven post-infection (Cunha-Júnior et al., 2016). Animals were divided into 13 groups, as follows: (0) Control, non-infected and non-treated (CNI); (1) Control, PBS with 1% DMSO, infected and non-treated (CI); subsequently, all groups correspond to infected and treated mice, as follows: MFS at 15.4 mg/kg (2), 7.7 mg/kg (3), 3.85 mg/kg (4); LPV at 493.2 mg/kg (5), 246.6 mg/kg (6); MFS + LPV, respectively, at 7.7 mg/kg + 493.2 mg/kg (7), 7.7 mg/kg + 246.6 mg/kg (8), 3.85 mg/kg + 493.2 (9), 3.85 mg/kg + 246.6 mg/kg (10), 1.92 mg/kg + 493.2 mg/kg (11), 1.92 mg/kg + 246.6 mg/kg (12). Each group was composed of at least five mice, and the experiment was repeated three times, independently.

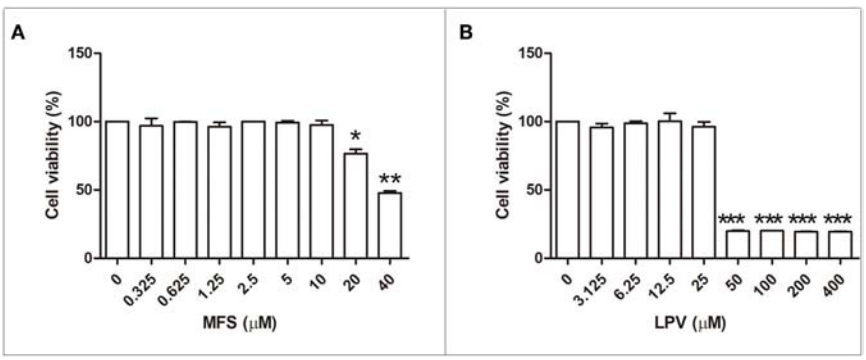

FIGURE 1 | Citotoxicity of MFS and LPV to peritoneal macrophages. Cells (1×10^6 cells/mL) were incubated in 96 well plates for 72 h in the presence of MFS **(A)** and LPV **(B)** at different concentrations. The viability of macrophages was assessed by using the Alamar blue assay. Data represent the mean (±SD) of three independent experiments. *$P < 0.05$, **$P < 0.01$, and ***$P < 0.001$.

Statistical Analyses

The results are presented as means ± standard deviation (SD) or standard error of the mean (SEM) of replicates samples from at least two independent assays. Paired comparisons between groups were carried out by Student's *t*-test or analysis. *P*-values equal or >0.05 were considered statistically significant.

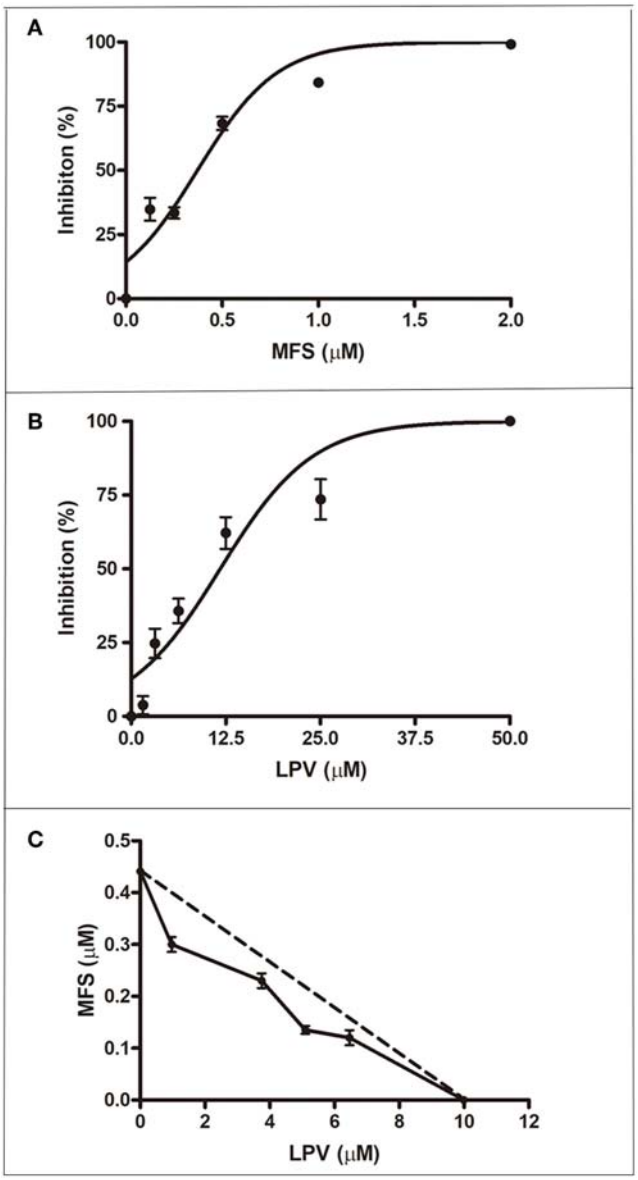

FIGURE 2 | Antiamastigote activity of MFS, LPV, and their combination. Peritoneal macrophages infected with *L. infantum* were treated with MFS **(A)**, LPV **(B)**, or both drugs associated **(C)** for 72 h at 37°C. **(C)** Isobologram analysis of antiamastigote activity of drugs combined in several proportions. Each plotted point in the isobolograms is the IC_{50} of the drug alone or in combination. The straight dashed line represents the theoretical line of additivity for each combination. Data are representative of three independent experiments and values are expressed in mean ± SD in **(A,B)** and ± SEM in **(C)**.

RESULTS

Evaluation of the *in vitro* Efficacy of LPV-MFS Combination

First, we aimed to determine the highest drug concentration of each compound that was not cytotoxic to macrophages under the assayed conditions, which were 25 and 20 μM for LPV and MFS, respectively (**Figure 1**). Then, the antiamastigote activity was evaluated for the drugs alone or associated in several proportions, as described in the materials and methods section. The antileishmanial activity of LPV and MFS was confirmed against intracellular *L. infantum* amastigotes, with IC_{50} of 9.89 ± 0.2 and 0.44 ± 0.3 μM, respectively (**Figures 2A,B**). The resulting effect of the drugs association was evaluated graphically by plotting the IC_{50} of the compounds alone or in combination as an isobologram (**Figure 2C**). In addition, the FICI value for each drug combination was calculated. The $\bar{x}$FICI was1.28 ± 0.24, indicating an additive interaction (Odds, 2003) between LPV and MFS (**Table S1**). Furthermore, none of the concentrations of the drugs tested in combination induced any significant toxicity as assessed by AlamarBlue assay (data not shown).

In vivo Efficacy of Drugs in the Murine VL Model

For *in vivo* assays, *L. infantum* infected BALB/c mice were treated with MFS at 15.4, 7.7, 3.85, and 1.92 mg per kg of body weight alone or in combination with LPV at 493.2 and 246.6 mg per kg of body weight. In MFS-treated mice, the hepatic and splenic amastigote loads were completed suppressed by 7.7 and 15.4 drug doses, respectively (**Figure 3**). This compound at 3.85 mg/kg promoted a significant reduction in the mean of parasitic load in liver (46.7% ± 7.1) and spleen (67% ± 10.5) (**Figure 3**). In LPV-treated mice the hepatic and splenic amastigote loads were statistically significant reduced by the treatment with 493.2 mg/kg to 40% (±20) and 52% (±16.4), respectively (**Figure 3**). In conclusion, as expected, MFS alone was able to reduce parasite burden compared to untreated infected control. Conversely, LPV at the highest dose tested presented a reduction in the parasite load that is not negligible.

Concerning the drug association at first, we showed that LPV did not exert any deleterious effect on MFS action by adding it at 493.2 and 246.6 mg/kg to a MFS dose that virtually eliminated the parasite (7.7 mg/kg) (**Figure 3**). Then, we tested the effect of LPV at the same concentrations on a MFS lower dose (3.85 mg/kg), which alone presented only an intermediary effect. The hepatic parasitic load was reduced in 70.15% (±4.6) and 71% (±5.6) in relation to single MFS treatment with 3.85 mg/kg or control infected mice, respectively, while no dose-response was observed between the two concentrations of LPV. In spleen, only the highest dose of LPV promoted a significant reduction (52.56% ± 16.4) in the parasite load, in relation to MFS alone (3.85 mg/kg). Finally, we analyzed the combination of MFS at 1.92 mg/kg with LPV at 493.2 and 246.6 mg/kg, this MFS dose has as a marginal effect based on the results at 3.85 mg/kg. The highest dose of LPV showed a significant reduction in hepatic (44.48% ± 20) and splenic (77% ± 6.5) parasite load (**Figure 3**).

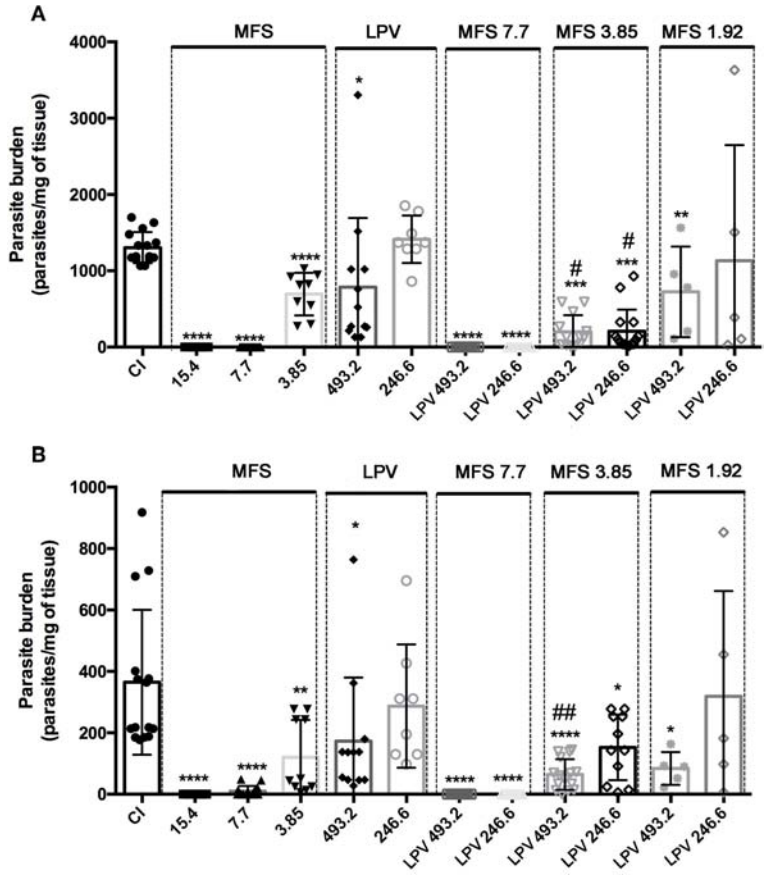

FIGURE 3 | Efficacy of MFS alone or in combination with LPV in *L. infantum in vivo* infection. Evaluation of hepatic **(A)** and splenic parasite burden **(B)** 30 days post-infection. CI, infected control. Animals were treated in day 7 post-infection by oral gavage twice daily for 5 days with a 12 h interval between doses. Data are presented as the mean ± SD. $^{*}P < 0.05$; $^{**}P < 0.01$; $^{****}P < 0.0001$ versus CI. $^{\#}P < 0.05$ vs. MFS 3.85; $^{\#\#}P < 0.01$ vs. MFS 3.85.

As expected, CI group presented a significant increase in spleen and liver relative weight when compared to CNI (**Figure 4**). A significant decrease in the liver weight in comparison to CI was only observed in the infected mice treated with 493.2/3.85 mg/kg of LPV/MFS (5.57% ± 0.82), while no statistical significance is observed when compared to CNI (**Figure 4A**), which indicates that a high dosage of LPV combined with MFS at 3.85 mg/kg reverted the liver weight to the levels of health individuals. The relative weight of spleen was significantly reduced in comparison to CI in mice treated with 493.2/7.7 and 493.2/3.85 mg/kg of LPV/MFS in 29.34% (SD 1.09) and 14.4% (SD 0.48), respectively (**Figure 4B**). Both treatments were able to revert the spleen weight to the levels of health individuals (**Figure 4B**). Finally, at the end of the treatment, the hepatic toxicity was evaluated by measuring the plasma levels of total bilirubin, ALT and AST (**Table S2**). No significant changes were observed in the bilirubin and ALT levels in comparison to CI. Increased circulation levels of AST were found in the serum of animals treated with MFS at 15.4 and 7.7 mg/kg, LPV at the highest dose (493.2 mg/kg) and in all combination doses. However, the AST values found for all doses tested are inside the normal range for mice (AST = 54-298 U/I) (Wege et al., 2012). The renal function was also evaluated and no significant changes for creatinine or urea levels in plasma of untreated and treated animals was observed (**Table S2**). Moreover, no differences were found in the serum cholesterol levels among all studied groups (**Table S2**). These data point out that the combined therapy did not present any relevant hepatotoxicity and impact on mice, under the assayed parameters.

DISCUSSION

The aim of this study was to evaluate the antileishmanial effect of LPV and MFS combination in an infection caused by *L. infantum* using *in vitro* and *in vivo* murine model of VL. The nature of interaction between the drugs was first determined as additive *in vitro*. This prompted us to assay the association *in vivo* in BALB/c mice infected with *L. infantum*, and the additive effect of both drugs observed *in vitro* was reproduced *in vivo*.

MFS interferes on *L. donovani* lipid metabolism, inducing an increase in sphingolipid and ergosterol content (Armitage et al., 2018). Sterol biosynthesis is a crucial pathway that leads to the production of ergosterol in *Leishmania* parasites, and therefore, it is an interesting chemotherapeutic target. Unlike mammalian cells, trypanosomatids synthesize C24-alkylated and ergostane-based sterols (Goad et al., 1984; McCall et al., 2015). Therefore, compounds that interfere with the sterol pathway are promising drugs in treating leishmaniasis. In addition, drugs that act synergistically on different points of the same pathway represent an attractive strategy for antimicrobial chemotherapy (Roberts et al., 2003; Andrade-Neto et al., 2016). In this sense, our group showed that LPV also alters the lipid composition on *L. amazonensis*, mainly interfering in sterol composition and causing a pronounced accumulation of cholesterol-ester in treated parasites (Rebello et al., 2018). Although the intracellular target or death mechanism of the HIV-PIs are not totally elucidated in trypanosomatids, it is also likely that they interact and inhibit trypanosomatids aspartyl peptidases (Santos et al., 2013; Castilho et al., 2018). Therefore, considering the multiple and diverse targets of each compound, the additive effect reported here was expected.

Recently, Valdivieso et al. reported the effects of the combined therapy with nelfinavir, another HIV-PI, and MFS in a murine infection by *L. infantum* (MCAN/ES/98/LLM-724) (Valdivieso et al., 2018). Mice experimentally infected were treated in day 15 by intraperitoneal injection of nelfinavir and MFS during 15 days, and then parasitemia was measured. This treatment is in high contrast to our scheme, which was oral gavage twice a day, for only 5 days in the seventh day post-infection. Mice were then sacrificed on day 30-post infection, therefore, before parasitemia was assessed, mice continued alive with no treatment during 18 days. Although Valdivieso et al. recently reported a more prominent combined effect, the treatment scheme reported here, strongly challenge the compounds efficacy, and the oral gavage, more closely resembles the administration route that is used for human patients, since MFS and HIV-PIs are oral drugs (Jha et al., 1999; Dorlo et al., 2012; Crabtree-Ramírez et al., 2016).

In the scenario of increasing cases of HIV/Leishmania co-infection, the data presented herein from oral-treated mice during only 5 days can help to guide the design of clinical trials for the specific management of co-infected individuals. The oral combined therapy of LPV-MFS was effective in reducing the parasite loads in animal models of visceral Leishmaniasis and boosted the effect of lower doses of MFS. We demonstrated the potential value of combining available oral and safer drugs as a promising strategy to treat VL/HIV co-infection patients, and envision the possibility of achieving the same treatment outcome with lower compounds dosages, which can prevent or delay drug resistance and reduce side effects in patients.

DATA AVAILABILITY

All datasets generated for this study are included in the manuscript and/or the **Supplementary Files.**

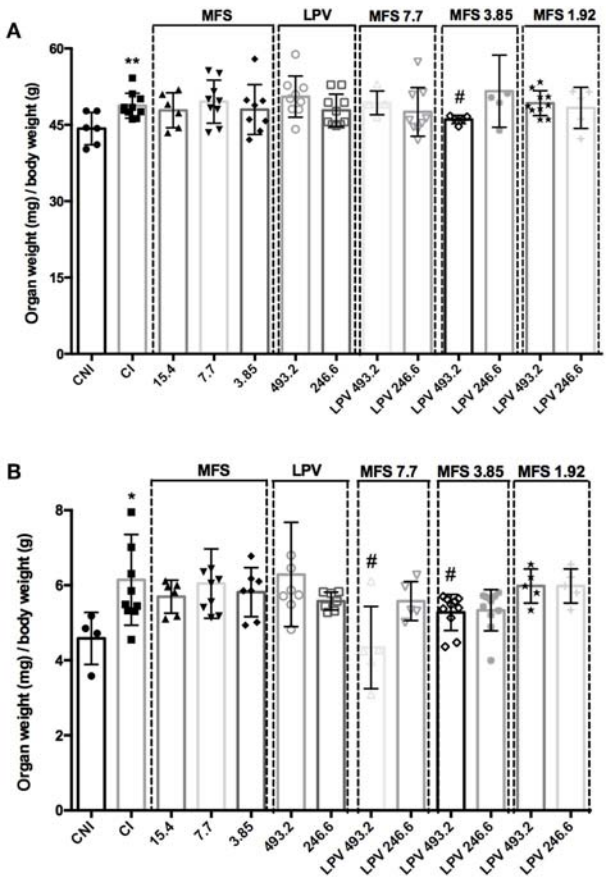

FIGURE 4 | Relative organ weights of mice in different treatment with MFS alone or in combination with LPV. **(A)** Liver, **(B)** Spleen. Animals were treated in day 7 post-infection by oral gavage twice daily for 5 days with a 12 h interval between doses. The control group (CI) was treated with 1% DMSO in saline via the oral route. A non-infected and non-treated control group (CNI) was also evaluated. $^{*}P < 0.05$ vs. CNI; $^{**}P < 0.01$ vs. CNI; $^{\#}P < 0.05$ vs. CI.

ETHICS STATEMENT

This study was carried out in accordance with the protocols approved by the Ethics Committee for Animal Use of the Instituto Oswaldo Cruz (CEUA-FIOCRUZ, license number: L-026/2015).

AUTHOR CONTRIBUTIONS

KR and VA-N performed experiments and data analysis. CG and MS provided reagents. MB and AS gave some advices for the work and provided valuable support with the writing. ET-S and Cd'A-L directed and coordinated the study. KR wrote the manuscript and all authors participated in editing it.

FUNDING

This work was supported by the Fundação Carlos Chagas Filho de Amparo à Pesquisa do Estado do Rio de Janeiro (FAPERJ),

Conselho Nacional de Desenvolvimento Científico e Tecnológico (CNPq), Coordenação de Aperfeiçoamento de Pessoal de Nível Superior (CAPES, financial code 001), and Fundação Oswaldo Cruz. KR and VA-N are supported by the FAPERJ grade 10 program. MB, AS, ET-S and Cd'A-L are CNPq research productivity fellows.

ACKNOWLEDGMENTS

We thank the Program of Technological Development in Tools for Health-PDTIS-FIOCRUZ for use of its facilities.

SUPPLEMENTARY MATERIAL

The Supplementary Material for this article can be found online at: https://www.frontiersin.org/articles/10.3389/fcimb.2019.00229/full#supplementary-material

Table S1 | IC_{50}, $FICI_{50}$, and $\Sigma FICI_{50}$ of LPV-MFS combination against *L. infantum* intracellular amastigotes.

Table S2 | Comparison of biochemical parameters between untreated (CI, control infected) and treated parasites with MFS or LPV administered alone or in combination. Levels of creatinine, urea, total bilirubin, cholesterol, AST (Alanine amino transferase), and ALT (Aspartate amino transferase) are shown. The data are mean ± SD of three independent experiments. $^{*}P < 0.05$, $^{**}P < 0.01$.

REFERENCES

Adriaensen, W., Dorlo, T. P. C., Vanham, G., Kestens, L., Kaye, P. M., and Van Griensven, J. (2017). Immunomodulatory therapy of visceral leishmaniasis in human immunodeficiency virus-coinfected patients. *Front. Immunol.* 8:1943. doi: 10.3389/fimmu.2017.01943

Agostoni, C., Dorigoni, N., Malfitano, A., Caggese, L., Marchetti, G., Corona, S., et al. (1998). Mediterranean leishmaniasis in HIV-infected patients: epidemiological, clinical, and diagnostic features of 22 cases. *Infection* 26, 93–99. doi: 10.1007/BF02767767

Alvar, J., Aparicio, P., Aseffa, A., Den Boer, M., Cañavate, C., Dedet, J. P., et al. (2008). The relationship between leishmaniasis and AIDS: the second 10 years. *Clin. Microbiol. Rev.* 21, 334–359. doi: 10.1128/CMR.00061-07

Andrade-Neto, V. V., Pereira, T. M., Canto-Cavalheiro, Md., and Torres-Santos, E. C. (2016). Imipramine alters the sterol profile in *Leishmania amazonensis* and increases its sensitivity to miconazole. *Parasit. Vectors* 9:183. doi: 10.1186/s13071-016-1467-8

Armitage, E. G., Alqaisi, A. Q. I., Godzien, J., Peña, I., Mbekeani, A. J., Alonso-Herranz, V., et al. (2018). Complex interplay between sphingolipid and sterol metabolism revealed by perturbations to the leishmania metabolome caused by miltefosine. *Antimicrob. Agents Chemother.* 62, e02095–e02017. doi: 10.1128/AAC.02095-17

Buffet, P. A., Sulahian, A., Garin, Y. J., Nassar, N., and Derouin, F. (1995). Culture microtitration: a sensitive method for quantifying *Leishmania infantum* in tissues of infected mice. *Antimicrob. Agents Chemother.* 39, 2167–2168. doi: 10.1128/AAC.39.9.2167

Burza, S., Croft, S. L., and Boelaert, M. (2018). Leishmaniasis. *Lancet* 392, 951–970. doi: 10.1016/S0140-6736(18)31204-2

Burza, S., Mahajan, R., Sinha, P. K., Van Griensven, J., Pandey, K., Lima, M. A., et al. (2014). Visceral leishmaniasis and HIV co-infection in Bihar, India: long-term effectiveness and treatment outcomes with liposomal amphotericin B (AmBisome). *PLoS Negl. Trop. Dis.* 8:e3053. doi: 10.1371/journal.pntd.0003053

Castilho, V. V. S., Gonçalves, K. C. S., Rebello, K. M., Baptista, L. P. R., Sangenito, L. S., Santos, H. L. C., et al. (2018). Docking simulation between HIV peptidase inhibitors and *Trypanosoma cruzi* aspartyl peptidase. *BMC Res. Notes* 11:825. doi: 10.1186/s13104-018-3927-z

Crabtree-Ramírez, B., Caro-Vega, Y., Shepherd, B. E., Grinsztejn, B., Wolff, M., Cortes, C. P., et al. (2016). Time to HAART initiation after diagnosis and treatment of opportunistic infections in patients with AIDS in Latin America. *PLoS ONE* 11:e0153921. doi: 10.1371/journal.pone.0153921

Cunha-Júnior, E. F., Andrade-Neto, V. V., Lima, M. L., Da Costa-Silva, T. A., Galisteo Junior, A. J., Abengóza, M. A., et al. (2017). Cyclobenzaprine raises ROS levels in *Leishmania infantum* and reduces parasite burden in infected mice. *PLoS Negl. Trop. Dis.* 11:e0005281. doi: 10.1371/journal.pntd.0005281

Cunha-Júnior, E. F., Martins, T. M., Canto-Cavalheiro, M. M., Marques, P. R., Portari, E. A., Coelho, M. G., et al. (2016). Preclinical studies evaluating subacute toxicity and therapeutic efficacy of LQB-118 in experimental visceral leishmaniasis. *Antimicrob. Agents Chemother.* 60, 3794–3801. doi: 10.1128/AAC.01787-15

Dorlo, T. P., Balasegaram, M., Beijnen, J. H., and De Vries, P. J. (2012). Miltefosine: a review of its pharmacology and therapeutic efficacy in the treatment of leishmaniasis. *J. Antimicrob. Chemother.* 67, 2576–2597. doi: 10.1093/jac/dks275

Ezra, N., Ochoa, M. T., and Craft, N. (2010). Human immunodeficiency virus and leishmaniasis. *J. Glob. Infect. Dis.* 2, 248–257. doi: 10.4103/0974-777X.68528

Goad, L. J., Holz, G. G. Jr., and Beach, D. H. (1984). Sterols of *Leishmania* species. implications for biosynthesis. *Mol. Biochem. Parasitol.* 10, 161–170. doi: 10.1016/0166-6851(84)90004-5

Jha, T. K., Sundar, S., Thakur, C. P., Bachmann, P., Karbwang, J., Fischer, C., et al. (1999). Miltefosine, an oral agent, for the treatment of Indian visceral leishmaniasis. *N. Engl. J. Med.* 341, 1795–1800. doi: 10.1056/NEJM199912093412403

Katsuno, K., Burrows, J. N., Duncan, K., Hooft Van Huijsduijnen, R., Kaneko, T., Kita, K., et al. (2015). Hit and lead criteria in drug discovery for infectious diseases of the developing world. *Nat. Rev. Drug Discov.* 14, 751–758. doi: 10.1038/nrd4683

Kulshrestha, A., Bhandari, V., Mukhopadhyay, R., Ramesh, V., Sundar, S., Maes, L., et al. (2013). Validation of a simple resazurin-based promastigote assay for the routine monitoring of miltefosine susceptibility in clinical isolates of *Leishmania donovani*. *Parasitol. Res.* 112, 825–828. doi: 10.1007/s00436-012-3212-3

Lima, I. D., Lima, A. L. M., Mendes-Aguiar, C. O., Coutinho, J. F. V., Wilson, M. E., Pearson, R. D., et al. (2018). Changing demographics of visceral leishmaniasis in northeast Brazil: lessons for the future. *PLoS Negl. Trop. Dis.* 12:e0006164. doi: 10.1371/journal.pntd.0006164

Lindoso, J. A., Cunha, M. A., Queiroz, I. T., and Moreira, C. H. (2016). Leishmaniasis-HIV coinfection: current challenges. *HIV AIDS* 8, 147–156. doi: 10.2147/HIV.S93789

Lukes, J., Mauricio, I. L., Schönian, G., Dujardin, J. C., Soteriadou, K., Dedet, J. P., et al. (2007). Evolutionary and geographical history of the *Leishmania donovani* complex with a revision of current taxonomy. *Proc. Natl. Acad. Sci. U.S.A.* 104, 9375–9380. doi: 10.1073/pnas.0703678104

McCall, L. I., El Aroussi, A., Choi, J. Y., Vieira, D. F., De Muylder, G., Johnston, J. B., et al. (2015). Targeting ergosterol biosynthesis in *Leishmania donovani*: essentiality of sterol 14 alpha-demethylase. *PLoS Negl. Trop. Dis.* 9:e0003588. doi: 10.1371/journal.pntd.0003588

Monge-Maillo, B., Norman, F. F., Cruz, I., Alvar, J., and López-Vélez, R. (2014). Visceral leishmaniasis and HIV coinfection in the Mediterranean region. *PLoS Negl. Trop. Dis.* 8:e3021. doi: 10.1371/journal.pntd.0003021

Nascimento, E. T., Moura, M. L., Queiroz, J. W., Barroso, A. W., Araujo, A. F., Rego, E. F., et al. (2011). The emergence of concurrent HIV-1/AIDS and visceral leishmaniasis in Northeast Brazil. *Trans. R. Soc. Trop. Med. Hyg.* 105, 298–300. doi: 10.1016/j.trstmh.2011.01.006

Odds, F. C. (2003). Synergy, antagonism, and what the chequerboard puts between them. *J. Antimicrob. Chemother.* 52:1. doi: 10.1093/jac/dkg301

Perron, G. G., Kryazhimskiy, S., Rice, D. P., and Buckling, A. (2012). Multidrug therapy and evolution of antibiotic resistance: when order matters. *Appl. Environ. Microbiol.* 78, 6137–6142. doi: 10.1128/AEM.01078-12

Pozio, E., and Morales, M. A. (2005). The impact of HIV-protease inhibitors on opportunistic parasites. *Trends Parasitol.* 21, 58–63. doi: 10.1016/j.pt.2004.11.003

Ready, P. D. (2014). Epidemiology of visceral leishmaniasis. *Clin. Epidemiol.* 6, 147–154. doi: 10.2147/CLEP.S44267

Rebello, K. M., Andrade-Neto, V. V., Zuma, A. A., Motta, M. C. M., Gomes, C. R. B., De Souza, M. V. N., et al. (2018). Lopinavir, an HIV-1 peptidase inhibitor, induces alteration on the lipid metabolism of *Leishmania amazonensis* promastigotes. *Parasitology* 145, 1304–1310. doi: 10.1017/S0031182018000823

Ritmeijer, K., Ter Horst, R., Chane, S., Aderie, E. M., Piening, T., Collin, S. M., et al. (2011). Limited effectiveness of high-dose liposomal amphotericin B (AmBisome) for treatment of visceral leishmaniasis in an Ethiopian population with high HIV prevalence. *Clin. Infect. Dis.* 53, e152–158. doi: 10.1093/cid/cir674

Roberts, C. W., Mcleod, R., Rice, D. W., Ginger, M., Chance, M. L., and Goad, L. J. (2003). Fatty acid and sterol metabolism: potential antimicrobial targets in apicomplexan and trypanosomatid parasitic protozoa. *Mol. Biochem. Parasitol.* 126, 129–142. doi: 10.1016/S0166-6851(02)00280-3

Santos, A. L. S. (2010). HIV aspartyl protease inhibitors as promising compounds against *Candida albicans* André Luis Souza dos Santos. *World J. Biol. Chem.* 1, 21–30. doi: 10.4331/wjbc.v1.i2.21

Santos, L. O., Marinho, F. A., Altoé, E. F., Vitorio, B. S., Alves, C. R., Britto, C., et al. (2009). HIV aspartyl peptidase inhibitors interfere with cellular proliferation, ultrastructure and macrophage infection of *Leishmania amazonensis*. *PLoS ONE* 4:e4918. doi: 10.1371/journal.pone.0004918

Santos, L. O., Vitório, B. S., Branquinha, M. H., Pedroso E Silva, C. M., Santos, A. L. S., and D'avila-Levy, C. M. (2013). Nelfinavir is effective in inhibiting the multiplication and aspartic peptidase activity of *Leishmania* species, including strains obtained from HIV-positive patients. *J. Antimicrob. Chemother.* 68, 348–353. doi: 10.1093/jac/dks410

Singh, S. (2014). Changing trends in the epidemiology, clinical presentation, and diagnosis of Leishmania-HIV co-infection in India. *Int. J. Infect. Dis.* 29, 103–112. doi: 10.1016/j.ijid.2014.07.011

Sinha, P. K., Van Griensven, J., Pandey, K., Kumar, N., Verma, N., Mahajan, R., et al. (2011). Liposomal amphotericin B for visceral leishmaniasis in human immunodeficiency virus-coinfected patients: 2-year treatment outcomes in Bihar, India. *Clin. Infect. Dis.* 53, e91–98. doi: 10.1093/cid/cir521

Stone, L. S., German, J. P., Kitto, K. F., Fairbanks, C. A., and Wilcox, G. L. (2014). Morphine and clonidine combination therapy improves therapeutic window in mice: synergy in antinociceptive but not in sedative or cardiovascular effects. *PLoS ONE* 9:e109903. doi: 10.1371/journal.pone.0109903

Sun, W., Sanderson, P. E., and Zheng, W. (2016). Drug combination therapy increases successful drug repositioning. *Drug Discov. Today* 21, 1189–1195. doi: 10.1016/j.drudis.2016.05.015

Trinconi, C. T., Reimão, J. Q., Yokoyama-Yasunaka, J. K., Miguel, D. C., and Uliana, S. R. (2014). Combination therapy with tamoxifen and amphotericin B in experimental cutaneous leishmaniasis. *Antimicrob. Agents Chemother.* 58, 2608–2613. doi: 10.1128/AAC.01315-13

Trudel, N., Garg, R., Messier, N., Sundar, S., Ouellette, M., and Tremblay, M. J. (2008). Intracellular survival of *Leishmania* species that cause visceral leishmaniasis is significantly reduced by HIV-1 protease inhibitors. *J. Infect. Dis.* 198, 1292–1299. doi: 10.1086/592280

Valdivieso, E., Mejias, F., Carrillo, E., Sanchez, C., and Moreno, J. (2018). Potentiation of the leishmanicidal activity of nelfinavir in combination with miltefosine or amphotericin B. *Int. J. Antimicrob. Agents* 52, 682–687. doi: 10.1016/j.ijantimicag.2018.06.016

Van Griensven, J. (2014). Visceral leishmaniasis and HIV coinfection in Bihar, India: a wake-up call? *Clin. Infect. Dis.* 59, 556–558. doi: 10.1093/cid/ciu334

Van Griensven, J., Carrillo, E., López-Vélez, R., Lynen, L., and Moreno, J. (2014a). Leishmaniasis in immunosuppressed individuals. *Clin. Microbiol. Infect.* 20, 286–299. doi: 10.1111/1469-0691.12556

Van Griensven, J., Diro, E., Lopez-Velez, R., Ritmeijer, K., Boelaert, M., Zijlstra, E. E., et al. (2014b). A screen-and-treat strategy targeting visceral leishmaniasis in HIV-infected individuals in endemic East African countries: the way forward? *PLoS Negl. Trop. Dis.* 8:e3011. doi: 10.1371/journal.pntd.0003011

Van Griensven, J., Zijlstra, E. E., and Hailu, A. (2014c). Visceral leishmaniasis and HIV coinfection: time for concerted action. *PLoS Negl. Trop. Dis.* 8:e3023. doi: 10.1371/journal.pntd.0003023

Wege, A. K., Florian, C., Ernst, W., Zimara, N., Schleicher, U., Hanses, F., et al. (2012). *Leishmania major* infection in humanized mice induces systemic infection and provokes a nonprotective human immune response. *PLoS Negl. Trop. Dis.* 6:e1741. doi: 10.1371/journal.pntd.0001741

Yimer, M., Abera, B., Mulu, W., Zenebe, Y., and Bezabih, B. (2014). Proportion of visceral leishmaniasis and human immune deficiency virus co-infection among clinically confirmed visceral leishmaniasis patients at the endemic foci of the Amhara National Regional State, North-West Ethiopia. *Am. J. Biomed. Life Sci.* 2, 1–7. doi: 10.11648/j.ajbls.20140201.11

Conflict of Interest Statement: The authors declare that the research was conducted in the absence of any commercial or financial relationships that could be construed as a potential conflict of interest.

frontiers in Cellular and Infection Microbiology

ORIGINAL RESEARCH
published: 10 July 2019
doi: 10.3389/fcimb.2019.00240

Intraspecies Polymorphisms in the Lipophosphoglycan of *L. braziliensis* Differentially Modulate Macrophage Activation via TLR4

Tamara da Silva Vieira[1], *Jeronimo Nunes Rugani*[1], *Paula Monalisa Nogueira*[1], *Ana Cláudia Torrecilhas*[2], *Celia Maria Ferreira Gontijo*[1], *Albert Descoteaux*[3] *and Rodrigo Pedro Soares*[1]*

[1] *Instituto René Rachou, Fundação Oswaldo Cruz - FIOCRUZ, Belo Horizonte, Brazil,* [2] *Universidade Federal de São Paulo, UNIFESP, Diadema, Brazil,* [3] *INRS-Institut Armand-Frappier, Université du Québec, Laval, QC, Canada*

Lipophosphoglycan (LPG) is the major *Leishmania* surface glycoconjugate having importance during the host-parasite interface. *Leishmania* (*Viannia*) *braziliensis* displays a spectrum of clinical forms including: typical cutaneous leishmaniasis (TL), mucocutaneous (ML), and atypical lesions (AL). Those variations in the immunopathology may be a result of intraspecies polymorphisms in the parasite's virulence factors. In this context, we evaluated the role of LPG of strains originated from patients with different clinical manifestations and the sandfly vector. Six isolates of *L. braziliensis* were used: M2903, RR051 and RR418 (TL), RR410 (AL), M15991 (ML), and M8401 (vector). LPGs were extracted and purified by hydrophobic interaction. Peritoneal macrophages from C57BL/6 and respective knock-outs (TLR2$^{-/-}$ and TLR-4$^{-/-}$) were primed with IFN-γ and exposed to different LPGs for nitric oxide (NO) and cytokine production (IL-1β, IL-6, IL-12, and TNF-α). LPGs differentially activated the production of NO and cytokines via TLR4. In order to ascertain if such functional variations were related to intraspecies polymorphisms in the LPG, the purified glycoconjugates were subjected to western blot with specific LPG antibodies (CA7AE and LT22). Based on antibody reactivity preliminary variations in the repeat units were detected. To confirm these findings, LPGs were depolymerized for purification of repeat units. After thin layer chromatography, intraspecies polymorphisms were confirmed especially in the type and/size of sugars branching-off the repeat units motif. In conclusion, different isolates of *L. braziliensis* from different clinical forms and hosts possess polymorphisms in their LPGs that functionally affected macrophage responses.

Keywords: ***Leishmania braziliensis*, virulence, lipophosphoglycan, clinical forms, macrophages, innate immunity**

OPEN ACCESS

Edited by:
Anabela Cordeiro-da-Silva, University of Porto, Portugal

Reviewed by:
Renato Augusto DaMatta, Universidade Estadual do Norte Fluminense Darcy Ribeiro, Brazil
Gaoqian Feng, Burnet Institute, Australia

***Correspondence:**
Rodrigo Pedro Soares
rodrigo.pedro@fiocruz.br

Specialty section:
This article was submitted to Parasite and Host, a section of the journal Frontiers in Cellular and Infection Microbiology

Received: *25 April 2019*
Accepted: *18 June 2019*
Published: *10 July 2019*

Citation:
Vieira TdS, Rugani JN, Nogueira PM, Torrecilhas AC, Gontijo CMF, Descoteaux A and Soares RP (2019) Intraspecies Polymorphisms in the Lipophosphoglycan of L. braziliensis Differentially Modulate Macrophage Activation via TLR4. Front. Cell. Infect. Microbiol. 9:240. doi: 10.3389/fcimb.2019.00240

INTRODUCTION

The Lipophosphoglycan (LPG) is the most studied glycoconjugate expressed by *Leishmania*. It is a pathogen-associated molecular pattern (PAMP) covering the entire promastigote surface and flagellum and is implicated in a wide variety of events during the interaction of the parasite with vertebrate and invertebrate hosts. Inter and intraspecies polymorphisms in the

LPGs and glycoinositolphospholipids (GIPLs) structures from several species have been reported as important for the virulence mechanisms especially during the innate immune compartment (Becker et al., 2003; de Veer et al., 2003; Spath et al., 2003; De Assis et al., 2012).

LPG comprises four distinct domains: a lipid anchor consisting of 1-*O*-alkyl-2-*lyso*-phosphatidylinositol, a central core represented by a heptassacaride Gal (α1,6)Gal(α1 (3)Gal_f(β1,3)[Glc(α1)-PO_4]Man(α1,3)Man(α1,4)-GlcN(α1), a conserved backbone of repeating Gal(β1,4)Man(α1)-PO_4 units and a terminal oligosaccharide named cap (Turco and Descoteaux, 1992). Most of the polymorphisms in the structure of LPG are located in the repeat units and cap structures. Several functions have been attributed to LPG including: inhibition of phagosome maturation and acidification (Desjardins and Descoteaux, 1997; Vinet et al., 2009), inhibition of PKC (Holm et al., 2001), induction of PKR (de Carvalho Vivarini et al., 2011), induction of extracellular neutrophil networks (NETs) (Guimaraes-Costa et al., 2009; Gabriel et al., 2010), induction of heme-oxygenase I (Luz et al., 2012), LTB4 (Tavares et al., 2014), PPAR-γ (Lima et al., 2017) and modulation of NO/cytokines, MAPKs and NF-kB translocation, TLR2/TLR4 agonist (De Assis et al., 2012; Ibraim et al., 2013; Paranaíba et al., 2015; Nogueira et al., 2016). However, there are still uncertainties in how intraspecies structural and compositional polymorphisms of LPG affect parasite virulence.

Polymorphisms in the repeat units of LPGs have already been reported in several species/strains of *Leishmania* from Old and New World (De Assis et al., 2012). Studies on intraspecies LPG polymorphisms are scarce and used a limited number of strains. For example, in Old World strains of *L. donovani* (1S-1D and MONGI) (Mahoney et al., 1999), *L. major* (FV1 and LV39) (Dobson et al., 2003) and *L. tropica* (L747, L810, and L863) (Soares et al., 2004). On the other hand, most of the studies have characterized LPG polymorphisms in New World strains including: *L. infantum* (14 strains) (Coelho-Finamore et al., 2011), *L. enriettii* (L88 and Cobaia) (Paranaíba et al., 2015), and *L. amazonensis* (PH8 and Josefa) (Nogueira et al., 2017). Studies on the glycobiology of *L. braziliensis* started in 2005, where the structure of the LPG strain M2903 was characterized as important during the interaction with the sandfly vector (Soares et al., 2005, 2010). In the procyclic form it has no side-chains branching-off the repeat units, whereas in the metacyclic stage it possesses 1-2 β-glucose side-chains (Soares et al., 2005). In mouse macrophages, *L. braziliensis* LPG was more pro-inflammatory than that of *L. infantum*. It was a stronger TLR2/TLR4 agonist inducing NO and cytokine production and NF-κB translocation (Ibraim et al., 2013). It is already known that intraspecies polymorphisms in the *L. infantum* LPG results in differential production of NO by murine macrophages (Coelho-Finamore et al., 2011). In this species, there are three types of LPG (I, II, and III) depending on the presence/absence of β-glucose side chains. Although *L. braziliensis* LPG is a very pro-inflammatory PAMP among different *Leishmania* species, nothing is known about intraspecies polymorphisms in this glycoconjugate.

In Americas, *L. braziliensis* causes either single cutaneous lesions (TL) at the site of the bite or metastasizes to the oronasopharyngeal mucosa (ML). Some lesions characterized as atypical (AL) of *L. braziliensis* have been previously reported by Guimarães et al. (2009) and more recently by Quaresma et al. (2018). Interestingly, some lesions are somewhat unusual, hindering correct clinical diagnosis. Those are so called atypical lesions (AL): they are lupoid, verrucous sometimes resembling to tumors that do not fit in the regular shape of the TL lesions. Previous findings showed a differential expression of cytokines/chemokines in AL patients compared to TL patients (Costa-Silva et al., 2014). AL lesions are more difficult to heal, and this was probably due to natural resistance to Sb-based chemotherapeutic schemes (Rugani et al., 2018). However, it is still unknown if LPGs from *L. braziliensis* may be responsible for the virulence degrees observed in several strains of this species.

Here, we intend to investigate if the intraspecies variability in LPGs from different clinical forms and hosts are associated to the immunopathological events in *L. braziliensis*.

MATERIALS AND METHODS

Ethics Statement

All animals were handled in strict accordance with animal practice as defined by Internal Ethics Committee in Animal Experimentation (CEUA) of Fundação Oswaldo Cruz (FIOCRUZ), Belo Horizonte, Minas Gerais (MG), Brazil (Protocol L-32/16). The procedures for strains isolation from humans were carried out in accordance with the recommendations of the National Committee for Research Ethics (CONEP # 355/2008).

Cell Culture

Leishmania braziliensis reference strains were used including: MHOM/BR/75/M2903 (TL), MHOM/BR/1996/M15991 (ML), IWELL/BR/1981/M8401 (vector). Other isolates included (RR051 and RR418) (TL) and RR410 (AL). Those strains were isolated from human patients in the Xakriabá indigenous community located in São João das Missões, Minas Gerais State, Brazil (Quaresma et al., 2018). Those strains were previously typed as reported (Rugani et al., 2018). Starter cultures of promastigotes were grown in supplemented Medium 199 as reported elsewhere (Soares et al., 2002).

Extraction and Purification of LPG

LPG extraction was performed as described elsewhere with solvent E (H_2O/ethanol/diethylether/pyridine/NH_4OH; 15:15:5:1:0.017) after a sequential organic solvent extraction. For purification, the solvent E extract was dried under N_2 evaporation, resuspended in 2 mL of 0.1N acetic acid/0.1 M NaCl, and applied onto a column with 2 mL of phenyl-Sepharose, equilibrated in the same buffer (Soares et al., 2002, 2004).

Macrophages, Nitrite, and Cytokines

Thioglycollate-elicited peritoneal macrophages were extracted from C57BL/6 and C57BL/6 (TLR2 and TLR4 knockouts) as previously reported (Ibraim et al., 2013; Nogueira et al., 2016). Briefly, recovered cells (3×10^5 cells/well) were washed with fresh RPMI and cultured in the same medium supplemented

with 2 mM glutamine, 50 U/ml of penicillin and 50 μg/mL streptomycin, 10% Fetal Bovine Serum in 96-well culture plates (37°C, 5% CO_2). Cells were primed with gamma interferon (IFN-γ) (3 IU/mL) for 18 h prior to incubation with LPGs (10 μg/mL) from all strains and controls for 48 h. Those included LPS (100 ng/mL, positive) and medium (negative). The nitrite concentration was measured by Griess reaction. For cytokine detection, supernatants were collected and IL-1β, IL-6, IL-12, and TNF-α were determined using BD CBA Mouse Cytokine assay kits according to the manufacturer's specifications (BD Biosciences, CA, USA). Flow cytometry measurements were performed on a FACS Calibur flow cytometry (BD Bioscience, Mountain View, CA, USA). Cell-Quest TM software package provided by the manufacturer was used for data acquisition and the FlowJo software 7.6.4 (Tree Star Inc., Ashland, OR, USA) was used for data analysis (Nogueira et al., 2016).

Western Blot

Purified LPGs (10 μg) were resolved by SDS-PAGE electrophoresis and transferred to nitrocellulose membrane. Blots were probed with monoclonal antibody (mAb) CA7AE (1:1,000), that recognizes the unsubstituted Gal(β1,4)Man(α1)-PO_4 repeat units (Tolson et al., 1989) and LT22 (1:1,000) that recognizes β-glucose/β-galactose side chains. After washing in PBS (3 × 5 min), the membrane was incubated for 1 h with antimouse IgG conjugated with peroxidase (1:10,000) and the reaction was visualized using luminol (Soares et al., 2005; Nogueira et al., 2017).

Biochemical Analysis

Promastigotes were radiolabeled during stationary phase 1.0 × 10^8-10^9 cells/mL with 90 uCi/ml_of [6-^{3}H]Gal at 26°C for 8 h as previously reported (Soares et al., 2005). [3H-Gal]-LPG was extracted and purified as described above. LPGs were depolymerized by mild acid hydrolysis (0.02 N HCl, 100°C, 5 min) in order to separate the repeating units and caps. Samples were subjected to the butanol: water partition (1:2) to remove core-PI motifs. Purified repeat units were recovered and subjected to enzymatic treatments with alkaline phosphatase prior to glycosidases (Mahoney et al., 1999). After enzymatic treatments, samples were desalted through a two-layered column of AG50W-X12(H+) over AG1-X8 (acetate). Phosphorylated oligosaccharides were treated with alkaline phosphatase in 15 mM Tris buffer, pH 9.0 (1 U, 16 h, 37°C). Neutral oligosaccharides were treated with sweet almond β-glucosidase in 200 mM ammonium acetate buffer, pH 5.0 (1 U, 16 h, 37°C). The repeat units treated with β-glucosidase were subject to thin layer chromatography technique (TLC). Samples were applied on silica plates and run in butanol pyridine water (6:4:3) solution for 20 h. Quantification of the radioactivity were performed using the Tri-Carb-1600 TR (Soares et al., 2002).

Data Analyses

Statistical analyses and graphics construction were performed using one-way ANOVA test with Software GraphPad Prism 6.0 (GraphPadSoftware Inc., San Diego, CA, EUA). The analyses were done after normality test of Kolmogorov-Smirnov. $P < 0.05$ was considered significant.

RESULTS

Macrophage Activation

Murine macrophages were exposed to LPGs from different strains to evaluate the impact on the innate immune response. In general, the various LPGs induced NO, IL-6, IL-12, and TNF-α production preferentially via TLR4 (**Figures 1**, **2**). However, this production varied among *L. braziliensis* strains. For example, LPG from M15991strain (ML) did not induce considerable levels of NO and cytokines. On the other hand, the LPG from the vector strain (M8401) was very proinflammatory inducing NO and cytokine levels similar to LPS (**Figures 1**, **2A–C**). In general, LPGs from AL/TL strains RR410/RR418 induced higher levels of NO and cytokines than LPG from TL strains M2903, RR051, and M15991 (ML) in the TLR2 KO but not WT macrophages (**Figures 1**, **2A–C**). No detectable IL-1β production was induced by the different LPGs used in this study (data not shown).

Biochemical Analysis

To detect if variations in macrophage responses could be functionally attributed to intraspecies polymorphisms among *L. braziliensis* LPGs, we performed a biochemical analysis of these molecules. First, a preliminary analysis using western blot with specific antibodies was conducted. In general, both antibodies recognized all purified LPGs confirming the success of the purification process. However, based on the profiles, the smears suggest the existence of polymorphisms (**Figures 3A,B**). For CA7AE, all LPGs were recognized by this antibody confirming the existence of Gal(β1,4)Man(α1)-PO_4 motifs common to all LPGs (Soares et al., 2005). Different from CA7AE, LT22 exhibited a more evident polymorphisms among strains. For example, RR051 followed by M2903 strain were strongly recognized by this antibody. Those data suggest the existence of sugars branching-off the repeat units in some of the strains. Interestingly, M15991 strain, who was weakly recognized by CA7AE, was also detected very poorly by LT22. Although the western blot analyses suggest the existence of polymorphisms in the repeat units, a deeper biochemical analysis using TLC was required. To this end, purified LPGs were depolymerized and subjected to TLC analysis. The repeat units from the M15991 (ML) and M8401 (vector) strains were similar and devoid of side-chains exhibiting only a disaccharide peak (**Figures 4A,B**). As expected, the repeat units of M2903 LPG (control) exhibited a di-, tri- and tetrasaccharide as previously reported (Soares et al., 2005) (**Figure 5A**). This profile was also observed for AL isolate RR410 (**Figure 5B**). The repeat units of RR051 isolate exhibited a tri- and a disaccharide (**Figure 5C**, closed circles). In order to confirm if the side-chains were composed by β-glucose residues that could justify its reactivity to LT22 (**Figure 3B**), treatment with β-glucosidase was performed. After enzymatic treatment, the trisaccharide disappeared and the disaccharide peak increased confirming the presence of β-glucoses as side-chains (**Figure 5C**, open circles). A similar result was observed for strain RR418 (data not shown).

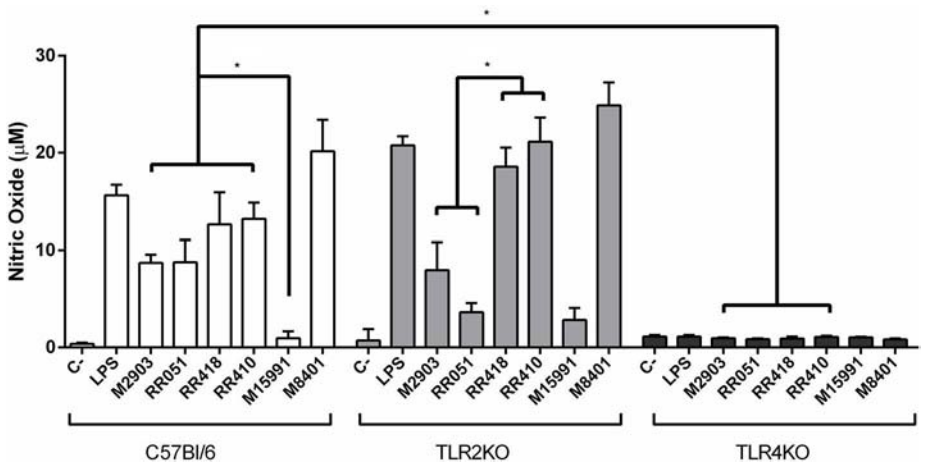

FIGURE 1 | Nitrite production by IFN-γ primed macrophages stimulated with *L. braziliensis* LPGs from patients with different clinical manifestations and the sandfly vector. Cells were pre-incubated with IFN-γ (3 IU/mL) for the 18 h prior to LPG exposure (10 μg/mL) and LPS (100 ng/mL, positive control) for 48 h. Fresh medium alone was used as negative control. Nitrite concentration was measured by Griess reaction. C, negative control; M2903, RR051, and RR418, *L. braziliensis* LPG isolated from typical lesions; RR410, LPG of *L. braziliensis* from atypical lesion; M15991, LPG isolated from mucocutaneous lesion; M8401, *L. braziliensis* LPG isolated from sandfly. *$P < 0.05$ was considered significant.

Altogether, those data indicate the presence of side-chains in the LPG repeat units of those strains.

DISCUSSION

Several factors may be related to the different levels of virulence among strains of a given *Leishmania* species. In the case of *L. braziliensis*, this species causes several clinical manifestations ranging from single lesions to atypical and/or severe mucocutaneous forms (Guimarães et al., 2016; Quaresma et al., 2018). Here, we investigated the role of LPG during the activation of macrophages from the innate immune compartment. An early and successful activation of this compartment is important for the fate of the acquired immune responses especially in parasitic diseases caused by Protozoa (Gazzinelli et al., 2004). Early studies with Old World *Leishmania* species already reported the role of LPG for the induction of cytokines, NO and MAPKs (Brittingham and Mosser, 1996; Feng et al., 1999). This triggered a lot of interest in establishing the TLRs involved in the innate immune responses in the hosts [revised by (Tuon et al., 2008)]. In this context, *L. major* LPG was the first TLR2 agonist reported for human natural-killer (NK) cells and murine macrophages. This activation triggers the production of TNF-γ and IFN-γ via MyD88 and is dependent on the integrity of the lipid anchor (Becker et al., 2003; de Veer et al., 2003). Consistent with those results, the integrity of the lipid anchor of *L. infantum* LPG was also required for the activation of PPAR-γ (Lima et al., 2017). In *L. braziliensis* (M2903 strain), it was previously reported that its LPG activates NO and cytokines production via TLR4/TLR2. A distinguishing feature of this LPG is the very pro-inflammatory profile compared to that of *L. infantum* (Ibraim et al., 2013). Here, this pro-inflammatory effect remained, but other strains (RR418, RR410, and M8401) exhibited a higher ability to induce NO and cytokines than M2903 especially in the TLR2 knockout. However, those differences were not observed in the WT. Those data confirmed that LPGs from different strains/isolates have variable immuno-modulatory activities toward murine macrophages. Based on our data, this activation was mediated by TLR4, similar to other dermotropic species such as *L. amazonensis* and *L. enriettii* (Paranaíba et al., 2015; Nogueira et al., 2016).

To investigate whether LPG polymorphisms correlated with clinical forms of leishmaniasis, macrophages were stimulated with glycoconjugates purified from *L. braziliensis* from different patients. The LPG from AL strain (RR410) induced a high NO and cytokine production than most of TL and ML strains. Interestingly, the LPG isolated from a vector strain (M8401), exhibited the highest pro-inflammatory activity, comparable to that of LPS. Our results confirm those in the literature that murine macrophages are able to produce NO in response to LPG, and that this production is variable among species/strains (Coelho-Finamore et al., 2011; Ibraim et al., 2013; Paranaíba et al., 2015; Nogueira et al., 2016). Cytokines are very important during immunopathology of Leishmaniasis. For example, IL-1β and IL-6 are important proinflammatory cytokines acting on endothelial cells by increasing the number of adhesion molecules and migration of leukocytes to the site of inflammation. This favor tissue damage by increasing inflammation by attracting and activating neutrophils (Castellucci et al., 2006; Boaventura et al., 2010; Sallusto et al., 2012). In our study, an important induction of IL-6 was noticed in most of the strains, suggesting the role of *L. braziliensis* LPG in this process. On the other hand, the reference strain from the mucocutaneous lesion (M15991) induced a very low production of NO and cytokines, a response similar to that of *L. infantum* LPG (Ibraim et al., 2013). Many aspects of the immunopathology of ML strains are still unknown, especially those related to metastasis from the bite

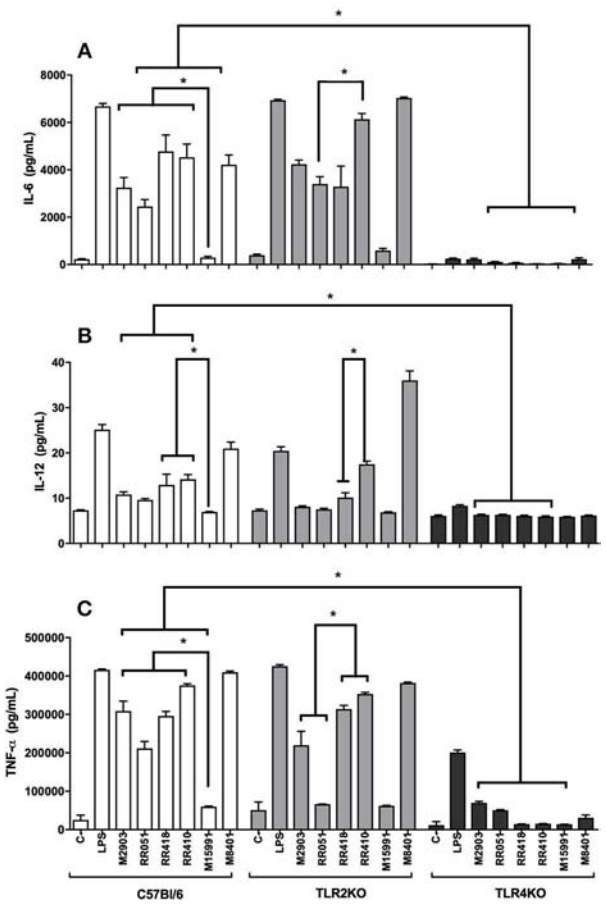

FIGURE 2 | Cytokine production by IFN-γ primed macrophages stimulated with *L. braziliensis* LPGs from patients with different clinical manifestations and the sandfly vector. Cells were pre-incubated with IFN-γ (3 IU/mL) for the 18 h prior to LPG exposure (10 μg/mL) and LPS (100 ng/mL, positive control) for 48 h. Fresh medium alone was used as negative control. Cytokine concentrations of IL-6 **(A)**, IL-12 **(B)**, and TNF-α **(C)** were determined by flow cytometry. C, negative control; M2903, RR051, and RR418, *L. braziliensis* LPG isolated from typical lesions; RR410, LPG of *L. braziliensis* from atypical lesion; M15991, LPG isolated from mucocutaneous lesion; M8401, *L. braziliensis* LPG isolated from sandfly. *$P < 0.05$ was considered significant.

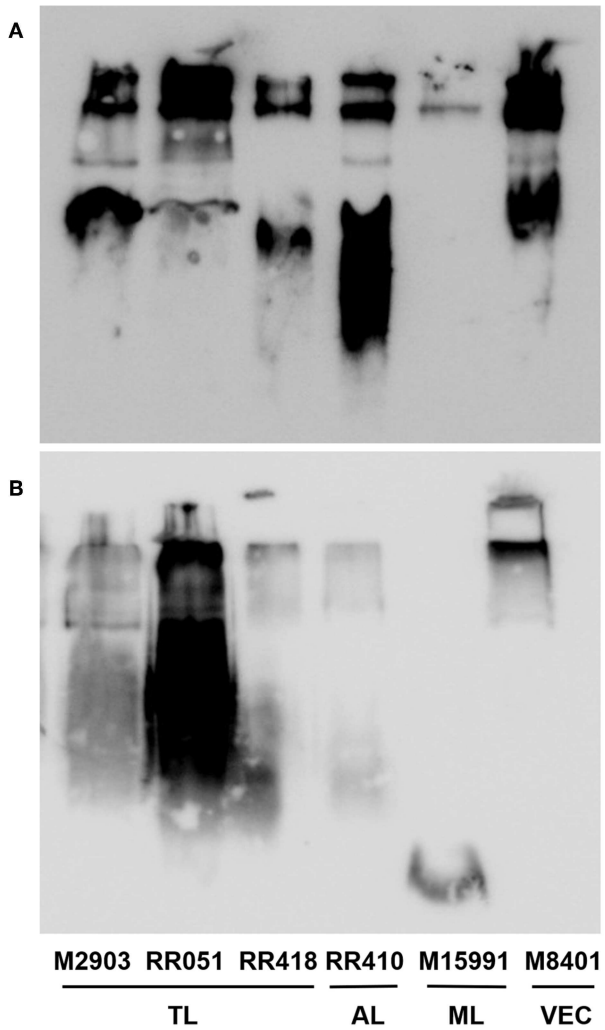

FIGURE 3 | Western blot of purified lipophosphoglycan (LPG). Purified LPG (10 μg per lane) from promastigotes of *L. braziliensis* strains (M2903, RR051, RR418, RR410, M15991, and M8401) were incubated with the antibody CA7AE (1:1,000) **(A)** and LT22 (1:1,000) **(B)**. LPG purified from *L. braziliensis* M2903 strain was used as positive control. TL, Typical lesions; AL, Atypical lesions; ML, Mucocutaneous strain; VEC, Vector strain.

site to the oropharyngeal mucosa. This low proinflammatory potential of the LPG from the ML strain strongly suggests that other molecules such as GP63, GIPLs, and PPGs could be important during macrophage response (De Assis et al., 2012). Consistent with this, M15991 strain does not possesses LRV1 (*Leishmaniavirus*) (Macedo et al., 2016), reinforcing that other strain-specific factors and perhaps from the host could be primarily involved in the immunopathology of ML. Interestingly, there was increased production of NO, IL-6, and TNF-α by the isolated strain from an atypical lesion (AL). AL lesions exhibited an aspect macroscopically different from the common TL lesion (ulcerated with elevated borders) (Costa-Silva et al., 2014; Quaresma et al., 2018). In general, the LPG of the RR410 strain was more pro-inflammatory than those of the TL/ML lesions mainly for the TLR2 knockout (IL-6 and IL-12). This reinforces that other factors such as genetics could be responsible for these unusual forms. Recently, it was reported that AL causing strains have a SNP in the 1,300 bp hsp70 gene fragment that clustered them in a group separated from TL/ML strains (Quaresma et al., 2018). Altogether our data show that the mechanisms underlying macrophage modulation by LPG clearly vary among strains/isolates of *L. braziliensis* and are not easily correlated with pathology.

To investigate whether those differences could be due to polymorphisms in the LPG, preliminary analyzes using western-blot were performed. All LPGs were recognized by the CA7AE antibody. The LPG from M15991 strain was weakly recognized by this antibody. However, most LPGs were recognized by this mAb suggesting that they possess most of

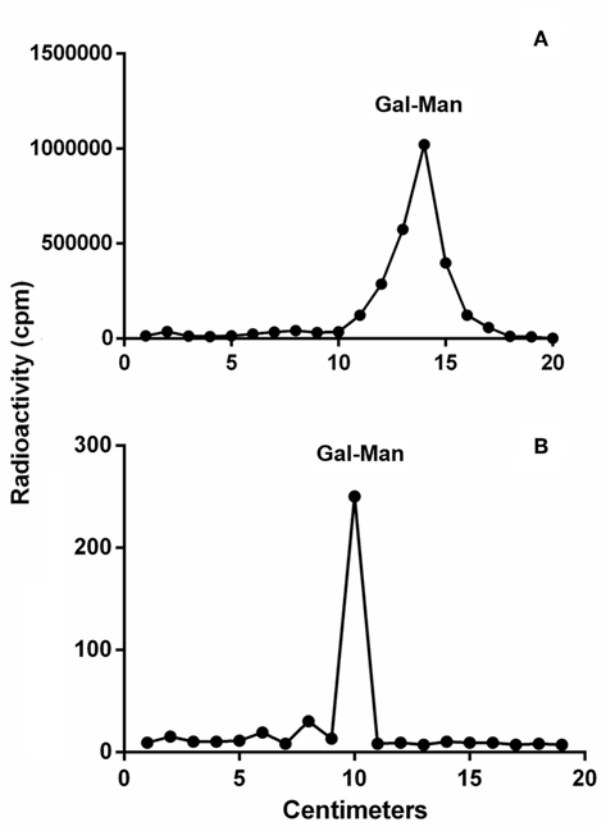

FIGURE 4 | Thin layer chromatography (TLC) of dephosphorylated [^{3}H]Gal-repeat units obtained from different *L. braziliensis* LPGs. **(A)** M15991 repeat units and **(B)** M8401 repeat units. Gal, galactose; Man, mannose.

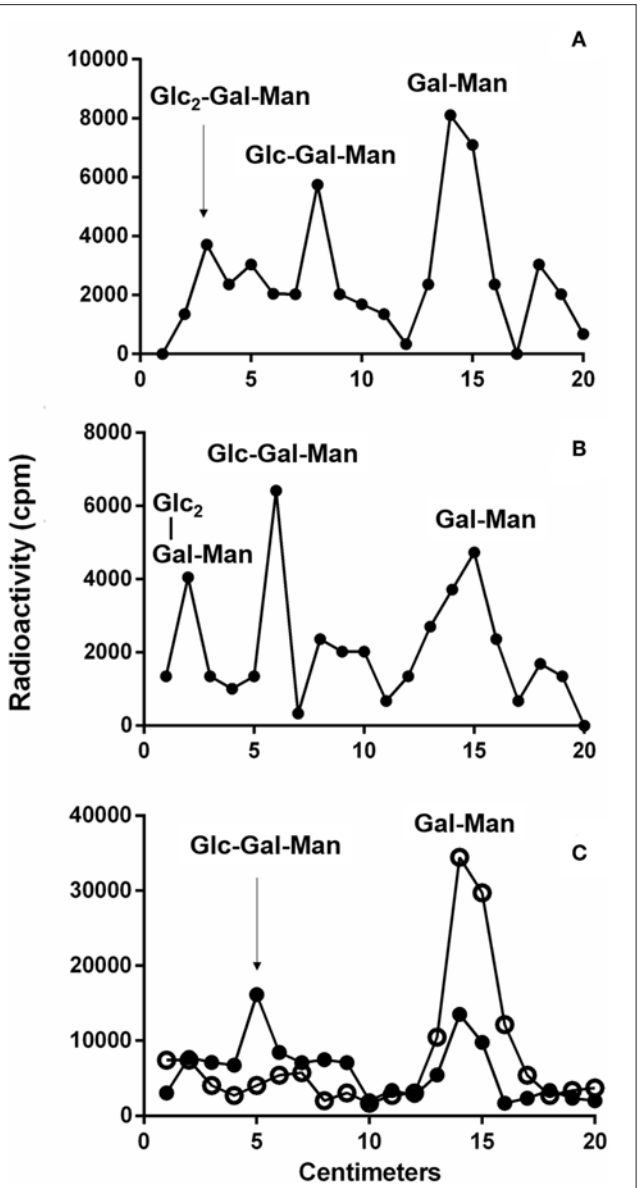

FIGURE 5 | Thin layer chromatography (TLC) of dephosphorylated [^{3}H]Gal-repeat units obtained from different *L. braziliensis* LPGs. **(A)** M2903 repeat units, **(B)** RR410, and **(C)** RR051 treated (open circles) or not (closed circles) with β-glucosidase. Glc, glucose; Gal, galactose; Man, mannose.

unsubstituted repeat units. This feature is commonly observed in *L. infantum* type I LPG (10 strains), *L. enriettii* (two strains), *Leishmania shawi*, and *L. donovani* (Sudan strain) (Sacks et al., 1995; Coelho-Finamore et al., 2011; Paranaíba et al., 2015; Passero et al., 2015). On the other hand, the presence of side-chains suggestive of glucoses (LT22 positive) was strongly detected in the LPG from RR051strain followed by M2903. This is consistent with the literature that the LPG of M2903 (positive control) from stationary phase possess 1-2 β-glucose side-chains (Soares et al., 2005). Those sugars are also observed in the LPG from *L. infantum* (strains PP75 and BH46), *L. amazonensis* (PH8 strain), and *L. donovani* (Mongi strain) (Mahoney et al., 1999; Soares et al., 2002; Coelho-Finamore et al., 2011; Nogueira et al., 2017). The other strains (RR418, RR410. M15991, and M8401) exhibited lower recognition by this mAb suggesting that some of the repeat units could be substituted with side-chains and this should be confirmed by TLC analysis. Those data suggest intraspecies polymorphisms in the purified repeat units from *L. braziliensis* LPGs.

To detect polymorphisms in the repeating units, we chose five *L. braziliensis* LPGs displaying different patterns, as assessed by western blots. LPGs were radioactively labeled to increase sensitivity, since *L. braziliensis* express lesser amounts of this glycoconjugate than other *Leishmania* species (Soares et al., 2005). The results indicated evident polymorphisms in the repeat units. The strains M15991 and M8401 possess LPGs without side chain confirming their basic structure of Gal(β1,4)Man(α1)-PO_4 (Sacks et al., 1995). Although LPG expressed by strain M15991 was weakly recognized by CA7AE, it exhibited a clear disaccharide peak confirming the existence of unbranched repeating units. As expected, TLC analysis of LPG from strain M2903 (control) confirmed the existence of di-, tri- and tetrasaccharides as previously described (Soares et al.,

2005). Confirming the western-blot data, in addition to a disaccharide, the LPG of RR051 also exhibited a tetrasaccharide peak. After enzymatic treatment with β-glucosidase this peak disappeared followed by an increase in the disaccharide peak. This confirmed the existence of β-glucoses as side-chains. Similar results were also observed for RR418 (data not shown), *L. infantum* and *L. mexicana* (Ilg et al., 1992; Soares et al., 2002). Those data confirmed that β-glucoses are the most common side chains found in the LPGs from New World species of *Leishmania*.

Those polymorphisms were functionally compared during macrophage studies. Depending on the cytokine/NO a correlation could be established. For example, the production of NO, TNF-α and IL-6 by WT murine macrophages was higher in response to glucosylated LPGs (M2903, RR051, and RR410) than that of unbranched LPG from M15991. However, for M8401 this correlation could not be established. It has an unbranched LPG but alike M15991 it exhibited a high pro-inflammatory activity. It is not likely that this feature is due to the presence of side-chains since it does not have it. Conversely, we could postulate that this could be due to a longer LPG size. This was already reported in another dermotropic species *L. enriettii*. Two strains of this species were compared and the LPG of L88 strain (longer size) was more pro-inflammatory than that of the Cobaia strain (short size) (Paranaíba et al., 2015). Those data suggested that LPG qualitative variations either in sugars branching-off the repeating units or size could differentially modulate macrophage responses. However, this is dependent on species/strains. For example, in *L. infantum* the presence of glycosylated LPGs (strains PP75 and BH46) triggered a higher NO production compared to unsubstituted (type I) LPGs (Coelho-Finamore et al., 2011). On the other hand, in *L. amazonensis*, polymorphisms in the sugar side-chains were not important for macrophage activation and this could be attributed to the lipid anchor (Nogueira et al., 2017).

In conclusion, our study showed that strains/isolates of *L. braziliensis* differentially activated murine macrophages via TLR4. We found considerable structural and compositional polymorphisms in the side-chains of these LPGs that could affect interaction with this TLR, although a clear correlation between structure and function could not be established. *Leishmania*-macrophage interaction process is very complex involving parasite and immune cells molecules. Our data reinforce the idea that not only LPG but other molecules play an important role during the interface parasite-host and perhaps affect the immunopathology. Based on our work, differences in virulence/pathogenicity are strongly dependent on species/strains. This is surely the case of the *L. braziliensis*, a species causing a spectrum of dermotropic diseases.

DATA AVAILABILITY

The raw data supporting the conclusions of this manuscript will be made available by the authors, without undue reservation, to any qualified researcher.

AUTHOR CONTRIBUTIONS

RS, AD, CG, and AT designed the experiments. JR, TV, PN, and AT performed the experiments. PN, TV, AD, CG, and RS analyzed the data. All authors contributed for the manuscript.

FUNDING

This work was supported by the Conselho Nacional de Pesquisa e Desenvolvimento (CNPq) (grant 305065/2016-5 to RS and 405336/2017-9 to PN) and Fundação de Amparo do Estado de Minas Gerais (FAPEMIG) (grant 00202-18 to RS). TV was the recipient of a scholarship from FAPEMIG and from the Emerging Leaders in the Americas Program (Global Affairs Canada). AT is supported by Fundação de Amparo do Estado de São Paulo (FAPESP) (grant 2016-01917-3). AD is supported by the Canadian Institutes of Health Research and is the holder of the Canada Research Chair on the Biology of intracellular parasitism. CG is a research fellow from CNPq. We also thank the Programa Print-Capes for financial support.

REFERENCES

Becker, I., Salaiza, N., Aguirre, M., Delgado, J., Carrillo-Carrasco, N., Kobeh, L. G., et al. (2003). Leishmania lipophosphoglycan (LPG) activates NK cells through toll-like receptor-2. *Mol. Biochem. Parasitol.* 130, 65–74. doi: 10.1016/S0166-6851(03)00160-9

Boaventura, V. S., Santos, C. S., Cardoso, C. R., De Andrade, J., Dos Santos, W. L. C., Clarêncio, J., et al. (2010). Human mucosal leishmaniasis: neutrophils infiltrate areas of tissue damage that express high levels of Th17-related cytokines. *Eur. J. Immunol.* 40, 2830–2836. doi: 10.1002/eji.200940115

Brittingham, A., and Mosser, D. (1996). Exploitation of the complement system by *Leishmania promastigotes*. *Parasitol. Today* 12, 444–447. doi: 10.1016/0169-4758(96)10067-3

Castellucci, L., Menezes, E., Oliveira, J., Magalhaes, A., Guimaraes, L. H., Lessa, M., et al. (2006). IL6-174 G/C promoter polymorphism influences susceptibility to mucosal but not localized cutaneous leishmaniasis in Brazil. *J. Infect. Dis.* 194, 519–527. doi: 10.1086/505504

Coelho-Finamore, J. M., Freitas, V. C., Assis, R. R., Melo, M. N., Novozhilova, N., Secundino, N. F., et al. (2011). *Leishmania infantum*: lipophosphoglycan intraspecific variation and interaction with vertebrate and invertebrate hosts. *Int. J. Parasitol.* 41, 333–342. doi: 10.1016/j.ijpara.2010.10.004

Costa-Silva, M. F., Gomes, L. I., Martins-Filho, O. A., Rodrigues-Silva, R., Freire, J., de, M., FláviaQuaresma P., et al. (2014). Gene expression profile of cytokines and chemokines in skin lesions from Brazilian Indians with localized cutaneous leishmaniasis. *Mol. Immunol.* 57, 74–85. doi: 10.1016/j.molimm.2013.08.008

De Assis, R. R., Ibraim, I. C., Nogueira, P. M., Soares, R. P., and Turco, S. J. (2012). Glycoconjugates in new world species of leishmania: polymorphisms in lipophosphoglycan and glycoinositolphospholipids and interaction with hosts. *Biochim. Biophys. Acta Gen. Subj.* 1820, 1354–1365. doi: 10.1016/j.bbagen.2011.11.001

de Carvalho Vivarini, A., Pereira, R. d. M. S., Dias Teixeira, K. L., Calegari-Silva, T. C., Bellio, M., Dalastra Laurenti M., et al. (2011). Human cutaneous leishmaniasis: interferon-dependent expression of double-stranded RNA-dependent protein kinase (PKR) via TLR2. *FASEB J.* 25, 4162–4173. doi: 10.1096/fj.11-185165

de Veer, M. J., Curtis, J. M., Baldwin, T. M., DiDonato, J. A., Sexton, A., McConville, M. J., et al. (2003). MyD88 is essential for clearance of *Leishmania*

major: possible role for lipophosphoglycan and Toll-like receptor 2 signaling. *Eur. J. Immunol.* 33, 2822–2831. doi: 10.1002/eji.200324128

Desjardins, M., and Descoteaux, A. (1997). Inhibition of phagolysosomal biogenesis by the leishmania lipophosphoglycan. *J. Exp. Med.* 185, 2061–2068.

Dobson, D. E., Mengeling, B. J., Cilmi, S., Hickerson, S., Turco, S. J., and Beverley, S. M. (2003). Identification of genes encoding arabinosyltransferases (SCA) mediating developmental modifications of lipophosphoglycan required for sand fly transmission of *Leishmania major*. *J. Biol. Chem.* 278, 28840–28848. doi: 10.1074/jbc.M302728200

Feng, G., Goodridge, H. S., Harnett, M. M., Wei, X., Nikolaev, A. V., Higson, A. P., et al. (1999). Extracellular signal-related kinase (ERK) and p38 mitogen-activated protein (MAP) kinases differentially regulate the lipopolysaccharide-mediated induction of inducible nitric oxide synthase and IL-12 in macrophages: *Leishmania phosphoglycans* subvert macr. *J. Immunol.* 163, 6403–6412. doi: 10.4049/jimmunol.166.3.1912

Gabriel, C., McMaster, W. R., Girard, D., and Descoteaux, A. (2010). *Leishmania donovani* promastigotes evade the antimicrobial activity of neutrophil extracellular traps. *J Immunol.* 185, 4319–4327. doi: 10.4049/jimmunol.1000893

Gazzinelli, R. T., Ropert, C., and Campos, M. A. (2004). Role of the Toll/interleukin-1 receptor signaling pathway in host resistance and pathogenesis during infection with protozoan parasites. *Immunol Rev.* 201, 9–25. doi: 10.1111/j.0105-2896.2004.00174.x

Guimarães, L. H., Machado, P. R. L., Lago, E. L., Morgan, D. J., Schriefer, A., Bacellar, O., et al. (2009). Atypical manifestations of tegumentary leishmaniasis in a transmission area of *Leishmania braziliensis* in the state of Bahia, Brazil. *Trans. R. Soc. Trop. Med. Hyg.* 103, 712–715. doi: 10.1016/j.trstmh.2009.04.019

Guimarães, L. H., Queiroz, A., Silva, J. A., Silva, S. C., Magalhães, V., Lago, E. L., et al. (2016). Atypical manifestations of cutaneous leishmaniasis in a region endemic for *Leishmania braziliensis*: clinical, immunological and parasitological aspects. *PLoS Negl. Trop. Dis.* 10:e0005100. doi: 10.1371/journal.pntd.0005100

Guimaraes-Costa, A. B., Nascimento, M. T. C., Froment, G. S., Soares, R. P. P., Morgado, F. N., Conceicao-Silva, F., et al. (2009). *Leishmania amazonensis* promastigotes induce and are killed by neutrophil extracellular traps. *Proc. Natl. Acad. Sci. U.S.A.* 106, 6748–6753. doi: 10.1073/pnas.0900226106

Holm, Å. V., Tejle, K., Magnusson, K. E., Descoteaux, A., and Rasmusson, B. (2001). *Leishmania donovani* lipophosphoglycan causes periphagosomal actin accumulation: correlation with impaired translocation of PKCα and defective phagosoem maturation. *Cell. Microbiol.* 3, 439–447. doi: 10.1046/j.1462-5822.2001.00127.x

Ibraim, I. C., De Assis, R. R., Pessoa, N. L., Campos, M. A., Melo, M. N., Turco, S. J., et al. (2013). Two biochemically distinct lipophosphoglycans from *Leishmania braziliensis* and *Leishmania infantum* trigger different innate immune responses in murine macrophages. *Parasites Vectors* 6, 1–11. doi: 10.1186/1756-3305-6-54

Ilg, T., Etges, R., Overath, P., McConville, M. J., Thomas-Oates, J., Thomas, J., et al. (1992). Structure of *Leishmania mexicana* lipophosphoglycan. *J. Biol. Chem.* 267, 6834–6840.

Lima, J. B., Araújo-Santos, T., Lázaro-Souza, M., Carneiro, A. B., Ibraim, I. C., Jesus-Santos, F. H., et al. (2017). *Leishmania infantum* lipophosphoglycan induced-Prostaglandin E2 production in association with PPAR-γ expression via activation of Toll like receptors-1 and 2. *Sci. Rep.* 7:14321. doi: 10.1038/s41598-017-14229-8

Luz, N. F., Andrade, B. B., Feijo, D. F., Araujo-Santos, T., Carvalho, G. Q., Andrade, D., et al. (2012). Heme oxygenase-1 promotes the persistence of *Leishmania chagasi* infection. *J. Immunol.* 188, 4460–4467. doi: 10.4049/jimmunol.1103072

Macedo, D. H., Menezes-Neto, A., Rugani, J. M., Rocha, A. C., Silva, S. O., Melo, M. N., et al. (2016). Low frequency of LRV1 in *Leishmania braziliensis* strains isolated from typical and atypical lesions in the State of Minas Gerais, Brazil. *Mol. Biochem. Parasitol.* 210, 50–54. doi: 10.1016/j.molbiopara.2016.08.005

Mahoney, A. B., Sacks, D. L., Saraiva, E., Modi, G., and Turco, S. J. (1999). Intra-species and stage-specific polymorphisms in lipophosphoglycan structure control *Leishmania donovani*—Sand fly interactions. *Biochemistry* 38, 9813–9823. doi: 10.1021/bi990741g

Nogueira, P. M., Assis, R. R., Torrecilhas, A. C., Saraiva, E. M., Pessoa, N. L., Campos, M. A., et al. (2016). Lipophosphoglycans from *Leishmania amazonensis* strains display immunomodulatory properties via TLR4 and do not affect sand fly infection. *PLoS Negl. Trop. Dis.* 10, 1–17. doi: 10.1371/journal.pntd.0004848

Nogueira, P. M., Guimarães, A. C., Assis, R. R., Sadlova, J., Myskova, J., Pruzinova, K., et al. (2017). *Lipophosphoglycan polymorphisms* do not affect *Leishmania amazonensis* development in the permissive vectors *Lutzomyia migonei* and *Lutzomyia longipalpis*. *Parasites Vectors* 10:608. doi: 10.1186/s13071-017-2568-8

Paranaíba, L. F., De Assis, R. R., Nogueira, P. M., Torrecilhas, A. C., Campos, J. H., Silveira, A. C. D. O., et al. (2015). *Leishmania enriettii*: biochemical characterisation of lipophosphoglycans (LPGs) and glycoinositolphospholipids (GIPLs) and infectivity to *Cavia porcellus*. *Parasites Vectors* 8, 1–14. doi: 10.1186/s13071-015-0633-8

Passero, L. F. D., Assis, R. R., da Silva, T. N. F., Nogueira, P. M., Macedo, D. H., Pessoa, N. L., et al. (2015). Differential modulation of macrophage response elicited by glycoinositolphospholipids and lipophosphoglycan from *Leishmania (Viannia) shawi*. *Parasitol. Int.* 64, 32–35. doi: 10.1016/j.parint.2015.01.006

Quaresma, P. F., Ferreira, C., Marteleto, J., Rugani, N., Freire, J. D. M., Baptista, R. D. P., et al. (2018). Distinct genetic profiles of *Leishmania (Viannia) braziliensis* associate with clinical variations in cutaneous-leishmaniasis patients from an endemic area in Brazil. *Parasitology* 145, 1161–1169. doi: 10.1017/S0031182018000276

Rugani, J. N., Quaresma, P. F., Gontijo, C. F., Soares, R. P., and Monte-Neto, R. L. (2018). Intraspecies susceptibility of *Leishmania (Viannia) braziliensis* to antileishmanial drugs: antimony resistance in human isolates from atypical lesions. *Biomed. Pharmacother.* 108, 1170–1180. doi: 10.1016/j.biopha.2018.09.149

Sacks, D. L., Pimenta, P. F., McConville, M. J., Schneider, P., and Turco, S. J. (1995). Stage-specific binding of *Leishmania donovani* to the sand fly vector midgut is regulated by conformational changes in the abundant surface lipophosphoglycan. *J. Exp. Med.* 181, 685–697. doi: 10.1084/jem.181.2.685

Sallusto, F., Zielinski, C. E., and Lanzavecchia, A. (2012). Human Th17 subsets. *Eur. J. Immunol.* 42, 2215–2220. doi: 10.1002/eji.201242741

Soares, R. P., Margonari, C., Secundino, N. C., MacÊdo, M. E., Da Costa, S. M., Rangel, E. F., et al. (2010). Differential midgut attachment of *Leishmania (Viannia) braziliensis* in the sand flies *Lutzomyia (Nyssomyia) whitmani* and *Lutzomyia (Nyssomyia) intermedia*. *J. Biomed. Biotechnol.* 2010:827851. doi: 10.1155/2010/439174

Soares, R. P. P., Barron, T., McCoy-Simandle, K., Svobodova, M., Warburg, A., and Turco, S. J. (2004). *Leishmania tropica*: intraspecific polymorphisms in lipophosphoglycan correlate with transmission by different Phlebotomus species. *Exp. Parasitol.* 107, 105–114. doi: 10.1016/j.exppara.2004.05.001

Soares, R. P. P., Cardoso, T. L., Barron, T., Araújo, M. S. S., Pimenta, P. F. P., and Turco, S. J. (2005). *Leishmania braziliensis*: a novel mechanism in the lipophosphoglycan regulation during metacyclogenesis. *Int. J. Parasitol.* 35, 245–253. doi: 10.1016/j.ijpara.2004.12.008

Soares, R. P. P., Macedo, M. E., Ropert, C., Gontijo, N. F., Almeida, I. C., Gazzinelli, R. T., et al. (2002). *Leishmania chagasi*: lipophosphoglycan characterization and binding to the midgut of the sand fly vector Lutzomyia longipalpis. *Mol. Biochem. Parasitol.* 121, 213–224. doi: 10.1016/S0166-6851(02)00033-6

Spath, G. F., Garraway, L. A., Turco, S. J., and Beverley, S. M. (2003). The role(s) of lipophosphoglycan (LPG) in the establishment of *Leishmania major* infections in mammalian hosts. *Proc. Natl. Acad. Sci. U.S.A.* 100, 9536–9541. doi: 10.1073/pnas.1530604100

Tavares, N. M., Araújo-Santos, T., Afonso, L., Nogueira, P. M., Lopes, U. G., Soares, R. P., et al. (2014). Understanding the mechanisms controlling *Leishmania amazonensis* infection *in vitro*: the role of LTB4 derived from human neutrophils. *J. Infect. Dis.* 210, 656–666. doi: 10.1093/infdis/jiu158

Tolson, D. L., Turco, S. J., Beecroft, R. P., and Pearson, T. W. (1989). The immunochemical structure and surface arrangement of *Leishmania donovani* lipophosphoglycan determined using monoclonal antibodies.

Mol. Biochem. Parasitol. 35, 109–118. doi: 10.1016/0166-6851(89)90113-8

Tuon, F. F., Amato, V. S., Bacha, H. A., Almusawi, T., Duarte, M. I., and Amato Neto, V. (2008). Toll-like receptors and leishmaniasis. *Infect. Immun.* 76, 866–872. doi: 10.1128/IAI.01090-07

Turco, S. J., and Descoteaux, A. (1992). The lipophosphoglycan of Leishmania parasites. *Annu. Rev. Microbiol.* 46, 65–94.

Vinet, A. F., Fukuda, M., Turco, S. J., and Descoteaux, A. (2009). The *Leishmania donovani* lipophosphoglycan excludes the vesicular proton-ATPase from phagosomes by impairing the recruitment of Synaptotagmin V. *PLoS Pathog.* 5:e1000628. doi: 10.1371/journal.ppat.1000628

Conflict of Interest Statement: The authors declare that the research was conducted in the absence of any commercial or financial relationships that could be construed as a potential conflict of interest.

frontiers in Cellular and Infection Microbiology

ORIGINAL RESEARCH
published: 12 July 2019
doi: 10.3389/fcimb.2019.00252

Thymic Microenvironment Is Modified by Malnutrition and *Leishmania infantum* Infection

Monica Losada-Barragán[1,2], Adriana Umaña-Pérez[3], Jonathan Durães[1], Sergio Cuervo-Escobar[4], Andrés Rodríguez-Vega[1], Flávia L. Ribeiro-Gomes[5], Luiz R. Berbert[6], Fernanda Morgado[1], Renato Porrozzi[1], Daniella Arêas Mendes-da-Cruz[6,7], Priscila Aquino[8], Paulo C. Carvalho[9], Wilson Savino[6,7], Myriam Sánchez-Gómez[3], Gabriel Padrón[1] and Patricia Cuervo[1]

[1] Laboratório de Pesquisa em Leishmanioses, Instituto Oswaldo Cruz, Fiocruz, Rio de Janeiro, Brazil, [2] Grupo de Investigación en Biología Celular y Funcional e Ingeniería de Biomoléculas, Departamento de Biologia, Universidad Antonio Nariño, Bogotá, Colombia, [3] Grupo de Investigación en Hormonas, Departamento de Química, Universidad Nacional de Colombia, Bogotá, Colombia, [4] Facultad de Ciencias, Universidad de Ciencias Aplicadas y Ambientales, Bogotá, Colombia, [5] Laboratório de Pesquisa em Malária, Instituto Oswaldo Cruz, Fiocruz, Rio de Janeiro, Brazil, [6] Laboratório de Pesquisas sobre o Timo, Instituto Oswaldo Cruz, Fiocruz, Rio de Janeiro, Brazil, [7] Instituto Nacional de Ciência e Tecnologia em Neuroimunomodulação, Fiocruz, Rio de Janeiro, Brazil, [8] Instituto Leônidas e Maria Deane, Fiocruz, Manaus, Brazil, [9] Computational Mass Spectrometry and Proteomics Group, Fiocruz, Rio de Janeiro, Brazil

OPEN ACCESS

Edited by:
Herbert Leonel de Matos Guedes, Federal University of Rio de Janeiro, Brazil

Reviewed by:
Iñaki Alvarez, Autonomous University of Barcelona, Spain
David Alfaro, Complutense University of Madrid, Spain

***Correspondence:**
Patricia Cuervo
patricia.cuervo@fiocruz.br;
patycescobar@gmail.com

Specialty section:
This article was submitted to Parasite and Host, a section of the journal Frontiers in Cellular and Infection Microbiology

Received: 23 April 2019
Accepted: 28 June 2019
Published: 12 July 2019

Citation:
Losada-Barragán M, Umaña-Pérez A, Durães J, Cuervo-Escobar S, Rodríguez-Vega A, Ribeiro-Gomes FL, Berbert LR, Morgado F, Porrozzi R, Mendes-da-Cruz DA, Aquino P, Carvalho PC, Savino W, Sánchez-Gómez M, Padrón G and Cuervo P (2019) Thymic Microenvironment Is Modified by Malnutrition and Leishmania infantum Infection. Front. Cell. Infect. Microbiol. 9:252. doi: 10.3389/fcimb.2019.00252

Detrimental effects of malnutrition on immune responses to pathogens have long been recognized and it is considered a main risk factor for various infectious diseases, including visceral leishmaniasis (VL). Thymus is a target of both malnutrition and infection, but its role in the immune response to *Leishmania infantum* in malnourished individuals is barely studied. Because we previously observed thymic atrophy and significant reduction in cellularity and chemokine levels in malnourished mice infected with *L. infantum*, we postulated that the thymic microenvironment is severely compromised in those animals. To test this, we analyzed the microarchitecture of the organ and measured the protein abundance in its interstitial space in malnourished BALB/c mice infected or not with *L. infantum*. Malnourished-infected animals exhibited a significant reduction of the thymic cortex:medulla ratio and altered abundance of proteins secreted in the thymic interstitial fluid. Eighty-one percent of identified proteins are secreted by exosomes and malnourished-infected mice showed significant decrease in exosomal proteins, suggesting that exosomal carrier system, and therefore intrathymic communication, is dysregulated in those animals. Malnourished-infected mice also exhibited a significant increase in the abundance of proteins involved in lipid metabolism and tricarboxylic acid cycle, suggestive of a non-proliferative microenvironment. Accordingly, flow cytometry analysis revealed decreased proliferation of single positive and double positive T cells in those animals. Together, the reduced cortical area, decreased proliferation, and altered protein abundance suggest a dysfunctional thymic microenvironment where T cell migration, proliferation, and maturation are compromised, contributing for the thymic atrophy observed in malnourished animals. All these alterations could affect the control of the local and systemic infection, resulting in an impaired response to *L. infantum* infection.

Keywords: thymus, thymic microenvironment, protein malnutrition, *Leishmania infantum*, visceral leishmaniasis, interstitial fluid, proteomics, fatty acid oxidation

INTRODUCTION

The thymus gland is the central lymphoid organ in the adaptive immune system, where maturation, proliferation, and exportation of T lymphocytes take place. The successful development of mature T cells depends on the constant migration of differentiating thymocytes through the thymic microenvironment. The mechanisms directing this migration are heavily dependent on the thymic microenvironment, which regulates the process of T cell development through surface molecules, extracellular matrix (ECM) proteins, matrix metallopeptidases, and by secreting soluble polypeptides as cytokines, chemokines, and hormones (Smythe et al., 1971; Schonland, 1972; Aref et al., 1982; Jambon et al., 1988; Aaby et al., 2002; Gameiro et al., 2010). However, the global complexity of soluble protein components that mediate T cell development in this environment is to be better defined, both in physiological and pathological conditions.

It is widely recognized that thymus is one of the most affected organs during malnutrition. In malnourished children, histological analyses revealed thymus atrophy (Schonland, 1972), with thymocyte depletion, increased intra and inter-lobular connective tissue, and decreased cortico-medullary limits (Smythe et al., 1971; Aref et al., 1982; Jambon et al., 1988). Importantly, it has been shown that a smaller thymus is a consistent and independent risk factor for mortality and is predictive of immune competence (Aaby et al., 2002; Garly et al., 2008).

Interestingly, several infectious diseases induce thymic atrophy and altered T cell subsets (Mendes-Da-Cruz et al., 2003; Savino et al., 2007; Andrade et al., 2008; Liu et al., 2014), thus sharing these characteristics with the effects of malnutrition in the thymus. In experimental models, the detrimental effects of malnutrition and infection on immunity have long been recognized (Savino and Dardenne, 2010; Ibrahim et al., 2013, 2017; Akuffo et al., 2018). Nevertheless, few studies evaluated the coexistence of infection and malnutrition (Savino, 2006; Perez et al., 2012; Cuervo-Escobar et al., 2014; Losada-Barragan et al., 2017; Zacarias et al., 2017). Acute infection by *Trypanosoma cruzi* leads to thymic atrophy and thymocyte depletion mainly in the cortical region of the organ (Savino and Dardenne, 2010), and this change is further exacerbated during protein malnutrition (Akingbemi et al., 1996).

We previously demonstrated that the thymus of protein malnourished mice infected with *L. infantum* presents severe atrophy and reduced absolute cellularity, including a drastic decrease of $CD4^+CD8^+$ thymocytes and significant decrease in single positive T cell total numbers (Cuervo-Escobar et al., 2014). In addition, parasites were detected in the thymus of both well-nourished and malnourished animals infected with *L. infantum* but amastigote nests were only observed in malnourished mice (Losada-Barragan et al., 2017). We also observed that protein malnutrition does affect thymocyte migration of *L. infantum*-infected animals, rather than increasing their apoptosis. In fact, protein malnutrition induced a significant reduction of thymic contents of chemokines such as CCL5, CXCL12, CXCL9, and CXCL10 as well as IGF1 in infected animals, suggesting altered migratory capabilities of developing T cells. However, since in this combined condition developing thymocytes were able to migrate *ex vivo* in response to chemotactic stimuli, our data indicated that malnutrition may compromise the thymic microenvironment rather than migratory capability of T cells *per se* (Losada-Barragan et al., 2017). Those results, together with the observation of an early increase in the splenic parasite load in malnourished animals, suggested that a precondition of malnutrition is affecting cell-mediated immune response to *L. infantum* (probably by altering local and systemic T cell migration) leading to an altered capacity of protein-deprived animals to control parasite spreading and proliferation (Losada-Barragan et al., 2017). In this work, we hypothesized that protein malnutrition alters thymic microarchitecture and abundance of intrathymic soluble proteins that mediate cell-matrix and cell-cytokine/chemokine mediated interaction leading to defects upon T cell maturation and migration, resulting in a severe clinical outcome during *L. infantum* infection. Accordingly, we conducted a quantitative mass spectrometry-based proteomics analysis of the interstitial fluid of the thymus in protein malnourished mice infected with *L. infantum* accompanied by a histopathological study of the thymic microarchitecture. This first descriptive work of the thymic microenvironment in the light of proteomics revealed significant intrathymic alterations related to T cell migration, maturation, and proliferation that could contribute to a defective immune response during visceral leishmaniasis.

MATERIALS AND METHODS

Ethics Statement

This study was carried out in accordance with the recommendations of the Guide for the Care and Use of Laboratory Animals of the National Institutes of Health—Eighth Edition. The protocol was approved by the Instituto Oswaldo Cruz committee for Animal Care and Use (License #LW-27/14). The *L. infantum* strain MCAN/BR/2000/CNV-FEROZ used in this study was provided by the Collection of *Leishmania* of the Instituto Oswaldo Cruz, Rio de Janeiro (Coleção de *Leishmania* do Instituto Oswaldo Cruz, CLIOC; http://clioc.fiocruz.br/). This collection is registered in the World Federation for Culture Collections (WFCC-WDCM 731) and is recognized as a Depository Authority by the Brazilian Ministry of the Environment (D.O.U. 05.04.2005).

Parasite Culture

Parasites were cultivated at 25°C in Schneider's medium containing 10% fetal calf serum (FCS) and were collected at the stationary phase by centrifugation at 1,800 *g* for 5 min. The parasites were then washed twice in PBS, pH 7.2.

Mice, Feeding Protocol, and Experimental Infection

BALB/c AnUnib (male, 3 weeks old) mice were purchased from Centro Multidisciplinar para Investigação Biológica na Área da Ciência em Animais de Laboratório da Universidade Estadual de Campinas (CEMIB-UNICAMP, http://www.cemib.unicamp.br/

servicos/cadastro_linhagens.php). Mice were kept in ventilated cages, in a 12/12 h light/dark cycle, in a specific pathogen–free area of the mouse facility of the Instituto Oswaldo Cruz (IOC-FIOCRUZ). Experimental infection was conducted as previously described (Cuervo-Escobar et al., 2014; Losada-Barragan et al., 2017). Animals were provided with a diet containing 14% protein (MP Biomedicals, Inc., USA, Catalog No. 960258). After 1 week of acclimation, animals were randomly divided into two groups: one group being fed 14% (13,79 g crude protein per 100 g food pellets; control protein, CP) and another group being fed a 4% protein content diet (4,59 g crude protein per 100 g food pellets; low protein, LP) (MP Biomedicals, Inc., USA, Catalog No 960254). These two diets are isocaloric; each providing 3.7 kcal/g. The caloric protein deficiency in the 4% protein diet was replaced by additional carbohydrate calories. The animals had free access to water and food. Food rations per cage were daily weighed and feed consumption was calculated (Sanchez-Gomez et al., 1999). After 7 days of diet, each group was divided into two subgroups, and one subgroup of each diet group was infected intravenously (tail vein) with 1×10^7 parasites, whereas the other group received saline solution. Diets were maintained after infection. Body weight was recorded every third day, but mice were monitored daily during the course of infection (14 days). The animals were euthanized after 14 days post-infection; euthanasia was conducted according to the protocol approved by license LW-27/14. Briefly, animals were anesthetized intraperitoneally with a mix of 10 mg/kg xylazine−200 mg/kg ketamine. When anesthetized, the animals were exposed to carbon dioxide gas. The thymus was removed, weighed, and subsequently processed for interstitial fluid (IF) extraction. Relative and absolute cell numbers in thymus were estimated by hemocytometer counting.

Flow Cytometry Analysis and Gating Strategies

The cells collected from the thymus were analyzed by flow cytometry according to previously described protocols (Cuervo-Escobar et al., 2014). Briefly, one million cells (1×10^6) were incubated with an anti-Fc-γ III/II (CD16/32) receptor Ab (2.4G2, BD Biosciences) in PBS containing 2% FCS, followed by surface staining with fluorochrome-conjugated antibodies for 20 min at 4°C. The following anti-mouse antibodies were used: APC anti-CD3 (17A2), PE anti-CD4 (GK1.5), APC-Cy7 anti-CD8a (53-6.7), or with IgG isotype-matched control antibodies. To analyze the percentage of proliferative cells, $CD4^+$, $CD8^+$, and $CD4^+CD8^+$ (DP) T cells were treated with the Foxp3 Fixation/Permeabilization Buffer (eBioscience) according to the manufacturer's instructions, and then stained with FITC anti-Ki67 (16A8) for 30 min at room temperature. All antibodies were from BioLegend. Acquisition (100,000 events) was performed in a FACSCanto™ flow cytometer. On-line analysis was performed with FlowJo™ Software, version 8.7. To identify the population of interest we performed the following gate strategy: by first gating on alive (SSC vs. FSC) and singlets (FSC-H vs. FSC-A) cells, we defined the CD4 T cells as $CD4^+CD8^-$, CD8 T cells as $CD4^-CD8^+$, and double positive (DP) T cells as $CD4^+CD8^+$ T cells. A Fluorescence Minus One (FMO) Control was used to identify and gate the $Ki67^+$ cells.

Isolation of Interstitial Fluid From the Thymus

Interstitial fluid (IF) was obtained by injection of PBS and gentle wash of the thymus with sterile needle syringes. Intact cells were pelleted by centrifugation and supernatants were recovered for proteomic analysis, these supernatants are considered as enriched IF from the thymus. The collected fluids were concentrated to a final volume of 100 μL using Amicon Centrifugal Filters 3K (Millipore). To each fluid sample was added 0.1% of Rapigest (Waters) for protein denaturation and rupture of exosomes membrane.

ITRAQ Labeling

In order to adjust the study within a single multiplex experiment, pools of samples from different mice were used instead of individual samples. Equal amounts of fluid samples from three animals within each experimental condition were mixed to produce one sample pool (**Figure 1**). Three sample pools of each group (P1, P2, P3) were used for a total of nine different animals in each experimental condition. Therefore, three biological replicates and two technical replicates for each treatment were incorporated into the multiplex iTRAQ design.

Pooled samples were digested with lysyl endopeptidase mass spectrometry grade (Wako) and sequencing grade modified trypsin (Promega, Madison, WI, USA). After digestion, Rapigest was precipitated and peptides were desalted using Spin Column C18 (Harvard Apparatus, USA) according to the manufacturer's protocol. Peptides were labeled with iTRAQ 4-plex (Reagents iTRAQ Applications 4-plex Kit; AB Sciex, Framingham, MA, USA) and mixed as follows: iTRAQ114 for sample pools of animals fed 14% protein diet); iTRAQ115 for sample pools of animals fed 4% protein diet; iTRAQ116 for sample pools of animals fed 14% protein diet and infected; and iTRAQ117 for sample pools of animals fed 4% protein diet and infected. Labeled peptides were further mixed (**Figure 1**), fractionated by strong cation exchange using Macro Spin Columns (Harvard Apparatus, USA) and desalted using Spin Column C18 (Harvard Apparatus, USA).

Mass Spectrometry Analysis

Tagged and desalinated fractions were subjected to nano-liquid chromatography coupled to mass spectrometry in tandem (nLC-MS/MS) in the mass spectrometry facility of the Carlos Chagas Institute—Fiocruz-Paraná. The nano-liquid chromatography system used was the *Easy NLC-1000* (*Thermo Fisher Scientific*). Injections were made in duplicate. In this system, peptides were loaded onto a reverse phase column packed in house with a flow of 500 nL/min with stationary phase ReprosilPur C18 Acqua (beads 1.9 m in diameter, Dr. Maisch) with a length of 30 cm and inner diameter of 75 μm. The elution of these peptides occurred with a flow of 250 nL/min applying a chromatographic gradient of 5–40% of phase B (5% DMSO, 0.1% formic acid in acetonitrile) for 180 min. Phase A was 5% DMSO in 0.1% formic acid.

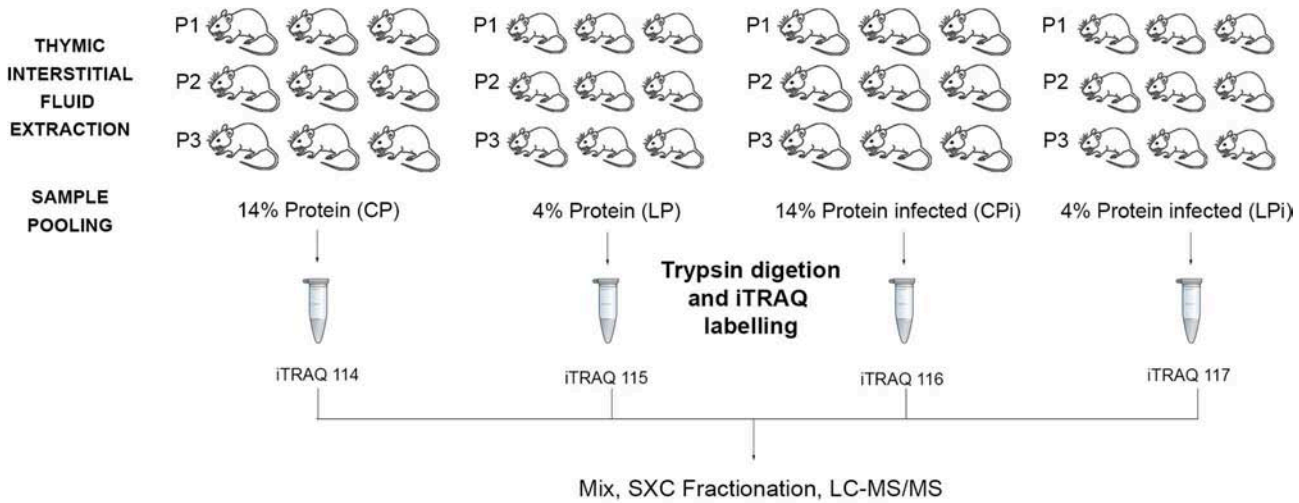

	iTRAQ114	iTRAQ115	iTRAQ116	iTRAQ117
	CP	LP	CPi	LPi
P1	3	3	3	3
P2	3	3	3	3
P3	3	3	3	3

FIGURE 1 | Workflow of the proteomics procedure for analyzing thymic interstitial fluid in protein malnourished and infected mice. Experimental workflow for the mass spectrometry-based identification and quantification of the IF proteins.

Spectra were acquired in a LTQ Orbitrap XL-ETD mass spectrometer (Thermo Fisher Scientific) by data dependent acquisition (DDA), automatically switching between full scan MS (m/z 300-2000) at resolution of 60,000 (m/z 100) and MS/MS with dynamic exclusion of 90s. The five most intense ions with +2 and +3 charges were isolated and fragmented by higher energy collision dissociation (HCD) using normalized collision energy of 45 and 30 ms of activation time. All scan functions of the mass spectrometer and the gradients in the nLC were controlled by Xcalibur 2.0 software (*Thermo Fisher Scientific*).

Protein Identification and Quantification

Protein identification was performed with PatternLab for Proteomics version 3.2.0.3 (http://patternlabforproteomics.org/) using the Comet PSM as search engine (Eng et al., 2013). *Mus musculus* protein sequences were download from UniProt database in February 2015 (http://www.uniprot.org/) with 83.653 entries. For estimation of false discovery rate (FDR), we subsequently generated a target-decoy database including the sequences of common mass spectra contaminants using the PatternLab's Search Database Generator (Carvalho et al., 2012). A cutoff score was established for accept a FDR of 1% based on the marked decoys from the database. The search parameters were tryptic and semi-tryptic peptide candidates, three missed cleavages, fixed modification of cysteine carbamidomethylation, fixed iTRAQ (+144.1 Da) at the N-terminal and in lysine (K) side chain with a 40 ppm mass tolerance of the precursor. Validation of the peptide-spectrum matches was done using Search Engine Processor (SEPro) integrated in the PatternLab for proteomics (Carvalho et al., 2012). The results were processed to accept only sequences with <5 ppm and two or more independent evidence of the presence of the protein in the sample (e.g., identifying a peptide with a different charge state, the same modified version of the unmodified peptide, or two different peptides for the same protein).

Relative quantification was performed using PatternLab's "Isobaric Analyzer" module. The SEPro file was used to produce a report of quantified peptides (Carvalho et al., 2009) A paired comparison analysis between the CP group and each of the other groups (LP, CPi, or LPi) was made, accepting at least 2 unique peptides per protein, 0.30 of "*peptide Log Fold Change Cutoff*" and 0.05 of "*Peptide p-value Cutoff*" for the *t*-paired test or *p* binomial value (Carvalho et al., 2016). Finally, corrected *p*-value was calculated according to the Benjamin–Hochberg procedure (Carvalho et al., 2016). The final report of quantification, containing only proteins with an absolute fold change ≥ 1.5 and $p \leq 0.05$, was exported to Microsoft Excel.

Ontological classification on cellular component, molecular function, and biological process was made through Gene Ontology database (http://geneontology.org/) using the Gene Ontology Explorer tool (GOEx) from the PatternLab (Carvalho et al., 2009). Interactome network analysis was mapped to KEGG pathways using the web-accessible program IIS- Integrated Interactome system (http://www.lge.ibi.unicamp.br/lnbio/IIS/) (Carazzolle et al., 2014). The enriched biological processes of the Gene Ontology database were calculated in each network using the hypergeometric distribution (Carazzolle et al., 2014).

The interaction network was viewed using Cytoscape version 2.8.3 (http://www.cytoscape.org/).

Signal Peptide, Alternative Secretion Pathway and Exosomal Origin Prediction

SignalP 4.1 server (http://www.cbs.dtu.dk/services/SignalP/) was used to predict the N-terminal signal peptide contained in classically secreted proteins (Petersen et al., 2011) and SecretomeP 2.0 server (http://www.cbs.dtu.dk/services/SecretomeP/) was used to predict non-classical *i.e.*, not signal peptide triggered protein secretion (Bendtsen et al., 2004) from our identified proteins. The proteins positively predicted by one of the servers was considered as secreted. The database (Release date: 29 July 2015) from ExoCarta (http://www.exocarta.org/) was used to identify exosomal proteins previously reported for *M. musculus*, *Rattus novergicus,* or *Homo sapiens*.

Measurement of Galectin-1 and Plasminogen by ELISA

Galectin-1 and plasminogen levels were measured in the thymic interstitial fluid by ELISA assays according to the manufacturer's procedures (Abcam Cambridge, UK, Cat. Ab119595 and ab197748). Levels of galectin-1 and plasminogen were expressed in pg/mL.

Histological Analysis of the Thymus

Fragments of the thymus embedded in OCT compound medium (Sakura TissueTek) were cut into 5 mm thick sections and mounted on microscope slides. Sections of the thymus were stained with Mayer's hematoxylin and examined by light microscopy (Nikon Eclipse E400-Tokyo, Japan). Cortical and medullar areas of the thymus were evaluated under a light microscope and quantified in at least 5 fields at 100x magnification and another 5 fields at 400x using the ImageJ 1.48v software (NIH, USA). Cortex:medulla ratio was calculated by dividing the media of cortex area by the media of medulla region of each animal.

Statistics

Statistical analysis was performed using two-way analysis of variance, ANOVA, with Bonferroni *post-hoc* test, or unpaired Student's *t*-test (GraphPad Prism version 6). Statistical significance was accepted at $p < 0.05$.

RESULTS

Protein Malnutrition Alters the Thymic Microarchitecture in BALB/c Mice

Histopathological analysis of the thymus revealed changes in the cortical and medullar areas of the thymus of infected and/or malnourished animals (**Figure 2A**). Quantitation of cortical and medullar areas revealed that malnourished animals (LP and LPi) presented a significant reduction in the cortical area showing a cortical: medullar ratio of 1.9 and 2.0, respectively (**Figure 2B**). These values represent a reduction of 46 and 43% cortical area, respectively, when compared to the control group (CP - cortex:medulla ratio = 3.5). In contrast, the CPi animals presented an increase in the cortical area relative to medulla, and the cortical:medullar ratio is higher in this group when compared to the control group (CP). However, such difference was not statistically significant.

Protein Malnutrition Alters Protein Abundance in the Thymic Interstitial Fluid in BALB/c Mice Infected With *L. infantum*

To gain insights into the effects of malnutrition in the thymic microenvironment during *L. infantum* infection, we used a quantitative proteomics approach for the identification of the global changes in the IF proteomes of malnourished BALB/c mice infected with *L. infantum*. We compared four groups of IF samples: animals fed 14% protein (iTRAQ labeled 114), animals fed 4% protein (iTRAQ labeled 115), animals fed 14% protein and infected with *L. infantum* (iTRAQ labeled 116), and animals fed 4% protein and infected with *L. infantum* (iTRAQ labeled 117).

In total, 3,098 peptides identified in the IF samples were assigned, with 1% FDR, to 280 proteins (**Supplementary Table 1**). Ninety percent (253/280) of the proteins were identified with at least two peptides and the remaining 10% (27/280) were accepted even with one peptide since they were unique or had more than one evidence of their presence in the sample (two or more spectra and/or two or more states of charge).

Many secreted proteins identified in the IF of the thymus are secreted *bona fide* moieties, including albumin, coagulation factors, complement factors, carrier proteins and apolipoproteins (**Supplementary Table 1**). Using SignalP and Secretome P servers we identified which proteins are secreted following classical or alternative pathways (**Supplementary Table 1**). Only for 3% proteins (7/280) were predicted a signal peptide, i.e., they are secreted by the classical pathway exclusively; 43% proteins (121/280) were predicted to be secreted by an alternative pathway exclusively and 14% proteins (39/280) were predicted as presenting both classical and non-classically signals for secretion. In total, 60% (167/280) proteins were identified as secreted proteins. Interestingly, 127 out of these 167 proteins have also been reported as secreted by exosomes. The remaining 40% (113/280) proteins were not predicted as secreted by any of the servers used here; however, 89% (100/113) of them were previously reported as exosomal proteins and 11% (13/113) were neither predicted as exosomal nor secreted by classical or non-classical secretion pathways (**Figure 3A** and **Supplementary Table 1**). In total, 81% (227/280) proteins identified in the thymic IF are secreted by exosomes. Previously reported thymic exosomal proteins were identified in our samples, such as galectin-1, macrophage migration inhibitory factor and plasminogen (Simpson et al., 2009; Turiak et al., 2011; Skogberg et al., 2015). Eight proteins were annotated as exclusively intracellular and 10 proteins do not have subcellular location information yet.

Proteins from CP group were considered as the reference *status* and variations in protein abundance in the other conditions were evaluated against that group. In total, 112, 55, and 109 proteins showed significant differences in abundance at

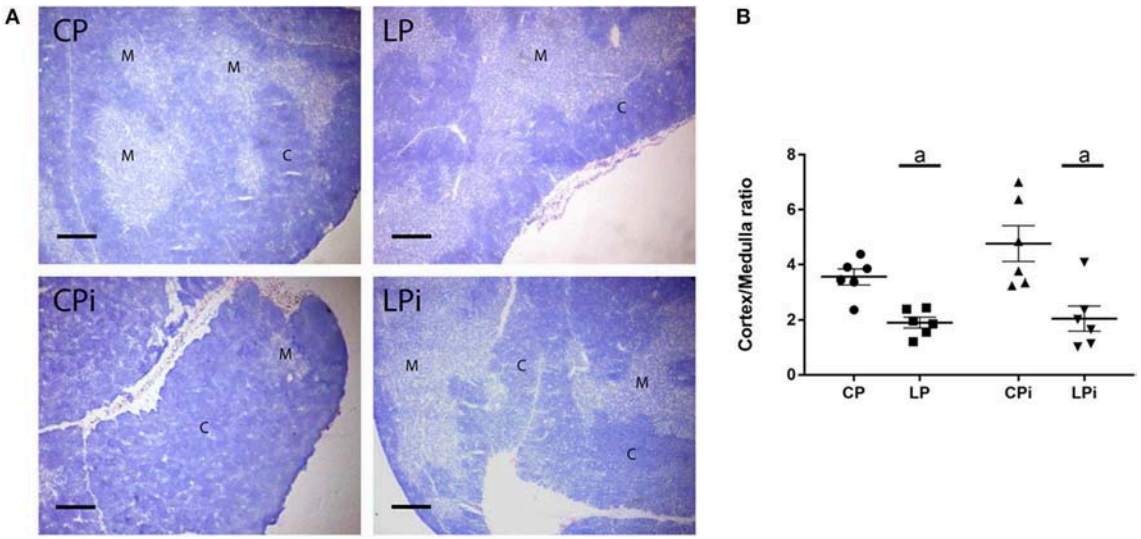

FIGURE 2 | Thymic cortical and medullary regions of BALB/c mice submitted to protein restriction and infected with *L. infantum*. Thymic sections were stained by hematoxylin and cortical or medullary regions were quantified as described in Experimental section. **(A)** Representative images of thymic cortical and medullary regions in each experimental group; **(B)** Cortex:medulla ratio, bars represent mean ± SEM. Data are representative of two independent experiments with 6 animals per group. Magnification bar: 200 μm. C, cortex; M, medulla. CP: animals fed 14% protein diet, LP: animals fed 4% protein diet, CPi: animals fed 14% protein diet and infected, LPi: animals fed 4% protein diet and infected. Two-way ANOVA analysis with Bonferroni *post-hoc* test. Statistical differences due to diet: **a** ($p < 0.0001$).

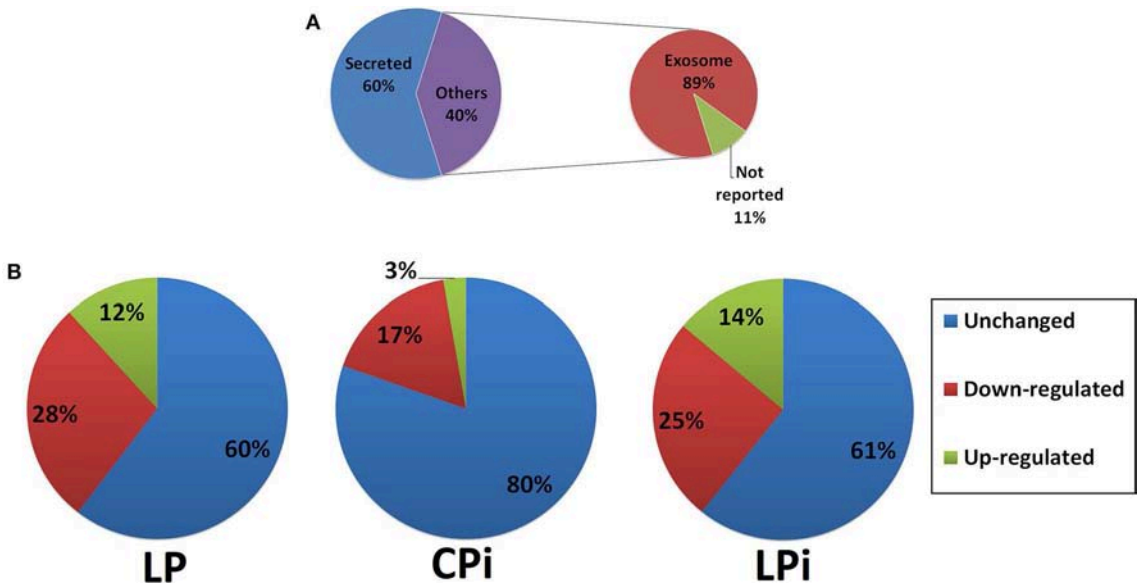

FIGURE 3 | Proteomics analysis of thymic interstitial fluid. **(A)** Percentage of secreted or exosomal proteins identified in the thymic IF of BALB/c mice. **(B)** Percentages of differentially abundant proteins identified in the thymic IF of CPi, LP, or LPi animals relative to CP mice. LP: animals fed 4% protein diet, CPi: animals fed 14% protein diet and infected, LPi: animals fed 4% protein diet and infected.

LP, CPi, and LPi animals, respectively, when compared to the CP group (**Supplementary Figure 1**).

Among the 112 proteins that significantly changed in LP mice, the relative abundance of 78 (28% of the total proteins identified, 78/280) was decreased whereas the relative abundance of 34 (12% of the total proteins identified, 34/280) was increased (**Figure 3B** and **Supplementary Table 1**). Thymic IF from CPi animals presented 55 proteins with altered abundance, 47 of which showed decreased relative abundance (17% of the total identified proteins, 47/280) and 8 increased (3% of the total identified proteins, 8/280) (**Figure 3B** and **Supplementary Table 1**). Differently, thymic IF from LPi mice

showed significant changes in the abundance of 109 proteins. The relative abundance of 71 (25% of the total identified proteins, 71/280) was significantly decreased whereas the relative abundance of 38 (14% of the total identified proteins, 38/280) was increased (**Figure 3B** and **Table 1**).

Differentially abundant proteins were classified according to the functional groups belonging to two main categories of gene ontology: *biological process* and *molecular function*. The highest number of positively regulated proteins in malnourished and infected animal samples was associated with *lipid and amino acid metabolism* and *developmental processes*, whereas negatively regulated proteins were mainly involved in *biosynthetic processes*, *biological regulation, and locomotion*. Many of the positively or negatively regulated proteins were associated with *catalytic and binding activities*. Some of the positively regulated proteins were classified into the group *transporter activity* whereas some negatively regulated proteins were associated with *binding protein activity to transcription factors*. These results are summarized in **Figure 4**.

Galectin-1 Is Significantly Decreased Whereas Plasminogen Is Increased in Malnourished-Infected Mice

In order to further verify, by an alternative method, the differences in protein abundance observed in the thymic IF by iTRAQ, galectin-1 (downregulated in malnourished mice) and plasminogen (upregulated in malnourished mice) were selected to be quantified in the thymic IF using commercial ELISA kits. Galectin-1 is a β-galactoside binding protein secreted by TECs that modulates crucial biological processes in thymus, such as cell adhesion, cell-cell interaction, migration, proliferation, and apoptosis of thymocytes (Baum et al., 1995; Perillo et al., 1998; Camby et al., 2006; Stillman et al., 2006). Plasminogen is the zymogen form of plasmin, a serine peptidase involved in fibrinolytic activities, which substrates include fibronectin, laminin, and von Willebrand factor, among others (Liotta et al., 1981). In the thymus, plasminogen may have an important role in tissue remodeling. In agreement with our proteomics data, analyses by ELISA revealed that the levels of galectin-1 were significantly reduced by malnutrition in the LP and LPi animals, relative to the CP group, whereas plasminogen levels were significantly increased in the thymic IF of malnourished and infected animals (LPi), in relation to the CP group (**Figure 5**).

Proteins Associated With Beta Oxidation of Fatty Acids or the Tricarboxylic Acid Cycle Are Significantly Increased in Malnourished Mice Infected With *L. infantum*

To explore which functions of IF proteins were altered by protein malnutrition and *L. infantum* infection we performed a functional pathway analysis using the IIS- interactome system web-accessible software. Interaction networks among differentially abundant proteins in each group were built to analyze the enriched biological processes shared by quantified proteins.

Proteins with altered abundance in the thymic IF of CPi animals were mostly less abundant when compared to the CP group (**Supplementary Figure 2A**). Groups of negatively regulated proteins that were better defined included: *tricarboxylic acid cycle* (FH, DLST, MDH1, MDH2) and *negative regulation of the apoptotic process* (PRDX3, NPM1, HSPD1, GSTP1). In addition, the proteins YWHAZ, NPM1, HSPD1, and VCP were also found with decreased relative abundance in the CPi group.

The LP group displayed two well-defined clusters of upregulated proteins: proteins associated with *fatty acid beta-oxidation* (HADHB, ACAA2, ECHS1); and proteins associated with the *tricarboxylic acid cycle* (DLST, DLAT, ACO2, PDHB). On the other hand, we observed several clusters of proteins with reduced abundance in LP animals: *mRNA processing* (PCPBP1, NHP2L1, KHSRP, LSM7, HNRNPA2B1); *cellular redox homeostasis* (TXN, PDIA3, SH3BGRT3); *oxidative stress response* (PRDX2, PEBP1, CA3, ATOX1); *drug response* (YWHAZ, DPYSL2, PEBP1); *transcription* (DPY30, ANP32A, CBX3); *metabolic process glutamate* (GOT1, GLUT); among others (**Supplementary Figure 2B**).

Similar to LP animals, the thymic IF of LPi mice exhibited two clusters of positively regulated proteins: (i) proteins associated with *beta oxidation of fatty acids* (HADH, HADHB, ACAA2, ECHS1) and (ii) proteins associated with the *tricarboxylic acid cycle* (DLST, DLAT, ACO2, FH, MDH1, MDH2) (**Figure 6**). A positive regulation was also observed in the group of *iron cellular homeostasis* (FH, FTH1). Several clusters of proteins whose abundance was reduced were evident in the network: *mRNA processing* (PCBP1, NHP2L1, LSM7, KHSRP, HNRNPA2B1); *protein ubiquitination* (VCP, UBE2I3, TCEB2); *cellular redox homeostasis* (TXN, PDIA3, SH3BGRT3); *glycolysis* (TPI1, PGK1); and *negative regulation of apoptotic processes* (KRT18, GSTP1). In addition, the biological process group termed *drug response* clustered both increased (UQCRFS1, SNCA, SOD1) and decreased proteins (YWHAZ, LGALS1, DPYSL2). Similar to the LP and CPi group, YWHAZ and VCP proteins were found with diminished abundance.

Although, LP and LPi show similar behaviors regarding the alteration of abundance of various groups of proteins, the LPi animals exhibit additional changes that were not observed in the LP group (**Supplementary Table 2**). For example, LPi animals exhibited decrease in the abundance of proteins involved in *negative regulation of apoptotic processes* that were not significantly altered in the LP group. Interestingly, this cluster was also significantly decreased in CPi group suggesting that infection *per se* is also modulating the abundance of proteins in LPi mice. In addition, LPi animals exhibited, for example, significant increase of *creatine kinase S-type* protein whereas LP animals showed decreased abundance of this protein (**Supplementary Table 2**).

Comparison between proteomics data from CPi and LPi animals also revealed that the eight proteins upregulated in CPi mice were not upregulated in LPi animals and three of them were even downregulated. For example, proteins that increased in response to infection in CPi animals, such as *microtubule-associated protein 4* and *thioredoxin domain-containing protein 17* (**Supplementary Table 2**) were unchanged or even decreased,

TABLE 1 | Differentially abundant proteins in the thymic interstitial fluid of malnourished BALB/c mice infected with *L. infantum* (LPi).

ProtID	Daltons	Sequence count	Spectral count	Avg Log fold	Fold change	Stouffers *P* value	Description	Gene	Abundance relative to CP
P56480	56247.46	1	2	1.581	4.9	0.011	ATP synthase subunit beta, mitochondrial	Atp5b	Down
P62830	14838.05	1	2	0.696	2.0	0.049	60S ribosomal protein L23	Rpl23	Down
Q9D0T1	14146.54	1	2	0.839	2.3	0.045	NHP2-like protein 1	Nhp2l1	Down
Q8K3C3	21505.1	1	2	0.719	2.1	0.035	Protein LZIC	Lzic	Down
Q91XV3	22055.58	1	2	0.945	2.6	0.023	Brain acid soluble protein 1	Basp1	Down
Q9CQQ8	11610.95	1	2	0.601	1.8	0.044	U6 snRNA-associated Sm-like protein LSm7	Lsm7	Down
P40142	67569.57	1	2	0.644	1.9	0.033	Transketolase	Tkt	Down
P60710	41691.72	1	2	0.988	2.7	0.029	Actin, cytoplasmic 1	Actb	Down
P68037	17832.23	1	2	0.71	2.0	0.010	Ubiquitin-conjugating enzyme E2 L3	Ube2l3	Down
Q8K1I7	50031.76	1	2	0.792	2.2	0.010	WAS/WASL-interacting protein family member 1	Wipf1	Down
P17751	32153.25	1	4	0.439	1.6	0.012	Triosephosphate isomerase	Tpi1	Down
Q9QXT0	20736.25	1	4	0.429	1.5	0.026	Protein canopy homolog 2	Cnpy2	Down
Q9DBP5	22133.28	1	4	0.504	1.7	0.010	UMP-CMP kinase	Cmpk1	Down
O08553	62220.58	1	4	0.443	1.6	0.026	Dihydropyrimidinase-related protein 2	Dpysl2	Down
P63158	24860.15	1	4	1.221	3.4	0.010	High mobility group protein B1	Hmgb1	Down
Q91WJ8	68479.01	1	4	1.2	3.3	0.010	Far upstream element-binding protein 1	Fubp1	Down
Q99KC8	87069.41	1	5	1.083	3.0	0.010	von Willebrand factor A domain-containing protein 5A	Vwa5a	Down
P30416	51521.93	1	5	1.07	2.9	0.010	Peptidyl-prolyl cis-trans isomerase FKBP4	Fkbp4	Down
Q9D8B3	24902.55	1	5	0.56	1.8	0.010	Charged multivesicular body protein 4b	Chmp4b	Down
Q9D1A2	52715.6	1	5	0.681	2.0	0.010	Cytosolic non-specific dipeptidase	Cndp2	Down
P16858	35769.2	1	5	0.705	2.0	0.010	Glyceraldehyde-3-phosphate dehydrogenase	Gapdh	Down
Q6NZB0	29776.36	1	5	0.915	2.5	0.010	DnaJ homolog subfamily C member 8	Dnajc8	Down
P32067	47708.95	1	5	1.558	4.7	0.010	Lupus La protein homolog	Ssb	Down
P50543	11057.48	1	6	0.92	2.5	0.010	Protein S100-A11	S100a11	Down
P63038	60899.38	1	6	1.054	2.9	0.035	60 kDa heat shock protein, mitochondrial	Hspd1	Down
P18760	18529.67	1	6	0.949	2.6	0.010	Cofilin-1	Cfl1	Down
P62774	12834.61	1	7	0.607	1.8	0.010	Myotrophin	Mtpn	Down
P99026	29079.32	1	7	0.653	1.9	0.010	Proteasome subunit beta type-4	Psmb4	Down
Q9JL35	45298.7	1	7	0.746	2.1	0.010	High mobility group nucleosome-binding domain-containing protein 5	Hmgn5	Down
P60335	37455.93	1	7	1.203	3.3	0.010	Poly(rC)-binding protein 1	Pcbp1	Down
P11031	14400.41	1	8	0.781	2.2	0.010	Activated RNA polymerase II transcriptional coactivator p15	Sub1	Down
Q99PT1	23374.8	1	8	0.605	1.8	0.010	Rho GDP-dissociation inhibitor 1	Arhgdia	Down
Q9CQR2	9117.54	1	8	0.801	2.2	0.010	40S ribosomal protein S21	Rps21	Down
O35685	38316.28	2	6	1.113	3.0	0.008	Nuclear migration protein nudC	Nudc	Down
Q05144	21409.07	2	7	1.799	6.0	0.006	Ras-related C3 botulinum toxin substrate 2	Rac2	Down

(Continued)

TABLE 1 | Continued

ProtID	Daltons	Sequence count	Spectral count	Avg Log fold	Fold change	Stouffers *P* value	Description	Gene	Abundance relative to CP
P28667	20135.44	2	7	1.17	3.2	0.008	MARCKS-related protein	Marcksl1	Down
Q62418	48651.6	2	8	0.644	1.9	0.005	Drebrin-like protein	Dbnl	Down
P19157	23576.1	2	8	0.451	1.6	0.006	Glutathione S-transferase P 1	Gstp1	Down
P63028	19431.54	2	8	2.293	9.9	0.007	Translationally-controlled tumor protein	Tpt1	Down
Q6IRU2	28432.42	2	9	1.843	6.3	0.008	Tropomyosin alpha-4 chain	Tpm4	Down
P09405	76658.76	2	9	1.444	4.2	0.007	Nucleolin	Ncl	Down
P00920	28996.49	2	10	0.662	1.9	0.008	Carbonic anhydrase 2	Ca2	Down
Q9JMG1	16340.9	2	11	1.952	7.0	0.005	Endothelial differentiation-related factor 1	Edf1	Down
P62869	13143.64	2	12	0.444	1.6	0.006	Transcription elongation factor B polypeptide 2	Tceb2	Down
P09411	44503.98	2	13	1.268	3.6	0.013	Phosphoglycerate kinase 1	Pgk1	Down
O08997	7315.65	2	13	0.499	1.6	0.005	Copper transport protein ATOX1	Atox1	Down
Q9CQM5	13987.73	2	14	0.738	2.1	0.009	Thioredoxin domain-containing protein 17	Txndc17	Down
P99024	49620.96	2	15	1.344	3.8	0.005	Tubulin beta-5 chain	Tubb5	Down
P27773	56624.67	3	15	0.521	1.7	0.003	Protein disulfide-isomerase A3	Pdia3	Down
P05784	47491.21	3	16	1.583	4.9	0.004	Keratin, type I cytoskeletal 18	Krt18	Down
Q91VW3	10452.26	3	20	0.744	2.1	0.002	SH3 domain-binding glutamic acid-rich-like protein 3	Sh3bgrl3	Down
O35381	28502.23	3	20	0.863	2.4	0.002	Acidic leucine-rich nuclear phosphoprotein 32 family member A	Anp32a	Down
O88569	37361.71	3	23	0.568	1.8	0.002	Heterogeneous nuclear ribonucleoproteins A2/B1	Hnrnpa2b1	Down
O70251	24660.23	3	24	0.689	2.0	0.002	Elongation factor 1-beta	Eef1b	Down
Q3U0V1	76709.7	4	18	0.985	2.7	0.001	Far upstream element-binding protein 2	Khsrp	Down
P28665	165174.53	4	18	1.176	3.2	0.001	Murinoglobulin-1	Mug1	Down
P34022	23563.7	4	21	0.832	2.3	0.001	Ran-specific GTPase-activating protein	Ranbp1	Down
Q9WVA4	22363.15	4	23	1.251	3.5	0.001	Transgelin-2	Tagln2	Down
Q6ZWZ6	14487.47	4	26	1.08	2.9	0.002	40S ribosomal protein S12	Rps12	Down
P99027	11625.82	4	26	1.736	5.7	0.001	60S acidic ribosomal protein P2	Rplp2	Down
P11679	54513.45	4	27	1.036	2.8	0.010	Keratin, type II cytoskeletal 8	Krt8	Down
P16045	14838.19	4	32	0.729	2.1	0.001	Galectin-1	Lgals1	Down
P63101	27735.73	5	23	1.264	3.5	0.001	14-3-3 protein zeta/delta	Ywhaz	Down
P10639	11649.63	5	37	1.136	3.1	0.000	Thioredoxin	Txn	Down
P16015	29329.63	6	39	0.826	2.3	0.000	Carbonic anhydrase 3	Ca3	Down
E9PZF0	30162.67	6	41	1.074	2.9	0.000	Nucleoside diphosphate kinase	Gm20390	Down
Q61599	22818.48	7	41	0.859	2.4	0.000	Rho GDP-dissociation inhibitor 2	Arhgdib	Down
P48036	35712.2	7	51	0.585	1.8	0.000	Annexin A5	Anxa5	Down
P26645	29625.81	7	52	1.267	3.6	0.000	Myristoylated alanine-rich C-kinase substrate	Marcks	Down
P07759	46831.98	10	61	1.296	3.7	0.000	Serine protease inhibitor A3K	Serpina3k	Down
Q01853	89247.71	12	52	1.026	2.8	0.000	Transitional endoplasmic reticulum ATPase	Vcp	Down
Q63918	46717.37	1	2	−0.903	2.5	0.036	Serum deprivation-response protein	Sdpr	Up
P10493	136432.48	1	2	−1.186	3.3	0.041	Nidogen-1	Nid1	Up
Q6P8J7	47425.31	1	2	−0.925	2.5	0.047	Creatine kinase S-type, mitochondrial	Ckmt2	Up

(Continued)

TABLE 1 | Continued

ProtID	Daltons	Sequence count	Spectral count	Avg Log fold	Fold change	Stouffers *P* value	Description	Gene	Abundance relative to CP
Q8BMF4	67880.67	1	2	−0.97	2.6	0.020	Pyruvate dehydrogenase complex component E2	Dlat	Up
Q8BKZ9	53947.22	1	2	−0.429	1.5	0.022	Pyruvate dehydrogenase protein X component, mitochondrial	Pdhx	Up
P37804	22543.37	1	2	−0.666	1.9	0.016	Transgelin	Tagln	Up
O55042	14458.17	1	2	−0.602	1.8	0.047	Alpha-synuclein	Snca	Up
P20918	90730.9	1	2	−0.983	2.7	0.036	Plasminogen	Plg	Up
Q61425	34423.87	1	3	−1.349	3.9	0.010	Hydroxyacyl-coenzyme A dehydrogenase, mitochondrial	Hadh	Up
P06151	36457.21	1	4	−0.616	1.9	0.010	L-lactate dehydrogenase A chain	Ldha	Up
P31786	9976.13	1	4	−0.415	1.5	0.014	Acyl-CoA-binding protein	Dbi	Up
P35505	46128.03	1	5	−0.607	1.8	0.036	Fumarylacetoacetase	Fah	Up
P56375	11852.05	1	6	−0.644	1.9	0.010	Acylphosphatase-2	Acyp2	Up
P09528	21035.25	1	6	−0.548	1.7	0.018	Ferritin heavy chain	Fth1	Up
Q9CR68	29331.19	1	7	−0.557	1.7	0.010	Cytochrome b-c1 complex subunit Rieske, mitochondrial	Uqcrfs1	Up
Q91XL1	37389.49	1	7	−0.458	1.6	0.024	Leucine-rich HEV glycoprotein	Lrg1	Up
Q91V76	34955.33	1	8	−0.641	1.9	0.010	Ester hydrolase C11orf54 homolog	C11orf54	Up
P99028	10409.97	1	8	−0.836	2.3	0.010	Cytochrome b-c1 complex subunit 6, mitochondrial	Uqcrh	Up
Q9WTP6	26433.69	1	8	−0.491	1.6	0.010	Adenylate kinase 2, mitochondrial	Ak2	Up
P08228	15914.79	1	16	−0.721	2.1	0.010	Superoxide dismutase [Cu-Zn]	Sod1	Up
Q99JY0	51335.4	2	5	−1.348	3.8	0.005	Trifunctional enzyme subunit beta, mitochondrial	Hadhb	Up
P52503	12993.66	2	5	−0.574	1.8	0.008	NADH dehydrogenase [ubiquinone] iron-sulfur protein 6, mitochondrial	Ndufs6	Up
Q9D2G2	48945.47	2	12	−0.773	2.2	0.006	2-oxoglutarate dehydrogenase complex component E2	Dlst	Up
Q6LD55	11293.81	2	14	−0.727	2.1	0.005	APOAII	Apoa2	Up
Q61171	21747.05	2	14	−0.495	1.6	0.006	Peroxiredoxin-2	Prdx2	Up
Q3THE6	20664.39	2	15	−0.757	2.1	0.005	Ferritin	Fth	Up
Q8BWT1	41785.43	2	15	−0.812	2.3	0.005	3-ketoacyl-CoA thiolase, mitochondrial	Acaa2	Up
P21614	53546.98	2	17	−0.499	1.6	0.009	Vitamin D-binding protein	Gc	Up
P97807	54304.06	3	10	−0.678	2.0	0.003	Fumarate hydratase, mitochondrial	Fh	Up
P14152	36470.07	3	13	−0.814	2.3	0.003	Malate dehydrogenase, cytoplasmic	Mdh1	Up
Q99LC5	34969.49	3	16	−0.768	2.2	0.003	Electron transfer flavoprotein subunit alpha, mitochondrial	Etfa	Up
P56391	10046.87	3	16	−0.779	2.2	0.003	Cytochrome c oxidase subunit 6B1	Cox6b1	Up
Q8BH95	31436.2	4	21	−1.269	3.6	0.001	Enoyl-CoA hydratase, mitochondrial	Echs1	Up
P08249	35570.75	4	22	−0.697	2.0	0.001	Malate dehydrogenase, mitochondrial	Mdh2	Up
Q99KI0	85392.01	7	33	−0.785	2.2	0.000	Aconitate hydratase, mitochondrial	Aco2	Up
Q91X72	51267.17	8	50	−0.418	1.5	0.000	Hemopexin	Hpx	Up
Q9DCW4	27587.97	8	51	−1.378	4.0	0.000	Electron transfer flavoprotein subunit beta	Etfb	Up
Q921I1	76655.71	12	87	−0.66	1.9	0.000	Serotransferrin	Tf	Up

Difference in protein abundance is relative to control mice (CP group).

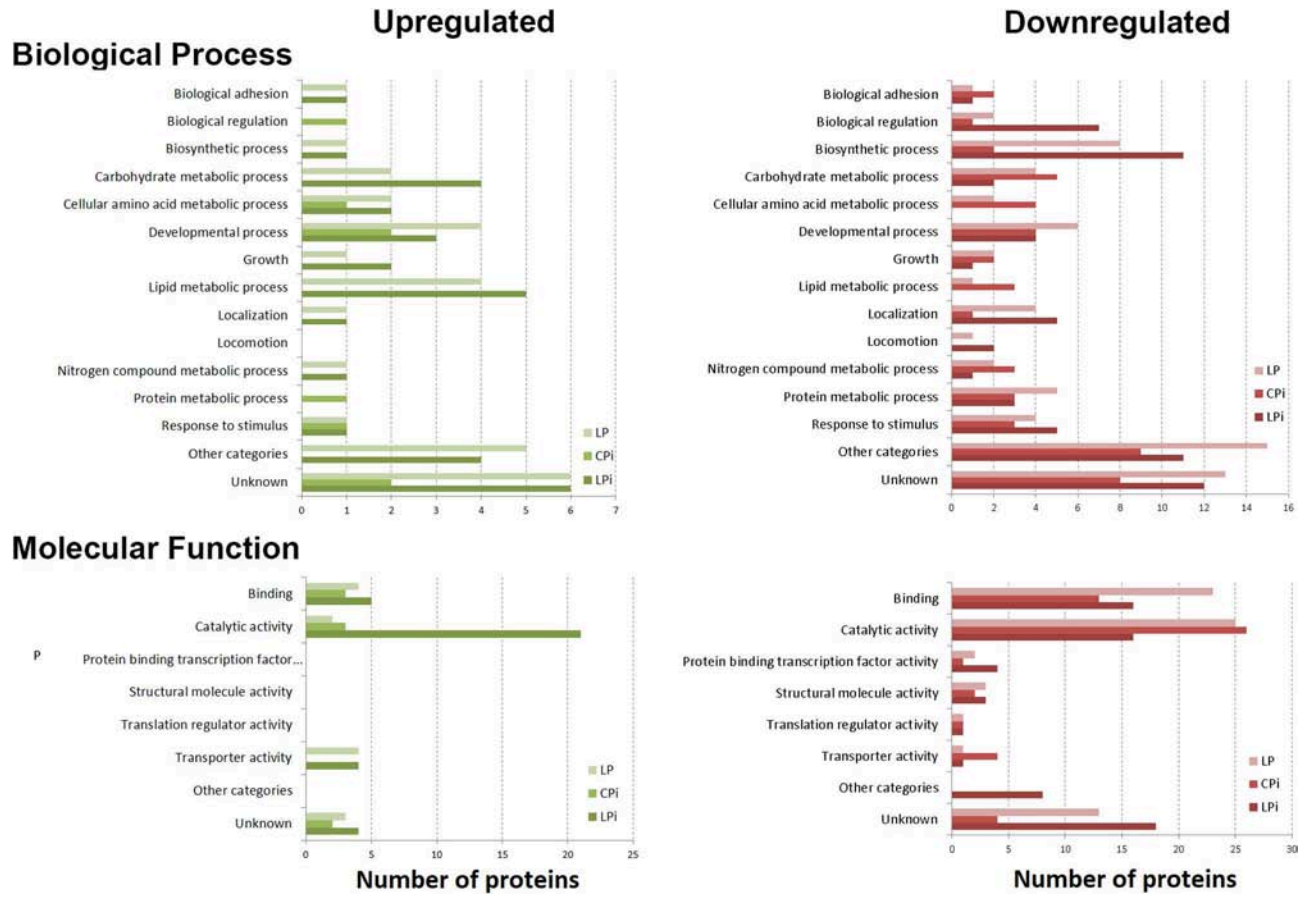

FIGURE 4 | Biological and molecular processes associated with altered protein abundance in the thymic IF of BALB/c mice. Functional annotation of biological process and molecular function assigned to the differentially abundant proteins as annotated in the Gene Ontology database. Differential abundance in LP, CPi, or LPi mice, relative to CP animals. LP: animals fed 4% protein diet, CPi: animals fed 14% protein diet and infected, LPi: animals fed 4% protein diet and infected.

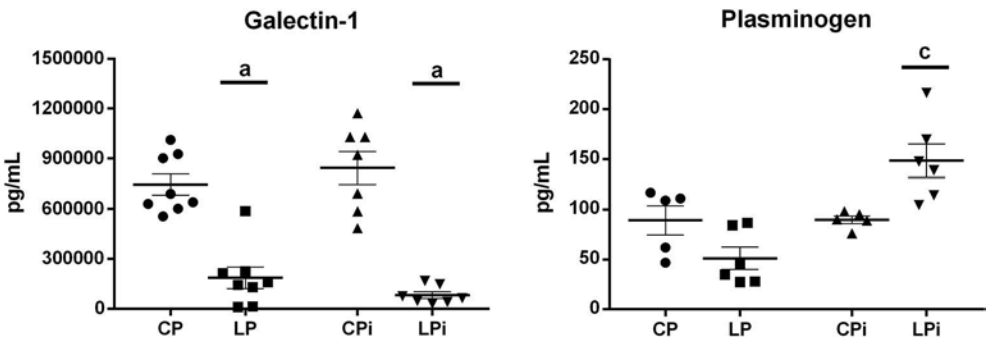

FIGURE 5 | ELISA quantification of proteins secreted into the thymic IF. Galectin-1 and plasminogen were quantified by a commercial ELISA kit and their values are expressed in pg/mL ($n = 5$–8 animal per group). Statistical differences due to diet: **a** ($p < 0.0001$), and interaction between diet and infection: **c** ($p < 0.05$) were determined using two-way ANOVA with Bonferroni *post-hoc* test. CP: animals fed 14% protein diet, LP: animals fed 4% protein diet, CPi: animals fed 14% protein diet and infected, LPi: animals fed 4% protein diet and infected.

respectively, in the LPi animals. In addition, infection in CPi induced downregulation of 47 proteins but 19 of them were upregulated by malnutrition in LPi. For instance, CPi animals showed a 6.7-fold reduction of *vitamin D-binding protein* whereas in LPi mice this protein was significantly upregulated (1.6-fold change). Those data emphasize that changes in protein abundance due to a precedent malnutrition could affect the immune response to infection.

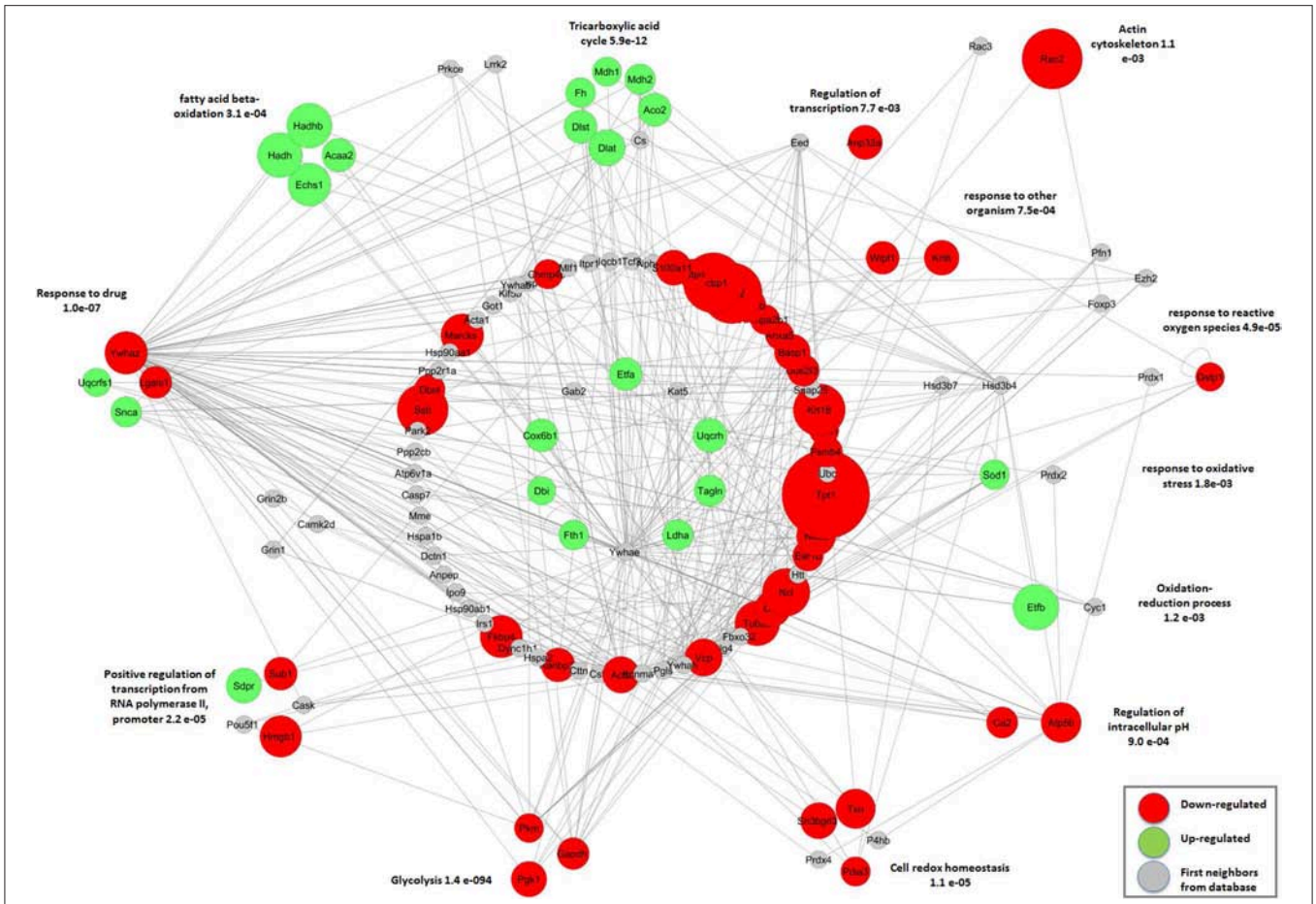

FIGURE 6 | Functional interaction network among differentially abundant proteins identified in the thymic IF of LPi mice grouped by biological process. The proteins with differential abundance in the LPi group relative to the CP group were grouped according to the biological process enriched with $p < 0.05$. The proteins represented in the central circles did not present clusters with significant enrichment in the biological process. Network was built using the IIS (Integrated interactome system) platform and viewed in Cytoscape software version 2.8.3.

Protein Malnutrition Decreases the Proliferation of Single Positive and Double Positive T Cells From the Thymus of *L. infantum*-Infected Mice

As proteomics data were suggestive of a non-proliferative thymic microenvironment, we evaluated the expression of Ki67 on T cell subsets from the thymus of malnourished animals infected with *L. infantum*. Flow cytometry analysis revealed that malnutrition impaired the proliferative capabilities of thymic lymphocyte subpopulations, altering the percentage of proliferative thymocytes (**Figure 7A** and **Supplementary Figure 4**). The percentage of proliferative ($Ki67^+$) single positive T cells ($CD4^+$ or $CD8^+$ T cells) was significantly decreased in the thymus of malnourished animals ($p < 0.001$). Infection with *L. infantum* in malnourished animals induced a still more accented decrease in the percentage of $CD4^+Ki67^+$ and $CD8^+Ki67^+$ T cells ($p < 0.001$). By contrast, CPi mice displayed a trend to increase the percentage of $CD4^+$ and $CD8^+$ T cells undergoing proliferation. Both independently and by interaction, protein malnutrition and infection induced a significant decrease in the percentage of double positive T cells ($CD4^+CD8^+$ T cells, DP) proliferating and that had recently proliferated, based on Ki67 expression, in the thymus of BALB/c mice ($p < 0.001$) (**Figure 7B**).

DISCUSSION

We previously demonstrated that interaction between protein malnutrition and *L. infantum* infection in BALB/c mice resulted in significant thymic atrophy, hypocellularity, changes in T cell subsets and thymic infection (Cuervo-Escobar et al., 2014; Losada-Barragan et al., 2017). These events were accompanied by significant alterations in the gene expression, at mRNA and protein levels, of chemokines, and adhesion molecules involved in T cell migration whereas mRNA and protein levels of proapoptotic molecules were not affected (Cuervo-Escobar et al., 2014; Losada-Barragan et al., 2017). All those alterations accelerated the pathological events observed during the course of infection with *L. infantum* resulting in an increased

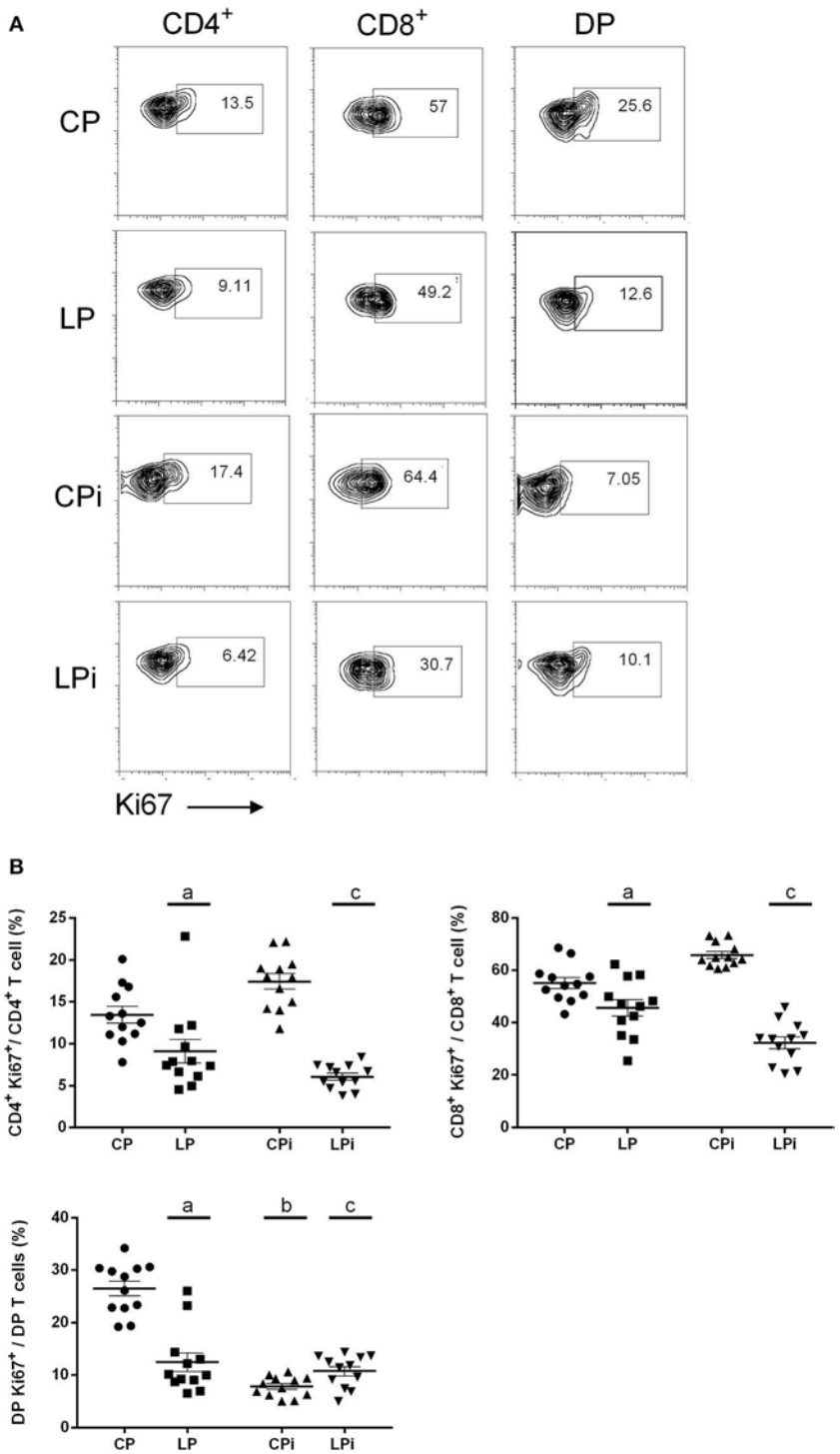

FIGURE 7 | Flow cytometry analysis of T cell subpopulations proliferating in the thymus of malnourished animals infected with *L. infantum*. Lymphocyte subpopulations from the thymus of the experimental groups were measured using FACS analysis as described in the Materials and Methods. **(A)** Representative plots of thymocyte subpopulations stained with Ki67. All images shown were selected from one single experiment and are representative of the phenotype obtained at each group; numbers indicate the percentages of the corresponding gate shown. Displacement of some subpopulations of thymocytes was observed during the analyzes and an adjust of the Ki67+ gate was necessary to distinguish proliferative and non-proliferative cells. The gates were defined using the same criteria described in **Supplementary Figure 4**. **(B)** Percentage of thymocytes subsets expressing Ki67 ($n = 12$ animals per group from two independent experiments with 6 animals each). CP: animals fed 14% protein diet; LP: animals fed 4% protein diet, CPi: animals fed 14% protein diet and infected; LPi: animals fed 4% protein diet and infected. Two-way ANOVA analysis with Bonferroni *post-hoc* test. Statistical differences due to diet: **a** ($p < 0.001$), infection: **b** ($p < 0.001$) and interaction between diet and infection: **c** ($p < 0.001$).

parasite load in spleen, without infection resolution in the liver, and an earlier drastic damage of splenic architecture (Cuervo-Escobar et al., 2014; Losada-Barragan et al., 2017). Such observations led us to suggest that instead of increasing T cell apoptosis, malnutrition seriously affected the migration of these cells (both central and peripheral migration), leading to defects in T cell-mediated immune responses to *L. infantum*. Remarkably, *ex vivo* assays revealed that thymocytes from LPi group stimulated with chemotactic stimuli did preserve their migratory capabilities, indicating that in malnourished mice the thymic microenvironment that mediates cell mobilization, including extracellular matrix molecules and protein milieu, are altered rather than the migratory capabilities of T cells *per se* (Cuervo-Escobar et al., 2014; Losada-Barragan et al., 2017). In the current study, we analyzed the thymus microarchitecture, the proteins circulating in the thymic microenvironment and the proliferation of thymocytes from malnourished BALB/c mice infected with *L. infantum* with the aim to identify the factors that could be influencing the pathophysiology of the organ in these conditions.

The thymic physiology is highly dependent of an ordered process for T-cell development, involving sequential migration of immature thymocytes through differentiated regions of the thymus that contribute for each cell to receive the proper signals and favor cell–cell interactions in a precise order and in a suitable microenvironment (Petrie and Zuniga-Pflucker, 2007). The thymic cortex is the location where β-selection and positive and negative selection occur and is mainly constituted by double negative (DN) and double positive (DP) T cell populations, whereas the thymic medulla is enriched of single positive (SP) $CD4^+$ and $CD8^+$ T cells expressing high levels of the αβTCR (Anderson et al., 2014). In this study, histopathological analysis of thymic microarchitecture of malnourished BALB/c mice infected or not with *L. infantum* revealed a significant ∼2-fold reduction of the cortex:medulla ratio. Remarkably, this reduction was accompanied by a significant ∼5-fold decrease in the abundance of cytokeratins K8 and K18, which are produced by TECs. These results could suggest that in malnourished mice (i) immune responses are not properly recruited to control thymic infection (Cuervo-Escobar et al., 2014; Losada-Barragan et al., 2017 and/or (ii) maturation and migration of T cells are not properly occurring in these animals in response to local and systemic infection. In fact, we observed that malnutrition drastically alters cellularity in infected animals, and total numbers of DP and SP T cells are significantly diminished in malnourished mice [(Cuervo-Escobar et al., 2014) and this study, **Supplementary Figure 3**]. During infection with other pathogens, it has been observed that recruiting of peripheral T cells back to the thymus has an important role in preventing the emergence and export of microorganism-tolerant T cells (Nobrega et al., 2013; Nunes-Alves et al., 2013). As we detected parasites in thymus of infected mice, it is possible to suggest that peripheral T cells reentry to the organ to control local infection; however, in malnourished animals, such responses could be altered. In addition, we previously reported a significant reduction in total DP (Cuervo-Escobar et al., 2014) and a significant increase of CCR7 expression in the thymus of LPi animals (Losada-Barragan et al., 2017). Thus, our results suggest that impairment of cortical area expansion due to malnutrition during *L. infantum* infection could alter key thymic processes such as (i) β-selection, (ii) proliferation, (iii) positive selection, and/or (iv) proper migration of DN and DP T cell populations, all of which occur in the cortex. In addition, our results also suggest that such alterations should be accompanied by dysregulations in distribution and location of ECM components that are essential to guide thymocyte differentiation and to drive the migration of thymocytes in the complexes with epithelial cells (Savino et al., 2000, 2004). However, such hypotheses remain to be further explored.

To analyze if the changes in the cortex:medulla ratio are accompanied by alterations in the levels of proteins secreted into the ECM milieu, composing a scenario where both structural and soluble factors would be affected by malnutrition, we performed a quantitative proteomics profiling of the thymic microenvironment for identification and quantification of proteins in IF samples. To our knowledge, this is the first quantitative proteomics study of the thymic IF and the first work showing the proteome changes occurring in the interstitial microenvironment of the thymus during interaction of two pathological conditions: protein malnutrition and *L. infantum* infection.

In total, we identified 280 proteins in thymic IF, and most of them (97%) are secreted by some predicted mechanism either exosomal, classical or alternative. Remarkably, we identified 81% proteins previously reported as exosomal. In general, exosomes and other secreted microvesicles typically carry ubiquitously expressed molecules, such as intracellular metabolic enzymes, cytoskeletal proteins, chaperones, and ribosomal proteins (Shin et al., 2009; Zhu et al., 2015). Exosomes are specifically enriched in molecules associated with their biogenesis or in molecules selectively packaged within them (Coakley et al., 2015). These proteins may constitute more than half of the secreted proteins as it has been observed in cancer cells (Wu et al., 2008). Despite our aim was not to characterize exosomes or extracellular vesicles, by comparison with previous studies reported elsewhere (Simpson et al., 2008; Skogberg et al., 2013, 2015; Lundberg et al., 2016) allow us to state that our IF samples contained proteins from exosomal origin. In fact, our proteomics data include typical exosomal markers and proteins often identified in exosomes such as: actin cytoplasmic 1 (ACTB), annexin A5 and 6 (ANXA5, ANXA6), cofilin-1 (CFL1), alpha-enolase (ENO1), phosphoglycerate kinase 1 (PGK1), pyruvate kinase PKM (PKM2), 14-3-3 protein zeta/delta (YWHAZ), serum albumin (ALB), L-lactate dehydrogenase A chain (LDHA), elongation factor 1-alpha 1 (EEF1A1), glyceraldehyde-3-phosphate dehydrogenase (GAPDH), and fructose-bisphosphate aldolase A (ALDOA) (http://www.exocarta.org/exosome_markers) (Simpson et al., 2009). Vesicles with hallmarks of exosomes have been described and characterized from primary cultures of thymic epithelial cells (TECs) (Simpson et al., 2009; Skogberg et al., 2013, 2015). Forty two percent of the proteins identified here were previously described as secreted by exosomes from TECs and/or in thymus of C57BL/6 mice (Skogberg et al., 2013, 2015; Lundberg et al., 2016). We also identified typical proteins

with a known expression in TECs such as cytokeratins K8 and K18 (Lundberg et al., 2016). These data indicate that proteins identified in the thymic IF have a mixed origin, with a significant proportion being secreted by TECs.

Several studies have shown that exosomes are capable of presenting antigens for T cells by themselves or indirectly via uptake by dendritic cells (DCs) (Raposo et al., 1996). Exosomes have several functions in the activation and suppression of immune cells (Montecalvo et al., 2012; Deng et al., 2013) and are also proposed to play a role in the development of diseases and tissue homeostasis (Valadi et al., 2007; Pegtel et al., 2010; Aswad et al., 2014; Ridder et al., 2014; Banfai et al., 2019). In the thymus, secreted exosomes from stromal medullary epithelial cells (mTECs) can contribute both to intercellular antigenic transfer by spreading antigens within the thymus and to the thymic physiology maintenance (Skogberg et al., 2015; Lundberg et al., 2016). Our proteomics dataset reveals exosomal secretion of different types of proteins mainly related with protein expression regulation and metabolism, suggesting the presence of intercellular transfer mechanisms that go beyond antigen presentation and could include further thymic cellular functions. Thus, our data provide molecular bases to hypothesize that secretion of proteins via exosomes is an important mechanism of cell communication in the thymic microenvironment. However, such hypothesis remains to be further explored.

Considering that its content is specific, it is possible to suggest that changes in the abundance of different types of exosomal proteins could reflect the communication that is happening among the thymus cells under pathological conditions. We found that the thymic IF of low protein diet groups (LP and LPi) particularly displayed down-regulation of proteins associated with transcription, translation, mRNA processing, and proteolysis, while the CPi group presented few differential changes of these kind of proteins. These findings highlight a dysregulation of the protein expression in thymic cells and consequently in the thymic microenvironment physiology. Thus, the reduced abundance of those type of proteins due to low protein diet may alter the regulation of the proteins that are going to be transcribed, translated and degraded during infection condition, reducing the local and systemic response to *L. infantum* infection.

Galectin-1 (LGALS1) is an exosomal protein with crucial role in thymus functionality (Perone et al., 2006); it is produced by TECs and binds to thymocytes modulating the interaction strength to the TCR, and therefore influencing its selection (Baum et al., 1995). Galectin-1 plays a critical role in apoptosis of negatively selected thymocytes (Perillo et al., 1998). Furthermore, LGALS1 mediates leukemic cell differentiation (Zhao et al., 2011) and has an important role in the adhesion of different cell types to the ECM via the cross-linking of glycoproteins with ECM components such as laminin and fibronectin (Gameiro et al., 2010). Alterations in LGALS1 production lead to aberrant thymic selection and altered T cell populations (Liu et al., 2008). Remarkably, we detected diminished levels of LGAS1 in the IF of the thymus of LPi mice. Since Gal-1 promotes the apoptosis of immature cortical thymocytes *in vitro* (Perillo et al., 1998), it is possible to suggest that diminished levels of this protein within the thymic microenvironment of malnourished mice could have a deleterious impact in the processes of positive and/or negative selection. Interestingly, LPi mice also exhibited increased levels of antiapoptotic markers (Losada-Barragan et al., 2017). These results, together with the observation that protein malnutrition modified the cortex:medulla ratio in the thymus of *L. infantum* infected mice, reinforces the hypothesis that an abnormal interaction of thymocytes with ECM components occurs in malnourished mice. Such defect would imply altered signalization during T cell differentiation and defective thymocyte selection in these animals. On the other hand, we observed a significant increase of plasminogen in malnourished mice. As this protein is involved in tissue remodeling, its increased abundance suggests a potential role in the alteration of the thymic microarchitecture in those animals. Interestingly, increase of plasminogen was accompanied by a decrease in von Willebrand factor, a known substrate for plasmin, reinforcing the hypothesis that plasminogen is actively participating in remodeling the thymic microenvironment of malnourished mice.

Thymic secreted proteins such as Rho GDP-dissociation inhibitor 1 and 2 (Rho GDIa and GDIb, respectively) have an important role in T cell development and egress (Ishizaki et al., 2006). Deficiency in Rho GDIa and GDIb is involved in defective intrathymic differentiation and T cell migration, particularly exported from the thymus (Ishizaki et al., 2006). In agreement with previous reports (Lundberg et al., 2016), we observed that these proteins are secreted in the thymus by exosomes. Moreover, these proteins were downregulated in malnourished mice, suggesting that thymocyte differentiation and T cell egress might be compromised in those animals. As a consequence, a reduction in peripheral T cell population, as observed previously (Cuervo-Escobar et al., 2014), might have a deleterious impact on parasite control. Together, our results show that malnutrition alters abundance of proteins involved in thymic remodeling, thymocyte adhesion and differentiation, and T cell migration, all of which contribute to thymic atrophy and defective peripheral T cell colonization.

Although available molecular data of thymic metabolism are relatively scarce, studies on cancer cell metabolism have helped to understand the metabolic requirements of proliferating cells, and have facilitated their study on T cells. In particular, studies on the bioenergetic profile of T cells have revealed that their metabolism change dynamically with the state of activation and differentiation (Wang and Green, 2012; Pearce et al., 2013; Lochner et al., 2015; Buck et al., 2016; Rambold and Pearce, 2018). Consistent with the metabolism of other non-proliferative cells, naive T cells and memory T cells maintain low glycolysis rates and predominantly oxidize pyruvate derived from glucose through oxidative phosphorylation (OxPhos) or involving fatty acids oxidation (FAO) to generate ATP (Pearce et al., 2013). Following activation, T cells switch to an anabolic growth program and accumulation of biomass to generate daughter cells; a process that requires a greater demand for ATP and metabolic resources. In addition, catabolic ATP generation pathways such as β-oxidation of fatty acids are actively suppressed (Wang and Green, 2012). However, it is unknown which metabolic pathways

are involved in the homeostasis of T cell proliferation and differentiation in the thymus. In this work, we found increased abundance of enzymes that participate in the catabolism of fatty acids via β-oxidation in malnourished animals. Enzymes such as enoyl-CoA hydratase (ECHS1), hydroxyl-coenzyme A dehydrogenase (HADH), 3-ketoacyl-CoA thiolase (ACAA2), and trifunctional beta subunit enzyme (HADHB) were significantly increased in that group. In addition, a high proportion of mitochondrial proteins participating in OxPhos and TCA were identified with greater abundance in malnourished (LP and LPi) mice in relation to CP animals. Such metabolic pattern seems to resemble a naïve or memory T cell metabolic profile and fits with a non-proliferative cell profile under malnutrition conditions in the thymus. Remarkably, such profiling is supported by the observation of a significant decrease in the percentage of proliferative SP and DP T cells in malnourished animals. Such results would also be in agreement with the microarchitecture alterations in the thymus of malnourished animals.

These findings could also be related with a diminished recirculation of peripheral T cells into the thymus and/or a defective proliferation and differentiation of thymocytes during protein malnutrition and *L. infantum* infection. In agreement, our results from flow cytometry analysis corroborated defective proliferation of SP and DP T cells in malnourished animals. Moreover, it is well-documented that during thymus infection by *Mycobacterium tuberculosis* and *Mycobacterium avium* there is an increased mobilization of mature peripheral T cells recirculating back into this organ, which seem to be related to controlling the thymic infection (De Meis and Savino, 2013; Nobrega et al., 2013). As we reported previously, the thymus is a direct target of *L. infantum* infection (Losada-Barragan et al., 2017) and therefore, according to the proteomic profile, it seems plausible that during a protein restricted diet, the mobilization of peripheral T cells back to the thymus could be diminished, affecting the control of the local infection (Losada-Barragan et al., 2017). In contrast, well-nourished infected animals exhibited a down-regulation of ECHS1 and ACAA2, suggesting a diminished rate of FAO and a proliferative profile in response to infection. However, further assays are needed to clarify this issue.

Additionally, in LPi mice we observed reduced abundance of proteins associated with differentiation processes, such as S100 calcium binding protein A11 (S100a11), endothelial differentiation-related factor 1 (EDF1) and transgelin-2 (TAGLN2). S100a11 has been implicated in the regulation of epidermal (Olsen et al., 1995), chondrocyte (Cecil and Terkeltaub, 2008) and keratinocyte differentiation (He et al., 2009). Furthermore, this protein is able to function as an unconventional inflammatory mediator of altered chondrocyte differentiation and matrix remodeling (Cecil and Terkeltaub, 2008). In cancer cells decreased levels of S100a11 have been associated with invasive forms (Ji et al., 2014; Zhang et al., 2015). EDF1 is a calmodulin binding protein that regulates calmodulin-dependent enzymes involved in the repression of endothelial cell differentiation (Mariotti et al., 2000). Moreover EDF1 is upregulated during early adipogenesis, since silencing of EDF1 in 3T3-L1 cells blocked adipose conversion, showing that its expression is required for the progression of the adipogenic program (Lopez-Victorio et al., 2013). TAGLN and TAGLN2 primarily participate in processes associated with a remodeling of actin cytoskeleton and their role in differentiation has been mainly described in tumor cells. However, the functional meaning of these proteins in the thymus remains to be defined. We presume that downregulation of TAGLN2 and upregulation of TAGLN levels together with downregulation of S100a11 and EDF1 in the IF of LPi mice could be also associated with defective differentiation processes in the thymus.

In general, malnutrition affected the thymus gland in such a way that when the animal is infected, it fails to respond properly to the infection due to all the defects caused by the previous malnutrition. Despite considering that malnutrition is the main detrimental factor for the thymus and therefore has very deleterious consequences in the immune response mediated by cells, we cannot rule out that the infection *per se* is also very harmful to the organ, as has been observed in other infections such as with *Trypanosoma cruzi* (Perez et al., 2012; Gonzalez et al., 2016). However, in this work we do not focus our attention on infection *per se*, because the course of infection is too short to draw conclusions about it. Instead, we call attention to the plethora of alterations that malnutrition induced in the thymic microenvironment and how those defects may impact the response to infection.

Characterization of thymus microarchitecture and thymic secreted proteins in malnourished animals infected with *L. infantum* allowed the identification of new elements in the thymus physiology under such conditions. We demonstrated that the abundance of thymic secreted proteins is altered by protein malnutrition in mice infected with *L. infantum*, likely affecting thymic intercellular communication and basic processes in the thymus. Together, the reduced cortical area, the increased abundance of OxPhos- and β-oxidation-related proteins and the decreased abundance of galectin-1, and Rho GDIa and GDIb, among others, may play a critical role in intrathymic proliferation, dysfunctional thymocyte differentiation and selection and defective T cell migration, all of which can contribute to exacerbate thymic atrophy observed in malnourished mice infected with *L. infantum*. In addition, these elements suggest that a protein-restricted diet modifies both structural and soluble thymic factors, resulting in a non-proliferative microenvironment in *L. infantum* infected mice that could affect the proper mobilization of peripheral T cells into the thymus and toward periphery, affecting the control of the local and systemic infection.

DATA AVAILABILITY

The datasets generated and analyzed for this study can be found in the Pride Archive https://www.ebi.ac.uk/pride/archive/ with the dataset identifier PXD010414.

ETHICS STATEMENT

This study was carried out in accordance with the recommendations of the Guide for the Care and Use of

Laboratory Animals of the National Institutes of Health—Eighth Edition. The protocol was approved by the Instituto Oswaldo Cruz committee for Animal Care and Use (License #LW-27/14). The *L. infantum* strain MCAN/BR/2000/CNV-FEROZ used in this study was provided by the Collection of Leishmania of the Instituto Oswaldo Cruz, Rio de Janeiro (Coleção de Leishmania do Instituto Oswaldo Cruz, CLIOC; http://clioc.fiocruz.br/). This collection is registered in the World Federation for Culture Collections (WFCC-WDCM 731) and is recognized as a Depository Authority by the Brazilian Ministry of the Environment (D.O.U. 05.04.2005).

AUTHOR CONTRIBUTIONS

Conceived and designed the experiments: PC, ML-B, AU-P, SC-E, GP. Performed the experiments: ML-B, JD, AR-V, AU-P, SC-E, FR-G, LB, FM, PA, PC. Analyzed the data: ML-B, AU-P, FR-G, RP, DM, PCC, WS, MS-G, GP, PC. Contributed reagents, materials, and analysis tools: AU-P, SC-E, RP, DM, WS, MS-G, PC. Contributed to the writing of the manuscript: ML-B, AU-P, FM, WS, GP, PC. All authors gave final approval of the version to be submitted to publication and agreed to be accountable for all aspects of the work in ensuring that questions related to the accuracy or integrity of any part of the article are appropriately investigated and resolved.

FUNDING

This research was funded by the Conselho Nacional de Desenvolvimento Científico e Tecnológico—CNPq (PC Universal grant No. 448007/2014-2 and Bilateral grant #490560/2013-0); CNPq-TWAS (Third World Academy of Sciences) [ML-B scholarship #190405/2011-2], FIOCRUZ-CNPq (PC, RP, FM, and ML-B PROEP grant #476727/2010-3); Departamento Administrativo de Ciencia, Tecnología e Innovación—Colciencias (MS-G, SC-E, and AU-P grants # 11263-576-2009; 110165843548; 614-2014); DIEB-Universidad Nacional de Colombia (AU-P grant # 37436); Fundação de Amparo à Pesquisa do Estado de Rio de Janeiro—FAPERJ (PC JCNE E-26/201.545/2014 and JCNE E-26/203.253/2017), and Mercosur Fund for Structural Convergence (FOCEM) #03/11. GP is a CAPES fellow of the Visitant Professor Program (Process No. 0344141). PC is a CNPq PQ-fellow (PQ Process No. 306393/2014-0 and 305796/2017-8). This work was partially developed in the framework of the Brazilian National Institute of Science and Technology on Neuroimmunomodulation.

ACKNOWLEDGMENTS

We thank Gabriela Meirelles for her guidance with the interactome analysis and all the staff of the proteomic facilities of Fiocruz-Paraná (Plataforma Proteômica RPT02H—FIOCRUZ) for technical help with mass spectrometric measurements. We thank all the staff of CLIOC—Fiocruz and Dr. Rosane Temporal - quality manager of LPL-Fiocruz for the technical assistance.

SUPPLEMENTARY MATERIAL

The Supplementary Material for this article can be found online at: https://www.frontiersin.org/articles/10.3389/fcimb.2019.00252/full#supplementary-material

REFERENCES

Aaby, P., Marx, C., Trautner, S., Rudaa, D., Hasselbalch, H., Jensen, H., et al. (2002). Thymus size at birth is associated with infant mortality: a community study from Guinea-Bissau. *Acta Paediatr.* 91, 698–703. doi: 10.1111/j.1651-2227.2002.tb03305.x

Akingbemi, B. T., Aire, T. A., Oke, B. O., Onwuka, S. K., and Ogwuegbu, S. O. (1996). Gossypol toxicosis in the rat associated with protein malnutrition and experimental infection with *Trypanosoma brucei*. *J. Comp. Pathol.* 115, 13–22. doi: 10.1016/S0021-9975(96)80024-7

Akuffo, H., Costa, C., Van Griensven, J., Burza, S., Moreno, J., and Herrero, M. (2018). New insights into leishmaniasis in the immunosuppressed. *PLoS Negl. Trop. Dis.* 12:e0006375. doi: 10.1371/journal.pntd.0006375

Anderson, G., Baik, S., Cowan, J. E., Holland, A. M., Mccarthy, N. I., Nakamura, K., et al. (2014). Mechanisms of thymus medulla development and function. *Curr. Top. Microbiol. Immunol.* 373, 19–47. doi: 10.1007/82_2013_320

Andrade, C. F., Gameiro, J., Nagib, P. R., Carvalho, B. O., Talaisys, R. L., Costa, F. T., et al. (2008). Thymic alterations in *Plasmodium berghei*-infected mice. *Cell. Immunol.* 253, 1–4. doi: 10.1016/j.cellimm.2008.06.001

Aref, G. H., Abdel-Aziz, A., Elaraby, I. I, Abdel-Moneim, M. A., Hebeishy, N. A., and Rahmy, A. I. (1982). A post-mortem study of the thymolymphatic system in protein energy malnutrition. *J. Trop. Med. Hyg.* 85, 109–114.

Aswad, H., Forterre, A., Wiklander, O. P., Vial, G., Danty-Berger, E., Jalabert, A., et al. (2014). Exosomes participate in the alteration of muscle homeostasis during lipid-induced insulin resistance in mice. *Diabetologia* 57, 2155–2164. doi: 10.1007/s00125-014-3337-2

Banfai, K., Garai, K., Ernszt, D., Pongracz, J. E., and Kvell, K. (2019). Transgenic exosomes for thymus regeneration. *Front. Immunol.* 10:862. doi: 10.3389/fimmu.2019.00862

Baum, L. G., Pang, M., Perillo, N. L., Wu, T., Delegeane, A., Uittenbogaart, C. H., et al. (1995). Human thymic epithelial cells express an endogenous lectin, galectin-1, which binds to core 2 O-glycans on thymocytes and T lymphoblastoid cells. *J. Exp. Med.* 181, 877–887. doi: 10.1084/jem.181.3.877

Bendtsen, J. D., Jensen, L. J., Blom, N., Von Heijne, G., and Brunak, S. (2004). Feature-based prediction of non-classical and leaderless protein secretion. *Protein Eng. Des. Sel.* 17, 349–356. doi: 10.1093/protein/gzh037

Buck, M. D., O'sullivan, D., Klein Geltink, R. I., Curtis, J. D., Chang, C. H., Sanin, D. E., et al. (2016). Mitochondrial dynamics controls T cell fate through metabolic programming. *Cell* 166, 63–76. doi: 10.1016/j.cell.2016.05.035

Camby, I., Le Mercier, M., Lefranc, F., and Kiss, R. (2006). Galectin-1: a small protein with major functions. *Glycobiology* 16, 137R−157R. doi: 10.1093/glycob/cwl025

Carazzolle, M. F., De Carvalho, L. M., Slepicka, H. H., Vidal, R. O., Pereira, G. A., Kobarg, J., et al. (2014). IIS–Integrated Interactome System: a web-based platform for the annotation, analysis and visualization of protein-metabolite-gene-drug interactions by integrating a variety of data sources and tools. *PLoS ONE* 9:e100385. doi: 10.1371/journal.pone.0100385

Carvalho, P. C., Fischer, J. S., Chen, E. I., Domont, G. B., Carvalho, M. G., Degrave, W. M., et al. (2009). GO Explorer: a gene-ontology tool to aid in the interpretation of shotgun proteomics data. *Proteome Sci.* 7:6. doi: 10.1186/1477-5956-7-6

Carvalho, P. C., Fischer, J. S., Xu, T., Cociorva, D., Balbuena, T. S., Valente, R. H., et al. (2012). Search engine processor: filtering and organizing peptide spectrum matches. *Proteomics* 12, 944–949. doi: 10.1002/pmic.201100529

Carvalho, P. C., Lima, D. B., Leprevost, F. V., Santos, M. D., Fischer, J. S., Aquino, P. F., et al. (2016). Integrated analysis of shotgun proteomic data with PatternLab for proteomics 4.0. *Nat. Protoc.* 11, 102–117. doi: 10.1038/nprot.2015.133

Cecil, D. L., and Terkeltaub, R. (2008). Transamidation by transglutaminase 2 transforms S100A11 calgranulin into a procatabolic cytokine for chondrocytes. *J. Immunol.* 180, 8378–8385. doi: 10.4049/jimmunol.180.12.8378

Coakley, G., Maizels, R. M., and Buck, A. H. (2015). Exosomes and other extracellular vesicles: the new communicators in parasite infections. *Trends Parasitol.* 31, 477–489. doi: 10.1016/j.pt.2015.06.009

Cuervo-Escobar, S., Losada-Barragan, M., Umana-Perez, A., Porrozzi, R., Saboia-Vahia, L., Miranda, L. H., et al. (2014). T-cell populations and cytokine expression are impaired in thymus and spleen of protein malnourished BALB/c mice infected with *Leishmania infantum*. *PLoS ONE* 9:e114584. doi: 10.1371/journal.pone.0114584

De Meis, J., and Savino, W. (2013). Mature peripheral T cells are important to preserve thymus function and selection of thymocytes during *Mycobacterium tuberculosis* infection. *Immunotherapy* 5, 573–576. doi: 10.2217/imt.13.41

Deng, Z. B., Zhuang, X., Ju, S., Xiang, X., Mu, J., Liu, Y., et al. (2013). Exosome-like nanoparticles from intestinal mucosal cells carry prostaglandin E2 and suppress activation of liver NKT cells. *J. Immunol.* 190, 3579–3589. doi: 10.4049/jimmunol.1203170

Eng, J. K., Jahan, T. A., and Hoopmann, M. R. (2013). Comet: an open-source MS/MS sequence database search tool. *Proteomics* 13, 22–24. doi: 10.1002/pmic.201200439

Gameiro, J., Nagib, P., and Verinaud, L. (2010). The thymus microenvironment in regulating thymocyte differentiation. *Cell Adh. Migr.* 4, 382–390. doi: 10.4161/cam.4.3.11789

Garly, M. L., Trautner, S. L., Marx, C., Danebod, K., Nielsen, J., Ravn, H., et al. (2008). Thymus size at 6 months of age and subsequent child mortality. *J. Pediatr.* 153, 683–688, 688 e681–683. doi: 10.1016/j.jpeds.2008.04.069

Gonzalez, F. B., Calmon-Hamaty, F., No Seara Cordeiro, S., Fernandez Bussy, R., Spinelli, S. V., D'attilio, L., et al. (2016). *Trypanosoma cruzi* experimental infection impacts on the thymic regulatory T cell compartment. *PLoS Negl. Trop. Dis.* 10:e0004285. doi: 10.1371/journal.pntd.0004285

He, H., Li, J., Weng, S., Li, M., and Yu, Y. (2009). S100A11: diverse function and pathology corresponding to different target proteins. *Cell Biochem. Biophys.* 55, 117–126. doi: 10.1007/s12013-009-9061-8

Ibrahim, M. K., Barnes, J. L., Anstead, G. M., Jimenez, F., Travi, B. L., Peniche, A. G., et al. (2013). The malnutrition-related increase in early visceralization of *Leishmania donovani* is associated with a reduced number of lymph node phagocytes and altered conduit system flow. *PLoS Negl. Trop. Dis.* 7:e2329. doi: 10.1371/journal.pntd.0002329

Ibrahim, M. K., Zambruni, M., Melby, C. L., and Melby, P. C. (2017). Impact of childhood malnutrition on host defense and infection. *Clin. Microbiol. Rev.* 30, 919–971. doi: 10.1128/CMR.00119-16

Ishizaki, H., Togawa, A., Tanaka-Okamoto, M., Hori, K., Nishimura, M., Hamaguchi, A., et al. (2006). Defective chemokine-directed lymphocyte migration and development in the absence of Rho guanosine diphosphate-dissociation inhibitors alpha and beta. *J. Immunol.* 177, 8512–8521. doi: 10.4049/jimmunol.177.12.8512

Jambon, B., Ziegler, O., Maire, B., Hutin, M. F., Parent, G., Fall, M., et al. (1988). Thymulin (facteur thymique serique) and zinc contents of the thymus glands of malnourished children. *Am. J. Clin. Nutr.* 48, 335–342. doi: 10.1093/ajcn/48.2.335

Ji, Y. F., Huang, H., Jiang, F., Ni, R. Z., and Xiao, M. B. (2014). S100 family signaling network and related proteins in pancreatic cancer (Review). *Int. J. Mol. Med.* 33, 769–776. doi: 10.3892/ijmm.2014.1633

Liotta, L. A., Goldfarb, R. H., Brundage, R., Siegal, G. P., Terranova, V., and Garbisa, S. (1981). Effect of plasminogen activator (urokinase), plasmin, and thrombin on glycoprotein and collagenous components of basement membrane. *Cancer Res.* 41, 4629–4636.

Liu, B., Zhang, X., Deng, W., Liu, J., Li, H., Wen, M., et al. (2014). Severe influenza A(H1N1)pdm09 infection induces thymic atrophy through activating innate CD8(+)CD44(hi) T cells by upregulating IFN-gamma. *Cell Death Dis.* 5:e1440. doi: 10.1038/cddis.2014.323

Liu, S. D., Whiting, C. C., Tomassian, T., Pang, M., Bissel, S. J., Baum, L. G., et al. (2008). Endogenous galectin-1 enforces class I-restricted TCR functional fate decisions in thymocytes. *Blood* 112, 120–130. doi: 10.1182/blood-2007-09-114181

Lochner, M., Berod, L., and Sparwasser, T. (2015). Fatty acid metabolism in the regulation of T cell function. *Trends Immunol.* 36, 81–91. doi: 10.1016/j.it.2014.12.005

Lopez-Victorio, C. J., Velez-Delvalle, C., Beltran-Langarica, A., and Kuri-Harcuch, W. (2013). EDF-1 downregulates the CaM/Cn/NFAT signaling pathway during adipogenesis. *Biochem. Biophys. Res. Commun.* 432, 146–151. doi: 10.1016/j.bbrc.2013.01.069

Losada-Barragan, M., Umana-Perez, A., Cuervo-Escobar, S., Berbert, L. R., Porrozzi, R., Morgado, F. N., et al. (2017). Protein malnutrition promotes dysregulation of molecules involved in T cell migration in the thymus of mice infected with Leishmania infantum. *Sci. Rep.* 7:45991. doi: 10.1038/srep45991

Lundberg, V., Berglund, M., Skogberg, G., Lindgren, S., Lundqvist, C., Gudmundsdottir, J., et al. (2016). Thymic exosomes promote the final maturation of thymocytes. *Sci. Rep.* 6:36479. doi: 10.1038/srep36479

Mariotti, M., De Benedictis, L., Avon, E., and Maier, J. A. (2000). Interaction between endothelial differentiation-related factor-1 and calmodulin *in vitro* and *in vivo*. *J. Biol. Chem.* 275, 24047–24051. doi: 10.1074/jbc.M001928200

Mendes-Da-Cruz, D. A., De Meis, J., Cotta-De-Almeida, V., and Savino, W. (2003). Experimental *Trypanosoma cruzi* infection alters the shaping of the central and peripheral T-cell repertoire. *Microbes Infect.* 5, 825–832. doi: 10.1016/S1286-4579(03)00156-4

Montecalvo, A., Larregina, A. T., Shufesky, W. J., Stolz, D. B., Sullivan, M. L., Karlsson, J. M., et al. (2012). Mechanism of transfer of functional microRNAs between mouse dendritic cells via exosomes. *Blood* 119, 756–766. doi: 10.1182/blood-2011-02-338004

Nobrega, C., Nunes-Alves, C., Cerqueira-Rodrigues, B., Roque, S., Barreira-Silva, P., Behar, S. M., et al. (2013). T cells home to the thymus and control infection. *J. Immunol.* 190, 1646–1658. doi: 10.4049/jimmunol.1202412

Nunes-Alves, C., Nobrega, C., Behar, S. M., and Correia-Neves, M. (2013). Tolerance has its limits: how the thymus copes with infection. *Trends Immunol.* 34, 502–510. doi: 10.1016/j.it.2013.06.004

Olsen, E., Rasmussen, H. H., and Celis, J. E. (1995). Identification of proteins that are abnormally regulated in differentiated cultured human keratinocytes. *Electrophoresis* 16, 2241–2248. doi: 10.1002/elps.11501601356

Pearce, E. L., Poffenberger, M. C., Chang, C. H., and Jones, R. G. (2013). Fueling immunity: insights into metabolism and lymphocyte function. *Science* 342:1242454. doi: 10.1126/science.1242454

Pegtel, D. M., Cosmopoulos, K., Thorley-Lawson, D. A., Van Eijndhoven, M. A., Hopmans, E. S., Lindenberg, J. L., et al. (2010). Functional delivery of viral miRNAs via exosomes. *Proc. Natl. Acad. Sci. U.S.A.* 107, 6328–6333. doi: 10.1073/pnas.0914843107

Perez, A. R., Berbert, L. R., Lepletier, A., Revelli, S., Bottasso, O., Silva-Barbosa, S. D., et al. (2012). TNF-alpha is involved in the abnormal thymocyte migration during experimental *Trypanosoma cruzi* infection and favors the export of immature cells. *PLoS ONE* 7:e34360. doi: 10.1371/journal.pone.0034360

Perillo, N. L., Marcus, M. E., and Baum, L. G. (1998). Galectins: versatile modulators of cell adhesion, cell proliferation, and cell death. *J. Mol. Med.* 76, 402–412. doi: 10.1007/s001090050232

Perone, M. J., Larregina, A. T., Shufesky, W. J., Papworth, G. D., Sullivan, M. L., Zahorchak, A. F., et al. (2006). Transgenic galectin-1 induces maturation of dendritic cells that elicit contrasting responses in naive and activated T cells. *J. Immunol.* 176, 7207–7220. doi: 10.4049/jimmunol.176.12.7207

Petersen, T. N., Brunak, S., Von Heijne, G., and Nielsen, H. (2011). SignalP 4.0: discriminating signal peptides from transmembrane regions. *Nat. Methods* 8, 785–786. doi: 10.1038/nmeth.1701

Petrie, H. T., and Zuniga-Pflucker, J. C. (2007). Zoned out: functional mapping of stromal signaling microenvironments in the thymus. *Annu. Rev. Immunol.* 25, 649–679. doi: 10.1146/annurev.immunol.23.021704.115715

Rambold, A. S., and Pearce, E. L. (2018). Mitochondrial dynamics at the interface of immune cell metabolism and function. *Trends Immunol.* 39, 6–18. doi: 10.1016/j.it.2017.08.006

Raposo, G., Nijman, H. W., Stoorvogel, W., Liejendekker, R., Harding, C. V., Melief, C. J., et al. (1996). B lymphocytes secrete antigen-presenting vesicles. *J. Exp. Med.* 183, 1161–1172. doi: 10.1084/jem.183.3.1161

Ridder, K., Keller, S., Dams, M., Rupp, A. K., Schlaudraff, J., Del Turco, D., et al. (2014). Extracellular vesicle-mediated transfer of genetic information between the hematopoietic system and the brain in response to inflammation. *PLoS Biol.* 12:e1001874. doi: 10.1371/journal.pbio.1001874

Sanchez-Gomez, M., Malmlof, K., Mejia, W., Bermudez, A., Ochoa, M. T., Carrasco-Rodriguez, S., et al. (1999). Insulin-like growth factor-I, but not growth hormone, is dependent on a high protein intake to increase nitrogen balance in the rat. *Br. J. Nutr.* 81, 145–152. doi: 10.1017/S0007114599000288

Savino, W. (2006). The thymus is a common target organ in infectious diseases. *PLoS Pathog.* 2:e62. doi: 10.1371/journal.ppat.0020062

Savino, W., Dalmau, S. R., and Dealmeida, V. C. (2000). Role of extracellular matrix-mediated interactions in thymocyte migration. *Dev. Immunol.* 7, 279–291. doi: 10.1155/2000/60247

Savino, W., and Dardenne, M. (2010). Nutritional imbalances and infections affect the thymus: consequences on T-cell-mediated immune responses. *Proc. Nutr. Soc.* 69, 636–643. doi: 10.1017/S0029665110002545

Savino, W., Dardenne, M., Velloso, L. A., and Silva-Barbosa, S. D. (2007). The thymus is a common target in malnutrition and infection. *Br. J. Nutr.* 98, S11–S16. doi: 10.1017/S0007114507832880

Savino, W., Mendes-Da-Cruz, D. A., Smaniotto, S., Silva-Monteiro, E., and Villa-Verde, D. M. (2004). Molecular mechanisms governing thymocyte migration: combined role of chemokines and extracellular matrix. *J. Leukoc. Biol.* 75, 951–961. doi: 10.1189/jlb.1003455

Schonland, M. (1972). Depression of immunity in protein-calorie malnutrition: a post-mortem study. *J. Trop. Pediatr. Environ. Child Health* 18, 217–224. doi: 10.1093/tropej/18.3.217

Shin, Y. K., Yoo, B. C., Hong, Y. S., Chang, H. J., Jung, K. H., Jeong, S. Y., et al. (2009). Upregulation of glycolytic enzymes in proteins secreted from human colon cancer cells with 5-fluorouracil resistance. *Electrophoresis* 30, 2182–2192. doi: 10.1002/elps.200800806

Simpson, R. J., Jensen, S. S., and Lim, J. W. (2008). Proteomic profiling of exosomes: current perspectives. *Proteomics* 8, 4083–4099. doi: 10.1002/pmic.200800109

Simpson, R. J., Lim, J. W., Moritz, R. L., and Mathivanan, S. (2009). Exosomes: proteomic insights and diagnostic potential. *Expert Rev. Proteomics* 6, 267–283. doi: 10.1586/epr.09.17

Skogberg, G., Gudmundsdottir, J., Van Der Post, S., Sandstrom, K., Bruhn, S., Benson, M., et al. (2013). Characterization of human thymic exosomes. *PLoS ONE* 8:e67554. doi: 10.1371/journal.pone.0067554

Skogberg, G., Lundberg, V., Berglund, M., Gudmundsdottir, J., Telemo, E., Lindgren, S., et al. (2015). Human thymic epithelial primary cells produce exosomes carrying tissue-restricted antigens. *Immunol. Cell Biol.* 93, 727–734. doi: 10.1038/icb.2015.33

Smythe, P. M., Brereton-Stiles, G. G., Grace, H. J., Mafoyane, A., Schonland, M., Coovadia, H. M., et al. (1971). Thymolymphatic deficiency and depression of cell-mediated immunity in protein-calorie malnutrition. *Lancet* 2, 939–943. doi: 10.1016/S0140-6736(71)90267-4

Stillman, B. N., Hsu, D. K., Pang, M., Brewer, C. F., Johnson, P., Liu, F. T., et al. (2006). Galectin-3 and galectin-1 bind distinct cell surface glycoprotein receptors to induce T cell death. *J. Immunol.* 176, 778–789. doi: 10.4049/jimmunol.176.2.778

Turiak, L., Misjak, P., Szabo, T. G., Aradi, B., Paloczi, K., Ozohanics, O., et al. (2011). Proteomic characterization of thymocyte-derived microvesicles and apoptotic bodies in BALB/c mice. *J. Proteomics* 74, 2025–2033. doi: 10.1016/j.jprot.2011.05.023

Valadi, H., Ekstrom, K., Bossios, A., Sjostrand, M., Lee, J. J., and Lotvall, J. O. (2007). Exosome-mediated transfer of mRNAs and microRNAs is a novel mechanism of genetic exchange between cells. *Nat. Cell Biol.* 9, 654–659. doi: 10.1038/ncb1596

Wang, R., and Green, D. R. (2012). Metabolic checkpoints in activated T cells. *Nat. Immunol.* 13, 907–915. doi: 10.1038/ni.2386

Wu, C. C., Chen, H. C., Chen, S. J., Liu, H. P., Hsieh, Y. Y., Yu, C. J., et al. (2008). Identification of collapsin response mediator protein-2 as a potential marker of colorectal carcinoma by comparative analysis of cancer cell secretomes. *Proteomics* 8, 316–332. doi: 10.1002/pmic.200700819

Zacarias, D. A., Rolao, N., De Pinho, F. A., Sene, I., Silva, J. C., Pereira, T. C., et al. (2017). Causes and consequences of higher Leishmania infantum burden in patients with kala-azar: a study of 625 patients. *Trop. Med. Int. Health* 22, 679–687. doi: 10.1111/tmi.12877

Zhang, Q., Zhu, M., Cheng, W., Xing, R., Li, W., Zhao, M., et al. (2015). Downregulation of 425G>a variant of calcium-binding protein S100A14 associated with poor differentiation and prognosis in gastric cancer. *J. Cancer Res. Clin. Oncol.* 141, 691–703. doi: 10.1007/s00432-014-1830-0

Zhao, X. Y., Zhao, K. W., Jiang, Y., Zhao, M., and Chen, G. Q. (2011). Synergistic induction of galectin-1 by CCAAT/enhancer binding protein alpha and hypoxia-inducible factor 1alpha and its role in differentiation of acute myeloid leukemic cells. *J. Biol. Chem.* 286, 36808–36819. doi: 10.1074/jbc.M111.247262

Zhu, Y., Chen, X., Pan, Q., Wang, Y., Su, S., Jiang, C., et al. (2015). A comprehensive proteomics analysis reveals a secretory path- and status-dependent signature of exosomes released from tumor-associated macrophages. *J. Proteome Res.* 14, 4319–4331. doi: 10.1021/acs.jproteome.5b00770

Conflict of Interest Statement: The authors declare that the research was conducted in the absence of any commercial or financial relationships that could be construed as a potential conflict of interest.

frontiers in Cellular and Infection Microbiology

ORIGINAL RESEARCH
published: 07 August 2019
doi: 10.3389/fcimb.2019.00280

Pathogen Evasion of Chemokine Response Through Suppression of CXCL10

*Alejandro L. Antonia[1], Kyle D. Gibbs[1], Esme D. Trahair[1], Kelly J. Pittman[1], Amelia T. Martin[1], Benjamin H. Schott[1], Jeffrey S. Smith[2], Sudarshan Rajagopal[2,3], J. Will Thompson[4], Richard Lee Reinhardt[5,6] and Dennis C. Ko[1,7]**

[1] Department of Molecular Genetics and Microbiology, School of Medicine, Duke University, Durham, NC, United States, [2] Department of Biochemistry, School of Medicine, Duke University, Durham, NC, United States, [3] Division of Cardiology, Department of Medicine, School of Medicine, Duke University, Durham, NC, United States, [4] Proteomics and Metabolomics Shared Resource, Center for Genomics and Computational Biology, School of Medicine, Duke University, Durham, NC, United States, [5] Department of Biomedical Research, National Jewish Health, Denver, CO, United States, [6] Department of Immunology and Microbiology, University of Colorado Anschutz Medical Campus, Aurora, CO, United States, [7] Division of Infectious Diseases, Department of Medicine, School of Medicine, Duke University, Durham, NC, United States

OPEN ACCESS

Edited by:
Claudia Ida Brodskyn, Gonçalo Moniz Institute (IGM), Brazil

Reviewed by:
Albert Descoteaux, Institut National de la Recherche Scientifique (INRS), Canada
Nicolaus Albert Borges Schriefer, Federal University of Bahia, Brazil

***Correspondence:**
Dennis C. Ko
dennis.ko@duke.edu;
@denniskoHiHOST

Specialty section:
This article was submitted to Parasite and Host, a section of the journal Frontiers in Cellular and Infection Microbiology

Received: *10 May 2019*
Accepted: *23 July 2019*
Published: *07 August 2019*

Citation:
Antonia AL, Gibbs KD, Trahair ED, Pittman KJ, Martin AT, Schott BH, Smith JS, Rajagopal S, Thompson JW, Reinhardt RL and Ko DC (2019) Pathogen Evasion of Chemokine Response Through Suppression of CXCL10. Front. Cell. Infect. Microbiol. 9:280. doi: 10.3389/fcimb.2019.00280

Clearance of intracellular pathogens, such as *Leishmania* (*L.*) *major*, depends on an immune response with well-regulated cytokine signaling. Here we describe a pathogen-mediated mechanism of evading CXCL10, a chemokine with diverse antimicrobial functions, including T cell recruitment. Infection with *L. major* in a human monocyte cell line induced robust *CXCL10* transcription without increasing extracellular CXCL10 protein concentrations. We found that this transcriptionally independent suppression of CXCL10 is mediated by the virulence factor and protease, glycoprotein-63 (*gp63)*. Specifically, GP63 cleaves CXCL10 after amino acid A81 at the base of a C-terminal alpha-helix. Cytokine cleavage by GP63 demonstrated specificity, as GP63 cleaved CXCL10 and its homologs, which all bind the CXCR3 receptor, but not distantly related chemokines, such as CXCL8 and CCL22. Further characterization demonstrated that CXCL10 cleavage activity by GP63 was produced by both extracellular promastigotes and intracellular amastigotes. Crucially, CXCL10 cleavage impaired T cell chemotaxis *in vitro,* indicating that cleaved CXCL10 cannot signal through CXCR3. Ultimately, we propose CXCL10 suppression is a convergent mechanism of immune evasion, as *Salmonella enterica* and *Chlamydia trachomatis* also suppress CXCL10. This commonality suggests that counteracting CXCL10 suppression may provide a generalizable therapeutic strategy against intracellular pathogens.

IMPORTANCE

Leishmaniasis, an infectious disease that annually affects over one million people, is caused by intracellular parasites that have evolved to evade the host's attempts to eliminate the parasite. Cutaneous leishmaniasis results in disfiguring skin lesions if the host immune system does not appropriately respond to infection. A family of molecules called chemokines coordinate recruitment of the immune cells required to eliminate infection. Here, we demonstrate a novel mechanism that *Leishmania (L.)* spp. employ to suppress host chemokines: a *Leishmania*-encoded protease cleaves chemokines known

to recruit T cells that fight off infection. We observe that other common human intracellular pathogens, including *Chlamydia trachomatis* and *Salmonella enterica,* reduce levels of the same chemokines, suggesting a strong selective pressure to avoid this component of the immune response. Our study provides new insights into how intracellular pathogens interact with the host immune response to enhance pathogen survival.

Keywords: CXCL10, CXCR3, *Leishmania*, gp63, leishmanolysin, *Chlamydia*, *Salmonella*, convergent evolution

INTRODUCTION

Proper immune clearance of intracellular pathogens requires precise cytokine and chemokine signaling. These cytokines coordinate the localization, activation, and polarization of innate and adaptive immune cell subsets. To study T cell recruitment and polarization in response to intracellular pathogens, parasites in the genus *Leishmania* have served as a paradigm (Reiner and Locksley, 1995). However, persistent gaps in the understanding of host and pathogen factors that influence T cell response and recruitment contribute to the dearth of immunotherapeutics and vaccines. With no available vaccine and limited treatment options, *Leishmania* spp. continue to cause 1.2 million cases of cutaneous leishmaniasis (CL) and 0.4 million cases of visceral leishmaniasis annually (VL) (Alvar et al., 2012). A better understanding of host immunity and pathogen evasion strategies is imperative to develop alternative approaches to current therapies, which are limited by variable efficacy, high cost, and growing drug resistance (Okwor and Uzonna, 2009). Of particular relevance may be instances where multiple diverse pathogens have evolved to evade or suppress the same key host immune signaling pathways (Finlay and McFadden, 2006; Hajishengallis and Lambris, 2011).

To clear *L. major* parasites, a causative agent of CL, the adaptive immune system must be coordinated to a type-1 response by appropriately recruiting immune cell subsets, particularly CD4+ T helper 1 (T_h1) cells and CD8+ cytotoxic T lymphocytes (CTLs; Scott and Novais, 2016). This recruitment is mediated by chemokines, a family of signaling molecules that regulate recruitment and localization of unique immune cell subsets. For example, T_h1 cells, which mediate a pro-inflammatory response effective at eliminating intracellular parasites, are recruited by chemokines such as CXCL10 through the CXCR3 receptor. By contrast, T_h2 cells, which promote immunity targeting extracellular parasites, are recruited by chemokines such as CCL22 through the CCR4 receptor (Kim et al., 2001). When infected with *L. major*, T_h2 responding mice develop non-healing lesions, whereas T_h1 responding mice effectively clear the parasite (Scott et al., 1988; Heinzel et al., 1989; Reiner and Locksley, 1993). As part of the broader type-1 immune response against *L. major* infection, parasite-specific CD8+ cells are also recruited, and have been implicated in productive immunity to primary and secondary infection (Muller et al., 1993, 1994; Belkaid et al., 2002; Uzonna et al., 2004). Corresponding observational studies in humans support this model where non-healing cutaneous lesions are characterized by T_h2 associated cytokines, and individuals resistant to lesion development have a higher predominance of T_h1 associated cytokines (Carvalho et al., 1995; Ajdary et al., 2000; Ritter and Körner, 2002; Castellano et al., 2009). Together these studies highlight the critical role of cytokine and chemokine signaling in specific immune cell subsets during infection.

One of the chemokines that specifically regulates localization and activity of CD4+ T_h1 and effector CD8+ T-cells is CXCL10, or IFNγ Inducible Protein 10 (IP10). CXCL10 is part of a family of highly homologous chemokines, including CXCL9 and CXCL11, which bind to and activate the CXCR3 chemokine receptor (reviewed in Groom and Luster, 2011). Multiple lines of investigation suggest that CXCL10 protects against *Leishmania* infection. First, the host upregulates *CXCL10* transcription throughout infection (Zaph and Scott, 2003; Antoniazi et al., 2004; Vargas-Inchaustegui et al., 2010) and cells expressing CXCR3 are expanded after infection (Oghumu et al., 2013). Second, BALB/c mice, which are unable to control *Leishmania* spp. infection, demonstrate a defect in CXCR3 upregulation (Barbi et al., 2007, 2008). Finally, exogenous CXCL10 is protective against both cutaneous and visceral leishmaniasis (Vester et al., 1999; Vasquez and Soong, 2006; Gupta et al., 2009, 2011). Therefore, the type-1 associated chemokine CXCL10 is important for host control of cutaneous leishmaniasis.

Beyond *Leishmania,* type-1 immunity and CXCL10-CXCR3 signaling are critical for clearing other intracellular pathogens. For the obligate intracellular bacterium *Chlamydia trachomatis*, T_h1 cells are required for clearance of infection while a T_h2 dominated response may lead to excessive pathology (Perry et al., 1997; Morrison and Caldwell, 2002; Gondek et al., 2009; Morrison et al., 2011). In mice, CXCL10 mRNA and protein are significantly induced after infection (Maxion and Kelly, 2002; Rank et al., 2010; Lijek et al., 2018). Similarly, T_h1 responses are crucial for an effective immune response to the facultative intracellular bacteria *Salmonella enterica* serovar Typhimurium based on studies in mice (Hess et al., 1996; Ravindran et al., 2005) and the predisposition of people with rare mutations in T_h1-promoting cytokines (IFNγ and IL12) to invasive Salmonellosis (Gilchrist et al., 2015). Further, M1-polarized macrophages, which restrict *Salmonella* intracellular replication (Lathrop et al., 2015; Saliba et al., 2016), robustly upregulate *CXCL10* transcription (Martinez et al., 2006; Goldberg et al., 2018). Finally, mice deficient for CXCR3 have increased susceptibility to *S. enterica* (Chami et al., 2017), *Toxoplasma* (*T.*) *gondii* (Khan et al., 2000), and *C. trachomatis* (Olive et al., 2011). Thus, the CXCL10-CXCR3 signaling axis coordinates an adaptive type-1 immune response to intracellular pathogens that promotes a successful healing response.

Here, we report that *L. major* suppresses extracellular CXCL10 protein levels, providing a potential mechanism for

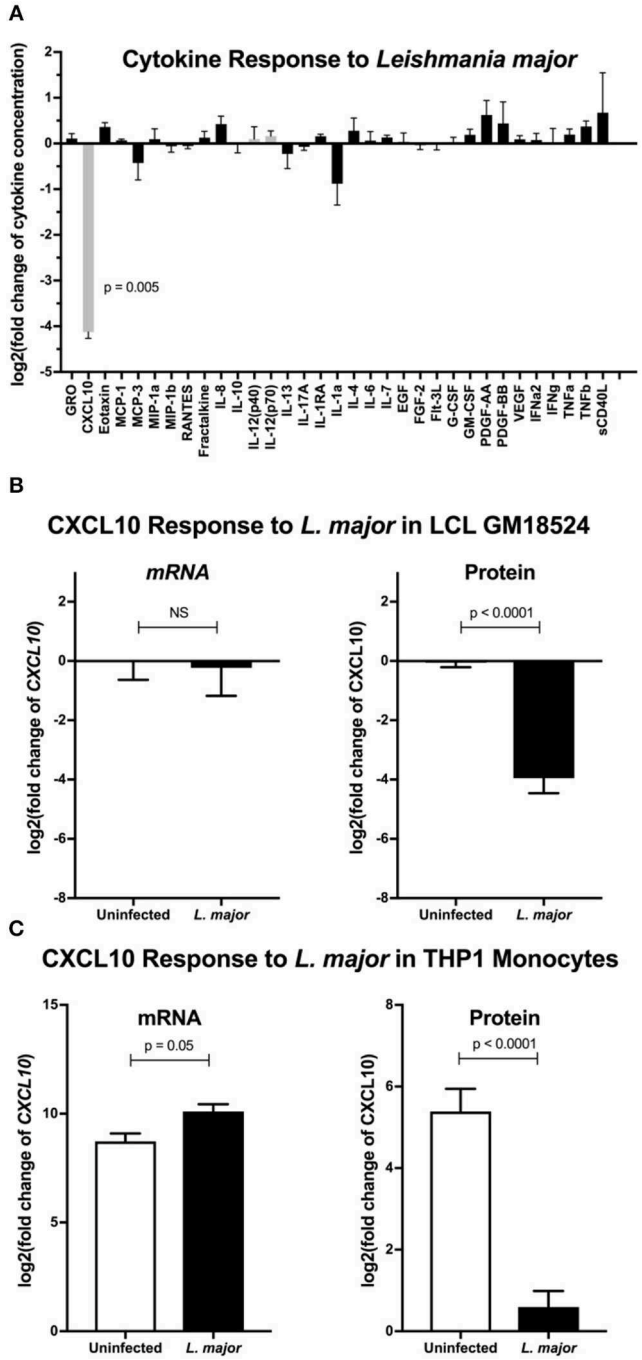

FIGURE 1 | *Leishmania major* suppresses CXCL10 post-transcriptionally in multiple human cell lines. **(A)** Cytokine screening of LCLs exposed to *L. major* demonstrated suppression of CXCL10. Three lymphoblastoid cell lines (LCL), GM07357, GM18524, and GM19203, were infected with *L. major.* Chemokines secreted into culture supernatants were analyzed by Luminex. Cytokines below the limit of detection were removed from the final analysis. Values are represented as $\log_2$ of the fold change relative to uninfected LCLs. Type-1 associated cytokines are represented in gray. *P*-value represents Dunnett's *post-hoc* test compared to 1, after repeated measures one-way ANOVA. **(B)** CXCL10 suppression by *L. major* is transcriptionally independent in LCL GM18524. LCL GM18524 was infected with *L. major* at MOI 10 to

(Continued)

FIGURE 1 | confirm the CXCL10 suppression phenotype. Despite significant reduction in CXCL10 protein, there was no change in relative *CXCL10* mRNA. *CXCL10* mRNA was measured by qRT-PCR TaqMan assay using the $\Delta\Delta C_t$ method with 18s as housekeeping gene, and CXCL10 protein was measured by ELISA. Four experimental replicates were used to calculate mRNA ($n = 4$) and ELISA ($n = 8$) fold change relative to uninfected LCL 18524. *P*-values calculated by Student's *t*-test. **(C)** CXCL10 produced by LPS stimulated THP-1 monocytes was suppressed by *L. major.* THP-1 monocytes were stimulated with LPS prior to *L. major* infection. Three experimental replicates were used to calculate mRNA ($n = 3$) and protein ($n = 6$) fold change relative to unstimulated, uninfected THP-1s. *P*-values calculated by Student's *t*-test.

evasion of the adaptive immune response. This suppression occurs through the proteolytic activity of the virulence factor glycoprotein-63 (GP63). GP63 cleavage of CXCL10 occurs throughout *in vitro* infection and abrogates CXCR3-dependent T cell migration. Furthermore, we observed CXCL10 suppression with other intracellular pathogens, including *S. enterica* and *C. trachomatis,* demonstrating that diverse intracellular pathogens have developed convergent mechanisms to suppress CXCL10.

RESULTS

L. major Infection Suppresses CXCL10 Protein, Despite Induction of *CXCL10* mRNA

To broadly screen for *L. major* manipulation of host immunity, we measured secreted levels of 41 cytokines following infection of lymphoblastoid cell lines (LCLs) with *L. major*. LCLs constitutively produce CXCL10, and incubation with *L. major* reduced CXCL10 levels by >90% (**Figure 1A**). We tested whether the decrease in CXCL10 is due to a change in transcript by repeating the infection in LCLs and assaying both *CXCL10* mRNA and CXCL10 protein. Despite no observed change in *CXCL10* mRNA we confirmed that *L. major* significantly suppressed CXCL10 protein (**Figure 1B**). To confirm this phenotype in a cell type that canonically senses *L. major* parasites, we next measured the CXCL10 response in LPS-stimulated human THP-1 monocytes infected with *L. major* (**Figure 1C**). Despite the reduction in CXCL10 protein in culture supernatants, THP-1s exposed to *L. major* had 2.5-fold higher *CXCL10* mRNA relative to uninfected (**Figure 1C**). Therefore, *L. major* suppresses CXCL10 protein through a transcriptionally independent mechanism.

The *L. major* Matrix-Metalloprotease, Glycoprotein-63 (GP63), Is Necessary and Sufficient for CXCL10 Protein Suppression

To test whether an *L. major*-secreted factor is responsible for CXCL10 protein suppression, we treated recombinant human CXCL10 with cell-free conditioned media obtained from cultured *L. major* promastigotes. Again, CXCL10 was reduced by 90% with the conditioned media (**Figure 2A**). These results were consistent with proteolytic degradation by a pathogen-secreted protease. We hypothesized that CXCL10 suppression

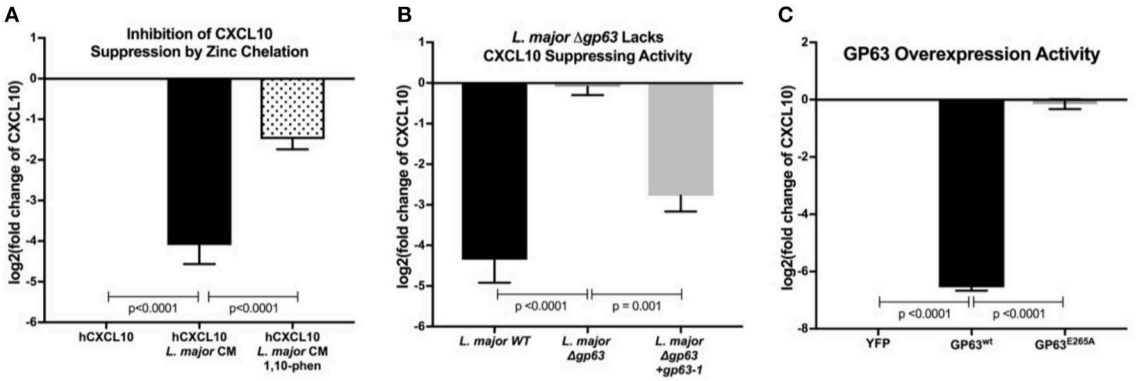

FIGURE 2 | *Leishmania major* matrix-metalloprotease, glycoprotein-63, is necessary and sufficient to cleave CXCL10. **(A)** Zinc chelation prevents CXCL10 suppression. Concentration of human recombinant CXCL10 was measured by ELISA after incubation for 12 h with filtered conditioned media from *L. major* WT promastigote culture and addition of the zinc-chelator 1,10-phenanthroline ($n = 8$ from 4 experiments). **(B)** *gp63* is required for *L. major* CXCL10 suppression. Human recombinant CXCL10 concentrations were measured by ELISA after 12 h incubation with conditioned media from *L. major* WT, *Δgp63*, or *Δgp63+1* ($n = 6$ from 3 experiments). **(C)** GP63 expressed and secreted by HEK293Ts is sufficient for CXCL10 suppression. Human recombinant CXCL10 concentrations were measured by ELISA after 12 h incubation with culture supernatant from HEK293Ts transfected with pCDNA3.1-gp63^{WT} or pCDNA3.1-gp63^{E285A} ($n = 6$ from 3 experiments). Concentration is represented as fold change relative to supernatants from YFP transfection control. *P*-values calculated by one-way ANOVA with Tukey's *post-hoc* test. Error bars represent standard error of the mean.

was mediated by glycoprotein-63 (GP63), a zinc-metalloprotease conserved among the *Trypanasoma* family of parasites and expressed in both the extracellular promastigote and intracellular amastigote life stages (Voth et al., 1998; Olivier et al., 2012; Valdivia et al., 2015; Fernandes et al., 2016). To test if GP63 is required to suppress CXCL10, we used a known GP63 inhibitor, the zinc-chelator 1,10-phenanthroline (Chaudhuri et al., 1989). 1,10-phenanthroline inhibited CXCL10-suppressive activity in *L. major* conditioned media (**Figure 2A**). Consistent with GP63-mediated degradation of CXCL10, conditioned media from a promastigote culture of *L. major* deficient for *gp63* (*Δgp63;* Joshi et al., 2002) did not suppress CXCL10, whereas complementation with a single copy of *gp63* (*L. major Δgp63*+1) restored CXCL10 suppression (**Figure 2B**). As relevant controls in using these *L. major* strains, we found the strains contained similar levels of metacyclic parasites based on flow cytometric measurement (Saraiva et al., 2005) and metacyclic enrichment with peanut agglutinin (**Figure S1A**). Furthermore, heterologously expressed GP63 secreted from mammalian HEK293T cells was sufficient for complete CXCL10 suppression, while a single point mutation in the catalytic site of GP63 (E265A) abrogated suppression (**Figure 2C**). Therefore, GP63 is both necessary and sufficient for CXCL10 suppression by *L. major*.

GP63 Selectively Cleaves the CXCL10-related Family of Chemokines at the Start of the C-terminal Alpha-Helix

As GP63 has a diverse set of identified *in vitro* substrates (Olivier et al., 2012), we examined the specificity of GP63 across a spectrum of chemokines. Based on the initial cytokine screen (**Figure 1A**), we hypothesized GP63 cleavage would be restricted to CXCL10 and highly related chemokines. To experimentally test for GP63 cleavage, purified recombinant chemokines were incubated with conditioned media from *L. major* WT, *L. major Δgp63,* or *L. major Δgp63+1*. GP63 cleavage was observed for CXCL9 (38.14% amino acid identity with CXCL10) and CXCL11 (30.85% amino acid identity with CXCL10; **Figures 3A,B**), which both signal through CXCR3. By contrast, no cleavage of CXCL8 (IL-8; a neutrophil-attracting chemokine) or CCL22 (MDC; a Th2-attracting chemokine) was detected (**Figure 3B**). Thus, chemokine cleavage by GP63 appears to preferentially degrade chemokines involved in CXCR3 signaling.

Although western blot analysis supported GP63-dependent cleavage through loss of CXCL10 immunoreactivity, it did not reveal the cleavage site or potential cleavage products. The GP63 consensus cleavage site has been described as polar, hydrophobic, and basic amino acids at positions P1, P1′, and P2′ (Bouvier et al., 1990). Following this pattern, there are three potential cleavage sites in the mature CXCL10 protein (from amino acid position 22-96) that are conserved between human and murine CXCL10 (68.37% amino acid identity; **Figure 3A**). In order to characterize the cleavage product(s), we incubated GP63 with human recombinant CXCL10 and visualized a shift in size by total protein stain (**Figure 3C**). Intact CXCL10 and the largest cleavage products were determined to be 8.8 and 6.6 kD, respectively, by capillary electrophoresis-mass spectrometry (CE-MS; **Figure 3D**). After running the sample on a PAGE gel, the 8.8 kD (intact, "Hi") product, 6.6 kD (cleaved, "Lo") product, and an uncleaved control ("Ctrl") were sequenced by trypsin digestion followed by liquid chromatography-tandem mass spectrometry (LC-MS/MS). Comparison of peptides after trypsin digest revealed a peptide from amino acids (AA) 74-81 that was exclusively present in the cleaved CXCL10 band, but notably absent in the uncleaved band (**Figure 3E**). Conversely, distal peptide fragments such as AA84-91 were only present in the uncleaved CXCL10. This analysis demonstrated cleavage occurring in between A81 and I82, resulting in the loss

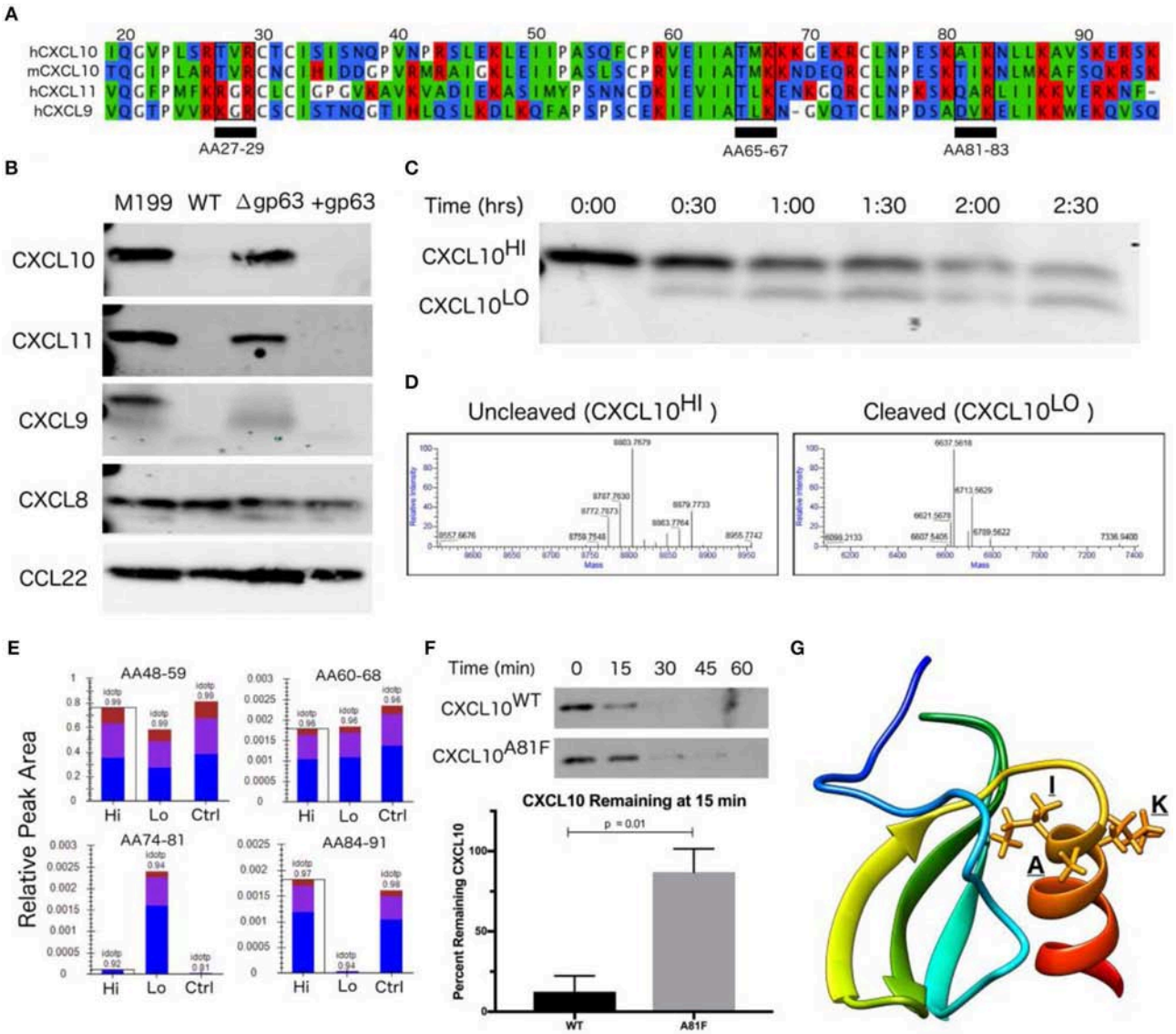

FIGURE 3 | CXCL10 cleavage by GP63 occurs between positions A81 and I82. **(A)** CXCL9/10/11 share significant homology at the amino-acid level. Multisequence alignment demonstrates that physical characteristics of amino acids are conserved across the CXCL10 family of chemokines. There are three putative GP63 cleavage sites (underlined) based on the consensus sequence of polar (P1), hydrophobic (P1′), basic (P2′) (Bouvier et al., 1990). **(B)** GP63 selectively cleaves chemokine ligands of the CXCR3 receptor. Conditioned media from *L. major WT, Δgp63,* and *Δgp63+1* was incubated with human recombinant chemokines for 12 h and product detected by western blot. Cleavage is only detected for the CXCL9/10/11 family. Representative blots are shown from at least two independent experiments. **(C)** Cleavage by GP63 generates a smaller molecular weight protein. A time course of cleavage of human CXCL10 by heterologously expressed GP63 demonstrated an intermediate cleavage product, resolved by PAGE and Coomassie staining. **(D)** Cleavage by GP63 results in a change in CXCL10 molecular weight of 2.2 kD. Capillary electrophoresis-Mass Spectrometry (CE-MS) determined the molecular weight of the uncleaved ($CXCL10^{Hi}$) and cleaved ($CXCL10^{Lo}$) bands as 8.8 and 6.6 kD, respectively. **(E)** Comparative analysis by trypsin digest of cleaved and uncleaved CXCL10 reveals cleavage occurring between A81-I82. Liquid chromatography-mass spectrometry (LC-MS) following trypsin digest of $CXCL10^{Hi}$ and $CXCL10^{Lo}$ identified peptide ending at A81, exclusively in the $CXCL10^{Lo}$ band, and a corresponding lack of peptide coverage from AA84-91. **(F)** Mutation of A81F significantly impairs GP63 cleavage of CXCL10. In the presence of GP63, $CXCL10^{A81F}$ ($n = 4$ from 4 experiments) remains stable for up to 45 min whereas $CXCL10^{WT}$ ($n = 3$ from 3 experiments) degradation is nearly complete by 15 min. Percentage of GP63 remaining at 15 min is plotted. *P*-value calculated by Student's *t*-test. **(G)** The GP63 cleavage site is found on the C-terminal alpha-helix loop of CXCL10. Based on the NMR crystal structure of CXCL10 (Booth et al., 2002), the A81, I82, K83 (P1, P1′, P2′) GP63 cleavage motif maps to an exposed alpha-helical region.

of detectable peptides beyond those amino acids in cleaved CXCL10. This is consistent with the fragment size based on intact molecular weight CE-MS, and notably AIK (AA 81-83) is one of the three potential cleavage sites identified in our comparative analysis (see **Figure 3A**). To confirm this site as preferred for GP63 cleavage, we used site-direct mutagenesis to mutate the residues in the proposed cleavage motif. Mutation of the identified P1 residue significantly slowed CXCL10 cleavage in

a time course experiment (**Figure 3F**). Mapping the residues onto the crystal structure of CXCL10 (Booth et al., 2002) demonstrated that cleavage occurs at the beginning of the C-terminal alpha-helix of CXCL10 (**Figure 3G**).

GP63 Produced by *L. major* Promastigotes or Amastigotes Can Cleave CXCL10 Protein

Immediately after injection by the sand-fly vector, *Leishmania* parasites exist as an extracellular, flagellated promastigote but are rapidly phagocytized where they transform into the intracellular, aflagellated amastigote parasite stage. We hypothesized that GP63 would continue to be able to suppress CXCL10 through both stages of infection, as transcriptomics indicate GP63 expression during both stages (Fernandes et al., 2016) while microarray expression analysis (Akopyants et al., 2004) and proteomics (de Rezende et al., 2017) have identified GP63 in lesion derived amastigotes. To test the capacity of *L. major* to suppress CXCL10 in both the promastigote and amastigote stage of infection, we utilized PMA differentiated THP-1 monocytes as an intracellular macrophage model of infection. Differentiated THP-1 monocytes were infected at an MOI of 20 with promastigotes from *L. major WT, Δgp63,* or *Δgp63+1.* Extracellular promastigote activity was assessed in the supernatant at 24 h post-infection, followed immediately by washing to remove the extracellular promastigotes and GP63 protein in the media, and subsequently assessing intracellular amastigote activity at 48 h post-infection. The differentiation of parasites into amastigotes was confirmed by observing a reduction in expression of the promastigote specific developmental stage gene, *L. major 07.1160* (Rochette et al., 2008) (**Figure S1B**).

This model demonstrated CXCL10 protein suppression by GP63 in both stages of the parasite life cycle. *L. major WT* promastigotes had no induction of CXCL10 protein relative to uninfected cells, while *L. major Δgp63* infection resulted in a significant induction of CXCL10 protein (**Figure 4A**). Similarly, the *L. major WT* amastigotes continued to suppress CXCL10 protein while *L. major Δgp63* infection significantly induced CXCL10 protein (**Figure 4A**). In contrast to CXCL10 protein, all three *L. major* strains cause comparable induction of *CXCL10* mRNA (**Figure 4B**). The complementation observed with the *L. major Δgp63+1* strain is significant, though incomplete in the promastigote stage and further reduced in the amastigote stage. This is attributable to the incomplete complementation of *L. major Δgp63+1* as evidenced by lower expression of *gp63* mRNA relative to *L. major* WT in both promastigotes and amastigotes (**Figure 4C**).

In order to assess whether CXCL10 cleavage is occurring intracellularly or extracellularly during infection, we harvested THP-1 monocytes at 24 h post-infection with either *L. major WT, Δgp63,* or *Δgp63+1,* counted the number of living cells, and measured CXCL10 in both the supernatants and cell lysates. All three parasite strains induced similar percent cell death (**Figure S2A**). Although there was again a significant GP63 dependent reduction in CXCL10 extracellularly, there was no difference in intracellular CXCL10 between *WT, Δgp63,* or *Δgp63+1* infections (**Figure 4D**) despite a relatively higher parasite burden in *L. major* WT infection (**Figures S2B,C**). These results indicate that CXCL10 mRNA is induced during *Leishmania* infection, but protein levels are reduced by GP63 extracellularly during both parasite life cycle stages involved in infection in mammalian hosts.

GP63-cleaved CXCL10 Is Unable to Recruit CXCR3 Expressing T Cells

Because CXCL10 coordinates the recruitment of CXCR3+ T cells during infection, we next tested if GP63 cleavage of CXCL10 impacts T cell recruitment. We tested the chemotactic ability of cleaved CXCL10 to recruit Jurkat T cells expressing CXCR3. The basal chamber of a transwell system was seeded with CXCL10 in the presence of conditioned media from *L. major WT, L. major Δgp63,* or *L. major Δgp63+1.* Conditioned media from *L. major* WT and *L. major Δgp63+1* abrogated CXCL10 induced migration of CXCR3+ Jurkat T cells, whereas the *L. major Δgp63* conditioned media did not impair chemotaxis (**Figure 4E**). Together these data support a model whereby the host attempts to produce CXCL10 to coordinate recruitment of CXCR3 expressing immune cells, but *L. major* produces GP63 to inactivate CXCL10 and impair T cell chemotaxis (**Figure 4F**).

CXCL10 Suppression Has Evolved Independently in Multiple Intracellular Pathogens

Finally, we tested whether this mechanism of immune evasion is conserved across *Leishmania* spp. and other intracellular pathogens. *Leishmania* spp. are incredibly diverse and frequently classified according to geographic origin (Old World vs. New World), genetic relatedness (*leishmania* vs. *viannia* subgenera), and clinical manifestation (cutaneous, visceral, and atypical manifestations such as mucocutaneous) (Burza et al., 2018). Although the *gp63* gene is conserved in all *Leishmania* spp., it is highly polymorphic in amino acid sequence and copy number variation (Alvarez-Valin et al., 2000; Victoir et al., 2005; Valdivia et al., 2015). Despite this variation, we found that all *Leishmania* spp. screened were able to cleave recombinant CXCL10 (**Figure 5A**) including: the *L. major* Friedlin strain, *L. tropica* (old world; *leishmania* subgenus; cutaneous), *L. donovani* (old world; *leishmania* subgenus; visceral), *L. venezuelenesis* (new world; *leishmania* subgenus; cutaneous), and *L. braziliensis* (new world; *viannia* subgenus; mucocutaneous). Therefore, CXCL10 suppression is found in *Leishmania* spp. encompassing diverse geographic origins, genetic backgrounds, and clinical manifestations.

Given that CXCL10 mediates a type-1 immune response that protects against a broad range of intracellular pathogens, we asked if suppression of CXCL10 has evolved in other parasites and bacteria. CXCL10 levels in LCL supernatants was measured by ELISA after exposure to a variety of pathogens including *Toxoplasma* (*T.*) *gondii*, *Plasmodium* (*P.*) *bergei*, *Salmonella* (*S.*) *enterica* serovar Typhimurium, *Chlamydia* (*C.*) *trachomatis*, *Mycobacterium* (*M.*) *marinum, Mycobacterium* (*M.*)

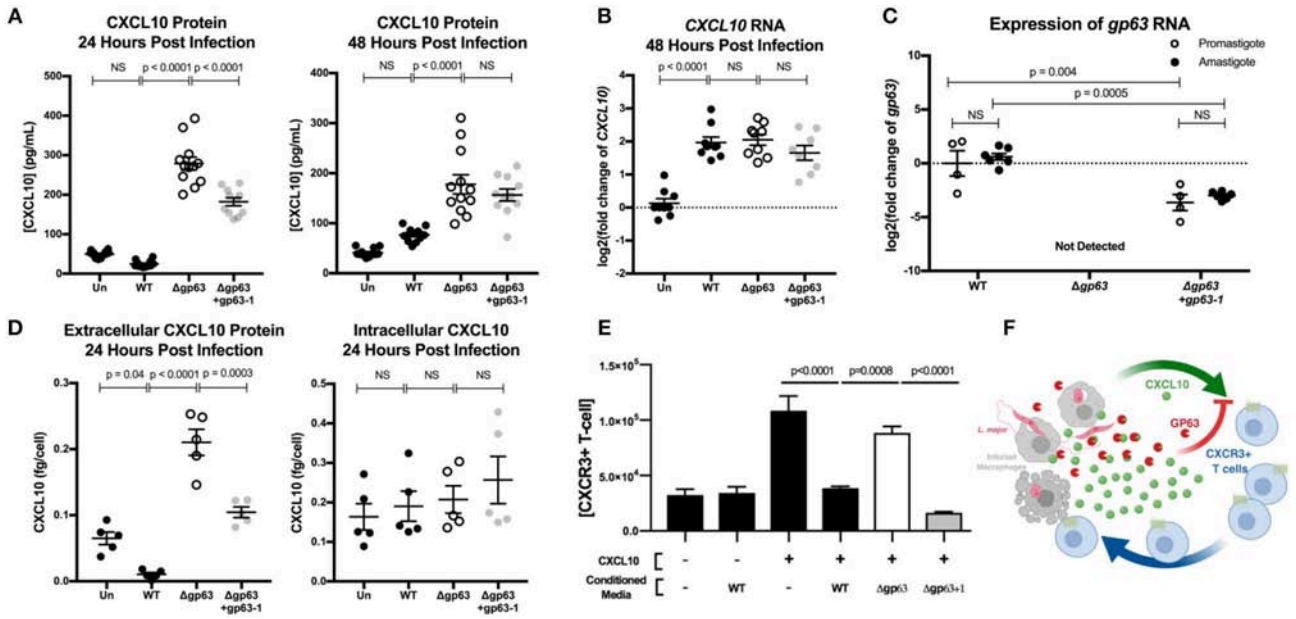

FIGURE 4 | GP63 produced by *L. major* promastigotes and amastigotes cleaves CXCL10 and abolishes its chemotactic activity. **(A)** *Leishmania major* promastigotes suppress CXCL10 through GP63 activity at 24 and 48 h post-infection. THP-1 monocytes were differentiated using 100 ng/mL of PMA prior to infection, infected at MOI 20 with *L. major* promastigotes, and extracellular promastigotes were washed away from the differentiated THP-1 monocytes at 24 h post-infection. CXCL10 concentration was assessed in the supernatant by ELISA. Data analyzed by one-way ANOVA with Tukey's *post-hoc* test ($n = 12$ from 4 experiments) **(B)** *Leishmania major* induces similar levels of *CXCL10* mRNA, independent of GP63 genotype. At 48 h post-infection, mRNA was extracted from PMA differentiated THP-1 monocytes and CXCL10 mRNA was measured by qRT-PCR TaqMan assay using the $\Delta\Delta C_t$ method with 18s as housekeeping gene. For **(B)** data analyzed by one-way ANOVA with Tukey's *post-hoc* test ($n = 9$ from 3 experiments). **(C)** Expression of *gp63* mRNA in *L. major Δgp63+1* does not fully rescue wildtype *gp63* expression in promastigote or amastigotes stages. Promastigote RNA ($n = 4$ from 4 experiments) was derived from day 5 of parasite culture before preparing for infection, and amastigote RNA ($n = 7$ from 3 experiments) was derived from intracellular THP-1s as described above. *gp63* mRNA was measured by qRT-PCR using Sybr Green and relative expression calculated with the $\Delta\Delta C_t$ method using rRNA45 as housekeeping gene. Data analyzed by two-way ANOVA with Tukey's *post-hoc* test. **(D)** GP63 cleavage of CXCL10 only occurs extracellularly. THP-1 macrophages were treated with PMA and infected as described above. At 24 h post-infection, supernatants were collected and cells were removed from the plate by pipetting with cold PBS. The concentration of living cells was determined using 7AAD staining and counting cells with a Guava easyCyte flow cytometer. Cells were then lysed with RIPA buffer supplemented with protease inhibitor tablet and 10 μM 1,10-phenanthroline. CXCL10 in the supernatants and cell lysates ($n = 5$ from 2 experiments) was measured by ELISA and is expressed per concentration of living cells in each replicate prior to analysis by one-way ANOVA with Tukey's *post-hoc* test. **(E)** CXCL10 incubated with GP63 is unable to chemoattract CXCR3+ cells *in vitro.* Jurkat T cells stably transfected with CXCR3 were seeded on the apical surface of a 5 μm transwell insert, with human recombinant CXCL10 pre-incubated with conditioned media from either *L. major WT, Δgp63,* or *Δgp63+1* in the basal chamber. The number of CXCR3+ Jurkats in the basal chamber after 4 h were counted to assess chemotactic capacity of CXCL10 after exposure to GP63. **(F)** Proposed model where the host attempts to upregulate CXCL10 in response to infection, but through the activity of GP63 *L. major* is able to impair signaling through the CXCR3 receptor.

smegmatis, *Staphylococcus* (*S.*) *aureus,* and *Cryptococcus* (*C.*) *neoformans.* CXCL10 suppression of at least 80% was observed with two additional intracellular pathogens: *S.* Typhimurium and *C. trachomatis.* In contrast, other pathogens, including the extracellular pathogens *S. aureus* and *C. neoformans,* exhibited modest to no suppression of CXCL10 (**Figure 5B**).

Confirmation and characterization of CXCL10 suppression in different cell lines demonstrated that diverse intracellular pathogens impair chemokine accumulation. Using a second LCL, we confirmed that *S.* Typhimurium and *C. trachomatis* infection suppress CXCL10 (**Figures 5C,D**). We then assessed the generalizability of CXCL10 suppression in host cell types known to be commonly infected by each pathogen. THP-1 monocytes stimulated with LPS upregulate significant production of CXCL10 protein, but infection with live *S.* Typhimurium dramatically impaired this CXCL10 induction (**Figure 5E**). Similarly, the cervical epithelial cell line A2EN produces CXCL10 at baseline, but this is significantly reduced after infection with *C. trachomatis* (**Figure 5F**). Thus, multiple intracellular pathogens that pose significant health burdens around the globe have independently evolved the ability to suppress CXCL10 in the cell types relevant to their infective niche.

DISCUSSION

We describe a mechanism used by intracellular pathogens to evade host chemokine response. Specifically, *L. major* can significantly reduce CXCL10 and impair its chemotactic activity through the matrix-metalloprotease, GP63. This strategy is likely to be highly beneficial to the parasite as CXCL10 protects against *L. major* (Vester et al., 1999), *L. amazonensis* (Vasquez and Soong, 2006), and *L. donovani* infection (Gupta et al., 2009, 2011). A similar phenotype of immune evasion

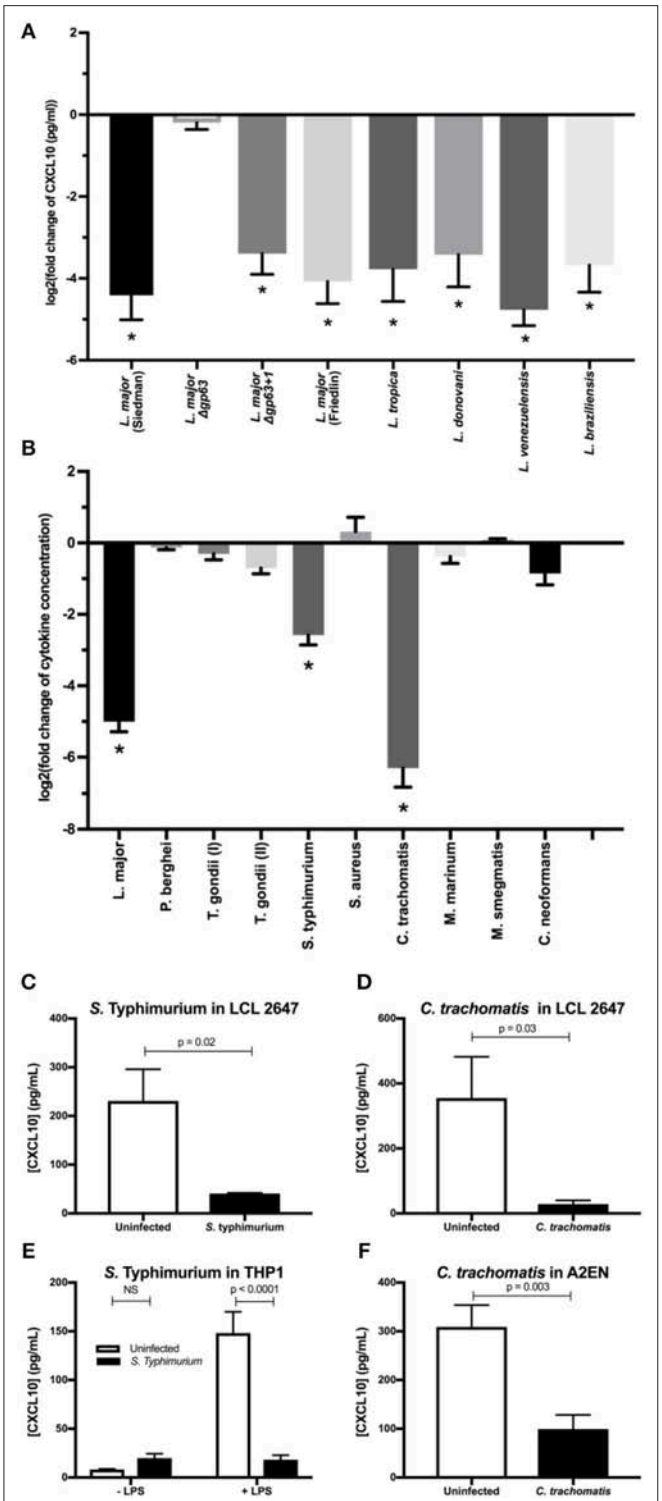

FIGURE 5 | Multiple intracellular pathogens have evolved a mechanism for CXCL10 suppression. **(A)** *Leishmania* spp. with diverse geographic origin, genetic background, and clinical manifestations suppress CXCL10. 1×10^6 live promastigotes from day 5 cultures of *L. major* Seidman *WT* ($p = 0.0001$), *L. major* Seidman *Δgp63* ($p = 0.81$), *L. major* Seidman *Δgp63+1* ($p = 0.0001$), *L. major* Friedlin ($p = 0.0001$), *L. tropica* ($p = 0.0001$),

(Continued)

FIGURE 5 | *L. donovani* ($p = 0.0001$), *L. venezuelensis* ($p = 0.0001$), and *L. braziliensis* ($p = 0.0001$) were incubated in 50 μl of M199 supplemented with 1 ng/μl of human recombinant CXCL10 at 37°C for 24 h. **(B)** LCL 18524 was used to screen *L. major* ($p = 0.0001$), *P. berghei* ($p = 0.99$), *T. gondii* I (RH) ($p = 0.44$), *T. gondii* II (Prugniaud A7) ($p = 0.011$), *S. enterica* serovar Typhimurium ($p = 0.0001$), *S. aureus* ($p = 0.12$), *C. trachomatis* ($p = 0.0001$), *M. marinum* ($p = 0.37$), *M. smegmatis* ($p > 0.99$), *and C. neoformans* ($p = 0.010$) for CXCL10 suppressing activity ($n = 2$–4 for each pathogen). For **(A,B)** CXCL10 concentration was measured by ELISA and is represented as the $\log_2$ of fold change relative to uninfected controls. *P*-values calculated by one-way ANOVA with Dunnett's *post-hoc* test comparing non-log transformed values to 1, which would represent no change relative to uninfected $^*p < 0.01$. **(C,D)** *S.* Typhimurium and *C. trachomatis* suppress CXCL10 in a second LCL. Infections were performed in the LCL HG02647 for *S.* Typhimurium ($n = 6$; two experiments) and *C. trachomatis* ($n = 5$; three experiments). Mean ± standard error of the mean is plotted and *P*-values calculated by Student's *t*-test. **(E)** *S.* Typhimurium suppresses production of CXCL10 in THP-1 monocytes. THP-1 monocytes were stimulated with 1 μg/mL of purified LPS from *S.* Typhimurium at the time of infection. CXCL10 concentration in culture supernatant at 24 hpi was assayed by ELISA. Mean ± standard error the mean is plotted, and *P*-values calculated by two-way ANOVA with Tukey's *post-hoc* test. **(F)** *Chlamydia trachomatis* suppresses CXCL10 in the human endocervical epithelial cell line A2EN. CXCL10 concentration in culture supernatant at 72 hpi was assayed by ELISA. Mean ± standard error of the mean is plotted and *P*-values calculated by Student's *t*-test.

that is shared by diverse intracellular pathogens points to a critical conserved role for CXCL10 in immunity to intracellular pathogens.

Consistent with CXCL10 playing a protective role during infection, multiple studies show that recruitment of CXCR3-expressing cells actively shapes the immune response. In response to *Leishmania* spp. specifically, CXCL10 is critical for the recruitment and activation of several cell types that contribute to the coordination of a protective type-1 immune response: natural killer (NK) cells, CD8+ T cells, dendritic cells, and CD4+ T_h1 cells. With the early upregulation of *CXCL10* transcript (Zaph and Scott, 2003), NK cells recruited during infection produce IFNγ that contributes to T_h1 differentiation (Vester et al., 1999; Muller et al., 2001). Specific subsets of effector CD8+ T cells are recruited by CXCL10 after infection (Majumder et al., 2012; Oghumu et al., 2013). Finally, dendritic cells exposed to CXCL10 produce increased IL12, a cytokine that promotes T_h1 polarization, and T_h1 cells exposed to CXCL10 produce greater amounts of IFNγ (Vasquez et al., 2008), a signal which infected macrophages require for efficient parasite killing (Scott and Novais, 2016). Beyond *Leishmania*, CXCR3-expressing cells have also been reported to play important roles in other infectious and inflammatory models (Qin et al., 1998; Cella et al., 1999; Thomas et al., 2003; Nanki et al., 2009; Groom and Luster, 2011; Oghumu et al., 2013). After infection with lymphocytic choriomeningitis virus, CXCR3 deletion leads to impaired production and localization of effector CD8+ T cells (Hu et al., 2011), and CXCL10 precisely coordinates effector CD8+ T cells to the site of *Toxoplasma gondii*, another intracellular eukaryotic pathogen (Harris et al., 2012). In response to the bacterial pathogen *S.* Typhimurium, which we identified as also suppressing CXCL10, mice have a significant expansion of CXCR3+ T_h1 cells which border bacteria-rich granulomas in the

spleen (Goldberg et al., 2018). These diverse examples highlight the importance of evading the CXCL10-CXCR3 signaling axis for pathogens.

Current limitations regarding the complexity of GP63 related proteases may contribute to an incomplete picture of the impact of GP63 on chemokine suppression. First, sequencing *L. major* revealed proteins distantly homologous to GP63 (∼35% amino acid identity) on chromosomes 28 and 31, in addition to the tandem array of *gp63* genes on chromosome 10 (Ivens et al., 2005; Valdivia et al., 2015). These related proteases may suppress CXCL10 during different stages of infection or cleave an additional set of host substrates, even though they are not required for CXCL10 cleavage under our *in vitro* conditions. Second, *L. major Δgp63+1* has one of the seven chromosome-10 *gp63* copies which does not complement *gp63* mRNA to wild-type levels (**Figure 4C**) in the absence of G418 selection making the currently available GP63 strains sub-optimal for *in vivo* experiments. Finally, the *in vitro* THP-1 infection assay used in this study is unable to identify the route of GP63 release during intracellular infection. Although there was no observed GP63 dependent difference in cell death (**Figure S2A**), we are unable to distinguish whether GP63 is actively secreted or passively released from host cells after cell death. Despite these limitations, we demonstrate that GP63 cleavage of CXCL10 is selective, rapid, and renders the chemokine non-functional. Further investigation beyond the scope of this manuscript will be required to elucidate the implications of CXCL10 cleavage in other infection contexts and animal models.

An effective vaccine to protect against leishmaniasis has been a tantalizing strategy for disease control with unrealized potential due to an incomplete understanding of how the parasites interact with the immune system. Historically, inoculation with live parasites in unexposed areas of skin has effectively prevented future infections (Seyed et al., 2018); however, this strategy poses significant risks (Lindoso et al., 2014; Monge-Maillo et al., 2014; Singh, 2014) and subsequent vaccine development efforts failed to confer long-term protection in human studies (Seyed et al., 2018). Recent studies highlight the importance of chemokine recruitment in mounting an efficient secondary immune response. Specifically, transcription of *Cxcl10* is upregulated in T resident-memory (T_{rm}) cells after secondary infection, and antibody blockade of CXCR3 prevents recruitment of circulating CD4+ T cells to the site of infection (Glennie et al., 2015; Glennie and Scott, 2016; Romano et al., 2017). Together with our finding that CXCR3 substrates are cleaved by *L.* major, this suggests that one of the goals of vaccine development should be to overcome parasite-encoded CXCR3 escape upon secondary infection. Promisingly, GP63-specific CD4+ T cells elicit strong IFNγ and T_h1 responses (Julia and Glaichenhaus, 1999) while GP63 based vaccines elicit long term immunity in mice that is correlated with T_h1 responses (Bhowmick et al., 2008; Sachdeva et al., 2009; Mazumder et al., 2011a,b); a phenotype that could be enhanced by anti-GP63 antibodies functionally blocking cleavage of CXCR3 ligands. A complete understanding of how the parasite alters chemokine recruitment upon secondary infection may facilitate development of a vaccine that can provide long term immunity to leishmaniasis.

The relevance of these insights into immune evasion is made more impactful by the observation that CXCL10 suppression is conserved across *Leishmania* spp. and has arisen in multiple intracellular pathogens. We found that in addition to *Leishmania* spp., *S.* Typhimurium, and *C. trachomatis* independently evolved the ability to suppress CXCL10, which indicates that suppression of CXCR3 inflammatory signaling is advantageous for multiple intracellular pathogens. In addition to *S.* Typhimurium and *C. trachomatis,* several other commensal and pathogenic bacteria have been reported to suppress CXCL10, including *Lactobacillus paracasei*, *Streptococcus pyogenes, Finegoldia magna*, and *Porphymonas gingivalis* (Karlsson et al., 2009; von Schillde et al., 2012; Jauregui et al., 2013). Similarly, the fungal pathogen *Candida albicans* produces a signaling molecule to inhibit *CXCL10* transcription (Shiraki et al., 2008). Among viruses, Hepatitis C virus (HCV) upregulates host proteases to modify CXCL10 (Casrouge et al., 2011), Epstein-Barr virus (EBV) decreases transcription through chromatin remodeling at the *CXCL10* locus (Harth-Hertle et al., 2013), and Zika virus (ZIKV) blocks translation of CXCL10 (Bowen et al., 2017; Chaudhary et al., 2017). The repeated and independent evolution of CXCL10 evasion suggests that this chemokine poses a significant evolutionary pressure on common human pathogens. These diverse pathogens heavily impact global morbidity and mortality. Understanding how pathogens manipulate the CXCR3 signaling axis to their advantage may enable therapeutic countermeasures that circumvent or prevent pathogen suppression of CXCR3 signaling.

MATERIALS AND METHODS

Cell Lines

LCLs from the International HapMap Project (Consortium, 2005) (GM18524 from Han Chinese in Beijing, China, GM19203 from Yoruba in Ibadan, Nigeria, GM7357 from Utah residents with Northern and Western European ancestry from the CEPH collection, and HG02647 of Gambian ancestry isolated in Gambia) were purchased from the Coriell Institute. LCLs were maintained at 37°C in a 5% CO2 atmosphere and were grown in RPMI 1640 media (Invitrogen) supplemented with 10% fetal bovine serum (FBS), 2 mM glutamine, 100 U/ml penicillin-G, and 100 mg/ml 790 streptomycin. THP-1 monocytes, originally from ATCC, were obtained from the Duke Cell Culture Facility and maintained in RPMI 1640 as described above. HEK293T cells were obtained from ATCC and maintained in DMEM complete media (Invitrogen) supplemented with 10% FBS, 100 U/ml penicillin-G, and 100 mg/ml 790 streptomycin. Jurkat cells (an immortalized T cell line) stably expressing CXCR3 were generated by transfecting a linearized pcDNA3.1 expression vector encoding *CXCR3* and resistance to Geneticin (G-418), selecting for transfected cells with 1000 μg/mL Geneticin, and collecting highly expressing CXCR3 cells by FACS. Cells were maintained in RPMI 1640 media (Sigma) supplemented with 10% FBS, 1% Penicillin/Streptomycin, 0.23% Glucose, 10 mM HEPES, 1 mM Sodium Pyruvate, and 250 μg/mL Geneticin. The A2EN cell line was provided by Raphael Valdivia and maintained in Keratinocyte serum free

media (Gibco; 17005-042) supplemented with 10% heat-inactivated FBS, Epidermal Growth Factor 1–53, and Bovine Pituitary Extract.

Pathogen Culture and Infections

The following *Leishmania* spp. were obtained from BEI or ATCC: *L. major* Seidman *WT* [(MHOM/SN/74/Seidman), NR-48819], *L. major Δgp63* [(MHOM/SN/74/SD) *Δgp63 1-7,* NR-42489], *L. major Δgp63+1* [(MHOM/SN/74/SD) *Δgp63 1-7 + gp63-1,* NR-42490], *L. major* Friedlin V1 [(MHOM/IL/80/FN) NR-48815], *L. tropica* [(MHOM/AF/87/RUP) NR-48820], *L. donovani* [(MHOM/SD/62/1S) NR-48821], *L. venezuelensis* [(MHOM/VE/80/H-16) NR-29184], *L. braziliensis* [(MHOM/BR/75/M2903) ATCC-50135]. Parasites were maintained at 27°C in M199 media (Sigma-Aldrich, M1963), supplemented with 100 μ/ml penicillin/streptomycin, and 0.05% Hemin (Sigma-Aldrich, 51280). Cultures were split 1:20 every 5 days into 10 mL of fresh culture media. To prepare parasites for infection, 8 mL of a 5-day-old culture was spun at 1,200 g for 10 min and washed with 5 mL of HBSS prior to counting promastigotes with a hemocytometer and resuspending at the indicated concentration.

For *Leishmania major* infections of LCLs and THP-1 monocytes, 1×10^5 cells were placed in 100 μl of RPMI 1640 assay media as described above, with no penicillin/streptomycin added. In the case of THP-1 monocytes, cells were then stimulated with 1 μg/mL of LPS derived from *Salmonella enterica* serovar Typhimurium S-form' (Enzo Bioscience, ALX-581-011-L001). Finally, 1×10^6 *L. major* promastigotes were added in 50 μL of RPMI 1640 assay media for a multiplicity of infection (MOI) of 10. Culture supernatants and cell pellets or mRNA were collected after 24 h of infection. For phorbol 12-myristate 13-acetate (PMA) differentiation of THP-1 monocytes, 1.2×10^6 cells were placed in 2 mL of complete RPMI 1640 media supplemented with 100 ng/mL of PMA for 8 h after which the RPMI media was replaced and cells allowed to rest for 36 h. Parasites were then washed and counted as described above and added at an MOI of 20. At 24 h post-infection, the culture supernatant was removed, spun at 1,200 g for 10 min to separate extracellular parasites, and stored at −20°C for downstream cytokine analysis. Cells were then washed 3 times with 1 mL of PBS followed by one additional wash with 2 mL of RPMI media to remove the remaining extracellular promastigotes. At 48 h post-infection the culture supernatant was collected and stored for downstream analysis. To assess intracellular CXCL10 in differentiated THP-1 monocytes, at 24 h post-infection, cells were removed from the plate by pipetting with cold PBS. The concentration of living cells was determined using 7AAD staining and counting cells with a Guava EasyCyte flow cytometer. Cells were then lysed with RIPA buffer supplemented with protease inhibitor tablet (Roche, 11836153001) and 10 μM 1,10-phenanthroline. For downstream mRNA extraction (RNeasy Mini Kit, Qiagen, 74106), cells were stored in 1 mL of RNAprotect (Qiagen, 76526) at −20°C.

Screening GM18524 CXCL10 after infection with *Salmonella enterica* serovar Typhimurium 14028s*, Chlamydia trachomatis* serovar L2, and *Toxoplasma gondii* (RH and Prugniaud A7) were performed as described previously (Wang et al., 2018). For *Staphylococcus aureus,* LCLs were plated at 40,000 cells per 100 μl RPMI assay media in 96-well-plates prior to inoculation at an MOI of 10 with *S. aureus* Sanger-476. Cells were spun at 200 × g for 5 min prior to incubation at 37°C for 1 h. Gentamicin was added at 50 μg/ml and then supernatant was collected at 24 h. For *Cryptococcus neoformans,* LCLs were plated at 40,000 cells per 100 μl RPMI assay media in 96-well-plates prior to inoculation at an MOI of 5 with *C. neoformans* H99 strain. Cells were incubated at 37°C for 24 h prior to collection of supernatant. For *Plasmodium berghei* infections, LCLs were plated at 40,000 cells per 100 μl RPMI assay media in 96-well-plates prior to inoculation with 17,000 *P. berghei*-Luciferase sporozoites isolated from *Anopheles stephensi* from the New York University Insectary Core Facility. Cells were spun at 1,000 × g for 10 min prior to incubation at 37°C for 48 h. Cell death was monitored by 7AAD staining and quantified using a Guava easyCyte HT flow cytometer. To harvest supernatants, LCLs were centrifuged at 200 × g for 5 min prior to removing supernatant and storing at −80°C prior to quantifying chemokines production by ELISA. For *Mycobacterium marinum* and *Mycobacterium smegmatis* infections, LCLs were plated at 40,000 cells per 100 μl RPMI assay media without FBS and supplemented with 0.03% bovine serum albumin (BSA) prior to infection with 400,000 bacteria per well. Cells were spun at 100 x g for 5 min prior to incubation at 33°C for 3 h, after which 50 μl of streptomycin in RPMI media was added for a final concentration of 200 μg/ml streptomycin with 10% FBS, and incubation was continued at 33°C for 24 h. Cell death was monitored by 7AAD staining and quantified using a Guava easyCyte HT flow cytometer. To harvest supernatants, LCLs were centrifuged at 200 x g for 5 min prior to removing supernatant and storing at −80°C prior to quantifying chemokines by ELISA.

Confirmation of suppression by *S.* Typhimurium and *C. trachomatis* in LCL HG02647 was performed in 24 well-plate format. For *S.* Typhimurium infection, 5×10^5 cells were washed with antibiotic free RPMI assay media and plated in 500 μl of RPMI assay media prior to infection at MOI 30. At 1 h post-infection, gentamycin was added at 50 μg/mL to kill the remaining extracellular bacteria. At 2 h post-infection, gentamycin was diluted to 18 μg/mL to prevent killing of intracellular bacteria. For *C. trachomatis* infection, 2×10^5 cells were washed and plated in 500 μl of RPMI assay media prior to infection at MOI 5 followed by centrifugation at 1,500 g for 30 min. For *S.* Typhimurium infection of THP-1 monocytes, cells were washed once with antibiotic free RPMI assay media and resuspended at a concentration of 1×10^5 in 100 μl of RPMI assay media on a 96-well-plate. Cells were then treated with 1 μg/mL of LPS diluted in RPMI assay media or the equivalent volume of media and *S.* Typhimurium added at an MOI of 10. At 1 h post-infection, gentamycin was added at 50 μg/mL. At 2 h post-infection, gentamycin was diluted to 25 μg/mL. For *C. trachomatis* infection of A2EN cells, 1×10^5 cells were plated in a 96 well-plate the day prior to infection. *C. trachomatis* was added at an MOI of 5 and centrifuged for 30 min at 1,500 g. For all *S.* Typhimurium infections, culture supernatants were harvested at 24 h post-infection. For *C. trachomatis* infection, culture supernatants were collected cells at 72 h post-infection to assess cytokine production.

Cytokine Measurements and Detection

Cytokines were detected by ELISA, Luminex, western blot, or total protein as indicated. Luminex platform based assay for detection of multiple cytokines from Millipore was used to screen *L. major*. The following cytokines and chemokines were included: eotaxin, MCP-1, MCP-3, MIP-1α, MIP-1β, RANTES, Fractalkine, IL8, IL10, IL12p40, IL12p17, IL13, IL17A, IL1RA, IL1α, IL4, IL6, *7,* EGF, FGF2, FLT-3L, G-CSF, GM-CSF, PDGF-AA, PDGF-BB, VEGF, IFNα2, IFNγ, TNFα, TNFβ, sCD40L, IL15, IL1β, IL2, IL3, IL5, IL8, TGFα, and MDC (Millipore). Cytokines below or above the limit of detection were excluded from analyses.

To interrogate the effect of GP63 on individual substrates, the following recombinant chemokines were used: human CXCL10 (R&D, 266-IP), mouse CXCL10 (R&D, 466-CR), human CXCL11 (R&D, 672-IT), human CXCL9 (Peprotech, 300-26), human CXCL8 (Peprotech, 200-08A), and human CCL22 (Peprotech, 300-36A). To separate chemokines based on size, all chemokines except for CXCL9 (which antibody required non-reducing conditions) were incubated at 97°C for 10 min in SDS-loading buffer in the presence of βME prior to loading in a 4–20% bis-tris polyacrylamide gels and running at 120 V for 1 h. For total protein, the Colloidal Blue Staining kit (Thermo Scientific, LC6025) was used per manufacturer's protocol. For western blotting, protein was transferred to a PVDF membrane using a Hoefer TE77X semi-dry transfer system. LiCor Odyssey (TBS) Blocking Buffer (VWR, 102971-244) was used to block for 1 h at room temperature. The following primary antibodies were used to detect chemokines: human CXCL9 (R&D, MAB392-SP), human CXCL11 (MAB672-SP), human CXCL8 (Novus, MAB208-SP), human CCL22 (Novus, MAB336-SP). Primary antibodies were detected with IRDye secondary antibodies (Li-Cor) and developed using a LiCor Odyssey Infrared Imaging System (Li-Cor, 9120). Relative protein quantification based on band intensity was performed using the FIJI gel analysis function (Schindelin et al., 2012).

Parasite mRNA Quantification

RNA was obtained from promastigotes collected from day 5 to 6 of culture after preparation for infection or amastigotes from THP-1 monocytes at 48 h post-infection as described above. Two microgram of RNA was then subject to genomic DNA removal using the TURBO DNase (Ambion) kit. Incubation with TURBO DNase was extended to 1 h and repeated twice. RNA cleanup was performed with the RNeasy MinElute Cleanup Kit (74204, Qiagen). Reverse transcriptase was carried out using 1 μg RNA per sample with the iScript Reverse Transcriptase Kit (Biorad, 1708840) in 20 μl. cDNA was diluted 1:5 prior to adding to PCR reaction with ITaq universal SYBR Green supermix (BioRad, 172-5124), 50 nM of each primer, and 4 μl cDNA for gene targets or 1 μl cDNA for housekeeping gene in a final volume of 10 μl. To determine the relative expression of *gp63-1*, primers (Forward: CCGTCACCCGGGCCTT; Reverse: CAGCAACGAAGCATGTGCC) were designed using the *L. major* Friedlin reference gene 10.0480 which has 100% sequence similarity with the *gp63-1* gene in *L. major* Seidman WT and *Δgp63+1* (Button and McMaster, 1988). To monitor for stage specific expression, we used previously described primers for *L. major* Fd gene *07.1160* (Rochette et al., 2008), a gene identified and confirmed as highly expressed specifically in the promastigote stage (Akopyants et al., 2004; Rochette et al., 2008; Fernandes et al., 2016). For housekeeping gene, previously described primers for the *rRNA45* gene were used, which has been demonstrated to be stable across parasite life-cycle stages (Ouakad et al., 2007). cDNA was quantified using either a StepOne Plus Real-Time PCR system (Applied Biosystems) or a QuantStudio 6 Flex Real-Time PCR system (Applied Biosystems). After an initial denaturation stage of 95°C for 20 s, samples were amplified for 40 cycles of denaturation at 95°C for 3 s and annealing at 61°C for 30 s. For melt curve analysis, samples underwent denaturation at 95°C for 15 s, annealing at 53°C for 30 s, and a Step and Hold stage (+0.3°C every 5 s). All PCR reactions were performed in triplicate. Samples containing products with peaks outside of the expected melt temperature ±0.5°C were excluded. To monitor the efficiency of genomic DNA removal, a control reaction for each sample was performed with by amplifying the housekeeping gene from RNA not subject to cDNA synthesis.

In vitro T Cell Migration

RPMI 1640 media (Sigma) was supplemented with 2% FBS and CXCL10 at a starting concentration of 100 nM. This was pre-incubated at a ratio of 1:1 with conditioned media from either *L. major WT, Δgp63,* or *Δgp63+1*. After 12 h of pre-incubation, 600 μl of CXCL10/conditioned media mix was added to a 24 well-plate. Five hundred thousand Jurkat T cells stably transfected with *CXCR3* were seeded onto the apical membrane of the 5 μm transwell insert (Corning, 3421), and allowed to incubate at 37°C for 4 h. The transwell insert was removed and the concentration of cells in the basal chamber determined using a Guava easyCyte HT flow cytometer (Millipore).

Parasite Quantification by DAPI Staining

THP-1 macrophages (1.2×10^5) were treated with 100 ng/mL PMA in 200 mL on a poly-D lysine treated 8-well-chamber slide for 8 h and subsequently allowed to rest for 1 day prior to infection. Cells were then infected at MOI 20 with the indicated *L. major* strain. At 24 h post-infection, media was removed and cells were fixed with 4% paraformaldehyde for 20 min. After washing 3 times with PBS, cells were incubated in blocking and permeabilization buffer (PBS supplemented with 0.5% Saponin and 0.2% Normal Donkey Serum) for 30 min at room temperature after which the blocking buffer was aspirated and replaced with 5 μM DAPI in PBS for 30 min. Cells were then washed three times with PBS prior to mounting. Images were acquired using a fluorescence microscope (Leica DM4B) with attached CCD microscope camera (Leica DFC3000g) at 400x total magnification. One field of view was recorded for each well and image quantification was performed by two independent experimenters using the cell counter plug-in in FIJI (Schindelin et al., 2012; Schneider et al., 2012). Quantification from the two independent experimenters was averaged prior to plotting.

Expression of Recombinant GP63 and Site-Directed Mutagenesis

Expression of CXCL10 and GP63 were performed by transfection in HEK293T cells. HEK293Ts were maintained in complete DMEM media supplemented with 10% FBS. Two days prior to transfection, 250,000 cells were washed and plated in a 6-well-tissue culture treated plate in 2 mL of serum free, FreeStyle 293 Expression Media (ThermoFisher, 12338018). One hour prior to transfection, media was replaced with fresh FreeStyle media. Transfection was performed with 2.5 total μg of endotoxin free plasmid DNA using the Lipofectamine 3000 Transfection Reagent Kit per manufacturer's instructions. Transfected HEK293Ts were incubated at 37°C for 48 h prior to harvesting culture supernatant and storing in polypropylene, low-binding tubes (Corning, 29442-578) at −80°C until use.

The CXCL10 plasmid was obtained from Origene (NM_001565), and contains C-terminal Myc and Flag epitope tags. For GP63, a codon optimized plasmid was obtained from GenScript on the pcDNA3.1/Hygro plasmid backbone. Following a kozak sequence and secrecon to enhance secretion (Kozak, 1989; Barash et al., 2002; Güler-Gane et al., 2016), GP63-1 based on the *L. major* Fd sequence (Q4QHH2-1) was inserted with the *Leishmania* specific secretion signal and GPI anchor motif removed (V100-N577) (Schlagenhauf et al., 1998), and epitope tagged with Myc and His sequences placed at the C-terminus. Point mutations in CXCL10 and GP63 were made using the Agilent QuikChange Site Directed Mutagenesis kit according to manufacturer's instructions.

Mass Spectrometry

CXCL10 exposed to GP63 for 5 h, along with a negative (untreated) control was delivered in PAGE loading buffer at an approximate concentration of 30 ng/uL. Mass spectrometry was carried out by the Duke Proteomics and Metabolomics Shared Resource. Molecular weight analysis of intact and cleaved CXCL10 from gel loading buffer was performed using a ZipChip CE system (908 Devices, Inc.) coupled to a Q Exactive HF Orbitrap mass spectrometer (Thermo Scientific). Ammonium acetate was added to the sample to a final concentration 0.1 M, and 5 μL of the loading buffer was pipetted manually into a HR ZipChip. Capillary electrophoresis (CE) separation was performed at 500 V/cm with a 30 s injection in Metabolite BGE (908 Devices, Inc.). Mass spectrometry used positive electrospray with 120,000 Rs scan, 500–2,000 m/z, 3e6 AGC target and 100 ms max ion injection time. Mass deconvolution was performed in Proteome Discoverer 2.2.

Tandem mass spectrometric sequencing of the cleaved and uncleaved fragments of CXCL10 after GP63 treatment, as well as an untreated control sample, were performed after gel separation on a 4–12% NuPAGE gel (Invitrogen). Gel bands were isolated after colloidal Coomassie staining, destained in acetonitrile/water, reduced with 10 mM DTT, alkylated with 20 mM iodoacetamide, and digested overnight at 37°C with 300 ng sequencing grade trypsin (Promega) in 50 mM ammonium bicarbonate at pH 8. Peptides were extracted in 1% formic acid and dried on a speedvac, then resuspended in a total of 10 μL 97/2/1 v/v/v water/acetonitrile/TFA. Four microliter of each sample was injected for analysis by LC-MS/MS using a 90 min, 5–30% MeCN LC gradient and a top 12 DDA MS/MS method with MS1 at 120 k and MS2 at 15 k resolution. The data files were searched on Mascot v 2.5 with the UniProt database (downloaded November 2017) and *Homo sapiens* taxonomy selected, semitryptic specificity, along with fixed modification carbamidomethyl (C) and variable modifications oxidated (M), and deamidated (NQ). The results of the database searches were compiled into Scaffold v4 for curation. Using the search results as a spectral library, Skyline v4.1 was used to extract peak intensities for peptides which looked to be a part of the cleavage region (residues 74–91) or non-cleaved region (residues 48–68), in order to more definitively localize the specific cleavage location (**Figure 3E**). Intensity was expressed as the peak area normalized to the protein region from residues 29–52, in order to control for protein abundance differences between the samples. The Skyline file has been made publicly available at Panoramaweb.org (https://goo.gl/4xsLsF).

Statistical Analysis

All statistical analysis was performed using GraphPad Prism. Unpaired Student's *t*-test, one-way ANOVA, and two-way ANOVA with Tukey's *post-hoc* test were used as appropriate where indicated. The number of biological replicates (N) are indicated in the figure legend for each experiment and defined as follows. For *in vitro* cell culture and protein assessment each well of cells or chemokine prior to experimental manipulation (such as infection with parasite or addition of chemokine and/or inhibitor) was treated as a unique biological replicate. When technical replicates, repeated use of the same biological sample in a readout assay, were used they are indicated in the figure legend text and averaged values were combined into the single biological replicate prior to calculating statistics.

DATA AVAILABILITY

All datasets generated for this study are included in the manuscript and/or **Supplementary Files**.

AUTHOR CONTRIBUTIONS

All authors critically reviewed the manuscript and contributed input to the final submission. AA, DK, KG, and RR wrote the manuscript. AA, DK, RR, JS, SR, and JT contributed to strategy and project planning. AA, KG, ET, KP, AM, BS, JS, JT, RR, and DK carried out experiments and analysis.

FUNDING

AA, KG, ET, KP, BS, and DK were supported by Duke Molecular Genetics and Microbiology startup funds, Duke University Whitehead Scholarship, Butler Pioneer Award, and NIH U19AI084044. ET was supported by the Duke Summer Research Opportunity Program (SROP). AM was supported by the Duke Department of Molecular Genetics and Microbiology Summer Undergraduate Research Experience (MGM SURE). JS

and SR were supported by NIH GM122798 and the Burroughs Wellcome Fund Career Award for Medical Scientists. RR was supported by NIH AI119004.

ACKNOWLEDGMENTS

We thank Robyn Guo for assistance with immunoblotting, Sarah Rains for assistance with sample prep for CXCL10 cleavage site identification, and Jeffrey S. Bourgeois for thoughtful discussion about experimental design and analysis. For assistance with screening additional pathogens for CXCL10 cleavage we thank Emily Derbyshire, Maria Toro-Moreno, David Tobin, Ana-María Xet-Mull, Raphael Valdivia, Qin Yan, Vance Fowler, Jennifer Tenor, and John Perfect. We thank the Duke University School of Medicine for the use of the Proteomics and Metabolomics Shared Resource.

SUPPLEMENTARY MATERIAL

The Supplementary Material for this article can be found online at: https://www.frontiersin.org/articles/10.3389/fcimb.2019.00280/full#supplementary-material

REFERENCES

Ajdary, S., Alimohammadian, M. H., Eslami, M. B., Kemp, K., and Kharazmi, A. (2000). Comparison of the immune profile of nonhealing cutaneous Leishmaniasis patients with those with active lesions and those who have recovered from infection. *Infect. Immun.* 68, 1760–1764. doi: 10.1128/IAI.68.4.1760-1764.2000

Akopyants, N. S., Matlib, R. S., Bukanova, E. N., Smeds, M. R., Brownstein, B. H., Stormo, G. D., et al. (2004). Expression profiling using random genomic DNA microarrays identifies differentially expressed genes associated with three major developmental stages of the protozoan parasite *Leishmania major*. *Mol. Biochem. Parasitol.* 136, 71–86. doi: 10.1016/j.molbiopara.2004.03.002

Alvar, J., Vélez, I. D., Bern, C., Herrero, M., Desjeux, P., Cano, J., et al. (2012). Leishmaniasis worldwide and global estimates of its incidence. *PLoS ONE* 7:e35671. doi: 10.1371/journal.pone.0035671

Alvarez-Valin, F., Tort, J. F., and Bernardi, G. (2000). Nonrandom spatial distribution of synonymous substitutions in the GP63 gene from Leishmania. *Genetics* 155, 1683–1692.

Antoniazi, S., Price, H. P., Kropf, P., Freudenberg, M. A., Galanos, C., Smith, D. F., et al. (2004). Chemokine gene expression in toll-like receptor-competent and -deficient mice infected with *Leishmania major*. *Infect. Immun.* 72, 5168–5174. doi: 10.1128/IAI.72.9.5168-5174.2004

Barash, S., Wang, W., and Shi, Y. (2002). Human secretory signal peptide description by hidden Markov model and generation of a strong artificial signal peptide for secreted protein expression. *Biochem. Biophys. Res. Commun.* 294, 835–842. doi: 10.1016/S0006-291X(02)00566-1

Barbi, J., Brombacher, F., and Satoskar, A. R. (2008). T cells from *Leishmania major*-susceptible BALB/c mice have a defect in efficiently up-regulating CXCR3 upon activation. *J. Immunol.* 181, 4613–4620. doi: 10.4049/jimmunol.181.7.4613

Barbi, J., Oghumu, S., Rosas, L. E., Carlson, T., Lu, B., Gerard, C., et al. (2007). Lack of CXCR3 delays the development of hepatic inflammation but does not impair resistance to *Leishmania donovani*. *J. Infect. Dis.* 195, 1713–1717. doi: 10.1086/516787

Belkaid, Y., Von Stebut, E., Mendez, S., Lira, R., Caler, E., Bertholet, S., et al. (2002). CD8+ T cells are required for primary immunity in C57BL/6 mice following low-dose, intradermal challenge with *Leishmania major*. *J. Immunol.* 168, 3992–4000. doi: 10.4049/jimmunol.168.8.3992

Bhowmick, S., Ravindran, R., and Ali, N. (2008). gp63 in stable cationic liposomes confers sustained vaccine immunity to susceptible BALB/c mice infected with *Leishmania donovani*. *Infect. Immun.* 76, 1003–1015. doi: 10.1128/IAI.00611-07

Booth, V., Keizer, D. W., Kamphuis, M. B., Clark-Lewis, I., and Sykes, B. D. (2002). The CXCR3 binding chemokine IP-10/CXCL10: structure and receptor interactions. *Biochemistry* 41, 10418–10425. doi: 10.1021/bi026020q

Bouvier, J., Schneider, P., Etges, R., and Bordier, C. (1990). Peptide substrate specificity of the membrane-bound metalloprotease of Leishmania. *Biochemistry* 29, 10113–10119. doi: 10.1021/bi00495a015

Bowen, J. R., Quicke, K. M., Maddur, M. S., O'Neal, J. T., McDonald, C. E., Fedorova, N. B., et al. (2017). Zika virus antagonizes type I interferon responses during infection of human dendritic cells. *PLoS Pathog.* 13:e1006164. doi: 10.1371/journal.ppat.1006164

Burza, S., Croft, S. L., and Boelaert, M. (2018). Leishmaniasis. *Lancet* 392, 951–970. doi: 10.1016/S0140-6736(18)31204-2

Button, L. L., and McMaster, W. R. (1988). Molecular cloning of the major surface antigen of leishmania. *J. Exp. Med.* 167, 724–729. doi: 10.1084/jem.167.2.724

Carvalho, E. M., Correia Filho, D., Bacellar, O., Almeida, R. P., Lessa, H., and Rocha, H. (1995). Characterization of the immune response in subjects with self-healing cutaneous leishmaniasis. *Am. J. Trop. Med. Hyg.* 53, 273–277. doi: 10.4269/ajtmh.1995.53.273

Casrouge, A., Decalf, J., Ahloulay, M., Lababidi, C., Mansour, H., Vallet-Pichard, A., et al. (2011). Evidence for an antagonist form of the chemokine CXCL10 in patients chronically infected with HCV. *J. Clin. Invest.* 121, 308–317. doi: 10.1172/JCI40594

Castellano, L. R., Filho, D. C., Argiro, L., Dessein, H., Prata, A., Dessein, A., et al. (2009). Th1/Th2 immune responses are associated with active cutaneous leishmaniasis and clinical cure is associated with strong interferon-gamma production. *Hum. Immunol.* 70, 383–390. doi: 10.1016/j.humimm.2009.01.007

Cella, M., Jarrossay, D., Facchetti, F., Alebardi, O., Nakajima, H., Lanzavecchia, A., et al. (1999). Plasmacytoid monocytes migrate to inflamed lymph nodes and produce large amounts of type I interferon. *Nat. Med.* 5, 919–923. doi: 10.1038/11360

Chami, B., Yeung, A., Buckland, M., Liu, H. M., Fong G., Tao K. (2017). CXCR3 plays a critical role for host protection against Salmonellosis. *Sci. Rep.* 7:10181. doi: 10.1038/s41598-017-09150-z

Chaudhary, V., Yuen, K. S., Chan, J. F., Chan, C. P., Wang, P. H., Cai, J. P., et al. (2017). Selective activation of type II interferon signaling by Zika virus NS5 protein. *J. Virol.* 91:e00163-17. doi: 10.1128/JVI.00163-17

Chaudhuri, G., Chaudhuri, M., Pan, A., and Chang, K. P. (1989). Surface acid proteinase (gp63) of *Leishmania mexicana*. A metalloenzyme capable of protecting liposome-encapsulated proteins from phagolysosomal degradation by macrophages. *J. Biol. Chem.* 264, 7483–7489.

Consortium, I. H. (2005). A haplotype map of the human genome. *Nature* 437, 1299–1320. doi: 10.1038/nature04226

de Rezende, E., Kawahara, R., Pena, M. S., Palmisano, G., and Stolf, B. S. (2017). Quantitative proteomic analysis of amastigotes from *Leishmania* (L.) amazonensis LV79 and PH8 strains reveals molecular traits associated with the virulence phenotype. *PLoS Negl. Trop. Dis.* 11:e0006090. doi: 10.1371/journal.pntd.0006090

Fernandes, M. C., Dillon, L. A., Belew, A. T., Bravo, H. C., Mosser, D. M., and El-Sayed, N. M. (2016). Dual transcriptome profiling of Leishmania-infected human macrophages reveals distinct reprogramming signatures. *MBio* 7:e00027-16. doi: 10.1128/mBio.00027-16

Finlay, B. B., and McFadden, G. (2006). Anti-immunology: evasion of the host immune system by bacterial and viral pathogens. *Cell* 124, 767–782. doi: 10.1016/j.cell.2006.01.034

Gilchrist, J. J., MacLennan, C. A., and Hill, A. V. (2015). Genetic susceptibility to invasive *Salmonella* disease. *Nat. Rev. Immunol.* 15, 452–463. doi: 10.1038/nri3858

Glennie, N. D., and Scott, P. (2016). Memory T cells in cutaneous leishmaniasis. *Cell. Immunol.* 309, 50–54. doi: 10.1016/j.cellimm.2016.07.010

Glennie, N. D., Yeramilli, V. A., Beiting, D. P., Volk, S. W., Weaver, C. T., and Scott, P. (2015). Skin-resident memory CD4+ T cells enhance protection against *Leishmania major* infection. *J. Exp. Med.* 212, 1405–1414. doi: 10.1084/jem.20142101

Goldberg, M. F., Roeske, E. K., Ward, L. N., Pengo, T., Dileepan, T., Kotov, D. I., et al. (2018). *Salmonella* persist in activated macrophages in T cell-sparse granulomas but are contained by surrounding CXCR3 ligand-positioned Th1 cells. *Immunity* 49, 1090–1102.e7. doi: 10.1016/j.immuni.2018.10.009

Gondek, D. C., Roan, N. R., and Starnbach, M. N. (2009). T cell responses in the absence of IFN-gamma exacerbate uterine infection with *Chlamydia trachomatis*. *J. Immunol.* 183, 1313–1319. doi: 10.4049/jimmunol.0900295

Groom, J. R., and Luster, A. D. (2011). CXCR3 ligands: redundant, collaborative and antagonistic functions. *Immunol. Cell Biol.* 89, 207–215. doi: 10.1038/icb.2010.158

Güler-Gane, G., Kidd, S., Sridharan, S., Vaughan, T. J., Wilkinson, T. C., and Tigue, N. J. (2016). Overcoming the refractory expression of secreted recombinant proteins in mammalian cells through modification of the signal peptide and adjacent amino acids. *PLoS ONE* 11:e0155340. doi: 10.1371/journal.pone.0155340

Gupta, G., Bhattacharjee, S., Bhattacharyya, S., Bhattacharya, P., Adhikari, A., Mukherjee, A., et al. (2009). CXC chemokine-mediated protection against visceral leishmaniasis: involvement of the proinflammatory response. *J. Infect. Dis.* 200, 1300–1310. doi: 10.1086/605895

Gupta, G., Majumdar, S., Adhikari, A., Bhattacharya, P., Mukherjee, A. K., Majumdar, S. B., et al. (2011). Treatment with IP-10 induces host-protective immune response by regulating the T regulatory cell functioning in *Leishmania donovani*-infected mice. *Med. Microbiol. Immunol.* 200, 241–253. doi: 10.1007/s00430-011-0197-y

Hajishengallis, G., and Lambris, J. D. (2011). Microbial manipulation of receptor crosstalk in innate immunity. *Nat. Rev. Immunol.* 11, 187–200. doi: 10.1038/nri2918

Harris, T. H., Banigan, E. J., Christian, D. A., Konradt, C., Tait Wojno, E. D., Norose, K., et al. (2012). Generalized Levy walks and the role of chemokines in migration of effector CD8(+) T cells. *Nature* 486, 545–8. doi: 10.1038/nature11098

Harth-Hertle, M. L., Scholz, B. A., Erhard, F., Glaser, L. V., Dölken, L., Zimmer, R., et al. (2013). Inactivation of intergenic enhancers by EBNA3A initiates and maintains polycomb signatures across a chromatin domain encoding CXCL10 and CXCL9. *PLoS Pathog.* 9:e1003638. doi: 10.1371/journal.ppat.1003638

Heinzel, F. P., Sadick, M. D., Holaday, B. J., Coffman, R. L., and Locksley, R. M. (1989). Reciprocal expression of interferon gamma or interleukin 4 during the resolution or progression of murine leishmaniasis. Evidence for expansion of distinct helper T cell subsets. *J. Exp. Med.* 169, 59–72. doi: 10.1084/jem.169.1.59

Hess, J., Ladel, C., Miko, D., and Kaufmann, S. H. (1996). *Salmonella typhimurium* aroA- infection in gene-targeted immunodeficient mice: major role of CD4+ TCR-alpha beta cells and IFN-gamma in bacterial clearance independent of intracellular location. *J. Immunol.* 156, 3321–3326.

Hu, J. K., Kagari, T., Clingan, J. M., and Matloubian, M. (2011). Expression of chemokine receptor CXCR3 on T cells affects the balance between effector and memory CD8 T-cell generation. *Proc. Natl. Acad. Sci. U.S.A.* 108, E118–E127. doi: 10.1073/pnas.1101881108

Ivens, A. C., Peacock, C. S., Worthey, E. A., Murphy, L., Aggarwal, G., Berriman, M., et al. (2005). The genome of the kinetoplastid parasite, *Leishmania major*. *Science* 309, 436–442. doi: 10.1126/science.1112680

Jauregui, C. E., Wang, Q., Wright, C. J., Takeuchi, H., Uriarte, S. M., and Lamont, R. J. (2013). Suppression of T-cell chemokines by *Porphyromonas gingivalis*. *Infect. Immun.* 81, 2288–2295. doi: 10.1128/IAI.00264-13

Joshi, P. B., Kelly, B. L., Kamhawi, S., Sacks, D. L., and McMaster, W. R. (2002). Targeted gene deletion in *Leishmania major* identifies leishmanolysin (GP63) as a virulence factor. *Mol. Biochem. Parasitol.* 120, 33–40. doi: 10.1016/S0166-6851(01)00432-7

Julia, V., and Glaichenhaus, N. (1999). CD4(+) T cells which react to the *Leishmania major* LACK antigen rapidly secrete interleukin-4 and are detrimental to the host in resistant B10.D2 mice. *Infect. Immun.* 67, 3641–3644.

Karlsson, C., Eliasson, M., Olin, A. I., Morgelin, M., Karlsson, A., Malmsten, M., et al. (2009). SufA of the opportunistic pathogen finegoldia magna modulates actions of the antibacterial chemokine MIG/CXCL9, promoting bacterial survival during epithelial inflammation. *J. Biol. Chem.* 284, 29499–29508. doi: 10.1074/jbc.M109.025957

Khan, I. A., MacLean, J. A., Lee, F. S., Casciotti, L., DeHaan, E., Schwartzman, J. D., et al. (2000). IP-10 is critical for effector T cell trafficking and host survival in *Toxoplasma gondii* infection. *Immunity* 12, 483–494. doi: 10.1016/S1074-7613(00)80200-9

Kim, C. H., Rott, L., Kunkel, E. J., Genovese, M. C., Andrew, D. P., Wu, L., et al. (2001). Rules of chemokine receptor association with T cell polarization *in vivo*. *J. Clin. Invest.* 108, 1331–1339. doi: 10.1172/JCI13543

Kozak, M. (1989). The scanning model for translation: an update. *J. Cell Biol.* 108, 229–241. doi: 10.1083/jcb.108.2.229

Lathrop, S. K., Binder, K. A., Starr, T., Cooper, K. G., Chong, A., Carmody, A. B., et al. (2015). Replication of *Salmonella enterica* Serovar Typhimurium in human monocyte-derived macrophages. *Infect Immun.* 83.2661–2671. doi: 10.1128/IAI.00033-15

Lijek, R. S., Helble, J. D., Olive, A. J., Seiger, K. W., and Starnbach, M. N. (2018). Pathology after *Chlamydia trachomatis* infection is driven by nonprotective immune cells that are distinct from protective populations. *Proc. Natl. Acad. Sci. U.S.A.* 115, 2216–2221. doi: 10.1073/pnas.1711356115

Lindoso, J. A., Cota, G. F., da Cruz, A. M., Goto, H., Maia-Elkhoury, A. N., Romero, G. A., et al. (2014). Visceral leishmaniasis and HIV coinfection in Latin America. *PLoS Negl. Trop. Dis.* 8:e3136. doi: 10.1371/journal.pntd.0003136

Majumder, S., Bhattacharjee, S., Paul Chowdhury, B., and Majumdar, S. (2012). CXCL10 is critical for the generation of protective CD8 T cell response induced by antigen pulsed CpG-ODN activated dendritic cells. *PLoS ONE* 7:e48727. doi: 10.1371/journal.pone.0048727

Martinez, F. O., Gordon, S., Locati, M., and Mantovani, A. (2006). Transcriptional profiling of the human monocyte-to-macrophage differentiation and polarization: new molecules and patterns of gene expression. *J. Immunol.* 177, 7303–7311. doi: 10.4049/jimmunol.177.10.7303

Maxion, H. K., and Kelly, K. A. (2002). Chemokine expression patterns differ within anatomically distinct regions of the genital tract during *Chlamydia trachomatis* infection. *Infect. Immun.* 70, 1538–1546. doi: 10.1128/IAI.70.3.1538-1546.2002

Mazumder, S., Maji, M., and Ali, N. (2011b). Potentiating effects of MPL on DSPC bearing cationic liposomes promote recombinant GP63 vaccine efficacy: high immunogenicity and protection. *PLoS Negl. Trop. Dis.* 5:e1429. doi: 10.1371/journal.pntd.0001429

Mazumder, S., Maji, M., Das, A., and Ali, N. (2011a). Potency, efficacy and durability of DNA/DNA, DNA/protein and protein/protein based vaccination using gp63 against *Leishmania donovani* in BALB/c mice. *PLoS ONE* 6:e14644. doi: 10.1371/journal.pone.0014644

Monge-Maillo, B., Norman, F. F., Cruz, I., Alvar, J., and Lopez-Velez, R. (2014). Visceral leishmaniasis and HIV coinfection in the Mediterranean region. *PLoS Negl. Trop. Dis.* 8:e3021. doi: 10.1371/journal.pntd.0003021

Morrison, R. P., and Caldwell, H. D. (2002). Immunity to murine chlamydial genital infection. *Infect. Immun.* 70, 2741–2751. doi: 10.1128/IAI.70.6.2741-2751.2002

Morrison, S. G., Farris, C. M., Sturdevant, G. L., Whitmire, W. M., and Morrison, R. P. (2011). Murine *Chlamydia trachomatis* genital infection is unaltered by depletion of CD4+ T cells and diminished adaptive immunity. *J. Infect. Dis.* 203, 1120–1128. doi: 10.1093/infdis/jiq176

Muller, I., Kropf, P., Etges, R. J., and Louis, J. A. (1993). Gamma interferon response in secondary *Leishmania major* infection: role of CD8+ T cells. *Infect. Immun.* 61, 3730–3738.

Muller, I., Kropf, P., Louis, J. A., and Milon, G. (1994). Expansion of gamma interferon-producing CD8+ T cells following secondary infection of mice immune to *Leishmania major*. *Infect. Immun.* 62, 2575–2581.

Muller, K., van Zandbergen, G., Hansen, B., Laufs, H., Jahnke, N., Solbach, W., et al. (2001). Chemokines, natural killer cells and granulocytes in the early course of *Leishmania major* infection in mice. *Med. Microbiol. Immunol.* 190, 73–76. doi: 10.1007/s004300100084

Nanki, T., Takada, K., Komano, Y., Morio, T., Kanegane, H., Nakajima, A., et al. (2009). Chemokine receptor expression and functional effects of chemokines on B cells: implication in the pathogenesis of rheumatoid arthritis. *Arthritis Res. Ther.* 11:R149. doi: 10.1186/ar2823

Oghumu, S., Dong, R., Varikuti, S., Shawler, T., Kampfrath, T., Terrazas, C. A., et al. (2013). Distinct populations of innate CD8+ T cells revealed in a CXCR3 reporter mouse. *J. Immunol.* 190, 2229–2240. doi: 10.4049/jimmunol.1201170

Okwor, I., and Uzonna, J. E. (2009). Immunotherapy as a strategy for treatment of leishmaniasis: a review of the literature. *Immunotherapy* 1, 765–776. doi: 10.2217/imt.09.40

Olive, A. J., Gondek, D. C., and Starnbach, M. N. (2011). CXCR3 and CCR5 are both required for T cell-mediated protection against *C. trachomatis* infection in the murine genital mucosa. *Mucosal Immunol.* 4, 208–216. doi: 10.1038/mi.2010.58

Olivier, M., Atayde, V. D., Isnard, A., Hassani, K., and Shio, M. T. (2012). Leishmania virulence factors: focus on the metalloprotease GP63. *Microbes Infect.* 14, 1377–1389. doi: 10.1016/j.micinf.2012.05.014

Ouakad, M., Bahi-Jaber, N., Chenik, M., Dellagi, K., and Louzir, H. (2007). Selection of endogenous reference genes for gene expression analysis in *Leishmania major* developmental stages. *Parasitol. Res.* 101, 473–477. doi: 10.1007/s00436-007-0491-1

Perry, L. L., Feilzer, K., and Caldwell, H. D. (1997). Immunity to *Chlamydia trachomatis* is mediated by T helper 1 cells through IFN-gamma-dependent and -independent pathways. *J. Immunol.* 158, 3344–3352.

Qin, S., Rottman, J. B., Myers, P., Kassam, N., Weinblatt, M., Loetscher, M., et al. (1998). The chemokine receptors CXCR3 and CCR5 mark subsets of T cells associated with certain inflammatory reactions. *J. Clin. Invest.* 101, 746–754. doi: 10.1172/JCI1422

Rank, R. G., Lacy, H. M., Goodwin, A., Sikes, J., Whittimore, J., Wyrick, P. B., et al. (2010). Host chemokine and cytokine response in the endocervix within the first developmental cycle of Chlamydia muridarum. *Infect. Immun.* 78, 536–544. doi: 10.1128/IAI.00772-09

Ravindran, R., Foley, J., Stoklasek, T., Glimcher, L. H., and McSorley, S. J. (2005). Expression of T-bet by CD4 T cells is essential for resistance to *Salmonella* infection. *J. Immunol.* 175, 4603–4610. doi: 10.4049/jimmunol.175.7.4603

Reiner, S. L., and Locksley, R. M. (1993). Cytokines in the differentiation of Th1/Th2 CD4+ subsets in leishmaniasis. *J. Cell. Biochem.* 53, 323–328. doi: 10.1002/jcb.240530409

Reiner, S. L., and Locksley, R. M. (1995). The regulation of immunity to *Leishmania major*. *Annu. Rev. Immunol.* 13, 151–177. doi: 10.1146/annurev.iy.13.040195.001055

Ritter, U., and Körner, H. (2002). Divergent expression of inflammatory dermal chemokines in cutaneous leishmaniasis. *Parasite Immunol.* 24, 295–301. doi: 10.1046/j.1365-3024.2002.00467.x

Rochette, A., Raymond, F., Ubeda, J. M., Smith, M., Messier, N., Boisvert, S., et al. (2008). Genome-wide gene expression profiling analysis of *Leishmania major* and *Leishmania infantum* developmental stages reveals substantial differences between the two species. *BMC Genomics* 9:255. doi: 10.1186/1471-2164-9-255

Romano, A., Carneiro, M. B. H., Doria, N. A., Roma, E. H., Ribeiro-Gomes, F. L., Inbar, E., et al. (2017). Divergent roles for Ly6C+CCR2+CX3CR1+ inflammatory monocytes during primary or secondary infection of the skin with the intra-phagosomal pathogen *Leishmania major*. *PLoS Pathog.* 13:e1006479. doi: 10.1371/journal.ppat.1006479

Sachdeva, R., Banerjea, A. C., Malla, N., and Dubey, M. L. (2009). Immunogenicity and efficacy of single antigen Gp63, polytope and polytopeHSP70 DNA vaccines against visceral Leishmaniasis in experimental mouse model. *PLoS ONE* 4:e7880. doi: 10.1371/journal.pone.0007880

Saliba, A. E., Li, L., Westermann, A. J., Appenzeller, S., Stapels, D. A., Schulte, L. N., et al. (2016). Single-cell RNA-seq ties macrophage polarization to growth rate of intracellular *Salmonella*. *Nat. Microbiol.* 2:16206. doi: 10.1038/nmicrobiol.2016.206

Saraiva, E. M., Pinto-da-Silva, L. H., Wanderley, J. L., Bonomo, A. C., Barcinski, M. A., and Moreira, M. E. (2005). Flow cytometric assessment of *Leishmania* spp metacyclic differentiation: validation by morphological features and specific markers. *Exp. Parasitol.* 110, 39–47. doi: 10.1016/j.exppara.2005.01.004

Schindelin, J., Arganda-Carreras, I., Frise, E., Kaynig, V., Longair, M., Pietzsch, T., et al. (2012). Fiji: an open-source platform for biological-image analysis. *Nat. Methods* 9, 676–682. doi: 10.1038/nmeth.2019

Schlagenhauf, E., Etges, R., and Metcalf, P. (1998). The crystal structure of the *Leishmania major* surface proteinase leishmanolysin (gp63). *Structure* 6, 1035–1046. doi: 10.1016/S0969-2126(98)00104-X

Schneider, C. A., Rasband, W. S., and Eliceiri, K. W. (2012). NIH image to ImageJ: 25 years of image analysis. *Nat. Methods* 9, 671–675. doi: 10.1038/nmeth.2089

Scott, P., Natovitz, P., Coffman, R. L., Pearce, E., and Sher, A. (1988). CD4+ T cell subsets in experimental cutaneous leishmaniasis. *Mem. Inst. Oswaldo Cruz.* 83(Suppl. 1), 256–259. doi: 10.1590/S0074-02761988000500006

Scott, P., and Novais, F. O. (2016). Cutaneous leishmaniasis: immune responses in protection and pathogenesis. *Nat. Rev. Immunol.* 16, 581–592. doi: 10.1038/nri.2016.72

Seyed, N., Peters, N. C., and Rafati, S. (2018). Translating observations from leishmanization into non-living vaccines: the potential of dendritic cell-based vaccination strategies against Leishmania. *Front. Immunol.* 9:1227. doi: 10.3389/fimmu.2018.01227

Shiraki, Y., Ishibashi, Y., Hiruma, M., Nishikawa, A., and Ikeda, S. (2008). Candida albicans abrogates the expression of interferon-gamma-inducible protein-10 in human keratinocytes. *FEMS Immunol. Med. Microbiol.* 54, 122–128. doi: 10.1111/j.1574-695X.2008.00457.x

Singh, S. (2014). Changing trends in the epidemiology, clinical presentation, and diagnosis of Leishmania-HIV co-infection in India. *Int. J. Infect. Dis.* 29, 103–112. doi: 10.1016/j.ijid.2014.07.011

Thomas, S. Y., Hou, R., Boyson, J. E., Means, T. K., Hess, C., Olson, D. P., et al. (2003). CD1d-restricted NKT cells express a chemokine receptor profile indicative of Th1-type inflammatory homing cells. *J. Immunol.* 171, 2571–2580. doi: 10.4049/jimmunol.171.5.2571

Uzonna, J. E., Joyce, K. L., and Scott, P. (2004). Low dose *Leishmania major* promotes a transient T helper cell type 2 response that is down-regulated by interferon gamma-producing CD8+ T cells. *J. Exp. Med.* 199, 1559–1566. doi: 10.1084/jem.20040172

Valdivia, H. O., Scholte, L. L., Oliveira, G., Gabaldón, T., and Bartholomeu, D. C. (2015). The Leishmania metaphylome: a comprehensive survey of Leishmania protein phylogenetic relationships. *BMC Genomics* 16:887. doi: 10.1186/s12864-015-2091-2

Vargas-Inchaustegui, D. A., Hogg, A. E., Tulliano, G., Llanos-Cuentas, A., Arevalo, J., Endsley, J. J., et al. (2010). CXCL10 production by human monocytes in response to Leishmania braziliensis infection. *Infect. Immun.* 78, 301–308. doi: 10.1128/IAI.00959-09

Vasquez, R. E., and Soong, L. (2006). CXCL10/gamma interferon-inducible protein 10-mediated protection against *Leishmania amazonensis* infection in mice. *Infect. Immun.* 74, 6769–6777. doi: 10.1128/IAI.01073-06

Vasquez, R. E., Xin, L., and Soong, L. (2008). Effects of CXCL10 on dendritic cell and CD4+ T-cell functions during *Leishmania amazonensis* infection. *Infect. Immun.* 76, 161–169. doi: 10.1128/IAI.00825-07

Vester, B., Müller, K., Solbach, W., and Laskay, T. (1999). Early gene expression of NK cell-activating chemokines in mice resistant to *Leishmania major*. *Infect. Immun.* 67, 3155–3159.

Victoir, K., Arevalo, J., De Doncker, S., Barker, D. C., Laurent, T., Godfroid, E., et al. (2005). Complexity of the major surface protease (msp) gene organization in Leishmania (Viannia) braziliensis: evolutionary and functional implications. *Parasitology* 131, 207–214. doi: 10.1017/S0031182005007535

von Schillde, M. A., Hörmannsperger, G., Weiher, M., Alpert, C. A., Hahne, H., Bäuerl, C., et al. (2012). Lactocepin secreted by Lactobacillus exerts anti-inflammatory effects by selectively degrading proinflammatory chemokines. *Cell Host Microbe* 11, 387–396. doi: 10.1016/j.chom.2012.02.006

Voth, B. R., Kelly, B. L., Joshi, P. B., Ivens, A. C., and McMaster, W. R. (1998). Differentially expressed *Leishmania major* gp63

genes encode cell surface leishmanolysin with distinct signals for glycosylphosphatidylinositol attachment. *Mol. Biochem. Parasitol.* 93, 31–41. doi: 10.1016/S0166-6851(98)00013-9

Wang, L., Pittman, K. J., Barker, J. R., Salinas, R. E., Stanaway, I. B., Williams, G. D., et al. (2018). An atlas of genetic variation linking pathogen-induced cellular traits to human disease. *Cell Host Microbe* 24, 308–323.e6. doi: 10.1016/j.chom.2018.07.007

Zaph, C., and Scott, P. (2003). Interleukin-12 regulates chemokine gene expression during the early immune response to *Leishmania major*. *Infect. Immun.* 71, 1587–1589. doi: 10.1128/IAI.71.3.1587-1589.2003

Conflict of Interest Statement: The authors declare that the research was conducted in the absence of any commercial or financial relationships that could be construed as a potential conflict of interest.

frontiers in Cellular and Infection Microbiology

BRIEF RESEARCH REPORT
published: 30 August 2019
doi: 10.3389/fcimb.2019.00311

Macrophages From Subjects With Isolated GH/IGF-I Deficiency Due to a GHRH Receptor Gene Mutation Are Less Prone to Infection by *Leishmania amazonensis*

Mônica R. Barrios[1], Viviane C. Campos[2], Nalu T. A. Peres[1,3], Laís L. de Oliveira[1], Rodrigo A. Cazzaniga[1], Márcio B. Santos[1], Murilo B. Aires[1], Ricardo L. L. Silva[1], Aline Barreto[1], Hiro Goto[4,5], Roque P. Almeida[1], Roberto Salvatori[5], Manuel H. Aguiar-Oliveira[2†] and Amélia M. R. Jesus[1†]*

[1] Division of Immunology and Molecular Biology Laboratory, Federal University of Sergipe, Aracaju, Brazil, [2] Division of Endocrinology, Federal University of Sergipe, Aracaju, Brazil, [3] Department of Microbiology, Institute of Biological Sciences, Federal University of Minas Gerais, Belo Horizonte, Brazil, [4] Laboratório de Soroepidemiologia e Imunobiologia, Instituto de Medicina Tropical de São Paulo, Universidade de São Paulo, São Paulo, Brazil, [5] Division of Endocrinology, Diabetes and Metabolism, The Johns Hopkins University School of Medicine, Baltimore, MD, United States

Isolated growth hormone (GH) deficiency (IGHD) affects approximately 1 in 4,000 to 1 in 10,000 individuals worldwide. We have previously described a large cohort of subjects with IGHD due to a homozygous mutation in the GH releasing hormone (GHRH) receptor gene. These subjects exhibit throughout the life very low levels of GH and its principal mediator, the Insulin Growth Factor-I (IGF-I). The facilitating role of IGF-I in the infection of mouse macrophages by different *Leishmania* strains is well-known. Nevertheless, the role of IGF-I in *Leishmania* infection of human macrophages has not been studied. This study aimed to evaluate the behavior of *Leishmania* infection *in vitro* in macrophages from untreated IGHD subjects. To this end, blood samples were collected from 14 IGHD individuals and 14 age and sex-matched healthy controls. Monocytes were isolated and derived into macrophages and infected with a strain of *Leishmania amazonensis*. In addition, IGF-I was added to culture medium to evaluate its effect on the infection. Cytokines were measured in the culture supernatants. We found that macrophages from IGHD subjects were less prone to *Leishmania* infection compared to GH sufficient controls. Both inflammatory and anti-inflammatory cytokines increase only in the supernatants of the control macrophages. Addition of IGF-I to the culture medium increased infection rates. In conclusion, we demonstrated that IGF-I is crucial for *Leishmania* infection of human macrophages.

Keywords: growth hormone deficiency, insulin growth factor-I deficiency, macrophages, leishmaniasis, phagocytosis, infection, immunology

OPEN ACCESS

Edited by:
Anabela Cordeiro-da-Silva, University of Porto, Portugal

Reviewed by:
Fátima Ribeiro-Dias, Universidade Federal de Goiás, Brazil
Diego Luis Costa, National Institute of Allergy and Infectious Diseases (NIAID), United States

****Correspondence:***
Amélia M. R. Jesus
ameliaribeirodejesus@gmail.com

† These authors have contributed equally to this work and share senior authorship

Specialty section:
This article was submitted to Parasite and Host, a section of the journal Frontiers in Cellular and Infection Microbiology

Received: *20 April 2019*
Accepted: *16 August 2019*
Published: *30 August 2019*

Citation:
Barrios MR, Campos VC, Peres NTA, de Oliveira LL, Cazzaniga RA, Santos MB, Aires MB, Silva RLL, Barreto A, Goto H, Almeida RP, Salvatori R, Aguiar-Oliveira MH and Jesus AMR (2019) Macrophages From Subjects With Isolated GH/IGF-I Deficiency Due to a GHRH Receptor Gene Mutation Are Less Prone to Infection by Leishmania amazonensis. Front. Cell. Infect. Microbiol. 9:311. doi: 10.3389/fcimb.2019.00311

INTRODUCTION

Growth Hormone (GH) and its peripheral effector Insulin Growth Factor-I (IGF-I) have mitogenic and anabolic actions in various cells, including immune cells. This observation created an interest in understanding the role of GH in the endocrine-immune axis (Wells, 1999). The effect of IGF-I in pathogen-macrophage interaction has been described in *Leishmania* and *M. leprae* infections (Reis et al., 2013; Batista-Silva et al., 2016).

Leishmania is an obligate intracellular parasite that infects macrophages. In humans, it causes a broad clinical spectrum of diseases, such as cutaneous, mucosal, and visceral leishmaniasis. This diversity of manifestations depends on the parasite species, environmental, biological, or genetic factors of the host, particularly the immune response (Oryan and Akbari, 2016). The model of infection using *Leishmania* is easy to culture and manipulate, and has been widely used in studies that seek to understand the immune response to intracellular infections (de Oliveira et al., 2015; Silva et al., 2017).

Goto et al. (1998) showed that IGF-I enhanced, *in vitro,* the growth of promastigotes and amastigotes in mouse macrophages (Goto et al., 1998) and that IGF-I-pre-treated *Leishmania* have enhanced infectivity (Gomes et al., 2000). Furthermore, IGF-I increases the expression and activity of arginase I (that promotes the parasite survival), and blocks the induction of NOS2, an enzyme involved in nitric oxide production, essential to kill *Leishmania* (Vendrame et al., 2007, 2015). In addition, recent studies have shown that during infection, *M. leprae* induces the production of IGF-I in both macrophages and Schwan cells, an important mechanism for the survival of this pathogen (Rodrigues et al., 2010; Batista-Silva et al., 2016). These data suggest that IGF-I plays an important role in the survival and proliferation of these intracellular pathogens. The use of hormonal pathways by intracellular pathogens to evade the immune system may be one important mechanism of these pathogens to explain their adaptation to survive in human cells.

In Itabaianinha County, in Northeast Brazil, we identified a large cohort of individuals with severe isolated GH deficiency (IGHD) caused by the *null* homozygous (c.57 + 1 A→ G) mutation in the growth hormone releasing hormone (GHRH) receptor gene (*GHRHR*) (Salvatori et al., 1999). This is the largest cohort of patients with IGHD described to date. This mutation leads to a complete abolition of the GHRHR function and consequently affects GH secretion (Souza et al., 2005), leading to very low levels of GH and IGF-I (Aguiar-oliveira et al., 1999; Salvatori et al., 2006). These IGHD individuals have proportional short stature, doll face, high-pitched voices, and central obesity (Aguiar-Oliveira and Bartke, 2018). They have relatively reduced spleen volume (Oliveira et al., 2008), reduced total serum IgG levels, and present smaller papule diameter after streptokinase injection. Despite these abnormalities, they seem to have normal immune function and do not exhibit increased frequency of infections (Campos et al., 2016). Not surprisingly, they exhibit normal longevity, and some reached centenarian age (Aguiar-Oliveira et al., 2010; Aguiar-Oliveira and Bartke, 2018).

Most of the adult IGHD individuals have never been treated with GH replacement therapy, and therefore provide a unique model to evaluate the role of IGF-I on immune cells in a variety of conditions. The purpose of this study was to evaluate the behavior of *Leishmania* infection *in vitro* in macrophages of these IGHD subjects.

MATERIALS AND METHODS

Subjects

Fourteen IGHD individuals with genotype proven homozygosis for the C.57 + 1G > A *GHRHR* mutation, and 14 age and sex-matched normal statured local controls proven to be homozygous for the wild-type *GHRHR* allele were included in this study. The Research Ethical Committee at Federal University of Sergipe approved this study (CAAE 0152.0.107.000-07). After signing informed consent form, the participants were submitted to clinical examination, measurement of height, weight and venipuncture to collect peripheral blood. Two of the IGHD subjects had received GH therapy for 6 years, completed more than 15 years prior to this study.

Hormones Measurements

IGF-I was measured by a solid-phase, enzyme labeled chemiluminescent immunometric assay IMMULITE 2000 (Siemens Healthcare Diagnostics Products Ltd, Malvern, PA, USA), with a sensitivity of 25 ng/ml. Prolactin was measured by fluoroimmunoassay (Perkin Elmer Life and Analytical Science, Wallac Oy Turku, Finland) with sensitivity of 1.44 ng/ml.

IGF-I and IGF-I Receptor (IGF-IR) mRNA Expression in PBMC

Peripheral blood mononuclear cells (PBMC) were isolated by Ficoll gradient from whole blood. Total RNA was extracted by Trizol reagents (ThermoFisher), and 1 μg RNA was converted into cDNA using the High Capacity cDNA Synthesis Kit (ThermoFischer), following the manufacturers' protocol. qPCR was performed using Taqman probes (hs01547656_m1– IGF-I and hs00609566_m1 – IGF-IR), in the 7500 Fast Real Time PCR System (Applied Biosystems). Normalization was performed using the GAPDH gene (hs99999905_m1), and relative gene expression was represented by the $2^{-\Delta Ct}$ method (Livak and Schmittgen, 2001).

Macrophage Infection

Macrophage cultures and infection with *Leishmania* were processed according to previous publications (de Oliveira et al., 2015; Silva et al., 2017). Briefly, PBMC were fractioned by Ficoll-Hypaque (Histopaque® 1077, Sigma). The monocytes were isolated by adherence to plastic plates and maintained in culture medium RPMI supplemented (albumin and antibiotics) for 6 days in a humid incubator (37°C and 5%CO^2) to differentiate into macrophages in LabTek (de Oliveira et al., 2015). *Leishmania amazonensis* (LTCP 9667) were cultured in medium supplemented with Schneider (ThermoFisher) in a dry incubator (26°C) and were used to infect macrophages (5:1) for 2 h in a humid incubator (37°C and 5% CO2). Macrophages from healthy controls ($n = 6$) and IGHD individuals ($n = 4$) were also infected with *Leishmania* without or with IGF-I

addition (75 ng/ml) 2 h before infection, or infected with IGF-I pre-treated *Leishmania* (50 ng/ml) for 5 min and washed off with saline supplemented with 1% albumin (ThermoFisher) ($n = 4$), as previously described by Gomes et al. (2000). We measured the number of amastigotes in 100 macrophages at 2 h of *Leishmania* infection. The supernatants were collected and stored at −80°C and macrophages slides were stained after 2, 24, 48, and 72 h post infection. The macrophages slides infected with IGF-I-treated macrophages and *Leishmania* pre-treated with IGF-I were stained 2, 24, and 48 h post infection. Slides were fixed and then stained with Instant Prov (NEW/PROV, Paraná, Brazil). Three blinded scientists counted the number of infected macrophages per 100 macrophages, and the number of amastigotes per 100 infected macrophages.

Cytokine Measures

The cytokines IL-12p70, TNF-α, IFN-γ, IL-1β, IL-6, IL-10, GM-CSF, IL-4, IL-33, and IL-27 were measured in the macrophage supernatants previously stored at −80°C. Cytokines quantification was done by multiplex assay (Procarta, Thermo, Waltham, MA USA).

Statistical Analysis

Data analyses were processed in GraphPad Prism Software (v.4.0). Values for parametric variables were expressed as mean (standard deviation). Variables with non-parametric distribution (IGF-I levels) were expressed as median (interquartile range). Gender was compared with the Fisher's exact test. D'Agostino and Pearson and Shapiro–Wilk normality tests were used to verify if the groups follow a normal distribution. Student *t*-test was used for comparisons between two variables with normal distribution and Mann–Whitney *U*-test for those with non-Gaussian distribution, adopting 95% as confidence interval and significance values when $p < 0.05$.

RESULTS

Demographic Characteristics and Levels of IGF-I and Prolactin, and IGF-I and IGF-I Receptor mRNA Expression of the Study Subjects

Clinical and demographic data, IGF-I and prolactin levels are shown in **Table 1**. There were no differences in age and sex distribution between IGHD and controls. As expected, height, weight, and IGF-I levels were lower ($p < 0.0001$) in the IGHD group than controls. Most IGF-I levels in IGHD group were lower than the sensitivity of assay, emphasizing the severity of IGF-I deficiency. There was no difference in prolactin levels between the groups (**Table 1**). No differences in the mRNA expression of IGF-I was observed between IGHD subjects and controls, but higher levels of IGF-1R mRNA was found in PBMC from IGHD subjects as compared to controls (**Figure 1**).

TABLE 1 | Demographic and serum levels of IGF-I and prolactin in subjects with isolated GH deficiency due to a GHRH receptor gene mutation and controls.

Variables		IGHD ($n = 14$)	Control ($n = 14$)	*P*
Age (years)	Mean (SD)	40.4 (10.7)	41.3 (14.3)	0.84
	Range	27–58	21–61	
Male		09 (60%)	08 (50%)	0.58
Height (cm)	Mean (SD)	131.8 (8.1)	168.9 (7.7)	< 0.0001
	Range	119–143	157–187	
Weight (kg)	Mean (SD)	38.5 (7.1)	73.5 (13.1)	< 0.0001
	Range	27.4–51.7	52.5–105	
Serum IGF-I (ng/ml)	Median (Interquartile)	25 (0)	170 (55)	< 0.0001
	Range	25–52.8	104–340	
Serum prolactin (ng/ml)	Mean (SD)	15.2 (7.9)	11.8 (5.9)	0.38
	Range	2.07–23.4	3.7–26.3	

Age, height, weight, and prolactin were compared by the unpaired T-Test; gender by the Fisher's Exact Test; and IGF-I by the Mann–Whitney Test.

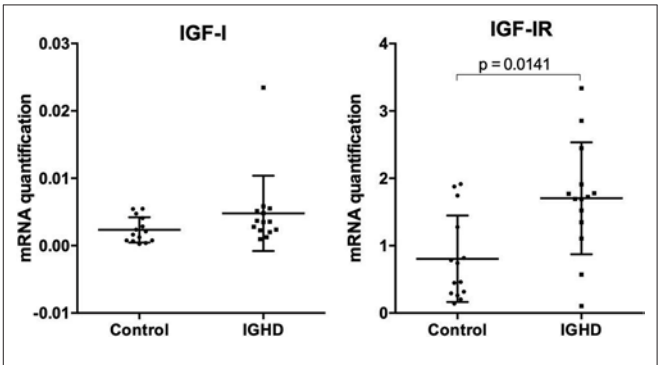

FIGURE 1 | mRNA expression of IGF-I and IGF-I receptor in PBMC of IGHD and control subjects. Total RNA was extracted from PBMC of 14 IGHD individuals and 14 controls, and qPCR was performed using Taqman probes. Normalization was performed using the GAPDH gene, and relative gene expression is represented by the $2^{-\Delta Ct}$ method.

Macrophages Infection

The infection curve of *L. amazonensis* in macrophages from IGHD subjects and controls demonstrate both a lower number of infected macrophages and parasitic load (number of amastigotes per 100 infected macrophages) in IGHD group, in the early hours of exposure to the parasite ($p < 0.05$) (**Figure 2A**). **Figure 2B** is a Photomicrography of 2 h-infected macrophages from controls subjects and IGHD subjects showing an example of the differences between the infection in these two hosts. While macrophage from the control subjects have many parasites inside the cytosol, the macrophages from IGHD subjects have parasites around the membrane and very few parasites inside the cytosol.

Cytokine Levels

The levels of cytokines in the supernatants of these cultures revealed a significant increase in TNF-α (**Figure 3A**), IFN-γ (**Figure 3B**), IL-10 (**Figure 3C**), and GM-CSF (**Figure 3D**) only in the control group after 24 h of *L. amazonensis* infection, with a gradual increase until 72 h post-infection, as compared to the IGHD subjects ($p < 0.05$). An inverse correlation was

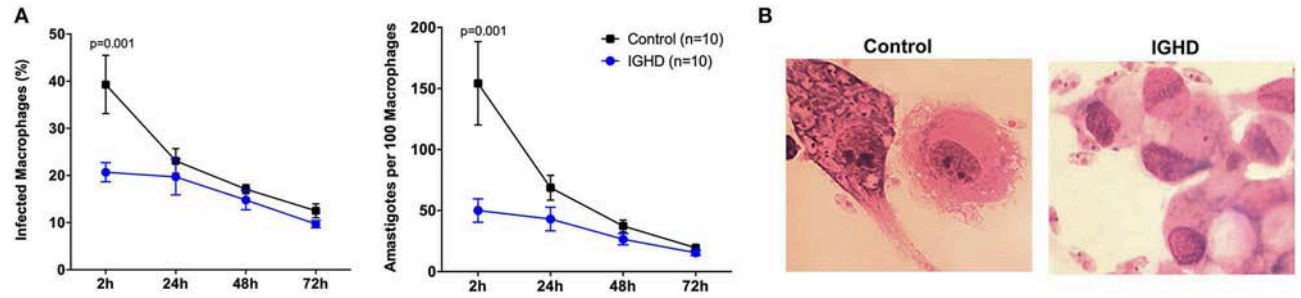

FIGURE 2 | *Leishmania amazonensis* infection curves in human macrophages from IGHD subjects and controls. **(A)** Number of macrophages infected with *L. amazonensis* in 100 macrophages and number of amastigotes in 100 macrophages from IGHD patients and healthy controls. **(B)** Photomicrography of 2 h-infected macrophages from controls subjects and IGHD subjects.

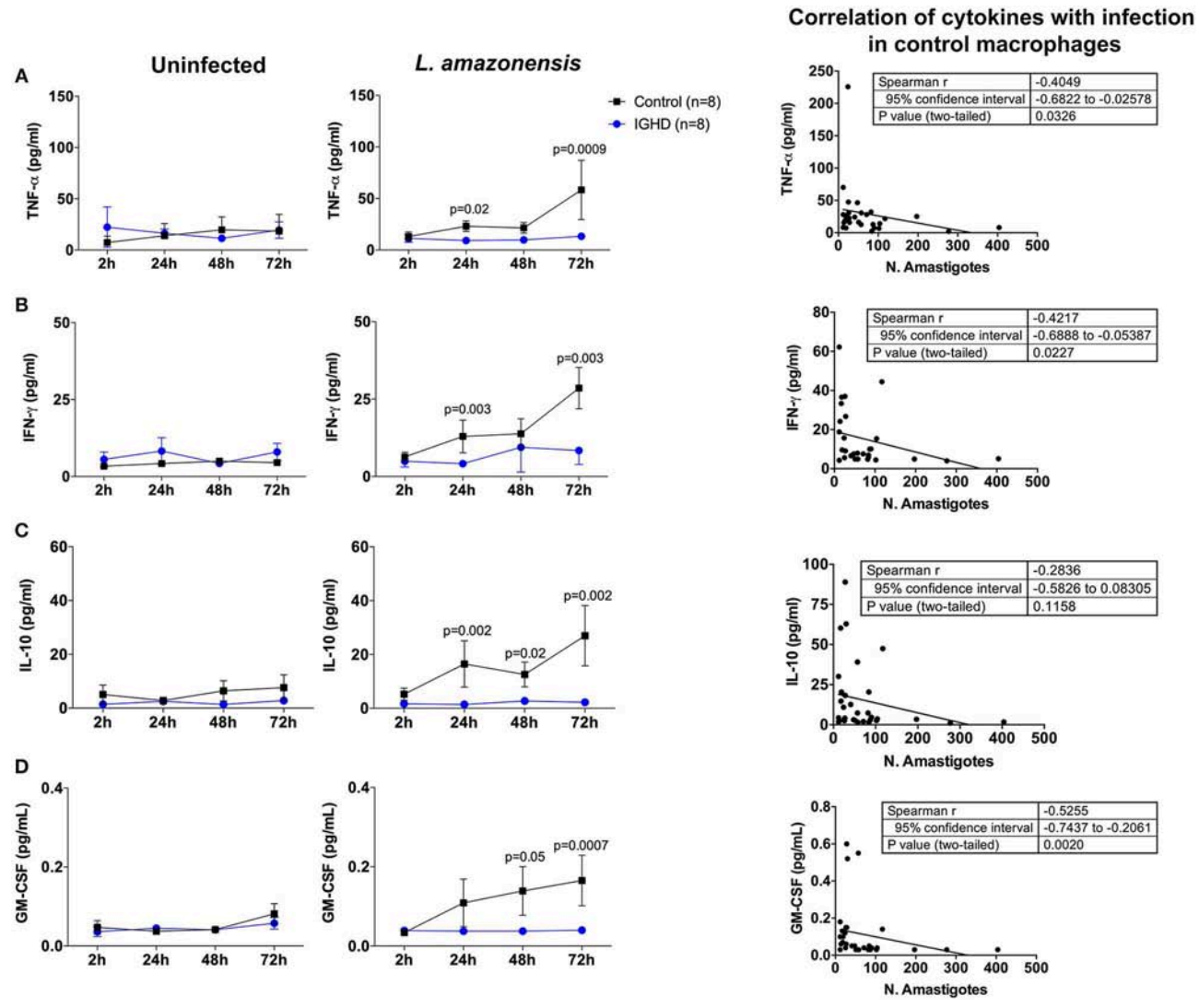

FIGURE 3 | Cytokines produced by human macrophages from IGHD subjects and controls during *in vitro Leishmania amazonensis* infection. The levels of the cytokine were measured by luminex in the culture supernatants, and correlation with infection determined in control macrophages. **(A)** TNF-α, **(B)** IFN-γ, **(C)** IL-10, and **(D)** GM-CSF.

observed between the levels of TNF-α (rS = 0.40, $p = 0.03$), IFN-γ (rS = 0.42, $p = 0.02$), and GM-CSF (rS = 0.52, $p = 0.002$) with the parasite numbers. No correlation was observed between the levels of IL-10 with the number of parasites. No differences were observed in the levels of IL-12p70, IL-1β, IL-6, IL-4, IL-33, IL-27 either during the time-points of infection or between the two groups. Addition of IGF-I to the macrophage cultures, or pre-treatment of the leishmania with IGF-1 increased *L. amazonensis* infection in control macrophages at 2 h of the infection (**Figure 4**), but not at 24 and 48 h (data not shown). However, this treatment did not affect the infection in macrophages from the IGHD subjects (**Figure 4**).

DISCUSSION

Our study shows that macrophages of IGHD individuals with very low serum IGF-I levels present lower levels of infection by *L. amazonensis*, as compared to control macrophages. We hypothesize that IGHD subjects have reduced phagocytic uptake of *Leishmania*, or possibly reduced phagocytic entry of this parasite into the macrophages. This, together with the demonstration that pre-treatment of *Leishmania* with IGF-I increases macrophage infection of control macrophages, is the first report of a prominent role of IGF-I in *Leishmania* infection in humans. These data agree with previous studies in mouse. In this animal, Goto et al. have shown that IGF-I may be used by *Leishmania* as a growth factor (Gomes et al., 1997, 1998; Goto et al., 1998). In addition, IGF-I increases, *in vitro,* the infectivity of this parasite in mouse macrophages (Vendrame et al., 2007, 2015), and *in vivo*, in experimental models of cutaneous leishmaniasis, with strains of *Leishmania mexicana* and *L. amazonensis* (Gomes et al., 2000).

Due to the high homology between GH and prolactin receptors, and the possibility of a cross talk between the two ligands and receptors (Fu et al., 1992), we decided to include prolactin measurements in this protocol. The lack of difference in serum prolactin in the two groups exclude any role of this hormone in reduction of L. *amazonensis* uptake by the macrophages of IGHD subjects.

IGF-IR is expressed in 97% of monocytes, 88% of B lymphocytes and 2% of T lymphocytes (Schwartz et al., 1993; Oberlin et al., 2009). Activation of this receptor leads to stimulation of cell proliferation and differentiation, angiogenesis, and apoptosis inhibition (Juul, 2003). IGF-I also promotes increased expansion of granulocyte and macrophage colonies (Schwartz et al., 1993). Moreover, autocrine production of IGF-I in cells such as macrophages acting on innate immunity indicates a role of IGF-I in modulating the immune response and phagocytosis (Oberlin et al., 2009).

The previously published proposed mechanism to explain the increase of parasite load by IGF-I includes the observation that this hormone increases arginase activity and the production of urea and L-ornithine, nutrients for parasite growth, and inhibits the NOS2 pathway and the production of nitric oxide (NO) (De Souza et al., 2016). It is possible that IGF-I is used as an adaptation mechanism, developed by *Leishmania* to counteract the immune system and to establish the infection. Another finding that reinforces the hypothesis of a role of IGF-I in favoring infection is the presence of a receptor antigenically similar to the human IGF-I receptor (IGF-IR) alpha chain in the promastigote forms of *Leishmania* (Gomes et al., 2001).

Here we demonstrate reduced uptake of *Leishmania* from IGHD macrophages. Interestingly, the addition of IGF-I to the macrophages culture media during infection, or the pre-treatment of *L. amazonensis* with IGF-I, increased the parasite load at the initial stages of infection only in the control group, suggesting that IGF-I favors *Leishmania* infection. We cannot explain why the addition of IGF-I in the macrophages from the IGHD subjects did not have a similar effect, although we observed a higher level of IGF-IR mRNA in PBMC from IGHD subjects, compared to controls. More experiments will be needed to establish if this difference in the expression of this receptor is also confirmed on the macrophage surface. Given that the macrophages from IGHD subjects are able to express IGF-IR, a possible explanation is that the chronic absence of the IGF-I

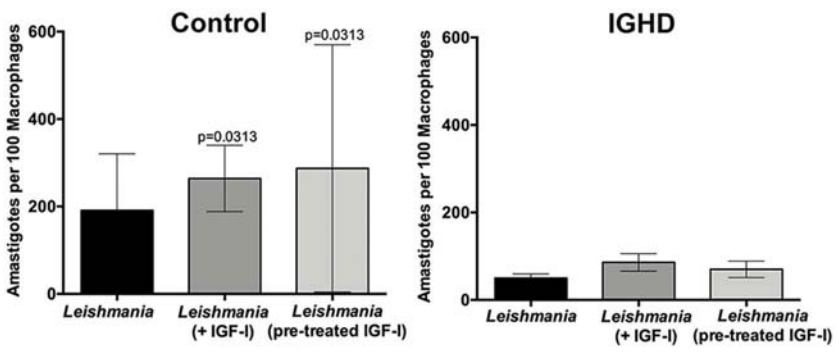

FIGURE 4 | *Leishmania amazonensis* infection in human macrophages from IGHD subjects and controls, in the absence or presence of IGF-I. Infection of macrophages from healthy controls ($n = 6$) and IGHD subjects ($n = 4$) without or with IGF-I addition (75 ng/ml) 2 h before infection, or infected with pre-treated leishmania (50 ng/ml) for 5 min and washed off with saline supplemented with 1% albumin ($n = 4$). The graphs show the number of amastigotes in 100 macrophages at 2 h of *Leishmania* infection.

stimuli in these subjects throughout their lives might decrease its activation pathway.

The conditions that can affect the macrophages polarization and their implication on infectious diseases remain unclear. It is believed that this gap can be the key to understand several infectious diseases (Sridharan et al., 2015). The production of IGF-I and IGF-IR by the macrophages suggest an auto/paracrine function on these cells. Furthermore, it has been shown that IGF-I favors a M2 differentiation (Barrett et al., 2015). Recent studies have shown that *M. leprae* infection *in vitro* induces IGF-I production by macrophages and Schwan cells, favoring the establishment of the infection in these cells (Rodrigues et al., 2010; Batista-Silva et al., 2016).

The cytokine profile showed that both inflammatory and anti-inflammatory cytokines increases only in the control macrophages supernatants, concomitantly with the decrease of parasite load. Macrophages from individuals with IGHD were not infected by *Leishmania*, nor did they produce any of these cytokines in their supernatants. These data do not corroborate the hypothesis that the IGHD subjects, who are not exposed to the effects of IGF-I, present macrophages with increased inflammatory and microbicidal ability. Additional studies should be performed to clarify the mechanism of the reduced uptake of *Leishmania* by the macrophages from IGHD subjects.

Our hypothesis is that individuals with IGHD have a reduced phagocytic or non-phagocytic uptake of *Leishmania*. The clinical relevance of these findings still needs to be clarified. One limitation of this study is its descriptive nature, as we could not identify a clear mechanism that explains our findings in IGHD subjects. While we did not find differences in the measured cytokines between IGHD and controls, many other additional cytokines and other mediators, independent of IGF-I, could be analyzed which could, in future studies, shed a light on the molecular mechanism of the identified resistance. As the State of Sergipe is endemic for visceral leishmaniasis, but not for cutaneous forms, a protective role against *Leishmania* infection may have reduced the frequency of the visceral endemic form in the IGHD group. In agreement, during the 25-year follow-up of this cohort, no case of cutaneous or visceral leishmaniasis was recorded (Campos et al., 2016). In addition, the lower uptake of this and possibly other intracellular infectious agents may have contributed to the survival of individuals with IGHD over many generations, and to the spread of this particular mutation in this tropical area. Interestingly, Tripanosomiasis was recorded in normal homozygous controls, but not in IGHD subjects even if they have lived at the same address for decades (Campos et al., 2016).

In summary, this study demonstrates that a unique population of subjects that are genetically deficient in GH/IGF-I that present a reduced uptake of *L. amazonensis* infection, confirming a role of IGF-I in the first events of this infection in human macrophages. These findings indicate genetic advantage of this IGHD cohort against at least this particular pathogen, and confirm immune benefits of this endocrine deficiency.

DATA AVAILABILITY

All datasets generated for this study are included in the manuscript and/or the supplementary files.

ETHICS STATEMENT

The manuscript includes human studies. The local Ethical Committee of the Federal University of Sergipe approval was received for the studies (CAAE 0152.0.107.000-07), and the informed consent of all participating subjects or their legal guardians was obtained.

AUTHOR CONTRIBUTIONS

MB, VC, and LO performed the majority of the experiments. VC, MA-O, and RSa are endocrinologists and assisted the IGHD individuals, helped to recruit them for this study, and discussed the experimental design with the immunology group. MA, RSi, and AB helped with the macrophage infection experiments. MS helped in the Luminex experiments and statistical analysis. NP, RC, HG, RA, and AJ helped in the experimental design. MB and VC draft the manuscript. NP, MA-O, RSa, and AJ revised the manuscript. AJ was also responsible for the grants to perform this study and is the advisor of MB and LO, during Ph.D. and Masters, respectively. MA-O is the advisor of VC, during Ph.D.

FUNDING

This work was funded by Fundação de Apoio à Pesquisa e à Inovação Tecnológica do Estado de Sergipe (FAPITEC)/SE/FUNTEC/Conselho Nacional de Desenvolvimento Científico e Tecnológico (CNPq, Brazil), Grants: CNPq n°12/2009, Process n° 019.203.02712/2009 (AJ). Chamada MCTIC/CNPq N° 28/2018—Universal, Process 421060/2018-2 (AJ). MB's fellowship was suported by Fundação Coordenação de Aperfeiçoamento de Pessoal de Nível Superior (CAPES), Edital 032/2010 (AJ). LO's fellowship was also suported by CAPES. AJ and RA are CNPq investigators.

ACKNOWLEDGMENTS

We would like to thank the residents and endocrinologists of Endocrinology Clinic, HU/UFS. The funders had no role in study design, data collection and analysis, decision to publish or manuscript preparation.

REFERENCES

Aguiar-Oliveira, M. H., and Bartke, A. (2018). Growth hormone deficiency: health and longevity. *Endocr. Rev.* 40, 575–601. doi: 10.1210/er.2018-00216

Aguiar-Oliveira, M. H., Gill, M. S., Miraki-moud, F., Menezes, C. A., Souza, A. H. O., Martinelli, C. E., et al. (1999). Effect of severe growth hormone (GH) deficiency due to a mutation in the GH-releasing hormone receptor on insulin-like growth factors (IGFs), IGF-binding proteins, and

ternary complex formation throughout life. *J. Clin. Endocrinol. Metab.* 84, 4118–4126.

Aguiar-Oliveira, M. H., Oliveira, F. T., Pereira, R. M., Oliveira, C. R. P., Blackford, A., Valenca, E. H., et al. (2010). Longevity in untreated congenital growth hormone deficiency due to a homozygous mutation in the GHRH receptor gene. *J. Clin. Endocrinol. Metab.* 95, 714–721. doi: 10.1210/jc.2009-1879

Barrett, J. P., Minogue, A. M., Falvey, A., and Lynch, M. A. (2015). Involvement of IGF-1 and Akt in M1/M2 activation state in bone marrow-derived macrophages. *Exp. Cell Res.* 335, 258–268. doi: 10.1016/j.yexcr.2015.05.015

Batista-Silva, L. R., Rodrigues, L. S., Vivarini Ade, C., Costa Fda, M., Mattos, K. A., Costa, M. R., et al. (2016). Mycobacterium leprae-induced Insulin-like Growth Factor i attenuates antimicrobial mechanisms, promoting bacterial survival in macrophages. *Sci. Rep.* 6:27632. doi: 10.1038/srep27632

Campos, V. C., Barrios, M. R., Salvatori, R., de Almeida, R. P., de Melo, E. V., Nascimento, A. C., et al. (2016). Infectious diseases and immunological responses in adult subjects with lifetime untreated, congenital GH deficiency. *Endocrine* 54, 182–190. doi: 10.1007/s12020-016-1061-z

de Oliveira, F. A., Barreto, A. S., Bomfim, L. G., Leite, T. R., Dos Santos, P. L., de Almeida, R. P., et al. (2015). Soluble CD40 ligand in sera of subjects exposed to leishmania infantum infection reduces the parasite load in macrophages. *PLoS ONE* 10:e0141265. doi: 10.1371/journal.pone.0141265

De Souza, L. D., Vendrame, C. M., De Jesus, A. R., Carvalho, M. D., Magalhães, A. S., Schriefer, A., et al. (2016). Insulin-like growth factor-I serum levels and their biological effects on Leishmania isolates from different clinical forms of American tegumentary leishmaniasis. *Parasit. Vectors* 9:335. doi: 10.1186/s13071-016-1619-x

Fu, Y. K., Arkins, S., Fun, G., Cunningham, B. C., Wells, J. A., Fong, S., et al. (1992). Growth hormone augments superoxide anion secretion of human neutrophils by binding to the prolactin receptor. *J. Clin. Invest.* 89, 451–457. doi: 10.1172/JCI115605

Gomes, C. M., Goto, H., Corbett, C. E., and Gidlund, M. (1997). Insulin-like growth factor-1 is a growth promoting factor for Leishmania promastigotes. *Acta Trop.* 64, 225–228. doi: 10.1016/S0001-706X(96)00633-X

Gomes, C. M., Goto, H., Magnanelli, A. C., Monteiro, H. P., Soares, R. P., Corbett, C. E., et al. (2001). Characterization of the receptor for insulin-like growth factor on Leishmania promastigotes. *Exp. Parasitol.* 99, 190–197.

Gomes, C. M., Goto, H., Ribeiro Da Matta, V. L., Laurenti, M. D., Gidlund, M., and Corbett, C. E. (2000). Insulin-like growth factor (IGF)-I affects parasite growth and host cell migration in experimental cutaneous leishmaniasis. *Int. J. Exp. Pathol.* 81, 249–255. doi: 10.1046/j.1365-2613.2000.00157.x

Gomes, C. M., Monteiro, H. P., Gidlund, M., Corbett, C. E. P., and Goto, H. (1998). Insulin-like growth factor-I induces phosphorylation in Leishmania (Leishmania) mexicana promastigotes and amastigotes. *J. Eukaryot. Microbiol.* 45, 352–355. doi: 10.1111/j.1550-7408.1998.tb04548.x

Goto, H., Gomes, C. M., Corbett, C. E., Monteiro, H. P., and Gidlund, M. (1998). Insulin-like growth factor I is a growth-promoting factor for Leishmania promastigotes and amastigotes. *Proc. Natl. Acad. Sci. U.S.A.* 95, 13211–13216. doi: 10.1073/pnas.95.22.13211

Juul, A. (2003). Serum levels of insulin-like growth factor I and its binding proteins in health and disease. *Growth Horm. IGF Res.* 13, 113–70. doi: 10.1016/S1096-6374(03)00038-8

Livak, K. J., and Schmittgen, T. D. (2001). Analysis of relative gene expression data using real- time quantitative PCR and the $2^{-\Delta\Delta CT}$ method. *Methods* 25, 402–408. doi: 10.1006/meth.2001.1262

Oberlin, D., Fellbaum, C., and Eppler, E. (2009). Insulin-like growth factor I messenger RNA and protein are expressed in the human lymph node and distinctly confined to subtypes of macrophages, antigen-presenting cells, lymphocytes and endothelial cells. *Immunology* 128, 342–350. doi: 10.1111/j.1365-2567.2009.03136.x

Oliveira, C. R., Salvatori, R., Nóbrega, L. M., Carvalho, E. O., Menezes, M., Farias, C. T., et al. (2008). Sizes of abdominal organs in adults with severe short stature due to severe, untreated, congenital GH deficiency caused by a homozygous mutation in the GHRH receptor gene. *Clin. Endocrinol.* 69, 153–158. doi: 10.1111/j.1365-2265.2007.03148.x

Oryan, A., and Akbari, M. (2016). Worldwide risk factors in leishmaniasis. *Asian Pac. J. Trop. Med.* 9, 925–932. doi: 10.1016/j.apjtm.2016.06.021

Reis, L. C., Ramos-Sanchez, E. M., and Goto, H. (2013). The interactions and essential effects of intrinsic insulin-like growth factor-I on Leishmania (Leishmania) major growth within macrophages. *Parasite Immunol.* 35, 239–244. doi: 10.1111/pim.12041

Rodrigues, L. S., da Silva Maeda, E., Moreira, M. E., Tempone, A. J., Lobato, L. S., Ribeiro-Resende, V. T., et al. (2010). Mycobacterium leprae induces insulin-like growth factor and promotes survival of Schwann cells upon serum withdrawal. *Cell. Microbiol.* 12, 42–54. doi: 10.1111/j.1462-5822.2009.01377.x

Salvatori, R., Hayashida, C. Y., Aguiar-Oliveira, M. H., Phillips, J. A., Souza, A. H., Gondo, R. G., et al. (1999). Familial dwarfism due to a novel mutation of the growth hormone- releasing hormone receptor gene. *J. Clin. Endocrinol. Metab.* 84, 917–923. doi: 10.1210/jc.84.3.917

Salvatori, R., Serpa, M. G., Parmigiani, G., Britto, A. V., Oliveira, J. L., Oliveira, C. R., et al. (2006). GH response to hypoglycemia and clonidine in the GH-releasing hormone resistance syndrome. *J. Endocrinol. Invest.* 29, 805–808. doi: 10.1007/BF03347374

Schwartz, G. N., Hudgins, W. R., and Perdue, J. F. (1993). Glycosylated insulin-like growth factor II promoted expansion of granulocyte-macrophage colony-forming cells in serum-deprived liquid cultures of human peripheral blood cells. *Exp. Hematol.* 21, 1447–1454.

Silva, R. L., Santos, M. B., Almeida, P. L., Barros, T. S., Magalhães, L., Cazzaniga, R. A., et al. (2017). sCD163 levels as a biomarker of disease severity in leprosy and visceral leishmaniasis. *PLoS Negl. Trop. Dis.* 11:e0005486. doi: 10.1371/journal.pntd.0005486

Souza, A. H. O., Salvatori, R., Martinelli, C. E. Jr., Carvalho, W. M. O., Menezes, C. A., and de A Barretto, E. S., et al. (2005). Growth or somatotrophic hormone: new perspectives in isolated GH deficiency after description of the mutation in the GHRH receptor gene in individuals of Itabaianinha County, Brazil. *Arq. Bras. Endocrinol. Metabol.* 48, 406–413. doi: 10.1590/S0004-27302004000300013

Sridharan, R., Cameron, A. R., Kelly, D. J., Kearney, C. J., and O'Brien, F. J. (2015). Biomaterial based modulation of macrophage polarization: a review and suggested design principles. *Mater. Today* 18, 313–325. doi: 10.1016/j.mattod.2015.01.019

Vendrame, C. M., Carvalho, M. D., Rios, F. J., Manuli, E. R., Petitto-Assis, F., and Goto, H. (2007). Effect of insulin-like growth factor-I on *Leishmania amazonensis* promastigote arginase activation and reciprocal inhibition of NOS2 pathway in macrophage in vitro. *Scand. J. Immunol.* 66, 287–296. doi: 10.1111/j.1365-3083.2007.01950.x

Vendrame, C. M., Carvalho, M. D., Tempone, A. G., and Goto, H. (2015). Insulin-like growth factor-I induces arginase activity in *Leishmania amazonensis* amastigote-infected macrophages through a cytokine-independent mechanism. *Mediators Inflamm.* 2014:475919. doi: 10.1155/2014/475919

Wells, J. A. (1999). *Advances in Protein Chemistry*, *Vol. 52, Cytokines* (Redwood City, CA: Academic Press).

Conflict of Interest Statement: The authors declare that the research was conducted in the absence of any commercial or financial relationships that could be construed as a potential conflict of interest.

frontiers in Cellular and Infection Microbiology

ORIGINAL RESEARCH
published: 06 September 2019
doi: 10.3389/fcimb.2019.00319

Leishmania braziliensis: Strain-Specific Modulation of Phagosome Maturation

Tamara da Silva Vieira[1,2†], Guillermo Arango Duque[2†], Kévin Ory[2,3], Celia Maria Gontijo[1], Rodrigo Pedro Soares[1] and Albert Descoteaux[2*]*

[1] Fundação Oswaldo Cruz - FIOCRUZ, Centro de Pesquisas René Rachou, Belo Horizonte, Brazil, [2] INRS - Centre Armand-Frappier Santé Biotechnologie, Université du Québec, Laval, QC, Canada, [3] Université de Rennes 1, CHU Rennes, INSERM, Rennes, France

OPEN ACCESS

Edited by:
Herbert Leonel de Matos Guedes, Federal University of Rio de Janeiro, Brazil

Reviewed by:
Camila I. De Oliveira, Oswaldo Cruz Foundation (Fiocruz), Brazil
Thiago DeSouza-Vieira, National Institute of Allergy and Infectious Diseases (NIAID), United States
Ricardo Silvestre, University of Minho, Portugal

***Correspondence:**
Rodrigo Pedro Soares
rodrigo.pedro@fiocruz.br
Albert Descoteaux
albert.descoteaux@iaf.inrs.ca

†These authors have contributed equally to this work

Specialty section:
This article was submitted to Parasite and Host, a section of the journal Frontiers in Cellular and Infection Microbiology

Received: 29 March 2019
Accepted: 26 August 2019
Published: 06 September 2019

Citation:
da Silva Vieira T, Arango Duque G, Ory K, Gontijo CM, Soares RP and Descoteaux A (2019) Leishmania braziliensis: Strain-Specific Modulation of Phagosome Maturation. Front. Cell. Infect. Microbiol. 9:319. doi: 10.3389/fcimb.2019.00319

Leishmania (*Viannia*) *braziliensis* is responsible for the largest number of American tegumentary leishmaniasis (ATL) in Brazil. ATL can present several clinical forms including typical (TL) and atypical (AL) cutaneous and mucocutaneous (ML) lesions. To identify parasite and host factors potentially associated with these diverse clinical manifestations, we first surveyed the expression of two virulence-associated glycoconjugates, lipophosphoglycan (LPG) and the metalloprotease GP63 by a panel of promastigotes of Leishmania braziliensis *(L. braziliensis)* strains isolated from patients with different clinical manifestations of ATL and from the sand fly vector. We observed a diversity of expression patterns for both LPG and GP63, which may be related to strain-specific polymorphisms. Interestingly, we noted that GP63 activity varies from strain to strain, including the ability to cleave host cell molecules. We next evaluated the ability of promastigotes from these *L. braziliensis* strains to modulate phagolysosome biogenesis in bone marrow-derived macrophages (BMM), by assessing phagosomal recruitment of the lysosome-associated membrane protein 1 (LAMP-1) and intraphagosomal acidification. Whereas, three out of six *L. braziliensis* strains impaired the phagosomal recruitment of LAMP-1, only the ML strain inhibited phagosome acidification to the same extent as the *L. donovani* strain that was used as a positive control. While decreased phagosomal recruitment of LAMP-1 correlated with higher LPG levels, decreased phagosomal acidification correlated with higher GP63 levels. Finally, we observed that the ability to infect and replicate within host cells did not fully correlate with the inhibition of phagosome maturation. Collectively, our results revealed a diversity of strain-specific phenotypes among *L. braziliensis* isolates, consistent with the high genetic diversity within *Leishmania* populations.

Keywords: *Leishmania braziliensis*, virulence, lipophosphoglycan, GP63, macrophage, phagosome, intracellular survival

INTRODUCTION

The various species of the protozoan parasite *Leishmania* cause a spectrum of human diseases ranging from a relatively confined cutaneous lesion to a progressive and potentially fatal visceral infection (Alvar et al., 2012). Upon delivery in the vertebrate host by an infected sand fly, metacyclic *Leishmania* promastigotes are engulfed by phagocytes. To avoid destruction, these

parasites have evolved efficient means of disarming the microbicidal functionality of their host cells (Arango Duque and Descoteaux, 2015; Podinovskaia and Descoteaux, 2015; Atayde et al., 2016; Martínez-López et al., 2018). To achieve this, infectious promastigotes rely on a panoply of virulence factors including two abundant components of their surface coat, the glycolipid lipophosphoglycan (LPG) and the GPI-anchored zinc metalloprotease GP63 (Moradin and Descoteaux, 2012; Olivier et al., 2012; Arango Duque and Descoteaux, 2015; Atayde et al., 2016). The use of mutants defective in either LPG or GP63 revealed that these molecules are indeed important for the colonization of phagocytic cells by promastigotes of *Leishmania donovani (L. donovani)* (Desjardins and Descoteaux, 1997; Lodge et al., 2006), *Leishmania major (L. major)* (Späth et al., 2000; Joshi et al., 2002), and *Leishmania infantum (L. infantum)* (Lázaro-Souza et al., 2018), all of which live in tight individual vacuoles. These virulence factors exert a profound impact on infected cells, altering signaling pathways (Descoteaux et al., 1991; Shio et al., 2012), inducing the production of inflammatory cytokines (Arango Duque et al., 2014), activating the inflammasome (de Carvalho et al., 2019), and inhibiting phagolysosomal biogenesis and functionality (Desjardins and Descoteaux, 1997; Späth et al., 2003; Lodge et al., 2006; Vinet et al., 2009; Matheoud et al., 2013; Matte et al., 2016). Of note, defective synthesis of LPG has no measurable effect on the ability of *Leishmania mexicana (L. mexicana)*, which lives in large communal vacuoles, to replicate in cultured macrophages and cause lesions in mice (Ilg, 2000; Ilg et al., 2001). These findings underline the fact that the relative contribution of a given virulence factor in the ability of promastigotes to colonize mammalian hosts varies among *Leishmania* species.

Leishmania braziliensis (subgenus *Viannia*) is responsible for the largest number of American tegumentary leishmaniasis cases in Brazil (ATL) (Alvar et al., 2012; PAHO/WH1O, 2017). ATL may exhibit several clinical forms including typical (TL), atypical (AL), and mucocutaneous (ML) lesions. TL may be confined at the bite site or metastasize to the oronasopharyngeal mucosa to give rise to ML. *L. braziliensis* AL lesions are scarce and they have been previously reported by Guimarães et al. in Bahia State (Guimarães et al., 2009) and by Quaresma et al. in the Minas Gerais State (Quaresma et al., 2018). Those lesions do not resemble classical TL lesions (round, ulcerated with elevated borders) and their ambiguous nature hinders correct diagnosis. Whether variations in GP63 and LPG levels are associated to the various clinical manifestations of ATL has not been investigated. In this regard, studies aimed at characterizing *GP63* in *L. braziliensis* revealed the presence of nearly 40 copies of this gene, as well as important sequence polymorphisms among clinical isolates (Medina et al., 2016). Characterization of LPG from *L. braziliensis* promastigotes revealed structural and compositional similarities to that of *L. donovani* (Soares et al., 2005), as well its strain-dependent capacity to induce inflammatory mediator release (Vieira Td et al., 2019).

To date, studies on the modulation of phagolysosome biogenesis by *Leishmania* promastigotes and on the contribution of LPG and GP63 to this process have focused mainly on species of the subgenus *Leishmania*. In the present study, we examined the levels of LPG and GP63 in a panel of *L. braziliensis* strains and surveyed their ability to interfere with phagosome maturation.

MATERIALS AND METHODS

Ethics Statement

This study was carried out in accordance with the recommendations the Canadian Council on Animal Care on animal handling practices. Protocol 1706-07 was approved by the *Comité Institutionel de Protection des Animaux* of the INRS-Institut Armand-Frappier. *Leishmania braziliensis* field strains were obtained from patients living in the Xakriabá indigenous community located in São João das Missões municipality, Minas Gerais State, Brazil. Isolates from other endemic areas were obtained from the outpatient care facility at *Centro de Referência em Leishmanioses*—Instituto René Rachou/Fiocruz Minas from 1993 to 1998. Patient samples were obtained under informed consent procedures approved by the IRR Research Ethics Committee in Human Research, the National Committee for Research Ethics (*Comissão Nacional de Ética em Pesquisa*—CONEP) n° 355/2008, and the National Indian Foundation (*Fundação Nacional do Índio*—FUNAI) n° 149/CGEP/08.

Cell Culture

Bone marrow-derived macrophages (BMM) were obtained from the bone marrow of 6–8 week-old female C57BL/6 mice and differentiated in complete DMEM [containing L-glutamine (Life Technologies), 10% v/v heat-inactivated fetal bovine serum (FBS) (Life Technologies), 10 mM HEPES (Bioshop) at pH 7.4, and penicillin-streptomycin (Life Technologies)] supplemented with 15% v/v L929 cell-conditioned medium (LCM) as a source of macrophage colony-stimulating factor. To render BMM quiescent prior to experiments, cells were transferred to tissue culture-treated plates containing glass coverslips for 16 h in complete DMEM without LCM (Descoteaux and Matlashewski, 1989). BMM were kept in a humidified 37°C incubator with 5% CO_2.

Promastigotes were grown in *Leishmania* medium [M199-1X (Sigma) with 10% heat-inactivated FBS, 40 mM HEPES at pH 7.4, 100 μM hypoxanthine, 5 μM hemin, 3 μM biopterin,

TABLE 1 | Leishmania strains used in this study.

Strain/Isolate	Geographical origin	Lesion type
MHOM/BR/75/M2903	Pará state, Brazil	TL
MHOM/BR/1995/RR051	Belo Horizonte, Minas Gerais State	TL
MHOM/BR/2009/RR418	São João das Missões, Minas Gerais State	TL
MHOM/BR/2008/RR410	São João das Missões, Minas Gerais State	AL
MHOM/BR/1996/M15991	Belém, Pará State	ML
IWELL/BR/1981/M8401	Belém, Pará State	N/A (strain isolated from vector)
MHOM/ET/67/Hu3:LV9	Ethiopia	Visceral
MHOM/SN/74 NIH clone A2 (A2WF)	Senegal	TL

1 μM biotin, MEM vitamin solution 1X, and penicillin-streptomycin] in a 26°C incubator (Soares et al., 2002; Arango Duque et al., 2014). The *L. braziliensis* strains used in this study (**Table 1**) include the World Health Organization reference strain (MHOM/BR/75/M2903), a ML isolate (MHOM/BR/1996/M15991), and a strain derived from *P. welcomei* sand flies (IWELL/BR/1981/M8401). The *L. braziliensis* RR051 strain was isolated from a TL lesion in the Minas Gerais State, and the RR418 (TL) and RR410 (AL) strains from lesions found in the Xakriabá community (Quaresma et al., 2018). These strains have been molecularly typed as *L. braziliensis* (Quaresma et al., 2018; Rugani et al., 2018). *Leishmania donovani* LV9 and *L. major* Seidman A2 promastigotes were freshly differentiated from splenic or ear lesion-derived amastigotes, respectively.

Infections and Phagosome Acidification Assays

Late stationary phase promastigotes (5-day cultures at $> 50 \times 10^6$ promastigotes/ml) from an early passage, or zymosan particles, were opsonised with serum from C5-deficient DBA/2 mice, resuspended in cold complete DMEM and fed to BMM (10:1 ratio) that had been seeded onto glass coverslips. Cells were incubated at 4°C for 5 min, and centrifuged for 2 min at 1,200 rpm (Arango Duque et al., 2013). Particle internalization was triggered by transferring cells to 37°C (Vinet et al., 2008; Arango Duque et al., 2014). Two hours post-internalization, infected macrophages were washed 3X with 1 ml warm DMEM to remove non-internalized promastigotes. Macrophages were either left at 37°C for an extra 22 h, or prepared for confocal microscopy. To assay phagosome acidification, BMM were incubated for 2 h with the acidotropic LysoTracker Red dye (diluted 1:1,000; Molecular probes) prior to the 2 h infection. In the case of the 24 h infection, infected macrophages were incubated in diluted LysoTracker for 2 h prior to the end of the infection time point. Cells were then washed and fixed.

For intracellular colonization assays, 6, 24, and 72 h-infected BMM seeded on coverlips were washed with PBS1X, stained with the Hema 3™ Stat Pack (Fisher), briefly washed with deionized water, and air-dried for 10 min. Coverslips were mounted onto a drop of Fluoromount-G and sealed. Images were acquired with a Qimaging camera (Teledyne Technologies International Corp) mounted on a Nikon Eclipse E800 microscope (60X objective). Images were compiled and analyzed with the ImageJ (Rueden et al., 2017) interphase of the Icy image analysis software (de Chaumont et al., 2012). Threshold segmentation was used to differentiate and enumerate BMM and intracellular *Leishmania* nuclei.

Confocal Immunofluorescence Microscopy

Infected cells on coverslips were fixed with 2% paraformaldehyde (Thermo Scientific) for 20 min and blocked and permeabilized for 17 min with a solution of 0.1% Triton X-100, 1% BSA, 6% non-fat milk, 20% goat serum, and 50% FBS. This was followed by a 2 h incubation with a monoclonal rat antibody to Lysosome-associated membrane protein 1 (LAMP-1) (developed by J. T. August (1D4B) and purchased through the Developmental Studies Hybridoma Bank at the University of Iowa and the National Institute of Child Health and Human Development) diluted 1:200 in PBS1X. Subsequently, cells were incubated for 35 min in a solution containing an anti-rat antibody conjugated to Alexa-488 (diluted 1:500; Molecular Probes) and DAPI (1:40,000; Molecular Probes). Coverslips were washed three times with PBS1X after every step. After the final wash, coverslips were mounted cell-side facing a drop of Fluoromount-G (Southern Biotechnology Associates) that was placed on a glass slide (Fisher); coverslips were sealed with nail polish (Sally Hansen). Infected macrophages were imaged with the 63X objective of an LSM780 confocal microscope (Carl Zeiss Microimaging) and image processing was done with the ZEN 2012 software. In regards to LysoTracker-treated cells, fixed samples were incubated in diluted DAPI for 35 min prior to mounting. Recruitment was evaluated by scoring the presence of staining on the phagosome membrane (LAMP-1) and/or the phagosome lumen (LysoTracker) (Vinet et al., 2009; Arango Duque et al., 2014). One hundred phagosomes per coverslip were scored for every experimental condition, each done in duplicate.

Electrophoresis, Western Blotting, and Zymography

Before lysis, stationary phase promastigotes, or infected BMM were washed with cold PBS1X containing 1 mM sodium orthovanadate and 5 mM 1,10-phenanthroline (Sigma). Pelleted parasites were resuspended in a lysis buffer containing 1% NP-40, 50 mM Tris-HCl (pH 7.5), 150 mM NaCl, 1 mM EDTA (pH 8), 15 mM 1,10-phenathroline and phosphatase and protease inhibitors (Roche). Samples were incubated at −70°C, sonicated with 20 s and thereafter centrifuged at 4°C for 15 min to remove insoluble material. After protein quantification, 30 μg of protein (10 μg in the case of promastigote lysate) was boiled (100°C) for 6 min in SDS sample buffer and migrated in SDS-PAGE gels. Proteins were transferred onto PDVF (phosphoglycan blots) or nitrocellulose membranes and thereafter blocked for 2 h in TBS1X-0.1% Tween containing 5% BSA. Membranes were subsequently probed (overnight at 4°C) with a mouse mAb (CA7AE; Cedarlane) that recognizes unbranched Galβ1,4Manα1-PO_4 phosphoglycan moieties (Tolson et al., 1989), and detects *L. braziliensis* LPG (Vieira Td et al., 2019). Membranes were also probed for the presence of GP63 (mouse mAb #235 targeting the membrane-anchored version of *L. major* GP63) (Button et al., 1993; Macdonald et al., 1995); VAMP8 and syntaxin-5 (Stx5) (rabbit pAbs from Synaptic Systems). Anti-*L. donovani* aldolase (rabbit pAb, a kind gift from A. Jardim) and β-actin (Sigma) were used as loading controls. After washing, membranes were probed with suitable HRP-conjugated secondary antibodies for 1 h at room temperature, and incubated in ECL (GE Healthcare). Immunodetection was achieved via chemiluminescence (Arango Duque et al., 2014). To assess GP63 proteolysis via zymography, lysates were incubated at 50°C for 5 min in sample buffer without DTT, and then migrated in 10–12% SDS-PAGE gels containing 0.12% gelatin (Sigma) (Hassani et al., 2014; Arango Duque et al., 2019). Gels were incubated for 2 h in the presence of 50 mM Tris pH 7.4, 2.5% Triton X-100, 5 mM $CaCl_2$ and

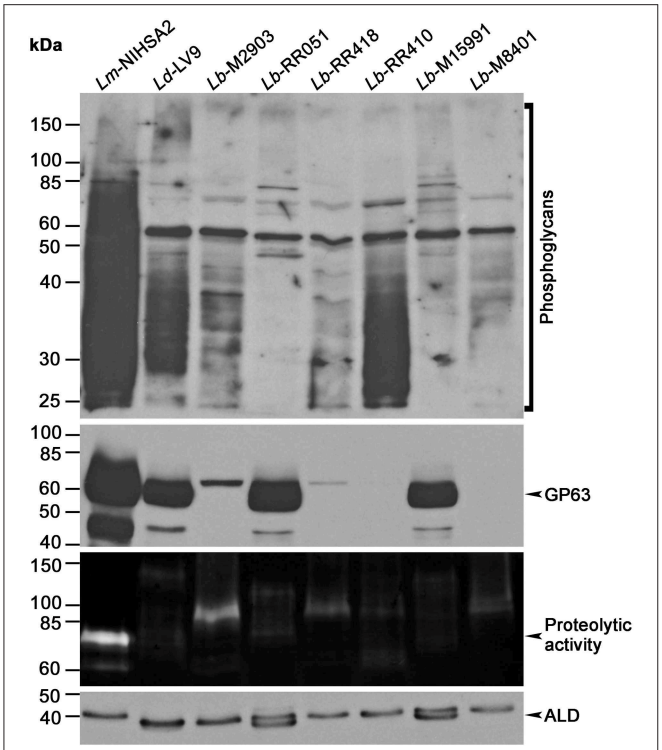

FIGURE 1 | Expression of virulence-associated glycoconjugates in different *L. braziliensis* strains. *Leishmania* promastigote lysates were assayed for LPG, GP63, and aldolase expression by Western blot, and GP63 activity was probed via gelatin zymography. Images are representative of two independent experiments. *Lm, L. major; Ld, L. donovani; Lb, L. braziliensis; ALD, Ld aldolase*.

1 mM $ZnCl_2$, followed by an overnight incubation at 37°C in a buffer containing 50 mM Tris pH 7.4, 5 mM $CaCl_2$, 1 mM $ZnCl_2$, and 0.01% NaN_3. Protease activity was visualized by gradually distaining gels that were incubated in 0.5% Coomassie Brilliant blue (Sigma) for 1 h.

Statistical Analysis

Statistical differences in recruitment levels were assessed using one-way ANOVA followed by Bonferroni *post-hoc* tests. Data were considered statistically significant when $p < 0.05$ and univariate column scatter graphs were constructed using GraphPad Prism 6.0 (GraphPad Software Inc).

RESULTS

Expression of LPG and GP63 Varies Among Strains of *L. braziliensis*

The ability of *Leishmania* promastigotes to colonize host cells and impair phagosome maturation and functionality is mediated to a large extent by the virulence factors LPG and GP63 (Chaudhuri et al., 1989; Späth et al., 2003; Moradin and Descoteaux, 2012; Atayde et al., 2016; Matte and Descoteaux, 2016). Here, we sought to determine the relative levels of LPG and GP63 expressed by promastigotes of a panel of *L. braziliensis* strains differing in their origin (**Table 1**). We included in our analysis *L. major* (NIH Seidman A2) and *L. donovani* (LV9) promastigotes as controls. Western blot analysis performed on promastigote lysates showed notable variations in the levels of LPG among the tested strains (**Figure 1**). Particularly, whereas the levels of LPG expressed by *L. braziliensis* RR410 were similar to those observed for *L. donovani* LV9, the levels detected in the other *L. braziliensis* strains were lower. In the case of GP63, we observed important differences among the *L. braziliensis* strains (**Figure 1**). Both *L. braziliensis* strains RR051 and M15991 expressed GP63 at levels comparable to those observed for *L. donovani* LV9. In contrast, GP63 levels were very low in the other strains. Interestingly, when we assessed the proteolytic activity of GP63 present in the *Leishmania* promastigotes lysates, we observed a lack of correlation with the GP63 levels detected by Western blot (**Figure 1**). Notably, *L. braziliensis* strains with low levels of GP63 (M2903 and RR418) showed high GP63 proteolytic activity, whereas *L. braziliensis* strains expressing higher GP63 levels (RR051 and M15991) showed reduced GP63 activity. These observations clearly demonstrated important intra-specific variations in the levels of detected LPG and GP63 (as well as GP63 activity) expressed by *L. braziliensis* strains isolated from patient with diverse ATL manifestations and from the insect vector.

Cleavage of GP63 Substrates by *L. braziliensis* Strains

Given the variations in GP63 levels and activity observed among the *L. braziliensis* isolates, we investigated the impact of these differences on the cleavage of phagosomal host cell proteins known to be targeted by GP63 (Matheoud et al., 2013). To this end, we performed Western blot analyses to assess the levels and integrity of the soluble *N*-ethylmaleimide-sensitive-factor attachment protein receptors (SNAREs) VAMP8 and Stx5, in lysates of BMM infected for 6 h with promastigotes of selected *L. braziliensis* strains (M2903, RR418, M15991, and M8401) and promastigotes of *L. major* NIHS A2 as control. As shown in **Figure 2**, VAMP8 was cleaved to the same extent by all *L. braziliensis* strains and by *L. major* NIHS A2, regardless of the levels and activity of GP63 detected in the cell lysates. In contrast, cleavage of the endoplasmic reticulum (ER)- and Golgi-resident SNARE Stx5 was strain-dependent and did not entirely correlate with the levels and activity of GP63 detected in the cell lysates (**Figure 2**). Collectively, these results indicate that cleavage of host cell GP63 substrates occurs in BMM infected with all *L. braziliensis* strains tested, albeit with some differences in the extent of cleavage. These findings also suggest that sensitivity to GP63 cleavage is substrate-specific.

L. braziliensis Impairs Phagosomal Recruitment of LAMP-1 in a Strain-Specific Manner

Given the variations observed among our panel of *L. braziliensis* strains in LPG and GP63 levels and activity, as well as substrate cleavage, we investigated the impact of *L. braziliensis* promastigotes on phagosome maturation. To this end, we incubated BMM with promastigotes from our panel of *L. braziliensis* strains for 2 and 24 h and assessed the

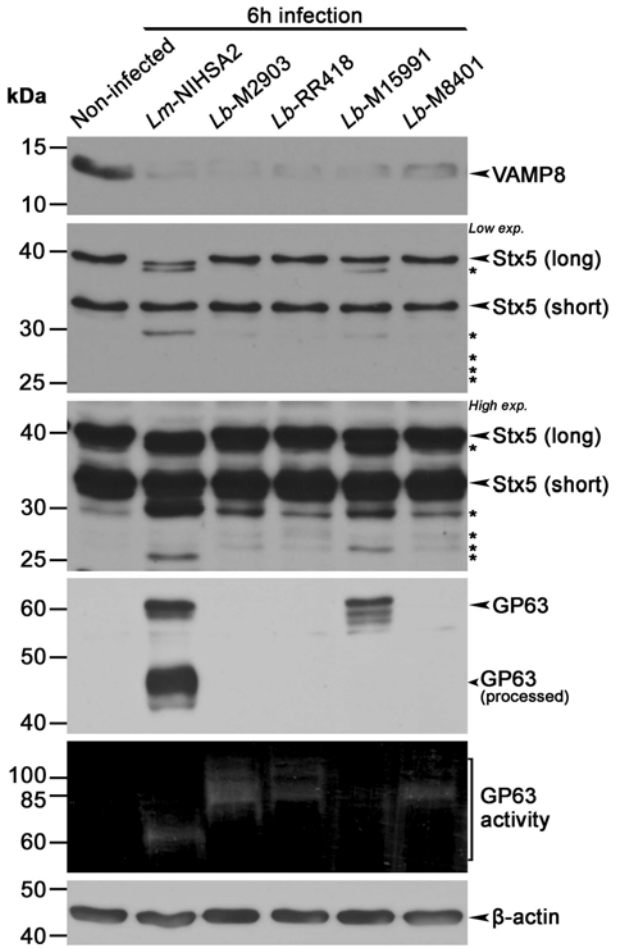

FIGURE 2 | Proteolytic cleavage of phagosome-associated proteins by *Leishmania braziliensis (L. braziliensis).* BMM were infected with opsonized stationary phase promastigotes from selected *L. braziliensis* strains, and the cleavage of phagosomal proteins VAMP8 and Stx5 was assessed via Western blot. GP63 activity was also assayed via gelatin zymography and β-actin was used as loading control. The long form of Stx5 is localized at the Golgi and ER, and the short one at the Golgi. Asterisks denote cleavage fragments. *Lm*, *L. major*; *Lb*, *L. braziliensis*.

recruitment of the lysosomal marker LAMP-1 to phagosomes. Promastigotes of *L. donovani* (LV9 strain), which efficiently inhibit phagosome maturation and phagosomal recruitment of LAMP-1 (Scianimanico et al., 1999), and zymosan were used as controls. At 2 h after the initiation of phagocytosis, we observed a higher recruitment of LAMP-1 to phagosomes containing *L. braziliensis* strains RR051 and M15991 compared to phagosomes containing *L. donovani* LV9 (**Figures 3A,B**). As expected, recruitment of LAMP-1 to phagosomes containing zymosan was higher to that observed for phagosomes induced by promastigotes of *L. donovani* LV9 and of those from *L. braziliensis* isolated from an AL lesion (RR410) (**Figure 3**). At 24 h post-infection, the presence of LAMP-1 on phagosomes harboring *L. donovani* promastigotes LV9 remained very low, as was also the case for phagosomes containing *L. braziliensis* M2903, RR410, and RR418. However, recruitment of LAMP-1 to phagosomes harboring *L. braziliensis* RR051 and M8401 was significantly higher than the levels observed for phagosomes containing the other *L. braziliensis* strains and *L. donovani* LV9 (**Figure 3**). These results suggest that the ability *L. braziliensis* promastigotes to interfere with phagosome maturation varies among strains.

Phagosome Acidification Is Differentially Modulated by *L. braziliensis* Strains

Consistent with their ability to inhibit phagolysosome biogenesis (Desjardins and Descoteaux, 1997), we previously reported that *L. donovani* promastigotes efficiently impair phagosome acidification (Vinet et al., 2009). To further characterize the impact of *L. braziliensis* promastigotes on phagosome maturation, we used the lysotropic dye LysoTracker Red to monitor acidification kinetics of phagosomes harboring the various *L. braziliensis* strains. Consistent with previous studies, at 2 h post-infection, acidification occurred in the majority of zymosan-harboring phagosomes but was hindered in phagosomes containing *L. donovani* LV9 promastigotes (**Figures 4A,B**). Similar impairment of phagosome acidification was observed for all *L. braziliensis* strains, with the exception of the strain isolated from an AL lesion (RR410) (**Figures 4A,B**). At 24 h post-infection, most phagosomes harboring *L. donovani* LV9 (80%) and the *L. braziliensis* ML isolate (M15991) (70%) remained negative for LysoTracker Red (**Figure 4**). In contrast, over 70% of phagosomes containing *L. braziliensis* isolates RR418 and RR410 were positive for LysoTracker Red at 24 h (**Figure 4B**). These data indicate that most *L. braziliensis* strains in our panel inhibit phagosome acidification during the early phase of macrophage infection. However, at later time points, the capacity to hinder phagosome acidification varies in a strain-specific manner.

Colonization of Macrophages by *L. braziliensis* Strains Does Not Fully Correlate With the Ability to Inhibit Phagosome Maturation and Acidification

Previous studies with *L. donovani* and *L. major* (Desjardins and Descoteaux, 1997; Späth et al., 2003; Vinet et al., 2009) revealed a correlation between the ability of these parasites to impair phagosome maturation and the ability to colonize macrophages. To investigate whether such a correlation exists for the *L. braziliensis* strains under study, we incubated BMM for 2 h with promastigotes of selected strains (M2903, RR418, M15991, and M8401) and promastigotes of *L. major* NIHS A2 as control. We then quantified the number of parasites per 100 macrophages and the percentage of infected macrophages at 6, 24, and 72 h post-phagocytosis. As shown in **Figure 5**, the ability to survive and replicate over time within BMM varied among the *L. braziliensis* strains analyzed. At the exception of strain M2903, which displayed reduced ability to survive in BMM over 72 h, all the other strains persisted and two of them (RR418 and M8401) replicated as was the case for *L. major* NIHS A2. Interestingly, *L. braziliensis* strain M2903, which survived poorly in BMM,

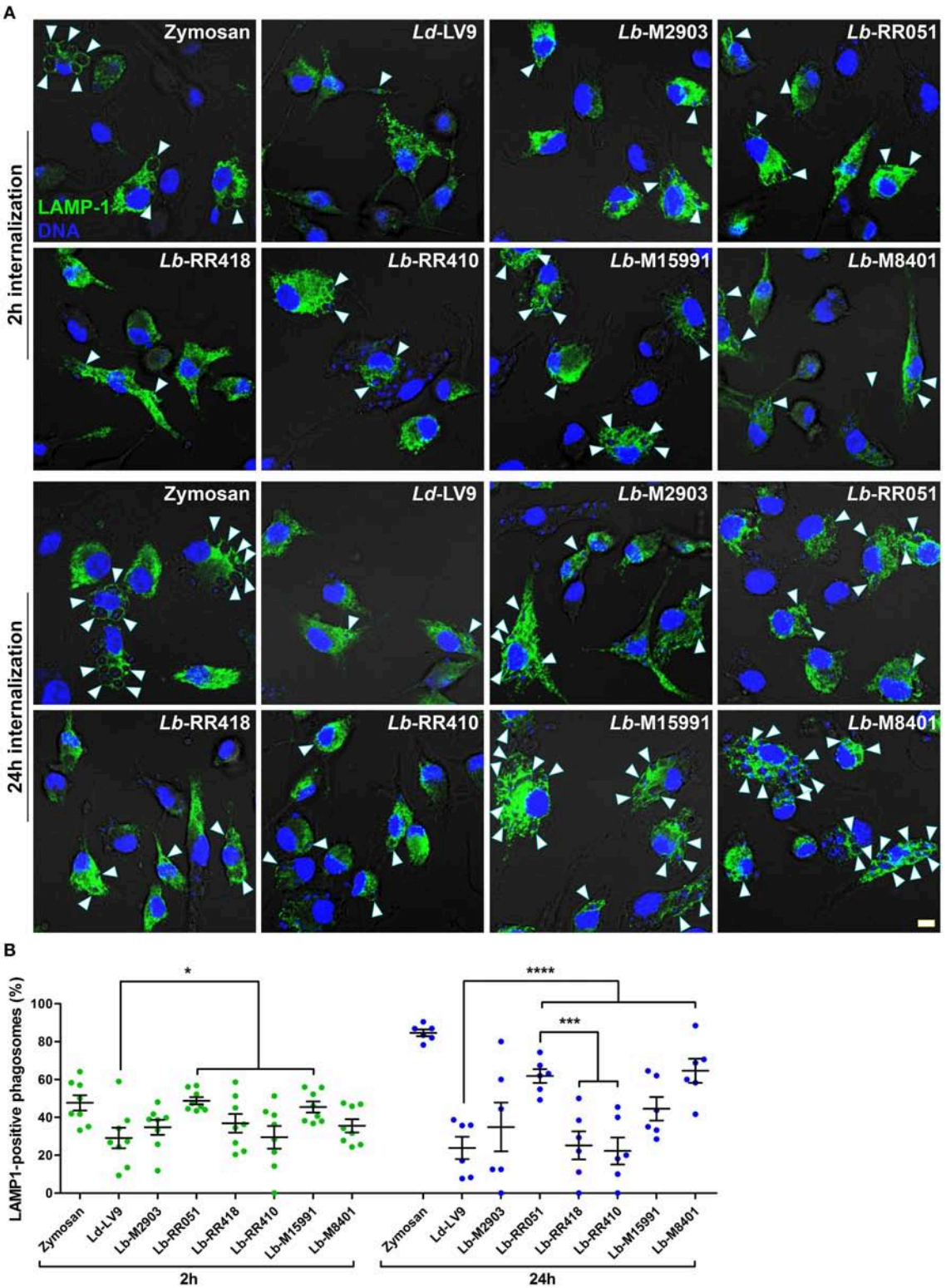

FIGURE 3 | LAMP-1 recruitment to parasitophorous vacuoles harboring *L. braziliensis* parasites. **(A)** BMM were infected with opsonized stationary phase promastigotes from different *L. braziliensis* strains, and LAMP-1 (green) recruitment to parasite-containing phagosomes was visualized via immunofluorescence at 2 and 24 h post-internalization. DNA is shown in blue; scale bar = 5 μm. White arrowheads indicate LAMP1 recruitment. **(B)** Quantification of LAMP-1-positive phagosomes at 2 h (green dots) and 24 h (blue dots) post-phagocytosis. Bars depict the mean ± SEM of % positive phagosomes counted over three independent experiments done at least in duplicate coverslips. *$p < 0.05$; ***$p < 0.001$; ****$p < 0.0001$. *Ld*, *L. donovani*; *Lb*, *L. braziliensis*.

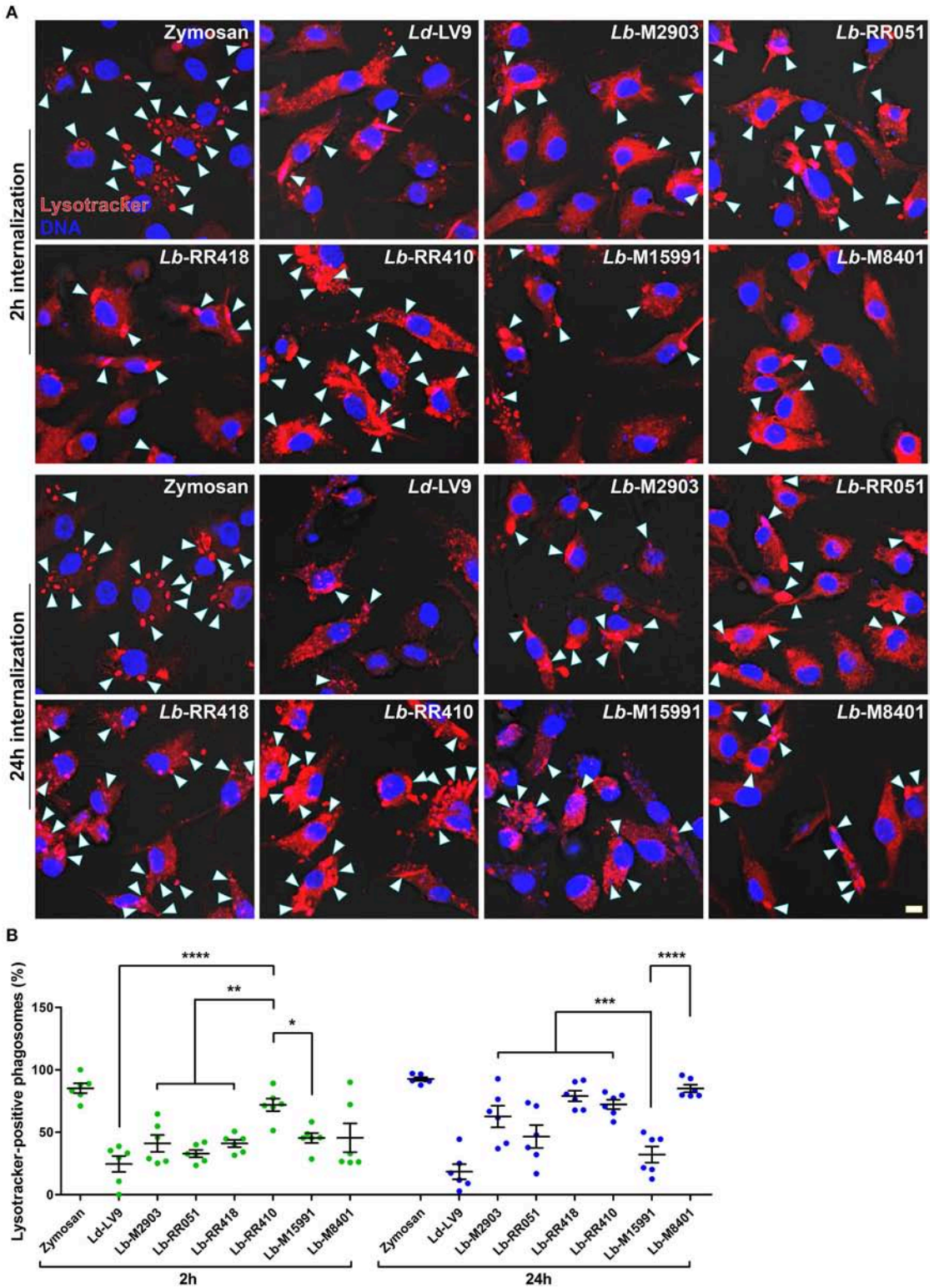

FIGURE 4 | Acidification of parasitophorous vacuoles harboring *L. braziliensis* parasites. **(A)** Bone marrow-derived macrophages (BMM) were infected with opsonized stationary phase promastigotes from different *L. braziliensis* strains, and acidification of parasite-containing vacuoles was assayed via LysoTracker staining (red) at 2 and 24 h post-internalization. DNA is shown in blue; scale bar = 5 μm. White arrowheads indicate LysoTracker-positive phagosomes. **(B)** Quantification of LysoTracker-positive phagosomes at 2 h (white bars) and 24 h (gray bars) post-phagocytosis. Bars depict the mean ± SEM of % positive phagosomes counted over three independent experiments done in duplicate. *$p < 0.05$; **$p < 0.01$; ***$p < 0.001$; ****$p < 0.0001$. *Ld*, *L. donovani*; *Lb*, *L. braziliensis*.

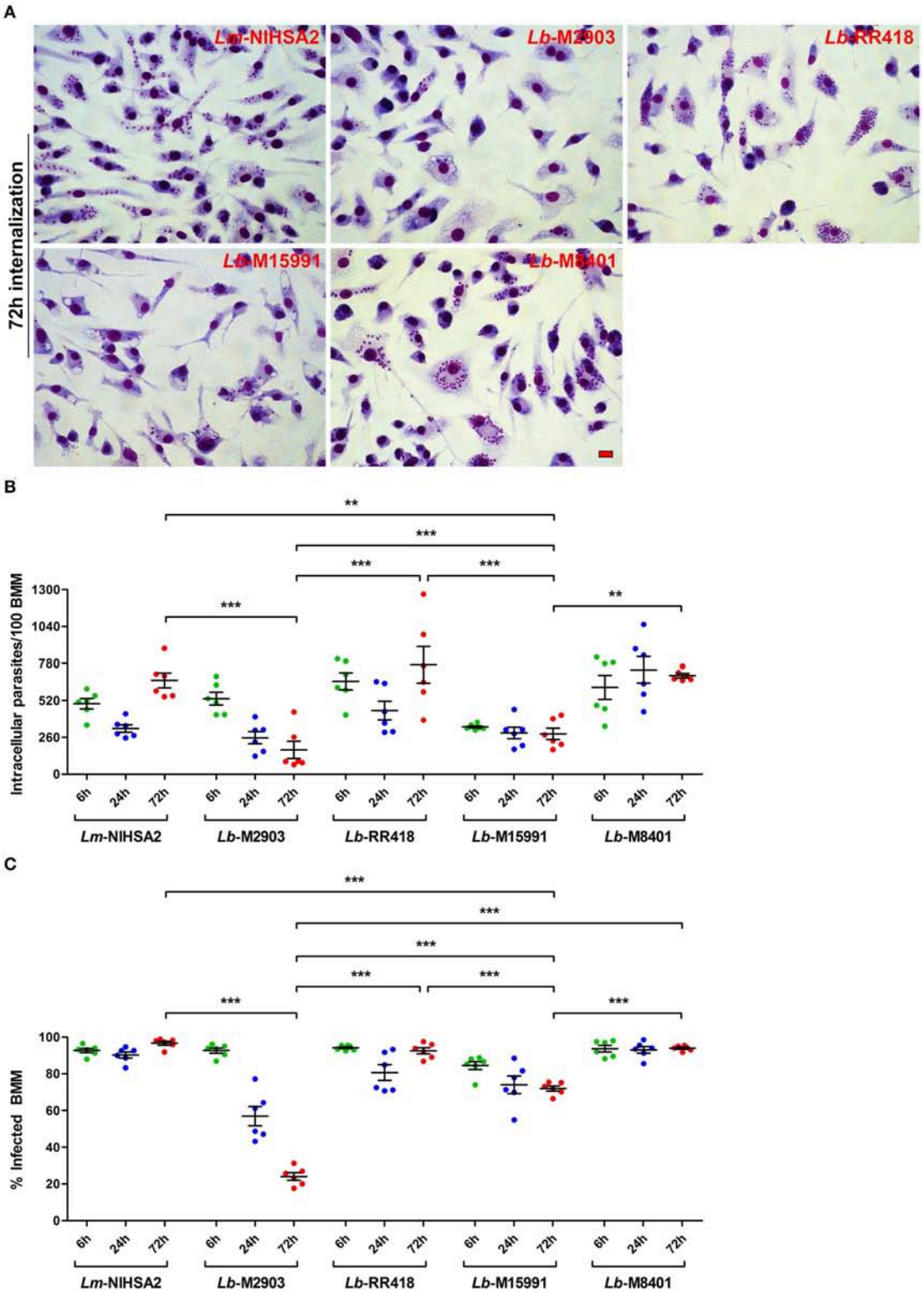

FIGURE 5 | Intracellular survival and replication of *L. braziliensis* parasites. BMM were infected with opsonized stationary phase promastigotes from selected *L. braziliensis* strains, and intracellular survival was quantified in Hema 3-stained cells. **(A)** Representative images of the 72 h time point. Scale bar = 10 μm. Intracellular survival at 6 (green dots), 24 (blue dots), and 72 h (red dots) post-infection was assessed via the quantification of internalized parasites in 100 macrophages **(B)** and the percentage of infected cells **(C)**. In both **(B,C)**, bars depict the mean ± SEM of two independent experiments done in triplicate coverslips. $^{**}p < 0.01$; $^{***}p < 0.001$. *Lm*, *L. major*; *Lb*, *L. braziliensis*.

was among the most efficient strains at inhibiting phagosome maturation (**Figures 3**, **4**). For strains RR418 and M8401, their ability to replicate in BMM correlated with their capacity to impair the phagosomal recruitment of LAMP-1 and acidification during the early phases of infection (**Figures 3**, **4**). These data are consistent with the notion that factor(s) other than the capacity to impair phagosome maturation are required for colonization of host cells by *L. braziliensis*.

DISCUSSION

The *Leishmania* virulence factors LPG and GP63 contribute to the ability of promastigotes to colonize phagocytic cells by targeting key host cell host defense mechanisms, including the biogenesis of microbicidal phagolysosomes. In the present study, we sought to examine the levels of LPG and GP63 expressed by promastigotes of *L. braziliensis* (subgenus *Viannia*) strains isolated from patients exhibiting various clinical manifestations of ATL and from the insect vector. We also characterized the ability of these *L. braziliensis* strains to impair phagosome maturation and to infect and replicate within macrophages.

Our results revealed an unexpected diversity of expression patterns for both LPG and GP63 among the evaluated *L. braziliensis* strains. Although some strains expressed LPG levels similar to those of *L. donovani* LV9 promastigotes, other strains expressed very low LPG levels. Similarly, some *L. braziliensis* strains expressed GP63 levels comparable to those observed in *L. donovani* LV9, whereas other strains expressed very low GP63 levels. Interestingly, we noted that GP63 activity varies from strain to strain, and does not correlate with GP63 levels detected by Western blot. Whether the polymorphims detected in the *GP63* genes of *L. braziliensis* (Medina et al., 2016) affected the recognition of GP63 by our anti-GP63 antibody is however unclear. Clearly, the significance of these observations deserves to be further investigated.

As part of their strategy to colonize host phagocytes, *Leishmania* promastigotes alter the composition and properties of the parasitophorous vacuole (Moradin and Descoteaux, 2012; Séguin and Descoteaux, 2016). Phagosomal recruitment of the lysosomal protein LAMP-1 is a widely used marker of phagosome maturation (Huynh et al., 2007). In the case of *Leishmania* promastigotes, delayed phagosomal acquisition of LAMP-1 following phagocytosis supported the notion that these parasites impair phagolysosomal biogenesis (Scianimanico et al., 1999; Lerm et al., 2006; Verma et al., 2017). Interestingly, we found that the ability to inhibit the phagosomal recruitment of LAMP-1 varies significantly among our panel of *L. braziliensis* strains. Phagosome acidification is an important consequence of the maturation process and we previously reported that it is efficiently inhibited by *L. donovani* promastigotes (Vinet et al., 2009). Similar to the recruitment of LAMP-1, we observed an important variation among promastigotes of the *L. braziliensis* strains tested in their capacity to inhibit phagosomal acidification. Interestingly, whereas promastigotes of *L. donovani* LV9 efficiently inhibited both phagosome acidification and recruitment of LAMP-1, we observed no correlation between the ability to inhibit phagosomal recruitment of LAMP-1 and phagosome acidification among the *L. braziliensis* strains. Previous work from our group revealed that acquisition of LAMP-1 and of the v-ATPase by phagosomes occurs through two distinct mechanisms (Vinet et al., 2009). In the case of *L. donovani*, LPG is the molecule responsible for inhibiting both the phagosomal recruitment of LAMP-1 and acidification (Scianimanico et al., 1999; Vinet et al., 2009). However, the ability of *L. braziliensis* strains to interfere with phagosome maturation does not appear to correlate with LPG levels.

In addition to LPG, *Leishmania* promastigotes use the metalloprotease GP63 to modulate the composition and function of phagosomes through the cleavage of host proteins such as VAMP3, VAMP8, and Synaptotagmin XI (Matheoud et al., 2013; Arango Duque et al., 2014; Casgrain et al., 2016; Matte and Descoteaux, 2016; Matte et al., 2016). Since VAMP8 is required for antigen cross-presentation (Matheoud et al., 2013), its cleavage by the various *L. braziliensis* strains suggests that they efficiently inhibit antigen cross-presentation. Future experiments will specifically address this issue. On the other hand, the endoplasmic reticulum- and Golgi-resident SNARE Stx5 is partially cleaved, to varying extents, by our *L. braziliensis* strains. This SNARE regulates trafficking between the phagosome and the secretory pathway (Cebrian et al., 2011; Arango Duque et al., 2019) and contributes to the expansion of communal parasitophorous vacuoles harboring *L. amazonensis* (Canton and Kima, 2012). The significance of its cleavage by *L. braziliensis* for establishment and replication within macrophages is an issue that will deserve further investigation.

In *L. braziliensis*, *GP63* is present on chromosome 10 and strains isolated from different clinical manifestations from the same geographical region have conserved domains and display specific polymorphisms in their catalytic sites (Medina et al., 2016; Sutter et al., 2017; Quaresma et al., 2018). This variability could result in different virulence patterns and clinical outcomes. Of interest, a recent genomic analysis of *Leishmania* clinical isolates revealed important differences among genetically highly related *Leishmania* strains, including both in amplification and in loss of genes linked to parasite infectivity such as *GP63* (Bussotti et al., 2018). Whether the diversity of GP63 levels and activity portrayed by the *L. braziliensis* strains is the consequence of gene amplification associated to environmental adaptation is a likely possibility that deserves further investigation. Similar to LPG and GP63, GIPLs are highly expressed on the *Leishmania* surface (Assis et al., 2012). They are inhibitory molecules impairing NO and cytokine production by murine macrophages and their role on phagosome maturation and intracellular survival will be assayed in prospective studies. Together, our findings underline the importance of performing functional genetic analyses with these clinical *L. braziliensis* strains to directly assess the importance of LPG and GP63 in the colonization of host phagocytes, and ultimately in the pathogenesis of ATL.

For the past several decades, research on virulence or immune subversion mechanisms of *Leishmania* has been for the most part performed with reference or laboratory strains. Results obtained with those strains allowed for the discovery of several biological processes. For instance, the Th1/Th2 dichotomy and

the importance of IL-4 in mediating susceptibility to infection were discovered using a particular *L. major* strain (Heinzel et al., 1989). However, studies using other *L. major* strains led to opposite results (Noben-Trauth et al., 1996, 1999). In the case of *L. braziliensis* ATL strains, our study revealed an unexpected diversity in terms of expression of virulence molecules and ability to interfere with phagosome maturation. Clearly, these studies highlight the fact that it is important to exert caution when drawing broad conclusions based on observations obtained with a single strain or isolate of a given *Leishmania* species.

DATA AVAILABILITY

All datasets generated for this study are included in the manuscript and/or the supplementary files.

ETHICS STATEMENT

Mice were manipulated under the guidelines of protocol 1706-07 of the Comité Institutionel de Protection des Animaux of the INRS-Institut Armand-Frappier, which respects animal handling practices promulgated by the Canadian Council on Animal Care. *Leishmania braziliensis* field strains were obtained from patients living in the Xakriabá indigenous community located in São João das Missões municipality, Minas Gerais State, Brazil. Isolates from other endemic areas were obtained from the outpatient care facility at Centro de Referência em Leishmanioses—Instituto René Rachou/Fiocruz Minas from 1993 to 1998. Patient samples were obtained under informed consent procedures approved by the IRR Research Ethics Committee in Human Research, the National Committee for Research Ethics (Comissão Nacional de Ética em Pesquisa—CONEP) n° 355/2008, and the National Indian Foundation (Fundação Nacional dÍo ndio—FUNAI) n° 149/CGEP/08.

AUTHOR CONTRIBUTIONS

GA, TS, RS, and AD conceived and designed the study, contributed to the data analysis, and drafted and revised the manuscript. GA, TS, and KO performed the experiments. CG provided the *L. braziliensis* strains. GA, TS, RS, and AD wrote and revised the manuscript. All authors read and approved the final version of this manuscript.

FUNDING

This work was supported by the Canadian Institutes of Health Research (CIHR) (grants PJT-156416 and MOP-125990 to AD), by the Conselho Nacional de Pesquisa e Desenvolvimento (CNPq) (grant 305065/2016-5 to RS), and the Fundação de Amparo do Estado de Minas Gerais (FAPEMIG) (grant 00202-18 to RS). AD was the holder of the Canada Research Chair on the Biology of intracellular parasitism. TS was the recipient of a scholarship from FAPEMIG and from the Emerging Leaders in the Americas Program (Global Affairs Canada). GA was supported by a CIHR Banting and Best Doctoral Award.

ACKNOWLEDGMENTS

We thank W. R. McMaster (University of British Columbia) for providing antibodies against GP63, A. Jardim (McGill University) for providing the aldolase antiserum, and J. Tremblay for assistance with confocal immunofluorescence experiments.

REFERENCES

Alvar, J., Vélez, I. D., Bern, C., Herrero, M., Desjeux, P., Cano, J., et al. (2012). Leishmaniasis worldwide and global estimates of its incidence. *PLoS ONE* 7:e35671. doi: 10.1371/journal.pone.0035671

Arango Duque, G., and Descoteaux, A. (2015). *Leishmania* survival in the macrophage: where the ends justify the means. *Curr. Opin. Microbiol.* 26, 32–40. doi: 10.1016/j.mib.2015.04.007

Arango Duque, G., Fukuda, M., and Descoteaux, A. (2013). Synaptotagmin XI regulates phagocytosis and cytokine secretion in macrophages. *J. Immunol.* 190, 1737–1745. doi: 10.4049/jimmunol.1202500

Arango Duque, G., Fukuda, M., Turco, S. J., Stäger, S., and Descoteaux, A. (2014). *Leishmania* promastigotes induce cytokine secretion in macrophages through the degradation of synaptotagmin XI. *J. Immunol.* 193, 2363–2372. doi: 10.4049/jimmunol.1303043

Arango Duque, G., Jardim, A., Gagnon, É., Fukuda, M., and Descoteaux, A. (2019). The host cell secretory pathway mediates the export of *Leishmania* virulence factors out of the parasitophorous vacuole. *PLoS Pathog.* 15:e1007982. doi: 10.1371/journal.ppat.1007982

Assis, R. R., Ibraim, I. C., Noronha, F. S., Turco, S. J., and Soares, R. P. (2012). Glycoinositolphospholipids from *Leishmania braziliensis* and *L. infantum*: Modulation of Innate Immune System and Variations in Carbohydrate Structure. *PLoS Neglected Tropical Dis.* 6:e1543. doi: 10.1371/journal.pntd.0001543

Atayde, V. D., Hassani, K., da Silva Lira Filho, A., Borges, A. R., Adhikari, A., Martel, C., et al. (2016). *Leishmania* exosomes and other virulence factors: Impact on innate immune response and macrophage functions. *Cell. Immunol.* 309, 7–18. doi: 10.1016/j.cellimm.2016.07.013

Bussotti, G., Gouzelou, E., Côrtes Boité M., Kherachi, I., Harrat, Z., Eddaikra, N., et al. (2018). *Leishmania* genome dynamics during environmental adaptation reveal strain-specific differences in gene copy number variation, karyotype instability, and telomeric amplification. *mBio* 9:e01399–18. doi: 10.1128/mBio.01399-18

Button, L. L., Wilson, G., Astell, C. R., and McMaster, W. R. (1993). Recombinant *Leishmania* surface glycoprotein GP63 is secreted in the baculovirus expression system as a latent metalloproteinase. *Gene* 134, 75–81. doi: 10.1016/0378-1119(93)90176-4

Canton, J., and Kima, P. E. (2012). Targeting host syntaxin-5 preferentially blocks *Leishmania* parasitophorous vacuole development in infected cells and limits experimental leishmania infections. *Am. J. Pathol.* 181, 1348–1355. doi: 10.1016/j.ajpath.2012.06.041

Casgrain, P. A., Martel, C., McMaster, W. R., Mottram, J. C., Olivier, M., and Descoteaux, A. (2016). Cysteine peptidase B regulates *Leishmania mexicana* virulence through the modulation of GP63 expression. *PLoS Pathog.* 12:e1005658. doi: 10.1371/journal.ppat.1005658

Cebrian, I., Visentin, G., Blanchard, N., Jouve, M., Bobard, A., Moita, C., et al. (2011). Sec22b regulates phagosomal maturation and antigen crosspresentation by dendritic cells. *Cell* 147, 1355–1368. doi: 10.1016/j.cell.2011.11.021

Chaudhuri, G., Chaudhuri, M., Pan, A., and Chang, K. P. (1989). Surface acid proteinase (gp63) of *Leishmania mexicana*. A metalloenzyme capable of protecting liposome-encapsulated proteins from phagolysosomal degradation by macrophages. *J. Biol. Chem.* 264, 7483–7489.

de Carvalho, R. V. H., Andrade, W. A., Lima-Junior, D. S., Dilucca, M., de Oliveira, C. V., Wang, K., et al. (2019). *Leishmania* lipophosphoglycan triggers caspase-11 and the non-canonical activation of the NLRP3 inflammasome. *Cell Rep*. 26:e5. doi: 10.1016/j.celrep.2018.12.047

de Chaumont, F., Dallongeville, S., Chenouard, N., Hervé N., Pop, S., Provoost, T., et al. (2012). Icy: an open bioimage informatics platform for extended reproducible research. *Nat. Methods* 9:690. doi: 10.1038/nmeth.2075

Descoteaux, A., and Matlashewski, G. (1989). c-fos and tumor necrosis factor gene expression in *Leishmania donovani*-infected macrophages. *Mol. Cell Biol*. 9, 5223–5227. doi: 10.1128/MCB.9.11.5223

Descoteaux, A., Turco, S. J., Sacks, D. L., and Matlashewski, G. (1991). *Leishmania donovani* lipophosphoglycan selectively inhibits signal transduction in macrophages. *J. Immunol*. 146, 2747–2753.

Desjardins, M., and Descoteaux, A. (1997). Inhibition of phagolysosomal biogenesis by the *Leishmania* lipophosphoglycan. *J. Exp. Med*. 185, 2061–2068. doi: 10.1084/jem.185.12.2061

Guimarães, L. H., Machado, P. R., Lago, E. L., Morgan, D. J., Schriefer, A., Bacellar, O., et al. (2009). Atypical manifestations of tegumentary leishmaniasis in a transmission area of *Leishmania braziliensis* in the state of Bahia, Brazil. *Trans R Soc. Trop. Med. Hyg*. 103, 712–715. doi: 10.1016/j.trstmh.2009.04.019

Hassani, K., Shio, M. T., Martel, C., Faubert, D., and Olivier, M. (2014). Absence of metalloprotease GP63 alters the protein content of *Leishmania* exosomes. *PLoS ONE* 9:e95007. doi: 10.1371/journal.pone.0095007

Heinzel, F. P., Sadick, M. D., Holaday, B. J., Coffman, R. L., and Locksley, R. M. (1989). Reciprocal expression of interferon gamma or interleukin 4 during the resolution or progression of murine leishmaniasis. Evidence for expansion of distinct helper T cell subsets. *J. Exp. Med*. 169, 59–72. doi: 10.1084/jem.169.1.59

Huynh, K. K., Eskelinen, E. L., Scott, C. C., Malevanets, A., Saftig, P., and Grinstein, S. (2007). LAMP proteins are required for fusion of lysosomes with phagosomes. *EMBO J*. 26, 313–24. doi: 10.1038/sj.emboj.7601511

Ilg, T. (2000). Lipophosphoglycan is not required for infection of macrophages or mice by *Leishmania mexicana*. *EMBO J*. 19, 1953–1962. doi: 10.1093/emboj/19.9.1953

Ilg, T., Demar, M., and Harbecke, D. (2001). Phosphoglycan repeat-deficient *Leishmania mexicana* parasites remain infectious to macrophages and mice. *J. Biol. Chem*. 276, 4988–4997. doi: 10.1074/jbc.M008030200

Joshi, P. B., Kelly, B. L., Kamhawi, S., Sacks, D. L., and McMaster, W. R. (2002). Targeted gene deletion in *Leishmania major* identifies leishmanolysin (GP63) as a virulence factor. *Mol. Biochem. Parasitol*. 120, 33–40. doi: 10.1016/S0166-6851(01)00432-7

Lázaro-Souza, M., Matte, C., Lima, J. B., Arango Duque, G., Quintela-Carvalho, G., de Carvalho Vivarini, Á., et al. (2018). *Leishmania infantum* lipophosphoglycan-deficient mutants: a tool to study host cell-parasite interplay. *Front. Microbiol*. 9:626. doi: 10.3389/fmicb.2018.00626

Lerm, M., Holm, A., Seiron, A., Särndahl, E., Magnusson, K. E., and Rasmusson, B. (2006). *Leishmania donovani* requires functional Cdc42 and Rac1 to prevent phagosomal maturation. *Infect Immun*. 74, 2613–2618. doi: 10.1128/IAI.74.5.2613-2618.2006

Lodge, R., Diallo, T. O., and Descoteaux, A. (2006). *Leishmania donovani* lipophosphoglycan blocks NADPH oxidase assembly at the phagosome membrane. *Cell Microbiol*. 8, 1922–1931. doi: 10.1111/j.1462-5822.2006.00758.x

Macdonald, M. H., Morrison, C. J., and McMaster, W. R. (1995). Analysis of the active site and activation mechanism of the *Leishmania* surface metalloproteinase GP63. *Biochim. Biophys*. 1253, 199–207. doi: 10.1016/0167-4838(95)00155-5

Martínez-López, M., Soto, M., Iborra, S., and Sancho, D. (2018). *Leishmania* hijacks myeloid cells for immune escape. *Front. Microbiol*. 9:883. doi: 10.3389/fmicb.2018.00883

Matheoud, D., Moradin, N., Bellemare-Pelletier, A., Shio, M. T., Hong, W. J., Olivier, M., et al. (2013). *Leishmania* evades host immunity by inhibiting antigen cross-presentation through direct cleavage of the SNARE VAMP8. *Cell Host Microbe* 14, 15–25. doi: 10.1016/j.chom.2013.06.003

Matte, C., Casgrain, P.-A., Séguin, O., Moradin, N., Hong, W. J., and Descoteaux, A. (2016). *Leishmania major* promastigotes evade LC3-associated phagocytosis through the action of GP63. *PLoS Pathog*. 12:e1005690. doi: 10.1371/journal.ppat.1005690

Matte, C., and Descoteaux, A. (2016). Exploitation of the host cell membrane fusion machinery by leishmania is part of the infection process. *PLoS Pathog*. 12:e1005962. doi: 10.1371/journal.ppat.1005962

Medina, L. S., Souza, B. A., Queiroz, A., Guimarães, L. H., Lima Machado, P. R., Carvalho, M., et al. (2016). The *gp63* gene cluster is highly polymorphic in natural *Leishmania* (*Viannia*) *braziliensis* populations, but functional sites are conserved. *PLoS ONE* 11:e0163284. doi: 10.1371/journal.pone.0163284

Moradin, N., and Descoteaux, A. (2012). *Leishmania* promastigotes: building a safe niche within macrophages. *Front Cell Infect. Microbiol*. 2:121. doi: 10.3389/fcimb.2012.00121

Noben-Trauth, N., Kropf, P., and Müller, I. (1996). Susceptibility to *Leishmania major* infection in interleukin-4-deficient mice. *Science* 271, 987–990. doi: 10.1126/science.271.5251.987

Noben-Trauth, N., Paul, W. E., and Sacks, D. L. (1999). IL-4- and IL-4 receptor-deficient BALB/c mice reveal differences in susceptibility to *Leishmania major* parasite substrains. *J. Immunol*. 162, 6132–6140.

Olivier, M., Atayde, V. D., Isnard, A., Hassani, K., and Shio, M. T. (2012). *Leishmania* virulence factors: focus on the metalloprotease GP63. *Microbes Infect*. 14, 1377–1389. doi: 10.1016/j.micinf.2012.05.014

PAHO/WH1O (2017). *Leishmaniasis: Epidemiological Report of the Americas Washington: Pan American Health Organization [cited 2019 February 25]*. 5. Available online at: http://www.paho.org/leishmaniasis

Podinovskaia, M., and Descoteaux, A. (2015). *Leishmania* and the macrophage: a multifaceted interaction. *Fut. Microbiol*. 10, 111–129. doi: 10.2217/fmb.14.103

Quaresma, P. F., de Brito, C. F. A., Rugani, J. M. N., Freire Jd, M., Baptista Rd, P., Moreno, E. C., et al. (2018). Distinct genetic profiles of *Leishmania* (*Viannia*) *braziliensis* associate with clinical variations in cutaneous-leishmaniasis patients from an endemic area in Brazil. *Parasitology* 145, 1161–1169. doi: 10.1017/S0031182018000276

Rueden, C. T., Schindelin, J., Hiner, M. C., DeZonia, B. E., Walter, A. E., Arena, E. T., et al. (2017). ImageJ2: imageJ for the next generation of scientific image data. *BMC Bioinform*. 18:529. doi: 10.1186/s12859-017-1934-z

Rugani, J. N., Quaresma, P. F., Gontijo, C. F., Soares, R. P., and Monte-Neto, R. L. (2018). Intraspecies susceptibility of *Leishmania* (*Viannia*) *braziliensis* to antileishmanial drugs: antimony resistance in human isolates from atypical lesions. *Biomed. Pharmacother*. 108, 1170–1180. doi: 10.1016/j.biopha.2018.09.149

Scianimanico, S., Desrosiers, M., Dermine, J. F., Méresse, S., Descoteaux, A., and Desjardins, M. (1999). Impaired recruitment of the small GTPase rab7 correlates with the inhibition of phagosome maturation by *Leishmania donovani* promastigotes. *Cell Microbiol*. 1, 19–32. doi: 10.1046/j.1462-5822.1999.00002.x

Séguin, O., and Descoteaux, A. (2016). *Leishmania*, the phagosome, and host responses: the journey of a parasite. *Cell. Immunol*. 309, 1–6. doi: 10.1016/j.cellimm.2016.08.004

Shio, M. T., Hassani, K., Isnard, A., Ralph, B., Contreras, I., Gómez, M. A., et al. (2012). Host cell signalling and *Leishmania* mechanisms of evasion. *J. Trop. Med*. 2012:819512. doi: 10.1155/2012/819512

Soares, R. P., Cardoso, T. L., Barron, T., Araújo, M. S. S., Pimenta, P. F., and Turco, S. J. (2005). *Leishmania braziliensis*: a novel mechanism in the lipophosphoglycan regulation during metacyclogenesis. *Int. J. Parasitol*. 35, 245–253. doi: 10.1016/j.ijpara.2004.12.008

Soares, R. P., Macedo, M. E., Ropert, C., Gontijo, N. F., Almeida, I. C., Gazzinelli, R. T., et al. (2002). *Leishmania chagasi*: lipophosphoglycan characterization and binding to the midgut of the sand fly vector *Lutzomyia longipalpis*. *Mol. Biochem. Parasitol*. 121, 213–224. doi: 10.1016/S0166-6851(02)00033-6

Späth, G. F., Epstein, L., Leader, B., Singer, S. M., Avila, H. A., Turco, S. J., et al. (2000). Lipophosphoglycan is a virulence factor distinct from related glycoconjugates in the protozoan parasite *Leishmania major*. *Proc. Natl. Acad. Sci. U.S.A*. 97, 9258–9263. doi: 10.1073/pnas.160257897

Späth, G. F., Garraway, L. A., Turco, S. J., and Beverley, S. M. (2003). The role(s) of lipophosphoglycan (LPG) in the establishment of *Leishmania major* infections in mammalian hosts. *Proc. Natl. Acad. Sci. U.S.A*. 100, 9536–9541. doi: 10.1073/pnas.1530604100

Sutter, A., Antunes, D., Silva-Almeida, M., Costa MGd, S., and Caffarena, E. R. (2017). Structural insights into leishmanolysins encoded on chromosome 10 of *Leishmania* (*Viannia*) *braziliensis*. *Memórias do Instituto Oswaldo Cruz* 112, 617–625. doi: 10.1590/0074-02760160522

Tolson, D. L., Turco, S. J., Beecroft, R. P., and Pearson, T. W. (1989). The immunochemical structure and surface arrangement of *Leishmania donovani* lipophosphoglycan determined using monoclonal antibodies. *Mol. Biochem. Parasitol.* 35, 109–118. doi: 10.1016/0166-6851(89)90113-8

Verma, J. K., Rastogi, R., and Mukhopadhyay, A. (2017). *Leishmania donovani* resides in modified early endosomes by upregulating Rab5a expression via the downregulation of miR-494. *PLoS Pathog.* 13:e1006459. doi: 10.1371/journal.ppat.1006459

Vieira Td, S., Rugani, J. N., Nogueira, P. M., Torrecilhas, A. C., Gontijo, C. M. F., Descoteaux, A., et al. (2019). Intraspecies polymorphisms in the lipophosphoglycan of *L. braziliensis* differentially modulate macrophage activation via TLR4. *Front. Cell. Infect. Microbiol.* 9:240. doi: 10.3389/fcimb.2019.00240

Vinet, A. F., Fukuda, M., and Descoteaux, A. (2008). The exocytosis regulator synaptotagmin V controls phagocytosis in macrophages. *J. Immunol.* 181, 5289–5295.doi: 10.4049/jimmunol.181.8.5289

Vinet, A. F., Fukuda, M., Turco, S. J., and Descoteaux, A. (2009). The *Leishmania donovani* lipophosphoglycan excludes the vesicular proton-ATPase from phagosomes by impairing the recruitment of synaptotagmin V. *PLoS Pathog.* 5:e1000628. doi: 10.1371/journal.ppat.1000628

Conflict of Interest Statement: The authors declare that the research was conducted in the absence of any commercial or financial relationships that could be construed as a potential conflict of interest.

frontiers in Cellular and Infection Microbiology

REVIEW
published: 19 September 2019
doi: 10.3389/fcimb.2019.00330

Leishmania Spp-Host Interaction: There Is Always an Onset, but Is There an End?

Fatima Conceição-Silva[1]* *and Fernanda N. Morgado*[2]*

[1] Laboratory of Immunoparasitology, Oswaldo Cruz Institute, IOC/Fiocruz, Rio de Janeiro, Brazil, [2] Laboratory of Leishmaniasis Research, Oswaldo Cruz Institute, IOC/Fiocruz, Rio de Janeiro, Brazil

For a long time Leishmaniasis had been considered as a neglected tropical disease. Recently, it has become a priority in public health all over the world for different aspects such as geographic spread, number of population living at risk of infection as well as the potential lethality and/or the development of disfiguring lesions in the, respectively, visceral and tegumentary forms of the disease. As a result, several groups have been bending over this issue and many valuable data have been published. Nevertheless, parasite-host interactions are still not fully known and, consequently, we do not entirely understand the infection dynamics and parasite persistence. This knowledge may point targets for modulation or blockage, being very useful in the development of measures to interfere in the course of infection/ disease and to minimize the risks and morbidity. In the present review we will discuss some aspects of the *Leishmania* spp—mammalian host interaction in the onset of infection and after the clinical cure of the lesions. We will also examine the information already available concerning the parasite strategy to evade immune response mainly at the beginning of the infection, as well as during the parasite persistence. This knowledge can improve the conditions of treatment, follow-up and cure control of patients, minimizing the potential damages this protozoosis can cause to infected individuals.

Keywords: leishmaniasis, parasite evasion mechanisms, immune response, parasite-host interaction, parasite persistence

OPEN ACCESS

Edited by:
Sarman Singh,
All India Institute of Medical Sciences, India

Reviewed by:
Celio Geraldo Freire-de-Lima,
Federal University of Rio de Janeiro, Brazil
Lucas Carvalho,
Federal University of Bahia, Brazil

***Correspondence:**
Fatima Conceição-Silva
fconcei@ioc.fiocruz.br
Fernanda N. Morgado
morgado@ioc.fiocruz.br

Specialty section:
This article was submitted to Parasite and Host, a section of the journal Frontiers in Cellular and Infection Microbiology

Received: *30 April 2019*
Accepted: *04 September 2019*
Published: *19 September 2019*

Citation:
Conceição-Silva F and Morgado FN (2019) Leishmania Spp-Host Interaction: There Is Always an Onset, but Is There an End? Front. Cell. Infect. Microbiol. 9:330. doi: 10.3389/fcimb.2019.00330

LEISHMANIASIS: A BRIEF INTRODUCTION

Leishmaniasis is an infectious disease caused by parasites of the genus *Leishmania* that affect humans and other animals. They are transmitted by insects popularly known as sand flies (Order Diptera, family *Psychodidae*, subfamily Phlebotominae) and can cause different clinical presentations, from cutaneous, and/or mucosal lesions (tegumentary leishmaniasis) up to visceral infection with tropism by the lymphohematopoietic system (visceral leishmaniasis). Due to its potential for lethality, mainly in visceral forms, as well as its dispersion in several continents with large population groups under infection risk, it is considered by WHO as one of the priority attention diseases (World Health Organization, 2010, 2017; Alvar et al., 2012).

The resolution WHA60.13, published during the World Health Assembly in 2007, aims to develop different actions all over the world in order to promote leishmaniasis control both by improving diagnosis and treatment access and by establishing or fortifying national control programs (World Wealth Assembly, 2007). Nowadays, leishmaniasis is described in 98

countries and several others are under risk of infection due to climate changes and/or population mobility (by migration and travel) (Ait Kbaich et al., 2017; Azimi et al., 2017; Baylis, 2017; World Health Organization, 2017, among others). In this sense, several diagnostic possibilities have emerged in recent years, and the serological test rK39 is among the most promising rapid tests due to its high sensitivity and specificity for the diagnosis of visceral leishmaniasis in symptomatic and asymptomatic patients (Maia et al., 2012; Boelaert et al., 2014; Bangert et al., 2018).

In order to develop new drugs and less invasive diagnostic procedure, it is necessary to better understand the parasite-host interaction and the factors that can promote disease severity and control. Several factors have been implicated in determining, or at least facilitating, the development of leishmaniasis in humans (reviewed by Conceição-Silva et al., 2018), and the consensus indicates that the presence of clinically detectable leishmaniasis occurs due to multiple factors related to both parasite and host. In this connection, in the last few years, an increased number of evidences have pointed several mechanisms that can take place according to the necessity for survival from both sides.

At the host side, the presence of malnutrition, comorbidities, extremes of age, amongst others may facilitate the evolution of leishmaniasis to more severe forms, since many of these factors act direct or indirectly on the ability of the immune system to respond adequately to the presence of the parasite (reviewed by Conceição-Silva et al., 2018). For example, in HIV-*Leishmania* coinfection patients, VL quickly accelerates the onset of AIDS and shortens their life-expectancy. Also, HIV increases the risk of clinical VL and the risk of atypical leishmaniasis (Freitas-Junior et al., 2012; Távora et al., 2015; Henn et al., 2018). In addition, during thousands of years, parasites and humans have co-evolved and, consequently, their surviving systems have been structured to avoid danger and damage. As a result, parasites have developed intricate strategies to subvert, modify and/or inhibit the host immune response. Positive selection pressure has improved species survival into the host environment based on more adapted individuals. Thus, the "good" parasite is that one capable of surviving while causing minimal damage to its host. The result of this encounter may lead to equilibrium (parasitic persistence) or disequilibrium (disease) of the parasite-host relationship. This point is easily demonstrated by the clinical disease onset in individuals under immunosuppressive status (recently reviewed by Akuffo et al., 2018; Conceição-Silva et al., 2018) even with no previous story of infection.

Two natural events proving the persistence of parasite are represented by 1- mucosal lesions produced years after primary cutaneous lesions (Leite et al., 2012; Ávila et al., 2018), and 2- the Post-Kal-azar dermal leishmaniasis (PKDL) after VL recovering (Ganguly et al., 2010; Singh et al., 2012; Zijlstra, 2016). In both cases, the same *Leishmania* species is able to produce, after healing, a different clinical form from primary manifestations. Although these manifestations appear in part of patients, since mainly *Leishmania donovani* is responsible for PKDL, and just few *Leishmania* species can produce mucosal forms, the importance of parasite in these late clinical manifestations is evident. Furthermore, isolates obtained from PKDL patients genetically differ from strains of patients who present just VL (Mishra et al., 2013). These differences may play a role in the pathogenesis of PKDL and in drug resistance to sodium antimony gluconate, miltefosine, and paromomycin (Mishra et al., 2013).

At the parasite side, different pathways to avoid or subvert the immune response have been demonstrated (reviewed by Duque and Descoteaux, 2015; Mandell and Beverley, 2016; Conceição-Silva et al., 2018, among others). The mechanisms of escape of *Leishmania* spp in their hosts is so varied that we decided to focus on some aspects of the interaction, notably those strategies observed at the beginning of infection, escape from NETs, cleavage of molecules from complement system, strategies to entry, and to survive inside permissive cells and subversion of macrophages and lymphocytes, as well as the capacity to use the normal regulatory immunological mechanisms to replicate and to establish infection.

One of the first steps of the *Leishmania*-host interaction occurs by the metacyclic promatigostes inoculation during the female sand fly feed.

HOW PARASITE PROMOTES SURVIVAL IN A NON-FRIENDLY ENVIRONMENT?

The First Step: Infection

Infection begins when a female sand fly interacts with the skin host and injects metacyclic promastigotes into the dermis. The proportion of metacyclic promastigotes delivered by the female sand fly into the skin is responsible for the success of the infection (Giraud et al., 2019). Flies infected for more days contain more parasite burden and are able to deliver higher numbers of parasites into the skin and their infective dose is enriched by non-metacyclic promastigotes (low-quality dose) (Giraud et al., 2019). This fact influences the pathology caused by *Leishmania mexicana* leading to exacerbated cutaneous lesions, enriched by neutrophils, and associated with low parasite load in the skin of mammalians (Giraud et al., 2019). A high-quality dose containing low quantity of promastigotes (∼100–1,000 parasites) but enriched by metacyclic promastigotes generates milder lesions with higher parasite load and is more effective in transmitting to other sand flies, showing the influence of parasite-vector relationship on the skin inflammatory response and on the final parasite load in the mammalian host (Giraud et al., 2019). Moreover, the traumatic changes caused by the contact of proboscides with skin and the disruption of the epidermis layers associated with the sand fly saliva induce the endothelial activation and neutrophil infiltration (Peters et al., 2008; Peters and Sacks, 2009). The inflammatory infiltrate generated creates a toxic environment from which promastigotes have to escape to survive. For this, promastigotes have to escape from extracellular toxic environment, enter the host cells, and convert into amastigote form. In this context, components in the sand fly saliva may help promastigotes in this issue. For example, saliva contains endonuclease, which digests Neutrophil Extracellular Traps (NETs) and inhibits blood coagulation, possibly allowing the local spread of promastigotes (Chagas et al., 2014).

Resident macrophages together with infiltrated neutrophils are the first cells to interact with *Leishmania* parasite upon infection. Neutrophils may exert a variety of effector mechanisms, such as phagocytosis, enzymes, and antimicrobial proteins release and NET formation (Kennedy and De Leo, 2009). *Leishmania amazonensis* promastigotes induce NET formation (Guimarães-Costa et al., 2009) and NETs were also demonstrated in active and chronic lesions of Tegumentary Leishmaniasis (TL) caused by *Leishmania braziliensis*, showing that even amastigotes may induce NET formation (Guimarães-Costa et al., 2009; Morgado et al., 2015). In *in vitro* system, NETs exerted restraint and toxic effects for *L. amazonensis* promastigotes (Guimarães-Costa et al., 2009), which could be reverted by the expression of *Leishmania* - 3'Nucleotidase/Nuclease activity digesting NETs and escaping killing by released NETs (Guimarães-Costa et al., 2014). In patients infected with *L. braziliensis*, ecto-nucleotidase activity is correlated with clinical manifestations: isolates from mucosal lesions presented higher ecto-nucleotidase activity than skin lesions (Leite et al., 2012). Furthermore, higher ecto-nucleotidase activity is also correlated with higher parasite load, and modulation of immune response by inhibiting dendritic cell activation and NO production (Leite et al., 2012). The interaction between NETs and macrophages favor the survival and persistence of parasites since it stimulates the M2 profile of macrophages, which are susceptible to *L. amazonensis* infection but unable to kill the parasite (Guimarães-Costa et al., 2017). Recently, *L. panamensis* resistant strains to miltefosine and meglumine antimoniate were described (Regli et al., 2018). These strains were able to modulate neutrophils stimulating the release of NETs and ROS production and survived better within neutrophils than the drug-susceptible strains (Regli et al., 2018). Altogether, these published data suggest that the induction of NET formation may lead to escape from extracellular effector immune mechanisms, facilitating the access of a permissive cell to parasite infection and persistence.

Still in the extracellular milieu, promastigotes have to survive from the effect of complement molecules. For this, LPG present in the parasite surface interferes with the complement cascade (Hermoso et al., 1991) and with the insertion of membrane attack complex (Puentes et al., 1990). In addition, the metallopeptidase GP63 cleaves the C3b molecule (Brittingham et al., 1995).

To enter host cells, *Leishmania* spp. uses manose-fucose (Akilov et al., 2007), Fc (Kima et al., 2000), fibronectin (Brittingham et al., 1999), and Toll-like receptors (Kropf et al., 2004), as well as CR1 and CR3 complement receptors (Blackwell et al., 1985; Wenzel et al., 2012). Inside the phagolysossoma, *Leishmania* spp have to escape from the acid environment, the action of enzymes and the microbicidal effects from oxygen and nitrogen radicals. In *L. donovani* experimental infection, the inhibition of phagolysosomes biogenesis was observed (Matheoud et al., 2013). As an effect of the metallopeptidase GP63 that mediates the cleavage of SNAREs, *L. donovani* infection prevented NADPH oxidase complex from assembling, altering the pH and phagosome degradative properties (Matheoud et al., 2013). As a result, antigen presentation via MHC-I was impaired, reducing the T cell activation (Matheoud et al., 2013).

During parasite-host macrophage interaction, *Leishmania* spp. infection may exert some impacts on signaling pathways leading to the inability of macrophages to kill intracellular parasites (Awasthi et al., 2003). For example, in experimental infection of BALB/c mice with *Leishmania major*, the CD40 signaling pathway is impaired (Awasthi et al., 2003). Thus, it results in the impairment of protein kinase C (PKCα, βI, βII, and ε) (Sudan et al., 2012) and the consequent reduction in p38MAPK phosphorylation and NOS2 expression, resulting in an impairment in killing *Leishmania* amastigotes (Awasthi et al., 2003). On the other hand, *L. major* infection enhances PKCδ, ζ, and λ isoforms, promoting ERK1/ERK2 phosphorilation, IL-10 production, and parasite growth (Sudan et al., 2012). These effects can be reverted using anisomycin, a p38MAPK activator, establishing a host-protective memory T cell response (Awasthi et al., 2003). *Leishmania donovani* infection differentially regulates small G-proteins: enhances N-Ras expression, whereas it inhibits K-Ras and H-Ras expression (Husein et al., 2018). It also increases extracellular signal–regulated kinase 1/2 phosphorylation and simultaneously decreases p38 phosphorylation, leading to the reduction of IL-12 and the increase of IL-10 expression (Husein et al., 2018). In macular PKDL patients, *L. donovani* infection decreased leucocyte rolling (L-selectin shedding) and induced up-regulation of the cellular signaling factors involved in pathogenesis (ERK1/2) as well as down regulated the signaling elements (p38 MAPK) involved in the Th1 response (Singh et al., 2018). The role of IL-10-induced immunosuppression in parasite persistence in visceral leishmaniasis and PKDL has already been described (Zijlstra, 2016; Lima et al., 2017; Bunn et al., 2018; Viana et al., 2019). *Leishmania infantum* subverts the host inflammatory response through the adenosine $A2_A$ receptor by inducing $CD4^+FOXP3^+$ T cells and IL-10 expression impairing the development of Th1-type adaptive immunity and promoting the establishment of infection (Lima et al., 2017). In experimental infection with *L. donovani*, the absence of IL-10 resulted in the control of parasite replication, but also caused tissue damage and the rupture of splenic microarchitecture (Bunn et al., 2018). PKDL is characterized by an intermediate position between a Th2 and Th1 response: the Th2 response shows the presence and persistence of IL-10 in the skin that was already present during VL, while systemically the Th1 response that was induced after VL therapy persists with IFN-γ production (Zijlstra, 2016).

Although not observed in *L. major* infection (Späth et al., 2008), in *L. donovani* infection, the inhibition of nitric oxide production by the protein tyrosine phosphatase (SHP-1) in mice macrophages was demonstrated *in vitro* and *in vivo* (Forget et al., 2006). The authors demonstrated that *Leishmania major* was able to inhibit the activation of JAK2 and ERK1/2 and the transcription factors NF-kB and AP-1 since SHP-1 is a negative regulator of these transcription factors (Forget et al., 2006; Blanchette et al., 2008). In addition, infection of macrophages with *L. major* induces the expression of Monarch-1, a negative regulator of NF-kB activation (Fata et al., 2013). *Leishmania infantum* infection induces the activation of phosphatidylinositol 3-kinase/Akt and extracellular signal-regulated kinase 1/2 and promotes the cleavage of the nuclear factor-kB $p65^{RelA}$ subunit

TABLE 1 | Main evasion mechanisms already described for *Leishmania* species.

Leishmania species	Escape mechanisms mainly described	Reference
L. major	Impairment in CD40 signaling.	Awasthi et al., 2003
	Impairment of protein kinase C (PKCα, βI, βII and ε) and enhancement of PKCδ, ζ and λ isoforms, promoting ERK1/ERK2 phosphorilation, IL-10 production and parasite growth.	Sudan et al., 2012
	Suppression of IL-2Rα expression by peripheral human T lymphocytes.	Khodadadi et al., 2013
	Induction of Monarch-1 expression by macrophages, a negative regulator of NF-kB activation.	Fata et al., 2013
	Hijack of host cell autophagy machinery to reduce T-cell proliferation.	Crauwels et al., 2015
	Induction of apoptosis of lymphocytes by the downregulation of Bcl-2 and over-expression of p53 and caspase-3.	Moshrefi et al., 2017
L. donovani	Inhibition of nitric oxide production and the activation of JAK2 and ERK1/2 and the transcription factors NF-kB and AP-1 by the protein tyrosine phosphatase (SHP-1) in macrophages.	Forget et al., 2006; Blanchette et al., 2008
	Different regulation of small G-proteins, enhancing N-Ras expression, and inhibiting K-Ras and H-Ras expression.	Husein et al., 2018
	Induction of PD-1 and CTLA-4 expression by lymphocytes.	Murphy et al., 1998
	Induction of PD-L2 expression by macrophages.	Medina-Colorado et al., 2017
	Inhibition of phagolysosomes biogenesis, NADPH oxidase complex assembling, altering the pH and phagosome degradative properties, and inhibiting antigen presentation via MHC-I.	Matheoud et al., 2013
	Induction of the transcription factor IRF-5 that limits CD8 T cells expansion and inhibits IL-12 expression.	Hammami et al., 2015
L. braziliensis	Reduction of NO production and high infection index *in vitro*.	Campos et al., 2008
	Decrease of BLT1 receptor, which recognizes the lipid leukotriene B4 (LTB4).	Morato et al., 2014
	Increase of superoxide dismutase 1 (SOD1) by macrophages.	Khouri et al., 2014
	Ecto-nucleotidase activity.	Leite et al., 2012
L. amazonensis	Phosphatidylserine exposition.	Wanderley et al., 2009
	Activation of NF-kB repressor complex p50/p50 that negatively regulates NOS2 expression interfering with NO production.	Calegari-Silva et al., 2009
	Induction of NETs and stimulation of M2 profile.	Guimarães-Costa et al., 2017
	Increase of superoxide dismutase 1 (SOD1) by macrophages.	Khouri et al., 2014
	Downregulation of macrophage iNOS expression via Histone Deacetylase 1 (HDAC1).	Calegari-Silva et al., 2018
L. infantum	Use of apoptosis from host cell as a mean to survive and replicate. The mechanism should be clarified.	Moreira et al., 2013
	Expression of 3'Nucleotidase/Nuclease activity.	Guimarães-Costa et al., 2014
	Manipulation of AMPK activation.	Moreira et al., 2015
	Production of the enzyme ornithine descarboxylase, which plays a role in the synthesis of tripanothione and the modulation of the immune response and pathogenesis.	Yadav et al., 2015
	Lower expression of TLR2, TLR9, HLA-DR and TNF-α, resulting in less control of parasite load.	Viana et al., 2018
	Induction of MHC Class IIhigh DC to polarize CD4+ T Cells toward a nonprotective T-bet+ IFN-g+IL-10+ phenotype.	Resende et al., 2013
L. guyanensis	Induction of the up-regulation of the A20 protein, avoiding the inflammasome pathways.	Hartley et al., 2018

by infected DCs (Neves et al., 2010). Therefore, *Leishmania* can inhibit microbicidal oxygen and nitrogen radicals, enabling them to escape from effector mechanisms upon phagocytosis. Some of these effects could be reversed *in vitro* using meglumine antimoniate, but nitric oxide production was only recovered using the drug associated with TNF-α (Muniz-Junqueira and de Paula-Coelho, 2008).

In human cutaneous leishmaniasis, the oxidative burst of monocytes is higher than that from healthy donors (Carneiro et al., 2016). However, NO alone is not sufficient to control the parasite load (Carneiro et al., 2016). This capacity to resist or interfere with NO production by macrophages depends on the *Leishmania* species involved (**Table 1**; Campos et al., 2008). Therein, *L. braziliensis* isolated from Mucosal Leishmaniasis patients showed the highest infection index and the lowest NO production *in vitro* by macrophages when compared to the infection by the other species of subgenus *Viannia* (Campos et al., 2008). In contrast, *L. naiffi*, which generally causes a benign and autoresolutive infection in humans, showed the lowest infection index and the highest NO production (Campos et al., 2008). In another study, promastigotes isolated from patients with mucosal leishmaniasis express more thiol-specific antioxidant protein, and were more resistant to nitric oxide and H_2O_2 than strains obtained from localized cutaneous leishmaniasis (Ávila et al., 2018). *Leishmania amazonensis*, which is capable of inducing severe diffuse cutaneous form cursing with high parasite load and inactivation of macrophages, also developed strategies to escape from oxidative effects from phagocytes. For example, *L. amazonensis* activates the NF-kB repressor complex p50/p50 that negatively regulates NOS2 expression interfering with NO production (Calegari-Silva et al., 2009). *Leishmania donovani* produces ornithine decarboxylase, which plays a role in the synthesis of tripanothione, the major reduced thiol responsible for the modulation of the immune response and pathogenesis in visceral leishmaniasis (Yadav et al., 2015). In this last study, the effects of a recombinant ornithine decarboxylase from *L. donovani* (r-LdODC) on the immune response of peripheral blood mononuclear cells of patients affected by visceral leishmaniasis were observed (Yadav et al., 2015). The r-LdODC induced the production of IL-10 from CD4 T cells and

the reduced IL-12 and NO production (Yadav et al., 2015). The induction of proinflammatory mediators such as TNF-α and IL-6 through the transcription factor IRF-5 by *L. donovani* has also been demonstrated (Hammami et al., 2015). IRF-5 also limits CD8 T cell expansion and inhibits IL-12 expression, favoring the establishment of persistent infection (Hammami et al., 2015).

Leishmania spp can also interfere with immune cell-cell communication, inhibiting an efficient immune response. For example, *L. major* can suppress IL-2Rα expression by peripheral human T lymphocytes (Khodadadi et al., 2013). This suppression impacts the proliferation of T cells, stimulation of NK cells, and IFN-γ production, thus resulting in a failure of immune response. In this sense, *L. infantum* may induce MHC Class II^{high} DC to polarize $CD4^+$ T Cells toward a non-protective T-bet^+ IFN-g^+IL-10^+ phenotype, which is associated with chronicity and prolonged parasite persistence (Resende et al., 2013). Differences in the capability to modulate the effector response from monocytes by both species have also been demonstrated (Viana et al., 2018). *Leishmania infantum* infections lead to lower expression of TLR2, TLR9, HLA-DR and TNF-α, resulting in less control of parasite load, which may reflect upon the distinct clinical course observed in patients presenting visceral and tegumentary leishmaniasis (Viana et al., 2018).

Once the parasite converts into intracellular amastigotes, the next step is dissemination. A study comparing *L. major*—promastigotes and amastigotes infection of macrophages—showed that while infection with promastigotes induced inflammatory mediators, such as TNF-α and chemokines, amastigote infection was silent resulting in increased parasite load (Wenzel et al., 2012).

The Infection Continuity: A Question of Response Subversion to Promote *Leishmania* spp Survival

Sand fly saliva is composed of multiple components with a variety of functions and is able to immunomodulate macrophages (Lerner et al., 1991; Morris et al., 2001; Oliveira et al., 2008). Maxadilan, the most well-defined component from *Lutzomyia longipalpis* saliva, alone decreases TNF-α, IL-10 and increases IL-6, IL-8, and IL-12 production in LPS stimulated human macrophages (Costa et al., 2004). In addition, saliva from *Lutzomyia longipalpis* increases the anti-inflammatory mediator PGE2 and reduces the lipid leukotriene B4 (LTB4), favoring *L. infantum* infection in C57BL6 mice (Araújo-Santos et al., 2014). *Leishmania* spp. may also affect macrophage profile and functions. Infection with *L. braziliensis* leads to the decrease of BLT1 receptor, which recognizes LTB4 (Morato et al., 2014). LTB4-BLT1 recognition activates pro-inflammatory responses and stimulates the leishmanicidal activity of macrophages and neutrophils by inducing ROS secretion (Morato et al., 2014; Plagge and Laskay, 2017). Depending on the species, *Leishmania* can differently modulate macrophages. For example, infection with *L. baziliensis* promotes the infiltration of intermediate monocytes that express TNF and IL1β and enhance the inflammatory response in human patients (Passos et al., 2015; Santos et al., 2018). LPG from *L. braziliensis* was able to induce higher TNF-α, IL-6, IL-1β, and NO production by infected macrophages than LPG from *L. infantum* (Ibraim et al., 2013). In addition, *L. braziliensis* activates NF-kB, while no ERK activation by *L. infantum* LPG was demonstrated (Ibraim et al., 2013). In fact, the production of IL-1β by cutaneous leishmaniasis patients is associated with chronic inflammation and tissue damage (Novais et al., 2017). *L. amazonensis* induces HDAC1, which negatively regulates NOS2 expression contributing to the hyporeactive state of macrophages and to the replication of amastigotes (Calegari-Silva et al., 2018). *Leishmania infantum* is able to modulate host macrophage mitochondrial metabolism by hijacking the SIRT1-AMPK axis (Moreira et al., 2015). Parasites alter the macrophage metabolism toward aerobic glycolysis (Warburg effect) with a concomitant decrease of mitochondrial function, leading to the accumulation of intracellular ATP (Moreira et al., 2015). Consequently, an activation of AMPK is observed and leads to catabolic processes to restore intracellular energy and nutrients that can nourish the parasite (Moreira et al., 2015). Besides that, *Leishmania* parasites activate the PERK/eIF2α/ATF-4 pathway in cultured macrophages and infected human tissue protecting themselves from the harmful consequences of cellular stress, thus contributing to parasite survival and progression of the infection (Dias-Teixeira et al., 2017). Recently, the modulation of human macrophages by *L. infantum*—MicroRNA hsa-miR-346 demonstrated to play a role in regulating macrophage functions since several MHC- or interferon-associated genes are targets for this miRNA (Diotallevi et al., 2018).

Apoptosis is a process of cell death that maintains tissue homeostasis (Trahtemberg and Mevorach, 2017). Apoptotic cells present morphological and functional characteristics, such as chromatin condensation, pyknotic, and fragmented nuclei, apoptotic bodies formation, and phosphatidylserine (PS) exposition (Elmore, 2007; Trahtemberg and Mevorach, 2017). PS is recognized by regulatory receptors, such as TIM-3, which inhibits the inflammatory response (Kerr et al., 2018). As an escape mechanism, promastigotes may also inhibit the inflammatory process due to exposition of PS (Wanderley et al., 2009). Different from amastigotes whose entire population expresses PS, part of *L. amazonensis* promastigotes are PS^+ and modulate inflammatory infiltrate, while PS^- promastigotes are able to successfully infect macrophages and survive intracellularly due to host phagocyte inactivation and reduction of NO production (Wanderley et al., 2009). Apoptotic parasites stimulate TGF-β production, silencing macrophages and favoring the survival of viable parasites (Aga et al., 2002; van Zandbergen et al., 2004). Therefore, efficient *in vivo* and *in vitro* infection occurred only when PS positive and negative promastigotes subpopulations were added simultaneously (Wanderley et al., 2009). Apoptotic-like *Leishmania* also uses host cell autophagy machinery (Crauwels et al., 2015). Therefore, T cell proliferation is inhibited favoring the overall population survival (Crauwels et al., 2015). Autophagy machinery plays a role during homeostasis by clearing apoptotic bodies in a process known as LC3-associated phagocytosis and promotes an anti-inflammatory response with production of IL-10 and TGF-β and hampering the production

of proinflammatory cytokines, such as TNF-α, IL-1B, and IL-6 (Crauwels et al., 2015), generating a microenvironment favorable to *Leishmania* survival and replication.

Still at the beginning of infection, the infiltrating neutrophils rapidly respond to the infection and phagocytize the promastigotes and die generating apoptotic bodies that inhibit the response of macrophages (Afonso et al., 2008; Ribeiro-Gomes and Sacks, 2012). In established infection, apoptosis of host cells has been correlated with disease progression and increase of parasite load, suggesting the parasite can use the normal regulatory process to escape from effector mechanisms from leucocytes (Moreira et al., 2013). *Leishmania major* infection induces apoptosis of lymphocytes by the down-regulation of Bcl-2 and over-expression of p53 and caspase-3 (Moshrefi et al., 2017). However, how *Leishmania* spp may use this mechanism to evade immune response has yet to be clarified. In fact, apoptosis of inflammatory cells may occur as a result of cellular exhaustion (Liu et al., 2018). Cellular exhaustion was first described in chronic viral infection and manifested at the beginning of infection, being characterized by the expression of PD-1 receptor (Programmed Death 1) (Barber et al., 2006). PD-1 expression is induced by repeated antigenic stimulation of T and B lymphocytes (Eichbaum, 2011). The PD-ligand 1 (PD-L1) is constitutively expressed by B and T lymphocytes, macrophages and dendritic cells from spleen (Eichbaum, 2011). PD-1 activation induces apoptosis, down-regulates cellular proliferation and cytokine expression (Joshi et al., 2009). PD-1 and CTLA-4 expression by CD8 cells from peripheral blood and spleen were demonstrated in human VL (Gautam et al., 2014) and in *L. donovani*-infected mice (Murphy et al., 1998). The exhaustion pathway blockage with anti-CTLA-4 antibody increased IFN-γ and IL-4 expression in murine spleen and liver, as well as accelerated the development of hepatic granulomatous response associated with the reduction of parasite load (Joshi et al., 2009).

Esch et al. (2013) studied dogs with VL that showed $CD4^+PD\text{-}1^+$ and $CD8^+PD\text{-}1^+$ cells in peripheral blood. These cells presented reduced proliferation index, as wells as reduced IFN-γ expression. Blockage of the exhaustion pathway *in vitro* recovered the T cell effector functions, such as proliferation index and oxidative radical production. As a result, the parasite load was partially controlled by monocytes. Exhaustion of macrophages has also been demonstrated in *L. donovani* infection (Medina-Colorado et al., 2017). The blockage of PD-L2 was able to induce a reduction in arginase-1 and to control the parasite load; however, no alterations in IFN-γ nor NOS2 were demonstrated (Medina-Colorado et al., 2017). Despite the Th1 response induced and the IFN-γ expression detected during leishmaniasis, amastigotes are able to survive probably by using normal regulatory mechanisms developed by the immune system that prevents tissue damage and maintains the homeostasis. In this context (Kong et al., 2017), observed that IFN-γ enhanced *L. donovani* growth and induced the counter-regulatory molecules STAT3, IL-10, Arg1, Ido1, and Irg1 in splenic macrophages, which suggests that splenic macrophages in VL are conditioned to respond to macrophage activation signals with a counter-regulatory response, which is ineffective and even disease-promoting (Kong et al., 2017). M2 macrophages were also observed during *Leishmania* spp infection (Moreira et al., 2016; Hu et al., 2018; Kumar et al., 2018; Lee et al., 2018). The M2 profile has been described as a cell type that participates in the processes of cellularity reduction in the inflammatory infiltrate, tissue remodeling, and healing (Tomiotto-Pellissier et al., 2018). In this regard, it produces IL-10, TGF-b, and endothelium growth factors make a cell unable to express NOS2 and kill intracellular amastigotes, favoring *Leishmania* replication and persistence.

Recently, the capacity of *Leishmania* spp to modify its genome constitution in order to better adapt to different environments has been demonstrated for *L. donovani, L. major,* and *L. tropica* complexes (Prieto Barja et al., 2017; Bussotti et al., 2018). Aneuploidy has been described for *Leishmania* parasites and this phenomenon generates karyotypic fluctuations that are correlated with phenotypic variations, impacting the proliferative, and infectivity capacities (Prieto Barja et al., 2017). *Leishmania* clones containing beneficial haplotypes selected by the environment give rise to specific copy number variation profiles that could represent a fitness gain to new hostile environments (Bussotti et al., 2018). Therefore, *Leishmania* is able to change its chromosome and gene copy number to adapt to environmental changes (Prieto Barja et al., 2017; Bussotti et al., 2018). In this sense, the microenvironment generated by immune cells from the mammalian host or by anti-*Leishmania* drugs may constitute a bottle neck for the selection of better adapted clones, enabling the persistence of parasites. For example, the allopurinol-resistance of *L. infatum* strain was associated with chromosome and gene copy number variations (Yasur-Landau et al., 2018). The gene encoding the s-adenosylmethionine synthetase (METK) showed diminished copy numbers in allopurinol-resistance strains (Yasur-Landau et al., 2018). The deletion of the gene LinJ.36.2510 that encodes 24-sterol methyltransferase was associated to amphotericin B-resistance (Rastrojo et al., 2018). And whole genomic sequencing of *L. mexicana* strain showed an association between anphotericin B resistance and mutation of the sterol biosynthesis gene (Pountain et al., 2019). Moreover, a comparative proteomic analysis revealed the role of the iron superoxide dismutase in miltefosine resistance of *L. donovani* strains (Veronica et al., 2019). In another study, genomic analysis of *L. infantum* strains evidenced an association between deletion or mutations in LiMT and LiRos3 genes and miltefosine-resistance (Mondelaers et al., 2016). Finally, the increase of thiol levels was associated to antimony-resistance indicating that the redox metabolism has a role in the antimony-resistance of new world VL isolates (Magalhães et al., 2018).

Once the parasite is able to successfully establish growth and survival in the cells from mammalian host, clinical disease can be detected. However, a certain number of infected individuals are able to control parasite replication as well as the immune response, becoming permissive to parasite persistence. In this case they are considered infected but not sick. In this context, patients with subclinical infection with *L. braziliensis* may present more $CD8^+IFN\text{-}\gamma^+$ cells and less Cytotoxic $CD8^+$ T cells than patients manifesting cutaneous leishmaniasis (Cardoso et al.,

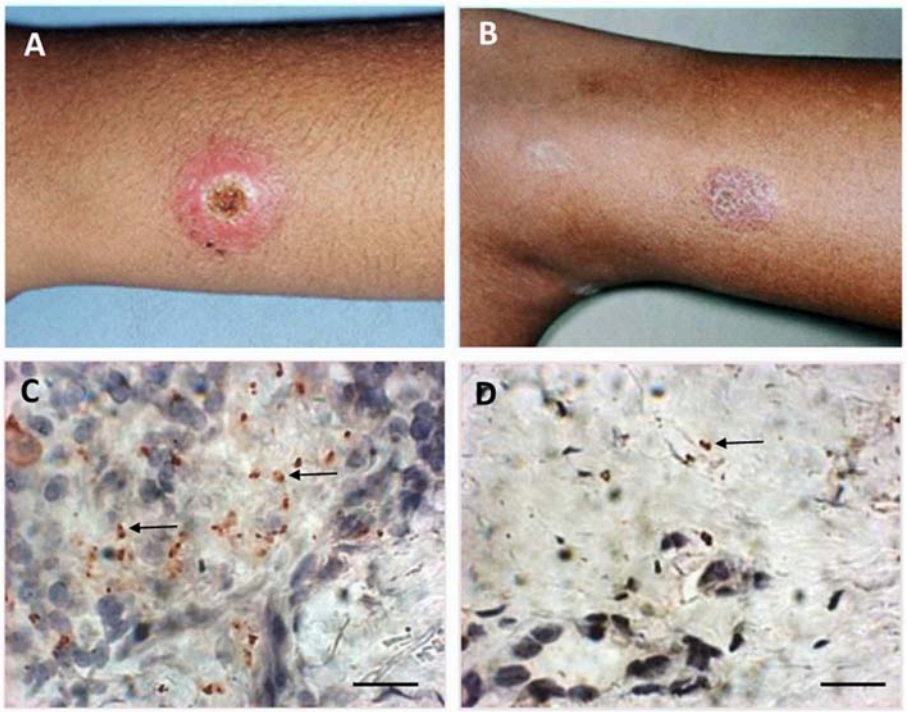

FIGURE 1 | Macroscopic and microscopic aspects of active lesion and scar of American Tegumentary Leishmaniasis. **(A)** Active lesion—single ulcer with elevated borders and granulomatous aspect in center. **(B)** Scar—atrophic scar after successful treatment. **(C)** Several amastigotes detected by immunohistochemistry (arrows) involved by a granulomatous reaction in an active lesion. **(D)** Two amastigotes (arrow) detected by immunohistochemistry near a discrete inflammatory reaction characterized by cell niches in a scar. Magnification bar = 10 μm.

2015). However, even these subclinical patients maintain latent parasites that may reactivate in case of immunosuppression (Conceição-Silva et al., 2018). How do parasites persist in mammalian tissues? How does mammalian host contain parasite replication? Answering these questions is crucial to understand the role of both sides to survive without serious damage. Consequently, this knowledge may improve the design of new methods for diagnosis, the development of new drugs, as well as the way to construct a vaccine.

IS THERE AN END IN *LEISHMANIA* SPP INFECTION? AN UPDATE

Recently, some factors enrolled in parasite persistence were reviewed (Conceição-Silva et al., 2018). In this connection, the *Leishmania* spread and persistence in different sites have been well-characterized by different authors. Thus, it was already described that in active cutaneous leishmaniasis patients, the parasite can be present in extralesional sites (Romero et al., 2010; Canário et al., 2019). In this subject, Canário et al. (2019) showed that positivity in healthy mucosa was high in patients with more severe cutaneous lesions and those who needed to be treated longer. However, we still do not know whether parasite burden can influence parasite persistence. Evidences of parasite persistence were not restricted to cutaneous leishmaniasis. In visceral leishmaniasis, parasites may persist after clinical cure of primary manifestations leading to PKDL (Ganguly et al., 2010; Singh et al., 2012; Zijlstra, 2016) or to visceral leishmaniasis reactivation in HIV patients (Freitas-Junior et al., 2012; Távora et al., 2015; Henn et al., 2018). In addition, the presence of some differences in evasion mechanisms according to *Leishmania* infection produced by different species (de Freitas et al., 2016, among others) has been shown.

Direct or indirect evidences of parasite persistence after healing have been demonstrated since the 1990's (reviewed by Conceição-Silva et al., 2018) (**Figure 1**). Thus, the importance of the mouse genetic background in the development of disease or parasite persistence has been explored by different research groups (reviewed by Launois et al., 1997; Fowell and Locksley, 1999; Conceição-Silva et al., 2018). In addition, *Leishmania* profile has also been implicated in different degrees of infection and healing (De Luca and Macedo, 2016). It was already discussed the *Leishmania* capacity to modify its genome in order to increase the survival in hostile environment (Prieto Barja et al., 2017; Bussotti et al., 2018, see above). This phenomenon would help parasite to survive either during active disease or healing phase.

One of the first pieces of information about how parasite could persist after leishmaniasis healing showed that parasites could subvert the production of reactive nitrogen and oxygen intermediates and modulate the cytokine production, such as interleukin 12, by the host cells (Bogdan et al., 1996; Stenger

et al., 1996; Bogdan and Röllinghoff, 1998). These functions have been detected both *in vitro* and *in vivo* using mouse model of *L. major* infection. Later on, in animal model, it was shown that, in addition to the parasites inside macrophages, 40% of the persistent parasites were associated with fibroblasts with reduced expression of NOS2, pointing the importance of these cells to promote parasite survival (Bogdan et al., 2000). It was also demonstrated that GP63 metalloprotease from parasite can inhibit key microbicidal activity by altering antigen presentation and important metabolic and signaling pathways subverting macrophage function in controlling parasite growth (reviewed by Duque and Descoteaux, 2015; Soulat and Bogdan, 2017). In addition, it was also shown that *Leishmania* parasites harboring *Leishmania* RNA virus 1 (LRV1) can promote macrophage survival via LRV1 recognition through TLR-3. The authors showed in an *in vitro* model the possibility of LRV1 interference leading therefore to an increased infection in macrophages (Eren et al., 2016). Hence, the concomitant presence of parasitized macrophages and fibroblasts could produce a balance between death and survival, which would allow the control of parasite growth via continuous immunological stimulus and at the same time would allow a continuous presence of live parasites. In this sense, the persistence parasite at the primary infection site and as a result the continuous antigenic stimulus that leads to long-lasting immunity to reinfection was discussed previously (Okwor and Uzonna, 2008). Nowadays, pieces of evidence of parasite persistence in leishmaniasis are getting more robust. However, we still do not know a real percentage of patients that maintain a tissue parasitism and exactly how the host keeps the parasite under control. Hence, detailed information of how it does occur and the implication of this persistence in the protection to reinfection are still under construction. As tissue parasite distribution seems to be heterogeneous, and different methodological approaches can influence the positivity, one cannot affirm that negative cases reached a sterile healing. In this context, Morgado et al. (2010) showed by immunohistochemistry a gradual reduction of inflammatory reaction after clinical cure, which could be observed even in 3-year-old scars (Morgado et al., 2010). The maintenance of inflammatory profile restrict to niches of cells was associated with the evidence of parasites in 2 scars from evaluated patients (Conceição-Silva et al., 2010; Morgado et al., 2010).

PCR detection of parasites has been widely used as a method to identify *Leishmania* spp in different tissues, but the primer design is considered crucial to detect parasites, since it has been shown that the use of different primers can produce different percentage of positivity (Romero et al., 2010). Nevertheless, parasites have been detected by PCR in different tissues upon infection, even in the absence of clinical disease. Authors have reported the presence of viable parasites in nasal, oral and conjunctival mucosa as well as in blood mononuclear cells, tonsils and normal skin in asymptomatic individuals and also in patients with isolated cutaneous lesions, demonstrating parasite dissemination without evidences of disease (Martinez et al., 1992; de Oliveira Camera et al., 2006; Vergel et al., 2006; Figueroa et al., 2009; Romero et al., 2010; Rosales-Chilama et al., 2015, among others). Figueroa et al. (2009) showed the presence of *Leishmania* spp in 81% of nasal tissues of patients with active cutaneous leishmaniasis without clinical signs of nasal lesion. In addition, Martinéz-Valencia et al. (2017) detected by PCR-Southern blot a percentage of positivity in 30% of the healed patients evaluated 13 weeks after treatment initiation. Rosales-Chilama et al. (2015) detected parasites in 40% of healthy individuals living in endemic areas and presenting positivity to Montenegro skin test (MST+). These authors were able to demonstrate parasite viability in 59% of the MST+ individuals. Interestingly, they were also able to detect parasites in few negative MST volunteers. Taken together, these results confirm the dissemination of *Leishmania* parasites in different host tissues during the active disease. They also confirm the persistence of parasites in humans after healing, and most importantly, even in healthy individuals without clinical signs of past active or healed tegumentary leishmaniasis.

Protozoan persistence seems to be very frequent in infected individuals, and the onset of an immunosuppression can lead to a recrudescent disease, even in those cases in which the primo infection was silent (discussed in Conceição-Silva et al., 2018). In leishmaniasis, the distribution of the parasite in the tissues from mammalian host appears to occur very early during the infection. In this sense, these results presented above confirm that, at least in leishmaniasis caused by the subgenus *Viannia*, parasites are precociously located in the mucosae of the upper airways and digestive tracts. However, it has not yet been proven whether this fact facilitates the appearance of secondary mucosal lesions.

What are the advantages or disadvantages of parasite persistence to the host? One possibility is to protect individuals against new infection. However, it was already demonstrated that, at least in mouse model, the immune response elicited by the persistent parasite do not always avoid the possibility of a re-infection (Mandell and Beverley, 2016, among others). On the other hand, the infection does not necessarily evolve into the disease, and even if reinfection is not avoided, the persistence of the parasite may prevent the development of clinical manifestations as long as the immune system is competent. The understanding of this complex host-parasite interaction and the identification of favorable and effective immune responses capable maintaining this equilibrium could be used in vaccine development (Okwor and Uzonna, 2008; De Luca and Macedo, 2016). In addition, Mandell and Beverley (2016) discussed that persistent infection of *L. major* would work as a "natural vaccination" in a condition known as concomitant immunity. Although concomitant immunity seems to be an advantage for the host, this interaction also promotes a potential dangerous condition since if one of the actors modifies the profile (i.e., increased parasite virulence or immunosuppression) the host-parasite equilibrium can be broken leading to the development of severe disease. In this context, the authors showed in a mouse model of leishmaniasis resistance that after a secondary challenge parasites are able to colonize and persist as much as the parasites from the primary infection. However, disease is weak when compared with the primary clinic onset. According to the authors, these results indicated that this strategy would facilitate the generation of parasite diversity during the life cycle maintenance. The same authors (Mandell

and Beverley, 2017), using mouse model of *Leishmania major* infection, described the presence of two parasite populations: one with normal replication rate and a second one with very low replication. In addition, they also demonstrated parasites inside NOS^+ cells, indicating a dynamic control of parasite burden as the number of parasites keeps almost the same throughout the study. They concluded that the constant parasite replication and death are implicated in concomitant immunity and thus are beneficial to both parasite and host. It was not observed an attenuation of NO production by the increase of substrate competition. Both NOS2 and arginase utilize L-arginine as substrate and Paduch et al. (2019) demonstrated that Arginase I (Arg1)-deficient C57BL/6 mice were able to control *Leishmania* infection as much as the wild type. The absence of Arg1 did not affect parasite burden, NO production, or host cell parasitism. In wild type, they detected Arg1 in skin during active lesions but not in healed tissue. The authors also showed parasites in NOS2 negative areas enriched by myeloid cells and fibroblasts. In conclusion, the authors indicated that Arg1 is not essential to parasite control and lesion healing. On the other hand, arginase was already detected in *Leishmania* parasites, mainly in glycosomes (da Silva et al., 2012; Soares-Bezerra et al., 2013). Arginase pathway is necessary to produce polyamines, which have multiple roles in stabilizing nucleic acids and membranes, as well as regulating cell growth and differentiation. In this context, it has been demonstrated the importance of arginase activity in parasites, since replication is mainly dependent on polyamines (Badirzadeh et al., 2017). Nevertheless, it has already been demonstrated a NO production by *Leishmania* parasites (Géigel and Leon, 2003; Genestra et al., 2003a,b,c), and *Leishmania*-NO seems to have a role during host-parasite interaction (Temporal et al., 2005; Badirzadeh et al., 2017).

Recently, Holowka et al. (2016) studied the influence of *Leishmania*-encoded othologs of macrophage migration inhibitory factor in parasite survival and persistence, using KO parasites ($mif^{-/-}$) to cytokine macrophage migration inhibitory factor (MIF) and a wild type ($mif^{+/+}$) as control. The results showed that mice infected with $mif^{-/-}$ parasites had three times less parasites, a decrease in antigen presenting cells activation, as well as in T cell priming and CD4 effector cells, leading to diminished inflammation signs. On the other hand, the infection promoted differences in the expression of exhaustion markers when compared with the infection produced by the $mif^{+/+}$ *Leishmania major*. Taken the results together, the authors pointed out the influence of MIF produced by *L. major* to facilitate parasite persistence. In this aspect, Soulat and Bogdan (2017) reviewed the influence of parasites and host phosphatases on the host immune response mainly by modulating macrophage function. This group of molecules would act deactivating phagocytes' host, by inhibiting or stimulating different pathways of activation. One example, amongst others, is the reduced ROS release provoked by GP63, one of the most abundant *Leishmania* surface molecules. Other phosphatases can also act on macrophages function, allowing parasite survival (reviewed by Soulat and Bogdan, 2017).

FINAL CONSIDERATIONS

In summary, results published until now point out an important influence of *Leishmania* species and their intrinsic diversity to promote and sustain parasite survival and persistence after infection. It could be detected in patients after clinical disease healing as well as in healthy individuals from endemic areas, without any signs of past sickness, and in tissues where no clinical signs of lesion were observed. Understanding the dynamic of parasite spread and tropism (if any), and the evasion mechanisms enrolled in persistence can indicate new steps for the design of new drugs and vaccines in order to control leishmaniasis.

AUTHOR CONTRIBUTIONS

FC-S and FM conceived the manuscript and wrote, reviewed, and approved the manuscript. FC-S conceived the figure. FM conceived the table.

FUNDING

This study was funded by PAEF-IOC-Fiocruz (IOC-023-FIO-18-2-47) and by CNPq-Universal (421223/2018-9).

ACKNOWLEDGMENTS

We would like to thank Drs. A. Schubach, M. Lyra, and M. I. F. Pimentel from the LaPClin Vigileish-Evandro Chagas National Institute of Infectious Diseases -INI- Fiocruz for the photos in **Figure 1**, and Dr. L. L. Leon for the valuable discussion on parasite NO and arginase.

REFERENCES

Afonso, L., Borges, V. M., Cruz, H., Ribeiro-Gomes, F. L., Dos Reis, G. A., Dutra, A. N., et al. (2008). Interactions with apoptotic but not with necrotic neutrophils increase parasite burden in human macrophages infected with *Leishmania amazonensis*. *J. Leukoc. Biol.* 84, 389–396. doi: 10.1189/jlb.0108018

Aga, E., Katschinski, D. M., van Zandbergen, G., Laufs, H., Hansen, B., Müller, K., et al. (2002). Inhibition of the spontaneous apoptosis of neutrophil granulocytes by the intracellular parasite *Leishmania major*. *J. Immunol.* 169, 898–905. doi: 10.4049/jimmunol.169.2.898

Ait Kbaich, M., Mhaidi, I., Ezzahidi, A., Dersi, N., El Hamouchi, A., Riyad, M., et al. (2017). New epidemiological pattern of cutaneous leishmaniasis in two pre-Saharan arid provinces, southern Morocco. *Acta Trop.* 173, 11–16. doi: 10.1016/j.actatropica.2017.05.016

Akilov, O. E., Kasuboski, R. E., Carter, C. R., and McDowell, M. A. (2007). The role of mannose receptor during experimental leishmaniasis. *J. Leukoc. Biol.* 81, 1188–1196. doi: 10.1189/jlb.0706439

Akuffo, H., Costa, C., van Griensven, J., Burza, S., Moreno, J., and Herrero, M. (2018). New insights into leishmaniasis in the immunosuppressed. *PLoS Negl. Trop. Dis.* 12:e0006375. doi: 10.1371/journal.pntd.0006375

Alvar, J., Vélez, I. D., Bern, C., Herrero, M., Desjeux, P., Cano, J., et al. (2012). Control team. *Leishmaniasis* worldwide and global estimates of its incidence. *PLoS ONE* 7:e35671. doi: 10.1371/journal.pone.0035671

Araújo-Santos, T., Prates, D. B., França-Costa, J., Luz, N. F., Andrade, B. B., Miranda, J. C., et al. (2014). Prostaglandin E2/leukotriene B4 balance induced by *Lutzomyia longipalpis* saliva favors *Leishmania infantum* infection. *Parasit. Vect*. 7:601. doi: 10.1186/s13071-014-0601-8

Ávila, L. R., Gomes, C. M., Oliveira, P. G., Gomes, R. S., Vinaud, M. C., Dorta, M. L., et al. (2018). Promastigote parasites cultured from the lesions of patients with mucosal leishmaniasis are more resistant to oxidative stress than promastigotes from a cutaneous lesion. *Free Radical. Biol. Med.* 129, 35–45. doi: 10.1016/j.freeradbiomed.2018.09.005

Awasthi, A., Mathur, R., Khan, A., Joshi, B. N., Jain, N., Sawant, S., et al. (2003). CD40 signaling is impaired in *L. major*-infected macrophages and is rescued by a p38MAPK activator establishing a host-protective memory T cell response. *J. Exp. Med.* 197, 1037–1043. doi: 10.1084/jem.20022033

Azimi, F., Shirian, S., Jangjoo, S., Ai, A., and Abbasi, T. (2017). Impact of climate variability on the occurrence of cutaneous Leishmaniasis in Khuzestan Province, southwestern Iran. *Geospat. Health*. 12:478. doi: 10.4081/gh.2017.478

Badirzadeh, A., Taheri, T., Taslimi, Y., Abdissamadi, Z., Heidari-Kharaji, M., Gholami, E., et al. (2017). Arginase activity in pathogenic and non-pathogenic species of *Leishmania*-parasites. *PLoS Negl. Trop. Dis.* 11:e0005774. doi: 10.1371/journal.pntd.0005774

Bangert, M., Flores-Chávez, M. D., Llanes-Acevedo, I. P., Arcones, C., Chicharro, C., García, E., et al. (2018). Validation of rK39 immunochromatographic test and direct agglutination test for the diagnosis of Mediterranean visceral leishmaniasis in Spain. *PLoS Negl. Trop. Dis*. 12:e0006277. doi: 10.1371/journal.pntd.0006277

Barber, D. L., Wherry, E. J., Masopust, D., Zhu, B., Allison, J. P., Sharpe, A. H., et al. (2006). Restoring function in exhausted CD8 T cells during chronic viral infection. *Nature* 439, 682–687. doi: 10.1038/nature04444

Baylis, M. (2017). Potential impact of climate changes on emerging vector-borne and other infections in the UK. *Environ. Health* 16:112. doi: 10.1186/s12940-017-0326-1

Blackwell, J. M., Ezekowitz, R. A., Roberts, M. B., Channon, J. Y., Sim, R. B., and Gordon, S. (1985). Macrophage complement and lectin-like receptors bind *Leishmania* in the absence of serum. *J. Exp. Med*. 162, 324–331. doi: 10.1084/jem.162.1.324

Blanchette, J., Abu-Dayyeh, I., Hassani, K., Whitcombe, L., and Olivier, M. (2008). Regulation of macrophage nitric oxide production by the protein tyrosine phosphatase Src homology 2 domain phosphotyrosine phosphatase 1 (SHP-1). *Immunology* 127, 123–133. doi: 10.1111/j.1365-2567.2008.02929.x

Boelaert, M., Verdonck, K., Menten, J., Sunyoto, T., van Griensven, J., Chappuis, F., et al. (2014). Rapid tests for the diagnosis of visceral leishmaniasis in patients with suspected disease. *Cochrane Database Syst. Rev.* 2014:CD009135. doi: 10.1002/14651858.CD009135.pub2

Bogdan, C., Donhauser, N., Döring, R., Röllinghoff, M., Diefenbach, A., and Rittig, M. G. (2000). Fibroblasts as host cells in latent leishmaniosis. *J. Exp. Med*. 191, 2121–2130. doi: 10.1084/jem.191.12.2121

Bogdan, C., Gessner, A., Solbach, W., and Röllinghoff, M. (1996). Invasion, control and persistence of *Leishmania* parasites. *Curr. Opin. Immunol.* 8, 517–525. doi: 10.1016/S0952-7915(96)80040-9

Bogdan, C., and Röllinghoff, M. (1998). The immune response to *Leishmania*: mechanisms of parasite control and evasion. *Int. J. Parasitol.* 28, 121–134. doi: 10.1016/S0020-7519(97)00169-0

Brittingham, A., Chen, G., McGwire, B. S., Chang, K. P., and Mosser, D. M. (1999). Interaction of *Leishmania* gp63 with cellular receptors for fibronectin. *Infect. Immun*. 67, 4477–4484.

Brittingham, A., Morrison, C. J., McMaster, W. R., McGwire, B. S., Chang, K. P., and Mosser, D. M. (1995). Role of the Leishmania surface protease gp63 in complement fixation, cell adhesion, and resistance to complement-mediated lysis. *J. Immunol.* 155, 3102–3111.

Bunn, P. T., Montes de Oca, M., de Labastida Rivera, F., Kumar, R., Ng, S. S., Edwards, C. L., et al. (2018). Distinct roles for CD4+ Foxp3+ regulatory T cells and IL-10-mediated immunoregulatory mechanisms during experimental visceral *Leishmaniasis* caused by *Leishmania donovani*. *J. Immunol.* 201, 3362–3372. doi: 10.4049/jimmunol.1701582

Bussotti, G., Gouzelou, E., CôrtesBoité, M., Kherachi, I., Harrat, Z., Eddaikra, N., et al. (2018). *Leishmania* genome dynamics during environmental adaptation reveal strain-specific differences in gene copy number variation, karyotype instability, and telomeric amplification. *MBio* 9:e01399–e01318. doi: 10.1128/mBio.01399-18

Calegari-Silva, T. C., Pereira, R. M., De-Melo, L. D., Saraiva, E. M., Soares, D. C., Bellio, M., et al. (2009). NF-kappaB-mediated repression of iNOS expression in *Leishmania amazonensis* macrophage infection. *Immunol. Lett*. 127, 19–26. doi: 10.1016/j.imlet.2009.08.009

Calegari-Silva, T. C., Vivarini, A. C., Pereira, R. M. S., Dias-Teixeira, K. L., Rath, C. T., Pacheco, A. S. S., et al. (2018). *Leishmania amazonensis* downregulates macrophage iNOS expression via histone deacetylase 1 (HDAC1): a novel parasite evasion mechanisms. *Eur. J. Immunol.* 48, 1188–1198. doi: 10.1002/eji.201747257

Campos, M. B., De Castro Gomes, C. M., de Souza, A. A., Lainson, R., Corbett, C. E., and Silveira, F. T. (2008). *In vitro* infectivity of species of *Leishmania (Viannia)* responsible for American cutaneous leishmaniasis. *Parasitol. Res*. 103, 771–776. doi: 10.1007/s00436-008-1039-8

Canário, A., Queiroz, M., Cunha, G., Cavalcante, T., Riesz, V., Sharma, R., et al. (2019). Presence of parasite DNA in clinically unaffected nasal mucosa during cutaneous leishmaniasis caused by *Leishmania (Viannia) braziliensis*. *Clin. Microbiol. Infect*. 25, 515.e5–515.e7. doi: 10.1016/j.cmi.2018.12.027

Cardoso, T. M., Machado, Á., Costa, D. L., Carvalho, L. P., Queiroz, A., Machado, P., et al. (2015). Protective and pathological functions of CD8+ T cells in Leishmania braziliensis infection. *Infect. Immun*. 83, 898–906. doi: 10.1128/IAI.02404-14

Carneiro, P. P., Conceição, J., Macedo, M., Magalhães, V., Carvalho, E. M., and Bacellar, O. (2016). The role of nitric oxide and reactive oxygen species in the killing of leishmania braziliensis by monocytes from patients with cutaneous *Leishmaniasis*. *PLoS ONE* 11:e0148084. doi: 10.1371/journal.pone.0148084

Chagas, A. C., Oliveira, F., Debrabant, A., Valenzuela, J. G., Ribeiro, J. M., and Calvo, E. (2014). Lundep, a sand fly salivary endonuclease increases *Leishmania* parasite survival in neutrophils and inhibits XIIa contact activation in human plasma. *PLoS Pathog.* 10:e1003923. doi: 10.1371/journal.ppat.1003923

Conceição-Silva, F., Leite-Silva, J., and Morgado, F. N. (2018). The binomial parasite-host immunity in the healing process and reactivation of human tegumentary leishmaniasis. *Front. Microbiol.* 9:1308. doi: 10.3389/fmicb.2018.01308

Conceição-Silva, F., Morgado, F. N., Costa-Santos, M., Miranda-Nascimento, C., and Oliveira-Mendes, S. (2010). *Leishmania braziliensis* and *in situ* host immune response: dispute or partnership? *Rev. Soc. Bras. Med. Trop*. 43, 63–70.

Costa, D. J., Favali, C., Clarêncio, J., Afonso, L., Conceição, V., Miranda, J. C., et al. (2004). *Lutzomyia longipalpis* salivary gland homogenate impairs cytokine production and costimulatory molecule expression on human monocytes and dendritic cells. *Infect. Immun*. 72, 1298–1305. doi: 10.1128/IAI.72.3.1298-1305.2004

Crauwels, P., Bohn, R., Thomas, M., Gottwalt, S., Jäckel, F., Krämer, S., et al. (2015). Apoptotic-like *Leishmania* exploit the host's autophagy machinery to reduce T-cell-mediated parasite elimination. *Autophagy* 11, 285–297. doi: 10.1080/15548627.2014.998904

da Silva, M. F. L., Zampieri, R. A., Muxil, S. M., Beverley, S. M., and Floeter-Winter, L. M. (2012). *Leishmania amazonensis* arginase compartimentalization in the glycosome is important for parasite infectivity. *PLoS ONE* 7:234022. doi: 10.1371/journal.pone.0034022

de Freitas, E. O., Leoratti, F. M., Freire-de-Lima, C. G., Morrot, A., and Feijó, D. F. (2016). The contribution of immune evasive mechanisms to parasite persistence in visceral leishmaniasis. *Front. Immunol.* 7:153. doi: 10.3389/fimmu.2016.00153

De Luca, P. M., and Macedo, A. B. (2016). Cutaneous *Leishmaniasis* vaccination: a matter of quality. *Front. Immunol.* 7:151. doi: 10.3389/fimmu.2016.00151

de Oliveira Camera, P., Junger, J., do Espírito Santo Silva Pires, F., Mattos, M., Oliveira-Neto, M. P., Fernandes, O., et al. (2006). Haematogenous dissemination of *Leishmania (Viannia) braziliensis* in human American tegumentary leishmaniasis. *Trans. R. Soc. Trop. Med. Hyg.* 100, 1112–1117. doi: 10.1016/j.trstmh.2006.02.014

Dias-Teixeira, K. L., Calegari-Silva, T. C., Medina, J. M., Vivarini, Á. C., Cavalcanti, Á., Teteo, N., et al. (2017). Emerging role for the PERK/eIF2α/ATF4 in

human cutaneous *Leishmaniasis*. *Sci. Rep*. 7:17074. doi: 10.1038/s41598-017-17252-x

Diotallevi, A., De Santi, M., Buffi, G., Ceccarelli, M., Vitale, F., Galluzzi, L., et al. (2018). *Leishmania* infection induces microRNA hsa-miR-346 in human cell line-derived macrophages. *Front. Microbiol*. 9:1019. doi: 10.3389/fmicb.2018.01019

Duque, G. A., and Descoteaux, A. (2015). *Leishmania* survival in macrophages: were the ends justify the means. *Curr. Opin. Microbiol*. 26, 32–40. doi: 10.1016/j.mib.2015.04.007

Eichbaum, Q. (2011). PD-1 signaling in HIV and chronic viral infection–potential for therapeutic intervention? *Curr. Med. Chem*. 18, 3971–3980. doi: 10.2174/092986711796957239

Elmore, S. (2007). Apoptosis: a review of programmed cell death. *Toxicol. Pathol*. 35, 495–516. doi: 10.1080/01926230701320337

Eren, R. O., Reverte, M., Rossi, M., Hartley, M. A., Castiglioni, P., Prevel, F., et al. (2016). Mammalian innate immune response to a *Leishmania*-resident RNA virus increases macrophage survival to promote parasite persistence. *Cell Host Microbe*. 20, 318–328. doi: 10.1016/j.chom.2016.08.001

Esch, K. J., Juelsgaard, R., Martinez, P. A., Jones, D. E., and Petersen, C. A. (2013). Programmed death 1-mediated T cell exhaustion during visceral leishmaniasis impairs phagocyte function. *J. Immunol*. 191, 5542–5550. doi: 10.4049/jimmunol.1301810

Fata, A., Mahmoudian, M., Varasteh, A., and Sankian, M. (2013). Monarch-1 activation in murine macrophage cell line (J774 A.1) infected with iranian strain of *Leishmania major*. *Iran J. Parasitol*. 8, 207–211.

Figueroa, R. A., Lozano, L. E., Romero, I. C., Cardona, M. T., Prager, M., Pacheco, R., et al. (2009). Detection of *Leishmania* in unaffected mucosal tissues of patients with cutaneous leishmaniasis caused by *Leishmania (Viannia)* species. *J. Infect. Dis*. 200, 638–646. doi: 10.1086/600109

Forget, G., Gregory, D. J., Whitcombe, L. A., and Olivier, M. (2006). Role of host protein tyrosine phosphatase SHP-1 in *Leishmania donovani*-induced inhibition of nitric oxide production. *Infec. Immun*. 74, 6272–6279. doi: 10.1128/IAI.00853-05

Fowell, D. J., and Locksley, R. M. (1999). *Leishmania major* infection of inbred mice: unmasking genetic determinants of infectious diseases. *Bioessays* 21, 510–518. doi: 10.1002/(SICI)1521-1878(199906)21:6<510::AID-BIES7>3.0.CO;2-5

Freitas-Junior, L. H., Chatelain, E., Kim, H. A., and Siqueira-Neto, J. L. (2012). Visceral leishmaniasis treatment: what do we have, what do we need and how to deliver it? *Int. J. Parasitol*. 2, 11–19 doi: 10.1016/j.ijpddr.2012.01.003

Ganguly, S., Das, N. K., Barbhuiya, J. N., and Chatterjee, M. (2010). Post-kala-azar dermal leishmaniasis – an overview. *Int. J. Dermatol*. 49, 921–931. doi: 10.1111/j.1365-4632.2010.04558.x

Gautam, S., Kumar, R., Singh, N., Singh, A. K., Rai, M., Sacks, D., et al. (2014). CD8 T cell exhaustion in human visceral leishmaniasis. *J. Infect. Dis*. 209, 290–299. doi: 10.1093/infdis/jit401

Géigel, L. F., and Leon, L. L. (2003). Cyclic 3'-5'guanoside monophosphate-dependent activity in *Leishmania amazonensis*. *Mem. Inst. Oswaldo Cruz*. 98, 499–500. doi: 10.1590/S0074-02762003000400012

Genestra, M., de Souza, W. J., Cysne-Finkelstein, L., and Leon, L. L. (2003b). Comparative analysis of the nitric oxide production by *Leishmania* sp. *Med. Microbiol. Immunol*. 192, 217–223. doi: 10.1007/s00430-003-0176-z

Genestra, M., Echevarria, A., Cysne-Finkelstein, L., Vignólio-Alves, L., and Leon, L. L. (2003a). Effect of amidine derivatives on nitric oxide production by *Leishmania amazonensis* promastigotes and axenic amastigotes. *Nitric Oxide* 8, 1–6. doi: 10.1016/S1089-8603(02)00129-5

Genestra, M. S., Cysne-Finkelstein, L., Guedes-Silva, D., and Leon, L. L. (2003c). Effect of L-arginine analogs and a calcium chelator on nitric oxide (NO) production by *Leishmania* sp. *J. Enzyme Inhib. Med. Chem*. 18, 445–452. doi: 10.1080/1475636031000138787

Giraud, E., Martin, O., Yakob, L., and Rogers, M. (2019). Quantifying *Leishmania* metacyclic promastigotes from individual sandfly bites reveals the efficiency of vector transmission. *Commun. Biol*. 2:84. doi: 10.1038/s42003-019-0323-8

Guimarães-Costa, A. B., De Souza-Vieira, T. S., Paletta-Silva, R., Freitas-Mesquita, A. L., Meyer-Fernandes, J. R., and Saraiva, E. M. (2014). 3'-nucleotidase/nuclease activity allows *Leishmania* parasites to escape killing by neutrophil extracellular traps. *Infect. Immun*. 82, 1732–1740. doi: 10.1128/IAI.01232-13

Guimarães-Costa, A. B., Nascimento, M. T., Froment, G. S., Soares, R. P., Morgado, F. N., Conceição-Silva, F., et al. (2009). *Leishmania amazonensis* promastigotes induce and are killed by neutrophil extracellular traps. *Proc. Natl. Acad. Sci. U.S.A*. 106, 6748–6753. doi: 10.1073/pnas.0900226106

Guimarães-Costa, A. B., Rochael, N. C., Oliveira, F., Echevarria-Lima, J., and Saraiva, E. M. (2017). Neutrophil extracellular traps reprogram IL-4/GM-CSF-induced monocyte differentiation to anti-inflammatory macrophages. *Front. Immunol*. 8:523. doi: 10.3389/fimmu.2017.00523

Hammami, A., Charpentier, T., Smans, M., and Stäger, S. (2015). IRF-5-mediated inflammation limits CD8+ T cell expansion by inducing HIF-1α and impairing dendritic cell functions during *Leishmania* infection. *PLoS Pathog*. 11:e1004938. doi: 10.1371/journal.ppat.1004938

Hartley, M. A., Eren, R. O., Rossi, M., Prevel, F., Castiglioni, P., Isorce, N., et al. (2018). *Leishmania guyanensis* parasites block the activation of the inflammasome by inhibiting maturation of IL-1β. *Microb. Cell*. 5, 137–149. doi: 10.15698/mic2018.03.619

Henn, G. A. L., Ramos Júnior, A. N., Colares, J. K. B., Mendes, L. P., Silveira, J. G. C., Lima, A. A. F., et al. (2018). Is visceral *Leishmaniasis* the same in HIV-coinfected adults? *Braz. J. Infect. Dis*. 22, 92–98. doi: 10.1016/j.bjid.2018.03.001

Hermoso, T., Fishelson, Z., Becker, S. I., Hirschberg, K., and Jaffe, C. L. (1991). Leishmanial protein kinases phosphorylate components of the complement system. *EMBO J*. 10, 4061–4067. doi: 10.1002/j.1460-2075.1991.tb04982.x

Holowka, T., Castilho, T. M., Garcia, A. B., Sun, T., McMahon-Pratt, D., and Bucala, R. (2016). *Leishmania*-encoded orthologs of macrophage migration inhibitory factor regulate host immunity to promote parasite persistence. *FASEB J*. 30, 2249–2265. doi: 10.1096/fj.201500189R

Hu, S., Marshall, C., Darby, J., Wei, W., Lyons, A. B., and Körner, H. (2018). Absence of tumor necrosis factor supports alternative activation of macrophages in the liver after infection with *Leishmania major*. *Front. Immunol*. 9:1. doi: 10.3389/fimmu.2018.00001

Husein, A., Jamal, A., Ahmed, M. Z., Arish, M., Ali, R., Tabrez, S., et al. (2018). *Leishmania donovani* infection differentially regulates small G-proteins. *J. Cell. Biochem*. 119, 7844–7854. doi: 10.1002/jcb.27186

Ibraim, I. C., de Assis, R. R., Pessoa, N. L., Campos, M. A., Melo, M. N., Turco, S. J., et al. (2013). Two biochemically distinct lipophosphoglycans from *Leishmania braziliensis* and *Leishmania infantum* trigger different innate immune responses in murine macrophages. *Parasit. Vect*. 6:54. doi: 10.1186/1756-3305-6-54

Joshi, T., Rodriguez, S., Perovic, V., Cockburn, I. A., and Stäger, S. (2009). B7-H1 blockade increases survival of dysfunctional CD8(+) T cells and confers protection against *Leishmania donovani* infections. *PLoS Pathog*. 5:e1000431. doi: 10.1371/journal.ppat.1000431

Kennedy, A. D., and De Leo, F. R. (2009). Neutrophil apoptosis and the resolution of infection. *Immunol. Res*. 43, 25–61. doi: 10.1007/s12026-008-8049-6

Kerr, D., Tietjen, G. T., Gong, Z., Tajkhorshid, E., Adams, E. J., and Lee, K. Y. C. (2018). Sensitivity of peripheral membrane proteins to the membrane context: a case study of phosphatidylserine and the TIM proteins. *BBA* 1860, 2126–2133. doi: 10.1016/j.bbamem.2018.06.010

Khodadadi, A., Rahdar, M., Hossainpour, A., and Khademvatan, S. (2013). An *in vitro* study on suppressive effects of *Leishmania major* on IL-2Rα expression on peripheral human T lymphocyte. *Trop. Biomed*. 30, 526–534.

Khouri, R., Santos, G. S., Soares, G., Costa, J. M., Barral, A., Barral-Netto, M., et al. (2014). SOD1 plasma level as a biomarker for therapeutic failure in cutaneous leishmaniasis. *J. Infect. Dis*. 210, 306–310. doi: 10.1093/infdis/jiu087

Kima, P. E., Constant, S. L., Hannum, L., Colmenares, M., Lee, K. S., Haberman, A. M., et al. (2000). Internalization of *Leishmania mexicana* complex amastigotes via the Fc receptor is required to sustain infection in murine cutaneous leishmaniasis. *J. Exp. Med*. 191, 1063–1068. doi: 10.1084/jem.191.6.1063

Kong, F., Saldarriaga, O. A., Spratt, H., Osorio, E. Y., Travi, B. L., Luxon, B. A., et al. (2017). Transcriptional profiling in experimental visceral Leishmaniasis reveals a broad splenic inflammatory environment that conditions macrophages toward a disease-promoting phenotype. *PLoS Pathog*. 13:e1006165. doi: 10.1371/journal.ppat.1006165

Kropf, P., Freudenberg, M. A., Modolell, M., Price, H. P., Herath, S., Antoniazi, S., et al. (2004). Toll-like receptor 4 contributes to efficient control of infection with the protozoan parasite *Leishmania major*. *Infect. Immun*. 72, 1920–1928. doi: 10.1128/IAI.72.4.1920-1928.2004

Kumar, A., Das, S., Mandal, A., Verma, S., Abhishek, K., Kumar, A., et al. (2018). *Leishmania* infection activates host mTOR for its survival by M2 macrophage polarization. *Parasite Immunol*. 40:e12586. doi: 10.1111/pim.12586

Launois, P., Louis, J. A., and Milon, G. (1997). The fate and persistence of *Leishmania major* in mice of different genetic backgrounds: an example of exploitation of the immune system by intracellular parasites. *Parasitology* 115 (Suppl):S25–S32. doi: 10.1017/S0031182097001777

Lee, S. H., Charmoy, M., Romano, A., Paun, A., Chaves, M. M., Cope, F. O., et al. (2018). Mannose receptor high, M2 dermal macrophages mediate nonhealing *Leishmania major* infection in a Th1 immune environment. *J. Exp. Med*. 215, 357–375. doi: 10.1084/jem.20171389

Leite, P. M., Gomes, R. S., Figueiredo, A. B., Serafim, T. D., Tafuri, W. L., de Souza, C. C., et al. (2012). Ecto-nucleotidase activities of promastigotes from *Leishmania (Viannia) braziliensis* relates to parasite infectivity and disease clinical outcome. *PLoS Negl. Trop. Dis*. 6:e1850. doi: 10.1371/journal.pntd.0001850

Lerner, E. A., Ribeiro, J. M., Nelson, R. J., and Lerner, M. R. (1991). Isolation of maxadilan, a potent vasodilatory peptide from the salivary glands of the sand fly *Lutzomyia longipalpis*. *J. Biol. Chem*. 266, 11234–11236.

Lima, M. H. F., Sacramento, L. A., Quirino, G. F. S., Ferreira, M. D., Benevides, L., Santana, A. K. M., et al. (2017). Leishmania infantum parasites subvert the host inflammatory response through the Adenosine A2A receptor to promote the establishment of infection. *Front. Immunol*. 8:815. doi: 10.3389/fimmu.2017.00815

Liu, Y., Liu, S., He, B., Wang, T., Zhao, S., Wu, C., et al. (2018). PD-1 blockade inhibits lymphocyte apoptosis and restores proliferation and anti-viral immune functions of lymphocyte after CP and NCP BVDV infection *in vitro*. *Vet Microbiol*. 226, 74–80. doi: 10.1016/j.vetmic.2018.10.014

Magalhães, L. S., Bomfim, L. G., Mota, S. G., Cruz, G. S., Corrêa, C. B., Tanajura, D. M., et al. (2018). Increased thiol levels in antimony-resistant *Leishmania* infantum isolated from treatment-refractory visceral leishmaniasis in Brazil. *Mem. Inst. Oswaldo Cruz*. 113, 119–125. doi: 10.1590/0074-02760170289

Maia, Z., Lírio, M., Mistro, S., Mendes, C. M., Mehta, S. R., and Badaro, R. (2012). Comparative study of rK39 Leishmania antigen for serodiagnosis of visceral leishmaniasis: systematic review with meta-analysis. *PLoS Negl. Trop. Dis*. 6:e1484. doi: 10.1371/journal.pntd.0001484

Mandell, M. A., and Beverley, S. M. (2016). Concomitant immunity induced by persistent *Leishmania major* does not preclude secondary re-infection: implications for genetic exchange, diversity and vaccination. *PLoS Negl. Trop. Dis*. 10:e0004811. doi: 10.1371/journal.pntd.0004811

Mandell, M. A., and Beverley, S. M. (2017). Continual renewal and replication of persistent *Leishmania major* parasites in concomitantly immune hosts. *Proc. Natl. Acad. Sci. U.S.A*. 114, E801–E810. doi: 10.1073/pnas.1619265114

Martinez, J. E., Alba Arias, L., Escobar, M. A., and Saravia, N. G. (1992). Haemoculture of *Leishmania (Viannia) braziliensis* from two cases of mucosal Leishmaniasis: re-examination of haematogenous dissemination. *Trans. R Soc. Trop. Med. Hyg*. 86, 392–394. doi: 10.1016/0035-9203(92)90233-3

Martinéz-Valencia, A. J., Daza-Rivera, C. F., Rosales-Chilama, M., Cossio, A., Casadiego Rincón, E. J., Desai, M. M., et al. (2017). Clinical and parasitological factors in parasite persistence after treatment and clinical cure of cutaneous leishmaniasis. *PLoS Negl. Trop. Dis*. 11:e0005713. doi: 10.1371/journal.pntd.0005713

Matheoud, D., Moradin, N., Bellemare-Pelletier, A., Shio, M. T., Hong, W. J., Olivier, M., et al. (2013). *Leishmania* evades host immunity by inhibiting antigen cross-presentation through direct cleavage of the SNARE VAMP8. *Cell Host Microbe* 14, 15–25. doi: 10.1016/j.chom.2013.06.003

Medina-Colorado, A. A., Osorio, E. Y., Saldarriaga, O. A., Travi, B. L., Kong, F., Spratt, H., et al. (2017). Splenic CD4+ T cells in progressive visceral leishmaniasis show a mixed effector-regulatory phenotype and impair macrophage effector function through inhibitory receptor expression. *PLoS ONE* 12:e0169496. doi: 10.1371/journal.pone.0169496

Mishra, J., Madhubala, R., and Singh, S. (2013). Visceral and post-Kala-Azar dermal leishmaniasis isolates show significant difference in their in vitro drug susceptibility pattern. *Parasitol. Res.* 112, 1001–1009. doi: 10.1007/s00436-012-3222-1

Mondelaers, A., Sanchez-Cañete, M. P., Hendrickx, S., Eberhardt, E., Garcia-Hernandez, R., Lachaud, L., et al. (2016). Genomic and molecular characterization of miltefosine resistance in *Leishmania infantum* strains with either natural or acquired resistance through experimental selection of intracellular amastigotes. *PLoS ONE* 11:e0154101. doi: 10.1371/journal.pone.0154101

Morato, C. I., da Silva, I. A. Jr, Borges, A. F., Dorta, M. L., Oliveira, M. A., Jancar, S., et al. (2014). Essential role of leukotriene B4 on *Leishmania (Viannia) braziliensis* killing by human macrophages. *Microbes Infect*. 16, 945–953. doi: 10.1016/j.micinf.2014.08.015

Moreira, D., Rodrigues, V., Abengozar, M., Rivas, L., Rial, E., Laforge, M., et al. (2015). *Leishmania infantum* modulates host macrophage mitochondrial metabolism by hijacking the SIRT1-AMPK axis. *PLoS Pathog*. 11:e1004684. doi: 10.1371/journal.ppat.1004684

Moreira, P. R., Bandarra, M., Magalhães, G. M., Munari, D. P., Machado, G. F., and Prandini, M. M. (2013). Influence of apoptosis on the cutaneous and peripheral lymph node inflammatory response in dogs with visceral leishmaniasis. *Vet. Parasitol*. 192, 149–157. doi: 10.1016/j.vetpar.2012.09.029

Moreira, P. R., Fernando, F. S., Montassier, H. J., André, M. R., and de Oliveira Vasconcelos, R. (2016). Polarized M2 macrophages in dogs with visceral leishmaniasis. *Vet. Parasitol*. 226, 69–73. doi: 10.1016/j.vetpar.2016.06.032

Morgado, F. N., Nascimento, M. T., Saraiva, E. M., de Oliveira-Ribeiro, C., Madeira, M., and da Costa-Santos, M. (2015). Are neutrophil extracellular traps playing a role in the parasite control in active American tegumentary Leishmaniasis lesions? *PLoS ONE* 10:e0133063. doi: 10.1371/journal.pone.0133063

Morgado, F. N., Schubach, A., Vasconcellos, E., Azeredo-Coutinho, R. B., Valete-Rosalino, C. M., Quintella, L. P., et al. (2010). Signs of an *in situ* inflammatory reaction in scars of human American tegumentary leishmaniasis. *Parasite Immunol*. 32, 285–295. doi: 10.1111/j.1365-3024.2009.01188.x

Morris, R. V., Shoemaker, C. B., David, J. R., Lanzaro, G. C., and Titus, R. G. (2001). Sandfly maxadilan exacerbates infection with *Leishmania major* and vaccinating against it protects against *L. Major* infection. *J. Immunol*. 167, 5226–5230. doi: 10.4049/jimmunol.167.9.5226

Moshrefi, M., Spotin, A., Kafil, H. S., Mahami-Oskouei, M., Baradaran, B., Ahmadpour, E., et al. (2017). Tumor suppressor p53 induces apoptosis of host lymphocytes experimentally infected by *Leishmania major*, by activation of Bax and caspase-3: a possible survival mechanism for the parasite. *Parasitol. Res*. 116, 2159–2166. doi: 10.1007/s00436-017-5517-8

Muniz-Junqueira, M. I., and de Paula-Coelho, V. N. (2008). Meglumine antimonate directly increases phagocytosis, superoxide anion and TNF-alpha production, but only via TNF-alpha it indirectly increases nitric oxide production by phagocytes of healthy individuals, *in vitro*. *Int. Immunopharmacol*. 8, 1633–1638. doi: 10.1016/j.intimp.2008.07.011

Murphy, M. L., Cotterell, S. E., Gorak, P. M., Engwerda, C. R., and Kaye, P. M. (1998). Blockade of CTLA-4 enhances host resistance to the intracellular pathogen, *Leishmania donovani*. *J. Immunol*. 161, 4153–4160.

Neves, B. M., Silvestre, R., Resende, M., Ouaissi, A., Cunha, J., Tavares, J., et al. (2010). Activation of phosphatidylinositol 3-kinase/Akt and impairment of nuclear factor-kappaB: molecular mechanisms behind the arrested maturation/activation state of *Leishmania infantum*-infected dendritic cells. *Am. J. Pathol*. 177, 2898–2911. doi: 10.2353/ajpath.2010.100367

Novais, F. O., Carvalho, A. M., Clark, M. L., Carvalho, L. P., Beiting, D. P., Brodsky, I. E., et al. (2017). CD8+ T cell cytotoxicity mediates pathology in the skin by inflammasome activation and IL-1β production. *PLoS Pathog*. 13:e1006196. doi: 10.1371/journal.ppat.1006196

Okwor, I., and Uzonna, J. (2008). Persistent parasites and immunologic memory in cutaneous Leishmaniasis: implications for vaccine designs and vaccination strategies. *Immunol. Res*. 41, 123–136. doi: 10.1007/s12026-008-8016-2

Oliveira, F., Lawyer, P. G., Kamhawi, S., and Valenzuela, J. G. (2008). Immunity to distinct sand fly salivary proteins primes the anti-*Leishmania* immune response towards protection or exacerbation of disease. *PLoS Negl. Trop. Dis*. 2:e226. doi: 10.1371/journal.pntd.0000226

Paduch, K., Debus, A., Rai, B., Schleicher, U., and Bogdan, C. (2019). Resolution of cutaneous *Leishmaniasis* and persistence of *Leishmania major* in the absence of arginase 1. *J. Immunol*. 202, 1453–1464. doi: 10.4049/jimmunol.1801249

Passos, S., Carvalho, L. P., Costa, R. S., Campos, T. M., Novais, F. O., Magalhães, A., et al. (2015). Intermediate monocytes contribute to pathologic immune response in *Leishmania braziliensis* infections. *J. Infect. Dis.* 211, 274–282. doi: 10.1093/infdis/jiu439

Peters, N. C., Egen, J. G., Secundino, N., Debrabant, A., Kimblin, N., Kamhawi, S., et al. (2008). *In vivo* imaging reveals an essential role for neutrophils in Leishmaniasis transmitted by sand flies. *Science* 321, 970–974. doi: 10.1126/science.1159194

Peters, N. C., and Sacks, D. L. (2009). The impact of vector-mediated neutrophil recruitment on cutaneous Leishmaniasis. *Cell Microbiol.* 11, 1290–1296. doi: 10.1111/j.1462-5822.2009.01348.x

Plagge, M., and Laskay, T. (2017). Early production of the neutrophil-derived lipid mediators LTB4 and LXA4 is modulated by intracellular infection with *Leishmania major*. *Biomed. Res. Int*. 2017:2014583. doi: 10.1155/2017/2014583

Pountain, A. W., Weidt, S. K., Regnault, C., Bates, P. A., Donachie, A. M., Dickens, N. J., et al. (2019). Genomic instability at the locus of sterol C24-methyltransferase promotes amphotericin B resistance in Leishmania parasites. *PLoS Negl. Trop. Dis*. 13:e0007052. doi: 10.1371/journal.pntd.0007052

Prieto Barja, P., Pescher, P., Bussotti, G., Dumetz, F., Imamura, H., Kedra, D., et al. (2017). Haplotype selection as an adaptive mechanism in the protozoan pathogen *Leishmania donovani*. *Nat. Ecol. Evol.* 1, 1961–1969. doi: 10.1038/s41559-017-0361-x

Puentes, S. M., Da Silva, R. P., Sacks, D. L., Hammer, C. H., and Joiner, K. A. (1990). Serum resistance of metacyclic stage *Leishmania major* promastigotes is due to release of C5b-9. *J. Immunol.* 145, 4311–4316.

Rastrojo, A., García-Hernández, R., Vargas, P., Camacho, E., Corvo, L., Imamura, H., et al. (2018). Genomic and transcriptomic alterations in *Leishmania donovani* lines experimentally resistant to antileishmanial drugs. *Int. J. Parasitol. Drug. Resist.* 8, 246–264. doi: 10.1016/j.ijpddr.2018.04.002

Regli, I. B., Fernández, O. L., Martínez-Salazar, B., Gómez, M. A., Saravia, N. G., and Tacchini-Cottier, F. (2018). Resistance of *Leishmania (Viannia) Panamensis* to meglumine antimoniate or miltefosine modulates neutrophil effector functions. *Front. Immunol.* 9:3040. doi: 10.3389/fimmu.2018.03040

Resende, M., Moreira, D., Augusto, J., Cunha, J., Neves, B., Cruz, M. T., et al. (2013). *Leishmania*-infected MHC class IIhigh dendritic cells polarize CD4+ T cells toward a nonprotective T-bet+ IFN-γ+ IL-10+ phenotype. *J. Immunol.* 191, 262–273. doi: 10.4049/jimmunol.1203518

Ribeiro-Gomes, F. L., and Sacks, D. (2012). The influence of early neutrophil-*Leishmania* interactions on the host immune response to infection. *Front. Cell Infect. Microbiol.* 2:59. doi: 10.3389/fcimb.2012.00059

Romero, I., Téllez, J., Suárez, Y., Cardona, M., Figueroa, R., Zelazny, A., et al. (2010). Viability and burden of *Leishmania* in extralesional sites during human dermal leishmaniasis. *PLoS Negl. Trop. Dis.* 4:e819. doi: 10.1371/journal.pntd.0000819

Rosales-Chilama, M., Gongora, R. E., Valderrama, L., Jojoa, J., Alexander, N., Rubiano, L. C., et al. (2015). Parasitological confirmation and analysis of *Leishmania* diversity in asymptomatic and subclinical infection following resolution of cutaneous Leishmaniasis. *PLoS Negl. Trop. Dis.* 9:e0004273. doi: 10.1371/journal.pntd.0004273

Santos, D., Campos, T. M., Saldanha, M., Oliveira, S. C., Nascimento, M., Zamboni, D. S., et al. (2018). IL-1β production by intermediate monocytes is associated with immunopathology in cutaneous *Leishmaniasis*. *J. Invest. Dermatol.* 138, 1107–1115. doi: 10.1016/j.jid.2017.11.029

Singh, A. K., Das, V. N. R., Amit, A., Dikhit, M. R., Mahantesh, V., Singh, S. K., et al. (2018). Cytokines and chemokines differentially regulate innate immune cell trafficking during post kala-azar dermal leishmaniasis. *J. Cell Biochem.* 119, 7406–7418. doi: 10.1002/jcb.27048

Singh, R. P., Picado, A., Alam, S., Hasker, E., Singh, S. P., Ostyn, B., et al. (2012). Post-kala-azar dermal Leishmaniasis in visceral leishmaniasis-endemic communities in Bihar, India. *Trop. Med. Int. Health* 17, 1345–1348. doi: 10.1111/j.1365-3156.2012.03067.x

Soares-Bezerra, R. J., Leon, L. L., Echevaria, A., Reis, C. M., Gomes-Silva, L., Agostinho, C. G., et al. (2013). *In vitro* evaluation of 4-phenyl-5-5(4'-X-phenyl)-1,3,4-thiadiazolium-2-phynylamide chlorides and 3[N-4'-X-phenyl]-1,2,3-oxadiazolium-5-olate derivatives on nitric oxide synthase and arginase activities of *Leishmania amazonensis*. *Exp. Parasitol.* 135, 50–54. doi: 10.1016/j.exppara.2013.05.008

Soulat, D., and Bogdan, C. (2017). Function of macrophage and parasite phosphatases in leishmaniasis. *Front. Immunol.* 8:1838. doi: 10.3389/fimmu.2017.01838

Späth, G. F., McDowell, M. A., and Beverley, S. M. (2008). *Leishmania major* intracellular survival is not altered in SHP-1 deficient mev or CD45-/- mice. *Exp. Parasitol.* 120, 275–279. doi: 10.1016/j.exppara.2008.07.003

Stenger, S., Donhauser, N., Thüring, H., Röllinghoff, M., and Bogdan, C. (1996). Reactivation of latent Leishmaniasis by inhibition of inducible nitric oxide synthase. *J. Exp. Med.* 183, 1501–1514. doi: 10.1084/jem.183.4.1501

Sudan, R., Srivastava, N., Pandey, S. P., Majumdar, S., and Saha, B. (2012). Reciprocal regulation of protein kinase C isoforms results in differential cellular responsiveness. *J. Immunol.* 188, 2328–2337. doi: 10.4049/jimmunol.1101678

Távora, L. G. F., Nogueira, M. B., and Gomes, S. T. (2015). Visceral Leishmaniasis/HIV co-infection in northeast Brazil: evaluation of outcome. *Braz. J. Infect. Dis.* 19, 651–656. doi: 10.1016/j.bjid.2015.07.004

Temporal, R. M., Cysne-Finkeltein, L., Echevarria, A., Silva-Gonçalves, A. J., Leon, L. L., and Genestra, M. S. (2005). Amidine derivatives and *Leishmania amazonensis*: na evaluation of the effect of nitric oxide (NO) production on the parasite-macrophage interaction. *Enzyme Inhib. Med. Chem.* 20, 13–18. doi: 10.1080/14756360400015207

Tomiotto-Pellissier, F., Bortoleti, B. T. D. S., Assolini, J. P., Gonçalves, M. D., Carloto, A. C. M., Miranda-Sapla, M. M., et al. (2018). Macrophage polarization in Leishmaniasis: broadening horizons. *Front. Immunol.* 9:2529. doi: 10.3389/fimmu.2018.02529

Trahtemberg, U., and Mevorach, D. (2017). Apoptotic cells induced signaling for immune homeostasis in macrophages and dendritic cells. *Front. Immunol.* 8:1356. doi: 10.3389/fimmu.2017.01356

van Zandbergen, G., Klinger, M., Mueller, A., Dannenberg, S., Gebert, A., Solbach, W., et al. (2004). Cutting edge: neutrophil granulocyte serves as a vector for *Leishmania* entry into macrophages. *J. Immunol.* 173, 6521–6525. doi: 10.4049/jimmunol.173.11.6521

Vergel, C., Palacios, R., Cadena, H., Posso, C. J., Valderrama, L., Perez, M., et al. (2006). Evidence for *Leishmania (viannia)* parasites in the skin and blood of patients before and after treatment. *J. Infect. Dis.* 194, 503–511. doi: 10.1086/505583

Veronica, J., Chandrasekaran, S., Dayakar, A., Devender, M., Prajapati, V. K., Sundar, S., et al. (2019). Iron superoxide dismutase contributes to miltefosine resistance in *Leishmania donovani*. *FEBS J.* 286, 3488–3503. doi: 10.1111/febs.14923

Viana, A. G., Magalhães, L. M. D., Giunchetti, R. C., Dutra, W. O., and Gollob, K. J. (2018). Infection of human monocytes with *Leishmania infantum* strains induces a downmodulated response when compared with infection with *Leishmania braziliensis*. *Front. Immunol.* 8:1896. doi: 10.3389/fimmu.2017.01896

Viana, A. G., Magalhães, L. M. D., Giunchetti, R. C., Dutra, W. O., and Gollob, K. J. (2019). *Leishmania infantum* induces expression of the negative regulatory checkpoint, CTLA-4, by human naïve CD8+ T cells. *Parasite Immunol.* 24:e12659. doi: 10.1111/pim.12659

Wanderley, J. L., Pinto da Silva, L. H., Deolindo, P., Soong, L., Borges, V. M., Prates, D. B., et al. (2009). Cooperation between apoptotic and viable metacyclics enhances the pathogenesis of Leishmaniasis. *PLoS ONE* 4:e5733. doi: 10.1371/journal.pone.0005733

Wenzel, U. A., Bank, E., Florian, C., Förster, S., Zimara, N., Steinacker, J., et al. (2012). *Leishmania major* parasite stage-dependent host cell invasion and immune evasion. *FASEB J.* 26, 29–39. doi: 10.1096/fj.11-184895

World Health Organization (WHO) (2010). *Control of Leishmaniasis.* IN: Repoprt of a meeting of the WHO expert committee on the control of leishmaniasis. Geneve (WHO Technical Report Series, 949).

World Health Organization [WHO] (2017). Global Leishmaniasis update, 2006–2015: a turning point in Leishmaniasis surveillance. *Wkly. Epidemiol. Rec.* 38, 557–572.

World Wealth Assembly (WHA) (2007). *Resolution From the 16° World Health Assembly, May 21, 2007*. Available online at: www.who.int/neglected_diseases/mediacentre/WHA_60.13_Eng.pdf

Yadav, A., Amit, A., Chaudhary, R., Chandel, A. S., Mahantesh, V., Suman, S. S., et al. (2015). *Leishmania donovani*: impairment of the cellular immune response against recombinant ornithine decarboxylase protein as a possible

evasion strategy of *Leishmania* in visceral leishmaniasis. *Int. J. Parasitol.* 45, 33–42. doi: 10.1016/j.ijpara.2014.08.013

Yasur-Landau, D., Jaffe, C. L., David, L., Doron-Faigenboim, A., and Baneth, G. (2018). Resistance of *Leishmania infantum* to allopurinol is associated with chromosome and gene copy number variations including decrease in the S-adenosylmethionine synthetase (METK) gene copy number. *Int. J. Parasitol. Drugs Drug Resist.* 8, 403–410. doi: 10.1016/j.ijpddr.2018.08.002

Zijlstra, E. E. (2016). The immunology of post-kala-azar dermal leishmaniasis (PKDL). *Parasites Vect.* 9:464. doi: 10.1186/s13071-016-1721-0

Conflict of Interest: The authors declare that the research was conducted in the absence of any commercial or financial relationships that could be construed as a potential conflict of interest.

frontiers in Cellular and Infection Microbiology

ORIGINAL RESEARCH
published: 04 October 2019
doi: 10.3389/fcimb.2019.00338

Transcriptional Analysis of Human Skin Lesions Identifies Tryptophan-2,3-Deoxygenase as a Restriction Factor for Cutaneous *Leishmania*

Vasco Rodrigues[1†], Sónia André[1], Hasnaa Maksouri[2], Tarik Mouttaki[2], Soumiya Chiheb[2,3], Myriam Riyad[2,4*], Khadija Akarid[5*] and Jérôme Estaquier[1,6*]*

[1] CNRS-ERL3649, Université Paris Descartes, Paris, France, [2] Research Team on Immunopathology of Infectious and Systemic Diseases, Laboratory of Cellular and Molecular Pathology, Faculty of Medicine and Pharmacy, Hassan II University of Casablanca, Casablanca, Morocco, [3] Department of Dermatology, University Hospital Ibn Rochd of Casablanca, Casablanca, Morocco, [4] Laboratory of Parasitology, Faculty of Medicine and Pharmacy, University of Hassan II Casablanca (UH2C), Casablanca, Morocco, [5] Molecular Genetics and Immunophysiopathology Research Team, Health and Environment Laboratory, Aïn Chock Faculty of Sciences, University of Hassan II Casablanca (UH2C), Casablanca, Morocco, [6] Faculty of Medicine, Centre Hospitalier Universitaire (CHU) de Québec Research Center, Laval University, Quebec, QC, Canada

Disease manifestation after infection with cutaneous *Leishmania* species is the result of a complex interplay of diverse factors, including the immune status of the host, the infecting parasite species, or the parasite load at the lesion site. Understanding how these factors impact on the pathology of cutaneous leishmaniasis (CL) may provide new targets to manage the infection and improve clinical outcome. We quantified the relative expression of 170 genes involved in a diverse range of biological processes, in the skin biopsies from patients afflicted with CL caused by infection with either *L. major* or *L. tropica*. As compared to healthy skin, CL lesions bear elevated levels of transcripts involved in the immune response, and conversely, present a significant downregulation in the expression of genes involved in epidermal integrity and arginine or fatty acid metabolism. The expression of transcripts encoding for cytotoxic mediators and chemokines in lesions was inversely correlated with the expression of genes involved in epidermal integrity, suggesting that cytotoxicity is a major mediator of CL pathology. When comparing the transcriptional profiles of lesions caused by either *L. major* or *L. tropica*, we found them to be very similar, the later presenting an aggravated inflammatory/cytotoxic profile. Finally, we identified genes positively correlated with the parasite load in lesions. Among others, these included Th2 or regulatory cytokines, such as *IL4* or *IL10*. Remarkably, a single gene among our dataset, encoding for tryptophan-2,3-deoxygenase (TDO), presented a negative correlation with the parasite load, suggesting that its expression may restrict parasite numbers in lesions. In agreement, treatment of macrophages infected with *L. major in vitro* with a TDO inhibitor led to an increase in parasite transcripts. Our work provides new insights into the factors that impact CL pathology and identifies TDO as a restriction factor for cutaneous *Leishmania*.

Keywords: cutaneous leishmanaisis, tryptophan-2,3-dioxygenase, *Leishmania tropica*, *Leishmania major*, parasite load

OPEN ACCESS

Edited by:
Elvira Saraiva, Federal University of Rio de Janeiro, Brazil

Reviewed by:
Iris Bruchhaus, Bernhard Nocht Institute for Tropical Medicine (BMITM), Germany
Valeria Borges, Oswaldo Cruz Foundation (Fiocruz), Brazil

***Correspondence:**
Vasco Rodrigues
vteixeir@curie.fr
Myriam Riyad
myr.riyad@yahoo.com
Khadija Akarid
kakarid@yahoo.fr
Jérôme Estaquier
estaquier@yahoo.fr

†Present address:
Vasco Rodrigues, Institut Curie, PSL Research University, INSERM U932, Paris, France

Specialty section:
This article was submitted to Parasite and Host, a section of the journal Frontiers in Cellular and Infection Microbiology

Received: *12 May 2019*
Accepted: *18 September 2019*
Published: *04 October 2019*

Citation:
Rodrigues V, André S, Maksouri H, Mouttaki T, Chiheb S, Riyad M, Akarid K and Estaquier J (2019) Transcriptional Analysis of Human Skin Lesions Identifies Tryptophan-2,3-Deoxygenase as a Restriction Factor for Cutaneous Leishmania. Front. Cell. Infect. Microbiol. 9:338. doi: 10.3389/fcimb.2019.00338

INTRODUCTION

Protozoan parasites of the genus *Leishmania* cause a group of diseases collectively known as leishmaniasis, with a clinical spectrum ranging from localized skin lesions to systemic visceral disease. *Leishmania* shuttles between an insect vector and a mammalian host to successfully complete its life cycle. In the gut of female sandflies, *Leishmania* promastigotes go through a maturation process that gives rise to infectious metacyclic forms, which are transmitted to a mammal's skin during blood feeding. These inoculated promastigotes are rapidly taken up by resident or recruited phagocytes and differentiate into the intracellular amastigote stage that spreads the infection (Kaye and Scott, 2011).

The cutaneous form of leishmaniasis remains a public health problem across many regions of the globe, with an estimated global incidence of 1 million cases (David and Craft, 2009; Alvar et al., 2012). In the Old World, cutaneous leishmaniasis (CL) is usually caused by *L. major, L. tropica,* or *L. aethiopica*, while in the Americas, the infecting species are typically *L. braziliensis* or *L. amazonensis* (Murray et al., 2005; WHO, 2013). In Morocco, CL is caused mainly by *L. major* and *L. tropica* and remains a significant health problem, with a steady increase in the number of reported cases since the beginning of the century, as a result of the emergence of several new foci (Aoun and Bouratbine, 2014; Mniouil et al., 2017).

Cutaneous *Leishmania* infection starts with an asymptomatic period of variable duration, characterized by parasite proliferation. This silent phase ends with the appearance of a small erythema at the site of the bite, indicating the onset of an inflammatory response in the infected tissue. The progressive infiltration of neutrophils, macrophages, eosinophils, or T cells heightens the inflammatory response and leads to the development of a papule or a nodule that grows slowly, over several weeks. A crust appears centrally and eventually falls off, exposing the ulcerated lesion. Ulcers generally present raised and indurated margins, healing gradually over months or years (Murray et al., 2005; Reithinger et al., 2007). Disease manifestation is highly variable, depending on the immune status of the host and the infecting parasite species. For instance, in North Africa, cutaneous lesions caused by *L. major* tend to be exudative or "wet," large and complicated by superficial and secondary bacterial infections. They are typically multiple and located on limbs. Spontaneous healing but with indelible scars is obtained in <8 months. Lesions caused by *L. tropica* are often "dry" with a central crust, mainly single and located on the face. Some *L. tropica* lesions last more than 1 year, confirming the chronic tendency of this form of CL. Relapses and treatment failures are also not exceptional. Hence, infection caused by *L. tropica* seems to be more insidious compared with *L. major* infection, with a longer incubation period. However, multiple, inflammatory, and infiltrative diffuse lesions were described in some Moroccan outbreaks (Aoun and Bouratbine, 2014).

Over the past decades, countless studies in animal models and human patients helped to elucidate how immune responses are orchestrated during CL and how they translate into the wide spectrum of clinical manifestations observed in CL patients (Scott and Novais, 2016). The crucial role played by Th1 immune responses in the resolution of infection is well-established, as it leads to the production of IFN-γ and TNF that activate macrophages to kill intracellular amastigotes. However, the excessive induction of Th1 responses may lead to immunopathology. Similarly, the presence of CD8 T cells expressing cytotoxic markers, such as perforin and granzymes, in lesional tissue has recently been associated with tissue damage that manifests as skin ulceration (Scott and Novais, 2016; Novais et al., 2017). In contrast, the action of immune-regulatory factors such as IL-10 or TGF-β promotes parasite persistence and lesion chronicity. These cytokines impair the induction of protective responses and may lead to an aggravated form of the disease known as diffuse cutaneous leishmaniasis (DCL), whose hallmark is a depressed cellular immunity as evidenced by a negative delayed type hypersensitivity response (Scott and Novais, 2016).

Studies in human CL patients have classically evaluated the capacity of circulating leukocytes to produce cytokines or proliferate when exposed to parasite antigens (Farajnia et al., 2005; Vargas-Inchaustegui et al., 2010; Shahi et al., 2013). While they may provide good correlates of protection, these systemic responses seldom reflect the immune environment in the infected tissue. More recently, transcriptomic and proteomic approaches provided a more detailed picture of the local immune response at the lesion site (Maretti-Mira et al., 2012; da Silva Santos et al., 2015; Novais et al., 2015; Christensen et al., 2016). Nevertheless, studies comparing the transcriptional signatures of CL lesions caused by different *Leishmania* species are still lacking. Also, the parasite load appears to impact the inflammatory and general transcriptional signatures of the lesions (Christensen et al., 2016). However, such knowledge has not yet been explored to identify factors that may promote or restrict parasite growth.

We quantified the transcript abundance of genes involved in inflammation, immunity, metabolism, and epidermal integrity from the skin of human CL patients infected with either *L. major* or *L. tropica*, recovered from Moroccan endemic areas. Confirming previous observations, we found that lesions are transcriptionally distinct from healthy skin, exhibiting a strong co-induction in the transcript levels of immune mediators, genes related with Th1 immune responses or metabolic enzymes. Conversely, genes associated with epidermal integrity and Th2 immune responses were either downregulated or remained unchanged. *L. major* and *L. tropica* lesions had very similar transcriptional signatures, the latter exhibiting an aggravated pro-inflammatory profile. Employing differential gene expression analysis, we also identified several functionally-related genes whose expression was associated with lesions bearing a high parasite load. These included immunoregulatory genes, and genes related with the metabolic function. Conversely, the expression of the tryptophan-catabolizing enzyme tryptophan-2,3-dioxigenase (TDO) correlated negatively with parasite transcripts. Importantly, treating cultured macrophages with a specific TDO inhibitor augmented *L. major* transcripts. Altogether, our results reveal novel gene signatures associated with CL and identify TDO as a restriction factor for cutaneous *Leishmania.*

MATERIALS AND METHODS

Ethics Statement

This work was conducted according to the principles specified in the Declaration of Helsinki and under the local ethical guidelines of the Ethics Committee for Biomedical Research (Faculty of Medicine and Pharmacy, Hassan II University of Casablanca, Morocco) that approved this research. The team explained to the patients the objectives of the survey, and why it needed a cutaneous biopsy, which is used routinely at the Department of Dermatology (University Hospital Ibn Rochd, Casablanca) for the parasitological confirmation of cutaneous leishmaniasis diagnosis before any treatment prescription. The dermatologist asked for the patients' consent (for adults) or from the parents for children. The sampling was done only if the patients or their tutors gave their oral consent. At the time of biopsy sampling (between 2012 and 2014), oral consent was the sole requirement imposed by the Ethics Committee to allow for patient tissue sampling for research purposes and thus written consent was not obtained. Oral consent was also obtained from the healthy skin donors. Finally, the team guaranteed the confidentiality of their personal and clinical data and that the results would be processed anonymously.

Peripheral blood was obtained from healthy adult donors (Etablissement Français du sang, Paris, France). All donors signed informed consent allowing the use of their blood for research purposes.

Study Subjects, Dermal Samples, Diagnostic, and Species Typing

Nineteen (19) patients presenting cutaneous lesions suggestive of CL were received and sampled at the Department of Dermatology -Ibn Rochd Hospital, Casablanca. Before the beginning of the treatment course, a skin biopsy was collected under sterile conditions from the border of active skin lesions. Normal skin samples were taken from three volunteers that were living in non endemic areas and without a history of cutaneous leishmaniasis. Sampled biopsies were immediately conserved in RNA Later (QIAGEN) at −80°C until RNA extraction.

Diagnosis of cutaneous leishmaniasis was confirmed by direct examination of amastigotes in Giemsa-stained smears of syringe-sucked dermal fluid, by parasite culture in NNN medium from recovered dermal fluid, or by PCR amplification of the kDNA minicircle region using the primer pair 13A/13B, as described (Reale et al., 1999).

Leishmania species typing in the lesions was carried out using the Internal Transcriber Sequence-1 (ITS1) PCR-RFLP assay, as previously described (Mouttaki et al., 2014).

RNA Extraction and Quantitative PCR

Skin biopsies, genotyped as *L. major* or *L. tropica*, or healthy skin controls, were grinded into a fine powder in liquid nitrogen using a mortar and pestle. One mL of TRIzol reagent (Thermo Fisher Scientific) was added to the powder, homogenized, and spun to remove particulate matter. Two hundred microliters of chloroform were added to TRIzol and the aqueous phase recovered after centrifugation. RNA was precipitated with one volume of isopropanol, washed two times in ethanol (70% v/v), and solubilized in H_2O. The concentration, purity and integrity of the extracted RNAs were verified in a Nanodrop 2000 spectrophotometer and the Experion Automated Electrophoresis System (Bio-Rad).

RNA was reverse transcribed using the AffinityScript QPCR cDNA synthesis kit (Stratagene), following the manufacturer's instructions. Quantitative PCR was performed in 10 μL reactions using the Sybr Green technology and the 7900HT Fast Real-Time PCR System (Applied Biosystems). The thermal cycle consisted of a hold of 15 min at 95°C, followed by 40 cycles of denaturation (95°C, 15 s), annealing (60°C, 30 s) and extension (72°C, 30 s). Primers for host genes used in this study were designed using the AutoPrime software, and their sequence is provided in **Table S1**. To quantify the relative parasite load in patient biopsies, we employed primers against the *Leishmania* genus-specific genes *KMP11* and *RRNA45*, whose transcript abundance is constant during the parasite life cycle, and have been previously employed as reference genes for quantitative PCR studies in *Leishmania* (Moreira et al., 2012; Zangger et al., 2013).

The delta threshold cycle (Δct) values for each tested gene were obtained by calculating the difference between the ct value for the gene of interest and the geometric mean of the ct values of two housekeeping genes (*GAPDH* and *RPS18*). Data was centered and normalized by calculating the ΔΔct value. For each gene evaluated, we subtracted the geometric mean of the Δct values for the healthy control samples to the Δct for every sample, to obtain the ΔΔct values. The ΔΔct values were directly employed in all subsequent analyses and are provided in **Table S2**.

Differential Gene Expression Analysis

To identify genes differentially expressed between healthy and lesioned skin and between *L. tropica* and *L. major* lesions, we employed the Comparative Marker Selection package from the GenePattern platform (v3.9.2, Broad Institute) (Gould et al., 2006). All differentially-expressed genes (DEGs) (*t* test, $P < 0.05$) between the two classes under analysis were extracted using the Extract Comparative Marker Selection package and are provided in **Tables S3**, **S4**.

Hierarchical Clustering, Principal Component Analysis, and Correlation Matrices

The R Language and Environment for Statistical Computing (R) (v3.2.2) along with the RStudio interface (v0.99.892) were employed for PCA, Hierarchical Clustering, and plotting heatmaps and correlation matrixes. The *FactoMineR* and *factoextra* R packages were employed to perform PCA for genes and samples. The *hclust* R function was employed to cluster samples. The *heatmap.2* and *cormat* functions were employed to plot heatmaps and correlation matrices, respectively.

Parasite and Mouse Macrophage Cell Line Culture

A *L. major* reference strain (MHOM/IL/81/Friedlin) was maintained in culture by weekly sub-passage 1X M199, 25 mM

of HEPES, 1X Penicillin-Streptomycin, 1X glutamine, 0.0001% of biotin, 10 μg/mL of folic acid, 100 μM of adenosine, 5 μg/mL of hemin and 10% of heat inactivated FBS. The murine macrophage cell line J774 was acquired from ATCC and maintained in culture by regular sub-passage in RPMI culture media supplemented with FBS and antibiotics.

Human Monocyte-Derived Macrophage (MDM) Differentiation

Peripheral blood mononuclear cells (PBMC) were purified from the peripheral blood using Ficoll-Paque (GE Healthcare) and density centrifugation. Monocytes were isolated by positive selection using CD14+ magnetic microbeads (Miltenyi) and differentiated into macrophages by culture in RPMI supplemented with 5% fetal calf serum (FCS; Gibco), 5% human serum (Sigma), penicillin-streptomycin (Gibco), and 25 ng/ml macrophage colony-stimulating factor (M-CSF; ImmunoTools).

In vitro Infections and Quantitative PCR

Human MDMs and J774 macrophages were infected with *L. major* stationary-phase promastigotes at a parasite-to-cell ratio of 10-to-1, for 4 h, after which non-internalized parasites were removed through extensive washing in PBS. Cells were then treated with a TDO-specific inhibitor (680C91, Sigma Aldrich) at a concentration of 20 μM, previously determined as non-toxic for both parasite and cells, or DMSO (vehicle). At 48 h after incubation at, cells were lysed in 800 μL of TRIzol reagent (Thermo Fisher Scientific. RNA was purified and reverse transcription and quantitative PCR using SensiFAST cDNA synthesis kit (Bioline) followed by a qPCR (SensiFAST SYBR Hi-ROX kit, Bioline). For gene amplification, mixtures were composed of SensiFAST buffer (2X, Bioline) and 200 nM of forward and reverse primer. Assays were performed in 10 μl reactions volume with 15 ng of cDNA sample. Thermocycling settings consisted of one hold of 2 min at 95°C followed by a two-step temperature (95°C for 15 s and 60°C for 30 s) over 40 cycles in a CFX384 touch real time PCR detection system (Bio-rad). To calculate the relative intracellular parasite growth between DMSO-treated and TDO-inhibitor treated cells, we quantified the parasite-specific transcripts *KMP11* and *RRNA45*, using *GAPDH* and *RPS18* as host reference genes.

TABLE 1 | Demographic and clinical data from the subjects included in the cohort.

Reference	Age/years	Gender	Lesion evolution/months*	*Leishmania* species
Healthy#1	32	M	–	–
Healthy#2	47	F	–	–
Healthy#3	53	F	–	–
CL#1 L02/12	57	F	2	*L. major*
CL#2 L07/12	26	M	9	*L. major*
CL#3 L45/12	56	F	2	*L. major*
CL#4 LC10/12	1	F	7	*L. major*
CL#5 LC11/12	28	M	3	*L. major*
CL#6 LC13/12	62	F	36	*L. major*
CL#7 LC14/13	65	F	9	*L. major*
CL#8 LC16/14	11	M	6	*L. major*
CL#9 LC20/14	26	M	7	*L. major*
CL#10 LC21/14	19	F	8	*L. major*
CL#11 L27/12	1	F	4	*L. tropica*
CL#12 L12/12	5	F	7	*L. tropica*
CL#13 LC13/13	32	F	6	*L. tropica*
CL#14 L29/12	6	M	7	*L. tropica*
CL#15 L32/12	85	F	2	*L. tropica*
CL#16 LC05/12	29	M	6	*L. tropica*
CL#17 LC06/12	62	F	6	*L. tropica*
CL#18 LC08/12	18	F	2	*L. tropica*
CL#19 LC12/12	6	F	6	*L. tropica*

**Time span, in months, between the appearance of the lesions and the medical consultation.*

RESULTS

Cutaneous Leishmaniasis Is Associated With the Induction of a Pro-Inflammatory Gene-Signature and the Downregulation of Genes Associated With Epidermal Integrity and Fatty Acid and Arginine Metabolism

To compare the transcriptional profile of human CL lesions with healthy skin, we performed a qPCR analysis on 19 biopsies recovered from patients residing or visiting endemic regions in Morocco and three healthy skin controls from non endemic Moroccan areas (**Table 1**). We evaluated the transcript levels of a total of 170 genes. These were categorized according to the biological processes they are involved in (**Table S1**). Among these, 71 genes are involved in the inflammatory/immune responses, including cytokines, chemokines, and immune cell surface markers. Interferon-stimulated genes (ISGs) were also included in the analysis (44 genes) as they have been implicated in the innate response to *Leishmania* infection *in vitro* (Favila et al., 2014), as well as in mice (Schleicher et al., 2018), but have not so far been examined with detail in cutaneous lesions from human patients. We further included 47 genes whose products fulfill metabolic roles that have a known impact on immune cell activation and function (Pearce and Pearce, 2013), as *Leishmania* has been described as capable of modulating the metabolic profile of the host cell (Moreira et al., 2015). Finally, we also included genes that ensure the maintenance of the skin barrier function (8 genes), as cutaneous leishmaniasis negatively impacts on epidermal integrity (Novais et al., 2015). Thus, the diversity of this group of selected genes should enable us to, first identify new genes that are differentially expressed between normal skin and lesions; second, to define a gene signature allowing the distinction of CL lesions caused by different species of *Leishmania* and, third, to identify genes whose expression in lesions is impacted by the parasite load.

A principal component analysis (PCA) on the whole gene set resolved the samples into two groups, healthy controls and lesions, across the principal component-1, which accounted for

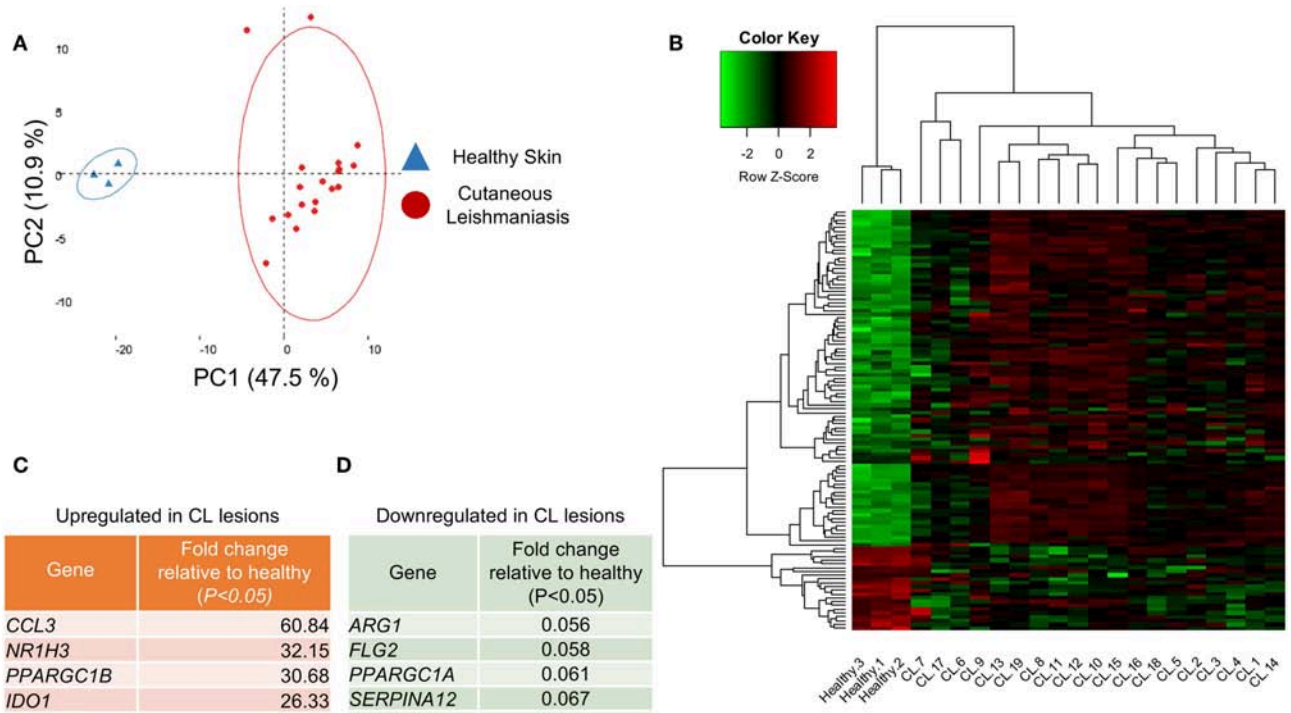

C

Upregulated in CL lesions

Gene	Fold change relative to healthy (*P*<0.05)
CCL3	60.84
NR1H3	32.15
PPARGC1B	30.68
IDO1	26.33
MB21D1	26.00
CXCL9	21.47
APOBEC3G	21.34
TBX21	20.99
IL17A	19.26
PKM	18.25

D

Downregulated in CL lesions

Gene	Fold change relative to healthy (P<0.05)
ARG1	0.056
FLG2	0.058
PPARGC1A	0.061
SERPINA12	0.067
CXCR1	0.082
SCGB2A2	0.098
SLC2A1	0.143
FABP4	0.178
NT5C3A	0.198
HPSE	0.239

FIGURE 1 | Healthy skin is transcriptionally distinct from cutaneous leishmaniasis lesions. **(A)** PCA analysis of the 170 analyzed genes from the 22 skin biopsies from either healthy skin (blue triangles) or CL patients (red dots). The two principal components (PC) are displayed on the axis along with the variance. Large circles denote the 95% confidence level. **(B)** Clustered heatmap of skin biopsies from CL patients according to their differential gene expression of healthy skin and CL lesions. **(C)** Table detailing the 10 most upregulated genes in CL lesions compared to healthy skin. **(D)** Table detailing the 10 most downregulated genes in CL lesions compared to healthy skin.

47.5% of the variation observed in the data (**Figure 1A**). Of the 170 evaluated genes, 111 were differentially expressed between normal and CL skin (**Table S3**, $P < 0.05$). Hierarchical clustering on differentially-expressed genes (**Figure 1B**, rows) showed that genes segregate into those that were significantly upregulated in CL skin, as compared to normal skin (89 genes, **Table S3**, $P < 0.05$), and those whose expression decreases in lesions (22 genes, **Table S3**, $P < 0.05$). **Figures 1C,D** show the most up- and down-regulated genes, respectively. The gene encoding the chemokine CCL3 was the most upregulated in lesions (**Figure 1C**), while *Arg1* expression decreased about 18 times in lesions, as compared to healthy skin and was the most down-regulated gene in our analysis (**Figure 1D**).

Among the significantly up-regulated genes were those associated with Th1 function (*IFNG, TNF, TBX21*) (**Figure S1A**), cytotoxicity (*PRF1, GZMB, GNLY)* (**Figure S1B**), or inflammatory chemokines (*CXCL9, CCL3, CCL5*) (**Figure S1C**). Similarly, genes encoding for inflammasome components (*NLRP3, CASP1, CASP4*) (**Figure S1D**) were significantly enriched in lesions, as compared to healthy skin, as well as genes encoding for Th17 cytokines (*IL17A, IL22*) (**Figure S1E**) and immune regulation (*IL10, TGFB1)* (**Figure S1F**). Finally, several Interferon-stimulated genes (ISGs) were also significantly upregulated in CL lesions (*TRIM56*, *TREX1*, *IFI44L*) (**Figure S1G**).

In contrast, genes associated with Th2 CD4 T cell function (*IL4, IL13*) remained unchanged in lesions (**Figure S1H**). Among the most downregulated genes were those involved in the epidermal barrier function (*SERPINA12, FLG2, HPSE*) and fatty acid biosynthesis (*ACACA, FABP4, FASN*) (**Figure 1D** and **Figures S1I,J**).

We further observed a significant upregulation of transcripts encoding for T cell surface markers (*CD4, CD8A, CD3G*) (**Figure S2A**), B cell markers (*MS4A1*) (**Figure S2B**) or neutrophils (*MPO*) (**Figure S2C**), but a significant decrease in the transcript levels of the blood monocyte marker *CD14* (**Figure S2D**).

Altogether, our data suggests that *Leishmania* induces the recruitment of immune cells to the site of cutaneous infection, triggering an immune response characterized by both pro-inflammatory and regulatory immune factors.

Up-Regulation of a Cytotoxic/Inflammatory Signature in CL Lesions Leads to Compromised Expression of Genes Involved in Epidermal Integrity and Arginine Metabolism

To gain additional insight into the transcriptional signatures operating in CL, we performed a new PCA, now limited to the 111 differentially-expressed genes identified above, and to the 19 biopsies recovered from CL patients (**Figure S3**). The two principal components accounted for about 50% of the variation observed across the lesion samples (**Figure S3**). To identify the genes, or groups of genes that contribute mostly to such variation, we plotted the individual contributions of each gene to these two principal components (**Figure 2A**). This approach should allow the identification of groups of genes that are co-induced or co-repressed in individual samples. We observed that a group of genes involved in the immune response (including *CD8*, *TBX21*, *PERF1*, *GZMB*, *IFNG,* and chemokines such as *CXCL19*, *CCL3*, *CCL4*) are clustered together in the PCA scores plot (**Figure 2A**, blue dots). Similarly, several ISGs (including *IRF9*, *IRF3*, *TREX1*, *IFI44L,* and *TRIM56*), appear closely grouped (**Figure 2A**, green dots), while a third group of functionally-diverse genes appear segregated ("Divergent") from both the "ISG" and "Immune Response" groups (**Figure 2A**, red dots). This latter group is comprised of genes whose expression decreases in lesions as compared with healthy skin, and play functions in epidermal integrity, and fatty acid and arginine metabolism, including, among others, *ARG2*, *ACACA*, or *FABP4* (**Figure 2A**, red dots).

Individual genes belonging to a given group should appear strongly co-induced or co-repressed in individual patients but present no association or correlate negatively with genes in other groups. To visualize this, we plotted the Pearson correlation coefficients for the genes selected for each of the three groups (**Figure 2B**). A complete Pearson correlation matrix for the whole differentially-expressed gene data set in patient biopsies is presented in **Figure S4**, and provides a comprehensive view of the simplified matrix presented in **Figure 2B**. Genes belonging to the "Immune Response" group, such as *IL10* and *IFNG*, present a strong positive correlation among them (**Figures 2B,C**), but bear no correlation with genes in the "ISGs" group (**Figures 2B,D**) or, instead, negatively correlate with most genes in the "Divergent" group, particularly those involved in epidermal integrity, or arginine metabolism (**Figures 2B,E**).

Similarly, individual genes in the "ISGs" group correlate positively with each other but have little association with genes in other groups (**Figures 2B,D,F**). These genes are also strongly induced in patient biopsies, as compared to healthy skin (**Table S3**). As the expression of ISGs is usually associated with viral infection, we assessed whether their induction in samples was due to the presence of the *Leishmania* RNA virus (LRV) (Zangger et al., 2013). Indeed, LRV2 was recently isolated from an Iranian strain of *L. major* (Hajjaran et al., 2016). However, LRV sequences were not detected in the skin biopsies of our cohort of patients (not shown).

These observations indicate that CL patients vary in their magnitude of induction of inflammatory genes and the potency of this program impacts on the mechanisms that maintain skin integrity.

Lesions Caused by *L. major* or *L. tropica* Lead to Very Similar Transcriptional Profiles, the Latter Presenting an Aggravated Inflammatory Signature

Among the 19 patients in our cohort, 10 presented lesions caused by *L. major*, while the remaining were infected with *L. tropica* (**Table 1**). We asked whether the variability in the transcriptional profiles observed across patients could be related to distinct transcriptional responses induced by the two species. A PCA on the whole gene data set and limited to the 19 biopsies from patients could not resolve the samples into lesions caused by either species (**Figure 3A**), providing an indication that the transcriptional profile induced by both *Leishmania* species are very similar. We then compared the transcriptional profile of the 10 lesions caused by *L. major* with the nine samples presenting *L. tropica* lesions to extract the genes that are differentially-expressed between lesions caused by the two species ($P < 0.05$, **Table S4**). Only three genes (*PIP*, *NT5C3A,* and *ATP5B*), that are functionally-unrelated, were significantly upregulated in *L. major* lesions as compared to CL caused by *L. tropica* ($P < 0.05$, **Figure 3B**, **Figure S5A**, and **Table S4**). Fourteen genes were significantly upregulated in *L. tropica* lesions, as compared to *L. major* (**Figure 3C**). Among these, many were involved in the CD8 T cell immune response (*GZMA*, *GZMB*, *PRF1*, and *CD8B*), and also included genes encoding for inflammatory chemokines such as *CCL5*, *CCL4* and its ligand *CCR5*, as well *CXCL19*, which plays a critical role in the recruitment of CD8 T cells (Hugues et al., 2007) (**Figure 3C**, **Figure S5B**, and **Table S4**). We also observed higher levels of *RORC* expression in *L. tropica* lesions, a transcriptional factor reported to be expressed by CD8 T cells of psoriatic skin lesions (Ortega et al., 2009). While most of these transcripts are also upregulated in *L. major* lesions as compared to normal skin (**Figure S5B**, **Table S3**), our analysis revealed that they are further enriched in CL caused by *L. tropica*.

We next asked whether the 17 differentially-expressed genes could constitute a signature able to distinguish and group together lesions caused by each of the species. For that, we clustered the samples from the 19 infected patients based on their expression levels of these 17 genes (**Figure 3D**). This approach yielded a relatively good separation of the samples according to the parasite species, since only one of the *L. major*-caused lesions segregated into the *L. tropica* group (CL10) (**Figure 3D**). We cannot exclude that additional host or environmental factors in this particular patient may contribute to blur the signatures induced by the two species.

We conclude that, within our gene dataset, both *Leishmania* species induce very similar gene signatures in the infected skin. Nevertheless, our results indicate that CL lesions caused by *L. tropica* bear an aggravated inflammatory profile as compared to *L. major* lesions that appears to result from increased CD8 T cell responses at the site of infection.

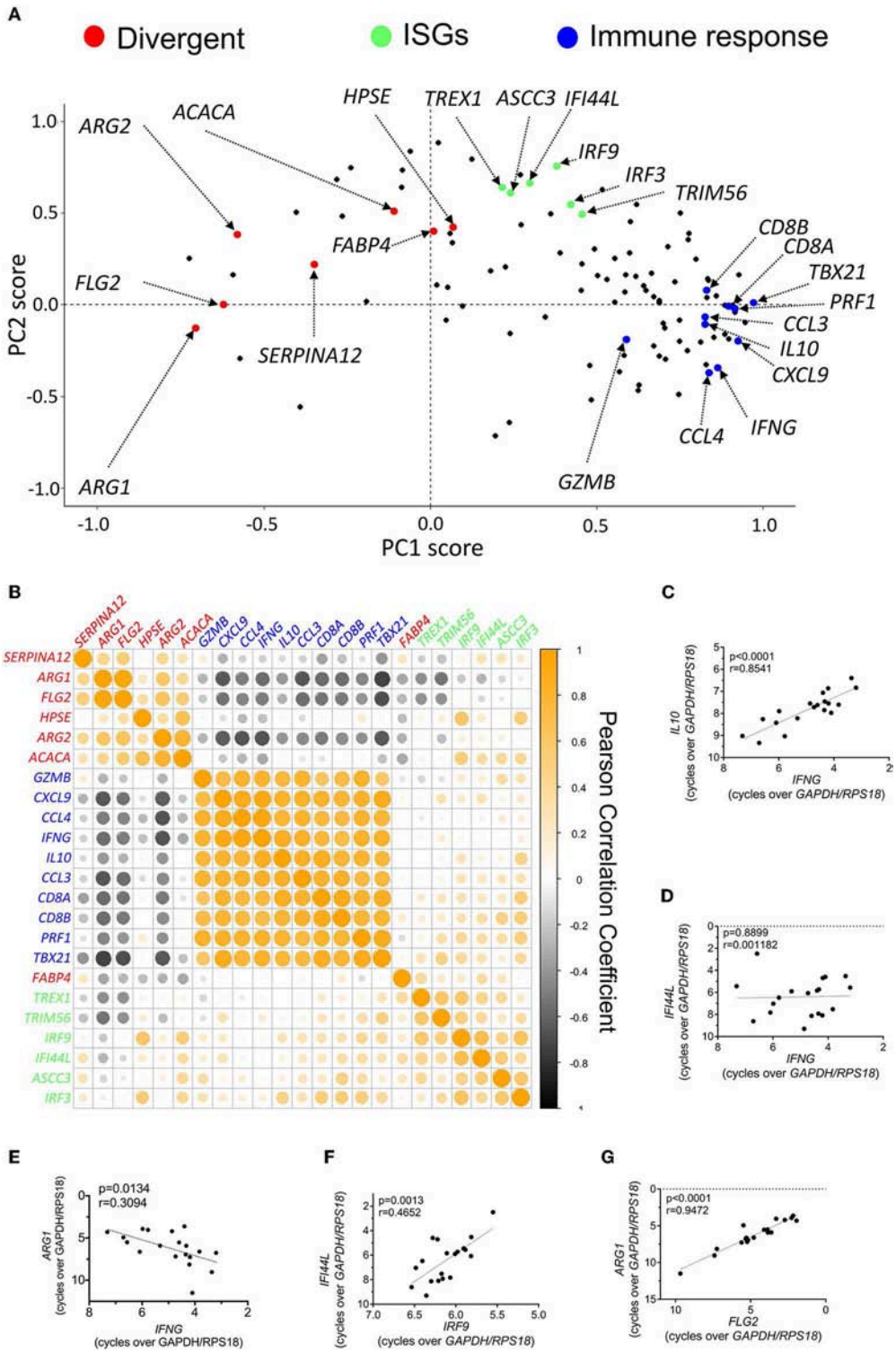

FIGURE 2 | Induction of a pro-inflammatory signature in CL skin is associated with a dampened expression of genes involved in epidermal integrity and arginine and fatty acid metabolism. **(A)** Scores plot from PCA of skin biopsies from CL patients showing the PCA scores for each of the 111 differentially-expressed genes. Certain groups of genes are highlighted due to their comparable PCA scores and functional relationship. **(B)** Clustered heatmap of Pearson correlation coefficients of the expression levels for the genes highlighted in **Figure 4A** in infected skin biopsies. **(C–G)** Pearson correlation of the expression levels of selected pairs of genes from **Figure 4B** across infected biopsies; **(C)** *IL10* vs. *IFNG*; **(D)** *IFI44L* vs. *IFNG*; **(E)** *ARG1* vs. *IFNG*; **(F)** *IFI44L* vs. *IRF9*; **(G)** *ARG1* vs. *FLG2*.

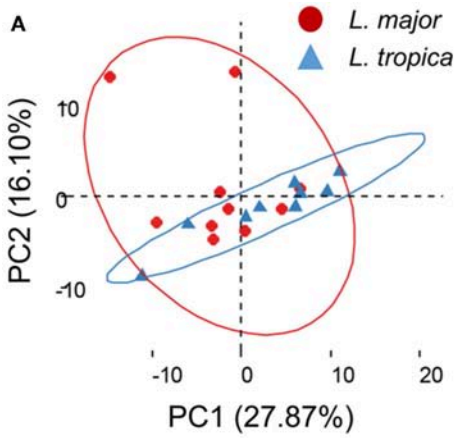

B

Enriched in *L. major* lesions	
Gene	Fold change (relative to *L. tropica* lesions) (p<0.05)
PIP	3.39
NT5C3A	3.18
ATP5B	1.35

C

Enriched in *L. tropica* lesions	
Gene	Fold change (relative to *L. major* lesions) (p<0.05)
RORC	11.74
CXCL9	2.56
GZMB	2.35
CCL4	2.13
PRF1	2.03
MPO	1.85
CCL5	1.71
CCR5	1.70
CD8B	1.69
SERP1	1.65
GZMA	1.57
ANKRD37	1.52
CASP4	1.34
LDHA	1.25

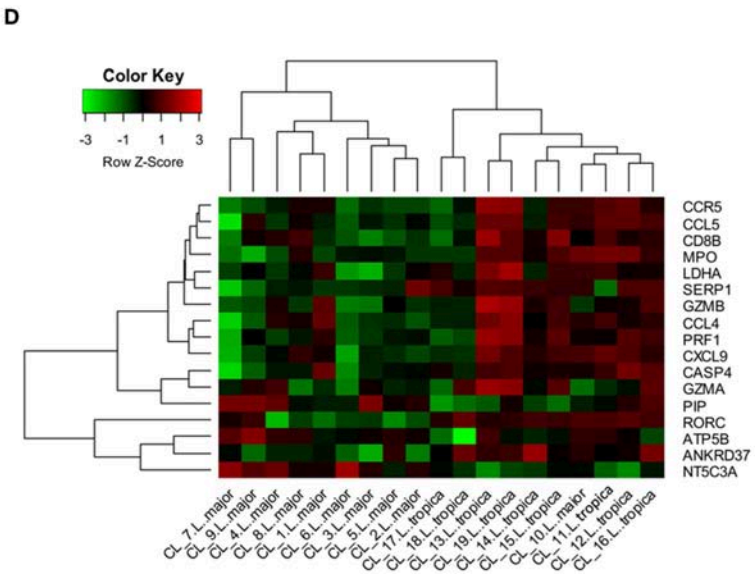

FIGURE 3 | Skin biopsies from CL patients caused by *L. major* or *L. tropica* are transcriptionally very similar, the latter presenting an aggravated inflammatory/cytotoxic signature. **(A)** PCA analysis of the 170 analyzed genes from the 19 CL skin biopsies caused by infection with either *L. major* (red dots) or *L. tropica* (blue triangles). The two principal components (PC) are displayed on the axis along with the variance. Large circles denote the 95% confidence level. **(B)** Table detailing the genes significantly ($P < 0.05$) enriched in *L. major* biopsies as compared with *L. tropica*. **(C)** Table detailing the genes significantly ($P < 0.05$) enriched in *L. tropica* biopsies as compared with *L. major*. **(D)** Clustered heatmap of skin biopsies from CL patients according to their expression of the genes differentially expressed between *L. major* and *L. tropica* lesions.

The Transcript Levels of the Tryptophan-Metabolizing Enzyme TDO Negatively Correlate With the Parasite Load in Lesions, and Inhibition of TDO Activity Promotes Intracellular *L. major* Growth in *in vitro*-Infected Macrophages

Recent data suggests that the parasite load in lesions impacts the type and magnitude of the immune responses induced during CL caused by *L. braziliensis* (Christensen et al., 2016). To evaluate whether a similar influence is present in lesions caused by *L. major* and *L. tropica*, we quantified the transcript levels of two parasite genes in the lesions, *KMP11* and *RRNA45*. These two genes are conserved across the *Leishmania* genus and stably expressed during the parasite's life cycle (Ouakad et al., 2007). They have also been validated as endogenous reference genes for gene expression studies in *Leishmania* (Moreira et al., 2012; Zangger et al., 2013), and thus should provide a precise quantification of the relative parasite load in samples. We observed that the transcript levels of these two parasite genes are strongly correlated with each other in skin biopsies, as expected (**Figure 4A**). At the limit of detection of our assay (CT $\leq$ 40), we could not amplify these transcripts from healthy skin samples (not shown). The variation in the parasite transcripts across the patients' samples wasn't due to the infecting species (**Figures 4A,B**), the patient's gender (**Figure 4C**), the patient's age

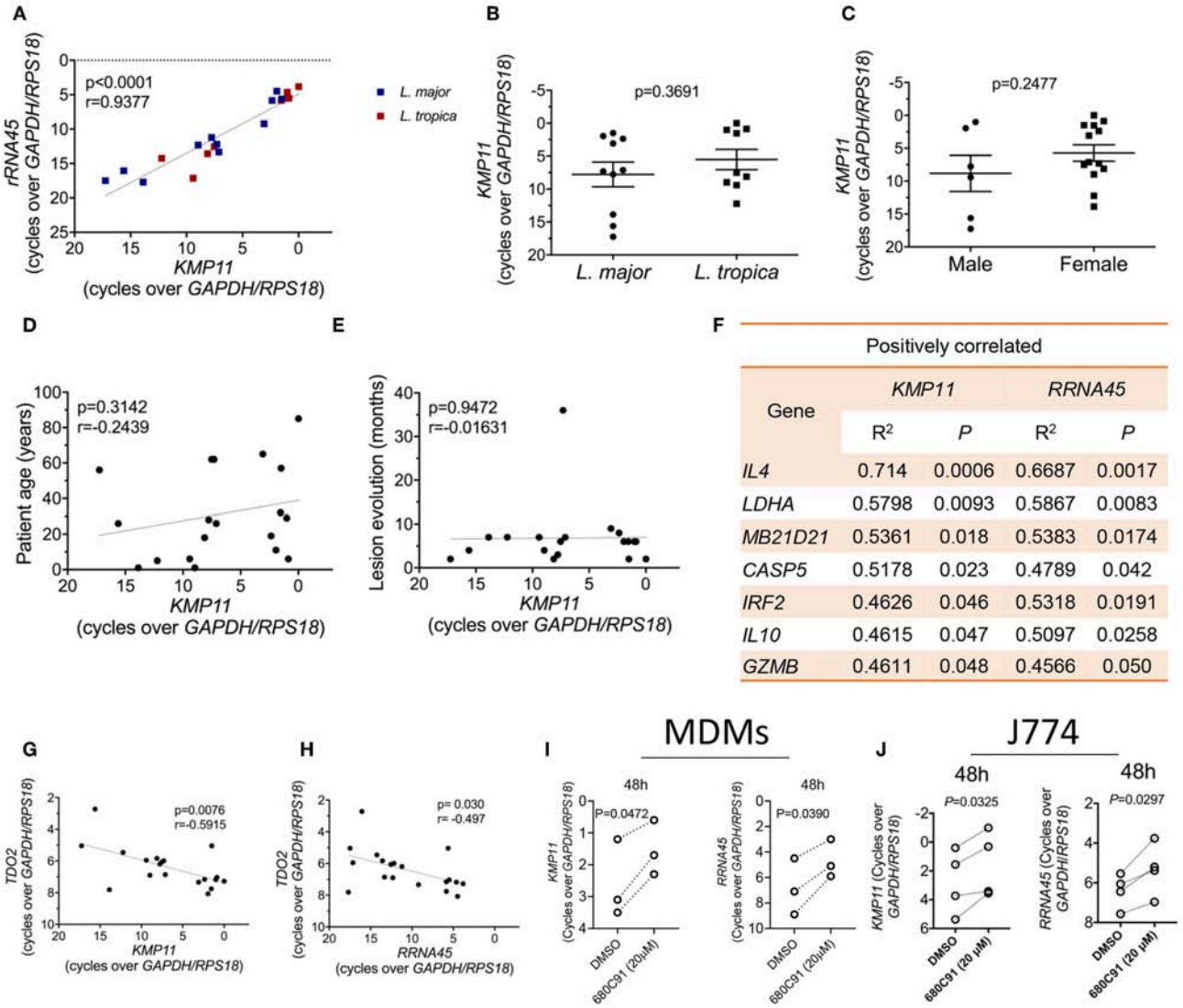

Gene	*KMP11*		*RRNA45*	
	R^2	*P*	R^2	*P*
IL4	0.714	0.0006	0.6687	0.0017
LDHA	0.5798	0.0093	0.5867	0.0083
MB21D21	0.5361	0.018	0.5383	0.0174
CASP5	0.5178	0.023	0.4789	0.042
IRF2	0.4626	0.046	0.5318	0.0191
IL10	0.4615	0.047	0.5097	0.0258
GZMB	0.4611	0.048	0.4566	0.050

FIGURE 4 | TDO gene expression is inversely correlated with the parasite load in lesions and inhibition of TDO boosts the parasite load in *L. major*-infected macrophages. **(A)** Correlation between the transcript levels of the *Leishmania* genes KMP11 and RRNA45 in CL biopsies from patients infected with *L. major* or *L. tropica* (Pearson correlation coefficient). **(B)** Comparison of the level of KMP11 expression between *L. major* and *L. tropica* biopsies (unpaired *T*-test). **(C)** Comparison of the level of *KMP11* expression between biopsies from male and female patients (unpaired *T*-test). **(D)** Correlation between the level of *KMP11* expression and the age of CL patients (Pearson correlation coefficient). **(E)** Correlation between the level of expression of *KMP11* and the time in months after lesion appearance (Pearson correlation coefficient). **(F)** Table of genes whose expression is significantly ($P < 0.05$) positively correlated with the expression levels of both *KMP11* and *RRNA45*. **(G)** Correlation between the levels of mRNA expression of *KMP11* and *TDO2* (Pearson correlation coefficient). **(H)** (Correlation between the levels of mRNA expression of *RRNA45* and *TDO2* (Pearson correlation coefficient). **(I,J)** MDMs **(I)** or J774 cells **(J)** were infected with *L. major* stationary phase promastigotes and subsequently treated with 20 μM of the TDO specific inhibitor, 680C91 or vehicle (DMSO). Cells were lysed for RNA extraction at 48 h after infection. The transcript levels of the *Leishmania* genes *KMP11* (left panels) or *RRNA45* (right panels) were quantified by qPCR and normalized by the expression of the host housekeeping genes (*GAPDH* and *RPS18*) (paired *T*-test). **(A–E,G,H)** Each dot represents an individual CL skin biopsy. **(I)** Each paired dot represents an independent blood donor ($n = 3$). **(J)** Each paired dot represents an independent experiment ($n = 4$).

(**Figure 4D**), or the time after lesion appearance (**Figure 4E**). We thus sought to identify host genes whose expression is either positively or negatively correlated with the parasite load. For that, we plotted the Pearson correlations between the expression levels of either *KMP11* or *RRNA45* and each of the host genes in our entire dataset. The expression of a total of seven genes were significantly positively correlated with the mRNA levels of both *KMP11* and *RRNA45* (**Figure 4F**). These include well-known susceptibility factors for CL, such as *IL4* or *IL10*. We also found that factors usually implicated in antiviral defense such as cGAS (*MB21D1)* and *IRF2* appear upregulated in lesions with higher parasite transcripts (**Figure 4F**).

Strikingly, among our entire dataset, a single gene, *TDO2*, which encodes for the tryptophan-catabolizing enzyme tryptophan 2,3-dioxygenase (TDO), negatively correlates with the expression levels of both *KMP11* and *RRNA45* (**Figures 4G,H**).

The negative correlation observed between the transcript levels of TDO and the parasite load in lesions, suggests that this enzyme may act as a restriction factor for cutaneous *Leishmania*. To test this hypothesis, we infected primary human monocyte-derived macrophages (MDMs) (**Figure 4I**) or the murine macrophage cell line J774 (**Figure 4J**) with *L. major* stationary phase promastigotes. After 4 h of infection, cells were treated with a specific TDO inhibitor, 680C91. We observed a significant increase in the levels of parasite transcripts at 48 h after treatment with 20 μM of 680C91, in both cell types, as measured by the expression of *KMP11* (**Figures 4I,J**, left panels). A similar result was observed when using *RRNA45* to quantify the parasite load (**Figures 4I,J**, right panels). We thus conclude that TDO restricts the intracellular growth of *Leishmania major* and its expression levels correlate negatively with the parasite transcripts in cutaneous biopsies.

DISCUSSION

The clinical presentation of CL results from a complex interplay of multiple factors, including the host's genetic background, its immunological status, and the parasite species (Scott and Novais, 2016). By exploring the variation in gene expression across lesion samples, we found that the induction of genes associated with immune responses was negatively correlated with the levels of transcripts encoding for genes ensuring epidermal integrity and fatty acid metabolism. This immune response group of genes was particularly enriched in genes involved the effector cytotoxic CD8 T cell function, including *CD8A, CD8B, PRF1* (perforin-1), and *GZMB* (granzyme B), as well as *TBX21* (T-bet). This group further comprised *CCL5* (Rantes) and *CCL4* (MIP-1β), which attract effector CD8 T cells to inflamed tissues (Franciszkiewicz et al., 2012). Our observations thus suggest that the magnitude of the CD8 cytotoxic response has a direct impact on the integrity of the skin and lesion pathology. Our data is in agreement with observations made on *L. braziliensis* lesions, where a similar relationship between the induction of a cytotoxic program and loss of epidermal integrity seems to operate (Novais et al., 2015, 2017).

We further observed the induction of a group of interferon-stimulated genes (ISGs) in CL biopsies, including transcripts encoding for IRF9, IRF3, IFI44L, and TRIM56. Interestingly, the induction of this type I IFN signature was independent of the main pro-inflammatory module and did not show any association with the expression of genes maintaining epidermal integrity or involved in fatty acid or arginine metabolism. Thus, our data suggests that the ISG signature does not directly contribute to the immunopathogenesis of CL, in contrast with what is observed in metastatic mucocutaneous leishmaniasis (MCL) (Rossi et al., 2017). As ISGs are generally induced following viral infection, we reasoned that the presence of LRV could explain the induction of these genes in a subset of the samples. We couldn't however detect LRV sequences in any of the biopsies of the cohort. Also, the induction of the ISG signature was independent of the parasite species and the parasite load. Thus, the factors that lead to the upregulation of these ISGs in a subset of CL lesions remain unidentified. It is possible that exogenous viral infections, known to be transmitted alongside *Leishmania* by the sand-fly vector, may trigger the detectable ISG response during CL (Rossi et al., 2017).

We further found a significant upregulation of genes encoding for inflammasome components in CL biopsies, including *NLRP3, CASP1,* and *CASP4*. Activation of the inflammasome at the site of *Leishmania* inoculation depends on co-transmission of microbes from the sand-fly gut, leading to IL-1β production and neutrophil recruitment (Dey et al., 2018), thus supporting observation of elevated *IL1B* levels as well as the neutrophil marker *MPO* in our cohort of biopsies.

A major novelty in our study is the direct comparison of the transcriptional profile of CL lesions caused by infection with two distinct *Leishmania* species. As both types of lesions were recovered from the same endemic areas, this analysis should provide an unbiased approach to assess the impact of the infecting species on the transcriptional profile of CL. Our data indicates that the transcriptional profiles of CL caused by *L. major* or *L. tropica* are very similar. Nevertheless, we found that lesions caused by *L. tropica* present an aggravated inflammatory profile with increased expression of genes associated with the CD8 T cell cytotoxic function and the inflammatory response. Conversely, we found that the expression of the gene encoding pyrimidine 5′-nucleotidase (NT5C3A) was significantly enriched in *L. major* lesions, as compared with *L. tropica*. NT5C3A suppresses cytokine production through inhibition of the NF-κB pathway (Al-Haj and Khabar, 2018) and may represent a negative feedback regulator of inflammatory cytokine signaling in *L. major*-caused CL, as compared with *L. tropica* lesions.

Clinically, lesions caused by *L. tropica* tend to be dryer and take longer to heal as compared to those caused by *L. major* (Masoudzadeh et al., 2017). This supports the idea that an aggravated inflammatory/ cytotoxic profile in *L. tropica* lesions prevents or delays the action of the mechanisms of skin regeneration. Future studies, employing larger gene sets, should aim to pinpoint whether the distinct clinical pictures observed in lesions caused by *L. major* and *L. tropica* conceal distinct transcriptional signatures. These studies can potentially be extended to additional parasite species that co-exist in the same endemic regions.

The impact of the parasite load on the transcriptional profile of CL lesions has been explored in a few studies (Kumar et al., 2009; Christensen et al., 2016; Pereira et al., 2017), but so far such knowledge has not been translated into the identification of genes that restrict parasite growth. Our approach of quantifying parasite transcripts as a proxy for the parasite load is validated by the finding that *IL4* was the host transcript that more significantly correlated with parasite transcripts in a positive manner. This confirms a previous study that uncovered a correlation between the levels of *IL4* expression and the parasite load in *L. tropica* lesions (Kumar et al., 2009). It is interesting to note that, in our

study, the expression levels of *IL4* are not significantly changed in CL lesions, as compared with healthy skin, which confirms the notion that, in humans, CL does not develop because of the abnormal expansion of Th2 cells. This suggests that the variability in the levels of *IL4* expression across individuals before infection is a major factor in determining the parasite load after infection. In this sense, it is interesting to note that polymorphisms at the level of the *IL4* promoter are associated with increased risk of developing CL (Kamali-Sarvestani et al., 2006). Additionally, CL patients with a concomitant helminth infection, known to drive a polarized Th2 response characterized by high IL-4 levels, bear lesions that take longer to heal as compared with helminth-free patients (O'Neal et al., 2007).

The transcript levels of the tryphophan-metabolizing enzyme TDO were negatively correlated with the parasite load in lesions. Furthermore, inhibition of TDO promoted an increase in parasite transcripts in human and mouse macrophages infected *in vitro* with *L. major*. TDO catalyzes the first, and rate-limiting, step in the biosynthesis of NAD+, by converting tryptophan to N-formylkynurenine (Platten et al., 2012). Its expression is particularly enriched in the liver, where it regulates the systemic levels of tryptophan, but other tissues such as the brain, lungs, or skin also appear to express low levels of the enzyme (van Baren and Van den Eynde, 2015). Unlike indoleamine 2,3-dioxygenase-1 (IDO), the other major enzyme involved in the degradation of tryptophan, TDO is not induced by inflammatory stimuli or cytokines (Lanz et al., 2017). Unlike IDO, the role of TDO during the immune response remains mostly unexplored. In our study, while *IDO1* was among the genes most highly induced in lesions as compared to healthy skin, the levels of *TDO2* remained unchanged. However, the abundance of *IDO1* transcripts had no correlation with the parasite load in lesions, while *TDO2* correlated negatively with the levels of parasite transcripts. *Leishmania* is auxotrophic for tryptophan (Nayak et al., 2018), which suggests that TDO may repress parasite growth by depleting intracellular tryptophan levels. However, within the inflammatory environment that characterizes CL and the consequent strong induction of IDO, the role of TDO in regulating tryptophan levels is probably negligible. As such, TDO may restrict cutaneous *Leishmania* through a mechanism not related to the depletion of tryptophan. Alternatively, the subcellular distribution of TDO may be distinct from IDO and allow it to selectively deplete tryptophan in the vicinity of parasite compartments. However, little is known about the subcellular localization of TDO. It is interesting to note that the growth of intracellular pathogens is differentially impacted by the inhibition of tryptophan degradation. For instance, the administration of an IDO inhibitor to *Leishmania major*-infected mice led to a better control of the infection and decreased the parasite load. In contrast, inhibition of IDO in *Toxoplasma gondii*-infected mice led to uncontrolled parasite growth, and accelerated mortality (Divanovic et al., 2012). Thus, the capacity of tryptophan-depleting enzymes to control intracellular parasites is pathogen-specific, likely depending on factors such as the replication kinetics of the parasite, or the localization of its intracellular niche, with TDO apparently being better suited to restrict *Leishmania* growth. Finally, given the strong expression of TDO in the liver, it is of the utmost interest to assess the impact of TDO inhibition on the growth of liver-targeting *Leishmania* species, such as *L. donovani*.

The relationship between the pathology of CL and the parasite load in the lesion is complex. In general, diffuse manifestations of cutaneous leishmaniasis (DCL), caused for instance by *L. aethiopica* are characterized by large numbers of parasites in lesions that spread over vast areas of the skin. These patients exhibit severe T cell anergy against parasite antigen as well as CD8 T cell exhaustion (Hernandez-Ruiz et al., 2010), that appear to be promoted by elevated levels of regulatory cytokines, such as IL10 (Scott and Novais, 2016). On the opposite side of the spectrum, lesions presenting an aggravated inflammatory profile, associated with extensive tissue destruction and immunopathology, such as MCL caused by *L. braziliensis*, tend to bear very low numbers of parasites (Scott and Novais, 2016). These lesions are characterized by extensive infiltration of CD4 T cells with a polarized Th1 profile, as well as cytotoxic CD8 T lymphocytes (Faria et al., 2005). Both of these extremes are characterized by severe pathology. In one case, due to parasite proliferation, and the other due to an excessive immune response (Scott and Novais, 2016). In patients with localized cutaneous leishmaniasis a compromise is attained in which the parasite load is kept in check by an immune response whose magnitude is regulated by the action of regulatory cytokines such as IL-10 or TGF-β (Scott and Novais, 2016). Indeed, we observed a co-induction of these immunoregulatory factors along with the pro-inflammatory mediators, suggesting that they act as brakes to moderate an excessive immune response. However, even localized CL lesions take long to heal, often leaving disfiguring scars that are a source of social stigma for individuals. In this context, novel therapeutic interventions, such as inducing the activation of TDO, that could adjuvate conventional anti-*Leishmania* drugs may allow for faster healing of the lesions in the context of a milder inflammatory response. This has a clear advantage over classical immunotherapeutic approaches, such as the neutralization of regulatory cytokines or the inhibition of immune checkpoints, that often result in exacerbated immune responses and concomitant pathology.

DATA AVAILABILITY STATEMENT

All datasets generated for this study are included in the manuscript/**Supplementary Files**.

ETHICS STATEMENT

This work was conducted according to the principles specified in the Declaration of Helsinki and under the local ethical guidelines of the Ethics Committee for Biomedical Research (Faculty of Medicine and Pharmacy, Hassan II University of Casablanca, Morocco) that approved this research. The team explained to the patients the objectives of the survey, and why it needed a cutaneous biopsy, which is used routinely at the Department of Dermatology (University Hospital Ibn Rochd, Casablanca) for the parasitological confirmation of cutaneous leishmaniasis

diagnosis before any treatment prescription. The dermatologist asked for the patients consent (for adults) or from the parents for children. The sampling was done only if the patients or their tutors gave their oral consent. At the time of biopsy sampling (between 2012 and 2014), oral consent was the sole requirement imposed by the Ethics Committee to allow for patient tissue sampling for research purposes and thus written consent was not obtained. Oral consent was also obtained from the healthy skin donors. Finally, the team guaranteed the confidentiality of their personal and clinical data and that the results would be processed anonymously.

AUTHOR CONTRIBUTIONS

VR, MR, KA, and JE planned research and coordinated the study. VR, SA, HM, and TM performed the experiments. SC provided the clinical samples. VR analyzed the data. VR and JE wrote the manuscript with contributions from MR and KA. All authors read and approved the submitted version of the manuscript.

FUNDING

This study was supported by a funding given by the Partenariat Hubert Curien (PHC) program (Volubilis, MA/11/262) (KA, MR, and JE). The research leading to these results has received funding from the European Community's Seventh Framework Programme under grant agreement No. 602773 Project KINDRED (JE). SA was supported by a post-doctoral fellowship from Fondation de la Recherche Médicale (FRM: SPF20160936115). VR was supported by a post-doctoral fellowship granted by the KINDReD consortium. The funders had no role in study design, data collection and analysis, decision to publish, or preparation of the manuscript.

SUPPLEMENTARY MATERIAL

The Supplementary Material for this article can be found online at: https://www.frontiersin.org/articles/10.3389/fcimb.2019.00338/full#supplementary-material

REFERENCES

Al-Haj, L., and Khabar, K. S. A. (2018). The intracellular pyrimidine 5'-nucleotidase NT5C3A is a negative epigenetic factor in interferon and cytokine signaling. *Sci. Signal*. 11:eaal2434. doi: 10.1126/scisignal.aal2434

Alvar, J., Velez, I. D., Bern, C., Herrero, M., Desjeux, P., Cano, J., et al. (2012). Leishmaniasis worldwide and global estimates of its incidence. *PLoS ONE* 7:e35671. doi: 10.1371/journal.pone.0035671

Aoun, K., and Bouratbine, A. (2014). Cutaneous leishmaniasis in North Africa: a review. *Parasite* 21:14. doi: 10.1051/parasite/2014014

Christensen, S. M., Dillon, L. A., Carvalho, L. P., Passos, S., Novais, F. O., Hughitt, V. K., et al. (2016). Meta-transcriptome profiling of the Human-*Leishmania braziliensis* cutaneous lesion. *PLoS Negl. Trop. Dis*. 10:e0004992. doi: 10.1371/journal.pntd.0004992

da Silva Santos, C., Attarha, S., Saini, R. K., Boaventura, V., Costa, J., Khouri, R., et al. (2015). Proteome profiling of human cutaneous leishmaniasis lesion. *J. Invest. Dermatol*. 135, 400–410. doi: 10.1038/jid.2014.396

David, C. V., and Craft, N. (2009). Cutaneous and mucocutaneous leishmaniasis. *Dermatol. Ther*. 22, 491–502. doi: 10.1111/j.-8019.2009.01272.x

Dey, R., Joshi, A. B., Oliveira, F., Pereira, L., Guimaraes-Costa, A. B., Serafim, T. D., et al. (2018). Gut microbes egested during bites of infected sand flies augment severity of leishmaniasis via inflammasome-derived IL-1beta. *Cell Host Microbe* 23, 134–143.e16. doi: 10.1016/j.chom.2017.12.002

Divanovic, S., Sawtell, N. M., Trompette, A., Warning, J. I., Dias, A., Cooper, A. M., et al. (2012). Opposing biological functions of tryptophan catabolizing enzymes during intracellular infection. *J. Infect. Dis*. 205, 152–161. doi: 10.1093/infdis/jir621

Farajnia, S., Mahboudi, F., Ajdari, S., Reiner, N. E., Kariminia, A., and Alimohammadian, M. H. (2005). Mononuclear cells from patients recovered from cutaneous leishmaniasis respond to Leishmania major amastigote class I nuclease with a predominant Th1-like response. *Clin. Exp. Immunol*. 139, 498–505. doi: 10.1111/j.1365-2249.2004.02702.x

Faria, D. R., Gollob, K. J., Barbosa, J. Jr., Schriefer, A., Machado, P. R., Lessa, H., et al. (2005). Decreased in situ expression of interleukin-10 receptor is correlated with the exacerbated inflammatory and cytotoxic responses observed in mucosal leishmaniasis. *Infect. Immun*. 73, 7853–7859. doi: 10.1128/IAI.73.12.7853-7859.2005

Favila, M. A., Geraci, N. S., Zeng, E., Harker, B., Condon, D., Cotton, R. N., et al. (2014). Human dendritic cells exhibit a pronounced type I IFN signature following Leishmania major infection that is required for IL-12 induction. *J. Immunol*. 192, 5863–5872. doi: 10.4049/jimmunol.1203230

Franciszkiewicz, K., Boissonnas, A., Boutet, M., Combadiere, C., and Mami-Chouaib, F. (2012). Role of chemokines and chemokine receptors in shaping the effector phase of the antitumor immune response. *Cancer Res*. 72, 6325–6332. doi: 10.1158/0008-5472.CAN-12-2027

Gould, J., Getz, G., Monti, S., Reich, M., and Mesirov, J. P. (2006). Comparative gene marker selection suite. *Bioinformatics* 22, 1924–1925. doi: 10.1093/bioinformatics/btl196

Hajjaran, H., Mahdi, M., Mohebali, M., Samimi-Rad, K., Ataei-Pirkooh, A., Kazemi-Rad, E., et al. (2016). Detection and molecular identification of leishmania RNA virus (LRV) in Iranian *Leishmania* species. *Arch. Virol*. 161, 3385–3390. doi: 10.1007/s00705-016-3044-z

Hernandez-Ruiz, J., Salaiza-Suazo, N., Carrada, G., Escoto, S., Ruiz-Remigio, A., Rosenstein, Y., et al. (2010). CD8 cells of patients with diffuse cutaneous leishmaniasis display functional exhaustion: the latter is reversed, *in vitro*, by TLR2 agonists. *PLoS Negl. Trop. Dis*. 4:e871. doi: 10.1371/journal.pntd.0000871

Hugues, S., Scholer, A., Boissonnas, A., Nussbaum, A., Combadiere, C., Amigorena, S., et al. (2007). Dynamic imaging of chemokine-dependent CD8+ T cell help for CD8+ T cell responses. *Nat. Immunol*. 8, 921–930. doi: 10.1038/ni1495

Kamali-Sarvestani, E., Rasouli, M., Mortazavi, H., and Gharesi-Fard, B. (2006). Cytokine gene polymorphisms and susceptibility to cutaneous leishmaniasis in Iranian patients. *Cytokine* 35, 159–165. doi: 10.1016/j.cyto.2006.07.016

Kaye, P., and Scott, P. (2011). Leishmaniasis: complexity at the host-pathogen interface. *Nat. Rev. Microbiol*. 9, 604–615. doi: 10.1038/nrmicro2608

Kumar, R., Bumb, R. A., and Salotra, P. (2009). Correlation of parasitic load with interleukin-4 response in patients with cutaneous leishmaniasis due to *Leishmania tropica*. *FEMS Immunol. Med. Microbiol*. 57, 239–246. doi: 10.1111/j.1574-695X.2009.00607.x

Lanz, T. V., Williams, S. K., Stojic, A., Iwantscheff, S., Sonner, J. K., Grabitz, C., et al. (2017). Tryptophan-2,3-Dioxygenase (TDO) deficiency is associated with subclinical neuroprotection in a mouse model of multiple sclerosis. *Sci. Rep*. 7:41271. doi: 10.1038/srep41271

Maretti-Mira, A. C., Bittner, J., Oliveira-Neto, M. P., Liu, M., Kang, D., Li, H., et al. (2012). Transcriptome patterns from primary cutaneous *Leishmania braziliensis* infections associate with eventual development of mucosal disease in humans. *PLoS Negl. Trop. Dis*. 6:e1816. doi: 10.1371/journal.pntd.0001816

Masoudzadeh, N., Mizbani, A., Taslimi, Y., Mashayekhi, V., Mortazavi, H., Sadeghipour, P., et al. (2017). *Leishmania tropica* infected human lesions: whole genome transcription profiling. *Acta Trop*. 176, 236–241. doi: 10.1016/j.actatropica.2017.08.016

Mniouil, M., Fellah, H., Amarir, F., Et-Touys, A., Bekhti, K., Adlaoui, E. B., et al. (2017). Epidemiological characteristics of visceral leishmaniasis

in Morocco (1990–2014): an update. *Acta Trop*. 170, 169–177. doi: 10.1016/j.actatropica.2016.10.016

Moreira, D., Rodrigues, V., Abengozar, M., Rivas, L., Rial, E., Laforge, M., et al. (2015). *Leishmania infantum* modulates host macrophage mitochondrial metabolism by hijacking the SIRT1-AMPK axis. *PLoS Pathog*. 11:e1004684. doi: 10.1371/journal.ppat.1004684

Moreira, D., Santarem, N., Loureiro, I., Tavares, J., Silva, A. M., Amorim, A. M., et al. (2012). Impact of continuous axenic cultivation in *Leishmania infantum* virulence. *PLoS Negl. Trop. Dis*. 6:e1469. doi: 10.1371/journal.pntd.0001469

Mouttaki, T., Morales-Yuste, M., Merino-Espinosa, G., Chiheb, S., Fellah, H., Martin-Sanchez, J., et al. (2014). Molecular diagnosis of cutaneous leishmaniasis and identification of the causative *Leishmania* species in Morocco by using three PCR-based assays. *Parasit. Vectors* 7:420. doi: 10.1186/1756-3305-7-420

Murray, H. W., Berman, J. D., Davies, C. R., and Saravia, N. G. (2005). Advances in leishmaniasis. *Lancet* 366, 1561–1577. doi: 10.1016/S0140-6736(05)67629-5

Nayak, A., Akpunarlieva, S., Barrett, M., and Burchmore, R. (2018). A defined medium for *Leishmania* culture allows definition of essential amino acids. *Exp. Parasitol*. 185, 39–52. doi: 10.1016/j.exppara.2018.01.009

Novais, F. O., Carvalho, A. M., Clark, M. L., Carvalho, L. P., Beiting, D. P., Brodsky, I. E., et al. (2017). CD8+ T cell cytotoxicity mediates pathology in the skin by inflammasome activation and IL-1beta production. *PLoS Pathog*. 13:e1006196. doi: 10.1371/journal.ppat.1006196

Novais, F. O., Carvalho, L. P., Passos, S., Roos, D. S., Carvalho, E. M., Scott, P., et al. (2015). Genomic profiling of human *Leishmania braziliensis* lesions identifies transcriptional modules associated with cutaneous immunopathology. *J. Invest. Dermatol*. 135, 94–101. doi: 10.1038/jid.2014.305

O'Neal, S. E., Guimaraes, L. H., Machado, P. R., Alcantara, L., Morgan, D. J., Passos, S., et al. (2007). Influence of helminth infections on the clinical course of and immune response to *Leishmania braziliensis* cutaneous leishmaniasis. *J. Infect. Dis*. 195, 142–148. doi: 10.1086/509808

Ortega, C., Fernandez, A. S., Carrillo, J. M., Romero, P., Molina, I. J., Moreno, J. C., et al. (2009). IL-17-producing CD8+ T lymphocytes from psoriasis skin plaques are cytotoxic effector cells that secrete Th17-related cytokines. *J. Leukoc. Biol*. 86, 435–443. doi: 10.1189/JLB.0109046

Ouakad, M., Bahi-Jaber, N., Chenik, M., Dellagi, K., and Louzir, H. (2007). Selection of endogenous reference genes for gene expression analysis in *Leishmania* major developmental stages. *Parasitol. Res*. 101, 473–477. doi: 10.1007/s00436-007-0491-1

Pearce, E. L., and Pearce, E. J. (2013). Metabolic pathways in immune cell activation and quiescence. *Immunity* 38, 633–643. doi: 10.1016/j.immuni.2013.04.005

Pereira, L. O., Moreira, R. B., de Oliveira, M. P., Reis, S. O., de Oliveira Neto, M. P., and Pirmez, C. (2017). Is *Leishmania (Viannia) braziliensis* parasite load associated with disease pathogenesis? *Int. J. Infect. Dis*. 57, 132–137. doi: 10.1016/j.ijid.2017.01.036

Platten, M., Wick, W., and Van den Eynde, B. J. (2012). Tryptophan catabolism in cancer: beyond IDO and tryptophan depletion. *Cancer Res*. 72, 5435–5440. doi: 10.1158/0008-5472.CAN-12-0569

Reale, S., Maxia, L., Vitale, F., Glorioso, N. S., Caracappa, S., and Vesco, G. (1999). Detection of *Leishmania infantum* in dogs by PCR with lymph node aspirates and blood. *J. Clin. Microbiol*. 37, 2931–2935.

Reithinger, R., Dujardin, J. C., Louzir, H., Pirmez, C., Alexander, B., and Brooker, S. (2007). Cutaneous leishmaniasis. *Lancet Infect. Dis*. 7, 581–596. doi: 10.1016/S1473-3099(07)70209-8

Rossi, M., Castiglioni, P., Hartley, M. A., Eren, R. O., Prevel, F., Desponds, C., et al. (2017). Type I interferons induced by endogenous or exogenous viral infections promote metastasis and relapse of leishmaniasis. *Proc. Natl. Acad. Sci. U.S.A*. 114, 4987–4992. doi: 10.1073/pnas.1621447114

Schleicher, U., Liese, J., Justies, N., Mischke, T., Haeberlein, S., Sebald, H., et al. (2018). Type I Interferon signaling is required for CpG-oligodesoxynucleotide-induced control of *Leishmania* major, but not for spontaneous cure of subcutaneous primary or secondary *L. major* Infection. *Front. Immunol*. 9:79. doi: 10.3389/fimmu.2018.00079

Scott, P., and Novais, F. O. (2016). Cutaneous leishmaniasis: immune responses in protection and pathogenesis. *Nat. Rev. Immunol*. 16, 581–592. doi: 10.1038/nri.2016.72

Shahi, M., Mohajery, M., Shamsian, S. A., Nahrevanian, H., and Yazdanpanah, S. M. (2013). Comparison of Th1 and Th2 responses in non-healing and healing patients with cutaneous leishmaniasis. *Rep. Biochem. Mol. Biol*. 1, 43–48.

van Baren, N., and Van den Eynde, B. J. (2015). Tryptophan-degrading enzymes in tumoral immune resistance. *Front. Immunol*. 6:34. doi: 10.3389/fimmu.2015.00034

Vargas-Inchaustegui, D. A., Hogg, A. E., Tulliano, G., Llanos-Cuentas, A., Arevalo, J., Endsley, J. J., et al. (2010). CXCL10 production by human monocytes in response to *Leishmania braziliensis* infection. *Infect. Immun*. 78, 301–308. doi: 10.1128/IAI.00959-09

WHO (2013). *Sustaining the Drive to Overcome the Global Impact of Neglected Tropical Diseases: Second WHO Report on Neglected Tropical Diseases*. Available online at: http://www.who.int/neglected_diseases/9789241564540/en/ (accessed March 26, 2014).

Zangger, H., Ronet, C., Desponds, C., Kuhlmann, F. M., Robinson, J., Hartley, M. A., et al. (2013). Detection of Leishmania RNA virus in *Leishmania* parasites. *PLoS Negl. Trop. Dis*. 7:e2006. doi: 10.1371/journal.pntd.0002006

Conflict of Interest: The authors declare that the research was conducted in the absence of any commercial or financial relationships that could be construed as a potential conflict of interest.

frontiers in Cellular and Infection Microbiology

ORIGINAL RESEARCH
published: 29 October 2019
doi: 10.3389/fcimb.2019.00353

Sertraline Delivered in Phosphatidylserine Liposomes Is Effective in an Experimental Model of Visceral Leishmaniasis

Maiara Maria Romanelli[1†], Thais Alves da Costa-Silva[1†], Edezio Cunha-Junior[2†], Daiane Dias Ferreira[1], Juliana M. Guerra[3], Andres Jimenez Galisteo Jr.[4], Erika Gracielle Pinto[5], Leandro R. S. Barbosa[6], Eduardo Caio Torres-Santos[2] and Andre Gustavo Tempone[1*]*

[1] Centre for Parasitology and Mycology, Instituto Adolfo Lutz, São Paulo, Brazil, [2] Fundação Oswaldo Cruz, Instituto Oswaldo Cruz, Pavilhão Leonidas Deane, Laboratório de Bioquímica de Tripanosomatídeos, Rio de Janeiro, Brazil, [3] Centre for Pathology, Instituto Adolfo Lutz, São Paulo, Brazil, [4] Faculdade de Medicina, Hospital das Clínicas HCFMUSP, Universidade de São Paulo, São Paulo, Brazil, [5] Drug Discovery Unit, Life Sciences, University of Dundee, Dundee, Scotland, [6] Instituto de Física da Universidade de São Paulo, Cidade Universitária, São Paulo, Brazil

Liposomes containing phosphatidylserine (PS) has been used for the delivery of drugs into the intramacrophage milieu. *Leishmania* (L.) *infantum* parasites live inside macrophages and cause a fatal and neglected viscerotropic disease, with a toxic treatment. Sertraline was studied as a free formulation (SERT) and also entrapped into phosphatidylserine liposomes (LP-SERT) against intracellular amastigotes and in a murine model of visceral leishmaniasis. LP-SERT showed a potent activity against intracellular amastigotes with an EC_{50} value of 2.5 μM. The *in vivo* efficacy of SERT demonstrated a therapeutic failure. However, when entrapped into negatively charged liposomes (−58 mV) of 125 nm, it significantly reduced the parasite burden in the mice liver by 89% at 1 mg/kg, reducing the serum levels of the cytokine IL-6 and upregulating the levels of the chemokine MCP-1. Histopathological studies demonstrated the presence of an inflammatory infiltrate with the development of granulomas in the liver, suggesting the resolution of the infection in the treated group. Delivery studies showed fluorescent-labeled LP-SERT in the liver and spleen of mice even after 48 h of administration. This study demonstrates the efficacy of PS liposomes containing sertraline in experimental VL. Considering the urgent need for VL treatments, the repurposing approach of SERT could be a promising alternative.

Keywords: leishmania, neglected diseases, drug delivery, liposomes, drug repurposing, sertraline

OPEN ACCESS

Edited by:
Herbert Leonel de Matos Guedes, Federal University of Rio de Janeiro, Brazil

Reviewed by:
Elaine Soares Coimbra, Juiz de Fora Federal University, Brazil
Lukasz Kedzierski, The University of Melbourne, Australia
Jose Angelo Lauletta Lindoso, University of São Paulo, Brazil

***Correspondence:**
Eduardo Caio Torres-Santos
ects@ioc.fiocruz.br
Andre Gustavo Tempone
andre.tempone@ial.sp.gov.br

[†]These authors have contributed equally to this work

Specialty section:
This article was submitted to Parasite and Host, a section of the journal Frontiers in Cellular and Infection Microbiology

Received: *01 June 2019*
Accepted: *30 September 2019*
Published: *29 October 2019*

Citation:
Romanelli MM, da Costa-Silva TA, Cunha-Junior E, Dias Ferreira D, Guerra JM, Galisteo AJ Jr, Pinto EG, Barbosa LRS, Torres-Santos EC and Tempone AG (2019) Sertraline Delivered in Phosphatidylserine Liposomes Is Effective in an Experimental Model of Visceral Leishmaniasis. Front. Cell. Infect. Microbiol. 9:353. doi: 10.3389/fcimb.2019.00353

INTRODUCTION

Leishmaniasis is a neglected infectious disease caused by an intracellular protozoan known as *Leishmania* spp. Visceral leishmaniasis (VL) is highly endemic in the South America, where it is caused by *Leishmania* (L.) *infantum*; in the Indian subcontinent; and in the east of Africa, where the etiologic agent is *Leishmania* (L.) *donovani*; the WHO (World Health Organization, 2017) estimates more than 400,000 new cases of VL every year. More than 90% of these cases are

concentrated in Bangladesh, Brazil, Ethiopia, India, Sudan, and Southern Sudan (Alvar et al., 2012; World Health Organization, 2017). VL is a chronic and systemic disease affecting liver, spleen, and bone marrow, and if not adequately treated, it results in 100% of death. The current therapy is challenging due to a limited number of available drugs, elevated costs due to hospitalization, high toxicity, parenteral administration, and the emergence of resistance to conventional drugs (Alvar et al., 2012). Limited options are available for the treatment of VL. In the Indian subcontinent, a single dose of AmBisome and combination therapy are the preferred treatment options. The combination of antimony with paromomycin is the choice in East Africa and Yemen. In the Mediterranean Basin, Middle East, and Central Asia, AmBisome remains the main choice. According to the recent PAHO guidelines, AmBisome, SbV, and conventional AmB are still the recommended drugs for the treatment of VL in the New World (Chakravarty and Sundar, 2019). Among candidate drugs for VL is paromomycin, an aminoglycoside antimicrobial, which showed efficacy as a parenteral drug and entered for Phase III in 2005 (Croft et al., 2005). Considering the lack of therapeutic options for the treatment of VL, the need for novel drugs is evident (Tempone et al., 2017).

Finding new uses for FDA-approved drugs is known as drug repositioning, and has been considered an excellent approach for neglected diseases to reduce the costs and time of the research (Andrews et al., 2014; Huang et al., 2015; Costa-Silva et al., 2017). Currently, all available drugs for the clinical treatment of leishmaniases were introduced by the repositioning approach. Pentamidine, an aromatic diamine, was first synthesized by May and Baker Co, during the preparation of antitrypanosomal (*Trypanosoma brucei*) compounds (Lourie and Yorke, 1939). The first report describing the activity of amphotericin B against *Leishmania* was in 1960 (Furtado et al., 1960). However, amphotericin B was initially licensed in 1959 for the treatment of progressive and potentially life-threatening fungal infections (Ostrosky-Zeichner et al., 2003). Miltefosine (hexadecylphosphocholine) was synthesized as part of an anti-inflammatory program in 1982 at the pharmaceutical company Burroughs Wellcome (USA) (Croft and Engel, 2006). A series of alkyl phospholipids analogs made by Takeda Co. demonstrated effective *in vitro* properties as antifungals (Tsushima et al., 1982), but only 2 years later, these compounds were selected for screening against *Leishmania* and trypanosomes at the Wellcome Research Laboratories (UK). Finally, paromomycin, an oral broad-spectrum aminoglycoside antibiotic synthesized in 1959 by Carlo Erba Co. (Botero, 1978), was studied as an antileishmanial candidate in 1975 (Mattock and Peters, 1975).

Drugs approved for central nervous system like antidepressants are usually safe and widely used worldwide. Antidepressants and tricyclic neuroleptic drugs have shown antileishmanial activity (Evans and Croft, 1994; Chan et al., 1998; Richardson et al., 2009). Another widely used antidepressant, imipramine, showed potential antileishmanial effect (Andrade-Neto et al., 2016), with promising *in vivo* efficacy (Mukherjee et al., 2014). Additionally, imipramine has shown to depolarize the transmembrane mitochondrial potential of *L.* (L.) *donovani* (Mukherjee et al., 2012) and altered the sterol level of *Leishmania* (L.) *amazonensis* (Andrade-Neto et al., 2016). In this context, sertraline (SERT), a selective serotonin reuptake inhibitor (SSRI), presents several therapeutic uses, ranging from management of depression, to control of obsessive–compulsive disorder and social phobia, to treatment of chronic pain (Kreilgaard et al., 2008; Santuzzi et al., 2012). Palit and Ali (2008) demonstrated the activity of SERT against the Indian etiologic agent of VL, *L.* (L.) *donovani*, and demonstrated both *in vitro* and *in vivo* efficacy at elevated doses.

The lethal action of sertraline was also investigated in *L. infantum* parasites. The drug induced respiration uncoupling, with a significant decrease of intracellular ATP level, and also induced oxidative stress in *Leishmania*. Metabolomics data demonstrated an extended metabolic disarray caused by sertraline, with a remarkable variation of the levels of thiol-redox and polyamine biosynthetic intermediates, suggesting a multitarget mechanism of action (Lima et al., 2018).

Drug delivery systems can direct antileishmanial substances to infected organs (Carvalheiro et al., 2015). Negatively charged nanoliposomes containing pentavalent antimony has shown superior efficacy than free pentavalent antimony for experimental VL treatment due to the targeting ability of these vesicles to bind host cell receptors, named scavenger receptors (ScavR) (Tempone et al., 2004).

In this work, we evaluated, for the first time, the *in vivo* efficacy of the antidepressant sertraline entrapped into negatively charged liposomes (LP-SERT) in a VL-experimental murine model and studied its immunomodulatory effect after treatment. Additionally, a delivery assay was developed to demonstrate the targeting ability of LP-SERT to spleen and liver organs. *In vitro* studies were also performed to evaluate host cell uptake, mammalian cytotoxicity, and *in vitro* efficacy.

MATERIALS AND METHODS

Drugs and Chemicals

3-[4,5-Dimethylthiazol-2-yl]-2,5-diphenyltetrazolium bromide (thiazol blue; MTT), sodium dodecyl sulfate (SDS), M-199 medium, RPMI-PR-1640 medium (w/o phenol red), and cholesterol were purchased from Sigma–Aldrich (St. Louis, MO, USA). Hydrogenated phospholipids were kindly donated by Lipoid GmbH (Ludwigshafen, Germany). Sertraline and other analytical reagents were purchased from Sigma–Aldrich (St. Louis, MO, USA). Molecular biology reagents are purchased from Life Technologies, and CBA (cytometric beads array) was purchased from BD (San Jose, CA, USA).

Parasites and Macrophages

L. (L.) *infantum* (MHOM/MA67ITMAP263) amastigotes were maintained by using promastigotes from the culture that were isolated from the liver of previously infected mice. The animals were infected with 1×10^8 amastigotes (100 μL) by intraperitoneal route. After 15 days post infection (d.p.i.), the animals were euthanized and the liver was macerated in a tissue grinder tube containing 5 ml of PBS and the amastigotes were separated by differential centrifugation to obtain a suspension of

parasites. Promastigotes were maintained in Schneider's medium supplemented with 10% fetal bovine serum (FBS) at 24°C. Macrophages were collected from the peritoneal cavity of BALB/c mice by washing with RPMI-1640 medium supplemented with 10% FBS and were maintained in a 5% CO_2-humidified incubator at 37°C (Cunha-Júnior et al., 2016).

Experimental Animals

BALB/c mice were obtained from the Instituto Adolfo Lutz of São Paulo State–Brazil, kept in sterile boxes with absorbent material, and received food and water *ad libitum*. BALB/c mice were infected each month with promastigotes from the culture to maintain the *Leishmania* strain. BALB/c mice were also used to obtain peritoneal macrophages. Animal experiments were performed with the approval of the Ethics Committee of Instituto Adolfo Lutz (project CEUA-IAL/Pasteur 04/2016) in accordance with the National Institutes of Health Guide for the Care and Use of Laboratory Animals (NIH Publications No. 8023).

Determination of 50% Effective Concentration (EC_{50}) of SERT and LP-SERT in Promastigotes and Amastigotes of *L.* (L.) *infantum*

To determine the 50% inhibitory concentration against promastigotes (final logarithmic phase of growth), SERT was dissolved in DMSO, and the standard drug (miltefosine) was dissolved in Mili-Q water; both drugs were diluted in Schneider's medium in 96-well microplates with an initial concentration of 100 μM. The promastigotes were counted in a Neubauer chamber and seeded at 1×10^6/well at the final volume of 150 μl. Controls with DMSO and without drugs were performed. The plate was incubated for 48 h, and the viability of promastigotes was determined by MTT assay. Promastigotes incubated without the drug was used as the viability control. The optical density was determined using a plate reader FilterMax at 570 nm and the data analysis was performed using GraphPad Prism 5.0 software (Mikus and Steverding, 2000).

To determine the EC_{50} value for SERT and LP-SERT against *L.* (L.) *infantum* intracellular amastigotes, peritoneal macrophages (1×10^5/well) were collected from the peritoneal cavity of BALB/c mice added to 16-well chamber slides (NUNC) and incubated for 24 h at 5% CO_2 and 37°C. A two-step washing procedure was performed to eliminate non-adherent cells. Promastigotes were added at a ratio of 10:1, using RPMI 1640 supplemented with 2% horse serum (Rebello et al., 2019), and after 4 h, the extracellular parasites were removed by washing; fresh medium containing SERT, LP-SERT, and control were added; and the cells were incubated at 37°C for 72 h. The initial concentration of SERT and miltefosine was 100 μM, and that for LP-SERT was 20 μM. At the end of the assay, the slides were stained with Giemsa and observed using a light microscopy. The EC_{50} was determined by the number of infected macrophages in 400 cells (Yardley and Croft, 2000).

Determination of Cytotoxicity of SERT and LP-SERT in Mammalian Cells

NCTC cells were seeded at 6×10^4 cells/well in 96-well microplates and incubated with SERT, LP-SERT, and miltefosine with 150 μM as the highest concentration, for 72 h at 37°C in a 5% CO_2 humidified incubator. The viability of the cells was determined by the MTT assay. Control cells were incubated in the presence of DMSO and without drugs. Viability of 100% was expressed based on the optical density of control NCTC cells, after normalization. The selectivity index (SI) was given by the ratio between the cytotoxicity in NCTC cells and the anti-parasitic activity of the drugs (Pinto et al., 2014).

In vitro Uptake of LP-SERT by Macrophages

Macrophages were obtained from the peritoneal cavity of BALB/c mice and seeded at 5×10^6/well for 24 h in 24-well plates. The cells were infected with promastigotes at a ratio of 1:10 (macrophage:parasites). After 4 h of infection, infected and uninfected cells were treated with rhodamine 123-labeled liposome (LP-SERT-R123) (10 μg/ml). The cells were scraped from their wells using a sterile cell scraper and the fluorescence intensity was measured by flow cytometry (Attune-Life technologies) up to 270 min. The excitation and emission wavelengths were 488 and 575 nm, respectively. A number of 10,000 events per sample/time were evaluated to observe the internalization of labeled liposomes. Untreated cells and liposomes without drug were used as controls.

SERT Entrapment in Liposomes

Encapsulation of SERT was performed as described by Reimão et al. (2012). Briefly, for the liposome preparation, 6 mg of sertraline was dissolved in methanol and sonicated in a bath sonicator for 10 min at 25°C (solution A). Solution B consisted of saturated egg phosphatidylcholine (25 mg), saturated egg phosphatidylserine (7.62 mg), and cholesterol (1.81 mg) at 7:2:1 mole ratio, dissolved in 1 ml of chloroform:methanol (1:1). The mixture of solutions A and B was further sonicated for 10 min. The mixture was evaporated in a rotary evaporator at 55°C for 40 min in a vacuum and protected from light. A pre-heated (55°C) isotonic solution of 2.25% glycerol (1 ml, v/v) was added to the lipid film using glass beads. The swelling process of the pre-formed liposomes was performed in a rotary evaporator at 55°C for 60 min without vacuum. The liposomes were sonicated in a bath sonicator under heating (55°C) for 30 min, followed by extrusion in membranes of 0.8, 0.4, and 0.2 nm. The untrapped SERT was separated from the liposomes by centrifugation (4,000 *g* for 15 min) (Reimão et al., 2012).

Quantification of SERT Into Liposomes

The concentration of the encapsulated SERT was determined using an ultra-high-performance liquid chromatography (UPLC) with a binary AT system (Prominence LC-20; Shimadzu Corp., Kyoto, Japan) and an ultraviolet photodiode detector array (PDA) SPDM20A on a reverse-phase ACE C4 column (4.6 mm × 250 mm, 5 μm particle size). The wavelength was set at 220 nm. The flow rate was 1 ml/minute using an isocratic method

with acetonitrile:methanol (7:3 v/v) and 0.1% trifluoroacetic acid (TFA). The SERT was diluted in isopropanol (1 mg/ml) to obtain standard solutions in a range of 3.125–400 μg/ml, and 20 μl samples were injected into the column. Results obtained were extrapolated from a standard curve using a linear regression curve. The encapsulation efficiency (%EE) was calculated using the following equation (Stewart, 1980; Ong et al., 2016). Free SERT is considered the non-entrapped drug. Liposomes were used in all assays immediately after preparation.

$$\%EE = (total\ SERT - free\ SERT)/(total\ SERT) \times 100$$

Dynamic Light Scattering (DLS)

DLS measurements were applied to obtain the vesicles' mean diameter in the absence and presence of SERT, through the apparent diffusion coefficient measurement. The DLS was performed in a ZetaSizer ZS90 equipment (Malvern, UK) using the detector positioned at 90° and a He–Ne laser, λ = 632.8 nm, as a light source. All measurements were performed at 22°C. Samples were diluted 20-fold to ensure no multiple scattering inside the cuvette during the experiments. The results show a unimodal distribution and represent the average of, at least, four experiments.

The apparent values of hydrodynamic diameter, which is related to the diffusional dynamics of a vesicle, were obtained with the autocorrelation functions and were analyzed by the cumulant analysis software provided by Malvern. The D_h determination was calculated by means of Stokes–Einstein, as the following equation:

$$D_h = \frac{k_B T}{3\pi \eta D_{app}}$$

where k_B is the Boltzmann constant, T is the absolute temperature, η is the viscosity of the solvent, and D_h and D_{app} are the hydrodynamic diameter and the apparent diffusion coefficient, respectively (Costa-Silva et al., 2017).

ζ-Potential

ζ-Potential measurements of PS-containing vesicles in the absence and presence of SERT were evaluated in order to check the effect of the drug on the vesicle effective surface charge. The ζ-potential was performed in a ZetaSizer ZS90 equipment (Malvern, UK) using the detector positioned at 173°, a He–Ne laser, λ = 632.8 nm, as a light source and applying PALS (phase analysis light scattering) and LDV (Laser Doppler Velocity) to calculate the electrophoretic mobility and the ζ-potential. The ζ-potential is a measure of the system stability, since it is able to give information about the net change at the vesicle surface. Actually, the ζ-potential is defined as the electrical potential in the beginning of the so-called double layer, i.e., the slipping plane of the vesicle surface. In this study, the ζ-potential was obtained using the electrophoretic mobility, based on the Helmholtz–Smoluchowski equation, which is used in water-based systems in the presence of ionic strength (I) > 1 mM and particle diameter (D_H), > 100 nm. The measurement for each sample was repeated for at least three times. In order to avoid multiple scattering, the samples were diluted 20-fold in the appropriate buffer before the measurements (Lamy et al., 1966; Costa-Silva et al., 2017). LP-SERT treatment was analyzed by culture microtitration as previously reported (Park and Lee, 2008).

Experimental Assay

Dose Translation

The initial dose was calculated based on the human dose, as follows:

$$Animal\ dose\ (mg/kg) = \left(\frac{human\ Km}{animal\ km}\right) \times\ human\ dose$$

where mouse Km = 3, human Km = 37 (Reagan-Shaw et al., 2008).

Determination of the Efficacy of SERT in L. (L.) Infantum-Infected Mice

Young female BALB/c mice were previously infected with *L.* (L.) *infantum* at 1 × 10^8 parasites/animal by intra-peritoneal route. The animals were treated at the 5th d.p.i. by the oral route for 10 consecutive days as follows: Group 1—untreated group; Group 2—SERT at 0.3 mg/kg/day; Group 3—SERT at 1 mg/kg/day. Each group consisted of five animals (n = 5/group). The animals were euthanized at the 16th d.p.i. and the parasitic load was analyzed by culture microtitration analysis (Buffet et al., 1995). Sertraline was dissolved and diluted in saline solution (0.9% m/v).

Determination of the Efficacy of LP-SERT in L. (L.) Infantum-Infected Mice

Young female BALB/c mice were previously infected with *L.* (L.) *infantum* at 1 × 10^8 parasites/animal by intra-peritoneal route. The animals were treated at the 5th d.p.i. by the subcutaneous route for 10 consecutive days as follows. Group 1—untreated group; Group 2—LP-SERT at 0.3 mg/kg/day; Group 3—LP-SERT at 1 mg/kg/day; Group 4—treated group with liposome in the absence of the drug. Each group consisted of five animals (n = 5/group). The animals were euthanized at the 16th d.p.i. and the parasitic load was analyzed by culture microtitration analysis (Buffet et al., 1995). As a control of this experiment, a study was performed using the free drug in the subcutaneous route in the same doses. Liposomal sertraline was diluted in isotonic glycerol solution (2.2% v/v).

Immunomodulatory Studies

Based on the results of the treatment with LP-SERT in *L.* (L.) *infantum*-infected mice, the group treated at 1 mg/kg/day was chosen for immunomodulatory studies. The serum cytokines were analyzed by flow cytometry using the CBA kit. The CBA kit quantifies the cytokines (IL-4, INF-γ, TNF-α, IL-6, IL-10, and IL-12) and chemokine MCP-1 involved in the inflammatory response (Costa-Silva et al., 2017). Six populations of beads with different intensities of fluorescence light conjugate with antibody of capture for each cytokine were mixed, and after the incubation with the serum, the samples were analyzed by flow cytometry (LSR Fortessa).

Histopathology Profile

After the treatment with LP-SERT, the animals were euthanized and the necropsy was performed with macroscopic and

microscopic evaluation of the organs (liver and spleen). Fragments of organs were immediately removed, preserved in 10% buffered formalin, and processed by usual histological techniques. After these procedures, the slides were stained with hematoxylin and eosin technique. The analyses were performed in light microscopy to characterize and describe histopathological lesions (Guerra et al., 2016).

Targeting of LP-SERT to Spleen and Liver

To confirm the targetability of LP-SERT to spleen and liver of animals, BALB/c mice were infected with 1×10^8 promastigotes of *L.* (L.) *infantum*; after 10 days of infection, the animals were treated (one dose) with LP-SERT labeled with fluorescent probe DIL C18. After 24 h of treatment, the animals were euthanized. The liver and spleen were removed, and imprint of the organs was done in glass slides, fixed with 3.5% formaldehyde for 6 min, and washed with phosphate buffered saline (PBS). The PGN solution (PBS, 0.2% gelatin and 0.15% NaN_3) was used for the permeabilization of the samples containing 0.1% of saponin. The nucleated cells were labeled with DAPI for 30 min (Tempone et al., 2010). The analyses of the samples were made in a fluorescent microscopy Nikon Eclipse 80i-D-FL-EPI.

Statistical Analysis

The data obtained were reported as the mean and standard deviation of duplicate samples from two or three independent assays. The data were analyzed using GraphPad Prism 5.0 software, using one-way ANOVA for significance testing ($P < 0.05$). For the immunomodulatory studies, the data were analyzed using the non-parametric *t*-test ($P < 0.05$).

RESULTS

Determination of the *in vitro* 50% Effective Concentration (EC_{50}) and 50% Cytotoxic Concentration (CC_{50})

SERT and the standard drug miltefosine were incubated with promastigotes of *L.* (L.) *infantum* and the viability was determined by the MTT assay. After 48 h of incubation, the drugs showed EC_{50} values of 0.7 and 16 μM, respectively (**Table 1**). SERT was also effective against intracellular amastigotes and showed an EC_{50} value of 4.2 μM. The liposomal formulation of SERT (LP-SERT) and miltefosine showed EC_{50} values of 2.5 μM and EC_{50} 3.1 μM, respectively. The mammalian cytotoxicity was evaluated using NCTC cells after 72 h of incubation, and the viability was determined by MTT assay. The free and liposomal drug (SERT and LP-SERT) showed CC_{50} values of 27.4 and 12.0 μM, respectively (**Table 1**).

TABLE 1 | *In vitro* 50% effective concentration (EC_{50}) of free and liposomal sertraline against *L.* (L.) *infantum* and mammalian cytotoxicity.

	EC_{50} (μM) ± SD			
Drugs	***L.* (L) *infantum* promastigotes**	***L.* (L) *infantum* amastigotes**	**Cytotoxicity NCTC cells**	**S.I.**
SERT	0.7 ± 0.4	4.2 ± 2.2	27.4 ± 0.8	6.4
LP-SERT	–	2.5 ± 1.6	12.0 ± 2.4	4.8
Miltefosine	16.2 ± 0.02	3.1 ± 1.6	127.7 ± 6.7	40.9

EC_{50}, 50% effective concentration; S.I., selectivity index [CC_{50} mammalian cells/EC_{50} L. (L) infantum amastigotes]; SERT, free sertraline; LP-SERT, liposomal sertraline; SD, standard deviation; EC_{50} values are representative of three independent assays.

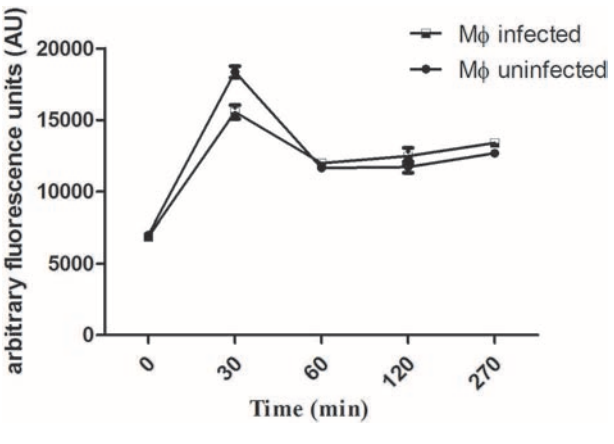

FIGURE 1 | Uptake of liposomal sertraline labeled with rhodamine 123 by *Leishmania*-infected and uninfected macrophages. The uptake was measured by the fluorescence intensity within macrophages using a flow cytometry (Attune-Thermofisher) for a period of 270 min. A number of 10,000 events were analyzed for each time.

Internalization of LP-SERT-R123 in Peritoneal Macrophages

The uptake capacity of *Leishmania*-infected macrophages and uninfected macrophages to internalize rhodamine 123-labeled liposomes was analyzed by flow cytometry. The peak of internalization of LP-SERT-R123 occurred within the first 30 min for both groups (infected and uninfected macrophages), with similar levels of fluorescence. At 60 min, the fluorescence levels dropped and remained sustained in both groups of macrophages until 270 min (**Figure 1**).

Physico-Chemical Characterizations of LP-SERT

In order to characterize the influence of SERT in PS-containing liposomes, DLS and ζ-potential experiments were performed. DLS measurements indicated that SERT was not able to alter the overall size of the liposomes, which showed an average diameter (*Z*-average) of ∼127 nm in the absence and 128 nm in the presence of SERT, respectively. PDI values were also calculated and remain 0.27 and 0.33 in the absence and presence of SERT, respectively. The liposome ζ-potential was also unchanged after the entrapment of SERT, which showed a negatively charged formulation of −64 ± 4 mV in the absence and −58 ± 5 mV in the presence of SERT. Taken together, both DLS and ζ-potential measurements indicated that the SERT was not able to change significantly either the vesicle effective diameter or its superficial charge. The quantification of SERT in liposomes was determined

by HPLC, using a standard curve of SERT. The Encapsulation Efficiency (%EE), resulted in a mean value of 80% ± 3%.

In vivo Efficacy of SERT

BALB/c mice were infected with *L.* (L.) *infantum* (1×10^8 promastigotes) and after 5 d.p.i. the animals were treated for 10 consecutive days with SERT by oral route at 0.3 and 1 mg/kg. The culture microtitration analysis demonstrated that the treatment with SERT was not able to reduce the parasite burden when compared with the untreated group (**Figure 2A**). Considering the therapeutic failure of SERT, the drug was entrapped into negatively charged liposomes and administered by subcutaneous route using the same doses. The results indicated that the treatment with LP-SERT was able to reduce the liver parasite burden by 72% at 0.3 mg/kg ($P < 0.05$) and by 89% at 1 mg/kg ($P < 0.05$) when compared with the untreated group. Free liposomes (without SERT) were used as a control and demonstrated no efficacy (**Figure 2B**). The efficacy of free SERT (unentrapped) was also evaluated by subcutaneous route and used as an internal control. The free drug was not able to eliminate the parasites in liver when administered by the subcutaneous route (**Figure 2C**). All animals survived after the treatment with SERT and LP-SERT. During the time of infection (15 days), 100% of animals survived in the untreated group.

In vivo Immunomodulatory Effect of LP-SERT

After 10 consecutive days of treatment with LP-SERT, the serum was collected and the cytokine levels of *L.* (L.) *infantum*-infected BALB/c mice were evaluated by flow cytometry. The results demonstrated a significant downregulation (two-fold) of the interleukin 6 (IL-6) levels of the group treated at 1 mg/kg. The chemokine MCP-1 levels were also significant upregulated in the treated group (**Figure 3**). Other cytokines showed undetectable levels in serum.

Histopathology Profile of BALB/c Mice Treated With LP-SERT

The spleen and the liver of untreated and animals treated (LP-SERT at 1 mg/kg) were evaluated using histopathological techniques. The light microscopy analysis of the slides demonstrated no significant differences between untreated infected animals and LP-SERT-treated groups. We observed the presence of a lymphoid hyperplasia in the spleen (**Figures 4A,B**) as well as an inflammatory infiltrate with the development of granulomas in liver (**Figures 4C,D**).

Targeting of LP-SERT to Spleen and Liver

The liposomal formulation of SERT was labeled with the fluorescent probe DIL C18 and administrated by subcutaneous route in infected *L.* (L.) *infantum* BALB/c mice. The fluorescence microscopy analyses demonstrated that LP-SERT was distributed to the liver and spleen of the infected animals after 24 h of administration (**Figure 5**).

DISCUSSION

VL affects millions of poor people worldwide and remains without safe therapeutic options; drug repurposing or repositioning has been an important approach, reducing time and cost of the research. Previous studies demonstrated that antidepressants like sertraline and others showed anti-*Leishmania* activity (Palit and Ali, 2008; Mukherjee et al., 2012). Palit and Ali (2008) have demonstrated that SERT eliminated 72 and 70% of parasite burden of spleen and liver, respectively, using a *L. donovani*-infected BALB/c mice model. SERT is a serotonin reuptake inhibitor approved by the Food and Drug Administration (FDA), and it is widely used in the treatment of depression (Santuzzi et al., 2012; Onaolapo et al., 2017). In this study, the therapeutic potential of SERT and LP-SERT against *L.* (L.) *infantum* was determined using *in vitro* and *in vivo* models.

Our studies demonstrated that SERT was 22 times more effective against promastigotes than the standard drug miltefosine. SERT was also able to eliminate 100% of intracellular amastigotes with similar activity to miltefosine, resulting in an SI of 6. Palit and Ali (2008) previously showed that SERT was effective against *L.* (L.) *donovani*, with EC_{50} values 1.6- and 10-fold smaller than our studies with *L.* (L.) *infantum* against promastigotes and intracellular amastigotes, respectively. Although *L.* (L.) *donovani* is also a viscerotropic species, the differences found in our studies could be ascribed to the differences in the species between *L.* (L.) *infantum* and *L.* (L.) *donovani*, resulting in different drug susceptibilities (Costa-Silva et al., 2015). Genetic markers for sensibility to specific drugs have been identified in viscerotropic *Leishmania* species, specifically *L.* (L.) *donovani* and *L.* (L.) *infantum*. The presence of Miltefosine Sensitivity Locus (MSL) in DNA resulted in a susceptible pattern to miltefosine, also modifying the clinical responsiveness to the drug. *Leishmania* parasites lacking MSL were shown to be resistant to miltefosine (Carnielli et al., 2018). Additionally, differences in DNA fingerprint analyses have been identified for *L.* (L.) *donovani* and *L.* (L.) *infantum* (Ellis and Crampton, 1991). Future genetic studies using *L.* (L.) *donovani* and *L.* (L.) *infantum* could demonstrate specific genetic markers that contribute to the response to sertraline.

The use of FDA-approved drugs for drug repositioning approach has considerable advantages, especially when one considers the available ADMET data of individual drugs. Data from the literature report that sertraline has a plasma half-life ($T_{1/2}$) of 8 h when orally administered in healthy patients, and more than 26 h for the plasma terminal $T_{1/2}$ (Murdoch and McTavish, 1992). Considering the *in vitro* potency of sertraline against *L.* (L.) *infantum*, we conducted an *in vivo* efficacy study in a murine model, using the following approach: (i) administration of SERT by oral route; (ii) administration of a daily single dose for 10 consecutive days; (iii) considering the HED index to translate doses human↔animal (Reagan-Shaw et al., 2008), a dose of 1 mg/kg was chosen based on the human equivalent dose of 0.1 mg/kg; a maximum human dose of sertraline as an antidepressant drug is 3 mg/kg, but this is followed by significant increase in adverse effects (Drugbank, 2017). This murine visceral model of Leishmaniasis has been useful for the

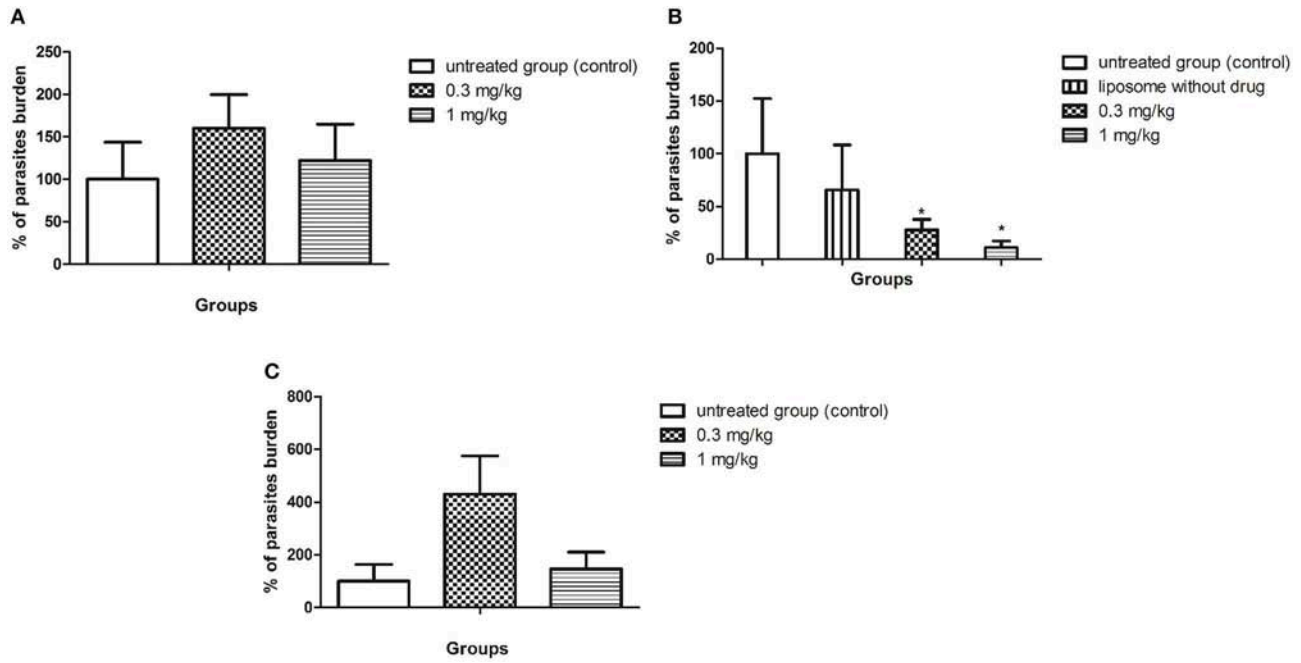

FIGURE 2 | *In vivo* efficacy of SERT. After 5 days of infection with *L.* (L.) *infantum*, BALB/c mice were treated for 10 consecutive days. **(A)** Parasite burden (%) of the treatment with free sertraline in oral administration. **(B)** Parasite burden (%) of the treatment with liposomal sertraline in subcutaneous administration. **(C)** Parasite burden (%) of the treatment with free sertraline in subcutaneous administration. $^*p < 0.05$.

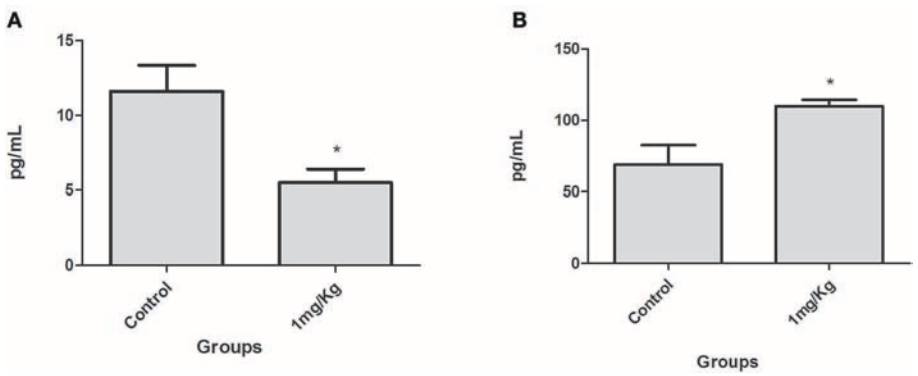

FIGURE 3 | Serum IL-6 **(A)** and chemokine MCP-1 **(B)** levels in BALB/c mice infected with *L.* (L.) *infantum* treated for 10 consecutive days with LP-SERT at a dose of 1 mg/kg. Cytokine levels (pg/ml) were determined by flow cytometry by the CBA kit (cytometric beads array—BD) ($^*p < 0.05$). It was considered 10,000 events per analysis. The control is defined by infected and untreated animals.

evaluation of drug candidates. Cunha-Junior et al. evaluated the time course of the infection using the same strain of *L.* (L.) *infantum* in BALB/c mouse. After intra-peritoneal infection with 1×10^8 stationary-phase promastigotes, the parasite burden was analyzed by the microtitration method at days 7, 14, 21, and 30. The infection was well-established after 7 days, with parasites in the spleen and liver, with increased and sustained infection for 30 days. Our *in vivo* assays of oral SERT showed no reduction of the parasite burden. This result could be ascribed to multiple factors, including a low oral absorption of SERT, a poor delivery of SERT, resulting in low tissue concentration of the drug in the spleen and liver, or the metabolization of SERT, which could have generated an inactive metabolite against *L.* (L.) *infantum*. Ronfeld et al. (1997) demonstrated that sertraline has low oral absorption in young human volunteers, with a T_{max} of 7 h. The authors also report a low absorption for sertraline after oral administration with a C_{max} value of 118 ng/ml. Additionally, data from DrugBank (https://www.drugbank.ca/drugs/DB01104) report that sertraline administered once daily at 50–200 mg for 14 days resulted in steady-state concentrations after 1 week. Additionally, the drug is extensively metabolized by the liver to form *N*-desmethylsertraline, which

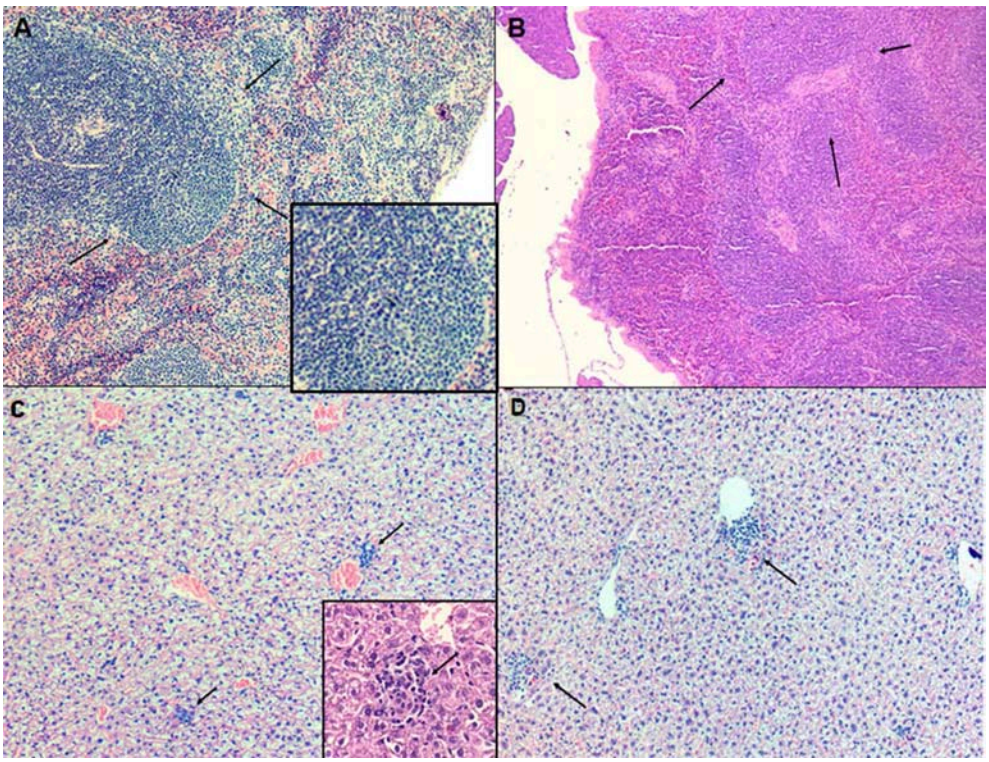

FIGURE 4 | Evaluation of histopathological profile of BALB c mice infected with *L.* (L.) *infantum*, after 10 consecutive days of treatment with liposomal sertraline. **(A)** Spleen of an animal representative of untreated group. **(B)** Spleen of an animal representative of the group treated with liposomal sertraline at 1 mg/kg. **(C)** Liver of an animal representative of the untreated control group. **(D)** Liver of an animal representative of the group treated with liposomal sertraline at 1 mg/kg. Presence of granulomas in all groups (arrows). Staining of H&E, 100× magnification.

has a lower pharmacological antidepressant effect than the parent compound.

Considering the therapeutic failure of free SERT, we performed the entrapment of the drug into negatively charged liposomes containing phosphatidylserine. Sertraline demonstrated a high entrapment (82%) into the formulation, resulting in the formation of nanovesicles covered by a negative charge. Drug delivery systems (DDS) as liposomes have been widely used in the pharmaceutical field (Kansal et al., 2014). In the clinical therapy of leishmaniases, DDS have been used for many years, as the liposomal amphotericin B (Ambisome), which provides reduced doses, higher safety, and increased therapeutic index (Ostrosky-Zeichner et al., 2003). In this work, we observed that the encapsulation of the SERT in negatively charged liposomes resulted in an *in vivo* efficacy of the drug, reducing 72% of the parasitic burden in the liver at doses below 1 mg/kg. At this dose (1 mg/kg), the parasite burden was reduced by 89% in the liver. In a previous study, miltefosine was administered to a BALB/c model infected with *L.* (L.) *infantum* (MHOM/MA67ITMAP263) and resulted in 100% suppression of the parasite burden in liver and spleen at 7.7 mg/kg (Rebello et al., 2019).

VL causes strong alterations in the immune system; Ansari et al. (2006) observed the serum of VL-patients and reported an increase of the cytokine IL-6, which was associated to the progressive form of the disease. Murray (2008) studied IL-6 knockout mice and observed a better outcome of animals treated with pentavalent antimonial and amphotericin B when compared to IL-6 competent mice. In our studies, significant differences of IL-6 levels were observed between treated and untreated groups. Additionally, the chemokine MCP-1 was analyzed, and we observed increased serum levels in mice treated with LP-SERT at 1 mg/kg. Chemokines constitute a family of chemoattractant cytokines and play a major role in selectively recruiting monocytes, neutrophils, and lymphocytes, as well as in inducing chemotaxis through the activation of G-protein-coupled receptors. Monocyte chemoattractant protein-1 (MCP-1/CCL2) is one of the key chemokines that regulate migration and infiltration of monocytes/macrophages (Deshmane et al., 2009). This chemokine is produced by macrophages, dendritic cells, and monocytes, and it is an important chemotactic factor for T cells and natural killer cells (Deshmane et al., 2009) for the formation of granulomas in the liver, promoting the extermination of the parasites (Cotterell et al., 1999; Dey et al., 2007). Our histopathological profile showed an increase of defense cells as macrophages and dendritic cells, besides the presence of hepatic granuloma and lymphoid hyperplasia in the spleen. This fact could be ascribed to a possible strategy of the organism to activate a response against the parasite after sertraline exposure. Additionally, these

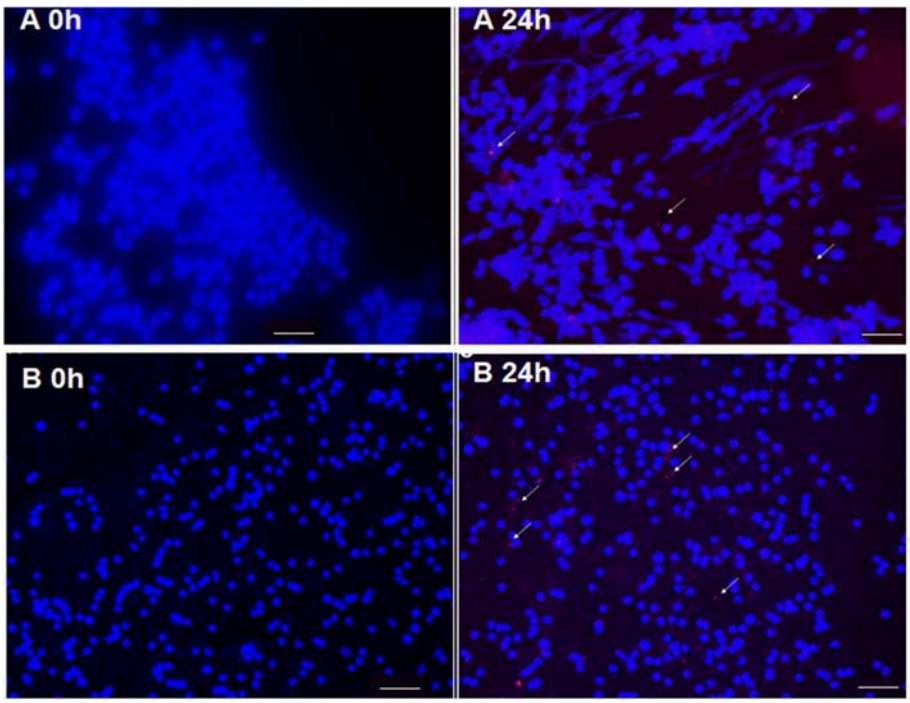

FIGURE 5 | Targeting of liposomes (arrow) labeled with DIL C18 (red) containing sertraline in spleen **(A)** and liver **(B)** of BALB/c mice. Ten days after infection, the animals were treated with LP-SERT, spleen and liver were removed, imprinting of each organ have been made in slides, and the samples were submitted to immunofluorescence analyses at 24 h. Nucleated cells were labeled with DAPI (blue). White bars represent 50 μm.

histopathological data corroborate the increased serum levels of the monocyte chemoattractant protein (MCP-1) and suggest the ability of LP-SERT to modulate the immune response of animals, eliminating *L.* (L.) *infantum* in liver. Although LP-SERT was able to reduce the parasite burden after a course of 10 days of treatment, the presence of hepatic granuloma and lymphoid hyperplasia demonstrates an active and unsolved inflammation. Future studies with higher courses (>10 days) of LP-SERT administration could contribute to tissue regeneration. Sertraline was also administered as a free formulation by the subcutaneous route. Our results demonstrate that free SERT was not able to reduce the parasite burden at any tested doses.

The physicochemical properties of liposomes drive the targeting ability of the formulation, and among them, the membrane charge and the vesicle size are critical issues. Negatively charged liposomes containing phosphatidylserine result in a higher uptake by macrophages via scavenger receptors (SRs), with an increased *in vitro* efficacy against *Leishmania* (Tempone et al., 2004), and the VL-mice model (Laverman et al., 1999; Mukherjee et al., 2012). The negative charge of vesicles (the modulus of the ζ-potential values >30 mV) also prevents aggregation of the vesicles, avoiding destabilization of the formulation (Walton et al., 2010). Another important characteristic is the vesicle size; large liposomes (>400 nm) are rapidly removed from the circulation when compared to smaller liposomes (<400 nm) (Faleiro et al., 2014). Considering that *Leishmania* is located inside the mononuclear monocyte system in spleen, liver, bone marrow, and lymph node (Lindoso et al., 2016), a formulation composed of nanostructures is essential. Reimão et al. (2012) demonstrated that liposomes smaller than 200 nm were able to reduce 80% of the parasite burden in bone marrow of *L.* (L.) *infantum*-infected hamsters.

The route of administration directly defines the therapeutic success of a drug. Previous studies of our group demonstrated that the subcutaneous route can increase the efficacy of negatively charged liposomes containing buparvaquone in an *in vivo* VL-model (Costa-Silva et al., 2017). Considering the efficacy of LP-SERT to reduce the parasite burden in liver of BALB/c mice, we studied the targetability of this formulation labeled with a fluorescent probe. After 24 h of the administration, it was possible to observe the presence of LP-SERT in the liver and spleen of previously infected animals. These data demonstrated that LP-SERT reached the *Leishmania* target organs, releasing the drug at or nearly the host cells when administrated subcutaneously. Additionally, our *in vitro* studies with infected macrophages demonstrated that LP-SERT-R123 was able to internalize into *Leishmania*-infected and uninfected macrophages at similar levels. Dhanikula et al. (2005) demonstrated that the pharmacokinetics parameters of the liposomal formulation of paclitaxel were widely distinct when administrated subcutaneously and intravenously; the drug bioavailability was improved by the subcutaneous route. Allen et al. (1993) observed the administration of liposomes in different routes (subcutaneous, intravenous, and intra-peritoneal); their

results showed undamaged liposomes in the bloodstream after passing for the lymphoid chain when administrated via the subcutaneous route. In our previous studies with liposomal buparvaquone, the subcutaneous route was also the best option to improve the drug efficacy and targeting ability.

CONCLUSION

The present study demonstrated that sertraline is a potent *in vitro* anti-*L.* (L.) *infantum* drug. For the first time in the literature, sertraline was encapsulated in phophatidylserine liposomes and studied in an experimental VL-murine model. The liposomal formulation of sertraline demonstrated the ability to reduce the parasite burden at low doses, being delivered to the liver and spleen of infected mice. The study also demonstrated that at higher doses, the liposomal sertraline can modulate the host immune response, affecting the course of the disease. Future pharmacokinetic studies may contribute to understand the action of this new formulation in VL.

DATA AVAILABILITY STATEMENT

The datasets generated for this study are available on request to the corresponding author.

ETHICS STATEMENT

Animal experiments were performed with the approval of the Ethics Committee of Instituto Adolfo Lutz (project CEUA-IAL/Pasteur 04/2016) in accordance with the National Institutes of Health guide for the care and use of Laboratory animals (NIH Publications No. 8023).

AUTHOR CONTRIBUTIONS

MR developed all experimental work. TC-S and DD developed part of the *in vitro* studies with sertraline. JG performed histopathology studies in animals. AG performed part of flow cytometry studies for cytokine detection. EC-J standardized animal studies with Leishmania. EP performed initial studies with sertraline in animals. ET-S standardized animal studies with Leishmania. LB performed physico-chemical characterization of liposomes. AT was responsible for the design and general idea of the work and analysis of *in vitro* and *in vivo* studies.

FUNDING

This work was funded by grants provided by the São Paulo State Research Foundation (FAPESP 2018/10279-6, 2015/23403-9, 2015/15822-1, and 2013/07275-5) and Conselho Nacional de Pesquisa e Desenvolvimento (CNPq) 306305/2017-8, 306943/2015-8, and 420567/2016-0.

ACKNOWLEDGMENTS

We thank Ms. Matilia Ana do Nascimento and Vicente Duarte for technical assistance in the laboratory. We also thank Coordenação de Aperfeiçoamento de Pessoal de Nível Superior (CAPES) for the scholarships.

REFERENCES

Allen, T. M., Hansen, C. B., and Guo, L. S. (1993). Subcutaneous administration of liposomes: a comparison with the intravenous and intraperitoneal routes of injection. *Biochim. Biophys. Acta* 1150, 9–16. doi: 10.1016/0005-2736(93)90115-G

Alvar, J., Vélez, I. D., Bern, C., Herrero, M., Desjeux, P., Cano, J., et al. (2012). Leishmaniasis Control Team. Leishmaniasis worldwide and global estimates of its incidence. *PLoS ONE* 5:e35671. doi: 10.1371/journal.pone.0035671

Andrade-Neto, V. V., Pereira, T. M., Canto-Cavalheiro, M.d, and Torres-Santos, E. C. (2016). Imipramine alters the sterol profile in *Leishmania amazonensis* and increases its sensitivity to miconazole. *Parasit. Vectors*. 9:183. doi: 10.1186/s13071-016-1467-8

Andrews, K. T., Fisher, G., and Skinner-Adams, T. S. (2014). Drug repurposing and human parasitic protozoan diseases. *Int. J. Parasitol. Drugs Drug Resist*. 4, 95–111. doi: 10.1016/j.ijpddr.2014.02.002

Ansari, N. A., Saluja, S., and Salotra, P. (2006). Elevated levels of interferon-gamma, interleukin-10, and interleukin-6 during active disease in Indian kala azar. *Clin. Immunol.* 119, 339–345. doi: 10.1016/j.clim.2006.01.017

Botero, D. (1978). Chemotherapy of human intestinal parasitic diseases. *Annu. Rev. Pharmacol. Toxicol.* 18, 1–15.

Buffet, P. A., Sulahian, A., Garin, Y. J., Nassar, N., and Derouin, F. (1995). Culture microtitration: a sensitive method for quantifying *Leishmania infantum* in tissues of infected mice. *Antimicrob. Agents. Chemother*. 39, 2167–2168. doi: 10.1128/AAC.39.9.2167

Carnielli, J. B. T., Crouch, K., Forrester, S., Silva, V. C., Carvalho, S. F. G., Damasceno, J. D., et al. (2018). A *Leishmania infantum* genetic marker associated with miltefosine treatment failure for visceral leishmaniasis. *EBioMedicine*. 36, 83–91. doi: 10.1016/j.ebiom.2018.09.029

Carvalheiro, M., Esteves, M. A., Santos-Mateus, D., Lopes, R. M., Rodrigues, M. A., Eleutério, C. V., et al. (2015). Hemisynthetic trifluralin analogues incorporated in liposomes for the treatment of leishmanial infections. *Eur. J. Pharm. Biopharm*. 93, 346–352. doi: 10.1016/j.ejpb.2015.04.018

Chakravarty, J., and Sundar, S. (2019). Current and emerging medications for the treatment of leishmaniasis. *Expert Opin. Pharmacother*. 20, 1251–1265. doi: 10.1080/14656566.2019.1609940

Chan, C., Yin, H., Garforth, J., McKie, J. H., Jaouhari, R., Speers, P., et al. (1998). Phenothiazine inhibitors of trypanothione reductase as potential antitrypanosomal and antileishmanial drugs. *J. Med. Chem*. 41, 148–156. doi: 10.1021/jm960814j

Costa-Silva, T. A., Galisteo, A. J., Lindoso, J. A., Barbosa, L. R., and Tempone, A. G. (2017). Nanoliposomal buparvaquone immunomodulates *Leishmania infantum*-infected macrophages and is highly effective in a murine model. *Antimicrob. Agents Chemother*. 61, e02297–e02316. doi: 10.1128/AAC.02297-16

Costa-Silva, T. A., Grecco, S. S., Sousa, F. S., Lago, J. H., Martins, E. G., Terrazas, C. A., et al. (2015). Immunomodulatory and antileishmanial activity of phenylpropanoid dimers isolated from nectandra leucanta. *J. Nat. Prod*. 78, 653–657. doi: 10.1021/np500809a

Cotterell, S. E., Engwerda, C. R., and Kaye, P. M. (1999). *Leishmania donovani* infection initiates T cell-independent chemokine responses, which are subsequently amplified in a T cell-dependent manner. *Eur. J. Immunol.* 29, 203–214.

Croft, S. L., Barrett, M. P., and Urbina, J. A. (2005). Chemotherapy of trypanosomiases and leishmaniasis. *Trends Parasitol.* 21, 508–12. doi: 10.1016/j.pt.2005.08.026

Croft, S. L., and Engel, J. (2006). Miltefosine-discovery of the antileishmanial activity of phospholipid derivatives. *Trans. R. Soc. Trop. Med. Hyg.* 100, S4–S8. doi: 10.1016/j.trstmh.2006.03.009

Cunha-Júnior, E. F., Martins, T. M., Canto-Cavalheiro, M. M., Marques, P. R., Portari, E. A., Coelho, M. G., et al. (2016). Preclinical studies evaluating subacute toxicity and therapeutic efficacy of LQB-118 in experimental visceral leishmaniasis. *Antimicrob. Agents Chemother.* 60, 3794–37801. doi: 10.1128/AAC.01787-15

Deshmane, S. L., Kremlev, S., Amini, S., and Sawaya, B. E. (2009). Monocyte chemoattractant protein-1(MCP-1): an overview. *J. Interferon. Cytokine. Res.* 29, 313–326. doi: 10.1089/jir.2008.0027

Dey, R., Majumder, N., Bhattacharyya Majumdar, S., Bhattacharjee, S., Banerjee, S., Roy, S., et al. (2007). Induction of host protective Th1 immune response by chemokines in *Leishmania donovani*-infected BALB/c mice. *Scand. J. Immunol.* 66, 671–683. doi: 10.1111/j.1365-3083.2007.02025.x

Dhanikula, A. B., Singh, D. R., and Panchagnula, R. (2005). *In vivo* pharmacokinetic and tissue distribution studies in mice of alternative formulations for local and systemic delivery of Paclitaxel: gel, film, prodrug, liposomes, and micelles. *Curr. Drug. Deliv.* 2, 35–44. doi: 10.2174/1567201052772852

Drugbank (2017). *Sertraline.* Retrieved from: https://www.Drugbank.Ca/Drugs/Db01104

Ellis, J. T., and Crampton, J. M. (1991). Differences between *Leishmania* (Leishmania) *chagasi*, *L.* (L.) *infantum* and *L.* (L.) *donovani* as shown by DNA fingerprinting. *Mem. Inst. Oswaldo Cruz.* 86, 479–481. doi: 10.1590/S0074-02761991000400022

Evans, A. T., and Croft, S. L. (1994). Antileishmanial actions of tricyclic neuroleptics appear to lack structural specificity. *Biochem. Pharmacol.* 48, 613–616. doi: 10.1016/0006-2952(94)90293-3

Faleiro, R. J., Kumar, R., Hafner, L. M., and Engwerda, C. R. (2014). Immune regulation during chronic visceral leishmaniasis. *PLoS. Negl. Trop. Dis.* 8:e2914. doi: 10.1371/journal.pntd.0002914

Furtado, T. A., Cisalpino, E. O., and Santos, U. M. (1960). *In vitro* studies of the effect of amphotericin B on *Leishmania brasiliensis.* Antibiot. *Chemother.* 10, 692–693.

Guerra, J. M., Fernandes, N. C. C. A., Kimura, L. M., Shirata, N. K., Magno, J. A., Abrantes, M. F., et al. (2016). Avaliação do exame imuno-histoquimico para o diagnóstico de *Leishmania* ssp. em amostras de tecidos caninos. *Rev. Do Inst Adolfo Lutz.* 75, 1–10.

Huang, H., Nguyen, T., Ibrahim, S., Shantharam, S., Yue, Z., and Chen, J. Y. (2015). DMAP: a connectivity map database to enable identification of novel drug repositioning candidates. *BMC. Bioinformatics.* 16 (Suppl. 13):S4. doi: 10.1186/1471-2105-16-S13-S4

Kansal, S., Tandon, R., Verma, A., Misra, P., Choudhary, A. K., Verma, R., et al. (2014). Coating doxorubicin-loaded nanocapsules with alginate enhances therapeutic efficacy against Leishmania in hamsters by inducing Th1-type immune responses. *Br. J. Pharmacol.* 171, 4038–4050. doi: 10.1111/bph.12754

Kreilgaard, M., Smith, D. G., Brennum, L. T., and Sánchez, C. (2008). Prediction of clinical response based on pharmacokinetic/pharmacodynamic models of 5-hydroxytryptamine reuptake inhibitors in mice. *Br. J. Pharmacol.* 155, 276–284. doi: 10.1038/bjp.2008.243

Lamy, L., Wonde, T., and Lamy, H. (1966). Action of amphotericin B on *Leishmania donovani* during multiplication in mouse macrophages maintained *in vitro*. *Bull. Soc. Pathol. Exot. Filiales.* 59, 964–968.

Laverman, P., Boerman, O. C., Oyen, W. J., Dams, E. T., Storm, G., and Corstens, F. H. (1999). Liposomes for scintigraphic detection of infection and inflammation. *Adv. Drug. Deliv. Rev.* 37, 225–235. doi: 10.1016/S0169-409X(98)00095-7

Lima, M. L., Abengózar, M. A., Nácher-Vázquez, M., Martínez-Alcázar, M. P., et al. (2018). Molecular basis of the leishmanicidal activity of the antidepressant sertraline as a drug repurposing candidate. *Antimicrob. Agents Chemother.* 62, e01928–e011946. doi: 10.1128/AAC.01928-18

Lindoso, J. A., Cunha, M. A., Queiroz, I. T., and Moreira, C. H. (2016). Leishmaniasis-HIV coinfection: current challenges. *HIV AIDS (Auckl).* 8, 147–156. doi: 10.2147/HIV.S93789

Lourie, E. M., and Yorke, W. (1939). Studies in chemotherapy. XXI: the trypanocidal action of certain aromatic diamidines. *Ann. Trop. Med. Parasitol.* 33, 289–304. doi: 10.1080/00034983.1939.11685073

Mattock, N. M., and Peters, W. (1975). The experimental chemotherapy of leishmaniasis. II. The activity in tissue culture of some antiparasitic and antimicrobial compounds in clinical use. *Ann. Trop. Med. Parasitol.* 69, 359–371. doi: 10.1080/00034983.1975.11687020

Mikus, J., and Steverding, D. (2000). A simple colorimetric method to screen drug cytotoxicity against *Leishmania* using the dye Alamar Blue. *Parasitol. Int.* 48, 265–269. doi: 10.1016/S1383-5769(99)00020-3

Mukherjee, S., Mukherjee, B., Mukhopadhyay, R., Naskar, K., et al. (2014). Imipramine exploits histone deacetylase 11 to increase the IL-12/IL-10 ratio in macrophages infected with antimony-resistant *Leishmania donovani* and clears organ parasites in experimental infection. *J Immunol.* 193, 4083–4094. doi: 10.4049/jimmunol.1400710

Mukherjee, S., Mukherjee, B., Mukhopadhyay, R., Naskar, K., Sundar, S., Dujardin, J. C., et al. (2012). Imipramine is an orally active drug against both antimony sensitive and resistant *Leishmania donovani* clinical isolates in experimental infection. *PLoS. Negl. Trop. Dis.* 6:e1987. doi: 10.1371/journal.pntd.0001987

Murdoch, D., and McTavish, D. (1992). Sertraline, A review of its pharmacodynamic and pharmacokinetic properties, and therapeutic potential in depression and obsessive-compulsive disorder. *Drugs* 44, 604–624. doi: 10.2165/00003495-199244040-00007

Murray, H. W. (2008). Accelerated control of visceral *Leishmania donovani* infection in interleukin-6-deficient mice. *Infect. Immun.* 76, 4088–4091. doi: 10.1128/IAI.00490-08

Onaolapo, O. J., Paul, T. B., and Onaolapo, A. Y. (2017). Comparative effects of sertraline haloperidol or olanzapine treatments on ketamine-induced changes in mouse behaviours. *Metab. Brain. Dis.* 32, 1475–1489. doi: 10.1007/s11011-017-0031-3

Ong, S. G., Ming, L. C., Lee, K. S., and Yuen, K. H. (2016). Influence of the encapsulation efficiency and size of liposome on the oral bioavailability of griseofulvin-loaded liposomes. *Pharmaceutics* 8:E25. doi: 10.3390/pharmaceutics8030025

Ostrosky-Zeichner, L., Marr, K. A., Rex, J. H., and Cohen, S. H. (2003). Amphotericin B: time for a new "gold standard". *Clin. Infect. Dis.* 37, 415–425. doi: 10.1086/376634

Palit, P., and Ali, N. (2008). Oral therapy with sertraline, a selective serotonin reuptake inhibitor, shows activity against *Leishmania donovani. J. Antimicrob. Chemother.* 61, 1120–1124. doi: 10.1093/jac/dkn046

Park, H. M., and Lee, W. M. (2008). Helmholtz-Smoluchowski velocity for viscoelastic electroosmotic flows. *J. Colloid. Interface. Sci.* 317, 631–636. doi: 10.1016/j.jcis.2007.09.027

Pinto, E. G., Santos, I. O., Schmidt, T. J., Borborema, S. E. T., Ferreira, V. F., Rocha, D. R., et al. (2014). Potential of 2-Hydroxy-3-Phenylsulfanylmethyl-[1,4]-Naphthoquinones against *Leishmania* (*L.*) *infantum*: biological activity and structure-activity relationships. *PLoS ONE* 9:e105127. doi: 10.1371/journal.pone.0105127

Reagan-Shaw, S., Nihal, M., and Ahmad, N. (2008). Dose translation from animal to human studies revisited. *FASEB J.* 22, 659–661. doi: 10.1096/fj.07-9574LSF

Rebello, K. M., Andrade-Neto, V. V., Gomes, C. R. B., de Souza, M. V. N., et al. (2019). Miltefosine-Lopinavir combination therapy against leishmania infantum infection: *in vitro* and *in vivo* approaches. *Front. Cell Infect. Microbiol.* 9:229. doi: 10.3389/fcimb.2019.00229

Reimão, J. Q., Colombo, F. A., Pereira-Chioccola, V. L., and Tempone, A. G. (2012). Effectiveness of liposomal buparvaquone in an experimental hamster model of *Leishmania* (L.) *infantum* chagasi. *Exp. Parasitol.* 195–199. doi: 10.1016/j.exppara.2012.01.010

Richardson, J. L., Nett, I. R., Jones, D. C., Abdille, M. H., Gilbert, I. H., and Fairlamb, A. H. (2009). Improved tricyclic inhibitors of trypanothione reductase by screening and chemical synthesis. *Chem. Med. Chem.* 4, 1333–1340. doi: 10.1002/cmdc.200900097

Ronfeld, R. A., Tremaine, L. M., and Wilner, K. D. (1997). Pharmacokinetics of sertraline and its N-demethyl metabolite in elderly and young male and female volunteers. *Clin. Pharmacokinet.* 32 (Suppl. 1), 22–30. doi: 10.2165/00003088-199700321-00004

Santuzzi, G. H., Futuro Neto, H. A., Pires, J. G., Gonçalves, W. L., Tiradentes, R. V., Gouvea, S. A., et al. (2012). Sertraline inhibits formalin-induced

nociception and cardiovascular responses. *Braz. J. Med. Biol. Res*. 45, 43–48. doi: 10.1590/S0100-879X2011007500154

Stewart, J. C. M. (1980). Colorimetric determination of phospholipids with ammonium ferrothiocyanate. *Anal. Biochem*. 104, 10–14. doi: 10.1016/0003-2697(80)90269-9

Tempone, A. G., Ferreira, D. D., Lima, M. L., Costa Silva, T. A., Borborema, S. E. T., Reimão, J. Q., et al. (2017). Efficacy of a series of alpha-pyrone derivatives against *Leishmania* (L.) *infantum* and *Trypanosoma cruzi*. *Eur. J. Med. Chem*. 139, 947–960. doi: 10.1016/j.ejmech.2017.08.055

Tempone, A. G., Mortara, R. A., Andrade, H. F., and Reimão, J. Q. (2010). Therapeutic evaluation of free and liposome-loaded furazolidone in experimental visceral leishmaniasi. *Int. J. Antimicrob. Agents* 36, 159–163. doi: 10.1016/j.ijantimicag.2010.04.006

Tempone, A. G., Perez, D., Rath, S., Vilarinho, A. L., Mortara, R. A., and Andrade, H. F. (2004). Targeting *Leishmania* (L.) *chagasi* amastigotes through macrophage scavenger receptors: the use of drugs entrapped in liposomes containing phosphatidylserine. *J. Antimicrob. Chemother*. 54, 60–68. doi: 10.1093/jac/dkh281

Tsushima, S., Yoshioka, Y., Tanida, S., Nomura, H., Nojima, S., and Hozumi, M. (1982). Syntheses and antimicrobial activities of alkyl lysophospholipids. *Chem. Pharm. Bull*. 30, 3260–3270. doi: 10.1248/cpb.30.3260

Walton, B. L., Leja, M., Vickers, K. C., Estevez-Fernandez, M., Sanguino, A., Wang, E., et al. (2010). Delivery of negatively charged liposomes into the atheromas of Watanabe heritable hyperlipidemic rabbits. *Vasc. Med*. 15, 307–313. doi: 10.1177/1358863X10374118

World Health Organization (2017). *Visceral Leishmaniasis*. Retrieved from: https://www.who.int/leishmaniasis/visceral_leishmaniasis/en/

Yardley, V., and Croft, S. L. (2000). A comparison of the activies of three amphotericin b lipid formulations against experimental visceral and cutaneous leishmaniasis. *Int. J. Antimicrob. Agents*. 13, 243–248. doi: 10.1016/S0924-8579(99)00133-8

Conflict of Interest: The authors declare that the research was conducted in the absence of any commercial or financial relationships that could be construed as a potential conflict of interest.

frontiers in Cellular and Infection Microbiology

ORIGINAL RESEARCH
published: 04 December 2019
doi: 10.3389/fcimb.2019.00403

Mapping Alterations Induced by Long-Term Axenic Cultivation of *Leishmania amazonensis* Promastigotes With a Multiplatform Metabolomic Fingerprint Approach

*Frederico Crepaldi[1,2†], Juliano Simões de Toledo[1,2†], Anderson Oliveira do Carmo[3], Leopoldo Ferreira Marques Machado[4], Daniela Diniz Viana de Brito[1], Angela Vieira Serufo[1], Ana Paula Martins Almeida[1], Leandro Gonzaga de Oliveira[1], Tiago Queiroga Nery Ricotta[1], Douglas de Souza Moreira[5], Silvane Maria Fonseca Murta[5], Ariane Barros Diniz[6], Gustavo Batista Menezes[6], Ángeles López-Gonzálvez[2], Coral Barbas[2] and Ana Paula Fernandes[1]**

[1] Clinical and Toxicological Analysis Department, School of Pharmacy, Federal University of Minas Gerais, Belo Horizonte, Brazil, [2] Centro de Metabolómica y Bioanálisis, Unidad Metabolómica, Interacciones y Bioanálisis (UMIB), Universidad CEU San Pablo, Boadilla del Monte, Spain, [3] Laboratory of Biotechnology and Molecular Markers, General Biology Department, Institute of Biological Science, Federal University of Minas Gerais, Belo Horizonte, Brazil, [4] Manchester Institute of Biotechnology, The University of Manchester, Manchester, United Kingdom, [5] René Rachou Research Center, Oswaldo Cruz Foundation, Belo Horizonte, Brazil, [6] Morphology Department, Institute of Biological Science, Federal University of Minas Gerais, Belo Horizonte, Brazil

OPEN ACCESS

Edited by:
Anabela Cordeiro-da-Silva, University of Porto, Portugal

Reviewed by:
Carlos Roberto Alves, Oswaldo Cruz Foundation (Fiocruz), Brazil
Patricia Sampaio Tavares Veras, Gonçalo Moniz Institute (IGM), Brazil

***Correspondence:**
Ana Paula Fernandes
apfernandes.ufmg@gmail.com

†These authors have contributed equally to this work

Specialty section:
This article was submitted to Parasite and Host, a section of the journal Frontiers in Cellular and Infection Microbiology

Received: *29 April 2019*
Accepted: *11 November 2019*
Published: *04 December 2019*

Citation:
Crepaldi F, de Toledo JS, do Carmo AO, Ferreira Marques Machado L, de Brito DDV, Serufo AV, Almeida APM, de Oliveira LG, Ricotta TQN, Moreira DdS, Murta SMF, Diniz AB, Menezes GB, López-Gonzálvez Á, Barbas C and Fernandes AP (2019) Mapping Alterations Induced by Long-Term Axenic Cultivation of Leishmania amazonensis Promastigotes With a Multiplatform Metabolomic Fingerprint Approach. Front. Cell. Infect. Microbiol. 9:403. doi: 10.3389/fcimb.2019.00403

Leishmaniases are widespread neglected diseases with an incidence of 1.6 million new cases and 40 thousand deaths per year. *Leishmania* parasites may show distinct, species-specific patterns of virulence that lead to different clinical manifestations. It is well known that successive *in vitro* passages (SIVP) lead to the attenuation of virulence, but neither the metabolism nor the pathways involved in these processes are well understood. Herein, promastigotes of a virulent *L. amazonensis* strain recently isolated from mice was compared to SIVP derived and attenuated promastigotes, submitted to 10, 40, and 60 axenic passages and named R10, R40, and R60, respectively. *In vitro* assays and *in vivo* tests were performed to characterize and confirmed the attenuation profiles. A metabolomic fingerprint comparison of R0, R10, and R60 was performed by means of capillary electrophoresis, liquid and gas chromatography coupled to mass spectrometry. To validate the metabolomic data, qPCR for selected loci, flow cytometry to measure aPS exposure, sensitivity to antimony tartrate and ROS production assays were conducted. The 65 identified metabolites were clustered in biochemical categories and mapped in eight metabolic pathways: ABC transporters; fatty acid biosynthesis; glycine, serine and threonine metabolism; β-alanine metabolism; glutathione metabolism; oxidative phosphorylation; glycerophospholipid metabolism and lysine degradation. The obtained metabolomic data correlated with previous proteomic findings of the SVIP parasites and the gene expression of 13 selected targets. Late SIVP cultures were more sensitive to Sb^{III} produced more ROS and exposed less phosphatidylserine in their surface. The correspondent pathways were connected to

build a biochemical map of the most significant alterations involved with the process of attenuation of *L. amazonensis*. Overall, the reported data pointed out to a very dynamic and continuous metabolic reprogramming process, accompanied by changes in energetic, lipid and redox metabolisms, membrane remodeling and reshaping of parasite-host cells interactions, causing impacts in chemotaxis, host inflammatory responses and infectivity at the early stages of infection.

Keywords: *L. amazonensis,* attenuation, metacyclogenesis, inflammation, multiplatform metabolomic fingerprint, metabolic pathways

INTRODUCTION

Leishmaniasis is a group of neglected diseases, endemic in 98 countries, which are caused by different species of the genus *Leishmania*. Collectively, the incidence of leishmaniasis reaches 1.6 million new cases and ∼40,000 deaths per year (WHO, 2010; Alvar et al., 2012; Courtenay et al., 2017). Among New World *Leishmania* species, *Leishmania amazonensis* has significant medical importance, being associated to all forms of leishmaniasis, including diffuse cutaneous leishmaniasis and visceral leishmaniasis, the former being a severe tegumentary form of the disease, while the latter is fatal if left untreated (Barral et al., 1991; Goto and Lindoso, 2010). *L. amazonensis* has evolved sophisticated mechanisms that allow resistance to extreme stress conditions, including oxidative burst and increased temperature in the host, as well as ways to subvert the host's immune system (McMahon-Pratt and Alexander, 2004; Soong et al., 2012; Carlsen et al., 2013).

To effectively achieve multiplication and transmission from one host to the other, *Leishmania* spp. undergoes several molecular, biochemical and morphological changes during its life cycle. The differentiation process undergone in the mammalian host involves the transformation of *Leishmania* from metacyclic promastigotes (introduced in the host's skin by the bite of a flebotominae sand fly) to amastigote forms (inside the host's macrophages). The differentiation process is more dynamic in the insect's gut and comprises several intermediate promastigote forms, including procyclic and metacyclic promastigotes. Metacyclogenesis is required for the detachment of promastigotes from the insect's gut and thus, effective transmission and infection of mammalian hosts (Bates and Rogers, 2004). While components on the insect's gut exert a selective pressure for maintenance of virulence factors (Sacks et al., 1985; da Silva and Sacks, 1987; McConville et al., 1992), successive *in vitro* passages (SIVP) are known to induce attenuation of virulence phenotype of *Leishmania* spp. (Moreira et al., 2012; Magalhães et al., 2014) and, accordingly, this procedure has been used to produce attenuated *Leishmania* for immunization (Saljoughian et al., 2014). Among several phenotypes that have been described, long-term axenic cultivation alters metacyclogenesis, amastigogenesis, calcium metabolism, and protease expression (da Silva and Sacks, 1987; Lu et al., 1997; Cysne-Finkelstein et al., 1998; Rebello et al., 2010; Moreira et al., 2012; Gomes et al., 2017). In agreement, a previous comparative proteomic analysis has revealed decreased virulence and several concomitant alterations in protein expression profile of *L. amazonensis* promastigotes generated through long-term SIVP (Magalhães et al., 2014). Recovery of virulence after *in vivo* passages has been also documented (Espiau et al., 2017). Moreover, it is possible to generate a diversity of sub-clones with reverting phenotypes from parasite clones with a given phenotype, disclosing the ability of continuous maintenance of parasite diversity for each *L. amazonensis* population (Espiau et al., 2017).

The -omics technologies have been widely applied in *Leishmania* studies to characterize parasite biology, disease phenotypes determinants and drug action mechanisms, as well as tools to discover new antigens (Paape et al., 2010; Coelho et al., 2012; Kaur and Rajput, 2014; Magalhães et al., 2014; McCall and McKerrow, 2014; Pawar et al., 2014). Despite previous–omics approaches, the mechanisms and the metabolic pathways related to SIVP and loss of virulence in *Leishmania* are still scantily described. Untargeted fingerprinting metabolomics has emerged as a powerful tool to unveil concomitant and global metabolic alterations occurring in a given biological condition, phenotype or in response to different stimuli (Lei et al., 2011). Fingerprinting studies usually generate a huge amount of data, requiring powerful bioinformatics analysis and additional metabolic and biological characterizations to be validated and integrated into pathways and with other–omics data to complement the information gathered from the post-genomic toolbox (Canuto et al., 2014; Villaveces et al., 2015). Metabolomics may have special relevance for *Leishmania,* due to the extremely high post-transcriptional regulation of gene expression (Canuto et al., 2014; Clayton, 2019). However, a single analytical system may be not sufficient to identify the broad range of metabolites potentially associated with such complex biological process (Canuto et al., 2014). Therefore, in this study we have applied a multi-analytical platform approach, encompassing liquid and gas chromatography and capilary eletrophoresis all coupled to mass spectometry (LC-MS, GC-MS and CE-MS, respectively) to identify as broadly as possible the highly diversified biochemical classes of metabolites associated with virulence attenuation in previously described SIVP parasites of *L. amazonensis* promastigotes (Magalhães et al., 2014). In parallel, additional assays were performed for biological characterization and validation of parasite infectivity, metacyclogenesis, phosphatidylserine exposure and sensitivity

to antimonial drugs. This untargeted metabolomics approach unveiled and linked several metabolites and biochemical pathways that are, in a concerted and dynamic way, associated to the adaptation of promastigotes to long-term axenic cultivation and attenuation.

MATERIALS AND METHODS

Ethics Statement

Experiments were performed in compliance with the National Guidelines of the Institutional Animal Care and Use Committee for the Ethical Handling of Research Animals (CEUA) from the Federal University of Minas Gerais (UFMG) (Law number 11.794, 2008), approved under protocol CETEA number 240/2016.

Mice, Cells, and Parasites

Female BALB/c mice (8 weeks old) were obtained from the breeding facilities of the Department of Biochemistry and Immunology, Institute of Biological Sciences, Federal University of Minas Gerais, and were maintained under specific pathogen-free conditions.

The L929 cell line was kindly supplied by Dr. Miriam Testassicca (Federal University of Ouro Preto, Brazil). The cells were maintained at 37°C with 5% CO_2 in DEMEM medium (GibcoBRL, Life Technologies) supplemented with L-glutamine 2 mM, HEPES 25 mM, Penicillin/100 IU/mL streptomycin and 100 mg/mL and 10% heat-inactivated fetal bovine serum (FBS).

The *L. amazonensis* strain (IFLA/BR/1967/PH-8) was originally provided by Dr. Maria Norma Mello, from the parasite collection of the Department of Parasitology, Federal University of Minas Gerais. All the SIVP cultures derived from this strain were provided by Dr. Eduardo Antonio Ferraz Coelho (Colégio Técnico, Federal University of Minas Gerais). These cultures were obtained as described by Magalhães et al. (2014). An axenic cell culture of the PH-8 strain, named R0, was recovered from the hind footpads of BALB/c mice after 8 weeks of infection and was used as the reference for a virulent profile. The other three derivate SIVP cultures, R10, R40, and R60 were obtained after 10, 40 and 60 successive *in vitro* passages (SIVP) from the R0 axenic culture. Parasites were grown at 26°C in M199 medium (GibcoBRL) at pH 7.4, supplemented with 10% heat-inactivated FBS, 20 mM L-glutamine, 100 UI/mL penicillin, 100 mg/mL streptomycin, adenine 10 mM, biotin 0.1% and hemine 0.25%.

In vitro Infection

Bone marrow cell suspensions were obtained by washing the femurs of BALB/c mice with sterile 0.9% saline. Suspensions with 2×10^5 parasites/mL were platted in Petri dishes in Complete Tissue Culture Medium (CTCM) [*Dulbecco's Modified Eagle's medium*–DMEM, supplemented with 10% inactivated BFS, L-glutamine 2 mM, penicilin G 100 UI/mL, 50 μM of β-mercaptoethanol (*Pharmacia Biotech, Uppsala*, Swiss) and HEPES 25 mM, pH 7.2]. L-929 cell conditioned medium (LCCM) was added (30%) at days 0 and 4 to induce cellular differentiation. At the 7th day of cultivation, promastigotes were incubated with BMMΦ at a 5:1 ratio. After 2 h, the infection was arrested and non-internalized promastigotes were removed with PBS (137 mM NaCl; 8 mM Na_2HPO_4; 2.7 mM KCl; 1.5 mM KH_2PO_4; pH 7.0). Infected cells were resuspended in CTCM at 8×10^5 cells/mL and plated in *Lab-tek* chamber slides (NUNC, Thermo Fisher Scientific). Cells were stained using Panotic (Laborclin, Pinhais, PR, Brazil) and infection rates were determined at 0, 3, 12, 24, and 48 h after infection. A microphotographic system with 400–1000X magnification on an optical microscope (Olympus CH30 Binocular Microscope) was used to observe and photograph the cells. These assays were repeated three times to determine the reproducibility of experimental data. The number of infected cells was calculated by counting at least 300 cells per well (Boltz-Nitulescu et al., 1987). Differences among groups were determined by One-way ANOVA, and $p < 0.05$ were considered as significant.

In vivo Infection

For *in vivo* infection, R0 and R60 promastigotes were collected at the 3rd day of the stationary phase and washed twice with cold PBS. The promastigotes were resuspended at 4×10^7 cells/mL and 25 μL of this suspension was inoculated in the right hind footpad of female BALB/c mice ($n = 10$ per group). The footpads of each group were measured weekly to follow development of the lesion. Lesion size measurements (mm) were considered as the size of infected paw minus the non-infected one (left hind). At the 2nd week post-infection, the mice were euthanized to collect spleen cells for cultivation and supernatant for ELISA.

Determination of Parasite Loads by Limiting Dilution Assay

Parasite burden in BALB/c mice hind footpads was determined by limiting dilution as previously described (Lima et al., 1997). Briefly, the footpads were homogenized in a douncer with M199 medium. Tissue debris was removed by centrifugation at 50 g at 4°C for 1 min. The supernatant was collected and centrifuged at 1540 g at 4°C for 10 min. The obtained pellet was resuspended in 500 μL of M199 medium and submitted to 1:10 serial dilution (in duplicate) in 96-well microplates at a final volume of 200 μL. Microplates were incubated at 26°C for 15 days and the presence of parasites was evaluated weekly. The final titer was considered as the last dilution in which at least one parasite could be identified in the well. Results were expressed as the negative logarithm of the number of parasites.

Soluble *Leishmania* Antigen Preparation

L. amazonensis from early stationary phase cultures were collected and washed twice in sterile PBS. The obtained pellets were submitted to seven cycles of freeze-thaw in liquid nitrogen (thawing at 37°C). Preparations were observed on an optical microscope for the presence of intact parasites (de Souza et al., 2010). Protein content was determined by Bradford (1976) and adjusted to 1 mg/mL. Antigen suspension was stored in aliquots, at −80°C.

Separation of *L. amazonensis* Promastigote Metacyclic Forms at Late Log (4th day) and Stationary (7th day) Phases From Axenic Cultures

Ficoll Gradient Separation Assay

A Ficoll gradient separation assay was performed using R0 and R60 promastigotes at the 4th and 7th days of cultivation. The cultures were separated in three sterile 15 mL conical tubes for each cell culture analyzed and the tubes were centrifuged at 50 g for 5 min at 4°C to remove dead parasites. Supernatants were transferred to new conical tubes and centrifuged at 1500 g at 4°C for 10 min. The obtained pellets were washed twice with 10 mL of cold PBS (4–8°C). After the second centrifugation, each pellet was suspended in Dulbecco's Modified Eagle's medium (DMEM) supplemented with 1% glucose (Sigma-Aldrich Inc.). 2.0 mL of suspensions with 1×10^7 parasites/mL were distributed in three 15 mL conical tubes. With the assistance of a Pasteur pipette, 2.0 mL of Ficoll 10% (Ficoll Type 400, Sigma-Aldrich Inc.) was added at the bottom of the tube. This solution was centrifuged at 1300 g at 25°C for 15 min, using acceleration 1 and deceleration 0 (Spath and Beverley, 2001). Procyclic and metacyclic promastigotes were used to determine the gates for FACS assays.

Determination of Metacyclic Forms Population by Flow Cytometry

The *L. amazonensis* R0 and R60 promastigotes at the 4th and 7th days of growth were washed twice with PBS and fixed in 300 μL of 1% formalin. The populations of procyclic and metacyclic promastigotes were then analyzed by flow cytometry (BD LSRFortessa™ cell analyze) (10 thousand events) and identified with the Flowjo software, version 10.1, using the gates previously established with the parasites separated by Ficoll gradient (**Supplemental Figure 2**). Metacyclic forms were considered to have lower granularity and smaller size (SSC × FSC), when compared to procyclic promastigotes, as previously described (da Silva et al., 2015). Statistical analyses were performed with Two-way ANOVA with Bonferroni post-test.

In vitro Infection of Bone Marrow-Derived Macrophages (BMMΦ) and L929 Strain Cell Culture

Murine cell strain L929 producing macrophage colony-stimulating factor (M-CSF) was cultivated in CTCM and HEPES [25 mM, pH 7.2] at an initial concentration of 2×10^5 cells/mL. Cells were incubated at 37°C with 5% of CO_2. On the 3rd day of growth, the supernatant was collected, centrifuged (1540 g, 4°C, 10 min), sterilized by filtration and then stored at −80°C, until further use.

Preparation of BMMΦ

BMMΦ were obtained using the protocol described by Boltz-Nitulescu et al. (1987). BALB/c mice were euthanized by cervical dislocation. Their thighbone and shinbone were surgically dissected, submerged in 70°GL alcohol for 2 min and washed with PBS supplemented with 5% inactivated FBS. The epiphyses were removed and the diaphysis were washed with PBS supplemented with 5% inactivated FBS, to obtain cells. The cells were suspended in differentiation medium DMEM (supplemented with 30% of supernatant from the L929 cell culture, 20% of FBS, 1% of L-glutamine and 100 UI/mL of penicilin G), distributed in Petri dishes and incubated at 37°C with 5% CO_2.

At the 4th and 7th days after bone marrow removal, more differentiation medium was added to the Petri dishes. At the 9th day of cultivation, the supernatant was aspirated and discarded. Each plate received 5 mL of a sterile solution of ethylenediamine tetraacetic acid (EDTA) 20 mM (Synth, Diadema, SP, Brazil) and was subsequently incubated at 37°C with 5% CO_2 for 20 min. At the end of the incubation period, 5 mL of FBS were added to each Petri dish. Cell scrappers were used to detach the cells. The subsequent cellular suspensions were transferred to sterile conical bottom tubes and washed with PBS. Concentrations were adjusted to 1×10^6 cells/mL in CTCM and final volumes of 2 mL (at 2×10^6 cells per well) were plated in polystyrene plates. An average of 30–33% of BMMΦ was obtained after the differentiation process.

BMMΦ Infection by R0 or R60

BMMΦ were infected with 2×10^6 promastigotes of either R0 or R60, grown for 7 days (late stationary phase) in axenic cultures. The parasites were centrifuged at 50 g for 10 min; dead parasites were discarded, and the viable ones were added to the BMMΦ culture in an average proportion of five parasites per BMMΦ. After 2 h of homogenization, the cells were washed with sterile PBS to eliminate the non-internalized parasites (time 0 h). The wells were analyzed after 3, 12, and 24 h (times 3, 12, and 24 h, respectively).

To evaluate *in vitro* infectivity, 8×10^5 cells/mL were plated in chamber slides (*Lab-tek chamber slides*, NUNC, Thermo Fisher Scientific). Panotic (Laborclin, Pinhais, PR, Brazil) was used to stain slides, following manufacturer instructions. Olympus BX50 optical microscopes *(Olympus, Center Valley, PA, USA)* were used for microscopic examination of slides to determine BMMΦ infectivity. A minimum of 300 BMMΦ per chamber well was analyzed for each SIVP cultures and for each time interval, and the numbers of infected and non-infected cells were determined. The experiment was performed in triplicate. Two-way ANOVA was used for statistical analyses.

Enzyme Linked Immunosorbent Assay (ELISA)

Spleens obtained after 2 weeks of infection with either R0 or R60 were collected and homogenized. The obtained suspensions had their concentrations adjusted to 5×10^6 cells/mL (CTCM, pH 7.2). The cells were distributed into 48 well plates and stimulated with 50 μg/mL of homolog *Leishmania* particulate antigen. 10 μg/mL of concanavalin A (ConA) was used as a positive control, while the CTCM with no stimulus was used as a negative control (Coelho et al., 2003). The plates were incubated for 48 h at 37°C with 5% CO_2 and then centrifuged at 706 g at room temperature for 5 min. Supernatants were collected and stored at −20°C for later cytokines assays.

Quantification of cytokines in culture supernatants was performed by enzyme-linked immune sorbent assay (ELISA). BD OptEIA (BD Biosciences, San Diego, CA, USA) kits were used for measurement of IFN-γ and IL-10, following the manufacturers' guidelines.

Metabolite Extraction for Metabolomic Fingerprint Analyses of Promastigotes

For each group, 10 biological replicates were collected at the 4th day of cultivation. Before extracting the metabolites, the culture bottle (10 mL volume) was shaken in an ethanol/dry-ice bath for 40 seconds for quenching. For UPLC-MS and CE-MS, 4×10^7 promastigotes were centrifuged at 2,000 g for 10 min at 4°C, washed 3 times in cold (4°C) PBS and lysed in 450 μL of cold (4°C) CH_3OH/H_2O (4:1, v/v). The cells were mechanically disrupted by 3 cycles of freeze/thaw in liquid N_2 and then by lysing for 10 min at 50 Hz in a TissueLyser LT (Qiagen) with glass beads (50 mg, 425–600 μm, Sigma-Aldrich). Cellular debris were removed by centrifugation at 15,700 g at 4°C for 10 min. For UPLC-MS, 200 μL of clarified supernatants were transferred to a glass vial and analyzed. For CE-MS, 200 μL of clarified supernatants were transferred to a new tube, dried, resuspended in 200 μL of formic acid (0.1 mmol/L) containing methionine sulphone (0.2 mmol/L–internal standard), vortex mixed for 1 min and then centrifuged at 15,700 g at 4°C for 10 min.

For GC-MS, the metabolites were extracted using 350 μL of $CH_3OH/CHCl_3/H_2O$ (3:1:1, v/v/v) at 4°C, lysed for 10 min at 50 Hz in a TissueLyser LT (Qiagen) with glass beads (50 mg, 425–600 μm, Sigma-Aldrich). The supernatants (200 μL) were clarified by centrifugation and evaporated until dry in a SpeedVac at 30°C. Afterwards, 10 μL of O-methoxyamine hydrochloride (15 mg/mL in pyridine) was added to each vial, mixed vigorously for 5 min with a vortex FB 15024 (Fisher Scientific, Spain) and incubated in darkness at room temperature for 16 h for methoximation. Later, 10 μL of BSTFA [N,O-bis(trimethylsilyl)trifluoroacetamida] with 1% TMCS (v/v) (trimethylchlorosilane) was added, the vials were vortexed for 5 min and incubated for 1 h at 70°C for the silylation reaction. Finally, 100 μL of 10 mg/mL of C18:0 methyl ester in heptane (internal standard) were added and the samples were vortexed. Two blank samples were prepared following the same procedures of extraction and derivatization.

Quality controls (QCs) were independently prepared for each technique by pooling equal volumes of each sample. They were evaluated at the beginning of each analysis to reach system equilibration and throughout each run to provide a measurement of the system's stability as well as the reproducibility of sample treatment procedure (Canuto et al., 2014).

Metabolomic Fingerprinting by UPLC-MS, CE-MS, and GC-MS

Samples were analyzed by UPLC-MS, CE-MS, and GC-MS, to ensure a wide coverage that would encompass hydrophobic, hydrophilic, acid, basic and neutral molecules. CE-MS and GC-MS were performed according to the methods previously described by Canuto et al. (2014). UPLC-MS was performed according to the methods previously described by Bujak et al. (2014) and Canuto et al. (2014).

Metabolomic Data Treatment and Statistical Analyses

The resulting data files (UPLC-MS and CE-MS) were cleaned of background noise and unrelated ions using the Molecular Feature Extraction (MFE) tool in the Mass Hunter Qualitative Analysis software (B.05.00, Agilent). Primary data treatment (filtering and alignment) was performed using the Mass Profiler Professional software (B.02.01, Agilent). Data treatment for the GC-MS analysis was conducted by using the Fiehn retention time locked (RTL) Library and the National Institute of Standards and Technology mass spectra library (Kind et al., 2009; Canuto et al., 2014), with the MSD ChemStation software (G1701EA E.02.00.493, Agilent) and a correct assignment based on the coincidence of retention times and spectrum profiles (Canuto et al., 2014). Features that did not appear in at least 50% of the QCs with a coefficient of variation lower than 30% were excluded from analysis in all analytical platforms. The Heatmap (**Figure 4B**) was constructed with R software (R x64 3.1.3), using gplots packages and Heatmap2 script. The clValid package with K-means script was applied to cluster metabolites into groups. The MBRole *on line* software (http://csbg.cnb.csic.es/mbrole/) was used to map pathways and the biological role of compounds.

The filtered masses were exported to SIMCA-P+ 12.0 (Umetrics) for multivariate statistical analysis. To approximate to a normal distribution, data were converted to the logarithmic scale before any statistical calculations (Canuto et al., 2014). To check for quality, principal component analysis (PCA-X) models were used to visualize QC clustering with the non-filtered data. Later, partial least square discriminant analysis (PLS-DA) models were built to discriminate the samples in the groups. The quality of these models was described by explained variance (R^2) and predicted variance (Q^2) the former explains variance and fitness, while the latter predicts variance and provides information about model predictability. The predictive ability of the multivariate models was confirmed in accordance to the orthogonal projection to latent structure discriminant analysis (OPLS-DA) (Canuto et al., 2014). Both PLS-DA and OPLS-DA were built using the filtered data. Unit variance (UV) scaling and logarithmic transformation (base 2) were used.

For LC-MS, GC-MS, and CE-MS data, differences among R0xR10, R0xR40, and R0xR60 were evaluated for individual metabolites using univariate statistical analysis (*t*-test for normal distribution or Mann-Whitney *U* test when the variable did not follow a normal distribution), using in-house algorithms in MATLAB, version 7.10 (MathWorks Inc., Natick, Massachusetts). Fold changes were calculated by averaging the abundance results between groups in Log_2.

Accurate masses of features representing significant differences ($p < 0.05$ in at least two statistical analyses) obtained from MS-based analyses were searched against the CEU mass mediator database (http://biolab.uspceu.com/mediator/). For each statistically significant mass, the formula proposed by

the MassHunter software (B.05.00, Agilent Technologies) was compared with the experimental isotopic pattern distribution.

For CE-MS data, commercial standards, when available, were used to confirm putative identifications, combining peaks of samples and peaks of standards at the same run. Confirmation of matches was performed by comparison of the migration time and isotopic distribution.

Evaluation of Cellular Oxidative Stress During SIVP Process

To evaluate the cellular oxidative stress, promastigotes from R0 and R60 were cultivated in M199 medium (Gibco) supplemented with 10% of fetal bovine serum (Gibco) and cultivated at 26°C. R0 and R60 cultures at late log (4th day) phase were used. Aliquots containing 10^6 parasites were centrifuged at 1,540 xg and washed with PBS twice. The cultures were treated as recommended by manufacturer of CellROX® Deep Red Reagent (Thermo Fisher Scientific). The levels of ROS were measured by flow cytometry using BD Fortessa. Experiments were performed in triplicates. The statistical analyses and graph plots were performed using GraphPad Prism 8.0.1

Susceptibility Assay of *L. amazonensis* SIVP Parasites to Antimony (Sb^{III})

L. amazonensis (R0, R10, R40, and R60) promastigotes at the 4th day of cultivation were submitted to Sb^{III} (Sigma-Aldrich, St. Louis, MO, USA) susceptibility tests. Suspensions of parasites at 2×10^6 cells/mL were incubated in 24-well plates with M199 medium at 26°C for 48 h. The parasites were incubated either in the absence of Sb^{III} or exposed to several different concentrations of that compound (18.7–374.3 μM). The effective concentrations required to kill 50% of the parasites (EC50) were determined using a model *Z1 Coulter Counter* (Beckman Coulter, Fullerton, CA, USA). EC50 values were determined from at least two independent measurements performed in triplicate, applying the method of linear interpolation (Huber and Koella, 1993). Statistical analyses were performed using GraphPad Prism Software v5.0, San Diego, CA.

Measurement of Phosphatidylserine Exposure by *L. amazonensis* SIVP Promastigotes Using FACS

The BD AnnexinV-PE Apoptosis Detection Kit was used to determine of aPS exposure by *L. amazonensis* submitted to SIVP. The protocol described by Rochael et al. (2013), with modifications was used. Suspensions of 5×10^5 cells/mL of promastigotes (R0, R10, R40, and R60) at the 4th and 7th days of growth were collected by centrifugation at 1,450 g, for 10 min at 4°C, washed twice in PBS and suspended in 100 μL of binding buffer (10 mM HEPES [pH 7.4], 150 mM NaCl, 5 mM KCl, 1 mM $MgCl_2$, and 1.8 mM $CaCl_2$). To each cell suspension, 2 μl of BD AnnexinV-PE and 2 μl of 7-Amino-Actinomycin (7-AAD) were added. No-labeled suspensions were used as negative controls, while positive controls were defined as those labeled either with AnnexinV-PE only or 7AAD only. The suspensions were incubated for 15 min in the dark, at room temperature. Triplicate analyses were performed for each SIVP. 7-AAD was used to determinate parasite viability, while AnnexinV-PE was used to measure aPS exposure. Graphs with PerCP-Cy5.5 (7-AAD) in the y axis and PE (annexinV) in the x axis were constructed, and gates were determined as following: lower left gates for no-labeled parasites; upper left gates for 7-AAD (dead parasites); upper right gates for 7-AAD+ annexinV (non-viable, aPS-exposing parasites); and finally lower right gates for AnnexinV-PE (viable, aPS-exposing parasites). Thus, the percentages of aPS exposure were calculated considering the number of parasites in the lower right gates (**Supplemental Figure 5**).

Results were obtained by flow cytometry, using a BD LSRFortessa™ cytometer. BD FACSDiva™ software was used for acquisition and analysis. Results were analyzed by FlowJo® V10. Statistical analyses were performed using GraphPad Prism Software v5.0, San Diego; CA. Two-way ANOVA was used for multiple group comparisons. Statistically significant values were defined as $p < 0.05$.

RNA Extraction and cDNA Synthesis

R0, R10, R40, and R60 promastigotes were cultivated in 20 mL of M199 medium until the 4th day of growth, as previously described. Cell suspensions were centrifuged at 5,000 g at 4°C for 10 min, using DNA/RNA-free tubes with 1.5 mL of sterile water. The parasites were suspended in 500 μL of RNA Later (Sigma-Aldrich, MO, USA) and stored at −80°C for further processing. When later processed, the suspensions were thawed and centrifuged at 5,000 g at 4°C for 10 min. RNA-Later supernatants were discarded. Total RNA was extracted with Tri-Reagent (Sigma-Aldrich, MO, USA), following the manufacturer's instructions. Quality, concentration and purity of the extracted RNA were measured by 1.5% agarose gel, Qubit 2.0 (Thermo) and NanoDrop (Thermo), respectively. Total RNA was treated with DNaseI (DNase I, RNase-free 1 U/μL, Thermo Fisher) following the manufacturer's instructions. cDNA was synthesized from 1 μg of total RNA with the High-Capacity cDNA kit (Thermo Fisher), following the manufacturer's instructions.

qPCR Analyses

Selected loci **(Supplemental Table 1)** were amplified using the Power Syber Green kit (Thermo Fisher) with 0.2 μM primers. The GAPDH locus was used as reference to normalized gene expression, while the R0 group was used as control. Quantitative PRC reactions were performed on the QuantiStudio 3 thermocycler (Thermo Fisher) with the following program: 50°C for 2 min, 95°C for 10 min, 40 cycles of 95°C for 15 s and 60°C for 1 min, followed by a dissociation curve of 60°C to 95°C (0.1°C/s). The values of Ct for each locus and each group were evaluated based on three different experiments. The expression levels were calculated using the ΔΔCT, as previously described (Pfaffl, 2001). Statistical analyses were performed using Two-way ANOVA with Bonferroni post-test.

RESULTS

L. amazonensis Parasites Resultant From SIVP Are Less Infective to Mice

In a previous study (Magalhães et al., 2014), the *L. amazonensis* PH-8 strain, recently isolated from mice (R0), was submitted to successive *in vitro* passages (SIVP) in axenic culture, generating the R10 and R30 parasites (obtained after 10 and 30 SIVP, respectively). Here, the R0 and R10 SIVP cultures, in addition to R40 and R60, also derived from R0, were further characterized through a metabolomics fingerprinting approach.

Initially, to validate that the SIVP process decreased infectivity, late stationary phase promastigotes (7th day of axenic growth) of R0 and R60 were used for *in vitro* infection of BALB/c mice bone marrow-derived macrophages (BMMΦ). As shown in **Figure 1A**, the percentages of BMMΦ infected with R60 were significantly lower as compared to R0, at all time points post-infection, indicating that R60 was less infective than R0. To determine if SIVP also diminished infectivity *in vivo*, BALB/c mice were infected at the right hind footpad with R0 and R60 and lesion development was monitored weekly. Differences in lesion size induced by R0 and R60 in BALB/c footpads were detected after 5 weeks of infection. Footpad swelling was significantly smaller in mice infected with R60, when compared to those infected with R0 (**Figure 1B**). After 2 weeks of infection, parasite loads (detected by limiting dilution assays) were also lower on BALB/c mice infected with R60 when compared to those infected with R0 (**Figure 1C**). These findings confirmed that, as expected, R60 promastigotes have impaired infectivity at the initial stages of infection in BALB/c mice.

Long-Term *in vitro* Cultivation Does Not Affect Growth Rates and the Promastigote Metacyclogenesis Process

To verify if SIVP interfered in the capacity of proliferation of the SIVP parasites, growth curves were evaluated (**Supplemental Figure 1**). R10, R40, and R60 displayed the same growth rates when compared to R0, indicating that, under the same conditions, SIVP did not impact on parasite growth rates.

Since metacyclogenesis is an important factor that affects *Leishmania* spp. infectivity and might be altered by long-term axenic growth (da Silva and Sacks, 1987; Cysne-Finkelstein et al., 1998), R0 and R60 promastigotes were also compared for their ability to differentiate *in vitro* from procyclic to metacyclic promastigote forms. Initially, enriched populations of procyclic and metacyclic were analyzed by a flow cytometry assay (FACS) to determine the gates that corresponded to each cell type (**Supplemental Figure 2**). FACS analysis was chosen because it allows discrimination of cells according to granularity and cellular volume and (FCS), and it is known that procyclics and metacyclics differ in size (Spath and Beverley, 2001; da Silva et al., 2015). Later R0 and R60 promastigotes were submitted

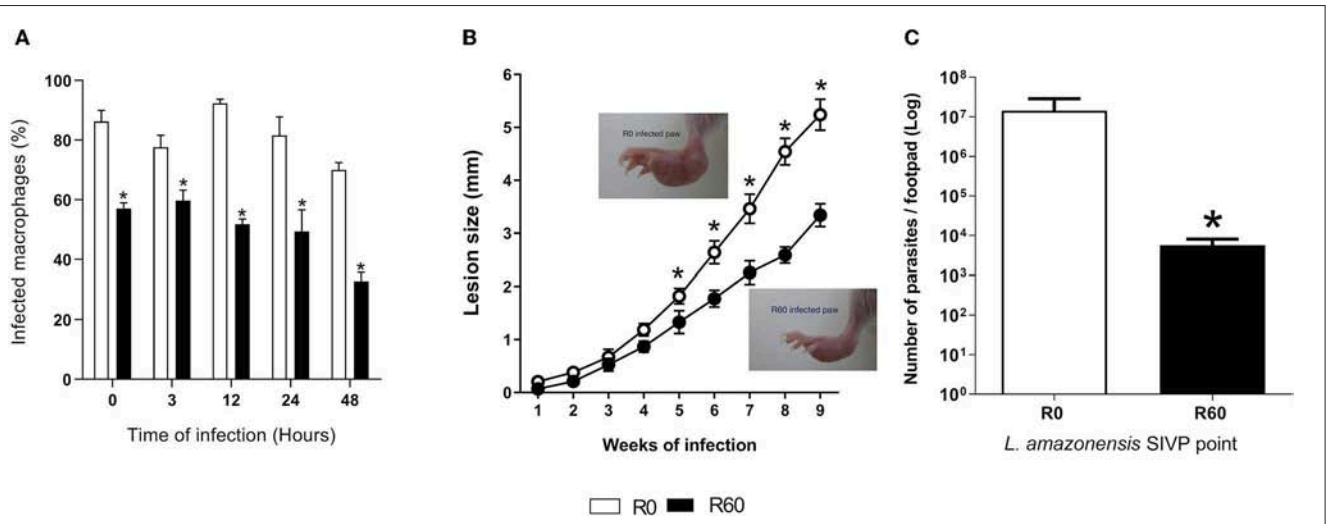

FIGURE 1 | *In vitro* BMMΦ infection, lesion size development and tissue parasitism in footpads of BALB/c infected with R0 and R60 strains. **(A)** Percentage of infected bone marrow-derived macrophages. BALB/c bone marrow-derived macrophages (2×10^5 cells/ml) were infected with R0 or R60 grown for 7 days, at late stationary phase (5 parasites/macrophage). The cells were fixed and stained with Giemsa after 3 h of exposure (defined as 0 h time) and after 3, 12, 24, and 48 h post infection. The percentage (%) of infected macrophages was obtained by manual counting using an optical microscope. 300 cells at three different wells were evaluated from two different assays. **(B)** Evaluation of footpad lesion size from BALB/c mice infected with 1×10^6 *L. amazonensis* R0 or R60 stationary phase promastigotes. Lesion size was weekly measured with a caliper, and represent the size of infected paw minus the size of the non-infected one. Each point represents an average of lesion size from six infected mice plus the standard error (95% confidence interval). In detail, photographs of R0 and R60 infected paws at 8 weeks post-infection. **(C)** Limiting dilution assay, performed at 2nd week post-infection. Infected BALB/c footpads were homogenized in a glass homogenizer with M199 medium. The obtained pellet was resuspended in 500 μl of M199 medium and submitted to serial dilution (in duplicate) 1:10 in 96-well micro plates at final volume of 200 μL and incubated at 26°C for 15 days. The last dilution at which viable parasites was observed was considered the final titer. Results were expressed as negative logarithm of the parasites title. Bars represent mean values of three biological replicates from four infected BALB/c footpads plus standard deviation of the mean. * indicates $p \leq 0.05$ (Two-way ANOVA with Bonferroni post-test).

to FACS analysis at the 4th and 7th days of cultivation (late log and stationary phases, respectively) (**Figures 2A,B**). The gates previously determined were used to indicate the populations that displayed low size and granularity. No significant differences were observed between R0 and R60 cultures at the analyzed time points, suggesting that the decreased infectivity of R60 is not associated with a decreased ability to generate metacyclics.

Infection With the Attenuated *L. amazonensis* R60 Promastigotes Is Associated With Increased Levels of Specific IFN-γ During the Early Stages of Infection in BALB/c Mice

Host immune responses modulate the course of *Leishmania* infection, while also reflecting its inflammatory responses to infection (Carneiro et al., 2015; Maspi et al., 2016; Conceicao-Silva et al., 2018). As previously shown, infection by R60 induced both smaller lesions and parasite loads in BALB/c mice, in relation to R0 promastigotes. To investigate if this profile could be associated to alterations in host immune responses, the levels of specific IFN-γ and IL-10, key cytokines enrolled, respectively in resistance and susceptibility to *Leishmania* infections, were measured in supernatants of splenocytes culture from BALB/c mice infected with R0 and R60. Two weeks post-infection, increased levels of IFN-γ were detected in spleen culture supernatants of mice infected with R60, when compared to those from R0 infected mice, after stimulation with promastigotes total protein extracts (**Figure 3A**). However, no significant differences were seen in IL-10 levels (**Figure 3B**).

The Metabolomic Multiplatform Fingerprint Approach Revealed the Biochemical Pathways Involved in *L. amazonensis'* Attenuation

To uncover the continuous metabolic changes occurring during SIVP, a multiplatform metabolomic fingerprint approach (GC-MS, LC-MS and CE-MS) was applied to obtain the metabolic profile of late log-phase (4th day of growth) promastigotes' extracts of R0, R10, R40, and R60, grown under the same conditions. QC samples, prepared by pooling aliquots of all samples, were used to monitor the entire analytical processes. These QC samples were applied recurrently at different intervals to monitor equipment performance.

The obtained metabolomics data were first filtered to exclude metabolites that presented extreme variations: more than 30% of quality controls (QC, %RSD) and in addition, those that were not present in at least 80% in each group (filtered by flags). Then, a PCA-x analysis was applied to the filtered features. The QC samples were very tightly clustered for each analytical method, indicating a precise analytical performance and high experimental reproducibility (**Supplemental Figure 3**). Subsequently, a supervised partial least squares discriminant analysis (PLS-DA) was performed. Samples from different SIVP promastigotes were clustered in well-defined groups, as a first indication of significant metabolic differences among the SIVP promastigotes (**Supplemental Figure 4**).

The chemometric analysis revealed significant changes in ionic abundance in 66 metabolites that could be associated to *L. amazonensis* SIVP. Of these, 30 metabolites were detected by GC-MS and had their identities confirmed by fragmentation pattern, using the Fiehn RTL Library (Agilent) (Kind et al., 2009); 17

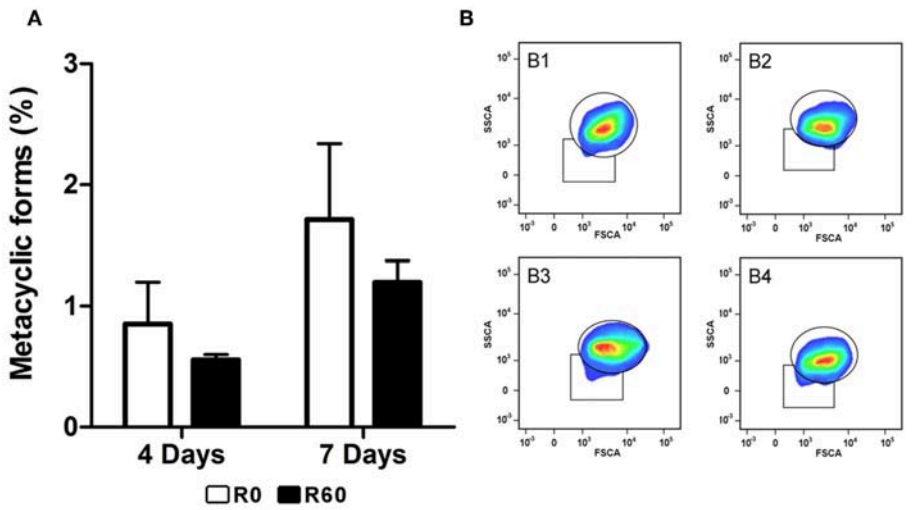

FIGURE 2 | Evaluation of metacyclogenesis in R0 and R60 cell lines. Promastigotes from R0 and R60 cell lines were cultivated in M199 medium (10% BFS, 26°C). R0 and R60 cultures at late log (4th day of growth) and stationary phases (7th day of growth) were analyzed by flow cytometry using BD Fortessa. **(A)** Percentages of promastigote metacyclic forms in R0 and R60 cell lines in late log (4 days) and stationary (7 days) phases. **(B)** B1 and B2 represent, respectively, R0 and R60 at the 4th day of growth. B3 and B4 represent, respectively, R0 and R60 at the 7th day of growth. The bars represent the average of two assays, minus and plus the standard deviation, in two independent analyses. Significant differences were investigated by Two-Way ANOVA.

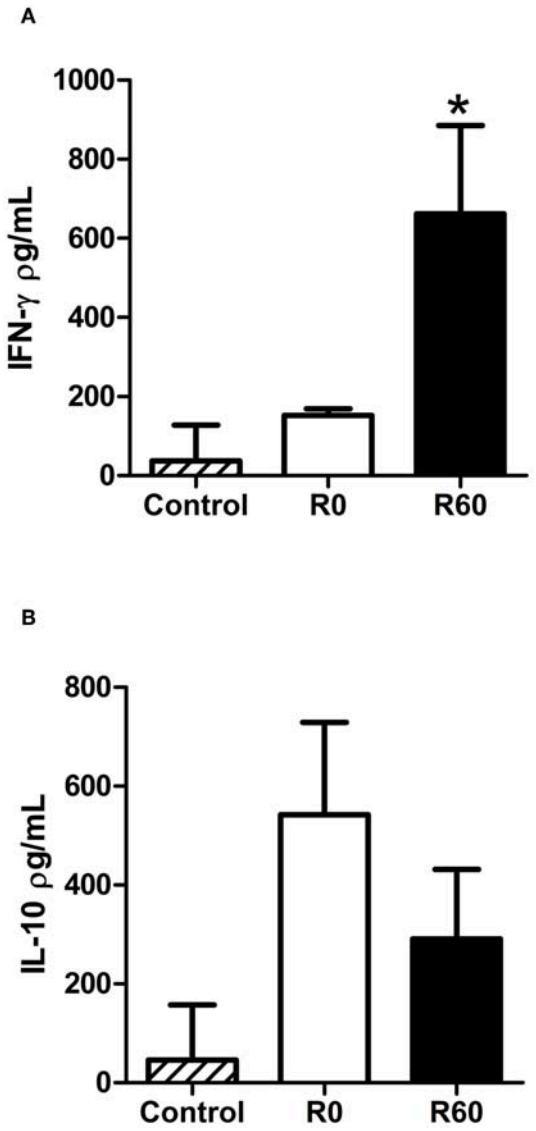

FIGURE 3 | Comparison of cytokine levels in spleen culture supernatants from BALB/c infected with R0 and R60 cell lines after 2 weeks of infection. For infection, 1×10^6 parasites were inoculated at the right footpad. Two weeks later, the animals were euthanized and RPMI medium (34°C, 5% CO_2) was used to cultivate spleen cells. The cultures were stimulated with soluble *Leishmania* antigen (SLA). Negative controls were non-stimulated spleen cells. 48 h after the stimulation, supernatant was collected and an ELISA assay was performed. **(A)** Levels of specific IFN-γ observed in spleen culture supernatants from BALB/c infected with R60 as compared to the levels produced by cells from mice infected with R0. **(B)** IL-10 levels in supernatant of splenocytes from R0 and R60. Bars represent mean values of three biological replicates from four infected BALB/c footpads, plus standard deviation of the mean. *indicates $p \leq 0.05$ (Two-way ANOVA with Bonferroni post-test).

compounds were putatively identified by LC-MS analysis in both positive and negative modes, while 19 compounds were identified using CE-MS; 10 compounds were confirmed by comparison with samples spiking off the corresponding standards (Naz et al., 2014), while nine were putative. Detailed results, including retention time (RT), theoretical and experimental compounds' mass, mass error in ppm and %RSD are shown in **Supplemental Table 2**.

The identified metabolites were, afterwards, grouped according to their chemical categories: 27% were classified as amino acids and amino acids derivatives, 18% as fatty acids, 16% as other organic compounds, 8% as nucleotides and nucleosides, 7% as phospholipids, 7% as organic acids, 5% as organic esters, 3% peptides, 3% as polyamines, 3% as lipids, and 3% as carbohydrates (**Figure 4A**). Altogether, 33% of the identified compounds were associated to fatty acids metabolism.

By comparing R0 with each of the other SIVP promastigotes, the fold changes of 65 metabolites' levels (except for proline) were hierarchically clustered and graphically represented in a heatmap (**Figure 4B**). Proline displayed a significant fold change increased throughout SIVP, starting from −1 and raising to 3.52 at R40 and 5.22 at R60, being far out of the heatmap scale for most of the other compounds, and thus was not represented in the heatmap. The HCA analysis clustered the metabolites in seven major clusters, according to the pattern of changes throughout SIVP (**Figure 4B**). Examination of this heat map, reveals that abundance of several metabolites significantly changed throughout the attenuation process, even as early as after 10 SIVP (R0xR10), suggesting that adaptation to this environmental change is a dynamic process and that metabolic alterations are continuously occurring, even after 40 SIVP.

Additionally, an enrichment analysis was performed, using the MBRole software (http://csbg.cnb.csic.es/mbrole/.) Of the 66 identified metabolites, 52 presented KEGG IDs and were used to map eight enriched metabolic pathways. The metabolites used by MBRole to identify the enriched pathways were plotted in individual graphs, as shown in **Figure 5**: ABC transporters (**Figure 5A**); fatty acid biosynthesis (**Figure 5B**); glycine, serine and threonine metabolism (**Figure 5C**); β-alanine metabolism (**Figure 5D**); glutathione metabolism (**Figure 5E**); oxidative phosphorylation (**Figure 5F**); glycerophospholipid metabolism (**Figure 5G**) and lysine degradation (**Figure 5H**). Taken as s whole, the metabolite's abundance decreased, except for lysine and succinic acid, which presented increased levels from R0 to R60 (**Figures 5A,F,H**). Some metabolites such as betaine, putrescine, and pipecolate showed increased levels until the 10th passage, but significant decreases were further observed in additional stages of axenic cultivation (**Figures 5A,C,E**). Other metabolites such as glycine, uracil, phosphate, myristic acid, stearic acid, palmitic acid, linoleic acid and arachidic acid showed decreased levels until the 40th passage, but their levels raised to those present in R0, in R60 (All **Figure 5**, except **Figure 5B**). Remarkably, phosphatidylserine (PS) was detected in low levels until the 10th passage but increased in further passages (**Figure 5C**).

Phosphatidylserine Analogs (aPS) Exposure by SIVP Promastigotes, as Revealed by Flow Cytometry Analysis

The metabolomic analysis revealed concomitant changes in the abundance of various lipids and glycerophospholipids,

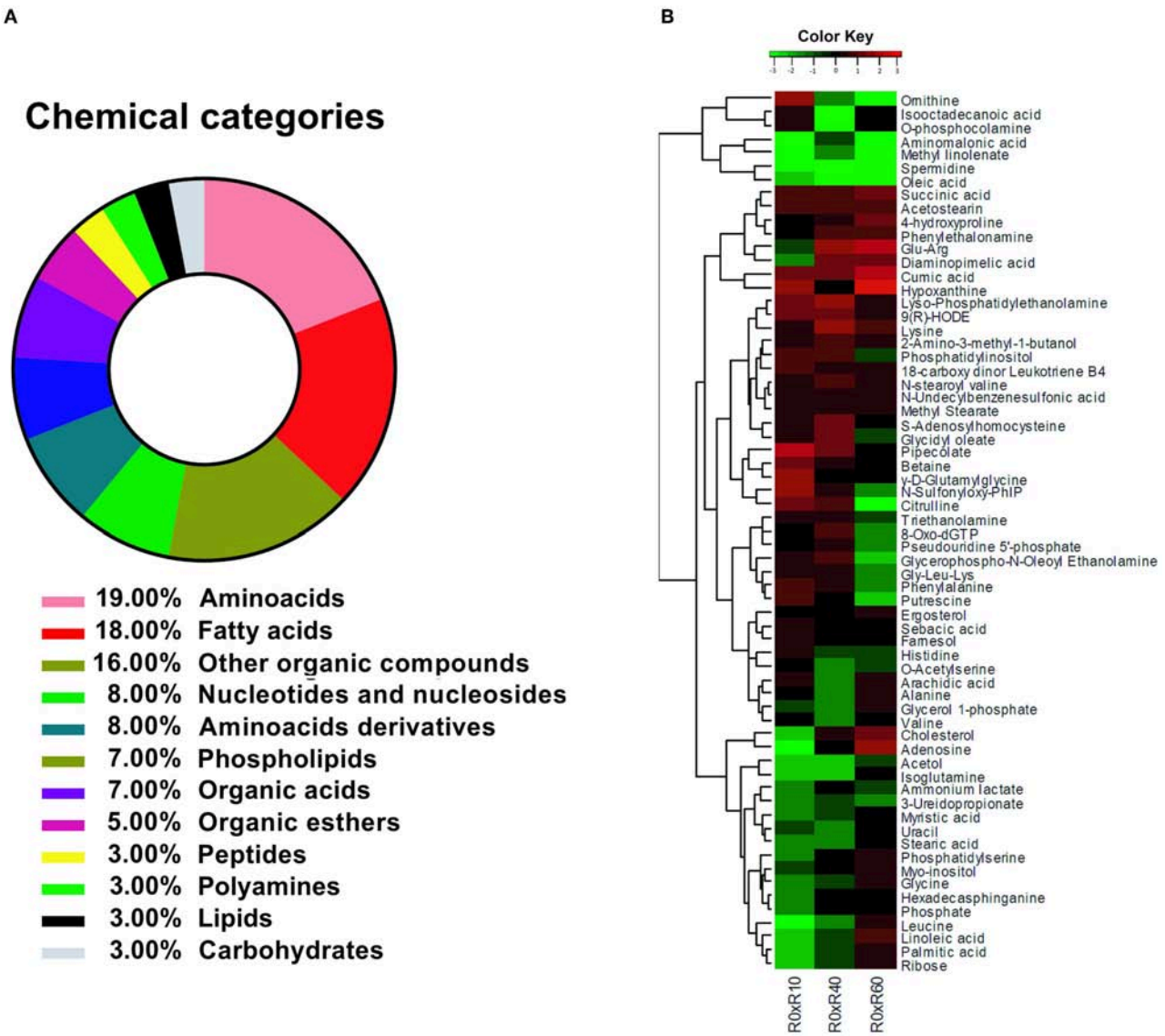

FIGURE 4 | Identification of *L. amazonensis* metabolites' changes during SIVP. **(A)** Biochemical categories for the identified metabolites in *L. amazonensis* attenuation process after SIVP, identified by multiplatform metabolomic fingerprint approach. Metabolites were classified according to their chemical category by MBRole online software. **(B)** Heatmap showing confirmed or putatively identified metabolites in log2-scale fold change. To obtain a Kinect metabolite profile, two intermediary strains were included in this analysis, R10 and R40 (10 and 40 SIVP, respectively). The dendogram shows the fold changes behavior for each metabolite among all metabolites (metabolome), except for Proline, which extrapolated the fold change for the majority of the metabolites and did not fit into the scale. Metabolites' fold changes were calculated by comparing the ionic abundance average (in Log_2) from each metabolite belonging from each attenuated lines (R10, R40, and R60) to the virulent one (R0). The Values varied from −3.0 (green) to 3.0 (red). Non-expressive fold changes (values next to zero) were shown in black. The heatmap were generated by the R x 64 3.1.3 software, using the gplots/heatmap2 package.

suggesting significant remodeling on membrane lipid composition during SIVP. Among glycerophospholipids, the increased exposure of analogs of phosphatidylserine (aPS) has been reported as important for *Leishmania* virulence (Franca-Costa et al., 2012; Rochael et al., 2013). There was a significant increase in the intracellular contents of PS in R40 and R60 parasites. However, R60 was less virulent than R0. This finding prompted the hypothesis that R60 exposes less aPS than R0. In order to confirm that aPS metabolism changed in attenuated parasites, we measured aPS exposure by flow cytometry (Franca-Costa et al., 2012; Rochael et al., 2013). The gates for aPS analysis were determined using non-labeled parasites (**Supplemental Figure 5A**, Q1), aPS labeled with only annexinV (PE) (**Supplemental Figure 5B**,

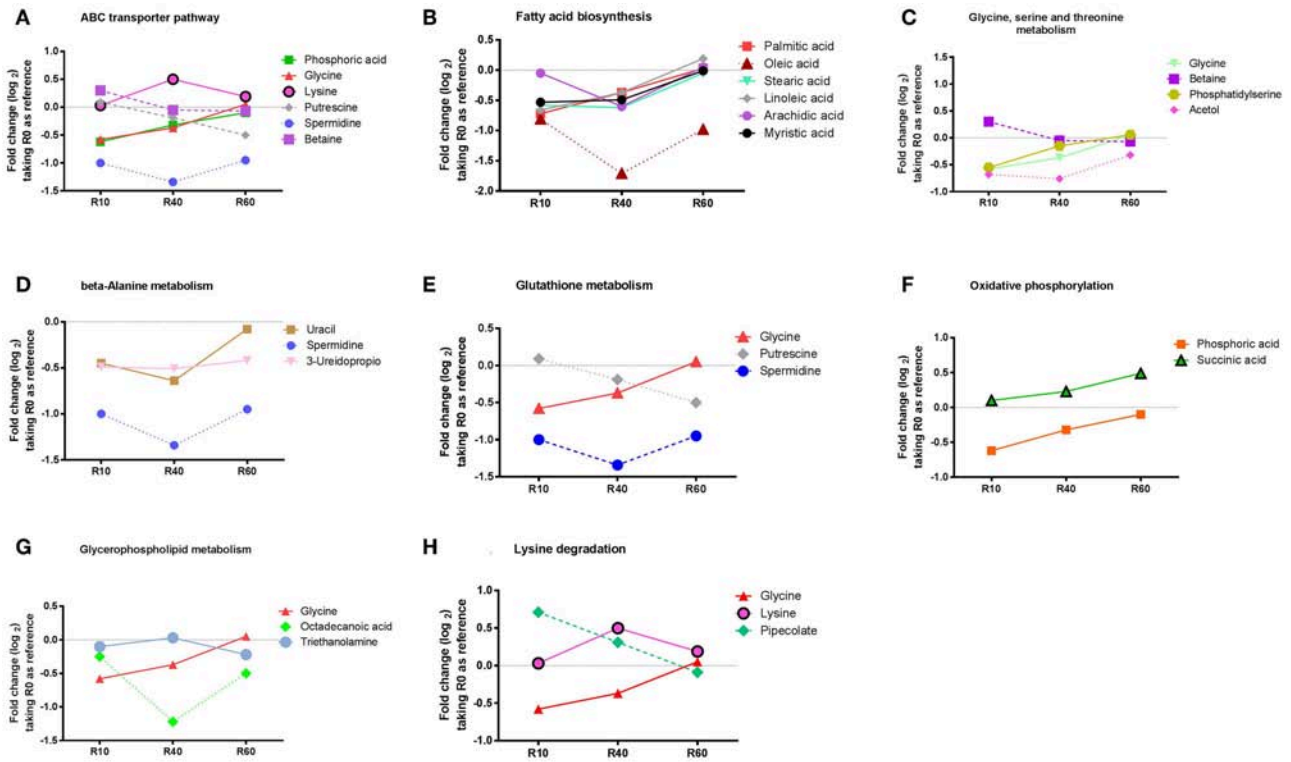

FIGURE 5 | Enriched and non-enriched pathways, identified by MBRole online software, form *L. amazonensis* metabolites associated with the attenuation process, as detected by the metabolomic fingerprint multiplatform approach. Identified metabolites were submitted to MBRole online software, using their KEGG IDs, with *L.* major pre-compiled reference, in order to map those biological pathways with statistic significance. Fifty-two metabolites could be identified with KEGG IDs and were mapped in 42 pathways. Eight pathways were mapped as enriched (statistic significant): ABC transporters **(A)**, Fatty acids Biosynthesis **(B)**, Glycine, serine and threonine metabolism **(C)**, B- beta-Alanine metabolism **(D)**, Glutathione metabolism **(E)**, Oxidative phosphorylation **(F)**, Glycerophospholipid metabolism **(G)**, Lysine degradation **(H)**. The metabolites responsible for identification of each enriched pathways are represented in graphics, showing Log_2 fold change, expressed as the average ionic abundance in R0xR10, R0xR40, and R0xR60, to obtain a kinetic analysis of metabolites during attenuation by SIVP.

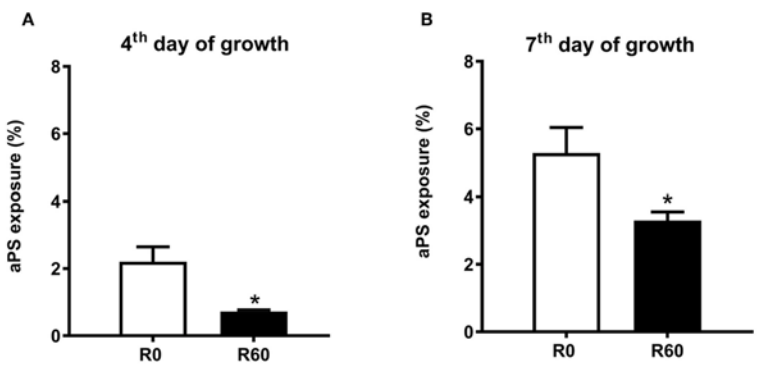

FIGURE 6 | aPs exposure by R0 and R60 promastigotes. **(A)** Profile of promastigotes grown for 4 days. **(B)** Profile of promastigotes grown for 7 days. 2×10^5 parasites from R0 and R60 were washed with PBS, suspended in binding buffer (BD-Anexin V-PE), and then incubated at room temperature for 15 min. At the moment of acquisition, 7AAD (PerCP-Cy5.5-A) was added as viability control, following manufacturer instructions. Data is shown as the difference between the geometric mean of the fluorescence intensity of unstained control samples (**Supplemental Figure 5**—Q1) compared to annexin V(PE) stained ones (**Supplemental Figure 5**—Q4). Viability was checked by 7AAD (PerCP-Cy5.5-A) parasites labeled (**Supplemental Figure 5**—Q2 and Q3). Data were collected in BD Fortessa and analyzed by FlowJo-X. At least 10,000 gated events were collected from each sample, in triplicates, from two essays. $^*p \leq 0.05$ Two-Way ANOVA.

Q4) and dead parasites labeled only with 7AAD (PerCP-Cy5.5) (**Supplemental Figure 5C**, Q2). Significant differences were observed in aPS exposure between R0 and R60, both at the 4th and 7th days of axenic growth (**Figures 6A,B**). Overall, lower aPS levels were presented by R60 than R0. This finding, in conjunction to the metabolomic data, may suggest that aPS are

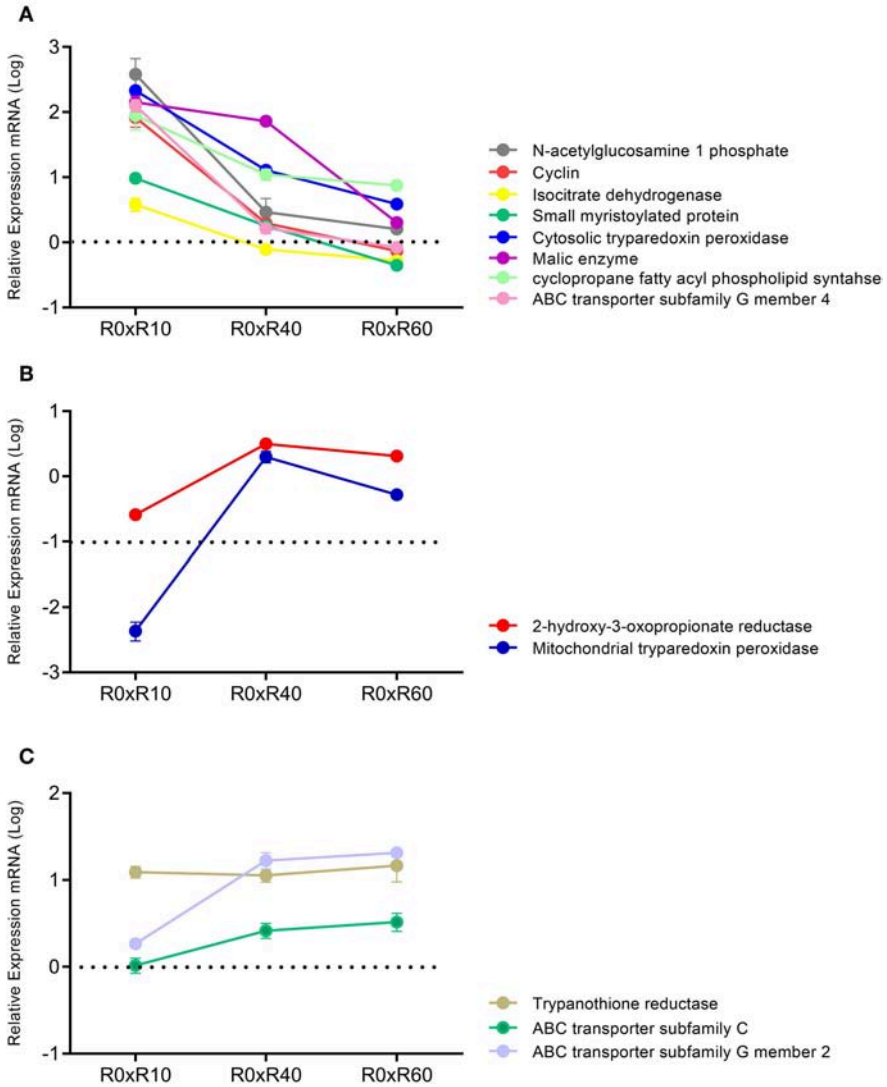

FIGURE 7 | qPCR analysis for expression of 13 genes related to the SIVP process. All measured loci were classified in three clusters, according to its expression. Data represent fold changes for R10, R40, R60, in relation to R0. **(A)** Cluster 1-N-acetylglucosamine 1 phosphate, Cyclin, Isocitrate dehydrogenase, Small myristoylated protein, Cytosolic tryparedoxin peroxidase, Malic enzyme, Cyclopropane fatty acyl phospholipid synthase, ABC transporter subfamily G member 4. **(B)** Cluster 2-2-hydroxy-3-oxopropionate reductase, Mitochondrial tryparedoxin peroxidase. **(C)** Cluster 3-Trypanothione reductase, ABC transporter subfamily C, ABC transporter subfamily G member 2. Samples were analyzed in duplicates, from three different experiments.

being accumulated in the promastigotes' cytoplasm and being less exposed at the cell surface.

qPCR Analysis of Selected Genes Involved in the Identified Pathways

Attempting to correlate the previous proteomic data of R0 and R30 (Magalhães et al., 2014) and the herein gathered metabolomic data, qPCR analyses of 13 selected genes linked to the proteins and metabolic pathways involved in attenuation after SIVP was carried out. Expression levels of GAPDH were used to normalize the expression levels of the selected loci. As shown in **Figure 7**, mRNAs expression profiles were classified in three clusters according to their expression pattern. The first cluster included the genes with increased gene expression in R10 related to R0 (N-acetylglucosamine 1-phosphate, cyclin, isocitrate dehydrogenase, small myristoylated protein, cytosolic tryparedoxin peroxidase, malic enzyme, cyclopropane fatty acyl phospholipid synthase and ABC transporter subfamily G member 4). However, their expression levels decreased progressively during further SIVP (R40 and R60) (**Figure 7A**). The second cluster, comprised by 2-hydroxy-3-oxopropionate reductase and mitochondrial tryparedoxin peroxidase, was characterized by decreased expression in R10 as compared to R0, and further increase, reaching levels similar to R0, in R40 and R60 (**Figure 7B**). The last cluster encompassed genes with increased expression during the entire SIVP process: ABC transporter subfamily G member

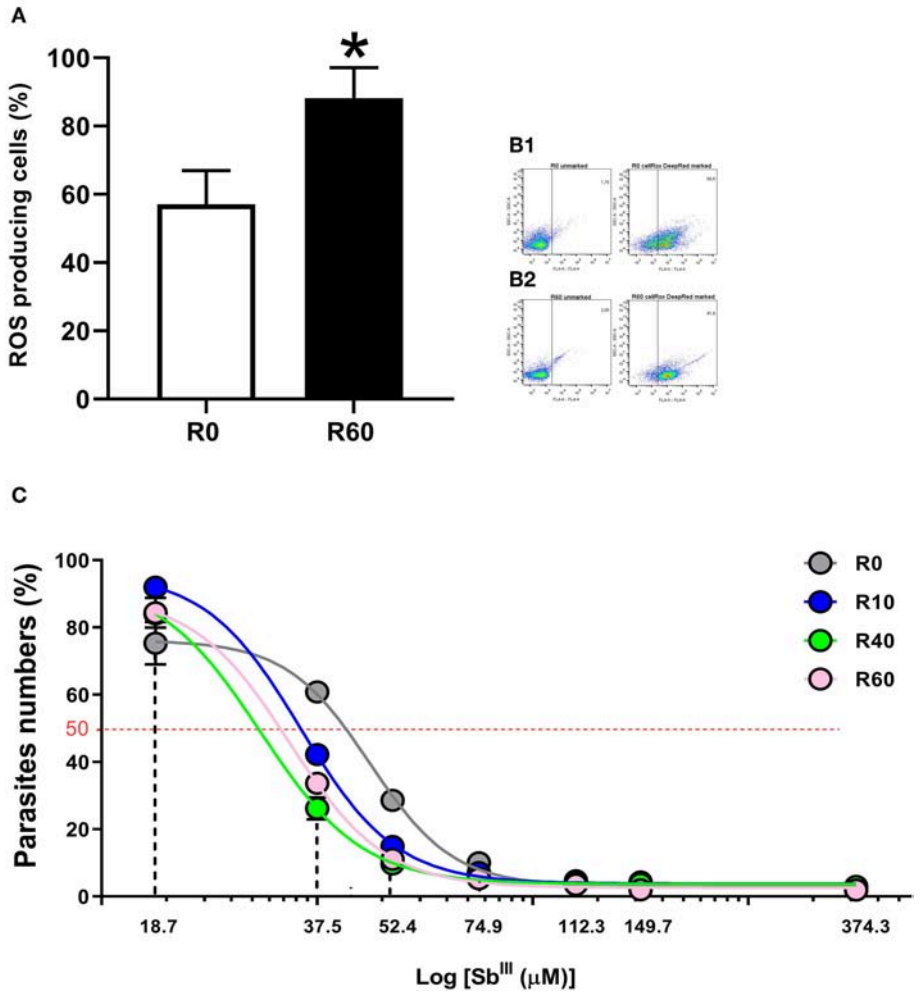

FIGURE 8 | Reactive oxygen species (ROS) measurement in *L. amazonensis* promastigotes after SIVP. R0 and R60 promastigotes were cultivated in M199 medium (10% BFS, 26°C). The level of ROS was assessed by CellROX Deep Red Reagent (Thermo Fisher Scientific). After treatment, R0 and R60 cultures at late log phase (4th day) were analyzed by flow cytometry (BD Fortessa). **(A)** Percentage of cells producing ROS from R0 and R60. **(B1,B2)** Gates used to determine the percentage of R0 and R60 ROS producing cells, respectively. The bars represent the average of tree assays minus or plus the standard deviation from two independent tests. **(C)** Cytotoxic effects of trivalent tartrate antimony (Sb^{III}) on *L. amazonensis* (R0, R10, R40, and R60) promastigotes at the 4th day of cultivation. Parasites were incubated in M199 medium at 2×10^6 cells/mL into 24-well plates (26°C), either in the absence or presence of several concentrations of Sb^{III} (18.71–374.32μM) for 48 h. The effective concentration required to decrease growth by 50% (EC_{50}) was determined using a Z1 Coulter Counter (Beckman Coulter, Fullerton, CA, USA). EC_{50} values were determined from at least three independent measurements performed in triplicate, using the linear interpolation method. Statistical analyses were performed using GraphPad Prism Software v6.0, San Diego, CA. The EC_{50} values were 47.09, 35.05, 29.52, 33.34 (μM; R0–R60, respectively; R2-values were >0.95 for all cell lines). *$p \leq 0.05$ by Two-Way ANOVA.

2, trypanothione reductase and ABC transporter subfamily C (**Figure 7C**).

SIVP Parasites Produced Increased Levels of ROS and Are More Sensitive to Antimony Tartrate

Energy metabolism, reactive oxygen species (ROS) production and cell detoxification pathways are tightly balanced. Shifts in this balance enable ROS to activate intracellular signaling and/or induce cellular damage and cell death (Liemburg-Apers et al., 2015). Since alterations in energetic metabolism and cell redox pathways were concomitantly by proteomics and metabolomics of SIVP parasites, we investigated if ROS levels were significantly altered in SIVP parasites, using a very specific reagent (CellRox deep red) that becomes oxidized and fluorescent when ROS is present. As shown in **Figure 8A**, R60 parasites displayed significantly increased levels of cell ROS, when compared to R0. **Figure 8B** show how gates were determined for this analysis.

Besides energy and glutathione metabolism, metabolomic, proteomic and qPCR data also pointed out significant alterations in the ABC transporters pathway. Since these pathways have been significantly associated to drug efflux and antimonial (Sb^{III})

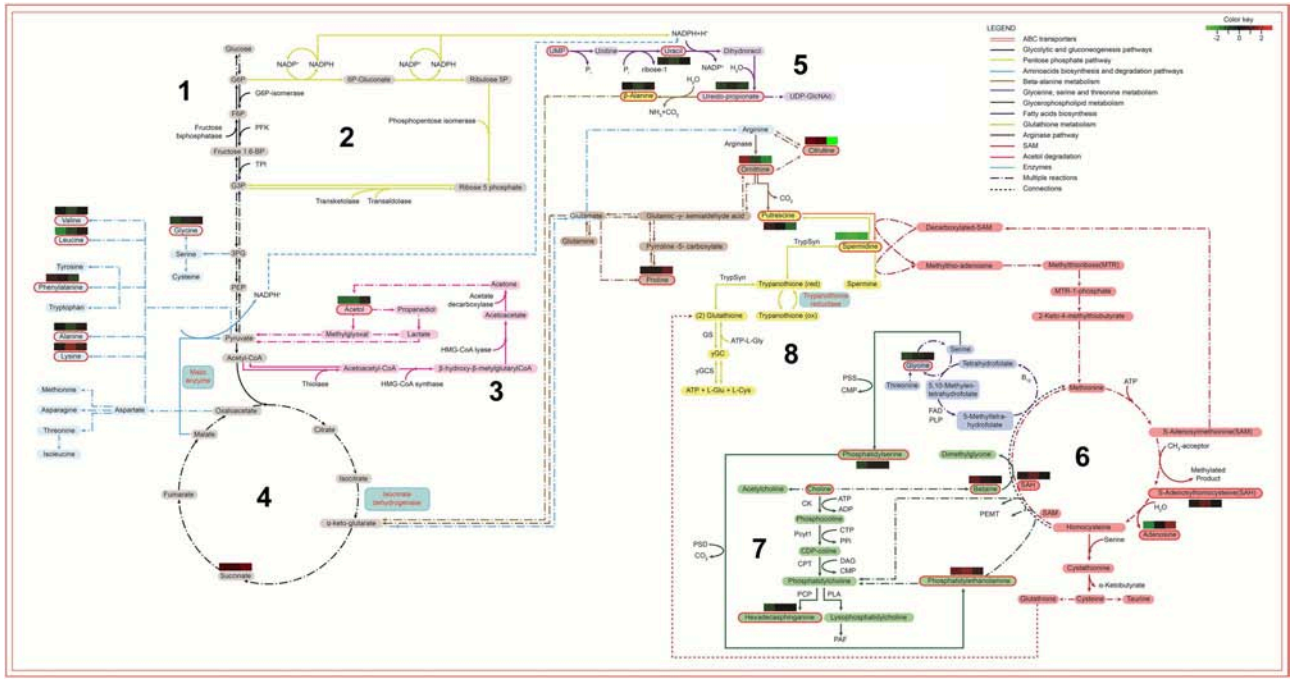

FIGURE 9 | Biochemical map of potential metabolic alterations occurred during axenization of *L. amazonensis*. Metabolites are represented by colored rectangles. Metabolites identified via metabolomic analysis are highlighted with a red contouring. The colored rectangles localized above/under metabolites represent the relative difference of abundance by comparing R10, R40, and R60 to R0 (left to right, respectively). Arrows represent reactions with enzymes, co-enzymes, metabolites or derivatives, indicated by their respective names or initials. Period-dash-period arrows indicate the occurrence of multiple reactions. Small dashes indicate interconnection of metabolic data between different metabolic pathways. The colors of arrows identify their respective pathways: 1. Black for energetic pathways (glycolytic and gluconeogenesis); 2. Yellow-green for pentose shunt (starting in G6P); 3. Light blue for amino acids biosynthesis; 4. Purple for fatty acids biosynthesis (receiving NADPH from pentose shunt and from malic enzyme reaction); 5. Light brown for β-alanine degradation (starting with ureidopropionate and culminating in α-keto-glutarate); 6. Dark brown for arginase and bright yellow for trypanothione (both pathways are connected in the production of putrescine); 7. Red for SAM or AdoMet pathway (interconnected to the Kennedy pathway, producer of phosphatidiletanolamine, phosphatidilcholine and phosphatidilserine); 8. Dark blue for glycine, serine and threonine biosynthesis. G6P, Glucose 6 phosphate; F6P, Fructose 6 phosphate; Fructose 1,6 bp, Fructose 6 bi-phosphate; PFK, phosphofructokinase; TPI, Triose phosphate isomerase; G3P, Glyceraldehyde 3-phosphate; 3PG, 3-phosphoglycerate; PEP, Phosphoenolpyruvate; UMP, Uridine monophosphate; UDP-GlcNac, Uridine diphosphate N- acetylglucosamine; HMG-CoA-Synthase, Hydroxymethylglutaryl-CoA synthase; NADPH, Nicotinamide adenine dinucleotide phosphate; ACP, Acyl carrier protein; TrypSyn, Trypanothione synthase; TrypRed, Trypanothione reductase; Gly, Glycine; Glu, Glutamine; ATP, Adenosine triphosphate; GS, Glutamine synthetase; SAH, S-adenosylhomocysteine; SAM, S-adennosylmethionine; PSS, phosphatidylserine synthase; PSD, Phosphatidylserine decarboxylase; CMP, Cytidine monophosphate; CK, Choline kinase; Pcyt1, Pyruvate carboxylase t1; CPT, Carnitine palmitoyltransferase; PLA, Phospholipase A; CTP, Phosphocholine cytidylyltransferase; ADP, Adenosine diphosphate; DAG, Diacylglycerol; PAF, Platelet-activating fator; PPi, Cytosolic pyrophosphate; PCP, Pyrrolidone carboxyl peptidase.

resistance in *Leishmania* (Wyllie et al., 2004; Leprohon et al., 2006), we hypothesized that these alterations in the cellular redox system and cell transport of the SIVP promastigotes may have affected their sensitivity to Sb^{III} tartrate. To test that, Sb^{III} tartrate EC_{50} was comparatively determined for all SIVP parasites. Sb^{III} tartrate ranged from 18.71 to 373.32 μM. As shown in **Figure 8C**, EC_{50} corresponded to 47.09, 35.05, 29.52, and 33.34 μM for R0, R10, R40, and R60, respectively. Therefore, SIVP promastigotes are significantly (all $R^2 > 0.95$) more sensitive to trivalent antimony when compared to R0, supporting our hypothesis.

Merging SIVP Metabolomics and Proteomics Data to Built a Biochemical Map

Finally, the metabolomic and the proteomic (Magalhães et al., 2014) data were merged into the enriched metabolomic pathways to build a comprehensive biochemical map, disclosing the metabolic alterations that occurred after long-term cultivation of *L. amazonensis* promastigotes. In this map (**Figure 9**), different colors and sequential numbers represent each pathway; metabolites are shown in colored blocks and proteins in blue squares. The identified metabolites were highlighted with red contouring and their fold changes represented by individual heatmaps (R0xR10, R0xR40, and R0xR60) either above or under their names. Proteomic data were represented by a blue square with blue contouring. The ABC transporter pathway was represented by a red double line square, contouring the whole map.

Considering that carbohydrate metabolism was retooled to supply demands from lipid metabolism, the glycolytic and gluconeogenic pathway (1) should be taken as a starting point on this map, followed by pentose phosphate pathway (2), acetol degradation (3) and tricarboxylic acid cycle (4). These pathways generate NADPH, which will be used for lipids biosynthesis (5) fatty acids biosynthesis; (6) SAM or AdoMet pathway, and (7) glycerophospholipids metabolism) and release a large amount of H^+ ions, culminating in a redox system overload (8) glutathione metabolism). Finally, the ABC transporters pathway were significantly altered and connected to metabolites of other pathways, since they are transmembrane proteins associated to lipid transport, glutathione metabolism and cell detoxification. The overloaded redox system and the lipid alterations make the parasite more vulnerable to ROS and less infective.

DISCUSSION

Maintenance of *Leishmania* promastigotes under long-term axenic cultivation may cause a wide variety of alterations that affect parasites virulence. This phenotypic variation is highly influenced by the parasites' species and original population, and the environmental conditions, including nutrient availability supplied by the culture medium and the number of passages in axenic culture. Such ability to adapt to environmental conditions and respond to selective pressures may be attributed to *Leishmania* genome plasticity, the clonal replicative structure of *Leishmania* populations, and the dynamic remodeling of its transcriptome and proteome, which will favor the maintenance of phenotypic diversity inside each population, for successful replication and perpetuation of the parasite genome (Rougeron et al., 2010; De Pablos et al., 2016; Laffitte et al., 2016; Espiau et al., 2017; Clayton, 2019). While cells are adapting to the new environment and gradually reaching homeostasis, significant fluctuations in protein and metabolites levels may also result from differences on the rates of differentiation from procyclic to metacyclics that takes place even in axenic conditions (Cysne-Finkelstein et al., 1998; Spath and Beverley, 2001; da Silva et al., 2015), as well as the occurrence of genomic alterations, such as single nucleotide polymorphisms and changes in gene copy numbers (Sinha et al., 2018). Although some pinpoint phenotypic alterations have been associated with attenuation after long-term axenic cultivation, several other concomitant metabolic alterations are likely to occur. In agreement, the previous comparative proteomic analysis of the SIVP promastigotes generated through long-term axenic cultures has revealed decreased virulence, which was validated herein, and several concomitant alterations in protein expression profile (Magalhães et al., 2014).

Changes in promastigotes' cell surface are determinants of host cells interactions, and are frequently associated to decreased promastigotes' infectivity. Metacyclogenesis affects mainly the *Leishmania spp* interactions with surface molecules on the vector's foregut, but also the parasite infectivity to the vertebrate host (da Silva and Sacks, 1987; McConville et al., 1992; Cysne-Finkelstein et al., 1998; Moreira et al., 2012), and correlates with modifications on phosphoglycan surface molecules, especially in LPG (Saraiva et al., 1995; Muskus and Marin Villa, 2002). Nevertheless, the lower infectivity of the *L. amazonensis* SIVP promastigotes could not be correlated to alterations in the percentage of metacyclics: both R0 and R60 displayed low numbers of metacyclics at the stationary growth phase. Therefore, other alterations rather than the metacyclogenesis seem to be important for *L. amazonensis* infectivity. In this sense, it has been shown that deficiency in LPG, as well as other PG containing molecules seems to be not sufficient to impair virulence in *L. mexicana* (Garami et al., 2001), a more closely phylogenetic related species to *L. amazonensis*.

Cellular immune responses are also key determinants in the course of *L. amazonensis* infection in mice. Besides the host inflammatory status, they may also reflect its ability to control parasite multiplication (McMahon-Pratt and Alexander, 2004; Soong et al., 2012; Carneiro et al., 2015; Maspi et al., 2016; Conceicao-Silva et al., 2018). IFN-γ is a biomarker of both inflammatory responses and activation of microbicidal mechanisms. It is important, through the induction of chemokine expression, for migration of CD^+ T cells and macrophages to lesion site and control of parasite replication (Carneiro et al., 2015). On the other hand, IL-10 is associated with macrophage deactivation and progressive infection (McMahon-Pratt and Alexander, 2004; Soong et al., 2012). Infection with R60 resulted in production of significant increased levels of IFN-γ, but similar levels of IL-10, which correlated with lower parasite burden and decreased lesion size, in comparison to R0. Therefore, the SIVP process induced metabolic changes in R60

that led to significant alterations in inflammatory responses upon infection in BALB/c mice, which correlated to improved control of parasite loads, at early stages of infection.

"Clustering in a heatmap the 66 compounds that were significantly altered in the SIVP metabolome", a very dymanic and continous adaptation process was disclosed. Altogether fatty acids, phospholipids, organic esthers, and lipids composed the major biochemical category of metabolites that changed during SIVP, suggesting that alterations in their metabolism were critical for the adaptation of *L. amazonensis* to long-term axenic conditions.

Among the identified fatty acids, linoleic acid, arachidic acid, 9-HODE, and palmitic acid showed a tendency of rising up, during SIVP, while stearic, and oleic acids decreased in R10 and R40, reaching similar levels in R60, as compared to R0. Fatty acids metabolism alters significantly the cell membrane fluidity and transport of substances and regulates neutrophil recruitment, host inflammatory responses, affecting several pathways related to trypanosomatid's virulence profile (Uttaro, 2014; Rodrigues et al., 2015). In agreement, these fatty acids seem to be quite important for amastigogenesis and their survival in the vertebrate host. Kloehn et al. (2015) have described that palmitic and stearic acid levels were similar in the host's serum and tissue amastigotes, but lower in cultivated promastigotes. In addition, oleic and linoleic acids were also significantly higher in promastigotes when compared to tissue amastigotes, while levels in amastigotes were higher compared to the host's plasma, and would be then predominantly synthesized by the parasite. Since mammalian hosts do not synthesize linoleic acid, amastigotes are dependent on the *de novo* synthesis of this compound (Kloehn et al., 2015). Therefore, increased levels of linoleic acid in promastigotes may be important for the early stages of amastigote differentiation and multiplication in the vertebrate host. Linoleic acid is produced from oleic acid by the action of desaturases, while oleic acid results from a desaturation of stearic acid, which ends from elongation of palmitic acid (Maldonado et al., 2006; Alloatti and Uttaro, 2011). Thus, the relative abundance of these fatty acids in the metabolomic analysis of SIVP promastigotes suggests that, while palmitic acid is constantly formed from the retooling of carbohydrates and protein metabolism, oleic and stearic acids are consumed to generate linoleic acid and its metabolites.

Arachidonic acid (AA) can modulate the expression of cyclooxygenase-2 (COX-2), a pivotal enzyme involved in skin inflammation and tissue reparation, which is responsible for the synthesis of prostaglandins (Chene et al., 2007). Various metabolites around AA metabolism were altered alongside the SIVP process, including, linoleic acid, a direct AA precursor and some AA derivates, such as 9-HODE and leukotriene B4. Previous studies have shown that AA induces parasites to release prostaglandins (Reiner and Malemud, 1985; Araujo-Santos et al., 2014), which affect the formation of lipid bodies. Increased levels of AA have been observed in lipid bodies of metacyclic forms and, during *L. chagasi* infection, the inhibition of prostaglandin receptor impairs parasite survival in macrophages (Araujo-Santos et al., 2014). Therefore, parasite-derived prostaglandins play a critical role in macrophage infection and are implicated in virulence. The fact that AA has not been found in the metabolomic fingerprint of SIVP promastigotes suggests a high consumption, given rise to the resultant metabolites of the lipoxygenase and prostaglandin synthase action, such as Leukotriene B4 (LTB4), or that its metabolism is significantly deviated to other pathways, such elongation of stearic acid and synthesis of 9-HODE. LTB4, which can be generated by the action of lipoxygenase on linoleic acid, is known as one of the most potent chemoattractant and activator of leukocytes involved in inflammatory diseases (Yokomizo et al., 2001). Moreover, macrophages from C3H/HePAS resistant mice produced higher levels of LTB4 upon *L. amazonensis* challenge than did those from susceptible BALB/c mice (Serezani et al., 2006). Treatment of human neutrophils with exogenous LTB4, prior to infection, significantly reduced the number of *L. amazonensis* viable parasites (Tavares et al., 2014), suggesting that, regardless of an endogenous or exogenous source, LTB4 might be required for protective responses against *L. amazonensis* infection. The 9 + 13 HODE byproducts of AA are also involved in inflammatory responses through regulation of cell adhesion molecules, neutrophil chemotaxis and degranulation, macrophage superoxide production, PPAR-γ activation, and inhibition of protein kinase C (Vangaveti et al., 2010; Rolin et al., 2014). Thus, 9 + 13 HODE may also assist in the control of neutrophil function, perhaps mitigating excessive neutrophil ROS, degranulation, and cell damage.

The ubiquitous ABC transporters protein family is composed by trans-membrane proteins, which are associated to lipid translocation across the membrane and are quite promiscuous regarding their lipid substrates. ABC transporters were already associated to increased intracellular levels of aPS, cholesterol, ergosterol, palmitic, myristic, linoleic acid, and arachidic acid, leukotriene B4, and other lipids, which were identified by the metabolomics of SIVP (Borst et al., 2000; van Meer et al., 2006; Zhang and Beverley, 2010). Interestingly, significant alterations in *L. donovani* ABC transporter genes have been seen by comparing the genome of early and late passages parasites, that have been associated to decreased virulence, including the presence of single nucleotide polymorphisms (Sinha et al., 2018). In *L. amazonensis*, a potential role of these proteins in cholesterol accumulation can be suggested, since this species lacks a *de novo* mechanism for cholesterol synthesis and, therefore, must scavenge this lipid from the host environment. In order to compensate for the lack of cholesterol synthesis, a lipid importing machinery would be required (De Cicco et al., 2012).

Phosphatidylserine, phenylethanolamine, lyso-phosphatidyletanolamine and phosphatidylinositol, as well as changes at hexadecasphinganine and O-phosphocholine were also detected in the long-term cultivation parasites. These metabolites are destined to the cell membrane and, therefore, also require transportation to their final location (Woehlecke et al., 2003; Wanderley et al., 2006; De Cicco et al., 2012; Campos-Salinas et al., 2013), which can be performed by members of the ABC transporters family. Since the enrichment analysis of metabolomic data revealed statistical significance for the ABC transporter pathway, we performed a qPCR analysis of some ABC transporters genes described in *L. amazonensis*. As expected, the SIVP promastigotes showed significant increase

in transcripts for ABC-C, ABC-G2 and ABC-G4 transporters. Recently, the ABC-G2 gene was shown to affect PS exposure and the ABC-G2 *L. major* knockout parasites displaying low PS exposure, are less virulent (Campos-Salinas et al., 2013). On the other hand, we have shown that ABC-G2 expression was increased during SIVP, while parasites accumulate aPS in the cell cytoplasm and expose less in the cell membrane, according to the FACS analysis. This apparent contrast with the previous effect reported for *Leishmania* ABC-G2 may be possibly explained by a competition for the ABC-G2 transporters among PS, other phospholipids, lipids, fatty acids and thiols, which are all increased in *L. amazonensis* SIVP parasites, as previously mentioned. The occurrence of point mutations or pseudogenes in ABC transporter genes, affecting their functionality, cannot be discarded as well, as this alterations have been previously reported in parasites submitted to SIVP (Sinha et al., 2018). Nonetheless the origin of these alterations, the transient non-exposure of aPS may have influenced the SIVP parasite's survival inside the macrophage, and thus, their attenuated profile, since PS exposure has been associated to increased virulence in *Leishmania* (Wanderley et al., 2006; Franca-Costa et al., 2012; Rochael et al., 2013).

In addition to ABC transporters, significant modulation on the expression of proteins related to membrane vesicular trafficking and remodeling, such as small GTP-binding protein Rab1, protein transport Sec13, actin and tubulin as well as of membrane-associated proteins, including the small myristoylated protein 3, enolase, and glucose regulated protein of 78 kDa were associated to SIVP, as disclosed by proteomics (Magalhães et al., 2014). The metabolite UDPG is essential for the N-glycosylation of membrane proteins and is linked to the metabolic pathway that includes UMP (uridine monophosphate), glycerol- 1 phosphate (Glc-1-P), ureidopropionate (Silva Pereira and Jackson, 2018); displaying decreased abundance in R60. In agreement, the expression of UDP-Glucose pyrophosphorilase, an enzyme that produces UDPG (Uridine Diphosphate-Glucose) and pyrophosphate (PPi), from Glc-1-P and UTP was also altered in SIVP proteomics (Magalhães et al., 2014). Myristoylation of proteins involves the addition of a myristoyl group, derived from myristic acid, and allows for weak protein–protein and protein–lipid interactions and, thus, links protein and lipids metabolism. Protein N-linked glycosylation is also an important mechanism for folding and/or oligomerization, and consequently to the correct trafficking and cellular addressing of proteins. Inhibition of myristoylation has been shown to have pleiotropic effects in *Leishmania* (Wright et al., 2015). Small myristoylated proteins localize in the inner leaflet of the *Leishmania* flagellar membrane and are associated with vesicular trafficking, stabilization of the flagellar membrane sterol- and sphingolipds reach domains (Tull et al., 2010; Wright et al., 2015). These functions are, therefore, consistent with the alterations in transcripts levels of the small myristoyled protein gene, as well as in the proteome (Magalhães et al., 2014) and metabolome of the SVIP promastigotes, especially during the first 10 SIVP.

Fatty acid metabolism is significantly affected during *Leishmania* lifecycle (Bouazizi-Ben Messaoud et al., 2017), reflecting the availability of nutrients and precursors that parasites found in a given environmental and the ability of the parasite to synthesize, metabolize or use them to compose membrane structures. Amastigotes obtain fatty acids from complex host lipids and use them as an alternative carbon source, but the lack of glyoxylate cycle enzymes needed to use acetyl-CoA in gluconeogenesis, suggests that *Leishmania* is unable to use fatty acids as the sole carbon source. While non-dividing promastigotes also use fatty acid β-oxidation as a secondary carbon source, this process occurs to a negligible extent in actively dividing promastigotes (McConville and Naderer, 2011). Accordingly, parasites recently recovered from the restricted nutritional microenvironment of host cells, are still metabolically adapted for the intracellular lifestyle, characterized by reduced metabolic activity (Burchmore and Barrett, 2001; Alcolea et al., 2010; Jara et al., 2017), decreased glucose utilization and increased fatty acid β-oxidation (Saunders et al., 2014). In contrast, in axenic culture, a less hostile environment than the parasitophorous vacuole and plentiful in nutrients, promastigotes channeled cell metabolism to anabolic reactions to support replication. The central metabolic hub of this adaptive metabolic process during SIVP seems to be the fatty acids biosynthesis, which requires adequate concentration of NADPH and acetyl-CoA. NADPH is generated in the pentose phosphate pathway (PPP), by the malic enzyme, which oxidizes malate into pyruvate and CO_2. Consistently, significant alterations in succinate, glycerol 1-phosphate and acetol were detected in the SIVP metabolomics. Similarly, cancer cells overexpress the malic enzyme to keep with the high demand of fatty acids (Sarfraz et al., 2018). Isocitrate dehydrogenase is another important enzyme that enables aerobic cells to fulfill their requirement for NADPH (Sarfraz et al., 2018). Likewise, changes in the levels of malic enzyme, isocitrate dehydrogenase and 2-hydroxy-3-oxopropionate reductase (another enzyme involved in the production of NADPH) that have been reported in promastigotes of *L. infantum* (Louassini et al., 1999) were also observed in the proteomic analysis of *L. amazonensis* promastigotes after 30 SIVP (Magalhães et al., 2014) and in the qPCR analysis of their transcripts in R0, R10, R40, and R60.

The increased intracellular levels of fatty acids observed in the metabolomic analyses may also reflect this metabolic retooling, which activates PPP to supply the cell with NADPH and nitrogenous bases for DNA and RNA synthesis, in order to support growth rates of SIVP promastigotes. To confirm this hypothesis, the mRNA levels of cyclin, a protein involved with cell cycle progression (Ali et al., 2010) and previously shown increased in the proteomics of SIVP promastigotes, was also measured by qPCR. As expected, cyclin expression increased significantly in R10 when compared to R0, reaching afterwards, in R40 and R60, similar levels to R0.

The shift to anabolic reactions requires intracellular reducing power of NADPH and a high activity of the parasite's redox system (Ilari et al., 2017). In agreement, the metabolome disclosed changes on the levels of proline, ornithine, citruline, spermidine, and putrescine, which are linked to parasite's redox system. Interestingly, pipecolate,

another metabolite related to proline-ornithine metabolism, but not previously reported in *Leishmania*, has been involved in protection of mammalian cells against oxidative stress, also increased during SIVP. The involvement of this pathway was corroborated by increased mRNA levels of trypanothione reductase and mitochondrial tryparedoxin peroxidase, as detected by qPCR in long-term cultivated parasites and in proteomics (Magalhães et al., 2014), inferring an overload of the glutathione pathway. S-adenosylhomocysteine was found increased in our analysis and could be linked to both glutathione and glycerophospholipid metabolisms (Kennedy pathway) (Pessi et al., 2005). In accordance to our main hypothesis, spermidine was synthesized from the pool of putrescine, while phosphatidylethanolamine originated from the glycerophospholipid metabolism. Therefore, it is possible that the SAM pathway had changed, leading to the increased levels of S-adenosylhomocysteine and betaine, observed during SIVP. Consistently, regulation of S-adenosylmethionine synthetase was associated to SIVP (Magalhães et al., 2014), further supporting this hypothesis.

Besides its significant role to control the parasite's intracellular redox state, trypanothione reductase is important in drug resistance in *Leishmania* and is inhibited by Sb^{III} in a NADPH-dependent reaction (Cunningham and Fairlamb, 1995; Baiocco et al., 2009; Cole, 2014). Moreover, ABC transporters are also involved in efflux of thiol and GSH-conjugated compounds, or may in same cases be stimulated by GSH (Leprohon et al., 2006). Accordingly, various ABC transporters subfamilies have been identified in *Leishmania*, which are responsible for the cellular transport of several compounds and have been connected with resistance to drugs, including antimonial compounds (Leprohon et al., 2006; Sauvage et al., 2009). Thus, it is plausible that long-term cultivated parasites may be more sensitive to drugs targeting trypanothione reductase and produce more reactive oxygen species (ROS). We hypothesized that fatty acid metabolism alterations induced glutathione system disequilibrium, with increased production of ROS that compromised the detox process and turned the parasites more sensitive to antimonials. In agreement, when we used Sb^{III} to disturb the redox system, SIVP parasites were more sensitive when compared to R0, again suggesting that the redox system was activated to counter balanced the oxidative state caused by anabolic reactions. Interestingly, the R60 parasites produced significantly higher levels of ROS than the R0 reference parasites, explaining, at least in part, the increased sensibility of R60 parasites to antimony. These results are also in agreement with significant alterations in glutathione metabolism and ABC transporters pathways, as indicated by qPCR results.

The SIVP process was accompanied by significant fluctuations in levels of the identified metabolites, indicating that *Leishmania* adaptation to a new environmental condition is a very dynamic process. As previously pointed out, successive changes in predominance of clones with different proliferative capacity and metabolic fitness may globally interfere with metabolite's levels. In addition, significant heterogeneity may result from developmental differentiation from procyclic to metacyclics and from genome alterations that takes place even in axenic conditions (Sinha et al., 2018). In agreement, late passages *L. donovani* parasites have significant higher numbers of pseudogenes, single nucleotide polymorphisms and alterations in gene copy number, as compared to early passages parasites, which directly impact in RNA and protein levels and activity (Sinha et al., 2018). Moreover, at each metabolomic measure, the individual metabolites levels may reflect reduced or increased production, consumption or their absorption from environment or host. For instance, it has been shown that, when the uptake rates were corrected for diffusion, the purine bases adenine and hypoxanthine were transported at a significantly slower rate than the purine nucleosides adenosine and inosine. In addition, adenine and hypoxanthine inhibited the uptake of one another competitively (Hansen et al., 1982). Considering these metabolites, it is also known that kinetoplastid protozoa are auxotrophs for purine bases, since *de novo* biosynthetic pathway is completely absent (Ullman and Carter, 1997). They are therefore dependent on recycling pre-formed purine nucleotides and acquiring purines from the host/environment. The salvage pathway recovers purines (adenine and guanine) from the degradation products of nucleotide metabolism and from hypoxanthine and xanthine. Then, we may hypothesize that levels of components of the nucleotide metabolism may decrease from R0 and R10, while cells are adapting from a quiescent condition (amastigotes in tissues), with low intracellular stocks, when DNA replication and energy metabolism is down-regulated to a highly replicative condition in an environment plenty of nutrients. Later, when cells are tending to achieve homeostasis, levels may increase, as gradually seen in R40 and R60. In agreement, proteome comparisons between purine-starved and purine-replete parasites have revealed a temporal and coordinated response to purine starvation (Martin et al., 2014). Purine transporters and enzymes involved in acquisition at the cell surface are up regulated within a few hours of purine removal from the media, while other key purine salvage components are up regulated later in the time-course and more modestly. Interestingly, significant fluctuations in protein expression could also be seen even in a short period of time (48 h), in deprived cells, unveiling extensive reprogramming of the parasite proteome and metabolome to adapt to the stress condition (Martin et al., 2014).

Some of the identified compounds were not or are rarely described in *Leishmania,* including the 2,6-diaminopimelic acid, a carbohydrate found in bacteria cell wall. According to Opperdoes et al. (2016), among trypanosomatids, *Leptomonas* and *Crithidia,* members of the Leishmaniinae subfamily, have acquired the capacity to convert this compound to lysine. Therefore, it is conceivable that *Leishmania* may also be able to metabolize this compound. Another compound is 2,6-farnesol, an isoprenoid resulting from mevalonic acid pathway, linked to the synthesis of sterols and dolichol. According to these same authors, enzymes synthesizing this long chain isoprenoids have been scarcely studied in trypanosomatids. The findings of these rarely seen compounds support the potential of our

fingerprinting metabolomics approach for better uncover of *Leishmania* metabolism.

It is noteworthy that plausible connections could be established among our findings and the previous preoteomic profile reported for the SIVP process (Magalhães et al., 2014). Therefore, we have merged proteome and metabolome data sets for a holistic view of metabolic pathways changed during SIVP process. Consistent with the predominance of lipids identified by metabolomics, the biochemical model led to a central hypothesis based on the adaptation to a nutrient rich environment. Promastigote's metabolism of carbohydrates (glicolitic and gluconeogenesis, pentose-phosphate pathway, acetol degradation), amino acid (amino acid biosynthesis and degradation, β-alanine, glycine and serine and arginase metabolisms) and purine, pyrimidine metabolism were retooled to supply the demands from increases in energy-intensive processes such as genome replication and protein synthesis and lipid metabolism (glycerophospholipids, fatty-acids biosynthesis), altering the cellular oxidative state. As a consequence, the redox homeostasis processes (SAM and glutathione metabolisms) changed to control the intracellular oxidative stress, resultant from the intense anabolic metabolism. A concerted alteration in expression of proteins associated with intracellular and membrane traffic of lipids, such as ABC transporters, led probably to significant remodeling of membrane lipid composition. This promastigotes' cell membrane remodeling and the lipid mediators may have, finally, affected significantly the parasite induced host inflammatory responses and the control of parasite replication, during early stages of infection.

In summary, our biochemical model point out to a very dynamic and continuous metabolic reprogramming process and the high capacity of *L. amazonensis* to adapt to the nutritional availability, modulating its metabolism and phenotype. This process was accompanied by changes in membrane remodeling, which, in turn, shaped parasite-host cells interactions to an attenuated profile. The clonal propagation structure, the plasticity in genome and gene expression are key elements to maintain heterogeneity inside each population, as well as to understand the alterations seen in metabolites' levels during the SIVP process. Although changes were detected in various metabolic pathways, most of them seemed to be metabolic adaptations to central alterations in the fatty acid and carbon metabolism, which acts as a metabolic hub, driving NADPH production. Anabolic reactions generate an oxidized intracellular state that is counterbalanced by the reducing power of NADPH and the parasite's redox system. Alterations in fatty acid composition secondarily affected parasite virulence due to membrane remodeling with an overall impact in chemotaxis and host inflammatory responses, at the early stages of *L. amazonensis* infection.

DATA AVAILABILITY STATEMENT

The raw data supporting the conclusions of this manuscript will be made available by the authors, without undue reservation, to any qualified researcher.

ETHICS STATEMENT

Experiments were performed in compliance with the National Guidelines of the Institutional Animal Care and Use Committee for the Ethical Handling of Research Animals (CEUA) from the Federal University of Minas Gerais (UFMG) (Law number 11.794, 2008), which approved under protocol CETEA number 240/2016.

AUTHOR CONTRIBUTIONS

FC, JT, AF, GM, and CB conceived and designed the experiments. FC, JT, AS, AC, LF, SM, AA, LO, DM, AD, and TR performed the experiments. ÁL-G, FC, SM, JT, CB, GM, and AF analyzed the data. JT, FC, ÁL-G, DB, and AF wrote the paper.

FUNDING

This work was supported by the Instituto Nacional de Ciência e Tecnologia em Vacinas (INCTv)/CNPq (Grant Nos. 573547/2008-4 and 465293/2014-0); Rede Mineira de Biomoléculas (FAPEMIG Grant No. red001214), Conselho Nacional de Desenvolvimento Científico e Tecnológico (CNPq); Fundação de Amparo à Pesquisa do Estado de Minas Gerais (FAPEMIG); Coordenação de Aperfeiçoamento de Pessoal de Nível Superior (CAPES), EADS-CASA and the Brazilian Air Force (FAB) mobility program.

ACKNOWLEDGMENTS

We thank Dr. Maria José Paiva for reviewing and discussing metabolomic data.

SUPPLEMENTARY MATERIAL

The Supplementary Material for this article can be found online at: https://www.frontiersin.org/articles/10.3389/fcimb.2019.00403/full#supplementary-material

Supplemental Figure 1 | Growth curves for R0, R10, R40, and R60 promastigotes, cultivated in medium M199 pH7.4, 26°C. Results correspond to average and SD of three different countings; two different experiments were performed.

Supplemental Figure 2 | Promastigotes from R0 and R60 were cultivated in M199 medium supplemented with 10% BFS, at 26°C, collected at 4th and 7th days of growth, separated by ficoll gradient and submitted to flow citometrry (BD, LSRFortessa cell analyser) to determine the gates for procyclic **(A)** and metacyclic **(B)** populations. To differentiate these populations, a merged graph **(C)** was constructed, showing the procyclic population in blue (circle) and the metacyclic population in red (square).

Supplemental Figure 3 | Scores plot for PCA-X. Models built with the filtered data set for each analytical technique obtained from R0, R10, R40, and R60 extract samples, provided by SINCA p+ statistical software demonstrating evident QC overlap (black) and good separation among the groups in unsupervised analysis. The predictive coefficients values demonstrated a strong statistical trend regardless the analytical techniques, in CE-MS [$R^2 = 0.904$, $Q^2 = 0.641$], GC-MS

[$R^2 = 0.715$, $Q^2 = 0.42$] and LC-MS [$R^2 = 0.314$, $Q^2 = 0.152$, in negative mode and $R^2 = 0.773$, $Q^2 = 0.193$ in positive mode].

Supplemental Figure 4 | Scores plot for PLS-DA. Models built with the filtered data set for each analytical technique obtained from R0, R10, R40, and R60 extract samples, provided by SINCA p+ statistical software demonstrating evident separation among the groups in supervised analysis, except for the LC-MS positive mode. The predictive coefficients values demonstrated a strong statistical trend regardless the analytical techniques, for CE-MS [$R^2 = 0.983$, $Q^2 = 0.947$], GC-MS [$R^2 = 0.594$, $Q^2 = 0.342$] and LC-MS [$R^2 = 0.582$, $Q^2 = 0.262$ in positive, and $R^2 = 0.744$, $Q^2 = 0.201$, in negative mode].

Supplemental Figure 5 | Determination of gates for aPS exposure. **(A)** Unlabeled parasites. **(B)** Parasites marked only with PE annexinV (aPS exposure). **(C)** Parasites marked only with 7-AAD (unviable parasites).

Supplemental Table 1 | Primers for RT-PCR of selected loci.

Supplemental Table 2 | List of all metabolites identified by the metabolomic multiplatform fingerprint approach. Confirmed indicates that the compound was putative or truly identified; Feature correspond to a peak or signal that represents a potential metabolite, which should be further identified, according to mass, charge and retention time. M/Z: molecular ion described by its molecular weight in Daltons; RT: retention time for each feature; AVG represent the average of the relative ion abundance present in each investigated group and each metabolite; pV: calculated *p*-value; Compound ID: compound's identification number in its respective database; Mass Theor: theoretical molecular mass; MH formula: theoretical formula; Score: probability of matched score from each identified metabolite; Ppm error: ppm error between the compound molecular weight and the found compound molecular weight.

REFERENCES

Alcolea, P. J., Alonso, A., Gomez, M. J., Moreno, I., Dominguez, M., Parro, V., et al. (2010). Transcriptomics throughout the life cycle of *Leishmania infantum*: high down-regulation rate in the amastigote stage. *Int. J Parasitol.* 40, 1497–1516. doi: 10.1016/j.ijpara.2010.05.013

Ali, N. O., Ibrahim, M. E., Grant, K. M., and Mottram, J. C. (2010). Molecular cloning, characterization and overexpression of a novel cyclin from *Leishmania mexicana*. *Pak. J. Biol. Sci.* 13, 775–784. doi: 10.3923/pjbs.2010.775.784

Alloatti, A., and Uttaro, A. D. (2011). Highly specific methyl-end fatty-acid desaturases of trypanosomatids. *Mol. Biochem. Parasitol.* 175, 126–132. doi: 10.1016/j.molbiopara.2010.10.006

Alvar, J., Velez, I. D., Bern, C., Herrero, M., Desjeux, P., Cano, J., et al. (2012). Leishmaniasis worldwide and global estimates of its incidence. *PloS ONE* 7:e35671. doi: 10.1371/journal.pone.0035671

Araujo-Santos, T., Rodriguez, N. E., Moura-Pontes, S., Dixt, U. G., Abanades, D. R., Bozza, P. T., et al. (2014). Role of prostaglandin F2alpha production in lipid bodies from *Leishmania infantum* chagasi: insights on virulence. *J. Infect. Dis.* 210, 1951–1961. doi: 10.1093/infdis/jiu299

Baiocco, P., Colotti, G., Franceschini, S., and Ilari, A. (2009). Molecular basis of antimony treatment in leishmaniasis. *J. Med. Chem.* 52, 2603–2612. doi: 10.1021/jm900185q

Barral, A., Pedral-Sampaio, D., Grimaldi Junior, G., Momen, H., D., McMahon-Pratt, A., et al. (1991). Leishmaniasis in Bahia, Brazil: evidence that *Leishmania amazonensis* produces a wide spectrum of clinical disease. *Am. J. Trop. Med. Hyg.* 44, 536–546. doi: 10.4269/ajtmh.1991.44.536

Bates, P. A., and Rogers, M. E. (2004). New insights into the developmental biology and transmission mechanisms of *Leishmania*. *Curr. Mol. Med.* 4, 601–609. doi: 10.2174/1566524043360285

Boltz-Nitulescu, G., Wiltschke, C., Holzinger, C., Fellinger, A., Scheiner, O., Gessl, A., et al. (1987). Differentiation of rat bone marrow cells into macrophages under the influence of mouse L929 cell supernatant. *J. Leukoc. Biol.* 41, 83–91. doi: 10.1002/jlb.41.1.83

Borst, P., Zelcer, N., and van Helvoort, A. (2000). ABC transporters in lipid transport. *Biochim. Biophys. Acta* 1486, 128–144. doi: 10.1016/S1388-1981(00)00053-6

Bouazizi-Ben Messaoud, H., Guichard, M., Lawton, P., Delton, I., and Azzouz-Maache, S. (2017). Changes in lipid and fatty acid composition during intramacrophagic transformation of *Leishmania donovani* complex promastigotes into amastigotes. *Lipids* 52, 433–441. doi: 10.1007/s11745-017-4233-6

Bradford, M. M. (1976). A rapid and sensitive method for the quantitation of microgram quantities of protein utilizing the principle of protein-dye binding. *Anal. Biochem.* 72, 248–254. doi: 10.1016/0003-2697(76)90527-3

Bujak, R., Garcia-Alvarez, A., Ruperez, F. J., Nuno-Ayala, M., Garcia, A., Ruiz-Cabello, J., et al. (2014). Metabolomics reveals metabolite changes in acute pulmonary embolism. *J. Proteome Res.* 13, 805–816. doi: 10.1021/pr400872j

Burchmore, R. J., and Barrett, M. P. (2001). Life in vacuoles–nutrient acquisition by Leishmania amastigotes. *Int. J. Parasitol.* 31, 1311–1320. doi: 10.1016/S0020-7519(01)00259-4

Campos-Salinas, J., Leon-Guerrero, D., Gonzalez-Rey, E., Delgado, M., Castanys, S., Perez-Victoria, J. M., et al. (2013). LABCG2, a new ABC transporter implicated in phosphatidylserine exposure, is involved in the infectivity and pathogenicity of *Leishmania*. *PLoS Negl. Trop. Dis.* 7:e2179. doi: 10.1371/annotation/6a3b1d53-4e80-45a9-8fab-f3fb56a134de

Canuto, G. A., Castilho-Martins, E. A., Tavares, M. F., Rivas, L., Barbas, C., and Lopez-Gonzalvez, A. (2014). Multi-analytical platform metabolomic approach to study miltefosine mechanism of action and resistance in *Leishmania*. *Anal. Bioanal. Chem.* 406, 3459–3476. doi: 10.1007/s00216-014-7772-1

Carlsen, E. D., Hay, C., Henard, C. A., Popov, V., Garg, N. J., and Soong, L. (2013). *Leishmania amazonensis* amastigotes trigger neutrophil activation but resist neutrophil microbicidal mechanisms. *Infect. Immun.* 81, 3966–3974. doi: 10.1128/IAI.00770-13

Carneiro, M. B., Lopes, M. E., Vaz, L. G., Sousa, L. M., dos Santos, L. M., de Souza, C. C., et al. (2015). IFN-gamma-dependent recruitment of CD4(+) T cells and macrophages contributes to pathogenesis during *Leishmania amazonensis* infection. *J. Interferon Cytokine Res.* 35, 935–947. doi: 10.1089/jir.2015.0043

Chene, G., Dubourdeau, M., Balard, P., Escoubet-Lozach, L., Orfila, C., Berry, A., et al. (2007). n-3 and n-6 polyunsaturated fatty acids induce the expression of COX-2 via PPARgamma activation in human keratinocyte HaCaT cells. *Biochim. Biophys. Acta* 1771, 576–589. doi: 10.1016/j.bbalip.2007.02.014

Clayton, C. (2019). Regulation of gene expression in trypanosomatids: living with polycistronic transcription. *Open Biol.* 9:190072. doi: 10.1098/rsob.190072

Coelho, E. A., Tavares, C. A., Carvalho, F. A., Chaves, K. F., Teixeira, K. N., Rodrigues, R. C., et al. (2003). Immune responses induced by the Leishmania (Leishmania) donovani A2 antigen, but not by the LACK antigen, are protective against experimental Leishmania (Leishmania) amazonensis infection. *Infect. Immun.* 71, 3988–3994. doi: 10.1128/IAI.71.7.3988-3994.2003

Coelho, V. T., Oliveira, J. S., Valadares, D. G., Chavez-Fumagalli, M. A., Duarte, M. C., Lage, P. S., et al. (2012). Identification of proteins in promastigote and amastigote-like *Leishmania* using an immunoproteomic approach. *PLoS Negl. Trop. Dis.* 6:e1430. doi: 10.1371/journal.pntd.0001430

Cole, S. P. (2014). Multidrug resistance protein 1 (MRP1, ABCC1), a "multitasking" ATP-binding cassette (ABC) transporter. *J. Biol. Chem.* 289, 30880–30888. doi: 10.1074/jbc.R114.609248

Conceicao-Silva, F., Leite-Silva, J., and Morgado, F. N. (2018). The binomial parasite-host immunity in the healing process and in reactivation of human tegumentary Leishmaniasis. *Front. Microbiol.* 9:1308. doi: 10.3389/fmicb.2018.01308

Courtenay, O., Peters, N. C., Rogers, M. E., and Bern, C. (2017). Combining epidemiology with basic biology of sand flies, parasites, and hosts to inform leishmaniasis transmission dynamics and control. *PLoS Pathog.* 13:e1006571. doi: 10.1371/journal.ppat.1006571

Cunningham, M. L., and Fairlamb, A. H. (1995). Trypanothione reductase from *Leishmania donovani*. Purification, characterisation and inhibition by trivalent antimonials. *Eur. J. Biochem.* 230, 460–468. doi: 10.1111/j.1432-1033.1995.0460h.x

Cysne-Finkelstein, L., Temporal, R. M., Alves, F. A., and Leon, L. L. (1998). *Leishmania amazonensis*: long-term cultivation of axenic amastigotes is associated to metacyclogenesis of promastigotes. *Exp. Parasitol.* 89, 58–62. doi: 10.1006/expr.1998.4276

da Silva, I. A. Jr., Morato, C. I., Quixabeira, V. B., Pereira, L. I., Dorta, M. L., de Oliveira, M. A., et al. (2015). *In vitro* metacyclogenesis of Leishmania (Viannia) braziliensis and Leishmania (Leishmania) amazonensis clinical field isolates, as evaluated by morphology, complement resistance, and infectivity to human macrophages. *BioMed Res. Int.* 2015:393049. doi: 10.1155/2015/393049

da Silva, R., and Sacks, D. L. (1987). Metacyclogenesis is a major determinant of *Leishmania* promastigote virulence and attenuation. *Infect. Immun.* 55, 2802–2806.

De Cicco, N. N., Pereira, M. G., Correa, J. R., Andrade-Neto, V. V., Saraiva, F. B., Chagas-Lima, A. C., et al. (2012). LDL uptake by *Leishmania amazonensis*: involvement of membrane lipid microdomains. *Exp. Parasitol.* 130, 330–340. doi: 10.1016/j.exppara.2012.02.014

De Pablos, L. M., Ferreira, T. R., and Walrad, P. B. (2016). Developmental differentiation in *Leishmania* lifecycle progression: post-transcriptional control conducts the orchestra. *Curr. Opin. Microbiol.* 34, 82–89. doi: 10.1016/j.mib.2016.08.004

de Souza, M. C., de Assis, E. A., Gomes, R. S., A., Marques da Silva Ede, Melo, M. N., Fietto, J. L., et al. (2010). The influence of ecto-nucleotidases on *Leishmania amazonensis* infection and immune response in C57B/6 mice. *Acta Tropica*. 115, 262–269. doi: 10.1016/j.actatropica.2010.04.007

Espiau, B., Vilhena, V., Cuvillier, A., Barral, A., and Merlin, G. (2017). Phenotypic diversity and selection maintain *Leishmania amazonensis* infectivity in BALB/c mouse model. *Mem. Inst. Oswaldo Cruz* 112, 44–52. doi: 10.1590/0074-02760160280

Franca-Costa, J., Wanderley, J. L., Deolindo, P., Zarattini, J. B., Costa, J., Soong, L., et al. (2012). Exposure of phosphatidylserine on *Leishmania amazonensis* isolates is associated with diffuse cutaneous leishmaniasis and parasite infectivity. *PLoS ONE* 7:e36595. doi: 10.1371/journal.pone.0036595

Garami, A., Mehlert, A., and Ilg, T. (2001). Glycosylation defects and virulence phenotypes of *Leishmania mexicana* phosphomannomutase and dolicholphosphate-mannose synthase gene deletion mutants. *Mol. Cell. Biol.* 21, 8168–8183. doi: 10.1128/MCB.21.23.8168-8183.2001

Gomes, C. B., Silva, F. S., Charret, K. D., Pereira, B. A., Finkelstein, L. C., R., et al. (2017). Increasing in cysteine proteinase B expression and enzymatic activity during *in vitro* differentiation of Leishmania (Viannia) braziliensis: First evidence of modulation during morphological transition. *Biochimie* 133, 28–36. doi: 10.1016/j.biochi.2016.11.015

Goto, H., and Lindoso, J. A. (2010). Current diagnosis and treatment of cutaneous and mucocutaneous leishmaniasis. *Exp. Rev. Anti Infect. Ther.* 8, 419–433. doi: 10.1586/eri.10.19

Hansen, B. D., Perez-Arbelo, J., Walkony, J. F., and Hendricks, L. D. (1982). The specificity of purine base and nucleoside uptake in promastigotes of *Leishmania braziliensis* panamensis. *Parasitology* 85 (Pt 2), 271–282. doi: 10.1017/S0031182000055256

Huber, W., and Koella, J. C. (1993). A comparison of three methods of estimating EC50 in studies of drug resistance of malaria parasites. *Acta Trop.* 55, 257–261. doi: 10.1016/0001-706X(93)90083-N

Ilari, A., Fiorillo, A., Genovese, I., and Colotti, G. (2017). Polyamine-trypanothione pathway: an update. *Fut. Med. Chem.* 9, 61–77. doi: 10.4155/fmc-2016-0180

Jara, M., Berg, M., Caljon, G., de Muylder, G., Cuypers, B., Castillo, D., et al. (2017). Macromolecular biosynthetic parameters and metabolic profile in different life stages of *Leishmania braziliensis*: amastigotes as a functionally less active stage. *PLoS ONE* 12:e0180532. doi: 10.1371/journal.pone.0180532

Kaur, G., and Rajput, B. (2014). Comparative analysis of the omics technologies used to study antimonial, amphotericin B, and pentamidine resistance in *Leishmania*. *J. Parasitol. Res.* 2014:726328. doi: 10.1155/2014/726328

Kind, T., Wohlgemuth, G., Y., Lee do, Lu, Y., Palazoglu, M., Shahbaz, S., et al. (2009). FiehnLib: mass spectral and retention index libraries for metabolomics based on quadrupole and time-of-flight gas chromatography/mass spectrometry. *Anal. Chem.* 81, 10038–10048. doi: 10.1021/ac9019522

Kloehn, J., Saunders, E. C., O'Callaghan, S., Dagley, M. J., and McConville, M. J. (2015). Characterization of metabolically quiescent *Leishmania* parasites in murine lesions using heavy water labeling. *PLoS Pathog.* 11:e1004683. doi: 10.1371/journal.ppat.1004683

Laffitte, M. N., Leprohon, P., Papadopoulou, B., and Ouellette, M. (2016). Plasticity of the *Leishmania* genome leading to gene copy number variations and drug resistance. *F1000Research* 5:2350. doi: 10.12688/f1000research.9218.1

Lei, Z., Huhman, D. V., and Sumner, L. W. (2011). Mass spectrometry strategies in metabolomics. *J. Biol. Chem.* 286, 25435–25442. doi: 10.1074/jbc.R111.238691

Leprohon, P., Legare, D., Girard, I., Papadopoulou, B., and Ouellette, M. (2006). Modulation of *Leishmania* ABC protein gene expression through life stages and among drug-resistant parasites. *Eukaryot. Cell* 5, 1713–1725. doi: 10.1128/EC.00152-06

Liemburg-Apers, D. C., Willems, P. H., Koopman, W. J., and Grefte, S. (2015). Interactions between mitochondrial reactive oxygen species and cellular glucose metabolism. *Arch. Toxicol.* 89, 1209–1226. doi: 10.1007/s00204-015-1520-y

Lima, H. C., Bleyenberg, J. A., and Titus, R. G. (1997). A simple method for quantifying *Leishmania* in tissues of infected animals. *Parasitol. Today* 13, 80–82. doi: 10.1016/S0169-4758(96)40010-2

Louassini, M., Foulquie, M., Benitez, R., and Adroher, J. (1999). Citric-acid cycle key enzyme activities during *in vitro* growth and metacyclogenesis of *Leishmania infantum* promastigotes. *J. Parasitol.* 85, 595–602. doi: 10.2307/3285729

Lu, H. G., Zhong, L., Chang, K. P., and Docampo, R. (1997). Intracellular Ca2+ pool content and signaling and expression of a calcium pump are linked to virulence in *Leishmania mexicana* amazonesis amastigotes. *J. Biol. Chem.* 272, 9464–9473. doi: 10.1074/jbc.272.14.9464

Magalhães, R. D., Duarte, M. C., Mattos, E. C., Martins, V. T., Lage, P. S., Chavez-Fumagalli, M. A., et al. (2014). Identification of differentially expressed proteins from *Leishmania amazonensis* associated with the loss of virulence of the parasites. *PLoS Negl. Trop. Dis.* 8:e2764. doi: 10.1371/journal.pntd.0002764

Maldonado, R. A., Kuniyoshi, R. K., Linss, J. G., and Almeida, I. C. (2006). Trypanosoma cruzi oleate desaturase: molecular characterization and comparative analysis in other trypanosomatids. *J. Parasitol.* 92, 1064–1074. doi: 10.1645/GE-845R.1

Martin, J. L., Yates, P. A., Soysa, R., Alfaro, J. F., Yang, F., Burnum-Johnson, K. E., et al. (2014). Metabolic reprogramming during purine stress in the protozoan pathogen *Leishmania donovani*. *PLoS Pathog.* 10:e1003938. doi: 10.1371/journal.ppat.1003938

Maspi, N., Abdoli, A., and Ghaffarifar, F. (2016). Pro- and anti-inflammatory cytokines in cutaneous leishmaniasis: a review. *Pathog. Global Health* 110, 247–260. doi: 10.1080/20477724.2016.1232042

McCall, L. I., and McKerrow, J. H. (2014). Determinants of disease phenotype in trypanosomatid parasites. *Trends Parasitol.* 30, 342–349. doi: 10.1016/j.pt.2014.05.001

McConville, M. J., and Naderer, T. (2011). Metabolic pathways required for the intracellular survival of *Leishmania*. *Ann. Rev. Microbiol.* 65, 543–561. doi: 10.1146/annurev-micro-090110-102913

McConville, M. J., Turco, S. J., Ferguson, M. A., and Sacks, D. L. (1992). Developmental modification of lipophosphoglycan during the differentiation of *Leishmania* major promastigotes to an infectious stage. *EMBO J.* 11, 3593–3600. doi: 10.1002/j.1460-2075.1992.tb05443.x

McMahon-Pratt, D., and Alexander, J. (2004). Does the *Leishmania* major paradigm of pathogenesis and protection hold for New World cutaneous leishmaniases or the visceral disease? *Immunol. Rev.* 201, 206–224. doi: 10.1111/j.0105-2896.2004.00190.x

Moreira, D., Santarem, N., Loureiro, I., Tavares, J., Silva, A. M., Amorim, A. M., et al. (2012). Impact of continuous axenic cultivation in *Leishmania infantum* virulence. *PLoS Negl. Trop. Dis.* 6:e1469. doi: 10.1371/journal.pntd.0001469

Muskus, C. E., and Marin Villa, M. (2002). [Metacyclogenesis: a basic process in the biology of *Leishmania*]. *Biomedica* 22, 167–177. doi: 10.7705/biomedica.v22i2.1156

Naz, S., Vallejo, M., Garcia, A., and Barbas, C. (2014). Method validation strategies involved in non-targeted metabolomics. *J. Chromatogr. A* 1353, 99–105. doi: 10.1016/j.chroma.2014.04.071

Opperdoes, F. R., Butenko, A., Flegontov, P., Yurchenko, V., and Lukes, J. (2016). Comparative metabolism of free-living bodo saltans and parasitic trypanosomatids. *J. Eukaryot. Microbiol.* 63, 657–678. doi: 10.1111/jeu.12315

Paape, D., Barrios-Llerena, M. E., Le Bihan, T., Mackay, L., and Aebischer, T. (2010). Gel free analysis of the proteome of intracellular *Leishmania mexicana*. *Mol. Biochem. Parasitol.* 169, 108–114. doi: 10.1016/j.molbiopara.2009.10.009

Pawar, H., Renuse, S., Khobragade, S. N., Chavan, S., Sathe, G., Kumar, P., et al. (2014). Neglected tropical diseases and omics science: proteogenomics analysis

of the promastigote stage of *Leishmania* major parasite. *Omics* 18, 499–512. doi: 10.1089/omi.2013.0159

Pessi, G., Choi, J. Y., Reynolds, J. M., Voelker, D. R., and Mamoun, C. B. (2005). *In vivo* evidence for the specificity of *Plasmodium falciparum* phosphoethanolamine methyltransferase and its coupling to the Kennedy pathway. *J. Biol. Chem.* 280, 12461–12466. doi: 10.1074/jbc.M414626200

Pfaffl, M. W. (2001). A new mathematical model for relative quantification in real-time RT-PCR. *Nucleic Acids Res.* 29:e45. doi: 10.1093/nar/29.9.e45

Rebello, K. M., Britto, C., Pereira, B. A., Pita-Pereira, D., Moraes, M. O., Ferreira, A. B., et al. (2010). Leishmania (Viannia) braziliensis: influence of successive *in vitro* cultivation on the expression of promastigote proteinases. *Exp. Parasitol.* 126, 570–576. doi: 10.1016/j.exppara.2010.06.009

Reiner, N. E., and Malemud, C. J. (1985). Arachidonic acid metabolism by murine peritoneal macrophages infected with *Leishmania donovani*: *in vitro* evidence for parasite-induced alterations in cyclooxygenase and lipoxygenase pathways. *J. Immunol.* 134, 556–563.

Rochael, N. C., Lima, L. G., Oliveira, S. M., Barcinski, M. A., Saraiva, E. M., Monteiro, R. Q., and Pinto-da-Silva, L. H. (2013). *Leishmania amazonensis* exhibits phosphatidylserine-dependent procoagulant activity, a process that is counteracted by sandfly saliva. *Mem. Inst. Oswaldo Cruz* 108, 679–685. doi: 10.1590/0074-0276108062013002

Rodrigues, H. G., Takeo Sato, F., Curi, R., and Vinolo, M. A. (2015). Fatty acids as modulators of neutrophil recruitment, function and survival. *Eur. J. Pharmacol.* 785, 50–58. doi: 10.1016/j.ejphar.2015.03.098

Rolin, J., Vego, H., and Maghazachi, A. A. (2014). Oxidized lipids and lysophosphatidylcholine induce the chemotaxis, up-regulate the expression of CCR9 and CXCR4 and abrogate the release of IL-6 in human monocytes. *Toxins* 6, 2840–2856. doi: 10.3390/toxins6092840

Rougeron, V., De Meeus, T., Kako Ouraga, S., Hide, M., and Banuls, A. L. (2010). Everything you always wanted to know about sex (but were afraid to ask) in *Leishmania* after two decades of laboratory and field analyses. *PLoS Pathog.* 6:e1001004. doi: 10.1371/journal.ppat.1001004

Sacks, D. L., Hieny, S., and Sher, A. (1985). Identification of cell surface carbohydrate and antigenic changes between noninfective and infective developmental stages of *Leishmania* major promastigotes. *J. Immunol.* 135, 564–569.

Saljoughian, N., Taheri, T., and Rafati, S. (2014). Live vaccination tactics: possible approaches for controlling visceral leishmaniasis. *Front. Immunol.* 5:134. doi: 10.3389/fimmu.2014.00134

Saraiva, E. M., Pimenta, P. F., Brodin, T. N., Rowton, E., Modi, G. B., and Sacks, D. L. (1995). Changes in lipophosphoglycan and gene expression associated with the development of *Leishmania* major in Phlebotomus papatasi. *Parasitology* 111(Pt 3), 275–287. doi: 10.1017/S003118200008183X

Sarfraz, I., Rasul, A., Hussain, G., Hussain, S. M., Ahmad, M., Nageen, B., et al. (2018). Malic enzyme 2 as a potential therapeutic drug target for cancer. *IUBMB Life* 70, 1076–1083. doi: 10.1002/iub.1930

Saunders, E. C., Ng, W. W., Kloehn, J., Chambers, J. M., Ng, M., and McConville, M. J. (2014). Induction of a stringent metabolic response in intracellular stages of *Leishmania mexicana* leads to increased dependence on mitochondrial metabolism. *PLoS Pathog.* 10:e1003888. doi: 10.1371/journal.ppat.1003888

Sauvage, V., Aubert, D., Escotte-Binet, S., and Villena, I. (2009). The role of ATP-binding cassette (ABC) proteins in protozoan parasites. *Mol. Biochem. Parasitol.* 167, 81–94. doi: 10.1016/j.molbiopara.2009.05.005

Serezani, C. H., Perrela, J. H., Russo, M., Peters-Golden, M., and Jancar, S. (2006). Leukotrienes are essential for the control of *Leishmania amazonensis* infection and contribute to strain variation in susceptibility. *J. Immunol.* 177, 3201–3208. doi: 10.4049/jimmunol.177.5.3201

Silva Pereira, S., and Jackson, A. P. (2018). UDP-glycosyltransferase genes in trypanosomatid genomes have diversified independently to meet the distinct developmental needs of parasite adaptations. *BMC Evol. Biol.* 18:31. doi: 10.1186/s12862-018-1149-6

Sinha, R., Mathu Malar, C., Raghwan, Das, S., Das, S., Shadab, M., et al. (2018). Genome plasticity in cultured *Leishmania donovani*: comparison of early and late passages. *Front. Microbiol.* 9:1279. doi: 10.3389/fmicb.2018.01279

Soong, L., Henard, C. A., and Melby, P. C. (2012). Immunopathogenesis of non-healing American cutaneous leishmaniasis and progressive visceral leishmaniasis. *Semin. Immunopathol.* 34, 735–751. doi: 10.1007/s00281-012-0350-8

Spath, G. F., and Beverley, S. M. (2001). A lipophosphoglycan-independent method for isolation of infective *Leishmania* metacyclic promastigotes by density gradient centrifugation. *Exp. Parasitol.* 99, 97–103. doi: 10.1006/expr.2001.4656

Tavares, N. M., Araujo-Santos, T., Afonso, L., Nogueira, P. M., Lopes, U. G., Soares, R. P., et al. (2014). Understanding the mechanisms controlling *Leishmania amazonensis* infection *in vitro*: the role of LTB4 derived from human neutrophils. *J. Infect. Dis.* 210, 656–666. doi: 10.1093/infdis/jiu158

Tull, D., Naderer, T., Spurck, T., Mertens, H. D., Heng, J., McFadden, G. I., et al. (2010). Membrane protein SMP-1 is required for normal flagellum function in *Leishmania*. *J. Cell Sci.* 123, 544–554. doi: 10.1242/jcs.059097

Ullman, B., and Carter, D. (1997). Molecular and biochemical studies on the hypoxanthine-guanine phosphoribosyltransferases of the pathogenic haemoflagellates. *Int. J. Parasitol.* 27, 203–213. doi: 10.1016/S0020-7519(96)00150-6

Uttaro, A. D. (2014). Acquisition and biosynthesis of saturated and unsaturated fatty acids by trypanosomatids. *Mol. Biochem. Parasitol.* 196, 61–70. doi: 10.1016/j.molbiopara.2014.04.001

van Meer, G., Halter, D., Sprong, H., Somerharju, P., and Egmond, M. R. (2006). ABC lipid transporters: extruders, flippases, or flopless activators? *FEBS Lett.* 580, 1171–1177. doi: 10.1016/j.febslet.2005.12.019

Vangaveti, V., Baune, B. T., and Kennedy, R. L. (2010). Hydroxyoctadecadienoic acids: novel regulators of macrophage differentiation and atherogenesis. *Ther. Adv. Endocrinol. Metab.* 1, 51–60. doi: 10.1177/20420188103 75656

Villaveces, J. M., Koti, P., and Habermann, B. H. (2015). Tools for visualization and analysis of molecular networks, pathways, and -omics data. *Adv. Appl. Bioinformatics Chem.* 8, 11–22. doi: 10.2147/AABC.S63534

Wanderley, J. L., Moreira, M. E., Benjamin, A., Bonomo, A. C., and Barcinski, M. A. (2006). Mimicry of apoptotic cells by exposing phosphatidylserine participates in the establishment of amastigotes of Leishmania (L) amazonensis in mammalian hosts. *J. Immunol.* 176, 1834–1839. doi: 10.4049/jimmunol.176.3.1834

WHO (2010). *Control of the Leishmaniasis: Report of a Meeting of the WHO Expert Committee on the Control of Leishmaniases*. Genova.

Woehlecke, H., Pohl, A., Alder-Baerens, N., Lage, H., and Herrmann, A. (2003). Enhanced exposure of phosphatidylserine in human gastric carcinoma cells overexpressing the half-size ABC transporter BCRP (ABCG2). *Biochem. J.* 376, 489–495. doi: 10.1042/bj20030886

Wright, M. H., Paape, D., Storck, E. M., Serwa, R. A., Smith, D. F., and Tate, E. W. (2015). Global analysis of protein N-myristoylation and exploration of N-myristoyltransferase as a drug target in the neglected human pathogen *Leishmania donovani*. *Chem. Biol.* 22, 342–354. doi: 10.1016/j.chembiol.2015.01.003

Wyllie, S., Cunningham, M. L., and Fairlamb, A. H. (2004). Dual action of antimonial drugs on thiol redox metabolism in the human pathogen *Leishmania donovani*. *J. Biol. Chem.* 279, 39925–39932. doi: 10.1074/jbc.M405635200

Yokomizo, T., Izumi, T., and Shimizu, T. (2001). Leukotriene B4: metabolism and signal transduction. *Arch. Biochem. Biophys.* 385, 231–241. doi: 10.1006/abbi.2000.2168

Zhang, K., and Beverley, S. M. (2010). Phospholipid and sphingolipid metabolism in *Leishmania*. *Mol. Biochem. Parasitol.* 170, 55–64. doi: 10.1016/j.molbiopara.2009.12.004

Conflict of Interest: The authors declare that the research was conducted in the absence of any commercial or financial relationships that could be construed as a potential conflict of interest.

frontiers in Cellular and Infection Microbiology

REVIEW
published: 18 December 2019
doi: 10.3389/fcimb.2019.00427

An Overview of Immunotherapeutic Approaches Against Canine Visceral Leishmaniasis: What Has Been Tested on Dogs and a New Perspective on Improving Treatment Efficacy

*Ana Alice Maia Gonçalves[1], Jaqueline Costa Leite[1], Lucilene Aparecida Resende[1], Reysla Maria da Silveira Mariano[1], Patricia Silveira[1], Otoni Alves de Oliveira Melo-Júnior[1], Helen Silva Ribeiro[1], Diana Souza de Oliveira[1], Diogo Fonseca Soares[1], Thaiza Aline Pereira Santos[1], Alexandre Ferreira Marques[2], Alexsandro Sobreira Galdino[3], Olindo Assis Martins-Filho[4], Walderez Ornelas Dutra[1], Denise da Silveira-Lemos[1] and Rodolfo Cordeiro Giunchetti[1]**

[1] Laboratory of Biology of Cell Interactions, Department of Morphology, Institute of Biological Sciences, Federal University of Minas Gerais, Belo Horizonte, Brazil, [2] Laboratory of Immuno-Proteome and Parasite Biology, Department of Parasitology, Institute of Biological Sciences, Federal University of Minas Gerais, Belo Horizonte, Brazil, [3] Laboratory of Biotechnology of Microorganisms, Federal University of São João Del-Rei, Divinópolis, Brazil, [4] Laboratory of Diagnostic and Monitoring Biomarkers, René Rachou Institute, FIOCRUZ-Minas, Belo Horizonte, Brazil

Visceral leishmaniasis (VL), caused by digenetic protozoa of the genus *Leishmania,* is the most severe form of leishmaniasis. *Leishmania infantum* is one of the species responsible for VL and the disease caused is considered a zoonosis whose main reservoir is the dog. Canine visceral leishmaniasis (CVL) can lead to the death of the animal if left untreated. Furthermore, the available pharmocologial treatment for CVL presents numerous disadvantages, such as relapses, toxicity, drug resistance, and the fact treated animals continue to be reservoirs when treatment fails to achieve parasitological cure. Moreover, the available VL control methods have not been adequate when it comes to controlling parasite transmission. Advances in immune response knowledge in recent years have led to a better understanding of VL pathogenesis, allowing new treatments to be developed based on immune system activation, often referred to as immunotherapy. In fact, well-defined protocols have been described, ranging from the use of immunomodulators to the use of vaccines. This treatment, which can also be associated with chemotherapy, has been shown to be effective in restoring or inducing an adequate immune response to reduce parasitic burden, leading to clinical improvement.

OPEN ACCESS

Edited by:
Herbert Leonel de Matos Guedes, Federal University of Rio de Janeiro, Brazil

Reviewed by:
Valentina Foglia Manzillo, University of Naples Federico II, Italy
Eva Spada, University of Milan, Italy
Yasuyuki Goto, The University of Tokyo, Japan
Angamuthu Selvapandiyan, Jamia Hamdard University, India

****Correspondence:***
Rodolfo Cordeiro Giunchetti
giunchetti@icb.ufmg.br; giunchetti@gmail.com

Specialty section:
This article was submitted to Parasite and Host, a section of the journal Frontiers in Cellular and Infection Microbiology

Received: *02 September 2019*
Accepted: *29 November 2019*
Published: *18 December 2019*

Citation:
Gonçalves AAM, Leite JC, Resende LA, Mariano RMdS, Silveira P, Melo-Júnior OAdO, Ribeiro HS, de Oliveira DS, Soares DF, Santos TAP, Marques AF, Galdino AS, Martins-Filho OA, Dutra WO, da Silveira-Lemos D and Giunchetti RC (2019) An Overview of Immunotherapeutic Approaches Against Canine Visceral Leishmaniasis: What Has Been Tested on Dogs and a New Perspective on Improving Treatment Efficacy. Front. Cell. Infect. Microbiol. 9:427. doi: 10.3389/fcimb.2019.00427

This review focuses on immunotherapy directed at dogs infected by *L. infantum,* including a literature review of what has already been done in dogs. We also introduce a promising strategy to improve the efficacy of immunotherapy.

Keywords: canine visceral leishmaniasis, *Leishmania infantum*, biomarkers, treatment, immunotherapy

INTRODUCTION

Leishmaniasis is a group of infectious parasitic diseases caused by protozoa of the *Leishmania* genus (Rossi and Fasel, 2017). Visceral leishmaniasis (VL) is the most severe form, which can result in a high mortality rate in humans if untreated (Alemayehu and Alemayehu, 2017). It is known that three species are responsible for causing VL; *Leishmania (Leishmania) donovani* (Laveran and Mesnil, 1903) and *Leishmania (Leishmania) infantum* (Nicolle, 1908) are found in the Old World, while *Leishmania* (*Leishmania*) *chagasi* (Cunha and Chagas, 1937) is found in the New World. Although they have different names and different geographical origins, molecular data suggest that *L. infantum* and *L. chagasi* are the same species (Maurício et al., 2000).

In recent years, cases of human VL have been reported in 76 countries (Organização Pan-Americana da Saúde, 2018) and, in 2017, 95% of the new cases occurred in seven countries: Brazil, Ethiopia, India, Kenya, Somalia, South Sudan, and Sudan (World Health Organization, 2018). Brazil accounts for 96% of the number of human VL cases in Latin America (Organização Pan-Americana da Saúde, 2018).

The VL, caused by *L. infantum,* is a zoonosis in which the dog (*Canis familiaris*) serves as the main domestic reservoir (World Health Organization, 2010; Roatt et al., 2014; Duarte et al., 2016). The disease in dogs may be manifested by inducing apparent clinical signs that, when present, may range from mild to severe, causing death (Maia-Elkhoury et al., 2008; Reis et al., 2009). During VL urbanization (Da Silva et al., 2017), dogs became responsible for spreading the disease throughout the Brazilian countryside, resulting in a rising number of human VL cases (Reis et al., 2010). Notably, cases of canine visceral leishmaniasis (CVL) precede human cases (Leite et al., 2018).

The applied VL control measures are not adequate when it comes to interrupting the spread of the disease. Moreover, *Leishmania* antigens are not able to induce a high immunogenicity regarding protection against infection in dogs (Giunchetti et al., 2019). Although, CVL treatment cannot induce parasite clearance, this measure has been largely employed, thus demonstrating the dogs' close relationship in our society. In this sense, immunotherapeutic treatments have shown to be promising against CVL, with the main objective of reestablishing dog immunity and, therefore, parasite control (Roatt et al., 2017). This approach can be performed alone or in combination with chemotherapy (Singh and Sundar, 2014). The focus of this review is on the immunotherapy methods already described for the CVL treatment, whether or not associated with chemotherapy. Taking into account the complexity of CVL transmission, we discuss some current aspects regarding immunology, resistance and susceptibility biomarkers, as well as available control measures and disease treatment.

GENERAL ASPECTS OF THE IMMUNOLOGICAL PROFILE AND BIOMARKERS REGARDING SUSCEPTIBILITY AND RESISTANCE IN CANINE VISCERAL LEISHMANIASIS

The immune response in CVL is of great importance for understanding the pathogenesis of the disease (Alvar et al., 2004; Ribeiro et al., 2018; Giunchetti et al., 2019). The immune response profile can trigger a resistance or susceptibility pattern during the parasite infection, resulting in different clinical forms of the disease (Moreno and Alvar, 2002; Leal et al., 2014; Giunchetti et al., 2019).

With regard to vector contact with the canine host, in addition to local lesion formation induced by vector feeding (Solano-Gallego et al., 2001; Giunchetti et al., 2006; Jacintho et al., 2018), the deposition of infective *L. infantum* promastigotes takes place in the dermis along with salivary content vector. This process recruits phagocytic cells to the site, such as neutrophils, macrophages, and dendritic cells, creating a pro-inflammatory environment (Soulat and Bogdan, 2017).

An *in vitro* study demonstrated that neutrophils are effector cells with the ability to control the initial infection, resulting in reduced parasite viability (Pereira et al., 2017). Furthermore, it has been observed that neutrophils have an ability to produce high levels of IFN-γ when stimulated with soluble antigen of *L. infantum* (Leal et al., 2014). Moreover, other molecules of the innate immunity have been correlated with ongoing CVL, such as TLRs (Toll-like receptors) (Hosein et al., 2015; Pereira-Fonseca et al., 2017) and chemokines (Menezes-Souza et al., 2012; Solcà et al., 2016).

It is known that the main immune response against the parasite is induced by the adaptive response, especially the type 1 immune response, characterized by IFN-γ, TNF-α, and IL-2 production related to the resistance profile. This type of immune response is related to the upregulation of the anti-leishmanial activity in macrophages (Koutinas and Koutinas, 2014), this being the main effector mechanism of the intracellular death of *Leishmania* amastigotes (Baneth et al., 2008). In this sense, the type 1 immune response induces cytokines, such as IFN-γ and TNF-α, predominant in asymptomatic dogs, demonstrating their protective potential against the disease (Costa-Pereira et al., 2015). Solano-Gallego et al. (2016) demonstrated that infected dogs presenting high levels of IFN-γ had lower parasite loads when compared to infected dogs that did not produce this cytokine. Dogs lacking this cytokine have more severe clinical symptoms, with higher parasitemia (Martínez-Orellana et al., 2017). Similarly, Th17 cells induce *L. infantum* control growth (Nascimento et al., 2015; Rodriguez-Cortes et al., 2017).

In contrast, the type 2 immune response, characterized IL-4, IL-5, IL-10, and TGF-β cytokines, is related to susceptibility in CVL (Sanches et al., 2014; Rodríguez-Cortés et al., 2016; Rodriguez-Cortes et al., 2017; Rossi et al., 2016; Solano-Gallego et al., 2016; Solcà et al., 2016; Tonin et al., 2016; De Martini et al., 2018). These susceptible dogs manifest a common pattern in the progression of clinical signs, with severity and variety of signs increasing with disease progression, in which most clinicopathological changes become evident after 12 months of infection (Foglia Manzillo et al., 2013). The type 2 immune response provides an anti-inflammatory cytokine microenviroment deactivating the cellular immune response against *L. infantum* infection (Rodriguez-Cortes et al., 2017). Moreover, a pronounced anti-*Leishmania* humoral response leads to the production of high levels of non-immunoprotective antibodies (Barbiéri, 2006; Gradoni, 2015), highlighting the polyclonal B cell response characteristic of susceptibility in CVL (Koutinas and Koutinas, 2014). There is still no consensus as to which IgG subclass is related to resistance or susceptibility in CVL (Lima et al., 2017; Chaabouni et al., 2018). Furthermore, excessive activation of humoral immunity may lead to the production of autoantibodies (Koutinas and Koutinas, 2014), such as antiactin and antitubulin (Pateraki et al., 1983), antinuclear (Smith et al., 2004; Ginel et al., 2008), and antitransferrin (Chaabouni et al., 2018).

Although the cellular and humoral immunity parameters help to understand the progression of CVL, as well as the mechanisms related to resistance or susceptibility, integrated studies of several biomarkers are needed for a better understanding of the disease (Solcà et al., 2016). In asymptomatic dogs, hematological and biochemical parameters usually remain unchanged, while in symptomatic dogs changes may occur (Maia and Campino, 2018). Symptomatic dogs showed a significant decrease in red cells, lymphocytes, eosinophils, and platelets (Lopes et al., 2018). The biochemical parameters can be used to assess the general health status in CVL. Ongoing CVL is characterized by hyperproteinemia, hypoalbuminemia, and changes in aspartate aminotransferase, alanine aminotransferase, alkaline phosphatase, urea, and creatinine concentrations (Heidarpour et al., 2012; Ribeiro et al., 2018). These parameters are interesting markers for therapeutic monitoring, especially those related to the kidney, since damage to this organ associated with the disease is almost unavoidable (Ribeiro et al., 2018). All of the biomarkers included in this section and regarding resistence or susceptibility in CVL are summarized in **Figure 1**.

CURRENT CONTROL METHODS BASED ON SANDFLY INTERFERENCE TO BLOCK CANINE VISCERAL LEISHMANIASIS TRANSMISSION

The approach to visceral leishmaniasis control needs to consider all elements in the transmission network, such as (i) sandfly vector, (ii) parasite reservoirs, and (iii) human health. In this sense, health control and surveillance measures, based on the Brazilian National Visceral Leishmaniasis Program of the Ministry of Health, determine: (i) the use of chemical insecticides and (ii) environmental management for vector population control and vector-human contact reduction, (iii) canine serological surveys, (iv) euthanasia of positive cases and timely diagnosis, and (v) adequate treatment of human cases to prevent severe forms of disease and death (Ministério da Saúde, 2014). However, it has been reported that an urgent revision in this control program is required, as its effectiveness ranges from low to moderate (Werneck et al., 2014).

In an attempt to reduce the adaptation of the vector population to the peridomic environment, the environmental management associated with chemical spraying can be used as a preventive action (Lara-Silva et al., 2017). However, this strategy is unsustainable in the long term due to the size of the area to be treated (Otranto and Dantas-Torres, 2013). The use of insecticides/repellents (mainly pyrethroids), impregnated in dog collars or used for individual human protection on the skin and/or clothing (Alexander and Maroli, 2003) aims to prevent contact with the vector. Deltamethrin, lead representative, impregnated in dog collars induced a reduction from 53 to 59% in the CVL incidence rate of infected sandflies (Kazimoto et al., 2018). In addition, uncollared dogs showed a higher frequency of clinical signs with faster progression when compared to collared dogs, demonstrating the anti-feeding effect (Foglia Manzillo et al., 2006), presenting an interesting combination of disease control and cost-effectiveness (Shimozako et al., 2017). Another type II pyrethroid, Flumethrin, applied pour-on in dogs resulted in a significant reduction on total mortality rate and in the blood-feeding index of sandflies (Jalilnavaz et al., 2016). Furthermore, the systemic insecticide Fluralaner (Bravecto®, MSD animal health) (Gomez and Picado, 2017; Miglianico et al., 2018) used in dogs has demonstrated induction of 40–60% mortality of phlebotomines using a membrane feeding assay (Gomez et al., 2018a) and 90% mortality when the vector was direct feeding (Gomez et al., 2018b). Moreover, sandfly feeding in vaccinated dogs with CaniLeish® resulted in a marked reduction in *Phlebotomus perniciosus* infection (Bongiorno et al., 2013).

Recently, a newly patented vaccine using non-salivary antigens from sandflies has shown promise as a vector control strategy because it impairs its life cycle in addition to blocking *Leishmania* infection in sandflies. This approach has been considered as the next vaccine frontier for controlling vector-borne diseases (Graciano et al., 2019).

Despite all existing control measures, preventing the spread of VL has been ineffective in Brazil (Romero and Boelaert, 2010). In this context, researchers advocate alternative control measures, such as mass vaccination and treatment of dogs, since these approaches are able to induce reduction in the parasite load and block *L. infantum* transmission in sandflies, thus providing evidence for reducing new canine and human VL cases (Pessoa-e-Silva et al., 2019).

CONVENTIONAL CANINE VISCERAL LEISHMANIAISIS TREATMENT

Treatment of CVL is characterized by high rates of relapse, regardless of the antileishmanial drugs used, either as a single drug or in combined drug therapy (Ribeiro et al., 2018).

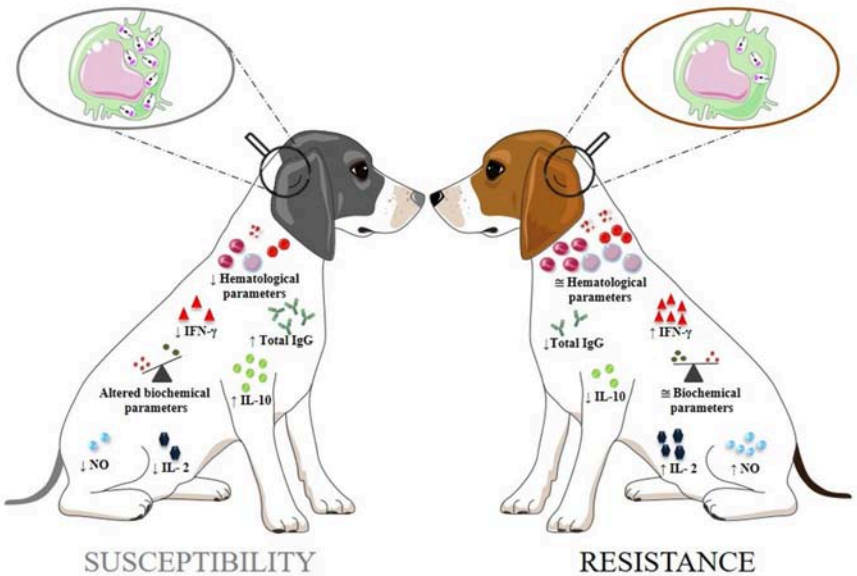

FIGURE 1 | The biomarkers of canine visceral leishmaniasis related to susceptibility or resistance. The arrows (↑ and ↓) indicate the increase and decrease in biomarker levels, respectively; ≅: approximate normal levels; ↓ Hematological parameters: decreased in red blood cells, lymphocytes, eosinophils, and platelets; Altered Biochemical parameters: hyperproteinemia, hypoalbuminemia, increased in aspartate aminotransferase, alanine aminotransferase, alkaline phosphatase, urea, and creatinine levels.

Moreover, clinical and parasitological cure is rarely achieved, not to mention the possibility of drug resistance (Travi, 2014; Marcondes and Day, 2019).

Drug therapy using miltefosine was originally developed as an anticancer agent in the 1990s and was first recorded for VL treatment in 2002 in India (Dorlo et al., 2012). In 2016, the Brazilian Ministry of Health and the Ministry of Agriculture Livestock and Supply approved the registration of Milteforan® (Virbac, Brazil) (Brasil, 2016). Although there was a notable improvement in the clinical symptoms when using this drug, it was not accompanied by parasitological clearance, suggesting that treatment with miltefosine should not be recommended (Andrade et al., 2011). Recently, miltefosine treatment against CVL revealed clinical improvement with a reduction in infectivity from *L. infantum*-infected dogs (Dos Santos Nogueira et al., 2019).

Allopurinol has a parasitostatic activity and its long-term administration maintains low parasite loads, thus contributing to the prevention of canine relapse (Koutinas et al., 2001). The association of this drug with miltefosine showed to be a promising combination for CVL treatment (Foglia Manzillo et al., 2009). However, induced resistance is also a problem associated with the use of allopurinol (Yasur-Landau et al., 2017).

In most parts of the world, meglumine antimoniate is the most commonly used treatment for human and canine leishmaniasis. Meglumine antimonate, combined with allopurinol, is considered the most effective therapy for CVL (Solano-Gallego et al., 2009); however, CVL treatment with the same human-used drugs is not recommended since it may induce parasite resistance (Travi, 2014).

The great challenge of CVL treatment is to identity a drug that (i) is not used in VL human treatment, (ii) does not induce kidney damage or any other adverse effect, (iii) provides a parasite load control, (iv) interferes in the sandflies' life cycle, and (v) blocks parasite transmission. In this sense, other treatment options should be studied, such as immunotherapy, in an attempt to improve CVL treatment efficacy.

IMMUNOTHERAPY AND IMMUNOCHEMOTHERAPY AS STRATEGIES FOR IMPROVING CANINE VISCERAL LEISHMANIASIS TREATMENT EFFICACY

Immunotherapy involves the use of biological substances or molecules to modulate immune responses for the purpose of achieving prophylactic and/or therapeutic success (Okwor and Uzonna, 2009; Musa et al., 2010; Khadem and Uzonna, 2014; Roatt et al., 2014; Singh and Sundar, 2014). For instance, immunotherapeutic agents exert their effect by directly or indirectly augmenting the host's natural defenses, restoring the impaired effector functions or reducing the host's excessive response (Oldham and Smalley, 1983; Okwor and Uzonna, 2009).

Since *Leishmania* is able to persist in host cells by evading or exploiting their immune mechanisms, the ability to develop a specific immune response could induce parasite replication control (Gupta et al., 2013). Thus, triggering the immune system with antigens or immunomodulators could be an alternative approach to combatting distinct infections such as leishmaniasis (Scott and Novais, 2016). In fact, cutaneous leishmaniasis (CL)

immunotherapy treatment was evaluated by Avila et al. (1982) using glucan immunotherapy, but without satisfactory results. In Brazil, the first study was carried out by Badaro et al. (1990), which demonstrated the immunotherapeutic ability of IFN-γ when concomitantly administered with pentavalent antimony in human visceral leishmaniasis. Notably, Mayrink et al. (1992) proposed immunotherapy using a mixture of five *Leishmania* strains and observed a 76% cure rate in human CL.

Distinct therapeutic approaches in CVL discussed in this section are summarized in **Table 1**. Since immunotherapeutic treatment against *Leishmania* infection has been successfully proved, the first study in dogs was performed by Neogy et al. (1994) using LiF2 antigen alone or combined with N-methylglucamine antimonate. These authors described that the immunochemotherapy protocol was more efficient for CVL treatment, demonstrating a 100% clinical cure rate, in which they did not observe any parasite in direct microscopic examination of bone-marrow aspirates. Another study demonstrated that the association of N-methyl D-glucamine antimoniate and *L. infantum* antigens (soluble antigen) showed an increase in the proportion of T lymphocytes; however, lymphnode aspirates remained positive (Guarga et al., 2002). Treatment using *L. braziliensis* promastigotes, alone or in association with Glucantime®, showed that chemotherapy alone was more effective, since the dogs had the lowest parasite load (Melo et al., 2002). Similarly, the *L. major* promastigote antigens and heat-killed *Mycobacterium vaccae* (SRL172) were compared to Glucantime® chemotherapy and revealed that both treatments were able to control parasitism, albeit slower in immunotherapy than in chemotherapy treatment (Jamshidi et al., 2011).

Immunomodulators have been described as triggering the immune system against *Leishmania* infection resulting in parasite control (Taslimi et al., 2016). Domperidone, for example, was able to induce clinical improvement in CVL in 86% of the animals with multiple clinical signs, with serum antibody titres decreased by 38% (Gómez-Ochoa et al., 2009). Moreover, the protein aggregate of magnesium–ammonium phospholinoleate–palmitoleate anhydride (P-MAPA) was used as a immunomodulator approach against CVL, inducing partial immunocompetence in symptomatic dogs (Santiago et al., 2013). Contrarily, the IMOD (Novel Herbal Immunomodulator Drug) used as immunotherapeutic treatment in experimental CVL did not trigger a proinflammatory immune response or induce parasite control, resulting in low therapeutic efficacy (Malmasi et al., 2014).

Vaccine therapy terminology has been employed in immunotherapy treatment, since the authors described the vaccinal antigens used for inducing cell-mediated immune response against CVL. Borja-Cabrera et al. (2004) evaluated the immunotherapeutic efficacy of FML-vaccine in asymptomatic dogs, which induced a positive DTH response in 79–95% of the animals and parasite control in bone marrow. Contrarily, vaccination with Leish111f (MML polyprotein) plus MPL®-SE failed to deter disease progression (Gradoni et al., 2005). Santos et al. (2007) administered enriched-Leishmune® vaccine (FML-Saponin) in symptomatic dogs, resulting in a reduction in clinical signs and parasitic burden on the liver, spleen, bone marrow, and blood. Immunotherapy using Leish-110f® with the adjuvant MPL-SE (Monophosphoril Lipid A), alone or in combination with Glucantime® (immunochemotherapy) in symptomatic dogs, was able to reduce the number of deaths, increase survival probability, and trigger specific cellular reactivity for parasite antigens (Miret et al., 2008). Beyond that, the recombinant polyprotein using Leish-111f® antigen with MPL-SE® provided a 75% cure rate, which was higher as compared to dogs treated with chemotherapy (64%) or immunochemotherapy (50%) (Trigo et al., 2010).

The immunotherapeutic protocol using *L. infantum* recombinant cysteine proteinase (rLdccys1) in combination with adjuvant *Propionibacterium acnes* induced high IFN-γ with low IL-10 cytokine production along with a reduction in the spleen parasite load (Ferreira et al., 2014). Notably, the vaccine composed of *L. braziliensis* antigens associated with MPL adjuvant (LBMPL vaccine) in symptomatic dogs was able to trigger increased $CD3^+$ T lymphocytes and their subpopulations, a reduction in $CD21^+$ B lymphocytes, and an increase in NK cells and $CD14^+$ monocytes. Moreover, the dogs exhibited an important decline in the number and intensity of disease symptoms, increased body weight, reduced splenomegaly, and a drop in the parasite burden (Roatt et al., 2017). Similarly, Viana et al. (2018) demonstrated that *L. amazonensis* antigens, alone or in association with saponin (LaSap therapeutic vaccine), used in symptomatic dogs improved their clinical status, reduced IgG serum levels, and triggered a lymphoproliferative profile using *L. infantum* antigens, resulting in an outstanding reduction in parasite load. Furthermore, the vaccine Leish-Tec® (*Leishmania* A2 protein plus saponin adjuvant—Ceva Saúde Animal Ltda) used as immunotherapy in asymptomatic dogs induced a curtailment in clinical progression and in mortality (Toepp et al., 2018).

The different protocols used for immunotherapy or immunochemotherapy generally lead to an improvement in clinical signs with a possibility to further reduce the parasite burden by being activated in the immune system against *Leishmania* infection. Taken together, these results showed that immunotherapy is a promising strategy for the treatment of CVL. However, parasite clearance in CVL has not yet been achieved, irrespective of treatment, and this is the strongest negative aspect in these studies. The search for new immunotherapeutic agents to improve the results in this type of treatment is of great interest, given its aim to improve parasite control and develop approaches to blocking CVL transmission. All immunotherapy-related immunological aspects described above are summarized in **Figure 2**.

DISCUSSION AND PERSPECTIVES: IMMUNOTHERAPEUTIC STRATEGIES TO TREAT AND BLOCK CANINE VISCERAL LEISHMANIASIS TRANSMISSION

Although the immunotherapeutic protocols described were able to induce clinical improvement, there is still a major impasse when it comes to obtaining parasitological cure, as the

TABLE 1 | Major immunotherapy and immunochemotherapy treatments evaluated in dogs against *L. infantum* infection.

Country	Type of infection/number of animals in the study	Immunotherapeutic agent/treatment scheme/number of animals	Chemotherapeutic agent/treatment scheme	Treatment efficacy/improvements	References
Corsica (French)	Naturally infected symptomatic dogs/24 animals	LiF2 antigen/3 IM doses at 7-day intervals/8 animals	Glucantime®/20 doses of 300 mg/kg by IM at 2-day intervals	100% cure rate	Neogy et al., 1994
Spain	Naturally infected dogs/10 animals	Soluble antigen of *L. infantum*/3 SC doses at 14- day intervals/5 animals	Glucantime®/21 consecutive doses of 100 mg/kg by SC	↑ proportion of T lymphocytes (CD4/TcRαβ$^+$ and CD4/CD45RA$^+$) in PBMCs	Guarga et al., 2002
Brazil	*L. infantum* experimentally infected with 1 × 10^7 amastigotes. Treatment starts at 150 dpi/32 animals	Dead promastigote of *L. brasiliensis*/3 SC cyles of 20 days with 10-day intervals/8 animals	Glucantime®/3 cyles of 20 days of 100 mg/kg by SC with 10-day intervals	↓ efficacy when compared with the group treated only with chemotherapy	Melo et al., 2002
Brazil	Naturally infected asymptomatic dogs/67 animals	FML-vaccine/3 doses/21 animals	–	Positive DTH response in 79–95% of the animals. Absence of parasite in bone marrow smears	Borja-Cabrera et al., 2004
Italy	Naturally infected asymptomatic dogs/15 animals	Leish111f+ MPL®-SE/3 SC doses at 28- day intervals with second three-dose after 1 year/9 animals	–	7 out of 9 animals progressed to a subsequent stage of infection, detected by PCR of bone marrow, lymph node aspiration, and serology	Gradoni et al., 2005
Brazil	*L. infantum* experimentally infected with 2 × 10^8 amastigotes. Treatment starts at 180 dpi/24 animals	enriched-Leishmune®/3 SC doses at 20- to 30-day intervals/12 animals	–	75% of the animals presented positive DTH with lower clinical scores and normal CD4+ counts	Santos et al., 2007
Brazil	Naturally infected symptomatic dogs/30 animals	Leish-110f® + MPL-SE/3 SC doses at 21-day intervals/6 animals	Glucantime®/2 cyles of 10 days of 100 mg/kg by IM with 10-day intervals	↓ deaths ↑ survival; specific cellular reactivity	Miret et al., 2008
Spain	Naturally infected dogs/98 animals	Domperidone/1 mg/Kg by OR every 12 h during 30 days/98 animals	–	Clinical improvement in 86% of animals with serum antibody titres decreased by 38%	Gómez-Ochoa et al., 2009
Brazil	Naturally infected symptomatic dog/59 animals	Leish-111f® + MPL-SE/4 SC doses at 7-day intervals/18 animals	Glucantime®/Daily doses of 20 mg/kg by IV during 30 days	75% cure rate in group treated only with immunotherapy	Trigo et al., 2010
Iran	*L. infantum* experimentally infected with 3 × 10^5 amastigotes. Treatment starts at 60 dpi/19 animals	*Leishmania major* antigen+ heat-killed *Mycobacterium vaccae*/3 ID doses at 30-day intervals/3 animals	Glucantime®/ 30 consecutive doses of 100 mg/kg by IM	Complete clearance of parasite with no relapse in the group treated only with immunotherapy	Jamshidi et al., 2011
Brazil	Naturally infected symptomatic dogs/20 animals	(P-MAPA)/2.0 mg/Kg by IM at 3-day intervals during 45 days/10 animals	–	↑ CD8$^+$ T cells, IL-2 and IFN-γ ↓ IL-10	Santiago et al., 2013

(Continued)

TABLE 1 | Continued

Country	Type of infection/number of animals in the study	Immunotherapeutic agent/treatment scheme/number of animals	Chemotherapeutic agent/treatment scheme	Treatment efficacy/improvements	References
Brazil	Naturally infected symptomatic dogs/30 animals	Recombinant cysteine proteinase of *L. infantum* (rLdccys1) + *P. acnes*/3 SC doses at 30-day intervals/10 animals	–	↑ IFN-γ; ↑ DTH; ↓ IL-10; ↓ spleen parasite load	Ferreira et al., 2014
Iran	*L. infantum* experimentally infected infection with 3×10^7 amastigotes. Treatment starts at 90 dpi/12 animals	IMOD + amastigotes/2 mg/kg over 1 h at 2-day intervals during 30 days/4 animals	–	↓ IFN-γ, IL- 2, IL- 4 e IL-10. All animals remained positive in parasitological evaluation in spleen biopsy	Malmasi et al., 2014
Brazil	Naturally infected symptomatic dogs/16 animals	*Leishmania braziliensis* antigens + MPL (LBMPL vaccine)/3 series of 10 SC doses at 10-day intervals/10 animals	–	↑ $CD3^+$ T lymphocytes and their subpopulations; ↑ NK cells and $CD14^+$; ↓ $CD21^+$ B lymphocytes; ↓ number and intensity of disease symptoms	Roatt et al., 2017
United States	Naturally infected asymptomatic dogs/495 animals	Leish-Tec® (*Leishmania* A2 protein + saponin)/3 SC doses at 14-day intervals/250 animals	–	↓clinical progression with ↓ mortality	Toepp et al., 2018
Brazil	Naturally infected symptomatic dogs/14 animals	LaSap (*Leishmania amazonenses* antigens + saponin)/5 SC doses at 7- day intervals/8 animals	–	Improvement in clinical status; ↓ IgG; ↑ lymphoproliferative capacity	Viana et al., 2018

The arrows (↑ and ↓) indicate the increase and decrease in biomarker levels, respectively, when compared to control groups. dpi, days post infection; IV, intravenous route; SC, subcutaneous route; IM, intramuscular route; OR, oral route; ID, intradermal route.

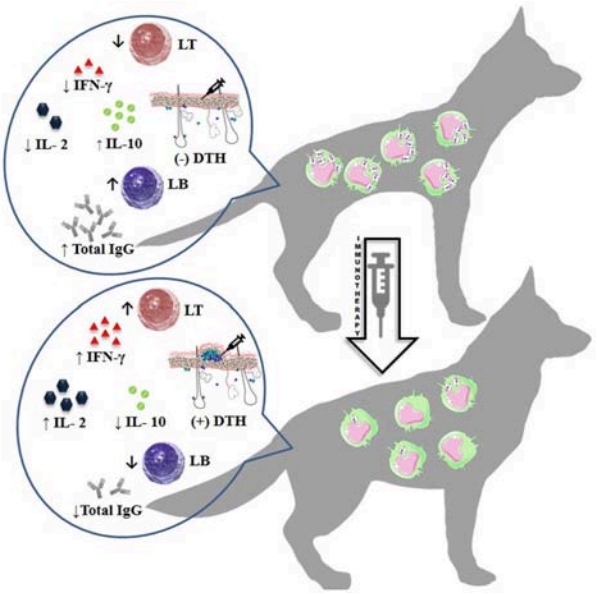

FIGURE 2 | Immunotherapy-related immunological aspects. ↑, decreased; ↑, increased; IFN-γ, *Interferon gamma;* IL-2, Interleukin 2; IL-10, Interleukin 10; (+), positive; (–), negative; DTH, delayed-type hypersensitivity; IgG, Immunoglobulin G; LT, T lymphocyte; LB, B lymphocyte.

L. infantum-infected dogs continue to be parasite reservoirs for sandfly vectors. Therefore, new protocols are needed to achieve a better efficacy in CVL treatment. Furthermore, innovative strategies can be incorporated into immunotherapy to interfere with the dynamics of disease transmission.

Considering that the sandfly's blood meal and the parasite's interaction with the invertebrate host are determining factors for *Leishmania* transmission, our research group has been developing studies focused on these factors so as to interfere with the parasite transmission dynamic (Graciano et al., 2019). The incorporation of vector antigens into new immunobiologicals is a promising strategy designed to disrupt the sandflies' life cycle, as well as block *L. infantum* transmission (Graciano et al., 2019). In fact, our research group has already identified different formulations with these capabilities that are currently being analyzed in addition to *Leishmania* antigens. The combination of parasite antigens with sandfly antigens in a single formulation as an immunotherapeutic protocol would provide more appropriate treatment. However, this new immunotherapeutic approach has not yet been tested in dogs. Finally, this type of immunotherapy could promote clinical improvement and efficient control of the parasite load, in addition to significantly reducing the risk of VL transmission and, thereby, lessening the number of canine and human cases.

AUTHOR CONTRIBUTIONS

AAG, JL, LR, and RM wrote the manuscript. AAG, PS, OM-J, HR, DO, DS, and TS reviewed the manuscript. AAG, AM, AG, OM-F, WD, DS-L, and RG drafted and critically evaluated the manuscript.

FUNDING

This research was financially supported through grants from CAPES (Coordination for the Improvement of High Higher Education Personnel, Brazil), CNPq (National Council for Scientific and Technological Development), Ministry of Health of Brazil (Decit/SCTIE/MS), Fundação de Amparo a Pesquisa do Estado de Minas Gerais (FAPEMIG), and Quatree (Granvita).

ACKNOWLEDGMENTS

The authors would also like to thank the CNPq for a fellowship to AM, AG, OM-F, WD, DS-L, and RG.

REFERENCES

Alemayehu, B., and Alemayehu, M. (2017). Leishmaniasis: a review on parasite, vector and reservoir host. *Healt. Sci. J.* 11, 1–6. doi: 10.21767/1791-809X.1000519

Alexander, B., and Maroli, M. (2003). Control of phlebotomine sandflies. *Med Vet. Entomol.* 17, 1–18. doi: 10.1046/j.1365-2915.2003.00420.x

Alvar, J., Cañavate, C., Molina, R., Moreno, J., and Nieto, J. (2004). Canine leishmaniasis. *Adv. Parasitol.* 57, 1–88. doi: 10.1016/S0065-308X(04)57001-X

Andrade, H. M., Toledo, V. P. C. P., Pinheiro, M. B., Guimarães, T. M. P. D., Oliveira, N. C., Castro, J. A., et al. (2011). Evaluation of miltefosine for the treatment of dogs naturally infected with *L. infantum* (=*L. chagasi*) in Brazil. *Vet. Parasit.* 181, 83–90. doi: 10.1016/j.vetpar.2011.05.009

Avila, J. L., Biondo, F., Monzón, H., and Convit, J. (1982). Cutaneous leishmaniasis in mice: resistance to glucan immunotherapy, either alone or combined with chemotherapy. *Am J Trop Med Hyg.* 31, 53–59. doi: 10.4269/ajtmh.1982.31.53

Badaro, R., Falcoff, E., Badaro, F. S., Carvalho, E. M., Pedral-Sampaio, D., Barral, A., et al. (1990). Treatment of visceral leishmaniasis with pentavalent antimony and interferon gamma. *N. Engl. J. Med.* 322, 16–21. doi: 10.1056/NEJM199001043220104

Baneth, G., Koutinas, A. F., Solano-Gallego, L., Bourdeau, P., and Ferrer, L. (2008). Canine leishmaniosis - new concepts and insights on an expanding zoonosis: part one. *Trends Parasitol.* 24, 324–330. doi: 10.1016/j.pt.2008.04.001

Barbiéri, C. L. (2006). Immunology of canine leishmaniasis. *Parasite Immunol.* 28, 329–337. doi: 10.1111/j.1365-3024.2006.00840.x

Bongiorno, G., Paparcone, R., Manzillo, V. F., Oliva, G., Cuisinier, A. M., and Gradoni, L. (2013). Vaccination with LiESP/QA-21 (CaniLeish®) reduces the intensity of infection in Phlebotomus perniciosus fed on *Leishmania infantum* infected dogs-A preliminary xenodiagnosis study. *Vet. Parasitol.* 197, 691–695. doi: 10.1016/j.vetpar.2013.05.008

Borja-Cabrera, G. P., Cruz, A., Paraguai, E., Souza, D., Hashimoto, L. Y., Antonio, F., et al. (2004). Effective immunotherapy against canine visceral leishmaniasis with the FML-vaccine. *Vaccine* 22, 2234–2243. doi: 10.1016/j.vaccine.2003.11.039

Brasil (2016). *Ministério da Agricultura Pecuária e Abastecimento*. Nota Técnica Conjunta n°001/2016. Available online at: http://www.sbmt.org.br/portal/wp-content/uploads/2016/09/nota-tecnica.pdf (accesed March 04, 2019).

Chaabouni, A., Elandoulsi, R. B., Mhadhbi, M., Gharbi, M., and Sassi, A. (2018). Comparative analysis of the *Leishmania infantum*-specific antibody repertoires and the autoantibody repertoires between asymptomatic and

symptomatic dogs. *Vet. Parasitol.* 261, 9–17. doi: 10.1016/j.vetpar.2018.07.011

Costa-Pereira, C., Moreira, M. L., Soares, R. P., Marteleto, B. H., Ribeiro, V. M., França-Dias, M. H., et al. (2015). One-year timeline kinetics of cytokine-mediated cellular immunity in dogs vaccinated against visceral leishmaniasis. *BMC Vet. Res.* 11, 1–10. doi: 10.1186/s12917-015-0397-6

Cunha, A. M., and Chagas, E. (1937). Estudos sobre o parasito. In: Leishmaniose visceral americana, nova entidade mórbida do homem na América do Sul. *Mem. Inst. Oswaldo Cruz.* 32, 329–337.

Da Silva, T. A. M., Coura-Vital, W., Barbosa, D. S., Oiko, C. S. F., Morais, M. H. F., Tourinho, B. D., et al. (2017). Spatial and temporal trends of visceral leishmaniasis by mesoregion in a southeastern state of Brazil, 2002-2013. *PLoS Negl. Trop. Dis.* 11:e0005950. doi: 10.1371/journal.pntd.0005950

De Martini, C. C., de Andrade, J. T., de Almeida, S. K. M., Silva, K. L. O., Eugenio, F. R., Santos, P. S. P., et al. (2018). Cellular apoptosis and nitric oxide production in PBMC and spleen from dogs with visceral leishmaniasis. *Comp. Immunol. Microb. Infec. Dis.* 57, 1–7. doi: 10.1016/j.cimid.2018.01.003

Dorlo, T. P. C., Balasegaram, M., Beijnen, J. H., and Vries, P. (2012). Miltefosine: a review of its pharmacology and therapeutic efficacy in the treatment of leishmaniosis. *J. Antimicrob. Chemother.* 67, 2576–2597. doi: 10.1093/jac/dks275

Dos Santos Nogueira, F., Avino, V. C., Galvis-Ovallos, F., Pereira-Chioccola, V. L., Moreira, M. A. B., Romariz, A. P. P. L., et al. (2019). Use of miltefosine to treat canine visceral leishmaniasis caused by *Leishmania infantum* in Brazil. *Parasites Vect.* 12:79. doi: 10.1186/s13071-019-3323-0

Duarte, M. C., Lage, D. P., Martins, V. T., Chávez-Fumagalli, M. A., Roatt, B. M., Menezes-Souza, D., et al. (2016). Recent updates and perspectives on approaches for the development of vaccines against visceral leishmaniasis. *Rev. Soc. Bras. Med.Trop.* 49, 398–407. doi: 10.1590/0037-8682-0120-2016

Ferreira, J. H. L., Silva, L. S., Longo-Maugéri, I. M., Katz, S., and Barbiéri, C. L. (2014). Use of a recombinant cysteine proteinase from *Leishmania (Leishmania)* infantum chagasi for the immunotherapy of canine visceral leishmaniasis. *PLoS Negl. Trop. Dis.* 8, 1–8. doi: 10.1371/journal.pntd.0002729

Foglia Manzillo, F., Paparcone, R., Cappiello, S., De Santo, R., Bianciardi, P., and Oliva, G. (2009). Resolution of tongue lesions caused by *Leishmania infantum* in a dog treated with the association miltefosine-allopurinol. *Parasites Vect.* 2, 4–7. doi: 10.1186/1756-3305-2-S1-S6

Foglia Manzillo, V., Di Muccio, T., Cappiello, S., Scalone, A., Paparcone, R., Fiorentino, E., et al. (2013). Prospective study on the incidence and progression of clinical signs in naïve dogs naturally infected by *Leishmania infantum*. *PLoS Negl. Trop.* 7:e2225. doi: 10.1371/journal.pntd.0002225

Foglia Manzillo, V., Oliva, G., Pagano, A., Manna, L., Maroli, M., and Gradoni, L. (2006). Deltamethrin-impregnated collars for the control of canine leishmaniasis: evaluation of the protective effect and influence on the clinical outcome of Leishmania infection in kennelled stray dogs. *Vet. Parasitol.* 142, 142–145. doi: 10.1016/j.vetpar.2006.06.029

Ginel, P. J., Camacho, S., and Lucena, R. (2008). Anti-histone antibodies in dogs with leishmaniasis and glomerulonephritis. *Res. Vet. Sci.* 85, 510–514. doi: 10.1016/j.rvsc.2008.01.007

Giunchetti, R. C., Mayrink, W., Genaro, O., Carneiro, C. M., Corrêa-Oliveira, R., Martins-Filho, O. A., et al. (2006). Relationship between canine visceral leishmaniosis and the *Leishmania (Leishmania) chagasi* burden in dermal inflammatory foci. *J. Comp. Pathol.* 135, 100–137. doi: 10.1016/j.jcpa.2006.06.005

Giunchetti, R. C., Silveira, P., Resende, L. A., Leite, J. C., de Oliveira Melo-Júnior, O. A., Rodrigues Alves, M. L., et al. (2019). Canine visceral leishmaniasis biomarkers and their employment in vaccines. *Vet. Parasitol.* 271, 87–97. doi: 10.1016/j.vetpar.2019.05.006

Gomez, S. A., Curdi, J. L., Hernandez, J. A. C., Peris, P. P., Gil, A. E., Velasquez, R. V. O., et al. (2018a). Phlebotomine mortality effect of systemic insecticides administered to dogs. *Parasit. Vect.* 11:230. doi: 10.1186/s13071-018-2820-x

Gomez, S. A., Lucientes, J., Castillo, J. A., Peris, M. P., Delacour, S., Ortega, P., et al. (2018b). A randomized, blinded, controlled trial to assess sand fly mortality of fluralaner administered orally in dogs. *Parasit Vect.* 11:627. doi: 10.1186/s13071-018-3231-8

Gomez, S. A., and Picado, A. (2017). Systemic insecticides used in dogs: potential candidates for phlebotomine vector control? *Trop. Med. Int. Health* 22, 755–764. doi: 10.1111/tmi.12870

Gómez-Ochoa, P., Castillo, J. A., Gascón, M., Zarate, J. J., Alvarez, F., and Couto, C. G. (2009). Use of domperidone in the treatment of canine visceral leishmaniasis: a clinical trial. *Vet. J.* 179, 259–263. doi: 10.1016/j.tvjl.2007.09.014

Graciano, R. C. D., Ribeiro, J. A. T., Macedo, A. K. S., Lavareda, J. P. S., Oliveira, P. R., Netto, J. B., et al. (2019). Recent patents applications in red biotechnology: a mini-review. *Recent Pat Biotechnol.* 13, 170–186. doi: 10.2174/1872208313666190114150511

Gradoni, L. (2015). Canine *Leishmania* vaccines: still a long way to go. *Vet. Parasitol.* 208, 94–100. doi: 10.1016/j.vetpar.2015.01.003

Gradoni, L., Manzillo, V. F., Pagano, A., Piantedosi, D., De Luna, R., Gramiccia, M., et al. (2005). Failure of a multi-subunit recombinant leishmanial vaccine (MML) to protect dogs from *Leishmania infantum* infection and to prevent disease progression in infected animals. *Vaccine* 23, 5245–5251. doi: 10.1016/j.vaccine.2005.07.001

Guarga, J. L., Moreno, J., Lucientes, J., Gracia, M. J., Peribanez, M. A., and Castillo, J. A. (2002). Evaluation of a specific immunochemotherapy for the treatment of canine visceral leishmaniasis. *Vet. Immunol. Immunopathol.* 88, 13–20. doi: 10.1016/S0165-2427(02)00128-9

Gupta, G., Oghumu, S., and Satoskar, A. R. (2013). Mechanisms of immune evasion in leishmaniasis. *Adv. Appl. Microb.* 82, 155–184. doi: 10.1016/B978-0-12-407679-2.00005-3

Heidarpour, M., Soltani, S., Mohri, M., and Khoshnegah, J. (2012). Canine visceral leishmaniasis: relationships between oxidative stress, liver and kidney variables, trace elements, and clinical status. *Parasitol. Res.* 111, 1491–1496. doi: 10.1007/s00436-012-2985-8

Hosein, S., Rodríguez-Cortés, A., Blake, D. P., Allenspach, K., Alberola, J., and Solano-Gallego, L. (2015). Transcription of toll-like receptors 2, 3, 4 and 9, FoxP3 and Th17 cytokines in a susceptible experimental model of canine *Leishmania infantum* infection. *PLoS ONE* 10:e0140325. doi: 10.1371/journal.pone.0140325

Jacintho, A. P. P., Melo, G. D., Machado, G. F., Bertolo, P. H. L., Moreira, P. R. R., Momo, C., et al. (2018). Expression of matrix metalloproteinase-2 and metalloproteinase-9 in the skin of dogs with visceral leishmaniasis. *Parasitol. Res.* 117, 1819–1827. doi: 10.1007/s00436-018-5868-9

Jalilnavaz, M. R., Abai, M., Vatandoost, H., Mohebali, M., Akhavan, A., Zarei, Z., et al. (2016). Original article application of flumethrin pour-on on reservoir dogs and its efficacy against sand flies in endemic focus of visceral leishmaniasis. *J Arthropod Borne Dis.* 10, 78–86.

Jamshidi, S. H., Avizeh, R., Mohebali, M., and Bokaie, S. (2011). Immunotherapy using autoclaved *L. major* antigens and *M. vaccae* with meglumine antimoniate, for the treatment of experimental canine visceral leishmaniasis. *Iranian J. Parasit.* 6, 26–34.

Kazimoto, T. A., Amora, S. S. A., Figueiredo, F. B., Magalhaes, J. M. E., Freitas, Y. B. M., Sousa, M. L. R., et al. (2018). Impact of 4% deltamethrin-impregnated dog collars on the prevalence and incidence of canine visceral leishmaniasis. *Vec. Borne Zoonotic Dis.* 18, 356–363. doi: 10.1089/vbz.2017.2166

Khadem, F., and Uzonna, J. E. (2014). Immunity to visceral leishmaniasis: implications for immunotherapy. *Future Microbiol.* 9, 901–915. doi: 10.2217/fmb.14.43

Koutinas, A. F., and Koutinas, C. K. (2014). Pathologic mechanisms underlying the clinical findings in canine leishmaniosis due to *Leishmania infantum*/chagasi. *Vet. Pathol.* 51, 527–538. doi: 10.1177/0300985814521248

Koutinas, A. F., Saridomichelakis, M. N., Mylonakis, M. E., Leontides, L., Polizopoulou, Z., Billinis, C., et al. (2001). A randomized, blinded, placebo-controlled clinical trial with allopurinol in canine leishmaniosis. *Vet. Parasitol.* 98, 247–261. doi: 10.1016/S0304-4017(01)00399-5

Lara-Silva, F. O., Michalsky, E. M., Fotes-Dias, C. L., Fiuza, V. O. P., and Dias, E. S. (2017). Evaluation of chemical spraying and environmental management efficacy in areas with minor previous application of integrated control actions for visceral leishmaniasis in Brazil. *Acta Trop.* 176, 109–113. doi: 10.1016/j.actatropica.2017.07.029

Laveran, A., and Mesnil, F. (1903). Sur un protozaire nouveau (Piroplasma donovani Lav. & Mesn.). Parasite d' une fièvrew de l'Inde. *Comp. R. Hébd. Séanc. Acad. Sci.* 137, 957–961.

Leal, G. G. D. A., Roatt, B. M., Aguiar-Soares, R. D. O., Carneiro, C. M., Giunchetti, R. C., Teixeira-Carvalho, A., et al. (2014). Immunological profile of resistance and susceptibility in naturally infected dogs by *Leishmania infantum*. *Vet. Parasitol.* 205, 472–482. doi: 10.1016/j.vetpar.2014.08.022

Leite, B. M. C., Solcà, M. D. S., Santos, L. C. S., Coelho, L. B., Amorim, L. D. A. F., Donato, L. E., et al. (2018). The mass use of deltamethrin collars to control and prevent canine visceral leishmaniasis: a field effectiveness study in a highly endemic área. *PLoS Negl. Trop. Dis.* 12:e0006496. doi: 10.1371/journal.pntd.0006496

Lima, L. V. D. R., Carneiro, L. A., Campos, M. B., Santos, T. V., Ramos, P. K., Laurenti, M. D., et al. (2017). Further evidence associating IgG1, but not IgG2, with susceptibility to canine visceral leishmaniasis caused by *Leishmania (L.) infantum chagasi* -infection. *Parasite* 24:37. doi: 10.1051/parasite/2017039

Lopes, V. V., Belo, V. S., Pereira, D. A., Coelho, M. B., Pena, H. P., Alves, N. R., et al. (2018). IgG avidity index and complete blood count as biomarkers of clinical disease in naturally infected dogs with *Leishmania infantum*. *Vet. Parasitol.* 15, 96–103. doi: 10.1016/j.vetpar.2018.08.016

Maia, C., and Campino, L. (2018). Biomarkers associated with *Leishmania infantum* exposure, infection, and disease in dogs. *Front. Cell. Infect. Microbiol.* 8:302. doi: 10.3389/fcimb.2018.00302

Maia-Elkhoury, A. N., Alves, W. A., Sousa-Gomes, M. L., Sena, J. M., and Luna, E. A. (2008). Visceral leishmaniasis in Brazil: trends and challenges. *Cad Saude Publica* 24, 2941–2947. doi: 10.1590/S0102-311X2008001200024

Malmasi, A., Ardestani, B. Z., Bayanolhagh, S., Mohebali, M., Khorshid, H. K., Sadrpour, P., et al. (2014). Assessment of the effects of a novel herbal immunomodulator drug (IMOD) on cytokine profiles in experimental canine visceral leishmaniasis: a preliminary survey. *Iran. J. Parasitol.* 9, 292–301.

Marcondes, M., and Day, M. J. (2019). Current status and management of canine leishmaniasis in Latin America. *Res. Vet. Sci.* 123, 261–272. doi: 10.1016/j.rvsc.2019.01.022

Martínez-Orellana, P., Marí-Martorell, D., Montserrat-Sangrà, S., Ordeix, L., Baneth, G., and Solano-Gallego, L. (2017). *Leishmania infantum*-specific IFN-γ production in stimulated blood from dogs with clinical leishmaniosis at diagnosis and during treatment. *Vet. Parasitol.* 248, 39–47. doi: 10.1016/j.vetpar.2017.10.018

Maurício, I. L., Stothard, J. R., and Miles, M. A. (2000). The strange case of *Leishmania chagasi*. *Parasitol. Today* 16, 188–189. doi: 10.1016/S0169-4758(00)01637-9

Mayrink, W., Magalhaes, P. A., Michalick, M. S., da Costa, C. A., Lima Ade, O., Melo, M. N., et al. (1992). Immunotherapy as a treatment of American cutaneous leishmaniasis: preliminary studies in Brazil. *Parassitologia*. 34, 159–165.

Melo, M. A., França-Silva, J. C., Azevedo, E. O., Tabosa, I. M., Da Costa, R. T., Da Costa, C. A., et al. (2002). Clinical trial on the efficacy of the N-methyl glucamine associated to immunotherapy in dogs, experimentally infected with *Leishmania* (*Leishmania*) *chagasi*. *Rev. Med. Vet.* 153, 75–84.

Menezes-Souza, D., Guerra-Sa, R., Carneiro, C. M., Vitoriano-Souza, J., Giunchetti, R. C., Teixeira-Carvalho, A., et al. (2012). Higher expression of CCL2, CCL4, CCL5, CCL21, and CXCL8 chemokines in the skin associated with parasite density in canine visceral leishmaniasis. *PLoS Negl. Trop. Dis.* 6:e1566. doi: 10.1371/journal.pntd.0001566

Miglianico, M., Eldering, M., Slater, H., Ferguson, N., Ambrose, P., Lees, R. S., et al. (2018). Repurposing isoxazoline veterinary drugs for control of vector-borne human diseases. *Proc. Natl. Acad. Sci. U.S.A.* 115, E6920–6. doi: 10.1073/pnas.1801338115

Ministério da Saúde, Secretaria de Vigilância em Saúde, and Departamento de Vigilância Epidemiológica (2014). *Manual de Vigilância e Controle da Leishmaniose Visceral. Série A. Normas e Manuais Técnicos* (Brasília), 120.

Miret, J., Nascimento, E., Sampaio, W., França, J. C., Fujiwara, R. T., Vale, A., et al. (2008). Evaluation of an immunochemotherapeutic protocol constituted of N-methyl meglumine antimoniate (Glucantime®) and the recombinant Leish-110f®+MPL-SE® vaccine to treat canine visceral leishmaniasis. *Vaccine* 26, 1585–1594. doi: 10.1016/j.vaccine.2008.01.026

Moreno, J., and Alvar, J. (2002). Canine leishmaniasis: epidemiological risk andthe experimental model. *Trends Parasitol.* 18, 399–405. doi: 10.1016/S1471-4922(02)02347-4

Musa, A. M., Noazin, S., Khalil, E. A. G., and Modabber, F. (2010). Immunological stimulation for the treatment of leishmaniasis: a modality worthy of serious consideration. *Trans. R. Soc. Trop. Med. Hyg.* 104, 1–2. doi: 10.1016/j.trstmh.2009.07.026

Nascimento, M. S. L., Albuquerque, T. D., Nascimento, A. F., Caldas, I. S., Do-Valle-Matta, M. A., Souto, J. T., et al. (2015). Impairment of interleukin-17A expression in canine visceral leishmaniosis is correlated with reduced interferon-γ and inducible nitric oxide synthase expression. *J. Comp. Pathol.* 153, 197–2015. doi: 10.1016/j.jcpa.2015.10.174

Neogy, A. B., Vouldoukis, I., da Costa, J. M., and Monjour, L. (1994). Exploitation of parasite-derived antigen in therapeutic success against canine visceral leishmaniosis. *Vet. Parasitol.* 54, 367–373. doi: 10.1016/0304-4017(94)90003-5

Nicolle, C. H. (1908). Culture des corps de Leishman isoles de la rate dans trois cãs d'anemicsptenique infantile. *Bull. Soc. Pathol.* 1:121.

Okwor, I., and Uzonna, J. E. (2009). Immunotherapy as a strategy for treatment of leishmaniasis: a review of the literature. *Immunotherapy* 1, 765–776. doi: 10.2217/imt.09.40

Oldham, R. K., and Smalley, R. V. (1983). Immunotherapy: the old and the new. *J. Biol. Response Mod.* 2, 1–37.

Organização Pan-Americana da Saúde (2018). *Leishmaniasis. Epidemiological Report of the Americas*. Available online at: https://www.paho.org/hq/index.php?option=com_topics&view=article&id=29&Itemid=40754&lang=pt (accesed January 17, 2019).

Otranto, D., and Dantas-Torres, F. (2013). The prevention of canine leishmaniasis and its impact on public health. *Trends Parasitol.* 29, 339–345. doi: 10.1016/j.pt.2013.05.003

Pateraki, E., Portocala, I. R., and Labrousse, H. (1983). Antiactin and antitubulin antibodies in canine visceral leishmaniasis. *Infect. Immunol.* 42, 496–500.

Pereira, M., Valério-Bolas, A., Santos-Mateus, D., Alexandre-Pires, G., Santos, M., Rodrigues, A., et al. (2017). Canine neutrophils activate effector mechanisms in response to *Leishmania infantum*. *Vet. Parasitol.* 248, 10–20. doi: 10.1016/j.vetpar.2017.10.008

Pereira-Fonseca, D. C. M., Oliveira-Rovai, F. M., Rodas, L. A. C., Beloti, C. A. C., Torrecilha, R. B. P., Ito, P. K. R. K., et al. (2017). Dog skin parasite load, TLR-2, IL-10 and TNF-α expression and infectiousness. *Parasite Immunol.* 39, 1–7. doi: 10.1111/pim.12493

Pessoa-e-Silva, R., Souza, V. V. A., Andrade, T. A. S., Silva, A. C. O., Oliveira, G. A., Trajano-Silva, L. A. M., et al. (2019). The diagnosis of canine visceral leishmaniasis in Brazil: confronting old problems. *Exp. parasitol.* 199, 9–16. doi: 10.1016/j.exppara.2019.02.012

Reis, A. B., Giunchetti, R. C., Carrillo, E., Martins-Filho, and, O. A., and Moreno, J. (2010). Immunity to Leishmania and the rational search for vaccines against canine leishmaniasis. *Trends Parasit.* 26, 341–349. doi: 10.1016/j.pt.2010.04.005

Reis, A. B., Martins-Filho, O. A., Teixeira-Carvalho, A., Giunchetti, R. C., Carneiro, C. M., Mayrink, W., et al. (2009). Systemic and compartmentalized immune response in canine visceral leishmaniasis. *Vet. Immunol. Immunopathol.* 128, 87–95. doi: 10.1016/j.vetimm.2008.10.307

Ribeiro, R. R., Michalick, M. S. M., da Silva, M. E., Dos Santos, C. C. P., Frézard, F. J. G., and da Silva, S. M. (2018). Canine leishmaniasis: an overview of the current status and strategies for control. *BioMed Res. Int.* 2018:3296893. doi: 10.1155/2018/3296893

Roatt, B. M., Aguiar-Soares, R. D., Coura-Vital, W., Ker, H. G., Moreira, N., Vitoriano-Souza, J., et al. (2014). Immunotherapy and immunochemotherapy in visceral leishmaniasis: promising treatments for this neglected disease. *Front. Immunol.* 5:272. doi: 10.3389/fimmu.2014.00272

Roatt, B. M., Aguiar-Soares, R. D., Reis, L. E., Cardoso, J. M., Mathias, F. A., de Brito, R. C., et al. (2017). A vaccine therapy for canine visceral leishmaniasis promoted significant improvement of clinical and immune status with reduction in parasite burden. *Front. Immunol.* 8:217. doi: 10.3389/fimmu.2017.00217

Rodríguez-Cortés, A., Carrillo, E., Martorell, S., Todolí, F., Ojeda, A., Martínez-Flórez, A., et al. (2016). Compartmentalized immune response in leishmaniasis: changing patterns throughout the disease. *PLoS ONE* 11:e0155224. doi: 10.1371/journal.pone.0155224

Rodriguez-Cortes, A., Martori, C., Martinez-Florez, A., Clop, A., Amills, M., Kubejko, J., et al. (2017). Canine leishmaniasis progression is associated

with Vitamin D deficiency. *Sci. Rep*. 7, 1–10. doi: 10.1038/s41598-017-03662-4

Romero, G. A., and Boelaert, M. (2010). Control of visceral leishmaniasis in Latin America - a systematic review. *PLoS Negl. Trop. Dis*. 4:e584. doi: 10.1371/journal.pntd.0000584

Rossi, C. N., Tomokane, T. Y., Batista, L. F., Marcondes, M., Larsson, C. E., and Laurenti, M. D. (2016). *In situ* cutaneous cellular immune response in dogs naturally affected by visceral leishmaniasis. *Rev. Inst. Med. Trop. São Paulo* 58, 3–10. doi: 10.1590/S1678-9946201658048

Rossi, M., and Fasel, N. (2017). How to master the host immune system? Leishmania parasites have the solutions! *Int. Immunol.* 30, 103–111. doi: 10.1093/intimm/dxx075

Sanches, F. P., Tomokane, T. Y., Da Matta, V. L., Marcondes, M., Corbett, C. E., and Laurenti, M. D. (2014). Expression of inducible nitric oxide synthase in macrophages inversely correlates with parasitism of lymphoid tissues in dogs with visceral leishmaniasis. *Acta Vet. Scand*. 7, 56–57. doi: 10.1186/s13028-014-0057-z

Santiago, M. E. B., Neto, L. S., Alexandre, E. C., Munari, D. P., Andrade, M. M. C., Somenzari, M. A., et al. (2013). Improvement in clinical signs and cellular immunity of dogs with visceral leishmaniasis using the immunomodulator P-MAPA. *Acta Trop*. 127, 174–180. doi: 10.1016/j.actatropica.2013.04.005

Santos, F. N., Borja-Cabrera, G. P., Miyashiro, L., Grechi, J., Reis, A. B., Moreira, M. A. B., et al. (2007). Immunotherapy against experimental canine visceral leishmaniasis with the saponin enriched-Leishmune® vaccine. *Vaccine* 25, 6176–6190. doi: 10.1016/j.vaccine.2007.06.005

Scott, P., and Novais, F. O. (2016). Cutaneous leishmaniasis: immune responses in protection and pathogenesis. *Nature Rev. Immunol.* 16, 581–592. doi: 10.1038/nri.2016.72

Shimozako, H. J., Wu, J., and Massad, E. (2017). The preventive control of zoonotic visceral leishmaniasis: efficacy and economic evaluation. *Comput. Math. Methods Med*. 2017:e4797051. doi: 10.1155/2017/4797051

Singh, O. P., and Sundar, S. (2014). Immunotherapy and targeted therapies in treatment of visceral leishmaniasis: current status and future prospects. *Front. Immunol*. 5:296. doi: 10.3389/fimmu.2014.00296

Smith, B. E., Tompkins, M. B., and Breitschwerdt, E. B. (2004). Antinuclear antibodies can be detected in dog sera reactive to *Bartonella vinsonii* subsp. berkhoffii, *Ehrlichia canis*, or *Leishmania infantum* Antigens. *J. Vet. Intern. Med*. 18, 47–51. doi: 10.1111/j.1939-1676.2004.tb00134.x

Solano-Gallego, L., Koutinas, A., Miró, G., Cardoso, L., Pennisi, M. G., Ferrer, L., et al. (2009). Directions for the diagnosis, clinical staging, treatment and prevention of canine leishmaniosis. *Vet. Parasitol*. 165, 1–18. doi: 10.1016/j.vetpar.2009.05.022

Solano-Gallego, L., Montserrrat-Sangrà, S., Ordeix, L., and Martínez-Orellana, P. (2016). *Leishmania infantum*-specific production of IFN-γ and IL-10 in stimulated blood from dogs with clinical leishmaniosis. *Parasit. Vect*. 9, 1–10. doi: 10.1186/s13071-016-1598-y

Solano-Gallego, L., Riera, C., Roura, X., Iniesta, L., Gallego, M., Valladares, J. E., et al. (2001). *Leishmania infantum* - specific IgG, IgG1 and IgG2 antibody responses in healthy and ill dogs from endemic areas. Evolution in the course of infection and after treatment. *Vet. Parasitol.* 96, 265–276. doi: 10.1016/S0304-4017(00)00446-5

Solcà, M. S., Andrade, B. B., Abbehusen, M. M., Teixeira, C. R., Khouri, R., Valenzuela, J. G., et al. (2016). Circulating biomarkers of immune activation, oxidative stress and inflammation characterize severe canine visceral leishmaniasis. *Sci. Rep*. 6:32619. doi: 10.1038/srep32619.

Soulat, D., and Bogdan, C. (2017). Function of macrophage and parasite phosphatases in leishmaniasis. *Front. Immunol.* 8:1838. doi: 10.3389/fimmu.2017.01838

Taslimi, Y., Zahedifard, F., and Rafati, S. (2016). Leishmaniasis and various immunotherapeutic approaches. *Parasitology* 145, 497–507. doi: 10.1017/S003118201600216X

Toepp, A., Larson, M., Wilson, G., Grinnage-Pulley, T., Bennett, C., Leal-Lima, A., et al. (2018). Randomized, controlled, double-blinded field trial to assess *Leishmania* vaccine effectiveness as immunotherapy for canine leishmaniosis. *Vaccine* 36, 6433–6441. doi: 10.1016/j.vaccine.2018.08.087

Tonin, A. A., Calado, A. M., Bottari, N. B., Dalenogare, D., Thomé, G. R., Duarte, T., et al. (2016). Novel markers of inflammatory response and hepatic dysfunction in canine leishmaniasis. *Comp. Immunol. Microb. Infec. Dis.* 44, 61–64. doi: 10.1016/j.cimid.2015.09.004

Travi, B. L. (2014). Ethical and epidemiological dilemmas in the treatment of dogs for visceral leishmaniosis in latin America. *Biomedica* 34, 7–12. doi: 10.7705/biomedica.v34i1.2153

Trigo, J., Abbehusen, M., Netto, E. M., Nakatani, M., Pedral-Sampaio, G., Jesus, R. S., et al. (2010). Treatment of canine visceral leishmaniasis by the vaccine Leish-111f+MPL-SE. *Vaccine* 28, 3333–3340. doi: 10.1016/j.vaccine.2010.02.089

Viana, K. F., Lacerda, G., Teixeira, N. S., Rodrigues Cangussu, A. S., Sousa Aguiar, R. W., and Giunchetti, R. C. (2018). Therapeutic vaccine of killed *Leishmania amazonensis* plus saponin reduced parasite burden in dogs naturally infected with *Leishmania infantum*. *Vet. Parasitol.* 254, 98–104. doi: 10.1016/j.vetpar.2018.03.010

Werneck, G. L., Costa, C. H. N., de Carvalho, F. A. A., Pires e Cruz, M., do, S., Maguire, J. H., and Castro, M. C. (2014). Effectiveness of insecticide spraying and culling of dogs on the incidence of *Leishmania infantum* infection in humans: a cluster randomized trial in Teresina, Brazil. *PLoS Negl. Trop. Dis.* 8:e3172. doi: 10.1371/journal.pntd.0003172

World Health Organization (2010). *Control of the Leishmaniases. Report of a Meeting of the WHO Expert Committee on the Control of Leishmaniases* (Geneva). Available online at: http://whqlibdoc.who.int/trs/WHO_TRS_949_eng.pdf?ua=1 (accesed January 23, 2019).

World Health Organization (2018). *Epidemiological Situation, 2018*. Available online at: https://www.who.int/leishmaniasis/burden/en/ (accessed January 17, 2019).

Yasur-Landau, D., Jaffe, C. L., Doron-Faigenboim, A., David, L., and Baneth, G. (2017). Induction of allopurinol resistance in *Leishmania infantum* isolated from dogs. *PLOS Neg. Trop. Dis.* 11:e0005910. doi: 10.1371/journal.pntd.0005910

Conflict of Interest: The authors declare that the research was conducted in the absence of any commercial or financial relationships that could be construed as a potential conflict of interest.

frontiers in Cellular and Infection Microbiology

MINI REVIEW
published: 14 January 2020
doi: 10.3389/fcimb.2019.00424

How to B(e)-1 Important Cell During *Leishmania* Infection

Luan Firmino-Cruz[1,2], *Debora Decote-Ricardo*[3], *Daniel Claudio de Oliveira Gomes*[4], *Alexandre Morrot*[5,6], *Celio Geraldo Freire-de-Lima*[7]* and *Herbert Leonel de Matos Guedes*[1,2,8]*

[1] Laboratório de Imunofarmacologia, Instituto de Biofísica Carlos Chagas Filho, Universidade Federal Do Rio de Janeiro, Rio de Janeiro, Brazil, [2] Laboratório Interdisciplinar de Pesquisas Médicas, Instituto Oswaldo Cruz, Fundação Oswaldo Cruz, Rio de Janeiro, Brazil, [3] Instituto de Veterinária, Universidade Federal Rural Do Rio de Janeiro, Seropédica, Brazil, [4] Núcleo de Doenças Infecciosas/Núcleo de Biotecnologia, Universidade Federal Do Espírito Santo, Vitoria, Brazil, [5] Laboratório de Imunopatologia, Instituto Oswaldo Cruz, Fundação Oswaldo Cruz, Rio de Janeiro, Brazil, [6] Faculdade de Medicina, Universidade Federal Do Rio de Janeiro, Rio de Janeiro, Brazil, [7] Laboratório de Imunomodulação, Instituto de Biofísica Carlos Chagas Filho, Universidade Federal Do Rio de Janeiro, Rio de Janeiro, Brazil, [8] Núcleo Multidisciplinar de Pesquisa UFRJ—Xerém em Biologia (NUMPEX-BIO), UFRJ Campus Duque de Caxias Professor Geraldo Cidade, Universidade Federal Do Rio de Janeiro, Duque de Caxias, Brazil

OPEN ACCESS

Edited by:
Javier Moreno, Carlos III Health Institute, Spain

Reviewed by:
Hira Nakhasi, Center for Biologics Evaluation and Research (FDA), United States
Salvador Iborra, Complutense University of Madrid, Spain
Angamuthu Selvapandiyan, Jamia Hamdard University, India

***Correspondence:**
Celio Geraldo Freire-de-Lima
celio@biof.ufrj.br
Herbert Leonel de Matos Guedes
herbert@ioc.fiocruz.br;
herbert@biof.ufrj.br;
herbert@xerem.ufrj.br

Specialty section:
This article was submitted to Parasite and Host, a section of the journal Frontiers in Cellular and Infection Microbiology

Received: *05 September 2019*
Accepted: *28 November 2019*
Published: *14 January 2020*

Citation:
Firmino-Cruz L, Decote-Ricardo D, Gomes DCO, Morrot A, Freire-de-Lima CG and de Matos Guedes HL (2020) How to B(e)-1 Important Cell During Leishmania Infection. Front. Cell. Infect. Microbiol. 9:424. doi: 10.3389/fcimb.2019.00424

B-1 cells are an innate-like population of B lymphocytes that are subdivided into B-1a and B-1b distinguished by the presence or absence of CD5, respectively. B-1 cells can act as regulatory B cells, are able to present antigen and produce IL-10. Leishmaniasis in humans is a complex of diseases caused by parasites of the genus *Leishmania*. More than 20 species can infect humans, with each species causing the development of different immunological responses in the host. Susceptibility is usually related to the production of anti-inflammatory cytokines while the production of Th1 cytokines is indicative of resistance. However, few studies have attempted to evaluate the role of B-1 cells during either the *in vivo* infection or *in vitro* interaction with *Leishmania* parasites. *In vivo* studies were performed using XID mice model, BALB/Xid mice have a mutation in the Bruton's tyrosine kinase, which is an important enzyme for developing B-1 and maturing B-2 lymphocytes leading to the presence of immature B-2 cells. Here, we compile these studies and assess the influence of B-1 cells on disease progression with different *Leishmania* species.

Keywords: Leishmaniasis, BALB/XID, B-1 cells, B-1CDP cells, IL-10

INTRODUCTION

B-1 cells are an innate-like population of B cells that are subdivided into B-1a and B-1b by the expression, or lack of, the cell marker CD5, respectively (Kantor et al., 1992; Stall et al., 1992). While the B-1a subset can be generated from precursors in the fetal liver (Tung et al., 2006), the B-1b subset is generated from precursors in the bone marrow (Tung et al., 2006) and can recognize a larger variety of antigens, including intracellular antigens (Cunningham et al., 2014). They are found mainly in the peritoneal and pleural cavities. B-1 cells have the ability to self-renew to survive long term, and have been shown to expand upon adoptive cell transfer. These cells can also secrete IgM without foreign antigen exposure (Kantor et al., 1992; Stall et al., 1992; Baumgarth, 2017), as well as naturally produce IL-10 (O'Garra and Howard, 1991).

The IL-10 production by B-1 cells was first suggested as an autocrine growth factor (O'Garra and Howard, 1991). However, a more recent study has shown that peritoneal B-1 cells from IL-10-knockout mice proliferate more than those from wild-type (WT) mice under LPS stimuli,

which suggests that IL-10 could act by downregulating B-1 proliferation (Sindhava et al., 2010). It has since been speculated that the IL-10 produced by B-1 cells acts as an autocrine and paracrine regulator factor (Sindhava and Bondada, 2012).

In contrast to conventional B cells (B-2 cells), B-1 cells are able to develop immunogenic memory (Alugupalli et al., 2003; De Lorenzo et al., 2007), they can act as regulatory B cells (De Lorenzo et al., 2007) and they are also related to the innate immunity through their ability to present antigens (Vigna et al., 2006).

Parasites of the genus *Leishmania* are present worldwide with more than 20 species that can infect humans. The clinical manifestations differ from species to species, forming a complex of diseases collectively named leishmaniasis. These can be subclassified based on tissue tropism as either cutaneous leishmaniasis (CL), mucocutaneous leishmaniasis (MCL), and visceral leishmaniasis (VL). In CL, the host presents a single ulcerative lesion with swollen edges filled with parasites; however, diffuse cutaneous leishmaniasis (DCL) also can occur, where the host presents many non-ulcerative lesions filled with parasites all over the body, usually when there is pre-existing immunosuppression. In VL, also known as kalazar, the host presents high parasite burdens in the spleen and liver, and when not treated it can be fatal in 95% of the cases. Finally, MCL is characterized by disfiguring lesions in the nose and mouth area that leads to loss of the whole nose and palate.

Most of what is known about resistance or susceptibility to infections with *Leishmania* spp. is based on the host cytokine profile. While T helper (Th) type 1 lymphocyte-related cytokines are generally associated with a good prognostic (IFN-γ and TNF-α), Th2-related cytokines (IL-4, IL-5, and IL-13) and anti-inflammatory cytokines (IL-10 and TGF-β) are associated with susceptibility (Scott et al., 1989; Heinzel et al., 1991; Reiner and Locksley, 1995).

Several studies have suggested a role of B cells in promoting infection with *Leishmania* spp. either directly or indirectly via production of antibody, IL-10 or PGE_2 (Hoerauf et al., 1994, 1995; Palanivel et al., 1996; Smelt et al., 2000; Colmenares et al., 2002; Buxbaum and Scott, 2005; Wanasen et al., 2008; Chu et al., 2010; Deak et al., 2010; Arcanjo et al., 2015, 2017a,b; Gonzaga et al., 2015, 2017; Geraldo et al., 2016). Taking CL as example, B cells are thought to be harmful to the host response. BALB/JhD, which lacks B cell (both B-1 and B-2), present lower lesions, antibodies and IL-10 than BALB/c mice when infected by *L. amazonensis* (Wanasen et al., 2008). Furthermore, in VL caused by *L. donovani* it is known that: mice which lack B cells are more resistant to infection (Smelt et al., 2000); marginal zone B cells impairs T cell responses (Bankoti et al., 2012); and the antibody production (Srinontong et al., 2018) as well as the presence of B cells (Silva-Barrios et al., 2016) are linked to pathogenesis. Besides conventional B-2 cells, B-1 cells also seem to be very important in this context (Hoerauf et al., 1994; Arcanjo et al., 2015, 2017a,b; Gonzaga et al., 2015, 2017; Geraldo et al., 2016) and here we visit several works trying to summarize the main findings in the field.

B-1 cells are related in the response to several intracellular pathogens, from opportunist infections such as microsporidia, in which they are important to control the infection upregulating T $CD8^+$ cells and proinflammatory cytokines (Langanke Dos Santos et al., 2018), to parasite infections. In the present work we aimed to review the current literature regarding the participation of B-1 cells in the development of *Leishmania* spp. infections in murine models.

THE ROLE OF B-1 CELL DURING *LEISHMANIA* MAJOR INFECTION

BALB/Xid mice have a mutation in the Bruton's tyrosine kinase, which is an important enzyme for developing B-1 and maturing B-2 lymphocytes (Tsukada et al., 1993) leading to the presence of immature B-2 cells (Oka et al., 1996). BALB/Xid mice infected in the footpad with *L. major* present delayed lesion development compared to WT BALB/c mice (Hoerauf et al., 1994). In addition, BALB/Xid mice have lower parasite loads at the inoculation site, draining lymph node and spleen at 3 weeks post-infection, but not at 5 weeks post-infection, compared to WT BALB/c mice (**Figure 1A**) (Hoerauf et al., 1994).

Peritoneal B cells (mainly B-1) were shown to produce IL-10 *in vitro*, and in the presence of *L. major* extract (Lm extract) and IL-4 stimulus per 66 h, the cells produce even more IL-10 than the non-stimulated control (Hoerauf et al., 1994). Moreover, intraperitoneal (i.p.) injection of Lm extract induces peritoneal B-1 cell proliferation and IL-10 production in BALB/c mice (**Figure 1A**), but not in C57BL/6 mice (Palanivel et al., 1996). However, peritoneal B-1 cells from C57BL/6 mice pre-stimulated with Lm extract i.p., when restimulated with the same extract *in vitro* are able to produce more IL-10 than the control. Peritoneal B-1 cells derived from BALB/c mice pre-stimulated with Lm extract i.p., present exacerbated IL-10 production when compared to the control (Palanivel et al., 1996). Besides that, it was shown that splenic B-1a cells are the main IL-10-producing B cell subtype during *L. major* infection, leading also to a strong Th2 signature (Ronet et al., 2010).

On the other hand, peritoneal B-1 cell-derived phagocytes (B-1CDP) are more susceptible than peritoneal macrophages to infection by *L. major in vitro*, with a higher percentage of infection, in terms of both the number of cells infected and the number of parasites per cell, as well as higher parasite proliferation (**Figure 1B**) (Arcanjo et al., 2015). This was attributed to the fact that B-1CDP produce more IL-10, lipid bodies and PGE_2 endogenously than the macrophages (**Figure 1B**), and when the B-1CDP are treated with anti-IL-10 or non-steroidal anti-inflammatory drugs that inhibit PGE_2 production these cells become as susceptible as macrophages (Freire-de-Lima et al., 2000, 2006; Decote-Ricardo et al., 2017). Besides that, the treatment with non-steroidal anti-inflammatory drugs decreases the level of IL-10 produced by B-1CDP and it becomes the same as the level of IL-10 produced by macrophages (Arcanjo et al., 2015). This indicates that the IL-10 production is the key factor in the susceptibility of B-1CDP cells to *L. major* infection. To further confirm this, B-1CDP from IL-$10^{-/-}$ mice are significantly less susceptible to *L. major* than those from WT mice, with lower infection ratios and reduced parasite proliferation (Arcanjo et al., 2015).

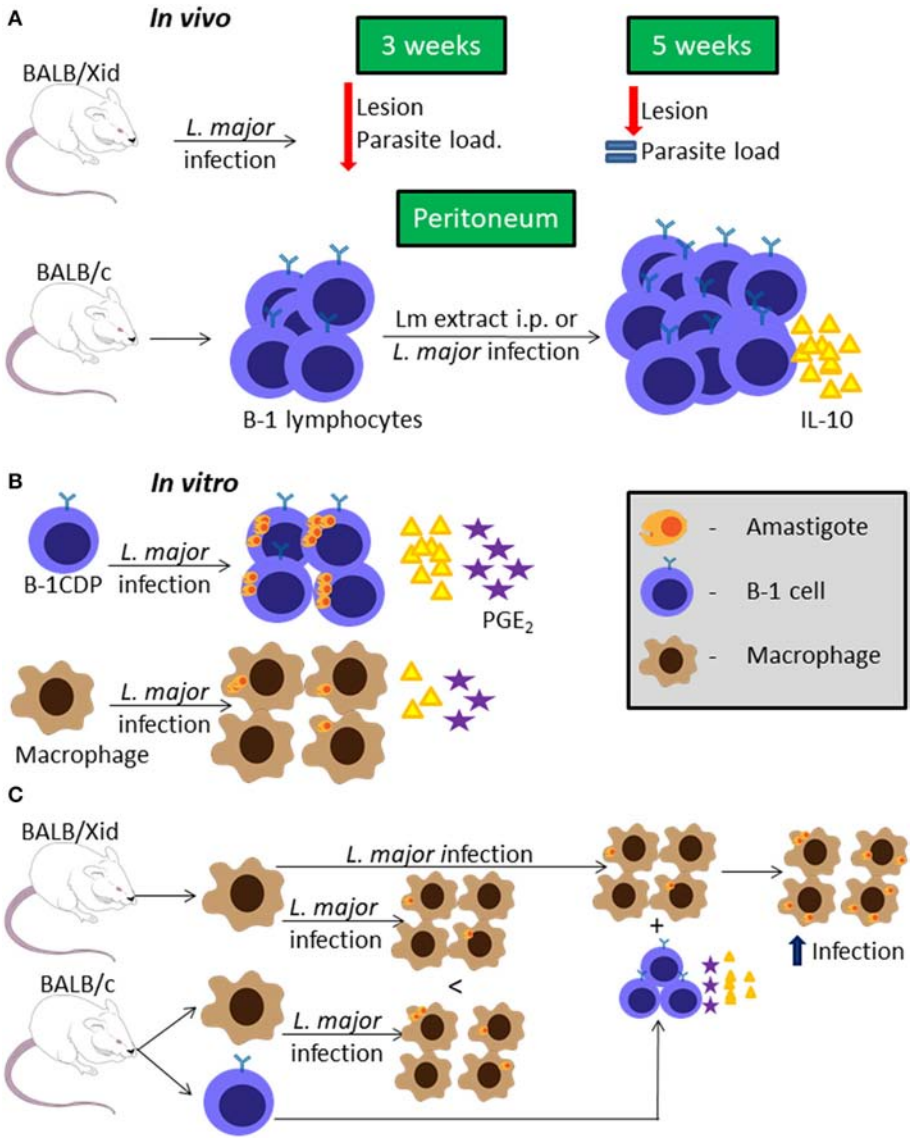

FIGURE 1 | B-1 cells and *Leishmania major* infection. Representative graphic scheme about *in vivo* infection with *L. major* or stimuli with *L. major* extract **(A)**; *in vitro* infection using BALB/c cells **(B)**; or *in vitro* infection comparing BALB/c and BALB/Xid derived cells **(C)**. The schemes show a compilation of the results obtained by different research groups.

Macrophages derived from BALB/Xid mice appear to be less susceptible to *L. major* infection than those derived from WT BALB/c mice (**Figure 1C**) (Arcanjo et al., 2017a). However, the presence of B-1 cells from WT BALB/c mice in the culture makes macrophages from both WT and BALB/Xid mice more susceptible to *L. major* infection *in vitro* and this phenomenon is not dependent on cell contact (**Figure 1C**) (Arcanjo et al., 2017a). Through the use of anti-IL-10 and non-steriodal anti-inflammatory drugs, it was again confirmed that this effect on macrophage susceptibility was due to IL-10 and PGE_2 (Arcanjo et al., 2017a). Furthermore, the presence of B-1 lymphocytes derived from IL-$10^{-/-}$ mice is not able to make macrophages susceptible as those derived from WT mice (Arcanjo et al., 2017a).

However, when BALB/c and C57BL/6 mice are lethally irradiated then reconstituted with autologous bone marrow, which leads to depletion of B-1 cells, there are no differences in the *L. major* disease progression between the B-1-depleted mice to their respective control, suggesting that B-1 cells may not be responsible for pathogenesis in this model (Babai et al., 1999).

THE ROLE OF B-1 CELL DURING *LEISHMANIA INFANTUM* INFECTION

In two different studies performed by two different groups, BALB/Xid mice were shown to be resistant to infection with *L. infantum* (same as *L. chagasi*), presenting lower splenomegaly and parasite loads in the spleen but not in the liver at final stages

of infection (Gonzaga et al., 2015; Arcanjo et al., 2017b) probably due to lower IL-10 level in the spleen (**Figure 2A**) (Arcanjo et al., 2017b). However, in the early stages of infection, there is resistance of BALB/Xid mice to infection in the liver but not in the spleen (**Figure 2A**) (Gonzaga et al., 2015).

Infection of mice with *L. infantum* leads to an increase in the percentage of $CD19^{+}CD23^{-}$ peritoneal B cells, and the B-1 cell repopulation of BALB/Xid mice leads to loss of the resistance by these transgenic mice and to a similar profile of $CD19^{+}CD23^{-}$ peritoneal B cell (**Figure 2A**) (Gonzaga et al., 2015). It was also demonstrated that the infection induces differences in intestinal compartment from mice. While BALB/c mice present decrease in the thickness of the submucosa and circular layer, BALB/Xid mice present increased thickness in those sites, but the repopulation with B-1 reduces the increase index in these mice (**Figure 2A**) (Souza et al., 2019). Besides that, the infection also caused impaired quantitative goblet cells change, in the sialomucins and sulphomucins-producing goblet cells and in the number of Paneth cells (**Figure 2A**) (Souza et al., 2019).

Moreover, IL-$10^{-/-}$ mice show resistance to *L. infantum* infection when compared to WT C57BL/6 mice, but when

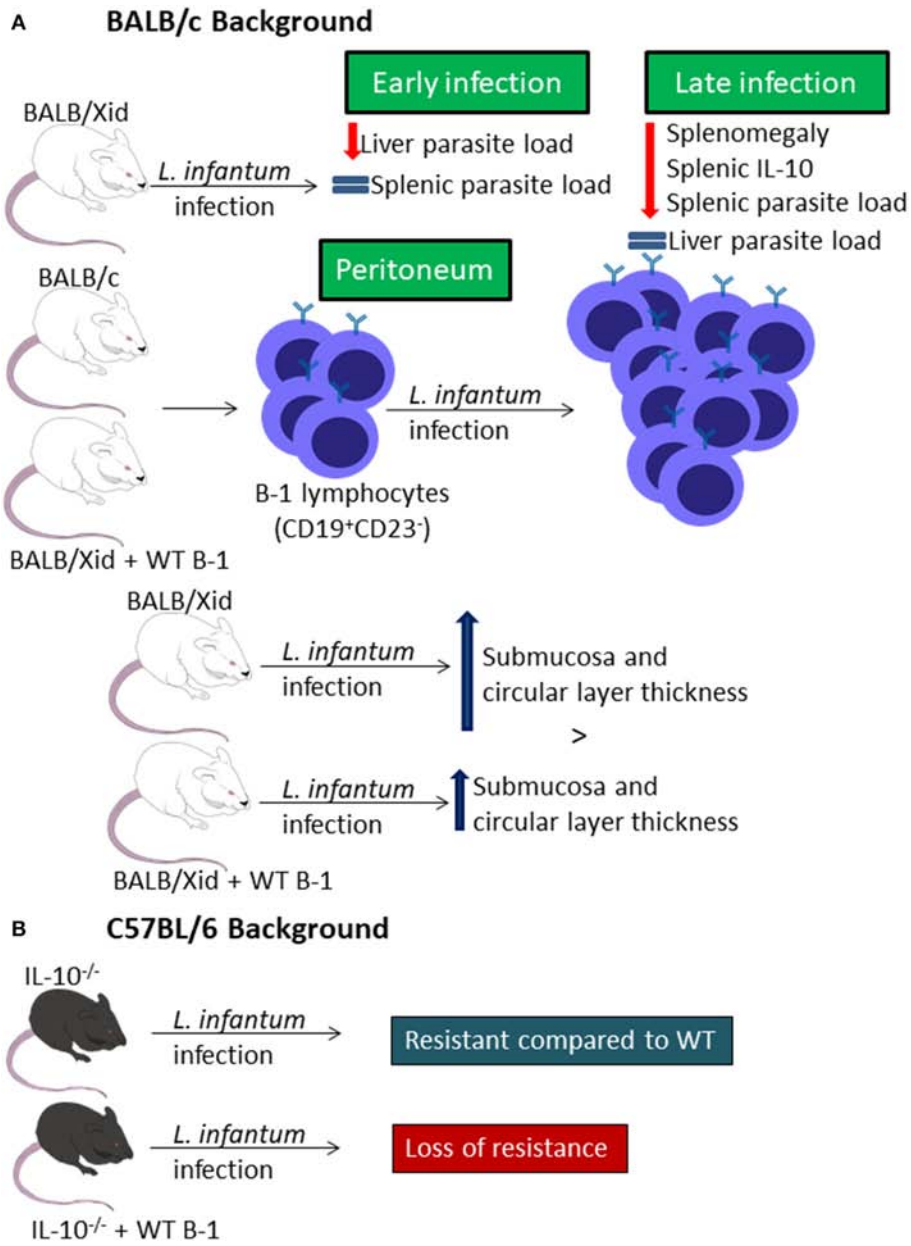

FIGURE 2 | B-1 cells and *Leishmania infantum* infection. Representative graphic scheme about experimental *in vivo* infection of BALB/c **(A)** or C57BL/6 **(B)** backgrounded mice. The schemes show a compilation of the results obtained by different research groups.

these mice receive an adoptive transfer of peritoneal B-1 cells they become as susceptible as WT C57BL/6 mice (**Figure 2B**) (Gonzaga et al., 2015).

THE ROLE OF B-1 CELL DURING *LEISHMANIA AMAZONENSIS* INFECTION

There are a few studies around the role of B-1 cells during *L. amazonensis* infection using two different strains, the Josefa strain (Firmino-Cruz et al., 2018) and the M2269 strain (Gonzaga et al., 2017). BALB/Xid mice showed resistance in lesion growth when compared to WT BALB/c mice in both studies (**Figure 3A**) (Gonzaga et al., 2017; Firmino-Cruz et al., 2018). Despite the similarities in the lesion development, there is some conflicting data regarding the parasite load, as BALB/Xid mice present higher parasite load in the footpad of mice infected with the M2269 strain compared to infected WT BALB/c mice (Gonzaga et al., 2017), but there is no differences between the groups infected with the Josefa strain (**Figure 3A**) (Firmino-Cruz et al., 2018). While one group claims that the, when repopulated with B-1 lymphocytes, BALB/Xid mice present the same phenotype as BALB/c (Gonzaga et al., 2017), the other claims that this repopulation is not able to change BALB/Xid phenotype (**Figure 3A**) (Firmino-Cruz et al., 2019).

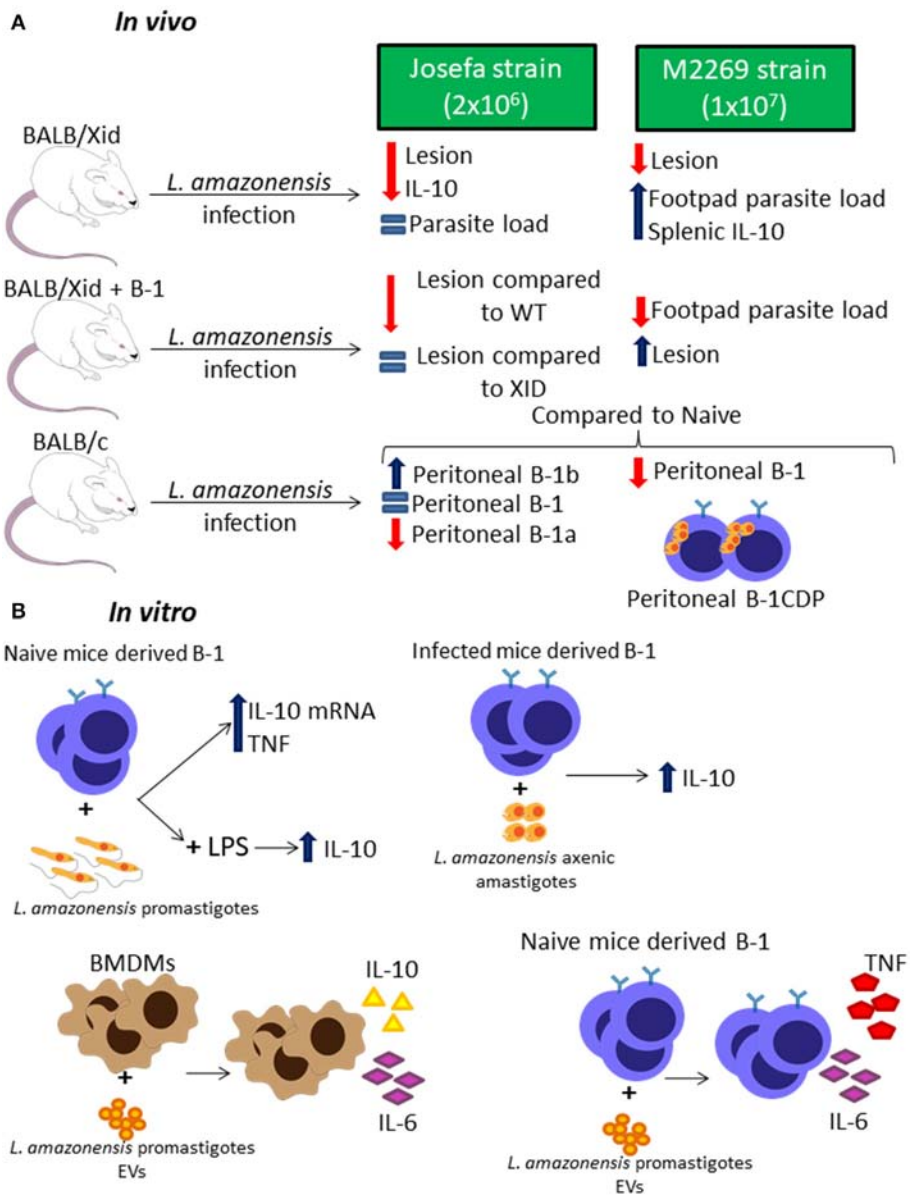

FIGURE 3 | B-1 cells and *Leishmania amazonensis* infection. Representative graphic scheme about *in vivo* **(A)** and *in vitro* **(B)** infection with *L. amazonensis* parasites. The schemes show a compilation of the results obtained by different research groups.

In addition, IL-10 production in these infected mice is also controversial since one group claims that BALB/Xid present a higher level of this cytokine in the spleen (Gonzaga et al., 2017), while the other shows that BALB/Xid present lower IL-10 levels in the footpads, spleen and draining lymph nodes when compared to WT BALB/c mice (**Figure 3A**) (Firmino-Cruz et al., 2018). It is very important to notice that the differences between these finding perhaps are related to the different parasite strain and load of infection used by each group, which can make a huge difference to the final phenotype (Loeuillet et al., 2016).

Interestingly, *L. amazonensis* infection modulates the B-1 cell profile in WT mice (**Figure 3A**) (Gonzaga et al., 2017; Firmino-Cruz et al., 2019). Besides that, the infection also alters the B-1 subtypes profile, increasing B-1b levels and severely decreasing B-1a levels (**Figure 3A**) (Firmino-Cruz et al., 2019). The interaction between peritoneal B-1 lymphocytes derived from naïve mice and *L. amazonensis* alone *in vitro* does not induce IL-10 production (Geraldo et al., 2016; Firmino-Cruz et al., 2019), even though there is an increase in the production of the mRNA of this cytokine (**Figure 3B**) (Geraldo et al., 2016). However, *L. amazonensis* is able to increase the IL-10 release caused by LPS and peritoneal B-1 cells derived from infected mice, when interacting to *L. amazonensis* axenic amastigotes, are able to produce more IL-10 than the ones derived from naïve mice (**Figure 3B**) (Firmino-Cruz et al., 2019). Moreover, the B-1 cell is able to induce the production of TNF in interaction with promastigotes (**Figure 3B**) (Geraldo et al., 2016). Recent studies have demonstrated that *L. amazonensis* promastigotes are able to release extracellular vesicles (EVs) which can induce bone marrow-derived macrophages (BMDMs) to increase the expression of IL-10 and IL-6, however those EVs act in B-1 cells differently, increasing IL-6 and TNF instead of IL-10 (**Figure 3B**) (Barbosa et al., 2018).

B-1 cells are not able to phagocytose *L. amazonensis*, however, B-1CDP cells can internalize more *L. amazonensis* parasites than peritoneal and medullar macrophages at 16 h and 24 h of infection (Geraldo et al., 2016). This phagocytic capacity was blocked by the presence of D-mannose and anti-complement receptor 3 (CR3) (Geraldo et al., 2016). B-1CDP cells can also phagocytose *L. amazonensis in vivo* (**Figure 3A**) (Geraldo et al., 2016).

CONCLUDING REMARKS

In conclusion, the role of B-1 cells in infection by *Leishmania* spp. is still unclear. While a few groups were able to link pathogenesis with the presence of B-1 cells (Hoerauf et al., 1994; Arcanjo et al., 2015, 2017a,b; Gonzaga et al., 2015, 2017) other have shown that *in vivo* this is more complex (Babai et al., 1999). The fact is that the presence of *Leishmania* spp. seems to induce responses in B-1 cells, such as cytokine production (Babai et al., 1999; Arcanjo et al., 2015, 2017b; Gonzaga et al., 2015, 2017; Geraldo et al., 2016; Firmino-Cruz et al., 2019) and lipid body formation (Arcanjo et al., 2015, 2017a). However, the B-1 cell susceptibility to *Leishmania* spp. infection seems to be linked to the production of IL-10 in most of cases (Hoerauf et al., 1994; Palanivel et al., 1996; Arcanjo et al., 2015, 2017a,b; Gonzaga et al., 2015, 2017; Geraldo et al., 2016) suggesting that this cytokine promotes infection, which is not restricted to B-1 cells endogenously, but also in relation to other cells, such as macrophages (Arcanjo et al., 2017a).

There are no many papers regarding the B-1 role during infection by genus *Leishmania*. Most have been done with *Leishmania major*, *Leishmania amazonensis,* and *Leishmania infantum*. Besides that, there still many open questions: Can B-1 cells migrate to the lesion site during CL? Can they migrate to lymph nodes and act as APCs? How physiologic is B-1 CDP and how they act during the each infection? And most important, do they act the same way between species and strains?

More studies are still necessary to gain a complete understanding of B-1 lymphocytes during *Leishmania* spp. infection, especially because there are many species of great clinical impact that have not been checked yet.

AUTHOR CONTRIBUTIONS

LF-C, DD-R, DCOG, AM, CGFL and HG wrote the review. All authors read and approved the final version of the manuscript.

FUNDING

We received financial support from Programa Jovem Cientista do Nosso Estado (FAPERJ - E-26/202.674/2018); Productivity Fellowships from Conselho Nacional de Desenvolvimento Científico e Tecnológico (304712/2016-7) and Agency for Support and Evaluation of Graduate Education (CAPES) Finance code 001. The funders had no role in study design, data collection and analysis, decision to publish, or preparation of the manuscript.

REFERENCES

Alugupalli, K. R., Gerstein, R. M., Chen, J., Szomolanyi-Tsuda, E., Woodland, R. T., and Leong, J. M. (2003). The resolution of relapsing fever borreliosis requires IgM and is concurrent with expansion of B1b lymphocytes. *J. Immunol.* 170, 3819–3827. doi: 10.4049/jimmunol.170.7.3819

Arcanjo, A. F., LaRocque-de-Freitas, I. F., Rocha, J. D., Zamith, D., Costa-da-Silva, A. C., Nunes, M. P., et al. (2015). The PGE_2/IL-10 axis determines susceptibility of B-1 cell-derived phagocytes (B-1CDP) to Leishmania major infection. *PLoS ONE* 10, 1–18. doi: 10.1371/journal.pone.0124888

Arcanjo, A. F., Nico, D., de Castro, G. M. M., da Silva Fontes, Y., Saltarelli, P., Decote-Ricardo, D., et al. (2017b). Dependency of B-1 cells in the maintenance of splenic interleukin-10 producing cells and impairment of macrophage resistance in visceral leishmaniasis. *Front. Microbiol.* 8, 1–7. doi: 10.3389/fmicb.2017.00978

Arcanjo, A. F., Nunes, M. P., Silva-Junior, E. B., Leandro, M., da Rocha, J. D. B., Morrot, A., et al. (2017a). B-1 cells modulate the murine macrophage

response to Leishmania major infection. *World J. Biol. Chem.* 8, 151–162. doi: 10.4331/wjbc.v8.i2.151

Babai, B., Louzir, H., Cazenave, P. A., and Dellagi, K. (1999). Depletion of peritoneal CD5+ B cells has no effect on the course of Leishmania major infection in susceptible and resistant mice. *Clin. Exp. Immunol.* 117, 123–129. doi: 10.1046/j.1365-2249.1999.00953.x

Bankoti, R., Gupta, K., Levchenko, A., and Stäger, S. (2012). Marginal zone B cells regulate antigen-specific T cell responses during infection. *J. Immunol.* 188, 3961–3971. doi: 10.4049/jimmunol.1102880

Barbosa, F. M. C., Dupin, T. V., Toledo, M. D. S., Reis, N. F. D. C., Ribeiro, K., Cronemberger-Andrade, A., et al. (2018). Extracellular vesicles released by *leishmania* (Leishmania) amazonensis promote disease progression and induce the production of different cytokines in macrophages and B-1 cells. *Front. Microbiol.* 9, 1–14. doi: 10.3389/fmicb.2018.03056

Baumgarth, N. (2017). A Hard(y) Look at B-1 cell development and function. *J. Immunol.* 199, 3387–3394. doi: 10.4049/jimmunol.1700943

Buxbaum, L. U., and Scott, P. (2005). Interleukin 10- and Fcγ receptor-deficient mice resolve leishmania mexicana lesions. *Infect. Immun.* 73, 2101–2108. doi: 10.1128/IAI.73.4.2101-2108.2005

Chu, N., Thomas, B. N., Patel, S. R., and Buxbaum, L. U. (2010). IgG1 is pathogenic in leishmania mexicana infection. *J. Immunol.* 185, 6939–6946. doi: 10.4049/jimmunol.1002484

Colmenares, M., Constant, S. L., Kima, P. E., and McMahon-Pratt, D. (2002). *Leishmania* pifanoi pathogenesis: Selective lack of a local cutaneous response in the absence of circulating antibody. *Infect. Immun.* 70, 6597–6605. doi: 10.1128/IAI.70.12.6597-6605.2002

Cunningham, A. F., Flores-Langarica, A., Bobat, S., Dominguez Medina, C. C., Cook, C. N., Ross, E. A., et al. (2014). B1b cells recognize protective antigens after natural infection and vaccination. *Front. Immunol.* 5, 1–11. doi: 10.3389/fimmu.2014.00535

De Lorenzo, B. H., Brito, R. R., Godoy, L. C., Lopes, J. D., and Mariano, M. (2007). Tolerogenic property of B-1b cells in a model of allergic reaction. *Immunol. Lett.* 114, 110–118. doi: 10.1016/j.imlet.2007.09.013

Deak, E., Jayakumar, A., Cho, K. W., Goldsmith-Pestana, K., Dondji, B., Lambris, J. D., et al. (2010). Murine visceral leishmaniasis: IgM and polyclonal B-cell activation lead to disease exacerbation. *Eur. J. Immunol.* 40, 1355–1368. doi: 10.1002/eji.200939455

Decote-Ricardo, D., Nunes, M. P., Morrot, A., and Freire-de-Lima, C. G. (2017). Implication of apoptosis for the pathogenesis of *Trypanosoma cruzi* infection. *Front. Immunol.* 8, 1–5. doi: 10.3389/fimmu.2017.00518

Firmino-Cruz, L., Ramos, T. D., da Fonseca-Martin, A. M., Maciel, D., da Silva, G. O., dos Santos, J. S., et al. (2019). B-1 lymphocytes are able to produce IL-10, but is not pathogenic during Leishmania (*Leishmania*) amazonensis infection. *Immunobiology*. doi: 10.1016/j.imbio.2019.10.006. [Epub ahead of print].

Firmino-Cruz, L., Ramos, T. D., da Fonseca-Martins, A. M., Maciel-Oliveira, D., Oliveira-Silva, G., Pratti, J. E. S., et al. (2018). Immunomodulating role of IL-10-producing B cells in Leishmania amazonensis infection. *Cell. Immunol.* 334, 20–30. doi: 10.1016/j.cellimm.2018.08.014

Freire-de-Lima, C. G., Nascimento, D. O., Soares, M. B., Bozza, P. T., Castro-Faria-Neto, H. C., de Mello, F. G., et al. (2000). Uptake of apoptotic cells drives the growth of a pathogenic trypanosome in macrophages. *Lett. Nat.* 403, 199–203. doi: 10.1038/35003208

Freire-de-Lima, C. G., Xiao, Y. Q., Gardai, S. J., Bratton, D. L., Schiemann, W. P., Henson, P. M. (2006). Apoptotic cells, through transforming growth factor-N_L, coordinately induce anti-inflammatory and suppress pro-inflammatory eicosanoid and NO synthesis in murine macrophages *. *J. Biol. Chem.* 281, 38376–38384. doi: 10.1074/jbc.M605146200

Geraldo, M. M., Costa, C. R., Barbosa, F. M., Vivanco, B. C., Gonzaga, W. F., Novaes E Brito, R. R., et al. (2016). *In vivo* and *in vitro* phagocytosis of *Leishmania* (Leishmania) amazonensis promastigotes by B-1 cells. *Parasite Immunol.* 38, 365–376. doi: 10.1111/pim.12324

Gonzaga, W. F., Xavier, V., Vivanco, B. C., Lopes, J. D., and Xander, P. (2015). B-1 cells contribute to susceptibility in experimental infection with *Leishmania* (Leishmania) chagasi. *Parasitology* 142, 1506–1515. doi: 10.1017/S0031182015000943

Gonzaga, W. F. K. M., Geraldo, M. M., Vivanco, B. C., Popi, A. F., Mariano, M., Batista, W. L., et al. (2017). evaluation of experimental infection with *L. (L.)* amazonensis in X-linked immunodeficient mice. *J. Parasitol.* 103, 708–717. doi: 10.1645/16-145

Heinzel, F. P., Sadick, M. D., Mutha, S. S., and Locksley, R. M. (1991). Production of interferon gamma, interleukin 2, interleukin 4, and interleukin 10 by CD4+ lymphocytes *in vivo* during healing and progressive murine leishmaniasis. *Proc. Natl. Acad. Sci. U.S.A.* 88, 7011–7015. doi: 10.1073/pnas.88.16.7011

Hoerauf, A., Solbach, W., Lohoff, M., and Röllinghoff, M. (1994). The xid defect determines an improved clinical course of murine leishmaniasis in susceptible mice. *Int. Immunol.* 6, 1117–1124. doi: 10.1093/intimm/6.8.1117

Hoerauf, A., Solbach, W., Röllinghoff, M., and Gessner, A. (1995). Effect of IL-7 treatment on Leishmania major-infected BALB.Xid mice: enhanced lymphopoiesis with sustained lack of B1 cells and clinical aggravation of disease. *Int. Immunol.* 7, 1879–1884.

Kantor, A. B., Stall, A. M., Adams, S., Herzenberg, L. A., and Herzenberg, L. (1992). A. Differential development of progenitor activity for three B-cell lineages. *Proc. Natl. Acad. Sci. U.S.A.* 89, 3320–3324. doi: 10.1073/pnas.89.8.3320

Langanke Dos Santos, D., Alvares-Saraiva, A. M., Xavier, J. G., Spadacci-Morena, D. D., Peres, G. B., and Dell'Armelina Rocha, P. R., et al. (2018). B-1 cells upregulate CD8 T lymphocytes and increase proinflammatory cytokines serum levels in oral encephalitozoonosis. *Microbes Infect.* 20, 196–204. doi: 10.1016/j.micinf.2017.11.004

Loeuillet, C., Bañuls, A. L., and Hide, M. (2016). Study of Leishmania pathogenesis in mice: experimental considerations. *Parasites Vect.* 9, 1–12. doi: 10.1186/s13071-016-1413-9

O'Garra, A., and Howard, M. (1991). Cytokines and Ly-1 (B1) B cells. *Int. Rev. Immunol.* 8, 219–234. doi: 10.3109/08830189209055575

Oka, Y., Rolink, A. G., Andersson, J., Kamanaka, M., Uchida, J., Yasui, T., et al. (1996). Profound reduction of mature B cell numbers, reactivities and serum Ig levels in mice which simultaneously carry the XID and CD40 deficiency genes. *Int. Immunol.* 8, 1675–1685. doi: 10.1093/intimm/8.11.1675

Palanivel, V., Posey, C., Horauf, A. M., Solbach, W., Piessens, W. F., and Harn, D. A. (1996). B-cell outgrowth and ligand-specific production of IL-10 correlate with Th2 dominance in certain parasitic diseases. *Exp. Parasitol.* 84, 168–177. doi: 10.1006/expr.1996.0102

Reiner, S. L., and Locksley, R. M. (1995). The regulation of immunity to leishmania major. *Annu. Rev. Immunol.* 13, 151–177. doi: 10.1146/annurev.iy.13.040195.001055

Ronet, C., Hauyon-La Torre, Y., Revaz-Breton, M., Mastelic, B., Tacchini-Cottier, F., Louis, J., et al. (2010). Regulatory B cells shape the development of Th2 immune responses in BALB/c mice infected with *Leishmania* major through IL-10 production. *J. Immunol.* 184, 886–894. doi: 10.4049/jimmunol.0901114

Scott, P., Pearce, E., Cheever, A. W., Coffman, R. L., and Sher, A. (1989). Role of cytokines and CD4+ T-cell subsets in the regulation of parasite immunity and disease. *Immunol. Rev.* 112, 161–182. doi: 10.1111/j.1600-065X.1989.tb00557.x

Silva-Barrios, S., Smans, M., Duerr, C. U., Qureshi, S. T., Fritz, J. H., Descoteaux, A., et al. (2016). Innate immune B cell activation by leishmania donovani exacerbates disease and mediates innate immune B cell activation by leishmania donovani exacerbates disease and mediates hypergammaglobulinemia. *Cell Rep.* 15, 2427–2437. doi: 10.1016/j.celrep.2016.05.028

Sindhava, V., Woodman, M. E., Stevenson, B., and Bondada, S. (2010). Interleukin-10 mediated autoregulation of murine B-1 B-cells and its role in borrelia hermsii infection. *PLoS ONE* 5, 1–17. doi: 10.1371/journal.pone.0011445

Sindhava, V. J., and Bondada, S. (2012). Multiple regulatory mechanisms control B-1 B cell activation. *Front. Immunol.* 3, 1–6. doi: 10.3389/fimmu.2012.00372

Smelt, S. C., Cotterell, S. E., Engwerda, C. R., and Kaye, P. M. (2000). B cell-deficient mice are highly resistant to leishmania donovani infection, but develop neutrophil-mediated tissue pathology. *J. Immunol.* 164, 3681–3688. doi: 10.4049/jimmunol.164.7.3681

Souza, K. D., Fernandes, E. P. A., Dos Santos, A. G. A., de Lima, L. L., Gonzaga, W. F. K. M., Xander, P., et al. (2019). Infection by Leishmania (Leishmania)

infantum chagasi causes intestinal changes B - 1 cells dependent. *Parasite Immunol.* 41, 1–8. doi: 10.1111/pim.12661

Srinontong, P., Wu, Z., Sato, K., Nagaoka, H., and Maekawa, Y. (2018). The circulating immunoglobulins negatively impact on the parasite clearance in the liver of Leishmania donovani -infected mice via dampening ROS activity. *Biochem. Biophys. Res. Commun.* 506, 20–26. doi: 10.1016/j.bbrc.2018.10.055

Stall, A. M., Adams, S., Herzenberg, L. A., and Kantor, A. B. (1992). Characteristics and development of the murine B-1b (Ly-1 B Sister) cell population. *Ann. N. Y. Acad. Sci.* 651, 33–43. doi: 10.1111/j.1749-6632.1992.tb24591.x

Tsukada, S., Saffran, D. C., Rawlings, D. J., Parolini, O., Allenm, R. C., Klisak, I., et al. (1993). Deficiente expression of a B cell cytoplasmic tyrosine kinase in human X-linked agammaglobulinemia. *Cell* 72, 279–290. doi: 10.1016/0092-8674(93)90667-F

Tung, J. W., Mrazek, M. D., Yang, Y., Herzenberg, L. A., and Herzenberg, L. A. (2006). Phenotypically distinct B cell development pathways map to the three B cell lineages in the mouse. *Proc. Natl. Acad. Sci. U.S.A.* 103, 6293–6298. doi: 10.1073/pnas.0511305103

Vigna, A. F., Almeida, S. R., Xander, P., Freymüller, E., Mariano, M., and Lopes, J. D. (2006). Granuloma formation in vitro requires B-1 cells and is modulated by *Paracoccidioides brasiliensis* gp43 antigen. *Microbes Infect.* 8, 589–597. doi: 10.1016/j.micinf.2005.06.033

Wanasen, N., Xin, L., and Soong, L. (2008). Pathogenic role of B cells and antibodies in murine Leishmania amazonensis infection. *Int. J. Parasitol.* 38, 417–429. doi: 10.1016/j.ijpara.2007.08.010

Conflict of Interest: The authors declare that the research was conducted in the absence of any commercial or financial relationships that could be construed as a potential conflict of interest.

frontiers in Cellular and Infection Microbiology

ORIGINAL RESEARCH
published: 24 January 2020
doi: 10.3389/fcimb.2019.00479

Inflammatory Dendritic Cells, Regulated by IL-4 Receptor Alpha Signaling, Control Replication, and Dissemination of *Leishmania major* in Mice

Ramona Hurdayal[1,2,3,4*†], *Natalie Eva Nieuwenhuizen*[2,3,5†], *Rethabile Khutlang*[6] *and Frank Brombacher*[2,3,4*]

[1] Department of Molecular and Cell Biology, University of Cape Town, Cape Town, South Africa, [2] International Centre for Genetic Engineering and Biotechnology, Cape Town Component, Cape Town, South Africa, [3] Division of Immunology, Department of Pathology, Faculty of Health Sciences, South African Medical Research Council on Immunology of Infectious Diseases, Institute of Infectious Diseases and Molecular Medicine, University of Cape Town, Cape Town, South Africa, [4] Faculty of Health Sciences, Wellcome Centre for Infectious Diseases Research in Africa, Institute of Infectious Diseases and Molecular Medicine, University of Cape Town, Cape Town, South Africa, [5] Department of Immunology, Max Planck Institute for Infection Biology, Berlin, Germany, [6] Identity Authentication Research Group, Defence and Security, Council for Scientific and Industrial Research, Pretoria, South Africa

OPEN ACCESS

Edited by:
Claudia Ida Brodskyn, Gonçalo Moniz Institute (IGM), Brazil

Reviewed by:
Vanessa Carregaro, University of São Paulo, Brazil
Celio Geraldo Freire-de-Lima, Federal University of Rio de Janeiro, Brazil

***Correspondence:**
Ramona Hurdayal
r.hurdayal@uct.ac.za
Frank Brombacher
brombacherfrank@gmail.com

†These authors have contributed equally to this work

Specialty section:
This article was submitted to Parasite and Host, a section of the journal Frontiers in Cellular and Infection Microbiology

Received: *30 August 2019*
Accepted: *27 December 2019*
Published: *24 January 2020*

Citation:
Hurdayal R, Nieuwenhuizen NE, Khutlang R and Brombacher F (2020) Inflammatory Dendritic Cells, Regulated by IL-4 Receptor Alpha Signaling, Control Replication, and Dissemination of Leishmania major in Mice. Front. Cell. Infect. Microbiol. 9:479. doi: 10.3389/fcimb.2019.00479

Leishmaniasis is a vector-borne disease caused by *Leishmania* parasites. Macrophages are considered the primary parasite host cell, but dendritic cells (DCs) play a critical role in initiating adaptive immunity and controlling *Leishmania* infection. Accordingly, our previous study in CD11c^{cre}IL-4Rα$^{-/lox}$ mice, which have impaired IL-4 receptor alpha (IL-4Rα) expression on CD11c^{+} cells including DCs, confirmed a protective role for IL-4/IL-13-responsive DCs in replication and dissemination of parasites during cutaneous leishmaniasis. However, it was unclear which DC subset/s was executing this function. To investigate this, we infected CD11c^{cre}IL-4Rα$^{-/lox}$ and control mice with *L. major* GFP^{+} parasites and identified subsets of infected DCs by flow cytometry. Three days after infection, CD11b^{+} DCs and CD103^{+} DCs were the main infected DC subsets in the footpad and draining lymph node, respectively and by 4 weeks post-infection, Ly6C^{+} and Ly6C^{-} CD11b^{+} DCs were the main infected DC populations in both the lymph nodes and footpads. Interestingly, Ly6C^{+}CD11b^{+} inflammatory monocyte-derived DCs but not Ly6C^{-}CD11b^{+} DCs hosted parasites in the spleen. Importantly, intracellular parasitism was significantly higher in IL-4Rα-deficient DCs. In terms of DC effector function, we found no change in the expression of pattern-recognition receptors (TLR4 and TLR9) nor in expression of the co-stimulatory marker, CD80, but MHCII expression was lower in CD11c^{cre}IL-4Rα$^{-/lox}$ mice at later time-points compared to the controls. Interestingly, in CD11c^{cre}IL-4Rα$^{-/lox}$ mice, which have reduced Th1 responses, CD11b^{+} DCs had impaired iNOS production, suggesting that DC IL-4Rα expression and NO production is important for controlling parasite numbers and preventing dissemination. Expression of the alternative activation marker arginase was unchanged in CD11b^{+} DCs in CD11^{cre}IL-4Rα$^{-/lox}$ mice compared to littermate controls, but RELM-α was

upregulated, suggesting IL-4Rα-independent alternative activation. In summary, *L. major* parasites may use Ly6C$^+$CD11b$^+$ inflammatory DCs derived from monocytes recruited to infection as "Trojan horses" to migrate to secondary lymphoid organs and peripheral sites, and DC IL-4Rα expression is important for controlling infection.

Keywords: *Leishmania major*, IL-4Rα, IL-4, dendritic cell, mice

INTRODUCTION

Leishmaniasis is a vector-borne parasitic infection caused by *Leishmania* species, obligate intracellular protozoans that are transmitted by the bite of infected female Phlebotominae sandflies. There are over 20 *Leishmania* species, and over 90 sandfly species known to transmit the parasites (Burza et al., 2018; WHO, 2019). According to the World Health Organization (WHO), ∼700,000-1 million new cases and 26,000-65,000 deaths occur annually (WHO, 2019). Cutaneous leishmaniasis is the most common form of the disease, causing disfiguring, often ulcerative skin lesions. Mucocutaneous leishmaniasis leads to destruction of the mucous membranes of the nose, mouth, and throat, while visceral leishmaniasis involves dissemination of the parasites to organs, such as the spleen, liver, and bone-marrow, and is usually fatal if left untreated (Burza et al., 2018). While vector control remains an important component in controlling disease transmission, other efforts have focused on the design of novel drugs or vaccines against *Leishmania* species (Handman, 2001).

Leishmania parasites have two morphological stages: a flagellated promastigote form that is found in the salivary glands of the insect vector and a non-motile amastigote form that is found intracellularly in the vertebrate host (Gutiérrez-Kobeh et al., 2018). Experimental infections in mouse models have shown that promastigotes infect macrophages and neutrophils that are present at the site of inoculation (Sunderkotter et al., 1993; Laskay et al., 2003; Hurdayal et al., 2013; Gutiérrez-Kobeh et al., 2018). The primary host cell for *Leishmania* species is considered the macrophage, wherein the parasites differentiate into amastigotes and divide within parasitophorous vacuoles (Lievin-Le Moal and Loiseau, 2016). The release of new amastigotes causes the infection to spread. Parasite killing is dependent on IFN-gamma (IFN-γ)-mediated classical activation of macrophages to induce killing effector molecules, such as nitric oxide (NO) (Liew et al., 1990; Stenger et al., 1994; Diefenbach et al., 1999; Holscher et al., 2006). Immunity to leishmaniasis therefore depends on the production of IL-12, which drives T helper 1 (Th1) responses and the production of IFN-γ. However, infection with *Leishmania* downregulates the capacity of macrophages to produce IL-12 (Belkaid et al., 1998). Dendritic cells (DCs), on the other hand, produce IL-12 upon taking up amastigote parasites (Woelbing et al., 2006). At the same time, they mature, upregulate MHCII and co-stimulatory molecules, and travel to the lymph nodes (LN), where they prime naïve T cells to differentiate into Th1 cells, producing IFN-γ. DCs therefore play a critical role in initiating adaptive immunity and controlling *Leishmania* infection.

Interestingly, optimal induction of Th1 responses by DCs requires the Th2 cytokine IL-4, which paradoxically promotes IL-12 production by dendritic cells via inhibition of IL-10 (Biedermann et al., 2001; Lutz et al., 2002; Yao et al., 2005; Hurdayal et al., 2013). In a previous study, we found that CD11c^{cre}IL-4Rα$^{-/lox}$ mice, in which DCs lack IL-4Rα and are thus impaired in IL-4/IL-13 signaling, were hypersusceptible to cutaneous *L. major* infection in comparison to littermate control mice (Hurdayal et al., 2013). This mouse strain showed increased footpad swelling and necrosis, increased Th2 responses as well as substantially increased parasite burdens in LN, spleens and peripheral organs, such as the liver and even the brain. Importantly, we also found that DCs themselves harbored parasites, and that iNOS production was impaired in IL-4Rα deficient CD11c^{hi}MHCII^{hi} DCs. The observation of infected DCs at peripheral sites suggested that DCs may play a role in disseminating *L. major*, and their effector responses could be important in controlling disease.

However, dendritic cells are recognized as a complex array of heterogeneous cell populations, and classified into different subsets by their surface markers, effector functions and ontogeny (Steinman and Inaba, 1999; Scott and Hunter, 2002; Zhou and Wu, 2017; Gutiérrez-Kobeh et al., 2018). Thus, we aimed to determine which subset of DCs is responsible for hosting and disseminating *L. major* parasites. We found that CD11b$^+$Ly6C$^+$ inflammatory DCs were most highly infected DC subset in CD11c^{cre}IL-4Rα$^{-/lox}$ mice, and that these DCs had impaired iNOS production in the absence of IL-4Rα signaling. This suggests that *L. major* parasites use inflammatory DCs as a "Trojan horse" to migrate to secondary lymphoid organs and peripheral sites, and that IL-4Rα signaling contributes to parasite control.

MATERIALS AND METHODS

Generation and Genotyping of CD11c^{cre}IL-4Rα$^{-/lox}$ BALB/c Mice

Generation, characterization and genotyping of CD11c^{cre}IL-4Rα$^{-/lox}$ mice was performed as previously described (Hurdayal et al., 2013). Briefly, *Cd11c*^{cre} mice were inter-crossed with IL-4Rα$^{lox/lox}$ BALB/c mice and homozygous IL-4Rα$^{-/-}$ BALB/c mice (Mohrs et al., 1999) to generate hemizygous CD11c^{cre}IL-4Rα$^{-/lox}$ mice, backcrossed to a BALB/c background for nine generations to generate CD11c^{cre}IL-4Rα$^{-/lox}$ BALB/c mice. Hemizygous littermates (IL-4Rα$^{-/lox}$) expressing functional IL-4Rα were used as wildtype controls in all experiments. All mice were housed in specific pathogen-free barrier conditions in individually ventilated cages at the University of Cape Town

biosafety level 2 animal facility. Experimental mice were age and sex matched and used between 8 and 12 weeks of age.

Ethics Statement

This study was performed in strict accordance with the recommendations of the South African national guidelines and University of Cape Town of practice for laboratory animal procedures. All mouse experiments were performed according to protocols approved by the Animal Research Ethics Committee of the Health Sciences Faculty, University of Cape Town (Permit Numbers: 009/042; 015/034). All efforts were made to minimize suffering of the animals.

Leishmania major Infection

Green-fluorescent protein (GFP)-labeled *L. major* IL81 (MHOM/IL/81/FEBNI) (Gonzalez-Leal et al., 2014) strains were maintained by continuous passage in BALB/c mice and prepared for infection as described previously (Hurdayal et al., 2013). Anesthetized mice were inoculated subcutaneously with 2×10^6 stationary phase promastigotes into the left hind footpad in a volume of 50 µl of sterile PBS. Swelling of infected footpads and weights of infected animals was monitored weekly using a Mitutoyo micrometer caliper (Brütsch, Zürich, Switzerland).

Isolation of Footpad, Lymph Node, and Spleen Cells

Single lymph node cell suspensions were prepared by pressing the draining popliteal lymph nodes through 40 µM cell-strainers. Single cell suspensions of spleen cells were isolated by pressing spleens through 70 µM cell-strainers followed by red blood cell lysis. To isolate a single cell population from the infected footpad, footpads were treated with DMEM medium supplemented with Collagenase IV (Sigma-Aldrich; 1 mg/ml) and DNase I (Sigma-Aldrich; 1 mg/ml) at 37°C for 60 min to digest muscle and collagen. Following incubation, single cell footpad suspensions were isolated by straining through 40 µM cell-strainers. All cell suspensions of lymph node, spleen and footpad were resuspended in complete DMEM (Gibco) supplemented with 10% FCS (Gibco) and penicillin and streptomycin (100 U/ml and 100 µg/ml, Gibco) and enumerated using trypan blue exclusion (Hurdayal et al., 2013).

Flow Cytometry

Antibodies against the following extracellular markers were used for flow cytometry: CD11c, CD11b, MHCII, F4/80, CD3, CD4, CD19, CD103, and Ly6C (all BD Bioscience, Erembodegem, Belgium). Footpad, pLN, and spleen cells (1×10^6) were stained with antibody cocktails in PBS containing 1% BSA/1% rat serum for 20 min at 4°C followed by fixing in 2% [w/v] PFA. For intracellular cytokine staining of dendritic cells, popliteal lymph node cells from *L. major* infected mice were seeded at 2×10^6 cells/well, surface-stained, fixed and permeabilized, and stained intracellularly for iNOS using rabbit anti-mouse iNOS (Abcam) with goat anti-rabbit PE (Abcam) and goat anti-mouse arginase (Santa Cruz Biotechnology) with donkey anti-goat PE (Abcam). Staining specificity was verified by isotype-matched antibody controls and compensation performed with BD compensation beads. Acquisition was performed using BD LSRFortessa (BD Biosciences), and data were analyzed using FlowJo software (Treestar, Ashland, OR, USA).

Ex vivo Restimulation of Footpad and Lymph Node Cells

Footpad and lymph node cells, resuspended in complete DMEM (Gibco) supplemented with 10% FCS (Gibco) and penicillin and streptomycin (100 U/ml and 100 µg/ml, Gibco) were cultured at 1×10^6 cells in 48-well plates together with 50 µg/ml soluble *Leishmania* antigen (SLA). Cells were incubated at 37°C in a humidified atmosphere containing 5% CO_2. Supernatants were collected after 72 h and stored at −80°C for cytokine analysis.

Enzyme-Linked Immunosorbent Assay (ELISA)

Cytokines (IL-4, IFN-γ, and TNF-α) in supernatants from restimulated footpad or lymph node cells were measured by indirect sandwich ELISA as previously described (Mohrs et al., 1999; Hurdayal et al., 2013).

Confocal Microscopy

OCT-embedded lymph node and spleen tissue from mice infected with GFP-*L. major* IL81 parasites for 4 weeks was cut into 10 µm cryosections. Following acetone fixation, dendritic cells were stained using biotinylated anti-CD11c mAb (BD Biosciences) and visualized by staining with a streptavidin-Cy3 conjugate (Sigma). Nuclei were stained with Hoechst. Coverslips were then mounted on sections using Mowiol® 4-88 mounting medium (Calbiochem) with anti-fade (Sigma). Images were acquired by Ziess LSM 510 confocal microscope and images quantified using a MatLab (MathWorks, Natick, Massachusetts) script developed for automated counting. A total of 16 fields were captured for each condition. At week 4 after GFP-*L. major* IL81 infection, lymph node B cells ($CD19^+CD3^-CD11c^-$) were isolated by cell sorting on a FACS Vantage cell sorter. Sorted cells were viewed live, directly in suspension in chamber slides for the presence of GFP^+ parasites by LSM 510 confocal microscopy.

Statistics

Data is given as mean ± SEM. Statistical analysis was performed using the unpaired Student's *t*-test or 1-way Anova with Bonferroni's post-test, defining differences to IL-4Rα$^{-/lox}$ mice as significant ($^*p \leq 0.05$; $^{**}p \leq 0.01$; $^{***}p \leq 0.001$) (Prism software; https://www.graphpad.com/scientific-software/prism/).

RESULTS

$Ly6C^+CD11b^+$ DCs Are the Predominant Infected DC Subset Associated With Dissemination in *L. major* Infected Mice

Previously, we found increased numbers of DCs containing GFP-expressing *L. major* parasites in CD11c^{cre}IL-4Rα$^{-/lox}$ mice compared to littermate controls using flow cytometry (Hurdayal et al., 2013). To confirm the presence of intracellular parasites in DC subsets by fluorescent imaging, CD11c^{cre}IL-4Rα$^{-/lox}$ and control mice were infected with GFP-expressing *L. major* in the hind footpad. As found previously (Hurdayal

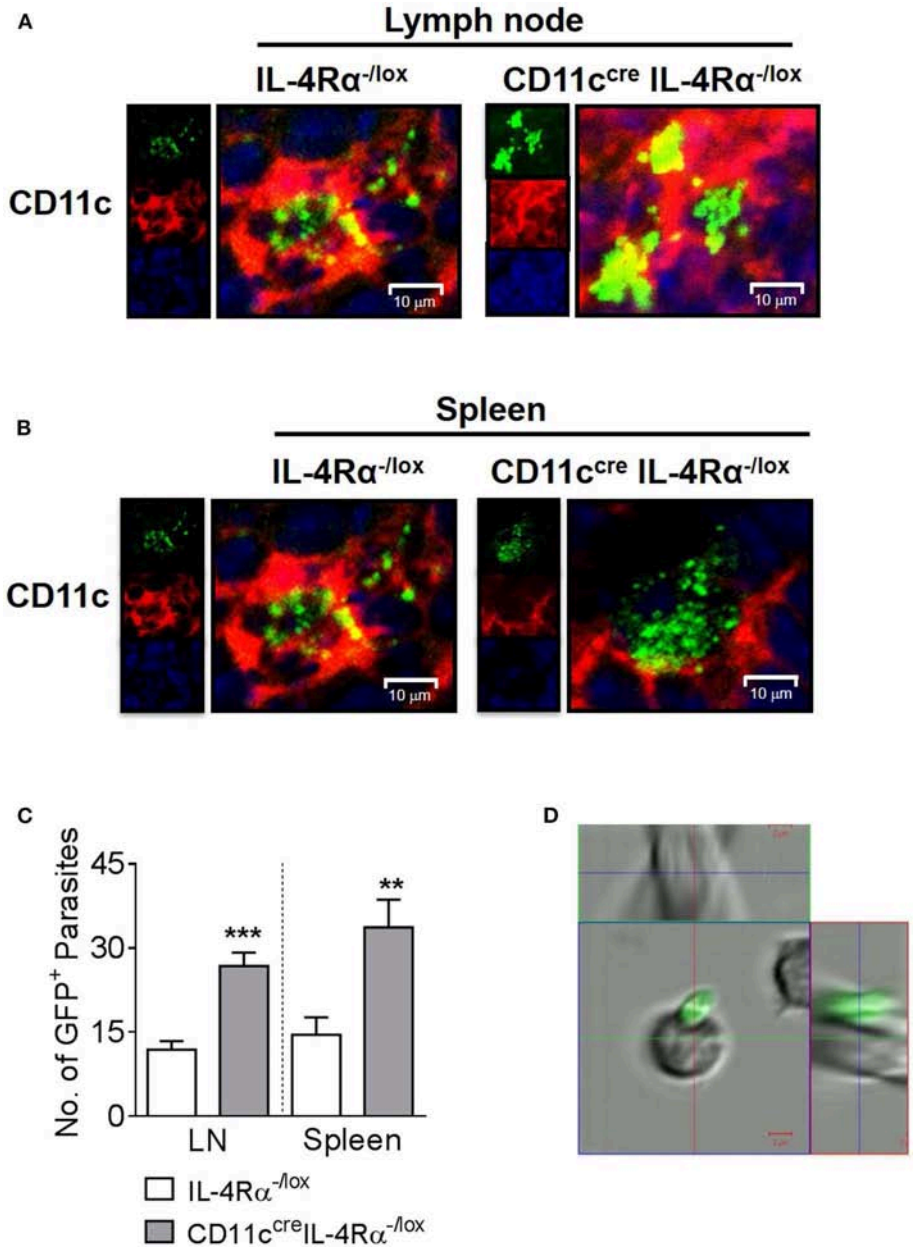

FIGURE 1 | Intracellular nature of GFP$^+$ *L. major* parasites in dendritic cells of lymph nodes and spleen. Mice were infected subcutaneously with 2 × 10^5 stationary phase GFP-expressing *L. major* IL81 promastigotes into the hind footpad. After 4 weeks of infection, frozen sections of lymph node and spleen were stained with a mAb against CD11c$^+$ dendritic cells. Representative micrographs of lymph node **(A)** and spleen cryosections **(B)** showing intracellular localization of GFP$^+$ *L. major*-infected (green) CD11c$^+$ dendritic cells (red) from CD11c^{cre}IL-4Rα$^{-/lox}$ and littermate mice (original magnification ×400). Insets show individual channels. The actual number of GFP$^+$ amastigote parasites in dendritic cells from CD11c^{cre}IL-4Rα$^{-/lox}$ and littermate control mice were quantified using MatLab software in 16 fields of multiple lymph node and spleen sections **(C)** from individual mice by confocal microscopy. At the same time-point, lymph node B cells (CD19$^+$CD3$^-$CD11c$^-$) were isolated on a FACS Vantage cell sorter after staining with specific mAbs **(D)**. Live sorted cells were viewed directly in suspension in chamber slides for the location of GFP$^+$ parasites by LSM 510 confocal microscopy. Data is expressed as mean ± SEM. Statistical analysis was performed defining differences to IL-4Rα$^{-/lox}$ mice (**$p \leq 0.01$; ***$p \leq 0.001$) as significant.

et al., 2013), by week 4 post-infection, CD11c^{cre}IL-4Rα$^{-/lox}$ mice presented with fulminant cutaneous leishmaniasis, and were hypersusceptible compared to littermate control mice (**Supplementary Figure S1**). Representative confocal images of the pLN (**Figure 1A**) and spleen (**Figure 1B**) demonstrate the intracellular amastigote nature of most of the GFP$^+$ parasites in CD11c$^+$ cells, indicating that these cell populations were harboring whole parasites and not fragments of GFP.

Automated quantification of intracellular GFP$^+$ *L. major* amastigote parasites in the cryo-fixed tissue sections using MatLab software revealed significantly increased numbers of parasites per cell in CD11c$^+$ cells of CD11c^{cre}IL-4Rα$^{-/lox}$ mice compared to littermate control mice in both the lymph node and spleen (**Figure 1C**) in accordance with previous flow cytometry data (Hurdayal et al., 2013). In contrast, confocal imaging of FACS-sorted B cells demonstrated GFP$^+$ parasites adhering to the outside of the cells and not intracellularly (**Figure 1D**) confirming that lymphocyte populations do not support replication of intracellular *Leishmania*. This illustrates the importance of confirming that GFP$^+$ cells actually harbor intracellular pathogens. Altogether, this strengthens and confirms previous data, in which CD11c-expressing cells served as a reservoir for pathogen replication (Heyde et al., 2018), and showed increased infection in the absence of IL-4-signaling via the IL-4Rα chain (Hurdayal et al., 2013).

Since DCs represent a highly heterogeneous cell population comprising various subsets defined by their effector functions and surface markers (Steinman and Inaba, 1999; Scott and Hunter, 2002; Zhou and Wu, 2017), we sought to investigate if any particular DC subset was important in harboring and disseminating *L. major* in infected mice. To determine which subsets harbor *L. major* after infection, CD11c^{cre}IL-4Rα$^{-/lox}$ and littermate control mice were infected in the footpads as above and infected cell populations were tracked by flow cytometry at early (day 3) and late (week 4) stages of infection. DC subsets were identified by their expression of particular cell-surface markers, focusing on the lymphoid and myeloid DC subsets. In line with their limited phagocytic ability (Pulendran et al., 1997), lymphoid-resident DCs (CD4$^+$CD11c^{hi}CD3$^-$ and CD8$^+$CD11c^{hi}CD3$^-$) DCs were the least infected DC population, both at day 3 and at week 4 post-*L. major* infection in both CD11c^{cre}IL-4Rα$^{-/lox}$ and littermate control mice. Myeloid-derived DCs are a migratory subset of conventional DCs, known to take up antigen at the infection site and migrate to the draining LN for presentation to antigen-specific T cells, with two major subsets being CD103$^+$ migratory tissue DCs and CD11b$^+$ DCs (Pulendran et al., 1997; Steinman and Inaba, 1999; Martinez-Lopez et al., 2015; Mayer et al., 2017). At day 3 post-*L. major* infection, CD11b$^+$ DCs (**Supplementary Figure S2**) were the main subset infected with *L. major* in the footpads of both CD11c^{cre}IL-4Rα$^{-/lox}$ mice and littermate controls (**Figure 2A**). However, in the LN of CD11c^{cre}IL-4Rα$^{-/lox}$ mice there was an increased number of GFP$^+$ CD103$^+$ DCs that had most likely carried *L. major* parasites from the tissue to the LNs (**Supplementary Figure S2** and **Figure 2B**). CD11b$^+$ DCs can be further divided into monocyte-derived/inflammatory DCs or non-monocyte derived, with monocyte-derived DCs (mo-DCs) typically expressing Ly6C and induced as part of the inflammatory response as infection progresses (Leon et al., 2007; Plantinga et al., 2013). Thus, at the later stage of infection (week 4), we included Ly6c as a marker to differentiate monocyte-derived DCs and non-monocyte derived DCs (**Supplementary Figure S2**). CD11b$^+$ DCs (both Ly6C$^+$ and Ly6C$^-$) were the main infected DC populations in both the footpads and lymph nodes at week 4 post-infection, and numbers of infected CD11b$^+$ DCs were greater in CD11c^{cre}IL-4Rα$^{-/lox}$ mice compared to littermate controls (**Figures 2C,D**). This indicates that monocyte-derived DCs that were recruited to the footpad also became infected with *L. major* parasites.

While it is known that parasites migrate from the site of infection to the lesion-draining lymph nodes, we were interested to determine if *L. major* parasites were using CD11b$^+$ Mo-DCs or CD11b$^+$ cDCs to disseminate to peripheral organs, and if IL-4/IL-13 signaling influenced this process. Therefore, we analyzed infected DC subsets in the spleens of CD11c^{cre}IL-4Rα$^{-/lox}$ and littermate control mice at 4 weeks post-*L. major* infection. The results showed that by week 4 post-infection, CD11b$^+$ DCs were the main subset containing GFP$^+$ *L. major* in the spleen (**Figure 2E**). Ly6C$^+$ CD11b$^+$ DCs consisted of two populations, Ly6C high (Ly6C^{hi}) and Ly6C intermediate (Ly6C^{int}). Both Ly6C^{hi} and Ly6C^{int} populations harbored intracellular *Leishmania*. In contrast, Ly6C$^-$ CD11b$^+$ DCs did not appear to be host cells for intracellular parasites. Importantly, the numbers of infected CD11b$^+$ DCs in FPs, LNs and spleens were higher in CD11c^{cre}IL-4Rα$^{-/lox}$ mice, suggesting a requirement for IL-4/IL-13 signaling in controlling dissemination of intracellular *Leishmania*. Taken together, these data suggest that *L. major* parasites utilize inflammatory CD11b$^+$Ly6C$^+$ DCs as "Trojan horses" to migrate to secondary lymphoid organs and that IL-4Rα-signaling contributes to parasite control in these cells.

Phenotype of CD11b$^+$ Dendritic Cells in CD11c^{cre}IL-4Rα$^{-/lox}$ Mice During *L. major* Infection

As CD11b$^+$ DCs were the most highly infected DC subset in CD11c^{cre}IL-4Rα$^{-/lox}$ mice at day 3 (footpad) and week 4 post-*L. major* infection, we checked whether the higher numbers of infected cells could be due to increased numbers of these cells overall, as a consequence of IL-4Rα-deficiency. At day 3 post-infection with GFP-expressing *L. major* IL81 parasites, similar levels of all DC subsets, including CD11b$^+$ DCs, was found in infected footpad (**Figure 3A**) and lymph node (**Figure 3B**). As there was no dissemination to the spleen at Day 3 post-infection (Hurdayal et al., 2013), analysis of DC subsets in the spleen was not performed at this time-point. The same trend in DC numbers was seen at week 4 post-infection, with similar numbers of all DC subsets, including CD11b$^+$ DCs, infiltrating the FP (**Figure 3C**), LN (**Figure 3D**), and spleen (**Figure 3E**) in CD11c^{cre}IL-4Rα$^{-/lox}$ mice and littermate controls. Moreover, analysis of CD11b$^+$ DCs in the spleen of naïve animals and at Day 1 and 3 found no difference in infiltration of CD11b$^+$ DCs between CD11c^{cre}IL-4Rα$^{-/lox}$ mice and littermate controls (**Supplementary Figure S3**). This suggests that altered effector functions of CD11b$^+$ DCs, and not increased numbers, contributed to increased parasites loads and dissemination in the absence of IL-4Rα signaling.

To investigate this further, we analyzed the effector functions of CD11b$^+$ DCs at early and late stages after *L. major* infection

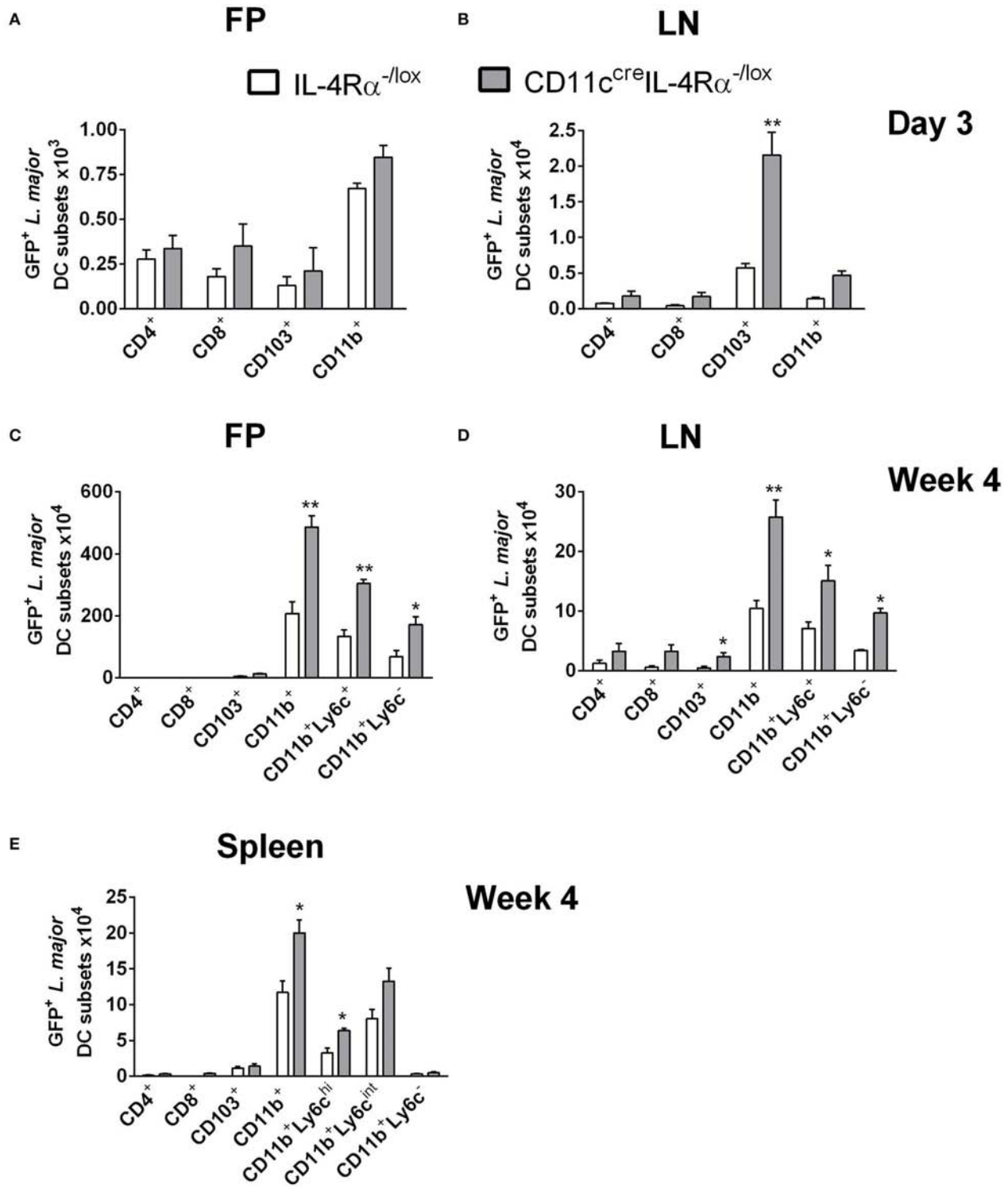

FIGURE 2 | CD11b$^+$ inflammatory dendritic cells in CD11c^{cre}IL-4R$\alpha^{-/lox}$ mice preferentially harbor *L. major* parasites during infection. CD11c^{cre}IL-4R$\alpha^{-/lox}$ and littermate mice were infected subcutaneously with GFP-labeled *L. major* IL81 promastigotes into the hind footpad. Number of GFP$^+$ *L. major* parasites was identified within dendritic cell subsets derived from footpad **(A,C)** and lymph node **(B,D)** at day 3 and week 4 after infection, respectively. Spleens were harvested to analyse GFP$^+$ *L. major* parasites in the indicated DC subsets **(E)** at week 4 after infection. Dendritic cell populations were gated as shown in **Supplementary Figure S1** and differentiated based on the following markers; conventional lymphoid-derived dendritic cells; CD4$^+$ DCs (CD11c$^+$CD4$^+$CD3$^-$), CD8$^+$ DCs (CD11c$^+$CD8$^+$CD3$^-$), and myeloid-derived dendritic cells; CD103$^+$ DCs (CD11c$^+$MHCII$^+$CD103$^+$), CD11b$^+$ DCs (CD11c$^+$CD11b$^+$MHCII$^+$), monocyte-derived DCs (CD11c$^+$CD11b$^+$MHCII$^+$Ly6C$^+$), and non-monocyte derived DCs (CD11c$^+$CD11b$^+$MHCII$^+$Ly6C$^-$). Statistical analysis was performed defining differences to IL-4R$\alpha^{-/lox}$ mice (*, $p \leq 0.05$; **, $p \leq 0.01$) as significant.

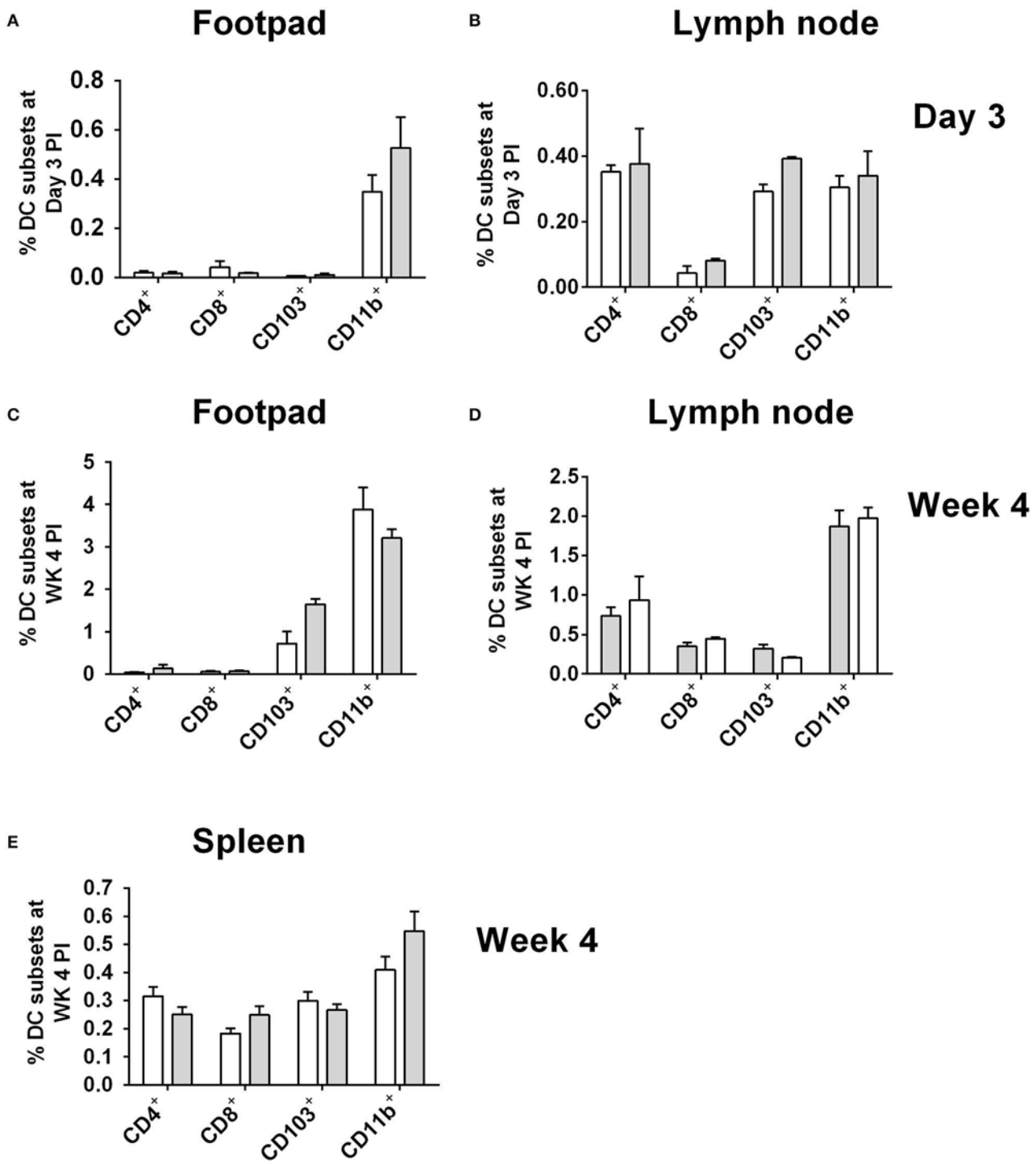

FIGURE 3 | Frequency of dendritic cells in during *L. major* IL81 infection in CD11c^{cre}IL-4Rα$^{-/lox}$ mice. CD11c^{cre}IL-4Rα$^{-/lox}$ and littermate mice were infected subcutaneously with GFP-labeled *L. major* IL81 promastigotes into the hind footpad. At day 3 and week 4 after infection, total footpad **(A,C)**, lymph node **(B,D)**, and spleen **(E)** cells were surface stained for total frequency of dendritic cells subsets. Cell populations were differentiated based on the following markers; conventional lymphoid-derived dendritic cells; CD4$^+$ DCs (CD11c$^+$CD4$^+$CD3$^-$), CD8$^+$ DCs (CD11c$^+$CD8$^+$CD3$^-$), and myeloid-derived dendritic cells; CD103$^+$ DCs (CD11c$^+$MHCII$^+$CD103$^+$), CD11b$^+$ DCs (CD11c$^+$CD11b$^+$MHCII$^+$), monocyte-derived DCs (CD11c$^+$CD11b$^+$MHCII$^+$Ly6C$^+$), and non-monocyte derived DCs (CD11c$^+$CD11b$^+$MHCII$^+$Ly6C$^-$).

in CD11c^{cre}IL-4Rα$^{-/lox}$ and control mice. DC activation, differentiation into subsets and subsequent parasite control has been linked to antigen recognition via pattern-recognition receptors (PRRs), specifically the Toll-like receptors (TLRs) (Faria et al., 2012). Since TLR4 and TLR9 are reportedly required for mounting an effective Th1 response (Faria et al., 2012) and hypersusceptible CD11c^{cre}IL-4Rα$^{-/lox}$ mice showed a shift toward Th2 responses in *L. major* infection (Hurdayal et al., 2013), we evaluated expression of these receptors on CD11b^{+} DCs by gating CD11c^{+}CD11b^{+}MHCII^{+} populations and analyzing mean fluorescence intensity of histograms of expression levels (**Supplementary Figure S2** and **Figure 4**). At Day 3 post-infection in the footpad, CD11b^{+} DCs from CD11c^{cre}IL-4Rα$^{-/lox}$ and littermate control mice expressed equivalent levels of TLR4 and TLR9 (**Figure 4A**). A similar trend was observed at week 4 post-infection in the footpad (**Figure 4B**). Once DCs are activated by pathogen products, they mature to express higher levels of MHCII and costimulatory molecules, such as CD80 and CD86, and can present antigen to prime naïve T cells (Pulendran et al., 1997), therefore we measured MHCII and CD80 expression on CD11b^{+} DCs in the lesion-draining lymph node. We and others have reported previously that lack of IL-4Rα signaling on DCs does not intrinsically alter expression of MHCII or co-stimulatory molecules, such as CD80, CD86, and CD40 *in vivo* (Cook et al., 2012; Hurdayal et al., 2013). At day 3 post-infection, CD11b^{+} DCs from CD11c^{cre}IL-4Rα$^{-/lox}$ and littermate control mice showed equivalent expression of MHCII and CD80 (**Figure 4C**), demonstrating that early activation of DCs was unaltered in the absence of IL-4Rα expression. At later time-points (week 4 post-infection), MHCII expression was lower in the absence of IL-4Rα on DCs (**Figures 4D,E**) whilst CD80 expression was similar between CD11c^{cre}IL-4Rα$^{-/lox}$ and littermate control mice (**Figure 4D**). Nevertheless, lower levels of MHCII expression did not correspond to differences in ability of DCs to prime differentiation of naïve Th cells into effector/memory T cells, since similar percentages and numbers of CD4^{+} T cells (gated FSC^{low}SSC^{low}CD3^{+}CD4^{+} as described in Hurdayal et al., 2017) were CD44^{+} in the LN of CD11c^{cre}IL-4Rα$^{-/lox}$ mice and littermate controls (**Figures 5A,B**). Similarly, we found similar levels of CD4^{+}CD44^{+} T cells in the spleens of CD11c^{cre}IL-4Rα$^{-/lox}$ and littermate control mice (**Figures 5C,D**). Taken together, these data suggest that IL-4Rα might play a role in regulation of DC maturation at the later stages of infection, but is not required for T cell activation in the lesion-draining lymph node.

IL-4Rα Regulates the Activation of CD11b^{+} DCs

Once phagocytosed, *Leishmania* parasites are eliminated by iNOS-induced nitric oxide production, which occurs predominantly in classically-activated macrophages in response to IFN-γ. In contrast, IL-4/IL-13 signaling via the IL-4Rα drives alternative activation of macrophages and arginase production, and this promotes parasite survival (Hurdayal and Brombacher, 2017). We measured cytokine production by cells from FPs of *L. major* infected mice restimulated with SLA, and found that IFN-γ production was significantly reduced in CD11c^{cre}IL-4Rα$^{-/lox}$ mice compared to littermate controls, whilst IL-4 production was dramatically increased, demonstrating a switch toward Th2-type responses at the site of infection (**Figures 6A,B**). Given the importance of inflammatory DCs in our model, we looked at production of the pro-inflammatory cytokine TNF-α by restimulated LN cells. Production of TNF-α was significantly higher in CD11c^{cre}IL-4Rα$^{-/lox}$ mice compared to those of littermate controls (**Figure 6C**). It has been shown that DCs may also be alternatively activated in schistosomiasis (Cook et al., 2012), and previously we found decreased iNOS in conventional DCs in spleens of *L. major* infected mice (Hurdayal et al., 2013). Therefore, we aimed to determine how IL-4Rα signaling affects the killing-effector phenotype of CD11b^{+} DCs in *L. major* infection. Intracellular staining of CD11b^{+} DCs in infected FPs demonstrated that intracellular iNOS expression was significantly lower in CD11b^{+} DCs of CD11c^{cre}IL-4Rα$^{-/lox}$ compared to those of littermate controls (**Figure 6D**). However, expression of the alternative activation marker arginase was unchanged in CD11b^{+} DCs in CD11c^{cre}IL-4Rα$^{-/lox}$ mice compared to littermate control mice (**Figure 6E**). Interestingly, RELMα, another marker associated with alternative activation of macrophages (Gordon, 2003) and DCs (Cook et al., 2012), was upregulated in CD11c^{cre}IL-4Rα$^{-/lox}$ mice (**Figure 6F**), suggesting IL-4/IL-4Rα-independent expression of RELMα on CD11b^{+} DCs.

DISCUSSION

Macrophages are considered the principal host cells of *Leishmania* parasites, and are key players in the parasite cycle of replication, release and entry into new host cells (Martinez-Lopez et al., 2018). However, dendritic cells can also be infected and appear to play an important role in disease progression (De Trez et al., 2009; Hurdayal et al., 2013). Dendritic cell-derived IL-12 is essential for the polarization of naïve T cells toward a Th1 subset and subsequent production of IFN-γ to control infection (Biedermann et al., 2001). In contrast, DC-derived IL-10 has been shown to dampen this process, leading to an environment that favors parasite replication and polarization of naïve T cells toward a Th2 subset (Yao et al., 2005). We previously demonstrated *in vivo* that IL-4 can instruct DCs to promote Th1 differentiation and effector iNOS production for killing of intracellular *L. major,* by using the cre/*loxP* recombination system to generate BALB/c mice deficient in the IL-4Rα gene under control of the *cd11c* locus (Hurdayal et al., 2013). In addition, we discovered that DCs function as important reservoirs for intracellular parasite replication and dissemination from the site of infection in the footpad.

DCs comprise a highly heterogeneous cell population consisting of various subsets with different characteristics (myeloid, lymphoid, migratory, plasmacytoid, and inflammatory) (Steinman and Inaba, 1999; Scott and Hunter, 2002; Zhou and Wu, 2017). They can be divided into three main groups: conventional DCs (cDCs), plasmacytoid DCs

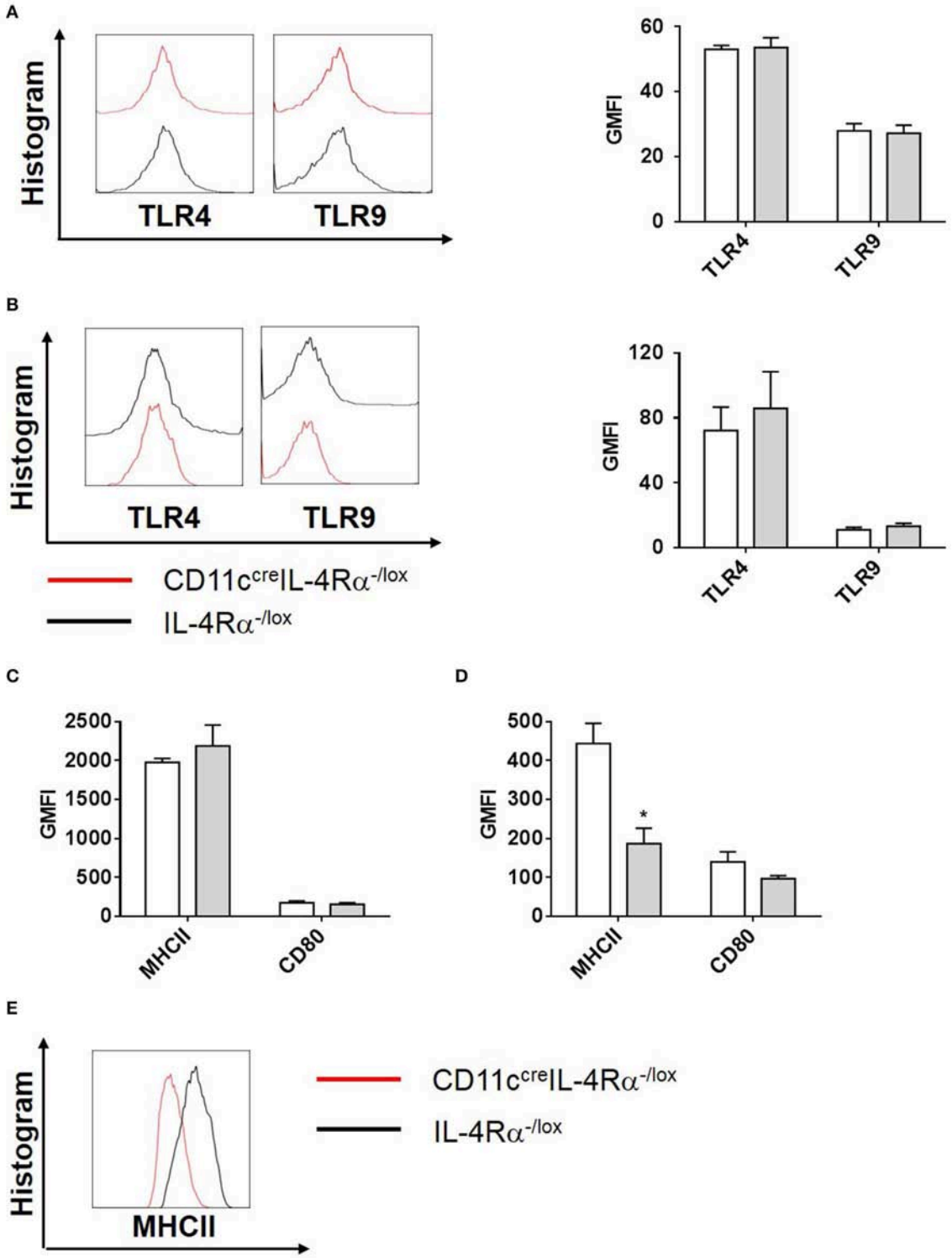

FIGURE 4 | Phenotype of CD11b^{+} DCs during *L. major* infection in CD11c^{cre}IL-4Rα$^{-/lox}$ mice and controls. CD11c^{cre}IL-4Rα$^{-/lox}$ and littermate mice were infected subcutaneously with GFP-labeled *L. major* IL81 promastigotes into the hind footpad. At week 4 after infection, total footpad cells were stained for levels of pattern-recognition receptors, TLR4 and TLR9 on CD11b^{+} DCs at day 3 **(A)** and week 4 **(B)** after infection. Similarly, activation markers (MHCII and CD80) on CD11c^{+}MHCII^{+}CD11b^{+} DCs in the footpad were analyzed at day 3 **(C)** and week 4 **(D)** after infection. Histogram plots of MHCII expression at week 4 after infection **(E)**. Statistical analysis was performed defining differences to IL-4Rα$^{-/lox}$ mice (*, $p \leq 0.05$) as significant.

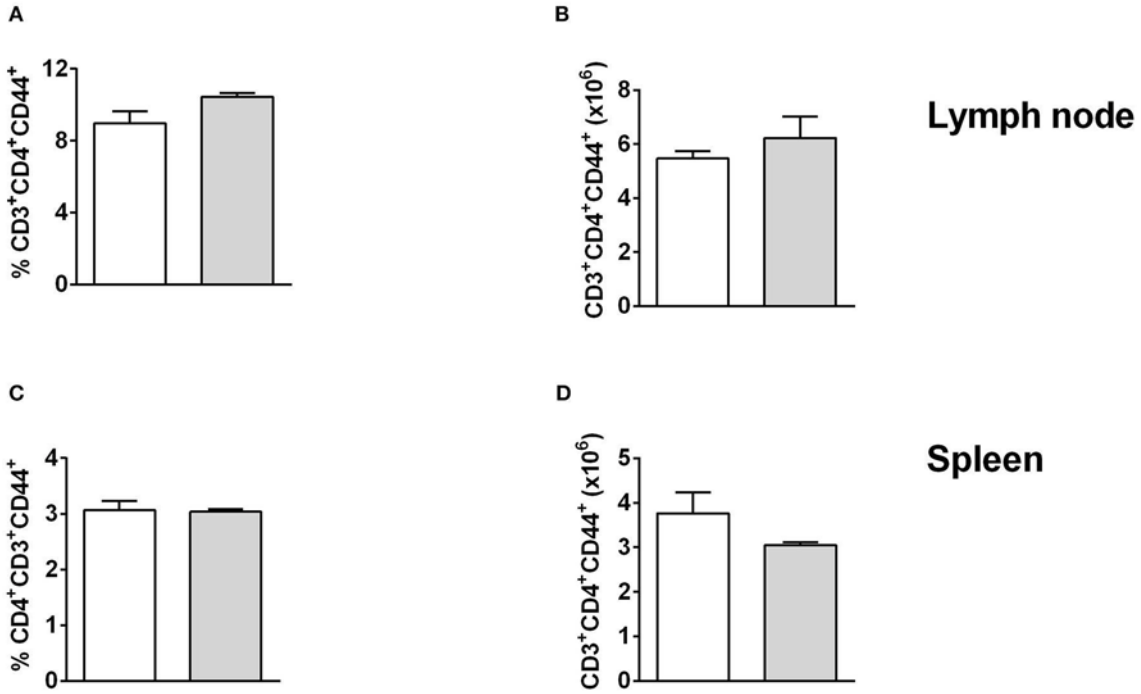

FIGURE 5 | T cell activation is unchanged in lymph node and spleen of CD11c^{cre}IL-4Rα$^{-/lox}$ mice and controls. CD11c^{cre}IL-4Rα$^{-/lox}$ and littermate mice were infected subcutaneously with GFP-labeled *L. major* IL81 promastigotes into the hind footpad. At week 4 after infection, total cells were stained for the frequency **(A,C)** and absolute number **(B**, **D)** of effector T helper cells (CD3$^+$CD4$^+$CD44$^+$) in the lesion-draining popliteal lymph node **(A,B)** and spleen **(C,D)**.

(pDCs), and monocyte-derived DCs (mo-DCs). DC-*Leishmania* interactions can vary depending on the different DC subsets involved, as they are equipped with different effector functions in terms of pathogen recognition, signal transduction and cytokine release. DCs are important for parasite uptake (via Toll-like receptors), processing, presentation, and subsequent activation of naïve T cells in adaptive immunity. They not only engulf apoptotic neutrophils harboring intracellular parasites but also engulf free extracellular promastigotes (Martinez-Lopez et al., 2018). It has also been shown that they can function as effector cells in killing of intracellular pathogens by expression of iNOS (De Trez et al., 2009; Hurdayal et al., 2013). Moreover, cytokine signaling has been shown to influence the effector function of DCs (Marovich et al., 2000; Girard-Madoux et al., 2015; Martinez-Lopez et al., 2015). After finding that mice with impaired IL-4Rα signaling on CD11c$^+$ cells (CD11c^{cre}IL-4Rα$^{-/lox}$ mice) were susceptible to *L. major* and showed increased numbers of infected DCs (Hurdayal et al., 2013), we wanted to determine which DC subset, regulated by IL-4, might be important for intracellular multiplication and the spread of *L. major* parasites during infection, and which effector functions were involved in the phenotype. To address this, we used GFP-labeled parasites to track infected DC populations and flow cytometry to identify subsets of dendritic cells infiltrating the footpad, LN and spleen during the early (Day 3) and late stages (week 4) of *L. major* infection.

During early stages of infection in the skin, recruited monocytes are believed to differentiate into effector cells for uptake, processing and transport of antigen to the draining LN. It is therefore not surprising that migratory CD103$^+$ DCs, which are derived from monocytes (Jakubzick et al., 2008; Del Rio et al., 2010), were the main source of infected cells in the draining popliteal LN at the early stage (day 3) of infection. CD103$^+$ DCs are reported to be the main source of IL-12 upon infection with *L. major* parasites, important in inducing local Th1 immunity (Martinez-Lopez et al., 2015). Interestingly, the absence of IL-4/IL-13 signaling in these cells increased the percentage of cells that contained parasites, while the number of CD103$^+$ DCs remained similar, suggesting that IL-4/IL-13 signaling to CD103$^+$ migratory DCs could represent an early control mechanism for establishment of infection in the LN. A previous study also reported that DCs were the primary infected cell population in the draining LN of *L. major* infected mice, but did not examine DC subsets (Muraille et al., 2003). Our study expands upon these findings by demonstrating that CD103$^+$ tissue DCs may be responsible for trafficking parasites to the draining LN at the onset of infection. This concept is supported by a study involving influenza virus infection in the lung, which demonstrated that CD103$^+$ DCs were the cells that carried intact viral protein to the draining LNs, and that this occurred as early as 12 h after inoculation, peaking at 48 h after infection (Helft et al., 2012). Previously we showed that pDCs also harbor parasites at the site of infection early (day 3) after parasite inoculation (Hurdayal et al., 2013).

During the later stage of infection (week 4), we found that CD11b$^+$ DCs, consisting of both monocyte-derived

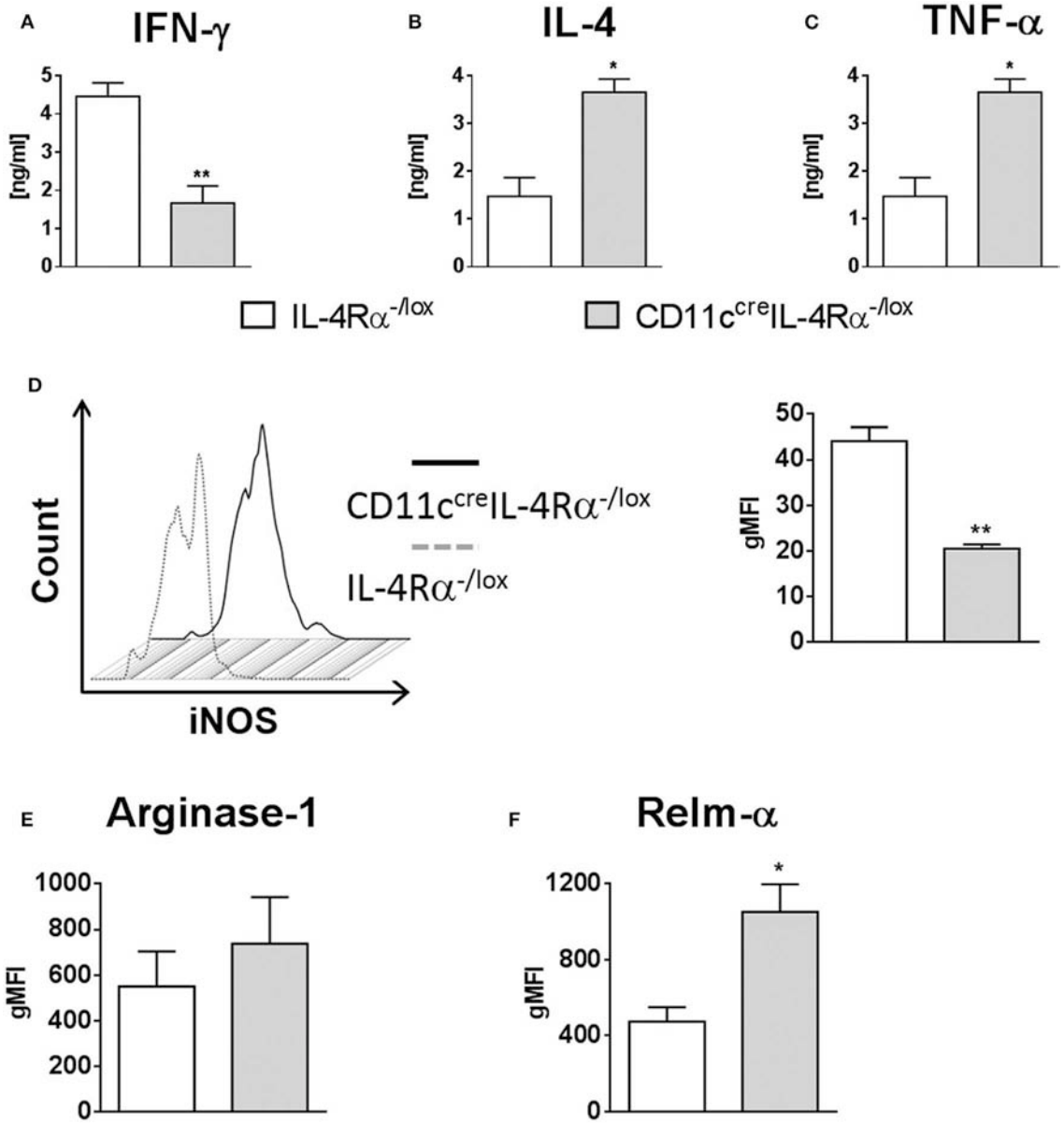

FIGURE 6 | IL-4Rα regulates the activation of CD11b$^+$ DCs during *L. major* infection in CD11c^{cre}IL-4Rα$^{-/lox}$ mice and controls. CD11c^{cre}IL-4Rα$^{-/lox}$ and littermate mice were infected subcutaneously with GFP-labeled *L. major* IL81 promastigotes into the hind footpad. At week 4 after infection, total footpad cells were re-stimulated with soluble *Leishmania* antigen (SLA) for 72 h and levels of IFN-γ **(A)** and IL-4 **(B)** was determined in cell supernatants by ELISA. TNF-α **(C)** was determined in draining lymph-node cells by ELISA following SLA stimulation. To analyse classical and alternate activation of DCs, CD11b$^+$ DCs of total footpad cells were stained for intracellular levels of inducible nitric oxide synthase (iNOS) **(D)**, arginase **(E)**, and resistin-like molecule alpha-RELM-α **(F)** at week 4 after *L. major* infection. Statistical analysis was performed defining differences to IL-4Rα$^{-/lox}$ mice (*, $p \leq 0.05$; **, $p \leq 0.01$) as significant.

inflammatory DCs (Ly6C$^+$) (Leon et al., 2007) and conventional DCs (Ly6C), were the main infected cells in both the FP and LN of BALB/c mice infected with *L. major*. Similar to what was seen with the CD103$^+$ DCs, the frequency of parasite-infected CD11b$^+$ DCs increased strikingly in the absence of IL-4-responsivness, suggesting that IL-4Rα-signaling on DCs contributes to intracellular parasitism of DCs themselves. In fact, all DCs subsets analyzed had increased parasite loads in the absence of IL-4Rα on DCs, while numbers of DCs infiltrating tissues were similar between CD11c^{cre}IL-4Rα$^{-/lox}$ mice and littermate controls. This suggests that differences in DC effector functions were responsible for the increased parasite replication and dissemination seen during infection. Our analysis demonstrated that hypersusceptibility, in the absence of IL-4-responsive DCs during *L. major* infection was not a consequence of altered expression of pattern recognition receptors (TLR4, TLR9) or expression of the co-stimulatory marker CD80. DC-derived MHCII levels were similar in CD11c^{cre}IL-4Rα$^{-/lox}$

mice and littermate controls at day 3, but at week 4 they were decreased in CD11c^{cre}IL-4Rα$^{-/lox}$ mice, although activation of Th cells as measured by CD44 expression was not affected. At week 4 in the spleen, *L. major* parasites were found primarily in Ly6C$^+$CD11b$^+$ DCs whereas Ly6C$^-$CD11b$^+$ DCs were minimally infected. This suggests that *L. major* uses Ly6C$^+$ monocyte-derived inflammatory CD11b$^+$ DCs to disseminate from primary LN organs during infection. This is in line with a previous study during *Mycobacterium tuberculosis* infection, in which activated inflammatory DCs (CD11c$^+$CD11b$^+$Ly6C$^+$ DCs) showed a unique tendency to disseminate to systemic sites (Schreiber et al., 2011). In combination with the impaired ability to kill parasites because of reduced iNOS expression in these DCs, this would explain how CD11c^{cre}IL-4Rα$^{-/lox}$ mice were more susceptible to dissemination of *L. major*.

The term "classical activation" is characteristically employed for IFN-dependent activation of macrophages and secretion of nitric oxide to kill intracellular pathogens, such as *L. major* (Gordon, 2003; Gordon and Pluddemann, 2017). However, the combined evidence of several studies demonstrates that DCs can also express iNOS in order to control intracellular parasites (Serbina et al., 2003; De Trez et al., 2009; Hurdayal et al., 2013). We demonstrated previously that iNOS expression was decreased in CD11c$^+$ DCs from CD11c^{cre}IL-4Rα$^{-/lox}$ mice compared to littermate controls, most likely as a consequence of decreased Th1 responses due to lack of IL-4 instruction of DCs (Biedermann et al., 2001; Hurdayal et al., 2013). Now we have expanded on this, showing that IL-4Rα-deficient CD11b$^+$ DCs secrete decreased iNOS, which could play a significant role in parasite replication and indicates impaired classical activation. iNOS and arginase share the substrate L-arginine, and in macrophages, alternative activation of macrophages via IL-4Rα signaling leads to upregulation of arginase-1, which can promote parasite growth by arginase-dependent synthesis of polyamines (Kropf et al., 2005). Alternative activation of DCs by IL-4/IL-4Rα has been documented, in which DCs upregulate markers, such as RELM-α and Ym1/2 (Cook et al., 2012), However, DCs of CD11c^{cre}IL-4Rα$^{-/lox}$ mice have impaired responsiveness to IL-4/IL-13. Therefore, given the impaired classical activation, we examined markers of alternative activation to see whether they were affected by the loss of DC IL-4Rα signaling. Interestingly, we found that arginase-1 expression was unchanged in CD11c^{cre}IL-4Rα$^{-/lox}$ mice compared to littermate control mice, consistent with previous work showing that IL-4 does not modulate arginase-1 expression in murine DCs (Cook et al., 2012). Surprisingly however, we found that RELM-α, another marker of alternate activation (Cook et al., 2012), was upregulated in DCs of CD11c^{cre}IL-4Rα$^{-/lox}$ mice compared to littermate controls. This suggests that IL-4/IL-13-independent alternative activation of DCs can occur during *L. major* infection. Recent studies have demonstrated other mechanisms of alternative activation of macrophages. For example, interleukin-4-indiced gene 1 (IL-4I1) has been defined as a strong modulator of alternative macrophage activation (Yue et al., 2015), and is also expressed on DCs (Aubatin et al., 2018).

Suppression of monocyte function can also occur by the IFN-induced tryptophan-catabolizing enzyme indoleamine 2,3-dioxygenase (IDO) (Musso et al., 1994). Activated IDO depletes tryptophan levels and this depletion induces cell cycle arrest of T cells, ultimately increasing their apoptosis and causing immunosuppressive effects (Bilir and Sarisozen, 2017). It has been shown that IL-4 can inhibit IDO expression (Musso et al., 1994), so in the absence of responsiveness to IL-4, it is possible that DCs of CD11c^{cre}IL-4R$^{\alpha-/lox}$ mice would have increased IDO expression, resulting in a more suppressive phenotype. Support for this hypothesis comes from the observation of increased TNF-α production by LN cells of CD11c^{cre}IL-4Rα$^{-/lox}$ mice compared to controls, as TNF-α has been shown to activate IDO secretion (Braun et al., 2005; Kim et al., 2015; Bilir and Sarisozen, 2017). However, the role of IDO remains to be investigated in hypersusceptible CD11c^{cre}IL-4Rα$^{-/lox}$ mice. The function of IDO appears to be regulation of tissue inflammation (Rani et al., 2012; Bilir and Sarisozen, 2017). DCs in the CD11c^{cre}IL-4Rα$^{-/lox}$ mice expressed RELM-α, another molecule that modulates inflammation (Osborne et al., 2013). IL-4Rα independent expression of RELM-α has been recently reported during hookworm infection (Sutherland et al., 2018), and was upregulated by Ym1, another molecule typically associated with alternative macrophage activation. Previously we have shown that in the absence of IL-4Rα signaling, IL-10 can induce markers of alternative macrophage activation, including Ym1 and mannose receptor (Dewals et al., 2010). Other cytokines, such as TGF-beta and activin A have also been associated with alternative macrophage activation (Ogawa et al., 2006; Gong et al., 2012; Zhang et al., 2016). Further investigations are needed in order to clarify how cytokine signaling regulates classical and alternative activation of DCs and their interaction with intracellular pathogens.

Various lines of evidence support a role for CD11c$^+$ cells in replication of *Leishmania* parasites (Leon et al., 2007; De Trez et al., 2009; Hurdayal et al., 2013; Heyde et al., 2018). A recent study by Heyde et al. (2018) described CD11c$^+$ cells as monocyte-derived dendritic cell-like, Ly6C$^+$CCR2$^+$ monocytes (Heyde et al., 2018). These cells were highly infected and harbored parasites with the highest proliferation rate at the site of infection. Depletion of these CD11c-expressing cells resulted in a significant reduction in pathogen burden suggesting that CD11c$^+$ cells represent a selective niche for *L. major* proliferation. Our study used a different substrain of *L. major*, but most likely, the cells observed by Heyde et al. were the same subset of inflammatory, monocyte-derived Ly6C$^+$ DCs that we observed in our study. In another study, CD11b$^+$ CD11c$^+$ Ly6C$^+$ MHCII$^+$ cells were the main infected population in the footpad lesions and draining LNs of *L. major*-infected C57BL/6 mice, and the main iNOS-producing cells (De Trez et al., 2009). Such iNOS-producing inflammatory DC have also been implicated in resistance to *Listeria monocytogenes* and *Brucella melitensis* infection, and have been termed TNF-iNOS-producing DC (TipDCs) or inflammatory DCs (Serbina et al., 2003; Copin et al., 2007; Geissmann et al., 2008). In a visceral leishmaniasis study using *L. donovani*, Ly6C^{hi} inflammatory

monocytes formed an important niche for parasite survival, and blocking their recruitment to the liver and spleen using CCR2 antagonists reduced bacterial burdens (Terrazas et al., 2017). In this study, the cells were identified as $CD11b^{+}Ly6C^{hi}Ly6G^{-}$ and they expressed CD115, CCR2, and intermediate levels of MHCII and F4/80, but they did not express CD11c. Why such cells express CD11c during *L. major* infection but not *L. donovani* infection is not known and remains to be elucidated.

Various markers have been used to identify inflammatory DCs, including Ly6C, F4/80, CD64 (FcγRI), FcεRI, CCR2, DC-SIGN (CD209), and mannose receptor (CD206) (De Trez et al., 2009; Hammad et al., 2010; Langlet et al., 2012; Plantinga et al., 2013; Segura and Amigorena, 2013; Min et al., 2018). CD64 alone is not able to discriminate cDCs and moDCs within $CD11b^{+}$ DCs (Min et al., 2018). In the lung, Ly6C was a specific but insensitive marker for discriminating cDCs and moDCs, since Ly6C expression formed a continuum within $CD11b^{+}$ lung DCs, with $Ly6C^{low}$ cells found to be cDCs and $Ly6C^{hi}$ cells found to be moDCs (Plantinga et al., 2013). The combination of CD64 and FcεRI was suggested as more specific for discriminating moDCs in lung tissue (Plantinga et al., 2013). In our study, we found clear populations of $Ly6C^{hi}$ and $Ly6C^{lo}$ $CD11b^{+}$ DCs containing parasites in the LN and FP, but in the spleen we also found a population of $Ly6C^{int}$ cells. $Ly6C^{hi}$ and $Ly6C^{int}$ $CD11b^{+}$ DC populations were infected with parasites in the spleen, whereas the $Ly6C^{lo}$ $CD11b^{+}$ DC population in the spleen was not. This suggests that the $Ly6C^{int}$ population we observed may also have been moDCs, and suggests that the continuum of Ly6C expression on DCs could be to some extent tissue- and/or disease-specific.

In summary, our data suggest that $CD103^{+}$ DCs play an important role in trafficking parasites to the draining LN at the onset of infection, while later during infection $CD11b^{+}$ DCs become infected. Importantly, dissemination to secondary lymphoid organs, such as the spleen appears to be driven by the migration of $CD11b^{+}Ly6c^{+}$ DC inflammatory DCs. In addition, control of parasites in DCs relies on IL-4Rα signaling for early priming of Th1 responses, IFN-γ release and the subsequent upregulation of iNOS. In the absence of IL-4Rα, $CD11b^{+}Ly6C^{+}$ DCs provide a safe-haven for parasite replication and dissemination in the infected host. Thus, targeting inflammatory moDC responses may represent a strategy for reducing *L. major* parasite burdens and dissemination.

DATA AVAILABILITY STATEMENT

The datasets generated for this study are available on request to the corresponding author.

ETHICS STATEMENT

The animal study was reviewed and approved by Faculty of Health Sciences, Research Animal Ethics Committee, University of Cape Town.

AUTHOR CONTRIBUTIONS

RH, NN, and FB designed the study. FB provided the gene-deficient mice. RH and NN performed the experiments and analyzed results. RK performed the confocal quantification. RH and FB acquired the funding. RH and NN wrote the original draft. RH, NN, and FB edited the final version of the manuscript. All authors read and approved the final manuscript.

FUNDING

This work was supported by grants from the National Research Foundation, South Africa and the University of Cape Town (UCT) to RH. FB was supported with grants from the South African Medical Research Council (SAMRC), National Research Foundation (NRF) of South Africa, Department of Science and Technology (DST), South African Research Chair Initiative, International Center for Genetic Engineering and Biotechnology, and Wellcome Center for Infectious Diseases. NN was funded by the Medical Research Council South Africa and the Claude Leon Foundation. RK was funded by the Department of Science and Technology of the Republic of South Africa. The funders had no role in study design, data collection and analysis or decision to publish.

ACKNOWLEDGMENTS

We thank the animal facility staff, the genotyping staff and Mrs. Lizette Fick for their excellent technical assistance, as well as Prof. Dirk Lang and Mrs. Susan Cooper (Department of Human Biology, UCT) for assistance with confocal microscopy. We also thank Dr. Suraj Parihar for sharing his knowledge on the confocal microscopy unit.

SUPPLEMENTARY MATERIAL

The Supplementary Material for this article can be found online at: https://www.frontiersin.org/articles/10.3389/fcimb.2019.00479/full#supplementary-material

Supplementary Figure 1 | $CD11c^{cre}IL\text{-}4R\alpha^{-/lox}$ BALB/c are hypersusceptible to cutaneous *Leishmania major* IL81 infection. Mice were infected subcutaneously with 2×10^{6} stationary phase virulent GFP-expressing *L. major* IL81 (MHOM/IL/81/FEBNI) parasite strain into the hind footpad. Footpad swelling was measured at weekly intervals. Statistical analysis was performed defining differences to $IL\text{-}4R\alpha^{-/lox}$ mice (**, $p \leq 0.01$) as significant.

Supplementary Figure 2 | Representative gating strategy for dendritic cell subsets during *Leishmania major* infection. $CD11c^{cre}IL\text{-}4R\alpha^{-/lox}$ BALB/c and control mice were infected subcutaneously with 2×10^{6} GFP-labeled *L. major* IL81 promastigotes into the hind footpad. At day 3 or week 4 post-infection, total cells (either footpad, lymph node or spleen) were FACS-stained and gated on FSC-H/FSC-A to obtain singlets. Macrophages and granulocytes were excluded by staining for F4/80 and Ly6G, respectively. The resulting F4/80-Ly6G-negative population was gated for various DC subsets and receptors based on cell-surface markers as depicted.

Supplementary Figure 3 | Number of $CD11b^{+}$ dendritic cells is unaltered in $CD11c^{cre}IL\text{-}4R\alpha^{-/lox}$ BALB/c and control mice. $CD11c^{cre}IL\text{-}4R\alpha^{-/lox}$ BALB/c and control mice were infected subcutaneously with 2×10^{6} GFP-labeled *L. major* IL81 promastigotes into the hind footpad. At Day 0, 1, 3, and Week 4 after infection, total spleen cells were stained for $CD11c^{+}CD11b^{+}$ dendritic cells by flow cytometry, and total cell numbers enumerated based on spleen cell counts.

REFERENCES

Aubatin, A., Sako, N., Decrouy, X., Donnadieu, E., Molinier-Frenkel, V., and Castellano, F. (2018). IL4-induced gene 1 is secreted at the immune synapse and modulates TCR activation independently of its enzymatic activity. *Eur. J. Immunol.* 48, 106-119. doi: 10.1002/eji.201646769

Belkaid, Y., Butcher, B., and Sacks, D. L. (1998). Analysis of cytokine production by inflammatory mouse macrophages at the single-cell level: selective impairment of IL-12 induction in *Leishmania*-infected cells. *Eur. J. Immunol.* 28, 1389-1400. doi: 10.1002/(SICI)1521-4141(199804)28:04<1389::AID-IMMU1389>3.0.CO;2-1

Biedermann, T., Zimmermann, S., Himmelrich, H., Gumy, A., Egeter, O., Sakrauski, A. K., et al. (2001). IL-4 instructs TH1 responses and resistance to *Leishmania major* in susceptible BALB/c mice. *Nat. Immunol.* 2, 1054-1060. doi: 10.1038/ni725

Bilir, C., and Sarisozen, C. (2017). Indoleamine 2,3-dioxygenase (IDO): only an enzyme or a checkpoint controller? *J. Oncolo. Sci.* 3, 52-56. doi: 10.1016/j.jons.2017.04.001

Braun, D., Longman, R. S., and Albert, M. L. (2005). A two-step induction of indoleamine 2,3 dioxygenase (IDO) activity during dendritic-cell maturation. *Blood* 106, 2375-2381. doi: 10.1182/blood-2005-03-0979

Burza, S., Croft, S. L., and Boelaert, M. (2018). Leishmaniasis. *Lancet* 392, 951-970. doi: 10.1016/S0140-6736(18)31204-2

Cook, P. C., Jones, L. H., Jenkins, S. J., Wynn, T. A., Allen, J. E., and Macdonald, A. S. (2012). Alternatively activated dendritic cells regulate CD4+ T-cell polarization *in vitro* and *in vivo*. *Proc. Natl. Acad. Sci. U.S.A.* 109, 9977-9982. doi: 10.1073/pnas.1121231109

Copin, R., De Baetselier, P., Carlier, Y., Letesson, J. J., and Muraille, E. (2007). MyD88-dependent activation of B220-CD11b+LY-6C+ dendritic cells during brucella melitensis infection. *J. Immunol.* 178, 5182-5191. doi: 10.4049/jimmunol.178.8.5182

De Trez, C., Magez, S., Akira, S., Ryffel, B., Carlier, Y., and Muraille, E. (2009). iNOS-producing inflammatory dendritic cells constitute the major infected cell type during the chronic Leishmania major infection phase of C57BL/6 resistant mice. *PLoS Pathog.* 5:e1000494. doi: 10.1371/journal.ppat.1000494

Del Rio, M. L., Bernhardt, G., Rodriguez-Barbosa, J. I., and Forster, R. (2010). Development and functional specialization of $CD103^+$ dendritic cells. *Immunol. Rev.* 234, 268-281. doi: 10.1111/j.0105-2896.2009.00874.x

Dewals, B. G., Marillier, R. G., Hoving, J. C., Leeto, M., Schwegmann, A., and Brombacher, F. (2010). IL-4Rα-independent expression of mannose receptor and Ym1 by macrophages depends on their IL-10 responsiveness. *PLoS Negl. Trop Dis.* 4:e689. doi: 10.1371/journal.pntd.0000689

Diefenbach, A., Schindler, H., Rollinghoff, M., Yokoyama, W. M., and Bogdan, C. (1999). Requirement for type 2 NO synthase for IL-12 signaling in innate immunity. *Science* 284, 951-955. doi: 10.1126/science.284.5416.951

Faria, M. S., Reis, F. C., and Lima, A. P. (2012). Toll-like receptors in *Leishmania* infections: guardians or promoters? *J. Parasitol. Res.* 2012:930257. doi: 10.1155/2012/930257

Geissmann, F., Auffray, C., Palframan, R., Wirrig, C., Ciocca, A., Campisi, L., et al. (2008). Blood monocytes: distinct subsets, how they relate to dendritic cells, and their possible roles in the regulation of T-cell responses. *Immunol. Cell Biol.* 86, 398-408. doi: 10.1038/icb.2008.19

Girard-Madoux, M. J. H., Kautz-Neu, K., Lorenz, B., Ober-Blobaum, J. L., Von Stebut, E., and Clausen, B. E. (2015). IL-10 signaling in dendritic cells attenuates anti-*Leishmania major* immunity without affecting protective memory responses. *J. Invest. Dermatol.* 135, 2890-2894. doi: 10.1038/jid.2015.236

Gong, D., Shi, W., Yi, S. J., Chen, H., Groffen, J., and Heisterkamp, N. (2012). TGFbeta signaling plays a critical role in promoting alternative macrophage activation. *BMC Immunol.* 13:31. doi: 10.1186/1471-2172-13-31

Gonzalez-Leal, I. J., Roger, B., Schwarz, A., Schirmeister, T., Reinheckel, T., Lutz, M. B., et al. (2014). Cathepsin B in antigen-presenting cells controls mediators of the Th1 immune response during *Leishmania major* infection. *PLoS Negl. Trop Dis.* 8:e3194. doi: 10.1371/journal.pntd.0003194

Gordon, S. (2003). Alternative activation of macrophages. *Nat. Rev. Immunol.* 3, 23-35. doi: 10.1038/nri978

Gordon, S., and Pluddemann, A. (2017). Tissue macrophages: heterogeneity and functions. *BMC Biol.* 15:53. doi: 10.1186/s12915-017-0392-4

Gutiérrez-Kobeh, L., Rodríguez-González, J., Argueta-Donohué, J., Vázquez-López, R., and Wilkins-Rodríguez, A. A. (2018). *Role of Dendritic Cells in Parasitic Infections*. London: IntechOpen.

Hammad, H., Plantinga, M., Deswarte, K., Pouliot, P., Willart, M. A., Kool, M., et al. (2010). Inflammatory dendritic cells–not basophils–are necessary and sufficient for induction of Th2 immunity to inhaled house dust mite allergen. *J. Exp. Med.* 207, 2097-2111. doi: 10.1084/jem.20101563

Handman, E. (2001). Leishmaniasis: current status of vaccine development. *Clin. Microbiol. Rev.* 14, 229-243. doi: 10.1128/CMR.14.2.229-243.2001

Helft, J., Manicassamy, B., Guermonprez, P., Hashimoto, D., Silvin, A., Agudo, J., et al. (2012). Cross-presenting CD103+ dendritic cells are protected from influenza virus infection. *J. Clin. Invest.* 122, 4037–4047. doi: 10.1172/JCI60659

Heyde, S., Philipsen, L., Formaglio, P., Fu, Y., Baars, I., Hobbel, G., et al. (2018). CD11c-expressing $Ly6C^+CCR2^+$ monocytes constitute a reservoir for efficient *Leishmania* proliferation and cell-to-cell transmission. *PLoS Pathog.* 14:e1007374. doi: 10.1371/journal.ppat.1007374

Holscher, C., Arendse, B., Schwegmann, A., Myburgh, E., and Brombacher, F. (2006). Impairment of alternative macrophage activation delays cutaneous leishmaniasis in nonhealing BALB/c mice. *J. Immunol.* 176, 1115-1121. doi: 10.4049/jimmunol.176.2.1115

Hurdayal, R., and Brombacher, F. (2017). Interleukin-4 receptor alpha: from innate to adaptive immunity in murine models of cutaneous leishmaniasis. *Front. Immunol.* 8:1354. doi: 10.3389/fimmu.2017.01354

Hurdayal, R., Ndlovu, H. H., Revaz-Breton, M., Parihar, S. P., Nono, J. K., Govender, M., et al. (2017). IL-4-producing B cells regulate T helper cell dichotomy in type 1- and type 2-controlled diseases. *Proc. Natl. Acad. Sci. USA*, 114, E8430–E8439. doi: 10.1073/pnas.1708125114

Hurdayal, R., Nieuwenhuizen, N. E., Revaz-Breton, M., Smith, L., Hoving, J. C., Parihar, S. P., et al. (2013). Deletion of IL-4 receptor alpha on dendritic cells renders BALB/c mice hypersusceptible to *Leishmania major* infection. *PLoS Pathog.* 9:e1003699. doi: 10.1371/journal.ppat.1003699

Jakubzick, C., Tacke, F., Ginhoux, F., Wagers, A. J., Van Rooijen, N., Mack, M., et al. (2008). Blood monocyte subsets differentially give rise to $CD103^+$ and $CD103^-$ pulmonary dendritic cell populations. *J. Immunol.* 180, 3019-3027. doi: 10.4049/jimmunol.180.5.3019

Kim, S., Miller, B. J., Stefanek, M. E., and Miller, A. H. (2015). Inflammation-induced activation of the indoleamine 2,3-dioxygenase pathway: relevance to cancer-related fatigue. *Cancer* 121, 2129-2136. doi: 10.1002/cncr.29302

Kropf, P., Fuentes, J. M., Fahnrich, E., Arpa, L., Herath, S., Weber, V., et al. (2005). Arginase and polyamine synthesis are key factors in the regulation of experimental leishmaniasis *in vivo*. *FASEB J.* 19, 1000-1002. doi: 10.1096/fj.04-3416fje

Langlet, C., Tamoutounour, S., Henri, S., Luche, H., Ardouin, L., Gregoire, C., et al. (2012). CD64 expression distinguishes monocyte-derived and conventional dendritic cells and reveals their distinct role during intramuscular immunization. *J. Immunol.* 188, 1751-1760. doi: 10.4049/jimmunol.1102744

Laskay, T., Van Zandbergen, G., and Solbach, W. (2003). Neutrophil granulocytes–trojan horses for *Leishmania major* and other intracellular microbes? *Trends Microbiol.* 11, 210-214. doi: 10.1016/S0966-842X(03)00075-1

Leon, B., Lopez-Bravo, M., and Ardavin, C. (2007). Monocyte-derived dendritic cells formed at the infection site control the induction of protective T helper 1 responses against *Leishmania*. *Immunity* 26, 519-531. doi: 10.1016/j.immuni.2007.01.017

Lievin-Le Moal, V., and Loiseau, P. M. (2016). *Leishmania* hijacking of the macrophage intracellular compartments. *FEBS J.* 283, 598-607. doi: 10.1111/febs.13601

Liew, F. Y., Millott, S., Parkinson, C., Palmer, R. M., and Moncada, S. (1990). Macrophage killing of *Leishmania* parasite *in vivo* is mediated by nitric oxide from L-arginine. *J. Immunol.* 144, 4794-4797.

Lutz, M. B., Schnare, M., Menges, M., Rossner, S., Rollinghoff, M., Schuler, G., et al. (2002). Differential functions of IL-4 receptor types I and II for dendritic cell maturation and IL-12 production and their dependency on GM-CSF. *J. Immunol.* 169, 3574-3580. doi: 10.4049/jimmunol.169.7.3574

Marovich, M. A., Mcdowell, M. A., Thomas, E. K., and Nutman, T. B. (2000). IL-12p70 production by *Leishmania major*-harboring human dendritic cells is a CD40/CD40 ligand-dependent

process. *J. Immunol.* 164, 5858-5865. doi: 10.4049/jimmunol.164.11.5858

Martinez-Lopez, M., Iborra, S., Conde-Garrosa, R., and Sancho, D. (2015). Batf3-dependent CD103+ dendritic cells are major producers of IL-12 that drive local Th1 immunity against *Leishmania major* infection in mice. *Eur. J. Immunol.* 45, 119-129. doi: 10.1002/eji.201444651

Martinez-Lopez, M., Soto, M., Iborra, S., and Sancho, D. (2018). *Leishmania* hijacks myeloid cells for immune escape. *Front. Microbiol.* 9:883. doi: 10.3389/fmicb.2018.00883

Mayer, J. U., Demiri, M., Agace, W. W., Macdonald, A. S., Svensson-Frej, M., and Milling, S. W. (2017). Different populations of CD11b(+) dendritic cells drive Th2 responses in the small intestine and colon. *Nat. Commun.* 8:15820. doi: 10.1038/ncomms15820

Min, J., Yang, D., Kim, M., Haam, K., Yoo, A., Choi, J. H., et al. (2018). Inflammation induces two types of inflammatory dendritic cells in inflamed lymph nodes. *Exp. Mol. Med.* 50:e458. doi: 10.1038/emm.2017.292

Mohrs, M., Ledermann, B., Kohler, G., Dorfmuller, A., Gessner, A., and Brombacher, F. (1999). Differences between IL-4- and IL-4 receptor alpha-deficient mice in chronic *Leishmaniasis* reveal a protective role for IL-13 receptor signaling. *J. Immunol.* 162, 7302-7308.

Muraille, E., De Trez, C., Pajak, B., Torrentera, F. A., De Baetselier, P., Leo, O., et al. (2003). Amastigote load and cell surface phenotype of infected cells from lesions and lymph nodes of susceptible and resistant mice infected with *Leishmania major*. *Infect Immun.* 71, 2704-2715. doi: 10.1128/IAI.71.5.2704-2715.2003

Musso, T., Gusella, G. L., Brooks, A., Longo, D. L., and Varesio, L. (1994). Interleukin-4 inhibits indoleamine 2,3-dioxygenase expression in human monocytes. *Blood* 83, 1408-1411. doi: 10.1182/blood.V83.5.1408.1408

Ogawa, K., Funaba, M., Chen, Y., and Tsujimoto, M. (2006). Activin A functions as a Th2 cytokine in the promotion of the alternative activation of macrophages. *J. Immunol.* 177, 6787-6794. doi: 10.4049/jimmunol.177.10.6787

Osborne, L. C., Joyce, K. L., Alenghat, T., Sonnenberg, G. F., Giacomin, P. R., Du, Y., et al. (2013). Resistin-like molecule alpha promotes pathogenic Th17 cell responses and bacterial-induced intestinal inflammation. *J. Immunol.* 190, 2292-2300. doi: 10.4049/jimmunol.1200706

Plantinga, M., Guilliams, M., Vanheerswynghels, M., Deswarte, K., Branco-Madeira, F., Toussaint, W., et al. (2013). Conventional and monocyte-derived CD11b(+) dendritic cells initiate and maintain T helper 2 cell-mediated immunity to house dust mite allergen. *Immunity* 38, 322-335. doi: 10.1016/j.immuni.2012.10.016

Pulendran, B., Lingappa, J., Kennedy, M. K., Smith, J., Teepe, M., Rudensky, A., et al. (1997). Developmental pathways of dendritic cells *in vivo*: distinct function, phenotype, and localization of dendritic cell subsets in FLT3 ligand-treated mice. *J. Immunol.* 159, 2222-2231. doi: 10.1016/S0165-2478(97)86082-8

Rani, R., Jordan, M. B., Divanovic, S., and Herbert, D. R. (2012). IFN-gamma-driven IDO production from macrophages protects IL-4Rα-deficient mice against lethality during *Schistosoma mansoni* infection. *Am. J. Pathol.* 180, 2001-2008. doi: 10.1016/j.ajpath.2012.01.013

Schreiber, H. A., Harding, J. S., Hunt, O., Altamirano, C. J., Hulseberg, P. D., Stewart, D., et al. (2011). Inflammatory dendritic cells migrate in and out of transplanted chronic mycobacterial granulomas in mice. *J. Clin. Invest.* 121, 3902-3913. doi: 10.1172/JCI45113

Scott, P., and Hunter, C. A. (2002). Dendritic cells and immunity to leishmaniasis and toxoplasmosis. *Curr. Opin. Immunol.* 14, 466-470. doi: 10.1016/S0952-7915(02)00353-9

Segura, E., and Amigorena, S. (2013). Inflammatory dendritic cells in mice and humans. *Trends Immunol.* 34, 440-445. doi: 10.1016/j.it.2013.06.001

Serbina, N. V., Salazar-Mather, T. P., Biron, C. A., Kuziel, W. A., and Pamer, E. G. (2003). TNF/iNOS-producing dendritic cells mediate innate immune defense against bacterial infection. *Immunity* 19, 59-70. doi: 10.1016/S1074-7613(03)00171-7

Steinman, R. M., and Inaba, K. (1999). Myeloid dendritic cells. *J. Leukoc. Biol.* 66, 205-208. doi: 10.1002/jlb.66.2.205

Stenger, S., Thuring, H., Rollinghoff, M., and Bogdan, C. (1994). Tissue expression of inducible nitric oxide synthase is closely associated with resistance to *Leishmania major*. *J. Exp. Med.* 180, 783-793. doi: 10.1084/jem.180.3.783

Sunderkotter, C., Kunz, M., Steinbrink, K., Meinardus-Hager, G., Goebeler, M., Bildau, H., et al. (1993). Resistance of mice to experimental leishmaniasis is associated with more rapid appearance of mature macrophages *in vitro* and *in vivo*. *J. Immunol.* 151, 4891-4901.

Sutherland, T. E., Ruckerl, D., Logan, N., Duncan, S., Wynn, T. A., and Allen, J. E. (2018). Ym1 induces RELMalpha and rescues IL-4Ralpha deficiency in lung repair during nematode infection. *PLoS Pathog.* 14:e1007423. doi: 10.1371/journal.ppat.1007423

Terrazas, C., Varikuti, S., Oghumu, S., Steinkamp, H. M., Ardic, N., Kimble, J., et al. (2017). Ly6C(hi) inflammatory monocytes promote susceptibility to *Leishmania* donovani infection. *Sci. Rep.* 7:14693. doi: 10.1038/s41598-017-14935-3

WHO (2019). Leishmaniasis. Available online at: https://www.who.int/en/news-room/fact-sheets/detail/leishmaniasis (accessed August 5, 2019).

Woelbing, F., Kostka, S. L., Moelle, K., Belkaid, Y., Sunderkoetter, C., Verbeek, S., et al. (2006). Uptake of *Leishmania major* by dendritic cells is mediated by Fcgamma receptors and facilitates acquisition of protective immunity. *J. Exp. Med.* 203, 177-188. doi: 10.1084/jem.20052288

Yao, Y., Li, W., Kaplan, M. H., and Chang, C. H. (2005). Interleukin (IL)-4 inhibits IL-10 to promote IL-12 production by dendritic cells. *J. Exp. Med.* 201, 1899-1903. doi: 10.1084/jem.20050324

Yue, Y., Huang, W., Liang, J., Guo, J., Ji, J., Yao, Y., et al. (2015). IL4I1 is a novel regulator of M2 macrophage polarization that can inhibit T cell activation via L-tryptophan and arginine depletion and IL-10 production. *PLoS ONE* 10:e0142979. doi: 10.1371/journal.pone.0142979

Zhang, F., Wang, H., Wang, X., Jiang, G., Liu, H., Zhang, G., et al. (2016). TGF-beta induces M2-like macrophage polarization via SNAIL-mediated suppression of a pro-inflammatory phenotype. *Oncotarget* 7, 52294-52306. doi: 10.18632/oncotarget.10561

Zhou, H., and Wu, L. (2017). The development and function of dendritic cell populations and their regulation by miRNAs. *Protein Cell* 8, 501-513. doi: 10.1007/s13238-017-0398-2

Conflict of Interest: The authors declare that the research was conducted in the absence of any commercial or financial relationships that could be construed as a potential conflict of interest.

frontiers in Cellular and Infection Microbiology

ORIGINAL RESEARCH
published: 07 February 2020
doi: 10.3389/fcimb.2020.00039

Endocytosis and Exocytosis in *Leishmania amazonensis* Are Modulated by Bromoenol Lactone

Anne C. S. Fernandes[1,2], Deivid C. Soares[1], Roberta F. C. Neves[1], Carolina M. Koeller[3], Norton Heise[3], Camila M. Adade[1], Susana Frases[4], José R. Meyer-Fernandes[2,5], Elvira M. Saraiva[1] and Thaïs Souto-Padrón[1,2†]*

[1] Centro de Ciências da Saúde, Instituto de Microbiologia Paulo de Góes, Universidade Federal Do Rio de Janeiro, Rio de Janeiro, Brazil, [2] Instituto Nacional de Ciência e Tecnologia de Biologia Estrutural e Bioimagem, Universidade Federal Do Rio de Janeiro, Rio de Janeiro, Brazil, [3] Instituto de Biofísica Carlos Chagas Filho, Universidade Federal Do Rio de Janeiro, Rio de Janeiro, Brazil, [4] Laboratório de Ultraestrutura Celular Hertha Meyer, Instituto de Biofísica Carlos Chagas Filho, Universidade Federal Do Rio de Janeiro, Rio de Janeiro, Brazil, [5] Centro de Ciências da Saúde, Instituto de Bioquímica Médica Leopoldo de Meis, Universidade Federal Do Rio de Janeiro, Rio de Janeiro, Brazil

OPEN ACCESS

Edited by:
Albert Descoteaux, Institut National de la Recherche Scientifique (INRS), Canada

Reviewed by:
Ethel Bayer-Santos, University of São Paulo, Brazil
Ana Claudia Torrecilhas, Federal University of São Paulo, Brazil

***Correspondence:**
Elvira M. Saraiva
esaraiva@micro.ufrj.br

†*In Memoriam*

Specialty section:
This article was submitted to Parasite and Host, a section of the journal Frontiers in Cellular and Infection Microbiology

Received: *05 September 2019*
Accepted: *21 January 2020*
Published: *07 February 2020*

Citation:
Fernandes ACS, Soares DC, Neves RFC, Koeller CM, Heise N, Adade CM, Frases S, Meyer-Fernandes JR, Saraiva EM and Souto-Padrón T (2020) Endocytosis and Exocytosis in Leishmania amazonensis Are Modulated by Bromoenol Lactone. Front. Cell. Infect. Microbiol. 10:39. doi: 10.3389/fcimb.2020.00039

In the protozoan pathogen *Leishmania*, endocytosis, and exocytosis occur mainly in the small area of the flagellar pocket membrane, which makes this parasite an interesting model of strikingly polarized internalization and secretion. Moreover, little is known about vesicle recognition and fusion mechanisms, which are essential for both endo/exocytosis in this parasite. In other cell types, vesicle fusion events require the activity of phospholipase A_2 (PLA_2), including Ca^{2+}-independent $iPLA_2$ and soluble, Ca^{2+}-dependent $sPLA_2$. Here, we studied the role of bromoenol lactone (BEL) inhibition of endo/exocytosis in promastigotes of *Leishmania amazonensis.* PLA_2 activities were assayed in intact parasites, in whole conditioned media, and in soluble and extracellular vesicles (EVs) conditioned media fractions. BEL did not affect the viability of promastigotes, but reduced the differentiation into metacyclic forms. Intact parasites and EVs had BEL-sensitive $iPLA_2$ activity. BEL treatment reduced total EVs secretion, as evidenced by reduced total protein concentration, as well as its size distribution and vesicles in the flagellar pocket of treated parasites as observed by TEM. Membrane proteins, such as acid phosphatases and GP63, became concentrated in the cytoplasm, mainly in multivesicular tubules of the endocytic pathway. BEL also prevented the endocytosis of BSA, transferrin and ConA, with the accumulation of these markers in the flagellar pocket. These results suggested that the activity inhibited by BEL, which is one of the irreversible inhibitors of iPLA2, is required for both endocytosis and exocytosis in promastigotes of *L. amazonensis*.

Keywords: *Leishmania amazonensis*, bromoenol lactone (BEL), endocytic pathways, exocytic pathways, ultrastructure, calcium-independent phospholipase A_2

INTRODUCTION

Leishmania is a digenetic protozoan parasite belonging to the *Trypanosomatidae* family that causes a variety of human diseases collectively known as the leishmaniasis. In their developmental cycle *Leishmania* display distinct morphological and functional forms that adapt to different living conditions in their two main hosts. Parasites taken up by the phlebotomine vector with a blood

meal, differentiate in the insect alimentary tract into procyclic promastigotes, which are flagellated and motile forms. After morphological and physiological modifications, in a process named metacyclogenesis, procyclics differentiate in a highly motile and infective metacyclic promastigotes, which are transmitted to the vertebrate host. Metacyclogenesis includes changes in gene expression, morphology, cell surface molecules expression, and in the type and amount of secreted/exocytosed molecules as well as, on the traffic of molecules in the compartments of parasite's endocytic/exocytic pathways (McConville et al., 2002; Morgan et al., 2002a,b; Besteiro et al., 2006; Lambertz et al., 2012).

As described for mammalian cells, exocytosis in *Leishmania* is mediated by both classical N-terminal secretion signal peptide and non-classical mechanism characterized by the secretion of extracellular vesicles (EVs) that accounts for at least 52% of the total protein secreted by the parasite (Silverman et al., 2008, 2010).

The total amount of secreted/excreted proteins by a cell is called exoproteome (a mixture of secreted proteins as well as those released in microvesicles and exosomes) and, in various parasites, has a different composition according to the parasite developmental form under consideration.

The use of trypanosomatids in intracellular traffic studies is particularly interesting because some developmental forms have a high rate of endocytosis and exocytosis, which occur mainly in a small area of the cell surface, the flagellar pocket membrane, whose dynamics regulates tightly the exposure of a variety of molecules on the cell surface (Naderer et al., 2004). Interestingly, endocytic and exocytic pathway organelles in these protozoa have structural and functional characteristics distinct from those of the corresponding compartments in mammalian cells (De Souza et al., 2009).

Protein trafficking along the endocytic and exocytic pathways requires membrane fusion events, which are dependent on membrane bilayer curvature modifications generated by the presence of specific phospholipids and their metabolites (Brown et al., 2003; Shin et al., 2012). A variety of studies have shown that cytoplasmic phospholipases are intimately involved in the modification of membrane phospholipids favoring the membrane deformation and consequently influencing membrane-trafficking events (Brown et al., 2003). Four of the cytoplasmic phospholipases, the $iPLA_1\gamma$ and three different PLA_2: $cPLA_2\alpha$, $iPLA_2\beta$ and platelet-activating factor acetylhydrolase Ib (PAFAH Ib) were shown to be directly associated to the Golgi complex or other compartments of the exocytic pathway regulating the Golgi structure, the retrograde trafficking from the *cis* Golgi and endoplasmic reticulum-Golgi intermediate compartment (ERGIC) to the endoplasmic reticulum, the export from the TGN and the receptor recycling from endosomes (Morikawa et al., 2009; San Pietro et al., 2009; Bechler et al., 2010, 2012; Ben-Tekaya et al., 2010; Bechler and Brown, 2013).

Phospholipase A activities have been linked to microorganism differentiation, pathogenesis, and host cell invasion but, the exact mechanism of PLA action in this context has not yet been determined (Connelly and Kierszenbaum, 1984; Saffer et al., 1989; Snijder and Dijkstra, 2000; Belaunzarán et al., 2007, 2011, 2013). Four types of PLA_2 have been described in bacteria, fungi and protozoa: the secreted, small molecular weight $sPLA_2$s, the large cytosolic Ca^{2+}-dependent $cPLA_2$s, the Ca^{2+}-independent $iPLA_2$s and platelet activating factor acetyl hydrolase (PAF-AH) (Murakami and Kudo, 2002; Köhler et al., 2006; Sitkiewicz et al., 2007; Belaunzarán et al., 2011).

Genes encoding putative PLA_2-like proteins have been identified in the genome of several species of *Leishmania* (TriTrypDB database), including a putative and not yet cloned PAF-AH in *L. amazonensis* MHOM/BR/71973/M2269 strain (Accession Number LAMA_000796800), that shares 29% protein sequence identity with phospholipase A2 from mice (Accession Number EDL23405). Previously, we showed that inhibition with dibucaine (a $iPLA_2$ inhibitor) alters Golgi architecture and reduces the rates of endocytosis, secretion, and protein recycling in *Trypanosoma cruzi* (Souto-Padrón et al., 2006), similarly to that observed in mammalian cells (Tolleshaugh et al., 1982; Hagiwara and Ozawa, 1990; Ramanadhan et al., 1993; Lennartz et al., 1997; De Figueiredo et al., 2001; Balboa et al., 2003; Fensome-Green et al., 2007). However, similar studies in *Leishmania* have not been formally addressed with the use of tools that target the function of these proteins specifically.

In the present study we report that bromoenol lactone (BEL) inhibition modulated the metacyclogenesis, the exocytosis/secretion of both tartrate sensitive and resistant acid phosphatases, the shedding of microvesicles, the intracellular localization of GP63 and transferrin receptor and the endocytosis of BSA, Concanavalin A and transferrin by promastigotes of *L. amazonensis,* suggesting a role for sensitive iPLA2.

MATERIALS AND METHODS

Parasites

The *Leishmania amazonensis* (MHOM/BR/75/Josefa) was maintained by inoculation into the base of the tails of BALB/c mice. Axenic promastigotes were cultured in Schneider's insect medium supplemented with 10% fetal calf serum (Gibco, Brazil) at 26°C. Promastigotes used in the experiments were harvested by centrifugation (1,500 × *g* for 12 min) from 1- to 2-day-old logarithmic phase cultures, washed and counted using a hemocytometer.

Drugs and Reagents

Bromoenol lactone (BEL), sodium tartrate, DAPI, poly-L-lysine, and all other common reagents were from Sigma–Aldrich Chemical Co (St. Louis, MO, USA). SDS-PAGE and Western blotting equipment and reagents were from Bio-Rad Laboratories (Hercules, CA, USA) and Amersham Biosciences (Piscataway, NJ, USA). Molecular weight markers LMW were from Fermentas Life Sciences (Waltham, Massachusetts, USA). The mouse polyclonal antibody against *Leishmania* GP63 was from Acris antibodies (Herford, Germany, cat. # AM01176SU-N), and the mouse monoclonal antibody against α-tubulin was from Sigma-Aldrich (cat. #: MFCD00145891). Secondary antibodies, albumin, transferrin and concancavalin A (ConA) conjugated to Alexa Fluor® 488, and the JC-1 dye, were from Molecular Probes

(Molecular Probes; Eugene, OR, USA). 1-palmitoyl-2-[6-[(7-nitro-2-1,3-benzoxadiazol-4-yl)amino]caproyl]-*sn*-glycero-3-phosphocholine (6C-NBD-PC) was purchased from Avanti Polar Lipids (Alabaster, AL, USA). [3-(4,5-dimethyl-2-thiazolyl)-5-(3-carboxymethoxy-phenyl)-2-(4-sulfo- phenyl)-2*H*-tetrazolium inner salt/5-methylphenazinium methyl sulfate] (MTS/PMS) reagent (CellTiter Aqueous MTS One Solution Cell Proliferation Assay, Promega, Madison, WI, USA). Electron microscopy resin PolyBed 812 was from Polysciences (Warrington, PA, USA).

In vitro Anti-proliferative and Anti-differentiation Effects

Promastigotes were grown in Schneider's insect medium supplemented with 10% fetal calf serum (Gibco, Brazil) at 26°C in the absence or in the presence of 2.5, 5, or 10 μM BEL, and then cells were counted daily for 7 days, using a hemacytometer. To analyze the effect of BEL in metacyclogenesis, parasites in the log growth phase were incubated in the presence of BEL (2.5 μM) throughout the growth period, and the percentage of metacyclic promastigotes analyzed in cell smears stained with Giemsa (1:20), in a Zeiss Axioplan II light microscope.

Inhibition of Phospholipase A_2 Activities

Promastigotes of *L. amazonensis* were incubated in RPMI without serum with 2.5 μM BEL according to Ackermann et al. (1995). The inhibition treatment was done for 1 h at 26°C. Stock solution of the inhibitor was prepared in dimethyl sulfoxide (DMSO), stored at −20°C, and diluted in RPMI medium without serum immediately before use. The final concentration of the diluent never exceeds 0.1%. DMSO at the same concentration used for treatment with BEL did not affect any of the experiments showed in the present study, thus, all controls shown in this study refer to parasites not exposed to either DMSO or BEL treatment.

Cytotoxicity Assays

To assess parasite viability, control and BEL-treated promastigotes were harvested (4,000 × *g* for 15 min), washed in Hank's balanced salt solution (HBSS) and then incubated with propidium iodide (PI; 15 μg/mL), at 37°C for 15 min. PI fluorescence associated with non-viable cells was measured by flow cytometry (544/602 nm excitation/emission) on a FACSCalibur (Becton-Dickinson, Franklin Lakes, NJ, USA). A positive control for cell lysis was prepared by treating the parasites with 0.1% saponin in PBS for 40 min, at 26°C. Flow cytometry data were analyzed using the CellQuest software (Scripps Research Institute, San Diego, CA, USA).

Viability Assay

Control and BEL-treated parasites (2.5 μM, 1 h) were washed with sterile PBS (pH 7.2) and diluted in RPMI medium without phenol red supplemented with 10 mM glucose. Then, 2×10^6 cells/well were seeded in 96-well tissue culture plate and 20 μl of a solution of 2 mg/ml MTS [3-(4,5-dimethylthiazol-2-yl)-5-(3-carboxymethoxyphenyl)-2-(4-sulfophenyl)-2H-tetrazolium salt) and 0.92 mg/ml PMS (phenazine methosulfate], prepared according to the manufacturer's instructions (Promega) were added. Samples were diluted to a final volume of 100 μl/well with RPMI without phenol red, and incubated for 3 h at 26°C. The formation of a soluble formazan product was measured using a microplate spectrophotometer reader (Spectra Max Molecular Devices M2e) at 490 nm. Negative controls for MTS/PMS consisting of promastigotes fixed with 0.4% formaldehyde for 10 min at 26°C.

Mitochondrial Membrane Potential Analysis

Mitochondrial membrane potential ($\Delta\Psi m$) was investigated using the JC-1 fluorochrome, as described by Macedo-Silva et al. (2011). Briefly, control an BEL-treated promastigotes (2.5 μM, 1 h) were harvested, washed in PBS pH 7.2, added to the reaction medium containing 125 mM sucrose, 65 mM KCl, 10 mM HEPES/K^+ pH 7.2, 2 mM Pi, 1 mM $MgCl_2$ and 500 μM EGTA and counted using a hemocytometer. To evaluate the $\Delta\Psi m$, 2.0×10^7 parasites were incubated with 10 μg/mL JC-1 for 25 min in the reaction medium, and readings were made every min immediately after the start of the 25-min incubation period, using a Molecular Devices Microplate Reader (SpectraMax spectrofluorometer). As a positive control for mitochondrial membrane depolarization, parasites were incubated with 2 μM trifluoromethoxy carbonylcyanide phenylhydrazone (FCCP). The relative $\Delta\Psi m$ value was obtained by calculating the ratio 590 nm (red)/530 nm (green).

Secretion Assay

Control and BEL-treated promastigotes (2.5 μM, 1 h) were washed twice in HBSS, and then incubated in this solution (2×10^8 parasites/mL) for 4 h at 26°C, to allow secretion to occur. Then, aliquots were centrifuged at 2,740 × g for 10 min, at room temperature, to remove intact parasites. The supernatant (containing soluble proteins and vesicles shed/secreted by the parasites) was spun at 11,000 × *g* for 30 min, at 4°C, to remove large cell debris. The resulting supernatant—referred to henceforth as the "conditioned medium"—was spun again at 4°C for 1 h at 100,000 ×*g* resulting in an "extracellular vesicles fraction" (EVs) in the pellet, and a "soluble fraction" in the supernatant. EVs were washed twice in HBSS (100,000 ×*g*, 1 h, 4°C). Total protein concentration in conditioned medium, in EV and in soluble fractions was determined by Bradford, using BSA as standard (Bradford, 1976). Absorbance at 595 nm was measured (after 10 min of reaction time) in a SpectraMax M2 plate reader (Molecular Devices).

Dynamic Light Scattering (DLS)

The conditioned media samples containing the vesicles obtained from the untreated controls and BEL-treated promastigotes as described above were diluted 100-fold in Hanks' Balanced Salt Solution (HBSS) without phenol red (Thermofisher). Particles concentration determined by Bradford was 26 mg/ml for untreated control and 10 mg/ml for BEL-treated ones. The effective diameter and the polydispersity of vesicle preparations were measured at 25°C by Dynamic Light Scattering (DLS) in an Omni Particle Sizing analyzer (Brookhaven Instruments Corp., Holtsville, NY). The multimodal distributions of particle size diameter were generated by a Non-Negatively constrained

Least Squares algorithm (NNLS) based on the intensity of light scattered by each particle. All vesicle samples were analyzed under the same conditions.

Phospholipase A_2 (PLA_2) Activity Assay

PLA_2 activity present in intact parasites and in conditioned medium fractions (EVs and soluble) were determined using the fluorescent substrate 6C-NBD-PC, according to Wittenauer et al. (1984). To measure PLA_2 activity in control and BEL treated parasites, 2×10^8 promastigotes were incubated in 4 ml RPMI for 3 h, 26°C. The intact parasites, the conditioned medium and its sub-fractions were obtained as described in the preceding section. Parasites were then washed twice in HBSS and suspended in 4 ml of PBS; the conditioned medium, and the soluble fraction were separated and kept at 4°C (to measure secreted PLA_2 activity). To concentrate protein samples from conditioned medium and from the soluble fraction, 4 mL aliquots of each sample were transferred to Amicon tubes (Amicon Ultra 15, Millipore) and centrifuged at 7,500 × *g* for 15 min, until the concentrated volume was 200 μL (50 X concentrated). EV fractions (obtained as described previously) were resuspended in 200 μL PBS, and 50 μL of each sample (parasite suspensions, concentrated conditioned media, soluble, and EV fractions) were added to wells of black 96-well plates (SLP Lifescience), C6-NBD-PC was added in the dark (5 μM final), and samples were diluted to the final volume of 200 μL/well with PBS. Fluorescence was monitored at 26°C for 60 min, in a SpectraMax M2/M2e microplate (460/534 nm excitation/emission). As a negative control, samples were analyzed without the addition of the fluorogenic substrate.

SDS-PAGE and Western Blotting

The intact cells and conditioned media from untreated control and BEL-treated parasites to be analyzed in SDS-PAGE were boiled in 60 mM Tris-HCl pH 6.8, 5% 2-mercaptoethanol, 10% glycerol and 0.01% bromophenol blue, fractionated into 10% polyacrylamide gels (Laemmli, 1970) and transferred to nitrocellulose membranes (Hybond, Amersham Biosciences) using the Bio-Rad mini vertical Trans-Blot Cell system. Membranes were blocked in 5% non-fat dried milk in TBS (50 mM Tris-HCl, 100 mM NaCl, pH 7.5) for 1 h at room temperature, washed 3 times in TBS with 0.05% Tween-20 (TBS-T; 10 min/wash), once with TBS (5 min), and then incubated (for 18 h at 4°C) with one of the following primary antibodies: purified polyclonal anti-GP63 (1:1,000; Russel and Wilhelm, 1986) or monoclonal anti-α-tubulin (1:4,000; Sigma-Aldrich) diluted in TBS with 3% BSA and 0.05% sodium azide. Membranes were washed as described above and incubated with alkaline phosphatase-conjugated anti-mouse IgG secondary antibody (KPL), diluted to 1:1,000 in TBS with 3% BSA, for 1 h at room temperature. After a final washing cycle, bound antibodies were detected with 0.03% BCIP (5-bromo-4-chloro-3-indolyl-phosphate)/0.02% NBT (nitro blue tetrazolium) reagent (Fermentas) in alkaline phosphatase buffer (100 mM Tris-HCl pH 9.5, 150 mM NaCl, 5 mM $MgCl_2$, 0.05% Tween-20). The densitometry of the gel bands was analyzed by using the Gel Doc XR+ System (Bio-Rad Laboratories, CA, USA) and the Image Lab® software.

Acid Phosphatase Activity Analysis

Control and BEL treated (2.5 μM, 1 h) parasites (2×10^7 cells/mL) were centrifuged, washed and incubated in RPMI without serum for 3 h, 26°C. Then the samples were centrifuged and the pellet of intact cells and the conditioned medium (50 μL) were incubated, at 26°C for 60 min, in a reaction mixture (0.5 mL) containing 5 mM *p*-nitrophenylphosphate (*p*-NPP), in 50 mM Mes-Hepes buffer (pH 5.0). Reactions were started by the addition of cells or conditioned medium aliquots, and stopped by the addition of 1.0 mL 1 N NaOH. Cells added after interruption of the reaction were used as a blank control. For determining the concentration of the product of p-NPP hydrolysis (*p*-nitrophenol, p-NP) released, cells were centrifuged at 1,500 × *g* for 15 min, at 26°C, and the supernatants were analyzed using a SpectraMax M2/M2e spectrofluorometer (Molecular Devices), at 425 nm, using a *p*-NP curve as standard (Gomes et al., 2006).

The analysis of phosphatase inhibition was assayed as described above, but with the addition of sodium tartrate, and the secreted acid phosphatase inhibitor at 10 mM (final concentration), immediately before the addition of either parasites, or conditioned medium. Measurements of phosphatase activity in the presence of inhibitors were normalized to control measurements in the absence of inhibitors.

Endocytosis Assay

Control and BEL-treated promastigotes (2×10^6 parasites/mL) were washed 3 times in PBS, pH 7.2, and then incubated at 26°C for 1–2 h in RPMI containing one of the following fluorescent markers: 30 μg/ml BSA-Alexa Fluor 488, 25 μg/ml transferrin-Alexa Fluor-488 and 10 μg/ml Concanavalin A (ConA)-Alexa Fluor-488 (all from Molecular Probes). After incubation with fluorescent tracers, cells were analyzed by flow cytometry, in FACSCalibur flow cytometer (Becton-Dickinson, Franklin Lakes, NJ, USA) equipped with the CellQuest software (Joseph Trotter, Scripps Research Institute, San Diego, CA, USA). Also these cells were washed in PBS (pH 7.2), fixed in 4% formaldehyde (in PBS), for 30 min at 4°C, washed in PBS, and then adhered to poly-L-lysine-coated glass coverslips for 20 min, at 26°C. Coverslips were then washed twice in PBS mounted onto slides using anti-fade solution (0.2N *n*-propyl-galate in glycerol), and observed either in a ZEISS Axioplan II epifluorescent microscope, or in a Leica TCS SPE confocal microscope.

Transmission Electron Microscopy (TEM)

Parasites were fixed with 2.5% glutaraldehyde in 0.1 M cacodylate buffer (pH 7.2) containing 5 mM calcium chloride and 2% sucrose, for 1 h at room temperature. Then samples were rinsed in 0.1 M cacodylate buffer (pH 7.2) containing 2% sucrose, post-fixed in 1% osmium tetroxide (OsO_4) in 0.1 M cacodylate buffer (pH 7.2) with 0.8% potassium ferrocyanide and 5 mM calcium chloride (for 1 h at room temperature), dehydrated in a graded acetone series, and embedded in PolyBed 812 resin. Ultrathin sections, obtained with a Leica (Nussloch, Germany) ultramicrotome, were stained with uranyl acetate and lead citrate,

and observed using a FEI Morgagni F 268 transmission electron microscope, operating at 80 kV. The observed effects were well-recurring phenomena and the differences between control and BEL-treated parasites were readily apparent.

Cytochemical Detection of Acid Phosphatases

Promastigotes were fixed in 1% glutaraldehyde and 3.7% sucrose in 0.1 M cacodylate buffer (pH 7.2), for 10 min at 4°C. Next, cells were washed once in 0.1 M cacodylate buffer (pH 7.2) containing 3.7% sucrose, incubated for 10 min in 0.1 M sodium acetate buffer (pH 5.0) containing 5% sucrose, and then incubated for 1 h (at 37°C, and under constant agitation) in 0.1 M sodium acetate buffer (pH 5.0) containing 2 mM sodium β-glycerophosphate, 2 mM cerium chloride and 5% sucrose. Negative control cells were incubated either in reaction medium without substrate or in reaction medium containing 10 mM of the phosphatase inhibitor sodium tartrate. After that cells were washed in sodium acetate (pH 5.0) and sodium cacodylate (pH 7.2) buffers, fixed again for 1 h in 2.5% glutaraldehyde, 3.7% sucrose and 0.1 M cacodylate buffer (26°C), and prepared for TEM (post-fixed, dehydrated, and embedded) and viewed as described above (see "Transmission Electron Microscopy").

Immunofluorescence

Cells were fixed in formaldehyde (4% in PBS), washed in PBS, adhered to poly-L-lysine-coated glass coverslips and washed twice in PBS. The excess of aldehyde was quenched by incubating in 50 mM ammonium chloride (in PBS), for 30 min at room temperature, and then samples were incubated in PBS containing 0.2% gelatin, 0.1% azide ("PGN" solution; Da Silva et al., 2006) for 30 min, at room temperature. Cells were permeabilized using 0.1% saponin in PGN, and then incubated with the anti-GP63 antibody (1:1,000 in PGN), for 1 h at room temperature. Then, coverslips were washed twice in PGN and incubated with Alexa Fluor 488-conjugated anti-mouse antibody (diluted to 1:400), for 1 h. Coverslips were mounted as above and observed in a ZEISS Axioplan II microscope equipped with a Color View XS camera. Negative controls were incubated with secondary antibody only (no parasite auto-fluorescence was detected).

Statistical Analysis

Each experiment was repeated at least 3 times, and data are presented as the mean plus SEM (standard error of the mean), analyzed using the Graph-Pad-Prism 5.0 software. Comparisons between 2 groups were analyzed using Student *t* test. The differences were considered statistically significant when $p \leq 0.05$.

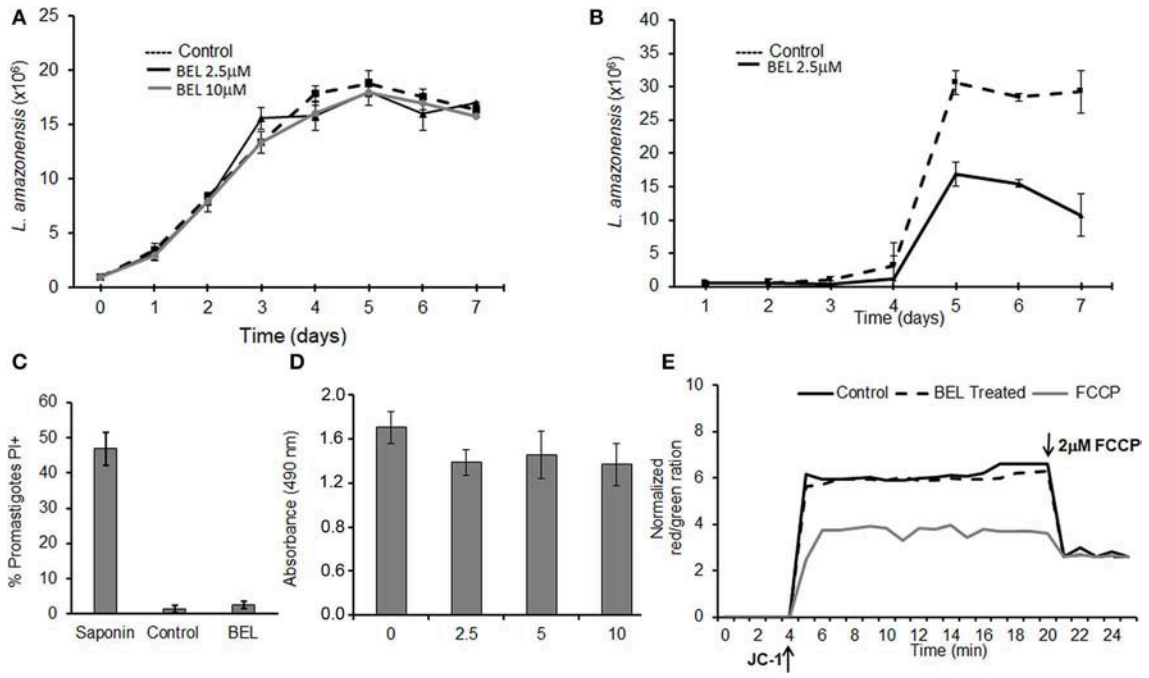

FIGURE 1 | Effects of bromoenol lactone (BEL) on *Leishmania amazonensis*. **(A)** Promastigotes were grown in the absence (control) or presence of 2.5 or 10 µM BEL, and cells counted daily for 7 days, using a hemacytometer. **(B)** *L. amazonensis* metacyclogenesis, Log growth phase promastigotes were incubated with 2.5 µM BEL and the percentage of metacyclic forms were evaluated daily over 7 days of growth using a hemocytometer. **(C)** Flow cytometry analysis of untreated control and BEL-treated promastigotes (2.5 µM, 1 h, 26°C) stained with 15 µg/mL propidium iodide (PI). Saponin treated-parasites were used as a positive control. **(D)** Untreated (0) and BEL-treated promastigotes at the indicated concentrations were stained with MTS/PMS for the viability assay. **(E)** Mitochondrial membrane potential ($\Delta\Psi m$), in cells labeled with JC-1. The values of $\Delta\Psi m$ were evaluated over 20 min, after which the "uncoupler" carbonyl cyanide-4-phenylhydrazone (FCCP) was added to the incubation medium, to abolish the $\Delta\Psi m$. The $\Delta\Psi m$ values are expressed as the ratio of aggregate [red]/monomer [green] measured at 590/530 nm. Data represent mean ± SEM values from three independent experiments, performed in triplicates.

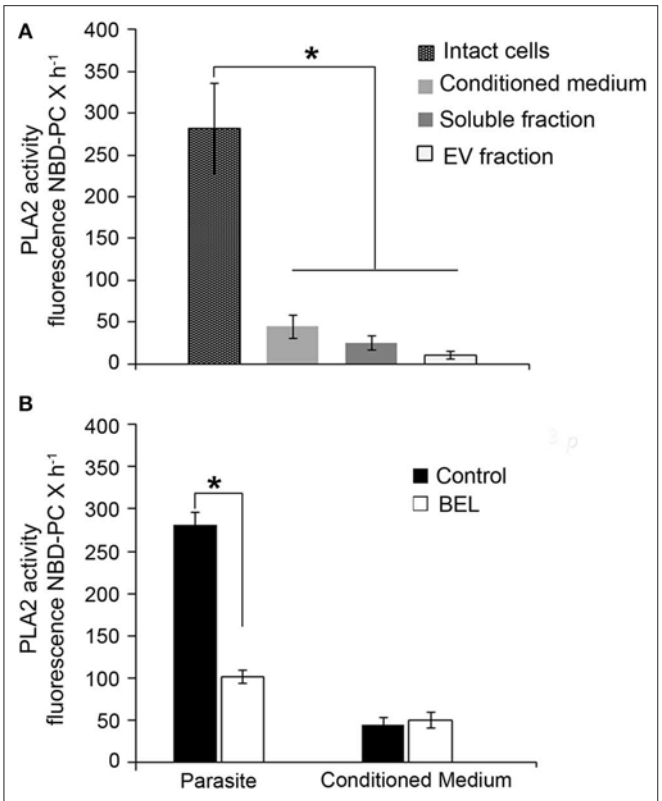

FIGURE 2 | Phospholipase A_2 (PLA_2) activity in promastigotes of *Leishmania amazonensis*. **(A)** PLA_2 activity was assayed in intact cells, in conditioned medium (from 2×10^8 promastigotes incubated in HBSS for 4 h, 26°C), and in soluble and extracellular vesicle (EV) fractions obtained from the conditioned medium, using the fluorogenic substrate 6C-NBD-PC. **(B)** Effect of the inhibitor in the PLA_2 activity of intact cells and conditioned media. Fluorescence measured as above was continuously monitored for 60 min 26°C in control untreated samples and in BEL treated promastigotes. Cells were treated with the inhibitor for 1 h, and then incubated for 3 h in culture medium lacking inhibitor. Data represent mean ± SEM values from three independent experiments, performed in triplicates (*$p < 0.05$).

RESULTS

Treatment With BEL Reduces Promastigotes Differentiation Into Metacyclics, but Does Not Affect Cell Growth or Viability

Previous studies using dibucaine, a non-specific inhibitor of phospholipase activity, showed the importance of $iPLA_2$ for exocytic and endocytic traffic in *Trypanosoma cruzi* (Souto-Padrón et al., 2006). These results prompted us to study the role of BEL in vesicular trafficking in other human pathogens from the Trypanosomatidae family, such as *Leishmania amazonensis*. It has been demonstrated that BEL was the most active PLA_2 inhibitor (Bordon et al., 2018), therefore we used this drug to characterize its role in some properties of promastigotes. Initially, we monitored the growth of *L. amazonensis* promastigotes for 7 days in Schneider's medium containing different concentrations of BEL (**Figure 1A**). Our results show that BEL, at the concentrations used, did not affect the growth of the parasites. In contrast, BEL treatment affects metacyclogenesis reducing about 65% the differentiation of promastigotes into metacyclics (**Figure 1B**). Importantly, parasite's membrane integrity, based on the absence of cytosolic leaky, the oxidoreductase activity and maintenance of the mitochondrial membrane potential, were not affected by BEL (**Figures 1C–E**). Interestingly, similar concentrations of BEL suppresses cell proliferation and leads to reduction in mitochondrial membrane potential and apoptosis induction in mammalian cells (Wilson et al., 2000; Fuentes et al., 2003; Zhang et al., 2006; Song et al., 2007; Ma et al., 2011). Based on the data described above, we chose to use 2.5 μM BEL in all the exocytosis and endocytosis experiments, since this dose did not affect parasite viability, even after more than 24 h treatment (**Figure 1A**).

BEL-Sensitive PLA_2 Activities in *L. amazonensis* Promastigotes

Leishmania promastigotes have a marked secretory activity, in the form of both soluble proteins and membrane-bound vesicles (Silverman et al., 2010). Thus, we assayed PLA_2 activities in intact parasites and in "conditioned medium" (HBSS after parasite incubation for 4 h). In addition, we fractionated the conditioned medium into extracellular vesicles (EVs) and soluble fractions, and then assayed the PLA_2 activity in these individual fractions.

Using the fluorogenic substrate 6C-NBD-PC, we detected marked PLA_2 activity in intact promastigotes (**Figure 2A**). PLA_2 activity was also detected in the conditioned medium and it was significantly higher in the soluble fraction compared with the EV fraction (**Figure 2A**). In order to identify if PLA_2 activity is present in the promastigotes, we used BEL treatment in intact parasites. Our results showed that BEL-sensitive activity accounted for approximately 60% of the total PLA_2 activity in the parasites (**Figure 2B**). BEL did not inhibit the phospholipase activity in the conditioned medium, suggesting no detectable $iPLA_2$ activity.

BEL Inhibits Exocytosis and Alters Golgi Morphology of Promastigotes

Inhibition of $iPLA_2$ by BEL prevents exocytosis and delays protein transport between intracellular compartments from endocytic/exocytic pathways in different mammal cells such as mammary epithelial cells, mast cells, and pancreatic cells (Ramanadhan et al., 1993; Péchoux et al., 2005; Fensome-Green et al., 2007). Next we assessed whether pre-treatment of cells with BEL affected protein secretion into the conditioned medium, and which was the result of exocytosis by promastigotes.

To examine in more detail the effect of BEL on promastigote exocytosis, we measured the amount of protein secreted by promastigotes in the conditioned medium, evaluated after 1 h of incubation with BEL followed by a wash and incubation for 1–4 h in HBSS (**Figure 3**). Our results showed that the amount of protein secreted by control cells increased with time (**Figure 3A**), and this was also observed in BEL-treated parasites, but these cells secreted ∼40% less protein in the conditioned medium

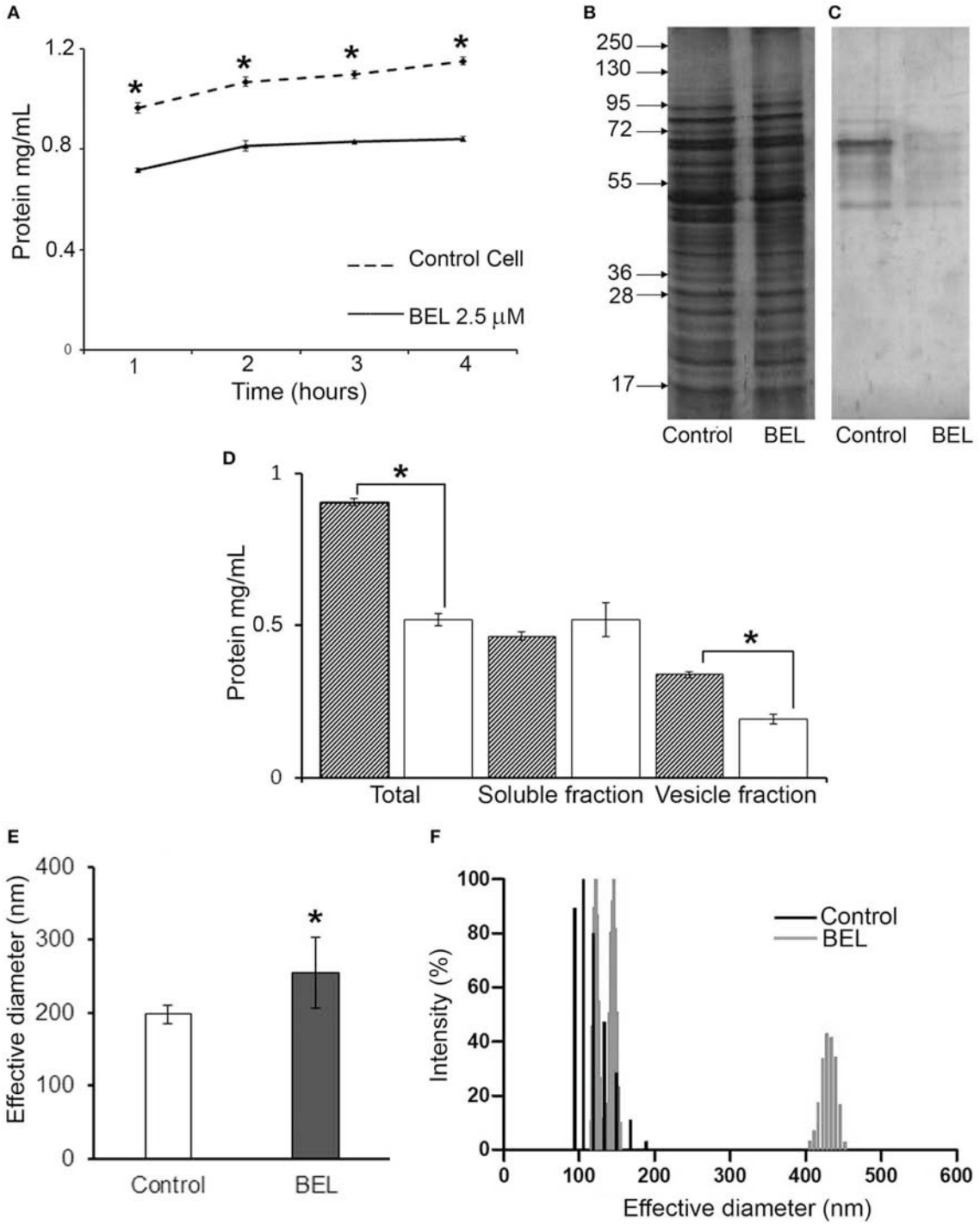

FIGURE 3 | Effect of bromoenol lactone (BEL) on the protein secretion by *Leishmania amazonensis* promastigotes. **(A)** Kinetics of protein secretion by promastigotes untreated (control) or treated with 2.5 μM of BEL for 1 h, and then incubated at 26°C for 4 h in Hank's balanced salt solution (HBSS). Protein concentrations in the conditioned medium were estimated using Bradford. Data represent mean ± SEM values from three independent experiments, performed in duplicates. *$p < 0.05$. **(B,C)** SDS-PAGE profile of intact cells **(B)** and of conditioned media **(C)** from untreated control and BEL-treated parasites (all lanes contain samples derived from equivalent numbers of cells). Molecular weight markers are indicated on the left. **(D)** Total amount of protein in the conditioned media (Total), soluble fractions and vesicle fraction of control (gray bars) and BEL-treated parasites (white bars). **(E,F)** Effective diameter and the polydispersity of *L. amazonensis* vesicles obtained from control and BEL-treated promastigotes were analyzed by dynamic light scattering (DLS). Results shown as effective diameter in nm and % of intensity of 5 different measurements *$p < 0.05$.

when compared to control cells. The protein profile analyzed by SDS-PAGE depicts a decrease in the intensity of the bands between 40 and 60 kDa (**Figure 3B**). SDS-PAGE profiles of conditioned medium from control and BEL-treated parasites contained protein bands ranging from 45 to 95 kDa, and a reduction in the intensity of bands of 67 and 48 kDa was evidenced in the profile from BEL-treated parasites (**Figure 3C**). After conditioned medium fractionation, we found that the reduction in protein concentration observed after BEL treatment is related to a reduction in the vesicle fraction (∼40% compared with the untreated control), since no difference was observed in the soluble fraction (**Figure 3D**). The size distribution evaluated by Dynamic light scattering (DLS) of the vesicles released by the promastigotes after 4 h incubation was increased after BEL treatment (**Figure 3E**), and contrary to the control cells, vesicles released after BEL-treatment were distributed in two populations ranging between of 100–150 and 400–450 nm of effective diameter.

We then analyze the ultrastructure of BEL-treated *L. amazonensis* promastigotes examining the endocytic and exocytic organelles (**Figures 4A–G**). As previously described in other cell types (De Figueiredo et al., 2000), BEL induced an intense Golgi and endoplasmic reticulum (ER) vesiculation in the parasite (**Figures 4F,G**). In some promastigotes the Golgi structure was reduced to only one or two cisterna, and the *trans*-Golgi region was filled with vesicles (**Figure 4F**), different from the Golgi of control cells showing preserved cisterna (**Figure 4A**). Aside from Golgi vesiculation, we also observed tubules with a branched aspect in the proximity of the flagellar pocket (**Figure 4G**, white arrows). A decrease in the number of vesicles inside the flagellar pocket was also observed after BEL treatment (**Figure 4G**). These data are in agreement with the reduction in the amount of protein in vesicle fraction after BEL treatment (**Figures 3C,D**).

BEL Interferes With the Traffic of Secreted but Not With GPI-Anchored Glycoproteins

Leishmania promastigotes secrete a significant amount of glycoproteins and also have, exposed in the cell membrane, a variety of trans-membrane and GPI-anchored proteins, aside from different kinds of glycolipids (McConville et al., 2002). Endocytosis and exocytosis occur mainly in the area of the flagellar pocket membrane in the anterior region of the cell, while internalized cargo accumulates at the posterior region, in late endosomes (Ghedin et al., 2001). This strikingly polarized organization of cargo trafficking facilitates the examination of both the endocytic and the exocytic pathways in these parasites. Therefore, we examined the effects of BEL on protein trafficking in promastigotes using as models two types of cargo proteins: secreted acid phosphatases and the GPI-anchored protease GP63.

Acid phosphatase activities derive from distinct molecular entities distributed in endosomes, lysosomes, Golgi, plasma membrane, and secreted through the flagellar pocket as well (Gottlieb and Dwyer, 1981, 1982). While secreted phosphatases are sensitive to the sodium tartrate, this inhibitor does not affect the activity of acid phosphatases found on the cell surface, as integral membrane proteins (Shakarian et al., 2002, 2003). Hence, to study the effect of BEL on different acid phosphatase activities in the *L. amazonensis* promastigotes, intact cells and the conditioned medium from control and BEL treated parasites were incubated in the presence of 10 mM sodium tartrate (**Figures 5A,B**). Phosphatase activities detected in the promastigotes cell surface (ecto-phosphatase activities), as well as those present in cell free supernatants were mostly resistant to sodium tartrate. Treatment with BEL increased by 21% the sodium tartrate-resistant activity in the cell surface (**Figure 5A**). Interestingly, 43% of the sodium tartrate-resistant phosphatase activity was reduced in the conditioned medium (**Figure 5B**). Sodium tartrate-sensitive phosphatase activity was low in the cells and almost not detected in the secretion. Propidium iodide (PI) labeling, performed after 3 h incubation in HBSS, confirmed parasite viability, and indicated that the enzyme activity present in the conditioned medium was not due to parasites' cell damage (data not shown). These results suggest that BEL inhibited significantly the secretion/release of both acid phosphatases: the sodium tartrate-resistant and -sensitive enzymes of *L. amazonensis* promastigotes.

We also examined the distribution of phosphatase activity in promastigotes treated with BEL, by cytochemical detection in TEM. Control cells had an electron dense precipitate (corresponding to phosphatase activity) on the whole cell surface, in the flagellar pocket lumen and on the flagellum and flagellar pocket membranes (**Figures 5C,D**). Contrasting, treatment with BEL led to a marked decrease in the amount of precipitate in the flagellar pocket, both in its lumen and membrane (**Figure 5E**) although it has not interfered with the intensity of reaction observed in the cell body and flagellar membranes. On the other hand, we observed an increase in acid phosphatase reactivity in intracellular compartments, including the Golgi (**Figure 5E**), vesicles located near the flagellar pocket and the tubulovesicular compartment or multivesicular tubule (MVT) (**Figures 5F,G**).

To evaluate the effect of BEL on the trafficking of a different type of surface protein, we examined the distribution of GP63 in BEL-treated parasites. GP63, the major surface protein of *Leishmania,* is a metalloprotease that occur as GPI-anchored (63 kDa) or unanchored or soluble (65 kDa) isoforms (Ellis et al., 2002; McGwire et al., 2002). Western blotting analysis of the GP63 contents in whole cell extracts of control and BEL-treated promastigotes revealed no significant difference in the intensity and in the pattern of bands (**Figure 6A**, lanes 1 and 2). However, in profiles of conditioned medium, we observed two major bands corresponding to the two GP63 isoforms in control samples. The total amount of GP63 was reduced after treatment with BEL (**Figure 6A**, lanes 3 and 4). Although we observed a reduction in the intensity in both isoforms, the 63 kDa GPI-anchored isoform was the one that suffered a larger reduction (**Figure 6A**, lanes 3 and 4). Flow cytometry of control and BEL-treated parasites permeabilized with saponin and labeled with anti-GP63 antibody showed that, in BEL-treated parasites, the intensity of labeling was slightly higher than that observed in the control (**Figure 6B**), but not statistically significant. We then asked if the increased fluorescence intensity of BEL-treated parasites was due to a reduction in GP63

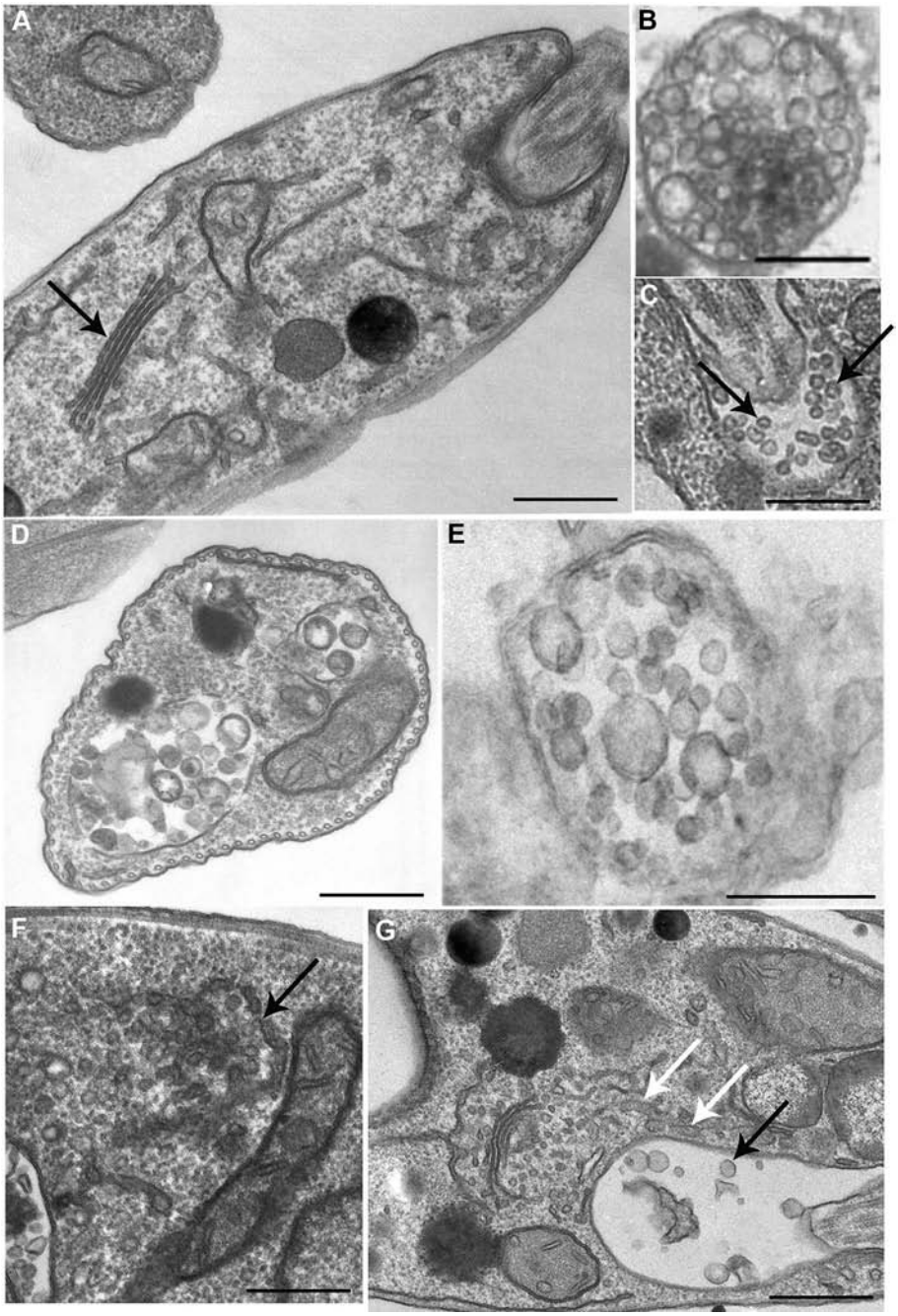

FIGURE 4 | Ultrastructure of endocytic/exocytic pathway organelles in untreated-control and BEL-treated promastigotes. In control cells **(A–C)** the Golgi complex appears as a compact organelle with aligned stacks (**A**, arrow), and cells profiles contain multivesicular bodies **(B,D,E)** and numerous small vesicles within the flagellar pocket (arrows in **C**). Treatment with BEL led to intensive Golgi vesiculation (arrow in **F**), some tubules with a branched aspect in the proximity of the flagellar pocket (white arrows in **G**) and a significant decrease in the number of small vesicles in the flagellar pocket (black arrow in **G**). Representative images of three independent experiments. Bars, 300 nm.

secretion, with intracellular retention and/or redistribution of GP63, as observed with the phosphatase activity (**Figure 5**). Immunofluorescence analysis of GP63 localization showed that, in control cells, labeling was more intense (**Figure 6C**) than in BEL-treated cells and we observed a significant increase in the protein labeling at the posterior region of the cell body, and also in tubular compartments that ran along the body of the parasite (**Figure 6E**).

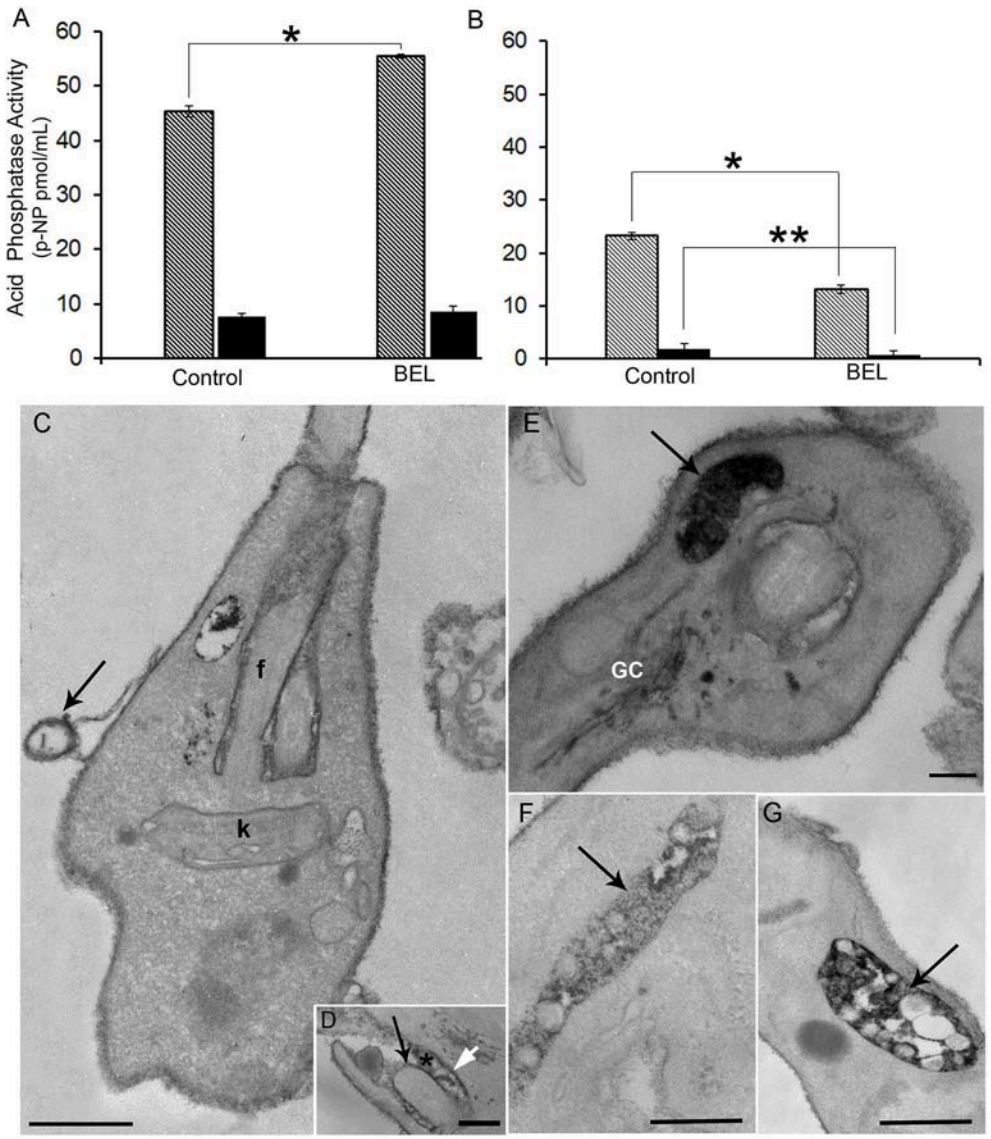

FIGURE 5 | Effect of bromoenol lactone (BEL) on the acid phosphatase activity and localization in promastigotes of *Leishmania amazonensis.* Quantitative analysis of acid phosphatase activity of **(A)** promastigotes and **(B)** conditioned media assayed in the presence or absence of sodium tartrate, in intact BEL-treated and untreated cells, and in conditioned media of untreated control cells and those incubated for 1 h in the presence of BEL as described in the Methods section. Data shown as p-nitrophenyl (p-NP) released, represent mean ± SEM of three independent experiments performed in triplicates. Hatched bars = Na-tartrate sensitive and black bars = Na-resistant tartrate phosphatases. $^{*}p < 0.05$; $^{**}p < 0.01$. **(C–G)** Cytochemical detection of acid phosphatases in control **(C,D)** and in BEL-treated parasites **(E,G)**, using sodium β-glycerophosphate as a substrate. In control parasites, electron dense precipitate indicative of acid phosphatase activity is localized mainly in the cell body, in the flagellar membrane (black arrow in **D**), in the membrane of microvesicles (arrow in **C**), in the membrane of the flagellar pocket (white arrow in **D**) and within the flagellar pocket (asterisk in **D**). In BEL-treated promastigotes acid phosphatase activity was also observed in the Golgi complex (GC), and concentrated in multivesicular tubules (MVTs, arrows in **E,F,G**). f, flagellum; K, kinetoplast. Representative images of three independent experiments. Bars, 300 nm.

BEL Reduces Endocytosis, in *L. amazonensis* Promastigotes

To study the effect of BEL on the endocytosis of promastigotes, we monitored the internalization of three fluorescent-labeled tracers: bovine serum albumin (BSA), transferrin (Tf) and ConA by flow cytometry and fluorescence microscopy, after 1 and 2 h incubation. We observed that the fluorescence intensity of control cells incubated with labeled BSA or transferrin (but not ConA) was ∼3 fold higher after 2 h incubation with the tracers, when compared with 1 h incubation (**Figures 7A–C**). In BEL-treated parasites incubated with fluorescent BSA we observed a reduction of ∼40 and 60% in the intensity of labeling compared with the control, after 1 and 2 h of incubation, respectively. BEL reduced by 70% the intensity of the transferrin labeling after 2 h, but it did not affect the labeling of promastigotes with ConA (**Figures 7B,C**). Moreover, we observed that in control cells,

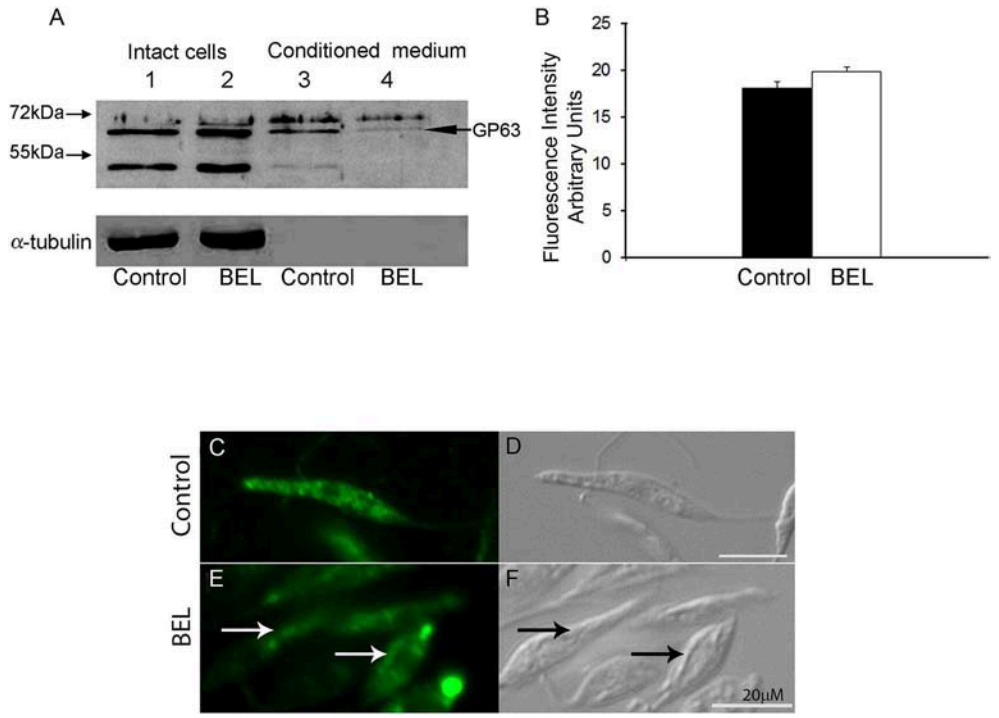

FIGURE 6 | Effect of bromoenol lactone (BEL) in the intracellular localization of GP63 in *Leishmania amazonensis* promastigotes. **(A)** Immunoblots of intact cell (lanes 1 and 2) and conditioned medium (lanes 3 and 4), probed with a polyclonal anti-GP63. Lanes 1 and 3, untreated controls; lanes 2 and 4, BEL-treated parasites. Molecular weight markers are indicated on the left, and the band corresponding to GP63 is indicated on the right. α-tubulin was used as loading control. **(B)** Flow cytometry analysis of GP63 intensity fluorescence in pre-fixed and permeabilized cells showing no statistically significant accumulation of the protein in BEL treated cells. **(C–E)** Fluorescence microscopy analysis of permeabilized cells labeled with anti-GP63 antibody. In control cells **(C,D)**, GP63 labeling was observed in small organelles distributed in the cell body **(C)**. In contrast, in BEL-treated cells **(E,F)**, labeling was less intense in the cytoplasm, and was concentrated in enlarged compartments in the anterior and posterior regions of the cell body, and in elongated structures that resembled the multivesicular tubule, running along the cell body (arrows in **E** and **F**). Bars, 20 μm.

after 2 h incubation, mostly of the fluorescent BSA labeling was concentrated at the posterior end of the parasite (**Figures 7D,E**), compatible with tracer localization in cytoplasmic compartments of the endocytic pathway, such as late endosomes, which are located in this area (Weise et al., 2000). In BEL treated cells, BSA (**Figure 7J**) signal was low occurring at the cell surface and in some cytoplasmic compartments.

Control parasites incubated with Tf showed a labeling concentration in cytoplasmic compartments in the posterior region of the parasite (**Figures 7F,G**). Although treatment with BEL did not modify the percentage of labeled cells, compared with the control, Tf fluorescence in BEL-treated cells was small and mostly on the surface and in the flagellar pocket (**Figures 7K,L**), rather than at the posterior end of the cell.

ConA-labeled promastigotes depicted a quite distinct staining pattern from that found in parasites labeled with the other two tracers. In control parasites, ConA fluorescence was concentrated on the cell surface, in the flagellar pocket, and in elongated structures (resembling the multivesicular tubule described in *L. mexicana*) near the kinetoplast and the nucleus (**Figures 7H,I**). In most BEL-treated parasites, cell surface and flagellar pocket labeling were still apparent, but only a few cells had clear labeling of elongated cytoplasmic structures resembling the tubular compartments (**Figures 7M,N**).

DISCUSSION

Our group produced the first evidence for PLA_2 role on endocytic and exocytic traffic in Trypanosomatids, in a study with epimastigotes of *T. cruzi* treated with dibucaine (Souto-Padrón et al., 2006). In that study, we observed effects suggestive of subversion of the regular traffic of proteases to the reservosomes; however, dibucaine is not a specific inhibitor of $iPLA_2$, and it is possible that some of the effects observed were off-target.

Here, we used BEL to study its effect on endo/exocytosis and traffic of different types of membrane proteins to the cell surface, in promastigotes of *L. amazonensis*. Although BEL is an irreversible and more specific $iPLA_2$ inhibitor, it has been described that BEL may also inhibit a magnesium-dependent phosphatidic acid phosphohydrolase, leading ultimately to apoptosis cell death in mammalian cells (Fuentes et al., 2003). Genes encoding putative phosphatidate phosphohydrolase proteins have been identified in the genome of several trypanosomatids (TriTrypDB database), including the *L. amazonensis* MHOM/BR/71973/M2269 strain, but none have

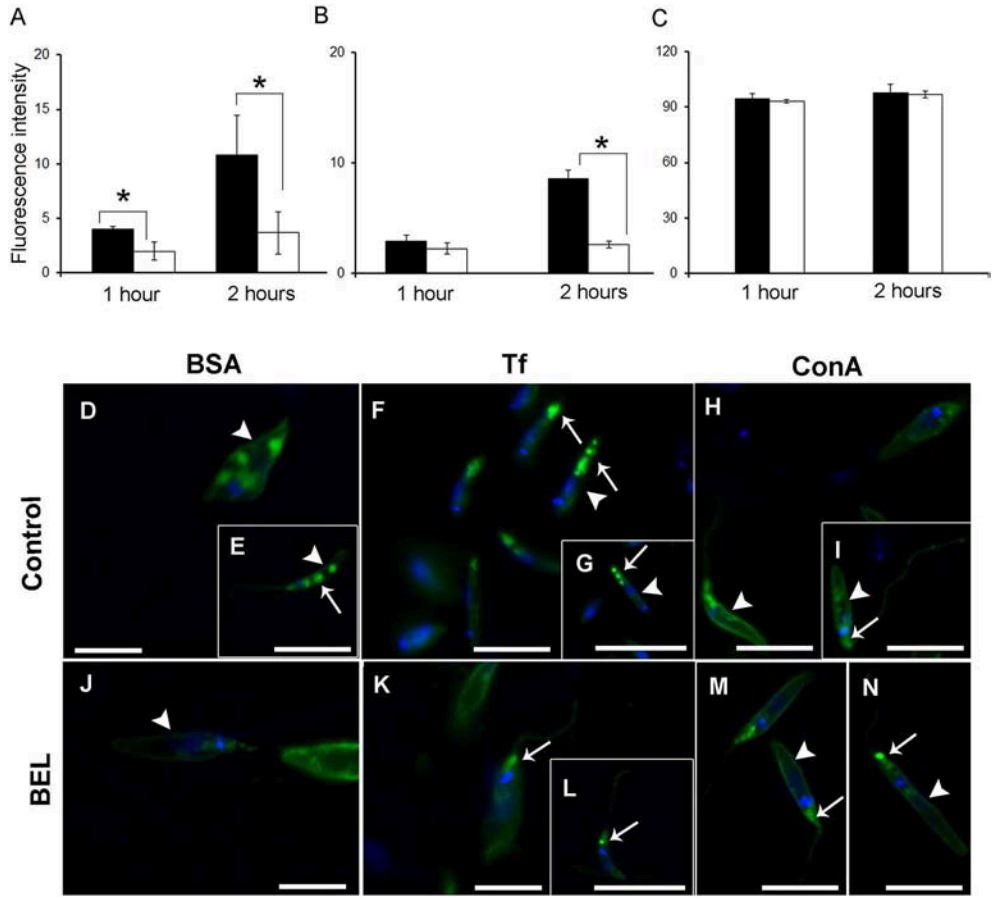

FIGURE 7 | Influence of bromoenol lactone (BEL) on the endocytic activity of *Leishmania amazonensis*. Promastigotes were incubated with **(A)** bovine serum albumin (BSA), **(B)** transferrin (Tf), and **(C)** Concanavalin A (ConA) tracers and the fluorescence intensity analysis by flow cytometry. Data represent mean ± SEM of three independent experiments, performed in duplicates. *$p < 0.05$. **(D–I)** Untreated controls and **(J–N)** BEL-treated promastigotes were incubated with Alexa Fluor 488-labeled BSA **(D,E,J)**, Tf **(F,G,K,L)**, and ConA **(H,I,M,N)** for 2 h. In control cells, labeled BSA and Tf **(D–G)** were observed on the cell surface (arrowheads) and in cytoplasmic compartments mainly the ones at the posterior end of the cells (arrows in **E–G**). In BEL treated cells, BSA **(J)** and transferrin **(K,L)** signal occur at the cell surface (arrowhead in **J**) and at the flagellar pocket (arrows in **K,L**). Control cells incubated with fluorescent ConA had intense signal on the cell surface (arrowheads in **H,I**), and in the flagellar pocket (arrow in **I**) and this labeling pattern was not altered by treatment with BEL **(M,N)**. The DNA was stained with DAPI. Bars: 20 μM.

been cloned or studied further yet. Among those, one type of phosphatidate phosphatase contains a conserved PAP-2 superfamily domain (Interpro IPR000326) and 3 putative genes coding for them were identified in the genome of *L. amazonensis* MHOM/BR/71973/M2269 strain (TriTrypDB Accession numbers LAMA 000277200, LAMA_000277300, and LAMA_000302500). The other type of magnesium-dependent phosphatidic acid phosphohydrolase identified in *L. amazonensis* (LAMA000023900) contains a Lipin (Interpro IPR007651) and Lipin/Ned1/Smp2 (Interpro IPR013209) conserved domains that strongly align with the sequences found in the yeast (NCBI AHY76617.1) and mice (NCBI NP_001186047.1) orthologs. Therefore, although not tested here, BEL might be also inhibiting another target enzyme in *Leishmania*. However, we could not found the characteristic alterations described for BEL-inhibition of magnesium-dependent phosphatidic acid phosphohydrolase (Fuentes et al., 2003) as the mitochondrial potential and apoptosis cell death in the parasites in our conditions. Moreover, treatment of *L. amazonensis* promastigotes with 2.5 μM BEL inhibited PLA_2 activity by 60% (**Figure 2B**) without causing cell death, even after more than 24 h treatment (**Figure 1A**). In contrast, this concentration of BEL is sufficient to reduce the mitochondrial membrane potential in different types of mammalian cells (Ma et al., 2011; Nordmann et al., 2014; Rauckhost et al., 2015). Contrary to mammalian cells, BEL did not inhibit *L. amazonensis* proliferation at our conditions (Sanchez and Moreno, 2002; Balboa et al., 2003; Song et al., 2007). However, treatment with BEL significantly reduced the differentiation of promastigotes into metacyclic forms (**Figure 1B**). In Trypanosomatids, metacyclogenesis is an important step that occurs in the insect vector which enables parasites to survive within the vertebrate host (Avila et al., 2003; Pinto-da-Silva et al., 2005). The structural changes and expression of molecules observed during metacyclogenesis

involve the activation of synthesis and degradative pathways that are dependent on the fusion of cytoplasmic compartments (Besteiro et al., 2007). We believe that changes in the fusion of these compartments caused by BEL, may participate in the reduction of metacyclogenesis rate in *L. amazonensis*.

In different pathogenic microorganisms (including bacteria and protozoa) PLA_2 activity is important for the pathogen interaction with host cells (Connelly and Kierszenbaum, 1984; Saffer and Schwartzman, 1991; Silverman et al., 1992). In *Leishmania,* different studies showed the presence of PLA_2 activity in *L. amazonensis* and of a platelet-activating factor acetylhydrolase (PAF-AH) in *L. major* (Henriques et al., 2003; Passero et al., 2008; Pawlowic and Zhang, 2012). Unlike that reported by Passero et al. (2008), we showed here that most PLA_2 activity in *L. amazonensis* promastigotes is present in the parasite and not in the culture supernatant (conditioned medium) (**Figure 2A**). A key difference that could explain this variation was that we evaluated PLA_2 activities in the intact parasite and not in cell lysates. Also, unlike what was shown by these authors for the inhibition of PLA_2 activity using betamethasone, we observed that BEL inhibited significantly the $iPLA_2$ activity in intact cells, but did not affect the PLA_2 activity secreted into the conditioned medium (**Figure 2B**).

In mammalian cells $iPLA_2$ regulates Golgi and ERGIC morphology, as well as membrane trafficking in and out of these organelles and $iPLA_2$ inhibition causes intense Golgi fragmentation (Mayorga et al., 1993; De Figueiredo et al., 1998, 1999, 2000; Ben-Tekaya et al., 2010; Bechler et al., 2012). We observed similar changes in the Golgi of promastigotes after BEL treatment (**Figures 4F,G**). BEL also led to enlargement of the MVT and other tubular structures located in the anterior region of the parasite (**Figures 4F,G**). In promastigotes this region is the site of intense endo/exocytic traffic. In analogy to other cellular models, it is likely that the enlargement of endocytic pathway compartments indicates changes in vesicular traffic that lead to inhibition of both exocytosis and endocytosis (Mayorga et al., 1993; Lennartz et al., 1997; De Figueiredo et al., 1998). In line with these observations, we detected that treatment with BEL reduced around 50% the overall amount of protein in the parasites and in the vesicle fraction. Images of the flagellar pocket of control cells showed a large number of vesicles of different sizes (**Figure 4C**), including small vesicles (50–100 nm) likely derived from exosomes exocytosis, and larger "microvesicles" (up to 300 nm in diameter), whose membrane derives directly from the flagellar pocket membrane. Microvesicles are also observed budding from the flagellar pocket membrane at the exit of flagellar pocket, from the cell body and the flagellar membranes.

Our data are consistent with that presented by Silverman et al. (2010), showing that exosome release is a major mechanism of protein secretion by *Leishmania*. However, we also noted a clear reduction in the number of microvesicles within and outside the flagellar pocket of treated parasites. Calcium-independent PLA_2 activity has been associated to the budding of microvesicles in lipid-rafts enriched plasma membrane (Mizuno-Kamiya et al., 2001; Nakano et al., 2009). Coincidentally, *Leishmania* plasma and flagellar membranes possess a high concentration of lipid rafts (Pimenta and De Souza, 1987) and an intense microvesicle budding activity (Saraiva et al., 1989; Vannier-Santos et al., 1992). In conclusion, our results suggest that BEL-sensitive target in *Leishmania* is also involved in controlling both the fusion of endocytic pathway compartments to the flagellar pocket membrane, which releases exosomes, and the direct budding of microvesicles from different regions of the parasite membrane. Interestingly, control parasites released microvesicles with similar size to that described by Barbosa et al. (2018). However, BEL-treated promastigotes besides the population alike the control cells, released also a second population of microvesicles, ranging from 400 to 450 nm of relative diameter.

In *Leishmania*, both acid phosphatases and GP63 are targeted to the plasma membrane, but may also be found free in the extracellular medium (Gottlieb and Dwyer, 1982; Jaffe and Dwyer, 2003). Inhibition by BEL increased the total acid phosphatase activity in promastigotes (**Figure 5A**), and changed the distribution of the tartrate-sensitive enzyme (**Figures 5C–G**). This activity, which is regularly secreted in control parasites, accumulated in MVTs after treatment with BEL, as seen in TEM images (**Figures 5E–G**). BEL treatment, however, did not affect the targeting of the sodium tartrate-resistant acid phosphatase to the plasma membrane, since cytochemical detection of phosphatases in BEL-treated parasites show an amount of cell surface precipitate similar to that observed in control cells (**Figures 5C,E**). The presence of a significant amount of tartrate-resistant phosphatase activity in the conditioned medium obtained from control parasites was in line with the ultrastructural data showing that control promastigotes released a higher amount of EVs in the conditioned medium. Its reduction after treatment with BEL is consistent with the decrease in the number of vesicles within the flagellar pocket also observed by TEM.

The GP63 is predominantly expressed on the surface of *Leishmania* promastigotes in a GPI-anchored form, associated with lipid rafts, or as an "unanchored" GP63 secreted into the extracellular medium (Weise et al., 2000; Denny et al., 2001; Ellis et al., 2002; McGwire et al., 2002). Treatment with BEL reduced the amount of GP63 released extracellularly and increased the labeling of compartments located in the posterior region of the parasite (**Figure 6E**), which include the MVT (Weise et al., 2000).

Anchored and unanchored GP63 isoforms are secreted by different routes that depend on the presence of GPI-anchor and N-glycosylation, respectively (Ellis et al., 2002). Our data suggest that changes in the structure of the ER and Golgi after BEL lead to changes in the glycosylation pattern of the unanchored GP63 and to their accumulation in the parasite as observed in the immunofluorescence image (**Figure 6E**). On the other hand GPI-anchored GP63, which targeting was previously described in *L. mexicana* (Ellis et al., 2002) as being regulated exclusively by the presence of a GPI anchor, appeared unaffected by BEL treatment as evidenced in **Figures 6C,E**. More

substantial changes were observed in the conditioned medium after BEL treatment that reduced around 40% the amount of secreted GP63. Among the two bands observed the most significant reduction was on the 63 kDa GPI anchored GP63. The GPI-anchored GP63 may be released from the cell surface by autoproteolytic cleavage (McGwire et al., 2002). As there are no reports of BEL action inhibiting autoproteolytic activities, we believe that the reduction of the 63 kDa band observed in the conditioned medium is related to the reduction in its release through the microvesicle secretion (Silverman et al., 2010). Indeed, our results suggest that the total amount of microvesicles in the incubation medium is reduced after treatment with BEL (**Figures 3G,I**).

We also determined whether BEL-target inhibition would be involved in the fusion of the endocytic compartments. As previously mentioned the uptake of molecules in *Leishmania* occurs through the flagellar pocket, and both fluid-phase endocytosis (of BSA and other tracers) and receptor-mediated endocytosis—of transferrin (Voyiatzaky and Soteriadou, 1992), LDL (Bastin et al., 1996), and hemoglobin (Singh et al., 2003)—have been reported. iPLA$_2$ inhibitors (such as dibucaine) decrease transferrin (Tf) endocytosis in rat muscle cells (Hagiwara and Ozawa, 1990), and BSA endocytosis in *T. cruzi* (Souto-Padrón et al., 2006). Our results using three different endocytosis tracers—BSA, Tf and Concanavalin A—showed that BEL-target inhibition is required for both fluid-phase and receptor mediated endocytosis. Nevertheless, BEL had different effects on the endocytosis of fluid-phase (BSA) and receptor-mediated (Tf) tracers by the promastigotes. Inhibition of BSA endocytosis by BEL was partial (∼60%), and similar to that observed in epimastigotes of *T. cruzi* treated with dibucaine (Souto-Padrón et al., 2006). This significant (albeit not full) reduction in BSA endocytosis contrasts with a more profound effect of BEL in Tf internalization (**Figures 7F,G,K,L**). Bromoenol lactone did not affect surface labeling of fluorescent Tf, suggesting that its target activity is not required for Tf receptor (TfR) recycling to the cell surface, differently from that described for HeLa cells and hepatocytes (De Figueiredo et al., 2001). Our data about the TfR trafficking are in agreement with the recently described trafficking of HbR in *Leishmania* (Bahl et al., 2015), which is independent of GP63 and secretory acid phosphatase pathway. In contrast, BEL-target activity appears essential for Tf uptake, since the endocytosis of this tracer was restricted to the flagellar pocket in BEL-treated cells, and was absent from internal endocytic compartments (**Figures 7F,G,K,L**). Further studies are required to confirm that BEL-target has a role in TfR endocytosis, but not in receptor recycling to the surface. Unlike procyclic/bloodstream *Trypanosoma brucei* (Brickman et al., 1995), *L. amazonensis* promastigotes did not internalize large amounts of labeled ConA, which was located primarily on the surface and flagellar pocket (**Figure 7**). However, some parasites displayed internal ConA labeling, in elongated structures that probably correspond to tubular compartments of the endocytic pathway. Internal labeling with ConA disappeared after BEL-treatment, and this lectin was concentrated in the flagellar pocket, reinforcing the notion that BEL-target activity (presumably at the flagellar pocket membrane) is important to initiate endocytosis by vesicle budding into the cytoplasm, regardless of the endocytic route used.

In conclusion, we showed that BEL-target activity is required for three key processes in *Leishmania*, namely: the internalization of nutrients by endocytosis, the secretion of vesicles and the differentiation of promastigotes into infective metacyclic forms. Interestingly, it has been shown that although their hepatotoxicity, BEL treatment decreased parasite load in a cutaneous murine model, suggesting further chemical modifications in the molecule that could decrease this side effect maintaining the leishmanicidal activity (Bordon et al., 2018).

DATA AVAILABILITY STATEMENT

The datasets generated for this study are available on request to the corresponding author.

ETHICS STATEMENT

The animal study was reviewed and approved by Ethics Committee for Animal Experimentation of the Health Sciences Center, Federal University of Rio de Janeiro (Protocol No. IBCCF-085).

AUTHOR CONTRIBUTIONS

TS-P conceived and designed the experiments. AF, DS, RN, CK, SF, NH, and CA performed the experiments. AF, DS, CK, SF, NH, CA, JM-F, ES, and TS-P analyzed the data. AF, DS, CK, NH, CA, SF, JM-F, ES, and TS-P wrote the manuscript. All authors read and approved the final version of the manuscript.

FUNDING

This study was provided by Conselho Nacional de Desenvolvimento Científico e Tecnológico (CNPq), Fundação de Amparo a Pesquisa do Estado do Rio de Janeiro (FAPERJ), Coordenação de Aperfeiçoamento de Pessoal de Nível Superior (CAPES), Finance code 001, and Instituto Nacional de Ciência e Tecnologia de Biologia Estrutural e Bioimagem (INBEB).

ACKNOWLEDGMENTS

We are grateful to Tarcísio Corrêa for valuable technical assistance, and to Unidade de Microscopia Multiusuário Souto-Padrón & Lins (UniMicro) for all the microscopy support.

REFERENCES

Ackermann, E. J., Conde-Frieboes, K., and Dennis, E. A. (1995). Inhibition of macrophage Ca(2+)-independent phospholipase A2 by bromoenol lactone and trifluoromethyl ketones. *J. Biol. Chem*. 270, 445–450. doi: 10.1074/jbc.270.1.445

Avila, A. R., Dallagiovanna, B., Yamada-Ogatta, S. F., Monteiro-Góes, V., Fragoso, S. P., Krieger, M. A., et al. (2003). Stage specific gene expression during *Trypanosoma cruzi* metacyclogenesis. *Genet. Mol. Res.* 2, 159–168.

Bahl, S., Parashar, S., Malhotra, H., Raje, M., and Mukhopadhyay, A. (2015). Functional characterization of monomeric GTPase Rab1 in the secretory pathway of Leishmania. *J. Biol. Chem*. 290, 29993–30005. doi: 10.1074/jbc.M115.670018

Balboa, M. A., Sáez, Y., and Balsinde, J. (2003). Calcium-independent phospholipase A2 is required for lysosyme secretion in U937 promonocytes. *J Immunol*. 170, 5276–5280. doi: 10.4049/jimmunol.170.10.5276

Barbosa, F. M. C., Dupin, T. V., Toledo, M. D. S., Reis, N. F. D. C., Ribeiro, K., Cronemberger-Andrade, A., et al. (2018). Extracellular vesicles released by *Leishmania* (*Leishmania*) amazonensis promote disease progression and induce the production of different cytokines in macrophages and B-1 cells. *Front. Microbiol*. 9:3056. doi: 10.3389/fmicb.2018.03056

Bastin, P., Stephan, A., Raper, J., Saint-Remy, J. M., Opperdoes, F. R., and Courtoy, P. J. (1996). An M(r) 145,000 low-density lipoprotein (LDL)-binding protein is conserved throughout the Kinetoplastida order. *Mol. Biochem. Parasitol*. 76, 43–56. doi: 10.1016/0166-6851(95)02537-5

Bechler, M. E., and Brown, W. J. (2013). PAFAH Ib phospholipase A2 subunits have distinct roles in maintaining Golgi structure and function. *Biochim. Biophys. Acta* 1831, 595–601. doi: 10.1016/j.bbalip.2012.12.004

Bechler, M. E., de Figueiredo, P., and Brown, W. J. (2012). A PLA1-2 punch regulates the Golgi complex. *Trends Cell Biol*. 22, 116–124. doi: 10.1016/j.tcb.2011.10.003

Bechler, M. E., Doody, A. M., Racoosin, E., Lin, L., Lee, K. H., and Brown, W. J. (2010). The phospholipase complex PAFAH Ib regulates of the functional organization of the Golgi complex. *J. Cell Biol*. 190, 45–53. doi: 10.1083/jcb.200908105

Belaunzarán, M. L., Lammel, M. J., and Isola, E. L. D. (2011). Phospholipases A in trypanosomatids. *Enz Res*. 2011:392082. doi: 10.4061/2011/392082

Belaunzarán, M. L., Wainszelbaum, M. J., Lammel, E. M., Gimenez, G., Aloise, M. M., Florin-Christensen, J., et al. (2007). Phospholipase A1 from Trypanosoma cruzi infective stages generates lipid messengers that activate host cell protein kinase C. *Parasitology* 134, 491–502. doi: 10.1017/S0031182006001740

Belaunzarán, M. L., Wilkowsky, S. E., Lammel, E. M., Giménez, G., Bott, E., Barbieri, M. A., et al. (2013). Phospholipase A1: a novel virulence factor in *Trypanosoma cruzi*. *Mol. Biochem. Parasitol*. 187, 77–86. doi: 10.1016/j.molbiopara.2012.12.004

Ben-Tekaya, H., Kahn, R. A., and Hauri, H. P. (2010). ADP ribosylation factors 1 and 4 and group VIA phospholipase A2 regulate morphology and intraorganellar traffic in the endoplasmic reticulum-Golgi intermediate compartments. *Mol. Biol. Cell* 21, 4130–4140. doi: 10.1091/mbc.e10-01-0022

Besteiro, S., Williams, R. A. M., Coombs, G. H., and Mottram, J. C. (2007). Protein turnover and differentiation in Leishmania. *Int. J. Parasitol*. 37, 1063–1075. doi: 10.1016/j.ijpara.2007.03.008

Besteiro, S., Williams, R. A. M., Morrison, L. S., Coombs, G. H., and Mottram, J. C. (2006). Endosome sorting and autophagy are essential for differentiation and virulence of Leishmania major. *J. Biol. Chem.* 281, 11384–11396. doi: 10.1074/jbc.M512307200

Bordon, M. L. A. C., Laurenti, M. D., Ribeiro, S. P., Toyama, M. H., Toyama, D. O., and Passero, L. F. D. (2018). Effect of phospholipase A(2) inhibitors during infection caused by Leishmania (L.) amazonensis. *J. Venom Anim Toxins Incl. Trop. Dis*. 24, 21–28. doi: 10.1186/s40409-018-0156-9

Bradford, M. M. (1976). A rapid and sensitive method for the quantitation of microgram quantities of protein utilizing the principle of protein-dye binding. *Anal. Biochem*. 72, 248–254. doi: 10.1016/0003-2697(76)90527-3

Brickman, M. J., Cook, J. M., and Balber, A. E. (1995). Low temperature reversibly inhibits transport from tubular endosomes to a perinuclear, acidic compartment in African trypanosomes. *J. Cell Sci.* 108, 3611–3621.

Brown, W. J., Chambers, K., and Doody, A. (2003). Phospholipase A2 (PLA2) enzymes in membrane trafficking: mediators of membrane shape and function. *Traffic* 4, 214–221. doi: 10.1034/j.1600-0854.2003.00078.x

Connelly, M. C., and Kierszenbaum, F. (1984). Modulation of macrophage interaction with *Trypanosoma cruzi* by phospholipase A2-sensitive components of the parasite membrane. *Biochem. Biophys. Res. Commun.* 121, 931–939. doi: 10.1016/0006-291X(84)90766-6

Da Silva, C. V., Luquetti, A. O., Rassi, A., and Mortara, R. A. (2006). Involvement of Ssp-4 related carbohydrate epitopes in mammalian cell invasion by *Trypanosoma cruzi* amastigotes. *Microb. Infect.* 8, 2120–2129. doi: 10.1016/j.micinf.2006.03.016

De Figueiredo, P., Doody, A., Polizotto, R. S., Drecktrah, D., Wood, S., Banta, M., et al. (2001). Inhibition of transferrin recycling and endosome tubulation by phospholipase A2 antagonists. *J. Biol. Chem*. 276, 47361–47370. doi: 10.1074/jbc.M108508200

De Figueiredo, P., Drecktrah, D., Katzenellenbogen, J. A., Strang, M., and Brown, W. J. (1998). Evidence that phospholipase A2 activity is required for Golgi complex and Trans-Golgi network membrane tubulation. *Proc. Natl. Acad. Sci. U.S.A*. 95, 8642–8647. doi: 10.1073/pnas.95.15.8642

De Figueiredo, P., Drecktrah, D., Polizotto, R. S., Cole, N. B., Lippincott-Schwartz, J., and Brown, W. J. (2000). Phospholipase A2 antagonists inhibit constitutive retrograde membrane traffic to the endoplasmic reticulum. *Traffic* 1, 504–511. doi: 10.1034/j.1600-0854.2000.010608.x

De Figueiredo, P., Polizotto, R. S., Drecktrah, D., and Brown, W. J. (1999). Membrane tubule-mediated reassembly and maintenance of the Golgi complex is disrupted by phospholipase A2 antagonists. *Mol. Biol. Cell.* 10, 1763–1782. doi: 10.1091/mbc.10.6.1763

De Souza, W., Sant'Anna, C., and Cunha-e-Silva, N. L. (2009). Electron microscopy and cytochemistry analysis of the endocytic pathway of pathogenic protozoa. *Prog. Histochem. Cytochem*. 44, 67–124. doi: 10.1016/j.proghi.2009.01.001

Denny, P. W., Field, M. C., and Smith, D. F. (2001). GPI-anchored proteins and glycoconjugates segregate into lipid rafts in Kinetoplastida. *FEBS Lett*. 491, 148–153. doi: 10.1016/S0014-5793(01)02172-X

Ellis, M., Sharma, D. K., Hilley, J. D., Coombs, G. H., and Mottram, J. C. (2002). Processing and trafficking of Leishmania mexicana GP63. Analysis using GP18 mutants deficient in glycosylphosphatidylinositol protein anchoring. *J. Biol. Chem*. 277, 27968–27974. doi: 10.1074/jbc.M202047200

Fensome-Green, A., Stannard, N., Li, M., Bolsover, S., and Cockcroft, S. (2007). Bromoenol lactone, an inhibitor of Group V1A calcium-independent phospholipase A2 inhibits antigen-stimulated mast cell exocytosis without blocking Ca2+ influx. *Cell Calcium*. 41, 145–153. doi: 10.1016/j.ceca.2006.06.002

Fuentes, L., Pérez, B., Nieto, M. L., and Balsinde, B. M. A. (2003). Bromoenol lactone promotes cell death by a mechanism involving phosphatidate phosphohydrolase-1 rather than calcium-independent phospholipase A2. *J. Biol. Chem*. 278, 44683–44690. doi: 10.1074/jbc.M307209200

Ghedin, E., Debrabant, A., Engel, J. C., and Dwyer, D. M. (2001). Secretory and endocytic pathways converge in a dynamic endosomal system in a primitive protozoan. *Traffic* 2, 175–188. doi: 10.1034/j.1600-0854.2001.020304.x

Gomes, S. A., Fonseca de Souza, A. L., Silva, B. A., Kiffer-Moreira, T., Santos-Mallet, J. R., Santos, A. L., et al. (2006). *Trypanosoma rangeli*: differential expression of cell surface polypeptides and ecto-phosphatase activity in short and long epimastigote forms. *Exp. Parasitol*. 12, 253–262. doi: 10.1016/j.exppara.2005.11.015

Gottlieb, M., and Dwyer, D. M. (1981). *Leishmania donovani*: surface membrane acid phosphatase activity of promastigotes. *Exp. Parasitol*. 52, 117–128. doi: 10.1016/0014-4894(81)90067-9

Gottlieb, M., and Dwyer, D. M. (1982). Identification and partial characterization of an extracellular acid phosphatase activity of *Leishmania donovani* promastigotes. *Mol. Cell Biol*. 2, 76–81. doi: 10.1128/MCB.2.1.76

Hagiwara, Y., and Ozawa, E. (1990). Suppression of transferring internalization in myogenic L6 cells by dibucaine. *Biochim. Biophys. Acta* 1051, 237–241. doi: 10.1016/0167-4889(90)90128-Z

Henriques, C., Atella, G. C., Bonilha, V. L., and De Souza, W. (2003). Biochemical analysis of proteins and lipids found in parasitophorous vacuoles containing *Leishmania amazonensis*. *Parasitol Res*. 89, 123–133. doi: 10.1007/s00436-002-0728-y

Jaffe, C. L., and Dwyer, D. M. (2003). Extracellular release of the surface metalloprotease, GP63 from Leishmania and insect trypanosomatids. *Parasitol. Res*. 91, 229–237. doi: 10.1007/s00436-003-0960-0

Köhler, G. A., Brenot, A., Haas-Stapleton, E., Agabian, N., Deva, R., and Nigam, S. (2006). Phospholipase A2 and Phospholipase B activities in fungi. *Biochim. Biophys. Acta* 1761, 1391–1399. doi: 10.1016/j.bbalip.2006.09.011

Laemmli, U. K. (1970). Cleavage of structural proteins during the assembly of head bacteriophage T4. *Nature* 227, 680–685. doi: 10.1038/227680a0

Lambertz, U., Silverman, J. M., Nandan, D., McMaster, W. R., Clos, J., Foster, L. J., et al. (2012). Secreted virulence factors and immune evasion in visceral leishmanisasis. *J. Leukoc. Biol*. 91, 887–899. doi: 10.1189/jlb.0611326

Lennartz, M. R., Yuen, A., Masi, S. M., Russell, D. G., Buttle, K. F., and Smith, J. J. (1997). Phospholipase A2 inhibition results in sequestration of plasma membrane into electronlucent vesiscles during IgG-mediated phagocytosis. *J. Cell Sci*. 110, 2041–2052.

Ma, M. T., Yeo, J. F., Farooqui, A. A., and Ong, W. Y. (2011). Role of calcium independent phospholipase A2 in maintaining mitochondrial membrane potential and preventing excessive exocytosis in PC12 cells. *Neurochem. Res*. 36, 347–354. doi: 10.1007/s11064-010-0340-y

Macedo-Silva, S. T., De Oliveira Silva, T. L., Urbina, J. A., De Souza, W., and Rodrigues, J. C. (2011). antiproliferative, ultrastructural and physiological effects of amiodarone on pormastigote and amastigote forms of *Leishmania amazonensis*. *Mol. Biol. Int*. 2011:876021. doi: 10.4061/2011/876021

Mayorga, L. S., Colombo, M. I., Lennartz, M., Brown, E. J., Rahman, K. H., Weiss, R., et al. (1993). Inhibition of endosome fusion by phospholipase A2 (PLA2) inhibitors points to a role for PLA2 in endocytosis. *Proc. Natl. Acad. Sci. U.S.A*. 90, 10255–10259. doi: 10.1073/pnas.90.21.10255

McConville, M. J., Mullin, K. A., Ilgoutz, S. C., and Teasdale, R. D. (2002). Secretory pathway of trypanosomatid parasites. *Microbiol. Mol. Biol. Rev*. 66, 122–154. doi: 10.1128/MMBR.66.1.122-154.2002

McGwire, B. S., O'Connel, W. A., Chang, K. P., and Engman, D. M. (2002). Extracellular release of the glycosylphospfatidylinositol (GPI)-linked Leishmania surface metalloprotease, GP 63, is independent of GPI phospholipolysis: implication for parasite virulence. *J. Biol. Chem*. 277, 8802–8809. doi: 10.1074/jbc.M109072200

Mizuno-Kamiya, M., Inokuchi, H., Kameyama, Y., Yashiro, K., and Fujita, A. (2001). Ca2+-independent phospholipase A2 activity in apical plasma membranes from the rat parotid gland. *Arch. Oral. Biol*. 46, 789–799. doi: 10.1016/S0003-9969(01)00050-4

Morgan, G. W., Hall, B. S., Denny, P. W., Carrington, M., and Field, M. C. (2002a). The kinetoplastida endocytic apparatus. Part I: a dynamic system for nutrition and evasion of host defences. *Trends Parasitol*. 18, 491–496. doi: 10.1016/S1471-4922(02)02391-7

Morgan, G. W., Hall, B. S., Denny, P. W., Field, M. C., and Carrington, M. (2002b). The endocytic apparatus of the kinetoplastida. Part II: machinery and components of the system. *Trends Parasitol*. 18, 540–546. doi: 10.1016/S1471-4922(02)02392-9

Morikawa, R. K., Aoki, J., Kano, F., Murata, M., Yamamoto, A., Tsujimoto, M., et al. (2009). Intracellular phospholipase A1γ (iPLA1γ) is a novel factor involved in coat protein complex I- and Rab6-independent retrograde transport between the endoplasmic reticulum and the Golgi complex. *J. Biol. Chem*. 284, 26620–26630. doi: 10.1074/jbc.M109.038869

Murakami, M., and Kudo, I. (2002). Phospholipase A2. *J. Biochem*. 131, 285–292. doi: 10.1093/oxfordjournals.jbchem.a003101

Naderer, T., Vince, J. E., and Mc Conville, M. J. (2004). Surface determinants of Leishmania parasites and their role in infectivity in the mammalian host. *Curr. Mol. Med*. 4, 649–665. doi: 10.2174/1566524043360069

Nakano, T., Inoue, I., Shinozaki, R., Matsui, M., Akatsuka, T. T. S., and Komoda, T. (2009). A possible role of lysophospholipids produced by calcium-independent phospholipase A2 in membrane-raft budding and fission. *Biochim. Biophys. Acta* 788, 2222–2228. doi: 10.1016/j.bbamem.2009.07.015

Nordmann, C., Strokin, M., Schönfeld, P., and Reiser, G. (2014). Putative roles of Ca2+-independent phospholipase A2 in respiratory chain-associated ROS production in brain mitochondria: influence of docosahexaenoid acid and bromoenol lactone. *J. Neurochem*. 131, 163–176. doi: 10.1111/jnc.12789

Passero, L. F., Laurenti, M. D., Tomokane, T. Y., Corbett, C. E., and Toyama, M. H. (2008). The effect of phospholipase A2 from Crotalus durissus collilineatus on Leishmania (Leishmania) amazonensis infection. *Parasitol. Res*. 102, 1025–1033. doi: 10.1007/s00436-007-0871-6

Pawlowic, M. C., and Zhang, K. (2012). Leishmania parasites possess a platelet-activating factor acetylhydrolase important for virulence. *Mol. Biochem. Parasitol*. 186, 11–20. doi: 10.1016/j.molbiopara.2012.08.005

Péchoux, C., Boisgard, R., Chanat, E., and Lavialle, F. (2005). Ca(2+)-independent phospholipase A2 participates in the vesicular transport of milk proteins. *Biochim. Biophys. Acta* 1743, 317–329. doi: 10.1016/j.bbamcr.2005.01.006

Pimenta, P. F., and De Souza, W. (1987). Leishmania mexicana: distribution of intramembranous particles and filipin sterol complexes in amastigotes and promastigotes. *Exp. Parasitol*. 63, 117–135. doi: 10.1016/0014-4894(87)90153-6

Pinto-da-Silva, L. H., Fampa, P., Soares, D. C., Oliveira, S. M., Souto-Padron, T., and Saraiva, E. M. (2005). The 3A1-La monoclonal antibody reveals key features of Leishmania (L) amazonensis metacyclic promastigotes and inhibits procyclics attachment to the sand fly midgut. *Int. J. Parasitol*. 35, 757–764. doi: 10.1016/j.ijpara.2005.03.004

Ramanadhan, S., Gross, R. W., Han, X., and Turk, J. (1993). Inhibition of arachidonate release by secretagogue-stimulated pancreatic islets suppresses both insulin secretion and the rise in beta-cell cytosolic calcium ion concentration. *Biochem* 32, 337–346. doi: 10.1021/bi00052a042

Rauckhost, A. J., Pfeiffer, D. R., and Broekemeier, K. M. (2015). The iPLA2γ is identified as the membrane potential sensitive phospholipase in liver mitochondria. *FEBS Lett*. 589, 2367–2371. doi: 10.1016/j.febslet.2015.07.016

Russel, D. G., and Wilhelm, H. (1986). The involvement of the major surface glycoprotein (GP 63) of Leishmania promastigotes in attachment to macrophages. *J. Immunol*. 136, 2613–2620.

Saffer, L. D., Long Krug, S. A., and Schwartzman, J. D. (1989). The role of phospholipase in host cell penetratrion by *Toxoplasma gondii*. *Am. J. Trop. Med. Hyg*. 40, 145–149. doi: 10.4269/ajtmh.1989.40.145

Saffer, L. D., and Schwartzman, J. D. (1991). A soluble phospholipase of *Toxoplasma gondii* associated with host cell penetration. *J. Protozool*. 38, 454–460. doi: 10.1111/j.1550-7408.1991.tb04816.x

San Pietro, E., Capestrano, M., Polishchuk, E. V., DiPentima, A., Trucco, A., Zizza, P., et al. (2009). Group IV phospholipase A2α controls the formation of inter-cisternal continuities involved in intra-Golgi transport. *PLoS Biol*. 7:e1000194. doi: 10.1371/journal.pbio.1000194

Sanchez, T., and Moreno, J. J. (2002). Calcium-independent phospholipase A2 through arachidonic acid mobilization is involved in Caco-2 cell growth. *J. Cell Physiol*. 193, 293–298. doi: 10.1002/jcp.10162

Saraiva, E. M., Vannier-Santos, M. A., Silva-Filho, F. C., and De Souza, W. (1989). Anionic site behavior in Leishmania and its role in the parasite-macrophage interaction. *J. Cell Sci*. 93, 481–489.

Shakarian, A. M., Joshi, M. B., Ghedin, E., and Dwyer, D. M. (2002). Molecular dissection of the functional domains of a unique tartrate-resistant, surface membrane acid phosphatase in the primitive human pathogen *Leishmania donovani*. *J. Biol. Chem*. 277, 17994–18001. doi: 10.1074/jbc.M200114200

Shakarian, A. M., Joshi, M. B., Yamage, M., Ellis, S. L., Debrabant, A., and Dwyer, D. M. (2003). Members of a unique histidine acid phosphatase family are conserved amongst a group of primitive eukaryotic human pathogens. *Mol. Cell Biochem*. 245, 31–41. doi: 10.1023/A:1022851914014

Shin, H. W., Takatsu, H., and Nakayama, K. (2012). Mechanisms of membrane curvature generation in membrane traffic. *Membranes* 2, 118–133. doi: 10.3390/membranes2010118

Silverman, D. J., Santucci, L. A., Meyers, N., and Sekeyova, Z. (1992). Penetration of host cells by *Rickettsia rickettsia* appears to be mediated by a phospholipase of rickettsial origin. *Infect. Immun*. 60, 2733–2740. doi: 10.1128/IAI.60.7.2733-2740.1992

Silverman, J. M., Chan, S. K., Robinson, D. P., Dwyer, D. M., Nandam, D., Foster, L., et al. (2008). Proteomic analysis of the secretome of *Leishmania donovani*. *Genome Biol*. 9:R35. doi: 10.1186/gb-2008-9-2-r35

Silverman, J. M., Clos, J., de'Oliveira, C. C., Shirvani, O., Fang, Y., Wang, C., et al. (2010). An exosome-based secretion pathway is responsible for protein export from Leishmania and communication with macrophages. *J. Cell Sci*. 123(Pt 6):842–852. doi: 10.1242/jcs.056465

Singh, S. B., Tandon, R., Krishnamurthy, G., Vikram, R., Sharma, N., Basu, S. K., et al. (2003). Rab5-mediated endosome-endosome fusion regulates haemoglobin endocytosis in *Leishmania donovani*. *EMBO J*. 21, 5712–5722. doi: 10.1093/emboj/cdg557

Sitkiewicz, I., Stockbauer, K. E., and Musser, M. J. (2007). Secreted bacterial phospholipase A2 enzymes: better living through phospholipolysis. *Trends Microbiol.* 15, 63–69. doi: 10.1016/j.tim.2006.12.003

Snijder, H. J., and Dijkstra, B. W. (2000). Bacterial phospholipase a: structure and function of an integral membrane phospholipase. *Biochim. Biophys. Acta*. 1488, 91–101. doi: 10.1016/S1388-1981(00)00113-X

Song, Y., Wilkins, P., Hu, W., Murthy, K. S., Chen, J., Lee, Z., et al. (2007). Inhibition of calcium-independent phospholipase A2 suppresses proliferation and tumorigenicity of ovarian carcinoma cells. *Biochem. J.* 406, 427–436. doi: 10.1042/BJ20070631

Souto-Padrón, T., Lima, A. P., and Ribeiro, R. O. (2006). Effects of dibucaine on the endocytic/exocytic pathways in *Trypanosoma cruzi*. *Parasitol. Res*. 99, 317–320. doi: 10.1007/s00436-006-0192-1

Tolleshaugh, H., Berg, T., and Holte, K. (1982). Effects of local anesthetics and related compounds on the endocytosis and catabolism of asialoglycoproteins in isolated hepatocytes. *Biochim. Biophys. Acta* 714, 114–121. doi: 10.1016/0304-4165(82)90132-5

Vannier-Santos, M. A., Saraiva, E. M., Martiny, A., Neves, A., and De Souza, W. (1992). Fibronectin shedding by Leishmania may influence the parasite-macrophage interaction. *Eur. J. Cell Biol*. 59, 389–397.

Voyiatzaky, C. S., and Soteriadou, K. P. (1992). Identification and isolation of the Leishmania transferring receptor. *J. Biol. Chem*. 267, 9112–9117.

Weise, F., Stierhof, Y. D., Kuhn, C., Wiese, M., and Overath, P. (2000). Distribution of GPI-anchored proteins in the protozoan parasite Leishmania, based on an improved ultrastructural description using high-pressure frozen cells. *J. Cell Sci*. 113, 4587–4603.

Wilson, H. A., Allred, D. V., O'Neil, K., and Bell, J. D. (2000). Activitis and interactions among phospholipases A2 during thapsigargin-induced S49 cell death. *Apoptosis* 5, 389–396. doi: 10.1023/A:1009647912056

Wittenauer, L. A., Shirai, K., Jackson, R. L., and Johnson, J. D. (1984). Hydrolysis of a fluorescent phospholipid substrate by phospholipase A2 and lipoprotein lipase. *Biochem. Biophys. Res. Commun*. 118, 894–901. doi: 10.1016/0006-291X(84)91479-7

Zhang, X. H., Zhao, C., Seleznev, K., Song, K., Manfredi, J. J., and Ma, Z. H. (2006). Disruption of G1-phase phospholipids turnover by inhibition of Ca2+-independent phospholipase A2 induces a p53-dependent cell-cycle arrest in G1 phase. *J. Cell Sci*. 119, 1005–1015. doi: 10.1242/jcs.02821

Conflict of Interest: The authors declare that the research was conducted in the absence of any commercial or financial relationships that could be construed as a potential conflict of interest.

frontiers in Cellular and Infection Microbiology

ORIGINAL RESEARCH
published: 27 May 2020
doi: 10.3389/fcimb.2020.00251

Clinical Proteomics Profiling for Biomarker Identification Among Patients Suffering With Indian Post Kala Azar Dermal Leishmaniasis

Priyank Jaiswal[1], Manab Ghosh[2†], Goutam Patra[1†], Bibhuti Saha[2] and Sumi Mukhopadhyay[1]*

[1] Department of Laboratory Medicine, School of Tropical Medicine, Kolkata, India, [2] Department of Tropical Medicine, School of Tropical Medicine, Department of Health & Family Welfare, Government of West Bengal, Kolkata, India

OPEN ACCESS

Edited by:
Claudia Ida Brodskyn,
Gonçalo Moniz Institute (IGM), Brazil

Reviewed by:
Eugenia Carrillo,
Carlos III Health Institute, Spain
Javier Moreno,
Carlos III Health Institute, Spain
Iraj Sharifi,
Kerman University of Medical Sciences, Iran

***Correspondence:**
Sumi Mukhopadhyay
drsumimukhopadhyay@gmail.com

[†]These authors share second authorship

Specialty section:
This article was submitted to Parasite and Host, a section of the journal Frontiers in Cellular and Infection Microbiology

Received: 20 August 2019
Accepted: 29 April 2020
Published: 27 May 2020

Citation:
Jaiswal P, Ghosh M, Patra G, Saha B and Mukhopadhyay S (2020) Clinical Proteomics Profiling for Biomarker Identification Among Patients Suffering With Indian Post Kala Azar Dermal Leishmaniasis. Front. Cell. Infect. Microbiol. 10:251. doi: 10.3389/fcimb.2020.00251

Background: Post Kala Azar Dermal Leishmaniasis (PKDL) is a non-fatal dermal sequel of Visceral Leishmaniasis (VL), affecting individuals worldwide. Available diagnostic tools lack sensitivity and specificity toward identifying macular (MAC) PKDL patients, due to low parasite load in patients' sample. Confirmatory test like punch biopsy are invasive and painful. Considering the rural nature of this disease and the prevailing situation of diagnostic scenario, PKDL patients mostly remains unattended from receiving proper medical care. They in turn act as "mobile parasite reservoir," responsible for VL transmission among healthy individuals (HI). This study aims to identify PKDL disease specific glycated protein biomarkers, utilizing the powerful LC-MS/MS technology, which is the tool of choice to efficiently identify and quantify disease specific protein biomarkers. These identified PKDL disease specific novel glycoproteins could be developed in future as immunochromatographic based assay for efficient case detection.

Methodology: Previously our lab had identified importance of glycated (Circulating Immune Complexes) CICs, among PKDL patients. This study aims to further characterize disease specific glycated protein biomarkers, among MAC PKDL patients for both diagnostic and prognostic evaluation of the disease. LC-MS/MS based comparative spectral count analysis of MAC PKDL to polymorphic (POLY) PKDL, HI, and Cured (CR) individuals were performed. Proteins level alterations among all study groups were confirmed by Western blot and enzyme-linked immunosorbant Assay (ELISA).

Results: Among MAC PKDL patients 43, 60, 90 proteins were altered compared to POLY PKDL, HI, and CR groups, respectively. Filtering for the most significant proteins, Plasminogen (PLG) and Vitronectin (VTN) were identified which promisingly identified MAC PKDL cases. Active surveillance results from endemic districts of West Bengal revealed drastic rise of MAC PKDL cases, alarming the urgency for field adaptive efficient biomarker.

Conclusion: This current study aims to establish PLG and VTN as novel diagnostic and prognostic protein biomarker for MAC and POLY PKDL cases management.

Keywords: PKDL, MAC, POLY, LC-MS/MS, CICs, proteomics, glycated biomarker

INTRODUCTION

PKDL is a non-fatal dermal sequel of VL, caused by protozoan parasite *Leishmania donovani*. On the global scenario, PKDL in mainly restricted to distinct zones of South Asia (India, Nepal and Bangladesh) and East Africa, mainly Sudan. In India, the most prominent fatal form of leishmaniasis present is VL, affecting entirely the eastern region of the country (Zijlstra et al., 2000; WHO, 2010; Desjeux and Ramesh, 2011; Alvar et al., 2012; Perry et al., 2013) The clinical presentation of VL and PKDL differ substantially; where VL patients suffer from sustained fever, hepatosplenomegaly, weight loss and anemia; PKDL patients on the other hand suffer from dermal lesions usually manifested in the form of MAC, Nodular and POLY. The lesion usually appear on face and subsequently gets spread to extremities. The predominance of PKDL patients suffering with MAC lesions varies among different regions; for example in Sudan, PKDL patients suffering with MAC lesions were reported to be 9% whereas in Indian scenario the percentage of PKDL patients suffering with MAC lesions ranges from 15 to 31%. The percentage of PKDL patients suffering with POLY lesions ranges from 69 to 85% in Indian scenario (Ganguly et al., 2010). Although, compared to VL, the mortality rate of PKDL patients is significantly lower, yet PKDL is observed as a stigmatizing disease that brings a substantial socioeconomic burden, further intensified by a hesitancy of patients, to obtain treatment, or due to noncompliance. Lesions, especially the POLY forms, are parasite-rich, concluding that PKDL patients plays a crucial role in the anthroponotic transmission of VL. PKDL patients suffering with MAC lesions, have comparatively lower parasitic load, and thus lack detection sensitivity with standard techniques like rK39 (73% sensitivity) (Salotra et al., 2001) Leishmanin skin test (54% sensitivity), histopathological studies with patients' skin biopsy sample (7–33% sensitivity) (WHO, 2015) and is often misdiagnosed as Vitiligo cases (Domínguez and Toraño, 1999; Jaiswal et al., 2018). In order to completely eliminate Kala-azar in Southeast Asia, proper identification of various routes responsible for the spread of the disease is essential (Zijlstra et al., 2003), which could efficiently distinguish between active PKDL patients and CR individuals as well as between active PKDL patients and other cross disease like Leprosy and Vitiligo. Most of the diagnostic methods for PKDL disease identification are based on highly invasive tissue biopsy methods (WHO, 2015) followed by PCR/qPCR; which requires high technical expertise. Till now very less work has been done toward identification of PKDL disease specific glycated CICs proteome biomarker from patients' plasma. Recent reports by active surveillance have suggested huge predominance of MAC PKDL cases, with very low parasitic load, and acts as efficient reservoir for spread of VL (Sengupta et al., 2018). Thus, there exists an urgent need for biomarkers for early MAC PKDL case detection.

Recent investigations from our group have demonstrated the importance of glycated CICs among PKDL patients (Jaiswal et al., 2018). Integral binding of antibody and antigens leads to the formation of Immune complexes (ICs). Inside human system, these ICs are subjected to various immunological responses like complement deposition, opsonisation (Domínguez and Toraño, 1999), phagocytosis or protease mediated cleaving. ICs accumulation inside patients' body results in various pro-inflammatory effects, including complement activation and cytokine secretion. Deposition of ICs inside tissue and vessel walls leads to inflammation, tissue damage and several other disease manifestations (Hoiby et al., 1986). ICs also induce various pro-inflammatory or anti-inflammatory cytokines which affect disease progression and outcome in several disorders (Rönnelid et al., 2003; Mathsson et al., 2006). ICs acts as complement activators, resulting in their solubilization and prevention of immune precipitation followed by their clearance through erythrocyte complement receptor 1 (CR1). Previous reports have repeatedly suggested association of parasite infections with high levels of CICs which directly leads to tissue damage (Moulds et al., 1992). Previous studies from our lab have reported the presence of high levels of CICs among PKDL patients (Datta et al., 2015; Jaiswal et al., 2018). Further high-throughput studies are required to identify the specific peptide fragments from PKDL patients' CICs, representing specific proteins, which could act as glycated CICs proteome biomarker for both diagnostic and prognostic care of PKDL patients after treatment completion.

Recently, experimental proteomics studies have been applied greatly for studying the pathophysiology of complex diseases, including both infectious and non-infectious ones. Few studies on Leishmaniasis have identified proteomic alteration in the plasma samples of VL patients compared with HI and reported significant alterations of plasma proteins (Rukmangadachar et al., 2011; Bag et al., 2014). Two comparative proteomics studies employing either quantitative (Rukmangadachar et al., 2011) or qualitative (Bag et al., 2014) approach, have reported 26 and 39 differentially expressed protein spots. Various acute-phase proteins were reported to be expressed differentially in VL patients compared to HI. Qualitative study reported up-regulation of α-1-acid glycoprotein and C1 inhibitor; and down regulation of retinol binding protein, whereas quantitative study reported up-regulation of α-1-antitrypsin, α-1-B glycoprotein, and amyloid-A1 precursor; and down regulation of vitamin-D binding protein. These studies highlight the role of proteomics in identifying disease specific protein markers that can help in detection of VL, when parasite load is scanty. Previous reports from our lab have reported altered CICs glycosylation status of PKDL patients (Datta et al., 2015; Jaiswal et al., 2018). High throughput proteomic analysis of PKDL patients' glycated CICs will assist in the identification of major PKDL disease specific protein biomarkers among Indian (MAC and POLY) PKDL population.

METHOD

Study Area and Population

PKDL study subjects were enrolled through the ongoing VL Elimination programme (2015-2016) at block and sub-block levels in the state of West Bengal, India. The study

Abbreviations: VL, Visceral Leishmaniasis; PKDL, Post Kala Azar Dermal Leishmaniasis; MAC PKDL, Macular PKDL; POLY PKDL; Polymorphic PKDL, CR, Cured individual; HI, Healthy individual; LC-MS/MS, Liquid Chromatography-Mass Spectrometry; CICs, Plasma, Circulating Immune Complexes.

subjects recruited were mainly from endemic zones of India namely *Malda and Darjeeling*. Taken together, 20 MAC PKDL patients, 20 POLY PKDL patients and 12 CR individuals were enrolled after taking thorough clinical examinations, information regarding history of VL and rk39 strip test positivity. Exclusion criteria included patients with underlying medical disorders e.g., Heamatological malignancies, Bleeding disorders, chronic liver disease, Diabetes mellitus, severe cardiorespiratory disease, renal disease. Cured (CR) group is described as individuals who have previously received treatment for PKDL and presently they are not suffering from any lesion severity. Additionally, 20 VL patients and 12 HI subjects were also enrolled for the study. Schematic representation of the quantitative proteomics study design by LC-MS/MS, ELISA and Western Blot is provided in the graphical abstract (**Figure 1**). Disease controls included subjects with similar disease manifestations like Vitiligo ($n = 12$) and Leprosy ($n = 12$), were enrolled from outdoor/indoor department of Dermatology and Tropical Medicine, School of Tropical Medicine, Kolkata.

Ethics Statement

After primary screening, 2 ml of venous blood was collected in heparinized vials. rK39 strip test was performed. For performing rK39 strip test, the following steps were done. 2ml of venous blood was collected in heparinized vials. rK39 strip test (Kala Azar ^{TM} Rapid Test InBios International, Seattle, WA, USA) as per Govt. guidelines, was performed by trained field medical assistants, according to the standardized protocol (as described by manufacturer). The ethical considerations at the study sites; both at the outdoor and indoor Departments of Dermatology and Tropical Medicine, Calcutta School of Tropical Medicine were reviewed and approved by the Clinical Research Ethics Committee of School of Tropical Medicine, Kolkata (CREC-STM/273 dated: 18.09.2015).

Sample Preparation

PKDL patients' plasma samples with different lesion gradations i.e., MAC, POLY and CR were pooled down separately; irrespective of gender biasness, along with HI to reduce sample complexity. Briefly, plasma from MAC PKDL ($n = 20$), POLY PKDL ($n = 20$) and CR ($n = 12$) individuals were pooled separately and CICs were precipitated by 50% saturated solution of ammonium sulfate as described by Moss et al. (1982). Next, the samples were dialyzed, using Dialysis tubing (Sigma-Aldrich), with repeated phosphate buffer saline (PBS) changes of 1000 ml for 48 h at 4°C.

Soluble *Leishmania donovani* Antigen (LDA) Preparation

Crude antigen preparation was performed with *L. donovani* strain MHOM/IN/83/AG83 after culturing them at log growth phase. Promastigotes (1×10^7cells/ml) were harvested in PBS solution (0.02M) and the pellets resuspended in lysis buffer (20 mMTris-HCl, 40 mM NaCl, pH 7.4) containing 2 mM PMSF, 1 mg/ml leupetin, 5 mM EDTA and 5 mM iodoacetamide. The lysates were preserved in −20°C until further use (Blum et al., 2001).

Parasite ELISA

For determination of anti-leishmanial antibody titer (IgG), parasite ELISA was performed (Bandyopadhyay et al., 2004). Briefly, soluble *L. donovani* antigen in PB (0.02 M, pH 7.2) was used as coating antigen at optimum concentration (1 μg/100 μl/well). After blocking non-specific sites, patient plasma (diluted 1:500; 100 μL/well) were added and incubated for 2 h at 4°C. The wells were then incubated for 1 h at RT with HRP-conjugated anti-human monoclonal IgG (1:15,000) (Sigma-Aldrich, Cat#:A0170), to measure the levels of IgG anti-leishmanial antibodies with Tetramethyl benzidine (TMB). Optical density (OD) was measured at 450 nm on micro plate reader (BIORAD PR4100).

Depletion of High Abundance Proteins

Depletion columns resins were used to remove high abundant plasma proteins to facilitate the detection of low abundant proteins. In this manner, high abundant protein like albumin was removed using Albumin Depletion kit (Pierce−85160) as per the manufacturer's instructions.

Isolation of Plasma Glycoproteins

Albumin depleted samples were treated with Glycine—HCL buffer as described by Jaiswal et al. (2018), to dissociate the antigen-antibody complex (Jaiswal et al., 2018). Next the acid dissociated CICs were affinity purified using equilibrated Protein A Sepharose 4B column (Invitrogen, USA), at room temperature (RT) for 45 minutes. Antibody free CICs' antigen fraction were collected and subjected to m-phenyl boronic acid column (sigma), overnight at RT, to purify the glycated CICs antigenic fraction (Stoll and Hounsell, 1987; Hageman and Kuehn, 1992). The Glycated fractions were eluted with 50 mM Taurin-NaOH solution, pH 8.7 (Bassil et al., 2004) and were subsequently dialyzed using Dialysis tubing (Sigma-Aldrich) with repeated PBS changes of 1,000 ml for 24 h at 4°C. Protein concentration was measured by Lowry method (Lowry et al., 1951).

De-glycosylation of Affinity Purified CIC Antigens

To characterize and reconfirm the glycation status, present in the affinity purified CIC antigens, the above column purified samples were de-glycosylated using *Arthrobacter ureafaciens* neuraminidase (Sigma-Aldrich) treatment according to manufacturer's instruction. Briefly, 50 μg of affinity purified CICs antigens were treated with 2 sigma units of neuraminidase in reaction buffer and incubated at 37°C for 3 h. The reaction mixtures were heated at 100°C for 5 min, followed by treatment with 5 units of N-Glycosidase F (Roche, USA), in reaction buffer (20 mM sodium phosphate, 10 mM EDTA, 0.5% (w/v) CHAPS and 0.05% (w/v) SDS), and incubated for 18 h at 37°C. Reactions were ultimately stopped by heating at 100°C for 5 min (Das et al., 2003).

Lectin Dot Blot

Glycation status of affinity purified CIC antigens were analyzed by DIG Glycan differentiation kit (Roche, USA) according to manufacturer's instruction. Briefly, 5 μg of affinity purified CIC

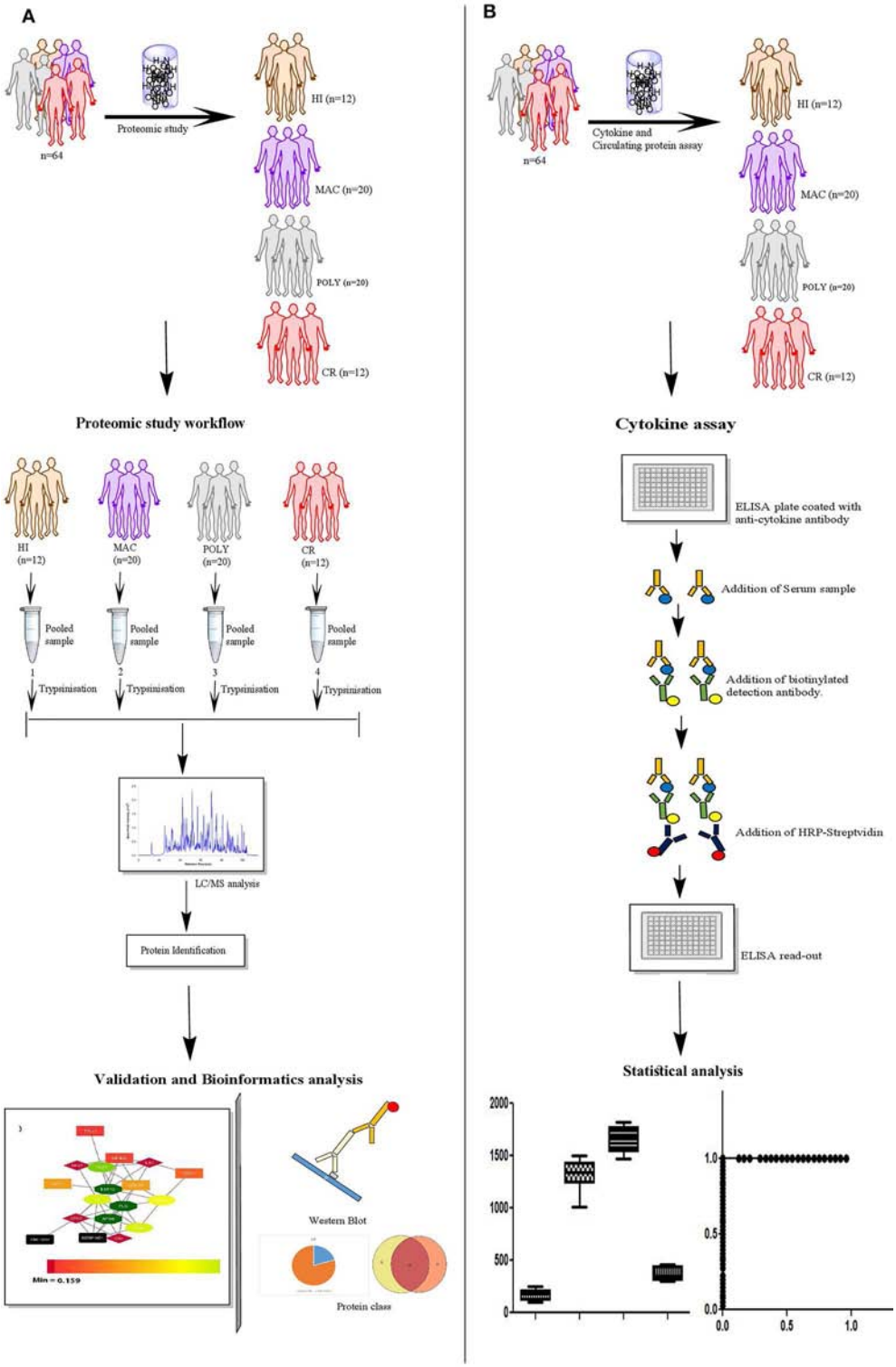

FIGURE 1 | Schematic representation of the experimental study design. **(A)** Sample selection strategy for the proteomics study; HI ($n = 12$), MAC ($n = 20$), POLY ($n = 20$) and CR ($n = 12$). **(B)** Experimental design used for the ELISA; HI ($n = 12$), MAC ($n = 20$), POLY ($n = 20$) and CR ($n = 12$). Patient population used for protein levels, belongs to the same patient population as that of the proteomics study. HI, Healthy Individuals; MAC, Macular PKDL patients; POLY, Polymorphic PKDL patients; CR, Cured Individuals.

antigens; both enzyme treated and untreated, as described above; were transferred to PVDF membrane followed by Lectin dot blot using DIG Glycan differentiation kit. Membranes were blot dried and analyzed (Sata et al., 1990).

Buffer Exchange of Affinity Purified CIC Fractions and In-Solution Digestion

Buffer exchange of quantified glycated CIC antigenic fractions, from PBS to triethylammonium bicarbonate buffer (0.5 M) was performed, using Amicon Ultra 0.5 mL Centrifugal filters, as previously described by Ray et al. (2012). In-solution digestion of the CIC fraction was performed by the addition of 1 μL denaturing solution containing 2.0% SDS to 45 μg of CIC samples. The CIC samples were incubated for 1 h at 60°C after subsequent addition of 2 μL of 50 mM reducing reagent (tris (2-carboxyethyl) phosphine). One microliter of cysteine blocking solution (iodoacetamide 100 mM) was added to the CIC samples and incubated for 10 min at RT. Next the CIC samples were treated with Trypsin (Pierce; Thermo Scientific), at a ratio of 1:30 (trypsin: protein) and incubated overnight at 37°C.

Zip-Tipping and LC-MS/MS

Protein samples were dried by speed-vacuum centrifugation and reconstituted in 40 μL of 0.1% formic acid eluted with acetonitrile and then dried. Samples were reconstituted in 15 μL of 0.1% formic acid. Prior to MS, different peptides present in polypeptide solution were separated with nano LC. Peptides were analyzed by electrospray ionization mass spectrometry using the Easy nano LC 1200 system [Thermo Scientific] coupled to a Q-Exactive Plus Orbitrap mass spectrometer [Thermo Scientific]. Briefly, tryptic digested peptides (6 μl injection volume) were loaded onto a nano-precolumn (Thermo Fisher Scientific Acclaim) PepMap 100 μm × 2 cm, nanoviper C18, 5 μm, 100A. Peptides were separated by a nano HPLC column ES 803 PepMap RSLC C18 2 μm, 100A, 75 μm × 50 cm, and separated with a linear gradient of water/ 80% acetonitrile/0.1% formic acid (v/v) and ion-sprayed into MS with a spray voltage of 1.90KV, capillary temperature 300°C. Further, raw files were analyzed to identify proteins of interest using Proteome Discoverer Software 2.2 (Thermo Scientific); with the following parameters: database; SequestHT Uniprot Homo sapiens database, Type of search; MS/MS Ion Search, Enzyme; Trypsin, Variable modifications; Oxidation (M), Mass values; Monoisotopic, Protein Mass; Unrestricted, Precursor Mass Tolerance; 10 ppm, Fragment Mass Tolerance; 0.05Da, Max Missed Cleavages; 2 and Instrument type; default. Searches were performed with the label-free quantification option selected (Nguyen et al., 2013). The liquid chromatography mass spectrometry (LC-MS/MS) proteomics data were deposited at the Proteome Xchange Consortium through the PRIDE partner repository. Data are available via Proteome Xchange with identifier numbers PXD012960 and 10.6019/PXD012960.

Determination of Circulating Proteins Titres

Circulating glyco-proteins, PLG and VTN were reported to interact directly with *L. donovani* parasite (Fatoux-Ardore et al., 2014). To evaluate their levels in PKDL infections, stored plasma of PKDL patients were thawed and levels of PLG and VTN were evaluated using standard ELISA kits (Ray Biotech, Suite, Georgia). The tests were carried out as per manufacturer's instruction. Samples used for this assay includes HI, MAC, POLY, CR, active VL, Vitiligo and Leprosy.

Western Blot Analysis

Affinity purified CICs antigens (30 μg) from plasma of PKDL patients were electrophoresed in SDS PAGE as described by Jaiswal et al. (2018). Samples were ran on 7.5% resolving gel prepared by 30% acrylamide and bisacrylamide solution, 1.5M Tris-HCl (pH-8.8), 10% SDS, 10% APS, and 5 μl TEMED. Electrophoresis was performed on mini protean tetra cell (Bio-Rad, USA) using electrophoresis buffer (Tris 0.025M, glycine 0.19M and SDS 0.1%). Western blot was performed using monoclonal biotin tagged PLG and VTN anti-human antibody (BIOSS, USA) followed by treatment with HRP- avidin anti-human IgG secondary antibody monoclonal IgG (1:1000) (Sigma-Aldrich, Cat#:A0170) and developed with DAB substrate kit (Pierce, USA) according to manufacturer's instruction (Singh et al., 2005).

Statistics

Values for each set of experiment were analyzed by calculating their respective medians and interquartile ranges (IQRs). Data representation was done by Box plots to show Tukey whiskers values, median and IQR. At first, all data sets were subjected for normality test using D'Agostino & Pearson omnibus normality test. Univariate non-parametric ANOVA analysis (i.e., Kruskal Wallis test) was performed and if data represents significant value, *post-hoc* (dunn) test was implemented for defining differences within each group with *p*-values smaller than 0.01 were statistically significant. Cut-off value of circulating glycoproteins (PLG and VTN) was determined by using Youden index. Efficiency of levels of circulating glycoproteins (PLG and VTN) and anti-leishmania antibody titer (IgG), for prediction of MAC PKDL and its further progression, were analyzed using receiver operating characteristic (ROC) curves. Sensitivity and specificity values for the same were calculated at different threshold points. Areas under curve (AUC) values were also calculated, which were statistically significant. Statistical analysis was performed using the Graph-Pad Prism statistics software (Graph-Pad Software Inc., San Diego, CA) and SPSS Inc (Chicago, IL).

Protein Network Analysis

Human gene symbols for identified proteins after LC-MS/MS analysis were uploaded to web-based STRING tool (version 10.5) to identify functional protein association network (Shannon et al., 2003). Gene ontology analysis was performed to retrieve overrepresented biological process terms (Maere et al., 2005).

RESULT

Plasma Proteomic Changes

Plasma samples from PKDL patients with MAC ($n = 20$), POLY ($n = 20$), CR ($n = 12$) and HI ($n = 12$) were isolated and processed for proteomics analysis, involving in-solution digestion, followed by analysis on a nano LC-MS/MS platform including an Q-Exactive Plus orbitrap mass spectrometer. Samples were arranged in groups: (i) MAC vs. HI, (ii) MAC vs. POLY and (iii) MAC vs. CR to identify relative abundance of proteins. All samples were run in triplicates. PKDL patients and HI characteristics are presented in **Table 1**. Of these 11, 42 and 19 proteins with > 2 peptide matches were differentially down-regulated in MAC vs. HI, MAC vs. POLY and MAC vs. CR, respectively and 31, 18 and 70 proteins were differentially up-regulated in MAC vs. HI, MAC vs. POLY and MAC vs. CR, respectively. Individual fold change values for identified proteins among all the patient groups. Proteins common in all the study groups; MAC vs. HI, MAC vs. POLY and MAC vs. CR; were chosen for further analysis to identify disease specific biomarkers that will allow the diagnosis as well as PKDL progression. Interestingly, several proteins, such as Profilin-1 and Alpha-2-macroglobulin were up-regulated (fold change >1.2) in all the study groups. Protein such as Galectin-1, Protein S100-A14, 60S Ribosomal protein L11, 40S ribosomal protein S2 and Fascin were up-regulated (fold change >1.2) in MAC vs. HI and MAC vs. CR whereas 60S Ribosomal protein L-37A was down-regulated (fold change <0.98) in MAC vs. POLY. Also proteins like Prothrombin, Fructose-bisphosphatealdolase, NF45 and Elongation factor-1 gamma were up-regulated (fold change >1.2) in MAC vs. POLY and MAC vs. CR groups. Proteins such as keratin type 1 cytoskeleton 14, Alpha-enolase and Galectin 7 were down-regulated (fold change <0.98) in MAC vs. HI and MAC vs. POLY group, whereas proteins such C4b-binding protein alpha chain, Keratin, type II cytoskeletal 2 epidermal, Fibronectin, Keratin, type I cytoskeletal 9, Clusterin, Afamin, Complement C5, Fibrinogen gamma chain, Hemopexin and Apolipoprotein A-II were down-regulated (fold change <0.98) in MAC vs. POLY and MAC vs. CR groups. Proteins such as PLG were significantly up-regulated among PKDL patients with MAC lesions as compared to PKDL patients with POLY lesions, HI and CR individuals whereas VTN is significantly up-regulated among PKDL patients with POLY lesions as compared to PKDL patients with MAC lesions, HI and CR individuals (**Figure 2**). Identification of *L. donovani* specific proteins were not included in the study as the main aim of the study was to identify proteomic alterations in the glycated CICs isolated from the plasma of PKDL patient in comparison to HI and CR individuals.

TABLE 1 | Patient and Healthy control characteristics.

	Patients ($n = 52$)	Control ($n = 12$)
Age		
Years (SD)	26.08 (16.26)	27.78 (7.78)
Gender		
Male	25	7
Female	27	5
Type of PKDL patient		
Macular	20	–
Polymorphic	20	–
Cured	12	–
Previous VL history	52	–

Comparison of Anti-Leishmanial Antibody Titres Among PKDL Patients and Control Individuals

Leishmania infection mounts humoral responses against *Leishmania* antigen in the form of immunoglobulins of isotypes IgG, which are important serological markers in the host. To assess the status of primary immunoglobulin responses, present study investigated IgG, antibody titres in the plasma of PKDL patients with respect to HI and CR individuals. Parameters involving plasma dilutions and antigen concentrations were standardized to set optimal ELISA condition for the serological assay. Anti-leishmanial antibody titres of IgG in plasma of PKDL patients showed enhanced responses. The performances of the sensitivities and the specificities of the ELISA with plasma from patients with PKDL were also evaluated. The reactivity of the IgG, antibodies from the plasma of patients with PKDL ($n = 40$) were significantly higher than those of the plasma from the HI but lower than CR ($p < 0.0001$). The "mean ± SEM" of anti-leishmanial IgG antibody titer in the plasma of MAC and POLY PKDL patients were 2.414 ± 0.062 and 2.275 ± 0.065 respectively in comparison to HI (1.772 ± 0.062) and CR individuals (2.733 ± 0.039) (**Figure 3A**). The sensitivity, specificity and AUC values for IgG ELISA among various experimental groups i.e., MAC vs. HI, MAC vs. POLY and MAC vs. CR is represented in **Table 3**. The respective AUC values for different experimental groups showed poor performance of IgG ELISA, in comparison to glyco-proteins PLG and VTN, for discriminating PKDL cases from controls (**Figures 5A–I**).

Protein Levels in Individual Samples

Significant variations in the levels of circulating glyco-proteins like PLG and VTN, were analyzed in individual samples of MAC ($n = 20$), POLY ($n = 20$), CR ($n = 12$), HI ($n = 12$), active VL ($n = 20$), Leprosy ($n = 12$) and Vitiligo ($n = 12$) by ELISA. PLG levels were significantly up-regulated in MAC with "mean ± SEM" value of 368.3 ± 11.48, as compared POLY (297.3 ± 6.387), CR (261.1 ± 12), HI (250.9 ± 7.080) (**Figure 3B**), active VL (286 ± 1.32), Vitiligo (239.6 ± 2.75) and Leprosy (218.17 ± 1.82) (**Figure 4A**) whereas VTN levels were up-regulated in POLY "mean ± SEM" value of 65.84 ± 4.835 as compared to MAC (46.64 ± 1.378), CR (32.44±1.751) and HI (30.46±1.88) (**Figure 3C**), active VL (38.95 ± 1.15), Vitiligo (24.75 ± 1.56) and Leprosy (28.25 ± 1.72) (**Figure 4B**).

Functional Data Analysis of Differentially Expressed Proteins

To identify the biological functions, associated with the proteins that exhibited changed abundance in plasma of PKDL patients

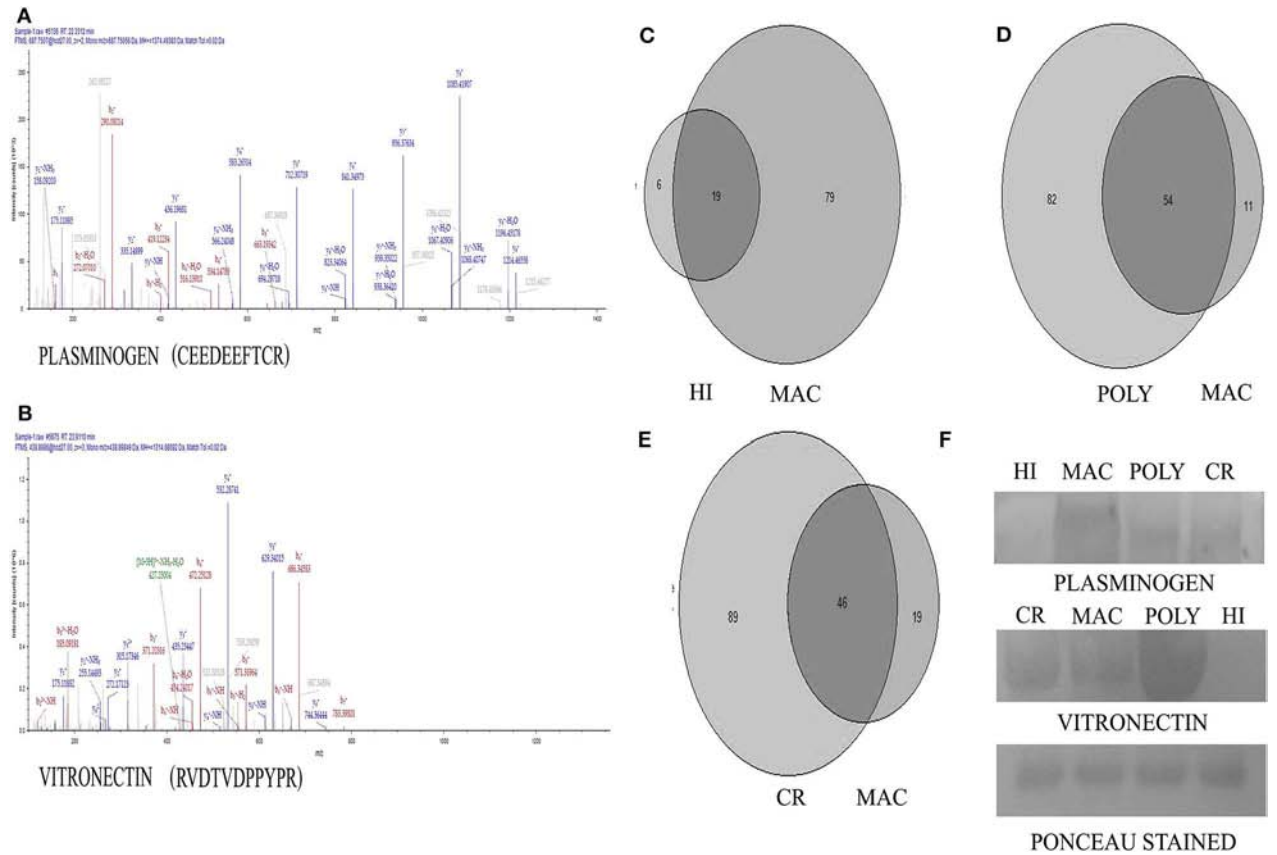

FIGURE 2 | Representative MS-MS spectra of significantly altered proteins obtained from Q-ExactivePlus Orbitrap mass spectrometer study. **(A)** MS-MS spectra of Plasminogen (PLG) protein. **(B)** MS-MS spectra of Vitronectin (VTN) protein. **(C)** Venn diagram showing number of common proteins in all the patients with MAC lesions compared to HI. **(D)** Venn diagram showing number of common proteins in all the patients with MAC lesions compared to POLY lesions. **(E)** Venn diagram showing number of common proteins in all the patients with MAC lesions compared to CR individuals. **(F)** Validation of Plasminogen and Vitronectin using western blotting image Ponceau stained image of the blot after transfer.

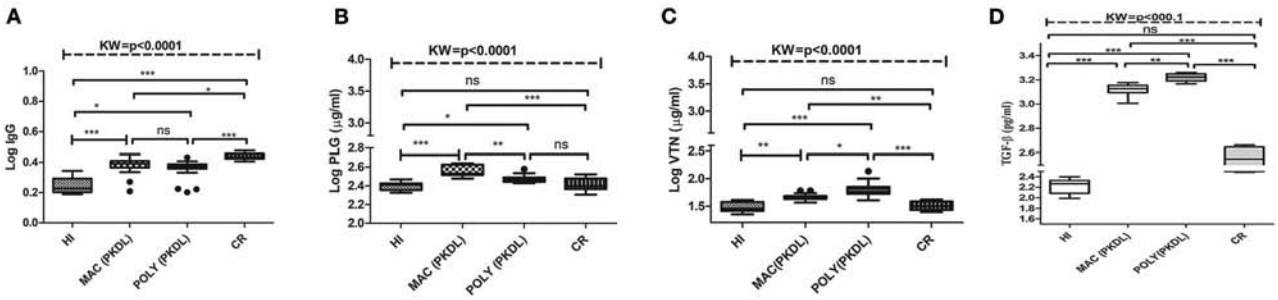

FIGURE 3 | Box plot of plasma level of **(A)** IgG **(B)** PLG (μg/ml) **(C)** VTN (μg/ml) **(D)** TGF-β (pg/ml) for HI, MAC PKDL patients, POLY PKDL patients and CR individuals. Whiskers calculated adopting the Tukey method. Outliers showed as dots. $^{*}p < 0.01$, $^{**}p < 0.001$, $^{***}p < 0.0001$, ns-not significant: Kruskal–Wallis test (K) followed by Dunn's multiple comparison test.

with MAC and POLY lesion manifestations as compared to HI and CR individuals, we performed STRING and Cytoscape analysis. Protein network were generated for the protein sets of all the groups (MAC vs. HI, MAC vs. POLY and MAC vs. CR) using STRING database (**Figure 6**). Gene ontology mining of the identified proteins revealed alteration in the biological functions, involved mostly in inflammatory and immune response and transporter activity (**Table 2**). List of various up-regulated and

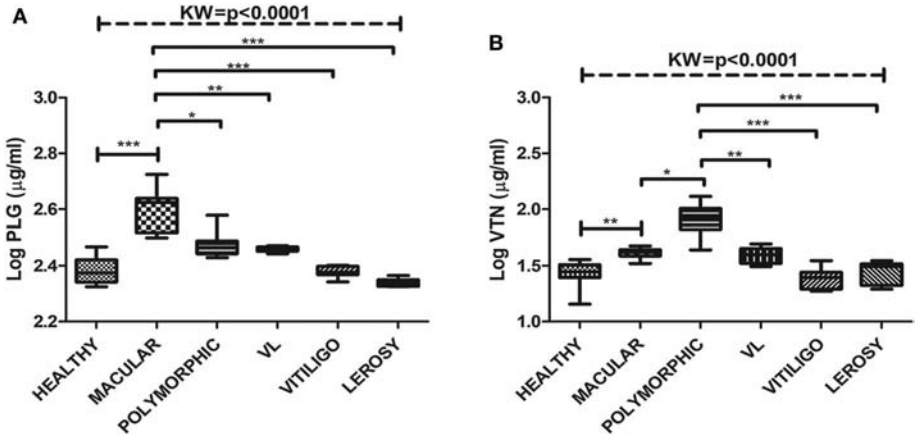

FIGURE 4 | Box plot of plasma level of **(A)** PLG (µg/ml) **(B)** VTN (µg/ml) for HI, MAC PKDL patients, POLY PKDL patients, Vitiligo and Leprosy patients. Whiskers calculated adopting the Tukey method. Outliers showed as dots. *$p < 0.01$, **$p < 0.001$, ***$p < 0.0001$, ns-not significant: Kruskal-Wallis test (K) followed by Dunn's multiple comparison test.

TABLE 2 | Overrepresented gene ontology (biological process) terms associated with differential proteins in MAC PKDL patients compared to POLY PKDL patients.

Protein	# Proteins regulation in PKDL	Biological process	Associated molecules
Down regulated	42	Inflammation response	APOD, C4BPA, C5, KRT1, SERPING1, VTN, FGA, HP, ORM1, FGA, HP, ORM1
		Immune system process	ACTG1, AMBP, APOA2, C1QB, C4BPA, C5, CLU, HPX, HSP90AA1, HSP90B1, KRT1, SERPING1, VTN, APOD, ORM1, C1QB, C4BPA, C5, CLU, SERPING1, GAPDH, AZGP1, FGA, HP, ITGB3
		Transport	ACTG1, AMBP, CLU, FGA, FGG, HBB, HP, HPX, HSP90AA1, HSP90B1, ITGB3, MYH9, SERPING1, VTN, AFM, APOA2, APOD, AZGP1, ORM1, RPL37, TTR
Up regulated	18	Transport	A2M, ALDOA, APOB, C4A, PFN1, PLG, TBC1D17

down-regulated proteins in various study groups i.e., MAC vs HI, MAC vs POLY and MAC vs CR are provided in **Tables S1–S6**.

Western Blot Protein Validation and Diagnostic Performance of Differentially Expressed Proteins

To confirm the results of proteomic analysis, western blots were performed which validated the presence of differentially expressed proteins, namely PLG and VTN. Western blot analysis was performed on pooled samples of PKDL patients with lesion gradations of MAC ($n = 20$) and POLY ($n = 20$) and among HI ($n = 12$) and CR ($n = 12$) individuals (**Figure 2**). Ponceau staining of the transferred blots indicated equal loading of each samples in each lane. Consistent with our proteomics findings, western blot analysis revealed PLG to be over-expressed in MAC patients compared to POLY patients, HI and CR individuals, whereas VTN was found to be significantly over-expressed in POLY patients as compared to MAC patients, HI and CR individuals.

To evaluate the individual performance of the circulating glyco-proteins PLG, VTN as efficient PKDL specific biomarkers, ROC curve was performed (**Figures 5D–I**). The area under the ROC curve (AUC) is a measure of how accurately the circulating glyco-proteins can distinguish between MAC and HI; MAC and POLY; MAC and CR. AUC values of PLG and VTN is represented in **Table 3**, which shows better performance of glycoprotein PLG and VTN as PKDL specific biomarkers in comparison to IgG based ELISA.

Prognostic Potential of Glyco-Protein PLG and VTN vs. Conventional Parasite ELISA

To evaluate the prognostic potential of glyco-protein PLG, VTN and anti-leishmanial antibody ELISA, longitudinal monitoring was performed among 10 paired PKDL samples at day 0 and >180 after drug administration. The glyco-protein PLG and VTN showed that all the 5 patients after treatment with Miltefosine (drug responsive group) demonstrated 2 fold decrease in the values (for PLG; $p = 0.0028$ and for VTN; $p = 0.0041$), indicating that these patients were responding to treatment, which was also confirmed clinically. Further, PLG and VTN glycoproteins could also identify 5 drug unresponsive patients (receiving LAmB) (for PLG; $p = 0.0191$ and for VTN; $p = 0.0252$) thus, indicating its utility for therapeutic monitoring. In comparison, the conventional anti-leishmanial antibody based ELISA failed to differentiate follow-up from baseline cases in both drug responsive and unresponsive groups, where the mean titer showed insignificant differences for both drug responsive ($p = 0.378$) and drug unresponsive ($p = 0.129$) cases.

DISCUSSION

PKDL patients are considered as an important reservoir of *L. donovani* parasite, responsible for VL infection (Molina

TABLE 3 | Sensitivity, Specificity and AUC value of IgG, PLG and VTN in different experimental groups of PKDL patients: MAC vs HI, MAC vs POLY and MAC vs CR.

	IgG			PLG			VTN		
	MAC vs HI	**MAC vs POLY**	**MAC vs CR**	**MAC vs HI**	**MAC vs POLY**	**MAC vs CR**	**MAC vs HI**	**MAC vs POLY**	**MAC vs CR**
Sensitivity (%)	85	75	100	95	85	91.67	95	95	100
Specificity (%)	100	65	70	100	90	90	100	80	90
AUC	0.945	0.686	0.897	1.00	0.907	0.956	0.987	0.882	0.979

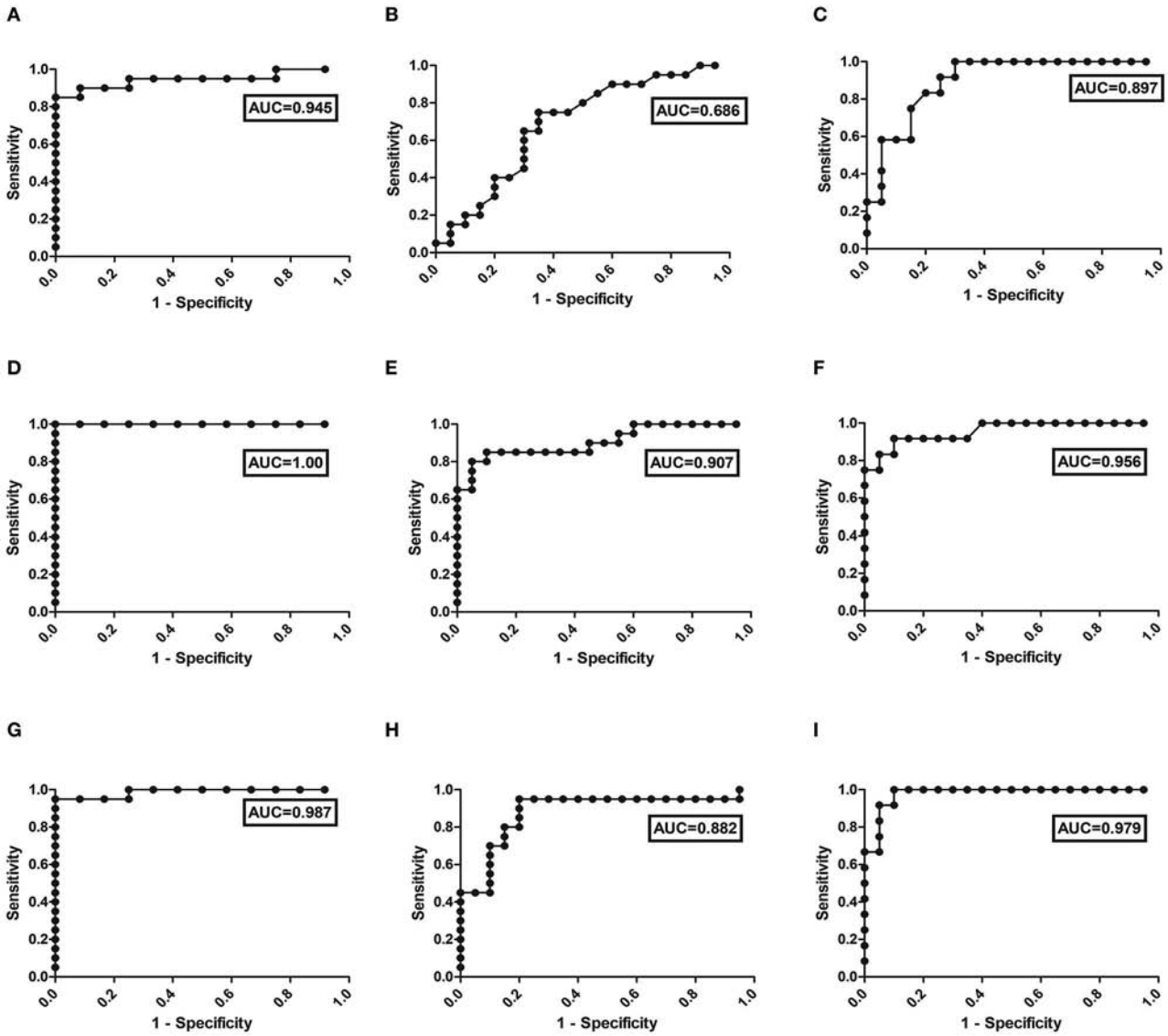

FIGURE 5 | ROC curve obtained from the ELISA values for the detection of: (I) IgG in different experimental groups i.e., **(A)** MAC vs. HI, **(B)** MAC vs. POLY, **(C)** MAC vs. CR; (II) PLG in different experimental groups i.e., **(D)** MAC vs. HI, **(E)** MAC vs. POLY, **(F)** MAC vs. CR; and (III) VTN in different experimental groups i.e., **(G)** MAC vs. HI, **(H)** MAC vs. POLY, **(I)** MAC vs. CR; from the plasma of PKDL patients' samples.

et al., 2017). PKDL patients residing in the endemic zones of West Bengal, are mostly from poor background and they show negligence toward default treatment due to two major concern; (i) the diagnostic test are highly invasive, painful and results in cosmetic scars, (ii) the mortality rate from PKDL disease is very less. Thus, absence of non-invasive and highly efficient diagnostic method for PKDL case detection, leaves most of these patients unattended. These PKDL patients acts

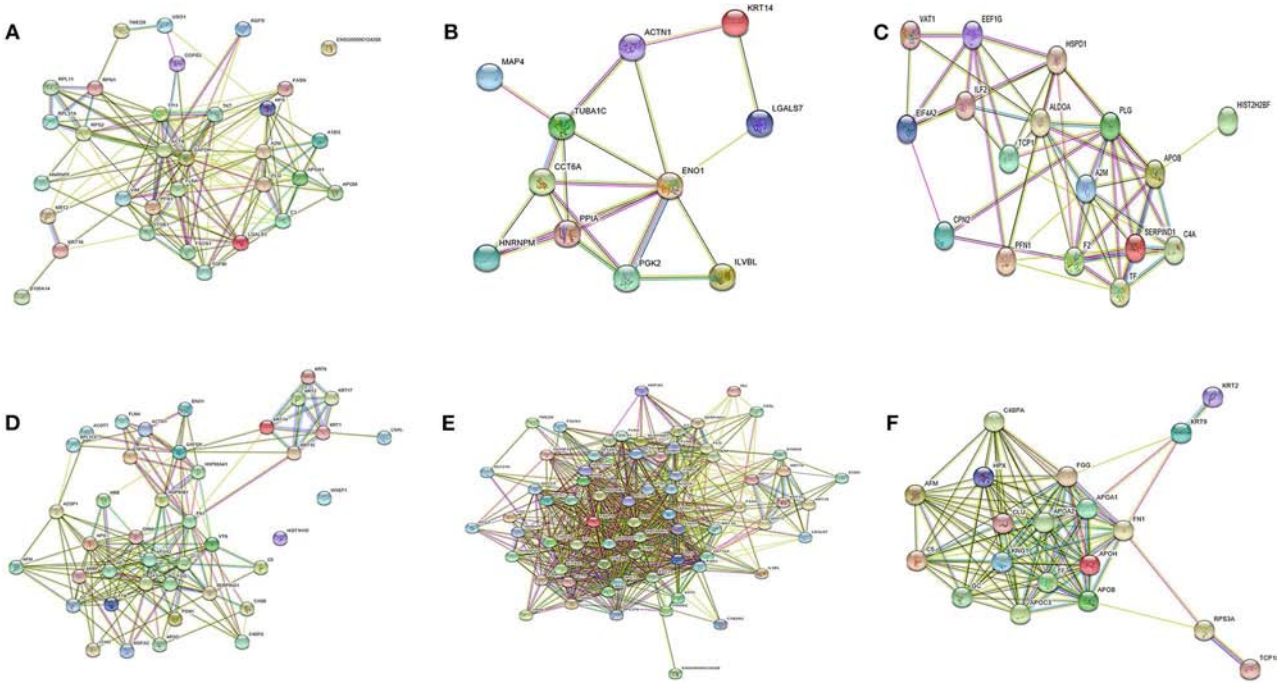

FIGURE 6 | Protein-protein interaction networks. Protein-protein interactions of differentially expressed protein in different study groups. **(A)** Up regulated proteins in MAC PKDL patients compared to HI individuals. **(B)** Down regulated proteins in MAC PKDL patients compared to HI individuals. **(C)** Up regulated proteins in MAC PKDL patients compared to POLY PKDL patients. **(D)** Down regulated proteins in MAC PKDL patients compared to POLY PKDL patients. **(E)** Up regulated proteins in MAC PKDL patients compared to CR individuals. **(F)** Down regulated proteins in MAC PKDL patients compared to CR individuals. Purple and green colored lines for experimental and textmining evidence of different interactions.

as parasite reservoir for spread of VL. This lack of efficient diagnostic methods and the negligence shown by PKDL patients toward treatment creates a huge socio-burden, which requires immediate action (Basher et al., 2012) in order to totally eliminate Kala Azar. For efficient identification and treatment of PKDL patients, confined to the endemic zones, government initiative has started since 2005, The Kala Azar Elimination Program, as a joint venture between India, Bangladesh and Nepal (Zijlstra et al., 2017). Recent report by Molina et al. (2017) and Moulik et al. (2018) suggested higher and/or equal infective potential and prevalence of PKDL patients suffering with MAC lesions, in contrast to PKDL patients suffering with POLY lesions, in endemic zone of West Bengal. The gold standard diagnostic approach, slit skin smear test shows very low parasite detection sensitivity, which ranges from 4 to 58% (Mondal et al., 2010; Zijlstra, 2016) for PKDL patients suffering with MAC lesions. Further most MAC PKDL patients are often misdiagnosed as pityriasis versicolor, due to similar dermal manifestation and very low number of LD bodies which is often missed out from detection. This prevents MAC PKDL patients from receiving prescribed diagnostic care (Das et al., 2011; Singh et al., 2015). Recent report suggested that PKDL patients suffering with MAC lesions harbor sufficient parasites, which in turn are transmitted by sandfly to HI (Moulik et al., 2018) resulting in active VL cases. The present available diagnostic methods fail to differentiate between fresh PKDL patients with active MAC lesions in comparison to CR individuals, after treatment completion.

The later situation arises due to persistence of high titres of anti-leishmanial antibody even after treatment completion (Desjeux et al., 2013). Moreover anti-leishmanial drugs requires longer duration, to reach the dermal site, due to partial skin diffusion (Zijlstra et al., 2017). The prescribed drugs of choice; Miltefosine and liposomal amphotericin B (LAmB), both lack efficacy toward parasite clearance. Miltefosine has been reported previously to show high efficacy toward parasite clearance in PKDL affected patients, but recent studies reported decline in its effectiveness in parasite clearance (Ghosh et al., 2015; Ramesh et al., 2015). Although LAmB has shown high efficacy in VL treatment, the drug efficacy in parasite clearance, especially for PKDL patients suffering with MAC lesions, is remarkably very low (Moulik et al., 2018). For proper disease administration, both diagnostic and prognostic management of PKDL patients stands as a crucial point. The goal of our present study is to identify glycated CICs protein biomarkers, to efficiently combat this gross disease situation.

In the current study, we have shown that the glycated CICs proteome of PKDL patients suffering with MAC and/or POLY lesion, differ significantly compared to HI and CR individuals. In addition, significant difference were observed among the CICs proteome of MAC PKDL patients, compared to

POLY PKDL patients. Exploiting the CICs proteome difference associated with different PKDL patients, HI and CR individuals, we were able to identify two differentially expressed glycated CICs protein, that have the potential to act as diagnostic and prognostic protein biomarker for efficient management of PKDL patients.

Previous studies reported the presence of altered proteomic profile among the plasma of VL patients. Plasma serves as a precious source for analysis of pathophysiological alterations associated with both disease identification and progression. Qualitative proteomic study on the plasma samples of VL patients' reported up-regulation of α-1-acid glycoprotein and C1 inhibitor and down regulation of retinol binding protein and transport protein transthyretin (Rukmangadachar et al., 2011), whereas quantitative study reported up-regulation of α-1-antitrypsin, α-1-B glycoprotein, and amyloid-A1 precursor; and down regulation of vitamin-D binding protein (Bag et al., 2014). These proteins were found to play important role in disease pathology, for example α-1-acidglycoprotein is elevated during systemic tissue inflammation and is involved in neutrophil inactivation, chemotaxis, and oxidative metabolism (Pucadyil et al., 2004). The importance of plasma proteome profile for identification of disease specific protein biomarkers among various diseases were previously reported for Dengue patients (Jadhav et al., 2017), for Rheumatoid arthritis patients (Ohyama et al., 2012) and for VL patients (Bag et al., 2014). No such studies were reported previously for PKDL patients. Study of this kind will be of immense importance for the identification of PKDL specific protein biomarker, further providing assistance toward disease progression and monitoring therapeutic response among PKDL patient.

In the present proteomic study targeting the glycated CICs, of PKDL patients, we have identified 32 up-regulated and 11 down-regulated proteins among MAC PKDL patients compared to HI. Similarly, 18 up-regulated and 42 down-regulated proteins were observed among MAC PKDL patients compared to POLY PKDL patients. Moreover, 71 up-regulated and 19 down-regulated proteins were observed among MAC PKDL patients compared to CR individuals. These proteins were largely linked to inflammatory response, immune system process and transport, which could be in accordance with various dermal manifestations linked with PKDL patients suffering with MAC and POLY lesions.

Previous reports have suggested that *Leishmania* parasite interacts with specific host cellular targets (dermal dendritic cells, mast cells and macrophages) (Kaye and Scott, 2011) as well as the promastigotes gets deposited into the dermal extracellular matrix (Moreno et al., 2010), for efficient infection. Recent works by direct binding assay with intact live *Leishmania* promastigotes, revealed the host interacting partners for efficient *Leishmania* infection. These studies identified various molecules, among which circulating glycoproteins PLG and VTN, have shown very high binding affinity with *L. donovani* promastigotes (Fatoux-Ardore et al., 2014). Our experimental data for the first time shows higher expression of circulating glycoproteins PLG and VTN, present in the glycated CICs of PKDL patients' plasma samples, in comparison to that of HI and CR individuals. Glycoprotein PLG is a member of the extracellular matrix (ECM) component and is critical for blood coagulation which assists in neutrophils and macrophage migration during wound healing (Serada et al., 2010).

Recent studies reported the binding of *L. donovani* parasite to PLG and to its activated form, plasmin (Fatoux-Ardore et al., 2014). This interaction is assisted by enolase secreting exocytic vesicle, which in turn traps the macrophages and possibly allows the parasite to migrate to dermis (Levin and Burgner, 2014; Fujimoto et al., 2015). Interaction of PLG with *L. donovani*, *Leishmania braziliensis, Leishmania tropica, Leishmania major,* and *Leishmania infantum* has recently been reported (Fatoux-Ardore et al., 2014). Studies suggest that the activation of TGF-β depends on availability of various molecules such as plasmin, urokinase plasminogen activator, M6P, etc.; which in turn depends on activation state macrophage (Song and Wang, 2015).

Glycoprotein VTN, found in blood and extracellular matrix, is a multifunctional glycoprotein which binds to glycosaminoglycan, collagen, PLG and urokinase-receptor (uPAR). It is also located in extracellular matrix and binds to PLG activation inhibitor-1, complement, heparin and thrombin-antithrombin III complexes. This results in cascade of immunological response and regulation of clot formation (Kadowaki et al., 2011). uPAR, a VTN binding protein, is found to associate with latent TGF-β and leads to TGF-β conversion, suggesting the role of VTN toward TGF-β availability, activation and degradation (Godár et al., 1999). Recently reported, VTN has been found to interact with parasite *L. donovani* and *Leishmania braziliensis,* indicating its possible role toward host parasite interaction (Fatoux-Ardore et al., 2014).

TGF-β is a growth regulatory protein known for its diversified biological activity like wound healing, growth, and differentiation and angiogenesis. Inside the cell, TGF-β is present in two milieu; latent form and active form (Sporn et al., 1986; Barnard et al., 1990; Massague et al., 1992; Roberts and Sporn, 1993). Previous studies targeting the immunological characterization of active TGF-β revealed its potential role as regulatory cytokine which suppresses iNOS synthase, IFN- gamma production and Th1 and Th2 cell production (Gantt et al., 2003) which in turn assists in survival of *Leishmania* parasite inside the macrophages. Further studies suggested that higher levels of TGF-β causes down regulation of IFN- gammaR among Indian PKDL patients (Ansari et al., 2006, 2008). In our studies, higher levels of TGF-β were observed among PKDL patients suffering from MAC and POLY lesions as compared to HI and CR individuals (**Figure 3D**).

For the first time, based on the proteomics study supported by western blot and ELISA, we report higher levels of circulating glycoproteins; PLG, VTN and plasma cytokine TGF-β, among PKDL patients with MAC and POLY lesions, compared to HI and CR. TGF-β activation plays an important role for *L. donovani* survival inside macrophages by enhancing the production of IL-10 cytokine (Mukhopadhyay et al., 2014). Previous studies have reported various methods of activation of TGF-β involving either one or both the above two circulating glycoproteins; PLG and VTN. Although no such studies has been conducted to reveal

the direct role of these proteins for disease progression among Indian PKDL patients. One study has revealed the binding of PLG and VTN directly on the surface *L. donovani* (Fatoux-Ardore et al., 2014) where as another study has revealed that the activation of TGF-β assist in survival of *Leishmania chagasi* inside macrophages (Gantt et al., 2003).

Taken together circulating glycoproteins PLG, VTN and cytokine TGF-β add up to PKDL disease severity. Based on the importance of PLG, VTN and TGF-β, each contributing individually toward PKDL progression, we studied the association of PLG and VTN with cytokine TGF-β. Positive association was observed between PLG-TGF-β ($p < 0.0001$) and VTN-TGF-β ($p < 0.0001$) which could be used as a prognostic marker for PKDL. TGF-β interacts directly with Plasmin- the activated form of PLG. Thus, our investigation revealed for the first time that circulating glycoprotein PLG and VTN could serve as severity biomarker for PKDL patients along with TGF-β; an important cytokine for PKDL severity, as reported previously by Saha et al. (2007).

Glycoprotein PLG and VTN could successfully differentiate between drug responsive and drug un-responsive PKDL patients. In this study 10 PKDL patients were longitudinally monitored, among which 5 PKDL patients were recognized as clinically CR as no dermal lesions was observed after treatment with Miltefosine. Among these patients the levels of PLG and VTN were significantly reduced and were at par with the PLG and VTN levels of CR individuals. Whereas, 5 PKDL patients treated with LAmB did not show regression of dermal lesion and PLG and VTN levels were at par with the MAC and POLY PKDL patients. The titer value "mean ± S.E.M" value of 405.7 ± 19.96 μg/ml and 236.4 ± 13.42 μg/ml was obtained, for PLG, for drug responsive cases at presentation with respect to follow up. Similarly for VTN, the titer value "mean ± S.E.M" value of 49.33 ± 3.55 μg/ml and 26.65 ± 0.654 was obtained, for drug responsive cases at presentation with respect to follow up. However, for drug un-responsive cases "mean ± S.E.M" value of 425.4 ± 39.04 μg/ml and 306.1 ± 5.246 μg/ml was obtained for PLG at presentation with respect to follow up. Similarly for VTN, the titer value "mean ± S.E.M" value of 70.98 ± 2.171 μg/ml and 60.05 ± 1.644 μg/ml was obtained for drug un-responsive cases, reflecting no significant decrease in titers even after treatment completion. Hence VTN and PLG were able to efficiently identify the drug unresponsiveness of these PKDL patient.

Conventional anti-leishmanial antibody based ELISA failed to efficiently differentiate between drug responsive and unresponsive groups. Due to limited number of PKDL patient samples, we were unable to analyse the effectiveness of these biomarker proteins; PLG and VTN, toward monitoring the specific drug dosage required for individual patient care. Future studies with higher patient pool will reveal the answer.

PKDL patients suffering with MAC lesions are tough to diagnose and are often misdiagnosed as Vitiligo or Pityriasis versicolor, having similar dermal lesions. Due to very less parasite load among MAC PKDL patients, most of the diagnostic tools lack sensitivity toward efficient case detection. The most commonly used rK39 strip test, Leishmania skin test (LST) and histopathological studies with patients' skin biopsy has only 73, 54, and 7–33% sensitivity, respectively toward detecting MAC PKDL patients (Zijlstra et al., 1994; Ramesh and Mukherjee, 1995; Sundar et al., 1998; Sharma et al., 2000; Salotra et al., 2001, 2003) With such difficult scenario to efficiently target and detect these PKDL patients, which in turn acts as a reservoir for transmission of *L. donovani* parasite and target healthy individuals resulting in VL, it becomes very essential to identify these patients efficiently.

To answer the above problem i.e., for efficient detection of PKDL patients suffering with MAC lesions, where parasite load is very less, we compared the differential fold change levels of PLG and VTN among PKDL patients suffering with MAC and POLY lesion. Our experimental LC-MS/MS data revealed up-regulation of PLG and down regulation of VTN among PKDL patients suffering with MAC lesions when compared to PKDL patients suffering with POLY lesions. This reveals that the ratio of VTN vs. PLG could serve as an efficient biomarker for efficient diagnosis for PKDL patients suffering with MAC lesions. Pathway analysis of various differentially expressed proteins, observed during the proteomic study of the glycated CICs of PKDL patients revealed alterations in transportation and immunological pathway (**Table 2**).

CONCLUSION

In conclusion, these novel observations from the proteomic profiling of the glycated CICs of PKDL patients revealed two important circulating glycoproteins PLG and VTN, with significantly higher titers in PKDL diseased individuals (MAC and POLY) in comparison to control groups (HI, VL, CR, Vitiligo, and Leprosy). Hence the above identified proteins have immense potential to act as PKDL diagnostic and prognostic biomarkers. This study opens a broad spectrum for efficient targeted drug designing for successful control and elimination of PKDL.

DATA AVAILABILITY STATEMENT

The datasets generated for this study can be found in the data are available via ProteomeXchange with identifier PXD012960.

ETHICS STATEMENT

The studies involving human participants were reviewed and approved by Clinical Research Ethics Committee School of Tropical Medicine (CREC-STM) Under Central drugs standard control organisation (CDSCO), Under Directorate General of Health Services, Ministry of Health And Family Welfare, Government of India. The patients/participants provided their written informed consent to participate in this study.

AUTHOR CONTRIBUTIONS

PJ and SM contributed to conceptualization, data curation, writing the original draft, and review and editing the manuscript. PJ, GP, MG, BS, and SM were responsible for the formal analysis. SM acquired the funding. PJ, MG, BS, and SM carried out the investigation. PJ worked on the methodology and visualization. MG, BS, and SM were responsible for administration, resources, and supervision. PJ and GP helped with the software and validation.

FUNDING

This study received financial funding from SERB (File no: YSS/2014/000934), Govt. of India. PJ was a recipient of CSIR Senior Research Fellowship (09/951(0005/2019-EMR-1).

ACKNOWLEDGMENTS

We acknowledge all study participants for their whole-hearted cooperation during the entire study period.

SUPPLEMENTARY MATERIAL

The Supplementary Material for this article can be found online at: https://www.frontiersin.org/articles/10.3389/fcimb.2020.00251/full#supplementary-material

REFERENCES

Alvar, J., Vélez, I. D., Bern, C., Herrero, M., Desjeux, P., Cano, J., et al. (2012). Leishmaniasis worldwide and global estimates of its incidence. *PLoS ONE* 7:e35671. doi: 10.1371/journal.pone.0035671

Ansari, N. A., Katara, G. K., Ramesh, V., and Salotra, P. (2008). Evidence for involvement of TNFR1 and TIMPs in pathogenesis of post-kala-azar dermal leishmaniasis. *Clin. Exp. Immunol.* 154, 391–398. doi: 10.1111/j.1365-2249.2008.03761.x

Ansari, N. A., Ramesh, V., and Salotra, P. (2006). Interferon (IFN)-gamma, tumor necrosis factor-alpha, interleukin-6, and IFN-gamma receptor 1 are the major immunological determinants associated with post-kala azar dermal leishmaniasis. *J. Infect. Dis.* 194, 958–965. doi: 10.1086/506624

Bag, A. K., Sutapa, S., Sundar, S., Saha, B., Chakrabarti, A., and Mandal, C. (2014). Comparative proteomics and glycoproteomics of plasma proteins in indian visceral leishmaniasis. *Proteome Sci.* 12:48. doi: 10.1186/s12953-014-0048-z

Bandyopadhyay, S., Chatterjee, M., Pal, S., Waller, R. F., Sundar, S., McConville, M. J., et al. (2004). Purification, characterization of o-acetylated sialoglycoconjugates-specific IgM, and development of an enzyme-linked immunosorbent assay for diagnosis and follow-up of indian visceral leishmaniasis patients. *Diagn. Microbiol. Infect. Dis.* 50, 15–24. doi: 10.1016/j.diagmicrobio.2004.04.014

Barnard, J. A., Lyons, R. M., and Moses, H. L. (1990). The cell biology of transforming growth factor β. *Biochim. Biophys. Acta*. 1032, 79–87. doi: 10.1016/0304-419X(90)90013-Q

Basher, A., Nath, P., Nabi, S. G., Selim, S., Rahman, Md. F., Abul, F., et al. (2012). A study on health seeking behaviors of patients of post-kala-azar dermal leishmaniasis. *Biomed. Res. Int.* 2015:314543. doi: 10.1155/2015/314543

Bassil, E., Hu, H., and Brown, P. H. (2004). Use of phenylboronic acids to investigate boron function in plants. Possible role of boron in transvacuolar cytoplasmic strands and cell-to-wall adhesion. *Plant physiol.* 136, 3383–3395. doi: 10.1104/pp.104.040527

Blum, J. J., Lehman, J. A., Horn, J. M., and Gomez-cambronero, J. (2001). Phospholipase D (PLD) is present in *Leishmania donovani* and its activity increases in response to acute osmotic stress. *J. Eukaryot. Microbiol.* 48, 102–110. doi: 10.1111/j.1550-7408.2001.tb00421.x

Das, N. K., Singh, S. K., Ghosh, S., Sarkar, A., Mukhopadhyay, D., Roy, S., et al. (2011). Case report: case series of misdiagnosis with rk39 strip test in indian leishmaniasis. *Am. J. Trop. Med. Hyg.* 84, 688–691. doi: 10.4269/ajtmh.2011.10-0590

Das, T., Sen, A. K., Kempf, T., Pramanik, S. R., Mandal, C., and Mandal, C. (2003). Induction of glycosylation in human c-reactive protein under different pathological conditions. *Biochem. J.* 373, 345–355. doi: 10.1042/bj20021701

Datta, S., Modak, D., Sarkar, S., Saha, B., and Mukhopadhyay, S. (2015). Identification and glycobiological characterization of circulating immune complexes in patients with visceral leishmaniasis and post kala azar dermal leishmaniasis. *Indian J. Exp. Biol.* 53, 321–328.

Desjeux, P., Ghosh, R. S., Dhalaria, P., Strub-Wourgaft, N., and Zijlstra, E. E. (2013). Report of the post kala-azar dermal leishmaniasis (PKDL) consortium meeting, New Delhi, India, 27–29 june 2012. *Parasit. Vectors*. 6:196. doi: 10.1186/1756-3305-6-196

Desjeux, P., and Ramesh, V. (2011). "Post-kala-azar dermal leishmaniasis: facing the challenge of eliminating kala-azar from South Asia," in *Kala Azar in South Asia*, eds T. Jha and E. Noiri (Dordrecht: Springer), 111–124. doi: 10.1007/978-94-007-0277-6_11

Domínguez, M., and Toraño, A. (1999). Immune adherence–mediated opsonophagocytosis: the mechanism of leishmania infection. *J. Exp. Med.* 189, 25–35. doi: 10.1084/jem.189.1.25

Fatoux-Ardore, M., Peysselon, F., Weiss, A., Bastien, P., Pratlong, F., and Ricard-Blum, S. (2014). Large-scale investigation of leishmania interaction networks with host extracellular matrix by surface plasmon resonance imaging. *Infect. Immun.* 82, 594–606. doi: 10.1128/IAI.01146-13

Fujimoto, M., Serada, S., Suzuki, K., Nishikawa, A., Ogata, A., Nanki, T., et al. (2015). Brief report: leucine-rich A2-glycoprotein as a potential biomarker for joint inflammation during anti-interleukin-6 biologic therapy in rheumatoid athritis. *Arthritis Rheumatol.* 67, 2056–2060. doi: 10.1002/art.39164

Ganguly, S., Das, N. K., Barbhuiya, J. N., and Chatterjee, M. (2010). Post-kala-azar dermal leishmaniasis – an overview. *Int. J. Dermatol.* 49, 921–931. doi: 10.1111/j.1365-4632.2010.04558.x

Gantt, K. R., Schultz-Cherry, S., Rodriguez, N., Jeronimo, S. M. B., Nascimento, E. T., Goldman, T. L., et al. (2003). Activation of TGF-β by *Leishmania chagasi* : importance for parasite survival in macrophages. *J. Immunol.* 170, 2613–2620. doi: 10.4049/jimmunol.170.5.2613

Ghosh, S., Das, N. K., Mukherjee, S., Mukhopadhyay, D., Barbhuiya, J. N., Hazra, A., et al. (2015). Inadequacy of 12-week miltefosine treatment for indian post-kala-azar dermal leishmaniasis. *Am. J. Trop. Med. Hyg.* 93, 767–769. doi: 10.4269/ajtmh.14-0721

Godár, S., Horejší, V., Weidle, U. H., Binder, B. R., Hansmann, C., and Stockinger, H. (1999). M6P/IGFII-receptor complexes urokinase receptor and plasminogen for activation of transforming growth factor-b1. *Eur. J. Immunol.* 29, 1004–1013.

Hageman, J. H., and Kuehn, G. D. (1992). Boronic acid matrices for the affinity purification of glycoproteins and enzymes. *Methods Mol. Biol.* 11, 45–72. doi: 10.1385/0-89603-213-2:45

Hoiby, N., Doring, G., and Schiotz, P. O. (1986). The role of immune complexes in the pathogenesis of bacterial infections. *Ann. Rev. Microbiol.* 40, 29–53. doi: 10.1146/annurev.mi.40.100186.000333

Jadhav, M., Nayak, M., Kumar, S., Venkatesh, A., Patel, S. K., Kumar, V., et al. (2017). Clinical proteomics and cytokine profiling for dengue fever disease severity biomarkers. *Omics* 21, 665–677. doi: 10.1089/omi.2017.0135

Jaiswal, P., Datta, S., Sardar, B., Chaudhuri, S. J., Maji, D., Ghosh, M., et al. (2018). Glycoproteins in circulating immune complexes are biomarkers of patients with indian PKDL: a study from endemic districts of West Bengal, India. *PLoS ONE* 13:e0192302. doi: 10.1371/journal.pone.0192302

Kadowaki, M., Sangai, T., Nagashima, T., Sakakibara, M., Yoshitomi, H., Takano, S., et al. (2011). Identification of vitronectin as a novel serum marker for early breast cancer detection using a new proteomic approach. *J. Cancer Res. Clin. Oncol.* 137, 1105–1115. doi: 10.1007/s00432-010-0974-9

Kaye, P., and Scott, P. (2011). Leishmaniasis: complexity at the host-pathogen interface. *Nat. Rev. Microbiol.* 9, 604–615. doi: 10.1038/nrmicro2608

Levin, M., and Burgner, D. (2014). Treatment of kawasaki disease with anti-TNF antibodies. *Lancet.* 383, 1700–1703. doi: 10.1016/S0140-6736(14)60131-8

Lowry, O. H., Rosebrough, N. J., Farr, A. L., and Randall,. R. J. (1951). Protein measurement with the folin phenol reagent. *J. Biol. Chem.* 193, 265–275.

Maere, S., Heymans, K., and Kuiper, M. (2005). BiNGO: a cytoscape plugin to assess over-representation of gene ontology categories in biological networks. *Bioinformatics* 21, 3448–3449. doi: 10.1093/bioinformatics/bti551

Massague, J., Cheifetz, S., Laiho, M., Ralph, D. A., Weis, F. M., and Zentella, A. (1992). Transforming growth factor-beta. *Cancer Surv.* 12, 81–103.

Mathsson, L., Lampa, J., Mullazehi, M., and Rönnelid, J. (2006). Immune complexes from rheumatoid arthritis synovial fluid induce FcγRIIa dependent and rheumatoid factor correlated production of tumour necrosis factor-α by peripheral blood mononuclear cells. *Arthritis Res. Ther.* 8:R64. doi: 10.1186/ar1926

Molina, R., Ghosh, D., Carrillo, E., Monnerat, S., Bern, C., Mondal, D., et al. (2017). Infectivity of post-kala-azar dermal leishmaniasis patients to sand flies: revisiting a proof of concept in the context of the kala-azar elimination program in the Indian. *Clin. Infect. Dis.* 65, 150–153. doi: 10.1093/cid/cix245

Mondal, D., Nasrin, K. N., Huda, M. M., Kabir, M., Hossain, M. S., Kroeger, A., et al. (2010). Enhanced case detection and improved diagnosis of PKDL in a kala-azar-endemic area of bangladesh. *PLoS Negl. Trop. Dis.* 4:e832. doi: 10.1371/journal.pntd.0000832

Moreno, I., Domínguez, M., Cabañes, D., Aizpurua, C., and Torañ, A. (2010). Kinetic analysis of *ex vivo* human blood infection by leishmania. *PLoS Negl. Trop. Dis.* 4:743. doi: 10.1371/journal.pntd.0000743

Moss, J., Woodrow, D. F., Guillon, J.-C., and Gresser, I. (1982). Tubular Aggregates and Interferon. *The Lancet.* 320, 1277–1278. doi: 10.1016/s0140-6736(82)90130-1

Moulds, J. M., Moulds, J. J., Brown, M., and Atkinson, J. P. (1992). Antiglobulin testing for CR1-related (knops/mcCoy/swain-langley/york) blood group antigens: negative and weak reactions are caused by variable expression of CR1. *Vox Sang.* 62, 230–235. doi: 10.1159/000462207

Moulik, S., Chaudhuri, S. J., Sardar, B., Ghosh, M., Saha, B., Das, N. K., et al. (2018). Monitoring of parasite kinetics in Indian post–kala-azar dermal leishmaniasis. *Clin. Infect. Dis.* 66, 404–410. doi: 10.1093/cid/cix808

Mukhopadhyay, D., Dalton, J. E., Kaye, P. M., and Chatterjee, M. (2014). Post kala-azar dermal leishmaniasis: an unresolved mystery. *Trends Parasitol.* 30, 65–74. doi: 10.1016/j.pt.2013.12.004

Nguyen, T. H., Trieu, H. T., Okamoto, K., Ninh, T. T. H., Ha, T. T. N., Morita, K., et al. (2013). Proteomic profile of circulating immune complexes in dengue infected patients. *J. Trop. Dis.* 1:109. doi: 10.4172/2329-891X.1000109

Ohyama, K., Kawakami, A., Tamai, M., Baba, M., Kishikawa, N., and Kuroda, N. (2012). Serum immune complex containing thrombospondin-1: a novel biomarker for early rheumatoid arthritis. *Ann. Rheum. Dis.* 71, 1916–1917. doi: 10.1136/annrheumdis-2012-201305

Perry, D., Dixon, K., Garlapati, R., Gendernalik, A., Poché, D., and Poché, R. (2013). Visceral leishmaniasis prevalence and associated risk factors in the saran district of Bihar, India, from 2009 to July of 2011. *Am. J. Trop. Med. Hyg.* 88, 778–784. doi: 10.4269/ajtmh.12-0442

Pucadyil, T. J., Tewary, P., Madhubala, R., and Chattopadhyay, A. (2004). Cholesterol is required for *Leishmania donovani* infection: implications in leishmaniasis. *Mol. Biochem. Parasitol.* 133, 145–152. doi: 10.1016/j.molbiopara.2003.10.002

Ramesh, V., and Mukherjee, A. (1995). Post-kala-azar dermal leishmaniasis. *Int. J. Dermatol.* 34, 85–91. doi: 10.1111/j.1365-4362.1995.tb03584.x

Ramesh, V., Singh, R., Kumar, A., Verma, A., Deep, D. K., Verma, S., et al. (2015). Decline in clinical efficacy of oral miltefosine in treatment of post kala-azar dermal leishmaniasis (PKDL) in India. *PLoS Negl. Trop. Dis.* 9:e0004093. doi: 10.1371/journal.pntd.0004093

Ray, S., Kamath, K. S., Srivastava, R., Raghu, D., Gollapalli, K., Jain, R., et al. (2012). Serum proteome analysis of vivax malaria: an insight into the disease pathogenesis and host immune response. *J. Proteomics.* 75, 3063–3080. doi: 10.1016/j.jprot.2011.10.018

Roberts, A. B., and Sporn, M. B. (1993). Physiological actions and clinical applications of transforming growth factor-β (TGF-β). *Growth Factors* 8, 1–9. doi: 10.3109/08977199309029129

Rönnelid, J., Tejde, A., Mathsson, L., Nilsson-Ekdahl, K., and Nilsson, B. (2003). Immune complexes from SLE sera induce IL10 production from normal peripheral blood mononuclear cells by an FcγRII dependent mechanism: implications for a possible vicious cycle maintaining B cell hyperactivity in SLE. *Ann. Rheum. Dis.* 62, 37–42. doi: 10.1136/ard.62.1.37

Rukmangadachar, L. A., Kataria, J., Hariprasad, G., Samantaray, J. C., and Srinivasan, A. (2011). Two-dimensional difference gel electrophoresis (DIGE) analysis of sera from visceral leishmaniasis patients. *Clin. Proteomics.* 8:4. doi: 10.1186/1559-0275-8-4

Saha, S., Mondal, S., Ravindran, R., Bhowmick, S., Modak, D., Mallick, S., et al. (2007). IL-10-and TGF-β-mediated susceptibility in kala-azar and post-kala-azar dermal leishmaniasis: the significance of amphotericin B in the control of Leishmania donovani infection in India. *J. Immunol.* 179, 5592–5603. doi: 10.4049/jimmunol.179.8.5592

Salotra, P., Sreenivas, G., Beena, K. R., Mukherjee, A., and Ramesh, V. (2003). Parasite detection in patients with post kala-azar dermal leishmaniasis in India: a comparison between molecular and immunological methods. *J. Clin. Pathol.* 56, 840–843. doi: 10.1136/jcp.56.11.840

Salotra, P., Sreenivas, G., Ramesh, V., and Sundar, S. (2001). A simple and sensitive test for field diagnosis of post kala-azar dermal leishmaniasis. *Br. J. Dermatol.* 145, 630–632. doi: 10.1046/j.1365-2133.2001.04434.x

Sata, T., Zuber, C., and Roth,. J. (1990). Lectin - digoxigenin conjugates: a new hapten system for glycoconjugate cytochemistry. *Histochemistry* 94, 1–11. doi: 10.1007/BF00266783

Sengupta, R., Chaudhuri, S. J., Moulik, S., Ghosh, M. K., Saha, B., Das, N. K., et al. (2018). Active surveillance identified a neglected burden of macular cases of post kala-azar dermal leishmaniasis in West Bengal. *PLoS Negl. Trop. Dis.* 13:e0007249. doi: 10.1371/journal.pntd.0007249

Serada, S., Fujimoto, M., Ogata, A., Terabe, F., Hirano, T., Iijima, H., et al. (2010). ITRAQ-based proteomic identification of ieucine-rich α-2 glycoprotein as a novel inflammatory biomarker in autoimmune diseases. *Ann. Rheum. Dis.* 69, 770–774. doi: 10.1136/ard.2009.118919

Shannon, P., Markiel, A., Ozier, O., Baliga, N. S., Wang, J. T., Ramage, D., et al. (2003). Cytoscape: a software environment for integrated models of biomolecular interaction networks. *Genome Res.* 13, 2498–2504. doi: 10.1101/gr.1239303

Sharma, M. C., Gupta, A. K., Verma, N., Das, V. N., Saran, R., and Kar, S. K. (2000). Demonstration of leishmania parasites in skin lesions of Indian post kala-azar dermal leishmaniasis (PKDL) cases. *J. Commun. Dis.* 32, 67–68.

Singh, A., Ramesh, V., and Ramam, M. (2015). Histopathological characteristics of post kala-azar dermal leishmaniasis: a series of 88 patients. *Int. J. Dermatol.* 55, 250–255. doi: 10.4103/0378-6323.148562

Singh, S. K., Bimal, S., Dinesh, D. S., Gupta, A. K., Sinha, P. K., Bimal, R., et al. (2005). Towards identifying immunogenic targets in visceral leishmaniasis: role of 17 kDa and 63 kDa phosphoproteins. *Am. J. Immunol.* 1, 96–100. doi: 10.3844/ajisp.2005.96.100

Song, W., and Wang, X. (2015). The role of TGFβ1 and LRG1 in cardiac remodelling and heart failure. *Biophys. Rev.* 7, 91–104. doi: 10.1007/s12551-014-0158-y

Sporn, M. B., Roberts, A. B., Wakefield, L. M., and Assoian, R. K. (1986). Transforming growth factor-β: biological function and chemical structure. *Science.* 233, 532–534. doi: 10.1126/science.3487831

Stoll, M. S., and Hounsell, E. F. (1987). Selective purification of reduced oligosaccharides using a phenylboronic acid bond elut column: potential application in HPLC, mass spectrometry, reductive amination procedures and antigenic/serum analysis. *Biomed. Chromatogr.* 2, 249–253. doi: 10.1002/bmc.1130020605

Sundar, S., Reed, S. G., Singh, V., P., Kumar, P, C., and Murray, H. (1998). Rapid accurate field diagnosis of indian visceral leishmaniasis. *Lancet* 351, 563–565. doi: 10.1016/S0140-6736(97)04350-X

WHO (2010). *Control of the Leishmaniases: Report of a Meeting of the WHO Expert Committee on the Control of Leishmaniasis*. Geneva. Available online at: https://apps.who.int/iris/bitstream/handle/10665/44412/WHO_TRS_949_eng.pdf?sequence=1 (accessed August 10, 2019).

WHO (2015). *Kala-azar Elimination Programme: Report of a WHO Consultation of Partners Leishmaniasis*. Geneva. Available online at: https://apps.who.int/iris/bitstream/handle/10665/185042/9789241509497__eng.pdf?sequence=1 (accessed August 10, 2019).

Zijlstra, E. E. (2016). The immunology of post-kala-azar dermal leishmaniasis (PKDL). *Parasit. Vectors.* 9:464. doi: 10.1186/s13071-016-1721-0

Zijlstra, E. E., Alves, F., Rijal, S., Arana, B., and Alvar, J. (2017). Post-kala-azar dermal leishmaniasis in the indian subcontinent: a threat to the south-east asia region kala-azar elimination programme. *PLoS Negl. Trop. Dis.* e0005877. doi: 10.1371/journal.pntd.0005877

Zijlstra, E. E., El-Hassan, A. M., Ismael, A., and Ghalib, H. W. (1994). Endemic kala-azar in eastern sudan: a longitudinal study on the incidence of clinical and subclinical infection and post kala-azar dermal leishmaniasis. *Am. J. Trop. Med. Hyg.* 51, 826–836. doi: 10.4269/ajtmh.1994.51.826

Zijlstra, E. E., Khalil, E. A. G., Kager, P. A., and El-Hassan, A. M. (2000). Post-kala-azar dermal leishmaniasis in the sudan: clinical presentation and differential diagnosis. *Br. J. Dermatol.* 143, 136–143. doi: 10.1046/j.1365-2133.2000.03603.x

Zijlstra, E. E., Musa, A. M., Khalil, E. A. G., El-Hassan, I. M., and El-Hassan, A. M. (2003). Post-kala-azar dermal leishmaniasis. *Lancet Infect. Dis.* 3, 87–98. doi: 10.1016/S1473-3099(03)00517-6

Conflict of Interest: The authors declare that the research was conducted in the absence of any commercial or financial relationships that could be construed as a potential conflict of interest.

Advantages of publishing in Frontiers

OPEN ACCESS
Articles are free to read for greatest visibility and readership

FAST PUBLICATION
Around 90 days from submission to decision

HIGH QUALITY PEER-REVIEW
Rigorous, collaborative, and constructive peer-review

TRANSPARENT PEER-REVIEW
Editors and reviewers acknowledged by name on published articles

Frontiers
Avenue du Tribunal-Fédéral 34
1005 Lausanne | Switzerland

Visit us: www.frontiersin.org
Contact us: info@frontiersin.org | +41 21 510 17 00

REPRODUCIBILITY OF RESEARCH
Support open data and methods to enhance research reproducibility

DIGITAL PUBLISHING
Articles designed for optimal readership across devices

FOLLOW US
@frontiersin

IMPACT METRICS
Advanced article metrics track visibility across digital media

EXTENSIVE PROMOTION
Marketing and promotion of impactful research

LOOP RESEARCH NETWORK
Our network increases your article's readership